



Calhoun: The NPS Institutional Archive
DSpace Repository

Theses and Dissertations

1. Thesis and Dissertation Collection, all items

2001-09

A coastal air-ocean coupled system for the East Asian marginal seas

Roth, Michael J.

Monterey, California. Naval Postgraduate School

<http://hdl.handle.net/10945/1461>

Downloaded from NPS Archive: Calhoun



Calhoun is a project of the Dudley Knox Library at NPS, furthering the precepts and goals of open government and government transparency. All information contained herein has been approved for release by the NPS Public Affairs Officer.

Dudley Knox Library / Naval Postgraduate School
411 Dyer Road / 1 University Circle
Monterey, California USA 93943

<http://www.nps.edu/library>

NAVAL POSTGRADUATE SCHOOL Monterey, California



THESIS

**A COASTAL AIR-OCEAN COUPLED SYSTEM FOR THE
EAST ASIAN MARGINAL SEAS**

by

Michael J. Roth

September 2001

Thesis Advisor:
Second Reader:

Peter C. Chu
Steven D. Haeger

Approved for public release; distribution is unlimited.

REPORT DOCUMENTATION PAGE			Form Approved OMB No. 0704-0188	
Public reporting burden for this collection of information is estimated to average 1 hour per response, including the time for reviewing instruction, searching existing data sources, gathering and maintaining the data needed, and completing and reviewing the collection of information. Send comments regarding this burden estimate or any other aspect of this collection of information, including suggestions for reducing this burden, to Washington headquarters Services, Directorate for Information Operations and Reports, 1215 Jefferson Davis Highway, Suite 1204, Arlington, VA 22202-4302, and to the Office of Management and Budget, Paperwork Reduction Project (0704-0188) Washington DC 20503.				
1. AGENCY USE ONLY (Leave blank)		2. REPORT DATE September 2001	3. REPORT TYPE AND DATES COVERED Master's Thesis	
4. TITLE AND SUBTITLE: A Coastal Air-Ocean Coupled System for the East Asian Marginal Seas			5. FUNDING NUMBERS	
6. AUTHOR(S) Michael J. Roth				
7. PERFORMING ORGANIZATION NAME(S) AND ADDRESS(ES) Naval Postgraduate School Monterey, CA 93943-5000			8. PERFORMING ORGANIZATION REPORT NUMBER	
9. SPONSORING / MONITORING AGENCY NAME(S) AND ADDRESS(ES) NAVOCEANO, Stennis Space Center, MS 39522-5001 Institute of Joint Warfare Analysis, NPS, Monterey, CA 93943			10. SPONSORING / MONITORING AGENCY REPORT NUMBER	
11. SUPPLEMENTARY NOTES The views expressed in this thesis are those of the author and do not reflect the official policy or position of the Department of Defense or the U.S. Government.				
12a. DISTRIBUTION / AVAILABILITY STATEMENT Approved for public release; distribution is unlimited.			12b. DISTRIBUTION CODE	
13. ABSTRACT (maximum 200 words) A coastal air-ocean coupled system (CAOCS) that includes the Princeton Ocean Model (POM) as the oceanic component and the Pennsylvania State University/National Center for Atmospheric Research (PSU/NCAR) Mesoscale Model Fifth Generation (MM5) as the atmospheric component was developed for the east Asian marginal seas (EAMS) – a littoral environment that is a common operating area for the United States Navy (USN). CAOCS output verified against surface wind data from the National Centers for Environmental Prediction (NCEP) and sea surface temperature (SST)/Sea Surface Salinity (SSS) data collected from buoy stations. CAOCS output clearly shows the significance of atmospheric and oceanic mesoscale features and their associated air-sea interaction processes such as coastal upwelling, Ekman transport, and enhancement of upward vertical motion during cyclogenesis. These mesoscale features and air-sea interaction processes occur during periods prior to summer monsoon onset as well as during time periods following summer monsoon onset. The study provides support that CAOCS does perform well in forecasting EAMS surface current circulation, SST/SSS structure, surface wind stress, and low-level atmospheric structure. Some weaknesses of CAOCS were identified that will aid in future improvement of the model.				
14. SUBJECT TERMS Numerical modeling and simulation, Oceanography, Yellow/East Sea, South China Sea, East China Sea, South China Sea, air-sea interaction, atmospheric forcing, oceanic forcing			15. NUMBER OF PAGES 590	
16. PRICE CODE				
17. SECURITY CLASSIFICATION OF REPORT Unclassified	18. SECURITY CLASSIFICATION OF THIS PAGE Unclassified	19. SECURITY CLASSIFICATION OF ABSTRACT Unclassified	20. LIMITATION OF ABSTRACT UL	

THIS PAGE INTENTIONALLY LEFT BLANK

Approved for public release; distribution is unlimited.

**A COASTAL AIR-OCEAN COUPLED SYSTEM FOR THE EAST ASIAN
MARGINAL SEAS**

Michael J. Roth
Lieutenant Commander, United States Navy
B.S., United States Naval Academy, 1992

Submitted in partial fulfillment of the
requirements for the degree of


**MASTER OF SCIENCE IN METEOROLOGY AND PHYSICAL
OCEANOGRAPHY**

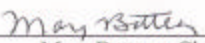
from the

**NAVAL POSTGRADUATE SCHOOL
September 2001**

Author: 
Michael J. Roth

Approved by: 
Peter C. Chu, Thesis Advisor


Steven D. Haeger, Second Reader


Mary Batteen, Chair
Department of Oceanography

THIS PAGE INTENTIONALLY LEFT BLANK

ABSTRACT

A coastal air-ocean coupled system (CAOCS) that includes the Princeton Ocean Model (POM) as the oceanic component and the Pennsylvania State University/National Center for Atmospheric Research (PSU/NCAR) Mesoscale Model Fifth Generation (MM5) as the atmospheric component was developed for the East Asian Marginal Seas (EAMS) – a littoral environment that is a common operating area for the United States Navy (USN). CAOCS output verified against surface wind data from the National Centers for Environmental Prediction (NCEP) and sea surface temperature (SST)/Sea Surface Salinity (SSS) data collected from buoy stations. CAOCS output clearly shows the significance of atmospheric and oceanic mesoscale features and their associated air-sea interaction processes such as coastal upwelling, Ekman transport, and enhancement of upward vertical motion during cyclogenesis. These mesoscale features and air-sea interaction processes occur during periods prior to summer monsoon onset as well as during time periods following summer monsoon onset.

The study provides support that CAOCS does perform well in forecasting EAMS surface current circulation, SST/SSS structure, surface wind stress, and low-level atmospheric structure. Some weaknesses of CAOCS were identified that will aid in future improvement of the model.

THIS PAGE INTENTIONALLY LEFT BLANK

TABLE OF CONTENTS

I.	INTRODUCTION	1
II.	OVERVIEW OF EAMS GEOGRAPHY, OCEANOGRAPHY, AND SEASONAL VARIATION OF ATMOSPHERIC SURFACE FORCING.....	5
A.	JES	5
B.	YES.....	7
1.	YS	7
2.	ECS.....	9
3.	Currents of the YES	9
C.	SCS.....	10
III.	CAOCS	13
A.	OCEAN COMPONENT – PRINCETON OCEAN MODEL (POM).....	13
1.	Model Description.....	13
2.	Boundary Conditions.....	13
3.	Initial Boundary Conditions and Model Initialization.....	13
B.	ATMOSPHERIC COMPONENT – MESOSCALE MODEL FIFTH GENERATION (MM5).....	14
1.	Model Description.....	14
2.	Land Surface Parameterization	14
3.	Initial Conditions and Lateral Boundary Conditions	14
C.	OCEAN-ATMOSPHERIC COUPLING.....	14
IV.	DATA ANALYSIS.....	15
A.	EXTRACTION AND VISUALIZATION OF DATA FROM OCEAN COMPONENT OF CAOCS	15
B.	EXTRACTION AND VISUALIZATION OF DATA FROM ATMOSPHERIC COMPONENT OF CAOCS	15
V.	CAOCS OUTPUT VERIFICATION.....	17
A.	VERIFICATION OF CAOCS ATMOSPHERIC OUTPUT.....	17
1.	Comparison of Interfacial Fluxes Between CAOCS Atmospheric Output and NCEP Data	17
2.	Comparison of 10-m Wind Fields Between CAOCS Atmospheric Output and NCEP Data	17
B.	VERIFICATION OF CAOCS OCEANIC OUTPUT.....	17
1.	Comparison of SST and SSS Values Between CAOCS Oceanic Output and Buoy Station Data	17
VI.	ATMOSPHERIC PROCESSES DURING MAY-JULY 1998	19
A.	MAY TIME PERIOD: MAY 13 THROUGH MAY 31, 1998	19
1.	JES	20
2.	YES.....	46
3.	SCS.....	64

B.	JULY TIME PERIOD: JULY 18 THROUGH JULY 31, 1998.....	74
1.	JES	74
2.	YES.....	92
3.	SCS	103
VII.	OCEANIC PROCESSES DURING MAY-JULY 1998.....	109
A.	MAY TIME PERIOD: MAY 13 THROUGH MAY 31, 1998	111
1.	Sea Surface Temperature (SST)	111
a.	<i>JES</i>	111
b.	<i>YES</i>.....	112
c.	<i>SCS</i>.....	114
2.	Sea Surface Velocity	115
a.	<i>JES</i>	115
b.	<i>YES</i>.....	117
c.	<i>SCS</i>.....	122
3.	Sea Surface Salinity (SSS).....	129
a.	<i>JES</i>	129
b.	<i>YES</i>.....	130
c.	<i>SCS</i>.....	130
B.	JULY TIME PERIOD: JULY 18 THROUGH JULY 31, 1998.....	131
1.	SST	131
a.	<i>JES</i>	131
b.	<i>YES</i>.....	132
c.	<i>SCS</i>.....	133
2.	Sea Surface Velocity	134
a.	<i>JES</i>	134
b.	<i>YES</i>.....	135
c.	<i>SCS</i>.....	137
3.	SSS.....	141
a.	<i>JES</i>	141
b.	<i>YES</i>.....	142
c.	<i>SCS</i>.....	142
VIII.	AIR-SEA INTERACTION	145
A.	MAY TIME PERIOD.....	145
B.	JULY TIME PERIOD	150
IX.	COMPARISON OF CAOCS OCEANIC COMPONENT OUTPUT WITH UNCOUPLED OCEAN MODEL OUTPUT	153
X.	CONCLUSIONS	155
APPENDIX A.	COMPONENTS OF THE EAMS	159
APPENDIX B.	JES GEOGRAPHY	161
APPENDIX C.	WINTER MONSOON.....	163
APPENDIX D.	SUMMER MONSOON	165
APPENDIX E.	SURFACE CURRENTS OF THE JES.....	167

APPENDIX F.	YES GEOGRAPHY	169
APPENDIX G.	SURFACE CURRENTS OF THE YES.....	171
APPENDIX H.	SCS GEOGRAPHY.....	173
APPENDIX I.	SCS SURFACE CIRCULATION PATTERN - WINTER	175
APPENDIX J.	SCS SURFACE CIRCULATION PATTERN - SUMMER.....	177
APPENDIX K.	SCS BIFURCATION REGIME OF THE KUC INTRUSION ...	179
APPENDIX L.	SCS LOOP REGIME OF THE KUC INTRUSION	181
APPENDIX M.	CAOCS OCEANIC BATHYMETRY AND OPEN BOUNDARY LATERAL TRANSPORT.....	183
APPENDIX N.	SAMPLES OF LOW LEVEL WIND FIELD VERIFICATION	185
APPENDIX O.	SAMPLES OF SST VERIFICATION	187
APPENDIX P.	SCS, YES, AND JES REGIONS FOR DISCUSSION OF ATMOSPHERIC AND OCEANIC PROCESSES	189
APPENDIX Q.	500-MB RELATIVE VORTICITY/GEOPOTENTIAL HEIGHT PLOTS OVER THE EAMS FOR THE MAY TIME PERIOD.....	191
APPENDIX R.	700-MB VERTICAL VELOCITY/GEOPOTENTIAL HEIGHT PLOTS OVER THE EAMS FOR THE MAY TIME PERIOD	201
APPENDIX S.	SEA LEVEL PRESSURE/SAT/SURFACE WIND PLOTS FOR THE JES FOR THE MAY TIME PERIOD	211
APPENDIX T.	SEA LEVEL PRESSURE/SAT/SURFACE WIND PLOTS FOR THE YES FOR THE MAY TIME PERIOD	231
APPENDIX U.	SEA LEVEL PRESSURE/SAT/SURFACE WIND PLOTS FOR THE SCS FOR THE MAY TIME PERIOD	251
APPENDIX V.	500-MB RELATIVE VORTICITY/GEOPOTENTIAL HEIGHT PLOTS OVER THE EAMS FOR THE JULY TIME PERIOD.....	271
APPENDIX W.	700-MB VERTICAL VELOCITY/GEOPOTENTIAL HEIGHT PLOTS OVER THE EAMS FOR THE JULY TIME PERIOD.....	287
APPENDIX X.	SEA LEVEL PRESSURE/SAT/SURFACE WIND PLOTS FOR THE JES FOR THE JULY TIME PERIOD	303
APPENDIX Y.	SEA LEVEL PRESSURE/SAT/SURFACE WIND PLOTS FOR THE YES FOR THE JULY TIME PERIOD	319
APPENDIX Z.	SEA LEVEL PRESSURE/SAT/SURFACE WIND PLOTS FOR THE SCS FOR THE JULY TIME PERIOD.....	335
APPENDIX AA.	SST AND SURFACE CURRENT VELOCITY PLOTS FOR THE JES FOR THE MAY TIME PERIOD	351

APPENDIX BB.	SST AND SURFACE CURRENT VELOCITY TENDENCY PLOTS FOR THE JES FOR THE MAY TIME PERIOD.....	361
APPENDIX CC.	SSS PLOTS FOR THE JES FOR THE MAY TIME PERIOD ..	371
APPENDIX DD.	SSS TENDENCY PLOTS FOR THE JES FOR THE MAY TIME PERIOD	381
APPENDIX EE.	SST AND SURFACE CURRENT VELOCITY PLOTS FOR THE YES FOR THE MAY TIME PERIOD	391
APPENDIX FF.	SST AND SURFACE CURRENT VELOCITY TENDENCY PLOTS FOR THE YES FOR THE MAY TIME PERIOD	401
APPENDIX GG.	SSS PLOTS FOR THE YES FOR THE MAY TIME PERIOD .	411
APPENDIX HH.	SSS TENDENCY PLOTS FOR THE YES FOR THE MAY TIME PERIOD	421
APPENDIX II.	SST AND SURFACE CURRENT VELOCITY PLOTS FOR THE SCS FOR THE MAY TIME PERIOD	431
APPENDIX JJ.	SST AND SURFACE CURRENT VELOCITY TENDENCY PLOTS FOR THE SCS FOR THE MAY TIME PERIOD	441
APPENDIX KK.	SSS PLOTS FOR THE SCS FOR THE MAY TIME PERIOD..	451
APPENDIX LL.	SSS TENDENCY PLOTS FOR THE SCS FOR THE MAY TIME PERIOD	461
APPENDIX MM.	SST AND SURFACE CURRENT VELOCITY PLOTS FOR THE JES FOR THE JULY TIME PERIOD	471
APPENDIX NN.	SST AND SURFACE CURRENT VELOCITY TENDENCY PLOTS FOR THE JES FOR THE JULY TIME PERIOD	479
APPENDIX OO.	SSS PLOTS FOR THE JES FOR THE JULY TIME PERIOD .	487
APPENDIX PP.	SSS TENDENCY PLOTS FOR THE JES FOR THE JULY TIME PERIOD	495
APPENDIX QQ.	SST AND SURFACE CURRENT VELOCITY PLOTS FOR THE YES FOR THE JULY TIME PERIOD.....	503
APPENDIX RR.	SST AND SURFACE CURRENT VELOCITY TENDENCY PLOTS FOR THE YES FOR THE JULY TIME PERIOD	511
APPENDIX SS.	SSS PLOTS FOR THE YES FOR THE JULY TIME PERIOD	519
APPENDIX TT.	SSS TENDENCY PLOTS FOR THE YES FOR THE JULY TIME PERIOD	527
APPENDIX UU.	SST AND SURFACE CURRENT VELOCITY PLOTS FOR THE SCS FOR THE JULY TIME PERIOD	535
APPENDIX VV.	SST AND SURFACE CURRENT VELOCITY TENDENCY PLOTS FOR THE SCS FOR THE JULY TIME PERIOD	543

APPENDIX WW. SSS PLOTS FOR THE SCS FOR THE JULY TIME PERIOD.	551
APPENDIX XX. SSS TENDENCY PLOTS FOR THE SCS FOR THE JULY TIME PERIOD	559
LIST OF REFERENCES	567
INITIAL DISTRIBUTION LIST.....	571

THIS PAGE INTENTIONALLY LEFT BLANK

LIST OF ABBREVIATIONS AND ACRONYMS

BS: Bohai Sea

CAOCS: coastal air-ocean coupled system

CGM: computer graphics metacode

COAMPS: coupled ocean-atmosphere mesoscale prediction system

COADS: Comprehensive Ocean and Atmosphere Data Set

EAMS: East Asian Marginal Seas

ECMWF: European Center for Medium-Range Weather Forecasts

ECS: East China Sea

EKWC: East Korean Warm Current

FORTRAN: Formula Translation

IDT: Interactive Display Tool

JES: Japan/East Sea

JNB: Japan Nearshore Branch

JSPW: Japan Sea Proper Water

KUC: Kuroshio Current

MATLAB: Matrix Laboratory

METOC: meteorology and oceanography

MLD: mixed layer depth

MM5: Mesoscale Model Fifth Generation

MMD: Marine Meteorology Division

NCAR: National Center for Atmospheric Research
NCEP: National Centers for Environmental Prediction

NKCC: North Korean Cold Current

NMOC: Naval Meteorology and Oceanography Command

NPS: Naval Postgraduate School

NRL: Naval Research Laboratory

NWL Eddy: eddy located northwest of Luzon Island

POM: Princeton Ocean Model

PSU: Pennsylvania State University

RIP: Read/Interpolate/Plot

RIPDP: RIP Data Preparation

SAT: surface air temperature

SCS: South China Sea

SCSBK: South China Sea Branch of the Kuroshio

SCSWC: South China Sea Warm Current

SPF: Subpolar Front

SSS: sea surface salinity

SST: sea surface temperature (SST)

TWC: Taiwan Warm Current

TsWC: Tsushima Warm Current

USN: United States Navy

YES: Yellow/East China Sea

YS: Yellow Sea

YSCW: Yellow Sea Cold Water

YSWC: Yellow Sea Warm Current

THIS PAGE INTENTIONALLY LEFT BLANK

ACKNOWLEDGMENTS

I would like to express my sincere appreciation to my advisor, Dr. Peter C. Chu, for his inspiration, enthusiasm, expertise, and guidance throughout the course of my thesis research at the Naval Postgraduate School. His positive attitude and moral support greatly enhanced my interest in the subject matter and helped make my thesis work a wonderful learning experience. I also would like to thank Chenwu Fan for his unfailing and prompt technical support and superb programming assistance. I especially want to thank my wife Yuko and son Bobby for providing me with their love, patience, and understanding necessary for me to achieve my academic goals.

THIS PAGE INTENTIONALLY LEFT BLANK

I. INTRODUCTION

The mission of the United States Naval Meteorology and Oceanography Command (NMOC) includes interpreting and applying meteorological and oceanographic data for tactical warfare deployment (Commander Naval Meteorology and Oceanography Command, 2001). United States Navy (USN) contingency planning and current operations emphasize the employment of naval forces to influence events in littoral regions of the world (Welch, 1999). In support of the NMOC mission and in consideration of the emphasis placed on naval operations in the littoral regions of the world, the focus of USN meteorology and oceanography (METOC) support is often on littoral regions at the mesoscale level and needs to be near-real time. One critical operating area of the USN, particularly for the 7th Fleet, is the East Asian Marginal Seas (EAMS). The EAMS is comprised of the South China Sea (SCS), Yellow/East China Sea (YES), and the Japan/East Sea (see Appendix A). In an effort to enhance the METOC support for this region a coastal air-ocean coupled system (CAOCS) has been developed at the Naval Postgraduate School (NPS).

The CAOCS is significant because it focuses on air-sea interaction at the mesoscale level for a littoral region. Air-sea interaction is crucial over the EAMS because the local monsoon system primarily forces the intermediate to upper layer oceanic circulation patterns of the EAMS and significantly alters the sea surface temperature (SST) and mixed layer depth (MLD) over regions of the EAMS (Wyrcki, 1961; Chu et al., 1997a; Chu et al., 1997b, Chu and Li, 2000, Shaw and Chao, 1994; Metzger and Hurlburt, 1996). Additionally, atmospheric forcing and local winds stress significantly contribute to the seasonal variation of the thermal structure of shallow oceanic areas of the EAMS (Chu et al., 1997a; Chu et al., 1997b)

Furthermore, CAOCS is significant because it is representative of the future capability of the USN METOC community's coupled ocean-atmosphere mesoscale prediction system (COAMPS) being further developed by the Marine Meteorology Division (MMD) of the Naval Research Laboratory (NRL). As of this date the oceanic component of the COAMPS is still under development and testing (NRL, 2001).

CAOCS is also significant because it is a source of near-real time data for USN METOC community officers and enlisted personnel.

Earlier studies on the oceanic component of CAOCS show the model is accurate in predicting the thermal structure and current system of the EAMS (Chu et al., 2000) as well as the multi-eddy structure of regions of the EAMS (Chu et al., 1999a). There have not been many studies that focus on the accuracy of the atmospheric component of CAOCS.

This paper focuses on the atmospheric processes of the lower level of the atmosphere, the oceanic processes at the surface of the ocean, and the air-sea interaction between the lower atmosphere and the surface of the ocean. These atmospheric and oceanic processes and the air-sea interaction are observed from model output of CAOCS between May and July 1998. More specifically, two time periods were identified that included significant oceanic and atmospheric mesoscale features present over the EAMS or in the vicinity of the EAMS in the lower atmosphere or at the surface of the ocean. The first time period was prior to the onset of the summer monsoon while the second time period was after the onset of the summer monsoon. Output of the atmospheric component of CAOCS was verified using available previously analyzed data. Output of the oceanic component of CAOCS was also verified against available previously collected data from buoy stations.

There are several intentions of this paper. First, it intends to provide further support that CAOCS does perform well in simulating the EAMS surface current circulation, SST structure, and sea surface salinity (SSS) structure. Secondly, it intends to provide support that CAOCS does perform well in simulating the EAMS surface wind stress and low level atmospheric structure. Thirdly, through analysis of CAOCS output, it intends to show how the atmosphere and ocean behave in a way that cannot be described climatologically due to the small temporal scales of the numerous mesoscale features present at the surface of the ocean and in the lower levels of the atmosphere even during a period following the onset of the summer monsoon. This will provide support regarding the usefulness of CAOCS over an uncoupled, climatologically forced ocean or atmospheric model. Fourthly, through analysis of CAOCS output, it intends to show the

significance of the air-sea interaction processes that occur between the lower atmosphere and the surface of the ocean and that CAOCS is indeed handling these air-sea interaction processes. Finally, the paper emphasizes the near-real time capability of CAOCS and in combination with all the above intentions, it intends to show that CAOCS is an excellent tool for USN METOC community personnel because the accurate, near-real time model output will contribute to increased meteorological, oceanographic, and acoustic forecasting skill in a littoral environment. A comparison is also made between the output of the ocean component of CAOCS and the available output of an uncoupled ocean model.

The following is a basic outline of the structure of the remainder of this paper. Section 2 provides a basic overview of EAMS geography, oceanography, and seasonal variation of atmospheric surface forcing. Section 3 discusses the oceanic and atmospheric components of CAOCS and what the model coupling entails. Section 4 is a discussion of the methods used to extract necessary data from CAOCS output as well as the software used to display CAOCS output. Section 5 discusses verification procedures and the results of the comparisons of CAOCS output with atmospheric data from National Centers for Environmental Prediction (NCEP) and oceanic data from available buoy stations. Section 6 discusses the atmospheric processes that were observed from the output of the atmospheric component of CAOCS during the May time period and the July time period. Section 7 discusses oceanic processes that were observed from the output of the oceanic component of CAOCS during the May time period and the July time period. Section 8 investigates air-sea interaction processes as observed from CAOCS output. Section 9 discusses the results of a comparison between some uncoupled oceanic model output with the output of the oceanic component of CAOCS.

All figures are included as appendices at the end of the thesis. Readers will be referred to the appropriate appendix.

THIS PAGE INTENTIONALLY LEFT BLANK

II. OVERVIEW OF EAMS GEOGRAPHY, OCEANOGRAPHY, AND SEASONAL VARIATION OF ATMOSPHERIC SURFACE FORCING

A. JES

The Japan Sea, known as the East Sea in Korea, is a semi-enclosed ocean basin covering an area of approximately 100,000 km² that contains a steep bottom topography (Chu et al., 2001). The JES is surrounded by the four countries of South Korea, North Korea, Russia, and Japan and has a maximum depth in excess of 3,700 m (see Appendix B). The JES is isolated from open oceans with the exception of a few narrow and shallow straits that connect it to the Pacific Ocean (Park and Chung, 1999; Minami et al., 1999). The Korean Strait is located in the southwest region and connects the JES to the Yellow Sea (YS) and the East China Sea (ECS). The Tsugaru Strait is located in the east region between Hokkaido, Japan and Honshu, Japan and connects the JES to the northwestern Pacific Ocean. The Soya and Tatar Straits in the northeast region connect the JES to the Sea of Okhotsk.

The JES contains three major basins called the Japan Basin, the Ulleng/Tsushima Basin, and the Yamato Basin as well as a high central seamount called the Yamato Rise. The scientific community often views the JES as a miniature prototype ocean since its basin wide circulation pattern, boundary currents, Subpolar Front (SPF), mesoscale eddy activity, and deep-water formation are similar to those in a large ocean (Chu et al., 2001).

The JES is subjected to the seasonal monsoon system (Chu et al., 2001). During the winter monsoon, from November through April, a cold northwest wind blows over the JES due to the presence of the Siberian High over the East Asian continent (see Appendix C). Radiative cooling and persistent cold air advection maintain cold air over the JES during the winter monsoon season. During the summer monsoon, from mid-May to mid-September, a weaker southeasterly wind blows over the JES due to the presence of the Manchurian Low over the East Asian continent and advects warm air into the region (see Appendix D).

There are several named currents present at the surface layer of the JES (see Appendix E). The Liman Current enters the northern JES from the Sea of Okhotsk via

the Tatar Strait and flows southward to southwestward along the Russian coast advecting cold water into the region. As the Liman Current approaches the east coast of North Korea it becomes the North Korean Cold Current (NKCC). Local forcing by wind and buoyancy flux are factors in the formation of the NKCC (Seung, 1994). The Tsushima Warm Current (TsWC) dominates the surface layer as it flows northeastward from the ECS through the Korean Strait and carries warm water into the JES (Chu et al., 2001; Minami et al., 1999). The TsWC is also the only supplier of heat and salt for the JES, especially in the southern JES (Lie and Cho, 1994). The TsWC separates north of 35°N into eastern and western channels (Chu et al., 2001). The eastern channel flow follows the Japanese west coast and is known as the Japan Nearshore Branch (JNB). The western flow follows the Korean east coast but begins to separate from the coast as it flows more northeastward and is known as the East Korean Warm Current (EKWC). Local forcing by wind and buoyancy flux are also factors in the separation from the coast of the EKWC (Seung, 1994). The EKWC undergoes a bifurcation at 37°N into an eastern and western branch.

The northeastward flowing eastern branch of the EKWC converges with the southwestward flowing NKCC at approximately 38°N with some meridional migration and forms the SPF that extends eastward across the basin to the west coast of Hokkaido, Japan (Seung and Yoon, 1995; Chu et al. 2001). The region is also a source of large meanders and associated warm and cold eddies. The western branch of the EKWC generally moves northward and forms a cyclonic eddy in the eastern Korean Bay (Chu et al. 2001). The JNB is generally weaker than the EKWC.

The very deep, cold, and nearly homogenous Japan Sea Proper Water (JSPW) lies below the TsWC, the EKWC, and the JNB and dominates the lower part of the basin (Minami et al., 1999). It accounts for roughly 80% of the total amount of water in the JES. The JSPW lies below approximately 500 m and has a water temperature lower than 1°C and salinity between 34.0 and 34.1 psu. A layer of minimum dissolved oxygen occurs between 1,000 and 1,500 m, but dissolved oxygen is richer in the northern part of the JES as compared to the southern part. The formation of JSPW is affected by the climate over the JES.

B. YES

1. YS

The YS is a semi-enclosed basin covering an area of approximately 295,000 km² (Yanagi and Takahashi, 1993). It is located between China and the Korean peninsula with the Bohai Sea (BS) to the northwest and the ECS to the south (Chu et al., 1997a) (see Appendix F). Four major rivers flow into it - the Yangtze River to the southwest, the Yellow River and the Liao River to the north, and the Han River to the east. The mixing of the fresh water runoff from the rivers with the ECS and Kuroshio Current (KUC) waters is a major contributing factor to the hydrographic character of YS water masses. Despite covering a relatively large area, the YS is quite shallow (Chu et al., 1997b). The water depth over most of the area is less than 50 m. The deepest water is confined to a north-south oriented trench located in the central portion of the YS reaching a maximum depth of 90 m.

Chu et al. (1997b) discuss two significant features of the YS depth distribution. First, the continental shelf is broad and shallow so that the water is readily affected by seasonally varying atmospheric forcing such as heating, cooling, and wind stress. This results in a large seasonal variation of the water masses of the YS. Second, the YS is characterized by east/west asymmetry. For example, extensive shoals less than 20 m are found in the western YS but are not generally found in the vicinity of the Korean peninsula and the 50-m isobath is located more than 100 km from the Chinese coast but only about 50 km from the South Korean coast. This east/west asymmetry plays a crucial role in the shoaling of the MLD.

As was the case for the JES, atmospheric forcing greatly contributes to the seasonal variation of the YS thermal structure (Chu et al., 1997a; Chu et al. 1997b). More specifically, the Asian monsoon circulation significantly alters the SST and greatly affects the MLD. During the winter monsoon season, the location of the Siberian High over the East Asian continent results in very cold northerly to north northwesterly surface winds over the YS region (see Appendix C). The polar front is to the north of the Philippines. The mean surface wind speed in February is roughly 28 m/s. The mean SST is 6°C at the northern extent of the YS and 10°C at the southeastern extent while the surface air temperature (SAT) varies between 0° and 8°C. With a SAT roughly 2°-6°C

cooler than the SST, surface heat is lost to the atmosphere resulting in an upward buoyancy flux at the air-ocean interface. The combination of the thermal forcing and the mechanical forcing associated with the strong wind stress generates turbulence and leads to the mixing of the surface water with the deeper water, entrainment, and a deepening of the MLD. The MLD often extends to the bottom during the winter.

The transition period between the winter and summer monsoon seasons usually begins in March as the SAT is generally 5°C warmer than in February and a rapid weakening of the Siberian High progresses into April. By late April, the polar front moves northward toward Korea. Frontally generated events often occur in late April and May resulting in highly variable winds, cloud amount, and precipitation. By May, the daily high SAT rises to 15°-16°C. The YS SST undergoes a 10°C average increase during the transition from winter to spring. Strong westerly winds carrying yellow desert sand caused by easterly migrating low-pressure systems originating in Mongolia occur periodically during this timeframe. In late May and early June an atmospheric low-pressure system forms in the north of the YS and migrates westward over Manchuria by late June.

By summer the polar front is located between 30 and 35°N. The Manchurian Low over the East Asian continent and the Bonin High to the southeast produce southerly winds that advect warm, moist air over the YS and establish the onset of the southwest summer monsoon (see Appendix D). The summer SAT is quite uniform and roughly 24°-26°C. With a SAT roughly 1.5°-2°C warmer than the SST and strong downward net radiation, surface heat is gained by the water surface resulting in a downward buoyancy flux at the air-ocean interface. The thermal forcing stabilizes the upper layer of the water and causes a shoaling of the MLD. A multi-layer structure is generally present during the summer months consisting of a mixed layer, thermocline, and sublayer. Additionally, a closed cyclonic circulation occurs above the thermocline, which is approximately 13 m in August, and may reach a speed of 15 cm/s (Bartz, 1972). The Yellow Sea Cold Water (YSCW) mass is found beneath the thermocline and remains unchanged and nearly motionless throughout the summer (Li and Yuan, 1992). October is the beginning of the transition back to winter conditions. The southerly winds weaken and the sea surface

slope reestablishes toward the winter pattern. The SST steadily decreases from October through January.

2. ECS

The ECS lies to the south of the YS and north of Taiwan (see Appendix F). The ECS is bounded by China to the west and by the Japanese Ryukyu Islands to the east. The Korean Strait is located in the northeast region and connects the YES to the JES. The Taiwan Strait is in the southwest region of the ECS and connects the ECS to the SCS. The ECS is part of the continental shelf with the exception of the Okinawa Trough west of the Ryukyu Islands that reaches 2,700 m in depth.

3. Currents of the YES

As was the case for the JES, there are several named currents present at the surface layer of the YES (see Appendix G). The KUC is a strong western boundary current that flows northeastward along the shelf break in the southern ECS. The TsWC flows northward from the KUC west of Kyushu, Japan and passes through the Korean Strait. The TsWC separation from the KUC occurs near the shelf break (Jacobs et al., 2000; Lie and Cho, 1994; Katoh et al., 1996). Additionally, the TsWC has been observed to split in the vicinity south of Cheju Island and the branch that turns northwestward and flows into the YS is often identified as the Yellow Sea Warm Current (YSWC) (Jacobs et al., 2000). A portion of the northwestward flow makes an anticyclonic turn entering the Cheju Strait and is known as the Cheju Warm Current (Lie et al., 1998). The Taiwan Warm Current (TWC) enters the ECS through the Taiwan Strait.

A characteristic feature of the YS is the YSWC that flows beneath the surface northward from region just west of Cheju Island (Jacobs et al., 2000; Lie and Cho, 1994). The YSWC is an important source of the advection of warm water into the YS. Near the surface of the YS during the summer there is northward flow. Near the surface of the YS within the YS during the fall and winter there is southward flow. The surface flow within the YS occurs as a direct response to the surface winds in the presence of highly stratified water. (Teague and Jacobs, 2000). During the winter and fall there is a mean northward flow below the surface within the YS to counter the southward mean surface flow induced by wind stress. The mean northward flow below the surface within the YS during winter and fall is a response to the pressure gradient set up by the north monsoon

winds and serves as a mass balance response to the pressure fields set up by the surface winds (Riedlinger and Jacobs, 2000). During the fall and winter northerly winds bursts generate the pressure gradient by forcing water from BS and northern YS and by intensifying the southward outflow along the Chinese coast.

The Chinese Coastal Current flows southward around the tip of the Shandong peninsula and along the Chinese Coast. The Chinese Coastal Current has been observed to flow along the entire Chinese coast to the Taiwan Strait especially during the winter (Zheng and Klemas, 1982; Jacobs et al., 2000). The Korean Coastal Current flows southward along the Korean peninsula (Zheng and Klemas, 1982). Also present during the summer is an influx of Yangtze River diluted water that has been observed as far east as Cheju Island (Park, 1986; Beardsley et al., 1985).

C. SCS

The SCS is a semi-enclosed tropical sea covering an area of approximately 3,500,000 km² (Chu et al. 1999a; Chu et al., 1999b). It is the largest marginal sea in the Southeast Asia (Chu and Li, 2000; Hu et al., 2000). It is located between the Asian landmass to the north and west, the Philippine Islands to the east, Borneo to the southeast, and Indonesia to the south (see Appendix H). It includes the shallow Gulf of Thailand and connects to the ECS through the Taiwan Strait, the Pacific Ocean (via the Philippine Sea) through the Luzon Strait, the Sulu Sea through the Mindoro Strait and Balabac Channel, the Java Sea through the Gasper and Karimata Straits, and the Indian Ocean through the Strait of Malacca. The center of the Gulf of Thailand is roughly 70 m deep. The straits are shallow with the exception of the Luzon Strait that has a sill depth of 2,400 m. The Luzon Strait, lying between Taiwan and the Philippines, is considered critical in determining the characteristics of SCS waters because of the connection to the Pacific Ocean and its relatively large width and deep sill depth (Chu and Li, 2000; Shaw 1991).

The topography of the SCS is complex (Chu et al., 1999a; Chu et al. 1999b). Broad shallows of the Sunda shelf are located in the south/southwest and form the submerged connection between Southeast Asia, Malaysia, Sumatra, Java, and Borneo with a depth of 100 m in the middle. The continental shelf of the Asian landmass in the north extends from the Gulf of Tonkin to the Taiwan Strait, is consistently near 70 m deep, and averages 150 km in width. Extensive continental shelves (less than 100 m

deep) exist in the western and southern SCS while deep slopes with almost no shelves are found in the eastern SCS. A deep, elliptical shaped basin is present in the center of the SCS at approximately 13°N that is 1,900 km along its major axis (oriented northeast-southwest) and approximately 1,100 km along its minor axis, and it extends to over 4,000 m depth. Numerous reef islands and underwater plateaus are also scattered throughout the SCS.

As was the case for the YES and the JES, the SCS is also subjected to the seasonal monsoon system (Wyrski, 1961). From November through March, the strong northeasterly winter monsoon winds create a maximum wind stress of roughly 0.3 N m^{-2} due to the presence of high pressure over the Asian continent (Chu and Li, 2000; Chu et al., 1999a; Chu et al. 1999b) (see Appendix C). The northeasterly winds advect relatively cooler, drier air over the SCS. The equatorial trough is located south of the equator (Ramage, 1971). As the winds cross the equator into the southern hemisphere they turn to the left due to Coriolis forcing and become north northwesterly to northwesterly.

During the summer the subtropical ridge over the Pacific Ocean is displaced poleward. The equatorial trough lies over the central Philippines and extends northwestward to the Tibetan Plateau (Ramage, 1971). Southeasterly surface winds from the southern hemisphere cross the equator into the southern SCS and they turn right due to Coriolis forcing and acquire a westerly component. From April to August, the relatively weaker, warm, and moist southwesterly summer monsoon winds due to the presence of heat lows over the Asian continent and higher pressure over the Pacific Ocean create a wind stress of just over 0.1 N m^{-2} (Chu and Li, 2000; Chu et al., 1999a; Chu et al. 1999b) (see Appendix D). Highly variable winds and surface currents characterize the transition periods between the winter and summer monsoons.

The complex dynamics involved in the oceanic flow of the SCS is related to the geometry of the SCS, its connectivity with the Pacific Ocean, and the strongly variable atmospheric forcing (Metzger and Hurlburt, 1996; Chu et al., 1999a). Water exchange between the SCS and ECS through the Taiwan Strait is also a contributing factor (Hu et al., 2000). The seasonally reversing monsoon winds play a crucial role in determining the upper-ocean circulation (Shaw and Chao, 1994). During the winter there is a

southward coastal jet off Vietnam and the general oceanic surface circulation of the SCS is cyclonic (Chu and Li, 2000; Chu and Fan, 2001; Hu et al., 2000) (see Appendix I). During the summer there is a northward coastal jet off Vietnam and the general oceanic surface circulation of the SCS is anticyclonic (see Appendix J).

Eddies are often present in the SCS (Dale, 1956; Uda and Nakao, 1972; Chu et al., 1997c; Chu and Fan, 2001; Chu and Chang, 1997). Chu et al. (1999b) note two distinct behaviors of eddies located in the SCS. First, cold core eddies are more common than warm core eddies. Second, bottom topography significantly affects eddies and they generally occur in regions of high current velocity.

One particular eddy, located northwest of Luzon Island (NWL eddy), plays an important role in determining the circulation pattern of the northeastern SCS (Chu and Fan, 2001). Chu and Fan (2001) characterize the circulation pattern present in the northeastern SCS as two separate regimes – bifurcation and loop. The KUC, originating from the North Equatorial Current, flows northward as a western boundary current east of Luzon. During the bifurcation regime the NWL eddy is cyclonic and KUC water enters the SCS through the entire Luzon Strait and bifurcates into northward and northwestward branches northeastward of the NWL eddy (see Appendix K). The northwestward branch makes a cyclonic turn around the NWL eddy while the northward branch of the KUC intrusion flows northward along the western coast of Taiwan. During the loop regime the NWL eddy is anticyclonic and KUC water flows into the SCS through the southern half of the Luzon Strait, makes an anticyclonic turn around the NWL eddy, and exits the SCS through the northern Luzon Strait to rejoin the KUC as it flows northward along the eastern coast of Taiwan (see Appendix L).

The waters of northern SCS are cold and saline with small annual variability in salinity due to inflow and diffusion of high salinity water from the Pacific Ocean through the Luzon Strait (Chu et al., 1999b). The waters of the southern SCS are warm and fresh. Where the two waters meet in the center of the SCS, there is a higher horizontal gradient of salinity with a larger temporal variability due to seasonal monsoon effects. The summer MLD in the SCS is generally 30 to 40 m while the winter MLD varies between 70 to 90 m.

III. CAOCS

A. OCEAN COMPONENT – PRINCETON OCEAN MODEL (POM)

1. Model Description

The oceanic component consists of the POM. POM is a time dependent, primitive equation circulation model on a three dimensional grid that includes realistic topography and a free surface (Chu et al. 1999a). Developed at Princeton University, the model was specifically designed to accommodate mesoscale phenomena, including the often non-linear processes commonly found in estuarine and coastal oceanography (Blumberg and Mellor, 1987). A rectilinear grid is used with horizontal spacing of 0.167° by 0.167° and 23 non-uniform vertical σ levels. The model uses realistic bathymetry data from the Naval Oceanographic Office (NOO) Digital Bathymetry Database with 5-minute resolution (DBDB5) (see Appendix M).

2. Boundary Conditions

Closed lateral boundaries, such as the modeled ocean bordered by land, were defined using a free slip condition for velocity and a zero gradient condition for temperature and salinity. No advective or diffusive heat, salt or velocity fluxes occur through these boundaries (Chu et al., 2000)

At open boundaries, monthly varying volume transports from a global inverse model were used (see Appendix M). When the water flows into the model domain, temperature and salinity at the open boundary are likewise prescribed from the climatological data. When water flows out of the domain, a radiation condition described by Chu et al. (2000) was applied.

3. Initial Boundary Conditions and Model Initialization

Prior to coupling with the MM5 POM was integrated for four years and four months from zero velocity and January climatological temperature and salinity fields. POM was forced by monthly mean surface wind stress from the Comprehensive Ocean and Atmosphere Data Set (COADS) and by the restoring-type surface heat and salinity fluxes that were relaxed to the surface monthly values. The final states of temperature, salinity, and velocity were used as the initial ocean conditions for May 1, 1998 (Chu et al. 2000).

B. ATMOSPHERIC COMPONENT – MESOSCALE MODEL FIFTH GENERATION (MM5)

1. Model Description

The atmospheric component consists of the Pennsylvania State University/National Center for Atmospheric Research (PSU/NCAR) MM5 version 3.4. MM5 is a limited-area, non-hydrostatic, terrain-following sigma-coordinate model designed to simulate or predict mesoscale and regional-scale atmospheric circulation (MM5 homepage, 2001).

2. Land Surface Parameterization

The horizontal resolution is 30 km. Sixteen pressure levels were used. A soil water availability function was used for computing the soil and water content by using 10 specified vegetation types (Chu et al. 2000).

3. Initial Conditions and Lateral Boundary Conditions

The initial conditions and the initial horizontal lateral boundary conditions for wind, temperature, water vapor, and surface pressure were interpolated from analyses of observations from the European Center for Medium-Range Weather Forecasts (ECMWF). They were projected onto a spectral T42 grid and a vertical resolution of 16 pressure levels. The initial conditions were the fields at 00Z May 1, 1998. The lateral boundary conditions were provided by a relaxation method and updated every 12 hours (Chu et al. 2000).

C. OCEAN-ATMOSPHERIC COUPLING

The model domain (67°-142°E, 7°S-55°N) covers the entire EAMS as well as surrounding lands and islands. The surface fluxes of water, heat (excluding solar radiation), and momentum are applied synchronously with opposite signs in the atmosphere and ocean. MM5 and POM update fluxes every 15 minutes. Flux adjustments were not used (Chu et al., 2000). The same MM5 flux parameterization was used for CAOCS with the one exception. The difference was the use of SST data. In a stand-alone MM5 model, SST is prescribed by a given parameter. In CAOCS, the POM SST is used at each time step of the MM5.

IV. DATA ANALYSIS

A. EXTRACTION AND VISUALIZATION OF DATA FROM OCEAN COMPONENT OF CAOCS

The oceanic component of CAOCS output was analyzed using a series of Formula Translation (FORTRAN) programs and Matrix Laboratory (MATLAB) coding. FORTRAN programs were created in order to convert the files that contained the CAOCS oceanic output, as well as the latitude and longitude data, into a format readable by MATLAB. Once the data was in a format compatible with MATLAB, MATLAB code was used to read in the various parameters of the oceanic data such as SST, SSS, and the u - and v - components of surface velocity. Since the CAOCS oceanic output was available at several times per day, a daily mean average was calculated as part of the MATLAB code. Additionally, MATLAB was a very effective tool for use in displaying the oceanic data.

B. EXTRACTION AND VISUALIZATION OF DATA FROM ATMOSPHERIC COMPONENT OF CAOCS

Conversion of the atmospheric component of CAOCS output into a series of files that could be easily ingested by MATLAB code was more complex. A FORTRAN program entitled Read/Interpolate/Plot (RIP), developed by Mark Stoelinga at both NCAR and the University of Washington (Stoelinga, 2000), was used for this purpose. More specifically, a component of RIP, RIP Data Preparation (RIPDP), was used to convert the atmospheric component of CAOCS output data file into a series of data files that contained all times and all variables. MATLAB code was designed to read in the various parameters of the atmospheric data such as surface latent heat flux. Additionally, MATLAB was a very effective tool for use in displaying the desired atmospheric parameters.

When MATLAB was not needed and only a visualization of the atmospheric data was necessary, two programs were available. The first program was RIP and the second program was GRAPH.

RIP was used to specify the desired plots by editing a formatted text file. RIP would create an NCAR Graphics file that was easily viewed with a metacode translator

application called Interactive Display Tool (IDT). The NCAR Graphics computer graphics metacode (CGM) file could also be converted into other formats using translators that are part of the NCAR Graphics library. RIP has the ability to convert from the sigma coordinate system to pressure level. Other benefits of RIP included the ability to control the appearance of all aspects of the plots such as color and labeling.

The GRAPH program is part of the NCAR Graphics library and generates simple diagnostics and plots for some standard meteorological variables (MM5 Home page, 2001). The user edits a series of formatted text files in order to specify the desired plots. Unlike RIP, the GRAPH program reads the atmospheric component of CAOCS output data file directly. The GRAPH program would create an NCAR Graphics file that was easily viewed with a metacode translator application called IDT. The NCAR Graphics CGM file could also be converted into other formats using translators that are part of the NCAR Graphics library. The GRAPH program also has the ability to convert from the sigma coordinate system to pressure level. Although the plots are not as enhanced as those of RIP, the GRAPH program was useful for plotting parameters such as the 10-meter wind fields.

V. CAOCS OUTPUT VERIFICATION

A. VERIFICATION OF CAOCS ATMOSPHERIC OUTPUT

1. Comparison of Interfacial Fluxes Between CAOCS Atmospheric Output and NCEP Data

The surface latent heat flux, surface sensible heat flux, surface longwave radiation flux, and surface shortwave radiation flux of the CAOCS atmospheric output were compared to NCEP data for verification purposes. Verification consisted of visual inspection of the respective parameter contour plots for both CAOCS atmospheric output and NCEP data.

Results of the visual inspections show values of surface latent heat flux, surface sensible heat flux, and surface shortwave radiation flux are in good agreement in both magnitude and position. Surface longwave radiation flux values for the CAOCS atmospheric output were too high in magnitude.

2. Comparison of 10-m Wind Fields Between CAOCS Atmospheric Output and NCEP Data

The 10-m wind fields for the CAOCS atmospheric output were compared to NCEP data for verification purposes. Verification consisted of visual inspection of the 10-m wind field vector plots for both CAOCS atmospheric output and NCEP data.

Results of the visual inspections show 10-m wind fields to be in good agreement in both magnitude and position. Some of the results are provided in the appendix. (see Appendix N).

B. VERIFICATION OF CAOCS OCEANIC OUTPUT

1. Comparison of SST and SSS Values Between CAOCS Oceanic Output and Buoy Station Data

The SST and SSS values for the CAOCS oceanic output were compared to archived buoy station data for verification purposes. Verification consisted of visual inspection of the SST and SSS values for both CAOCS oceanic output and the buoy station values.

A plot of the locations of the buoy stations is included in the appendix (see Appendix O). Results of the visual inspections show SST and SSS values to be in good agreement (see Appendix O).

VI. ATMOSPHERIC PROCESSES DURING MAY-JULY 1998

The visual plots of the analyzed data were examined and two significant time periods were chosen. The time periods are significant because they include major mesoscale oceanic and atmospheric events that take place prior to the onset of the summer monsoon and following the onset of the summer monsoon.

The first chosen time period was May 13, 1998 through May 31, 1998 and consisted of several major mesoscale atmospheric storms that either developed over the EAMS or transited across the EAMS prior to the onset of the summer monsoon. Additionally, mesoscale oceanic features were observed in the surface current velocity, SST, and SSS plots that were atypical of the climatologically discussed current structure within the EAMS.

The second chosen time period was from July 18, 1998 through July 31, 1998 and consisted of several major mesoscale atmospheric storms that either developed over the EAMS or transited across the EAMS after the onset of the summer monsoon. Additionally, mesoscale oceanic features were observed in the surface current velocity, SST, and SSS plots that were atypical of the climatologically discussed current structure within the EAMS.

The plots of the CAOCS atmospheric component output of the JES, YES, and SCS were broken down into regions to facilitate discussion of atmospheric processes that took place during the two time periods (see Appendix P). First the atmospheric processes that took place during the May time period will be discussed in detail for each of the three major seas that comprise the EAMS. Secondly, the atmospheric processes that took place during the July time period will be discussed in detail for each of the three major seas that comprise the EAMS. In the following chapter oceanic processes will be discussed.

A. MAY TIME PERIOD: MAY 13 THROUGH MAY 31, 1998

Readers should refer to Appendix Q for the 500-mb relative vorticity/geopotential height plots over the EAMS for the May period. The figures in Appendix Q are in time sequential order ever 12 hours from 00Z May 13 through 12Z May 31.

Readers should refer to Appendix R for the 700-mb vertical velocity/geopotential height plots over the EAMS for the May period. The figures in Appendix R are in time sequential order ever 12 hours from 00Z May 13 through 12Z May 31.

During this period the summer monsoon is not yet established. There is no semi-permanent 500-mb trough located over Manchuria and the 500-mb shortwave troughs that do occur over the Asian continent during this timeframe are rapid movers as they migrate from west to east. Additionally, the ridge associated with the Bonnin High that occurs during the summer monsoon is not yet present.

1. JES

Readers should refer to Appendix S for the surface level pressure/SAT/surface wind plots over the JES for the May period. The figures in Appendix S are in time sequential order ever 12 hours from 00Z May 13 through 12Z May 31.

From 00Z to 12Z May 13 a 500-mb trough is present over the JES that moves eastward. During the same time period a 700-mb trough is also present over the JES that moves eastward.

At 00Z May 13 a surface low lies east of the southeast region of the northern JES and affects the majority of the JES. A surface anticyclone lies to the southwest of the west region of the southern JES, centered at the southern boundary of the west region of the northern ECS, and affects the west region of the southern JES.

Surface winds in the northern JES, in the central JES, and in the east region of the southern JES make a cyclonic turn around the surface low lies east of the southeast region of the northern JES and are northeasterly at 15 knots in the northeast region of the northern JES, northeasterly to westerly at 5 to 10 knots in the southeast region of the northern JES, west northwesterly at 15 knots in the southwest region of the northern JES, westerly at 20 knots in the central JES, and westerly at 15 to 20 knots in the east region of the southern JES. Surface winds in the west region of the southern JES and Korean Strait are west northwesterly at 10 to 20 knots due to a surface anticyclone to the southwest that is centered at the southern boundary of the west region of the northern ECS.

At 12Z May 13 surface pressure over the JES rises while the pressure gradient weakens. The surface low has moved southeastward, is now located east of the southern

boundary of the northern JES, and its associated troughing continues to affect the southeast region of the northern JES and east region of the central JES. The surface anticyclone remains centered at the southern boundary of the west region of the northern ECS, but its associated ridging affects the majority of the eastern JES as well as the east region of the southern JES. A region of high pressure lies to the northeast of the northeast region of the northern JES and affects the northeast region of the northern JES. A surface cyclone is located northwest of the northeast region of the northern JES over Russia.

Surface winds throughout the JES weaken. Surface winds in the northeast region of the northern JES make an anticyclonic turn around high pressure to the northeast and are easterly to south southeasterly at 5 to 10 knots. Surface winds in the southeast region of the northern JES and in the east region of the central JES make a cyclonic turn due to troughing associated with a surface low east of the southern boundary of the northern JES and are easterly to northerly at 5 to 10 knots in the southeast region of the northern JES and northwesterly at 5 to 10 knots in east region of the central JES. Surface winds in the southwest region of the northern JES, in the west region of the central JES, in the southern JES, and in the Korean Strait make an anticyclonic turn due to ridging associated with the surface anticyclone centered at the southern boundary of the west region of the northern ECS and are west southwesterly to northwesterly at 3 to 5 knots in the southwest region of the northern JES, westerly to northwesterly at 5 to 15 knots in the west region of the central JES, northwesterly at 10 knots in the east region of the southern JES, westerly to north northwesterly at 5 knots in the west region of the southern JES, and north northwesterly at 10 knots in the Korean Strait.

From 00Z to 12Z May 14 a small shortwave 500-mb ridge moves eastward across the northern JES while a 500-mb trough remains over the central and southern JES. During the same time period, a small 700-mb ridge moves eastward across the northern JES and weakens while a 700-mb trough remains over the majority of the central and southern JES.

At 00Z May 14 surface pressure over the JES rises. The pressure gradient over the northeast region of the northern JES increases while the pressure gradient over the remainder of the JES continues to weaken. The surface anticyclone to the southwest is

now centered over China west of the northwest region of the central ECS, but its associated ridging affects the majority of the central and southern JES. The more northern surface anticyclone now lies east of the northeast region of the northern JES and affects the east region of the northern JES. The surface cyclone to northwest of the northeast region of the northern JES has moved eastward and affects the southwest region of the northern JES.

Surface winds in the east region of the northern JES make an anticyclonic turn around high pressure east of the northeast region of the northern JES and are southwesterly at 10 to 15 knots in the northeast region and easterly to southerly at 5 to 10 knots in the southeast region. Surface winds in the southwest region of the northern JES are south southwesterly to westerly at 3 to 5 knots due to the surface cyclone northwest of the northeast region of the northern JES. Surface winds in the east region of the central JES make a cyclonic turn and are light easterly to light northwesterly. Surface winds in the west region of the central JES, in the southern JES and in the Korean Strait make an anticyclonic turn due to ridging associated with the surface anticyclone over China west of the northwest region of the central ECS and are westerly to northwesterly at 3 to 5 knots in the west region of the central JES, northwesterly at 5 knots in the east region of the southern JES, northwesterly to northeasterly at 5 to 10 knots in the west region of the southern JES, and northeasterly at 10 to 15 knots in the Korean Strait.

At 12Z May 14 surface pressure falls over the northern JES. The pressure gradient over the northern JES increases. A surface anticyclone develops in the region of ridging that was present over the southern JES and is centered over the southern boundary of the central JES and affects the majority of the central and southern JES. The surface cyclone northwest of the northeast region of the northern JES has moved further eastward and affects the northern JES. A surface front associated with the surface cyclone lies inland and along the Russian coast in the vicinity of the northern JES.

Surface winds in the northern JES are west southwesterly to south southwesterly at 10 to 15 knots ahead of the surface front. Surface winds in the central JES are southwesterly at 10 to 15 knots in the northwest region and southwesterly at 5 to 10 knots in the northeast region due to the surface anticyclone centered over the southern

boundary of the central JES and the surface cyclone northwest of the northeast region of the northern JES. Surface winds in the south region of the central JES, in the southern JES, and in the Korean Strait make an anticyclonic turn around the surface anticyclone centered over the southern boundary of the central JES and are southerly to northeasterly at 5 to 10 knots in the south region of the central JES, northeasterly at 5 knots in the southern JES, and northeasterly at 10 knots in the Korean Strait.

From 00Z May 15 to 00Z May 16 a large 500-mb ridge propagates eastward across the JES. During the same time period, a large 700-mb ridge moves eastward across the JES.

At 00Z May 15 surface pressure continues to fall in the northern JES as the surface cyclone that was northwest of the northeast region of the northern JES continues to move eastward and is now located north of the northeast region of the northern JES. The surface front associated with the surface cyclone remains inland and along the Russian coast in the vicinity of the northern JES and dissipates. A second surface cyclone is located northwest of the southwest region of the northern JES. The pressure gradient over the northern JES does not change much while the pressure gradient in the central and southern JES increases as the surface anticyclone that remains centered over the southern boundary of the central JES builds.

Surface winds in the northern and central JES are southwesterly at 5 to 15 knots due to the surface anticyclone centered over the southern boundary of the central JES and the surface cyclone north of the northeast region of the northern JES. Surface winds in the southern JES and in the Korean Strait make an anticyclonic turn around the same central high pressure and are northerly to southerly at 3 to 5 knots in the southern JES and northeasterly at 10 to 15 knots in the Korean Strait.

At 12Z May 15 surface pressure increases over the JES because the surface cyclone that was north of the northeast region of the northern JES continues to move eastward and is now located northeast of the northeast region of the northern JES and also because the surface anticyclone that was centered over the southern boundary of the central JES moves eastward and is now centered over the southern boundary of the east region of the central JES and continues to build. The surface cyclone that was located

northwest of the southwest region of the northern JES moves eastward but remains northwest of the southwest region of the northern JES. The pressure gradient over the JES increases due to the building anticyclone centered over southern boundary of the east region of the central JES and the surface cyclone northwest of the southwest region of the northern JES.

Surface winds in the far north region of the northern JES slacken and become southerly to southwesterly at 5 knots while in the remainder of the northern JES they intensify to 20 knots and remain southwesterly. Surface winds in the central JES, in the southern JES, and in the Korean Strait make an anticyclonic turn around the surface high centered over the southern boundary of the east region of the central JES and are southerly to southwesterly at 10 to 20 knots in the northwest region of the central JES, south southeasterly to southerly at 10 knots in the southwest region of the central JES, southwesterly to west southwesterly at 10 to 20 knots in the northeast region of the central JES, south southeasterly to westerly at 5 knots in the southeast region of the central JES, easterly to east southeasterly at 5 to 10 knots in the east region of the southern JES, easterly to southeasterly at 10 knots in the west region of the southern JES, and easterly at 15 knots in the Korean Strait.

At 00Z May 16 the surface cyclone that was located northwest of the southwest region of the northern JES remains stationary but its associated troughing causes the pressure over the far north region of the northern JES to fall. Surface pressure increases over the remainder of the northern JES and over the majority of the central JES as the surface anticyclone that was centered over the southern boundary of the east region of the central JES moves northeastward so that it is now centered over Honshu, Japan to the east of the southeast region of the central JES while continuing to build. Surface pressure over the west region of the southern JES falls due a new surface cyclone that developed in a region of troughing over the eastern ECS and is centered over the east region of the northern ECS. The pressure gradient over the majority of the JES increases due to the building anticyclone centered east of the southeast region of the southern JES, the newly developed surface cyclone to the southwest of the southern JES, and the surface cyclone northwest of the southwest region of the northern JES.

Surface winds in the northern JES are southwesterly at 10 to 20 knots in the northeast region, southwesterly at 15 to 20 knots in the southeast region, and southerly at 10 knots in the southwest region. Surface winds in the east region of the central JES make an anticyclonic turn around the surface high east of the southeast region of the central JES and are southeasterly to southwesterly at 10 to 15 knots. Surface winds in the west region of the central JES experience divergence due to the surface anticyclone east of the southeast region of the central JES and the troughing associated with new surface cyclone centered in the middle of the east region of the northern ECS and are southeasterly to easterly at 10 to 15 knots in the southwest region and south southeasterly to southerly at 10 knots in the northwest region. Surface winds in the southern JES and in the Korean Strait make a cyclonic turn due to troughing associated with the surface cyclone centered in the middle of the east region of the northern ECS and are southeasterly to east southeasterly at 15 knots.

From 12Z May 16 through 00Z May 17 a small shortwave 500-mb trough propagates eastward across the southern and central JES while 500-mb ridging remains over the northern JES. During the same time period, a 700-mb trough begins to affect the southern and central JES as well as the majority of the northern JES while a 700-mb ridge is located over the northeast region of the northern JES.

At 12Z May 16 the surface cyclone that was located northwest of the southwest region of the northern JES moves eastward, but remains northwest of the southwest region of the northern JES. Surface pressure falls over the majority of the JES as the surface anticyclone that was east of the southeast region of the central JES moves northeastward so that it is east of the southern boundary of the northern JES and it also falls because the surface cyclone that was centered over the east region of the northern ECS moves northward so that it is now centered over the Korean peninsula. The pressure gradient over the majority of the JES remains strong due to the ridging associated with the anticyclone east of the southern boundary of the northern JES, the surface cyclone over the Korean peninsula, and the surface cyclone northwest of the southwest region of the northern JES.

Surface winds in the northeast region of the northern JES increase to 25 knots and remain southwesterly. Surface winds in the south region of the northern JES, in the east region of the central JES, in the northwest region of the central JES, and in the east region of the southern JES make an anticyclonic turn due to ridging from the surface high east of the southern boundary of the northern JES and are southerly to southwesterly at 10 to 20 knots in the southeast region of the northern JES, south southeasterly at 10 to 15 knots in the southwest region of the northern JES, southeasterly to south southeasterly at 10 to 15 knots in the northwest region of the central JES, south southeasterly to southerly at 5 to 15 knots in the east region of the central JES, and south southeasterly at 15 to 20 knots in the east region of the southern JES. Surface winds in the southwest region of the central JES, in the west region of the southern JES and in the Korean Strait make a cyclonic turn around the central low centered over the Korean peninsula and are southeasterly to northeasterly at 5 to 15 knots in the southwest region of the central JES, south southwesterly to southeasterly at 10 to 15 knots in the west region of the southern JES, and westerly to southwesterly at 10 to 15 knots in the Korean Strait.

At 00Z May 17 the surface cyclone that was located northwest of the southwest region of the northern JES moves southward, but remains northwest of the southwest region of the northern JES. Surface pressure falls over the majority of the JES due to the approaching surface cyclone northwest of the southwest region of the northern JES. Surface pressure also falls because the surface cyclone that was centered over the Korean peninsula has moved further northward so that it is west of the northwest region of the central JES. The pressure gradient over the majority of the JES remains strong due the troughing associated with these two surface cyclones.

Surface winds in the JES make a cyclonic turn due to troughing associated with the two cyclones and are south southwesterly and to 10 to 15 knots in the northern JES, south southwesterly at 15 knots in the east region of the central JES, southwesterly to south southwesterly at 15 knots in the west region of the central JES, southwesterly at 15 knots in the southern JES, and west southwesterly at 10 to 15 knots in the Korean Strait.

From 12Z May 17 through 00Z May 19 another shortwave 500-mb trough propagates eastward across the entire JES. During the same time period, a fairly intense 700-mb trough propagates eastward across the JES.

At 12Z May 17 the surface cyclone that was located northwest of the southwest region of the northern JES moves southeastward and is now located west of the northeast region of the northern JES. The surface cyclone has deepened and has combined with the surface low previously west of the northwest region of the central JES. A surface anticyclone lies east of the east region of the northern ECS. Surface pressure does not change, but the pressure gradient over the majority of the JES strengthens due to the surface low to the northwest and the surface high to the south.

Surface winds in the JES make a cyclonic turn around the central low pressure to the west of the northeast region of the northern JES and are southwesterly to easterly at 5 to 15 knots in the north region of the northern JES, southwesterly at 20 knots in the south region of the northern JES, southwesterly at 10 to 15 knots in the east region of the central JES, southwesterly at 20 knots in the west region of the central JES, west southwesterly at 10 to 15 knots in the southern JES, and westerly at 5 to 10 knots in the Korean Strait.

At 00Z May 18 the surface cyclone that was located west of the northeast region of the northern JES moves northeastward but remains west of the northeast region of the northern JES. A surface anticyclonic circulation is present over the tip of the Korean peninsula and there is slight ridging over the southern JES due to an anticyclone to the southeast. Surface pressure falls over most of the JES and the pressure gradient remains strong over the majority of the JES as the low pressure system to the northwest continues to move closer to the JES and a high pressure system remains to the south.

Surface winds in the northern and central JES make a cyclonic turn around the surface low west of the northeast region of the northern JES and are southwesterly to easterly at 5 to 10 knots in the northeast region of the northern JES, southwesterly at 15 to 20 knots in the southeast region, westerly to southwesterly at 10 to 20 knots in the southwest region of the northern JES, southwesterly at 10 to 15 knots in the east region of the central JES, and westerly to west southwesterly at 10 to 15 knots in the west region of

the central JES. Surface winds in the southern JES are westerly at 5 to 10 knots. Surface winds in the Korean Strait make an anticyclonic turn and are northerly to easterly at 3 to 5 knots.

At 12Z May 18 the surface cyclone that was located west of the northeast region of the northern JES has passed to the north of the northeast region of the northern JES and is now located northeast of the northeast region of the northern JES. A surface anticyclone is located to the northwest of the southwest region of the northern JES. A new anticyclonic circulation is located over the southeast region of the Korean peninsula. There is ridging over the southern JES due to a surface anticyclone to the southeast. Surface pressure rises over most of the northern JES and the pressure gradient weakens over the majority of the JES as the surface low to the northeast moves away from the JES.

Surface winds in the northern JES are northwesterly to westerly at 5 to 10 knots in the north region and southwesterly at 10 knots in the south region due to the surface low to the northeast of the northeast region of the northern JES. Surface winds in the east region of the central JES are southwesterly at 10 knots while in the west region they make an anticyclonic turn due to ridging associated with the surface anticyclone to the southeast of the JES and are south southwesterly to southwesterly at 5 to 10 knots. Surface winds in the southern JES make an anticyclonic turn and are westerly to northwesterly at 3 to 5 knots in the east region and southwesterly to northeasterly at 5 knots in the west region. Surface winds in the Korean Strait are northeasterly at 5 knots.

At 00Z May 19 the surface anticyclone that was located to the northwest of the southwest region of the northern JES has moved eastward and is now located northwest of the northeast region of the northern JES. A surface cyclone is located northwest of the southwest region of the northern JES. The anticyclonic circulation located over the southeast region of the Korean peninsula remains stationary. Surface pressure rises over most of the JES and the pressure gradient remains weak as the two surface anticyclones dominate the JES.

Surface winds in the north region of the northern JES make an anticyclonic turn around the surface high to the northwest of the northeast region of the northern JES and

are north northwesterly to northeasterly at 10 knots while in the southeast region they make a cyclonic turn and are northeasterly to north northwesterly at 5 to 10 knots. Surface winds in the southwest region of the northern JES are light and variable. Surface winds in the east region of the central JES are west northwesterly to westerly at 3 to 5 knots while in the west region they make an anticyclonic turn due to ridging associated with the surface anticyclonic circulation over the southeast region of the Korean peninsula and are west southwesterly to northwesterly at 5 to 10 knots. Surface winds in the east region of the southern JES are west northwesterly to northwesterly at 5 knots while in the west region they make an anticyclonic turn due to ridging associated with the anticyclonic circulation over the southeast region of the Korean peninsula and are north northwesterly to north northeasterly at 5 knots. Surface winds in the Korean Strait remain northeasterly at 5 knots.

At 12Z May 19 a 500-mb ridge is present over the JES. During the same time period, a fairly strong 700-mb ridge is located over the JES.

At 12Z May 19 the surface anticyclone that was located northwest of the northeast region of the northern JES has passed to the north of the northeast region of the northern JES and is now located northeast of the northeast region of the northern JES. The surface cyclone located northwest of the southwest region of the northern JES has moved eastward and is now located north-northwest of the southwest region of the northern JES. The anticyclonic circulation present over the southwest region of the Korean peninsula has moved eastward and is now centered over the southern boundary of the central JES. Surface pressure remains high over the JES and the pressure gradient remains weak as the two surface anticyclones continue to dominate the JES.

Surface winds in the east region of the northern JES make a slight anticyclonic turn around the central high pressure to the northeast of the northeast region of the northern JES and are easterly to southeasterly at 10 knots while in the southwest region they are southerly at 10 to 15 knots. Surface winds in the east region of the central JES and in the southern JES make an anticyclonic turn around the surface high over the southern boundary of the central JES and are northwesterly to northerly at 3 to 5 knots in the east region of the central JES, northeasterly at 5 knots in the east region of the

southern JES, and northeasterly to southerly at 3 to 5 knots in the west region of the southern JES. In the west region of the central JES they make a cyclonic turn due to troughing associated with the surface low north-northwest of the southwest region of the northern JES and are southwesterly to southerly at 5 to 15 knots. Northwesterly winds at 5 knots are present over the Korean Strait.

From 00Z May 20 through 12Z May 20 a strong 500-mb trough is present over the northern JES while a 500-mb ridge lies to the west of the central JES. During the same time period, a strong 700-mb trough is located over the northern JES while a 700-mb anticyclone lies to the west of the central JES.

At 00Z May 20 the surface cyclone previously located northwest of the southwest region of the northern JES has moved further eastward and is now located northwest of the northeast region of the northern JES. The surface high previously located over the southern boundary of the central JES has moved southeastward and is now centered over Honshu, Japan and lies east of the east region of the southern JES. Surface pressure falls over the northern JES and the pressure gradient strengthens over the northern JES as the surface cyclone continues to move toward the northern JES. Ridging associated with a surface high centered over the southern boundary of the central YS maintains higher pressure over the southern and central JES.

Surface winds in the northern JES, in the central JES and in the east region of the southern JES make a cyclonic turn around the central low northwest of the northeast region of the northern JES and are south southwesterly to southerly at 15 to 20 knots in the north region of the northern JES, northwesterly to southwesterly at 10 knots in the south region of the northern JES, southwesterly at 10 knots in the east region of the central JES, northwesterly to west southwesterly at 5 to 10 knots in the west region of the central JES, and southwesterly at 5 to 10 knots in the east region of the southern JES. Surface winds in the west region of the southern JES and in the Korean Strait make an anticyclonic turn due to ridging associated with a surface high centered over the southern boundary of the central YS and are westerly to northeasterly at 3 to 5 knots.

At 12Z May 20 the surface cyclone previously located northwest of the northeast region of the northern JES has moved further eastward and is now located north of the

northeast region of the northern JES. Surface pressure remains lower over the northern JES and the pressure gradient remains stronger over the northern JES as the surface cyclone passes north of the northeast region of the northern JES. A surface anticyclone has developed in the region of ridging that was previously present in the southern and central JES and is centered over the southern boundary of the central JES. Surface pressure over the southern and central JES rises due to the presence of the surface anticyclone.

Surface winds in the north region of the northern JES make a cyclonic turn around the central low to the north of the northeast region of the central JES and are westerly to southwesterly at 10 to 15 knots. Surface winds in the remainder of the JES make an anticyclonic turn around the central high centered over the southern boundary of the central JES and are southerly to westerly at 5 to 10 knots in the south region of the northern JES, westerly to northeasterly at 5 knots in the east region of the central JES, southeasterly to south southwesterly at 5 knots in the west region of the central JES, northeasterly at 5 knots in the east region of the southern JES, northeasterly to easterly at 5 knots in the west region of the southern JES, and northeasterly to northerly at 5 to 10 knots in the Korean Strait.

From 00Z May 21 through 00Z May 24 a strong 500-mb ridge propagates across the JES. During the same time period, a strong 700-mb ridge propagates eastward across the JES.

At 00Z May 21 the surface cyclone previously located north of the northeast region of the northern JES has moved further eastward and is now located northeast of the northeast region of the northern JES. A surface anticyclone is located north-northwest of the southwest region of the northern JES. Surface pressure rises over the JES and the pressure gradient weakens over the northern JES as the surface cyclone continues to move away from the JES and as the surface anticyclone centered over the southern boundary of the central JES remains stationary and builds.

Surface winds in the north region of the northern JES become northwesterly and increase to 10 to 15 knots. Surface winds in the remainder of the JES make an anticyclonic turn around the central high pressure centered over the southern boundary of

the central JES and are southwesterly to west northwesterly at 5 to 10 knots in the south region of the northern JES, west southwesterly to westerly at 5 to 10 knots in the east region of the central JES, southwesterly to west southwesterly at 5 to 10 knots in the west region of the central JES, westerly to northeasterly at 3 to 5 knots in the east region of the southern JES, east northeasterly to southeasterly at 3 to 5 knots in the west region of the southern JES, and northeasterly at 10 knots in the Korean Strait.

At 12Z May 21 the surface anticyclone previously located north-northwest of the southwest region of the northern JES has moved further eastward and is now located northwest of the northeast region of the northern JES. A surface cyclone lies northwest of the southwest region of the northern JES. Surface pressure rises over the northern JES as the more northerly surface anticyclone continues to move toward the JES. Surface pressure falls over the southern and central JES due to troughing associated with the surface cyclone northwest of the southwest region of the northern JES and also because the surface anticyclone previously centered over the southern boundary of the central JES has moved eastward while weakening and is now located over Honshu, Japan east of the east region of the southern JES.

Surface winds in the northern JES make an anticyclonic turn around the central high to the northwest of the northeast region of the northern JES and are northerly to northeasterly at 5 to 10 knots in the northeast region, northeasterly to southeasterly at 5 to 10 knots in the southeast region, and south southeasterly to southerly at 5 knots in the southwest region. Surface winds in the northeast region of the central JES are light and variable. Surface winds in the northwest region of the central JES make a cyclonic turn due to troughing associated with the surface low northwest of the southwest region of the northern JES and are southwesterly to south southwesterly at 10 to 15 knots. Surface winds in the remainder of the JES make an anticyclonic turn around the central high east of the east region of the southern JES and are southwesterly to west northwesterly at 5 knots in the southeast region of the central JES, southerly to southwesterly at 5 to 10 knots in the southwest region of the central JES, southeasterly to westerly at 3 to 5 knots in the east region of the southern JES, east southeasterly to southerly at 5 knots in the west region of the southern JES, and easterly at 5 knots in the Korean Strait.

At 00Z May 22 the surface anticyclone previously located northwest of the northeast region of the northern JES has moved further eastward and is now located north of the northeast region of the northern JES. The surface cyclone previously northwest of the southwest region of the northern JES has moved northeastward, but remains northwest of the southwest region of the northern JES. Surface pressure rises over the northern JES as the more northerly surface anticyclone passes north of the northeast region of the northern JES. The surface anticyclone previously located east of the east region of the southern JES remains stationary and continues to weaken.

Surface winds in the northern JES make an anticyclonic turn around the surface high north of the northeast region of the northern JES and are light and variable in the far north region, northeasterly to southeasterly at 3 to 5 knots in the remainder of the northeast region, easterly to southeasterly at 5 to 15 knots in the southeast region, and southeasterly at 5 to 10 knots in the southwest region. Surface winds in the east region of the central JES experience convergence as they make an anticyclonic turn around the same surface high as well as a cyclonic turn due to troughing associated with the surface low northwest of the southwest region of the northern JES and are south southwesterly to southeasterly at 5 to 10 knots. Surface winds in the west region of the central JES make a cyclonic turn due to troughing from the same central low and are southwesterly to south southeasterly at 5 to 10 knots. Surface winds in the east region of the southern JES are southwesterly at 3 to 5 knots while in the west region they make an anticyclonic turn due to ridging associated with the surface high east of the east region of the southern JES and are southeasterly to south southwesterly at 3 to 5 knots. Surface winds in the Korean Strait are easterly at 5 knots.

At 12Z May 22 the surface anticyclone previously located north of the northeast region of the northern JES has moved southeastward and is now located east of the northeast region of the northern JES. The surface cyclone previously northwest of the southwest region of the northern JES has moved eastward and is now located northwest of the northeast region of the northern JES. A surface low develops west of the northwest region of the central JES. Surface pressure falls over the JES as the surface anticyclone moves away from the JES and as the two surface cyclones approach the JES.

An east-west surface pressure gradient is present over the JES with slight ridging in the east and slight troughing in the west.

Surface winds in the east region of the northern JES make a slight anticyclonic turn around the central high east of the northeast region of the northern JES and are southeasterly to south southeasterly at 10 to 15 knots while in the southwest region they are southwesterly to southerly at 10 knots. Surface winds in the east region of the central JES make a slight anticyclonic turn around the same central high and are southeasterly to south southeasterly at 10 knots. Surface winds in the west region of the central JES experience some convergence as they make a cyclonic turn due to troughing associated with the surface low west of the northwest region of the central JES and an anticyclonic turn due to ridging associated with central high east of the northeast region of the northern JES and are westerly to southerly at 5 to 10 knots west of 132°E and south southeasterly to southerly at 10 knots east of 132°E. Surface winds in the southern JES are southeasterly at 5 to 10 knots in the east region and south southwesterly to southerly at 3 to 5 knots in the west region. Surface winds in the Korean Strait are westerly to southwesterly at 5 knots.

At 00Z May 23 the surface low previously located northwest of the northeast region of the northern JES has moved eastward and is now located north of the northeast region of the northern JES. A surface cold front, associated with this surface low is present to the west of the northern JES along and inland of the Russian coastline. The surface low west of the northwest region of the central JES remains stationary and fills. A surface anticyclone is located west of the southern border of the northeast region of the northern JES. Another surface anticyclone is located southeast of the east region of the central JES. Surface pressure falls over the northern JES as the surface cyclone passes north of the northeast region of the northern JES.

Surface winds in the north region of the northern JES make a cyclonic turn ahead of the surface cold front and are westerly to southwesterly at 5 to 10 knots. Surface winds in the south region of the northern JES experience divergence as they make a cyclonic turn ahead of the surface cold front as well as an anticyclonic turn around the surface high west of the southern border of the northeast region of the northern JES and

are northeasterly to southwesterly at 5 knots. Surface winds in the east region of the central JES are southwesterly at 5 to 10 knots while in the west region they make a sharp cyclonic turn and are northeasterly to southwesterly at 3 to 5 knots. Surface winds in the southern JES make an anticyclonic turn due to ridging associated with the surface high southeast of the east region of the central JES and are southerly to southwesterly at 5 to 10 knots in the east region and southeasterly to southwesterly at 3 to 5 knots in the west region. Surface winds in the Korean Strait are easterly at 5 knots.

At 12Z May 23 the surface high previously located west of the southern border of the northeast region of the northern JES has moved northeastward and is now located northwest of the northeast region of the northern JES. A surface low is located northwest of the southwest region of the northern JES. A weak surface low is located east of the southeast region of the northern JES. The surface anticyclone previously located southeast of the east region of the central JES moves eastward but remains southeast of the east region of the central JES. Surface pressure rises over the northern JES as the more northerly surface anticyclone approaches the northeast region of the northern JES. Surface pressure falls over the majority of the remainder of the JES because the more southerly surface anticyclone southeast of the east region of the central JES moves away from the JES and also because of troughing associated with the surface low northwest of the southwest region of the northern JES.

Surface winds in the far north region of the northern JES are light and variable while in the remainder of the east region they make a cyclonic turn around the weak surface low east of the southeast region of the northern JES and are easterly to northerly at 3 knots in the remainder of the northeast region and north northeasterly to north northwesterly at 3 to 5 knots in the southeast region. Surface winds in the southwest region of the northern JES are southeasterly to south southeasterly at 5 to 10 knots. Surface winds in the east region of the central JES are south southeasterly to southeasterly at 5 knots while in the west region they make a cyclonic turn due to troughing associated with the surface low northwest of the southwest region of the northern JES and are westerly to south southeasterly at 10 knots. Surface winds in the southern JES are southeasterly to south southeasterly at 5 knots in the east region and

south southwesterly to southerly at 5 to 10 knots in the west region. Surface winds in the Korean Strait are northeasterly at 5 knots.

At 00Z May 24 the surface high previously located northwest of the northeast region of the northern JES has passed to the north of the northeast region of the northern JES and is now located northeast of the northeast region of the northern JES. The surface low previously located northwest of the southwest region of the northern JES has moved northward but remains northwest of the southwest region of the northern JES. The surface anticyclone previously located southeast of the east region of the central JES continues to move eastward but remains southeast of the east region of the central JES. Surface pressure falls over the southern and central JES as the surface anticyclone southeast of the east region of the central JES continues to move away from the JES and as the surface low northwest of the southwest region of the northern JES remains in the vicinity of the JES. High pressure remains over the northern JES. An east-west pressure gradient is present over the JES.

Surface winds in the east region of the northern JES become southeasterly and increase to 10 to 15 knots while in the southwest region they are southerly at 10 knots. Surface winds in the east region of the central JES are southeasterly to southerly at 10 to 15 knots while in the west region they make a cyclonic turn due to troughing associated with the surface low northwest of the southwest region of the northern JES and are westerly to southerly at 10 to 15 knots. Surface winds in the southern JES are southerly at 10 to 15 knots in the east region and southwesterly to southerly at 5 to 10 knots in the west region. Surface winds in the Korean Strait are variable at 5 knots.

At 12Z May 24 a 500-mb trough is located over the JES. During the same time period, a 700-mb trough is located over the JES.

At 12Z May 24 the surface high previously located northeast of the northeast region of the northern JES has moved further eastward away from the JES. The surface low previously located northwest of the southwest region of the northern JES remains stationary and deepens. The surface anticyclone previously located southeast of the east region of the central JES continues to move eastward away from the JES. A surface low is located east of the central ECS. A ridge of high pressure associated with a surface

anticyclone west of the YES is located west of the northwest region of the central JES. A large surface trough is present over the JES. Surface pressure over the JES falls significantly. A strong east-west surface pressure gradient remains present over the east region of the northern and central JES.

Surface winds in the east region of the northern JES remain southeasterly and further increase to 15 to 20 knots while in the southwest region they make a cyclonic turn due to troughing associated with the surface low northwest of the southwest region of the northern JES and are northwesterly to southerly at 5 to 10 knots. Surface winds in the east region of the central JES are southeasterly to southerly at 15 knots while in the west region they make a cyclonic turn due to troughing associated with the surface low northwest of the southwest region of the northern JES and are northwesterly to southwesterly at 5 to 15 knots. Surface winds in the east region of the southern JES experience some convergence and are south southeasterly to southerly at 10 to 15 knots east of 136°E and southwesterly to southerly west of 136°E while in the west region they make a cyclonic turn due to troughing associated with the surface low northwest of the southwest region of the northern JES and are northwesterly to westerly at 10 to 15 knots. Surface winds in the Korean Strait are northwesterly at 15 to 20 knots.

From 00Z May 25 through 12Z May 28 a 500-mb ridge is located over the JES. During the same time period, a 700-mb trough is located over the JES on 00Z May 25, but between 12Z May 25 and 12Z May 28 a 700-mb ridge moves across the JES.

At 00Z May 25 the surface low previously located northwest of the southwest region of the northern JES continues to remain stationary and continues to deepen. The surface low previously located east of the central ECS has moved northeastward and is now located east of the southern border of the northern JES. The ridge of high pressure associated with the surface anticyclone west of the YES builds and extends into the southwestern JES between the two surface cyclones. Surface pressure over the southwestern JES begins to rise due to the building surface ridge. Surface pressure in the northeastern JES falls significantly due to the presence of the surface low east of the southern border of the northern JES. The surface pressure gradient intensifies over the

central JES due to the surface low east of the southern border of the northern JES and the surface ridge over the southwestern JES.

Surface winds in the far north part of the eastern region of the northern JES are southeasterly at 5 to 15 knots while in the central part they make a cyclonic turn due to troughing associated with the surface low east of the southern border of the northern JES and are southeasterly to westerly at 3 to 10 knots. Surface winds in the remainder of the eastern region of the northern JES are northwesterly at 15 to 20 knots. Surface winds in the southwest region of the northern JES make an anticyclonic turn due to ridging from the south and are southwesterly to northwesterly at 5 to 15 knots. Surface winds in the east region of the central JES make a slight cyclonic turn due to the surface low east of the southern border of the northern JES and are northwesterly to westerly at 15 to 20 knots while in the west region they make an anticyclonic turn due to ridging from the southwest and are north northwesterly to north northeasterly at 5 to 15 knots. Surface winds in the southern JES are northwesterly to north northwesterly at 15 to 20 knots in the east region and northerly at 15 to 20 knots in the west region. Surface winds in the Korean Strait are northerly at 15 knots.

At 12Z May 25 the surface low previously located northwest of the southwest region of the northern JES continues to remain stationary and continues to deepen. The surface low previously located east of the southern border of the northern JES has moved northward and is now located east of the northeast region of the northern JES. A surface anticyclone develops within the ridge of high pressure associated with the surface anticyclone now west of the ECS and is located over the east region of the central JES. Surface pressure over the southern JES rises due to the surface anticyclone. Surface pressure in the northern JES remains low due to the presence of the two surface cyclones in the vicinity. The surface pressure gradient is strong over the south region of the northern JES and the west region of the central JES.

Surface winds in the north region of the northern JES make a cyclonic turn around the central low pressure to the east of the northeast region of the northern JES and are north northeasterly to westerly at 5 to 15 knots while in the south region they make an anticyclonic turn around the central high over the east region of the central JES and are

south southwesterly to westerly at 15 to 20 knots. Surface winds in the central JES make an anticyclonic turn around the same central high and are southwesterly to north northeasterly at 5 to 10 knots in the east region and south southwesterly at 10 to 20 knots in the west region. Surface winds in the southern JES are northeasterly to northerly at 5 to 10 knots. Surface winds in the Korean Strait are northerly at 10 knots.

At 00Z May 26 the surface low previously located northwest of the southwest region of the northern JES continues to remain stationary. The surface low previously located east of the northeast region of the northern JES has moved eastward away from the JES but is still located east of the northeast region of the northern JES. The surface anticyclone previously located over the east region of the central JES has moved slightly southeastward and is now located over the southeast region of the central JES. Surface pressure over the JES rises due to the surface anticyclone. The surface pressure gradient remains stronger over the south region of the northern JES and the west region of the central JES.

Surface winds in the north region of the northern JES make a cyclonic turn due to troughing associated with the surface low east of the northeast region of the northern JES are northeasterly to westerly at 5 to 10 knots while in the south region they make an anticyclonic turn around the surface high over the southeast region of the central JES and are south southwesterly to west southwesterly at 10 to 15 knots. Surface winds in the east region of the central JES make an anticyclonic turn around the same surface high and are south southwesterly to southwesterly at 5 to 10 knots while in the west region they make a cyclonic turn due to troughing associated with the surface low northwest of the southwest region of the northern JES and are westerly to southwesterly at 10 knots. Surface winds in the east region of the southern JES are northeasterly at 3 to 5 knots while in the west region they make an anticyclonic turn and are southeasterly to north northeasterly at 3 to 5 knots. Surface winds in the Korean Strait are north northwesterly to northerly at 5 to 10 knots.

At 12Z May 26 the surface low previously located northwest of the southwest region of the northern JES continues to remain stationary. The surface anticyclone previously located over the southeast region of the central JES has moved northeastward

and is now located east of the central JES. The surface pressure gradient between the surface low and the surface high intensifies setting up a strong east-west pressure gradient over the middle of the northern and central JES.

Surface winds in the northern JES are southeasterly at 10 knots in the northeast region, southerly at 5 to 15 knots in the southeast region, and south southwesterly to southerly at 15 knots in the southwest region. Surface winds in the east region of the central JES make an anticyclonic turn around the surface high east of the central JES and are easterly to south southwesterly at 5 to 10 knots while in the west region they make a cyclonic turn due to troughing associated with the surface low northwest of the southwest region of the northern JES and are southwesterly to southerly at 10 to 15 knots. Surface winds in the east region of the southern JES make an anticyclonic turn and are easterly to south southeasterly at 5 knots while in the west region they make a cyclonic turn and are westerly to south southwesterly at 5 knots. Surface winds in the Korean Strait are westerly at 5 to 10 knots.

At 00Z May 27 the surface low previously located northwest of the southwest region of the northern JES moves northward but remains northwest of the southwest region of the northern JES. The surface anticyclone previously located east of the central JES has moved northeastward and is now located east of the southern border of the northern JES. A surface anticyclone is also located over the northern boundary of the west region of the central ECS and its associated ridging affects the west region of the southern JES and the Korean Strait. The surface pressure gradient over the northern JES remains strong due to the surface high to the east of the southern border of the northern JES and the surface low northwest of the southwest region of the northern JES.

Surface winds in the northern JES are southerly at 10 to 15 knots in the east region and south southwesterly to southerly at 10 knots in the southwest region. Surface winds in the east region of the central JES are south southeasterly to southerly at 5 to 10 knots while in the west region they make a cyclonic turn due to troughing associated with the surface low northwest of the southwest region of the northern JES and are westerly to southerly at 5 to 10 knots. Surface winds in the east region of the southern JES are south southeasterly to south southwesterly at 5 knots while in the west region they are west

northwesterly to west southwesterly at 5 knots. Surface winds in the Korean Strait make an anticyclonic turn due to ridging associated with the surface high over the northern boundary of the west region of the central ECS and are northwesterly to northerly at 5 knots.

At 12Z May 27 the surface anticyclone previously located east of the southern border of the northern JES remains stationary and builds. Lower pressure lies to the north of the northern JES. A surface anticyclone remains located over the northern boundary of the west region of the central ECS. The surface pressure gradient over the northern JES remains strong due to the surface high to the east of the southern border of the northern JES and the lower pressure to the north of the northern JES.

Surface winds in the northern JES make an anticyclonic turn due to the surface high east of the southern border of the northern JES and are south southwesterly at 15 knots in the northeast region, southerly to south southwesterly at 10 knots in the southeast region, and southerly at 10 knots in the southwest region. Surface winds in the central JES make an anticyclonic turn around the same surface high and are easterly to southerly at 5 knots in the east region and southerly at 10 knots in the west region. Surface winds in the southern JES are easterly at 5 to 10 knots in the east region and easterly to southerly at 5 to 10 knots in the west region. Surface winds in the Korean Strait are northeasterly to northwesterly at 5 knots.

At 00Z May 28 the surface anticyclone previously located east of the southern border of the northern JES has moved slightly southward and is now located east of the northeast region of the central JES and continues to build. Lower pressure lies to the north of the northeast region of the northern JES. A surface anticyclone previously located over the northern boundary of the west region of the central ECS is now located over the northern boundary of the ECS. A surface low is located west-northwest of the southwest region of the northern JES. Surface pressure continues to rise as the anticyclone to the east of the northeast region of the central JES continues to build and the east-west surface pressure gradient over the southern JES intensifies.

Surface winds in the east region of the northern JES make an anticyclonic turn due the surface high east of the northeast region of the central JES and are southerly to

southwesterly at 10 knots while in the southwest region they are south southeasterly at 10 to 15 knots. Surface winds in the east region of the central JES make an anticyclonic turn around the same surface high and are south southeasterly to southerly at 10 knots while in the west region they are south southeasterly to southerly at 10 to 15 knots. Surface winds in the southern JES are southeasterly at 10 knots. Surface winds in the Korean Strait are easterly at 5 to 10 knots.

At 12Z May 28 the surface anticyclone previously located east of the northeast region of the central JES has moved southeastward and is now located east of the southeast region of the central JES. A surface anticyclone previously located over the northern boundary of the ECS is now located over the northwest region of the central ECS. A surface low remains located west-northwest of the southwest region of the northern JES but deepens as another surface low that passed over the BS moves into the region. Surface pressure begins to fall over the majority of the JES as the ridging associated with the anticyclone east of the southeast region of the central JES retreats eastward and troughing associated with the deepening surface low west-northwest of the southwest region of the northern JES extends into the region. An east-west surface pressure gradient lies over the majority of the JES and tightens significantly although there is ridging present in the east regions of the northern and central JES and troughing present in the west regions of the central and southern JES.

Surface winds in the northern JES are southerly at 5 to 10 knots in the northeast region, southerly to southeasterly at 15 to 20 knots in the southeast region, and southerly to southeasterly at 15 to 20 knots in the southwest region. Surface winds in the east region of the central JES are southeasterly at 15 to 20 knots while in the west region they make a cyclonic turn around the surface low west-northwest of the southwest region of the northern JES and are southwesterly to south southeasterly at 15 knots. Surface winds in the southern JES are southeasterly to south southeasterly at 15 knots in the east region and southwesterly to southerly at 10 to 15 knots in the west region. Surface winds in the Korean Strait are southwesterly at 10 knots.

From 00Z May 29 through the end of the time period an intense 500-mb cyclone propagates eastward across the northern JES while its associated 500-mb troughing

passes over the central and southern JES. During the same time period, an intense 700-mb cyclone propagates eastward across the northern JES while its associated troughing passes over the central and southern JES.

At 00Z May 29 the surface anticyclone previously located east of the northeast region of the central JES has moved eastward away from the JES but is still located east of the southeast region of the central JES. The surface low located west-northwest of the southwest region of the northern JES has moved northward while continuing to deepen and is now located northwest of the southwest region of the northern JES. Surface pressure continues to fall over the majority of the JES as the ridging associated with the anticyclone east of the southeast region of the central JES continues to retreat eastward and troughing associated with the deepening surface low west-northwest of the southwest region of the northern JES continues to extend into the region. The pressure gradient is now oriented northeast-to-southwest and decreases in strength.

Surface winds in the northern JES are southeasterly at 10 knots in the northeast region, southerly to south southwesterly at 15 knots in the southeast region, and southwesterly at 10 to 15 knots in the southwest region. Surface winds in the east region of the central JES make an anticyclonic turn due to ridging associated with the surface high east of the southeast region of the central JES and are south southeasterly to south southwesterly at 10 to 15 knots while in the west region they make a cyclonic turn around the surface low northwest of the southwest region of the northern JES and are westerly to southwesterly at 5 to 10 knots. Surface winds in the southern JES are southerly at 3 to 5 knots in the east region and westerly at 3 to 5 knots in the west region. Surface winds in the Korean Strait make an anticyclonic turn and are northwesterly to northerly at 5 to 10 knots.

At 12Z May 29 the surface anticyclone previously located east of the northeast region of the central JES has moved northward and is now located east of the northeast region of the central JES. The surface low northwest of the southwest region of the northern JES has moved further northward but remains northwest of the southwest region of the northern JES. A weak surface low is present over Honshu, Japan to the east of the southern JES. A surface anticyclone is located northwest of the BS and west of the YS

and its associated ridging extends into the southwestern JES. Surface pressure falls in the northern JES and in the southeastern JES.

Surface winds in the northern JES make a cyclonic turn due to troughing associated with the surface low northwest of the southwest region of the northern JES and are south southwesterly to southeasterly at 10 to 15 knots in the northeast region and southwesterly at 5 to 15 knots in the south region. Surface winds in the northeast region of the central JES are light and variable while in the southeast region they make a cyclonic turn due to troughing associated with the weak surface low east of the southern JES and are easterly to northeasterly at 3 to 5 knots. Surface winds in the northwest region of the central JES are southwesterly at 5 to 15 knots while in the southwest region they make an anticyclonic turn due to ridging from the southwest and are westerly to northerly at 5 to 15 knots. Surface winds in the east region of the southern JES make a cyclonic turn due to troughing associated with the weak surface low east of the southern JES and are northeasterly to northerly at 5 knots while in the west region they make an anticyclonic turn due to ridging from the west and are northwesterly to northerly at 5 to 10 knots. Surface winds in the Korean Strait are northerly at 10 to 15 knots.

At 00Z May 30 the surface low to the northwest of the southwest region of the northern JES moves further northward but continues to remain northwest of the southwest region of the northern JES. The surface anticyclone previously northwest of the BS is now located west of the YS and its associated ridging continues to extend into the southwestern JES. Surface pressure continues to fall in the northern JES.

Surface winds in the northern JES make a cyclonic turn around the surface low northwest of the southwest region of the northern JES and are westerly to southeasterly at 5 to 10 knots in the east region and westerly at 10 knots in the southwest region. Surface winds in the central JES are anticyclonic due to ridging from the southwest and are westerly to northwesterly at 10 knots in the east region and westerly to north northwesterly at 5 to 10 knots in the west region. Surface winds in the southern JES are north northwesterly at 10 knots in the east region and northerly at 10 knots in the west region. Surface winds in the Korean Strait are northerly at 15 knots.

At 12Z May 30 the surface low to the northwest of the southwest region of the northern JES moves eastward and is now located northwest of the northeast region of the northern JES. The surface anticyclone previously west of the YS has moved eastward and is now centered over the west region of the YS. Its associated ridging now extends into the southern and central JES. Surface pressure continues to fall in the northern JES as the surface low approaches the JES. The surface pressure gradient intensifies over the JES.

Surface winds in the far north region of the JES make a cyclonic turn around the surface low northwest of the northeast region of the northern JES and are southwesterly to southeasterly at 3 to 10 knots while over the remainder of the JES they are southwesterly at 15 knots. Surface winds in the central JES are westerly at 10 to 15 knots. Surface winds in the southern JES are west northwesterly to northwesterly at 10 knots in the east region and west northwesterly to northwesterly at 10 to 15 knots in the west region. Surface winds in the Korean Strait are northwesterly at 10 to 15 knots.

At 00Z May 31 the surface low to the northwest of the northeast region of the northern JES has moved further eastward and is now located over the northeast region of the northern JES. The surface anticyclone previously centered over the west region of the YS has moved southward and is now centered over the west region of the northern ECS. Its associated ridging extends into the southern JES. Surface pressure continues to fall in the northern JES as the surface passes to the north of the northeast region of the northern JES. The surface pressure gradient further intensifies over the JES.

Surface winds in the northern JES are west southwesterly at 3 to 5 knots in the far north and west southwesterly at 20 knots elsewhere. Surface winds in the central JES are westerly at 20 knots. Surface winds in the east region of the southern JES are westerly to northwesterly at 10 to 15 knots while in the west region they make an anticyclonic turn due to ridging from the west and are west northwesterly to northwesterly at 10 knots. Surface winds in the Korean Strait are northerly at 10 knots.

At 12Z May 31 the surface low previously north of the northeast region of the northern JES has passed the northern JES and is now located east of the northeast region of the northern JES. The surface anticyclone previously centered over the west region of

the northern ECS remains stationary. The surface pressure gradient further remains intense over the JES.

Surface winds in the northeast region of the northern JES make a cyclonic turn around the surface low east of the northeast region of the northern JES and are northeasterly to westerly at 5 knots while in the south region they are southwesterly at 20 knots. Surface winds in the central JES are southwesterly at 20 knots. Surface winds in the southern JES are westerly at 10 to 15 knots. Surface winds in the Korean Strait are west northwesterly at 10 knots.

2. YES

Readers should refer to Appendix T for the surface level pressure/SAT/surface wind plots over the YES for the May period. The figures in Appendix T are in time sequential order every 12 hours from 00Z May 13 through 12Z May 31.

From 00Z May 13 through 00Z May 15 a 500-mb ridge propagates eastward across the YES. During the same time period, a 700-mb ridge propagates eastward across the YES).

At 00Z May 13 a surface anticyclone dominates the YES and is centered over the southern boundary of the west region of the northern ECS. A region of troughing is located north of the BS. Surface winds in the BS make a slight cyclonic turn due to troughing from the north and are westerly to southwesterly at 10 to 15 knots. Surface winds in the YS make an anticyclonic turn around the surface high centered over the southern boundary of the west region of the northern ECS and are southwesterly to west northwesterly at 10 to 15 knots. Surface winds in the ECS make an anticyclonic turn around the same surface high and are southwesterly to northwesterly at 5 to 10 knots in the west region of the northern ECS and are northwesterly to northeasterly at 5 to 15 knots in the remainder of the ECS.

At 12Z May 13 the surface anticyclone remains centered over the southern boundary of the west region of the northern ECS and continues to dominate the YES. Surface troughing affects the BS and the north region of the YS due to a region of low pressure north of the BS. Surface winds in the BS make a cyclonic turn due to troughing from the north and are westerly to southerly at 10 to 15 knots. Surface winds in the north

region of the YS are southerly at 5 to 15 knots. Surface winds in the central YS experience divergence due to troughing from the north and the surface high over the southern boundary of the west region of the northern ECS and are southerly at 5 to 10 knots to the north while in the south they make a slight anticyclonic turn and are west southwesterly to westerly at 5 knots. Surface winds in the southern YS and in the ECS make an anticyclonic turn around the same surface high and are south southwesterly to west northwesterly at 5 to 10 knots in the south region of the YS, south southeasterly to north northwesterly at 5 to 15 knots in the northern ECS, south southeasterly to northerly at 5 to 15 knots in the northwest region of the central ECS, north northwesterly to northwesterly at 10 to 15 knots in the east region of the central ECS, northerly to north northeasterly at 10 to 15 knots in the southwest region of the central ECS, and northerly to northeasterly at 10 to 15 knots in the southern ECS.

At 00Z May 14 the surface anticyclone moves westward and is located over China to the west of the northwest region of the central ECS. Surface troughing associated with a region of low pressure to the northwest of the BS affects the BS, the northern YS, and the west region of the central YS. Troughing associated with lower pressure east of the east region of the central ECS affects the east region of the northern ECS and the east region of the central ECS.

Surface winds in the BS are westerly at 10 to 15 knots. Surface winds in the northern YS and the west region of the central YS make a cyclonic turn due to troughing from the west and are westerly to southeasterly at 5 to 10 knots. Surface winds in the east region of the central YS are northerly at 3 to 5 knots. Surface winds in the southern YS are variable at 3 knots in the west region and northerly at 5 to 10 knots in the west region. Surface winds in the west region of the northern ECS are southerly at 5 knots in the west and northerly at 5 to 10 knots in the east. Surface winds in the east region of the northern ECS and in the east region of the central ECS make a slight cyclonic turn due to troughing from the east and are north northeasterly to north northwesterly at 10 to 15 knots. Surface winds in the west region of the central ECS and in the west region of the southern ECS make a slight anticyclonic turn due to the surface high west of the northwest region of the central ECS and are northerly to northeasterly at 10 to 20 knots. Surface winds in the east region of the southern ECS are northerly at 15 knots.

At 12Z May 14 the surface anticyclone moves northeastward and reestablishes itself over the west region of the southern YS. Troughing associated with lower pressure to the southeast of the east region of the central ECS affects the east region of the northern ECS and the east region of the central ECS. Surface winds in the BS are easterly at 5 knots in the north and westerly at 5 knots in the south. Surface winds in the northern YS experience divergence and are southeasterly at 5 knots in the west, southerly at 5 knots in the middle, and southwesterly at 5 knots in the east. Surface winds in the central and southern YS make an anticyclonic turn around the surface high over the west region of the southern YS and are west southwesterly to southerly at 5 to 15 knots. Surface winds in the west region of the northern ECS make an anticyclonic turn around the same surface high and are northerly to east southeasterly at 5 to 15 knots. Surface winds in the east region of the northern ECS and in the east region of the central ECS make a slight cyclonic turn due to troughing from the southeast and are northeasterly to northwesterly at 10 to 15 knots. Surface winds in the west region of the central ECS and the west region of the southern ECS make a slight anticyclonic turn and are northerly to northeasterly at 10 to 20 knots. Surface winds in the east region of the southern ECS are north northeasterly to north northwesterly at 10 to 15 knots.

At 00Z May 15 the surface anticyclone remains over the west region of the southern YS. Troughing associated with a region of lower pressure to the southeast of the east region of the central ECS affects the eastern ECS. Troughing associated with a region of low pressure to the north of the BS affects the BS. Surface winds in the BS make a cyclonic turn and are westerly to southerly at 5 to 15 knots. Surface winds in the YS and the west region of the northern ECS make an anticyclonic turn around the surface high over the west region of the southern YS and are south southeasterly to southeasterly at 5 knots in the northern YS, westerly to southerly at 3 to 5 knots in the west region of the central YS, northeasterly to southeasterly at 3 to 5 knots in the east region of the central YS, northeasterly to south southwesterly at 5 knots in the west region of the southern YS, northeasterly at 5 to 10 knots in the east region of the southern YS, and northeasterly to southeasterly at 5 to 10 knots in the west region of the northern ECS. Surface winds in the eastern ECS make a cyclonic turn due to troughing from the southeast and are northeasterly to north northeasterly at 10 to 15 knots in the east region

of the northern ECS, northeasterly to north northwesterly at 5 to 10 knots in the east region of the central ECS, and northerly to northwesterly at 5 to 15 knots in the east region of the southern ECS. Surface winds in the west region of the central ECS are northeasterly to northerly at 10 to 15 knots. Surface winds in the west region of the southern ECS make a slight anticyclonic turn and are northerly to northeasterly at 10 to 20 knots.

From 12Z May 15 through 00Z May 16 a small 500-mb shortwave trough is present over the YES. During the same time period a 700-mb trough is located over the YES.

At 12Z May 15 the surface anticyclone is now centered over the southern boundary of the west region of the central YS. Troughing associated with a region of low pressure to the south of the east region of the southern ECS affects the eastern ECS. This inverted trough is developing between the surface high over the southern boundary of the west region of the central YS and the surface anticyclone centered over the southern boundary of the east region of the central JES and is associated with a surface low centered over the east region of the northern SCS.

Surface winds in the BS, in the YS, and in the west region of the northern ECS make an anticyclonic turn around the surface high centered over the southern boundary of the west region of the central YS and are southeasterly south southeasterly at 5 to 15 knots. Surface winds in the eastern ECS make a cyclonic turn due to troughing associated with the surface low centered over the east region of the northern SCS and are easterly to north northeasterly at 10 knots in the east region of the northern ECS, southeasterly to northerly at 5 to 10 knots in the east region of the central ECS, and southwesterly to north northwesterly at 5 to 10 knots in the east region of the southern ECS. Surface winds in the west region of the central ECS and in the west region of the southern ECS make a slight anticyclonic turn and are northerly to north northeasterly at 10 to 15 knots in the west region of the central ECS and northerly to northeasterly at 10 to 15 knots in the west region of the southern ECS.

At 00Z May 16 the surface anticyclone is now located over the western part of the west region of the southern YS. A surface low has developed in the region of troughing

over the eastern ECS and is centered over the east region of the northern ECS. Surface winds in the BS, in the YS, and in the west region of the northern ECS make an anticyclonic turn around the surface high centered over the western part of the west region of the southern YS and are south southwesterly to northeasterly at 3 to 15 knots. Surface winds in the eastern ECS make a cyclonic turn around the surface low over the east region of the northern ECS and are south southeasterly to southwesterly at 5 to 10 knots. Surface winds in the west region of the central ECS are northerly to north northwesterly at 10 to 15 knots. Surface winds in the west region of the southern ECS make a slight anticyclonic turn and are northerly to northeasterly at 10 to 20 knots.

At 12Z May 16 a small 500-mb shortwave ridge is present over the YES and weakens through 12Z May 17. During the same time period a small 700-mb shortwave ridge is present over the YES and weakens through 12Z May 17.

At 12Z May 16 the surface anticyclone has moved southward and is now located over the northwest part of the west region of the central ECS. The surface low has moved northward and is now centered over the Korean peninsula. Troughing associated with a region of low pressure to the north of the BS affects the BS. Troughing associated with a region of low pressure to the south of the southern ECS associated with the surface low centered over the east region of the northern SCS affects the southern ECS.

Surface winds in the BS make a cyclonic turn due to troughing from the north and are westerly to south southeasterly at 5 to 15 knots. Surface winds in the YS make an anticyclonic turn around the surface high over the northwest part of the west region of the central ECS and are southerly to northwesterly at 5 to 15 knots. Surface winds in the western ECS make an anticyclonic turn due to the same surface high and are south southeasterly to northeasterly at 5 to 15 knots. Surface winds in the east region of the northern ECS and in the east region of the central ECS make a cyclonic turn due to the surface low pressure centered over the Korean peninsula and are northwesterly to west northwesterly at 5 to 15 knots. Surface winds in the east region of the southern ECS are variable at 3 to 5 knots.

At 00Z May 17 the surface anticyclone has moved eastward and is now located over the southern boundary of the east region of the northern ECS. The surface low over

the Korean peninsula has moved further northward and no longer affects the YES. Troughing associated with a surface low northwest of the southwest region of the northern JES affects the BS and the northern YS. Troughing associated with a surface low centered over the north part of the east region of the northern SCS and to the south of the southern ECS continues to affect the southern ECS.

Surface winds in the BS and the northern YS make a cyclonic turn due to troughing associated with the surface low northwest of the southwest region of the northern JES and are west northwesterly to south southwesterly at 15 knots. Surface winds in the YS and the northern and central ECS make an anticyclonic turn around the surface high over the southern boundary of the east region of the northern ECS and are southwesterly to south southwesterly at 3 to 15 knots. Surface winds in the southern ECS make a cyclonic turn due to troughing from the southwest and are southeasterly to easterly at 5 to 15 knots.

At 12Z May 17 the surface anticyclone has moved further eastward and is now east of the east region of the northern ECS, but its associated ridging continues to affect the majority of the YES. Troughing associated with a surface cyclone centered over the northeast part of the east region of the northern SCS affects the west region of the southern ECS. Surface winds in the BS are variable at 3 to 5 knots in the west part and southwesterly to west southwesterly at 10 to 15 knots in the east part. Surface winds in the YS make an anticyclonic turn due to ridging from the surface high to the east of the east region of the northern ECS and are southerly to southwesterly at 10 to 15 knots. Surface winds in the northern ECS and the north region of the central ECS make an anticyclonic turn due to ridging from the same surface high and are easterly to northerly at 5 to 10 knots. Surface winds in the south region of the central ECS are easterly at 5 to 10 knots. Surface winds in the east region of the southern ECS are variable at 3 to 5 knots while in the west region they make a cyclonic turn due to troughing from the southwest and are southerly to northeasterly at 10 to 20 knots.

From 00Z May 18 through 12Z May 19 a 500-mb trough moves eastward over the YES and the trailing 500-mb ridge builds over the BS. During the same time period, a

700-mb trough moves eastward over the YES while a trailing 700-mb ridge builds west of the YES. The 700-mb height gradient decreases over the time period.

At 00Z May 18 the surface low that was centered over the northeast part of the east region of the northern SCS has moved northeastward and is now centered over the southern boundary of the west region of the central ECS and affects the majority of the ECS. The surface precipitation plot for 00Z May 18, which is not included in any appendices, shows the surface low bringing some precipitation into the region. The surface anticyclone previously east of the east region of the northern ECS has moved northwestward and is now centered over the tip of the Korean peninsula to the east of the southern border of the central YS and its associated ridging continues to affect the majority of the YES.

Surface winds in the BS are southwesterly at 5 to 10 knots. Surface winds in the northern YS are southwesterly to south southwesterly at 5 to 10 knots in the west region and southerly at 10 knots in the east region. Surface winds in the central YS make an anticyclonic turn around the surface high east of the southern border of the central YS and are southeasterly to southwesterly at 3 to 5 knots in the east region and easterly to south southwesterly at 5 to 10 knots in the west region. Surface winds in the southern YS are easterly at 10 knots in the east region and southeasterly to northeasterly at 3 to 10 knots in the west region. Surface winds in the east region of the northern ECS make a slight anticyclonic turn and are east northeasterly to east southeasterly at 10 knots while in the west region they make a sharp cyclonic turn and are southerly to north northeasterly at 5 to 10 knots. Surface winds in the northwest region of the central ECS make an anticyclonic turn and are north northeasterly to southeasterly at 5 to 20 knots. Surface winds in the east region of the central ECS, in the southwest region of the central ECS, and in the southern ECS make a cyclonic turn around the surface low pressure over the southern boundary of the west region of the central ECS and are southerly to west southwesterly at 10 to 35 knots.

At 12Z May 18 the surface low has moved northeastward while filling and is now centered over the southern boundary of the central ECS and continues to affect the

majority of the ECS. The surface anticyclone previously east of the southern border of the central YS has moved westward and is now centered over the YS.

Surface winds in the BS and in the YS make an anticyclonic turn around the surface high centered over the YS and are southeasterly to southwesterly at 10 knots in the BS and south southeasterly to southeasterly at 5 to 10 knots in the YS. Surface winds in the ECS make a cyclonic turn around the central low pressure over the southern boundary of the central ECS and are northeasterly to east northeasterly at 5 to 30 knots.

By 00Z May 19 the surface low has filled considerably but its presence is still observed over the southern boundary of the central ECS. The surface anticyclone remains centered over the YS and builds. Surface winds in the BS and in the YS make an anticyclonic turn around the central high pressure centered in the middle of the YS and are southerly to south southeasterly at 5 to 10 knots. Surface winds in the east region of the northern ECS make a slight anticyclonic turn and are northeasterly to east northeasterly at 5 to 10 knots while in the west region they make sharp cyclonic turn and are easterly to north northwesterly at 5 to 10 knots. Surface winds in the central ECS make a cyclonic turn around the surface low over the southern boundary of the central ECS and are northeasterly at 10 knots in the northeast region, northeasterly to east northeasterly at 5 to 10 knots in the southeast region, and northeasterly to north northwesterly at 10 to 20 knots in the west region. Surface winds in the east region of the southern ECS make a cyclonic turn around the same surface low pressure and are south southwesterly to northwesterly at 10 to 15 knots while in the west region they experience some divergence and are northerly at 10 to 20 knots in the east and northeasterly at 15 knots in the west.

At 12Z May 19 the surface low is now observed over the southern boundary of the east region of the southern ECS but it has filled considerably. The surface anticyclone is now centered over the southern boundary of the central YS. Surface winds in the BS and in the northern YS make an anticyclonic turn around the surface high centered over the southern boundary of the central YS and are south southeasterly to southwesterly in the BS and southerly to westerly at 3 to 10 knots in the northern YS. Surface winds in the central and southern YS make an anticyclonic turn around the same

surface high and are southeasterly to northerly at 3 to 15 knots. Surface winds in the west region of the northern ECS make an anticyclonic turn around the same surface high and are north northeasterly to easterly at 5 to 15 knots. Surface winds in the east region of the northern ECS and in the east region of the central ECS make a slight anticyclonic turn and are northwesterly to east northeasterly at 5 to 10 knots. Surface winds in the west region of the central ECS are north northwesterly to north northeasterly at 10 to 15 knots. Surface winds in the east region of the southern ECS make a cyclonic turn around the surface low over the southern boundary of the east region of the southern ECS and are southeasterly to north northwesterly at 5 to 10 knots. Surface winds in the west region of the southern ECS experience some divergence and are northerly at 10 to 20 knots in the east and northeasterly at 15 knots in the west.

From 00Z May 20 through 12Z May 21 a 500-mb ridge propagates across the YES. During the same time period, a 700-mb ridge propagates across the YS while a 700-mb cyclone is present over the majority of the ECS and moves eastward while deepening.

At 00Z May 20 a closed cyclonic circulation is no longer present in the southern ECS, however troughing associated with a new developing low pressure system to the south of the ECS remains over the east region of the southern ECS. The surface anticyclone remains centered over the southern boundary of the central YS. Surface winds in the BS, in the YS, and in the northern ECS make an anticyclonic turn around the surface high centered over the southern boundary of the central YS and are south southwesterly to southerly at 5 to 15 knots. Surface winds in the central ECS are northeasterly at 10 to 15 knots in the east region and north northeasterly to northerly at 10 to 15 knots in the west region. Surface winds in the east region of the southern ECS make a cyclonic turn due to the troughing from the south and are east northeasterly to north northeasterly at 10 to 15 knots while in the west region they experience some divergence and are north northeasterly at 15 knots in the east and northeasterly at 15 to 20 knots in the west.

At 12Z May 20 the troughing associated with the surface low south of the ECS remains over the east region of the southern ECS. The surface anticyclone is now

centered over the central YS. Surface winds in the BS, in the YS, and in the northern ECS make an anticyclonic turn around the surface high centered over the central YS and are southeasterly to southwesterly at 10 to 15 knots in the BS and southerly to easterly at 5 to 15 knots in the YS and northern ECS. Surface winds in the central ECS are northeasterly to east northeasterly at 10 to 15 knots in the east region and northeasterly to north northeasterly at 10 to 15 knots in the west region. Surface winds in the east region of the southern ECS make a cyclonic turn around due to troughing from the south and are east northeasterly to northeasterly at 15 knots while in the west region they experience some divergence and are north northeasterly to northerly at 15 to 20 knots in the east and north northeasterly to northeasterly at 15 to 20 knots in the west.

At 00Z May 21 the troughing associated with the surface low pressure system to the south of the ECS extends further northward and is now over the central and southern ECS. The surface anticyclone is now centered over the southern boundary of the northern YS. Surface winds in the BS make a cyclonic turn due to troughing from the west and are southwesterly to southeasterly at 10 to 15 knots. Surface winds in the northern YS are southerly to southeasterly at 3 to 5 knots. Surface winds in the central YS are northeasterly at 10 knots in the east and variable at 3 to 5 knots in the west. Surface winds in the southern YS are northeasterly at 5 to 10 knots. Surface winds in the northern ECS are east northeasterly at 10 knots in the east and northeasterly at 10 to 15 knots in the west. Surface winds in the central ECS are east northeasterly at 15 to 20 knots in the east and northeasterly at 10 to 20 knots in the west. Surface winds in the east region of the southern ECS make a cyclonic turn due to troughing from the south and are easterly to east northeasterly at 15 to 20 knots while in the west region they experience some divergence and are northeasterly to northerly at 20 knots in the east and northeasterly at 15 to 20 knots in the west.

At 12Z May 21 the troughing associated with the surface low to the south of the ECS remains over the central and southern ECS. The surface anticyclone is now centered over the southern boundary of the west region of the central YS. Surface winds in the BS make an anticyclonic turn and are southeasterly to southwesterly at 10 to 15 knots. Surface winds in the YS and in the northern ECS make an anticyclonic turn around the surface high over the southern boundary of the west region of the central YS

and are south southeasterly to easterly at 3 to 10 knots. Surface winds in the central and southern ECS make a cyclonic turn due to troughing from the south and are easterly to northerly at 10 to 25 knots.

From 00Z May 22 through 00Z May 24 the 500-mb ridge now east of the YS weakens, a deepening 500-mb trough approaches the YS from the northwest and a 500-mb cyclone develops and then weakens east of the ECS. During the same time period, ridging associated with a closed 700-mb anticyclone northeast of the ECS moves eastward away from the YES, a 700-mb trough moves over the YES from the east, and the 700-mb cyclone east of the ECS deepens.

At 00Z May 22 the troughing associated with the surface low south of the ECS remains over the central and southern ECS. The surface anticyclone remains centered over the southern boundary of the west region of the central YS. Troughing associated with lower pressure to the northwest of the BS affects the BS and the northern YS. Surface winds in the BS and in the northern YS make a cyclonic turn due to troughing from the northwest and are west southwesterly to northerly at 5 to 15 knots. Surface winds in the YS and in the west region of the northern ECS make an anticyclonic turn around the surface high centered over the southern boundary of the west region of the central YS and are southerly to northeasterly at 3 to 10 knots. Surface winds in the east region of the northern ECS, in the central ECS, and in the southern ECS make a cyclonic turn due to troughing from the south and are easterly to north northeasterly at 5 to 25 knots.

At 12Z May 22 the troughing associated with the surface low south of the ECS remains over the central and southern ECS. The surface anticyclone remains centered over the southern boundary of the west region of the central YS. Surface winds in the BS make an anticyclonic turn due to ridging from the northwest and are northeasterly to southeasterly at 5 to 15 knots. Surface winds in the YS and in the northern ECS make an anticyclonic turn around the surface high over the southern boundary of the west region of the central YS and are south southwesterly to southeasterly at 5 to 10 knots. Surface winds in the central and southern ECS make a cyclonic turn due to troughing from the south and are northeasterly to north northeasterly at 10 to 25 knots.

At 00Z May 23 the troughing associated with the surface low now located east of the southern ECS remains over the central and southern ECS and begins to affect the east region of the northern ECS. A surface anticyclonic circulation is no longer present over the southern boundary of the west region of the central YS. A small surface cyclonic circulation develops over the southwestern part of the BS, but in general there is higher pressure northwest of the YES and lower pressure southeast of the YES. Surface winds in the BS make a cyclonic turn around a region of relatively lower pressure over the southwestern part of the BS and are southeasterly to southerly at 5 to 10 knots. Surface winds in the northern YS make a sharp anticyclonic turn and are northwesterly to east southeasterly at 3 to 10 knots. Surface winds in the central and southern YS make an anticyclonic turn and are north northeasterly to southeasterly at 3 to 10 knots. Surface winds in the west region of the northern ECS make a slight anticyclonic turn and are northeasterly to east northeasterly at 3 to 10 knots. Surface winds in the east region of the northern ECS, in the central ECS, and in the southern ECS make a cyclonic turn due to troughing associated with the surface low east of the southern ECS and are east northeasterly to northeasterly at 5 to 25 knots.

At 12Z May 23 the troughing associated with the deepening surface low, still located east of the southern ECS, remains over the central and southern ECS and continues to affect the east region of the northern ECS. Surface winds in the BS make a cyclonic turn and are northwesterly to southwesterly at 5 to 10 knots. Surface winds in the northern YS make a sharp anticyclonic turn and are south southwesterly to northwesterly at 3 to 10 knots. Surface winds in the east region of the central YS and in the east region of the southern YS are northerly to north northeasterly at 10 to 15 knots. Surface winds in the west region of the central YS, in the west region of the southern YS, and in the west region of the northern ECS make an anticyclonic turn due to ridging from the west and are west northwesterly to east northeasterly at 5 to 10 knots. Surface winds in the east region of the northern ECS, in the central ECS, and in the southern ECS are north northeasterly to northeasterly at 5 to 25 knots due to the passing surface cyclone to the east of the southern ECS and the higher pressure to the northwest of the YES.

At 00Z May 24 the troughing associated with the deepening surface low, still located east of the southern ECS, now covers the majority of the ECS. Ridging

associated with a strong anticyclone west of the YS affects the central and southern YS. Troughing associated with a surface low located northwest of the southwest region of the northern JES affects the northern YS and the BS. Surface winds in the BS and in the northern YS make a cyclonic turn due to troughing associated with surface low northwest of the southwest region of the northern JES and are northerly to north northeasterly at 15 to 25 knots in the BS and northerly to westerly at 10 to 15 knots in the northern YS. Surface winds in central and southern YS make a slight anticyclonic turn due to ridging associated with the surface anticyclone west of the YS and are westerly to north northwesterly at 10 knots. Surface winds in the eastern ECS make a cyclonic turn due to troughing associated with the surface low east of the southern ECS and are northeasterly to north northwesterly at 5 to 20 knots. Surface winds in the western ECS are north northwesterly to northeasterly at 10 to 20 knots.

From 12Z May 24 through 00Z May 26 the 500-mb trough that previously approached the YS from the northwest passes over the YES. During the same time period, the 700-mb cyclone that was east of the ECS is no longer present. A 700-mb trough propagates eastward across the YES.

At 12Z May 24 the deepening surface low is now located east of the central ECS. The strong surface anticyclone is now west of the YES. Troughing associated with a region of lower pressure to the north of the BS affects the BS. An east-west pressure gradient is present over the majority of the YES.

Surface winds in the BS are variable at 5 to 10 knots. Surface winds in the YS are northwesterly at 15 to 20 knots. Surface winds in the west region of the northern ECS and in the west region of the central ECS are north northwesterly at 15 to 20 knots. Surface winds in the east region of the northern ECS and in the east region of the central ECS are north northwesterly at 10 to 20 knots. Surface winds in the east region of the southern ECS are north northwesterly to northwesterly at 15 to 20 knots while in the west region they experience some divergence and are northerly to north northwesterly at 15 knots in the east and northerly to northeasterly at 10 to 15 knots in the west.

At 00Z May 25 a strong surface anticyclone remains west of the YES. Low pressure associated with a deepening surface low northwest of the southwest region of

the northern JES remains north of the BS. The surface low previously located east of the central ECS has moved northeastward and is now located east of the southern border of the northern JES. Lower pressure associated with troughing from this surface low is located east of the northern ECS. An east-west pressure gradient remains present over the majority of the YES although a north-south pressure gradient is present over the BS and the majority of the northern YS.

Surface winds in the BS and in the northern YS make a slight cyclonic turn and are west southwesterly to southwesterly at 5 to 15 knots. Surface winds in the west region of the central YS and in the west region of the southern YS make a sharp anticyclonic turn due to ridging associated with the surface high west of the YES and are west southwesterly to northerly at 5 to 10 knots. Surface winds in the east region of the central YS and in the east region of the southern YS are northerly at 10 knots. Surface winds in the east region of the northern ECS make a slight cyclonic turn due to troughing associated with lower pressure east of the northern JES and are north northeasterly to north northwesterly at 15 knots while in the west region they are northerly at 10 knots. Surface winds in the east region of the central ECS make a slight cyclonic turn due to troughing associated with the same region of lower pressure and are north northwesterly to northwesterly at 10 to 20 knots while in the west region they are north northwesterly at 10 to 15 knots. Surface winds in the east region of the southern ECS make a slight cyclonic turn due to troughing associated with the same region of low pressure and are north northwesterly to northwesterly at 10 to 15 knots while in the west region they experience some divergence and are northerly to north northwesterly at 10 to 15 knots in the east and northerly to northeasterly at 10 to 15 knots in the west.

At 12Z May 25 lower pressure associated with troughing from a surface low now located east of the northeast region of the northern JES remains east of the northern ECS. The strong surface anticyclone is now located to the west of the ECS and its associated ridging affects the majority of the YES. A region of lower pressure associated with a deepening surface low northwest of the southwest region of the northern JES is located in the vicinity of the BS.

Surface winds in the BS are south southwesterly to southwesterly at 15 knots. Surface winds in the YS and in the northern ECS make an anticyclonic turn due to ridging associated with the surface high west of the ECS and are southerly to northerly at 5 to 20 knots. Surface winds in the central ECS are northwesterly at 5 to 10 knots. Surface winds in the east region of the southern ECS are northwesterly at 5 to 10 knots while in the west region they experience some divergence and are north northwesterly at 5 to 10 knots in the east and northerly to northeasterly at 5 to 10 knots in the west.

At 00Z May 26 lower pressure associated with troughing from a surface low still located east of the northeast region of the northern JES remains east of the northern ECS. The strong surface anticyclone west of the ECS has moved eastward but remains west of the ECS and its associated ridging continues to affect the majority of the YES. A closed surface cyclonic circulation develops in the region of lower pressure associated with the deepening surface low northwest of the southwest region of the northern JES and is located west of the BS.

Surface winds in the BS are southwesterly at 10 to 15 knots in the south and northeasterly at 10 knots in the north. Surface winds in the YS and in the northern ECS make an anticyclonic turn due to ridging associated with the surface high west of the ECS and are south southwesterly to northerly at 5 to 15 knots. Surface winds in the central ECS make an anticyclonic turn due to ridging from the same surface high and are westerly to northwesterly at 5 to 10 knots. Surface winds in the east region of the southern ECS make a slight cyclonic turn due to troughing from the northeast and are north northwesterly to northwesterly at 5 to 10 knots while in the west region they make an anticyclonic turn due to ridging from the northwest and are north northwesterly to northeasterly at 10 to 15 knots.

From 12Z May 26 through 12Z May 27 500-mb flow becomes zonal. During the same time period a 700-mb ridge propagates across the YES.

At 12Z May 26 the surface anticyclone is centered over the northwest region of the central ECS and its associated ridging continues to affect the majority of the YES. A small closed surface anticyclonic circulation is present northwest of the BS while a small closed cyclonic circulation is present to the southwest of the BS. Surface winds in the BS

are north northeasterly at 10 to 15 knots. Surface winds in the YS and in the ECS make an anticyclonic turn around the surface high over the northwest region of the central ECS and are southerly to northeasterly at 5 to 25 knots.

At 00Z May 27 the surface anticyclone is centered over the northern boundary of the west region of the central ECS and its associated ridging affects the majority of the ECS. A region of high surface pressure is present north of the BS and its associated ridging affects the majority of the BS. A surface low is present west of the BS and its associated troughing affects the majority of the YS. Surface winds in the BS make a slight anticyclonic turn due to ridging from the north and are northeasterly to easterly at 10 to 15 knots. Surface winds in the northern YS are variable at 3 to 10 knots. Surface winds in the central and southern YS make a cyclonic turn due to troughing from the west and are west southwesterly to southerly at 5 to 15 knots. Surface winds in the ECS make an anticyclonic turn around the surface high over the northern boundary of the west region of the central ECS and are south southwesterly to northeasterly at 3 to 20 knots.

At 12Z May 27 the surface anticyclone remains centered over the northern boundary of the west region of the central ECS and its associated ridging continues to affect the majority of the ECS. A region of higher pressure is located to the north of the BS while the surface low west of the BS moves eastward and its associated troughing affects the majority of the YS and BS. Surface winds in the YS and BS make a cyclonic turn due to troughing from the west and are southwesterly to east southeasterly at 5 to 20 knots. Surface winds in the ECS make an anticyclonic turn around the surface high over the northern boundary of the west region of the central ECS and are southerly to southeasterly at 3 to 20 knots.

From 00Z May 28 through 12Z May 30 a 500-mb trough with a strong geopotential height gradient that is associated with an intense 500-mb cyclone north of the YES moves across the YES. During the same time period a 700-mb trough with a strong geopotential height gradient that is associated with an intense 700-mb cyclone north of the YES moves across the YES while a strong 700-mb ridge builds west of the YES.

At 00Z May 28 the surface anticyclone is centered over the northern boundary of the ECS. The surface low is now located over the western part of the BS and moves northeastward while deepening. Troughing associated with a surface low over the east region of the northern SCS extends northeastward and penetrates the eastern ECS. Surface winds in the BS are south southwesterly at 20 to 25 knots. Surface winds in the western YS are southwesterly to south southwesterly at 10 to 20 knots. Surface winds in the eastern YS are south southwesterly to southerly at 5 to 20 knots. Surface winds in the eastern ECS make a cyclonic turn due to troughing from the south and are easterly to north northeasterly at 5 to 10 knots. Surface winds in the western ECS make an anticyclonic turn around the surface high over the northern boundary of the ECS and are north northeasterly to south southwesterly at 5 to 10 knots in the west region of the northern ECS, north northeasterly to south southeasterly at 5 knots in the west region of the central ECS, and northeasterly to east northeasterly at 10 to 20 knots in the west region of the southern ECS.

At 12Z May 28 the surface anticyclone is centered over the northwest region of the central ECS. The surface low that passed over the BS is now located west-northwest of the southwest region of the northern JES and has deepened. The troughing associated with this surface low affects the BS and the northern and central YS. The more southerly surface low is now located south of Taiwan and it continues to deepen while moving northeastward. The troughing associated with the more southerly surface low affects the east region of the southern ECS and the east region of the central ECS.

The surface winds in the BS, in the northern YS, and in the central YS make a cyclonic turn due to troughing from the north and are north northwesterly to southwesterly at 15 to 30 knots. The surface winds in the southern YS and in the west region of the northern ECS make an anticyclonic turn around the surface high over the northwest region of the central ECS and are southerly to southwesterly at 3 to 15 knots. Surface winds in the west part of the east region of the northern ECS make an anticyclonic around the same surface high and are south southwesterly to northwesterly at 3 to 5 knots while in the east part of the of the east region of the northern ECS they make an anticyclonic turn due to ridging from the east and are southeasterly to southwesterly at 5 to 10 knots. Surface winds in the west region of the central ECS and in the west region

of the southern ECS make an anticyclonic turn around the same surface high and are easterly to northeasterly at 3 to 20 knots. Surface winds in the west part of the east region of the central ECS make an anticyclonic turn around the same surface high and are north northwesterly to north northeasterly at 5 knots while in the east part of the east region of the central ECS they make a cyclonic turn due to troughing from the southwest and are southeasterly to east southeasterly at 5 to 15 knots. Surface winds in the east region of the southern ECS make a cyclonic turn due to troughing from the southwest and are east southeasterly to northeasterly at 5 to 10 knots.

At 00Z May 29 the surface anticyclone is centered over the Shandong peninsula. A more intense surface anticyclone is located to the northwest of the BS. The ridging associated with these anticyclones affects the BS and the YS. The surface low to the south is now located east of Taiwan, continues to move northeastward, and brings The surface precipitation plot for 00Z May 29, which is not included in any appendices, shows the surface low bringing some precipitation into the region. The pressure gradient over the majority of the YES intensifies due to the surface high to the west and the transiting surface low in the southern ECS.

The surface winds in the BS, in the YS, and in the northern ECS make an anticyclonic turn around the surface high over the Shandong peninsula and are southwesterly to northeasterly at 5 to 25 knots. The surface winds in the central ECS are northeasterly to north northeasterly at 10 to 15 knots. The surface winds in the east region of the southern ECS are variable at 5 to 10 knots while in the west region they make a cyclonic turn around the surface low east of Taiwan and are northeasterly to northerly at 15 to 20 knots.

At 12Z May 29 the surface high previously northwest of the BS remains northwest of the BS and is also west of the YS. The southerly surface low is now centered in over the southern ECS, continues to move northeastward, and begins to fill. The pressure gradient over the majority of the YES remains strong. The surface winds in the BS are variable at 5 to 10 knots. The surface winds in the YS, in the northern ECS, and in the central ECS make an anticyclonic turn due to ridging associated with the surface high west of the YS and are northwesterly to southeasterly at 5 to 25 knots. The

surface winds in the southern ECS make a cyclonic turn around the surface low over the southern ECS and are southwesterly to north northwesterly at 5 to 20 knots.

At 00Z May 30 a strong surface anticyclone is centered west of the southern YS. The surface low to the south is no longer present but an extensive region of low pressure and cyclonic turning is present east of the ECS. The pressure gradient over the majority of the YES remains strong due to high pressure to the west and low pressure to the east. The surface winds in the BS, in the YS, in the northern ECS, in the central ECS, and in the west region of the southern ECS make an anticyclonic turn around the surface high west of the southern YS and are west southwesterly to northeasterly at 3 to 25 knots. Surface winds in the east region of the southern ECS make a cyclonic turn due to troughing from the northeast and are northerly to northwesterly at 5 to 20 knots.

At 12Z May 30 the surface anticyclone has moved eastward and is now centered over the west region of the southern YS. The surface winds in the YES make an anticyclonic turn around the surface high over the west region of the southern YS and are south southeasterly to southeasterly at 5 to 20 knots.

From 00Z May 31 through the end of the time period a 500-mb ridge propagates eastward across the YES. During the same time period the 700-mb ridge that had previously built up west of the YES moves over the YES.

At 00Z May 31 the surface anticyclone has moved southward and is now centered over the west region of the northern ECS. The surface winds in the YES make an anticyclonic turn around the surface high over the west region of the northern ECS and are south southwesterly to easterly at 3 to 20 knots.

At 12Z May 31 the surface anticyclone remains centered over the west region of the northern ECS. The surface winds in the YES make an anticyclonic turn around the central high pressure over the west region of the northern ECS and are east southeasterly to east northeasterly at 3 to 20 knots.

3. SCS

Readers should refer to Appendix U for the surface level pressure/SAT/surface wind plots over the SCS for the May period. The figures in Appendix U are in time sequential order every 12 hours from 00Z May 13 through 12Z May 31.

At 00Z May 13 a surface low develops over the west region of the northern SCS. Surface winds in the northern SCS make a cyclonic turn around the developing surface low centered over the west region of the northern SCS and are southeasterly to northeasterly at 5 to 20 knots in the east region and northeasterly to east southeasterly at 5 to 15 knots in the west region. Surface winds in the central SCS are predominantly east southeasterly to east northeasterly at 10 to 15 knots. Surface winds in the Gulf of Thailand make an anticyclonic turn and are east northeasterly to southeasterly at 3 to 5 knots. Surface winds in the southern are variable at 3 to 5 knots.

At 12Z May 13 a surface low continues to develop over the west region of the northern SCS. Surface winds in the northern SCS make a cyclonic turn around the developing surface low centered over the west region of the northern SCS and are northeasterly to east northeasterly at 3 to 15 knots. Surface winds in the central SCS are predominantly east northeasterly at 10 to 15 knots. Surface winds in the Gulf of Thailand are northeasterly at 3 to 5 knots. Surface winds in the southern SCS are easterly at 5 to 10 knots in the east part and remain variable at 3 to 5 knots elsewhere.

At 00Z May 14 a developing surface low remains over the west region of the northern SCS. Surface winds in the northern SCS continue to make a cyclonic turn around the developing surface low centered over the west region of the northern SCS and are northeasterly to east northeasterly at 3 to 15 knots. Surface winds in the central SCS are predominantly east southeasterly to northeasterly at 10 to 15 knots. Surface winds in the Gulf of Thailand are easterly at 5 knots. Surface winds in the southern SCS are northeasterly at 5 knots in the north part and variable at 3 to 5 knots elsewhere.

At 12Z May 14 the surface low deepens and remains stationary over the west region of the northern SCS. Surface winds in the northern SCS continue to make a cyclonic turn around the surface low centered over the west region of the northern SCS and are northeasterly to east northeasterly at 3 to 20 knots. Surface winds in the east region of the central SCS make a cyclonic turn and are easterly to northeasterly at 5 to 15 knots. Surface winds in the west region of the central SCS and in the Gulf of Thailand make an anticyclonic turn and are northeasterly to southerly at 3 to 10 knots. Surface

winds in the southern SCS are northeasterly at 5 knots in the north part and variable at 3 to 5 knots elsewhere.

At 00Z May 15 the surface low moves eastward and is centered over the northern SCS. Surface winds in the northern SCS continue to make a cyclonic turn around the surface low centered over the northern SCS and are northeasterly to east northeasterly at 3 to 20 knots. Surface winds in the east region of the central SCS are easterly at 5 to 10 knots. Surface winds in the west region of the central SCS and in the Gulf of Thailand make an anticyclonic turn and are easterly to southerly at 3 to 10 knots. Surface winds in the southern SCS are southwesterly to southerly at 3 to 5 knots.

At 12Z May 15 the surface low deepens, moves eastward, and is centered over the east region of the northern SCS. Surface winds in the northern SCS continue to make a cyclonic turn around the surface low centered over the east region of the northern SCS and are northeasterly to east northeasterly at 3 to 20 knots. Surface winds in the east region of the central SCS make a cyclonic turn and are southeasterly to easterly at 5 to 10 knots. Surface winds in the west region of the central SCS and in the Gulf of Thailand are calm to variable at 3 to 5 knots. Surface winds in the southern SCS make an anticyclonic turn and are southerly to southwesterly at 3 to 5 knots.

At 00Z May 16 the surface low remains centered over the east region of the northern SCS. Surface winds in the northern SCS and in the central SCS make a cyclonic turn around the surface low over the east region of the northern SCS and are northeasterly to east northeasterly at 5 to 20 knots. Surface winds in the Gulf of Thailand are southerly at 5 knots. Surface winds in the southern SCS make an anticyclonic turn and are southeasterly to west southwesterly at 3 to 5 knots.

At 12Z May 16 the surface low remains centered over the east region of the northern SCS and deepens. Surface winds in the northern SCS make a cyclonic turn around the surface low over the east region of the northern SCS and are northeasterly to east northeasterly at 5 to 30 knots. Surface winds in the east region of the central SCS are southeasterly at 5 knots in the east part and south southwesterly to southerly at 5 knots in the west part. Surface winds in the west region of the central SCS are southerly to south southeasterly at 5 knots. Surface winds in the Gulf of Thailand are westerly to

southerly at 5 knots. Surface winds in the southern SCS are south southeasterly to south southwesterly at 5 knots.

At 00Z May 17 the surface low moves northward and is now centered over the north part of the east region of the northern SCS. Surface winds in the northern SCS make a cyclonic turn around the surface low and are northeasterly to east northeasterly at 10 to 30 knots. Surface winds in the east region of the central SCS are southeasterly at 5 to 15 knots while in the west region of the central SCS they are southerly to south southeasterly at 3 to 5 knots. Surface winds in the Gulf of Thailand are southwesterly to south southwesterly at 3 to 5 knots. Surface winds in the southern SCS are south southeasterly to south southwesterly at 5 knots.

At 12Z May 17 the surface low moves northeastward and is now centered over the northeast part of the east region of the northern SCS. Surface winds in the northern SCS make a cyclonic turn around the surface low and are northeasterly to east northeasterly at 10 to 30 knots. Surface winds in the east part of the east region of the central SCS are southeasterly to south southeasterly at 10 knots. Surface winds in the west part of the east region of the central SCS, in the west region of the central SCS, and in the Gulf of Thailand make an anticyclonic turn and are easterly to southeasterly at 3 to 5 knots. Surface winds in the southern SCS are easterly at 5 knots in the east part and southerly at 5 knots in the west part.

At 00Z May 18 the surface low has moved northeastward and is now centered over the southern boundary of the west region of the central ECS. Surface winds in the northern SCS make a cyclonic turn due to the surface low and are northerly to southwesterly at 10 to 20 knots. Surface winds in the east region of the central SCS, in the east part of the west region of the central SCS, and in the east part of the southern SCS make an anticyclonic turn and are southeasterly to southwesterly at 5 to 10 knots. Surface winds in the west part of the west region of the central SCS and in the Gulf of Thailand make a cyclonic turn and are south southwesterly to southeasterly at 5 knots.

At 12Z May 18 the surface low has moved northeastward and is now centered over the southern boundary of the central ECS. Surface winds in the east region of the northern SCS make a cyclonic turn due to the surface low and are north northeasterly to

southwesterly at 10 to 15 knots. Surface winds in the west region of the northern SCS are northerly at 5 to 15 knots. Surface winds in the east region of the central SCS make a slight cyclonic turn and are southeasterly to northeasterly at 5 to 10 knots. Surface winds in the west region of the central SCS and in the Gulf of Thailand make a slight anticyclonic turn and are east southeasterly to southeasterly at 3 to 5 knots. Surface winds in the southern SCS make a slight anticyclonic turn and are southerly to east southeasterly at 5 knots.

At 00Z May 19 surface winds in the northern SCS make a cyclonic turn and are northeasterly to southwesterly at 5 to 15 knots in the east region and northeasterly to northerly at 3 to 5 knots in the west region. Surface winds in the east region of the central SCS are southeasterly at 5 to 10 knots. Surface winds in the west region of the central SCS and in the Gulf of Thailand make a slight anticyclonic turn and are southeasterly to south southeasterly at 5 knots. Surface winds in the southern SCS are southeasterly at 5 to 10 knots.

At 12Z May 19 a surface low begins to develop over the east part of the east region of the northern SCS. Surface winds in the east region of the northern SCS make a cyclonic turn around the developing surface low and are northeasterly to east northeasterly at 5 to 10 knots. Surface winds in the west region of the northern SCS are northeasterly to northerly at 5 to 10 knots. Surface winds in the east region of the central SCS make a slight cyclonic turn and are east southeasterly to easterly at 5 knots. Surface winds in the west region of the central SCS and in the Gulf of Thailand make a slight anticyclonic turn and are easterly to southerly at 3 to 5 knots. Surface winds in the southern SCS make a slight cyclonic turn and are southerly to east southeasterly at 5 to 10 knots.

At 00Z May 20 a surface low continues to develop over the east part of the east region of the northern SCS. Surface winds in the east region of the northern SCS make a cyclonic turn around the developing surface low and are northeasterly to east northeasterly at 5 to 20 knots. Surface winds in the west region of the northern SCS make an anticyclonic turn due to ridging associated with a surface high over the southern boundary of the central YS and are northeasterly to southeasterly at 3 to 5 knots. Surface

winds in the central SCS are southeasterly at 5 knots in the east region and calm to variable at 3 to 5 knots in the west region. Surface winds in the Gulf of Thailand make a slight anticyclonic turn and are southeasterly to southerly at 5 knots. Surface winds in the southern SCS make a slight cyclonic turn and are southerly to south southeasterly at 5 knots.

At 12Z May 20 a surface low continues to develop over the east part of the east region of the northern SCS. Surface winds in the east region of the northern SCS make a cyclonic turn around the developing surface low and are northeasterly to east northeasterly at 5 to 15 knots. Surface winds in the west region of the northern SCS are variable at 5 to 10 knots. Surface winds in the central SCS and in the Gulf of Thailand make a slight anticyclonic turn and are easterly to southerly at 3 to 5 knots. Surface winds in the west part of the southern SCS make a slight cyclonic turn and are southerly to southeasterly at 5 knots at 5 knots while in the east part they are calm.

At 00Z May 21 the surface low has moved northeastward and has joined a surface low that was south of the ECS. Surface winds in the east region of the northern SCS make a cyclonic turn due to the surface low south of the ECS and are northeasterly to southwesterly at 5 to 20 knots. Surface winds in the west region of the northern SCS are variable at 5 to 10 knots. Surface winds in the central SCS and in the southern SCS make a slight anticyclonic turn and are south southeasterly to southwesterly at 5 to 10 knots. Surface winds in the Gulf of Thailand are southerly at 5 knots.

At 12Z May 21 troughing associated with the surface low south of the ECS continues to affect the east region of the northern SCS. Surface winds in the east region of the northern SCS make a cyclonic turn due to the surface low south of the ECS and are north northeasterly to southwesterly at 5 to 20 knots. Surface winds in the west region of the northern SCS are variable at 3 to 5 knots. Surface winds in the central SCS and in the east part of the southern SCS make a slight anticyclonic turn and are southerly to westerly at 5 knots. Surface winds in the west part of the southern SCS make a slight cyclonic turn and are southerly to southeasterly at 5 knots. Surface winds in the Gulf of Thailand are south southeasterly at 5 knots.

At 00Z May 22 troughing associated with the surface low south of the ECS continues to affect the east region of the northern SCS. Surface winds in the east region of the northern SCS make a cyclonic turn due to the surface low south of the ECS and are northeasterly to southwesterly at 5 to 20 knots. Surface winds in the west region of the northern SCS are variable at 3 to 10 knots. Surface winds in the central SCS, in the southern SCS, and in the Gulf of Thailand make an anticyclonic turn due to higher pressure to the southeast of the east region of the central JES and are southeasterly to west southwesterly at 5 to 10 knots.

At 12Z May 22 troughing associated with the surface low south of the ECS continues to affect the east region of the northern SCS. Surface winds in the east region of the northern SCS make a slight cyclonic turn due to the surface low south of the ECS and are north northeasterly to northerly at 10 to 25 knots. Surface winds in the west region of the northern SCS are variable at 5 to 15 knots. Surface winds in the central SCS, in the southern SCS, and in the Gulf of Thailand make an anticyclonic turn due to higher pressure to the southeast of the east region of the central JES and are south southeasterly to southwesterly at 5 to 10 knots.

At 00Z May 23 troughing associated with the surface low that is now located east of the southern ECS continues to affect the east region of the northern SCS. An anticyclonic circulation is centered over Borneo. Surface winds in the east region of the northern SCS make a slight cyclonic turn and are north northeasterly to northerly at 5 to 20 knots. Surface winds in the west region of the northern SCS are variable at 3 to 15 knots. Surface winds in the central SCS, in the southern SCS, and in the Gulf of Thailand make an anticyclonic turn and are southeasterly to westerly at 5 to 15 knots.

At 12Z May 23 troughing associated with the deepening surface low east of the southern ECS affects the northern SCS. The anticyclonic circulation previously centered over Borneo has moved northwestward and is centered over the east part of the southern SCS. Surface winds in the northern SCS make a cyclonic turn and are northeasterly to north northwesterly at 5 to 20 knots. Surface winds in the central SCS, in the southern SCS, and in the Gulf of Thailand make an anticyclonic turn and are south southeasterly to westerly at 5 to 15 knots.

At 00Z May 24 troughing associated with the deepening surface low east of the southern ECS affects the northern SCS and the north part of the central SCS. The anticyclonic circulation previously centered over the east part of the southern SCS is no longer present, but ridging associated with higher pressure southeast of the east region of the central SCS affects the southern SCS, the Gulf of Thailand, and the central SCS. Surface winds in the northern SCS and in the north part of the central SCS make a cyclonic turn and are northeasterly to southwesterly at 5 to 20 knots. Surface winds in the remainder of the central SCS, in the southern SCS, and in the Gulf of Thailand make an anticyclonic turn and are southeasterly to west southwesterly at 5 to 15 knots.

At 12Z May 24 troughing associated with the deepening surface low that is now located east of the central ECS continues to affect the northern SCS and the north part of the central SCS. Surface winds in the northern SCS and in the north part of the central SCS make a cyclonic turn and are northeasterly to southwesterly at 5 to 20 knots. Surface winds in the remainder of the central SCS, in the southern SCS, and in the Gulf of Thailand make an anticyclonic turn and are southwesterly to west southwesterly at 5 to 15 knots.

At 00Z May 25 a surface low develops in the region of troughing that was located over the northern SCS. The surface low is centered over the south part of the east region of the northern SCS. Surface winds in the northern SCS and in the east region of the central SCS make a cyclonic turn around the surface low and are northeasterly to east northeasterly at 5 to 20 knots. Surface winds in the west region of the central SCS, in the southern SCS, and in the Gulf of Thailand make an anticyclonic turn and are southwesterly to westerly at 5 to 15 knots.

At 12Z May 25 the surface low is centered over the southern boundary of the east region of the northern SCS. Surface winds in the northern SCS and in the east region of the central SCS make a cyclonic turn around the surface low and are northeasterly to east northeasterly at 5 to 20 knots. Surface winds in the west region of the central SCS, in the southern SCS, and in the Gulf of Thailand make an anticyclonic turn and are southerly to westerly at 5 to 15 knots.

At 00Z May 26 the surface low has moved northward and is centered over the south part of the east region of the northern SCS. Surface winds in the northern SCS and in the north part of the east region of the central SCS make a cyclonic turn around the surface low and are northeasterly to east northeasterly at 5 to 20 knots. Surface winds in the remainder of the central SCS, in the southern SCS, and in the Gulf of Thailand make an anticyclonic turn and are southerly to westerly at 5 to 10 knots.

At 12Z May 26 the surface low remains centered over the south part of the east region of the northern SCS. Surface winds in the northern SCS and in the north part of the east region of the central SCS make a cyclonic turn around the surface low and are northeasterly to east northeasterly at 5 to 15 knots. Surface winds in the remainder of the central SCS, in the southern SCS, and in the Gulf of Thailand make an anticyclonic turn and are southerly to southwesterly at 5 to 10 knots.

At 00Z May 27 the surface low remains centered over the south part of the east region of the northern SCS. Surface winds in the northern SCS and in the north part of the east region of the central SCS make a cyclonic turn around the surface low and are northeasterly to east northeasterly at 5 to 15 knots. Surface winds in the remainder of the central SCS, in the southern SCS, and in the Gulf of Thailand make an anticyclonic turn and are south southeasterly to southwesterly at 5 to 10 knots.

At 12Z May 27 the surface low is centered over the east region of the northern SCS. Surface winds in the northern SCS and in the north part of the east region of the central SCS make a cyclonic turn around the surface low and are northeasterly to east northeasterly at 5 to 15 knots. Surface winds in the remainder of the central SCS, in the southern SCS, and in the Gulf of Thailand make an anticyclonic turn and are southeasterly to southwesterly at 5 to 10 knots.

At 00Z May 28 the surface low remains centered over the east region of the northern SCS. Surface winds in the northern SCS make a cyclonic turn around the surface low and are northeasterly to east northeasterly at 5 to 20 knots. Surface winds in the central SCS, in the southern SCS, and in the Gulf of Thailand make an anticyclonic turn and are southeasterly to west southwesterly at 5 to 15 knots.

At 12Z May 28 the surface low is located south of Taiwan. Surface winds in the northern SCS make a cyclonic turn and are north northeasterly to southwesterly at 5 to 20 knots. Surface winds in the central SCS, in the southern SCS, and in the Gulf of Thailand make an anticyclonic turn and are south southeasterly to southwesterly at 5 to 15 knots.

At 00Z May 29 the surface low is located east of Taiwan. Surface winds in the east region of the northern SCS make a cyclonic turn and are north northeasterly to southwesterly at 5 to 15 knots. Surface winds in the west region of the northern SCS are variable at 3 to 5 knots. Surface winds in the central SCS, in the southern SCS, and in the Gulf of Thailand make an anticyclonic turn and are south southeasterly to west southwesterly at 5 to 15 knots.

At 12Z May 29 a new surface low develops over the southern border of the northern SCS. Surface winds in the east region of the northern SCS are northeasterly to north northeasterly at 5 to 10 knots. Surface winds in the west region of the northern SCS make a slight cyclonic turn and are northeasterly to north northeasterly at 5 to 10 knots. Surface winds in the east region of the central SCS are southwesterly to southerly at 5 to 10 knots. Surface winds in the west region of the central SCS are westerly to southwesterly at 10 to 15 knots. Surface winds in the southern SCS make an anticyclonic turn and are southerly to southwesterly at 5 to 15 knots. Surface winds in the Gulf of Thailand are west southwesterly to southwesterly at 10 to 15 knots.

At 00Z May 30 the surface low remains over the southern border of the northern SCS. Surface winds in the northern SCS are variable at 3 to 10 knots. Surface winds in the east part of the east region of the central SCS make an anticyclonic turn and are southeasterly to southwesterly at 15 knots. Surface winds in the remainder of the central SCS, in the southern SCS, and in the Gulf of Thailand make an anticyclonic turn and are south southeasterly to west southwesterly at 5 to 20 knots.

At 12Z May 30 the surface low remains over the southern border of the northern SCS. A surface anticyclonic circulation develops over the east part of the southern SCS. Surface winds in the northern SCS and in the north part of the central SCS make a cyclonic turn around the surface low and are northeasterly to east northeasterly at 5 to 20 knots. Surface winds in the remainder of the central SCS, in the southern SCS, and in the

Gulf of Thailand make an anticyclonic turn and are south southeasterly to southeasterly at 3 to 20 knots.

At 00Z May 31 the surface low remains over the southern border of the northern SCS. Surface winds in the northern SCS and in the north part of the central SCS make a cyclonic turn around the surface low and are northeasterly to east northeasterly at 5 to 25 knots. Surface winds in the remainder of the central SCS, in the southern SCS, and in the Gulf of Thailand make an anticyclonic turn and are easterly to southwesterly at 3 to 20 knots.

At 12Z May 31 the surface low moves northeastward and is centered over the east region of the northern SCS. Surface winds in the northern SCS and in the north part of the central SCS make a cyclonic turn around the surface low and are northeasterly to east northeasterly at 5 to 15 knots. Surface winds in the remainder of the central SCS, in the southern SCS, and in the Gulf of Thailand make an anticyclonic turn and are east northeasterly to southwesterly at 3 to 10 knots.

B. JULY TIME PERIOD: JULY 18 THROUGH JULY 31, 1998

Readers should refer to Appendix V for the 500-mb relative vorticity/geopotential height plots over the EAMS for the July period. The figures in Appendix V are in time sequential order ever 12 hours from 00Z July 18 through 12Z July 31.

Readers should refer to Appendix W for the 700-mb vertical velocity/geopotential height plots over the EAMS for the July period. The figures in Appendix W are in time sequential order ever 12 hours from 00Z July 18 through 12Z July 31.

During this period the summer monsoon is established. The presence of the Manchurian Low and the Bonin High are clearly depicted at the 500-mb level of the model output.

1. JES

Readers should refer to Appendix X for the surface level pressure/SAT/surface wind plots over the JES for the July period. The figures in Appendix X are in time sequential order ever 12 hours from 00Z July 18 through 12Z July 31.

On July 18 a strong 500-mb ridge is present in the JES and mid-level flow is predominantly meridional. A 500-mb cyclone and its associated troughing are northwest

of the JES and remain stationary. An anticyclone and its associated ridging are clearly present in the JES at the 700-mb level. A 700-mb cyclone and its associated troughing lie to the northwest of the JES and remain stationary.

At 00Z July 18 a surface low is located to the northwest of the JES while a more southerly surface low is located over the southern boundary of the east region of the northern ECS. A surface high is located to the east of the northern JES.

Surface winds are very light throughout the JES. Surface winds in the northeast region of the northern JES are southwesterly at 5 knots while in the southeast region they make an anticyclonic turn due to ridging from the east and are easterly to southwesterly at 3 to 5 knots. Surface winds in the southwest region of the northern JES are southeasterly at 3 knots. Surface winds in the east region of the central JES are predominantly calm to variable at 3 knots, although northerly winds at 5 knots are present in the east part. Surface winds in the west region of the central JES are calm in the east part and easterly at 3 to 5 knots in the west part. Surface winds in the southern JES are variable at 3 knots in the east region and easterly at 5 knots in the west region. Surface winds in the Korean Strait are easterly at 10 knots.

At 12Z July 18 surface winds in the JES intensify as the surface pressure gradient tightens due to the surface high to the east of the JES, the surface low northwest of the JES, and the surface low that is now centered over the east region of the northern ECS.

Surface winds in the northern JES and in the north region and southeast region of the central JES make an anticyclonic turn around the surface high east of the JES and are southerly at 10 knots in the northeast region of the northern JES, northeasterly to southwesterly at 3 to 10 knots in the southeast region of the northern JES, southerly to southwesterly at 5 knots in the southwest region of the northern JES, northeasterly to southeasterly at 3 to 5 knots in the east region of the central JES, and southeasterly to easterly at 5 to 10 knots in the northwest region of the central JES. Surface winds in the southwest region of the central JES and in the southern JES make a cyclonic turn around the surface low over the east region of the northern ECS and are east southeasterly to easterly at 5 to 10 knots in the southwest region of the central JES, southeasterly at 5 to 10 knots in the east region of the southern JES, and southeasterly to easterly at 10 knots

in the west region of the southern JES. Surface winds in the Korean Strait are east southeasterly at 10 knots.

On July 19 the 500-mb anticyclone and its associated ridging remain over the majority of the JES although troughing from the 500-mb cyclone northwest of the JES extends southeastward over the southern JES. The 700-mb anticyclone and its associated ridging remain over the northern JES while troughing from the 700-mb cyclone northwest of the JES extends southeastward over the southern JES.

At 00Z July 19 the more southerly surface low continues to deepen and move northward so that it is centered over the Korean peninsula while the surface low pressure system northwest of the JES moves eastward but remains northwest of the JES. A surface high is east of the northern JES. Surface pressure over the JES falls while the pressure gradient over the southern and central JES intensifies.

Surface winds in the northeast region of the northern JES slacken and become variable at 3 to 5 knots while in the southeast region they make a slight anticyclonic turn due to the surface high to the east and are southeasterly to southerly at 3 to 5 knots. Surface winds in the southwest region of the northern JES, the central and southern JES, and in the Korean Strait make a cyclonic turn around the surface low over the Korean peninsula and are southeasterly to easterly at 5 knots in the southwest region of the northern JES, southerly to southeasterly at 3 to 10 knots in the east region of the central JES, southeasterly to easterly at 10 to 15 knots in the west region of the central JES, south southeasterly to southeasterly at 5 to 15 knots in the east region of the southern JES, southeasterly at 10 to 15 knots in the west region of the southern JES, and westerly to south southeasterly at 5 to 10 knots in the Korean Strait.

At 12Z July 19 the more southerly surface low moves eastward and is located over the southern JES while the surface low northwest of the JES remains stationary. Surface pressure over the JES remains low.

Surface winds in the east region of the northern JES make a slight anticyclonic turn and are northeasterly to easterly at 5 to 10 knots in the northeast region and easterly to southeasterly at 3 to 5 knots in the southeast region. Surface winds in the southwest region of the northern JES are southeasterly at 5 to 10 knots. Surface winds in the central

JES are southeasterly to east southeasterly at 5 to 10 knots in the east region and east southeasterly to easterly at 10 to 15 knots in the west region. Surface winds in the southern JES make a cyclonic turn the surface low over the southern JES and are southeasterly to east southeasterly at 5 to 10 knots in the east region and easterly to westerly at 3 to 5 knots in the west region. Surface winds in the Korean Strait are west northwesterly to westerly at 5 to 10 knots.

On July 20 the 500-mb anticyclone remains stationary and its associated ridging remains over most of the northern JES while the 500-mb cyclone moves slightly southward and its associated troughing continues to extend over the southern JES. The 700-mb anticyclone moves northwestward but its associated ridging remains over most of the northern JES while the 700-mb cyclone remains stationary and its associated troughing continues to extend over the southern JES.

At 00Z July 20 the surface low northwest of the JES moves westward but remains northwest of the JES. The surface low previously over the southern JES moves southeastward and is now south of the east region of the southern JES. Surface pressure over the JES increases.

Surface winds in the northeast region of the northern JES make an anticyclonic turn and are northerly to east southeasterly at 3 to 5 knots. Surface winds in the south region of the northern JES and in the central JES make a slight cyclonic turn and are east southeasterly to easterly at 5 to 10 knots in the southeast region of the northern JES, easterly at 5 knots in the southwest region of the northern JES, east southeasterly to easterly at 10 knots in the east region of the central JES, and easterly at 5 to 10 knots in the west region of the central JES. Surface winds in the east region of the southern JES are easterly to southeasterly at 5 knots. Surface winds in the Korean Strait and in the west region of the southern JES make a cyclonic turn due to troughing associated with the surface low northwest of the JES and are northwesterly to northerly at 3 to 5 knots.

At 12Z July 20 the surface low northwest of the JES remains stationary. The more southerly surface low moved eastward and is now southeast of the southern JES. Surface pressure over the JES rises with higher pressure to the northeast of the JES.

Surface winds in the northern JES are east southeasterly at 5 to 10 knots in the northeast region, east southeasterly at 10 to 15 knots in the southeast region, and easterly to east southeasterly in the southwest region. Surface winds in the north region of the central JES are east southeasterly to easterly at 10 knots. Surface winds in the south region of the central JES and in the southern JES make a slight anticyclonic turn and are easterly at 5 to 10 knots in the southeast region of the central JES, easterly to southeasterly at 5 to 10 knots in the southwest region of the central JES, east northeasterly to east southeasterly at 5 to 10 knots in the east region of the southern JES and southeasterly at 5 knots in the west region of the southern JES. Surface winds in the Korean Strait are variable at 5 knots.

On July 21 the 500-mb anticyclone remains stationary and its associated ridging is over most of the northeast region of the northern JES while the 500-mb cyclone continues to move slightly southward and its associated troughing now extends over the majority of the JES. The 700-mb anticyclone continues to move northwestward and its associated ridging is over most of the northeast region of the northern JES while the 700-mb cyclone moves southward and its associated troughing extend over the most of the JES.

At 00Z July 21 the surface low northwest of the JES remains stationary. A surface high is north of the northeast region of the northern JES. Surface pressure over the JES continues to rise as the surface high to the north builds.

Surface winds in the far north region of the northern JES are calm while in the remainder of the northeast region they make an anticyclonic turn and are northeasterly to easterly at 3 to 10 knots. Surface winds in the south region of the northern JES are easterly at 10 to 15 knots in the southeast region and easterly at 5 to 10 knots in the southwest region. Surface winds in the central JES are easterly to east southeasterly at 5 to 10 knots in the north region, easterly at 5 knots in the southeast region, and east southeasterly to easterly at 5 to 10 knots in the southwest region. Surface winds in the southern JES make an anticyclonic turn and are northeasterly to east southeasterly at 5 knots in the east region and southeasterly at 5 to 10 knots in the west region. Surface winds in the Korean Strait are southeasterly at 5 to 10 knots.

At 12Z July 21 surface pressure over the east region of the northern JES continues to increase as the surface high now northeast of the northern JES continues to build. The surface low northwest of the JES moves westward but is still northwest of the JES.

Surface winds in the northeast region of the northern JES make an anticyclonic turn and are easterly to southerly at 5 to 10 knots. Surface winds in the south region of the northern JES are easterly at 15 knots in the southeast region and easterly at 10 to 15 knots in the southwest region. Surface winds in the central and southern JES are easterly at 5 to 15 knots. Surface winds in the Korean Strait are easterly at 10 knots.

On July 22 the 500-mb anticyclone remains stationary and its associated ridging is over most of the northeast region of the northern JES while the 500-mb cyclone begins to dissipate. Troughing associated with a 500-mb cyclone northwest of the YS continues to extend over the majority of the JES. The 700-mb anticyclone moves northward and its associated ridging is over most of the east region of the northern JES while the 700-mb cyclone begins to dissipate. Troughing associated with a 700-mb cyclone northwest of the YS continues to extend over the most of the JES.

At 00Z July 22 surface pressure over the JES increases as the surface high now located north of the northeast region of the northern JES continues to build. Surface winds in the northern JES are easterly at 3 to 15 knots. Surface winds in the central JES are easterly to east northeasterly at 10 knots. Surface winds in the southern JES are northeasterly at 5 to 10 knots in the east region and easterly to northeasterly at 10 knots in the west region. Surface winds in the Korean Strait are easterly at 10 knots.

At 12Z July 22 surface pressure over the northern and central JES remains high due to the surface high now located northeast of the northern JES. A surface low is located over the northeast region of the central ECS. Troughing associated with this surface low extends northeastward and impacts the southeast region of the central JES and the east region of the southern JES.

Surface winds in the northeast region of the northern JES make an anticyclonic turn and are easterly to southerly at 5 to 15 knots. Surface winds in the south region of the northern JES are east northeasterly at 15 knots in the southeast region and east northeasterly to easterly at 10 knots in the southwest region. Surface winds in the north

region of the central JES are east northeasterly at 10 knots in the northeast region and east northeasterly at 5 to 10 knots in the northwest region. Surface winds in the southeast region of the central JES and in the east region of the southern JES make a cyclonic turn and are easterly to northeasterly at 10 knots. Surface winds in the southwest region of the central JES, in the west region of the southern JES, and in the Korean Strait make a slight anticyclonic turn and are northeasterly to easterly at 10 knots in the southwest region of the central JES, northeasterly to east northeasterly at 10 knots in the west region of the southern JES, and east northeasterly to easterly at 10 knots in the Korean Strait.

On July 23 the 500-mb anticyclone moves eastward and is located northeast of the northern JES. A 500-mb cyclone develops over the southeast region of the northern JES in the region of troughing over the JES associated with the 500-mb cyclone northwest of the YS. The 700-mb anticyclone remains stationary and is located north of the JES. A 700-mb cyclone develops over the south region of the northern JES in the region of troughing over the JES associated with a 700-mb cyclone northwest of the YS.

At 00Z July 23 surface pressure over the northern JES remains high due to the surface high now located north of the northern JES. Troughing associated with the surface low now centered over the southern boundary of the east region of the northern ECS affects the east region of the central JES.

Surface winds in the northern JES are easterly to east northeasterly at 5 to 10 knots in the northeast region, east northeasterly at 15 knots in the southeast region, and east northeasterly at 5 to 10 knots in the southwest region. Surface winds in the east region of the central JES make a cyclonic turn and are east southeasterly to northerly at 5 to 10 knots while in the west region they make an anticyclonic turn due to ridging from the north and are northeasterly to easterly at 5 to 10 knots. Surface winds in the east region of the southern JES are northerly to north northeasterly at 5 to 10 knots while in the west region they make an anticyclonic turn due to ridging from the north and are northeasterly to east northeasterly at 10 to 15 knots. Surface winds in the Korean Strait are easterly at 10 knots.

At 12Z July 23 surface pressure over the northern JES remains high due to the surface high north of the northern JES. Troughing associated with the surface low now

centered over the northeast region of the central ECS affects east region of the central JES and the southeast region of the northern JES. Surface winds in the northeast region of the northern JES are east southeasterly to east northeasterly at 5 to 15 knots. Surface winds in the southeast region of the northern JES make a slight cyclonic turn due to troughing from the south and are east northeasterly to northeasterly at 10 to 15 knots while in the southwest region they make a slight anticyclonic turn due to ridging from the north and are northeasterly to easterly at 3 to 10 knots. Surface winds in the east region of the central JES make a sharp cyclonic turn due to troughing from the south and are southerly to north northeasterly at 3 to 5 knots while in the west region they make a slight anticyclonic turn due to ridging from the north and are north northeasterly to easterly at 3 to 10 knots. Surface winds in the southern JES are northeasterly at 10 to 15 knots in the east region and easterly to northeasterly at 15 knots in the west region. Surface winds in the Korean Strait are easterly at 15 to 20 knots.

On July 24 a 500-mb cyclone remains northwest of the YS. The more recently developed 500-mb cyclone moves northeastward but remains over the majority of the northern JES. 500-mb ridging associated with a 500-mb anticyclone east of the southern JES lies over most of the southern JES. A 700-mb cyclone remains northwest of the YS. The more recently developed 700-mb cyclone moves northeastward but remains over most of the northeast region of the northern JES. A new 700-mb cyclone develops over the YS in the region of troughing over the YS associated with a 700-mb cyclone northwest of the YS. 700-mb ridging associated with a 700-mb anticyclone east of the JES covers most of the central and southern JES.

At 00Z July 24 surface pressure over the northern JES remains high and surface pressure increases over the majority of the central JES due to the surface high now located north of the northern JES. Slight surface troughing associated with a surface low centered over the north region of the central ECS affects the east region of the southern and central JES and the southeast region of the northern JES.

Surface winds in the northeast region of the northern JES are east northeasterly to northeasterly at 5 to 10 knots. Surface winds in the east region of the northern, central, and southern JES make a cyclonic turn due to troughing from the south and are east

northeasterly to northeasterly at 5 to 10 knots in the southeast region of the northern JES, south southeasterly to northeasterly at 5 to 10 knots in the east region of the central JES, and easterly to northeasterly at 5 to 15 knots in the east region of the southern JES. Surface winds are northeasterly at 5 knots in the southwest region of the northern JES. Surface winds in the west region of the central JES make a slight anticyclonic turn and are northeasterly to easterly at 5 to 10 knots. Surface winds in the west region of the southern JES are northeasterly at 15 knots. Surface winds in the Korean Strait are easterly at 15 knots.

At 12Z July 24 surface pressure over the northern and central JES remains high due to the surface high now located northwest of the northeast region of the northern JES. Slight surface troughing associated with the surface low now centered over the west part of the east region of the northern ECS affects the east region of the central and northern JES.

Surface winds in the northern JES are easterly at 10 knots in the far north region and northeasterly at 5 to 10 knots in the remainder of the northeast region. Surface winds in the southeast region of the northern JES make a slight cyclonic turn due to troughing from the south and are east southeasterly to east northeasterly at 5 knots while in the southwest region they make a slight anticyclonic turn due to ridging from the north and are east northeasterly to east southeasterly at 5 knots. Surface winds in the east region of the central JES make a cyclonic turn due to troughing from the south and are southeasterly to east northeasterly at 5 to 10 knots while in the west region they make a slight anticyclonic turn due to ridging from the north and are east northeasterly to easterly at 5 to 15 knots. Surface winds in the southern JES are easterly at 10 knots in the east region and east northeasterly at 15 knots in the west region. Surface winds in the Korean Strait are easterly at 15 knots.

On July 25 a 500-mb cyclone remains northwest of the YS and its associated troughing now extends over the west region of the southern JES. The 500-mb cyclone previously located over the majority of the northern JES moves northeastward and away from the JES. 500-mb ridging associated with a 500-mb anticyclone east of the southern JES now extends over most of the JES. A 700-mb cyclone remains northwest of the YS.

The 700-mb cyclone previously located over most of the northeast region of the northern JES moves northeastward and is now located east of the northeast region of the northern JES but its associated troughing remains over most of the northeast region of the northern JES. The troughing associated with the 700-mb cyclone over the YS now extends over most of the southern JES. The 700-mb ridging associated with a 700-mb anticyclone east of the JES continues to extend over most of the central JES.

At 00Z July 25 surface pressure over the northern and central JES remains high due to the surface high still located northwest of the northeast region of the northern JES. Slight surface troughing associated with the surface low now centered over the central part of the northern ECS affects the southeast region of the northern JES and the east region of the central JES.

Surface winds in the northeast region of the northern JES are north northeasterly to northerly at 3 to 5 knots while in the southeast region they make a slight cyclonic turn and are easterly to northeasterly at 3 to 5 knots. Surface winds in the southwest region of the northern JES are northeasterly at 5 to 10 knots. Surface winds in the east region of the central JES make a cyclonic turn and are southeasterly to northeasterly at 5 to 10 knots in the northeast region and southeasterly to easterly at 5 to 10 knots in the southeast region. Surface winds in the west region of the central JES are northeasterly to east northeasterly at 10 to 15 knots in the northwest region and east northeasterly at 15 knots in the southwest region. Surface winds in the southern JES are easterly at 5 to 15 knots in the east region and easterly at 15 to 20 knots in the west region. Surface winds in the Korean Strait are east southeasterly to easterly at 15 to 20 knots.

At 12Z July 25 surface pressure over the northern and central JES remains high due to the surface high still located northwest of the northeast region of the northern JES. The surface low now located over the northern boundary of the east region of the northern ECS deepens. The pressure gradient over most of the central and southern JES intensifies due to the deepening surface low to the southwest and the higher pressure to the north.

Surface winds in the northeast region of the northern JES are east northeasterly to northerly at 3 to 5 knots while in the southeast region they make a slight cyclonic turn

due to troughing from the south and are east northeasterly to northeasterly at 3 to 5 knots. Surface winds in the southwest region of the northern JES are northeasterly at 5 to 10 knots. Surface winds in the east region of the central JES make a cyclonic turn and are southeasterly to northeasterly at 5 to 10 knots in the northeast region and east southeasterly to east northeasterly at 5 to 10 knots in the southeast region. Surface winds in the west region of the central JES are northeasterly to east northeasterly at 10 to 15 knots in the northwest region and east northeasterly at 10 to 15 knots in the southwest region. Surface winds in the southern JES are easterly at 5 to 15 knots in the east region and easterly at 15 to 20 knots in the west region. Surface winds in the Korean Strait are east southeasterly to easterly at 20 knots.

On July 26 a 500-mb cyclone remains northwest of the YS and its associated troughing continues to extend over the west region of the southern JES. 500-mb ridging associated with a 500-mb anticyclone east of the southern JES continues to extend over most of the JES. A 700-mb cyclone remains northwest of the YS. The 700-mb cyclone previously located east of the northeast region of the northern JES moves away from the JES. The 700-mb cyclone previously centered over the YS moves eastward, is now centered over the Korean peninsula, and its associated troughing continues to extend over most of the southern JES. The 700-mb anticyclone previously east of the JES remains east of the JES and its associated ridging now extends over most of the central and northern JES.

At 00Z July 26 surface pressure over the northern and central JES remains high due to the surface high still located northwest of the northeast region of the northern JES. The surface low is now located over the east part of the east region of the northern ECS. The pressure gradient over most of the central and southern JES remains strong due to the surface low to the southwest and the higher pressure to the north.

Surface winds in the northeast region of the northern JES make an anticyclonic turn and are north northwesterly to northeasterly at 3 to 5 knots. Surface winds in the south region of the northern JES are east northeasterly to easterly at 5 to 10 knots in the southeast region and east northeasterly at 5 to 10 knots in the southwest region. Surface winds in the east region of the central JES make a slight cyclonic turn and are easterly to

east northeasterly at 10 knots while in the west region they are east northeasterly at 10 to 20 knots. Surface winds in the southern JES are easterly at 10 to 15 knots in the east region and easterly at 15 to 20 knots in the west region. Surface winds in the Korean Strait are easterly to east southeasterly at 15 knots.

At 12Z July 26 surface pressure over the northern JES remains high due to the surface high now located north of the northern JES while surface pressure over the southern and central JES falls as the surface low previously centered over east part of the east region of the northern ECS moves eastward but remains centered over the east part of the east region of the northern ECS. The pressure gradient over most of the south region of the central JES remains strong due to the surface low to the southwest and the higher pressure to the north.

Surface winds in the northern JES are easterly at 5 to 10 knots. Surface winds in the central JES are easterly to east northeasterly at 10 to 15 knots. Surface winds in the southern JES are easterly at 10 to 15 knots in the east region and east southeasterly to east northeasterly at 10 to 15 knots in the west region. Surface winds in the Korean Strait make a cyclonic turn and are easterly to northwesterly at 5 to 10 knots.

On July 27 a 500-mb cyclone remains northwest of the YS. A 500-mb cyclone develops over the southern JES in the region of troughing previously located over the west region of the southern JES. The 500-mb anticyclone previously east of the southern JES no longer affects the JES, however a strong 500-mb anticyclone located southeast of the JES and its associated ridging extends slightly over the central JES. A 500-mb ridge develops between the two 500-mb cyclones and is located west of the JES. 500-mb flow becomes zonal across the northern JES. A 700-mb cyclone remains northwest of the YS. The 700-mb cyclone previously centered over the Korean peninsula moves eastward, is now centered over the southern JES, and its associated troughing now extends over most of the western JES. The 700-mb anticyclone previously east of the JES no longer affects the JES, however a strong 700-mb anticyclone is located southeast of the JES and its associated ridging extends over most of the western JES. A 700-mb cyclone is located northeast of the JES and its associated troughing extends over most of the northern JES.

At 00Z July 27 surface pressure over the northern JES remains high due to the surface high still located north of the northern JES while surface pressure over the southern and central JES falls as the surface low is now centered over the south part of the west region of the southern JES.

Surface winds in the northern JES are calm in the far north region and east northeasterly at 5 knots in the remainder of the northeast region. Surface winds in the south region of the northern JES are east northeasterly at 10 knots in the southeast region and northeasterly at 10 to 15 knots in the southwest region. Surface winds in the central JES make a cyclonic turn around the surface low over the south part of the west region of the southern JES and are easterly to east northeasterly at 10 to 15 knots in the northeast region, east southeasterly to easterly at 10 knots in the southeast region, easterly to northeasterly at 10 to 15 knots in the northwest region, and easterly to north northeasterly at 10 to 15 knots in the southwest region. Surface winds in the southern JES make a cyclonic turn around the same surface low and are southeasterly to easterly at 10 knots in the east region and easterly to north northeasterly at 5 to 10 knots in the west region. Surface winds in the Korean Strait make a cyclonic turn around the same surface low and are east southeasterly to north northwesterly at 5 knots.

At 12Z July 27 surface pressure over the northern JES remains high due to the surface high now located northeast of the northern JES. The surface low remains stationary over the south part of the west region of the southern JES. Surface winds in the northeast region of the northern JES make an anticyclonic turn and are easterly to south southeasterly at 5 knots. Surface winds in the south region of the northern JES are east northeasterly at 10 to 15 knots. Surface winds in the central JES make a cyclonic turn around the central low pressure to the south of the west region of the southern JES and are easterly at 10 to 15 knots in the northeast region, east southeasterly to easterly at 10 knots in the southeast region, east northeasterly to northeasterly at 10 knots in the northwest region, and easterly to north northeasterly at 10 knots in the southwest region. Surface winds in the southern JES make a cyclonic turn around the same surface low and are southeasterly to easterly at 5 to 10 knots in the east region and easterly to north northeasterly at 5 to 10 knots in the west region. Surface winds in the Korean Strait make

a cyclonic turn around the same central low pressure and are east northeasterly to northerly at 5 knots.

On July 28 a 500-mb cyclone remains northwest of the YS. A 500-mb cyclone remains over the southern JES. The 500-mb anticyclone previously located southeast of the JES remains stationary and its associated ridging continues to extend slightly over the central JES. The 500-mb ridge previously west of the JES now lies over most of the northern JES. A 700-mb cyclone remains northwest of the YS. The 700-mb cyclone previously centered over the southern JES remains stationary and fills. The 700-mb anticyclone previously southeast of the JES remains stationary and its associated ridging now extends slightly over central JES. A 700-mb cyclone is located northeast of the JES and its associated troughing extends over most of the east region of the northern JES. A 700-mb ridge is located northwest of the northern JES.

At 00Z July 28 surface pressure over the northern JES remains high due to the surface high now located north of the northern JES. The surface low remains stationary over the south part of the west region of the southern JES. Surface winds in the north region of the northern JES are calm to variable at 3 knots in the far north region and east northeasterly at 5 knots in the remainder of the northeast region. Surface winds in the south region of the northern JES are northeasterly at 10 knots. Surface winds in the north region of the central JES are easterly to northeasterly at 5 to 10 knots in the northeast region and northeasterly at 10 knots in the northwest region. Surface winds in the south region of the central JES, in the southern JES, and in the Korean Strait make a cyclonic turn around the surface low centered over the south part of the west region of the southern JES and are southeasterly to easterly at 5 knots in the southeast region of the southern JES, east northeasterly to north northeasterly at 5 to 10 knots in the southwest region of the central JES, south southeasterly to easterly at 5 knots in the east region of the southern JES, easterly to north northeasterly at 5 knots in the west region of the southern JES, and easterly to northwesterly at 3 to 5 knots in the Korean Strait.

At 12Z July 28 surface pressure over the northern JES remains high due to the surface high now located northeast of the northern JES. The surface low has moved eastward and is now located south of the east region of the southern JES over Japan. The

pressure gradient over the northern JES increases. Surface winds in the northeast region of the northern JES make an anticyclonic turn and are easterly to south southeasterly at 5 knots. Surface winds in the south region of the southern JES make an anticyclonic turn and are northeasterly at 10 to 15 knots in the southeast region and east northeasterly to easterly at 10 to 15 knots in the southwest region. Surface winds in the central JES are northeasterly at 10 to 15 knots in the northeast region, east northeasterly at 10 knots in the southeast region, east northeasterly to easterly at 10 to 15 knots in the northwest region, and east northeasterly to northeasterly at 5 to 10 knots in the southwest region. Surface winds in the southern JES make a cyclonic turn around the surface low over Japan and south of the east region of the southern JES and are easterly to east northeasterly at 5 to 10 knots in the east region and east northeasterly to northeasterly at 5 to 10 knots in the west region. Surface winds in the Korean Strait make a cyclonic turn around the same surface low and are northeasterly to northwesterly at 5 knots.

On July 29 a 500-mb cyclone remains northwest of the YS. A 500-mb cyclone previously located over the southern JES fills although a 500-mb trough is located over most of the southern JES. The 500-mb anticyclone previously located southeast of the JES remains stationary but its associated ridging no longer affects the JES. The 500-mb ridge previously located over most of the northern JES remains stationary. A small 500-mb ridge forms over the Korean peninsula. A 700-mb cyclone remains northwest of the YS. The 700-mb cyclone previously centered over the southern JES fills. The 700-mb anticyclone previously southeast of the JES remains stationary but its associated ridging no longer affects the JES. A 700-mb cyclone is located northeast of the JES but its associated troughing no longer affects the JES. A 700-mb ridge remains northwest of the northern JES. The 700-mb flow is very weak over the JES.

At 00Z July 29 surface pressure over the northern JES remains high due to the surface high still northeast of the northern JES. The surface low has moved further eastward and is now located east of the east region of the southern JES over Honshu, Japan. The pressure gradient over the JES weakens.

Surface winds in the north region of the northern JES are calm in the far north region and easterly at 3 to 5 knots in the remainder of the northeast region. Surface

winds in the south region of the northern JES are easterly to east northeasterly at 10 knots in the southeast region and east northeasterly to easterly at 5 to 10 knots in the southwest region. Surface winds in the central JES are east northeasterly at 10 knots in the northeast region, east northeasterly to northeasterly at 5 to 10 knots in the southeast region, east northeasterly to easterly at 5 to 10 knots in the northwest region, and northeasterly to easterly at 5 to 10 knots in the southwest region. Surface winds in the southern JES are northeasterly at 3 to 5 knots in the east region and northeasterly at 5 knots in the west region. Surface winds in the Korean Strait make a cyclonic turn and are north northeasterly to northwesterly at 3 to 5 knots.

At 12Z July 29 surface pressure over the northern JES remains high due to the surface high pressure still located northeast of the northern JES. The surface low remains stationary east of the east region of the southern JES over Honshu, Japan.

Surface winds in the northern JES are east southeasterly to easterly at 3 to 10 knots. Surface winds in the east region of the central JES make a cyclonic turn around the surface low over Japan and are easterly to east northeasterly at 10 knots in the northeast region and easterly to northeasterly at 5 to 10 knots in the southeast region. Surface winds in the west region of the central JES experience divergence due to ridging from the north and troughing from the southeast and are east northeasterly to southeasterly at 5 to 10 knots in the northwest region and northeasterly to easterly at 5 to 10 knots in the southwest region. Surface winds in the southern JES and in the Korean Strait make a cyclonic turn around the surface low over Japan and are northeasterly to northwesterly at 5 knots in the east region of the southern JES, north northeasterly to northwesterly at 5 knots in the west region of the southern JES, and northwesterly to westerly at 5 knots in the Korean Strait.

From July 30 through July 31 a 500-mb cyclone remains northwest of the YS. The 500-mb anticyclone previously located southeast of the JES remains stationary but its associated ridging now extends northwestward over the majority of the JES. The 500-mb ridge previously located over most of the northern JES remains stationary. The small 500-mb ridge previously over the Korean peninsula moves eastward across the JES and is amplified by the ridging extending from the anticyclone southeast of the JES. A 700-mb

cyclone remains northwest of the YS. The 700-mb anticyclone previously southeast of the JES remains stationary but its associated ridging now extends northwestward over the majority of the JES.

At 00Z July 30 surface pressure over the northern JES remains high due to the surface high still northeast of the northern JES. The surface low remains stationary east of the east region of the southern JES over Honshu, Japan. Surface winds in the north region of the northern JES are calm in the far north region and easterly at 3 to 5 knots in the remainder of the northeast region. Surface winds in the southeast region of the northern JES are easterly at 10 knots while in the southwest region they make a slight anticyclonic turn and are easterly to east southeasterly at 5 to 10 knots. Surface winds in the east region of the central JES, in the southern JES and in the Korean Strait make a cyclonic turn around the surface low over Honshu Japan and are east northeasterly to northeasterly at 10 knots in the northeast region of the central JES, east northeasterly to north northeasterly at 10 knots in the southeast region of the central JES, north northeasterly to northwesterly at 5 knots in the east region of the southern JES, north northeasterly to northerly at 3 to 5 knots in the west region of the southern JES, and northerly to north northwesterly at 3 to 5 knots in the Korean Strait. Surface winds in the west region of the central JES experience divergence due to ridging from the north and troughing from the southeast and are northeasterly to southeasterly at 5 to 10 knots in the northwest region and north northeasterly to southeasterly at 5 to 10 knots in the southwest region.

At 12Z July 30 surface pressure over the northern JES remains high due to the surface high now east of the northeast region of the northern JES. The surface low remains stationary over Honshu, Japan to the east of the east region of the southern JES. The pressure gradient over the JES is fairly weak.

Surface winds in the northern JES make an anticyclonic turn and are southeasterly to south southwesterly at 3 to 10 knots in the northeast region, easterly to east northeasterly at 5 to 10 knots in the southeast region, and east southeasterly to southeasterly at 5 to 10 knots in the southwest region. Surface winds in the east region of the central JES and in the east region of the southern JES make a cyclonic turn around the

surface low over Honshu, Japan and are easterly to northeasterly at 5 to 10 knots in the east region of the central JES and north northeasterly to northerly at 5 knots in the east region of the southern JES. Surface winds in the west region of the central JES, in the west region of the southern JES, and in the Korean Strait make an anticyclonic turn due to ridging from the northeast and are easterly to southerly at 5 to 10 knots in the northwest region of the central JES, northeasterly to southerly at 5 to 10 knots in the southwest region of the central JES, northeasterly to easterly at 5 knots in the west region of the southern JES, and northerly to easterly at 5 knots in the Korean Strait.

At 00Z July 31 surface pressure is high over the JES due to the surface high still east of the northeast region of the northern JES. The surface low remains stationary over Honshu, Japan to the east of the east region of the southern JES and fills significantly. The pressure gradient over the JES weakens. Surface winds in the northern JES, in the north region of the central JES, in the southwest region of the northern JES, in the west region of the southern JES, and in the Korean Strait make an anticyclonic turn and are light and variable in the far north region of the northern JES, south southeasterly at 5 knots in the remainder of the northeast region of the northern JES, southeasterly at 5 knots in the southeast region of the northern JES, southerly at 5 knots in the southwest region of the northern JES, easterly to southeasterly at 3 to 5 knots in the northeast region of the central JES, southerly at 5 knots in the northwest region of the central JES, northeasterly to south southeasterly at 3 to 5 knots in the southwest region of the central JES, easterly to southeasterly at 5 to 10 knots in the west region of the southern JES, and southeasterly at 10 knots in the Korean Strait. Surface winds in the southeast region of the central JES make a cyclonic turn around the surface low over Honshu, Japan and are easterly to north northeasterly at 3 to 5 knots. Surface winds in the east region of the southern JES are north northeasterly to northeasterly at 5 knots.

At 12Z July 31 the surface high previously east of the northeast region of the northern JES moves eastward. The surface low over Honshu, Japan is no longer present. Surface pressure falls slightly over the JES. The pressure gradient over the JES remains weak. Surface winds in the northern JES are easterly at 3 to 5 knots in the far north region, southeasterly at 5 knots in the remainder of the northeast region, south southeasterly to southerly at 5 knots in the southeast region, and southerly at 5 to 10

knots in the southwest region. Surface winds in the central JES, in the southern JES, and in the Korean Strait make an anticyclonic turn and are easterly to south southeasterly at 5 to 10 knots in the central JES, easterly to south southeasterly at 3 to 10 knots in the southern JES, and southerly at 10 knots in the Korean Strait.

2. YES

Readers should refer to Appendix Y for the surface level pressure/SAT/surface wind plots over the YES for the July period. The figures in Appendix Y are in time sequential order ever 12 hours from 00Z July 18 through 12Z July 31.

At 00Z July 18 a strong 500-mb ridge is present in the JES. A 500-mb cyclone is located northwest of the YS and its associated troughing lies west of the YES. A strong 500-mb anticyclone is located southeast of the JES and its associated ridging extends westward into the southern ECS. A strong 700-mb anticyclone is present in the JES. A 700-mb cyclone is located northwest of the YS and its associated troughing lies over the YES. A strong 700-mb anticyclone is located southeast of the JES and its associated ridging extends westward into the southern ECS.

A surface low is centered over the southern boundary of the east region of the northern ECS. A surface anticyclone is located east of the northern SCS. A surface high is located east of the northern JES. Surface winds in the BS are variable at 5 knots. Surface winds in the northern YS are southeasterly at 5 to 10 knots. Surface winds in the central YS are variable at 3 to 5 knots in the west region and southeasterly at 5 to 10 knots in the east region. Surface winds in the west region of the southern YS and in the west region of the northern ECS make an anticyclonic turn and are northwesterly to easterly at 5 to 10 knots. Surface winds in the east region of the southern YS are variable at 5 knots. Surface winds in the east region of the northern ECS and in the east region of the central ECS make a cyclonic turn around the surface low centered over the southern boundary of the east region of the northern ECS and are north northeasterly to easterly at 5 to 15 knots. Surface winds in the west region of the central ECS make a cyclonic turn and are westerly to east northeasterly at 5 to 15 knots. Surface winds in the southern ECS make a slight anticyclonic turn and are southwesterly to westerly at 10 to 20 knots.

From 12Z July 18 through 00Z July 23 the 500-mb cyclone northwest of the YS moves southeastward towards the BS. A 500-mb anticyclone forms in the area of 500-mb ridging associated with the 500-mb anticyclone to the southeast of the JES and is located south of the ECS at 00Z July 22. The 500-mb geopotential height gradient remains strong and 500-mb flow remains zonal over the YES throughout this time period due to the 500-mb cyclone to the northwest and the 500-mb anticyclone to the south. The 700-mb cyclone northwest of the YS moves southeastward towards the BS. A 700-mb anticyclone forms in the area of 700-mb ridging associated with the 700-mb anticyclone to the southeast of the JES and is located south of the ECS at 00Z July 22. The 700-mb geopotential height gradient remains strong and 700-mb flow is predominantly cyclonic in the YS and slightly anticyclonic in the ECS throughout this time period due to the 700-mb cyclone to the northwest and the 700-mb anticyclone to the south.

At 12Z July 18 the surface low moves northward while deepening and is now centered over the east region of the northern ECS. A surface anticyclone remains east of the northern SCS. Surface winds in the BS are east southeasterly at 5 knots. Surface winds in the northern YS are easterly at 5 knots. Surface winds in the east region of the central YS, in the east region of the southern YS, and in the eastern ECS make a cyclonic turn around the surface low over the east region of the northern ECS and are east southeasterly to southerly at 5 to 20 knots. Surface winds in the west region of the central YS, in the west region of the southern YS, and in the west region of the northern ECS make an anticyclonic turn and are west northwesterly to east northeasterly at 5 to 15 knots. Surface winds in the west region of the central ECS are westerly at 15 to 20 knots. Surface winds in the west region of the southern ECS make a slight anticyclonic turn and are southwesterly to westerly at 15 to 20 knots.

At 00Z July 19 the surface low that was centered over the east region of the northern ECS has moved northward and is now centered over the Korean peninsula and continues to deepen. A surface anticyclone remains east of the northern SCS. Surface winds in the BS are variable at 3 knots in the north and west northwesterly to westerly at 5 to 10 knots in the south. Surface winds in the YS and in the northern ECS make a cyclonic turn around the surface low over the Korean peninsula and are northeasterly to westerly at 5 to 15 knots. Surface winds in the central ECS make a slight cyclonic turn

around the same surface low pressure and are west northwesterly to westerly at 10 to 20 knots. Surface winds in the east region of the southern ECS are westerly at 20 knots while in the west region they make a slight anticyclonic turn and are southwesterly to westerly at 15 to 20 knots.

At 12Z July 19 the surface anticyclone previously east of the SCS moves westward, but remains east of the northern SCS and its associated ridging affects the majority of the YES. The surface low previously centered over the Korean peninsula is now located over the southern JES. Surface winds in the BS are west southwesterly at 5 knots in the north and westerly to west northwesterly at 3 to 5 knots in the south. Surface winds in the northern YS are northerly to north northwesterly at 5 knots in the east region and south southwesterly to southerly in the west region. Surface winds in the central YS, in the southern YS, in the northern ECS, and in the west region of the central ECS make a slight anticyclonic turn due to ridging from the south and are west southwesterly to west northwesterly at 5 to 15 knots. Surface winds in the east region of the central ECS make a slight cyclonic turn and are west northwesterly to westerly at 15 knots. Surface winds in the west region of the southern ECS make a slight anticyclonic turn and are southwesterly to westerly at 10 to 20 knots while in the east region they are westerly at 15 to 20 knots.

At 00Z July 20 troughing associated with a surface low northwest of the JES affects the majority of the BS and YS. Ridging associated with the surface high east of the northern SCS affects the majority of the ECS. The surface low previously located over the southern JES moves southeastward and is now south of the east region of the southern JES. Surface winds in the BS and the YS make a cyclonic turn due to troughing from the northwest and are easterly to southerly at 5 to 15 knots. Surface winds in the northern ECS and in the west region of the central ECS make an anticyclonic turn due to ridging from the southwest and are westerly to northwesterly at 5 to 15 knots. Surface winds in the east region of the central ECS make a slight cyclonic turn due to troughing from the northeast and are northwesterly to westerly at 5 to 20 knots. Surface winds in the west region of the southern ECS make a slight anticyclonic turn and are southwesterly to west northwesterly at 10 to 20 knots while in the east region they are westerly at 15 to 20 knots.

At 12Z July 20 troughing associated with the surface low still northwest of the JES affects the majority of the BS and YS. Ridging associated with the surface high still located east of the northern SCS affects the majority of the ECS. Surface winds in the BS and YS make a cyclonic turn due to troughing from the northwest and are southwesterly to northeasterly at 5 to 10 knots. Surface winds in the ECS make an anticyclonic turn due to ridging from the south and are south southwesterly to northwesterly at 10 to 20 knots.

At 00Z July 21 a surface low develops over the southeast region of the central ECS. Ridging associated with surface high still east of the northern SCS affects the west region of the southern ECS. A surface low remains northwest of the JES and affects the BS, YS, and the west region of the northern ECS. Surface winds in the BS, in the YS, and in the west region of the northern ECS make a cyclonic turn and are northwesterly to easterly at 5 to 10 knots. Surface winds in the east region of the northern ECS are variable at 3 to 5 knots. Surface winds in the west region of the central ECS are southwesterly to northwesterly at 3 to 10 knots while in the east region they make a cyclonic turn around the surface low over the southeast region of the central ECS and are easterly to northwesterly at 5 to 15 knots. Surface winds in the west region of the southern ECS make a slight anticyclonic turn and are southwesterly to westerly at 10 to 20 knots while in the east region they make a slight cyclonic turn and are northwesterly to west northwesterly at 10 to 20 knots.

At 12Z July 21 the surface low previously northwest of the JES moves westward but remains northwest of the JES and affects the BS, the YS, and the west region of the northern ECS. The surface low previously centered over the southeast region of the central ECS has moved slightly northward and is now centered over the east region of the central ECS. Ridging associated with the surface high still east of the northern SCS continues to affect the west region of the southern ECS. Surface winds in the BS, in the YS and in the west region of the northern ECS make a cyclonic turn and are westerly to east northeasterly at 3 to 15 knots. Surface winds in the east region of the northern ECS are variable at 3 to 5 knots. Surface winds in the west region of the central ECS are west southwesterly at 5 to 10 knots in the northwest region and westerly at 10 to 15 knots in the southwest region. Surface winds in the east region of the central ECS make a cyclonic turn around the surface low over the east region of the central ECS and are

southeasterly to west southwesterly at 5 to 10 knots. Surface winds in the west region of the southern ECS make a slight anticyclonic turn and are southwesterly to west northwesterly at 15 knots while in the east region they make a slight cyclonic turn and are west northwesterly to westerly at 5 to 15 knots.

At 00Z July 22 a surface low remains centered over the east region of the central ECS. Ridging associated with surface high still east of the northern SCS continues to affect the west region of the southern ECS. Surface winds in the BS make an anticyclonic turn and are north northeasterly to northeasterly at 5 to 10 knots. Surface winds in the northern and central YS make a sharp cyclonic turn and are northerly to east southeasterly at 5 to 10 knots. Surface winds in the west region of the southern YS are variable at 5 knots while in the east region they make an anticyclonic turn and are easterly to southeasterly at 5 knots. Surface winds in the west region of the northern ECS are variable at 3 to 5 knots. Surface winds in the east region of the northern ECS, in the central ECS, and in the east region of the southern ECS make a cyclonic turn around the surface low centered over the east region of the central ECS and are north northeasterly to easterly at 3 to 20 knots. Surface winds in the west region of the southern ECS make a slight anticyclonic turn and are southwesterly to west northwesterly at 10 to 20 knots.

At 12Z July 22 the surface low has moved slightly northward and is now located over the northeast region of the central ECS. Ridging associated with the surface high still east of the northern SCS continues to affect the west region of the southern ECS. Surface winds in the BS are east southeasterly to northeasterly at 5 knots. Surface winds in the northern YS are southeasterly to easterly at 5 knots. Surface winds in the central YS, in the southern YS, and in the west region of the northern ECS are variable at 3 to 5 knots. Surface winds in the east region of the northern ECS, in the central ECS, and in the east region of the southern ECS make a cyclonic turn around the surface low and are east southeasterly to southerly at 5 to 15 knots. Surface winds in the west region of the southern ECS make a slight anticyclonic turn and are southwesterly to west northwesterly at 10 to 15 knots.

At 00Z July 23 the surface low has moved slightly northward and is now centered over the southern boundary of the east region of the northern ECS. Ridging associated

with the surface high still east of the northern SCS continues to affect the west region of the southern ECS. Surface winds in the BS, in the YS, and in the west region of the northern ECS are northeasterly to easterly at 5 to 10 knots. Surface winds in the east region of the northern ECS, in the central ECS, and in the east region of the southern ECS make a cyclonic turn around the surface low and are southeasterly to southwesterly at 3 to 15 knots. Surface winds in the west region of the southern ECS make an anticyclonic turn and are south southwesterly to northwesterly at 5 to 15 knots.

At 12Z July 23 the 500-mb cyclone northwest of the BS is no longer present but troughing associated with an intense 500-mb cyclone northwest of the YS remains over the area. A 500-mb cyclone forms in the southeast region of the northern JES in an area of troughing also associated with the 500-mb cyclone northwest of the YS. A 500-mb anticyclone remains south of the ECS. At 12Z July 23 the 700-mb cyclone northwest of the BS is no longer present but troughing associated with an intense 700-mb cyclone northwest of the YS remains over the area. A 700-mb cyclone forms in the southeast region of the northern JES in an area of troughing also associated with the 700-mb cyclone northwest of the YS. A 700-mb anticyclone remains south of the ECS.

At 12Z July 23 the surface low moves slightly southward and is now centered over the northeast region of the central ECS. Ridging associated with the surface high still east of the northern SCS continues to affect the west region of the southern ECS. Surface winds in the BS are easterly at 3 to 10 knots. Surface winds in the northern YS are east southeasterly to east northeasterly at 5 knots. Surface winds in the central YS, in the southern YS, and in the west region of the northern ECS are east northeasterly to easterly at 5 to 10 knots. Surface winds in the east region of the northern ECS, in the central ECS, and in the east region of the southern ECS make a cyclonic turn around the surface low pressure and are south southeasterly to southerly at 3 to 15 knots. Surface winds in the west region of the southern ECS make an anticyclonic turn and are south southwesterly to west northwesterly at 5 to 10 knots.

From 00Z July 24 through 00Z July 26 a 500-mb trough associated with the 500-mb cyclone northwest of the YS moves across the majority of the YES. By 00Z July 26 a 500-mb ridge associated with the 500-mb anticyclone south of the ECS is located west of

the YES. A 700-mb trough associated with the 700-mb cyclone northwest of the YS moves across the YES. By 12Z July 24 a 700-mb cyclone has formed in the area of troughing over the YES. By 00Z July 26 a 700-mb ridge is west of the YES.

At 00Z July 24 the surface low has deepened and moved westward so that it is centered over the north region of the central ECS. Surface winds in the BS make a slight anticyclonic turn and are northeasterly to east southeasterly at 5 to 10 knots. Surface winds in the YS, in the northern ECS, and in the central ECS make a cyclonic turn around the surface low and are south southeasterly to southerly at 3 to 20 knots. Surface winds in the west region of the southern ECS make a slight anticyclonic turn and are westerly to west northwesterly at 5 to 10 knots while in the east region they make a slight cyclonic turn and are northwesterly to southwesterly at 5 to 10 knots.

At 12Z July 24 the surface low moves slightly northward and deepens and is now centered over the west part of the east region of the northern ECS. Surface winds in the BS, in the YS, in the northern ECS, in the central ECS, and in the east region of the southern ECS make a cyclonic turn around the surface low and are east northeasterly to easterly at 5 to 30 knots. Surface winds in the west region of the southern ECS make a slight anticyclonic turn and are southwesterly to west northwesterly at 5 to 15 knots.

At 00Z July 25 the surface low continues to deepen and is now centered over the central part of the northern ECS. Surface winds in the BS, in the YS, in the northern ECS, in the central ECS, and in the east region of the southern ECS make a cyclonic turn around the surface low and are east northeasterly to easterly at 5 to 30 knots. Surface winds in the west region of the southern ECS make an anticyclonic turn and are southwesterly to northwesterly at 5 to 10 knots.

At 12Z July 25 the surface low continues to deepen, moves eastward, and is now centered over the northern boundary of the east region of the northern ECS. Surface winds in the BS, in the YS, in the northern ECS, in the central ECS, and in the east region of the southern ECS make a cyclonic turn around the surface low and are east northeasterly to easterly at 5 to 30 knots. Surface winds in the west region of the southern ECS make an anticyclonic turn and are southwesterly to northwesterly at 5 to 15 knots.

At 00Z July 26 the surface low continues to deepen, moves further eastward and is centered over the east part of the east region of the northern ECS. Surface winds in the BS, in the YS, and in the ECS make a cyclonic turn around the central low pressure over the east region of the northern ECS and are east northeasterly to west southwesterly at 5 to 25 knots.

From 12Z July 26 through July 28 the 500-mb ridge, associated with the 500-mb anticyclone previously south of the ECS and that is located southeast of the southern JES by 12Z July 28, moves eastward across the YES. By 12Z July 28 500-mb troughing associated with the 500-mb cyclone northwest of the YS begins to extend southeastward into the western YES. The 700-mb ridge previously located west of the YES weakens. The 700-mb cyclone previously centered over the YES moves eastward away from the YES, ridging associated with a 700-mb anticyclone southeast of the JES begins to extend northwestward into the southern ECS, and 700-mb troughing associated with the 700-mb cyclone northwest of the YS extends over the western YES.

At 12Z July 26 the surface low moves further eastward but remains over the east part of the east region of the northern ECS. Surface winds in the BS make an anticyclonic turn and are westerly to north northeasterly at 5 to 10 knots. Surface winds in the YS, in the northern ECS, in the central ECS, and in the east region of the southern ECS make a cyclonic turn around the surface low and are north northeasterly to westerly at 5 to 20 knots. Surface winds in the east part of the west region of the southern ECS are northwesterly at 10 knots while in the west part they make an anticyclonic turn due to ridging from the west and are north northwesterly to easterly at 3 to 5 knots.

At 00Z July 27 the surface low moves northeastward and is now centered over the south part of the west region of the southern JES. A surface high is located west of the YES. Surface winds in the BS make an anticyclonic turn and are northwesterly to north northwesterly at 5 to 10 knots. Surface winds in the YS, in the northern ECS, in the central ECS, and in the east region of the southern ECS make a cyclonic turn around the surface low and are northeasterly to westerly at 10 to 20 knots. Surface winds in the east part of the west region of the southern ECS are north northwesterly to northwesterly at 5

to 10 knots while in the west part they make an anticyclonic turn due to ridging from the west and are north northwesterly to east northeasterly at 5 to 10 knots.

At 12Z July 27 the surface low remains centered over the south part of the west region of the southern JES. The strong anticyclone west of the YES begins to move eastward. Surface winds in the BS are west northwesterly to west southwesterly at 5 to 10 knots in the north part and southwesterly to northwesterly at 3 to 10 knots in the south part. Surface winds in the YS make a slight anticyclonic turn due to ridging from the west and are northwesterly to north northeasterly at 10 to 15 knots. Surface winds in the northern ECS, in the central ECS, and in the east region of the southern ECS make a cyclonic turn and are northwesterly to west southwesterly at 10 to 15 knots. Surface winds in the east part of the west region of the southern ECS are north northeasterly to northwesterly at 5 to 10 knots while in the west part they make an anticyclonic turn due to ridging from the west and are north northwesterly to easterly at 5 to 10 knots.

At 00Z July 28 troughing associated with the surface low still over the south part of the west region of the southern JES affects the ECS while ridging associated with the surface high still west of the ECS affects the BS, YS, and west region of the southern ECS. Surface winds in the BS, in the YS, and in the west region of the northern ECS make an anticyclonic turn due to ridging from the west and are south southwesterly to northerly at 5 to 15 knots. Surface winds in the east region of the northern ECS, in the central ECS, and in the east region of the southern ECS make a cyclonic turn due to troughing from the northeast and are northerly to westerly at 5 to 15 knots. Surface winds in the west region of the southern ECS make an anticyclonic turn due to ridging from the west and are northwesterly to east northeasterly at 5 to 10 knots.

At 12Z July 28 troughing associated with the surface low now south of the east region of the southern JES affects the ECS while ridging associated with the surface high west of the YES affects the BS, YS, and west region of the southern ECS. Surface winds in the BS and YS make an anticyclonic turn due to ridging from the west and are south southwesterly to north northwesterly at 5 to 15 knots. Surface winds in the northern ECS, in the central ECS, and in the east region of the southern ECS make a cyclonic turn due to troughing from the northeast and are northwesterly to westerly at 5 to 15 knots.

Surface winds in the west region of the southern ECS make an anticyclonic turn due to ridging from the west and are northwesterly to northeasterly at 5 to 10 knots.

From July 29 through July 31 the 500-mb troughing over the western YS associated with the 500-mb cyclone northwest of the YS ceases. The 500-mb geopotential height gradient over the YES remains strong and 500-mb flow is predominantly zonal due to the 500-mb cyclone northwest of the YS and the 500-mb ridging to the south of the ECS associated with the 500-mb anticyclone southeast of the southern JES. The 700-mb troughing over the western YS associated with the 700-mb cyclone northwest of the YS persists and moves eastward so that by 12Z July 31 it is located over the Korean peninsula while the 700-mb ridging over the southern ECS associated with the 700-mb anticyclone southeast of the southern JES builds.

At 00Z July 29 troughing associated with the surface low now east of the east region of the southern JES affects the ECS while ridging associated with anticyclone to west of the YES affects the BS, YS, and west region of the southern ECS. Surface winds in the BS and YS make an anticyclonic turn due to ridging from the west and are south southwesterly to north northwesterly at 5 to 15 knots. Surface winds in the northern ECS, in the central ECS, and in the east region of the southern ECS make a cyclonic turn due to troughing from the northeast and are northwesterly to west southwesterly at 5 to 15 knots. Surface winds in the west region of the southern ECS make an anticyclonic turn due to ridging from the west and are northwesterly to northeasterly at 5 to 15 knots.

At 12Z July 29 the surface high is located west of the central ECS. Troughing associated with the surface east of the east region of the southern JES affects the majority of the eastern ECS. Surface winds in the BS, in the YS, and in the west region of the northern ECS make an anticyclonic turn due to ridging from the southwest and are southerly to north northwesterly at 5 to 15 knots. Surface winds in the east region of the northern ECS, in the central ECS, and in the east region of the southern ECS make a cyclonic turn due to troughing from the northeast and are northwesterly to west southwesterly at 5 to 15 knots. Surface winds in the west region of the southern ECS make an anticyclonic turn due to ridging from the west and are west northwesterly to easterly at 5 to 10 knots.

At 00Z July 30 the surface anticyclone remains west of the central ECS and builds. Troughing associated with the surface low still east of the east region of the southern JES affects the east region of the central ECS. Surface winds in the BS, in the YS, and in the northern ECS make an anticyclonic turn due to ridging from the southwest and are south southwesterly to north northwesterly at 5 to 15 knots. Surface winds in the east region of the central ECS make a cyclonic turn due to troughing from the northeast and are northwesterly to southwesterly at 5 to 10 knots. Surface winds in the west region of the central ECS and in the southern ECS make an anticyclonic around the surface high west of the central ECS and are west northwesterly to easterly at 5 to 10 knots.

At 12Z July 30 the surface high has moved eastward, is now centered over the west part of the southwest region of the central ECS, and builds. Troughing associated with the surface low still east of the east region of the southern JES affects the east region of the northern and central ECS. Surface winds in the BS, in the YS, and in the western ECS, and in the east region of the southern ECS make an anticyclonic turn around the surface high and are southwesterly to east southeasterly at 5 to 10 knots. Surface winds in the east region of the northern and central ECS make a cyclonic turn due to troughing from the northeast and are northwesterly to southwesterly at 3 to 10 knots.

At 00Z July 31 the surface high remains centered over the west part of the southwest region of the central ECS and continues to build. A surface low develops over the east region of the northern ECS. Surface winds in the west part of the BS make a sharp cyclonic turn and are southwesterly to east northeasterly at 5 to 15 knots while in the east part they are southerly at 10 to 15 knots. Surface winds in the northern YS are south southwesterly to southerly at 5 to 10 knots in the west region and south southeasterly at 5 knots in the east region. Surface winds in the central YS, in the southern YS, in the western ECS, and in the east region of the southern ECS make an anticyclonic turn around the surface high and are southerly to southeasterly at 5 to 10 knots. Surface winds in the east region of the northern and central ECS make a cyclonic turn around the surface low over the east region of the northern ECS and are north northwesterly to southeasterly at 5 to 10 knots.

At 12Z July 31 the surface high is now located over the west region of the central ECS. The surface low previously located over the east region of the northern ECS has moved northward and now located over the Korean peninsula. Surface winds in the south part of the BS make an a cyclonic turn and are southwesterly to south southwesterly at 3 to 20 knots while in the north part they are southwesterly at 10 knots. Surface winds in the northern YS are southerly at 5 to 10 knots in the west region and westerly at 5 knots in the east region. Surface winds in the central YS, in the southern YS, in the west region of the northern ECS, in the west region of the central ECS and in the east region of the southern ECS make an anticyclonic turn around the surface high over the west region of the central ECS and are southerly to east southeasterly at 3 to 10 knots. Surface winds in the east region of the northern and central ECS make a cyclonic turn around the surface low over the Korean peninsula and are northwesterly to south southwesterly at 5 to 15 knots. Surface winds in the west part of the west region of the southern ECS make a cyclonic turn and are south southwesterly to southeasterly at 5 to 10 knots while in the east part they are southerly to east southeasterly at 5 to 10 knots.

3. SCS

Readers should refer to Appendix Z for the surface level pressure/SAT/surface wind plots over the SCS for the July period. The figures in Appendix Z are in time sequential order ever 12 hours from 00Z July 18 through 12Z July 31.

At 00Z July 18 surface winds in the northern SCS and in the east region of the central SCS make an anticyclonic turn due ridging associated with a surface high east of the northern SCS and are southeasterly to southwesterly at 5 to 15 knots. Surface winds over the majority of the west region of the central SCS and in the east part of the southern SCS are calm to light and variable. Surface winds in the Gulf of Thailand are southerly at 3 to 5 knots. Surface winds in the west part of the southern SCS are southwesterly at 5 knots.

At 12Z July 18 surface winds in the northern and central SCS make an anticyclonic turn due ridging associated with a surface high east of the northern SCS and are easterly to southwesterly at 5 to 15 knots. Surface winds in the Gulf of Thailand are southerly to westerly at 3 to 5 knots. Surface winds in the remainder of the SCS are calm to variable at 3 to 5 knots.

At 00Z July 19 surface winds in the northern SCS and in the northeast part of the east region of the central SCS make an anticyclonic turn due ridging associated with a surface high east of the northern SCS and are southeasterly to southwesterly at 5 to 15 knots. Surface winds in the Gulf of Thailand and in the west region of the central SCS make an anticyclonic turn and are west southwesterly to northwesterly at 5 knots. Surface winds in the east part of the southern SCS and in the southwest part of the east region of the central ECS make a cyclonic turn and are northwesterly to southwesterly at 5 knots. Surface winds in the west part of the southern SCS are variable at 5 knots.

At 12Z July 19 surface winds in the northern SCS and in the east region of the central SCS make an anticyclonic turn due ridging associated with a surface high east of the northern SCS and are southeasterly to southwesterly at 3 to 15 knots. Surface winds in the Gulf of Thailand, in the west region of the central SCS, and in the southern SCS make a cyclonic turn due troughing associated with a surface low to the northwest and are southwesterly southerly at 5 knots.

At 00Z July 20 surface winds in the northern SCS make an anticyclonic turn due ridging associated with a surface high east of the northern SCS and are southeasterly to southwesterly at 3 to 15 knots. Surface winds in the remainder of the SCS make a cyclonic turn due to troughing associated with a surface low northwest of the Gulf of Tonkin and are westerly to southerly at 5 knots.

At 12Z July 20 surface winds in the northern SCS make an anticyclonic turn due ridging associated with a surface high east of the northern SCS and are east southeasterly to southwesterly at 3 to 15 knots. Surface winds in the remainder of the SCS make a cyclonic turn due to troughing associated with a surface low northwest of the Gulf of Tonkin and are westerly to southeasterly at 5 to 10 knots.

At 00Z July 21 surface winds in the east region of the northern SCS and in the northeast part of the east region of the central SCS make an anticyclonic turn due ridging associated with a surface high east of the northern SCS and are south southeasterly to southwesterly at 3 to 15 knots. Surface winds in the remainder of the SCS make a cyclonic turn due to troughing associated with a surface low northwest of the Gulf of Tonkin and are southwesterly to southerly at 5 to 15 knots.

At 12Z July 21 surface winds in the east region of the northern SCS and in the northeast part of the east region of the central SCS make an anticyclonic turn due ridging associated with a surface high east of the northern SCS and are southeasterly to southwesterly at 3 to 10 knots. Surface winds in the remainder of the SCS make a cyclonic turn due to troughing associated with a surface low northwest of the Gulf of Tonkin and are southwesterly to southerly at 5 to 15 knots.

At 00Z July 22 surface winds in the east region of the northern SCS and in the northeast part of the east region of the central SCS make an anticyclonic turn due ridging associated with a surface high east of the northern SCS and are southeasterly to westerly at 5 to 15 knots. Surface winds in the remainder of the SCS make a cyclonic turn due to troughing associated with a surface low northwest of the Gulf of Tonkin and are southwesterly to southerly at 10 to 15 knots.

At 12Z July 22 surface winds in the east region of the northern SCS are variable at 3 to 10 knots. Surface winds in the west region of the northern SCS are southwesterly to westerly at 5 to 15 knots. Surface winds in the central SCS are easterly to southerly at 3 to 5 knots in the east region and southerly at 5 to 10 knots in the west region. Surface winds in the southern JES are southwesterly at 5 knots in the northeast part, southwesterly at 5 to 10 knots in the south part, and southeasterly at 3 to 5 knots in the northwest part. Surface winds in the Gulf of Thailand are southwesterly at 10 knots.

At 00Z July 23 surface winds in the east region of the northern SCS and in the east part of the east region of the central SCS make an anticyclonic turn and are southerly to southwesterly at 5 to 10 knots. Surface winds in the remainder of the SCS are southwesterly at 5 to 15 knots.

At 12Z July 23 surface winds in the northern SCS are variable at 5 to 10 knots. Surface winds in the remainder of the SCS are southwesterly to southerly at 3 to 10 knots.

At 00Z July 24 surface winds in the northern SCS make an anticyclonic turn and are southwesterly to westerly 5 to 15 knots. Surface winds in the central SCS and in the Gulf of Thailand are predominantly southwesterly at 5 to 15 knots. Surface winds in the

southern SCS make an anticyclonic turn and are south southeasterly to west southwesterly at 5 knots.

At 12Z July 24 surface winds in the northern SCS are variable at 3 to 10 knots. Surface winds in the central SCS are predominantly southwesterly at 5 to 15 knots. Surface winds in the Gulf of Thailand are predominantly west southwesterly at 10 knots. Surface winds in the southern SCS make an anticyclonic turn and are southeasterly to southwesterly at 5 knots.

At 00Z July 25 surface winds in the northern SCS are variable at 3 to 5 knots. Surface winds in the central SCS make a cyclonic turn and are westerly to southerly at 5 to 15 knots. Surface winds in the Gulf of Thailand are predominantly southwesterly at 10 knots. Surface winds in the southern SCS are southwesterly to westerly at 3 to 5 knots.

At 12Z July 25 surface winds in the northern SCS are variable at 3 to 5 knots. Surface winds in the central SCS and in the Gulf of Thailand make a cyclonic turn and are westerly to southerly at 5 to 15 knots. Surface winds in the southern SCS are southerly to southwesterly 5 knots.

At 00Z July 26 surface winds in the northern SCS are variable at 3 to 5 knots. Surface winds in the remainder of the SCS make a cyclonic turn and are southwesterly to southerly at 5 to 15 knots.

At 12Z July 26 surface winds in the northern SCS are variable at 3 to 5 knots. Surface winds in the remainder of the SCS make a cyclonic turn and are westerly to southeasterly at 5 to 15 knots.

At 00Z July 27 surface winds in the northern SCS are variable at 3 to 5 knots. Surface winds in the remainder of the SCS make a cyclonic turn and are westerly to southerly at 5 to 10 knots.

At 12Z July 27 surface winds in the northern SCS are variable at 3 to 5 knots. Surface winds in the southern SCS make a sharp anticyclonic turn and are southeasterly to southwesterly at 5 to 10 knots. Surface winds in the remainder of the SCS make a sharp cyclonic turn and are westerly to easterly at 5 to 10 knots.

At 00Z July 28 surface winds in the northern SCS are variable at 3 to 5 knots. Surface winds in the southern SCS make an anticyclonic turn and are southerly to southwesterly at 5 to 10 knots. Surface winds in the west part of the Gulf of Thailand are southwesterly at 10 knots. Surface winds over the remainder of the SCS make a sharp cyclonic turn and are westerly to southerly at 5 to 10 knots.

At 12Z July 28 surface winds in the northern SCS are variable at 3 to 5 knots. Surface winds in the southern SCS make an anticyclonic turn and are southerly to southwesterly at 5 to 10 knots. Surface winds in the remainder of the SCS make a sharp cyclonic turn and are westerly to southerly at 5 to 10 knots.

At 00Z July 29 surface winds in the west region of the northern SCS are variable at 3 to 5 knots. Surface winds in the east region of the northern SCS make a cyclonic turn around a fairly small surface low and are northeasterly to east northeasterly at 5 to 20 knots. Surface winds in the remainder of the SCS make a cyclonic turn and are westerly to southerly at 5 to 15 knots.

At 12Z July 29 surface winds in the west region of the northern SCS are variable at 3 to 5 knots. Surface winds in the east region of the northern SCS continue to make a cyclonic turn around a fairly small surface low and are northeasterly to east northeasterly at 3 to 20 knots. Surface winds in the remainder of the SCS make a cyclonic turn and are westerly to southerly at 5 to 15 knots.

At 00Z July 30 surface winds in the west region of the northern SCS are variable at 3 to 5 knots. Surface winds in the east region of the northern SCS continue to make a cyclonic turn around a fairly small surface low and are northwesterly to east northeasterly at 3 to 15 knots. Surface winds in the remainder of the SCS make a cyclonic turn and are southwesterly to southerly at 5 to 15 knots.

At 12Z July 30 surface winds in the northern SCS are variable at 3 to 5 knots. Surface winds in the remainder of the SCS make an anticyclonic turn and are easterly to southerly at 5 to 10 knots.

At 00Z July 31 surface winds in the east region of the northern SCS, in the central SCS, and in southern SCS make an anticyclonic turn and are southeasterly to

southwesterly at 5 to 10 knots. Surface winds in the west region of the southern SCS are southwesterly to southeasterly at 3 to 5 knots. Surface winds in the Gulf of Thailand are southerly at 10 knots.

At 12Z July 31 surface winds in the north part of the east region of the northern SCS are variable at 3 to 5 knots. Surface in the remainder of the SCS make an anticyclonic turn and are northwesterly to southwesterly at 3 to 10 knots.

VII. OCEANIC PROCESSES DURING MAY-JULY 1998

The plots of the CAOCS oceanic component output of the JES, YES, and SCS were broken down into regions to facilitate discussion of oceanic processes that took place during these two time periods. The regions are identical to those described for the atmospheric processes (see Appendix P). The only difference is that MATLAB, rather than RIP, was used for their creation. Additionally, the JES appears smaller on the MATLAB plots as compared to the RIP plots because the ocean component of CAOCS had some difficulty in handling the open ocean boundary condition. MATLAB plots for the JES only extend eastward to 140°E whereas the RIP plots extend eastward to 142°E.

First the oceanic processes that took place during the May time period will be discussed in detail for each of the three major seas that comprise the EAMS. The SST for each major sea is discussed first, followed by the sea surface velocity and then the SSS. Secondly, the oceanic processes that took place during the July time period will be discussed in detail for each of the three major seas that comprise the EAMS.

Four types of plots are available for each of the three major seas. The first type of plot is the SST and surface current velocity and magnitude for each day of the time period. This plot is representative of the SST and surface current structure for each day. The second type of plot is the SST and surface current velocity and magnitude day-to-day tendency for the entire time period with the exception of the first day. This plot shows the actual change in the SST and surface current structure over the past 24 hours and is useful in determining changes that take place that may not be apparent in the first type of plot. The third type of plot is the SSS for each day of the time period. The fourth type of plot is the SSS day-to-day tendency for the entire time period with the exception of the first day.

Readers should refer to Appendix AA for the SST and surface current velocity and magnitude plot for each day of the May time period for the JES. Appendix BB contains the SST and surface current velocity and magnitude day-to-day tendency plot for the entire May time period for the JES with the exception of May 13. Appendix CC contains the SSS plot for each day of the May time period for the JES. Appendix DD

contains the SSS day-to-day tendency plot for the entire May period for the JES with the exception of May 13.

Readers should refer to Appendix EE for the SST and surface current velocity and magnitude plot for each day of the May time period for the YES. Appendix FF contains the SST and surface current velocity and magnitude day-to-day tendency plot for the entire May time period for the YES with the exception of May 13. Appendix GG contains the SSS plot for each day of the May time period for the YES. Appendix HH contains the SSS day-to-day tendency plot for the entire May period for the YES with the exception of May 13.

Readers should refer to Appendix II for the SST and surface current velocity and magnitude plot for each day of the May time period for the SCS. Appendix JJ contains the SST and surface current velocity and magnitude day-to-day tendency plot for the entire May time period for the SCS with the exception of May 13. Appendix KK contains the SSS plot for each day of the May time period for the SCS. Appendix LL contains the SSS day-to-day tendency plot for the entire May period for the SCS with the exception of May 13.

Readers should refer to Appendix MM for the SST and surface current velocity and magnitude plot for each day of the July time period for the JES. Appendix NN contains the SST and surface current velocity and magnitude day-to-day tendency plot for the entire July time period for the JES with the exception of July 18. Appendix OO contains the SSS plot for each day of the July time period for the JES. Appendix PP contains the SSS day-to-day tendency plot for the entire July period for the JES with the exception of July 18.

Readers should refer to Appendix QQ for the SST and surface current velocity and magnitude plot for each day of the July time period for the YES. Appendix RR contains the SST and surface current velocity and magnitude day-to-day tendency plot for the entire July time period for the YES with the exception of July 18. Appendix SS contains the SSS plot for each day of the July time period for the YES. Appendix TT contains the SSS day-to-day tendency plot for the entire May period for the YES with the exception of July 18.

Readers should refer to Appendix UU for the SST and surface current velocity and magnitude plot for each day of the July time period for the SCS. Appendix VV contains the SST and surface current velocity and magnitude day-to-day tendency plot for the entire July time period for the SCS with the exception of July 18. Appendix WW contains the SSS plot for each day of the July time period for the SCS. Appendix XX contains the SSS day-to-day tendency plot for the entire July period for the SCS with the exception of July 18.

A. MAY TIME PERIOD: MAY 13 THROUGH MAY 31, 1998

1. Sea Surface Temperature (SST)

a. JES

The SST contour plot of the JES for May 13 shows a region of warmer water in the vicinity of the west coast of Japan that corresponds to the location of the JNB. There is also a region of cooler water off the Russian coast in the northern JES that corresponds to the location of the southward to southwestward flowing Liman Current.

On May 14 a portion of the JNB in the west region of the southern JES warms and the majority of the JES south of 41°N also warms. On May 15 a large portion of the central and southern JES continues to warm. There is also warming off the Russian coast in the northeast region of the northern JES. On May 16 the southern JES cools while an area of the east region of the central JES warms. On May 17 there is cooling over the east region of the central JES and there is also some cooling off the Russian coast in the southeast region of the northern JES.

On May 18 the southern JES, especially the west region of the southern JES, warms. On May 19 the majority of the southern and central JES warms. There is also warming in the northeast region of the northern JES, and in areas of the southwest region of the northern JES. On May 20 the southern JES continues to warm. On May 21 the far west region of the central JES warms. Warming also occurs off the Russian coast in the southeast region of the northern JES. On May 22 warming occurs in the east region of the central JES and over the Korean Strait.

On May 23 the Korean Strait cools. The Japanese coastal regions in the east region of the southern JES and in the southeast part of the east region of the central

JES also cool. There is slight warming in the southeast region of the northern JES. On May 24 the JES cools. On May 25 the west region of the central and south region of the northern JES warm while the southern JES and the east region of the central JES experience surface cooling.

On May 26 the JES warms especially the east region of the central JES and the southern JES. On May 27 cooling occurs off the Russian coast in the northeast region of the northern JES while warming occurs over the majority of the east region of the central JES. On May 28 the southern and central JES cool while the east region of the northern JES warms. On May 29 the majority of the JES warms especially the south part of the west region of the southern JES. On May 30 the JES warms slightly. On May 31 the JES cools slightly.

b. YES

The SST contour plot of the YES for May 13 shows a strong northwest-southeast temperature gradient parallel to a line drawn from Taiwan to Kyusho, Japan that is associated with the KUC. The SST of the BS and northern YS are significantly cooler than elsewhere in the YES. A core of cooler water is centered over the northwest region of the central ECS.

On May 14 the southern YS warms dramatically. There is warming in the east region of the northern YS and in the region south of the Korean peninsula. The west part of the northwest region of the central ECS also warms and the core of cooler water previously centered over the northwest region of the central ECS diminishes in size. On May 15 there is surface cooling in the southern YS and over the southern border of the west region of the northern ECS. Surface warming continues in the region south of the Korean peninsula.

On May 16 there is warming in the northern and central YS. On May 17 there is cooling in the northern and western YS while slight warming occurs in the northern BS. On May 18 the northwestern YS warms, especially the northwest part of the west region of the southern YS. The western BS cools slightly. On May 19 the central and northern YS warm and a core of warmer water begins to form in the west region of the central YS. Surface cooling occurs over the southern BS and in the region

just south of the Shandong peninsula. There is also warming in the east region of the northern ECS in the vicinity of the Korean Strait.

On May 20 the southern and central YS warms significantly as the core of warm water increases significantly in size. There is also slight warming in the BS and in the east region of the northern YS. On May 21 the northern YS warms while the southern YS cools as the core of warm water moves northward. The western BS cools. On May 22 the northern YS cools as the warm core of water diminishes in size. The east region of the northern ECS in the vicinity of the Korean Strait warms. On May 23 cooling occurs in the east region of the northern YS and in the vicinity of the Korean Strait. Surface warming takes place in the west region of the northern ECS and in the northwest region of the central ECS.

On May 24 surface cooling occurs in the central YS, in the west region of the southern YS, and in the west region of the northern ECS, and to the south of the Korean peninsula. Additionally, the warm core of water previously present in the YS no longer exists. On May 25 surface warming occurs over the east part of the BS and over the majority of the YS. Surface cooling takes place over the southern border of the west region of the northern ECS and in the vicinity of the Korean Strait.

On May 26 surface warming occurs in the east part of the BS. Surface warming also occurs over the west region of the northern ECS and over the east region of the southern YS. On May 27 surface warming occurs in the north part of the BS, in the east region of the northern YS, and in the northwest region of the central ECS. On May 28 surface cooling occurs in the east part of the BS and in the northern YS. Warming also occurs in the west region of the northern ECS.

On May 29 surface cooling occurs over the east region of the central and southern YS as well as the northwest region of the central ECS. Surface warming takes place in the north part of the BS and in the west region of the northern YS. On May 30 significant warming occurs in the BS and in the western YS. On May 31 surface cooling occurs in the western YS and BS while surface warming takes place in the east region of the southern YS.

c. SCS

The SST contour plot of the SCS for May 13 shows a core of high surface temperature in the Gulf of Thailand off the coast of Malaysia. A second core of high surface temperature exists in the east part of the southern SCS off the northwest coast of Borneo. An intrusion of warmer surface water enters the east region of the central SCS through the middle of the Mindoro Strait. Cooler surface temperature exists in the Gulf of Tonkin. A relatively large area of cooler surface temperature is present in the east region of the northern SCS to the west of the Luzon Strait although an intrusion of warmer surface water associated with the KUC is observed entering through the Luzon Strait.

An area of warmer surface water is also centered over the southern boundary of the west region of the northern SCS to the east of Vietnam. An intrusion of warmer surface water associated with this area of higher SST extends northeastward into the northwest part of the east region of the northern SCS although cooler surface water is present over the continental shelf region off the Chinese coast in the northern SCS. During the May time period the SST over the SCS never changes by more than 1°C per day.

From May 14 through the end of the time period the warmer surface water that flows into the northwest part of the east region of the northern SCS from the area of high SST east of Vietnam and lies to the south of the cooler water over the continental shelf off the Chinese coast gradually retreats westward. The core of cooler water present in the east region of the northern SCS gradually expands in size.

On May 15 the west region of the central SCS and the east part of the Gulf of Thailand warms as a southwestward extension associated with the relatively large area of cooler surface temperature present in the east region of the northern SCS to the east of the Luzon Strait retreats northeastward. Surface warming also occurs in the east region of the central SCS off the west coast of Palawan Island as warmer water associated with the area of higher SST in the east part of the southern SCS off the northwest coast of Borneo moves northeastward. Surface cooling occurs at the northern most part of the Gulf of Thailand. From May 23 through May 24 surface cooling takes place in the west

part of the east region of the central SCS as cooler water to the north is pushed southward.

On May 31 cooling occurs over the southern border of the east region of the central SCS, off the northwest coast of Borneo, as cooler water from the northwest is pushed southeastward.

2. Sea Surface Velocity

a. JES

The surface velocity depiction of the JES for May 13 shows the JNB as it flows northward along the Japanese western coast. The southward to southwestward flowing Liman Current that enters the JES from the Sea of Okhotsk through the Tatar Strait is also present and strong.

On May 14 the Liman Current over the southeast region of the northern JES weakens while over the southwest region of the northern JES it strengthens and becomes southeasterly. The surface flow in the west part of the west region of the central JES becomes easterly and strengthens. On May 15 the surface flow in the northwest region of the central JES weakens while the EKWC in the southwest region of the central JES intensifies and flow to the east. In the southeast region of the northern JES the surface currents intensify and flow offshore and southeastward. An intense SPF is present over the majority of the central JES extending across the basin to the west coast of Hokkaido, Japan.

On May 16 the EKWC, JNB and SPF intensify as the surface flow over the southern and central JES becomes strong and northeastward to eastward. The previously offshore, southeastward flow in the vicinity of the Russian coast in the southeast region of the northern JES weakens significantly. On May 17 surface flow over the central JES remains strong and becomes southeastward. Over the southeast region of the northern JES, the surface flow intensifies and becomes eastward to northeastward. On May 18 the surface currents over the JES weaken. The Liman Current reestablishes and its presence is observed as far southward as the northwest region of the central JES. The SPF is no longer present as a westward current.

On May 19 the Liman Current retreats in its southward extension as the EKWC intensifies. The JNB over the southeast region of the northern JES also intensifies. On May 20 the JNB over the southeast region of the northern JES weakens while the Liman Current in the same region of the JES intensifies and flows more southeastward vice alongshore. The presence of the SPF is observed in the north region of the central JES as eastward flow that extends to Hokkaido, Japan. On 21 May the JNB intensifies over the southeast region of the northern JES and executes a cyclonic turn feeding into the now southwestward flow of the Liman Current. There is strong southward flow present in the north region of the central JES. On May 22 the JNB over the southeast region of the northern JES strengthens while the strength of the current elsewhere in the JES weakens considerably.

On May 23 the JNB over the southeast region of the northern JES weakens while the Liman Current in the same region of the northern JES intensifies. The EKWC over the southwest region of the central JES strengthens and flows eastward. The SPF flows eastward across the basin over the north region of the central JES and extends to Hokkaido, Japan. On May 24 the JNB intensifies over the southeast region of the northern JES and makes a cyclonic turn feeding into the Liman Current. The EKWC weakens while the surface flow within the central JES becomes southward to southeastward.

On May 25 the JNB over the southeast region of the northern JES weakens and the Liman Current strengthens and flows more offshore and southward to southeastward. The EKWC intensifies and the surface flow over the west region of the central JES intensifies significantly and flows eastward. On May 26 the JNB intensifies over the east region of the central JES and over the southeast region of the northern JES. The surface flow in the west region of the central JES weakens and becomes southeastward. The surface current in the east region of the central JES strengthens and remains eastward. In the southeast region of the northern JES the previously southward to southeastward surface flow becomes northeastward. On 27 May the EKWC and the SPF intensify. In the south part of the southeast region of the northern JES the previously northeastward surface current becomes eastward. Over the north part of the southeast

region of the northern JES, the Liman Current strengthens slightly while making a cyclonic turn at its southern extent and feeds into the eastward current.

On May 28 the JNB, SPF, and EKWC intensify. The surface current in the west region of the central JES intensifies and flows eastward. The Liman Current weakens slightly. An eastward surface flow lies over most of the central JES. On May 29 surface currents over the southern JES weaken and the SPF reverses direction and becomes westward. The strength of the Liman Current increases slightly. On May 30 the surface current over the northern and central JES intensifies and becomes southeastward. The SPF strengthens and reverses to its normal eastward direction. On May 31 strong southward to southeastward flow is present over the central JES and the south region of the northern JES.

b. YES

The surface velocity depiction of the YES for May 13 shows the KUC as it flows northward along the shelf break in the southern ECS and in the east region of the central ECS. The TsWC is observed flowing northward from the KUC west of Kyushu toward the Korean Strait. The TWC is observed entering through the Taiwan Strait and flowing northeastward inshore of the KUC. There is strong outflow from the BS to the YS. Over the BS and the northern and central YS the surface current is predominantly eastward. An anticyclonic circulation is present in the west region of the northern ECS, in the southern YS, and in the west region of the central ECS.

On May 14 the eastward current over the BS and northern YS decreases in strength. The center of the anticyclonic flow has shifted northward into the southern YS. The Korean Coastal Current intensifies and becomes southwestward. The TWC and TsWC strengthen.

On May 15 weak eastward current continues to prevail over the BS and northern YS. The Korean Coastal Current remains southwestward but weakens. Strong westward flow dominates the northern ECS, weak westward current is located over the southern YS, and an anticyclonic circulation is still present. Surface current in the central ECS to the west of the KUC and TWC flows mainly southwestward.

On May 16 the eastward flowing current in the BS strengthens and so does the outflow into the northern YS. In the northern YS the surface current strengthens and becomes northeastward to eastward. Along the western coast of the Korean peninsula the Korean Coastal Current intensifies and flows more southward vice southwestward. The TsWC and its outflow through the Korean Strait also intensify. In the southern YS an anticyclonic circulation is still present. The surface current south of the Shandong peninsula in the west region of the southern YS strengthens and flows northeastward. The surface current in the west part of the west region of the central ECS strengthens and flows northward. Surface current in the west region of the northern ECS weakens considerably. Surface current in the central ECS to the west of the KUC and TWC weakens but continues to flow southwestward. The TsWC and its outflow through the Korean Strait continue to increase.

On May 17 the surface current in the BS weakens. Surface current in the northern and central YS intensifies and flows eastward. The surface anticyclonic circulation is no longer present. The TWC, KUC, and TsWC intensify while the surface current in the west part of the west region of the central ECS also intensifies and flows northeastward. Surface current in the west region of the northern ECS intensifies and flows northward to northeastward. Surface current in the central ECS to the west of the KUC and TWC flows westward.

On May 18 the surface current in the BS flows northward. In the YS an anticyclonic circulation is present at the surface centered at approximately 37°N 124°E. The surface current in the west part of the west region of the central ECS weakens and flows northward. A branch of the KUC makes a cyclonic turn at 29°N and a cyclonic circulation is present at the surface of the central ECS centered at approximately 28°N 125°E. In the southeast part of the west region of the central ECS, westward of the TWC, the surface current intensifies and flows southwestward.

On May 19 the surface current in the BS intensifies and flows northeastward. The surface anticyclonic circulation in the YS is more extensive and is now centered at approximately 34°N 123°E. The Korean Coastal current intensifies and flows southward. In the northern ECS a cyclonic circulation is present at the surface at

approximately 33.5°N 124.5°E. The surface current in the west part of the west region of the central ECS weakens. A cyclonic circulation remains present at the surface of the central ECS and is now centered at approximately 28°N 125.5°E. In the east region of the southern ECS a branch of the KUC makes an anticyclonic circulation.

On May 20 the warm-core anticyclonic circulation in the YS increases in strength and the Korean Coastal Current intensifies and flows southwestward. The cyclonic circulation in the northern ECS dissipates and is no longer present. The surface current in the northern ECS strengthens and flows westward to northwestward. The surface current in the west region of the central ECS strengthens and flows westward to southwestward. The cyclonic circulation remains present at the surface of the central ECS still centered at approximately 28°N 125.5°E. In the east region of the southern ECS a branch of the KUC continues to make an anticyclonic circulation.

On May 21 the surface current in the BS and in the east region of the northern YS becomes northerly. A general surface anticyclonic circulation in the YS remains present and the surface current in the west region of the northern ECS and the southern YS flows westward. The Korean Coastal Current flows southwestward. The cyclonic circulation remains present at the surface of the central ECS still centered at approximately 28°N 124.5°E. The TsWC intensifies while the TWC weakens slightly. In the east region of the southern ECS a branch of the KUC continues to make an anticyclonic circulation.

On May 22 the surface current in the BS weakens. The surface current in the northern YS weakens and flows eastward. The Korean Coastal Current weakens slightly but continues to flow southwestward. The westward flowing current in the southern YS weakens. A general anticyclonic circulation remains present in the YS centered at approximately 36°N 124°E. The surface current in the west region of the northern ECS continues to flow westward. The cyclonic circulation remains present at the surface of the central ECS still centered at approximately 28°N 124.5°E. In the west region of the southern ECS, in the vicinity of the Taiwan Strait, the surface current intensifies and flows southwestward out of the strait while the TWC weakens. In the east

region of the southern ECS a branch of the KUC continues to make an anticyclonic circulation.

On May 23 the surface current in the BS remains weak. The surface current in the northern YS continues to weaken and flows southward. The Korean Coastal Current continues to flow southwestward. The current in the southern YS continues to flow westward and strengthens slightly. A general anticyclonic circulation remains in the YS centered at approximately 36°N 123.5°E . The surface current in the west region of the northern ECS continues to flow westward and intensifies. The cyclonic circulation remains present at the surface of the central ECS now centered at approximately 28°N 125°E . In the southern ECS at the vicinity of the Taiwan Strait the southwestward flowing surface current weakens and the TWC strengthens slightly. In the east region of the southern ECS a branch of the KUC continues to make an anticyclonic circulation.

On May 24 the surface current in the BS and northern YS strengthens and flows southeastward. The Korean Coastal Current flows southward. The current in the central and southern YS flows southward and strengthens slightly. The Chinese Coastal Current establishes and flows southward. An anticyclonic circulation is no longer present in the YS. The surface current in the west region of the northern ECS intensifies and flows westward to southwestward. The cyclonic circulation remains present at the surface of the central ECS now centered at approximately 28°N 125.5°E . The TWC strengthens. In the east region of the southern ECS a branch of the KUC continues to make an anticyclonic circulation.

On May 25 the surface current in the BS and northern YS strengthens and flows northeastward to eastward. The Korean Coastal Current flows southeastward. The current in the central and southern YS strengthens and flows northeastward to eastward. The Chinese Coastal Current is no longer present at the surface. The surface current in the northern ECS weakens. The cyclonic circulation at the surface of the central ECS is no longer present and the surface current over the west region of the central ECS is weak. The TWC continues to strengthen and the TsWC strengthens. In the east region of the southern ECS a branch of the KUC continues to make an anticyclonic circulation.

On May 26 the surface current in the BS strengthens but shifts direction and flows westward. The surface current in the northern YS weakens slightly and flows eastward. The Korean Coastal Current is no longer present at the surface. The current in the central and southern YS strengthens and flows eastward. The surface current in the west part of the west region of the northern ECS and southern YS, near the Chinese coast, intensify and flow northward to northeastward. The surface current over the central ECS remains weak. The TWC continues to strengthen. In the east region of the southern ECS a branch of the KUC continues to make an anticyclonic circulation.

On May 27 the surface current in the BS and northern YS flows northeastward. The surface current in the southern YS weakens slightly but continues to flow eastward. The surface current in the west part of the west region of the northern ECS and southern YS, near the Chinese coast, weakens slightly but continues to flow northward to northeastward. The surface current in the west region of the northern ECS strengthens slightly and flows northwestward. The surface current over the central ECS, west of the KUC, intensifies and flows westward. The TWC remains strong and the TsWC strengthens. In the east region of the southern ECS a branch of the KUC continues to make an anticyclonic circulation. In general a surface anticyclonic circulation exists over the eastern YES.

On May 28 the surface current in the BS intensifies and flows southeastward. The surface current in the YS flows southward to southeastward. The surface current in the west part of the west region of the southern YS, near the Chinese coast, weakens and flows westward. The surface current in the northern ECS west of the KUC weakens. The surface current in the west part of the west region of the central ECS continues to intensify and flows northward. In the east region of the southern ECS a branch of the KUC continues to make an anticyclonic circulation.

On May 29 surface current in the BS and northern YS weaken but flow eastward. In the central and southern YS surface current becomes anticyclonic and flows southward to westward. Surface currents in the northern and central ECS west of the KUC significantly intensify and flow westward to southwestward. A surface cyclonic circulation develops in the central ECS, west of the KUC, that is centered at

approximately 28°N 126°E. In the east region of the southern ECS a branch of the KUC continues to make an anticyclonic circulation.

On May 30 a general anticyclonic circulation is present over the eastern YES centered at approximately 35°N 124°E. The surface current in the northern YS significantly intensifies and flows southeastward. Surface currents in the northern and central ECS, west of the KUC weaken but continue to flow westward to southwestward. A surface cyclonic circulation remains in the southwest corner of the west region of the central ECS, west of the KUC, still centered at approximately 28°N 126°E. In the east region of the southern ECS a branch of the KUC continues to make an anticyclonic circulation.

On May 31 a general anticyclonic circulation remains present over the eastern YES. The surface current in the BS strengthens and flows eastward. The surface current in the northern YS and the Korean Coastal Current strengthen and flow southeastward. The surface current in the west part of the west region of the central ECS, near the Chinese coast, intensifies and flows northward. Surface current in the southwest region of the central ECS becomes westerly and the surface cyclonic circulation is no longer present in the southwest corner of the west region of the central ECS. The KUC in this area, however, continues to make a strong cyclonic turn. The TWC and TsWC intensify. In the east region of the southern ECS a branch of the KUC continues to make an anticyclonic circulation.

c. SCS

The surface velocity depiction of the SCS for May 13 shows surface current flowing northward into the southern SCS from the Gasper and Karimata Straits. The northward current makes an anticyclonic turn and flows eastward along the coast of Borneo. The eastward flow makes a cyclonic turn, intensifies, and flows northwestward to westward across the south part of the central SCS and into the Gulf of Thailand. As the westward surface current enters the Gulf of Thailand it weakens considerably.

A strong westward current enters the SCS through the central part of the Mindoro Strait. A branch of the westward current makes an immediate sharp anticyclonic turn and exits the SCS through the northern part of the Mindoro Strait.

Another branch of the westward flowing current further upstream makes a sharp anticyclonic turn that sets up a surface anticyclonic circulation centered at approximately 14.5°N 115°E.

The remainder of the westward current flows across the central SCS, makes an anticyclonic turn when it reaches the coast of Vietnam, and flows northward to Hainan Island. A branch of the northward flow makes a tight anticyclonic turn to the east of Vietnam in the east region of the northern SCS and forms a surface anticyclonic circulation centered at approximately 15.5°N 111°E. Upon approaching the southern coast of Hainan Island the northward surface current makes an anticyclonic turn, intensifies, and flows northeastward across the north part of the west region of the northern SCS exiting the SCS through the Taiwan Strait. This northeastward flowing current is known as the South China Sea Warm Current (SCSWC) (Hu et al., 2000). A branch of the SCSWC makes an immediate anticyclonic turn, flows southward, and makes a cyclonic turn creating a surface cyclonic circulation centered at approximately 17°N 112.5°E.

Another branch of the SCSWC further upstream makes a cyclonic turn and flows westward along the coastal region of China. Another branch of the SCSWC still further upstream makes an anticyclonic turn creating a surface anticyclonic circulation centered at approximately 19°N 116°E. Surface current in the Gulf of Tonkin is strong and cyclonic along the coast of China and Vietnam. A weak westward flowing surface current enters the northeast part of the east region of the northern SCS through the southern part of the Luzon Strait, makes a sharp anticyclonic turn, and exits the SCS through the northern part of the Luzon Strait. This is similar to the loop regime of the KUC intrusion described by Chu and Fan (2001). A branch of weak westward flowing surface current continues to flow southwestward and then westward south of the SCSWC and is known as the South China Sea Branch of the Kuroshio (SCSBK) (Hu et al., 2000).

On May 14 the cyclonic turning of the eastward flowing current along the Borneo coast is sharper and a westward surface flow prevails over the south part of the west region of the central SCS. At the southern border of the east region of the central SCS, a branch of the cyclonic turning continues northwestward and feeds into the

westward flowing current that enters the eastern SCS through the central part of the Mindoro Strait. Surface current intensifies and flows northwestward within the Gulf of Thailand. Surface current weakens slightly but remains cyclonic within the Gulf of Tonkin and in the west region of the northern SCS.

On May 15 the westward surface flow over the south part of the west region of the central SCS weakens. North of the weak westward flow, surface current also weakens but flows northward. The previously northwestward flow in the south part of the east region of the central SCS flows northward but continues to feed into the westward flowing current that enters the east region of the central SCS through the central part of the Mindoro Strait. A surface cyclonic circulation forms in the central SCS centered at approximately $11^{\circ}\text{N } 113.5^{\circ}\text{E}$. The KUC intrusion that is present in the northeast part of the east region of the northern SCS increases in strength. Surface current flows predominantly eastward within the Gulf of Thailand. Surface current weakens but remains cyclonic within the Gulf of Tonkin.

On May 16 the eastward surface current along the coast of Borneo intensifies. The westward surface flow over the south part of the west region of the central SCS continues to weaken. North of the weak westward flow, the previously northward surface current now flows southeastward. The previously northward flow in the south part of the east region of the central SCS now flows eastward countercurrent to the westward flowing current that enters the east region of the central SCS through the central part of the Mindoro Strait. This countercurrent intensifies the surface cyclonic circulation previously located in the middle of the east region of the central SCS and the intensified cyclonic circulation is now centered at approximately $11^{\circ}\text{N } 116^{\circ}\text{E}$. The surface cyclonic circulation previously located at $17^{\circ}\text{N } 112.5^{\circ}\text{E}$ is no longer present although a branch of the SCSWC continues to make an anticyclonic turn and flows southward but now makes a cyclonic turn that feeds into the anticyclonic circulation centered at $14.5^{\circ}\text{N } 115^{\circ}\text{E}$. The KUC intrusion continues to intensify. Surface current strengthens and remains cyclonic within the Gulf of Tonkin.

On May 17 the weak westward surface flow over the south part of the west region of the central SCS strengthens slightly. North of the weak westward flow,

surface current weakens and flows predominantly southward vice southeastward. The previously eastward flow in the east part of the southeast region of the central SCS now flows northward to northeastward and feeds into the westward current that enters the east region of the central SCS through the Mindoro Strait and the surface cyclonic circulation is no longer present. The KUC intrusion weakens. The SCSWC intensifies and flows out the Luzon Strait as well as the Taiwan Strait. Although there is westward flow in the middle of the east region of the northern SCS, the surface current is no longer related to the presence of the SCSBK, but is solely due to the branch of the SCSWC that makes an anticyclonic turn at 116°E. Surface current strengthens within the Gulf of Thailand. Surface current weakens within the Gulf of Tonkin.

On May 18 the westward surface flow in the south part of the west region of the central SCS strengthens significantly. The northward to northeastward flow in the southeast part of the east region of the central SCS now flows northeastward and intensifies. A branch of the westward flowing current that enters the east region of the central SCS through the central part of the Mindoro Strait now makes a cyclonic turn in the central SCS and forms a surface cyclonic circulation centered at approximately 11°N 114°E. The KUC intrusion strengthens. The SCSWC weakens and now only flows out the Taiwan Strait. The SCSBK reestablishes and again contributes to the presence of westward flow that forms the southern half of the surface anticyclonic circulation centered at 19°N 116°E. Surface current becomes northward within the Gulf of Thailand. Surface current continues to weaken within the Gulf of Tonkin.

On May 19 the westward surface flow over the south part of the west region of the central SCS strengthens and flows northwestward to northward. The northeastward flow in the southeast part of the east region of the central SCS weakens. The branch of the westward flowing current that enters the east region of the central SCS through the central part of the Mindoro Strait no longer makes a cyclonic turn in the middle of the east region of the central SCS and the surface cyclonic circulation previously centered at approximately 11°N 114°E is no longer present. Surface current become northeastward within the Gulf of Thailand. Surface current remains weak within the Gulf of Tonkin.

On May 20 surface current in the east part of the southern SCS intensifies and flows northwestward. The northwestward to northward surface flow over the south part of the west region of the central SCS significantly weakens. The northeastward flow in the southeast part of the east region of the central SCS strengthens and flows northward. A branch of the westward flowing current that enters the eastern SCS through the central part of the Mindoro Strait and makes a cyclonic turn in the central SCS reestablishes and a surface cyclonic circulation is again present centered at approximately 11°N 112°E. Surface current weakens within the Gulf of Thailand. Surface current remains weak within the Gulf of Tonkin.

On May 21 the northwestward surface flow in the east part of the southern SCS intensifies and flows eastward. The northward current in the southeast part of the east region of the central SCS no longer feeds into the westward flowing current that enters the eastern SCS through the central part of the Mindoro Strait. Instead, it intensifies, flows east northeastward and exists through the southern part of the Mindoro Strait. The KUC intrusion strengthens and so does the SCSBK. Surface current remains weak within the Gulf of Thailand. Surface current remains weak within the Gulf of Tonkin.

On May 22 northeastward surface flow is present over the south part of the east region of the central SCS. A strong eastward current flows across the middle of the central SCS south of the westward current that enters the east region of the central SCS through the Mindoro Strait and exits through the south part of the Mindoro Strait. The KUC intrusion weakens but the SCSBK strengthens. Surface current strengthens and flows eastward within the Gulf of Thailand. Surface current remains weak within the Gulf of Tonkin.

On May 23 a strong eastward current prevails across the Gulf of Thailand and the south region of the central SCS. In the middle of the central SCS and south of the westward surface current that enters the east region of the central SCS through the Mindoro Strait, a strong southeastward current prevails. Branching of the westward surface current that enters the east region of the central SCS through the Mindoro Strait make cyclonic turns that feed into the southeastward to eastward current that prevails

over the south part of the east region of the central SCS. The surface cyclonic circulation centered at approximately 11°N 112°E is no longer present. The SCSBK weakens. A surface cyclonic circulation is again present over the boundary between the east and west regions of the northern SCS and is centered at approximately 16°N 112.5°E. Surface current remains weak within the Gulf of Tonkin.

On May 24 the strong eastward surface current remains over the south region of the central SCS. In the west region of the central SCS a branch of the westward surface current that enters the east region of the central SCS through the Mindoro Strait makes a cyclonic turn and flows southeastward to southward over the middle of the central SCS. Branching of the westward surface current that enters the east region of the central SCS through the Mindoro Strait continue to make cyclonic turns that feed into the southeastward to eastward current that prevails over the south part of the east region of the central SCS. The KUC intrusion strengthens and the SCSBK strengthens. Surface current remains relatively strong and eastward within the Gulf of Thailand. Surface current strengthens within the Gulf of Tonkin.

On May 25, in the west region of the central SCS, a branch of the westward surface current that enters the east region of the central SCS through the Mindoro Strait continues to make a cyclonic turn and now flows southeastward to southwestward over the middle of the central SCS. Branching of the westward surface current that enters the east region of the central SCS through the Mindoro Strait continue to make cyclonic turns that feed into the southeastward to eastward current that prevails over the south part of the east region of the central SCS. Surface current remains strong and eastward within the Gulf of Thailand. Surface current weakens within the Gulf of Tonkin.

On May 26 the cyclonic branching of the westward surface current that enters the east region of the central SCS through the Mindoro Strait stops in the southern half of the central SCS. The surface currents over the southern half of the central SCS weaken considerably. The KUC intrusion and the SCSBK strengthen. Surface current weakens and remains eastward within the Gulf of Thailand. Surface current remains weak within the Gulf of Tonkin.

On May 27 the eastward surface flow in the east part of the southern SCS weakens. Surface current in the south part of the west region of the central SCS intensifies and flows northeastward. Surface current in the southeast part of the east region of the central SCS intensifies, flows northward to northeastward and exits through the southern part of the Mindoro Strait. An intense eastward to northeastward surface current flows across the middle of the central SCS south of the westward surface current that enters the east region of the central SCS through the Mindoro Strait. Branching of the westward surface current that enters the east region of the central SCS through the Mindoro Strait again make cyclonic turns that feed into the eastward to northeastward current that prevails over the middle of the central SCS. The KUC weakens and the SCSBK weakens. Surface current weakens within the Gulf of Thailand and within the Gulf of Tonkin.

On May 28 the surface flow in the east part of the southern SCS intensifies significantly and flows northward to northeastward. Strong eastward surface current prevails over the Gulf of Thailand and the south part of the central SCS. Branching of the westward surface current that enters the east region of the central SCS through the Mindoro Strait continue to make cyclonic turns that feed into the eastward current that prevails over the south part of the central SCS. The KUC intrusion strengthens slightly and the SCSBK strengthens. Surface current remains weak within the Gulf of Tonkin.

On May 29 the surface flow in the east part of the southern SCS intensifies significantly and flows eastward. A strong eastward surface current is present over the east part of the Gulf of Thailand and the southwest part of the west region of the central SCS. In the southeast part of the east region of the central SCS a strong eastward surface current is also present. The SCSBK and the SCSWC strengthens slightly. Surface current remains weak within the Gulf of Tonkin.

On May 30 surface flow in the east part of the southern SCS remains strong but flows southeastward. A strong eastward surface current remains present over the east part of the Gulf of Thailand, but in the southwest part of the west region of the central SCS the eastward surface current has weakened. A strong eastward surface current is no longer present in the southeast part of the east region of the central SCS

although a strong northward to northeastward surface current is present in the east part of the east region of the central SCS and exits through the southern part of the Mindoro Strait. A strong eastward surface current flows across the middle of the central SCS south of the westward surface current that enters the east region of the central SCS through the Mindoro Strait. The KUC intrusion, the SCSBK, and the SCSWC weaken slightly. Surface current weakens significantly and remains eastward within the Gulf of Thailand. Surface current remains weak within the Gulf of Tonkin.

On May 31 the cyclonic surface current in the southern SCS weakens. The surface current over the majority of the Gulf of Thailand and the south part of the west region of the central SCS weakens. The eastward surface current that flows across the middle of the central SCS, south of the westward surface current that enters the east region of the central SCS through the Mindoro Strait, remains present but has weakened considerably. A strong northward to northeastward surface current remains present in the east part of the east region of the central SCS and continues to exit through the southern part of the Mindoro Strait. Surface current remains weak within the Gulf of Tonkin.

3. Sea Surface Salinity (SSS)

a. JES

The SSS contour plot of the JES for May 13 shows the salinity of the JNB to be 34 to 34.1 PSU. Slightly fresher water is found along the North Korean and Russian coastal regions. The most saline water is located north of the Korean Strait. During the May time period the SSS over the JES never changes by more than 0.04 PSU per day.

From May 14 through May 23 the fresher water in the vicinity of the Russian and North Korean coastline in the west region of the central and southern JES gradually expands offshore while the more saline water over the southern JES gradually becomes slightly less saline. From May 24 through May 25 the salinity north of the Korean Strait in the southern JES and in the southeast region of the central JES increases slightly. From May 26 through the end of the timeframe the fresher water in the vicinity of the Russian and North Korean coastline continues to gradually expand offshore while the more saline water of the southern JES again slowly becomes slightly less saline.

b. YES

The SSS contour plot of the YES for May 13 shows a strong northwest-southeast salinity gradient parallel to a line drawn from Taiwan to Kyusho, Japan that is associated with the KUC. The KUC contains the highest salinity value within the YES of 34.5 PSU. The BS consists of relatively low salinity values and a strong salinity gradient from west to east. A salinity maximum is present in the northwest part of the west region of the southern ECS, north of the Taiwan Strait, and accurately the more saline TWC. A region of slightly less saline water is present along the western coast of the Korean peninsula, in the eastern YS, and accurately reflects the Korean Coastal Current. A core of saline water is present over the west region of the southern YS and west region of the northern ECS. During the May time period the SSS over the YES never changes by more than 0.06 PSU per day.

From May 14 through the end of the timeframe the KUC and TsWC gradually advect more saline water northward into the east region of the northern ECS. The tongue of slightly more saline water associated with the TWC gradually decreases in its northern extent. The salinity maximum in the west region of the southern YS and northern ECS gradually decreases in size.

On May 22 the SSS from the middle of the northern ECS eastward to the east part of the northern ECS decreases as less saline water surges southwestward from the Korean Strait. This surge of less saline water from the Korean Strait establishes a pool of less saline surface water over the middle of the YES that continues to persist throughout the remainder of the time period.

c. SCS

The SSS contour plot of the SCS for May 13 shows a core of slightly higher saline water on the eastern side of the Karimata Strait in the southern SCS. Less saline water is present over the remainder of the southern SCS. Less saline water is also present in the Gulf of Thailand. More saline water is found in the east region of the northern SCS associated with transport of more saline water from the KUC via the Luzon Strait. The salinity in the Gulf of Tonkin and along the continental shelf south of the Chinese coast is slightly less saline. An area of more saline water is also located in the west part of the west region of the central SCS over the coastal region in the vicinity of

the tip of the Zhongnan peninsula. During the May time period the SSS over the SCS never changes by more than 0.1 PSU per day.

From May 13 through the end of the timeframe the more saline water on the eastern side of the Karimata Strait in the southern SCS gradually extends northwestward. Additionally, the less saline water present in the Gulf of Thailand gradually extends southeastward. The core of more saline water located in the west part of the west region of the central SCS over the coastal region in the vicinity of the tip of the Zhongnan peninsula gradually moves northeastward. The salinity of the water in the south part of the east region of the central SCS gradually decreases as the less saline water along the northwest coast of Borneo in the east part of the southern SCS slowly surges northeastward.

From May 16 through May 17 and again on May 19 the surface salinity increases in the north part of the west region of the central SCS as the more saline water of the east region of the northern SCS extends slightly to the southwest. From May 24 through May 25 the salinity in the middle of the central SCS, in the vicinity of 10°N, increases as the southern extremity of the more saline water of the northern SCS surges southward.

B. JULY TIME PERIOD: JULY 18 THROUGH JULY 31, 1998

1. SST

a. JES

The SST contour plot of the JES for July 18 shows a region of warm water in the vicinity of the west coast of Japan in the east part of the east region of the central JES that corresponds to the location of the JNB. There is also a region of cooler water off the Russian coast in the east region of the northern JES that corresponds to the location of the southward to southwestward flowing Liman Current.

On July 19 the south part of the west region of the southern JES warms and the west part of the west region of the central JES cools. On July 20 the southern JES warms as warmer water is advected from the ECS through the Korean Strait into the southern JES. On July 21 the north part of the west region of the southern JES and the south part of the west region of the central JES warm as warm water from the JNB in the

west region of the southern JES is advected northward into the south part of the west region of the central JES. The southeast part of the east region of the central JES cools in the vicinity of the Japanese coast. On July 22 the east part of the east region of the central JES cools in the vicinity of the Japanese coast.

The SST of the Russian coast in the southeast region of the northern JES cools on July 23 as the Liman Current advects cooler water from the north into the area. On July 24 the east part of the east region of the central JES warms in the vicinity of the Japanese coast. On July 25 the west region of the southern JES cools as the influx of warmer water from the ECS through the Korean Strait slows. The majority of the east region of the central JES cools on July 26. There is also surface cooling in the southeast region of the northern JES off the Russian coast as the Liman Current intensifies.

SST warms along the Japanese coast in the southern JES from July 27 through July 28. On July 30 there is surface cooling in the southeast part of the east region of the central JES in the vicinity of the Japanese coast. The SST of the central JES and the southern region of the northern JES warm significantly on July 31.

b. YES

The SST contour plot of the YES for July 18 shows a strong northwest-southeast temperature gradient parallel to a line drawn from Taiwan to Kyusho, Japan that is associated with the KUC. The SST of the BS is significantly cooler than elsewhere in the YES. The SST is relatively warm to the north of the Taiwan Strait that coincides with the location of the TWC.

On July 19 there is surface warming east of the BS. Surface warming of the coastal region of the Korean peninsula in the east region of the southern YS occurs on July 20. There is also surface warming off the coast of the Korean peninsula north of the east region of the northern ECS. Surface warming occurs over the west part of the west region of the southern YS and also in the vicinity of the Korean Peninsula in the east region of the central YS on July 21.

On July 22 there is cooling in the west part of the west region of the southern YS off the coast of China. From July 24 through July 25 surface cooling occurs in the coastal region west of the Korean peninsula. On July 26 the northern BS warms by

a degree while the southern BS cools. On July 27 the eastern BS warms while the remainder of the BS cools. From July 30 through July 31 the SST of the southeast part of the east region of the central ECS warms. On July 31 a large degree of surface warming is noted in the BS.

c. SCS

The SST contour plot of the SCS for July 18 shows a core of high surface temperature in the Gulf of Thailand and in the northwest part of the southern SCS off the coast of Malaysia. A second core of high surface temperature exists in the east part of the southern SCS off the northwest coast of Borneo although its size is much smaller than it was during the May time period. A third core of high surface temperature is present in the coastal area of the west part of the west region of the central SCS. An intrusion of slightly cooler water is present on the eastern side of the Karimata Strait. An intrusion of warmer surface water enters the east region of the central SCS through the middle of the Mindoro Strait.

Cooler surface temperature exists in the Gulf of Tonkin and over the continental shelf region off the coast of China. A relatively large area of cooler surface temperature is present in the east region of the northern SCS to the west although an intrusion of warmer surface water associated with the KUC is observed entering through the Luzon Strait and is much stronger than during the May event. A tongue of warmer surface water associated with the SCSWC extends into the northwest part of the east region of the northern SCS from the west region of the northern SCS.

From July 19 through the end of the time period the tongue of warmer water extending into the northwest part of the east region of the northern SCS from the west region of the northern SCS and that lies to the south of the cooler water over the continental shelf off the Chinese coast gradually extends eastward. The KUC intrusion through the Luzon Strait gradually extends westward. The intrusion of slightly cooler water present on the eastern side of the Karimata Strait gradually extends northeastward.

From July 19 through July 27 the area of higher SST present in the coastal region of the west part of the west region of the central SCS cools but warms again between July 28 and the end of the time period.

From July 19 through July 22 the core of high surface temperature in the southwestern SCS off the coast of Malaysia cools and then warms again between July 23 and the end of the timeframe. On July 31 the SST of the southeast part of the east region of the central SCS and the east region of the southern SCS, particularly the coast of Borneo, warm significantly. Additionally, there is significant warming over the southwest part of the west region of the central SCS and along the Malaysian coast in the Gulf of Thailand and in the west part of the southern SCS.

2. Sea Surface Velocity

a. JES

The surface velocity depiction of the JES for July 18 shows the JNB as it flows northward along the Japanese western coast. The eastern and western branches of the EKWC are also present. The southward to southwestward flowing Liman Current that enters the JES from the Sea of Okhotsk through the Tatar Strait is also present but fairly weak.

On July 19 the JNB, EKWC, and SPF weaken in intensity in the southern JES. On July 20 the EKWC reestablishes itself in the west region of the southern JES and in the west region of the central JES. The presence of the SPF is observed in the north region of the central JES as eastward flow that extends across the basin to the west coast of Hokkaido, Japan. The JNB in the east part of the southeast region of the northern JES strengthens, makes a cyclonic turn, and feeds into the Liman Current. On July 21 the cyclonic turning of the JNB in the north part of the southeast region of the northern JES stops and the EKWC flows more northward vice northeastward. A westward current is present in the north part of the west region of the central JES.

The JNB in the southeast region of the northern JES intensifies and flows northwestward on July 22. The previous westward current in the north part of the west region of the central JES is no longer present. On July 23 the JNB in the southeast region of the northern JES weakens and returns to a northerly flow. On July 24 the Liman Current strengthens and extends further to the southwest while the JNB in the southeast region of the northern JES continues to weaken. The EKWC intensifies and becomes more northwesterly while the JNB in the east region of the southern JES also intensifies. On July 25 the Liman Current weakens while the JNB in the southeast region

of the northern JES strengthens. The EKWC remains strong but now flows northward vice northwestward. On July 26 the Liman Current strengthens. The western branch of the EKWC weakens and a northwestward current is present over the majority of the north part of the central JES. On July 27 the EKWC weakens. The northwestward current in the north part of the west region of the central JES now flows westward. On July 28 the Liman Current strengthens slightly and the JNB in the east region of the southern JES. The JNB in the southeast region of the northern JES intensifies and flows northwestward. On July 29 the northwestward flow of the JNB in the southeast region of the northern JES stops and the Liman Current weakens. The EKWC in the west region of the southern JES strengthens. On July 31 the southward extension of the Liman Current decreases and the EKWC strengthens. The JNB in the east part of the east region of the southern JES and in the south part of the east region of the central JES strengthens while JNB in the east part of the southeast region of the northern JES weakens.

b. YES

The surface velocity depiction of the YES for July 18 shows the KUC as it flows northward along the shelf break in the southern ECS and in the east region of the central ECS. The TsWC is observed flowing northward from the KUC west of Kyushu and passing through the Korean Strait. The TWC is observed entering through the Taiwan Strait and flowing northeastward inshore of the KUC. There is outflow from the BS through the Bohai Strait into the YS. The surface flow in the central YS and in the east region of the southern YS is southward while in the west region of the central ECS a strong southeastward surface current is present.

On July 19 the surface flow in the central YS, in the west region of the southern YS, and in the west part of the west region of the northern ECS flows eastward while the southeastward surface current previously located in the west region of the central ECS is no longer present.

On July 20 the surface current in the west region of the northern ECS increases and flows northwestward. The surface current in the west region of the central YS and in the northern YS flows northward and the surface current in the BS strengthens and flows northwestward. A cyclonic circulation is present over the YS and BS and there

is inflow to the BS through the Bohai Strait. The TWC intensifies. The TsWC also intensifies and outflow through the Korean Strait into the JES increases.

On July 21 the surface current over the YS and the west region of the northern ECS weakens and a cyclonic circulation is no longer present over the YS and BS. The TsWC continues to strengthen and the outflow through the Korean Strait and into the JES remains strong. A strong eastward and offshore surface current is present in the west part of the southwest region of the central ECS.

On July 22 the strong eastward and offshore surface current previously present in the west part of the southwest region of the central ECS is no longer present. The Korean Coastal Current strengthens slightly in the east part of the central and southern YS in the coastal region west of the Korean peninsula.

On July 23 surface current in the east region of the central and northern YS strengthens and flows northwestward. There is offshore, westward flow in the east region of the southern YS.

On July 24 a significant change is noted in the surface flow of the YS, the BS, and the western ECS. A strong cyclonic circulation is present with strong offshore flow from the Korean peninsula, an intensification of the southward flowing Chinese Coastal Current in the vicinity of the Chinese coast and stronger inflow to the BS through the Bohai Strait.

On July 25 the cyclonic circulation over the YS, the BS and the western ECS intensifies and the presence of the Chinese Coastal Current is observed extending as far southward as the Taiwan Strait. The flow into the BS from the YS increases as well. The cyclonic circulation feeds into the northeastward flowing KUC and TWC.

On July 26 the cyclonic circulation over the YS, the BS, and the western ECS remains present although the intensity weakens. The presence of the Chinese Coastal Current remains strong and still extends as far southward as the Taiwan Strait while the flow into the BS from the YS decreases.

On July 27 remnants of the cyclonic circulation are observed over the west region of the northern and central ECS but the diameter of the circulation significantly

decreases. The Chinese Coastal Current decreases in intensity and only extends southward to 29°N. The flow at the Bohai Strait shifts to outward flow from the BS to the YS. The majority of the flow within the YS is now southerly vice southwesterly and has weakened.

By July 28 the cyclonic circulation is no longer present at the surface of the YES. The eastward flow from the BS to the YS increases. The Chinese Coastal Current continues to weaken and further decreases in its southward extent. The Korean Coastal Current to the west of the Korean peninsula is quite strong and flows southward. Overall the strength of the surface current in the YS and western ECS weakens.

On 29 July the Chinese Coastal Current is no longer present at the surface and the flow in the vicinity of the Chinese coast is predominantly offshore, but weak. The Korean Coastal Current remains present but decreases slightly in strength. The eastward flow from the BS to the YS decreases.

On July 30 the Korean Coastal Current continues to weaken. There is weak northerly flow along the Chinese coast. The flow within the BS is weak and northeasterly. The TWC increases in intensity as it enters the ECS from the Taiwan Strait.

On July 31 there is fairly strong outflow from the BS to the YS. A strong anticyclonic turning surface current is present over the YS with southeastward, onshore flow to the west of the Korean peninsula and northeastward, offshore flow in the western YS. The TWC continues to increase in strength in the west part of the west region of the southern ECS. A branch of the TWC in the north part of the west region of the southern ECS is observed flowing onshore and northwestward toward the Chinese coast after entering the ECS through the Taiwan Strait. The surface flow from the ECS to the JES via the Korean Strait also increases with an associated strengthening of the TsWC.

c. SCS

The surface velocity depiction of the SCS for July 18 shows surface current flowing northward into the southern SCS from the Gasper and Karimata Straits. Strong southeastward surface current is located in the Gulf of Thailand. Upon exiting the

Gulf of Thailand a branch of the southeastward current turns cyclonically and flows northeastward along the Zhongnan peninsula in the west region of the central SCS.

The remainder of the southeastward current that exits the Gulf of Thailand continues flowing southeastward, reaches the coast of Borneo, and flows eastward to northeastward along the northwestern coast of Borneo and in the south east part of the east region of the central SCS.

As was the case for the May time period, a strong westward current enters the east region of the central SCS through the central part of the Mindoro Strait. The north part of the westward surface current contains branching that make anticyclonic turns that feed into an eastward countercurrent that is present over the majority of the south part of the east region of the northern SCS. The remainder of the westward surface current flows across the north part of the central SCS, converges with the northeastward current present in the west part of the west region of the central SCS and flows northward in the middle part of the west region of the of the northern SCS toward Hainan Island. A branch of the northward flow makes a tight anticyclonic turn and feeds into the eastward countercurrent north of the strong westward current.

The remainder of the northward flow, upon reaching the southern coast of Hainan Island, makes an anticyclonic turn, intensifies, and flows northeastward as the SCSWC along the Chinese coast exiting the SCS through the Taiwan Strait. A branch of the SCSWC makes an anticyclonic turn and feeds into the weak, southwestward flowing SCSBK. The KUC intrusion is fairly weak in strength. Unlike the May event, no westward countercurrent is observed along the coastal region of China. Surface current in the Gulf of Tonkin is strong and eastward.

The previously strong southeastward surface current in the Gulf of Thailand weakens on July 19. An eastward to northeastward surface current is now present across the south part of the central SCS, south of the strong westward current that enters the east region of the central SCS through the central part of the Mindoro Strait, and exits the SCS through the south part of the Mindoro Strait. The eastward countercurrent north of the strong westward current now flows southeastward and exits the SCS through the north part of the Mindoro Strait. The KUC intrusion strengthens

slightly. Surface current in the Gulf of Tonkin becomes anticyclonic along the coast of Vietnam and China.

The previously eastward to northeastward surface current present across the south part of the central SCS flows eastward on July 20. Additionally, it no longer exits the SCS through the south part of the Mindoro Strait. The previously southeastward countercurrent north of the strong westward current that enters the east region of the central SCS through the central part of the Mindoro Strait, now flows eastward, makes a cyclonic turn and flows northward in the southeast part of the east region of the northern SCS to the west of Luzon. Additionally, it no longer exits the SCS through the north part of the Mindoro Strait. The northeastward current along the Zhongnan peninsula in the west region of the central SCS strengthens. Surface current in the Gulf of Tonkin becomes northeastward.

The previously eastward surface current present across the south part of the central SCS weakens and flows eastward to southeastward on July 20. An eastward surface current is now present across the central part of the central SCS and becomes northeastward in the east part of the east region of the central SCS. There is now southeastward flow to the north of the strong westward current that enters the east region of the central SCS through the central part of the Mindoro Strait. Surface current in the Gulf of Tonkin strengthens and flows eastward.

On July 22 the surface current in the south part of the central SCS weakens with the exception of the northeastward current present along the Zhongnan peninsula in the west region of the central SCS. There is now eastward flow to the north of the strong westward current that enters the east region of the central SCS through the central part of the Mindoro Strait. Surface current in the Gulf of Tonkin remains eastward.

Weak eastward to northeastward surface current is present in the south part of the central SCS on July 23. There is now eastward to southeastward flow to the north of the strong westward current that enters the east region of the central SCS through the central part of the Mindoro Strait. Surface current in the Gulf of Tonkin weakens.

A more stronger and eastward surface current is present in the south part of the central SCS on July 24. There is now eastward to northeastward flow to the north of the strong westward current that enters the east region of the central SCS through the central part of the Mindoro Strait.

A southeastward surface current is present in the south part of the central SCS on July 25. There is now eastward flow to the north of the strong westward current that enters the east region of the central SCS through the central part of the Mindoro Strait. Surface current in the Gulf of Thailand strengthens and as it flows predominantly eastward. Surface current in the Gulf of Tonkin weakens.

The surface current is weak in the southeast part of the west region of the central SCS and in the southwest part of the east region of the central SCS on July 26. A strong northward to northeastward surface current is present in the east part of the east region of the central SCS. There is now eastward to southeastward flow to the north of the strong westward current that enters the east region of the central SCS through the central part of the Mindoro Strait. The KUC intrusion strengthens. The SCSBK strengthens. The surface current in the Gulf of Thailand weakens.

The surface current is strong and northeastward to eastward in the south part of the central SCS on July 27. A strong northward to northeastward surface current remains present in the east part of the east region of the central SCS. The strong westward current that enters the east region of the central SCS through the central part of the Mindoro Strait strengthens. The KUC intrusion weakens. The SCSBK weakens.

The surface current is strong and eastward in the south part of the central SCS on July 28. A strong northward to northeastward surface current remains present in the east part of the east region of the central SCS. The strong westward current that enters the east region of the central SCS through the central part of the Mindoro Strait weakens.

The surface current is strong and eastward in the south part of the central SCS on July 29. A strong eastward surface current is now present in the east part of the east region of the central SCS. The strong westward current that enters the east region of

the central SCS through the central part of the Mindoro Strait strengthens. The KUC intrusion strengthens. The SCSBK strengthens. The SCSWC strengthens.

The surface current is weak in the southeast part of the west region of the central SCS and in the southwest part of the east region of the central SCS on July 30. A northward to northwestward surface current is now present in the east part of the east region of the central SCS. The strong westward current that enters the east region of the central SCS through the central part of the Mindoro Strait continues to strengthen. The KUC intrusion continues to strengthen. The SCSWC continues to strengthen. A strong northwestward to northward surface current is present in the west part of the southern SCS. The surface current in the Gulf of Thailand intensifies and flows eastward to northeastward. The northeastward current present along the Zhongnan peninsula in the west region of the central SCS strengthens.

The surface current is weak in the southeast part of the west region of the central SCS and in the southwest part of the east region of the central SCS on July 31. A stronger northward to northeastward surface current is now present in the east part of the east region of the central SCS. A strong north northeastward surface current is present in the southwest part of the west region of the central SCS. The strong westward current that enters the east region of the central SCS through the central part of the Mindoro Strait weakens slightly. The KUC intrusion continues to strengthen. The SCSWC continues to strengthen. A stronger northwestward to northward surface current is present in the west part of the southern SCS. The surface current in the Gulf of Thailand continues to strengthen and flows northeastward. The northeastward current present along the Zhongnan peninsula in the west region of the central SCS continues to strengthen.

3. SSS

a. JES

The SSS contour plot of the JES for July 18 shows the salinity of the JNB to be 33.8 PSU. Slightly fresher water is found in the southeast region of the northern JES. The most saline water is located in the west region of the southern JES and in the southwest part of the west region of the central JES. During the July time period the SSS over the JES never changes by more than 0.04 PSU per day.

Between July 18 and July 22 the area of more saline water in the west region of the southern JES gradually becomes slightly less saline although an area of greater SSS remains present in the southwest part of the west region of the central JES. Between July 23 and July 28 the SSS of the northern most part of the west region of the southern JES gradually increases. From July 23 through July 25 the SSS of the Korean Strait increases. Between July 29 and July 31 the SSS of the northern most part of the west region of the southern JES gradually decreases.

b. YES

The SSS contour plot of the YES for July 18 shows a strong northwest-southeast salinity gradient parallel to a line drawn from Taiwan to Kyusho, Japan that is associated with the KUC. The KUC contains the highest salinity value within the YES of 34.5 PSU. The BS consists of relatively low salinity values and a strong salinity gradient from west to east. A salinity maximum is present in the west part of the west region of the southern ECS and accurately reflects the more saline TWC. A region of slightly less saline water is present along the western coast of the Korean peninsula, in the northeastern YS, and accurately the Korean Coastal Current. A core of less saline water is centered in the middle of the northern ECS. During the May time period the SSS over the YES never changes by more than 0.08 PSU.

From July 19 through the end of the timeframe the KUC and TsWC gradually advect some more saline water northeastward toward Kyushu, Japan. The TWC also gradually advects some more saline water northeastward. From July 19 through July 20 a core of slightly more saline water is present in the southwest part of the west region of the southern YS but is no longer present on July 21.

c. SCS

The SSS contour plot of the SCS for July 18 shows a core of more saline water on the eastern side of the Karimata Strait. Less saline water is present in the coastal region of the east part of the southern SCS and the southeast part of the east region of the central SCS. A core of less saline water is also located in the northern most part of the Gulf of Thailand. An area of higher salinity is present over the middle part of the east region of the northern SCS associated with transport of more saline water from the KUC via the Luzon Strait. Less saline water extends northward from the southwest

part of the west region of the central SCS into the northwest part of the west region of the central SCS and the middle part of the west region of the northern SCS. The tongue of less saline water then extends northeastward into the northwest part of the east region of the northern SCS. During the July time period the SSS over SCS never changes by more than 0.15 PSU per day.

From July 19 through the end of the timeframe the surface current associated with the more saline water on the eastern side of the Karimata Strait gradually advects more saline water northward. The SSS of the water in the southeast part of the east region of the northern SCS gradually increases as the more saline water from the northwest slowly advects southeastward. The SSS of the northwest part of the west region of the central SCS, the middle part of the west region of the northern SCS, and the northwest part of the east region of the northern SCS gradually decreases as less saline water from the southwest part of the west region of the central SCS advects northward and then northeastward. Additionally, the surge gradually extends further northeastward in the northwest part of the east region of the northern SCS.

THIS PAGE INTENTIONALLY LEFT BLANK

VIII. AIR-SEA INTERACTION

A. MAY TIME PERIOD

The number of atmospheric mesoscale features that either propagate across the EAMS or develop over the EAMS during the May time period is significant.

On May 13 a surface low develops in the west region of the northern SCS. From May 13 through May 17 the surface low deepens as it moves eastward to northward in the northern SCS. On May 18 it moves northeastward into the ECS and continues to move northeastward over the ECS while filling until May 20.

From May 13 through May 17 a surface high, initially centered over the southern boundary of the west region of the northern ECS, affects the majority of the YES and by 12Z May 17 is located east of the east region of the northern ECS. At 00Z May 18 the same surface high moves westward so that by 12Z May 18 it is located over the YS and remains present over the YS until May 22.

From 12Z May 13 through May 15 a surface low northwest of the northeast region of the northern JES moves eastward and passes north of the northeast region of the northern JES.

At 12Z May 14 a surface high develops over the southern boundary of the central JES. From May 15 through May 16 the surface high moves eastward and northeastward across the central and southern JES while building so that by 12Z May 16 it is located east of the southern boundary of the northern JES.

From May 15 through 00Z May 17 a surface low northwest of the southwest region of the northern JES moves eastward and then southward so that it is west of the northeast region of the northern JES. On May 16 a second surface low develops over the east region of the northern ECS and moves northward over the Korean peninsula. At 00Z May 17 the second surface low moves further northward so that it is west of the northwest region of the central JES. At 12Z May 17 the two surface lows combine. On May 18 the surface low moves northeastward and passes north of the northeast region of the northern JES.

From 12Z May 17 through May 18 a surface high east of the east region of the northern ECS moves northeastward so that by 12Z May 18 it is southeast of the southern JES.

From 12Z May 18 through May 19 a surface high northwest of the southwest region of the northern JES moves eastward and passes north of the northeast region of the northern JES.

From 12Z May 18 through 00Z May 20 a surface high over the tip of the Korean peninsula moves eastward across the southern JES to a location that is centered over Honshu Japan.

On May 19 a surface low develops in the east region of the northern SCS and remains present until May 20. On May 21 the surface low joins a surface low that was south of the ECS. From May 21 through May 24 the surface low south of the ECS deepens and moves northeastward passing to the east of the ECS. From May 25 through May 26 the same surface low continues moving northeastward while passing to the east of the JES.

From May 19 through May 20 a surface low northwest of the southwest region of the northern JES moves eastward and passes north of the northeast region of the northern JES.

From 12Z May 20 through 00Z May 22 a surface high develops over the southern boundary of the central JES, builds, and then moves eastward over Honshu, Japan and weakens.

From May 21 through 00Z May 22 a surface high north-northwest of the southwest region of the northern JES moves eastward and passes north of the northeast region of the northern JES.

From 12Z May 21 through 00Z May 23 a surface low northwest of the southwest region of the northern JES moves northeastward and eastward and passes north of the northeast region of the northern JES.

From 12Z May 22 through 00Z May 23 a surface low develops west of the northwest region of the central JES, remains stationary and fills.

From May 23 through 00Z May 24 a surface high west of the southern border of the northeast region of the northern JES moves northeastward and passes north of the northeast region of the northern JES.

From 12Z May 23 through 00Z May 27 a surface low northwest of the southwest region of the northern JES moves northward, then becomes stationary as it deepens, and then moves northward again.

On May 24 a surface high is present west of the YES that affects the majority of the YES through May 26. On May 27 the surface high moves eastward passing over the west region of the central ECS. On May 28 the surface high moves northward and westward so that by 00Z May 29 it has joined a more intense surface anticyclone northwest of the BS. From 12Z May 29 through May 31 the surface high builds and moves eastward and southward over the west region of the northern ECS.

On May 25 a surface low develops over the south part of the east region of the northern SCS. From May 26 through May 28 the surface low remains present over the east region of the northern SCS. On May 29 the same surface low moves northeastward, passes east of Taiwan and moves over the southern ECS while filling.

From 12Z May 25 through 00Z May 27 a surface high develops over the east region of the central JES and moves eastward and northeastward so that it is east of the southern border of the northern JES. At 12Z May 27 the surface high builds and remains stationary. From May 28 through 00Z May 29 the surface high moves southward and eastward so that it is east of the southeast region of the central JES. At 12Z May 29 the surface high moves northward to a location east of the northeast region of the central JES.

From May 27 a through May 28 a surface low west of the BS moves eastward, passes over the western part of the BS, and moves northeastward while deepening and combines with another surface low that is west-northwest of the southwest region of the northern JES. From May 29 through May 31 the surface low moves northward and eastward and passes over the northeast region of northern JES.

At 12Z May 29 a surface low develops over the southern border of the northern SCS that by 12Z May 31 it is centered over the east region of the northern SCS.

The CAOCS oceanic component output clearly shows the impact of these atmospheric mesoscale features. Several examples that demonstrate the effect of atmospheric forcing on the ocean SST, SSS, and surface velocity fields will be provided. These examples will include processes such as Ekman transport, coastal upwelling, and horizontal advection of temperature and salinity.

A strong pressure gradient over the JES is present at 12Z May 15 due to a building surface high centered over the southern boundary of the east region of the central JES and an approaching surface low northwest of the southwest region of the northern JES. Southwesterly winds at 20 knots are present over the majority of the north region of the central JES and over the south region of the northern JES. Surface winds in the south part of the west region of the central JES, in the southern JES, and in the Korean Strait make an anticyclonic turn around the central high at 10 to 15 knots. A more intense southeastward to eastward surface current is present in the southeast region of the northern JES due to Ekman transport from the wind stress. The majority of the SST over the central and southern JES warms due to warm subsiding air normally associated with a developing low-level anticyclone. Surface warming in this region is also due to horizontal advection of warmer water by the JNB and EKWC as they intensify due to Ekman transport by the easterly to southeasterly winds at 10 to 15 knots.

A surface high is to the east of the JES on May 16. There is a surface low over the Korean Peninsula and a second surface low to the northwest of the JES. Surface current in the JES is intense and northeastward to eastward in the east part of the west region of the central JES, in the east region of the central JES, and in the east region of the southern JES on May 16 due to Ekman transport by southeasterly winds at 15 to 20 knots. By 12Z May 17 the surface low to the northwest dominates the JES and surface winds make a cyclonic turn and are southwesterly to south southwesterly at 20 knots over most of the JES. The surface currents over the majority of the JES are intense and southeastward due to Ekman transport from the surface wind stress. Additionally, there is cooling over the east region of the central JES and there is also some cooling off the Russian coast in the southeast region of the northern JES. The southeast currents are advecting cooler water from the Liman Current in the southeast region of the northern

JES towards the JNB in the central JES. Coastal upwelling is occurring off the Russian coast.

A surface high moves over the YS on May 18 and remains stationary. The SAT of the surface high is warmer than the SST of the water over the same region. Heat is lost from the atmosphere to the surface of the ocean and in combination with the presence of anticyclonic surface winds around the surface high, a warm-core anticyclonic circulation develops and is clearly present over the YS by May 20. Only the surface of the ocean has been examined in this paper and additional research is required to determine the vertical extent in the ocean of this possible warm-core anticyclonic eddy over the YS that is present through May 23.

A surface high is centered west of the YES on May 24. A surface low is east of the ECS. A strong east-west pressure gradient is present over the YES and winds are north northwesterly at 20 knots. The SST of the central YS cools significantly due to cold air advection by the surface winds. By May 25 the surface low has moved northeastward away from the YES and ridging associated with the surface high now to the west of the ECS extends over the YS. The surface winds in the western YS are now southwesterly at 15 to 20 knots and the SST of the majority of the YS warms significantly due to warm air advection by the surface winds. The southerly component of wind stress in a region of shallow water results in Ekman transport and a strong northeastward to eastward surface current over the YS.

A surface high is northwest of the BS on May 29. A surface low is centered over the southern ECS. Surface winds in the east region of the central and southern YS are northerly at 20 knots. The northerly component of wind stress in a region of shallow water results in Ekman transport and the Korean Coastal Current flows southwestward and offshore in the east region of the southern YS. The result of the offshore flow is coastal upwelling in the vicinity of the east coast of the Korean peninsula. There is also surface cooling in the remainder of the east region of the southern YS and in the east part of the west region of the southern YS due to horizontal advection of the cooler water to the east by the southeastward surface current.

Troughing associated with a surface low east of the southern ECS is present over the northern SCS and the north part of the central SCS on May 24. A strong surface high is located southeast of the east region of the central SCS. Surface winds in the middle of the central SCS are west southwesterly at 15 knots. Surface current over this same area flow southeastward to southward due to Ekman transport. The SSS in this region increases as the southward to southeastward current advects the more saline water from the north into the region.

CAOCS also shows the impact of the ocean SST fields on the atmosphere. During the May time period, four surface lows developed in the northern SCS. Although the equatorial trough is a region favorable for cyclogenesis, the warm SST of the SCS contributes to upward vertical motion of the developing surface lows. Similarly, the 500-mb and 700-mb conditions were favorable for cyclogenesis in the east region of the northern ECS on May 16; however, the warmer SST of the KUC enforced the upward vertical motion in the lower levels of the atmosphere during the development of the surface low.

B. JULY TIME PERIOD

Although the onset of the summer monsoon and the more permanent features of the 500-mb level flow, such as the Manchurian Low, reduce the number of atmospheric mesoscale features that either propagate across the EAMS or develop over the EAMS, atmospheric mesoscale features still occur. The duration of these atmospheric mesoscale features, when they do occur, is often on a longer timescale because the nature of the mid-level atmospheric flow is less transitory.

Between July 18 and July 20 a surface low initially present over the east region of the northern ECS propagates over the southern JES to a position southeast of the southern JES by 12Z July 20.

Between July 21 and July 31 a surface low that initially develops over the southeast region of the central ECS slowly propagates over the southern JES to a position east of the east region of the southern JES at 00Z July 31.

Between July 27 and July 31 a surface high initially present west of the YES propagates moves over the YES so that it is located over the west region of the central ECS by 12Z July 31.

The CAOCS oceanic component output clearly shows the impact of these atmospheric mesoscale features that still occur during the summer monsoon season. Several examples that demonstrate the effect of atmospheric forcing on the ocean SST, SSS, and surface velocity fields will be provided.

A fairly stationary surface high northeast of the northern JES and a strong surface low over the northeast region of the central ECS result in strong east northeasterly winds at 15 knots across the southeast region of the northern JES on July 22. The surface velocity depiction of the YES for July 22 shows the JNB in the southeast region of the northern JES flowing northwestward across the basin towards the Russian coast due to Ekman transport by the surface wind stress. The SST tendency plot for July 22 shows slight warming in the vicinity of the Russian coast in the southeast region of the northern JES due to advection of warmer water from the southeast. A comparison of the SSS contour plot for July 21 and July 22 shows the slightly more saline water in the southeast part of the of the southeast region of the northern JES surging westward due to horizontal advection by the northwestward surface current in the area.

A surface low initially over the northeast region of the central JES significantly deepens and remains fairly stationary between July 23 and July 24. Comparison of the surface velocity depictions of the YES for July 23 and July 24 and the surface winds over the YES from 00Z July 23 through 12Z July 24 clearly demonstrates the impact of increased surface winds stress on the oceanic surface current circulation. The surface winds over the YES on July 23 are predominantly cyclonic around the surface low but are fairly weak. Surface winds remain cyclonic around the surface low on July 24 but significantly strengthen as the surface low deepens considerably. On July 24 a significant change is noted in the surface flow of the YS, the BS, and the western ECS as a strong cyclonic circulation is present with strong offshore flow from the Korean peninsula, an intensification of the southward flowing Chinese Coastal Current in the vicinity of the Chinese coast and stronger inflow to the BS through the Bohai Strait. The magnitude of

this cyclonic current is in excess of 1 m/s over the majority of the southern YS and over the west region of the northern ECS.

A comparison of the SST tendency plot for July 24, the surface velocity depictions of the YES for July 23 and July 24, and the surface winds over the YES from 00Z July 23 through 12Z July 24 demonstrates the impact of increased surface wind stress on SST through Ekman transport and coastal upwelling in a shallow water region of the ocean. The west side of the Korean peninsula cools by 1°C. The surface winds over this region change from east northeasterly at 5 knots to northeasterly at 30 knots. The increased wind stress causes the surface currents over this region to change from weak, off shore, westward flow to significantly stronger, offshore, west northwestward flow due to Ekman transport. The stronger off shore flow results in coastal upwelling and the region cools. The stronger northeasterly winds on July 24 advect cooler air from the northeast over the region also contributing to a lower SST.

CAOCS also shows the impact of the ocean SST fields on the atmosphere. During the July time period, a surface low develops over the southeast region of the central ECS at 00Z July 21. Although the 500-mb and 700-mb conditions were favorable for cyclogenesis in the southeast region of the central ECS on July 21, the warmer SST of the KUC enforced the upward vertical motion in the lower levels of the atmosphere during the development of the surface low.

IX. COMPARISON OF CAOCS OCEANIC COMPONENT OUTPUT WITH UNCOUPLED OCEAN MODEL OUTPUT

Surface velocity and SST data for the same region and for the same timeframe were available from an uncoupled POM run. The output from the uncoupled POM run was available at five-day intervals. During the May time period four dates were available for comparison with the CAOCS oceanic component output – May 16, May 21, May 26, and May 31. During the June time period 3 days were available for comparison with the CAOCS oceanic component output – June 20, June 25, and June 30.

Results of the comparison revealed some differences between the two models' SST contour plots and surface velocity depictions. These differences are attributed to the to the fact that the CAOCS oceanic component is consistently being updated in the coupling process whereas this is not the case for the uncoupled POM.

THIS PAGE INTENTIONALLY LEFT BLANK

X. CONCLUSIONS

The surface winds of the atmospheric component of CAOCS verified well against NCEP surface wind fields during May through July 1998. The net radiation of the CAOCS output appears to be too high due to higher values of surface longwave radiation flux. This discrepancy will be corrected in future work with CAOCS.

The higher values of net surface radiation flux lead to slightly higher values of SST over the EAMS. As the problem with the erroneously high surface longwave radiation flux of the CAOCS is corrected, the slightly higher values of the oceanic SST fields will adjust accordingly. In general, however, the oceanic component of CAOCS performs well in simulating the EAMS surface current circulation, SST structure, and SSS structure. CAOCS does have trouble with the open ocean boundary.

This study focused primarily on the lower levels of the atmosphere and on the surface layer of the ocean. It placed emphasis on the air-sea interaction processes that occur at these levels when the atmosphere and ocean behave in a way that cannot be described climatologically due to the small temporal scales of the numerous mesoscale features present at the surface of the ocean and in the lower levels of the atmosphere. Examination of the CAOCS air-sea interaction led to several conclusions. First, the impact of atmospheric wind stress on oceanic surface currents is significant. Even the strongest surface currents such as the KUC respond to significant changes in surface winds stress. In shallower regions of the EAMS such as the YS, atmospheric mesoscale features like migrating surface anticyclones and transiting surface low pressure systems clearly affect the entire surface velocity field over the region.

Secondly, the atmospheric forcing associated with major atmospheric mesoscale features alters the SST field of the ocean. SST values can increase by up to 4°C especially when a surface anticyclone remains over the region for several days. The response time for the oceanic SST values to return to normal conditions is often one day after the atmospheric mesoscale storm or anticyclone has dissipated or moved away from the region.

Thirdly, oceanic SSS fields over the EAMS are altered due to atmospheric forcing but to a lesser degree than the SST and surface velocity fields. Even during the presence of a significant storm or anticyclone, the SSS fields rarely changed by more than 1 PSU. The response time for the SSS fields to return to normal values appears to be one day after the atmospheric mesoscale storm or anticyclone has dissipated or moved away from the region.

Fourthly, CAOCS atmospheric and oceanic output is indicative of the impact of the ocean thermal structure on the lower level of the atmosphere. Analysis of CAOCS output revealed that warm SST values can often enhance upward vertical motion in the lower atmosphere and either support the development of atmospheric cyclones or trigger their actual development.

Examination of CAOCS output and verification of the surface wind fields during May through July 1998 clearly support the fact that atmospheric forcing prior to and following the onset of the summer monsoon is by no means a steady state. Significant atmospheric mesoscale features either develop over the EAMS or transit over the EAMS on relatively small temporal scales. The presence of southeasterly winds at 10 knots over the JES or southwesterly winds over the northern SCS after the onset of the summer monsoon is not always the case. This was made clear in the detailed description of the atmospheric processes that occurred during the May and July time periods from the 500-mb level to the surface.

A recent study by Chu et al. (2000) compared CAOCS model output over the EAMS for the period April through August 1998 with data collected during the international SCS Monsoon Experiment as well as data collected from USN air expendable bathythermograph (AXBT) surveys. The study found that CAOCS has the capability to predict the current system and thermal structure of the EAMS and successfully predicted the SCS multi-eddy structure. This study involved CAOCS model output over the EAMS for the same timeframe and verification involved a comparison of CAOCS oceanic output with available buoy station data that showed SST and SSS values to be in good agreement. Examination of CAOCS output and verification of oceanic surface velocity, SST, and SSS fields clearly support the fact that the oceanic structure is

by no means a steady state. Significant oceanic mesoscale features often develop over the EAMS such as a warm-core anticyclonic eddy over the YS and often have a temporal scale of a few days. The presence of the southward flowing Chinese Coastal Current along the east coast of China to the south of the Shandong peninsula is not always the case and is just one example of how a basic climatologic description of the oceanic current system and sea surface thermohaline structure of the EAMS is not always sufficient. This was made clear in the detailed description of the oceanic processes that occurred during the May and July time periods at the surface of the EAMS.

The air-sea interaction is an ongoing process and a direct reflection of the current mesoscale state of both the atmosphere and the ocean. A climatologically forced atmospheric or oceanic model will not represent these mesoscale features that occur on a relatively small temporal scale and are largely responsible for the air-sea interaction. A climatologically forced atmospheric or ocean model will be misrepresentative of the low-level atmospheric wind stress and the oceanic surface velocity, SST, and SSS fields.

Although atmospheric (oceanic) models that are forced with previously analyzed oceanic (atmospheric) model output have the ability to represent the significant mesoscale features of the ocean or atmosphere and are useful for research purposes the experienced delay involved in the process is insufficient for the near-real time requirement of USN METOC support to the fleet.

Differences were also noted between the uncoupled POM output and the CAOCS output. These differences are most likely attributable to the fact that the CAOCS oceanic component is constantly being updated in the coupling process whereas this is not the case for the uncoupled POM. Considering the fact that the atmospheric component of CAOCS as well as the oceanic component of CAOCS verified well against available previously analyzed and collected data it is possible that the oceanic component of CAOCS outperforms the uncoupled POM. A more detailed study that involves the comparison of the CAOCS oceanic component output, the uncoupled POM output, and previously analyzed or collected oceanic data should be conducted in further support of this apparent conclusion.

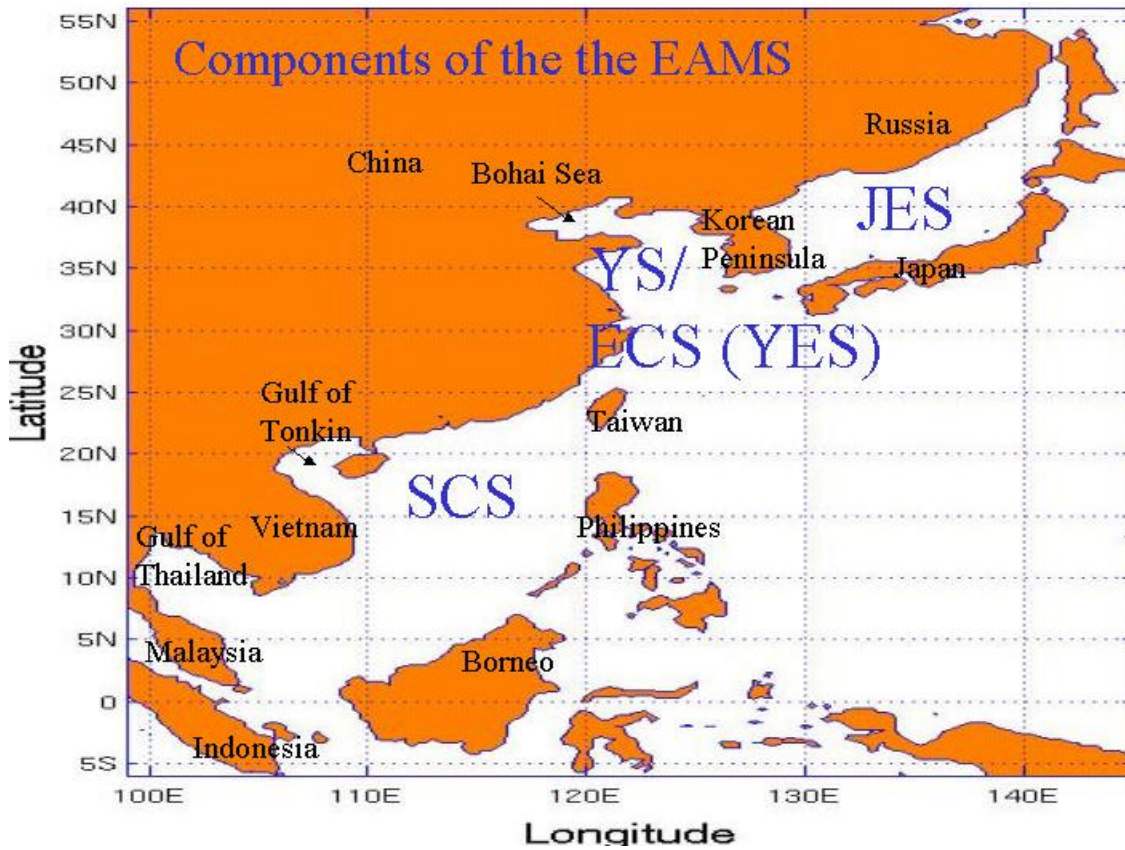
Although the surface wind field and structure of the atmospheric component of CAOCS verified well, no uncoupled MM5 model output was used in this study. Therefore, no conclusions concerning the overall better performer, atmospheric component of CAOCS versus uncoupled MM5, can be made. A more detailed study that involves the comparison of the CAOCS atmospheric component output, the uncoupled MM5 output, and previously analyzed NCEP atmospheric data is required for further conclusions regarding this matter.

This study has shown that CAOCS has the potential to be an extremely useful tool for USN METOC personnel because of its verification and near-real time capability at the mesoscale level of a littoral region. Accurate, real-time model output is essential to METOC personnel in order to properly analyze and forecast the ocean, atmosphere, and acoustical environment.

This study supports the concept behind NRL's COAMPS future capability. Once NRL COAMPS becomes a truly coupled system, it can easily be adopted at NPS as a replacement of CAOCS. It is highly recommended that future studies also involve comparison of the summer and winter monsoon using CAOCS as well as the impact of air-sea interaction at lower depths of the ocean using CAOCS. The inclusion of an acoustic prediction system as part of CAOCS has strong potential to be very useful in forecasting the ocean acoustic environment and once established should be compared in future studies to uncoupled prediction systems to determine the value added.

APPENDIX A. COMPONENTS OF THE EAMS

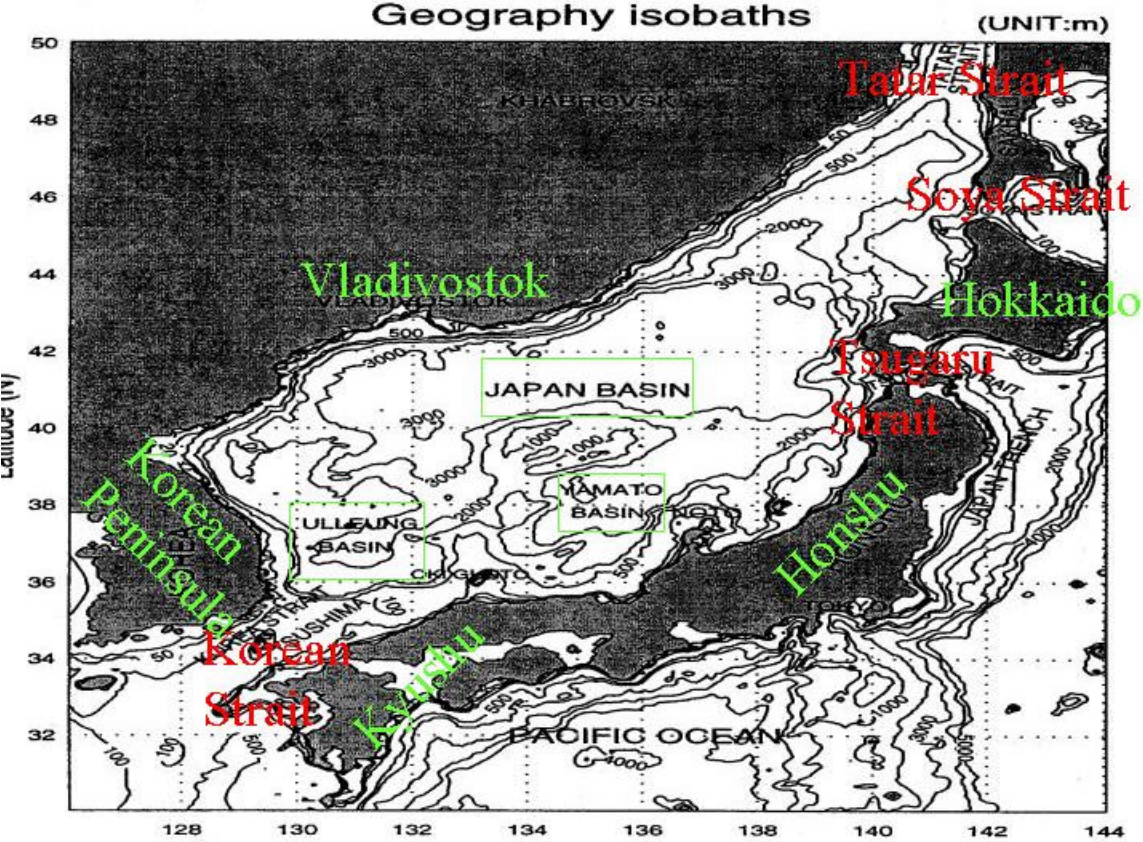
Appendix A consists of one figure that shows the three major seas that form the EAMs.



THIS PAGE INTENTIONALLY LEFT BLANK

APPENDIX B. JES GEOGRAPHY

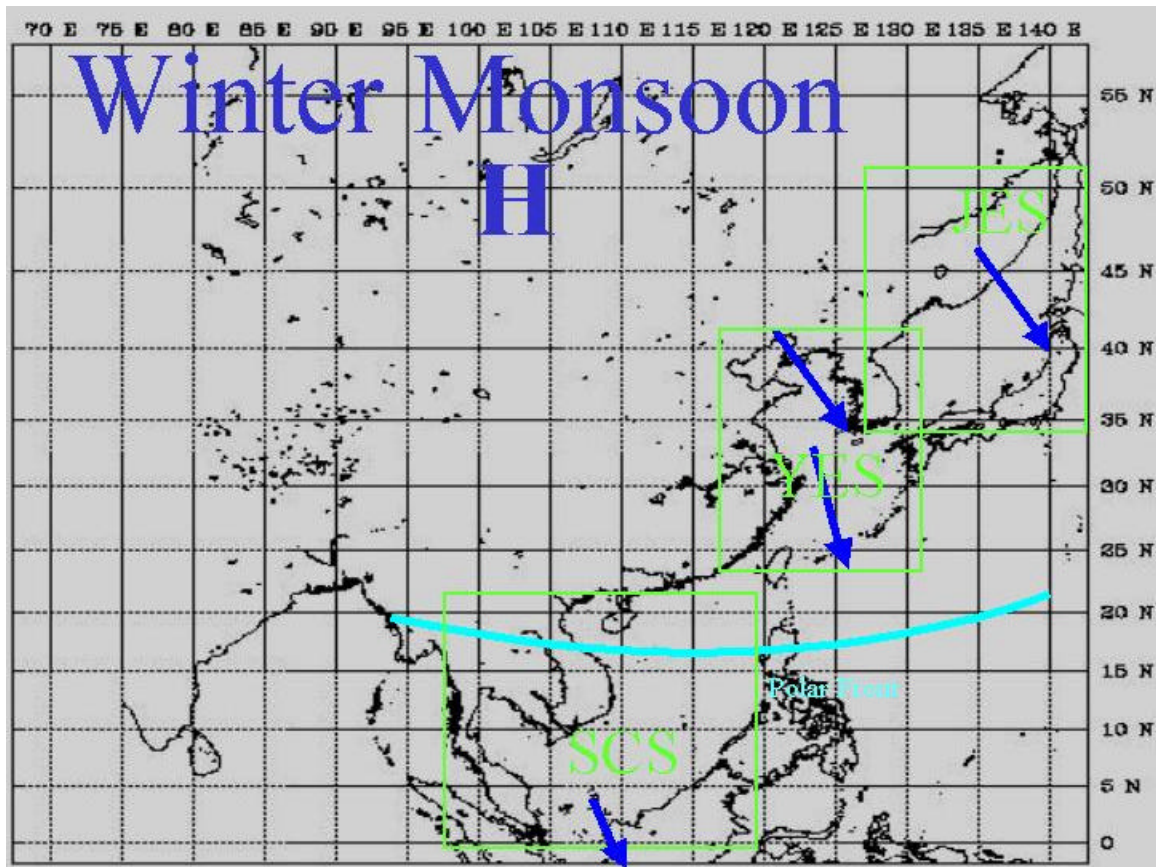
Appendix B consists of one figure that shows the geography and isobaths of the JES. Isobaths are in meters. This figure is a modified version of figure 1 from Chu et al. (2001).



THIS PAGE INTENTIONALLY LEFT BLANK

APPENDIX C. WINTER MONSOON

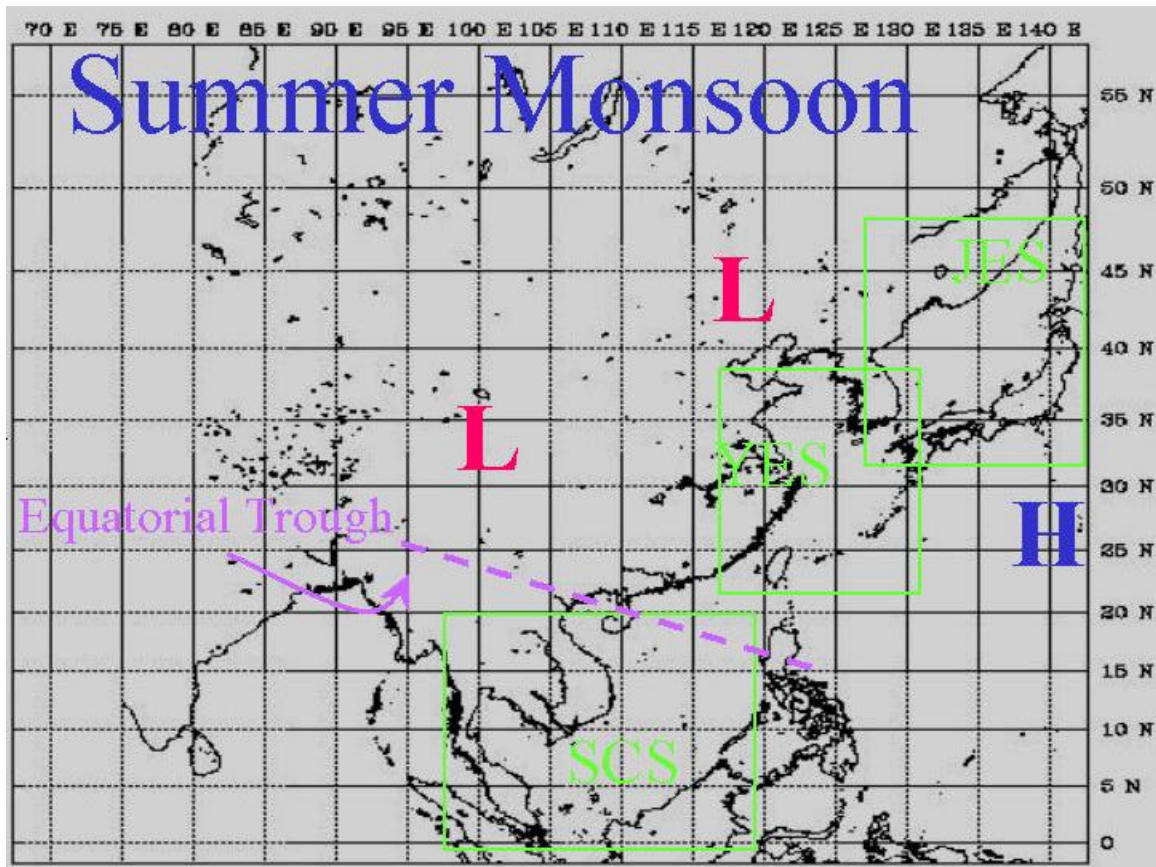
Appendix C consists of one figure that depicts the climatological direction of the winds over the EAMS, the climatological position of the synoptic scale surface pressure systems, and the position of the polar front during the winter monsoon.



THIS PAGE INTENTIONALLY LEFT BLANK

APPENDIX D. SUMMER MONSOON

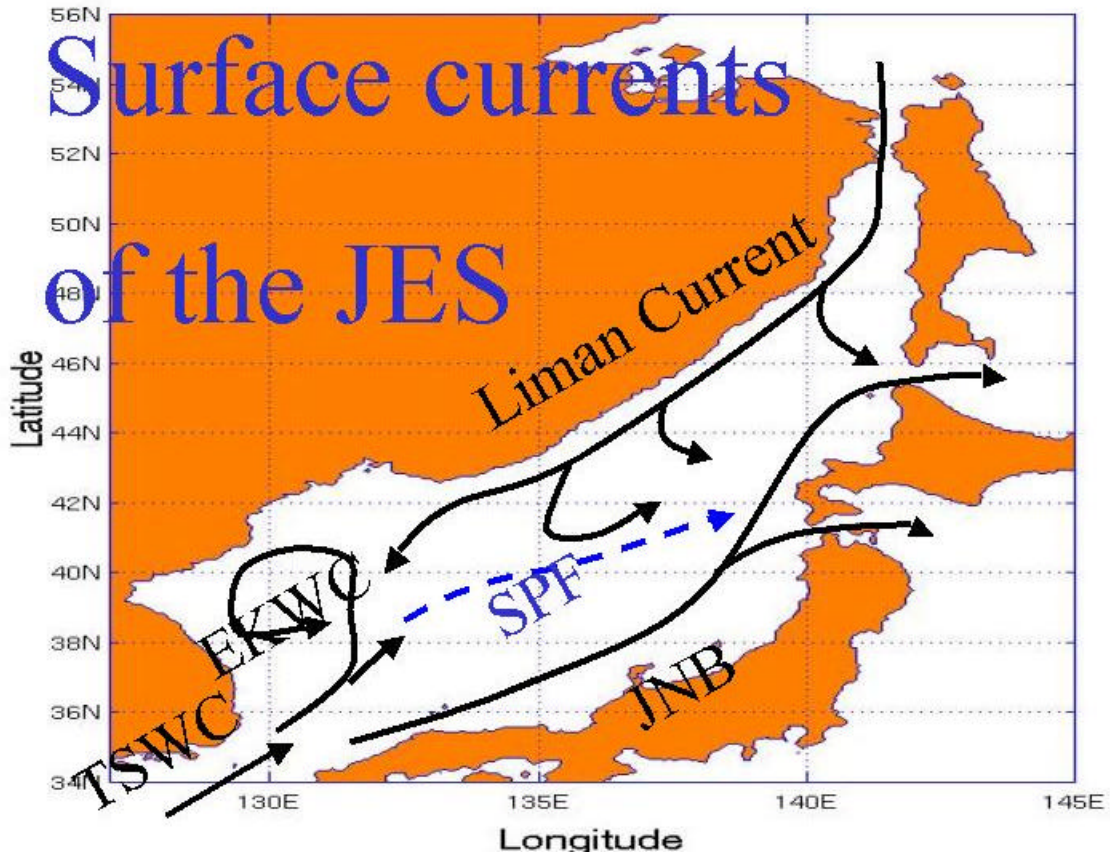
Appendix D consists of one figure that depicts the climatological direction of the winds over the EAMS, the climatological position of the synoptic scale surface pressure systems, and the position of the equatorial trough during the summer monsoon.



THIS PAGE INTENTIONALLY LEFT BLANK

APPENDIX E. SURFACE CURRENTS OF THE JES

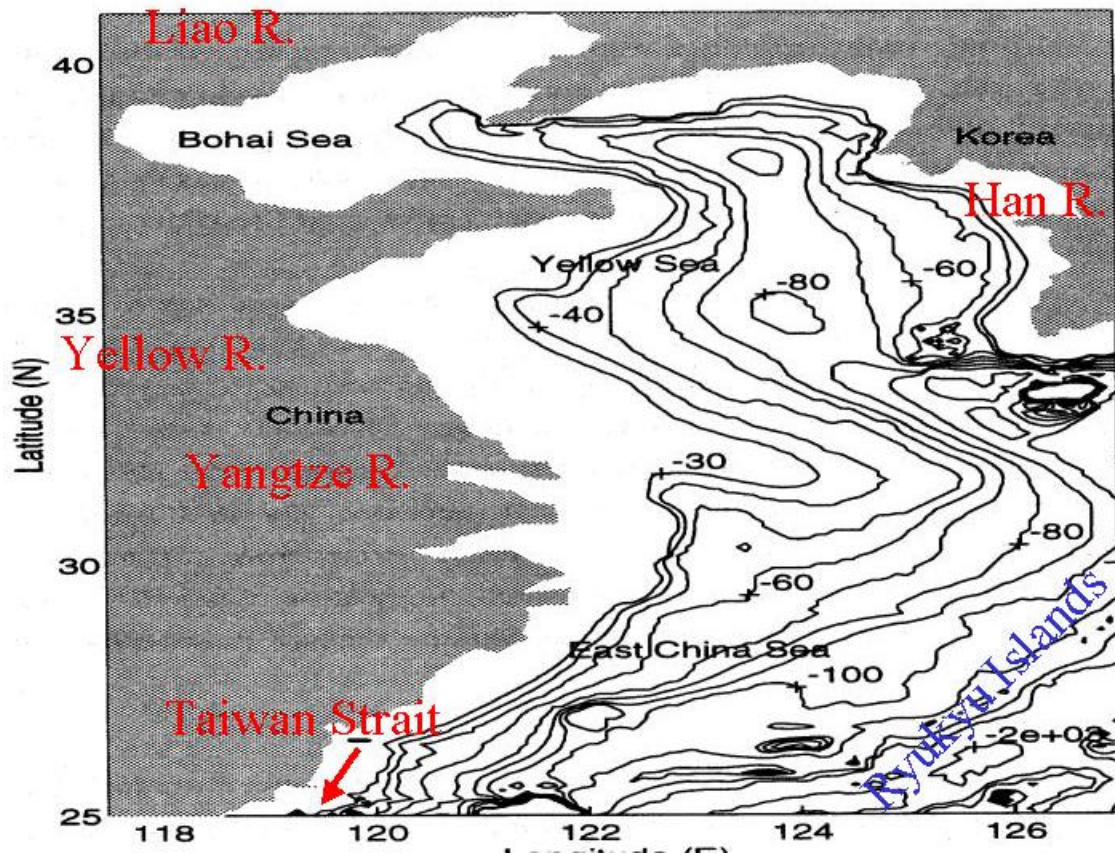
Appendix E consists of one figure that shows the positions of the major surface currents of the JES.



THIS PAGE INTENTIONALLY LEFT BLANK

APPENDIX F. YES GEOGRAPHY

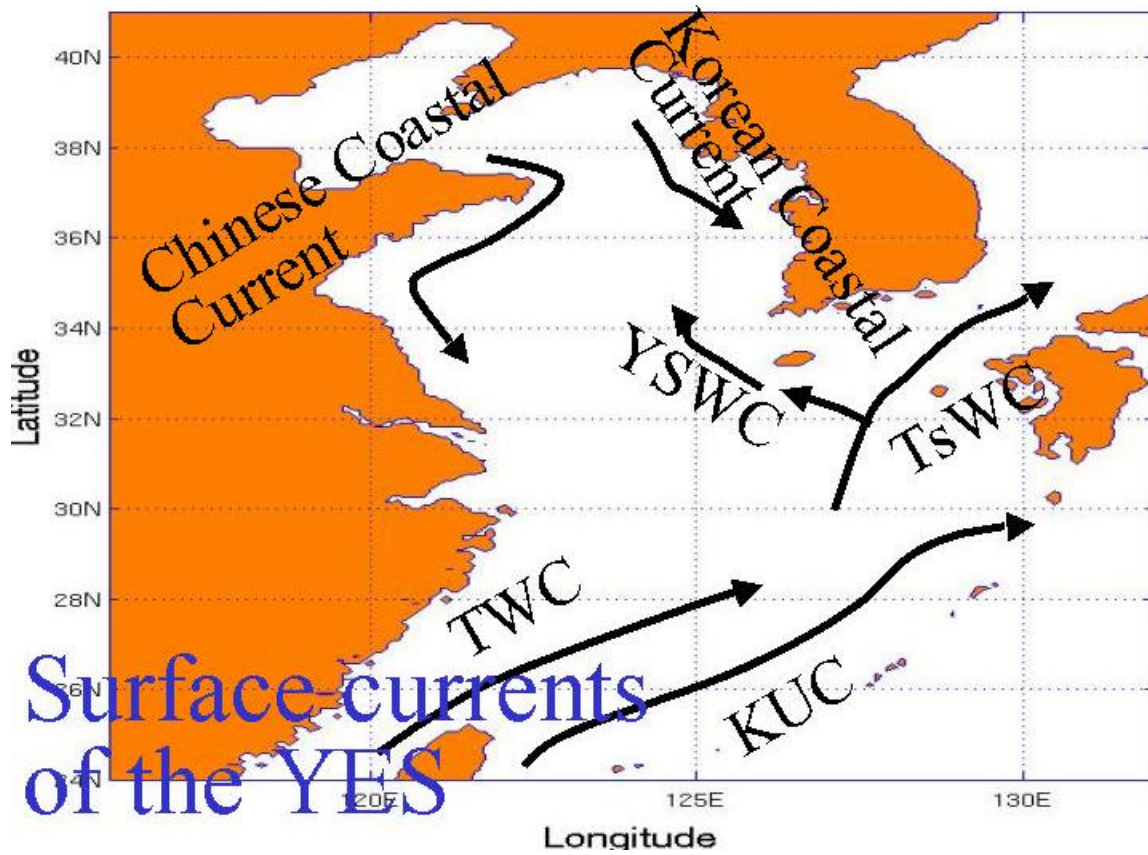
Appendix F consists of one figure that shows the geography and isobaths of the YES. Isobaths are in meters. This figure is a modified version of figure 2 from Chu et al. (1997a).



THIS PAGE INTENTIONALLY LEFT BLANK

APPENDIX G. SURFACE CURRENTS OF THE YES

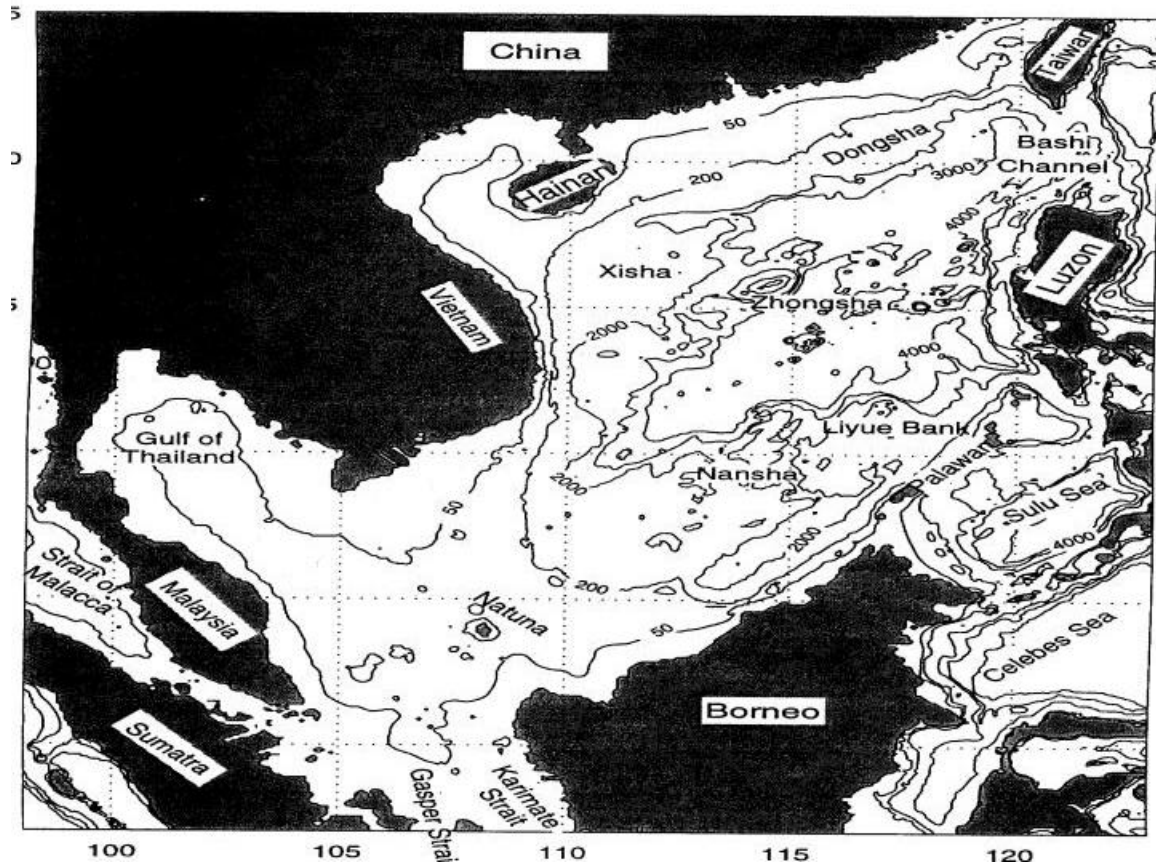
Appendix G consists of one figure that shows the positions of the major surface currents of the YES.



THIS PAGE INTENTIONALLY LEFT BLANK

APPENDIX H. SCS GEOGRAPHY

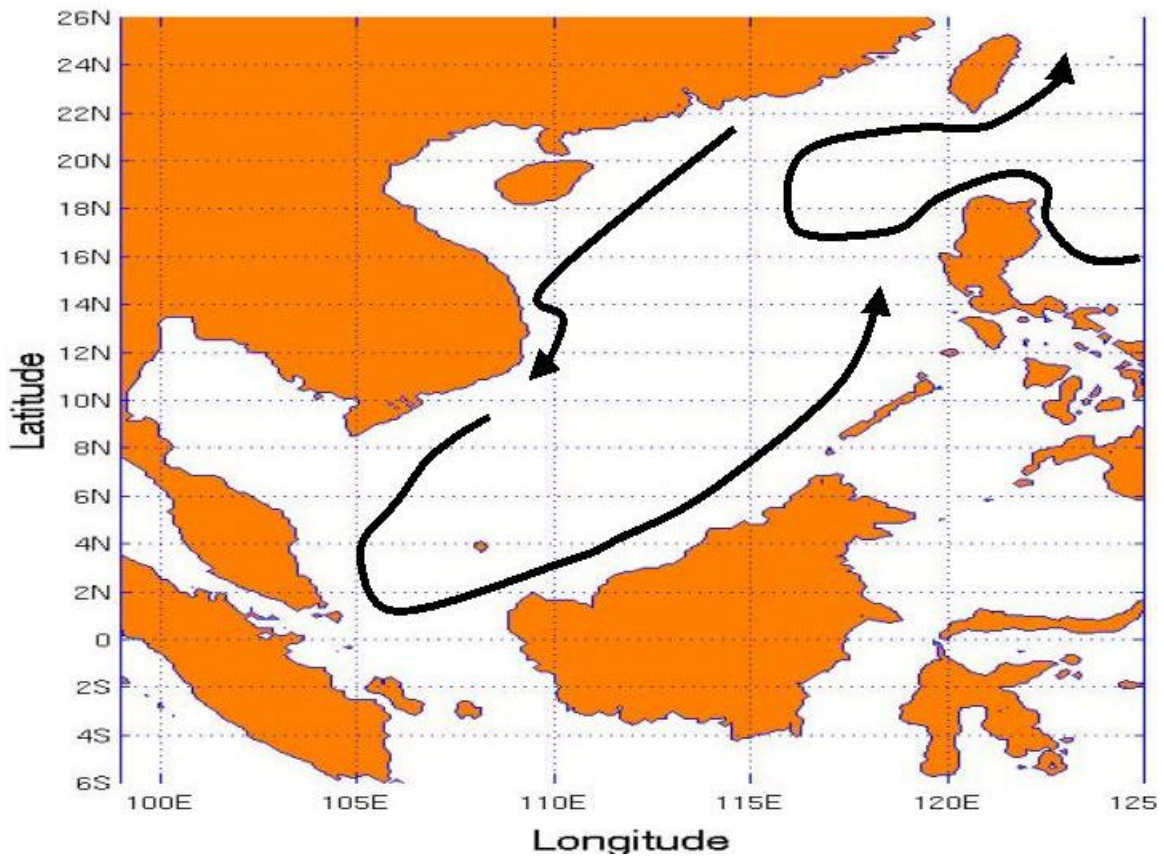
Appendix H consists of one figure that shows the geography and isobaths of the SCS. Isobaths are in meters. This figure is taken from Chu et al. (1999b).



THIS PAGE INTENTIONALLY LEFT BLANK

APPENDIX I. SCS SURFACE CIRCULATION PATTERN - WINTER

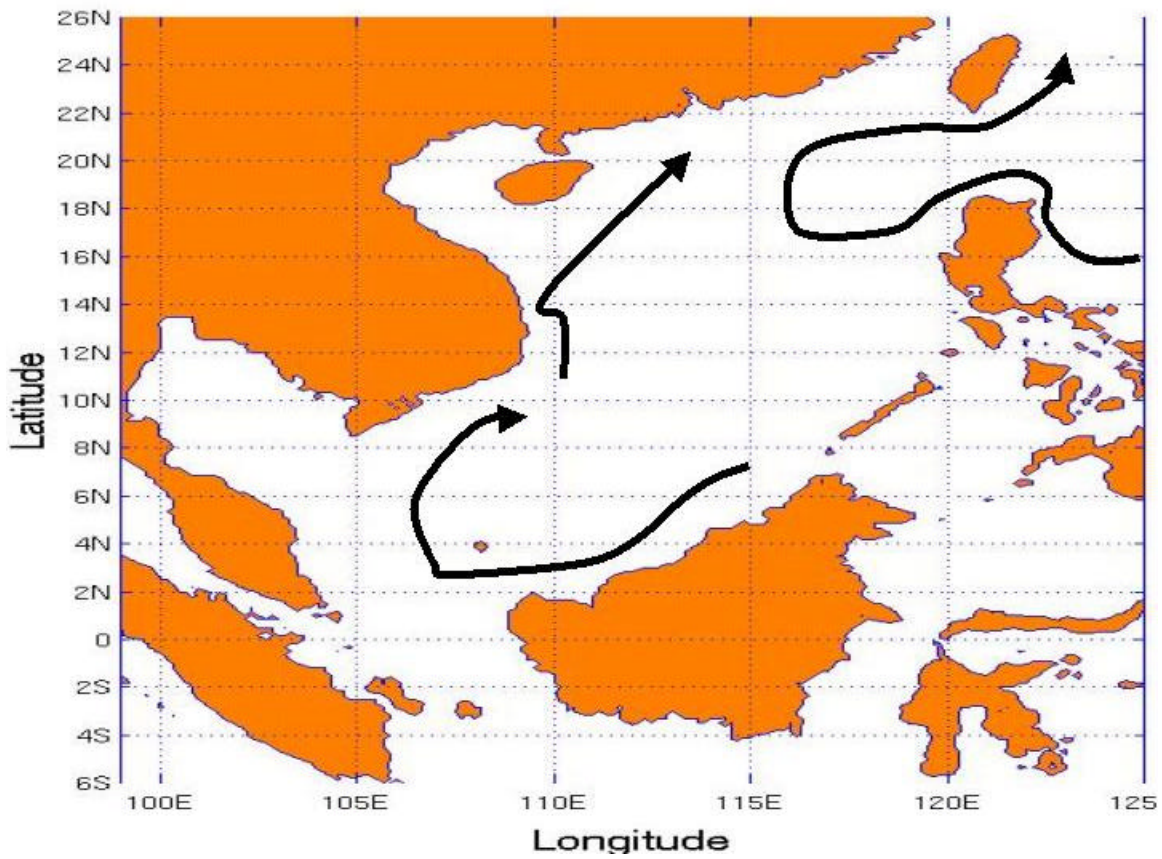
Appendix I consists of one figure that shows the general upper level oceanic circulation pattern for the SCS during the winter.



THIS PAGE INTENTIONALLY LEFT BLANK

APPENDIX J. SCS SURFACE CIRCULATION PATTERN - SUMMER

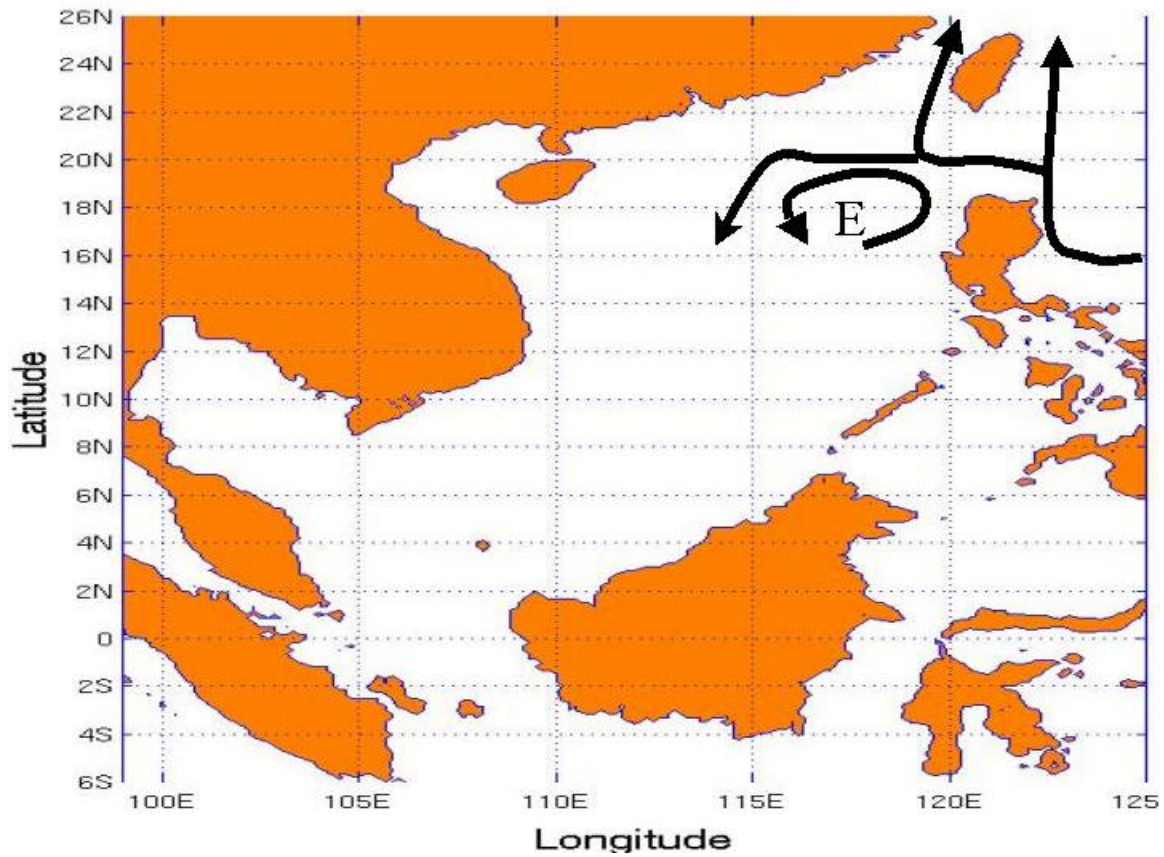
Appendix J consists of one figure that shows the general upper level oceanic circulation pattern for the SCS during the summer.



THIS PAGE INTENTIONALLY LEFT BLANK

APPENDIX K. SCS BIFURCATION REGIME OF THE KUC INTRUSION

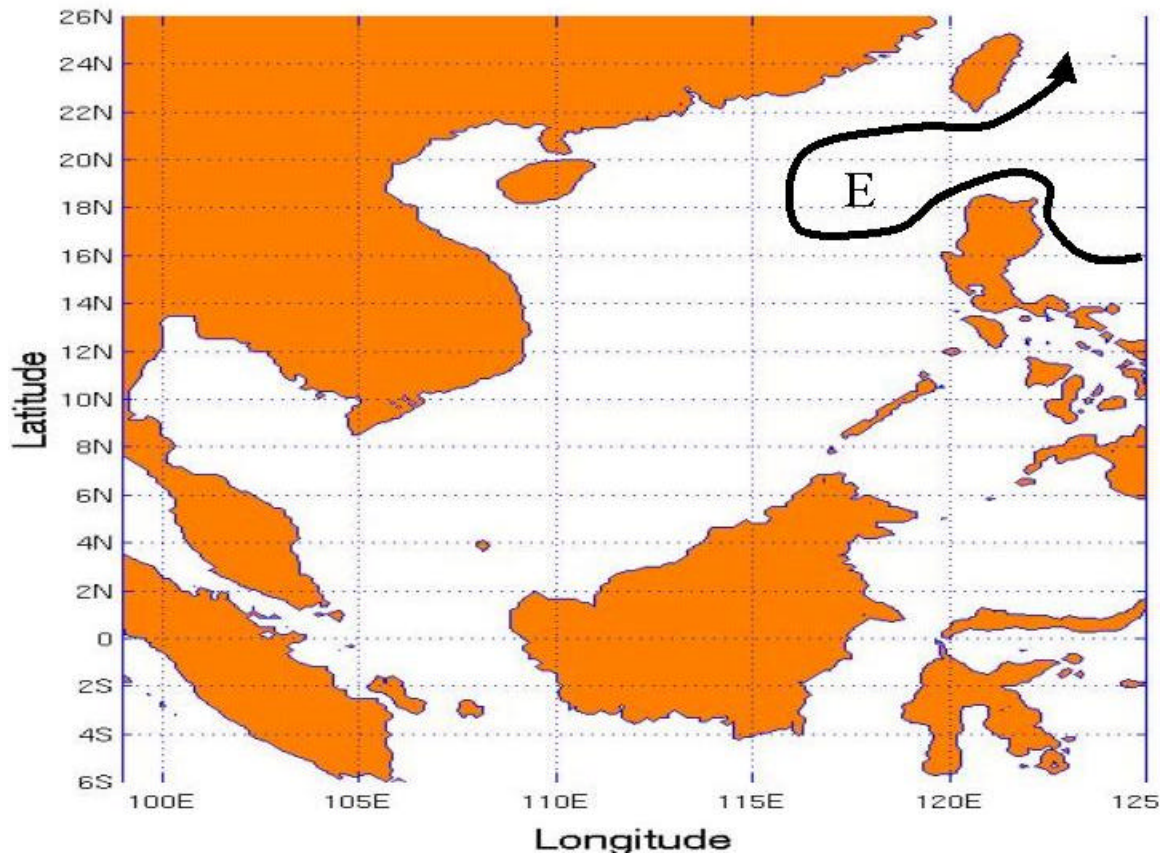
Appendix K consists of one figure that shows the bifurcation regime of the KUC intrusion. The E denotes the general location of the NWL eddy that is cyclonic during the bifurcation regime.



THIS PAGE INTENTIONALLY LEFT BLANK

APPENDIX L. SCS LOOP REGIME OF THE KUC INTRUSION

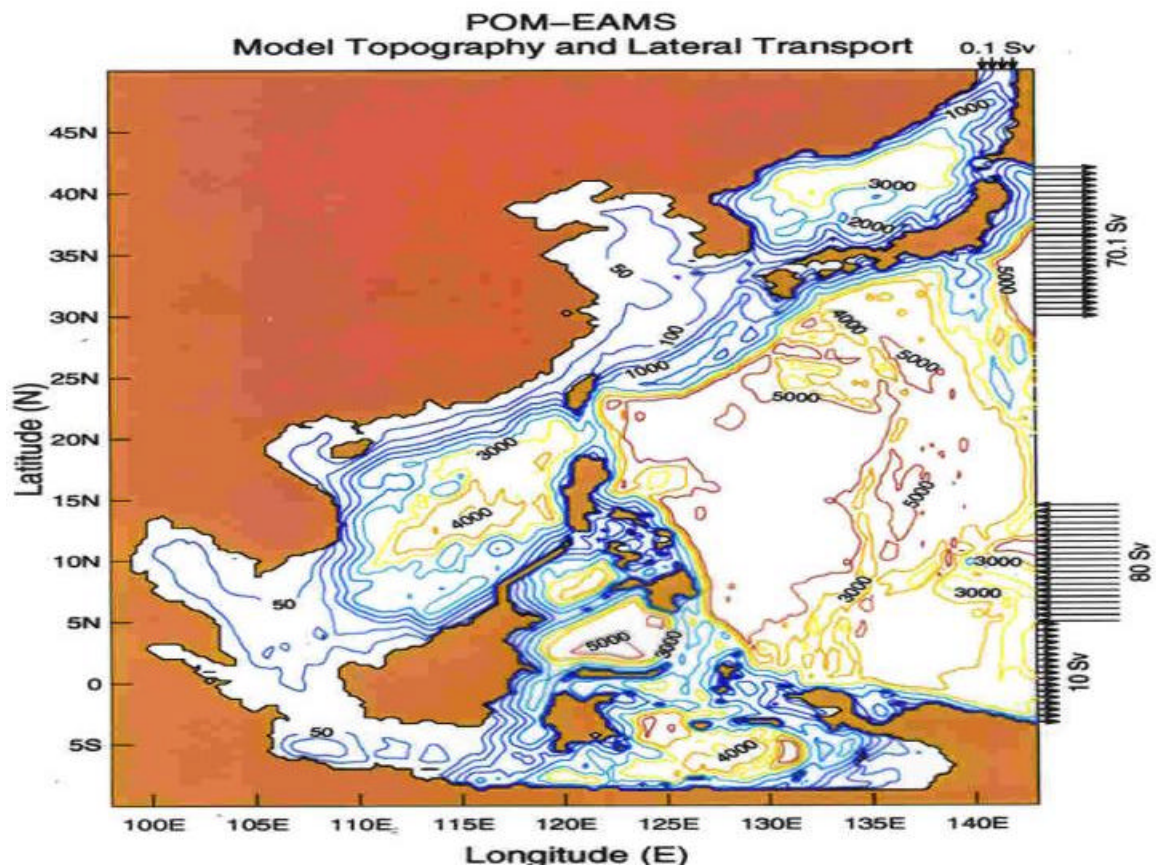
Appendix L consists of one figure that shows the loop regime of the KUC intrusion. The E denotes the general location of the NWL eddy that is anticyclonic during the loop regime.



THIS PAGE INTENTIONALLY LEFT BLANK

APPENDIX M. CAOCS OCEANIC BATHYMETRY AND OPEN BOUNDARY LATERAL TRANSPORT

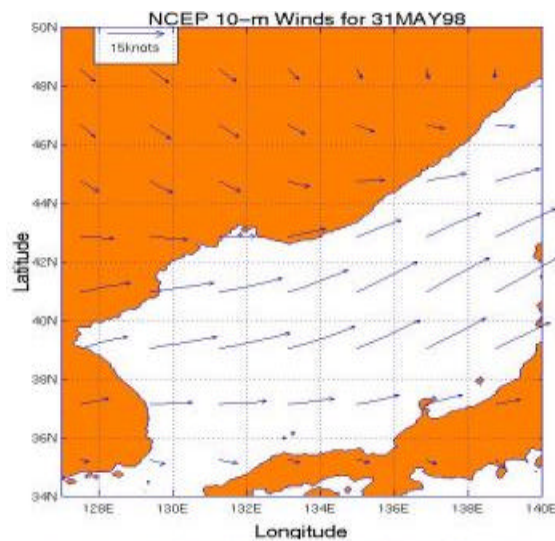
Appendix M consists of one figure that shows the bathymetry data of the oceanic component of CAOCS as well as the open boundary lateral transport of the model domain. Isobaths are in meters. Transport is in Sverdrups. This figure is taken from Chu et al. (2000).



THIS PAGE INTENTIONALLY LEFT BLANK

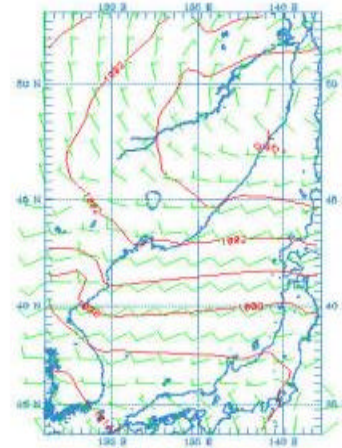
APPENDIX N. SAMPLES OF LOW LEVEL WIND FIELD VERIFICATION

Appendix N consists of four figures that compare NCEP 10-m wind fields with the CAOCS 10-m wind fields. NCEP Data is on the left and CAOCS output is on the right. The top comparison is for May 31 over the JES while the bottom comparison is for July 25 over the YES.



STORM #1 888 SEA PRESS (mb) 1 1998-05-31 12:00:00 + 1998-05-31 00 + 723.000 3000Hz #

STORM #2 982 SEA PRESS (mb) 1 1998-05-31 12:00:00 + 1998-05-31 00 + 723.000 3000Hz #

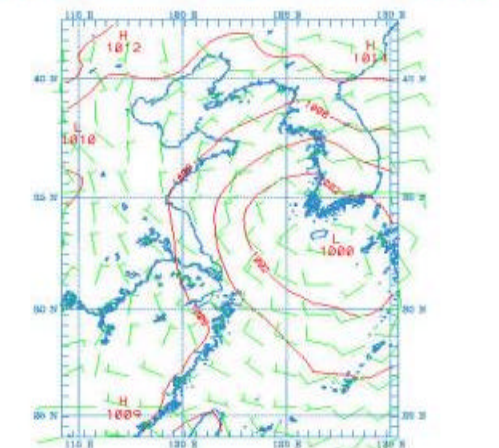
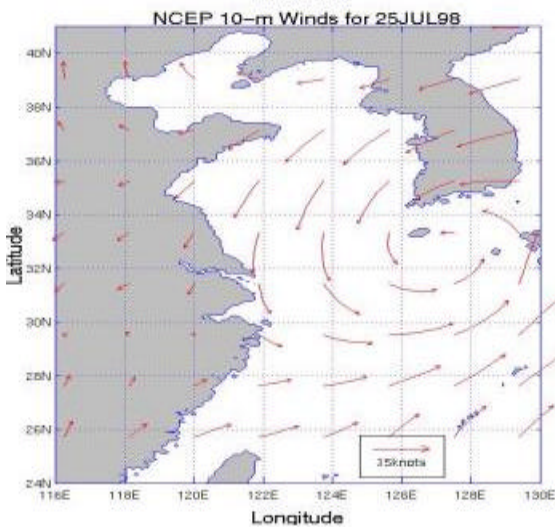


JES 10-m Winds for May 31, 1998

CENTRA FROM 90.00 TO 180.00 LATTER INTERVAL OF 3.0000 PTL:01- 1801.0

STORM #1 888 SEA PRESS (mb) 1 1998-07-25 12:00:00 + 1998-07-25 12 + 1000.000 3000Hz #

STORM #2 982 SEA PRESS (mb) 1 1998-07-25 12:00:00 + 1998-07-25 12 + 1000.000 3000Hz #



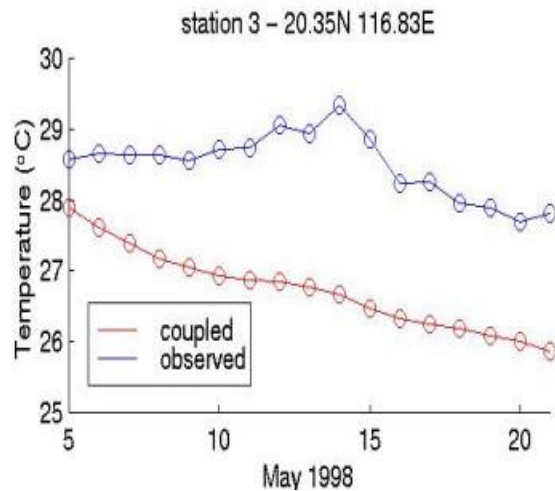
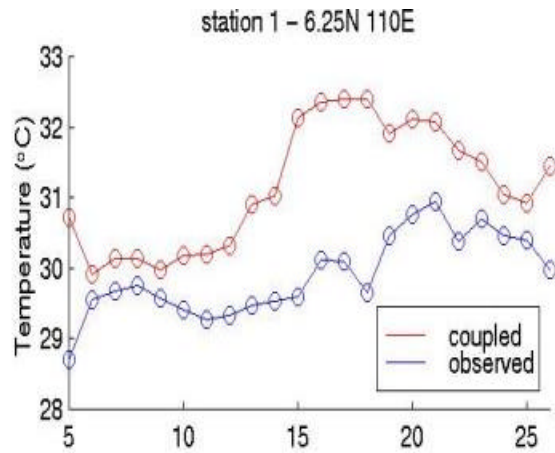
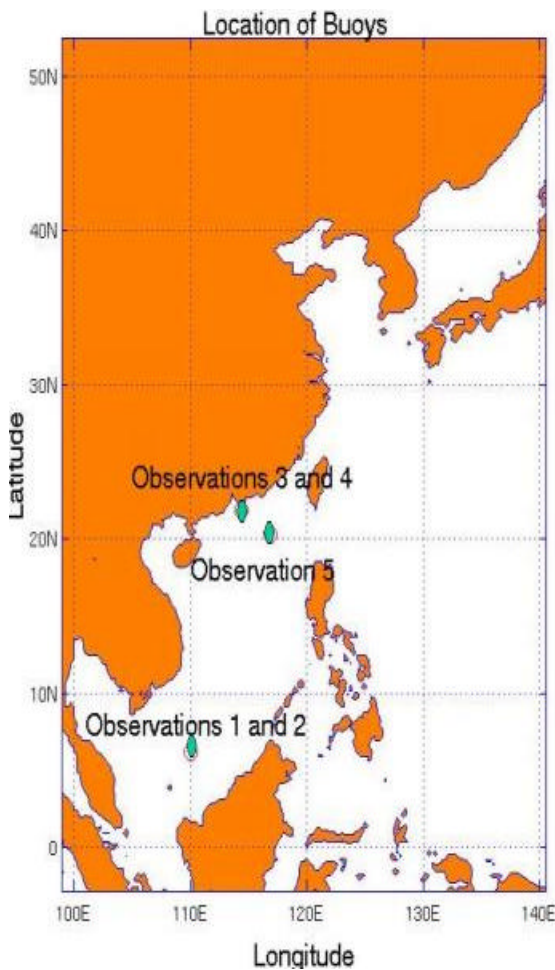
YES 10-m Winds for July 25, 1998

CENTRA FROM 90.00 TO 180.00 LATTER INTERVAL OF 3.0000 PTL:01- 1801.0

THIS PAGE INTENTIONALLY LEFT BLANK

APPENDIX O. SAMPLES OF SST VERIFICATION

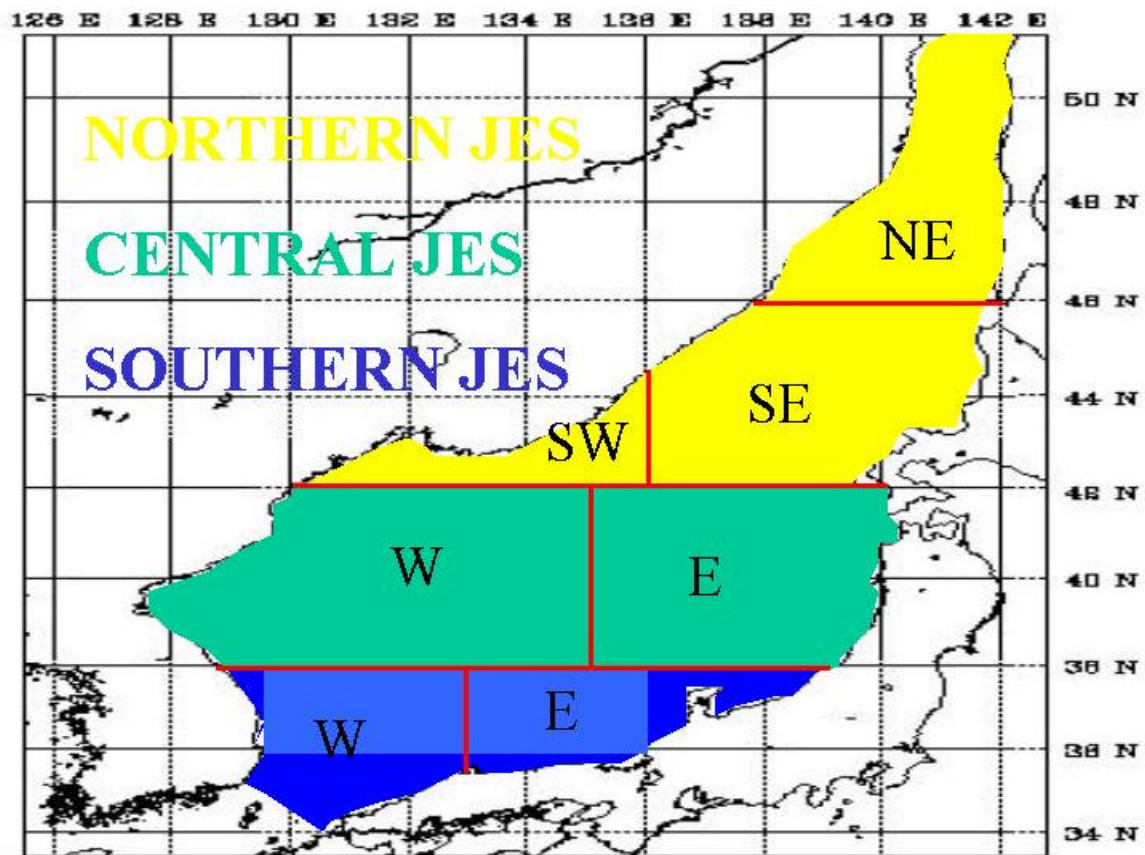
Appendix O consists of three figures that show verification of CAOCS oceanic component output. The left figure is the location of the buoy stations. The right top figure shows the CAOCS SST values in red and buoy station number 1 recorded SST values for the time period May 5 through May 26. The right bottom figure shows the CAOCS SST values in red and buoy station number 3 recorded SST values for the time period May 5 through May 21.

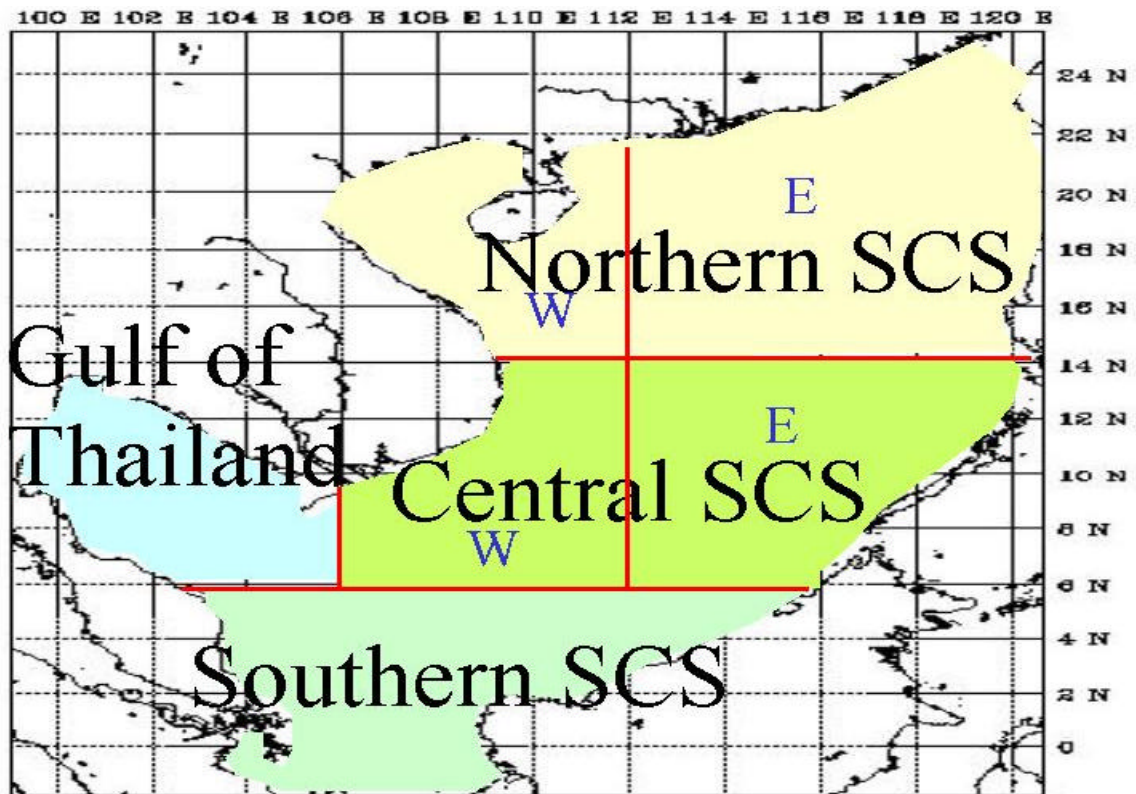
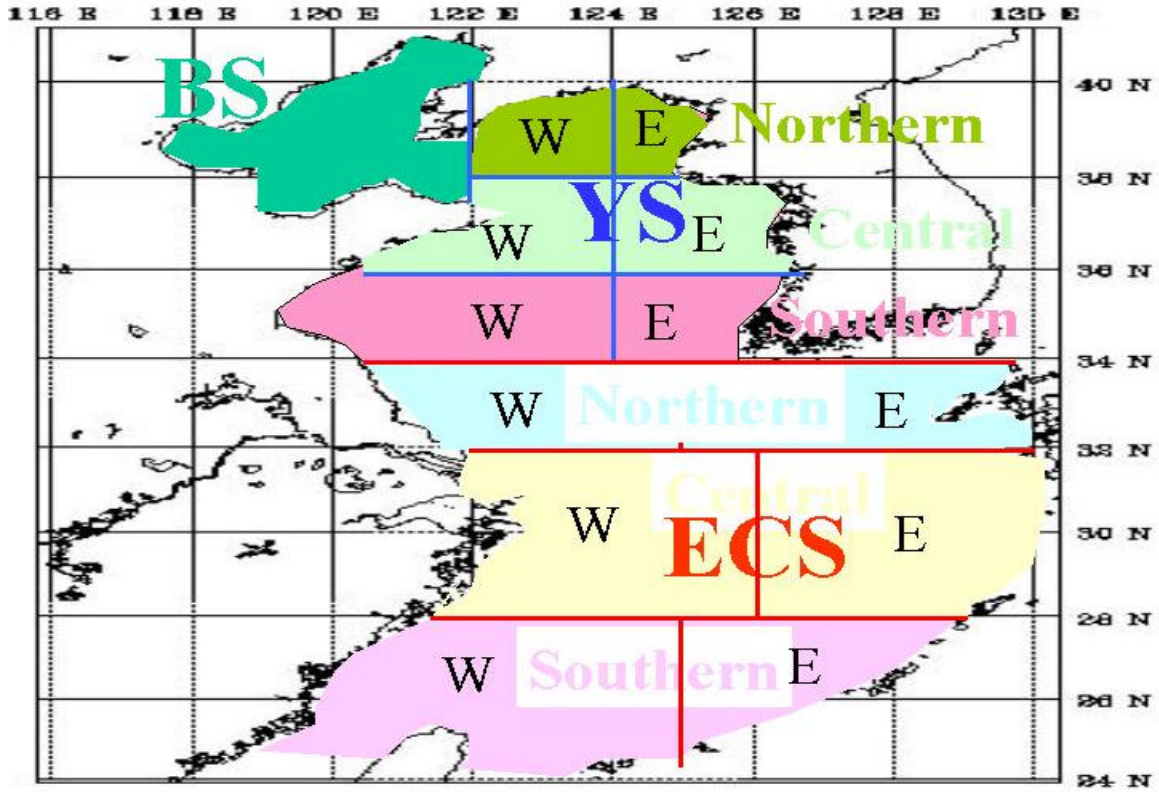


THIS PAGE INTENTIONALLY LEFT BLANK

APPENDIX P. SCS, YES, AND JES REGIONS FOR DISCUSSION OF ATMOSPHERIC AND OCEANIC PROCESSES

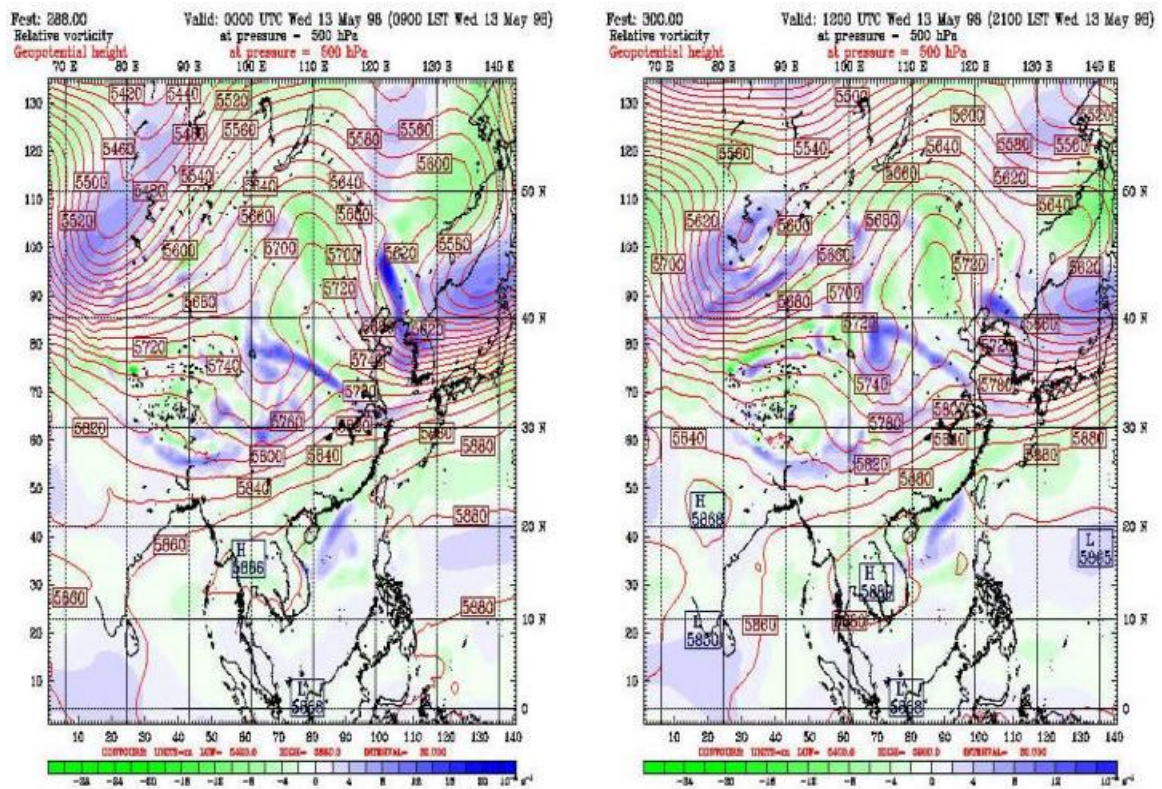
Appendix P consists of three figures that show how the YES, JES, and SCS were broken down into regions in order to facilitate discussion of atmospheric and oceanographic processes. Regions of each sea are color coded for identification. The first figure is for the JES, then the YES, and lastly the SCS.

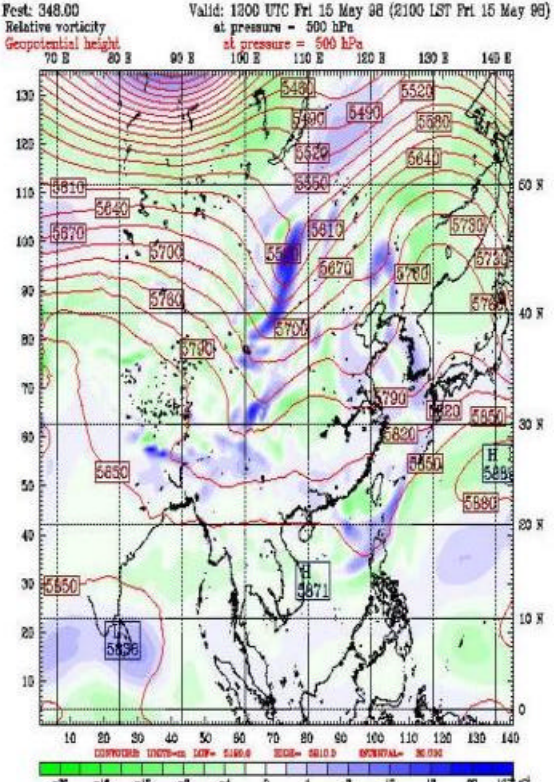
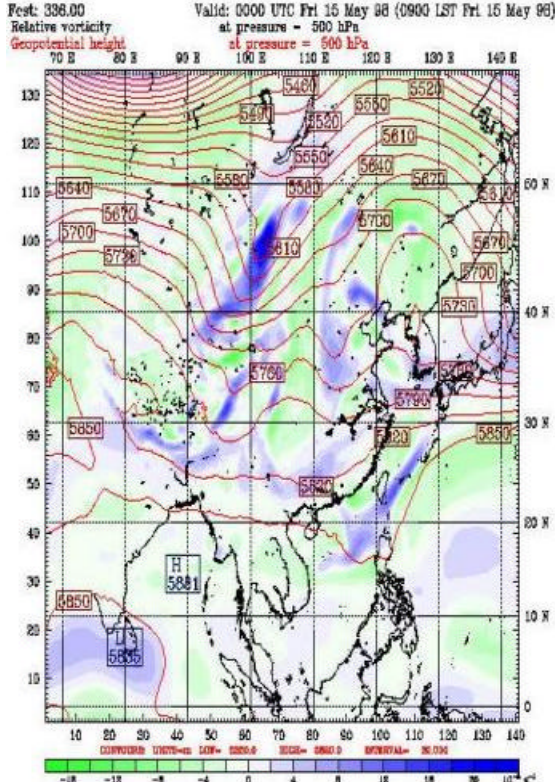
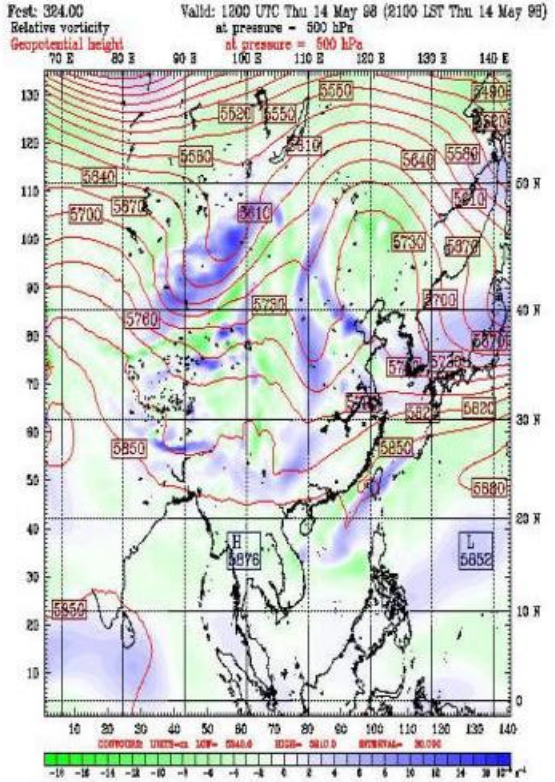
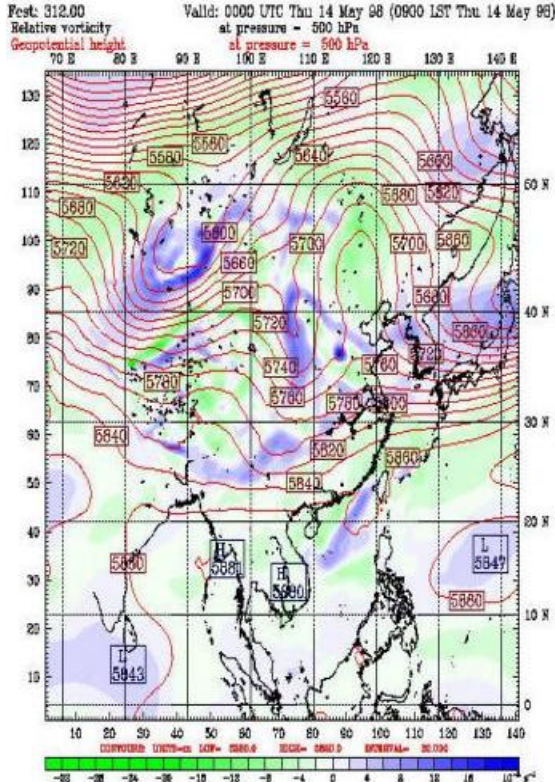


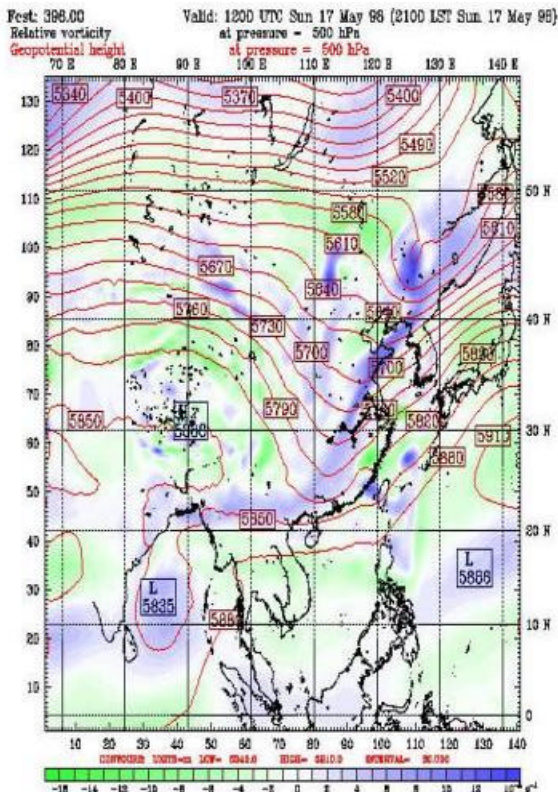
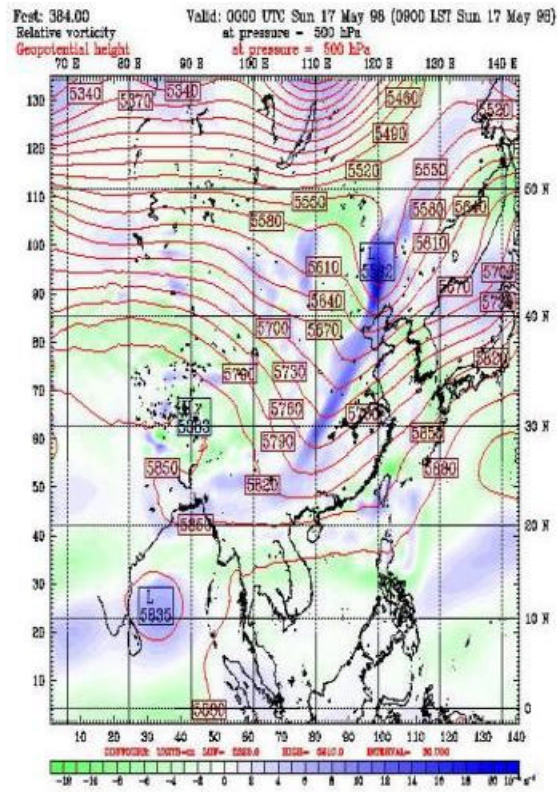
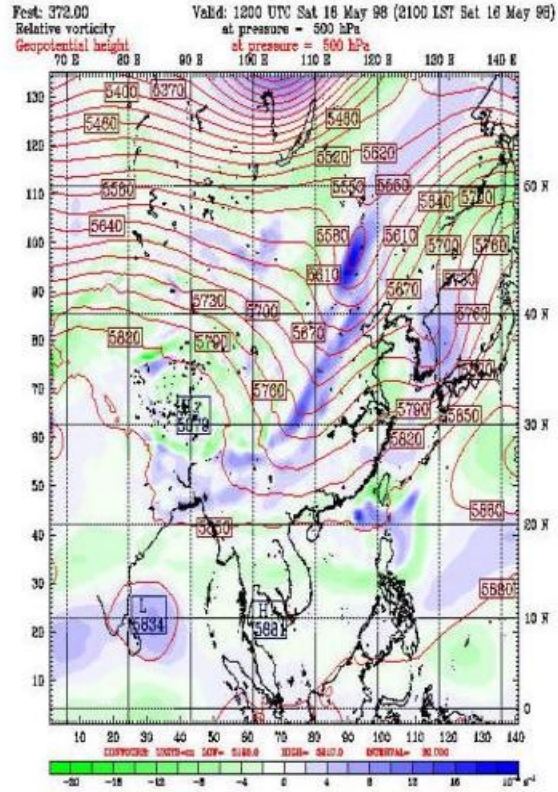
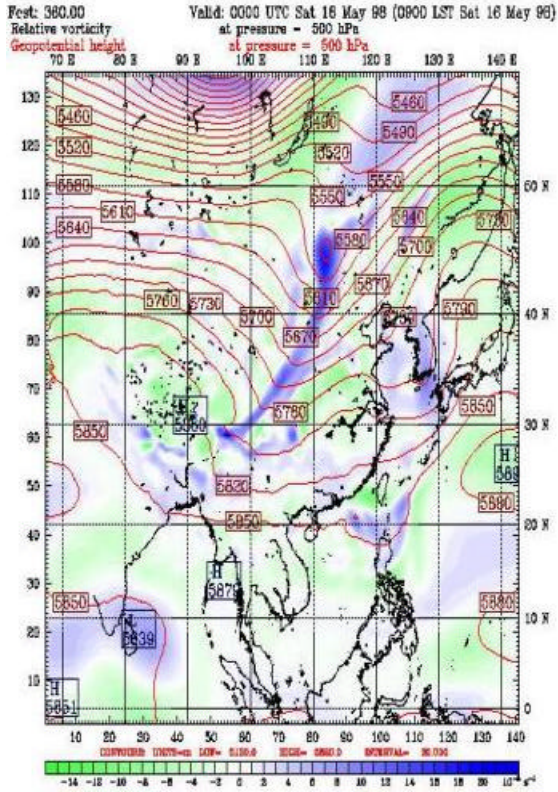


APPENDIX Q. 500-MB RELATIVE VORTICITY/GEOPOTENTIAL HEIGHT PLOTS OVER THE EAMS FOR THE MAY TIME PERIOD

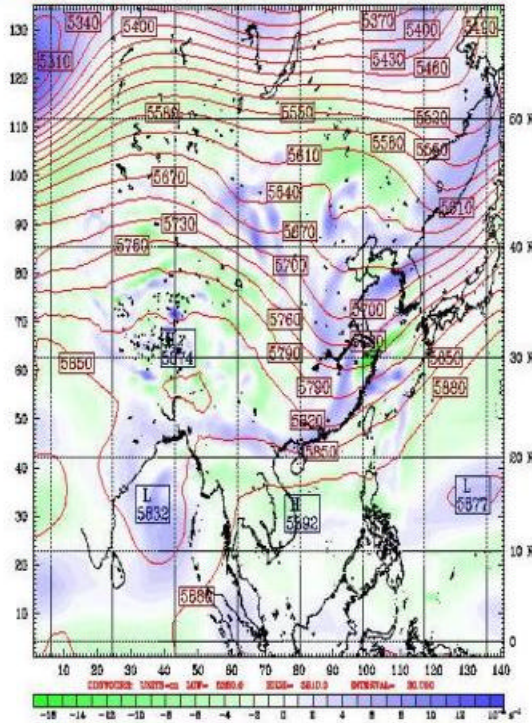
Appendix Q consists of 38 figures that show 500-mb relative vorticity and geopotential height for the May time period. The figures are in time sequential order with the left figure as the 00Z plot and the right figure as the 12Z plot from May 13 through May 31.



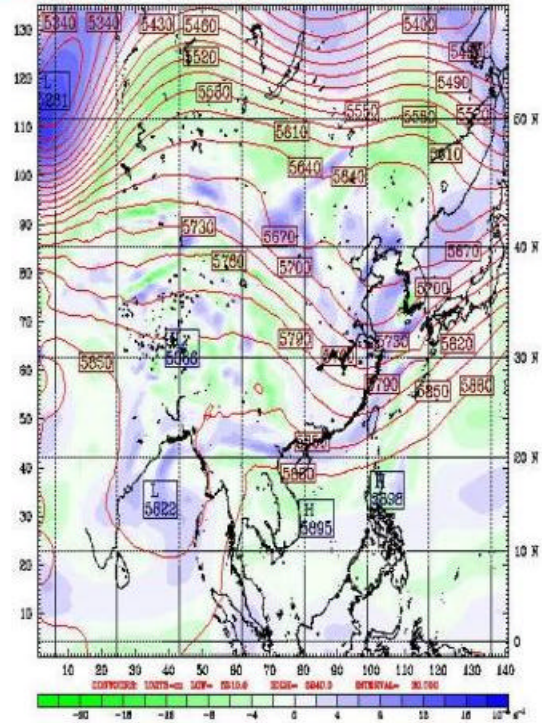




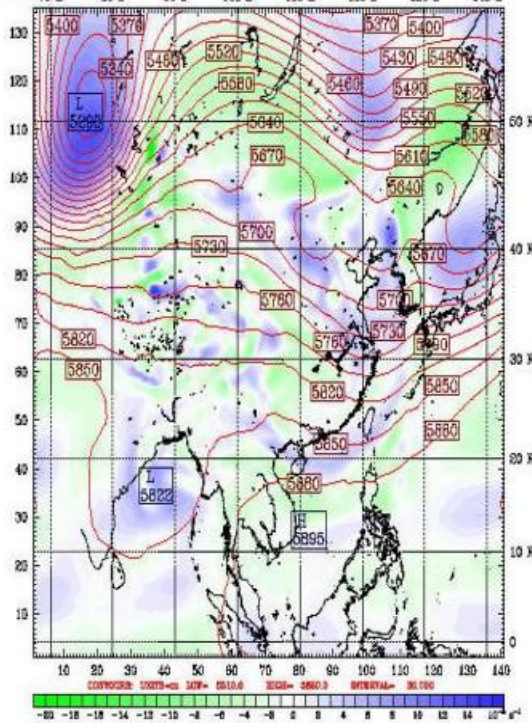
Feet: 408.00 Valid: 0000 UTC Mon 18 May 98 (0900 LST Mon 18 May 98)
Relative vorticity at pressure = 500 hPa
Geopotential height at pressure = 500 hPa



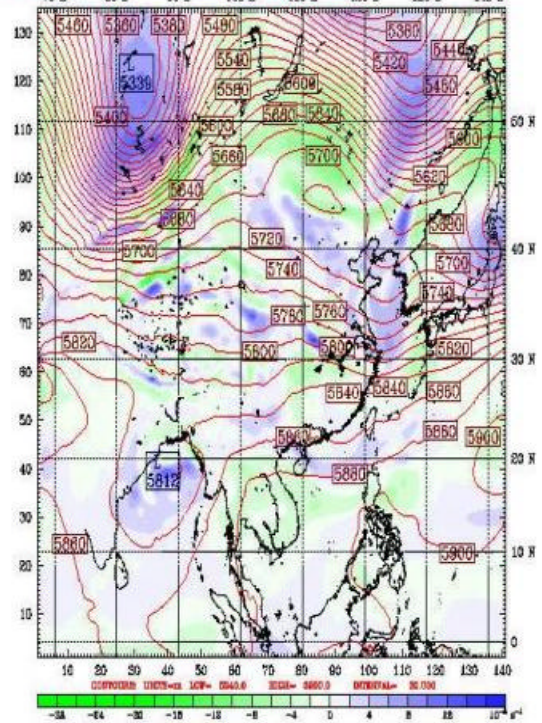
Feet: 420.00 Valid: 1200 UTC Mon 18 May 98 (2100 LST Mon 18 May 98)
Relative vorticity at pressure = 500 hPa
Geopotential height at pressure = 500 hPa

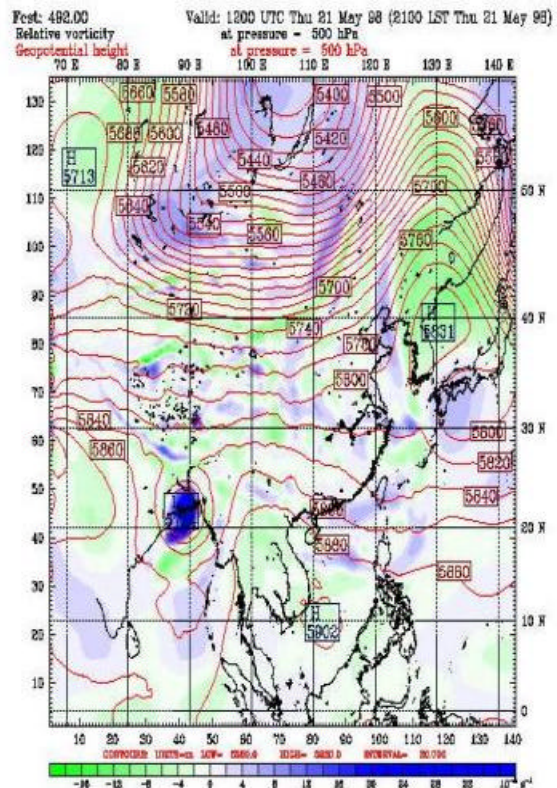
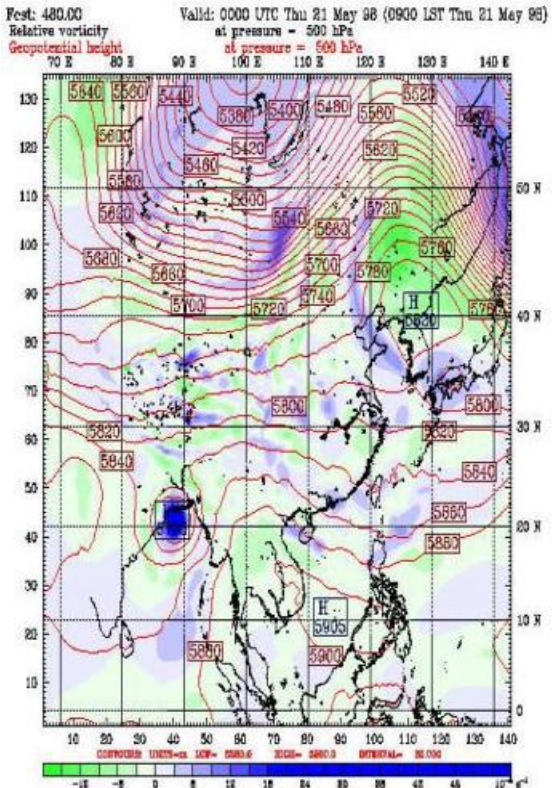
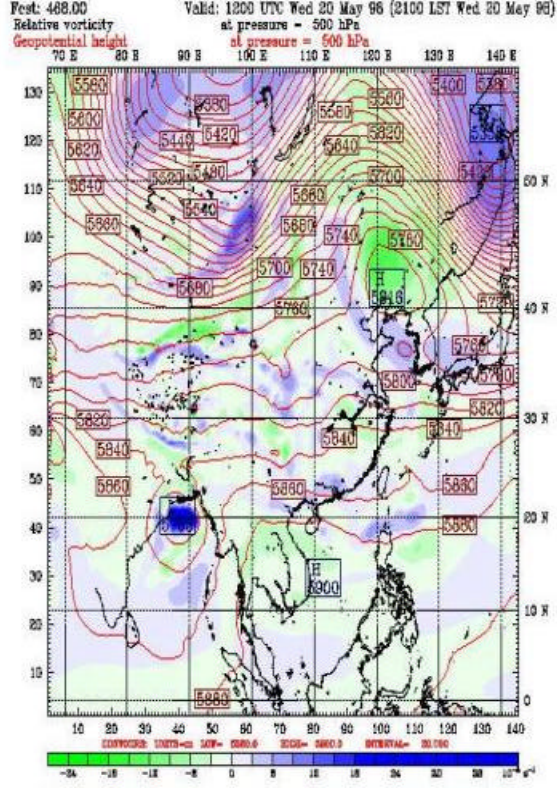
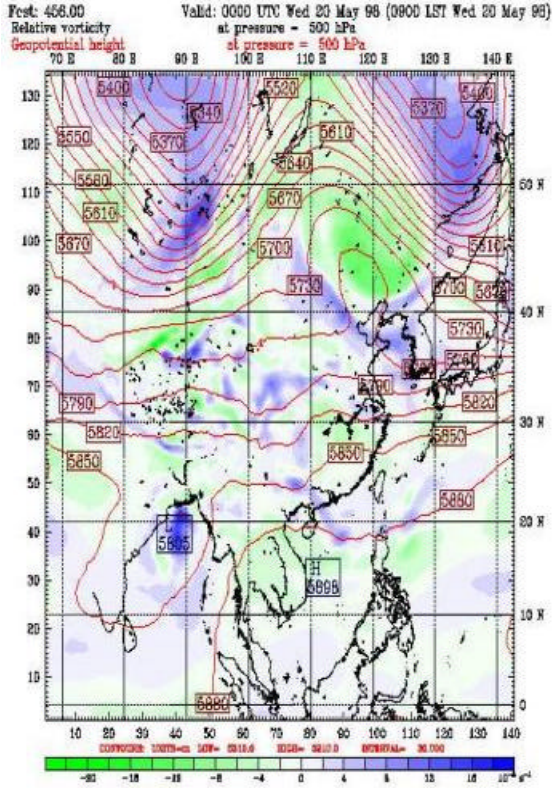


Feet: 432.00 Valid: 0000 UTC Tue 19 May 98 (0900 LST Tue 19 May 98)
Relative vorticity at pressure = 500 hPa
Geopotential height at pressure = 500 hPa

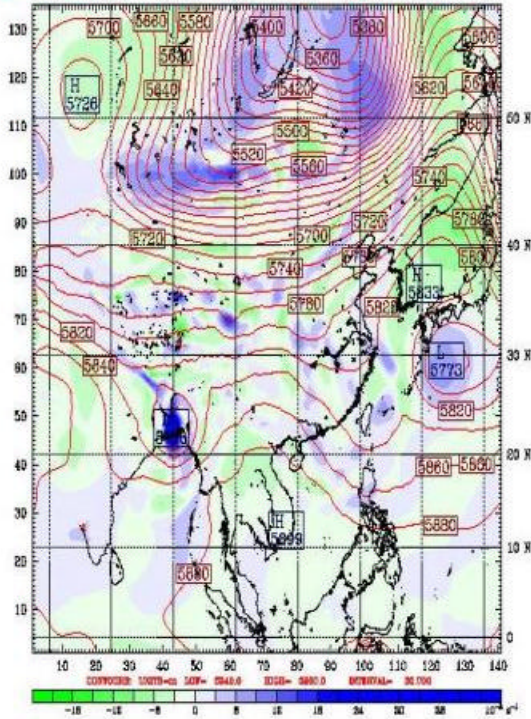


Feet: 444.00 Valid: 1200 UTC Tue 19 May 98 (2100 LST Tue 19 May 98)
Relative vorticity at pressure = 500 hPa
Geopotential height at pressure = 500 hPa

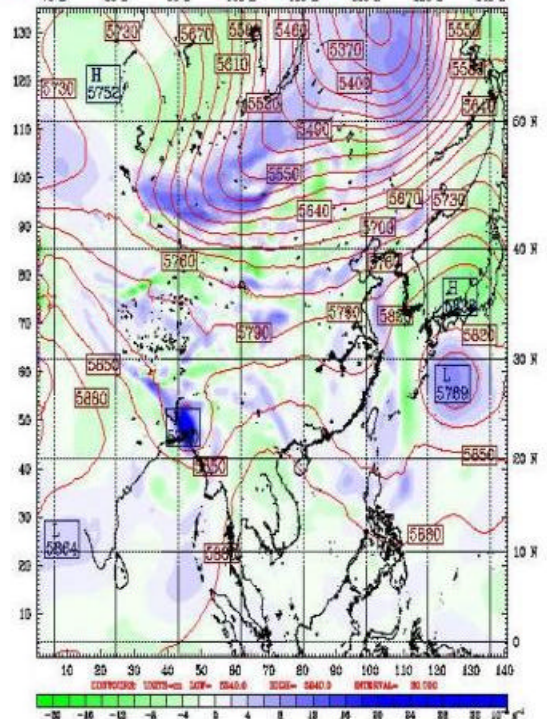




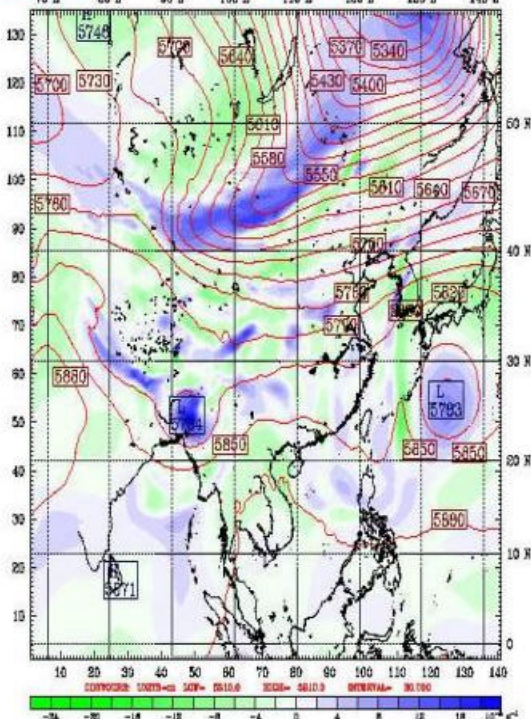
Feet: 504.00 Valid: 0000 UTC Fri 22 May 88 (0900 LST Fri 22 May 88)
 Relative vorticity at pressure = 500 hPa
 Geopotential height at pressure = 500 hPa



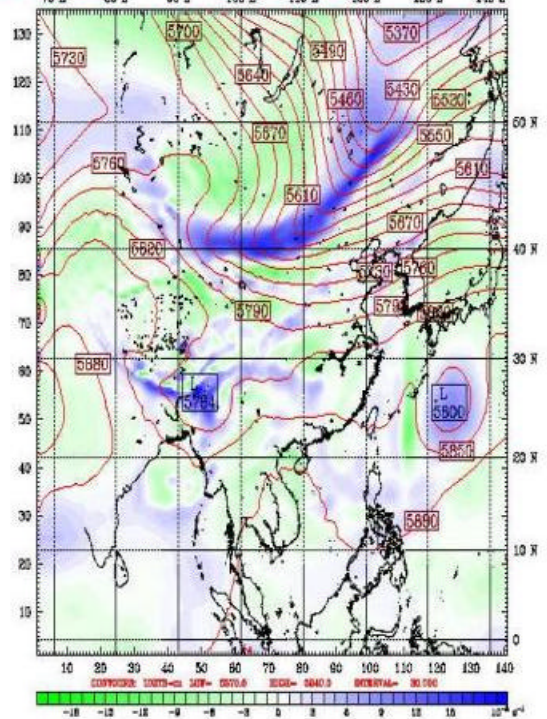
Feet: 516.00 Valid: 1200 UTC Fri 22 May 88 (2100 LST Fri 22 May 88)
 Relative vorticity at pressure = 500 hPa
 Geopotential height at pressure = 500 hPa



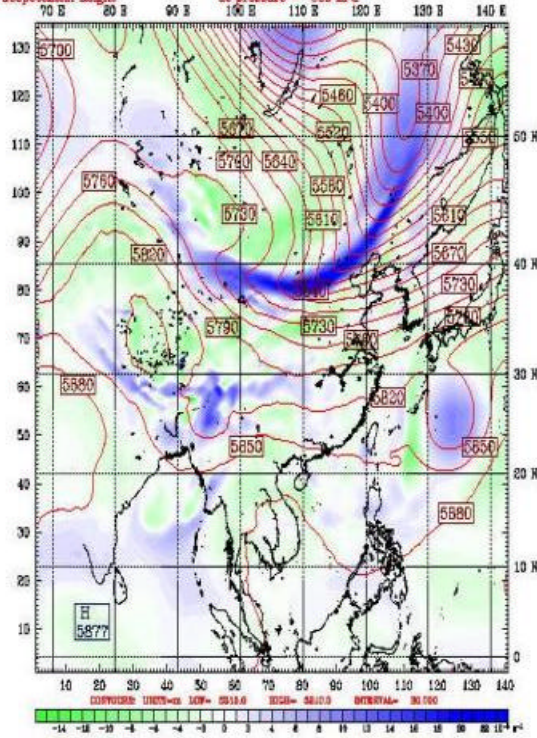
Feet: 528.00 Valid: 0000 UTC Sat 23 May 88 (0900 LST Sat 23 May 88)
 Relative vorticity at pressure = 500 hPa
 Geopotential height at pressure = 500 hPa



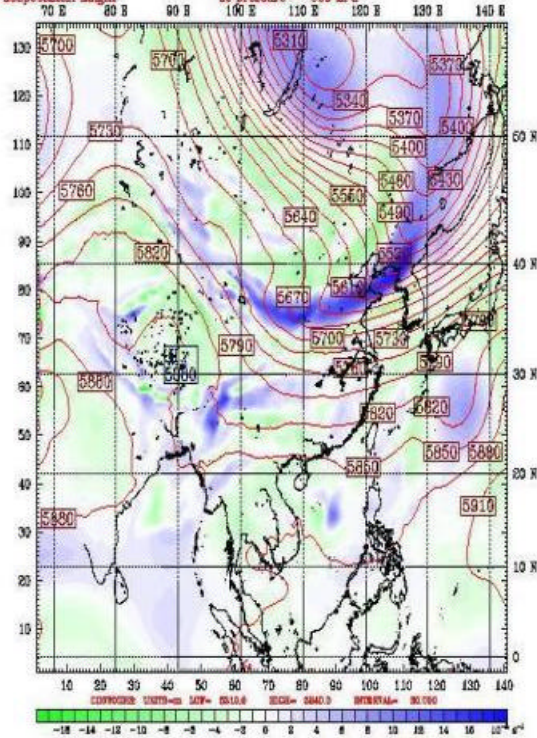
Feet: 540.00 Valid: 1200 UTC Sat 23 May 88 (2100 LST Sat 23 May 88)
 Relative vorticity at pressure = 500 hPa
 Geopotential height at pressure = 500 hPa



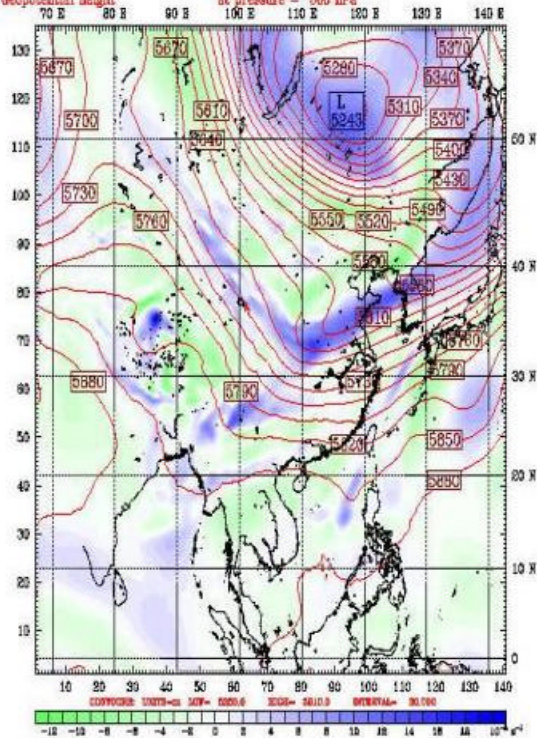
Best: 562.00 Valid: 0000 UTC Sun 24 May 96 (0900 LST Sun 24 May 96)
 Relative vorticity at pressure = 500 hPa
 Geopotential height at pressure = 500 hPa



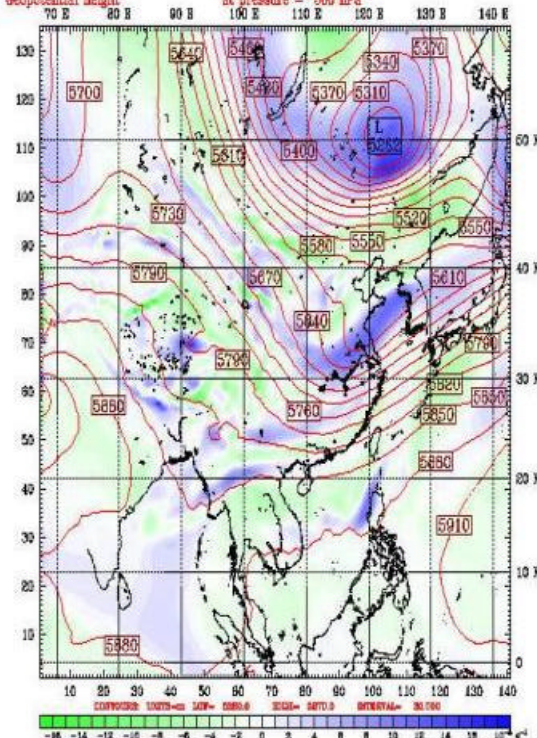
Best: 564.00 Valid: 1200 UTC Sun 24 May 96 (2100 LST Sun 24 May 96)
 Relative vorticity at pressure = 500 hPa
 Geopotential height at pressure = 500 hPa

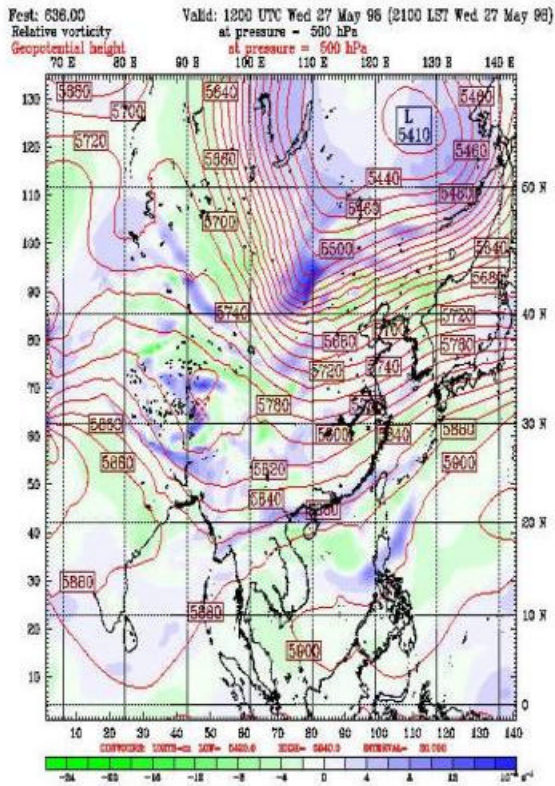
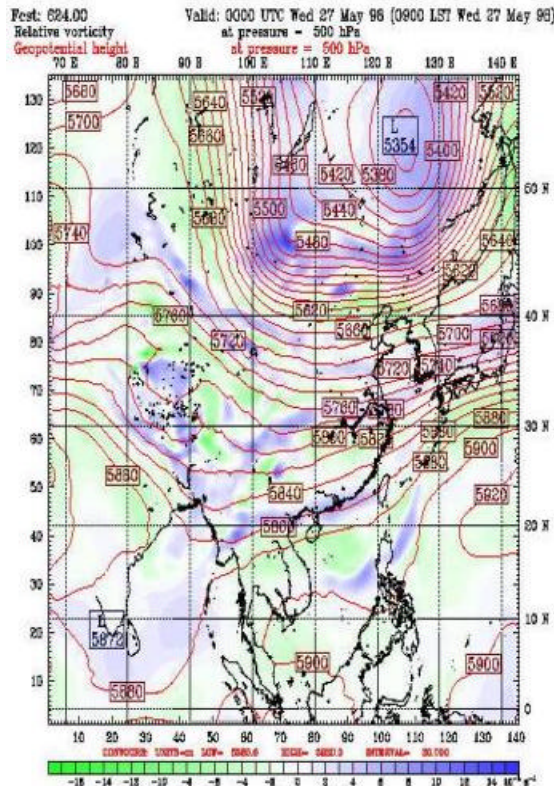
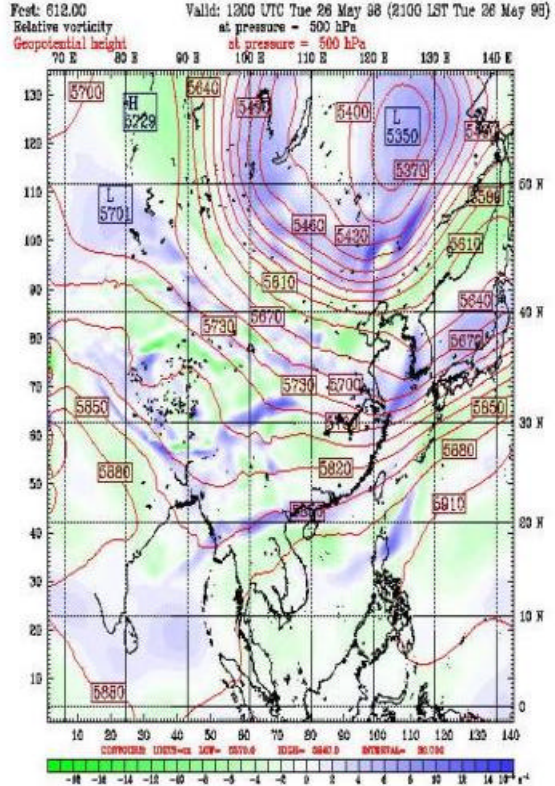
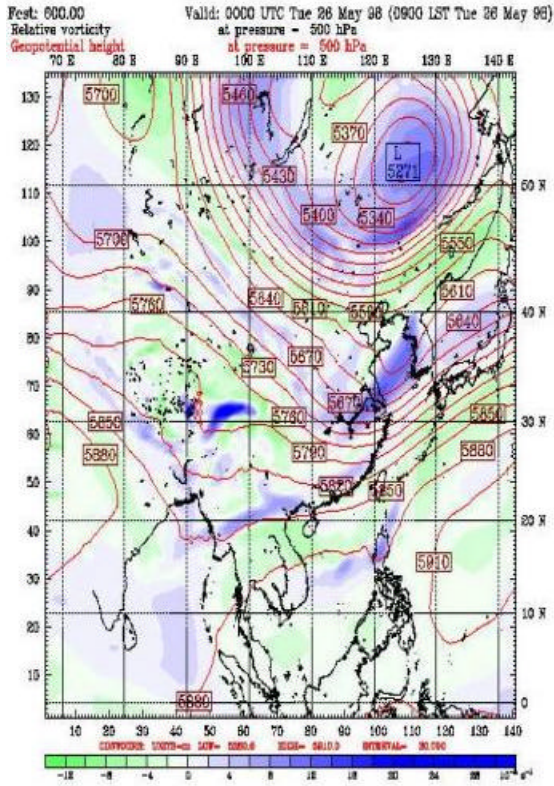


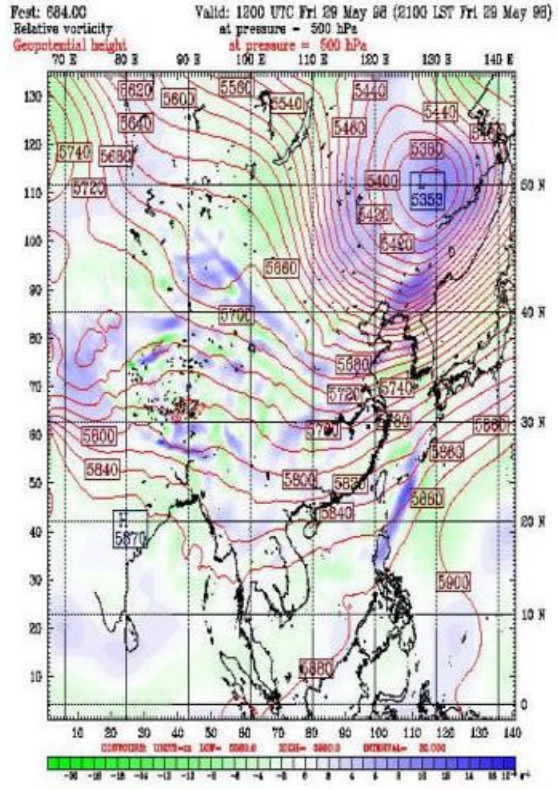
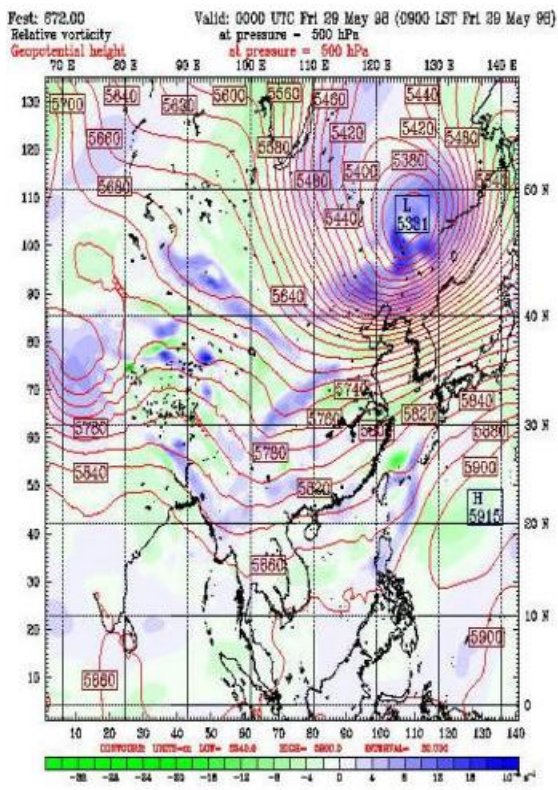
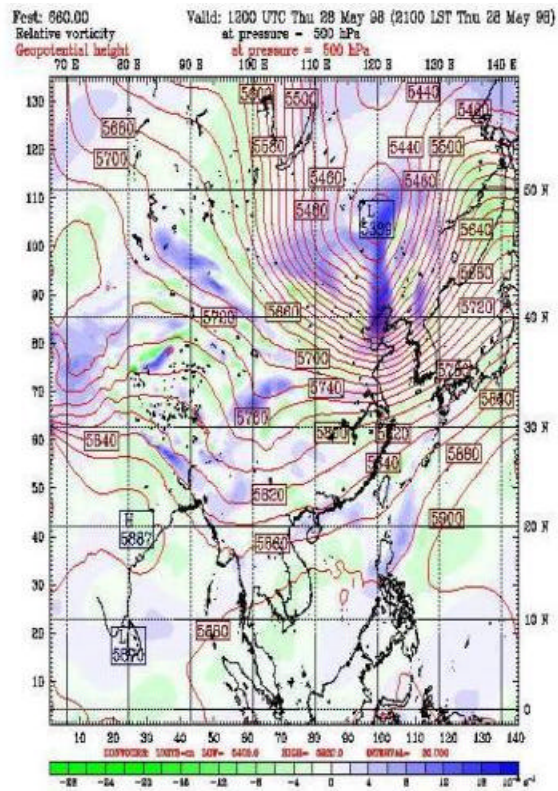
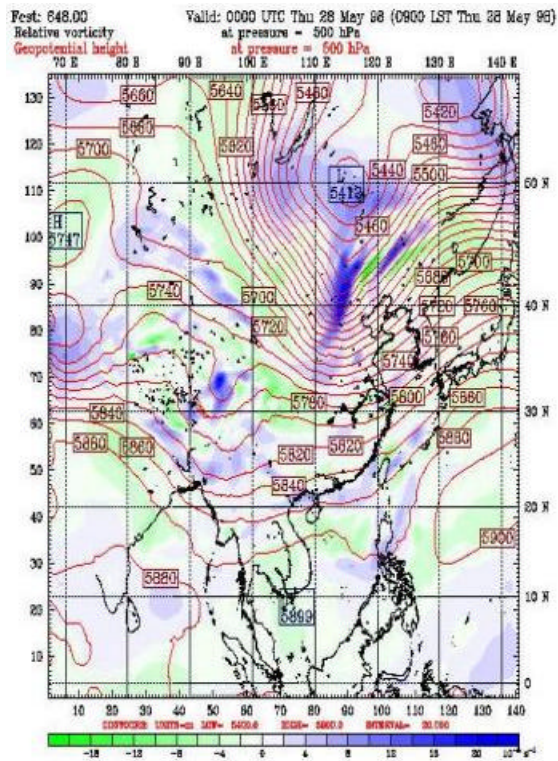
Best: 576.00 Valid: 0000 UTC Mon 25 May 96 (0900 LST Mon 25 May 96)
 Relative vorticity at pressure = 500 hPa
 Geopotential height at pressure = 500 hPa

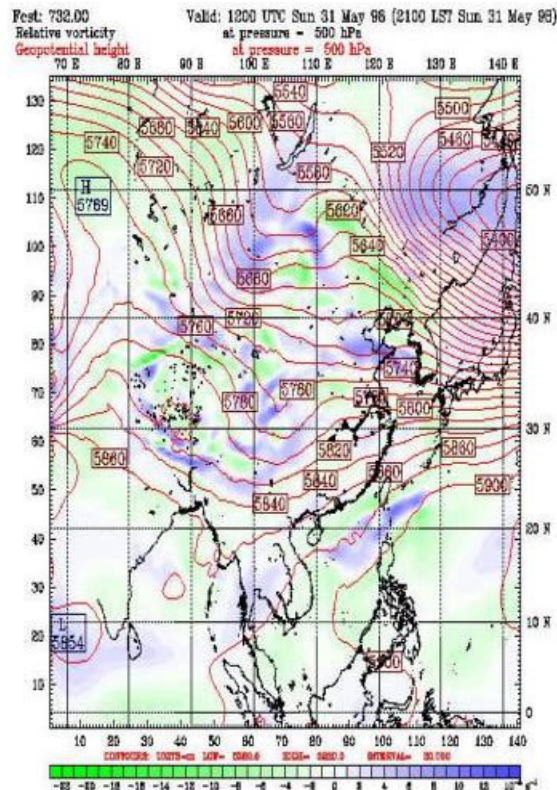
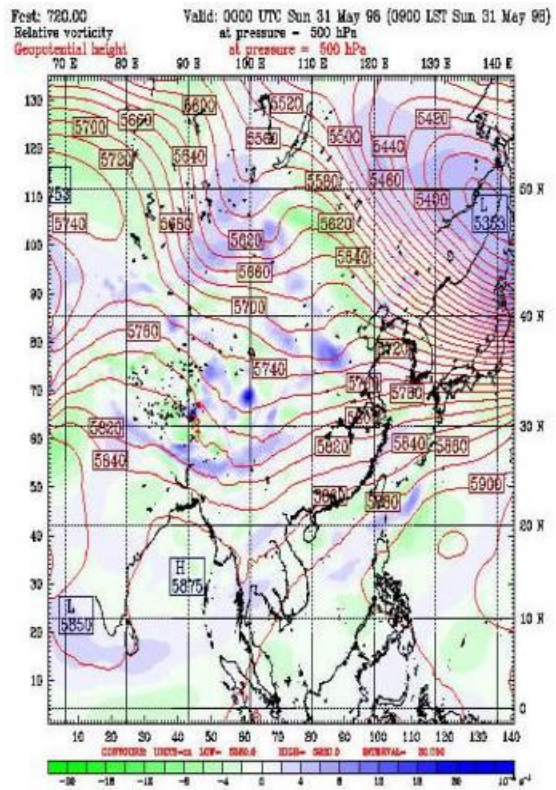
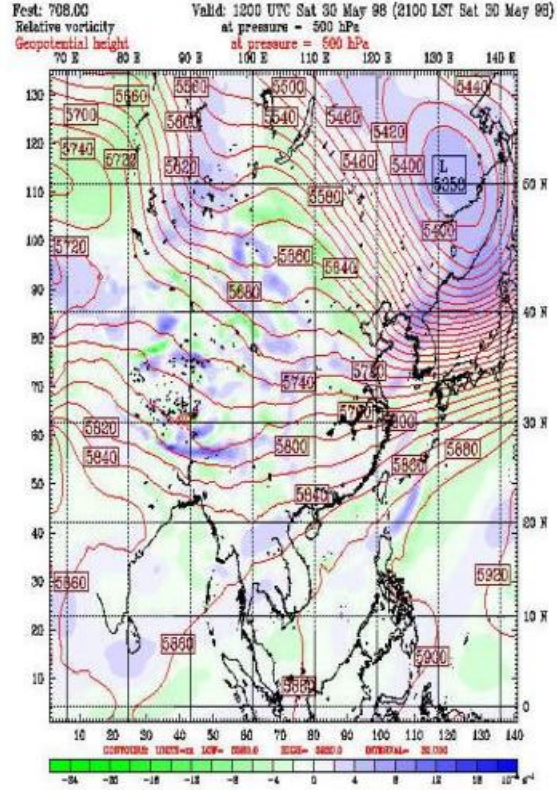
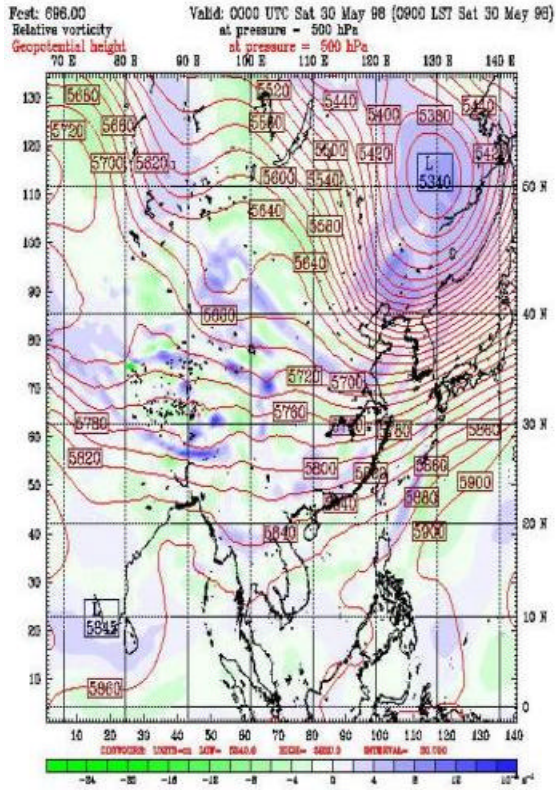


Best: 588.00 Valid: 1200 UTC Mon 25 May 96 (2100 LST Mon 25 May 96)
 Relative vorticity at pressure = 500 hPa
 Geopotential height at pressure = 500 hPa



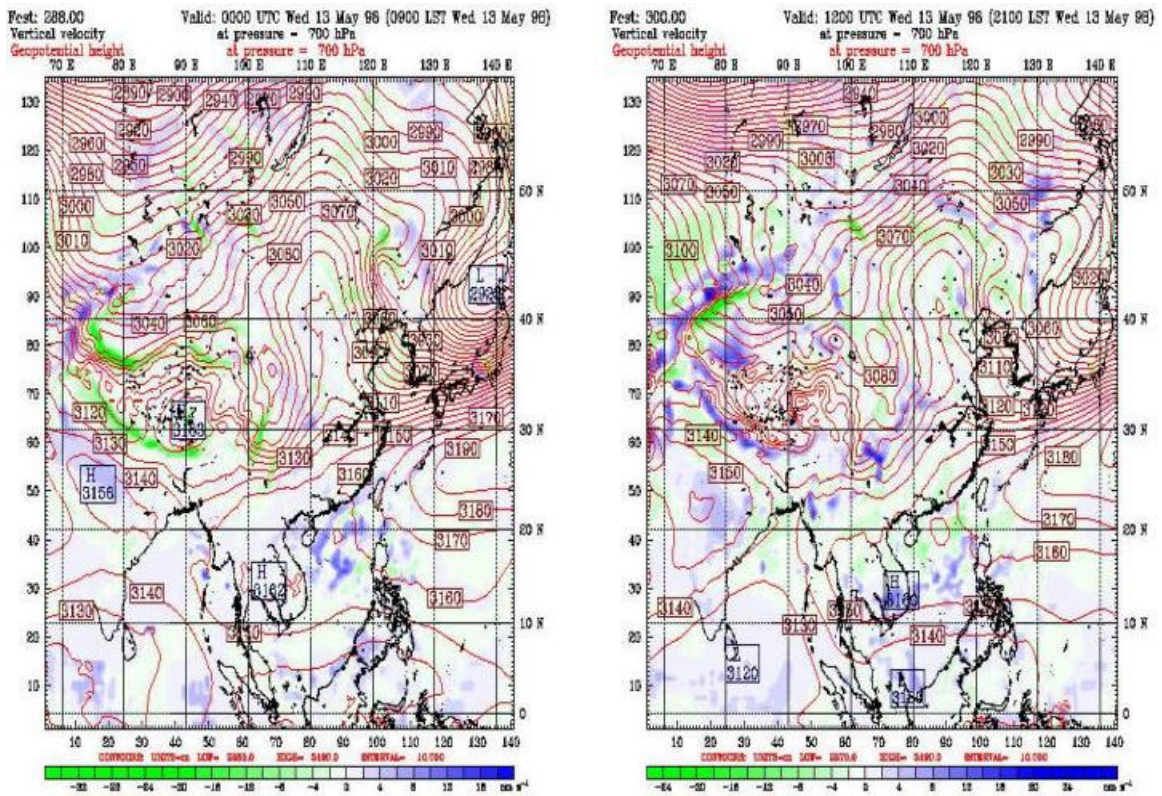


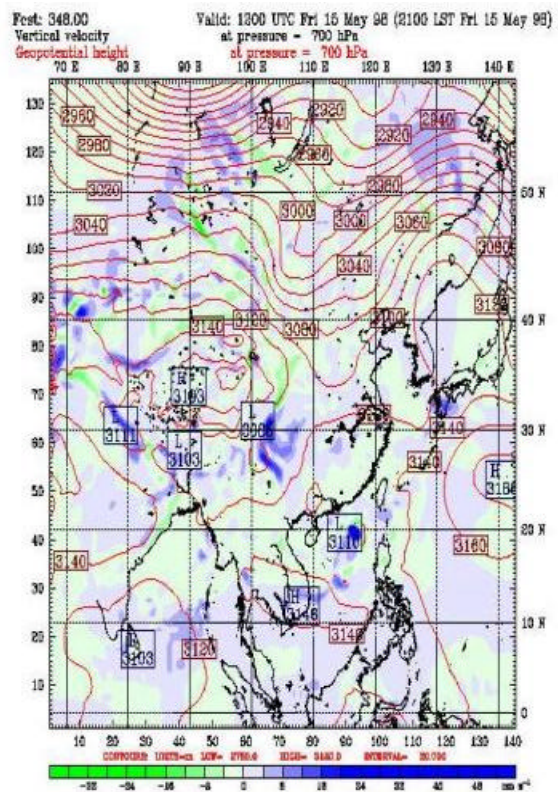
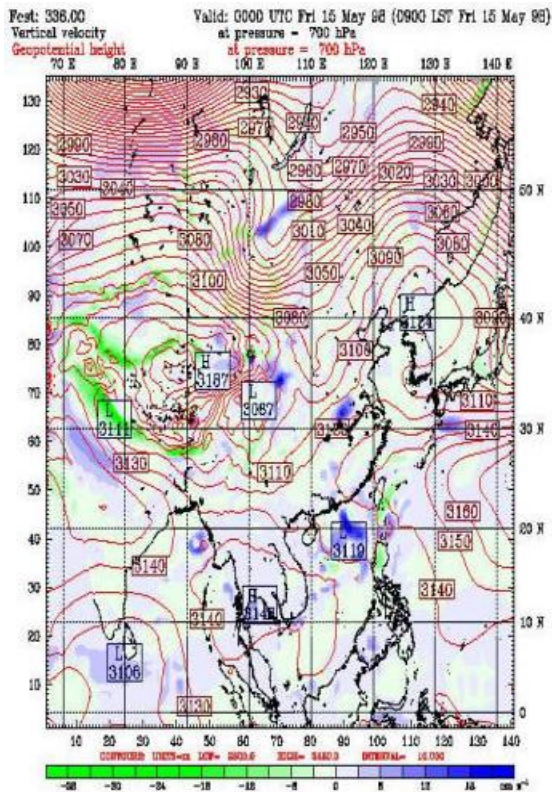
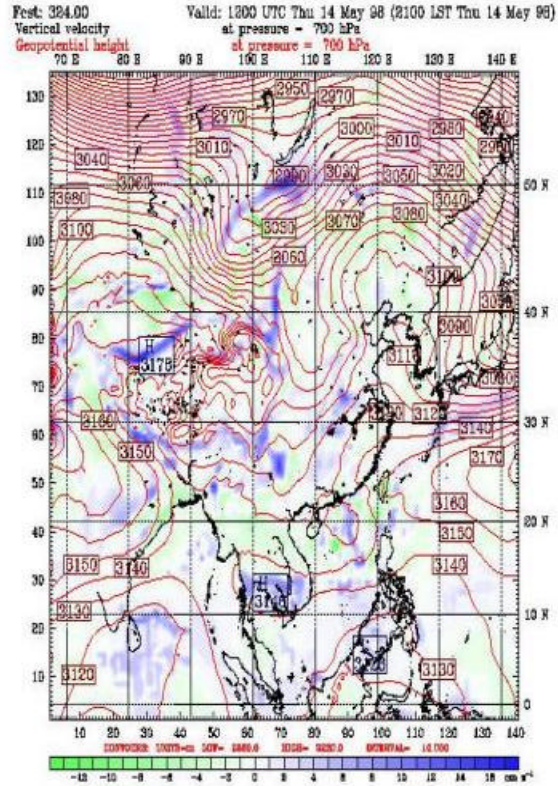
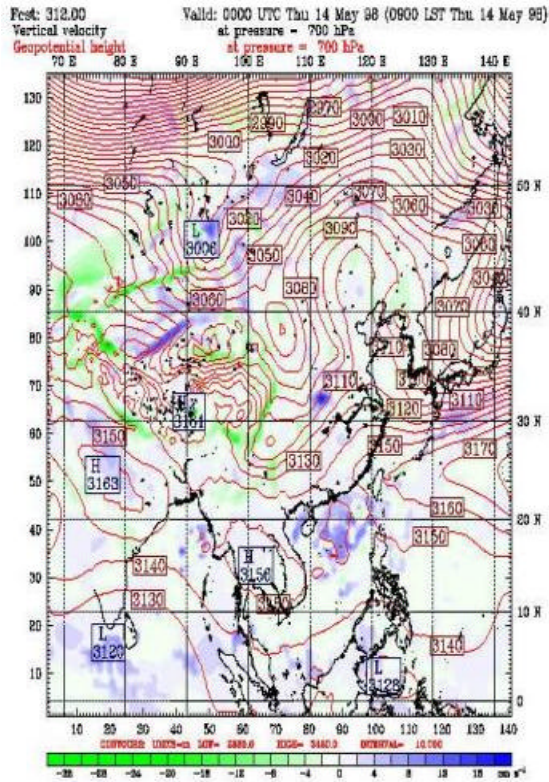




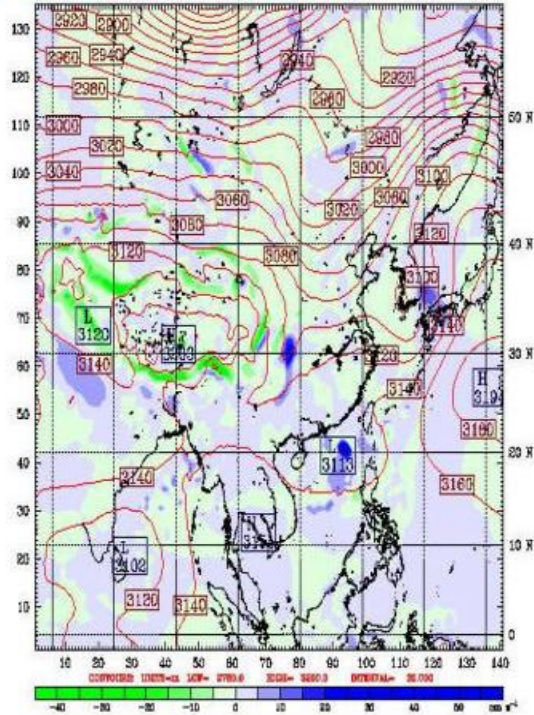
APPENDIX R. 700-MB VERTICAL VELOCITY/GEOPOTENTIAL HEIGHT PLOTS OVER THE EAMS FOR THE MAY TIME PERIOD

Appendix R consists of 38 figures that show 700-mb vertical velocity and geopotential height for the May time period. The figures are in time sequential order with the left figure as the 00Z plot and the right figure as the 12Z plot from May 13 through May 31.

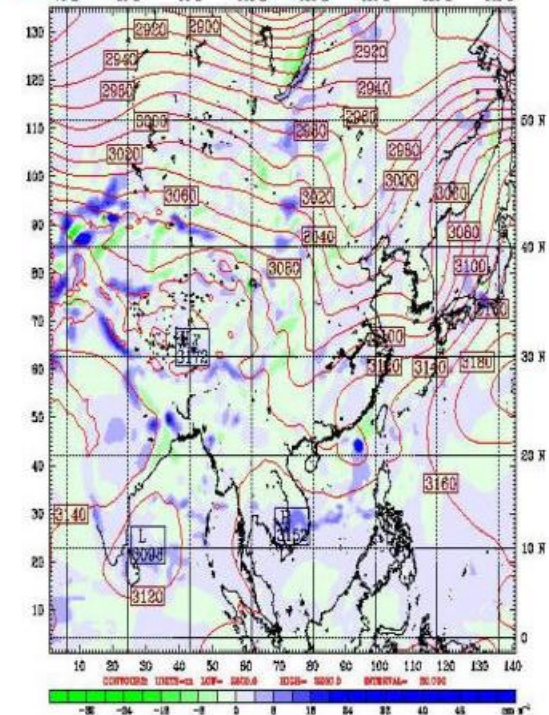




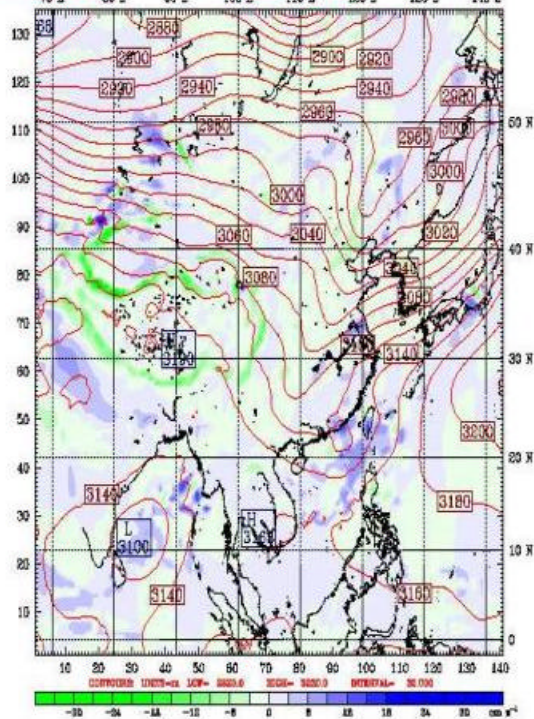
Feet: 360.00 Valid: 0000 UTC Sat 16 May 98 (0900 LST Sat 16 May 98)
 Vertical velocity at pressure = 700 hPa
 Geopotential height at pressure = 700 hPa



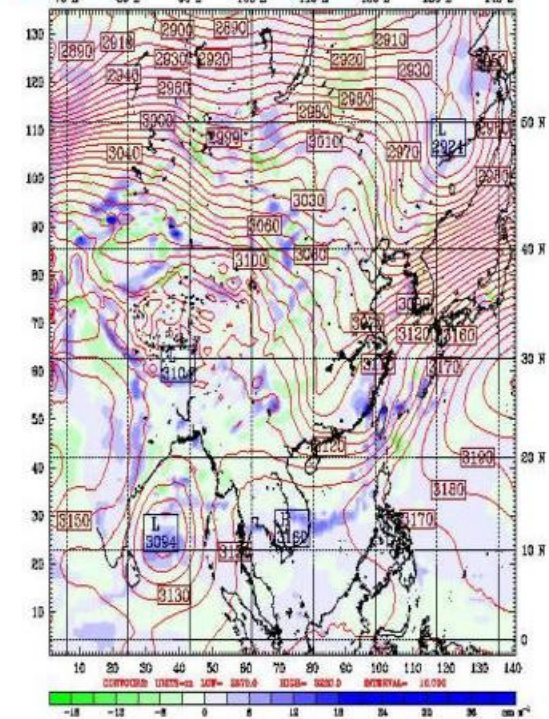
Feet: 372.00 Valid: 1200 UTC Sat 16 May 98 (2100 LST Sat 16 May 98)
 Vertical velocity at pressure = 700 hPa
 Geopotential height at pressure = 700 hPa

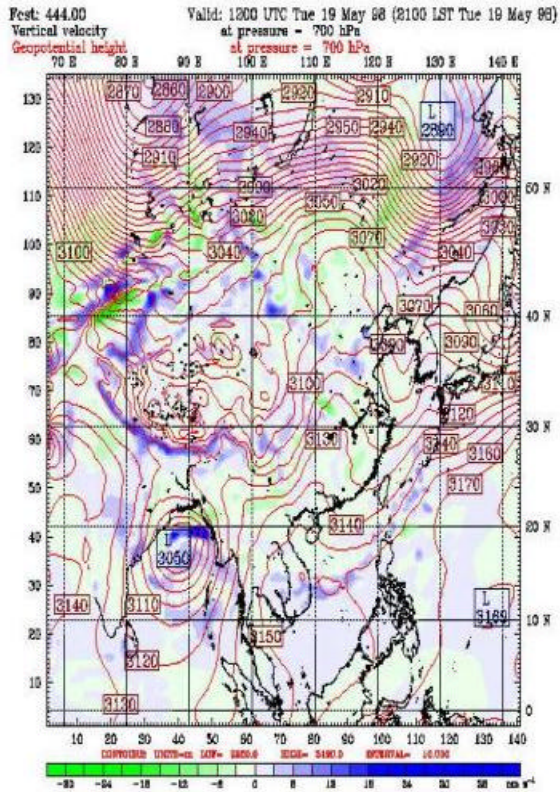
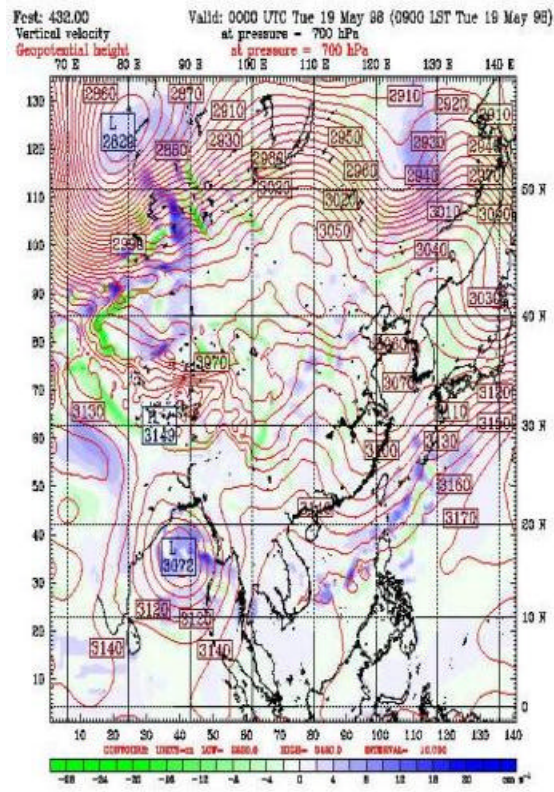
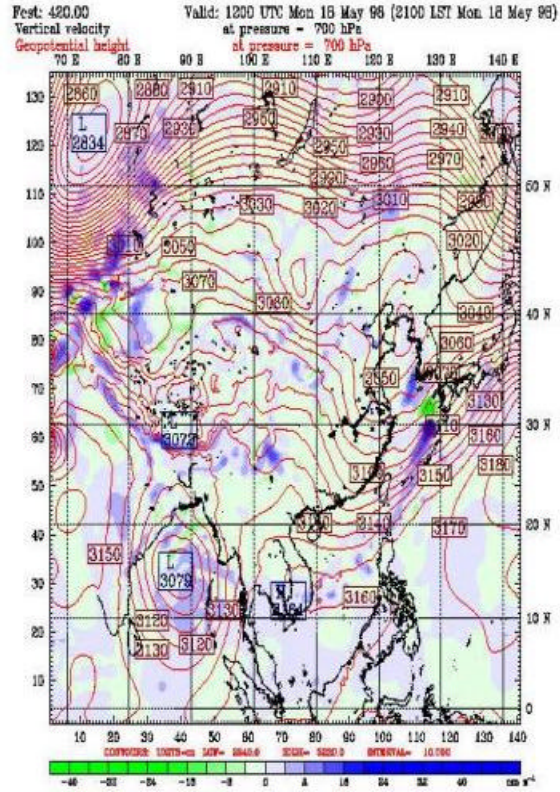
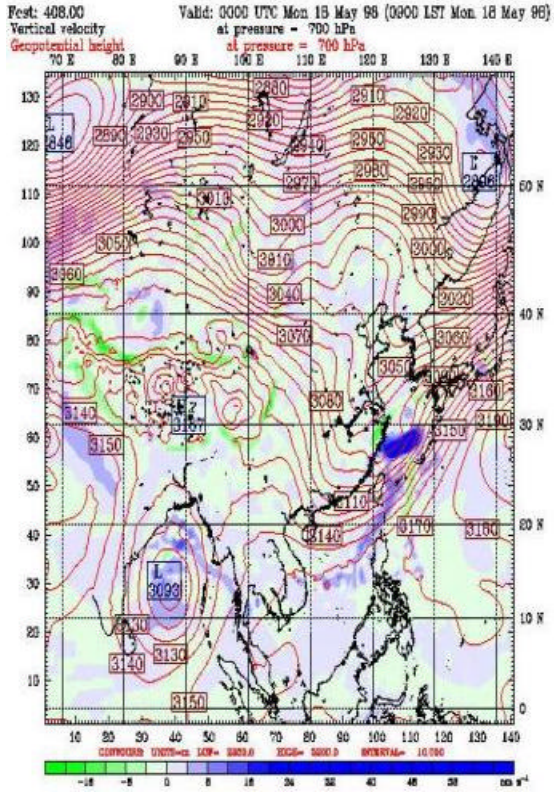


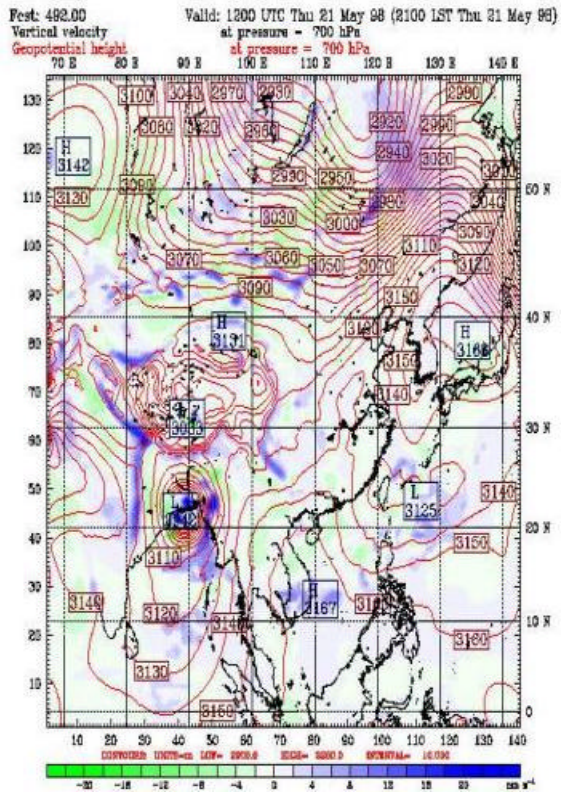
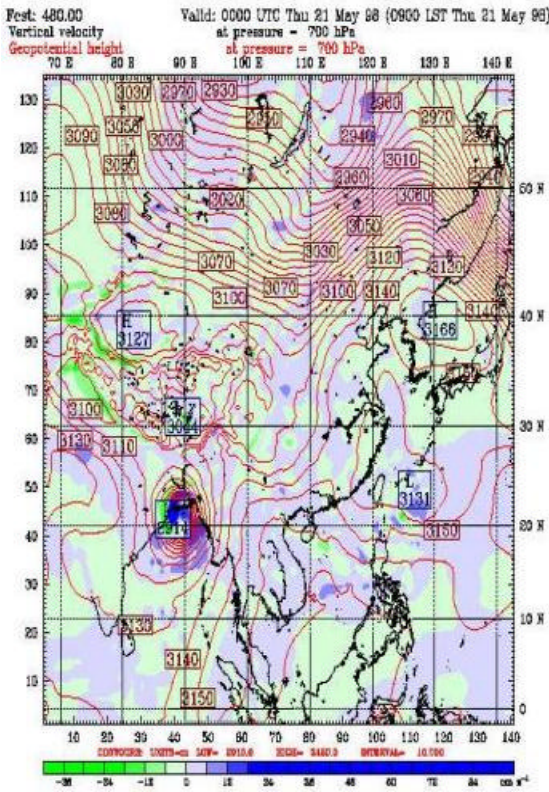
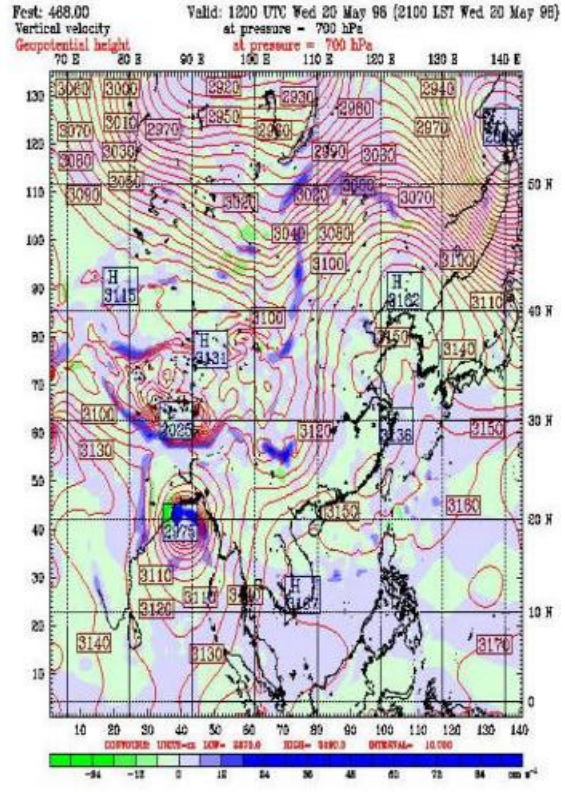
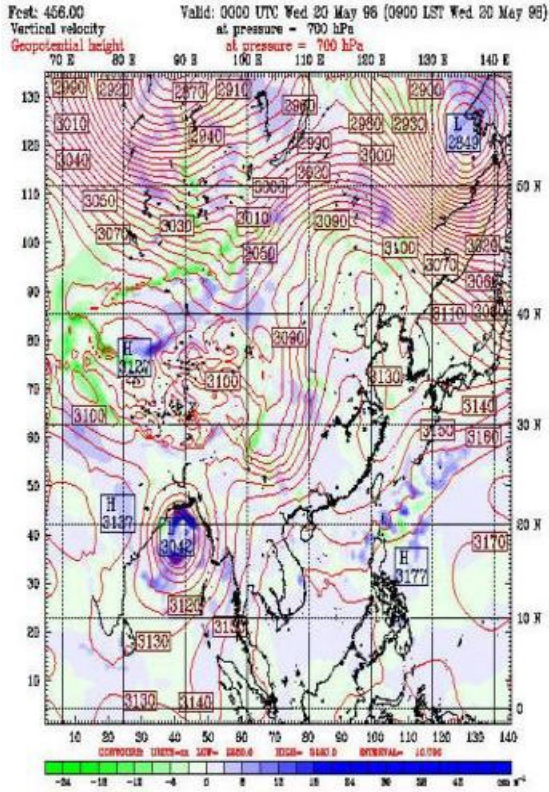
Feet: 384.00 Valid: 0000 UTC Sun 17 May 98 (0900 LST Sun 17 May 98)
 Vertical velocity at pressure = 700 hPa
 Geopotential height at pressure = 700 hPa

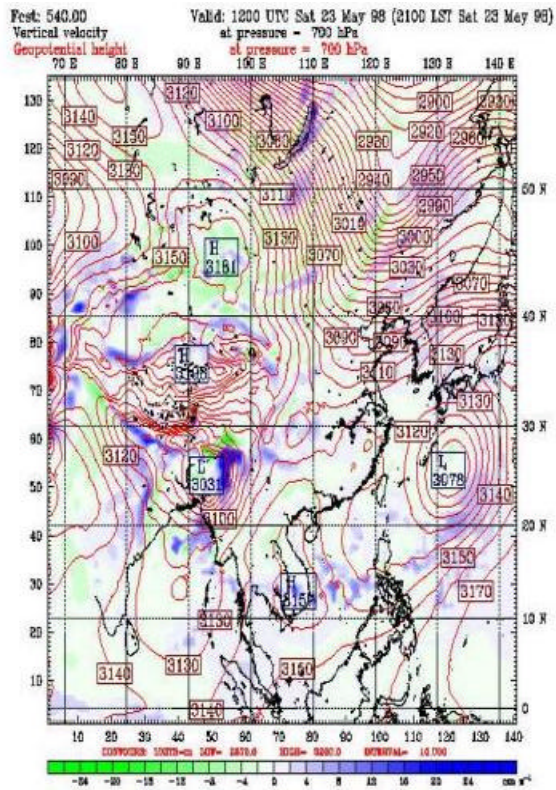
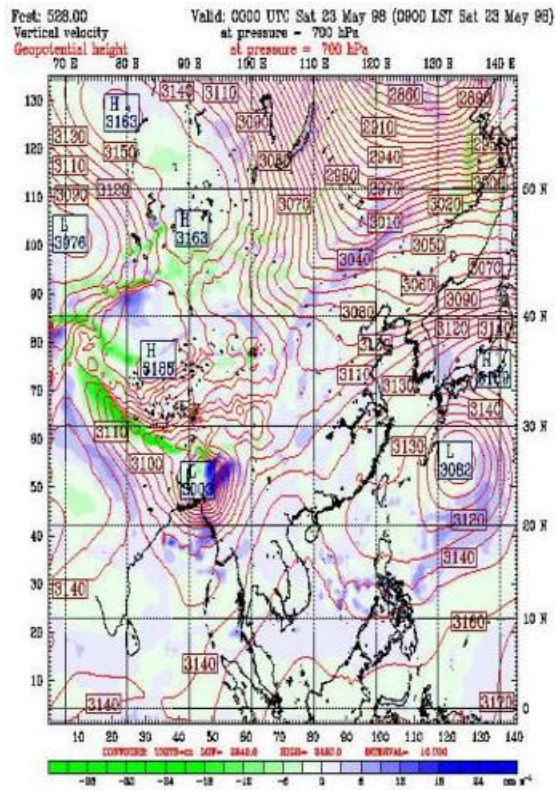
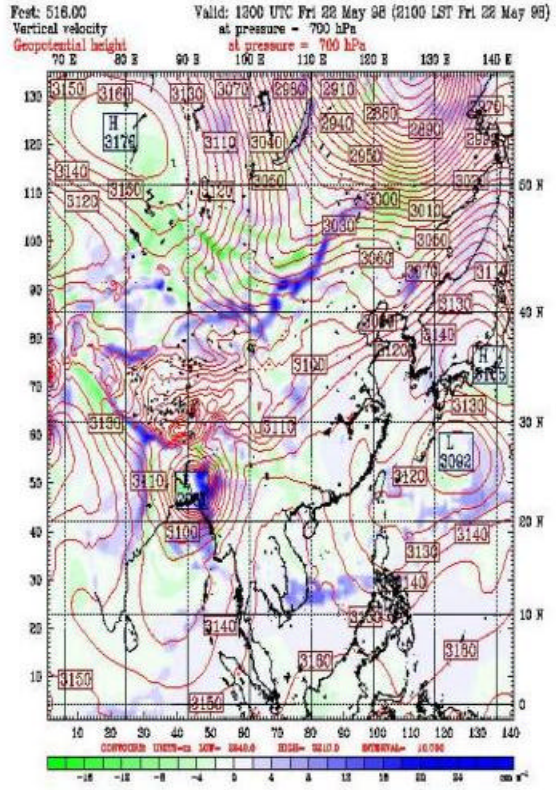
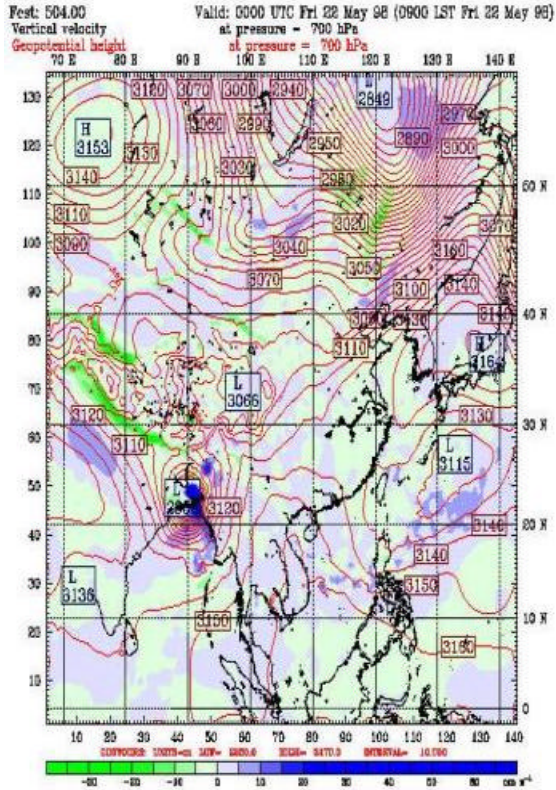


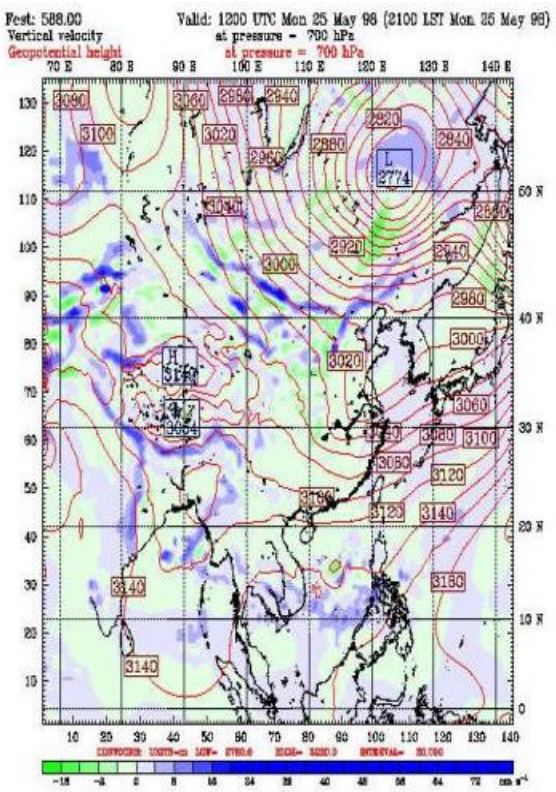
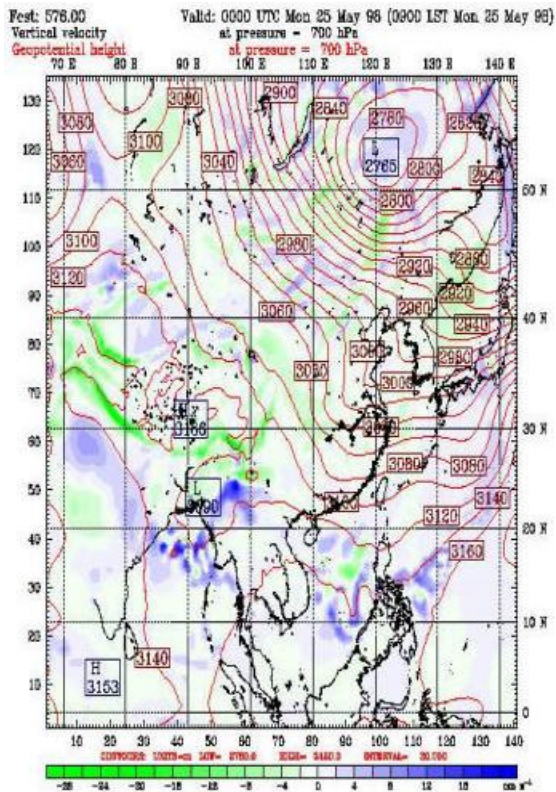
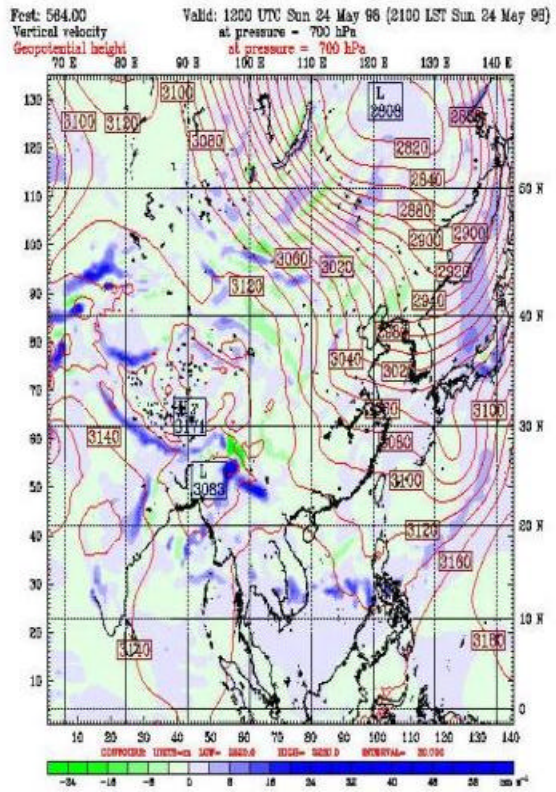
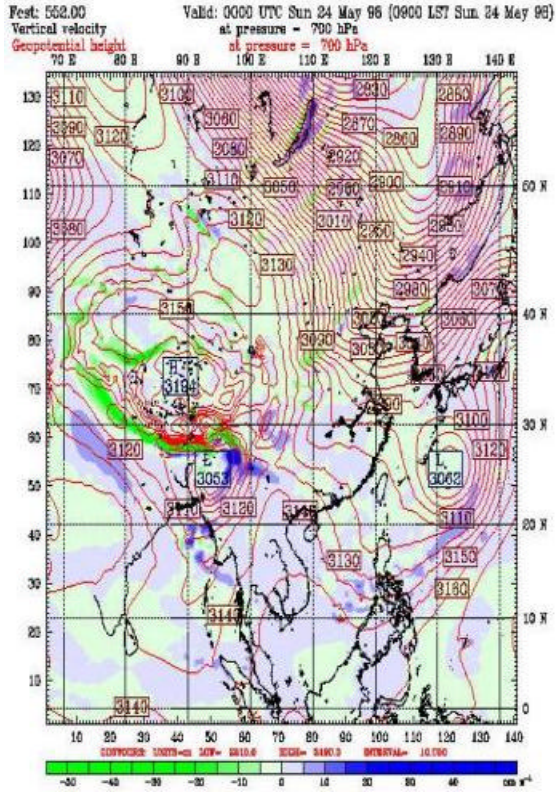
Feet: 386.00 Valid: 1200 UTC Sun 17 May 98 (2100 LST Sun 17 May 98)
 Vertical velocity at pressure = 700 hPa
 Geopotential height at pressure = 700 hPa

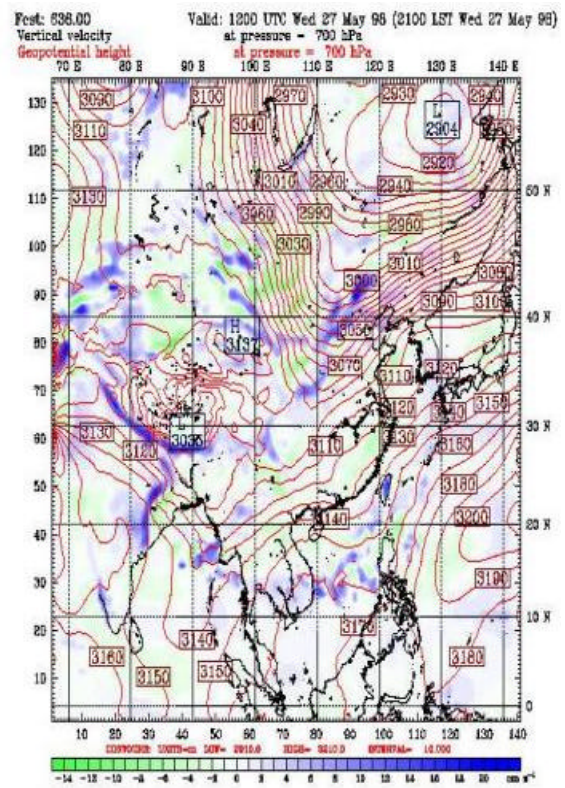
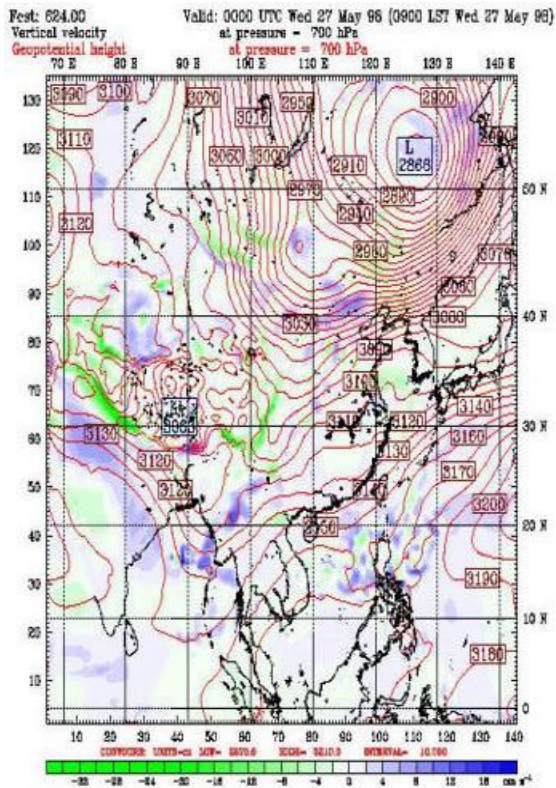
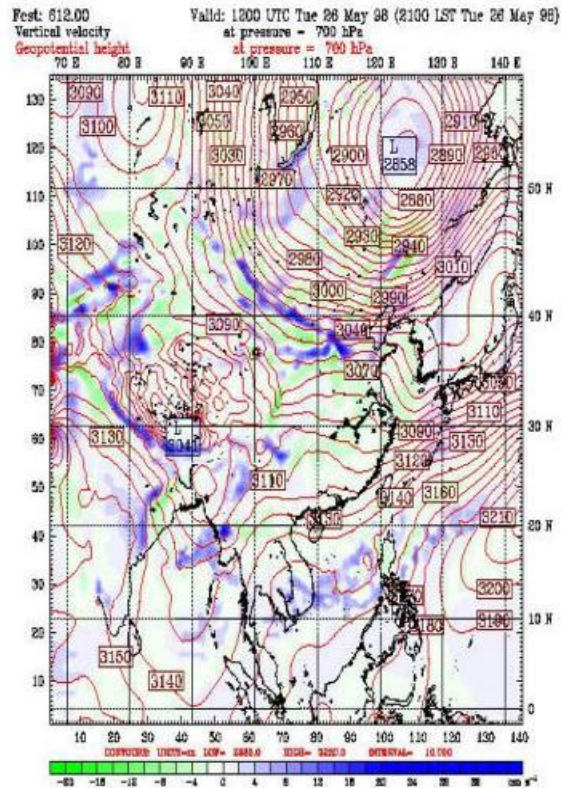
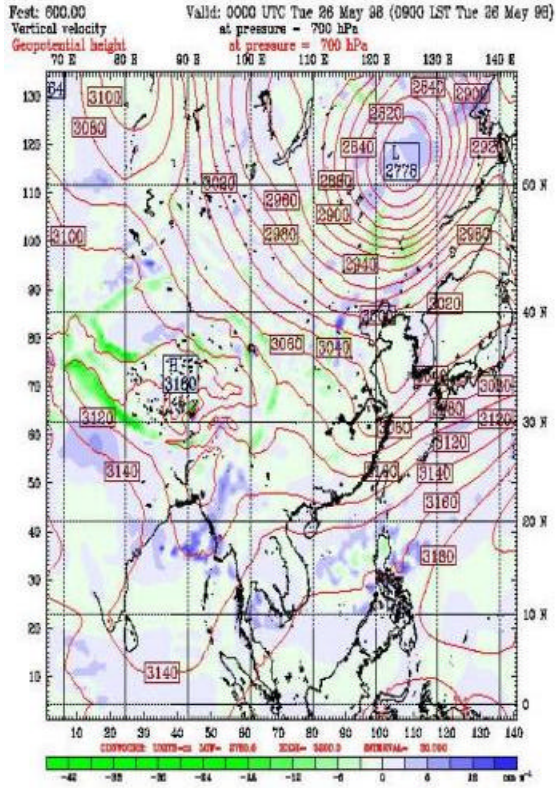


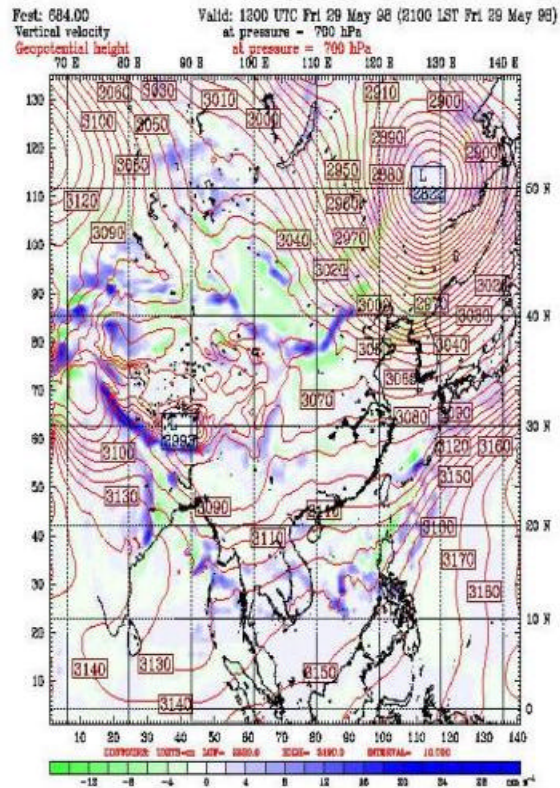
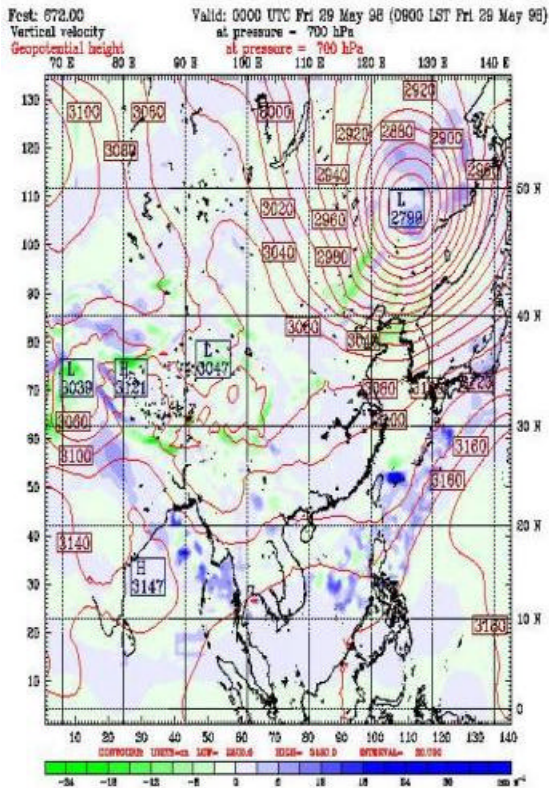
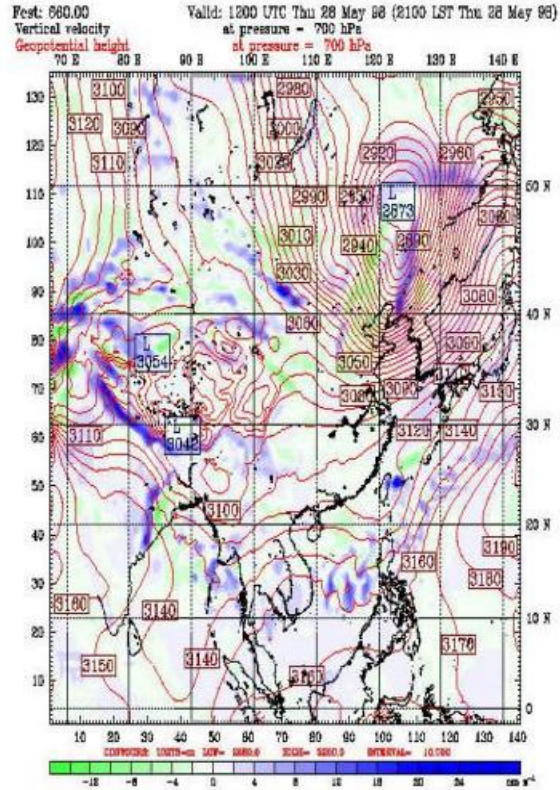
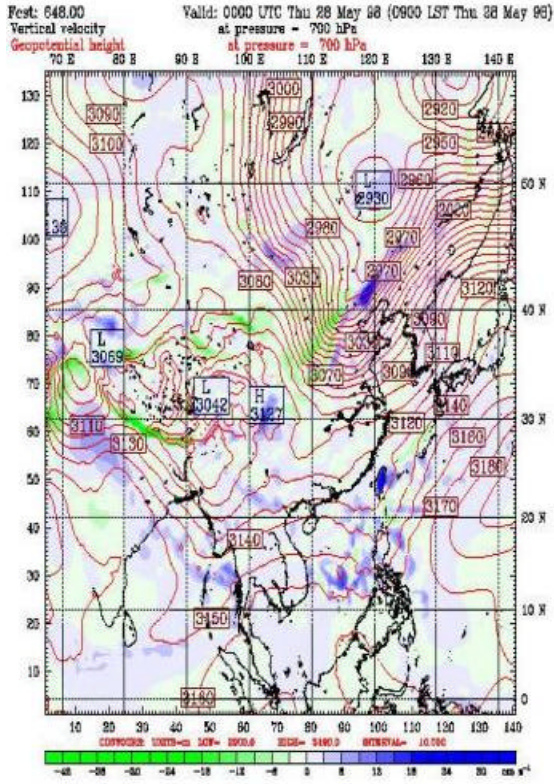




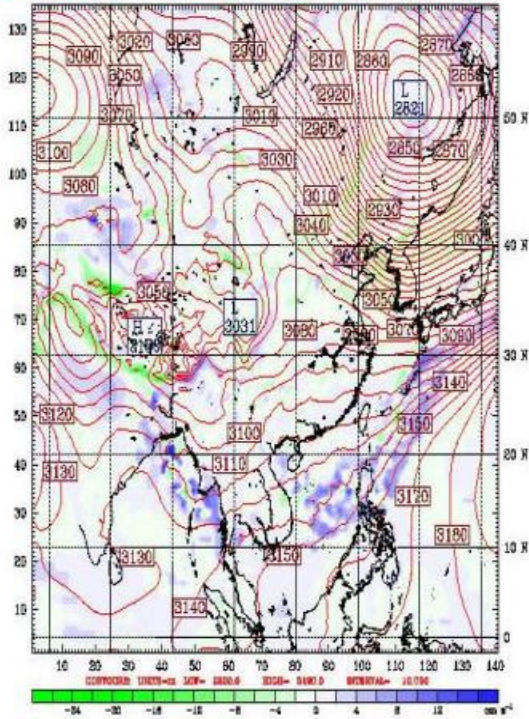




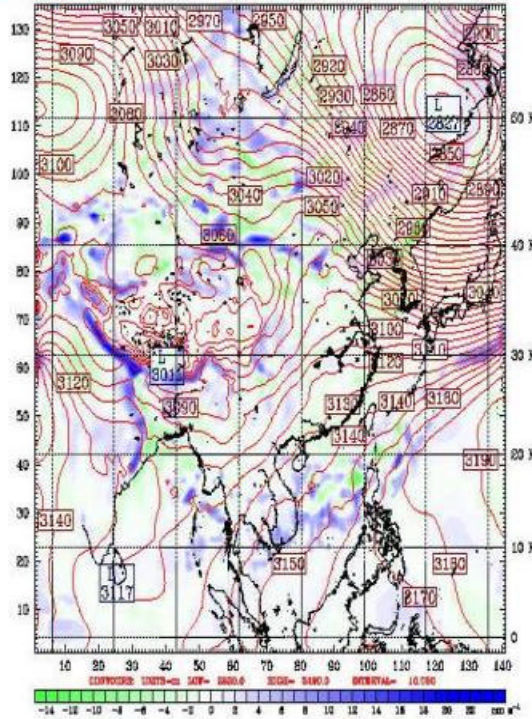




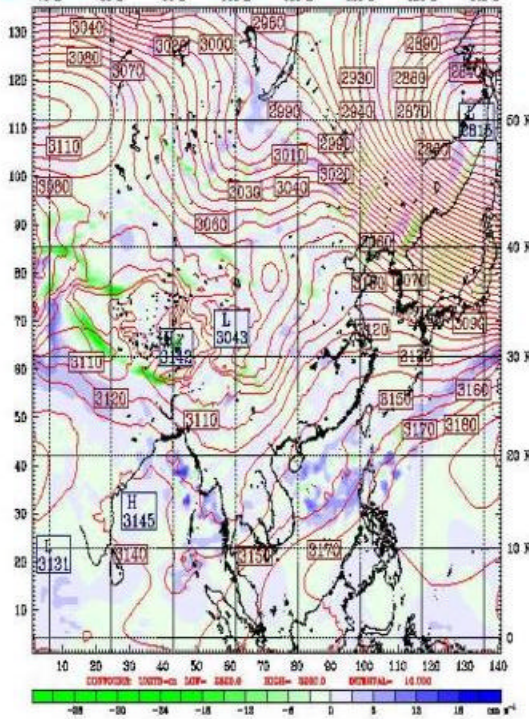
Feet: 896.00 Valid: 0000 UTC Sat 30 May 98 (0900 LST Sat 30 May 98)
 Vertical velocity at pressure = 700 hPa
 Geopotential height at pressure = 700 hPa



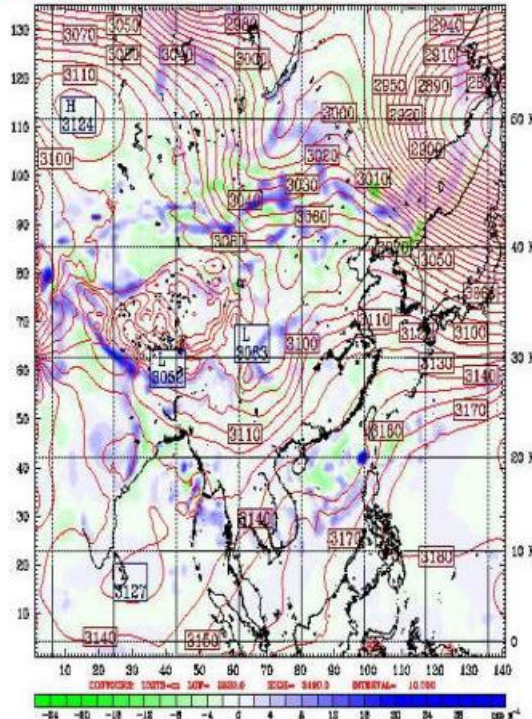
Feet: 708.00 Valid: 1200 UTC Sat 30 May 98 (2100 LST Sat 30 May 98)
 Vertical velocity at pressure = 700 hPa
 Geopotential height at pressure = 700 hPa



Feet: 780.00 Valid: 0000 UTC Sun 31 May 98 (0900 LST Sun 31 May 98)
 Vertical velocity at pressure = 700 hPa
 Geopotential height at pressure = 700 hPa

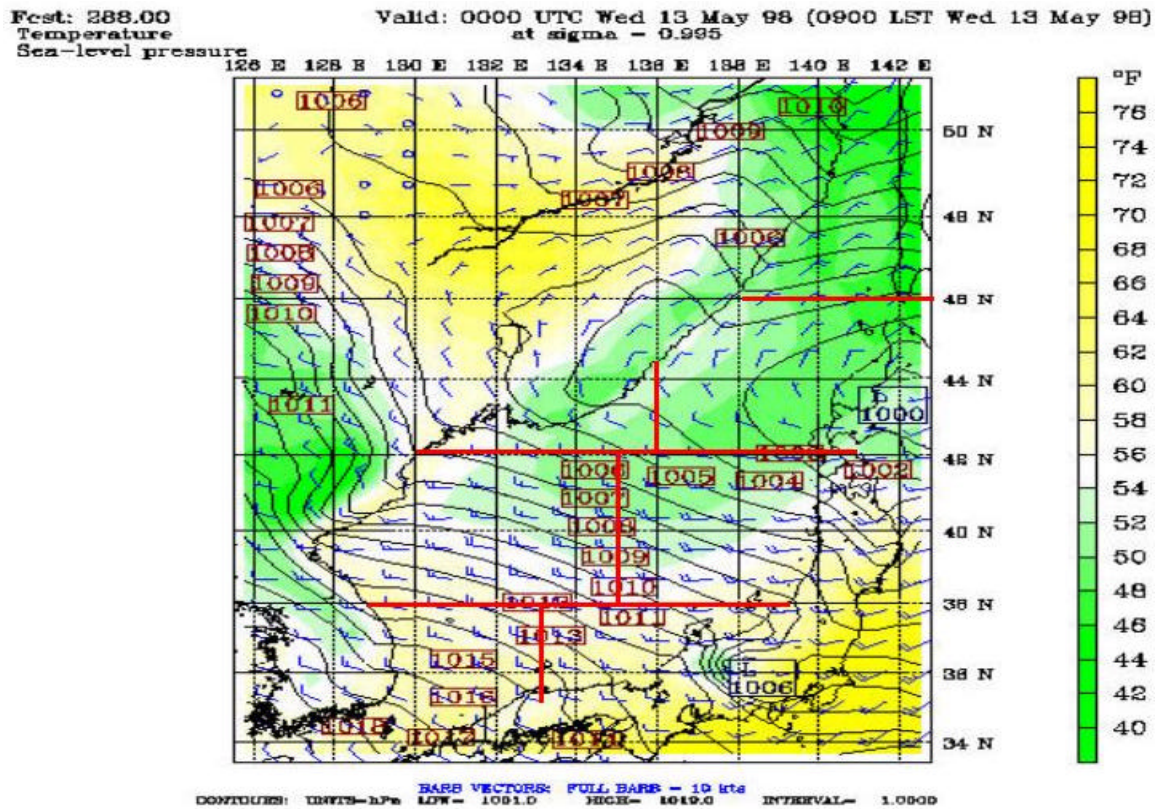


Feet: 732.00 Valid: 1200 UTC Sun 31 May 98 (2100 LST Sun 31 May 98)
 Vertical velocity at pressure = 700 hPa
 Geopotential height at pressure = 700 hPa



APPENDIX S. SEA LEVEL PRESSURE/SAT/SURFACE WIND PLOTS FOR THE JES FOR THE MAY TIME PERIOD

Appendix S consists of 38 figures that show sea level pressure, SAT, and surface winds for the May time period over the JES. The figures are in time sequential order from May 13 through May31.



Fcst: 300.00

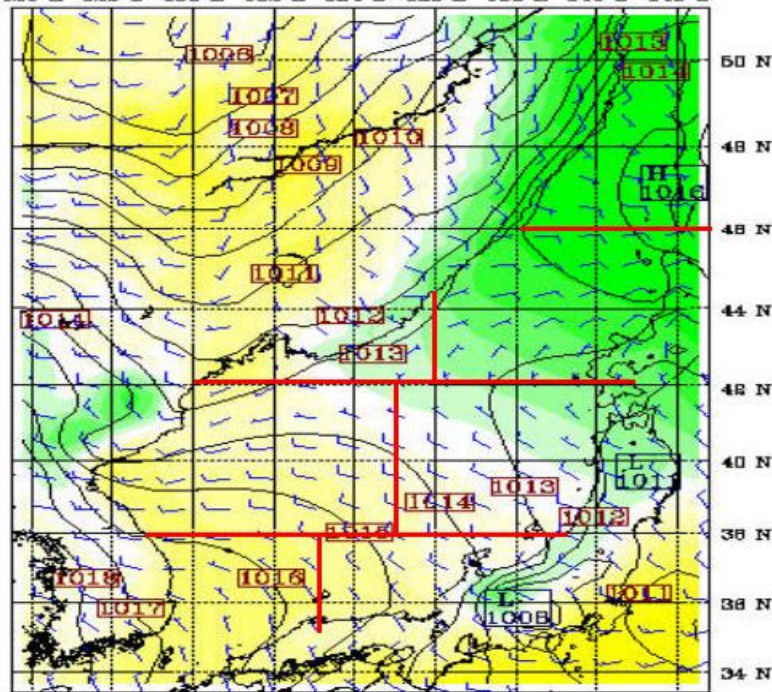
Temperature

Sea-level pressure

Valid: 1200 UTC Wed 13 May 98 (2100 LST Wed 13 May 98)

at sigma - 0.995

126 E 128 E 130 E 132 E 134 E 136 E 138 E 140 E 142 E



CONTIGUES: UNITS-hPa LFW- 1098.0 HGH- 1018.0 INTERVAL- 1.0000
BARR VECTORS: FULL BARR - 10 kts

Fcst: 312.00

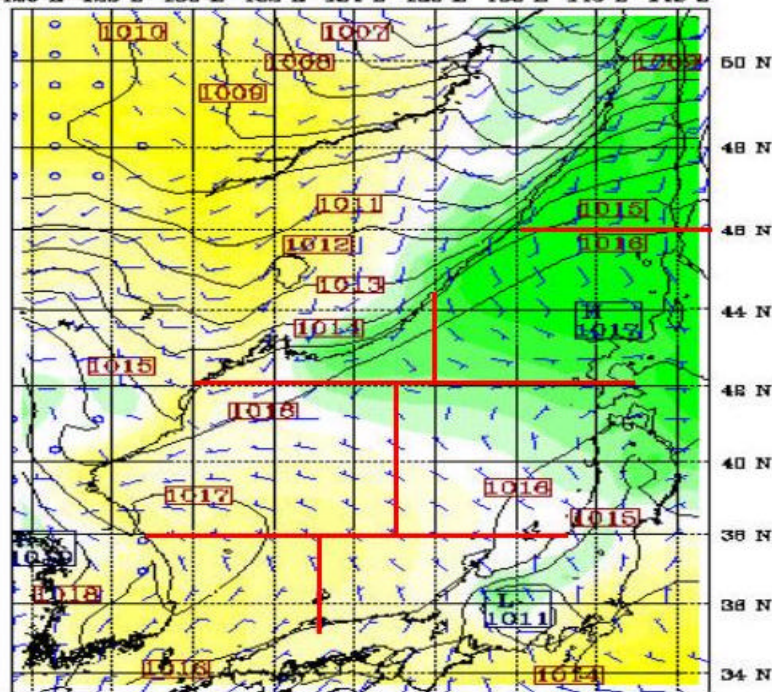
Temperature

Sea-level pressure

Valid: 0000 UTC Thu 14 May 98 (0900 LST Thu 14 May 98)

at sigma - 0.995

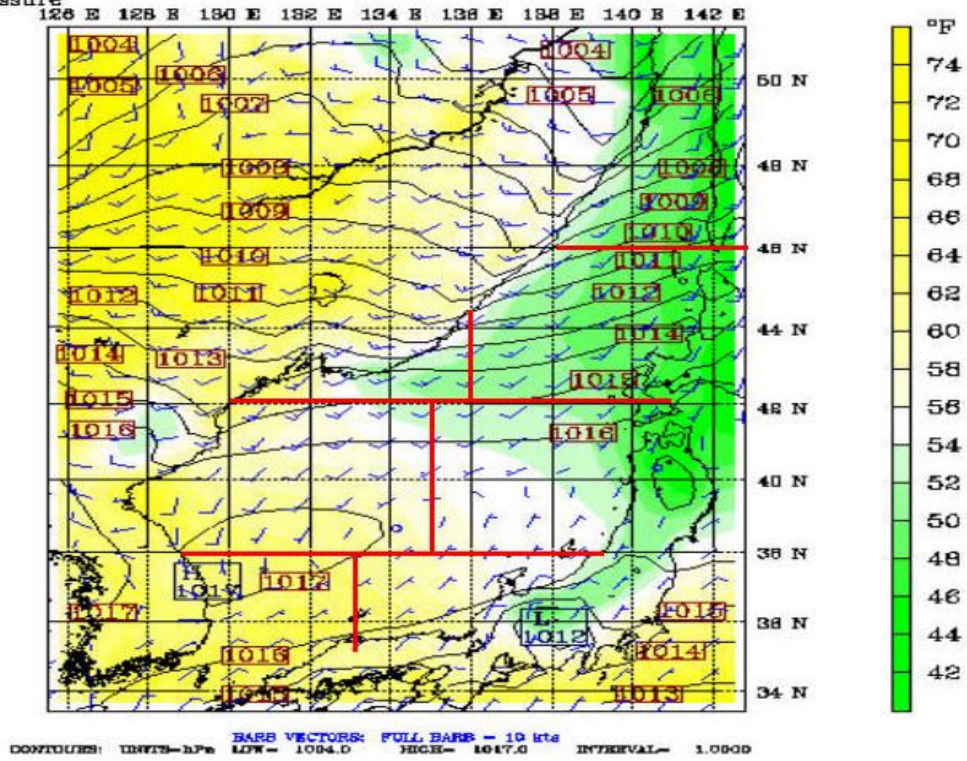
126 E 128 E 130 E 132 E 134 E 136 E 138 E 140 E 142 E



CONTIGUES: UNITS-hPa LFW- 1098.0 HGH- 1018.0 INTERVAL- 1.0000
BARR VECTORS: FULL BARR - 10 kts

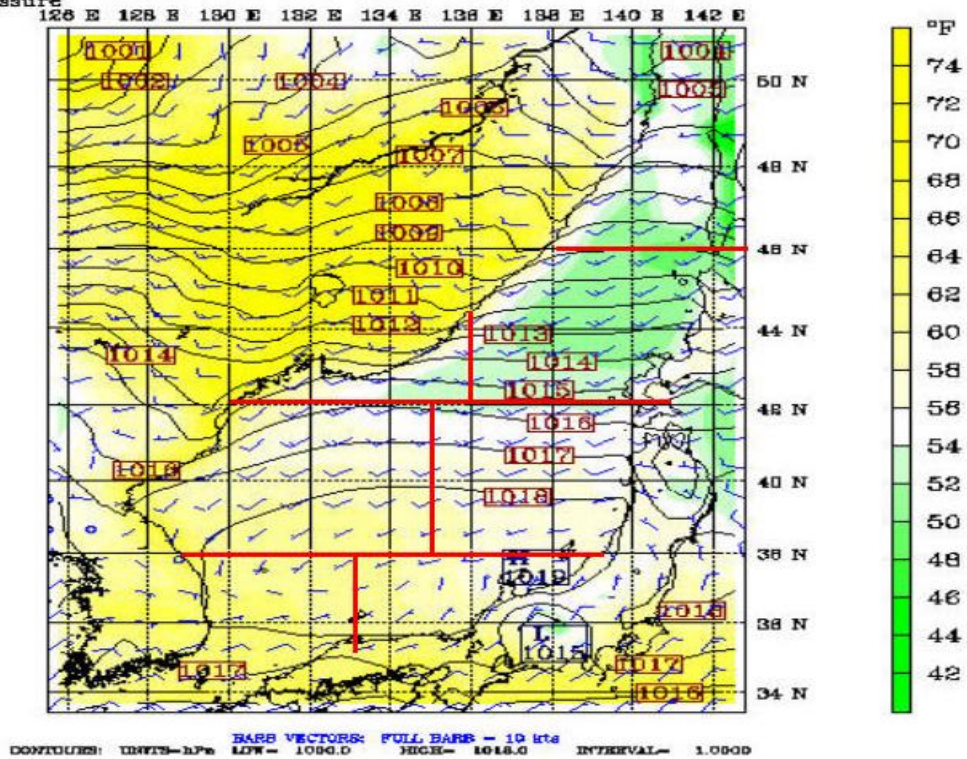
Fcst: 324.00
Temperature
Sea-level pressure

Valid: 1200 UTC Thu 14 May 98 (2100 LST Thu 14 May 98)
at sigma = 0.995



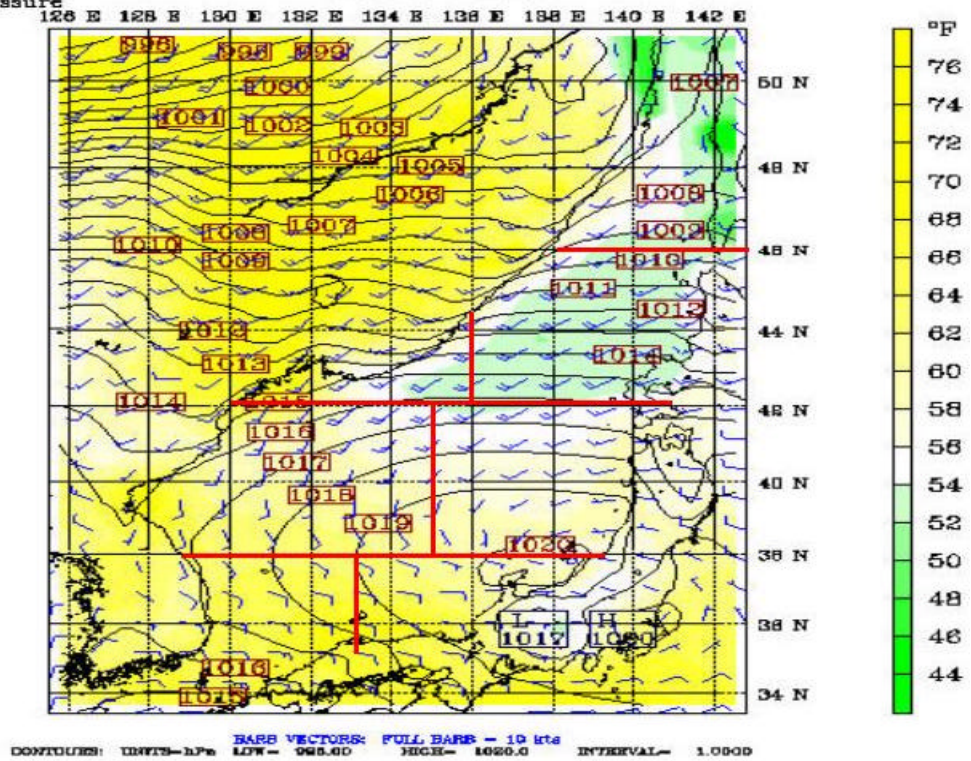
Fcst: 336.00
Temperature
Sea-level pressure

Valid: 0000 UTC Fri 15 May 98 (0900 LST Fri 15 May 98)
at sigma = 0.995



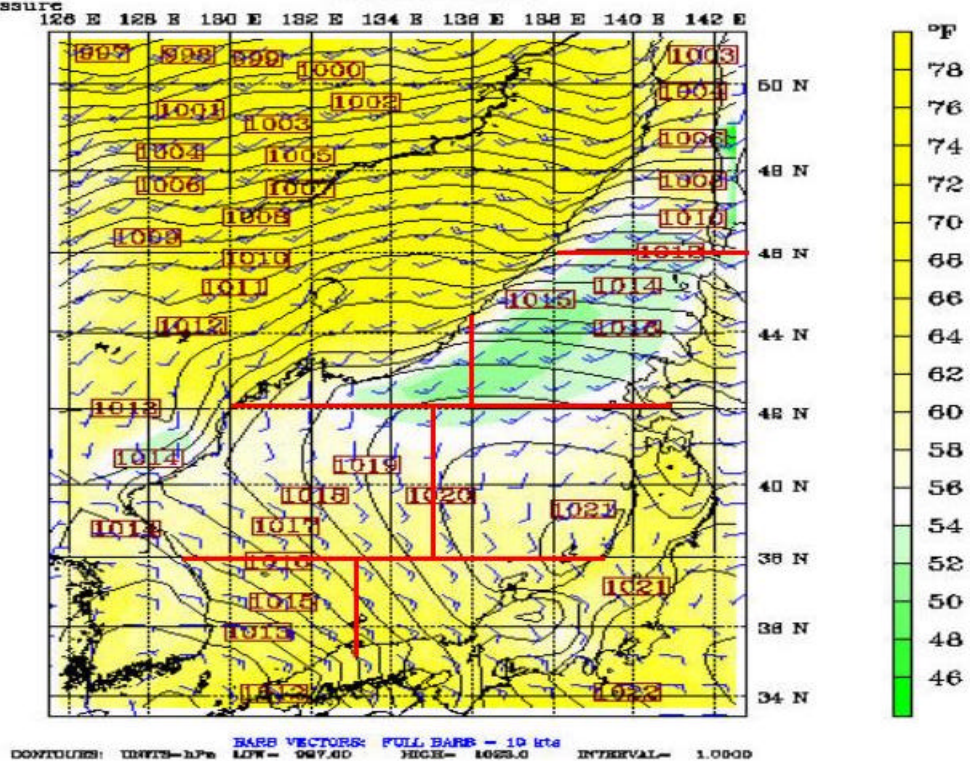
Fcst: 348.00
 Temperature
 Sea-level pressure

Valid: 1300 UTC Fri 15 May 98 (2100 LST Fri 15 May 98)
 at sigma = 0.995



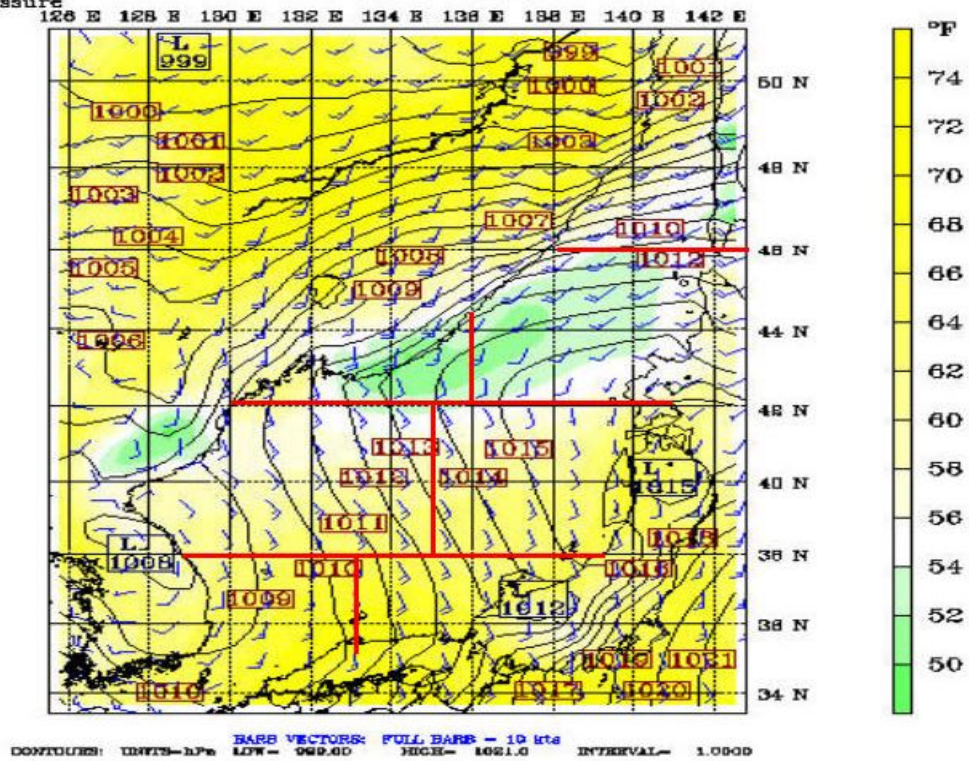
Fcst: 360.00
 Temperature
 Sea-level pressure

Valid: 0000 UTC Sat 16 May 98 (0900 LST Sat 16 May 98)



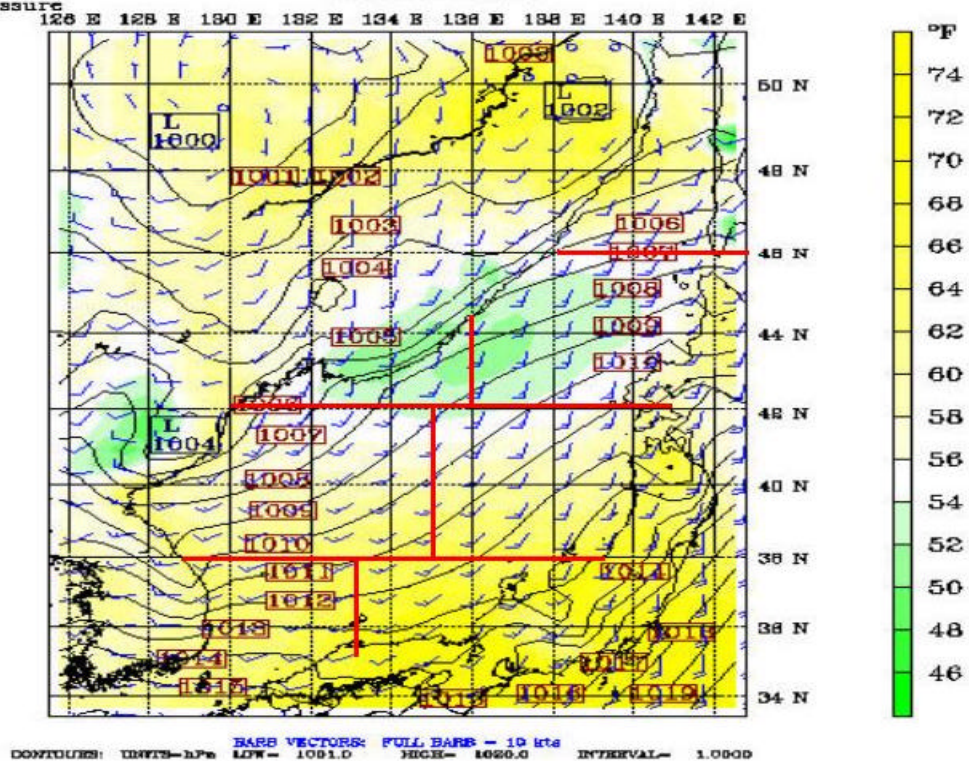
Fast: 372.00
 Temperature
 Sea-level pressure

Valid: 1200 UTC Sat 16 May 98 (2100 LST Sat 16 May 98)
 at sigma - 0.995



Fast: 384.00
 Temperature
 Sea-level pressure

Valid: 0000 UTC Sun 17 May 98 (0900 LST Sun 17 May 98)
 at sigma - 0.995



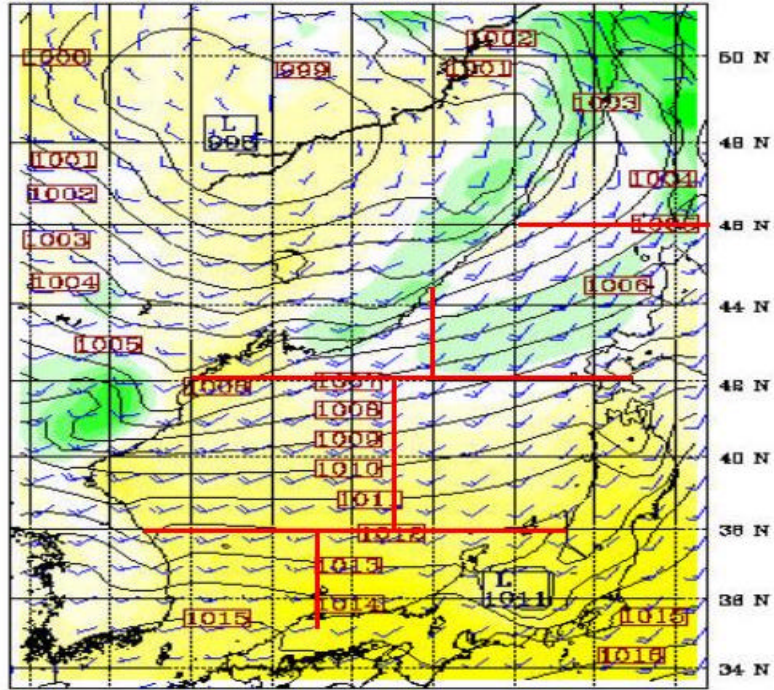
Fcst: 396.00

Temperature

Sea-level pressure

Valid: 1200 UTC Sun 17 May 98 (2100 LST Sun 17 May 98)
at sigma - 0.995

126 E 128 E 130 E 132 E 134 E 136 E 138 E 140 E 142 E



BARB VECTORS: FULL BARB - 10 kts
CONTIGUES: UNITS-hPa LOW- 998.00 HIGH- 1017.0 INTERVAL- 1.0000

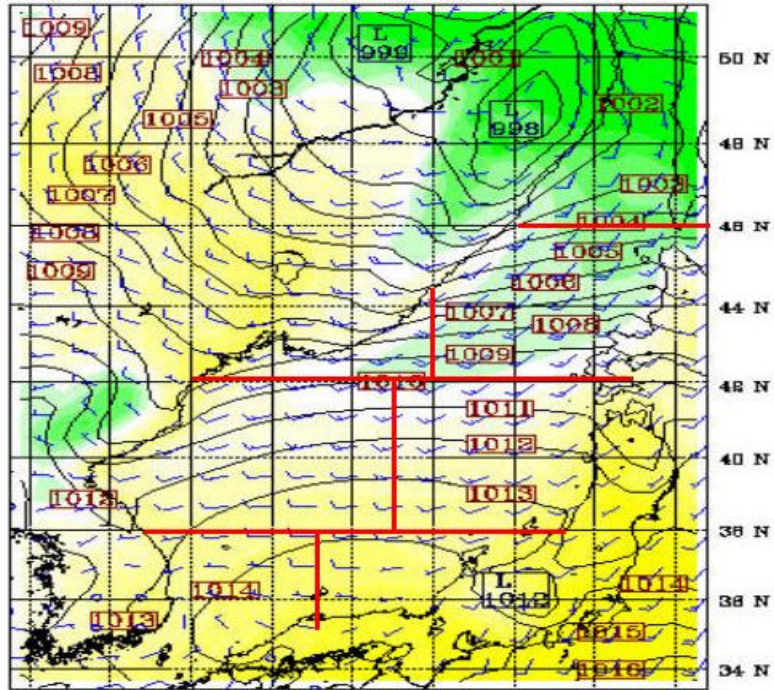
Fcst: 408.00

Temperature

Sea-level pressure

Valid: 0000 UTC Mon 18 May 98 (0900 LST Mon 18 May 98)
at sigma - 0.995

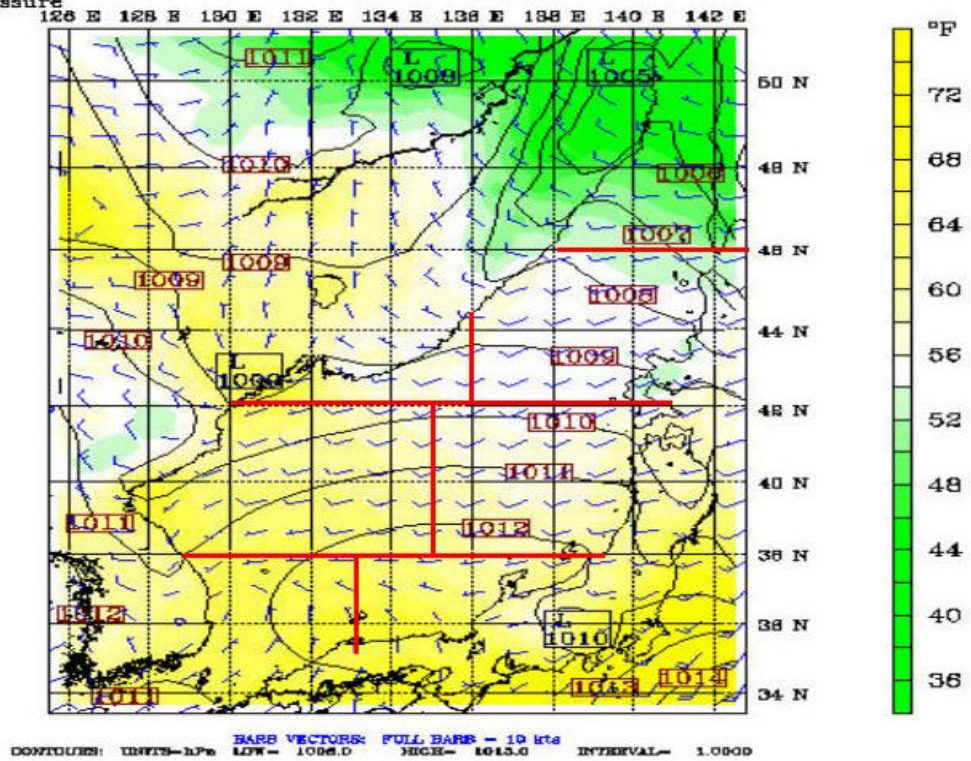
126 E 128 E 130 E 132 E 134 E 136 E 138 E 140 E 142 E



BARB VECTORS: FULL BARB - 10 kts
CONTIGUES: UNITS-hPa LOW- 998.00 HIGH- 1017.0 INTERVAL- 1.0000

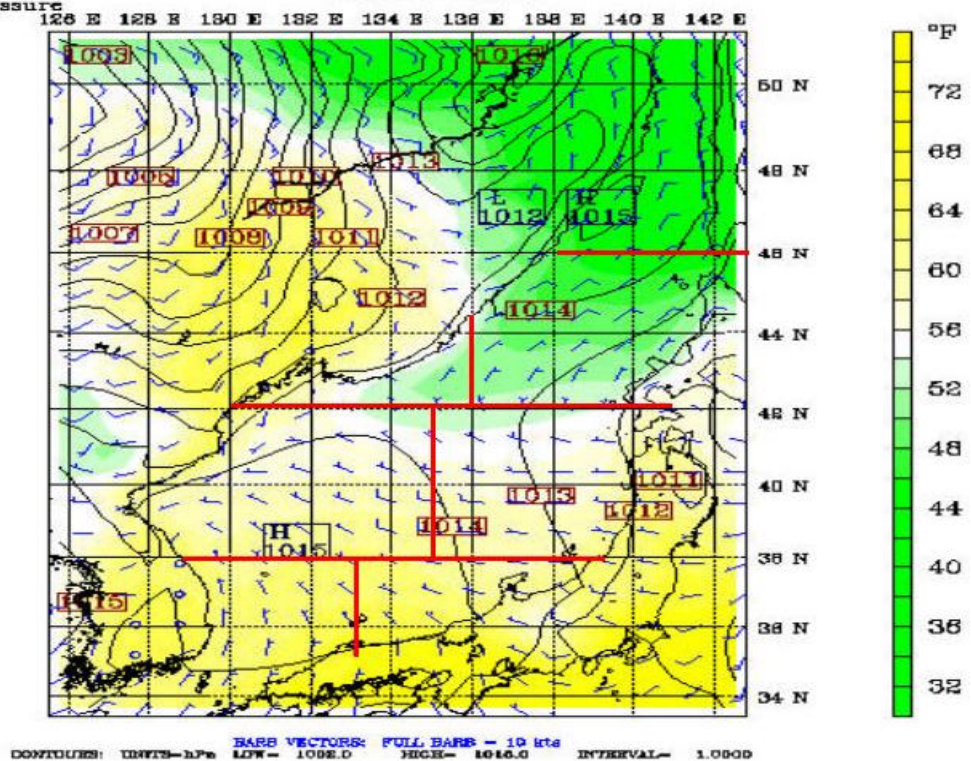
Fast: 420.00
Temperature
Sea-level pressure

Valid: 1200 UTC Mon 18 May 98 (2100 LST Mon 18 May 98)
at sigma = 0.995



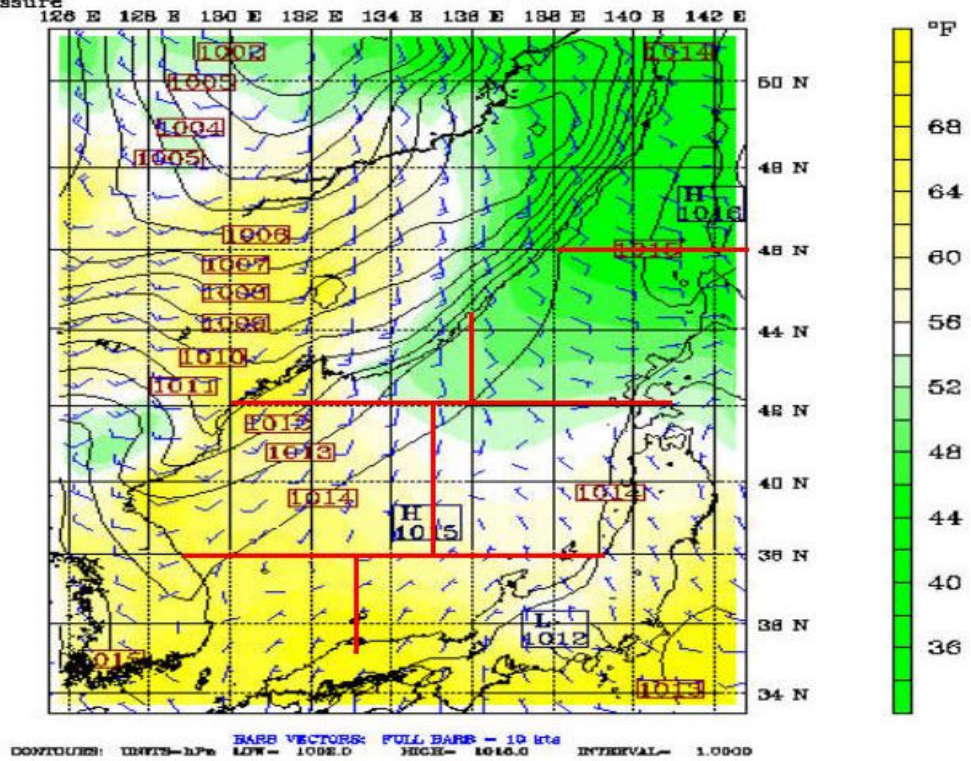
Fast: 432.00
Temperature
Sea-level pressure

Valid: 0000 UTC Tue 19 May 98 (0900 LST Tue 19 May 98)
at sigma = 0.995



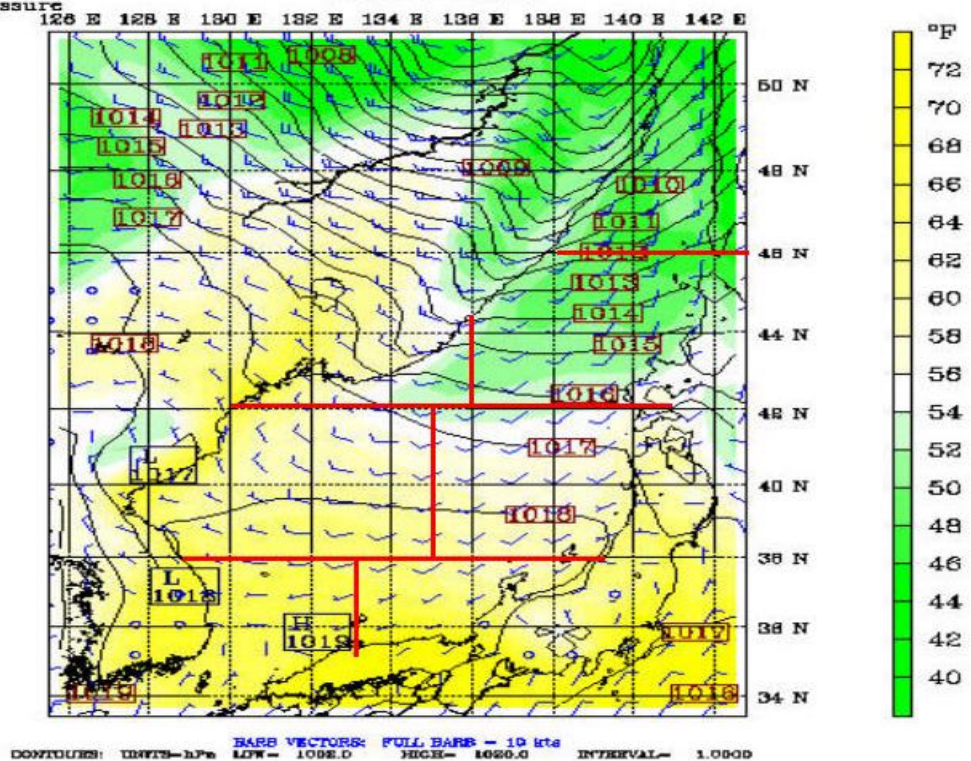
Fast: 444.00
 Temperature
 Sea-level pressure

Valid: 1200 UTC Tue 19 May 98 (2100 LST Tue 19 May 98)
 at sigma - 0.995



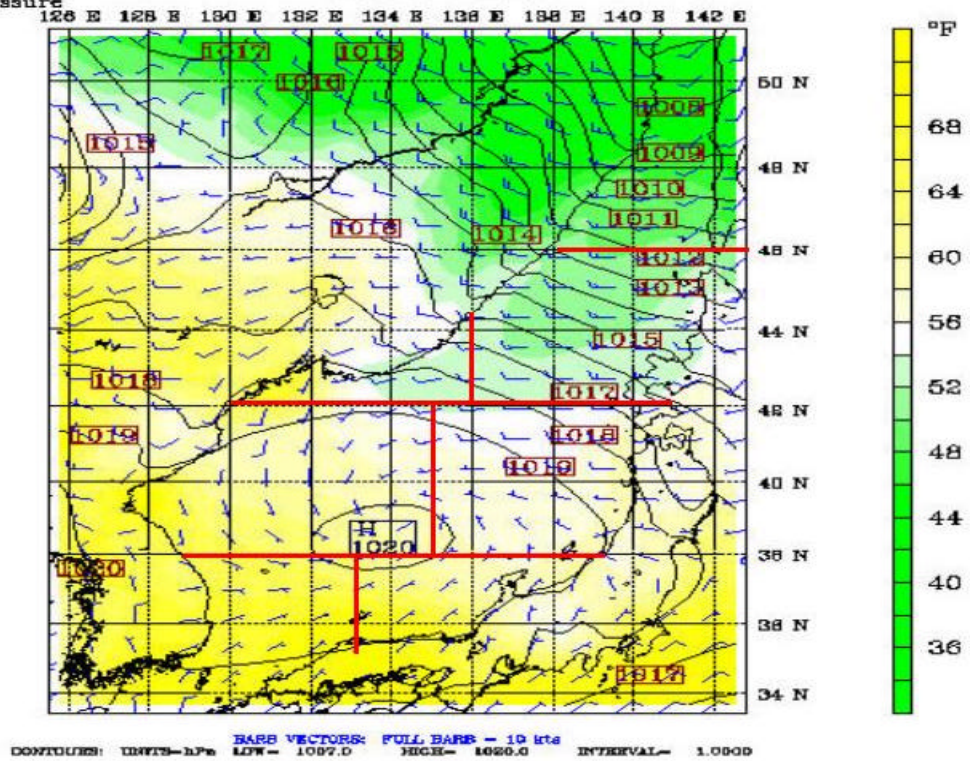
Fast: 458.00
 Temperature
 Sea-level pressure

Valid: 0000 UTC Wed 20 May 98 (0900 LST Wed 20 May 98)
 at sigma - 0.995



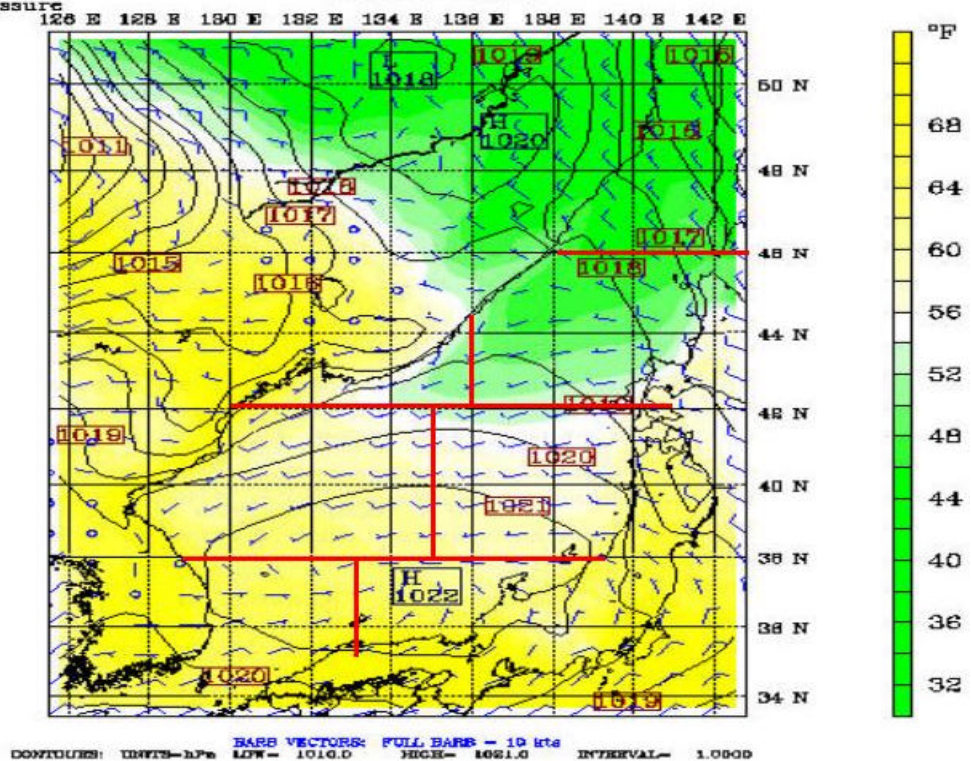
Fcst: 468.00
 Temperature
 Sea-level pressure

Valid: 1200 UTC Wed 20 May 98 (2100 LST Wed 20 May 98)
 at sigma - 0.995



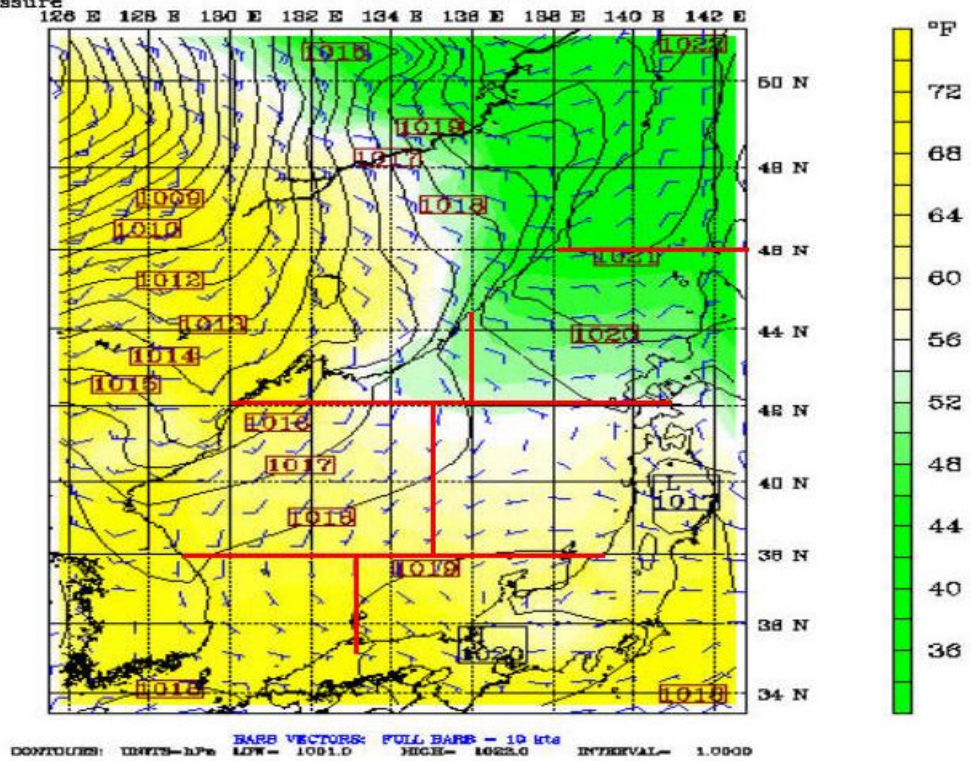
Fcst: 480.00
 Temperature
 Sea-level pressure

Valid: 0000 UTC Thu 21 May 98 (0900 LST Thu 21 May 98)



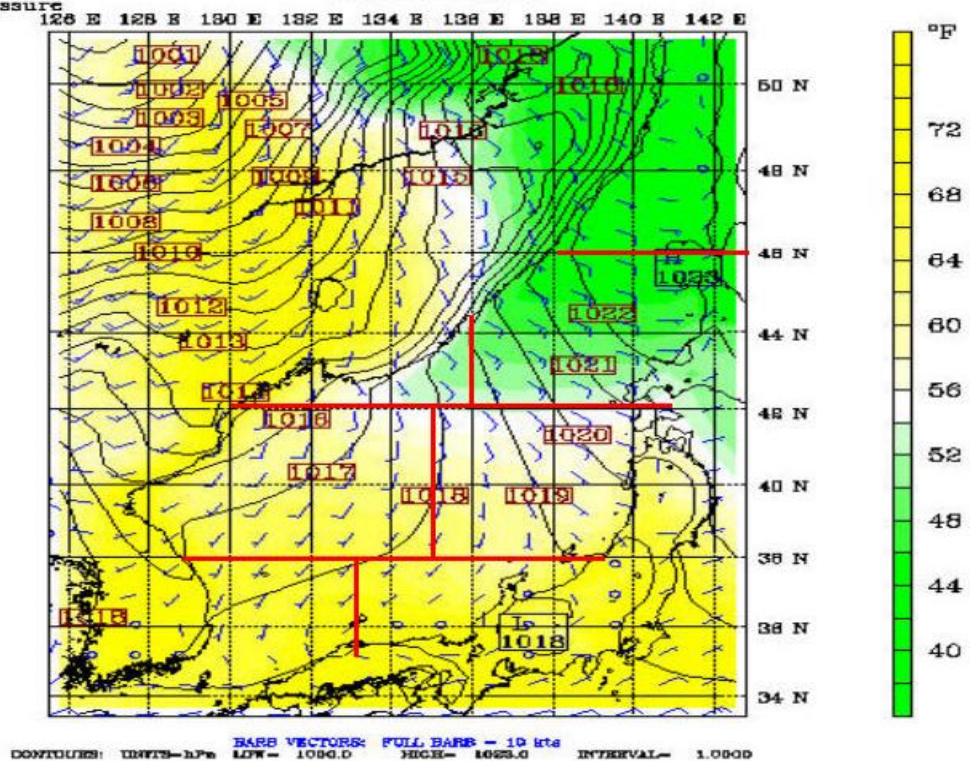
Fcst: 492.00
 Temperature
 Sea-level pressure

Valid: 1200 UTC Thu 21 May 98 (2100 LST Thu 21 May 98)
 at sigma = 0.995



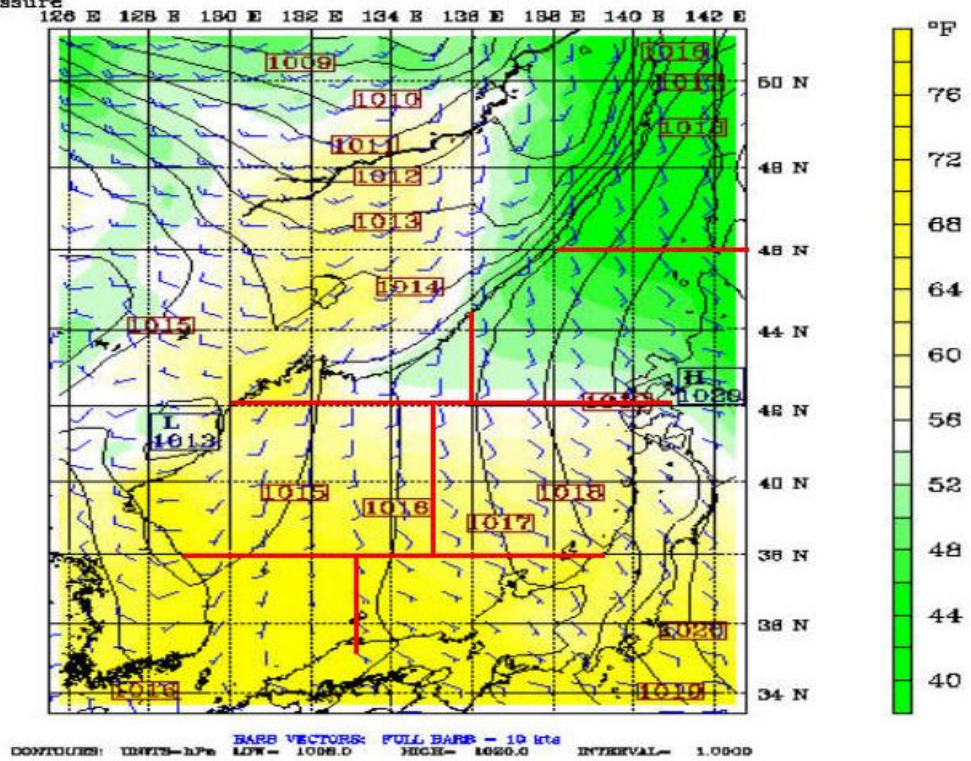
Fcst: 504.00
 Temperature
 Sea-level pressure

Valid: 0000 UTC Fri 22 May 98 (0900 LST Fri 22 May 98)
 at sigma = 0.995



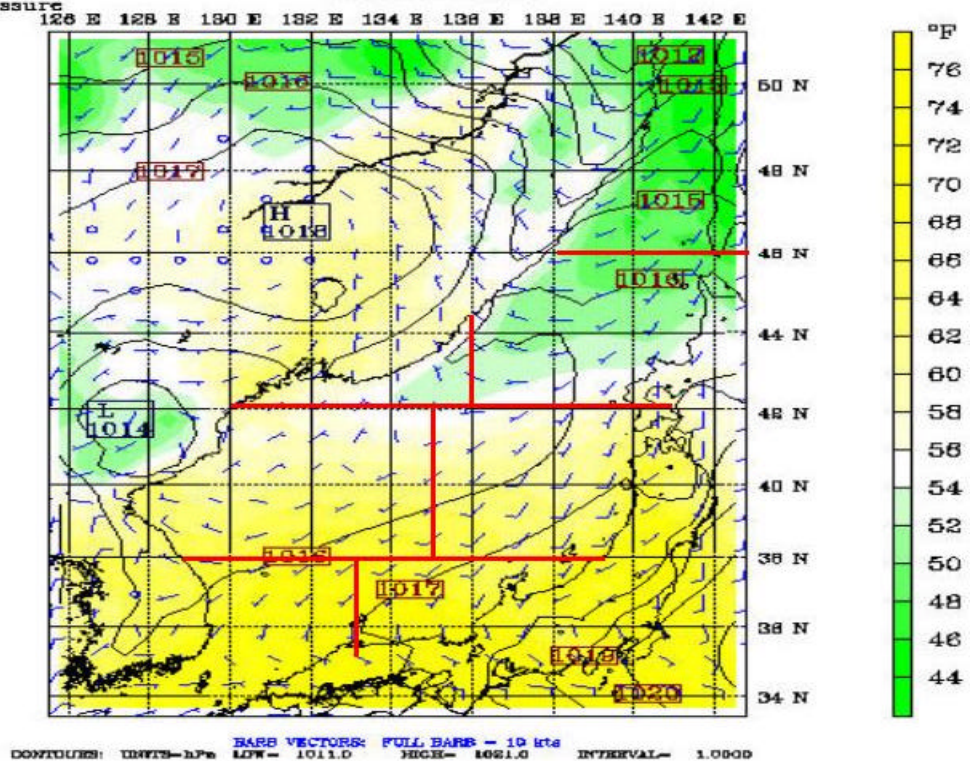
Fast: 516.00
Temperature
Sea-level pressure

Valid: 1300 UTC Fri 22 May 98 (2100 LST Fri 22 May 98)
at sigma - 0.995



Fast: 528.00
Temperature
Sea-level pressure

Valid: 0000 UTC Sat 23 May 98 (0900 LST Sat 23 May 98)
at sigma - 0.995



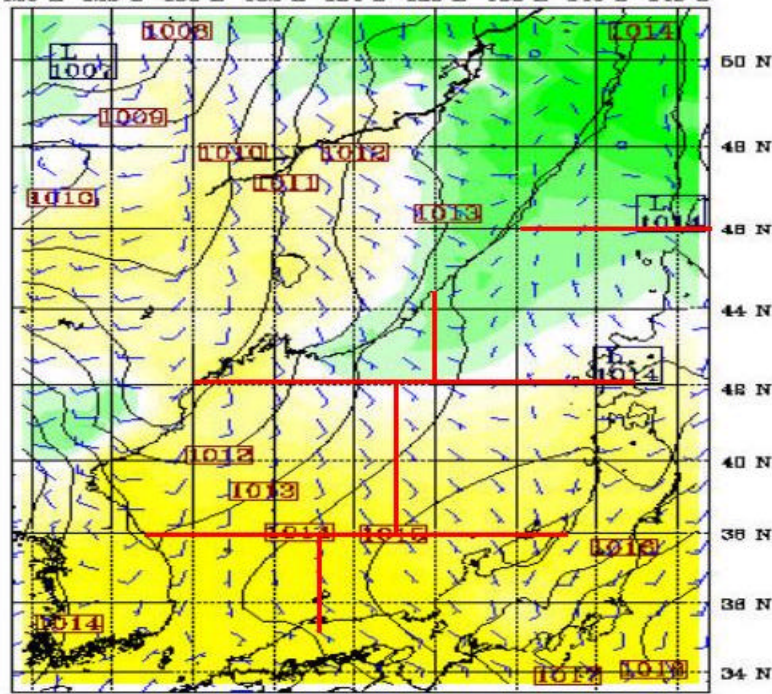
Fast: 540.00

Temperature

Sea-level pressure

Valid: 1200 UTC Sat 23 May 98 (2100 LST Sat 23 May 98)
at sigma - 0.995

126 E 128 E 130 E 132 E 134 E 136 E 138 E 140 E 142 E



BARB VECTORS: FULL BARB - 10 kts
CONTIGUES: UNITS-hPa LFW- 1088.0 HGH- 1018.0 INTERVAL- 1.0000

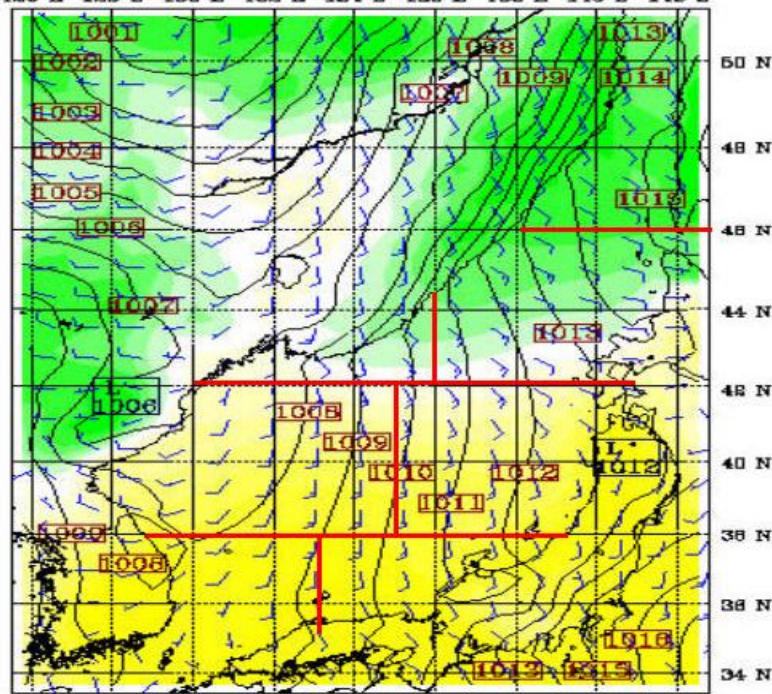
Fast: 552.00

Temperature

Sea-level pressure

Valid: 0000 UTC Sun 24 May 98 (0900 LST Sun 24 May 98)
at sigma - 0.995

126 E 128 E 130 E 132 E 134 E 136 E 138 E 140 E 142 E



BARB VECTORS: FULL BARB - 10 kts
CONTIGUES: UNITS-hPa LFW- 1088.0 HGH- 1017.0 INTERVAL- 1.0000

Fest: 564.00

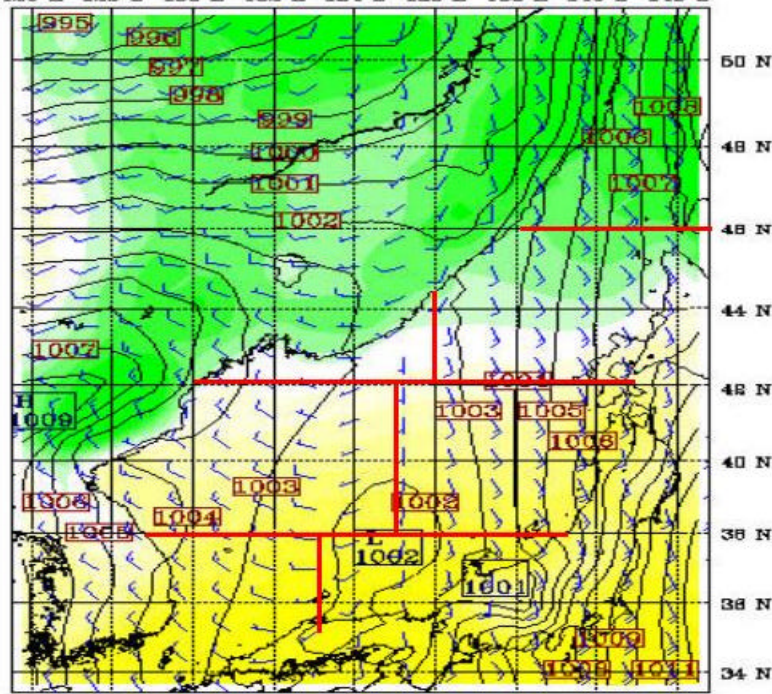
Valid: 1200 UTC Sun 24 May 98 (2100 LST Sun 24 May 98)

Temperature

at sigma - 0.995

Sea-level pressure

126 E 128 E 130 E 132 E 134 E 136 E 138 E 140 E 142 E



BARB VECTORS: FULL BARB = 10 kts
CONTIGUES: UNITS=hPa LOW= 995.00 HIGH= 1012.0 INTERVAL= 1.0000

Fest: 576.00

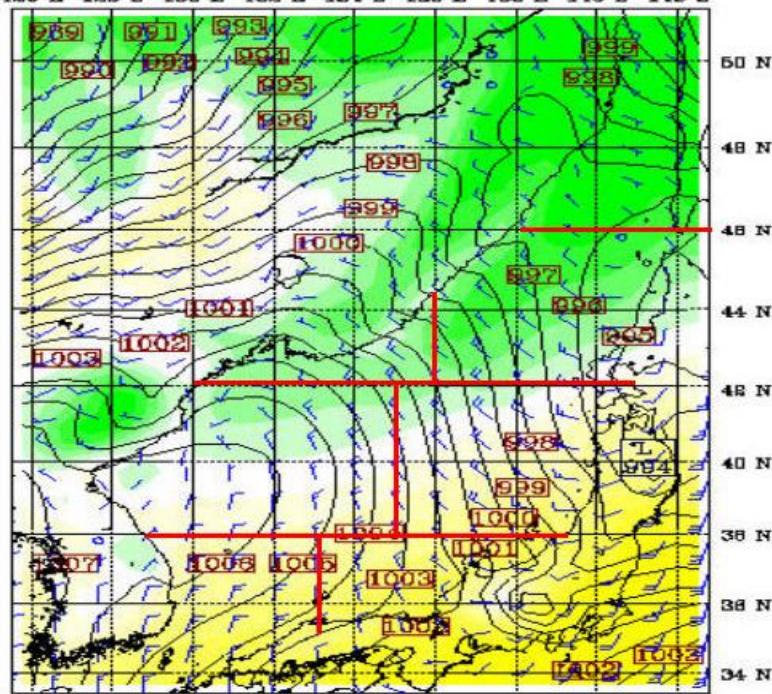
Valid: 0000 UTC Mon 25 May 98 (0900 LST Mon 25 May 98)

Temperature

at sigma - 0.995

Sea-level pressure

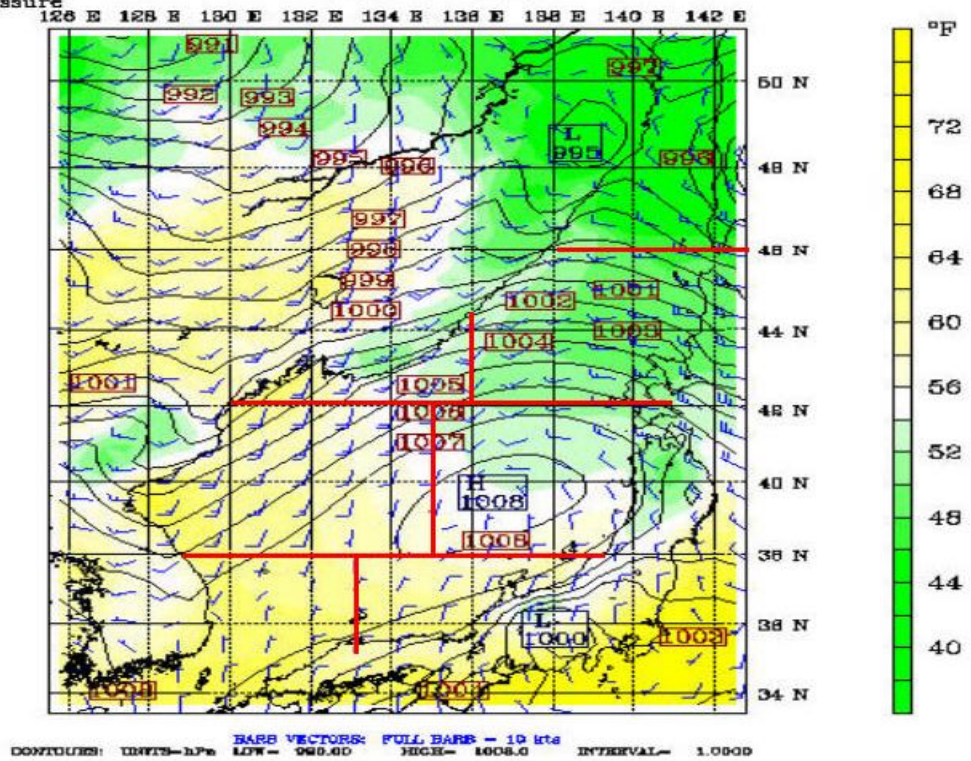
126 E 128 E 130 E 132 E 134 E 136 E 138 E 140 E 142 E



BARB VECTORS: FULL BARB = 10 kts
CONTIGUES: UNITS=hPa LOW= 993.00 HIGH= 1007.0 INTERVAL= 1.0000

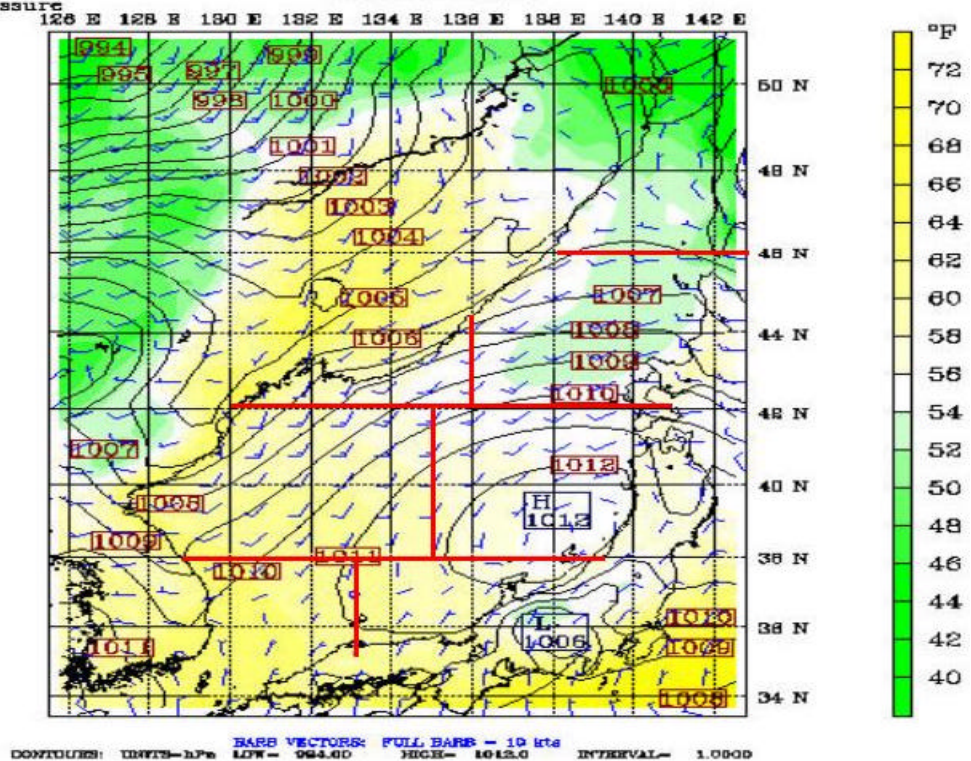
Fast: 588.00
Temperature
Sea-level pressure

Valid: 1200 UTC Mon 25 May 98 (2100 LST Mon 25 May 98)
at sigma - 0.995



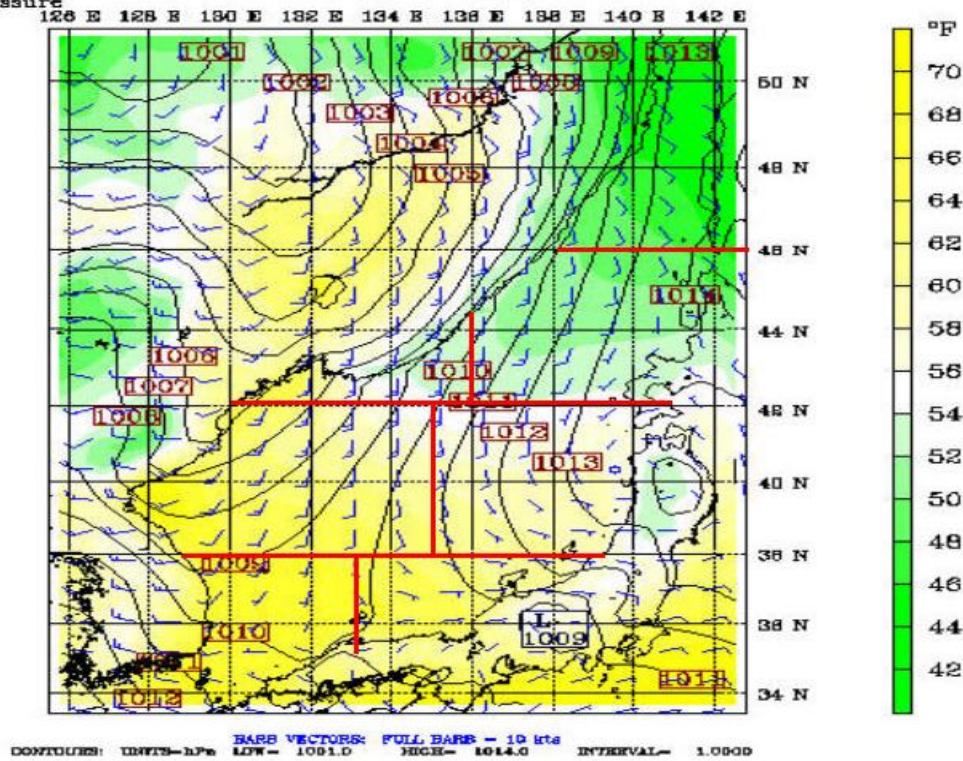
Fast: 600.00
Temperature
Sea-level pressure

Valid: 0000 UTC Tue 26 May 98 (0900 LST Tue 26 May 98)
at sigma - 0.995



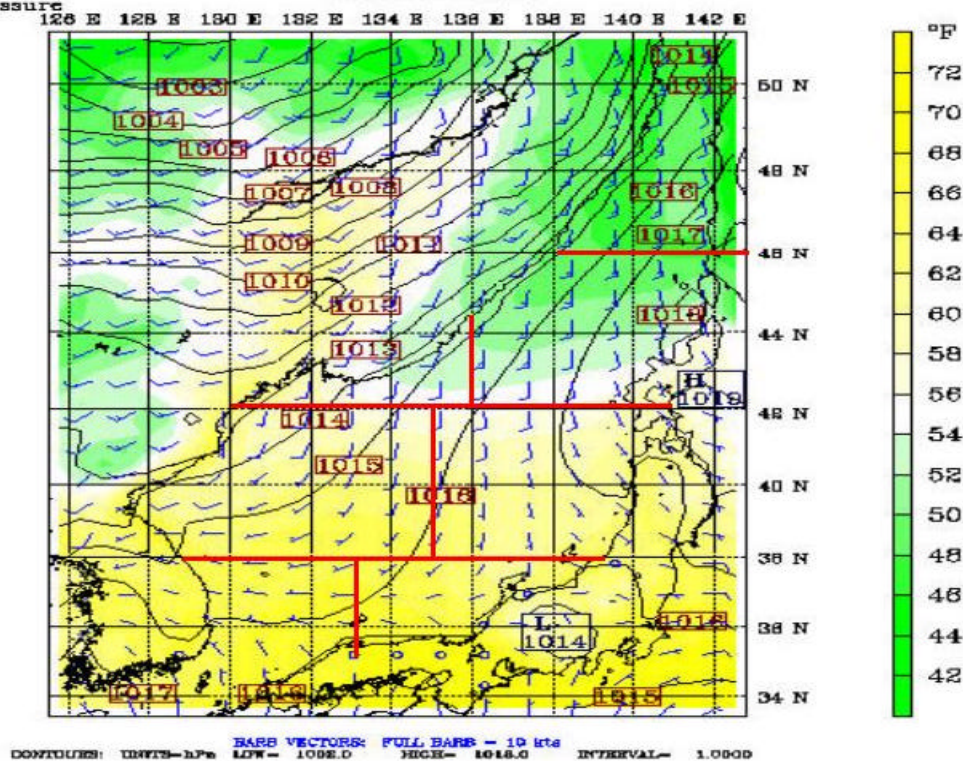
Fcst: 612.00
 Temperature
 Sea-level pressure

Valid: 1200 UTC Tue 26 May 98 (2100 LST Tue 26 May 98)
 at sigma - 0.995



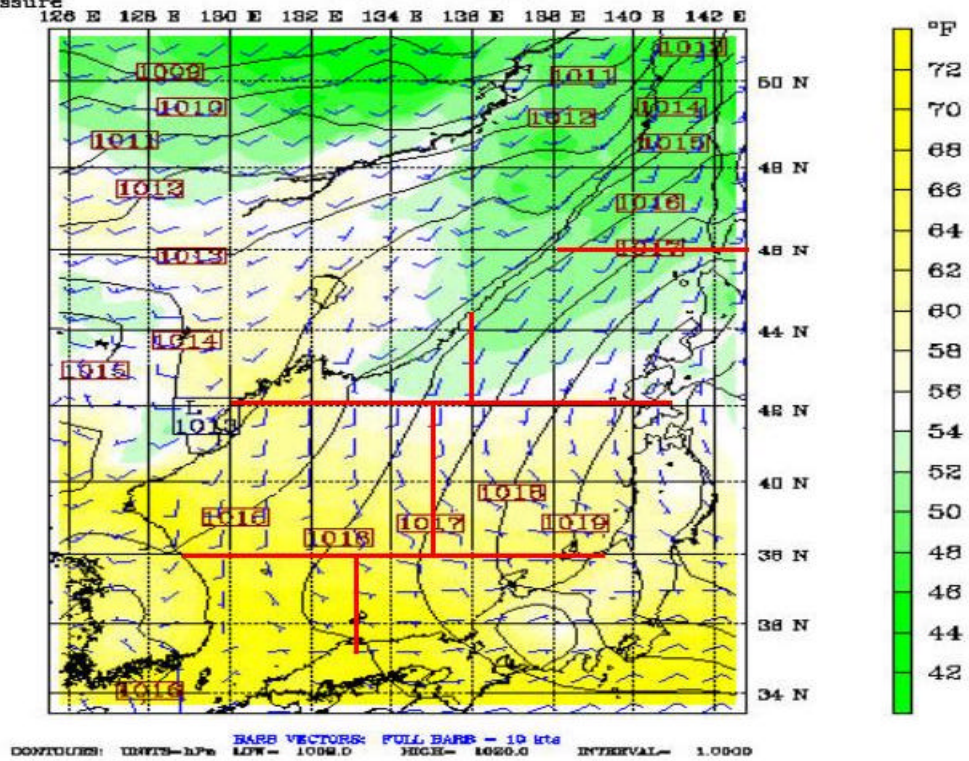
Fcst: 624.00
 Temperature
 Sea-level pressure

Valid: 0000 UTC Wed 27 May 98 (0900 LST Wed 27 May 98)



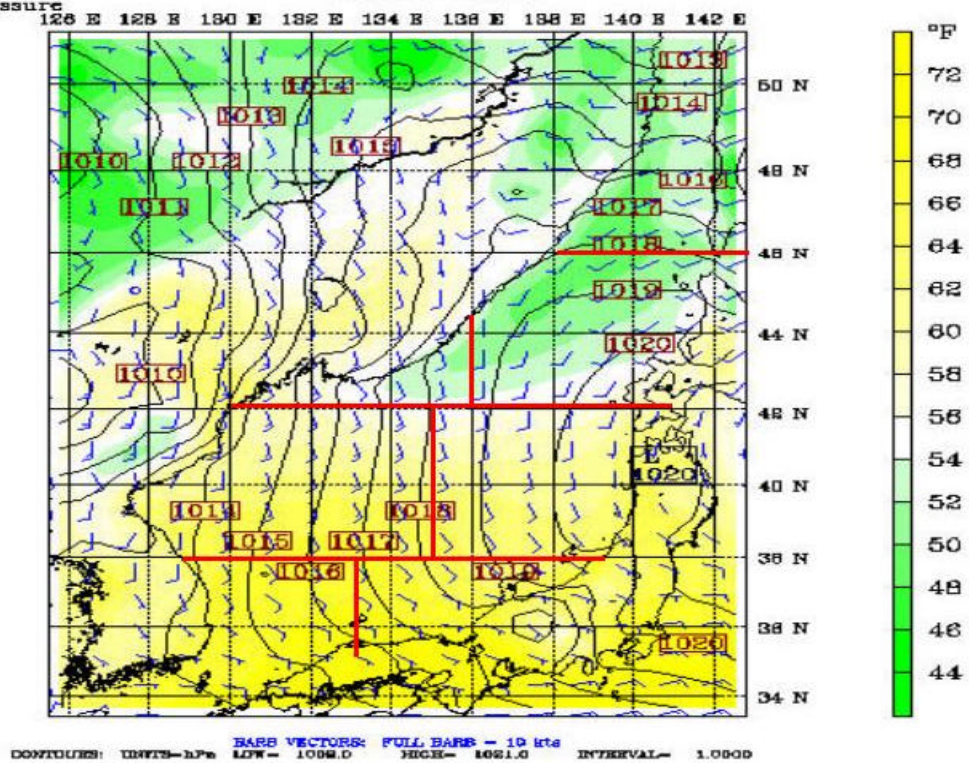
Fcst: 636.00
Temperature
Sea-level pressure

Valid: 1200 UTC Wed 27 May 98 (2100 LST Wed 27 May 98)
at sigma - 0.995



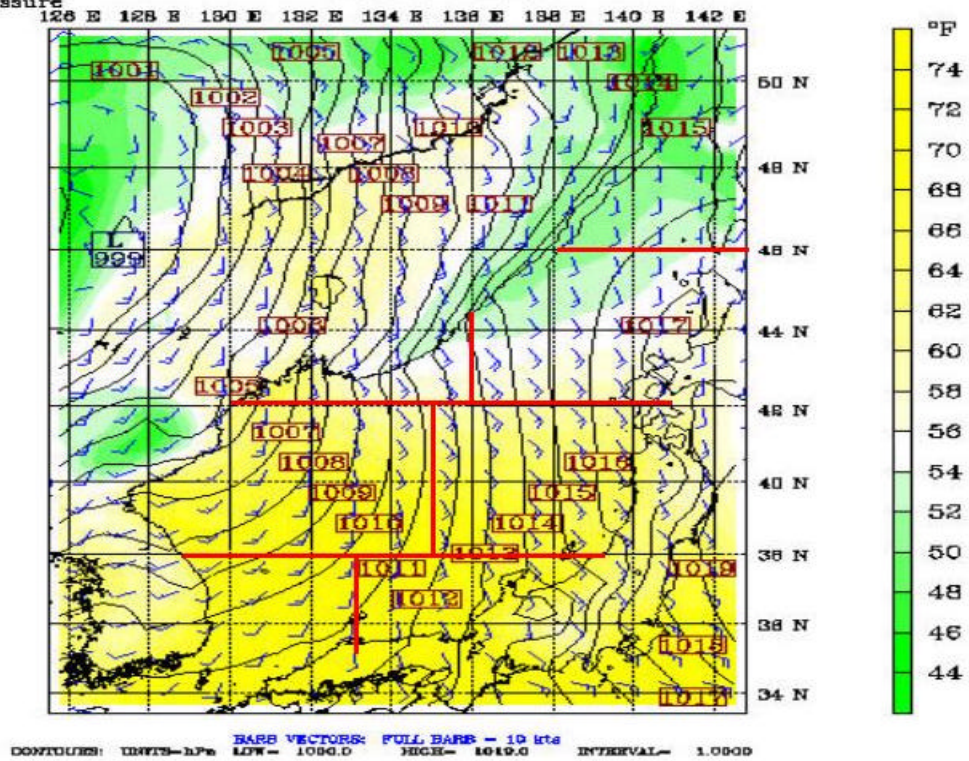
Fcst: 648.00
Temperature
Sea-level pressure

Valid: 0000 UTC Thu 28 May 98 (0900 LST Thu 28 May 98)
at sigma - 0.995



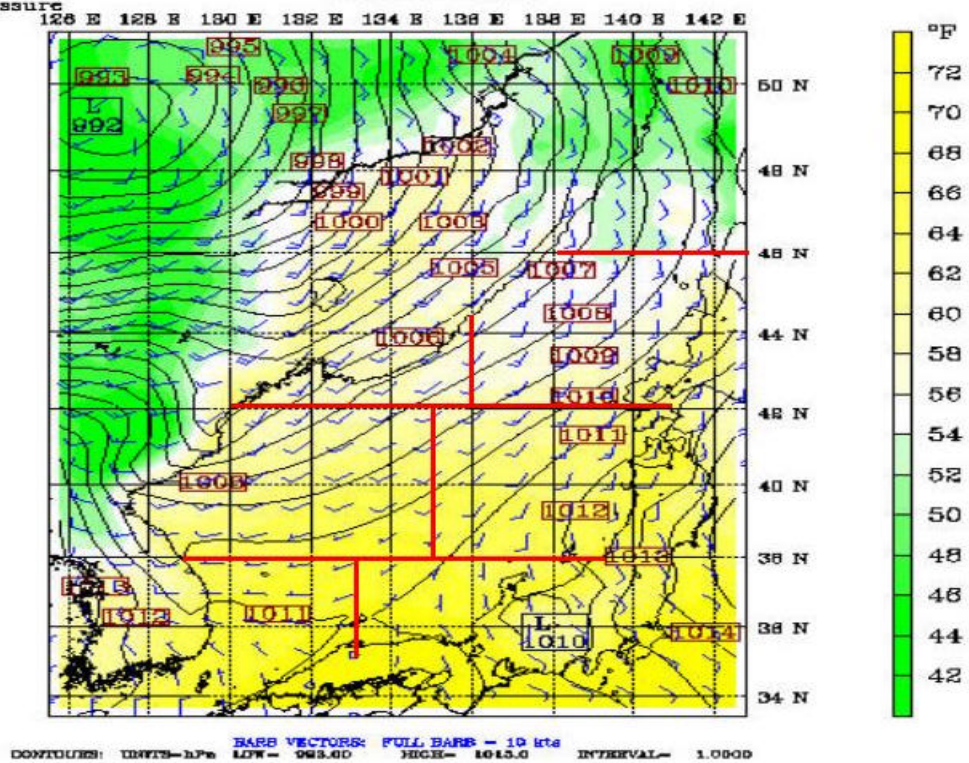
Fast: 660.00
Temperature
Sea-level pressure

Valid: 1200 UTC Thu 28 May 98 (2100 LST Thu 28 May 98)
at sigma - 0.995



Fast: 672.00
Temperature
Sea-level pressure

Valid: 0000 UTC Fri 29 May 98 (0900 LST Fri 29 May 98)
at sigma - 0.995



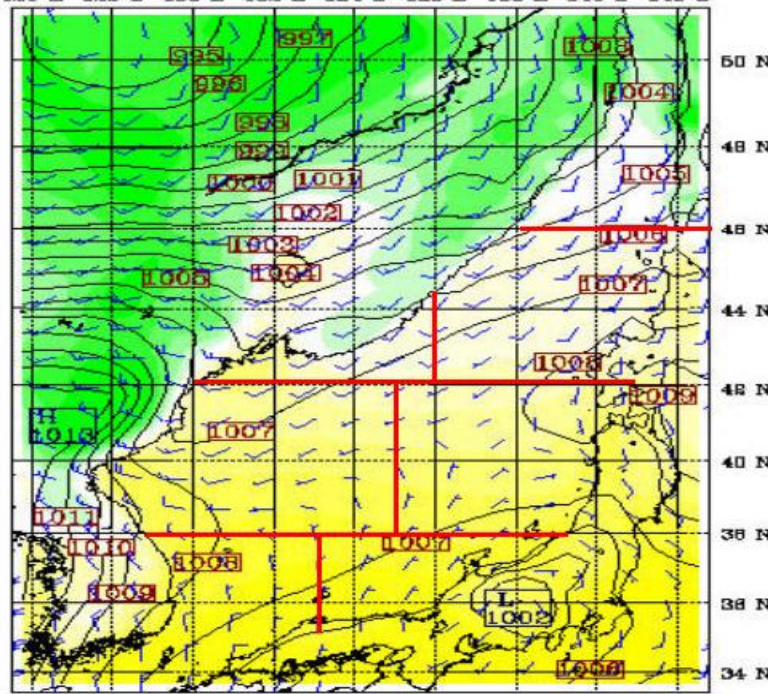
Fcst: 684.00

Temperature

Sea-level pressure

Valid: 1300 UTC Fri 29 May 98 (2100 LST Fri 29 May 98)
at sigma = 0.995

126 E 128 E 130 E 132 E 134 E 136 E 138 E 140 E 142 E



BARB VECTORS: FULL BARB = 10 kts
CONTIGUES: UNITS=hPa LFW= 995.00 HGH= 1013.0 INTERVAL= 1.0000

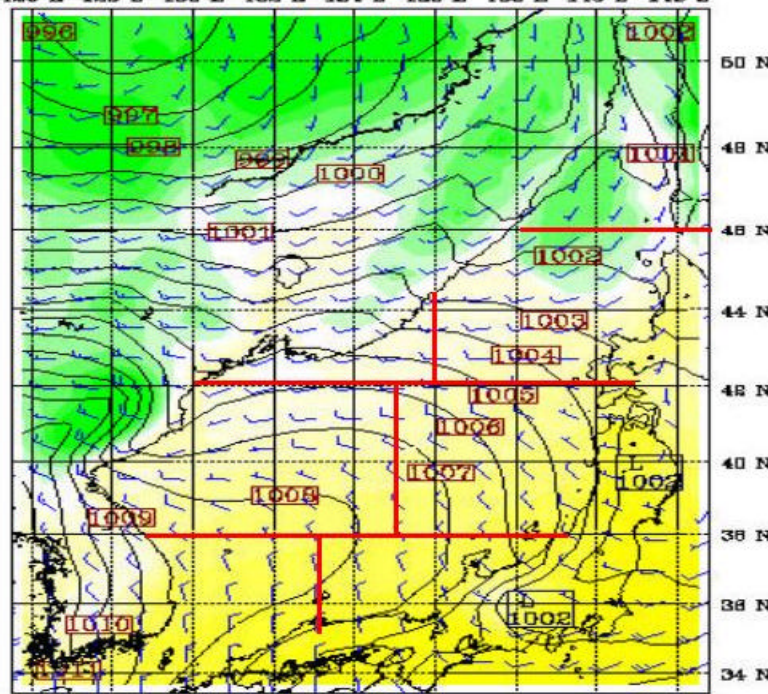
Fcst: 696.00

Temperature

Sea-level pressure

Valid: 0000 UTC Sat 30 May 98 (0900 LST Sat 30 May 98)
at sigma = 0.995

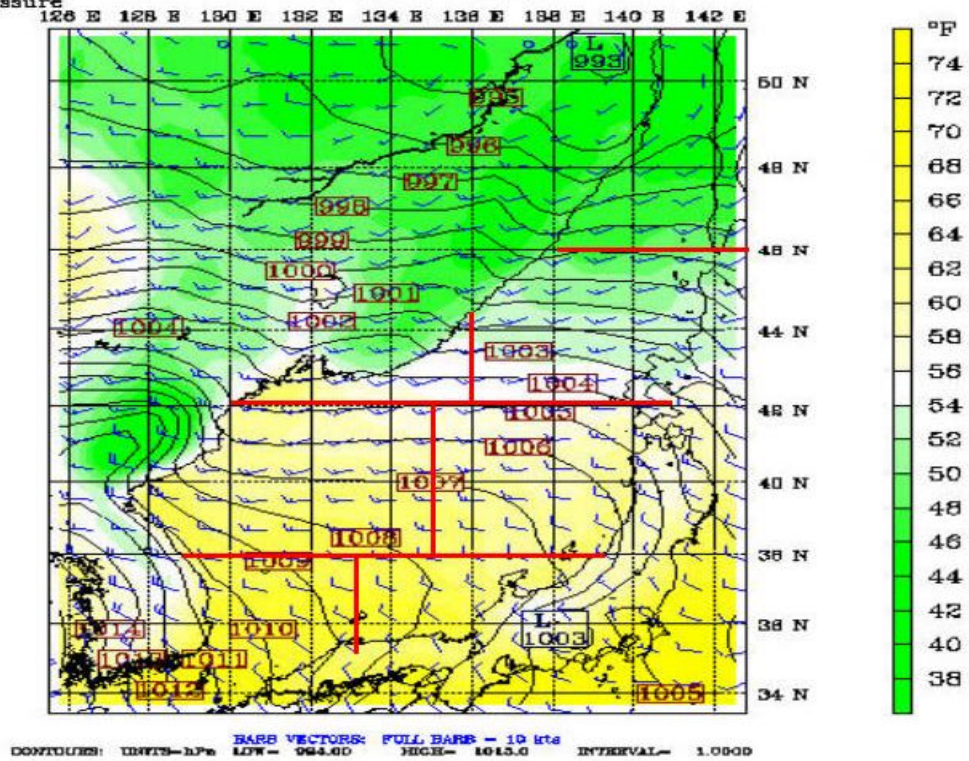
126 E 128 E 130 E 132 E 134 E 136 E 138 E 140 E 142 E



BARB VECTORS: FULL BARB = 10 kts
CONTIGUES: UNITS=hPa LFW= 995.00 HGH= 1013.0 INTERVAL= 1.0000

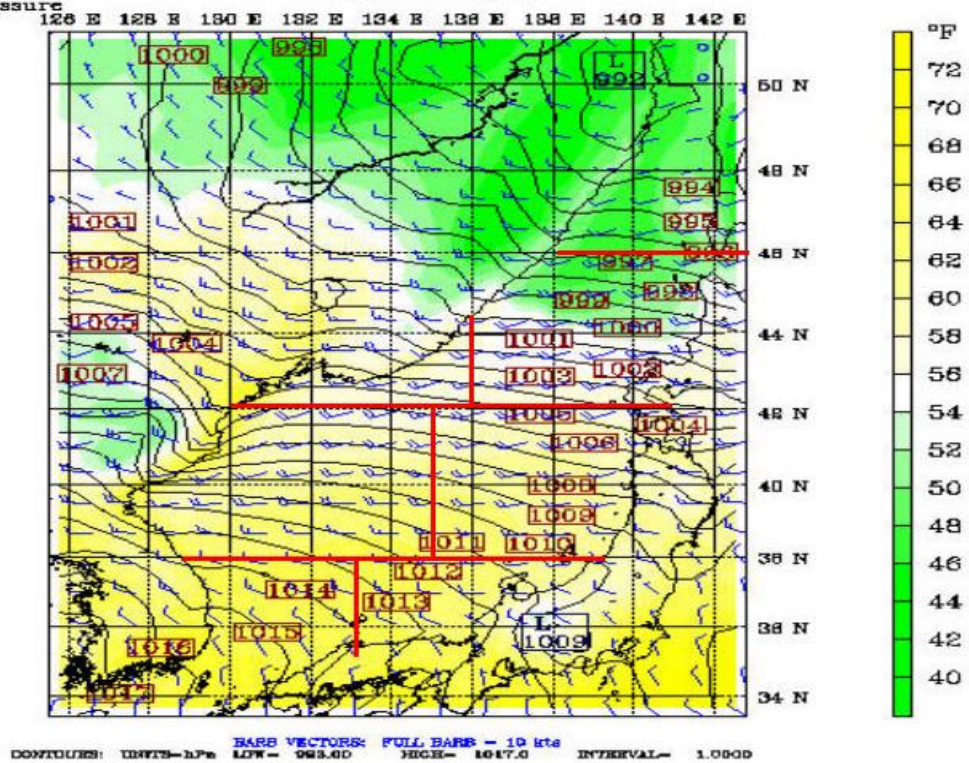
Fast: 708.00
 Temperature
 Sea-level pressure

Valid: 1200 UTC Sat 30 May 98 (2100 LST Sat 30 May 98)
 at sigma - 0.995



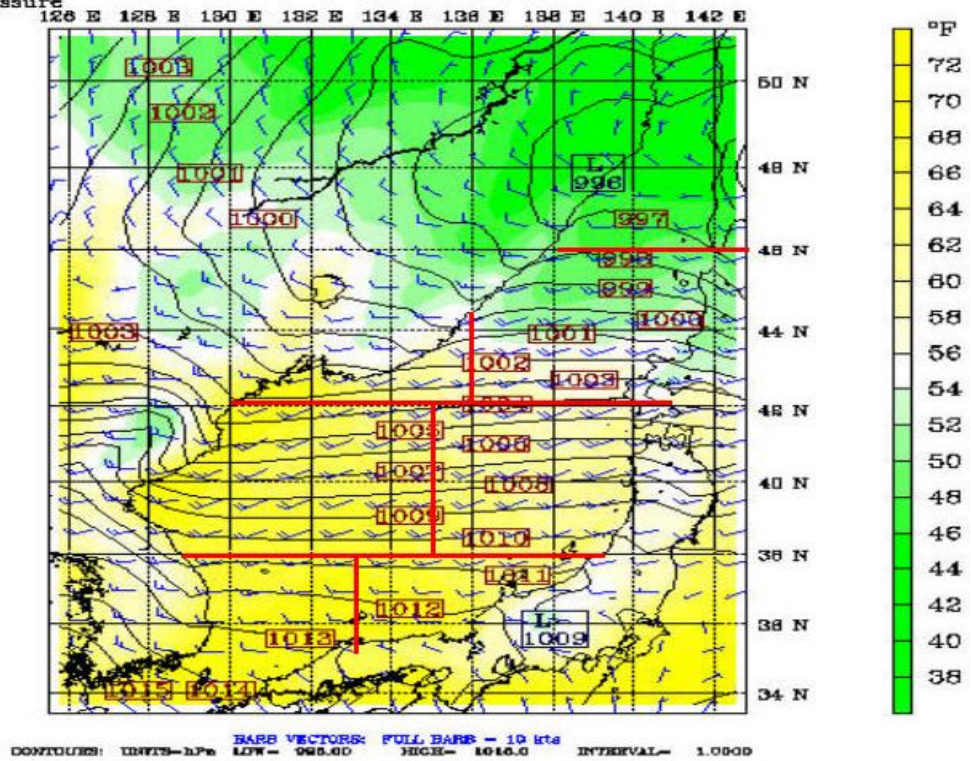
Fast: 720.00
 Temperature
 Sea-level pressure

Valid: 0000 UTC Sun 31 May 98 (0900 LST Sun 31 May 98)
 at sigma - 0.995



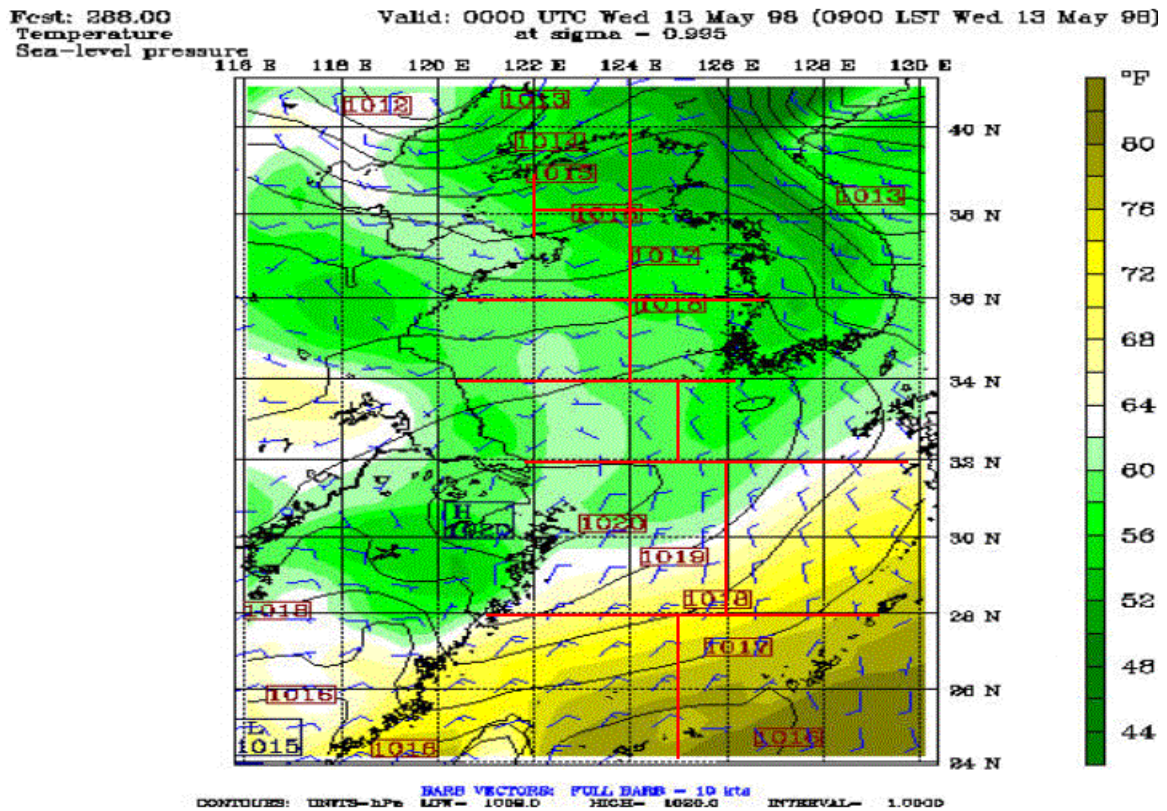
Fest: 732.00
Temperature
Sea-level pressure

Valid: 1200 UTC Sun 31 May 98 (2100 LST Sun 31 May 98)
at sigma = 0.995



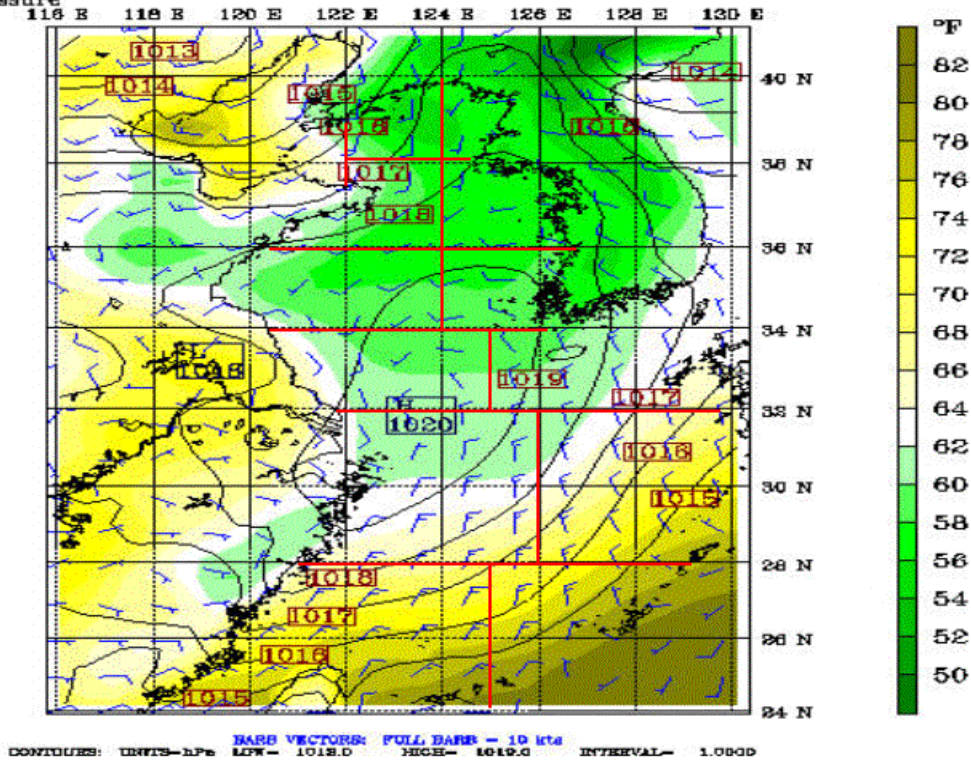
APPENDIX T. SEA LEVEL PRESSURE/SAT/SURFACE WIND PLOTS FOR THE YES FOR THE MAY TIME PERIOD

Appendix T consists of 38 figures that show sea level pressure, SAT, and surface winds for the May time period over the YES. The figures are in time sequential order from May 13 through May 31.



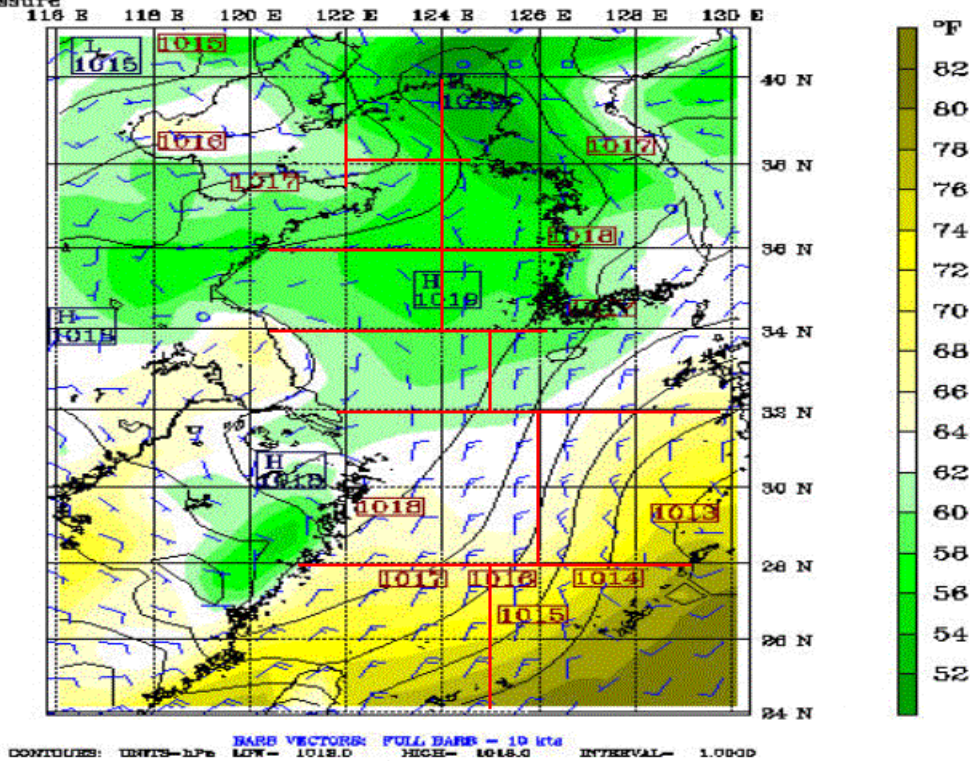
Fast: 300.00
Temperature
Sea-level pressure

Valid: 1200 UTC Wed 13 May 98 (2100 LST Wed 13 May 98)
at sigma - 0.995



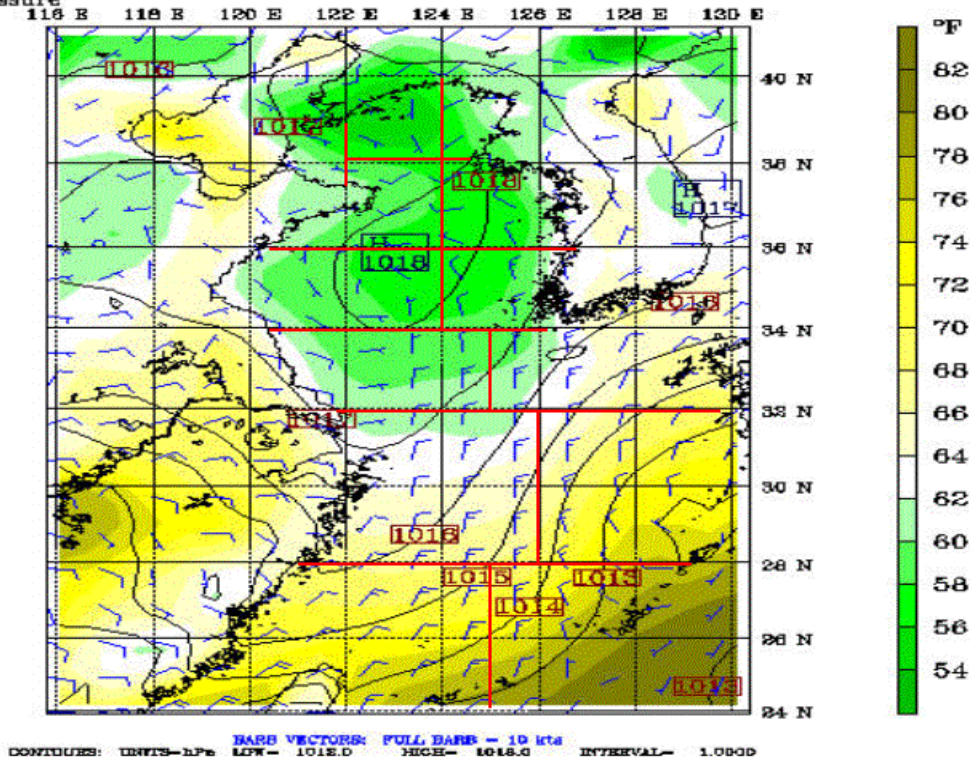
Fast: 312.00
Temperature
Sea-level pressure

Valid: 0000 UTC Thu 14 May 98 (0900 LST Thu 14 May 98)
at sigma - 0.995



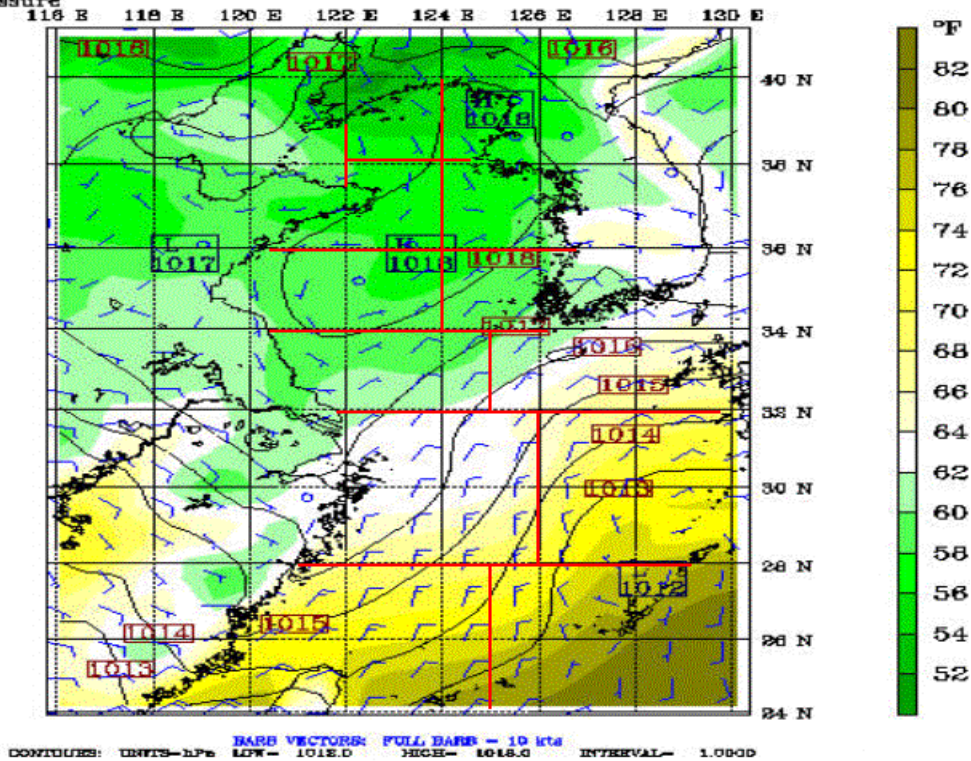
Fast: 324.00
Temperature
Sea-level pressure

Valid: 1200 UTC Thu 14 May 98 (2100 LST Thu 14 May 98)
at sigma - 0.995



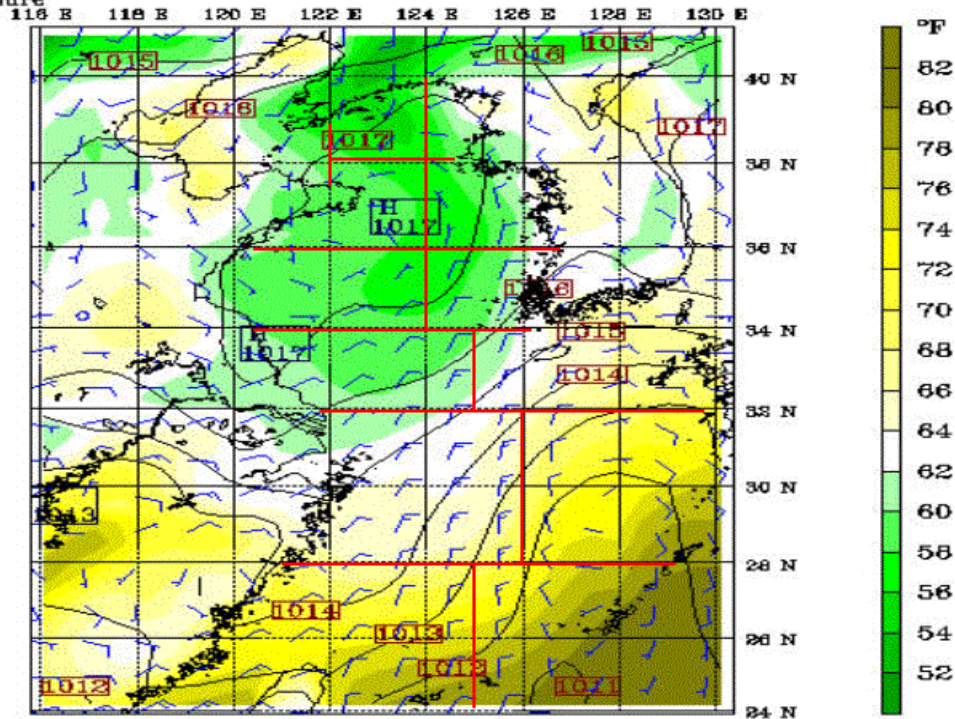
Fast: 336.00
Temperature
Sea-level pressure

Valid: 0000 UTC Fri 15 May 98 (0900 LST Fri 15 May 98)



Fast: 348.00
Temperature
Sea-level pressure

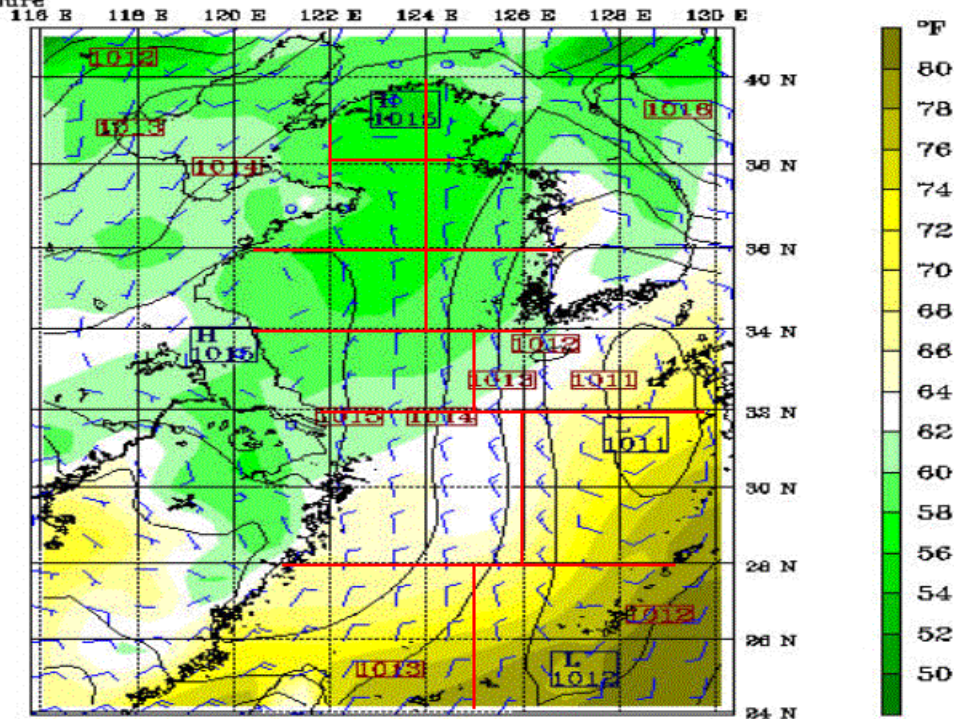
Valid: 1200 UTC Fri 15 May 98 (2100 LST Fri 15 May 98)
at sigma - 0.995



BARB VECTORS: FULL BARB - 10 kts
CONTOURS: UNITS-hPa LOW- 1011.0 HIGH- 1017.0 INTERVAL- 1.0000

Fast: 360.00
Temperature
Sea-level pressure

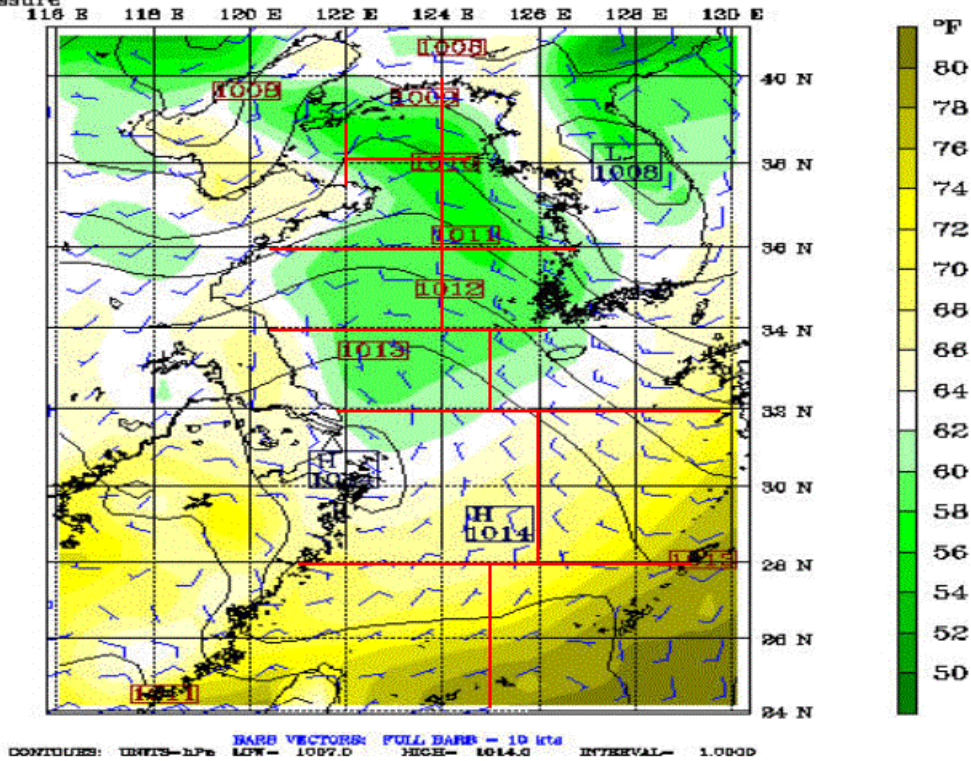
Valid: 0000 UTC Sat 16 May 98 (0900 LST Sat 16 May 98)
at sigma - 0.995



BARB VECTORS: FULL BARB - 10 kts
CONTOURS: UNITS-hPa LOW- 1011.0 HIGH- 1017.0 INTERVAL- 1.0000

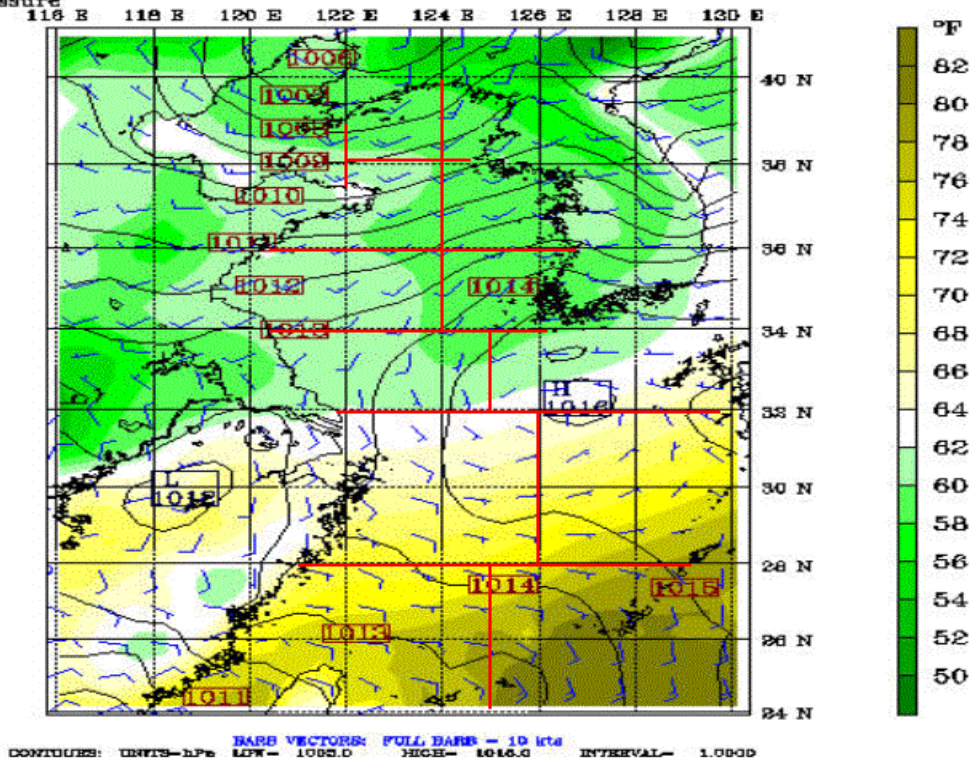
Fast: 372.00
Temperature
Sea-level pressure

Valid: 1200 UTC Sat 16 May 98 (2100 LST Sat 16 May 98)
at sigma - 0.995



Fast: 384.00
Temperature
Sea-level pressure

Valid: 0000 UTC Sun 17 May 98 (0900 LST Sun 17 May 98)
at sigma - 0.995



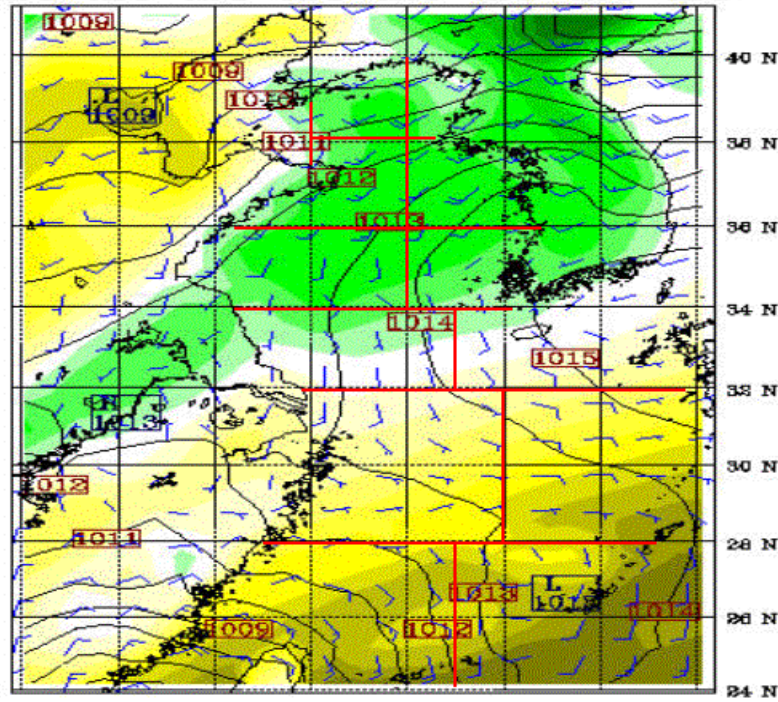
Fast: 396.00

Temperature

Sea-level pressure

Valid: 1200 UTC Sun 17 May 98 (2100 LST Sun 17 May 98)
at sigma - 0.995

118 E 118 E 120 E 122 E 124 E 126 E 128 E 130 E



BARB VECTORS: FULL BARB = 10 kts
CONTIGUES: UNITS-hPa LOW- 1008.0 HIGH- 1015.0 INTERVAL- 1.0000

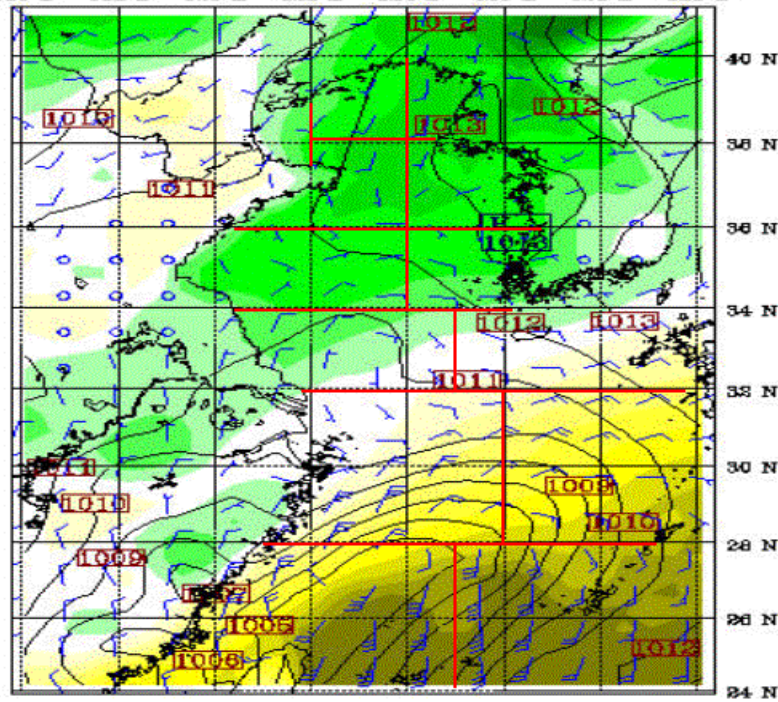
Fast: 408.00

Temperature

Sea-level pressure

Valid: 0000 UTC Mon 18 May 98 (0900 LST Mon 18 May 98)
at sigma - 0.995

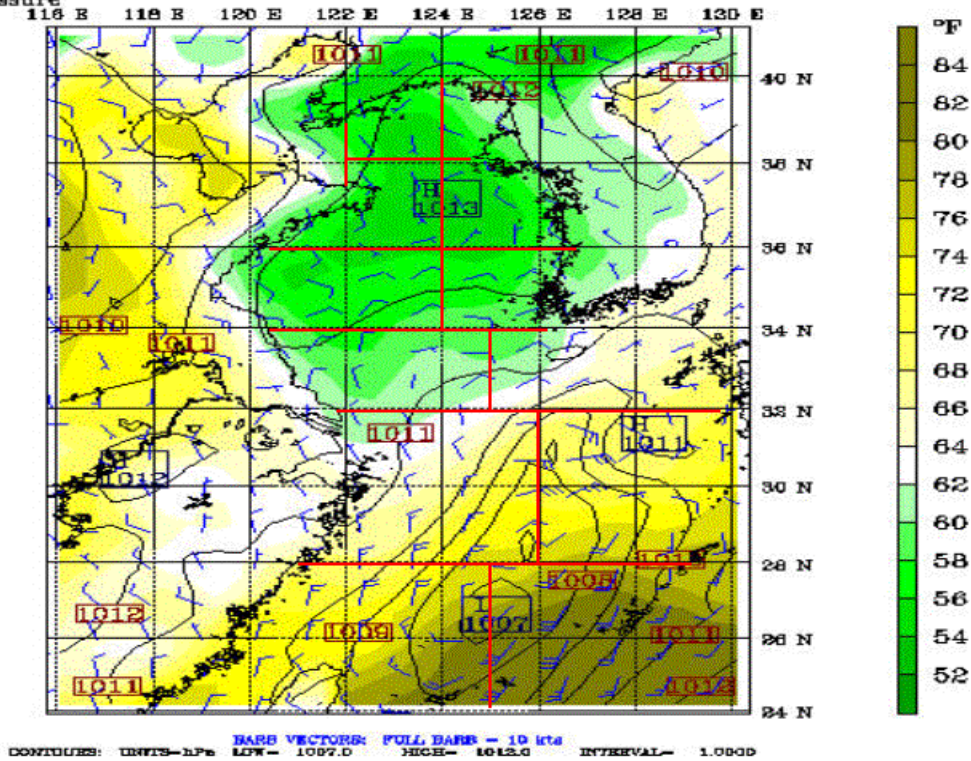
118 E 118 E 120 E 122 E 124 E 126 E 128 E 130 E



BARB VECTORS: FULL BARB = 10 kts
CONTIGUES: UNITS-hPa LOW- 1008.0 HIGH- 1014.0 INTERVAL- 1.0000

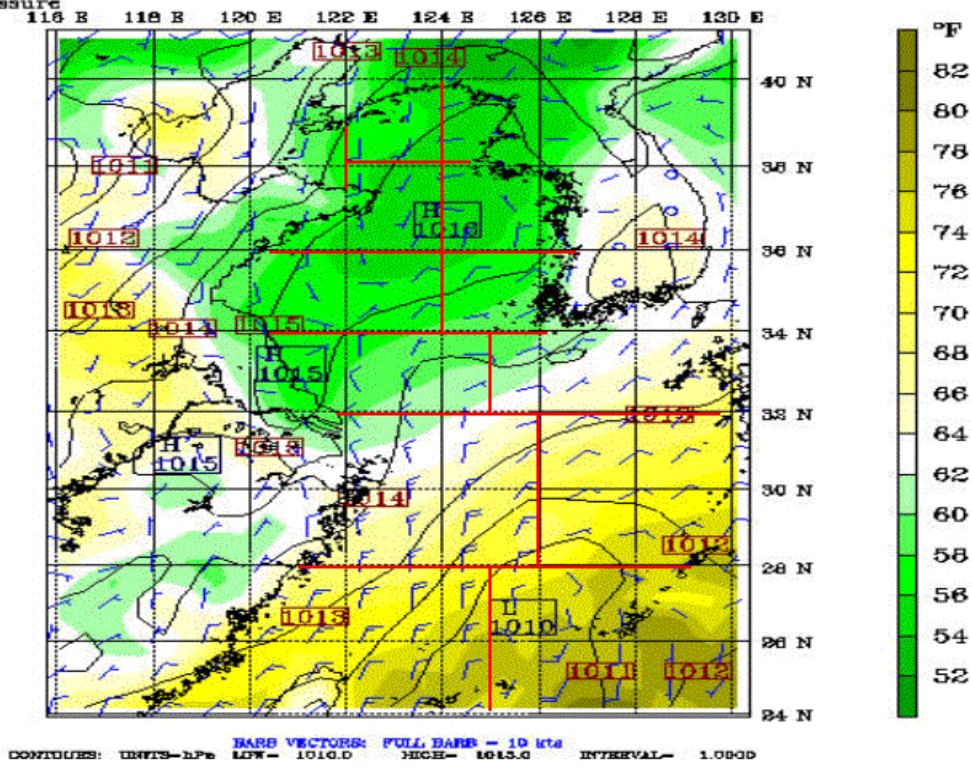
Fcst: 420.00
Temperature
Sea-level pressure

Valid: 1200 UTC Mon 18 May 98 (2100 LST Mon 18 May 98)
at sigma = 0.995



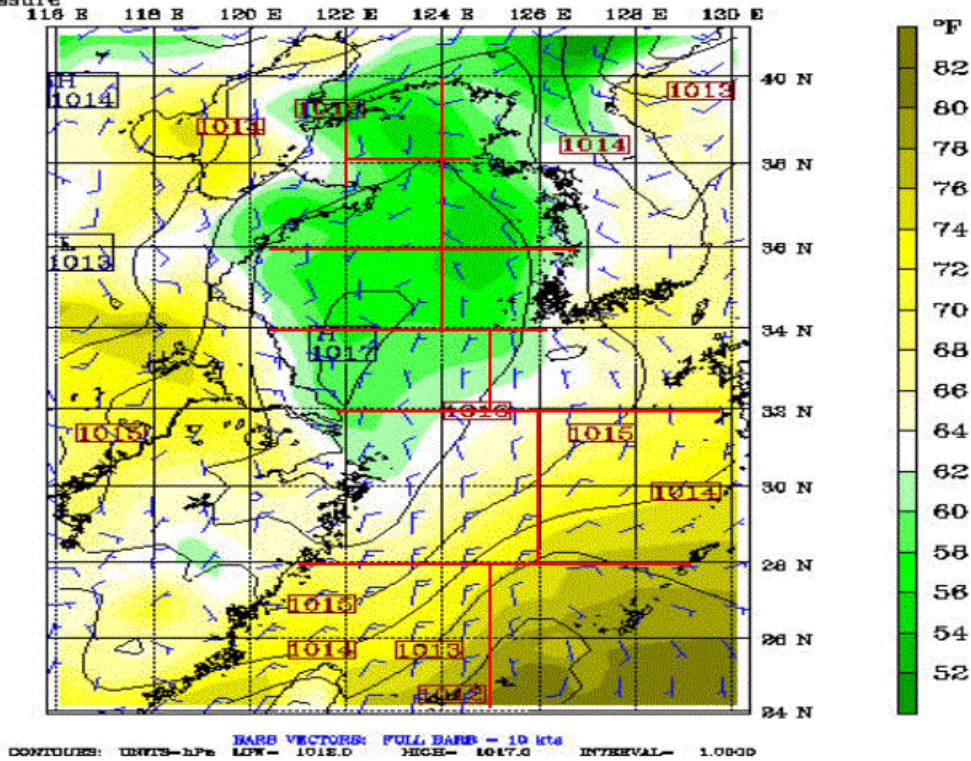
Fcst: 432.00
Temperature
Sea-level pressure

Valid: 0000 UTC Tue 19 May 98 (0900 LST Tue 19 May 98)
at sigma = 0.995



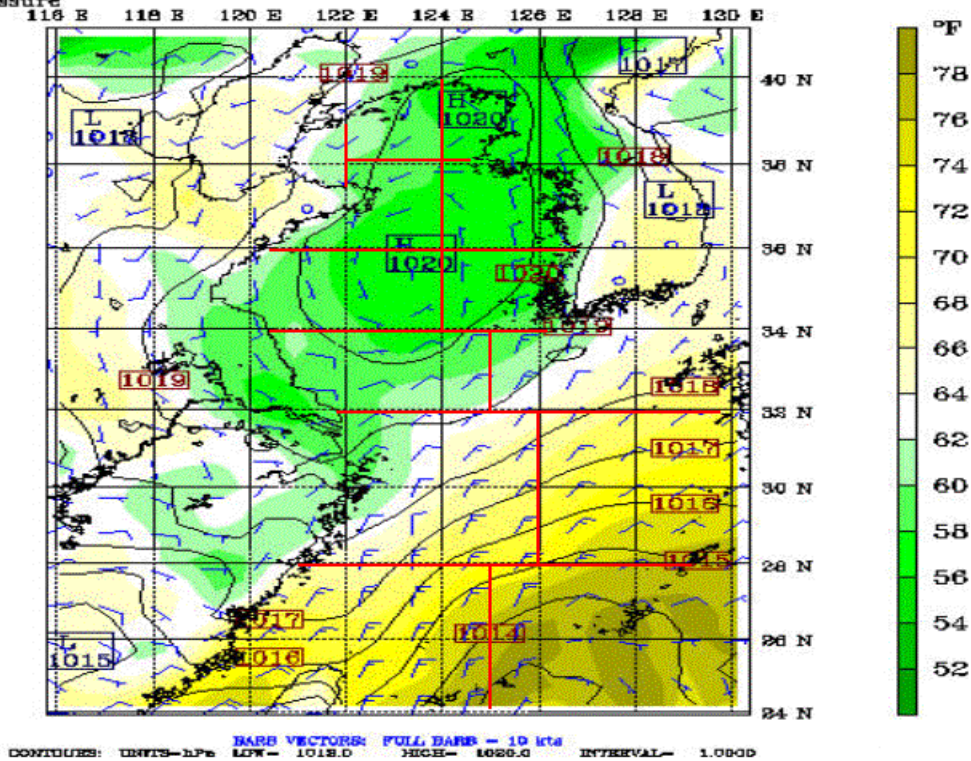
Fast: 444.00
Temperature
Sea-level pressure

Valid: 1200 UTC Tue 19 May 98 (2100 LST Tue 19 May 98)
at sigma - 0.995



Fast: 456.00
Temperature
Sea-level pressure

Valid: 0000 UTC Wed 20 May 98 (0900 LST Wed 20 May 98)
at sigma - 0.995

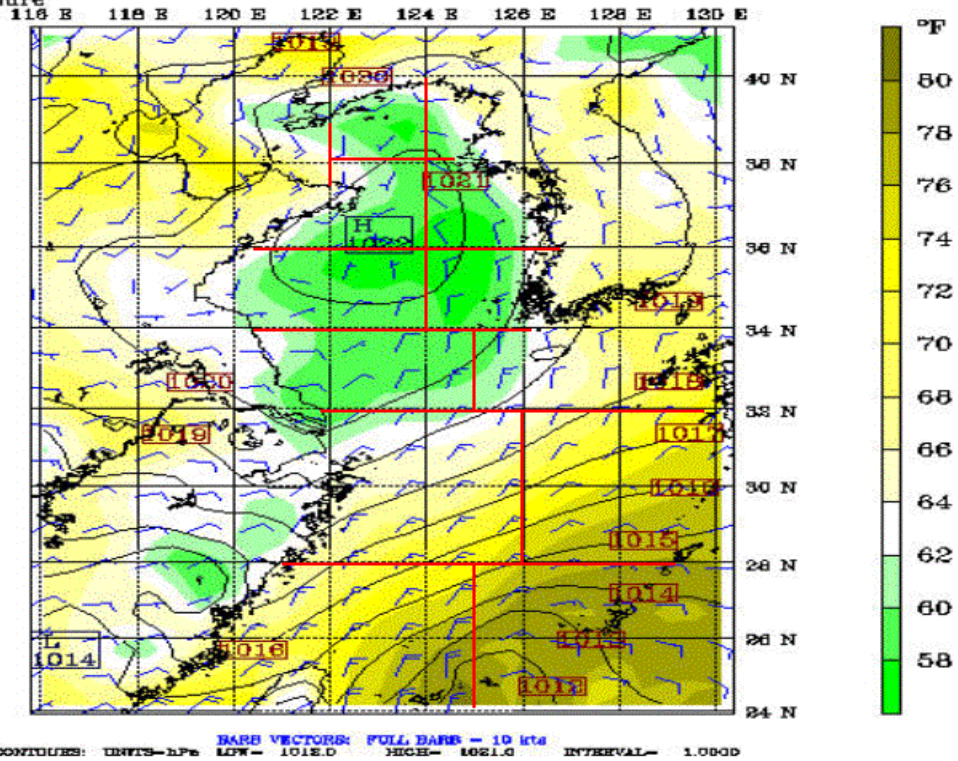


Fast: 468.00

Temperature

Sea-level pressure

Valid: 1200 UTC Wed 20 May 98 (2100 LST Wed 20 May 98)
at sigma - 0.995

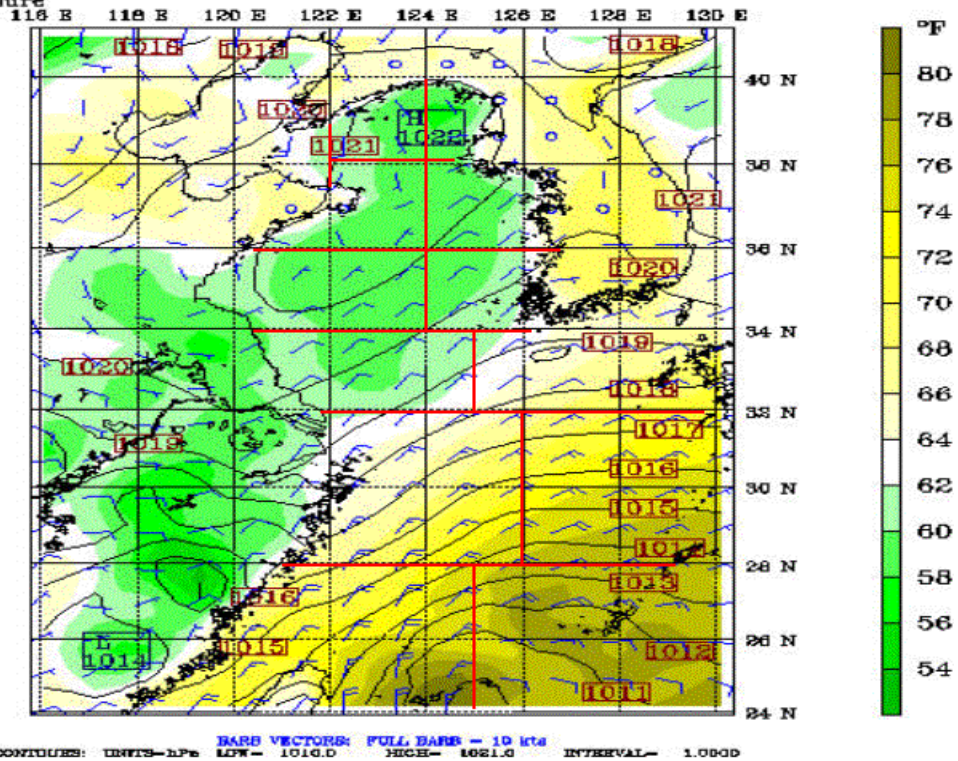


Fast: 480.00

Temperature

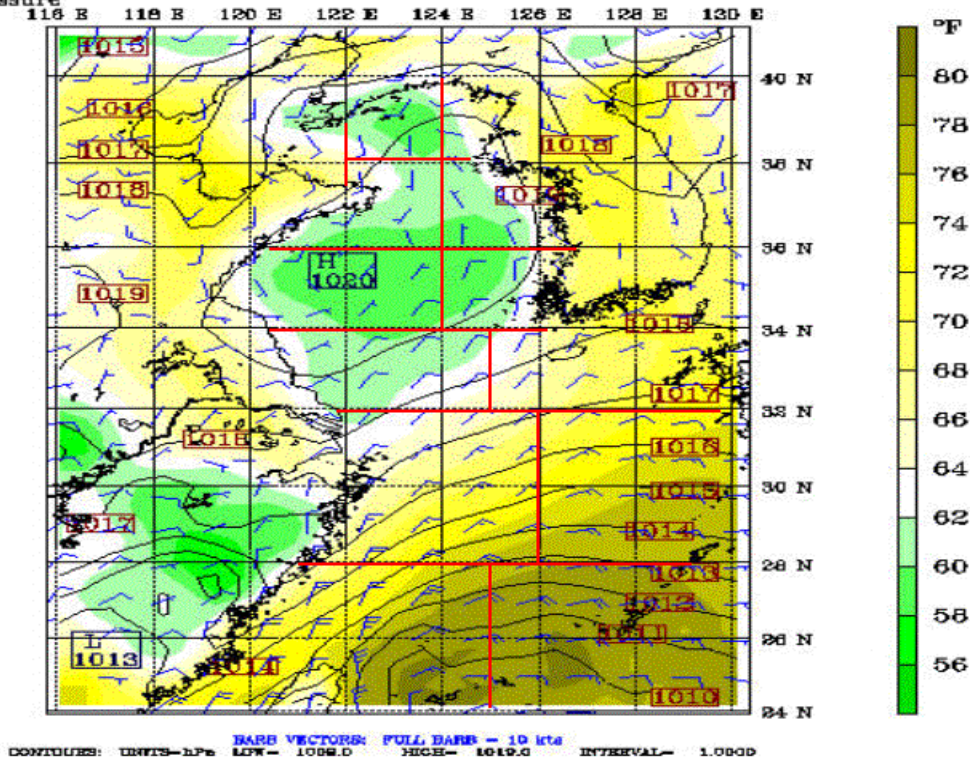
Sea-level pressure

Valid: 0000 UTC Thu 21 May 98 (0900 LST Thu 21 May 98)
at sigma - 0.995



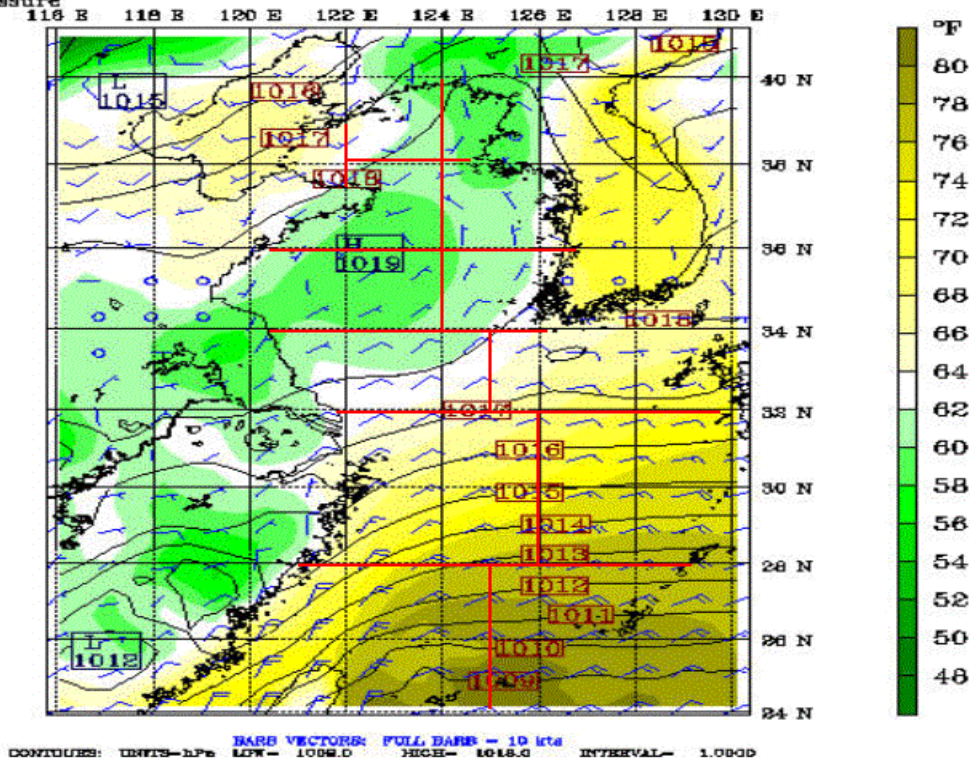
Fast: 492.00
Temperature
Sea-level pressure

Valid: 1200 UTC Thu 21 May 98 (2100 LST Thu 21 May 98)
at sigma - 0.995



Fast: 504.00
Temperature
Sea-level pressure

Valid: 0000 UTC Fri 22 May 98 (0900 LST Fri 22 May 98)
at sigma - 0.995



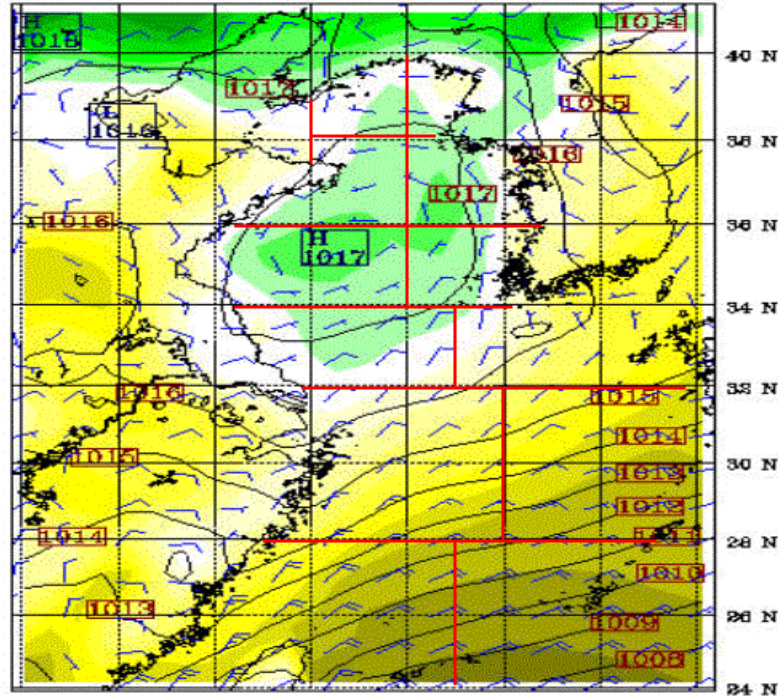
Fast: 516.00

Temperature

Sea-level pressure

Valid: 1200 UTC Fri 22 May 98 (2100 LST Fri 22 May 98)
at sigma - 0.995

118 E 118 E 120 E 122 E 124 E 126 E 128 E 130 E



BARB VECTORS: FULL BARB = 10 kts
CONTIGUES: UNITS-hPa LOW- 1008.0 HIGH- 1017.0 INTERVAL- 1.0000

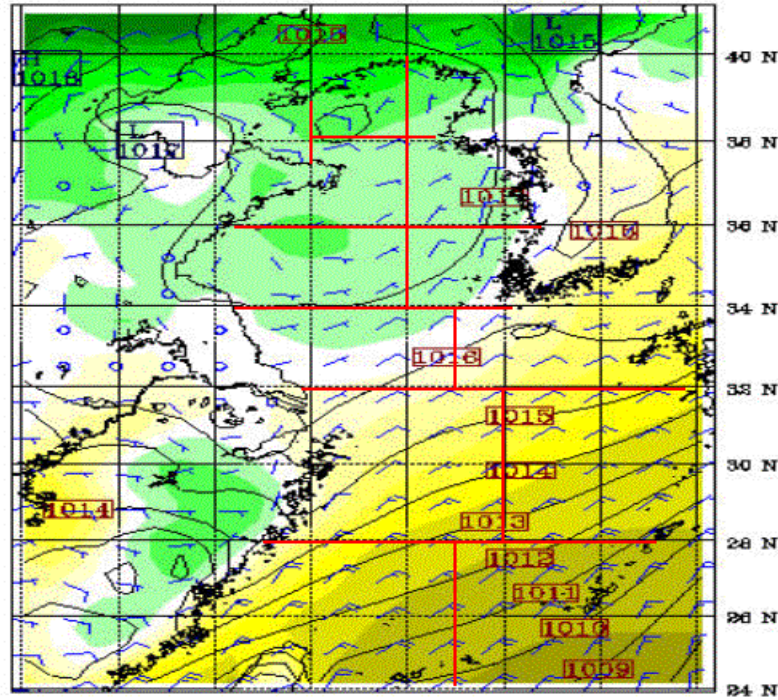
Fast: 528.00

Temperature

Sea-level pressure

Valid: 0000 UTC Sat 23 May 98 (0900 LST Sat 23 May 98)
at sigma - 0.995

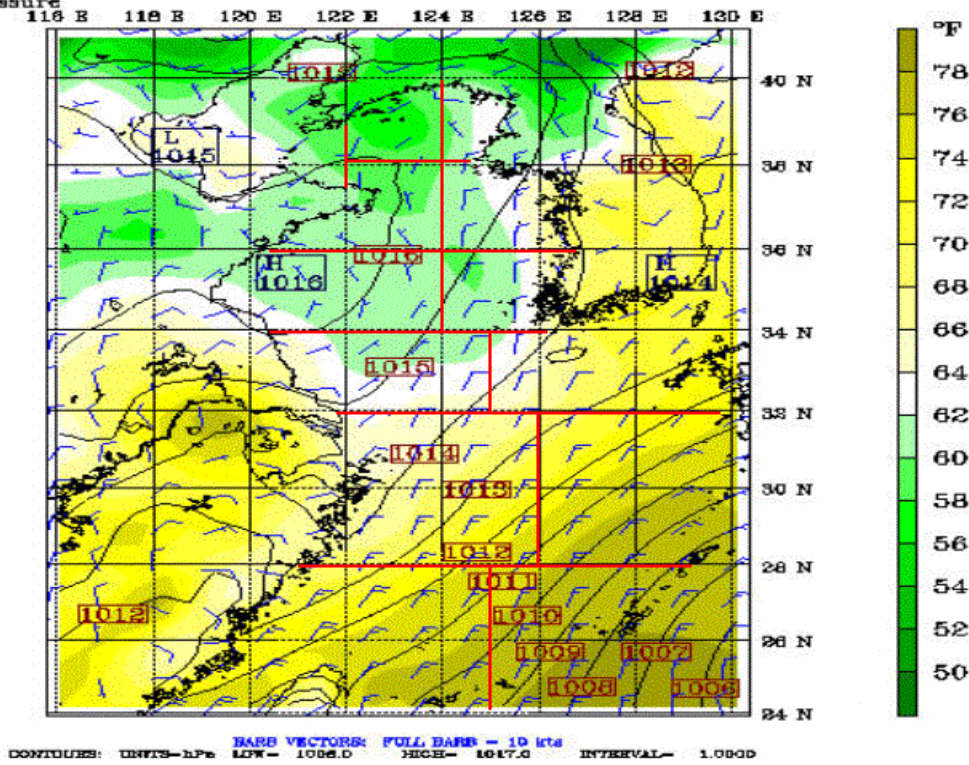
118 E 118 E 120 E 122 E 124 E 126 E 128 E 130 E



BARB VECTORS: FULL BARB = 10 kts
CONTIGUES: UNITS-hPa LOW- 1009.0 HIGH- 1018.0 INTERVAL- 1.0000

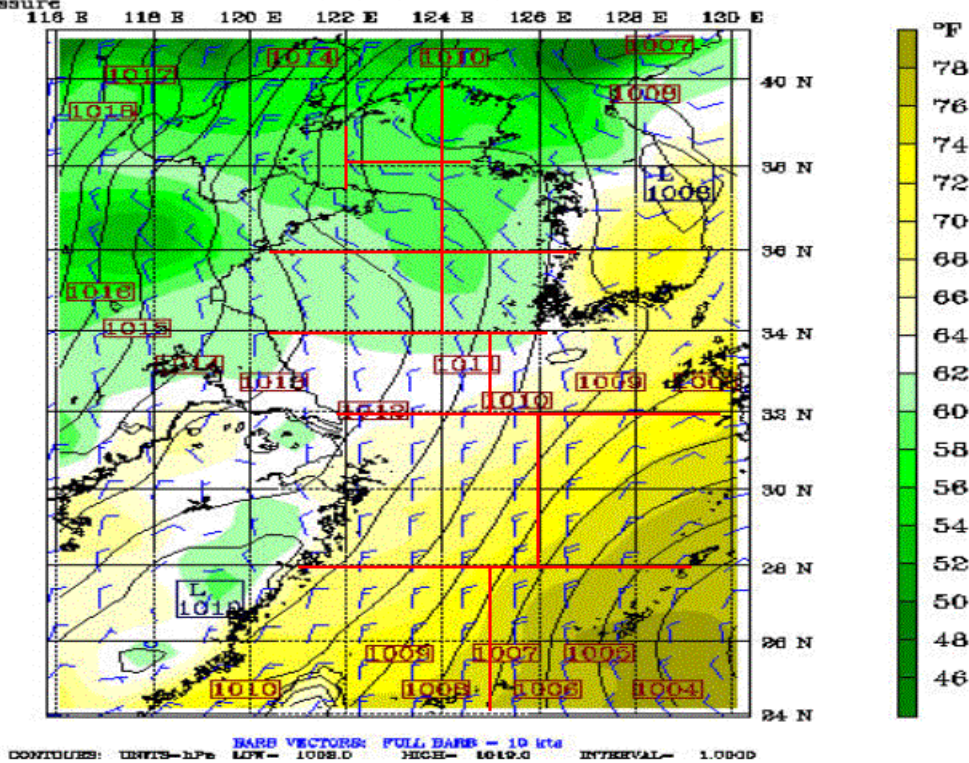
Fast: 540.00
Temperature
Sea-level pressure

Valid: 1200 UTC Sat 23 May 98 (2100 LST Sat 23 May 98)
at sigma - 0.995



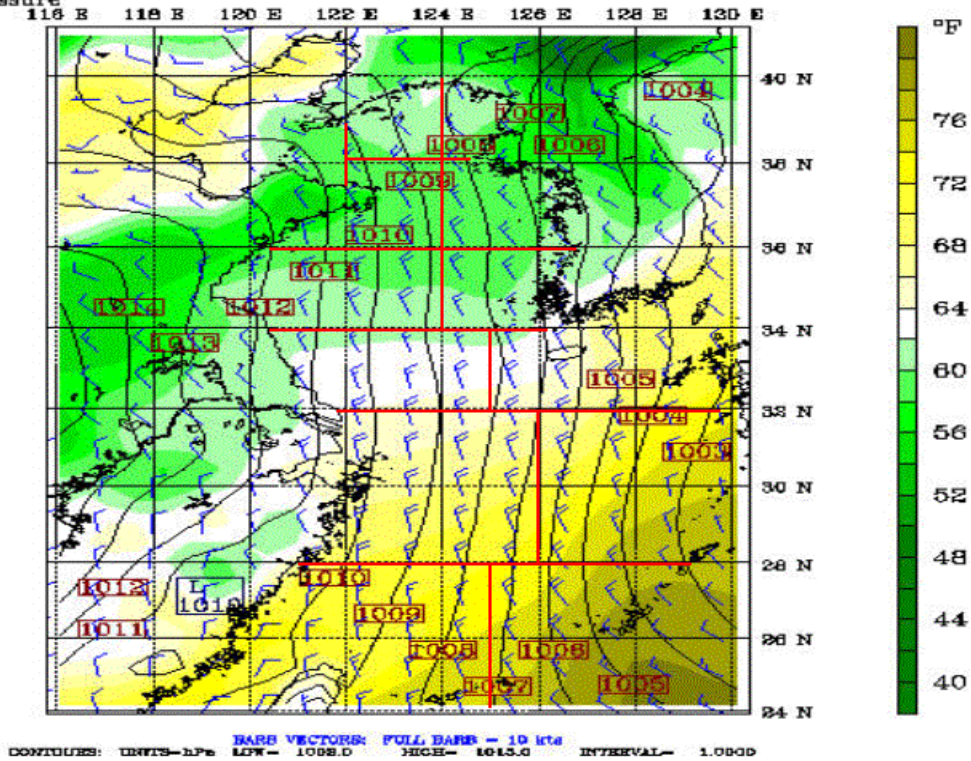
Fast: 552.00
Temperature
Sea-level pressure

Valid: 0000 UTC Sun 24 May 98 (0900 LST Sun 24 May 98)
at sigma - 0.995



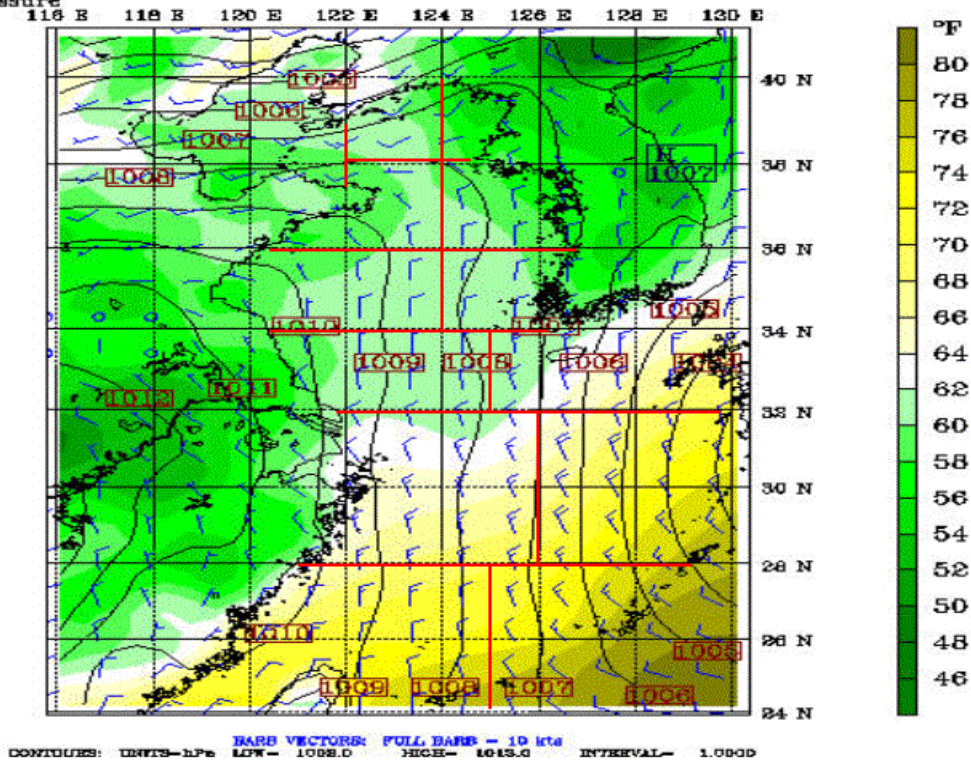
Fast: 564.00
Temperature
Sea-level pressure

Valid: 1200 UTC Sun 24 May 98 (2100 LST Sun 24 May 98)
at sigma - 0.995



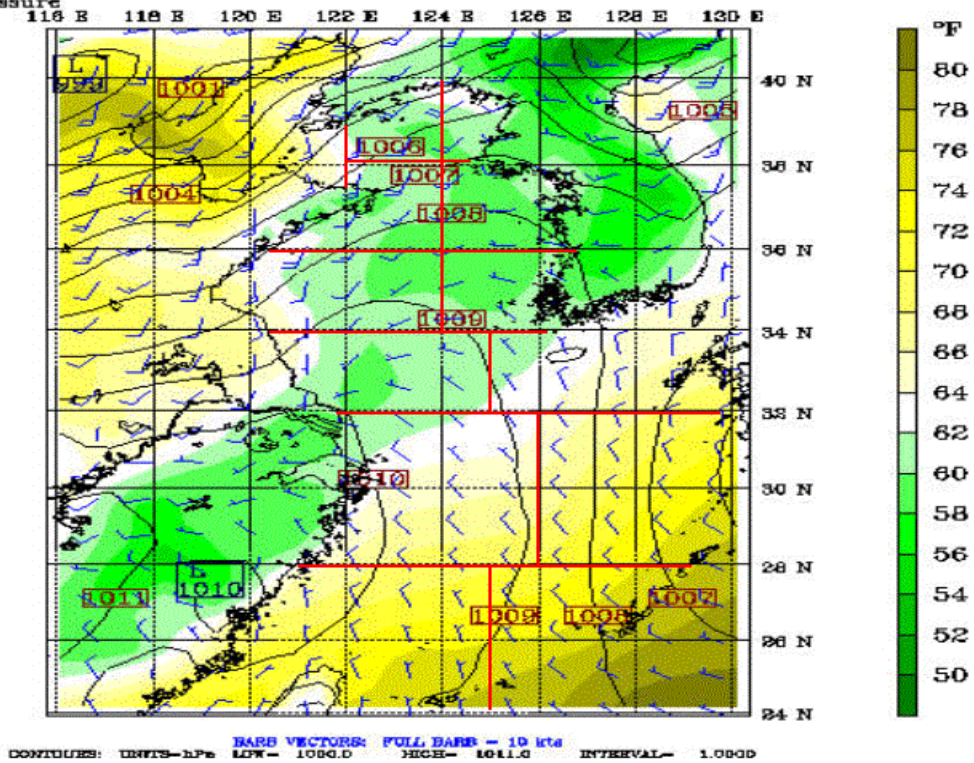
Fast: 576.00
Temperature
Sea-level pressure

Valid: 0000 UTC Mon 25 May 98 (0900 LST Mon 25 May 98)
at sigma - 0.995



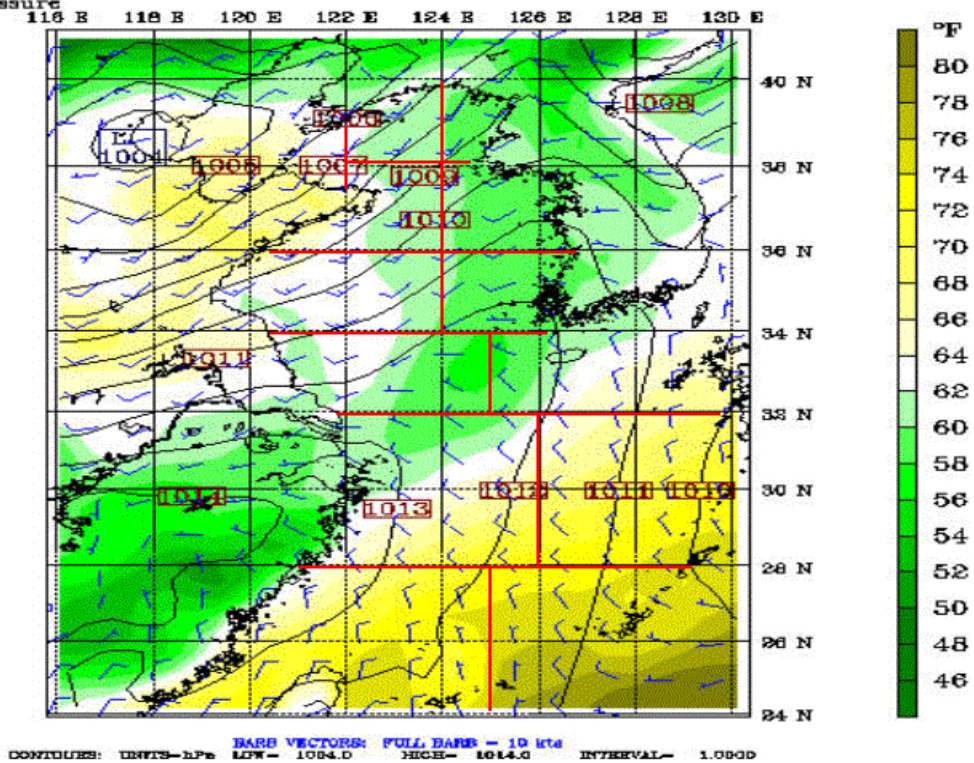
Fast: 588.00
Temperature
Sea-level pressure

Valid: 1200 UTC Mon 25 May 98 (2100 LST Mon 25 May 98)
at sigma = 0.995



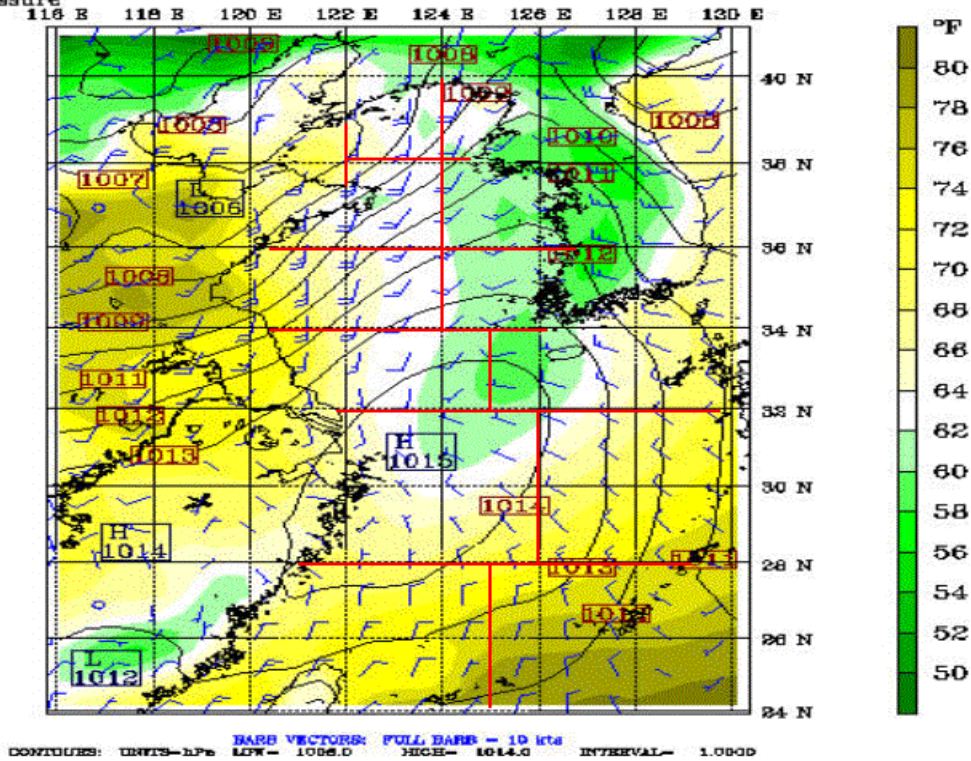
Fast: 600.00
Temperature
Sea-level pressure

Valid: 0000 UTC Tue 26 May 98 (0900 LST Tue 26 May 98)
at sigma = 0.995



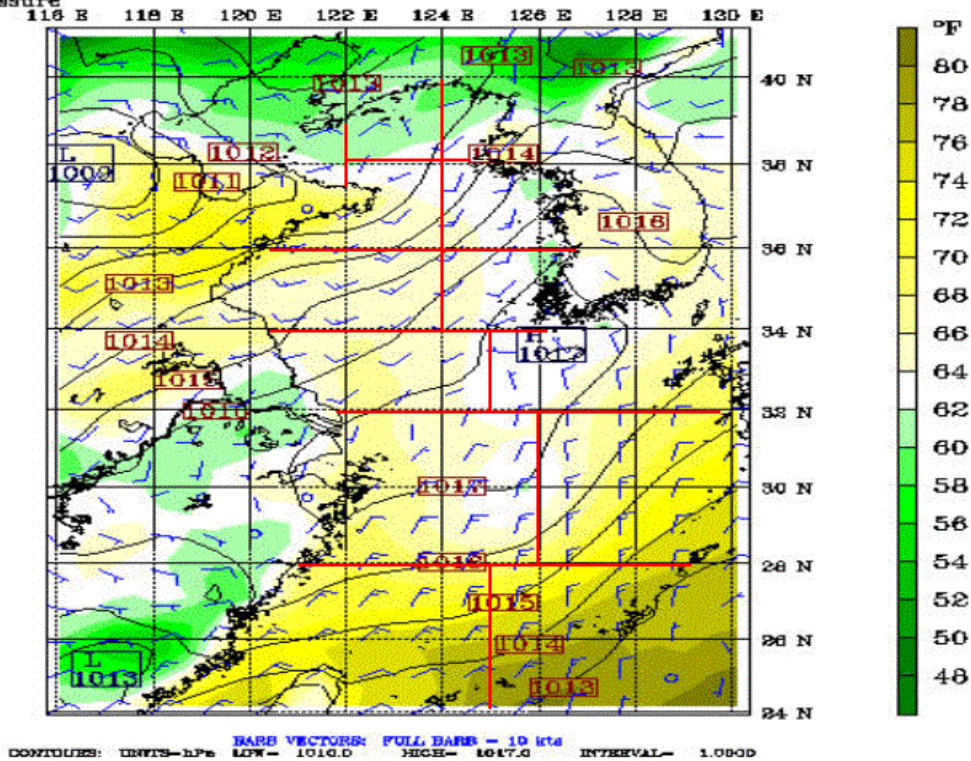
Fast: 612.00
Temperature
Sea-level pressure

Valid: 1200 UTC Tue 26 May 98 (2100 LST Tue 26 May 98)
at sigma - 0.995



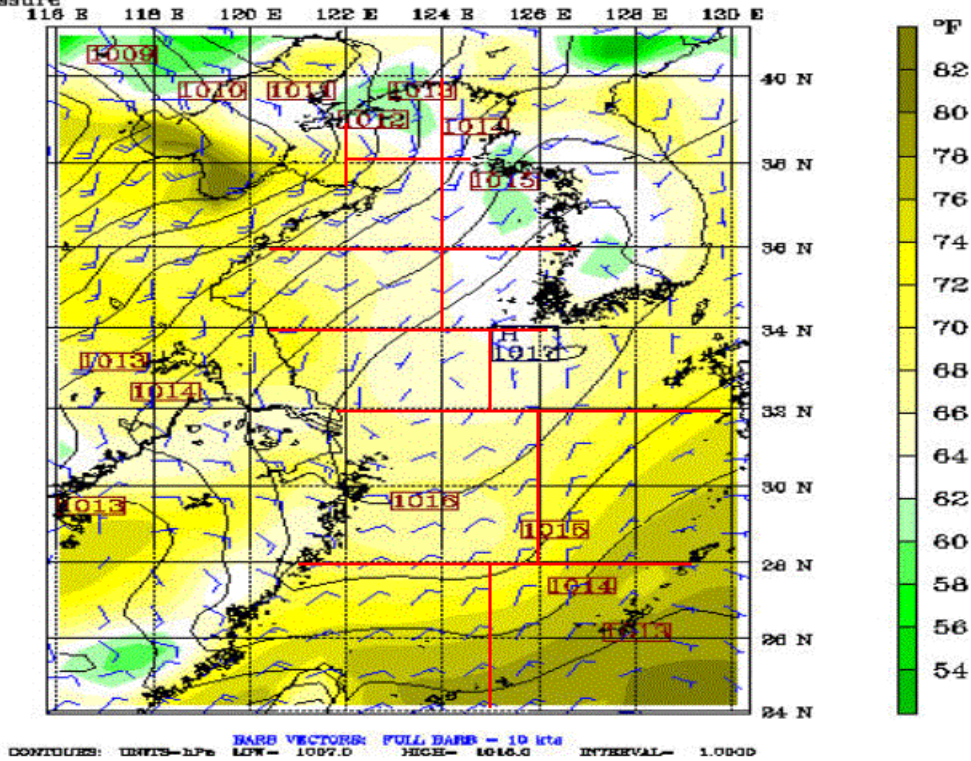
Fast: 624.00
Temperature
Sea-level pressure

Valid: 0000 UTC Wed 27 May 98 (0900 LST Wed 27 May 98)
at sigma - 0.995



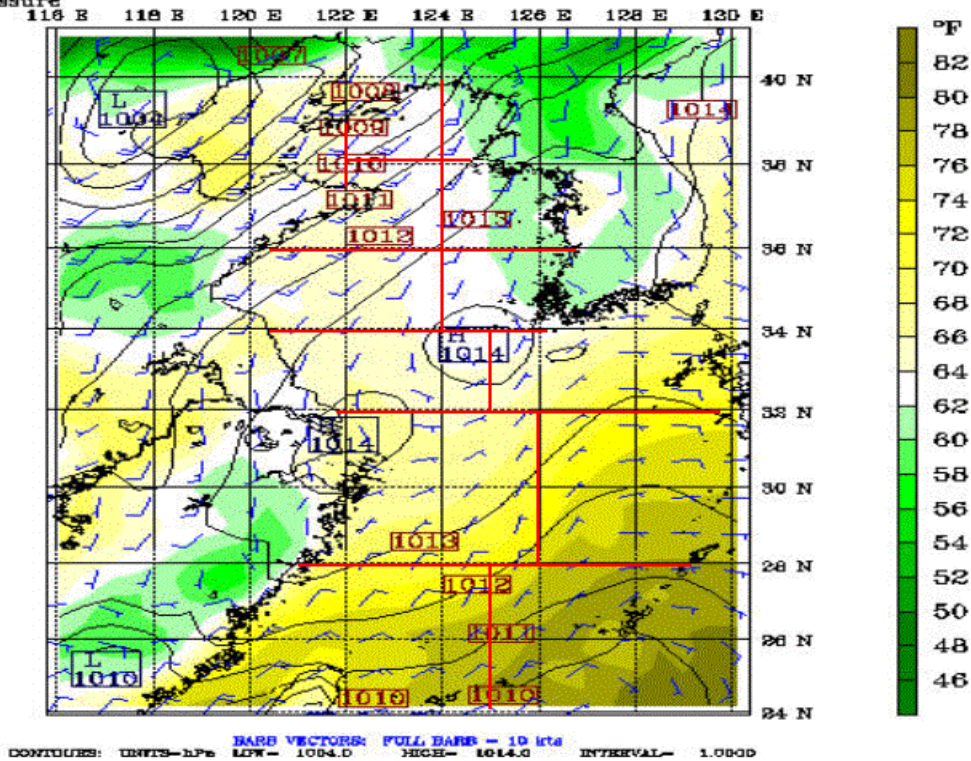
Fast: 636.00
Temperature
Sea-level pressure

Valid: 1200 UTC Wed 27 May 98 (2100 LST Wed 27 May 98)
at sigma - 0.995



Fast: 648.00
Temperature
Sea-level pressure

Valid: 0000 UTC Thu 28 May 98 (0900 LST Thu 28 May 98)
at sigma - 0.995



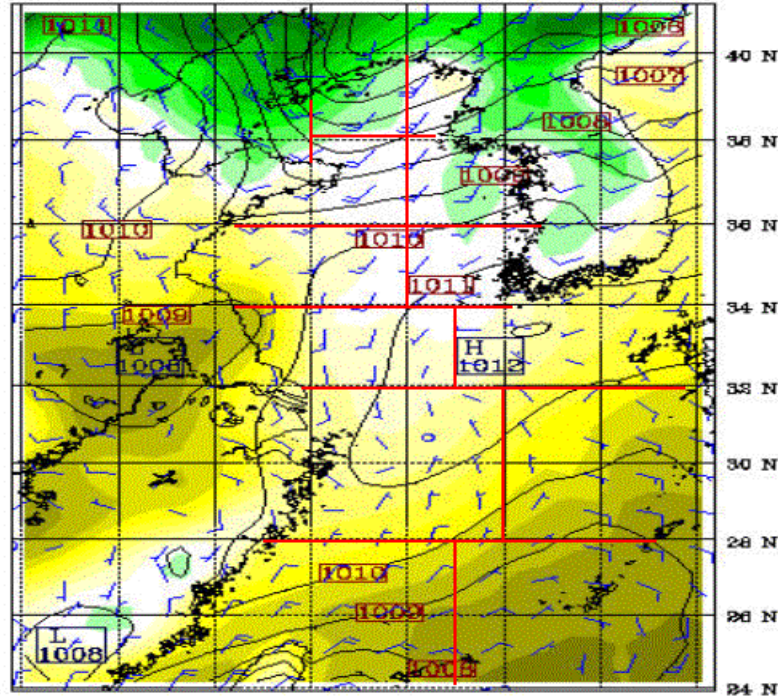
Fast: 660.00

Temperature

Sea-level pressure

Valid: 1200 UTC Thu 28 May 98 (2100 LST Thu 28 May 98)
at sigma - 0.995

118 E 118 E 120 E 122 E 124 E 126 E 128 E 130 E



BARB VECTORS: FULL BARB = 10 kts
CONTIGUES: UNITS-hPa LOW= 1008.0 HIGH= 1013.0 INTERVAL= 1.0000

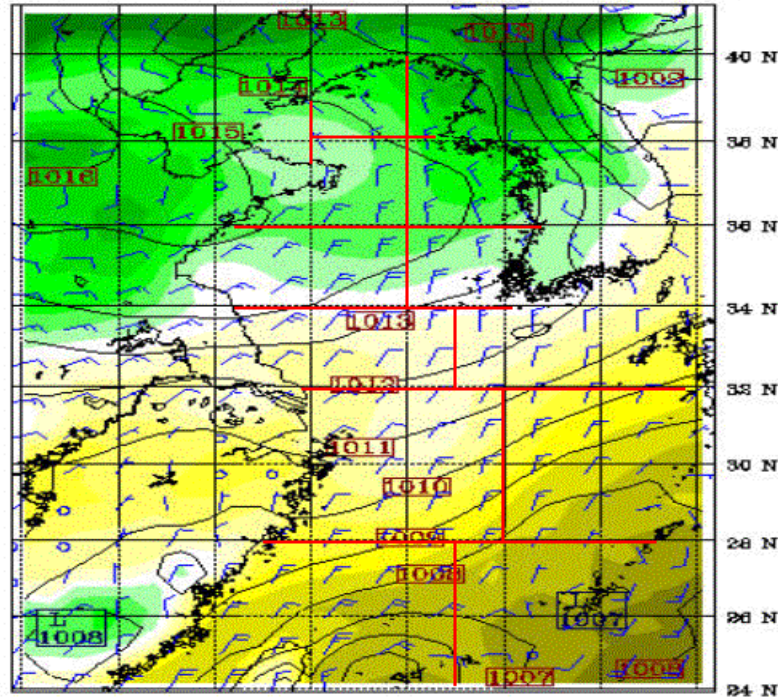
Fast: 672.00

Temperature

Sea-level pressure

Valid: 0000 UTC Fri 29 May 98 (0900 LST Fri 29 May 98)
at sigma - 0.995

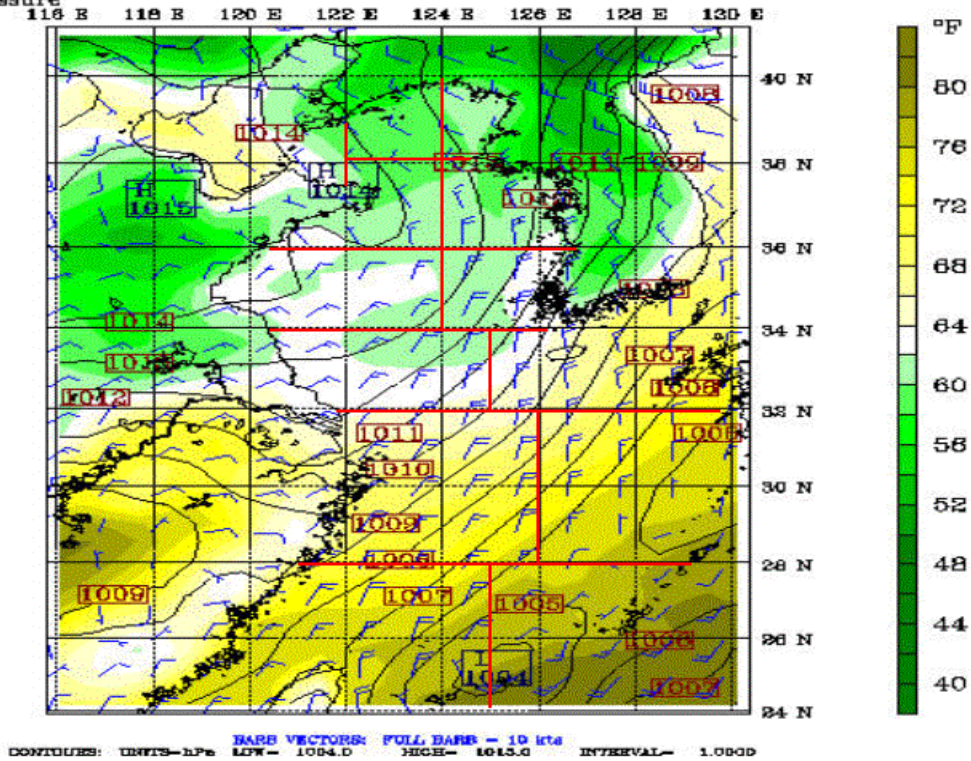
118 E 118 E 120 E 122 E 124 E 126 E 128 E 130 E



BARB VECTORS: FULL BARB = 10 kts
CONTIGUES: UNITS-hPa LOW= 1008.0 HIGH= 1013.0 INTERVAL= 1.0000

Fast: 684.00
Temperature
Sea-level pressure

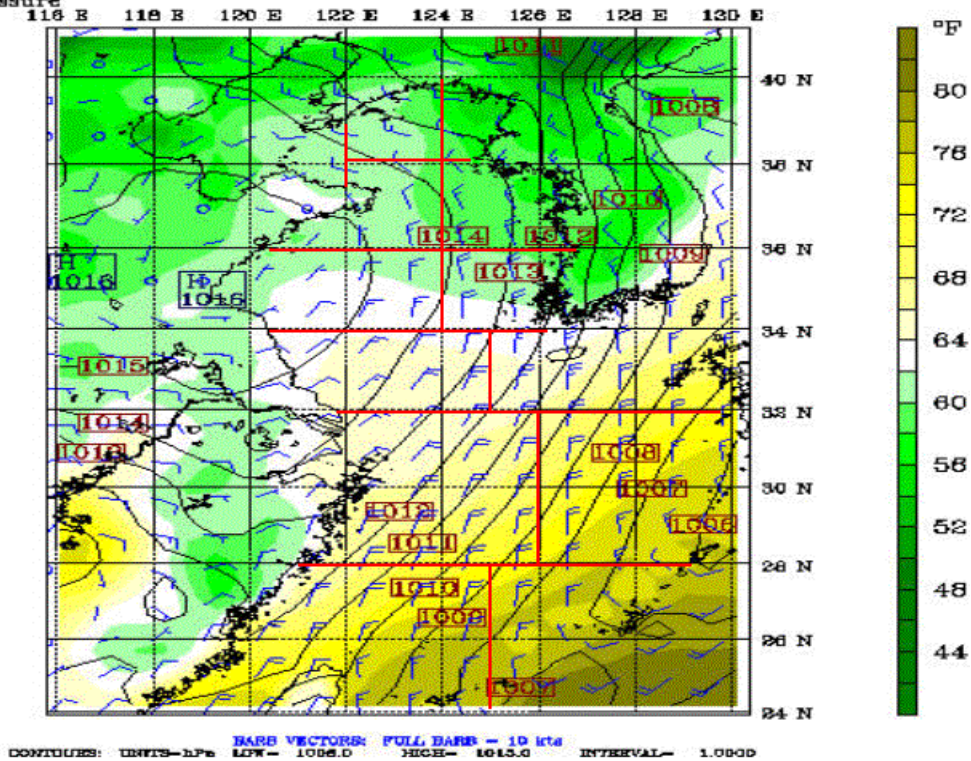
Valid: 1200 UTC Fri 29 May 98 (2100 LST Fri 29 May 98)
at sigma - 0.995



BARB VECTORS: FULL BARB = 10 kts
CONTIGUES: UNITS-hPa LOW- 1004.0 HIGH- 1015.0 INTERVAL- 1.0000

Fast: 696.00
Temperature
Sea-level pressure

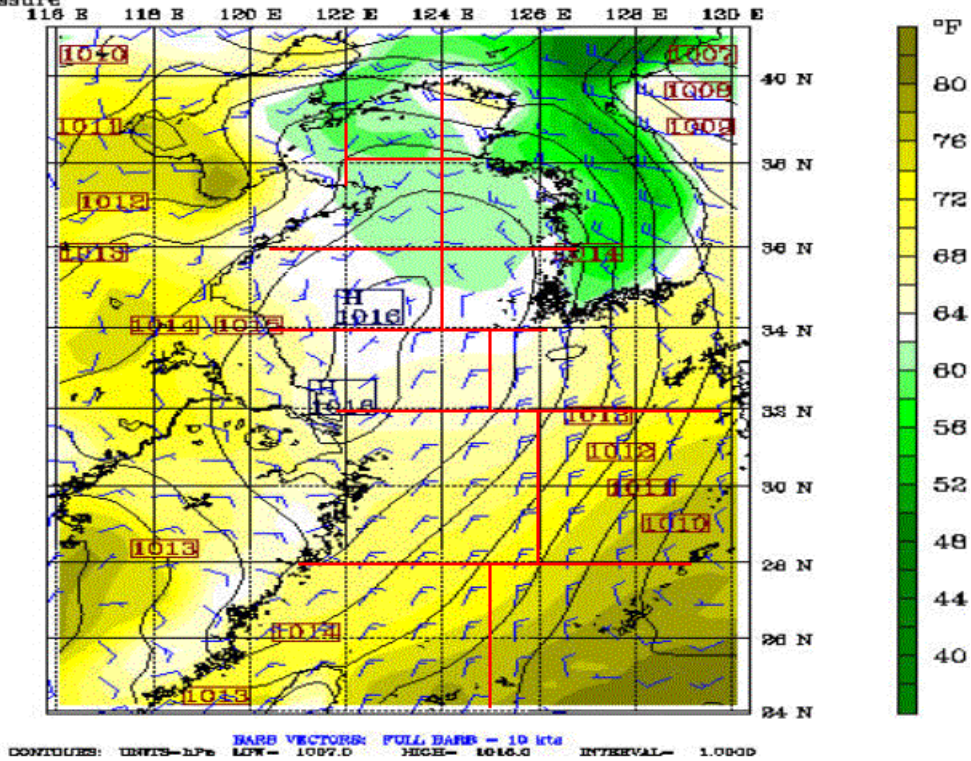
Valid: 0000 UTC Sat 30 May 98 (0900 LST Sat 30 May 98)
at sigma - 0.995



BARB VECTORS: FULL BARB = 10 kts
CONTIGUES: UNITS-hPa LOW- 1006.0 HIGH- 1015.0 INTERVAL- 1.0000

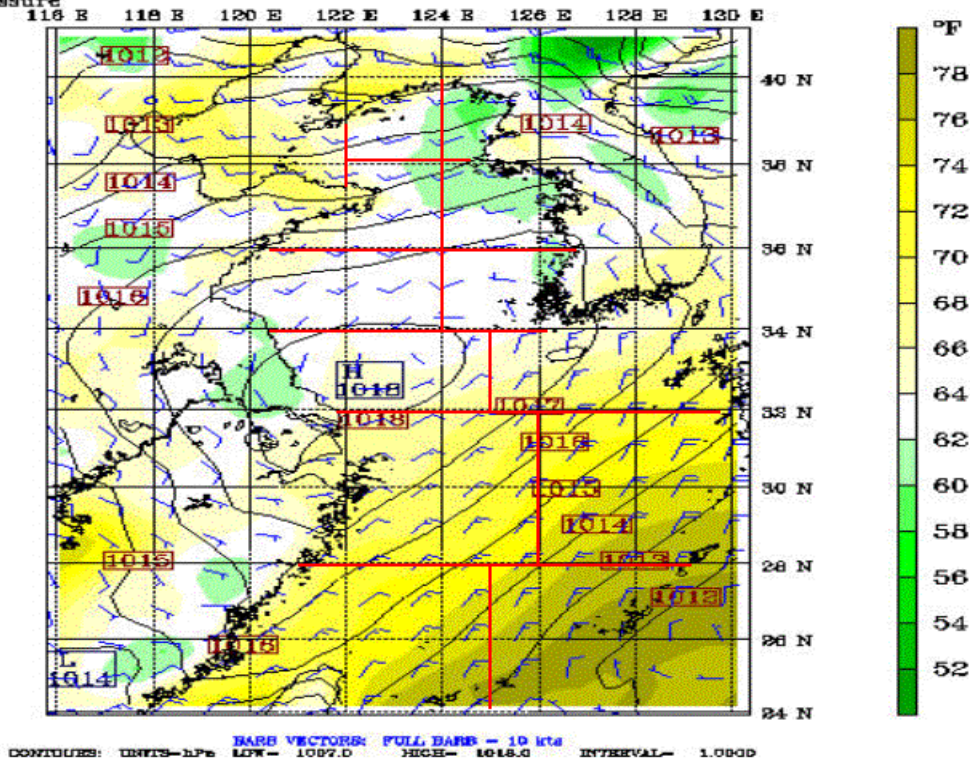
Fast: 708.00
Temperature
Sea-level pressure

Valid: 1200 UTC Sat 30 May 98 (2100 LST Sat 30 May 98)
at sigma - 0.995



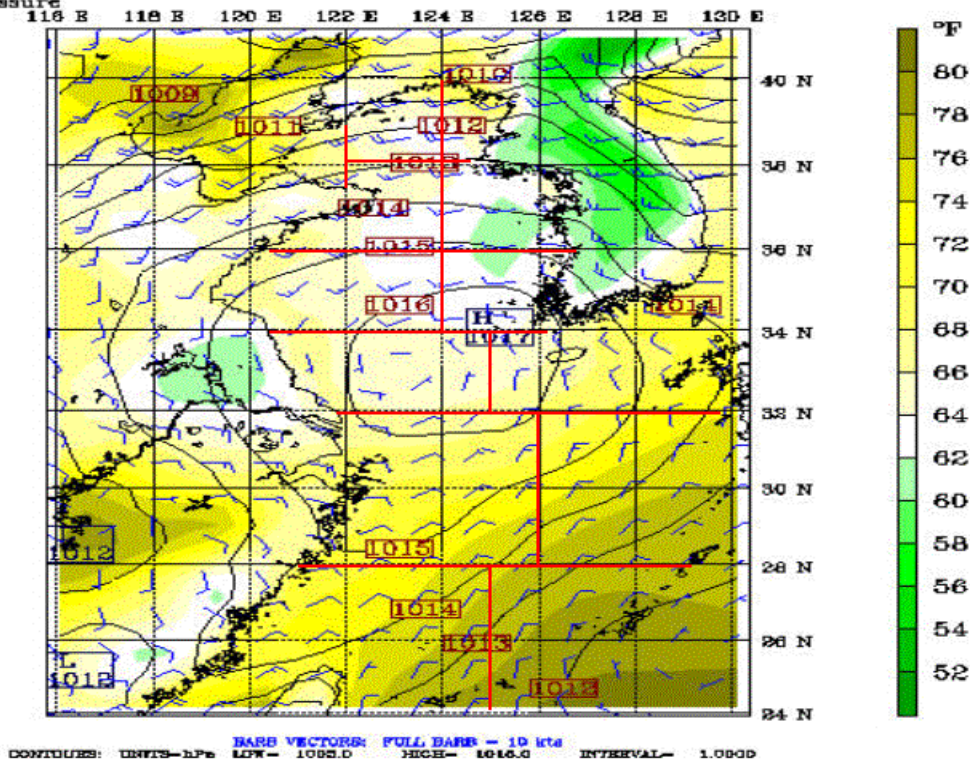
Fast: 720.00
Temperature
Sea-level pressure

Valid: 0000 UTC Sun 31 May 98 (0900 LST Sun 31 May 98)
at sigma - 0.995



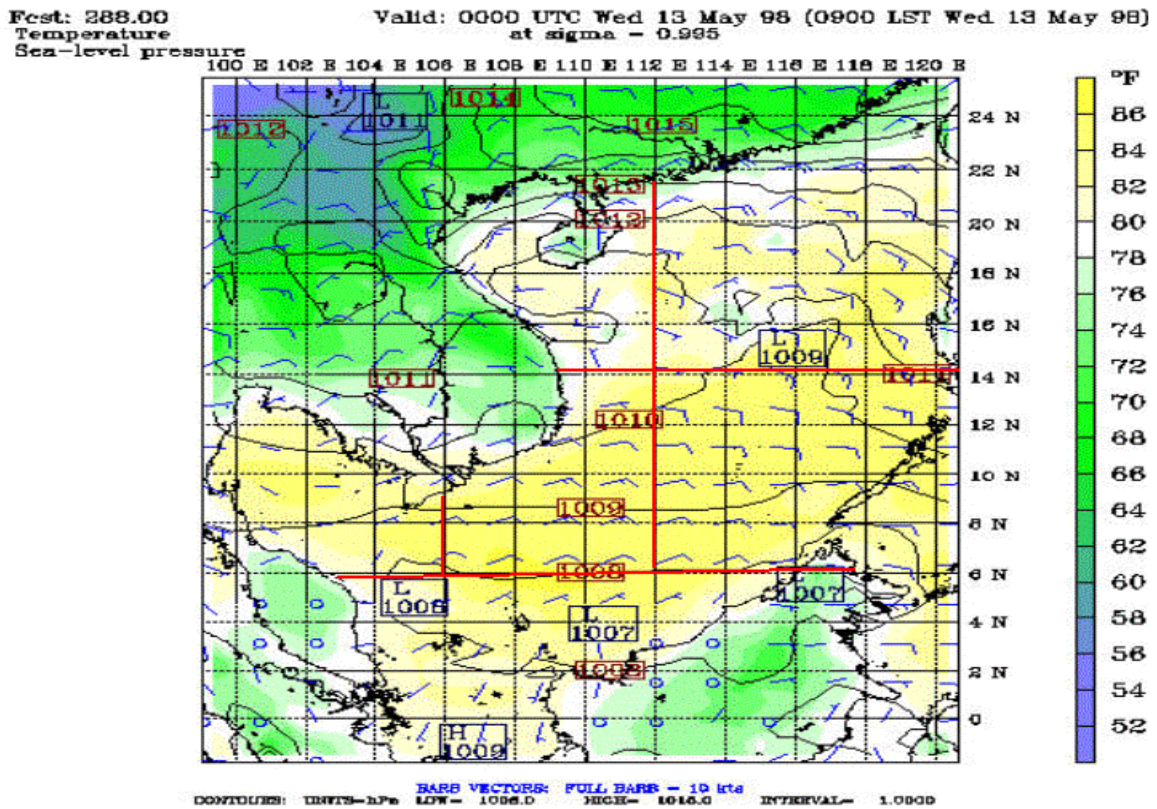
Post: 732.00
Temperature
Sea-level pressure

Valid: 1200 UTC Sun 31 May 98 (2100 LST Sun 31 May 98)
at sigma = 0.995



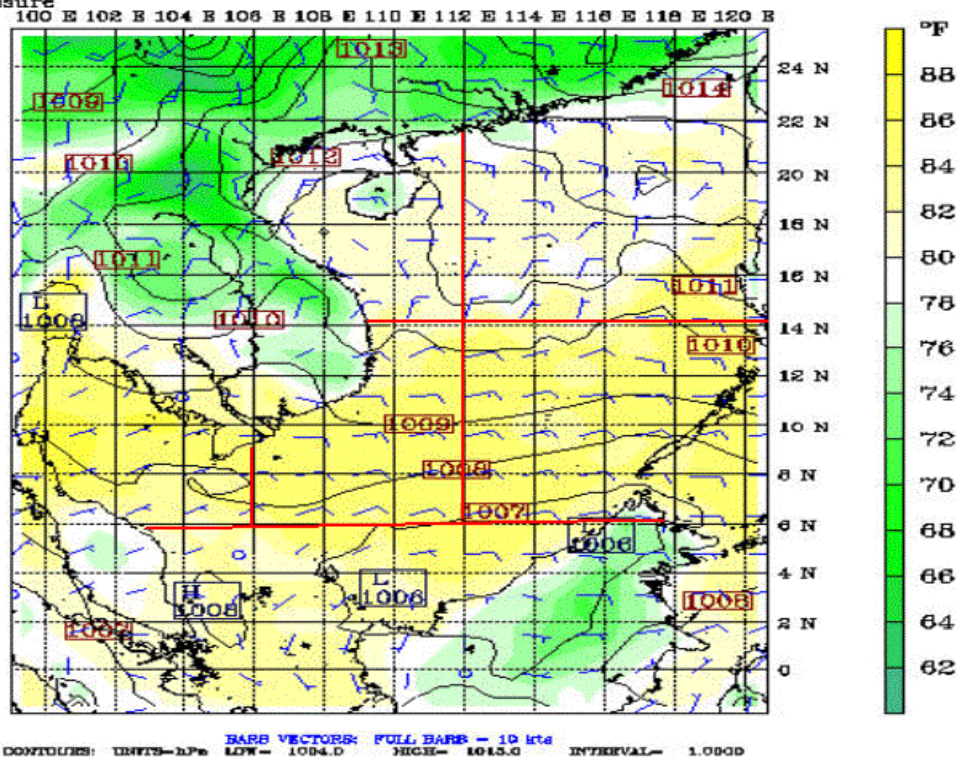
APPENDIX U. SEA LEVEL PRESSURE/SAT/SURFACE WIND PLOTS FOR THE SCS FOR THE MAY TIME PERIOD

Appendix T consists of 38 figures that show sea level pressure, SAT, and surface winds for the May time period over the YES. The figures are in time sequential order from May 13 through May31.



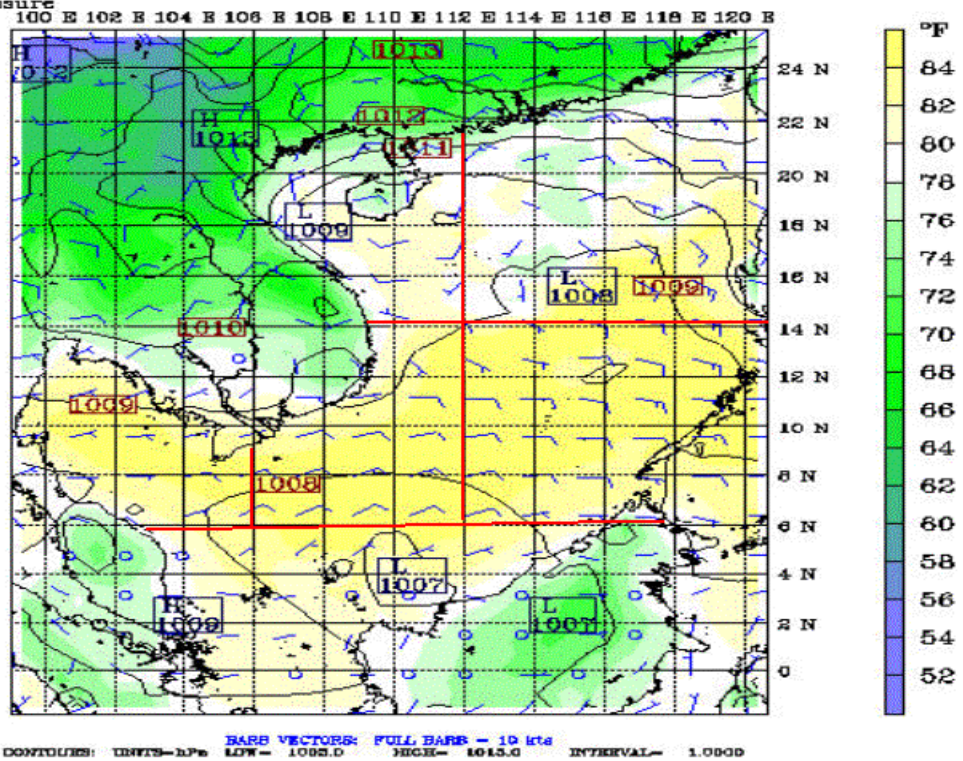
Fast: 300.00
Temperature
Sea-level pressure

Valid: 1200 UTC Wed 13 May 98 (2100 LST Wed 13 May 98)
at sigma - 0.995



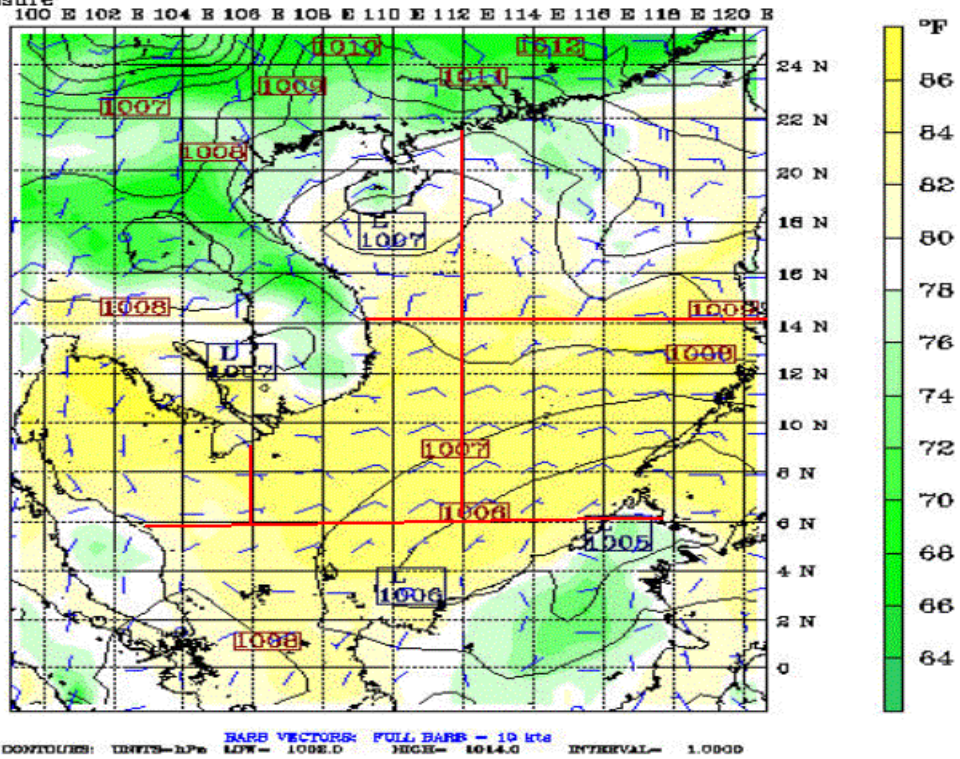
Fast: 312.00
Temperature
Sea-level pressure

Valid: 0000 UTC Thu 14 May 98 (0900 LST Thu 14 May 98)
at sigma - 0.995



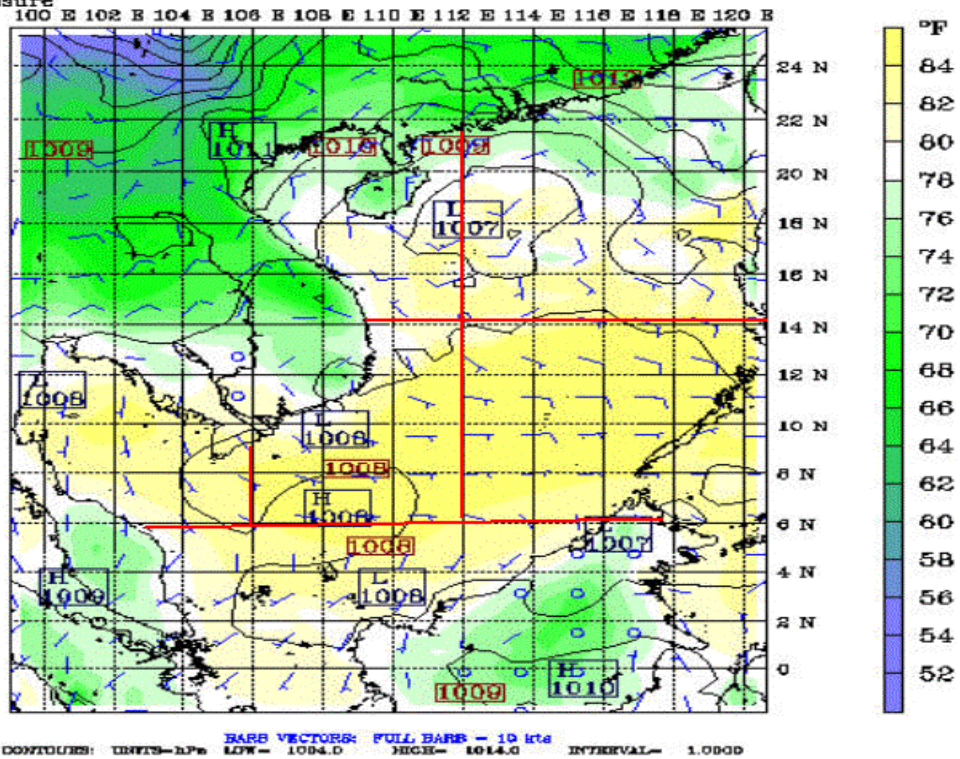
Fcst: 324.00
Temperature
Sea-level pressure

Valid: 1200 UTC Thu 14 May 98 (2100 LST Thu 14 May 98)
at sigma - 0.995



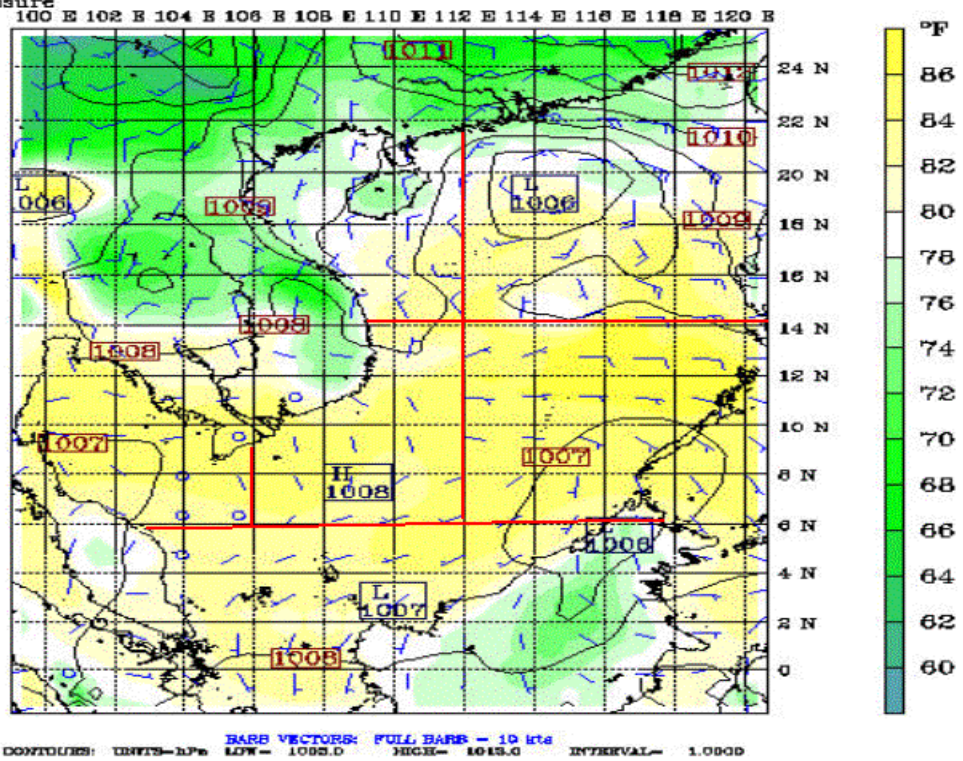
Fcst: 336.00
Temperature
Sea-level pressure

Valid: 0000 UTC Fri 15 May 98 (0900 LST Fri 15 May 98)
at sigma - 0.995



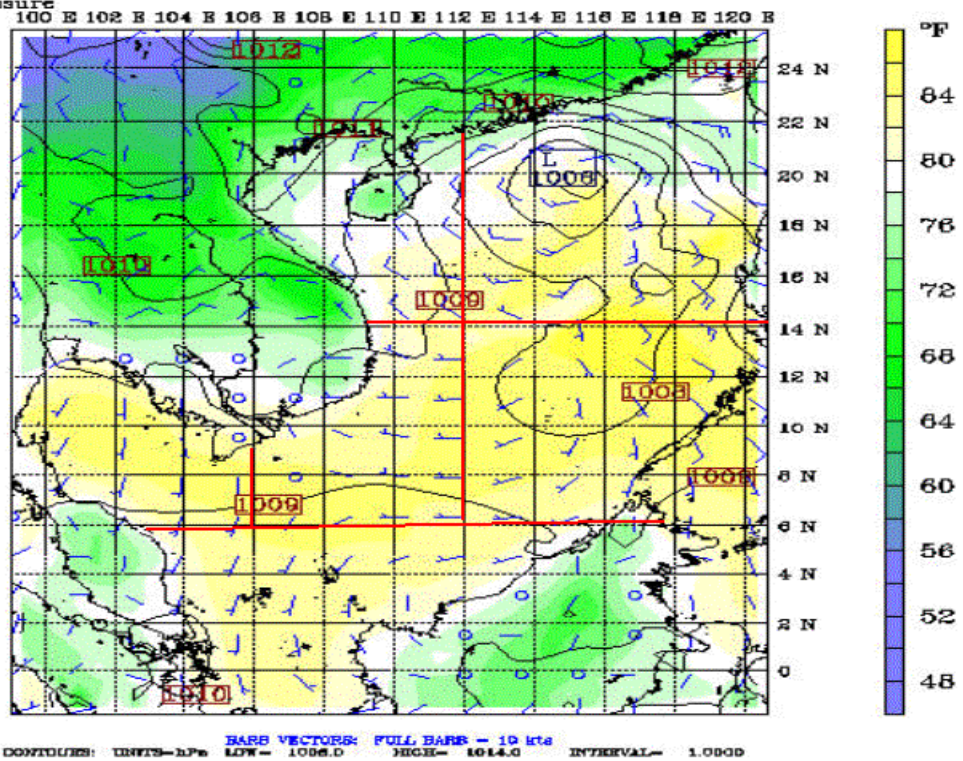
Fast: 348.00
Temperature
Sea-level pressure

Valid: 1200 UTC Fri 15 May 98 (2100 LST Fri 15 May 98)
at sigma - 0.995



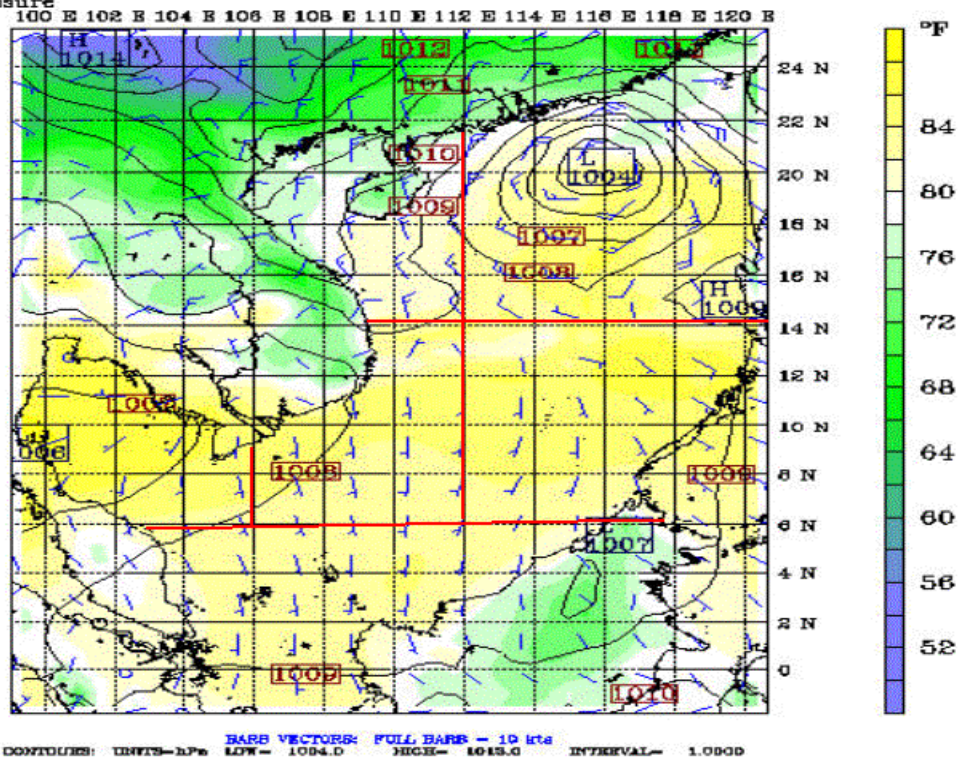
Fast: 360.00
Temperature
Sea-level pressure

Valid: 0000 UTC Sat 16 May 98 (0900 LST Sat 16 May 98)
at sigma - 0.995



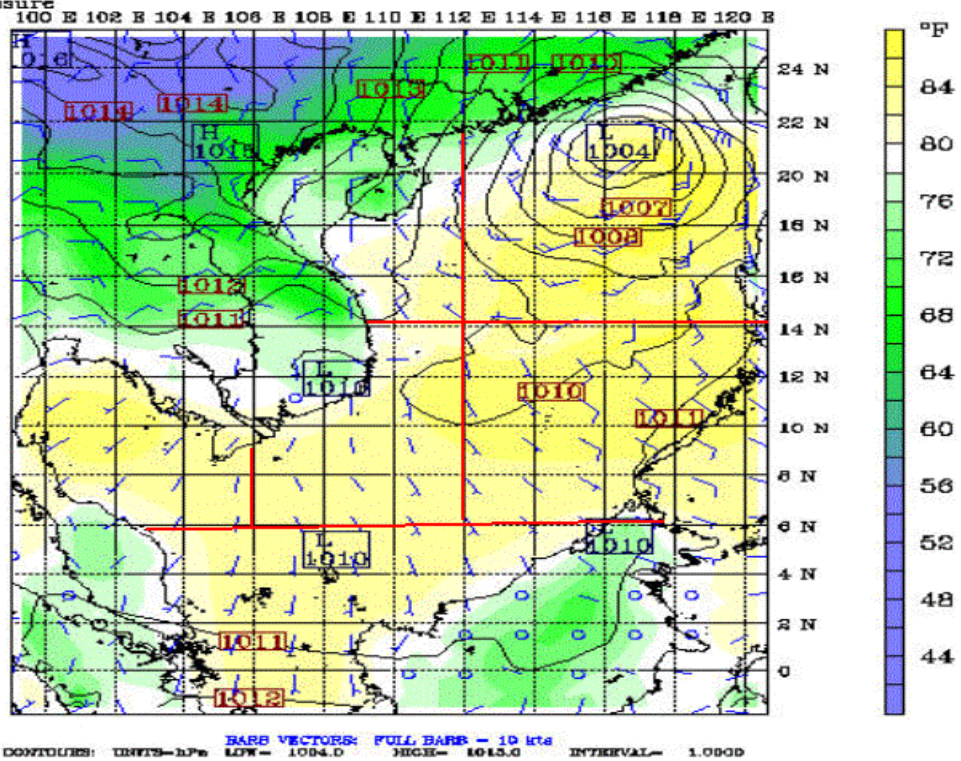
Fast: 372.00
Temperature
Sea-level pressure

Valid: 1200 UTC Sat 16 May 98 (2100 LST Sat 16 May 98)
at sigma - 0.995



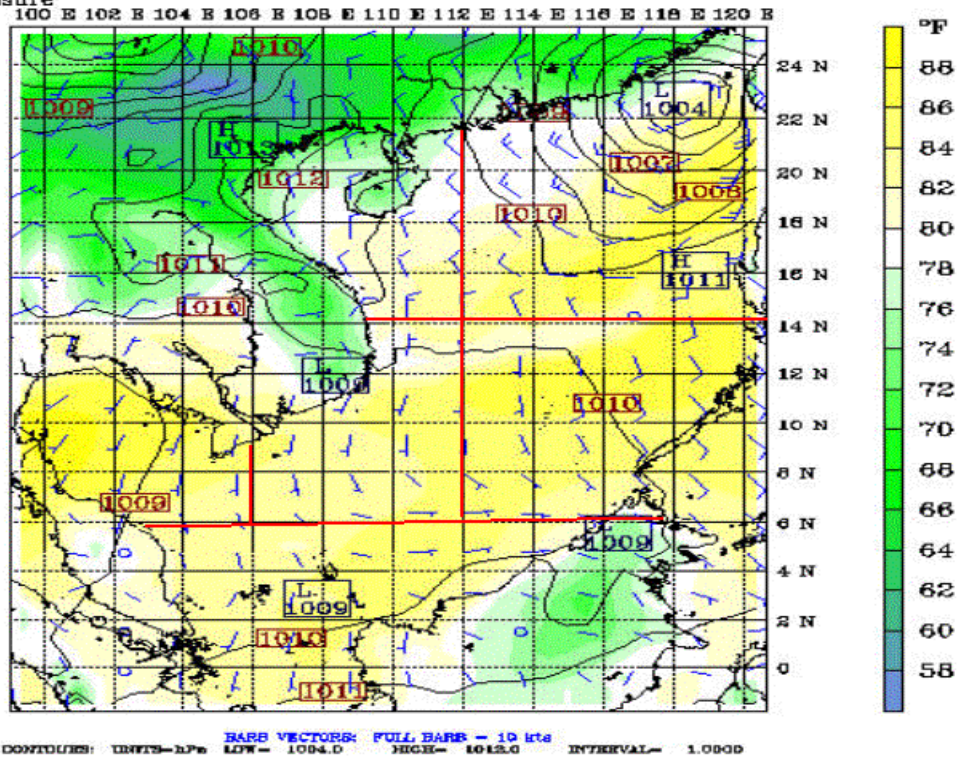
Fast: 384.00
Temperature
Sea-level pressure

Valid: 0000 UTC Sun 17 May 98 (0900 LST Sun 17 May 98)
at sigma - 0.995



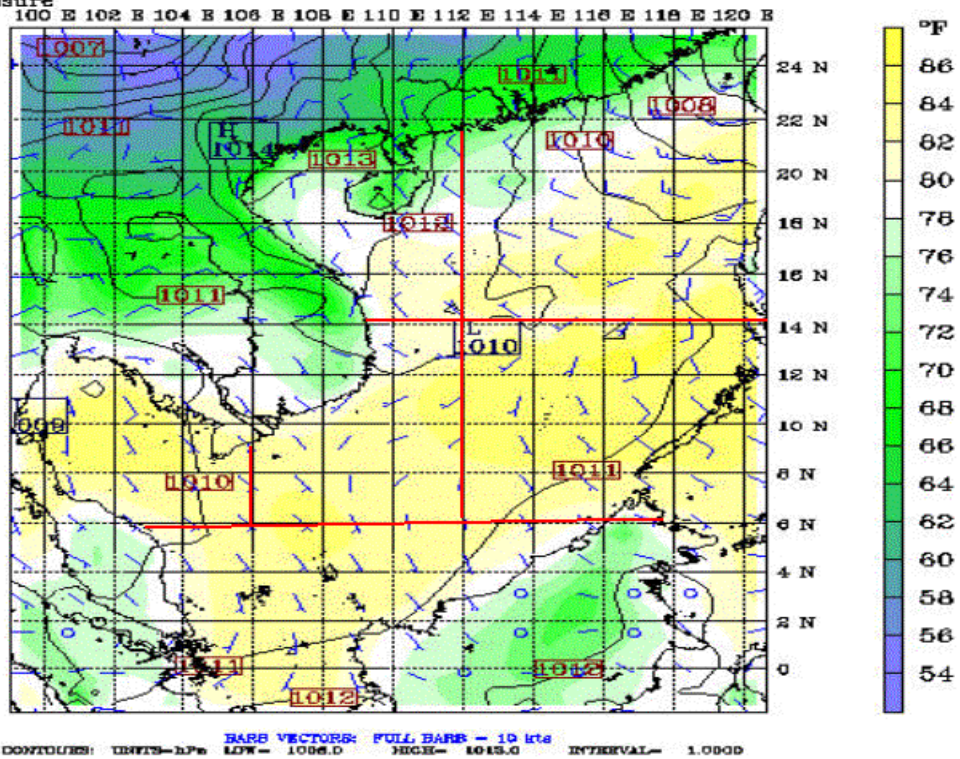
Fcst: 396.00
Temperature
Sea-level pressure

Valid: 1200 UTC Sun 17 May 98 (2100 LST Sun 17 May 98)
at sigma - 0.995



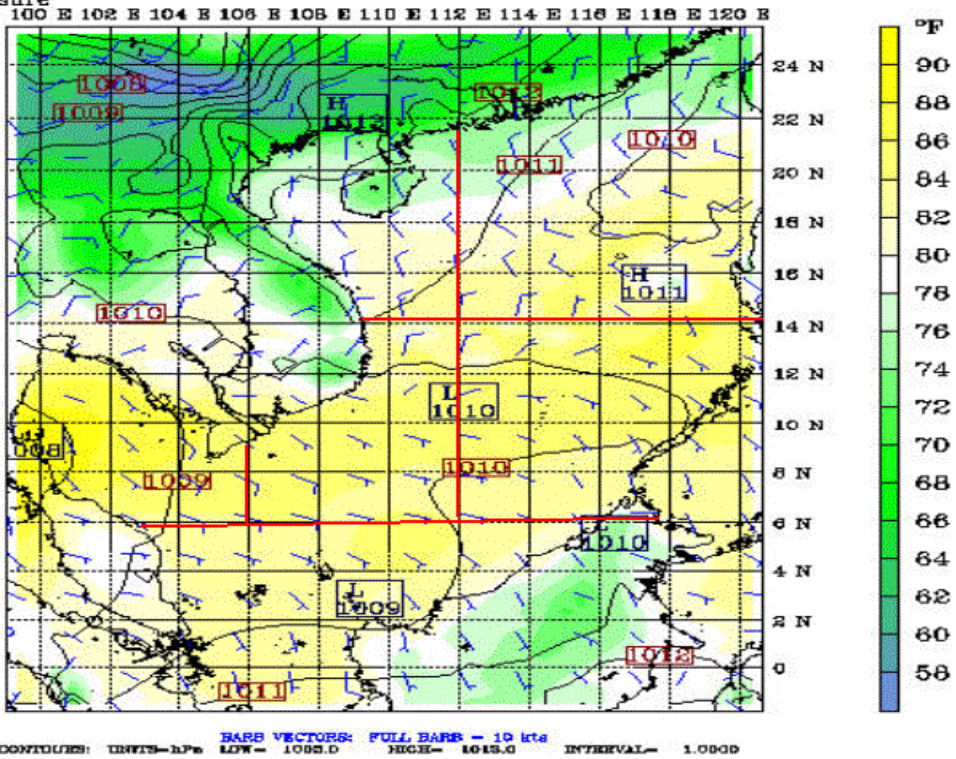
Fcst: 408.00
Temperature
Sea-level pressure

Valid: 0000 UTC Mon 18 May 98 (0900 LST Mon 18 May 98)
at sigma - 0.995



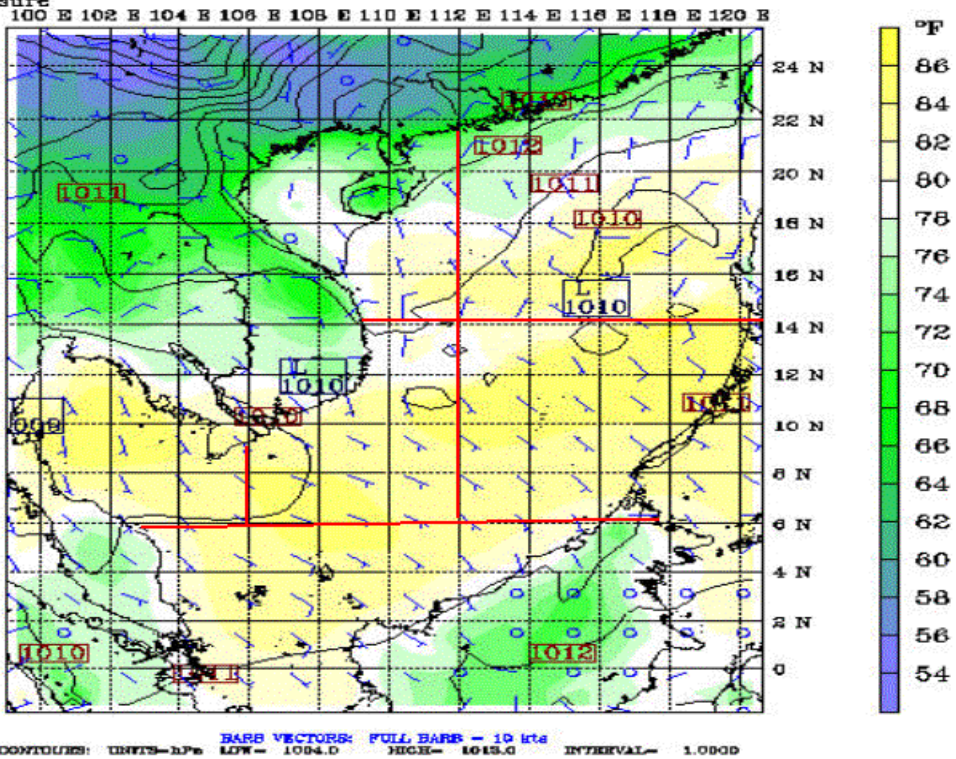
Fast: 420.00
Temperature
Sea-level pressure

Valid: 1200 UTC Mon 18 May 98 (2100 LST Mon 18 May 98)
at sigma - 0.995



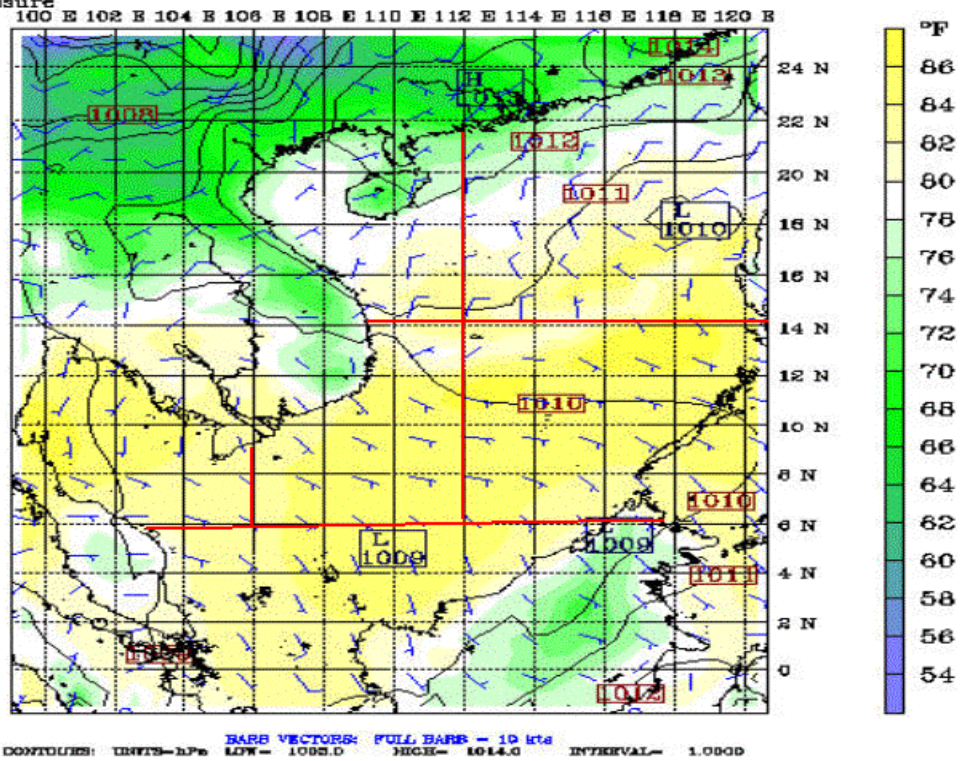
Fast: 432.00
Temperature
Sea-level pressure

Valid: 0000 UTC Tue 19 May 98 (0900 LST Tue 19 May 98)
at sigma - 0.995



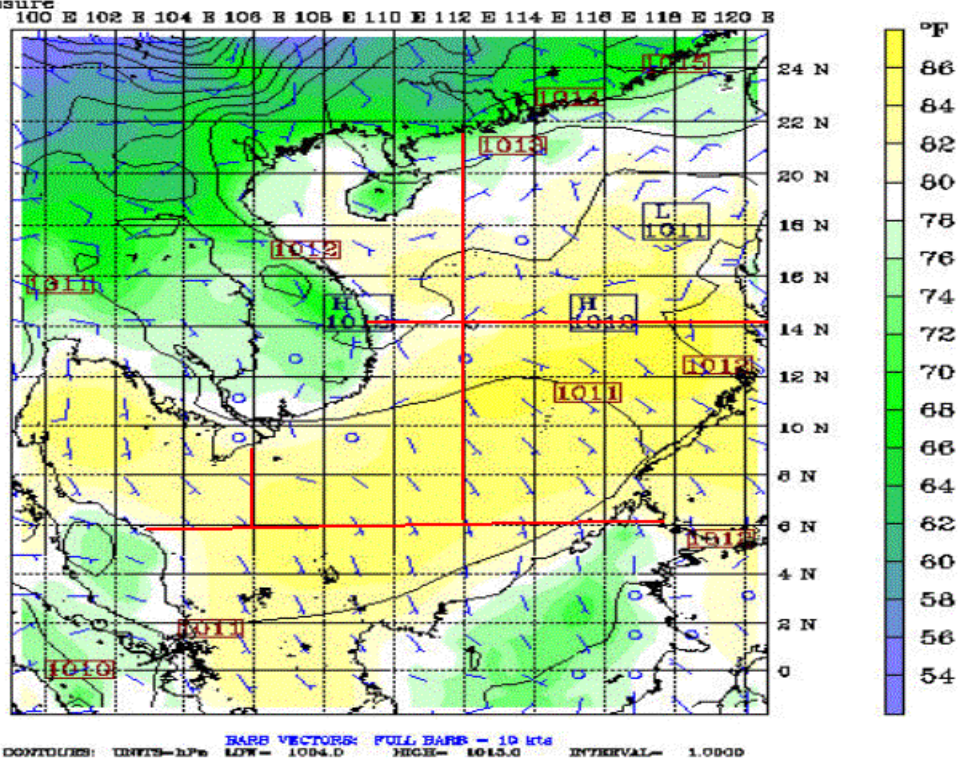
Fcst: 444.00
Temperature
Sea-level pressure

Valid: 1200 UTC Tue 19 May 98 (2100 LST Tue 19 May 98)
at sigma - 0.995



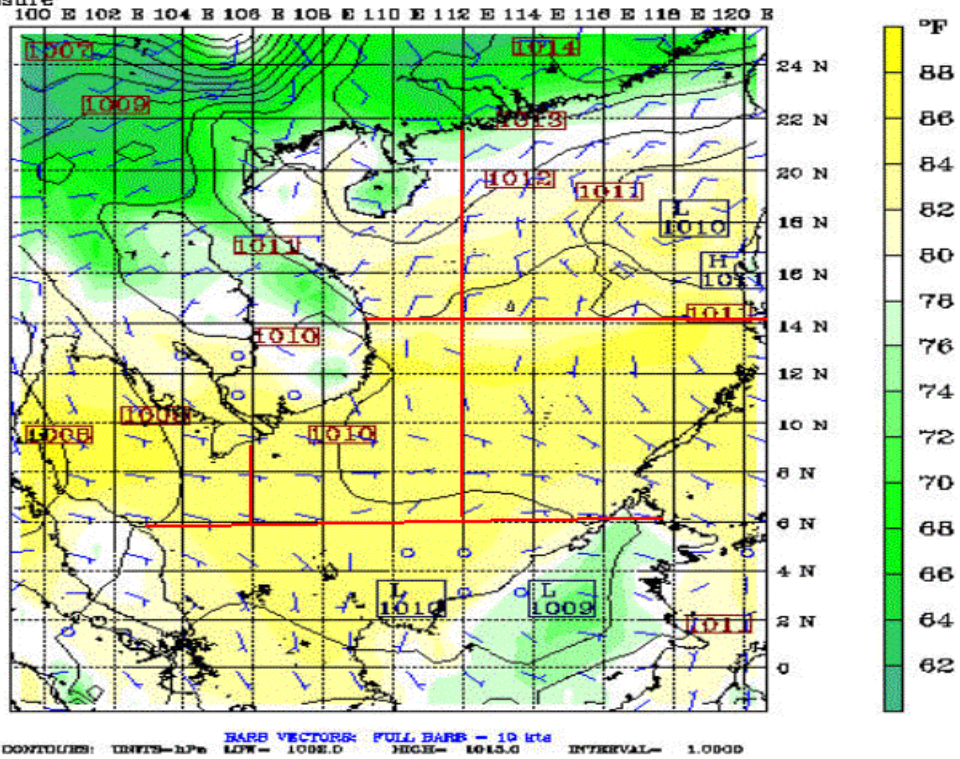
Fcst: 456.00
Temperature
Sea-level pressure

Valid: 0000 UTC Wed 20 May 98 (0900 LST Wed 20 May 98)
at sigma - 0.995



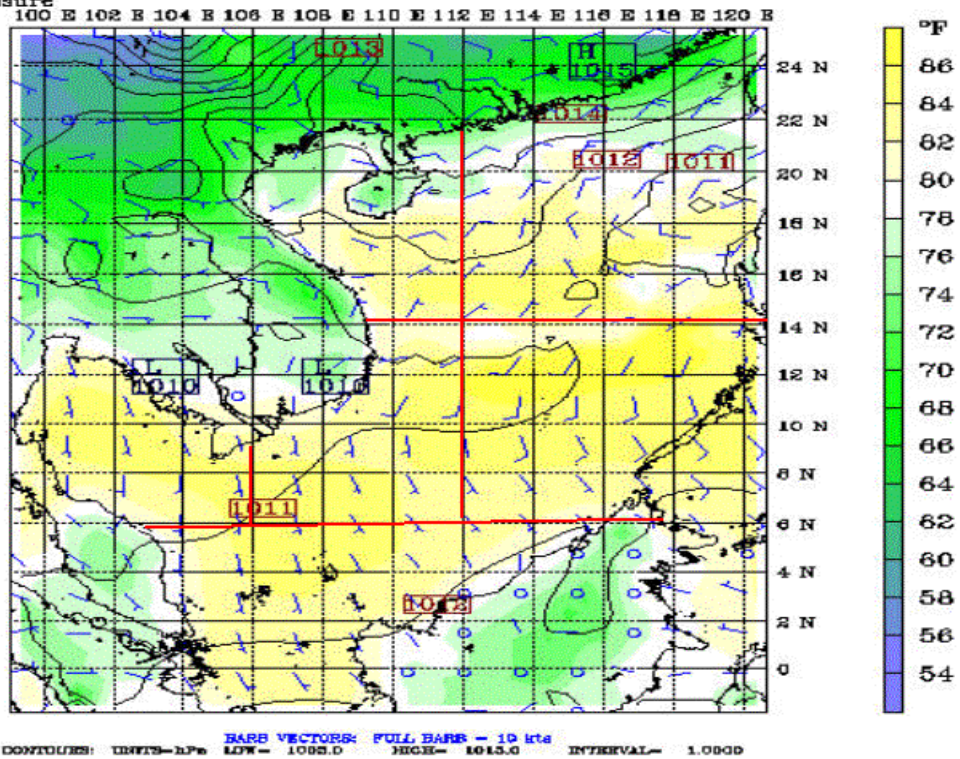
Fcst: 468.00
 Temperature
 Sea-level pressure

Valid: 1200 UTC Wed 20 May 98 (2100 LST Wed 20 May 98)
 at sigma = 0.995



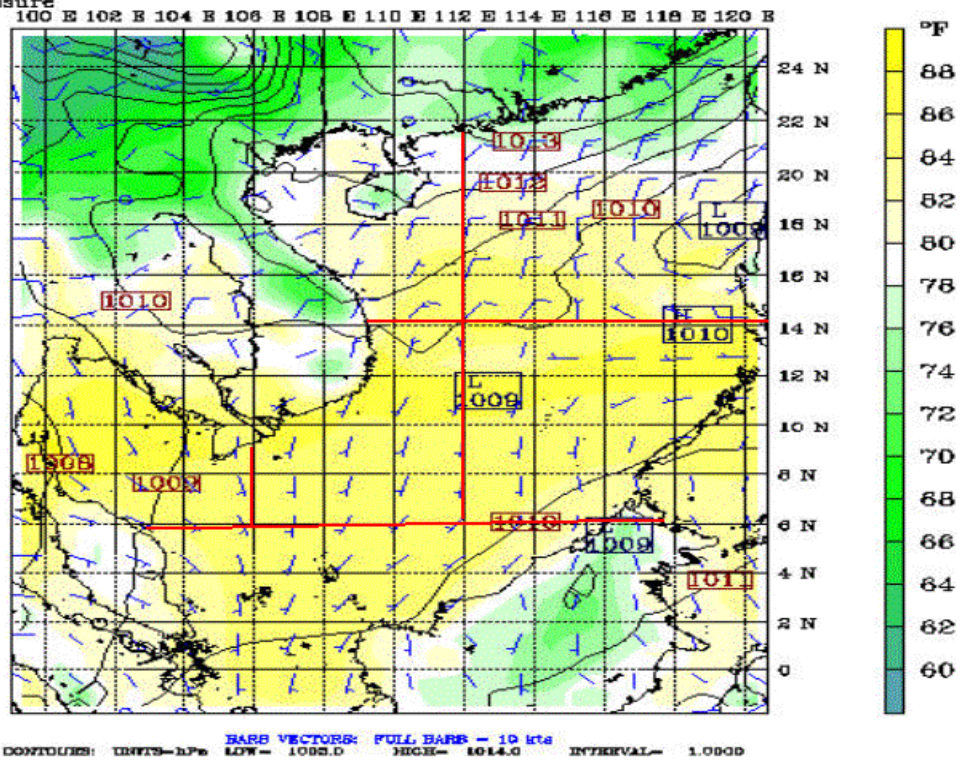
Fcst: 480.00
 Temperature
 Sea-level pressure

Valid: 0000 UTC Thu 21 May 98 (0900 LST Thu 21 May 98)
 at sigma = 0.995



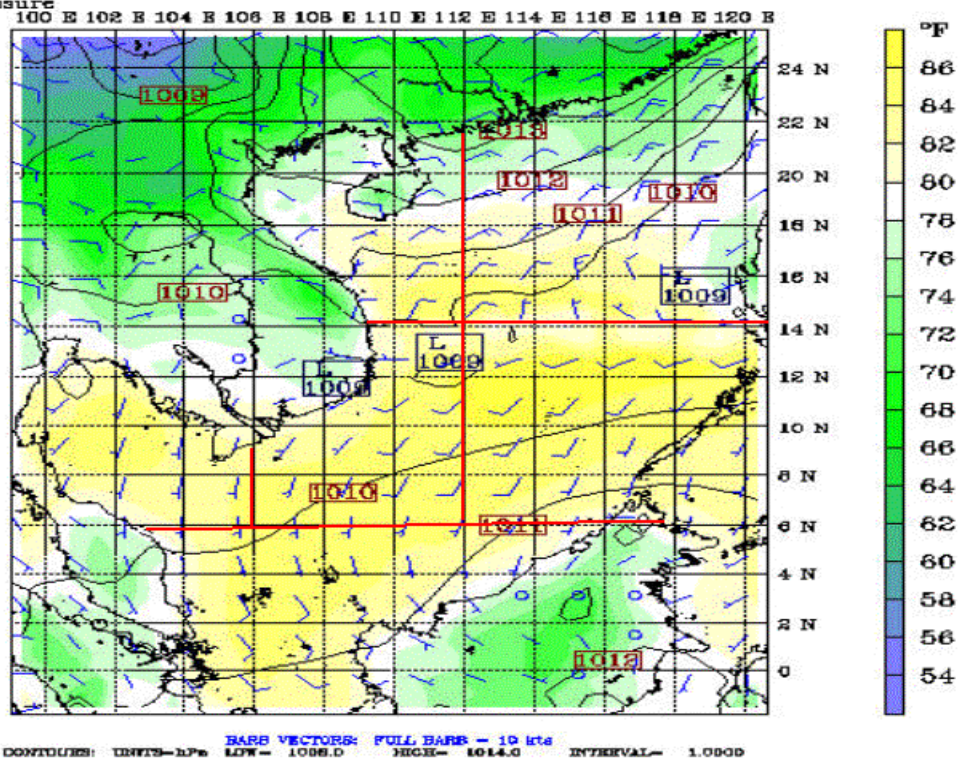
Fcst: 492.00
Temperature
Sea-level pressure

Valid: 1200 UTC Thu 21 May 98 (2100 LST Thu 21 May 98)
at sigma - 0.995



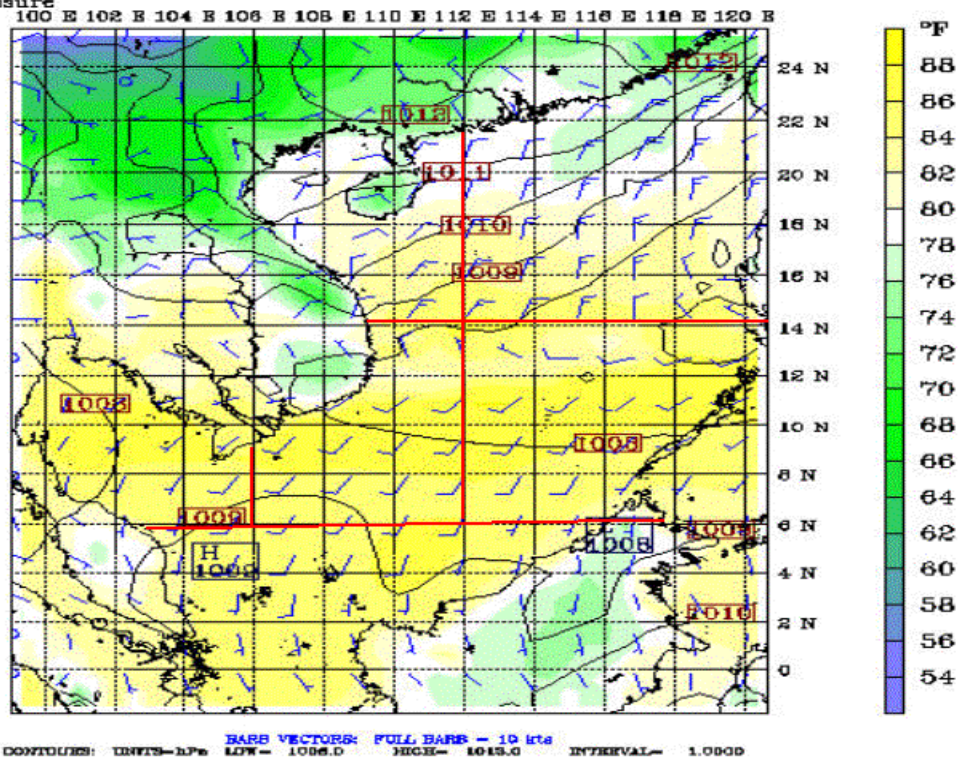
Fcst: 504.00
Temperature
Sea-level pressure

Valid: 0000 UTC Fri 22 May 98 (0900 LST Fri 22 May 98)
at sigma - 0.995



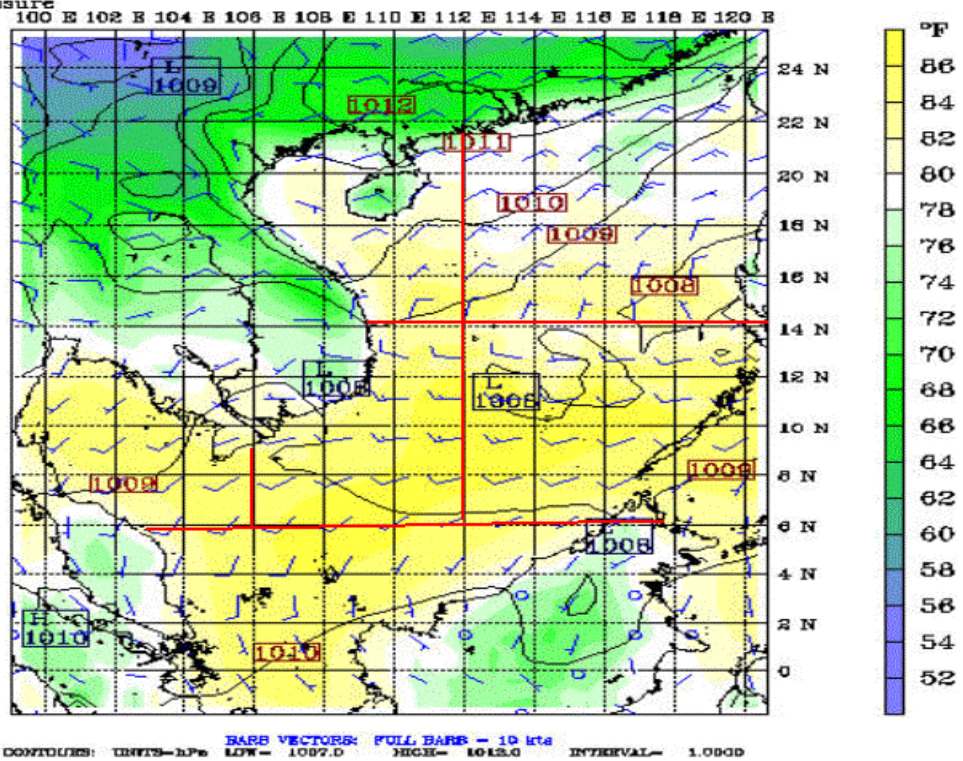
Fcst: 516.00
Temperature
Sea-level pressure

Valid: 1200 UTC Fri 22 May 98 (2100 LST Fri 22 May 98)
at sigma - 0.995



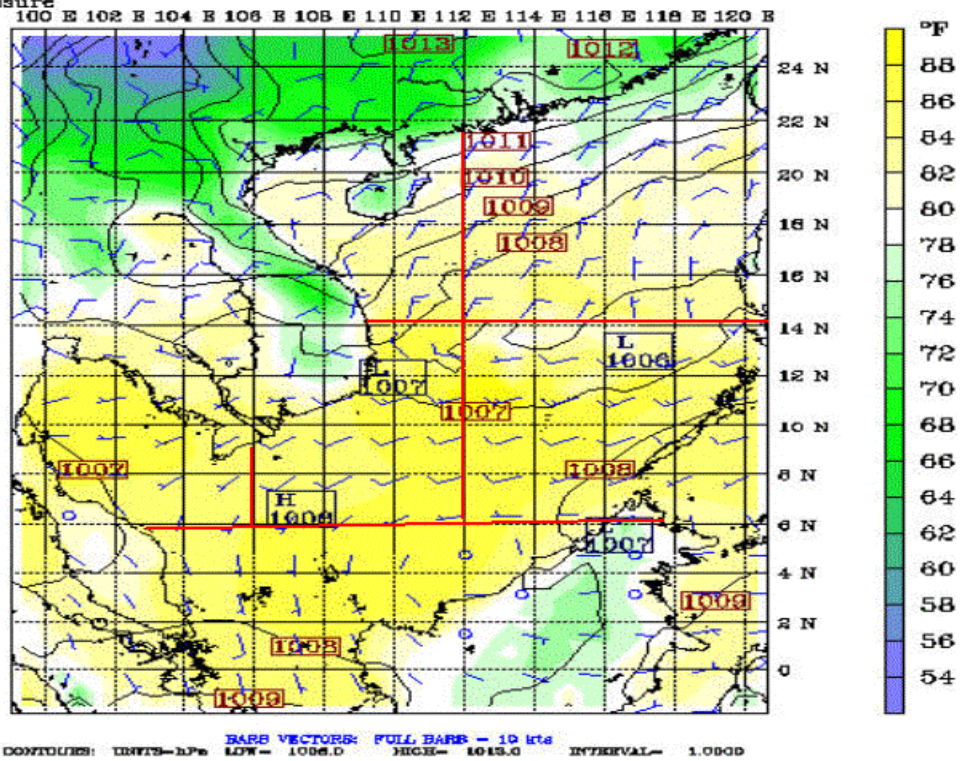
Fcst: 528.00
Temperature
Sea-level pressure

Valid: 0000 UTC Sat 23 May 98 (0900 LST Sat 23 May 98)
at sigma - 0.995



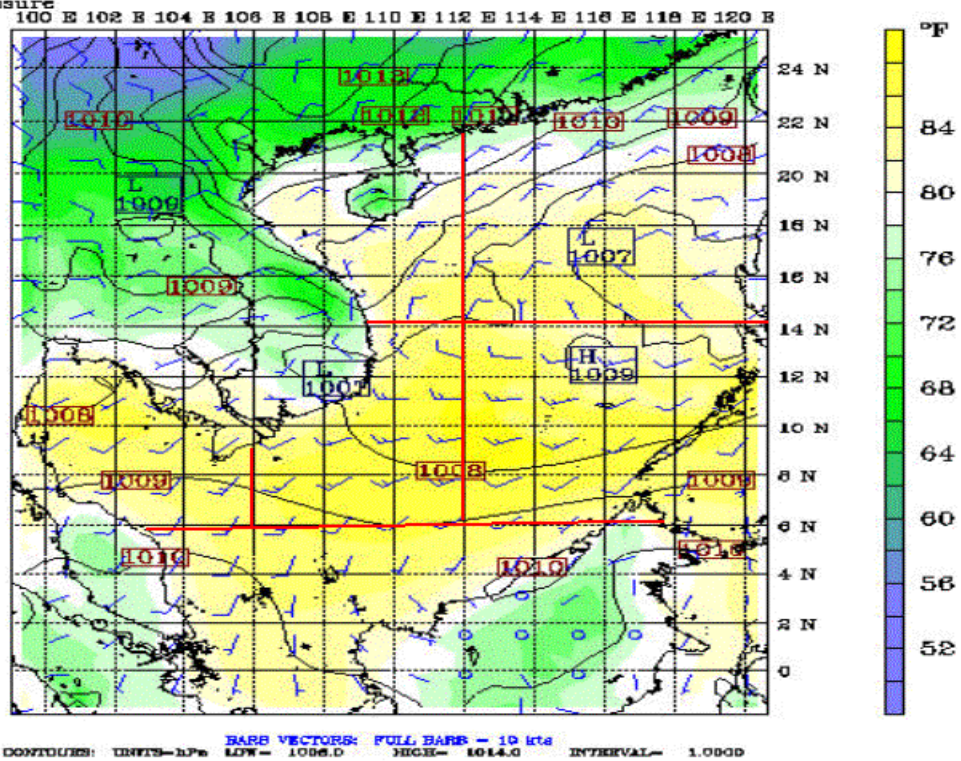
Fast: 540.00
Temperature
Sea-level pressure

Valid: 1200 UTC Sat 23 May 98 (2100 LST Sat 23 May 98)
at sigma - 0.995



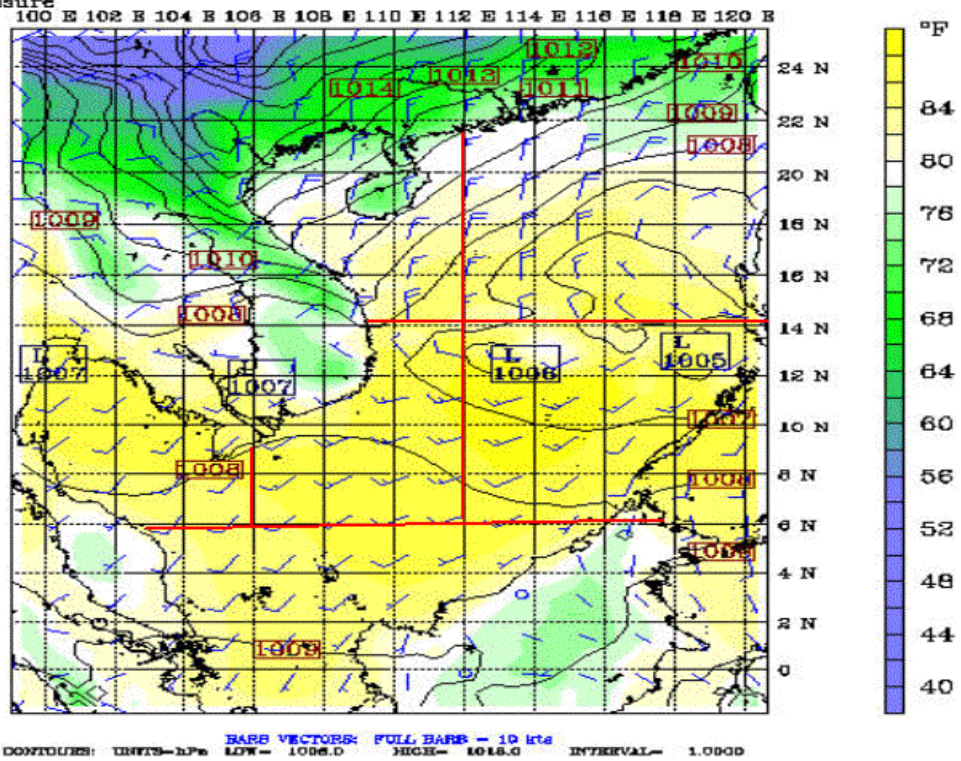
Fast: 552.00
Temperature
Sea-level pressure

Valid: 0000 UTC Sun 24 May 98 (0900 LST Sun 24 May 98)
at sigma - 0.995



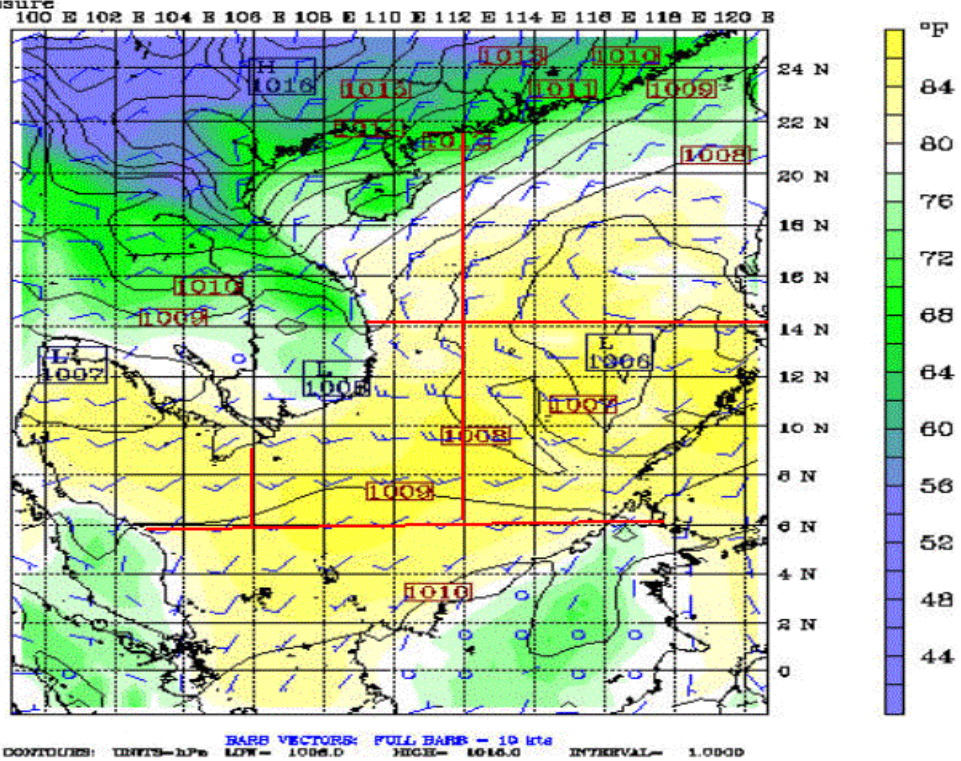
Fcst: 564.00
Temperature
Sea-level pressure

Valid: 1200 UTC Sun 24 May 98 (2100 LST Sun 24 May 98)
at sigma - 0.995



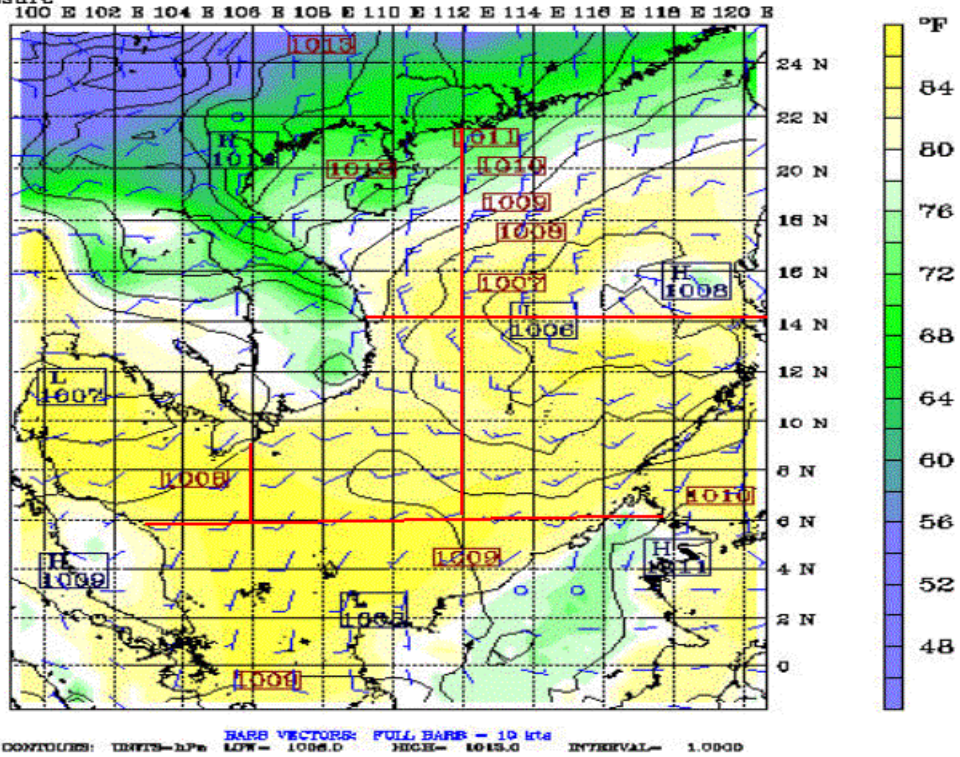
Fcst: 576.00
Temperature
Sea-level pressure

Valid: 0000 UTC Mon 25 May 98 (0900 LST Mon 25 May 98)
at sigma - 0.995



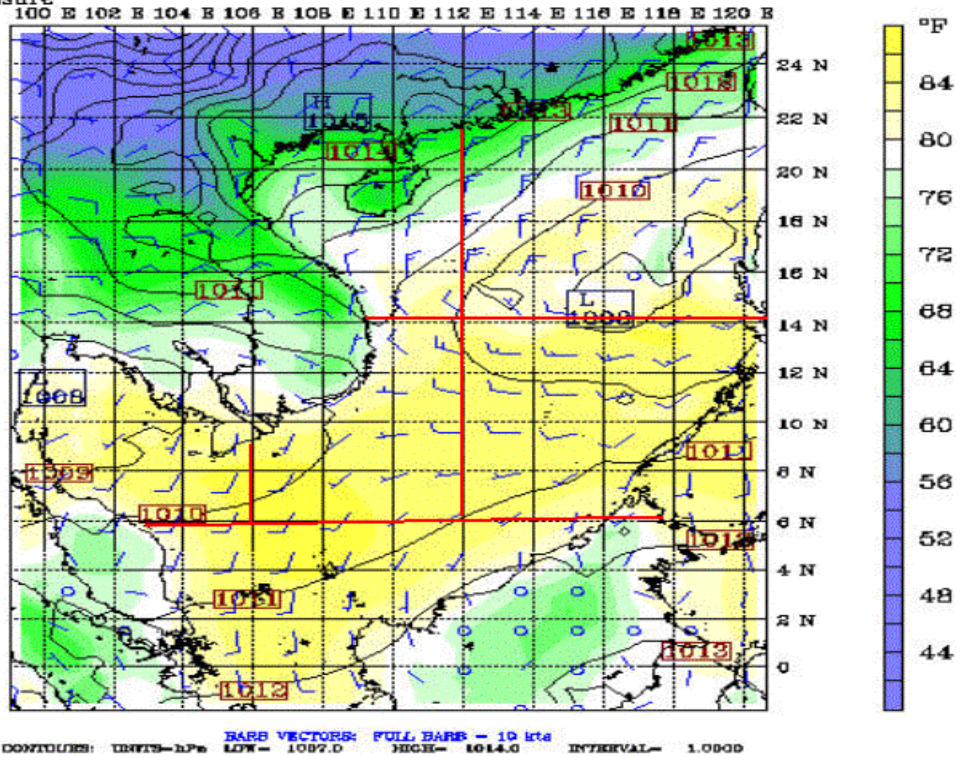
Fast: 588.00
Temperature
Sea-level pressure

Valid: 1200 UTC Mon 25 May 98 (2100 LST Mon 25 May 98)
at sigma - 0.995



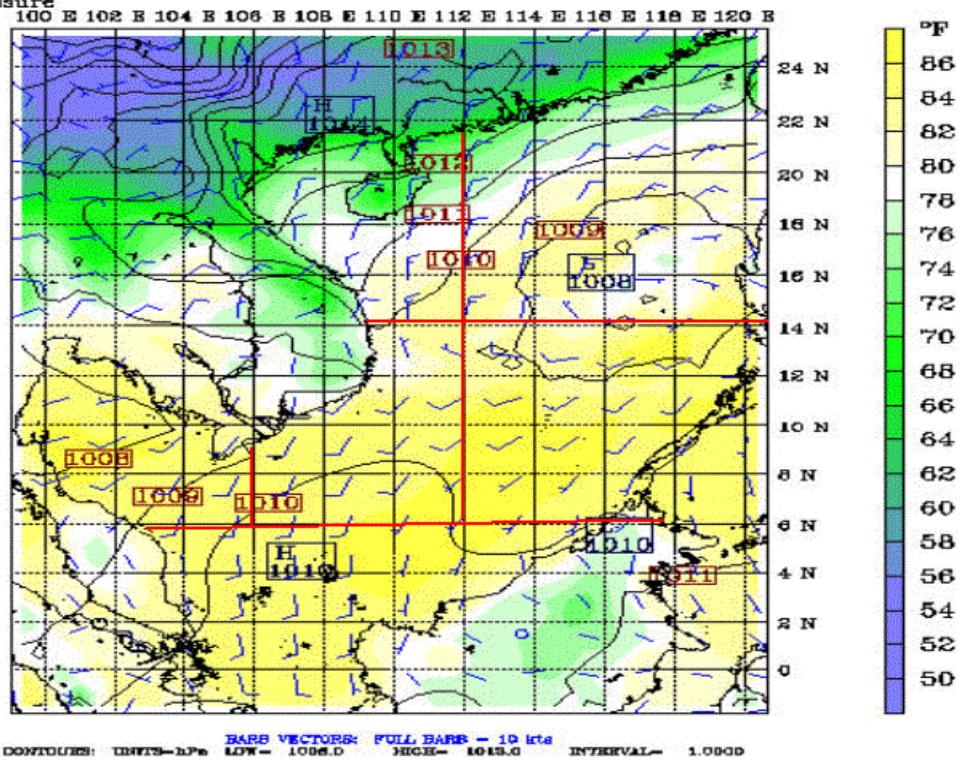
Fast: 600.00
Temperature
Sea-level pressure

Valid: 0000 UTC Tue 26 May 98 (0900 LST Tue 26 May 98)
at sigma - 0.995



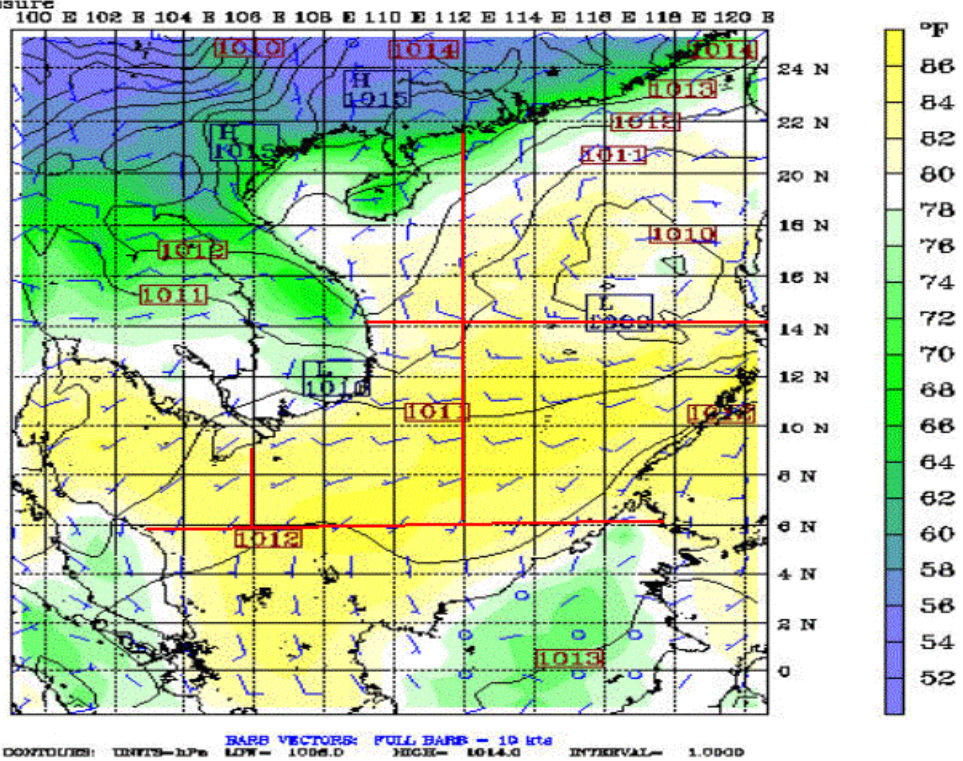
Fast: 612.00
Temperature
Sea-level pressure

Valid: 1200 UTC Tue 26 May 98 (2100 LST Tue 26 May 98)
at sigma - 0.995



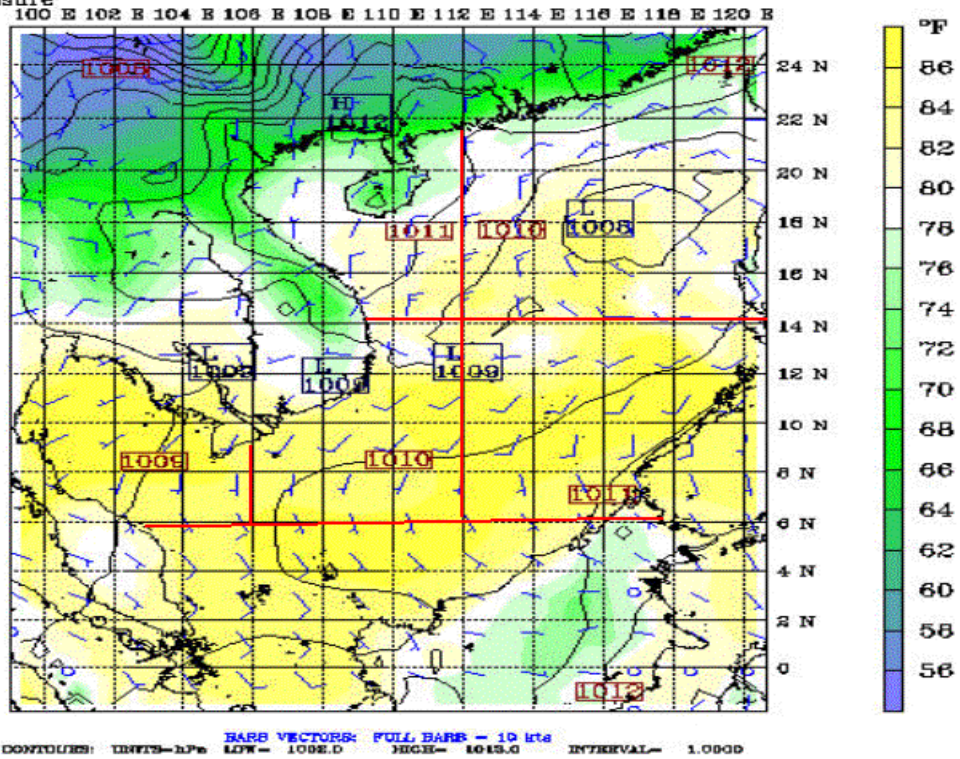
Fast: 624.00
Temperature
Sea-level pressure

Valid: 0000 UTC Wed 27 May 98 (0900 LST Wed 27 May 98)
at sigma - 0.995



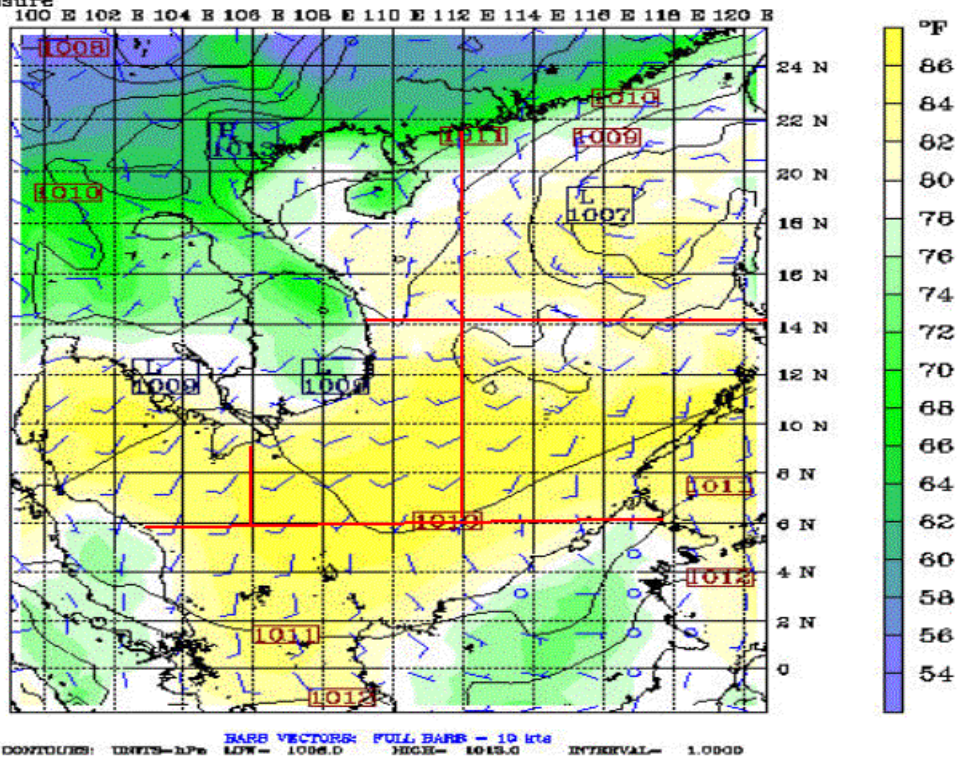
Fcst: 636.00
Temperature
Sea-level pressure

Valid: 1200 UTC Wed 27 May 98 (2100 LST Wed 27 May 98)
at sigma - 0.995



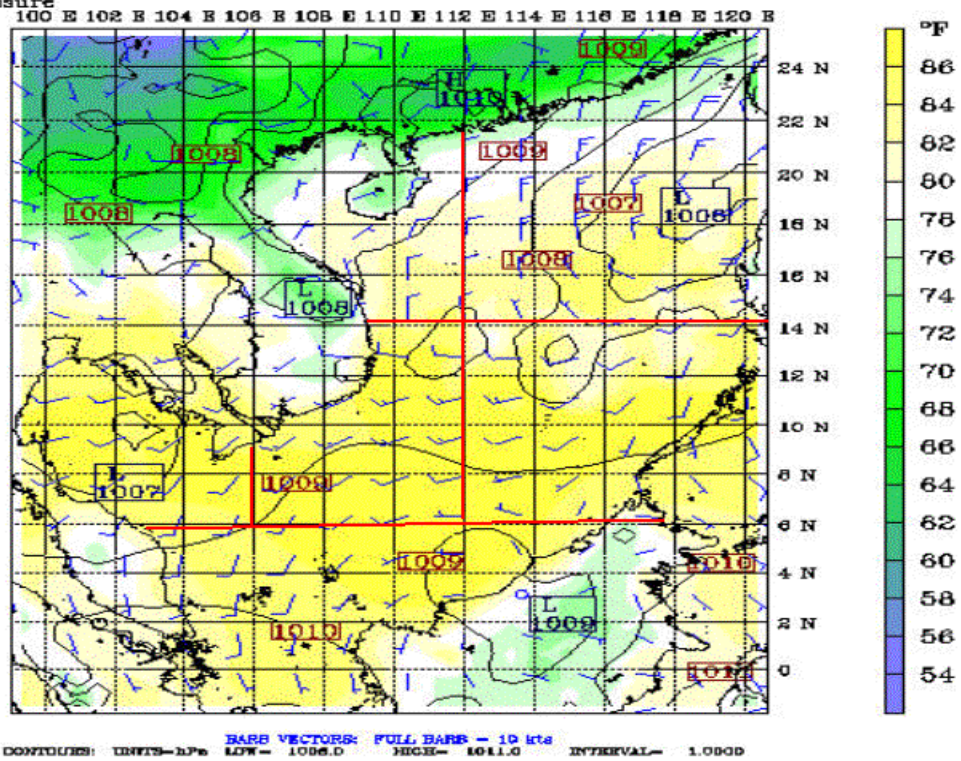
Fcst: 648.00
Temperature
Sea-level pressure

Valid: 0000 UTC Thu 28 May 98 (0900 LST Thu 28 May 98)
at sigma - 0.995



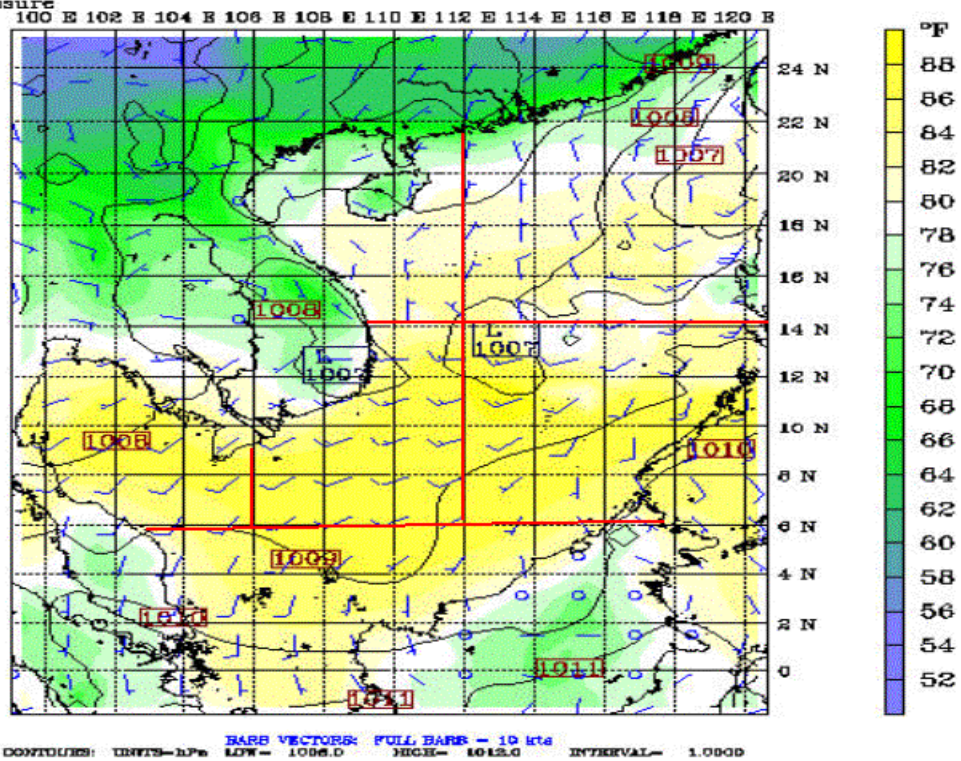
Fcst: 660.00
Temperature
Sea-level pressure

Valid: 1200 UTC Thu 28 May 98 (2100 LST Thu 28 May 98)
at sigma - 0.995



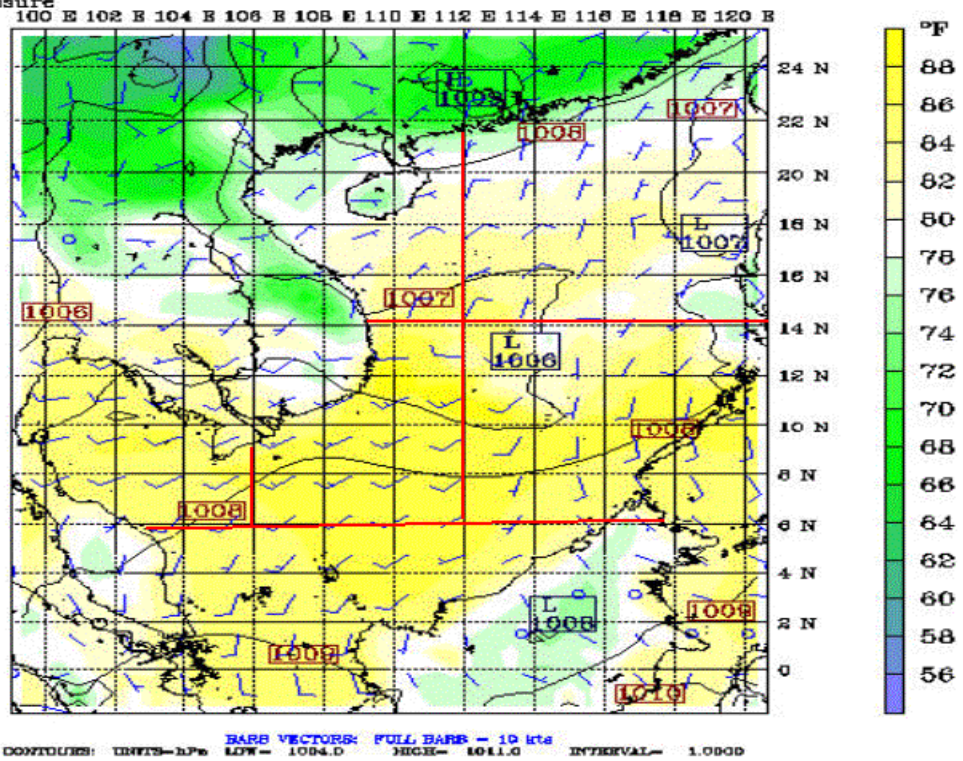
Fcst: 672.00
Temperature
Sea-level pressure

Valid: 0000 UTC Fri 29 May 98 (0900 LST Fri 29 May 98)
at sigma - 0.995



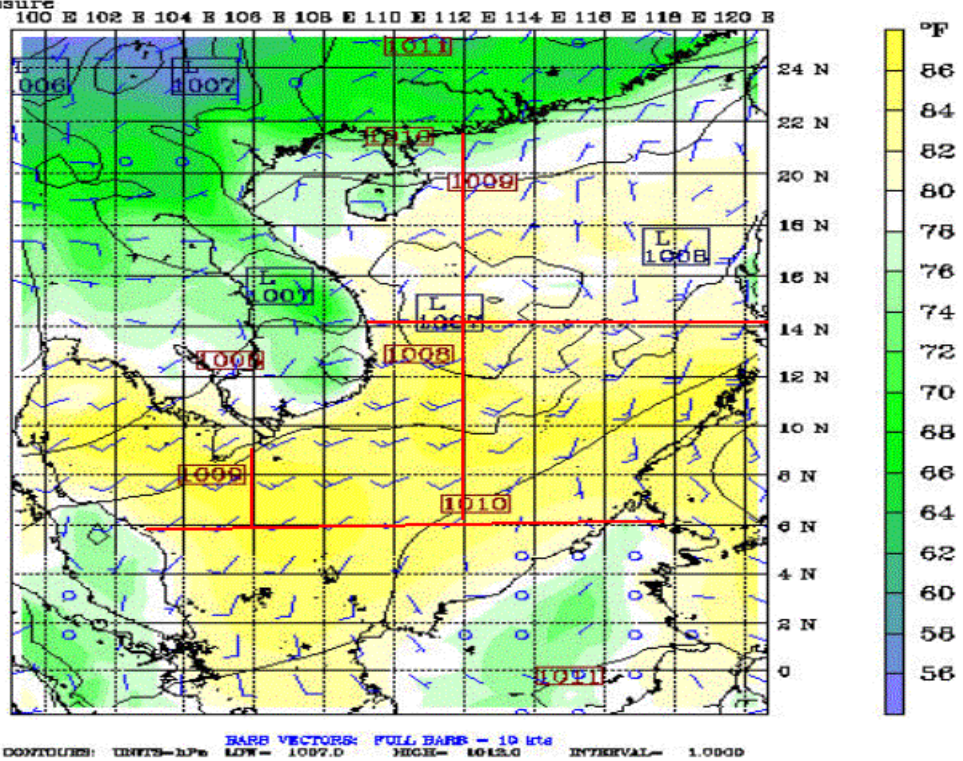
Fast: 684.00
Temperature
Sea-level pressure

Valid: 1200 UTC Fri 29 May 98 (2100 LST Fri 29 May 98)
at sigma - 0.995



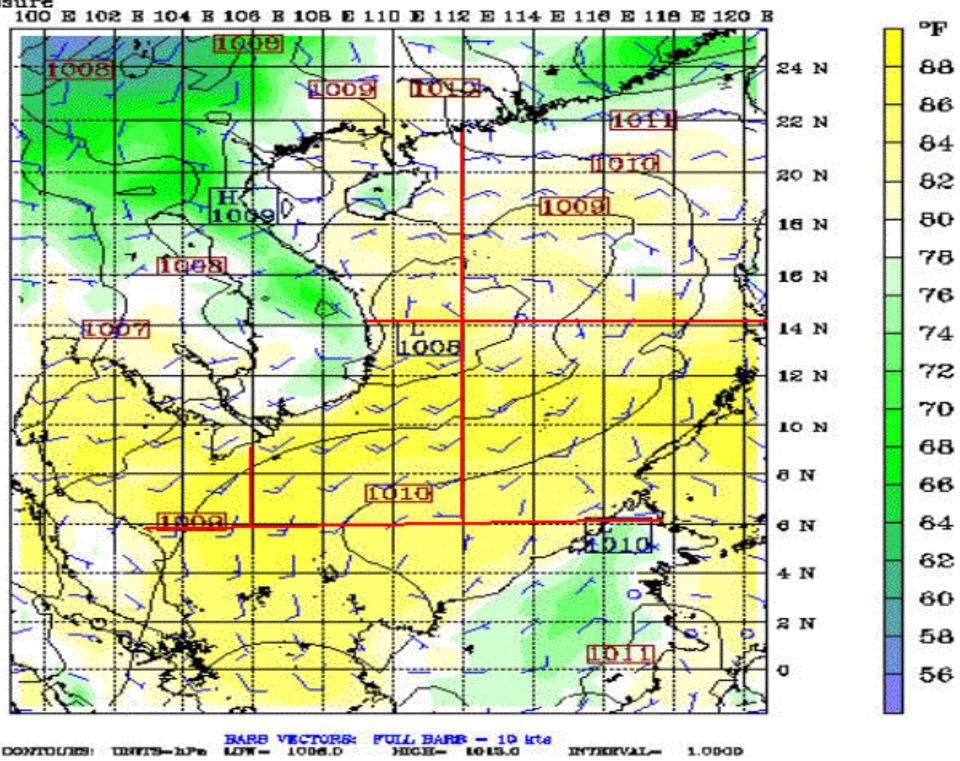
Fast: 696.00
Temperature
Sea-level pressure

Valid: 0000 UTC Sat 30 May 98 (0900 LST Sat 30 May 98)
at sigma - 0.995



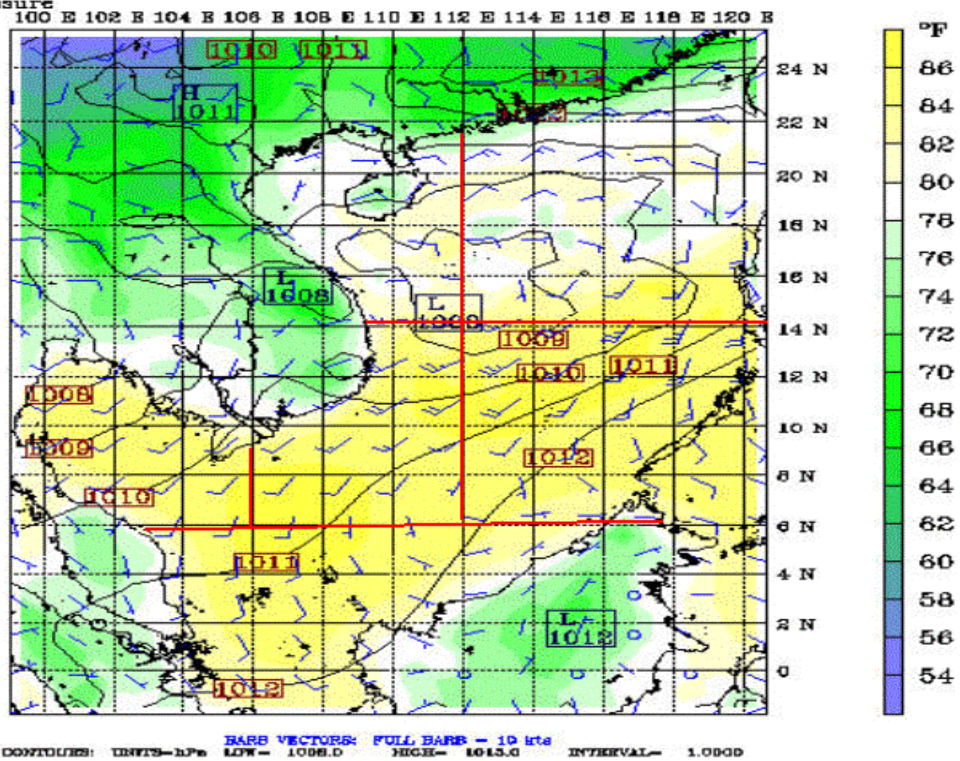
Fast: 708.00
Temperature
Sea-level pressure

Valid: 1200 UTC Sat 30 May 98 (2100 LST Sat 30 May 98)
at sigma - 0.995



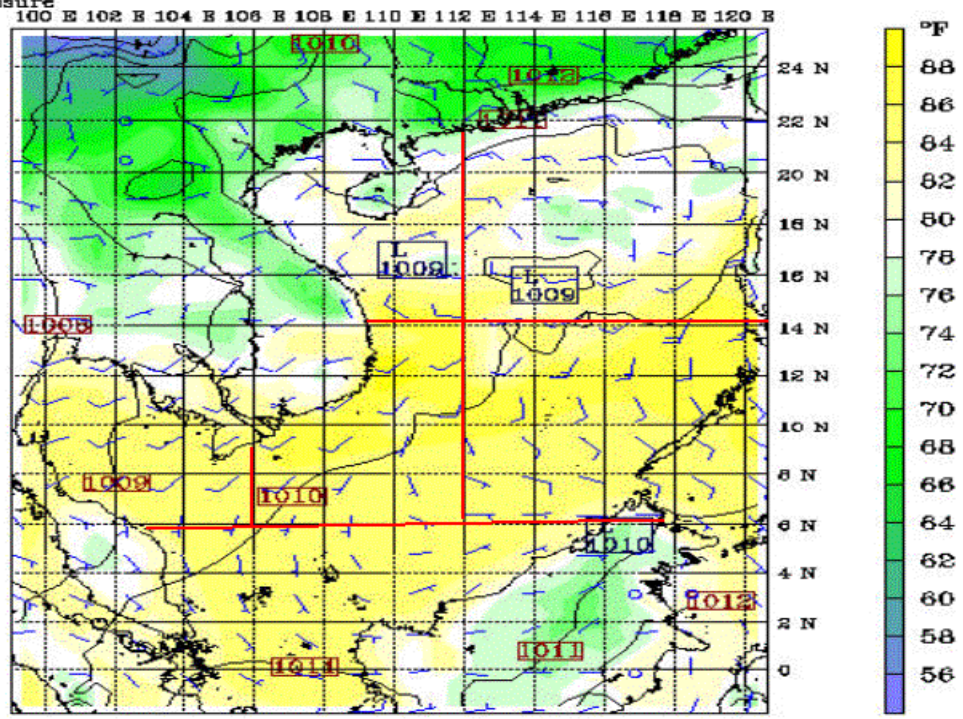
Fast: 720.00
Temperature
Sea-level pressure

Valid: 0000 UTC Sun 31 May 98 (0900 LST Sun 31 May 98)
at sigma - 0.995



Fcst: 732.00
Temperature
Sea-level pressure

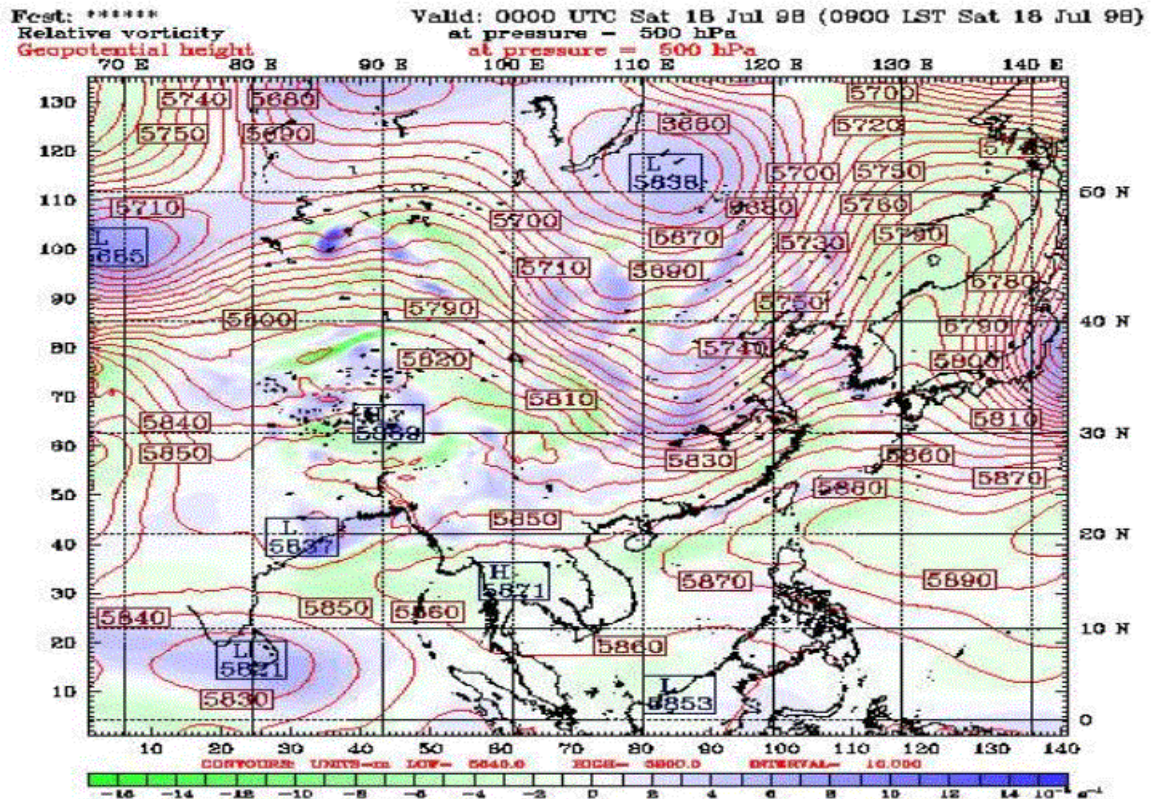
Valid: 1200 UTC Sun 31 May 98 (2100 LST Sun 31 May 98)
at sigma = 0.995



CONTOUTES: UNITS-hPa BARR VECTORS: FULL BARR = 10 kts
LOW = 1007.0 HIGH = 1014.0 INTERVAL = 1.0000

APPENDIX V. 500-MB RELATIVE VORTICITY/GEOPOTENTIAL HEIGHT PLOTS OVER THE EAMS FOR THE JULY TIME PERIOD

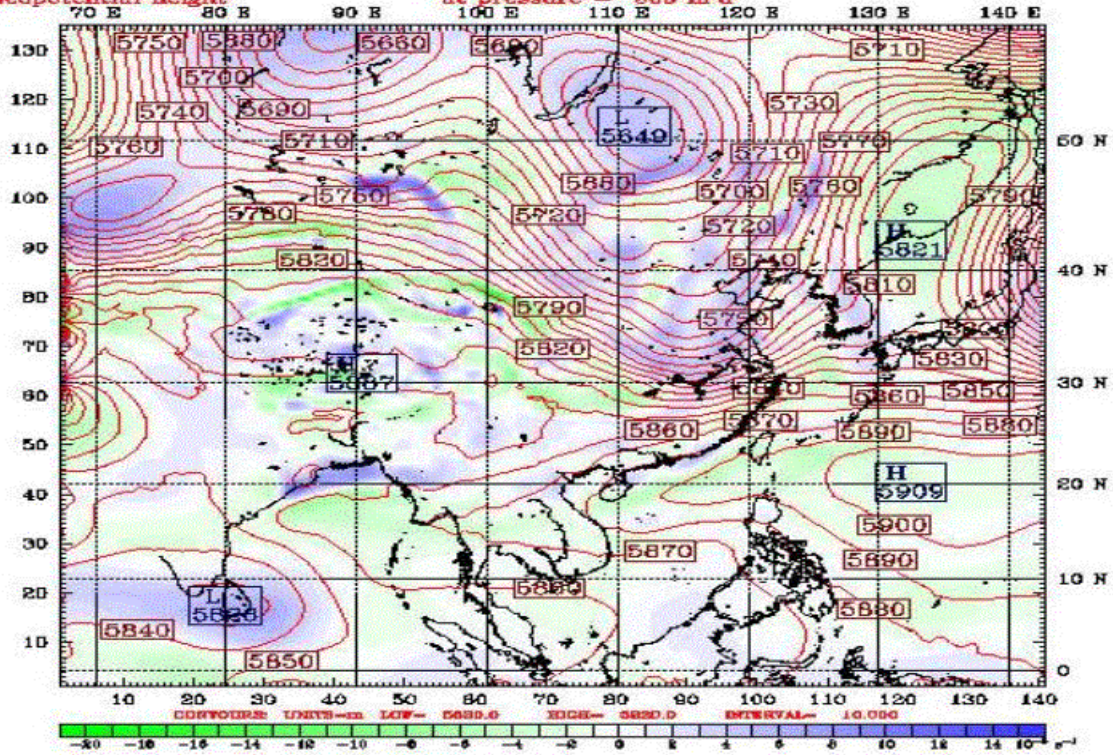
Appendix V consists of 28 figures that show 500-mb relative vorticity and geopotential heights for the May time period over the EAMS. The figures are in time sequential order from July 18 through July 31.



Fcst: *****

Relative vorticity
Geopotential height

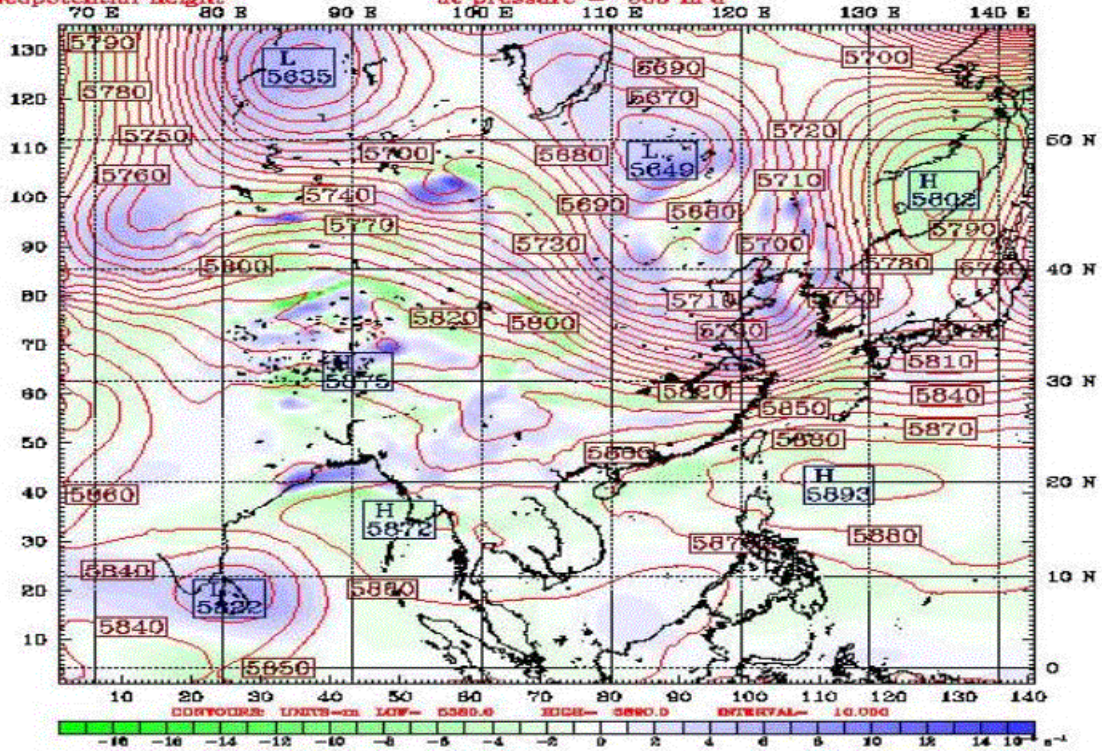
Valid: 1200 UTC Sat 18 Jul 98 (2100 LST Sat 18 Jul 98)
at pressure = 500 hPa
at pressure = 500 hPa



Fcst: *****

Relative vorticity
Geopotential height

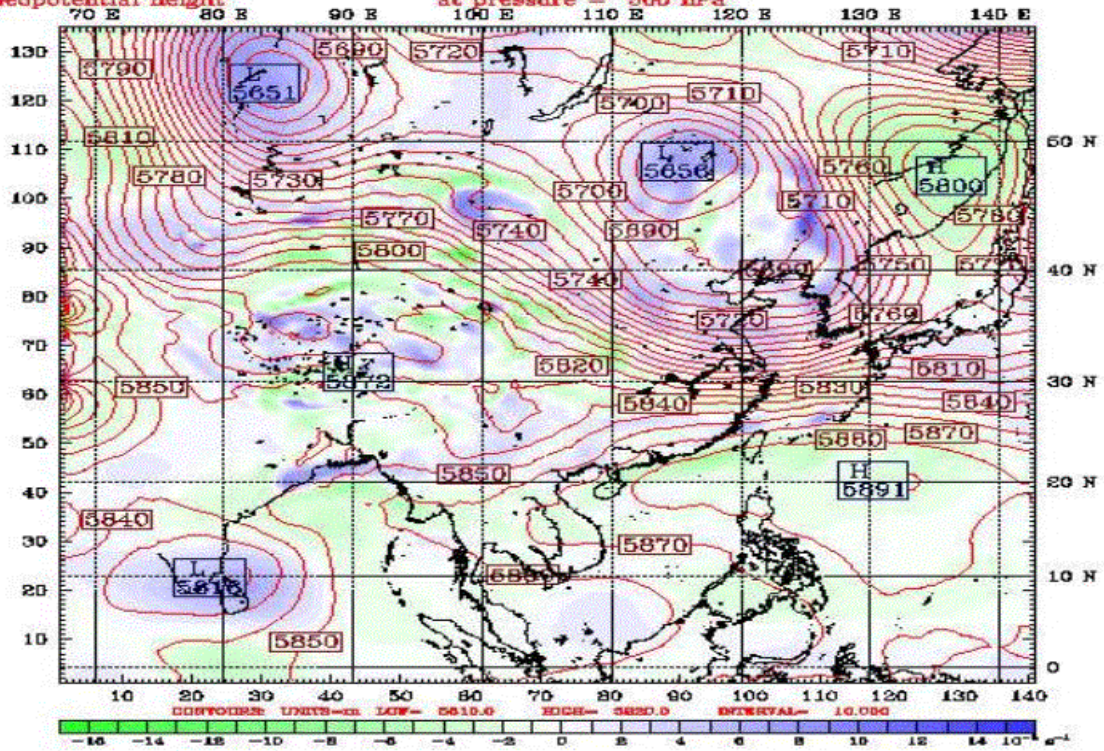
Valid: 0000 UTC Sun 19 Jul 98 (0900 LST Sun 19 Jul 98)
at pressure = 500 hPa
at pressure = 500 hPa



Fcst: *****

Relative vorticity
Geopotential height

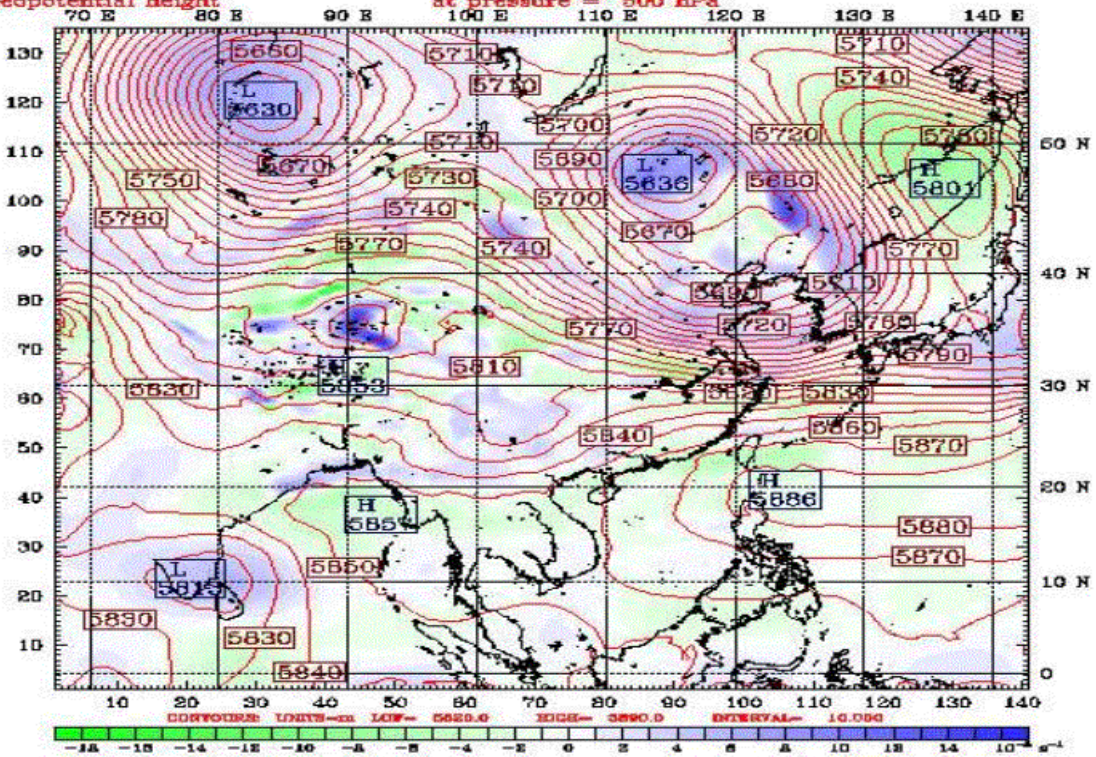
Valid: 1200 UTC Sun 19 Jul 98 (2100 LST Sun 19 Jul 98)
at pressure = 500 hPa
at pressure = 500 hPa



Fcst: *****

Relative vorticity
Geopotential height

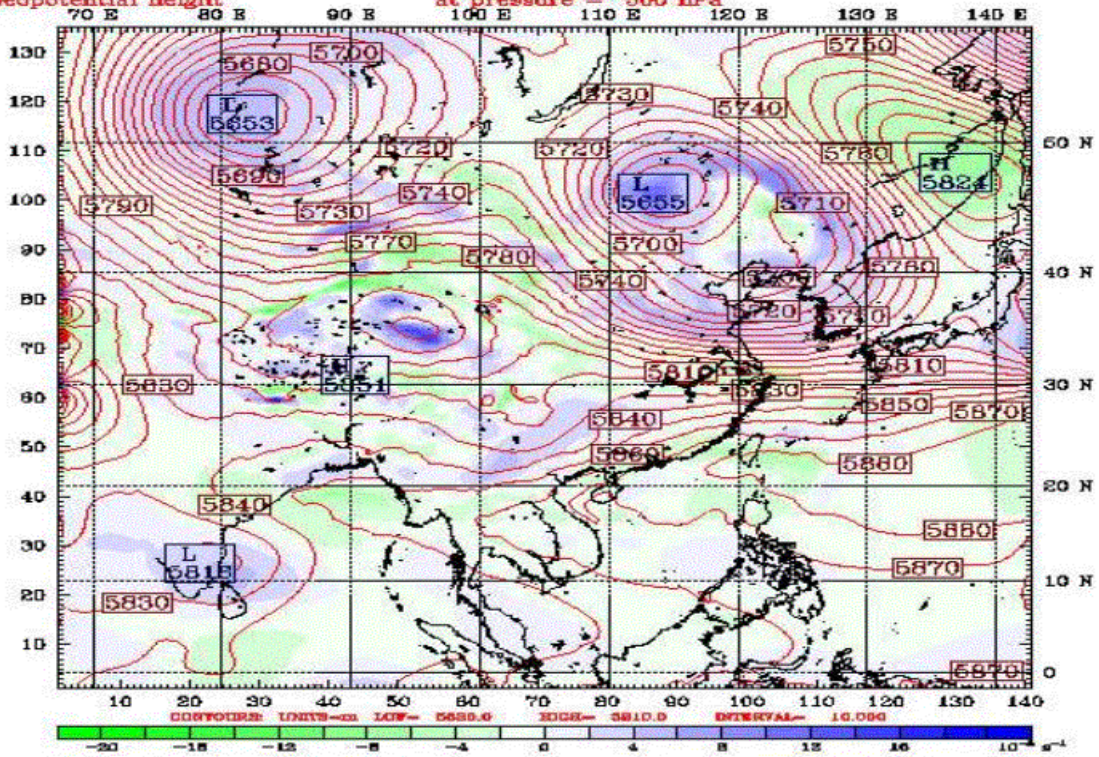
Valid: 0000 UTC Mon 20 Jul 98 (0900 LST Mon 20 Jul 98)
at pressure = 500 hPa
at pressure = 500 hPa



Fcst: *****

Relative vorticity
Geopotential height

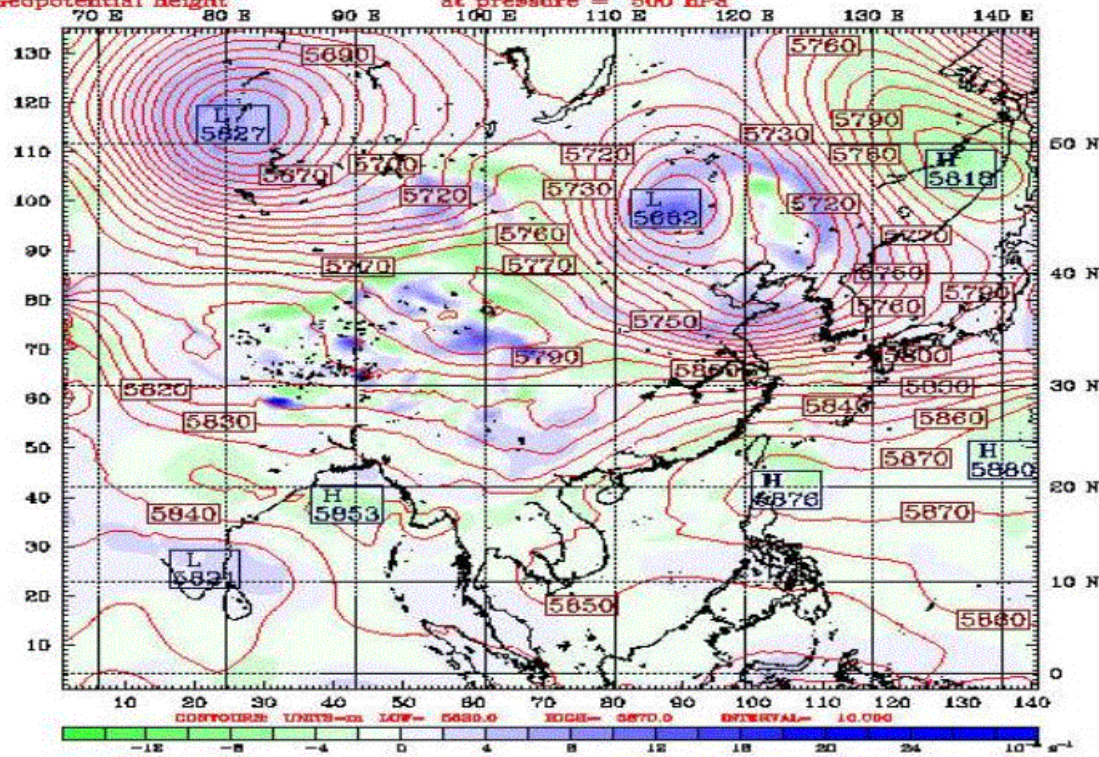
Valid: 1200 UTC Mon 20 Jul 98 (2100 LST Mon 20 Jul 98)
at pressure = 500 hPa
at pressure = 500 hPa



Fcst: *****

Relative vorticity
Geopotential height

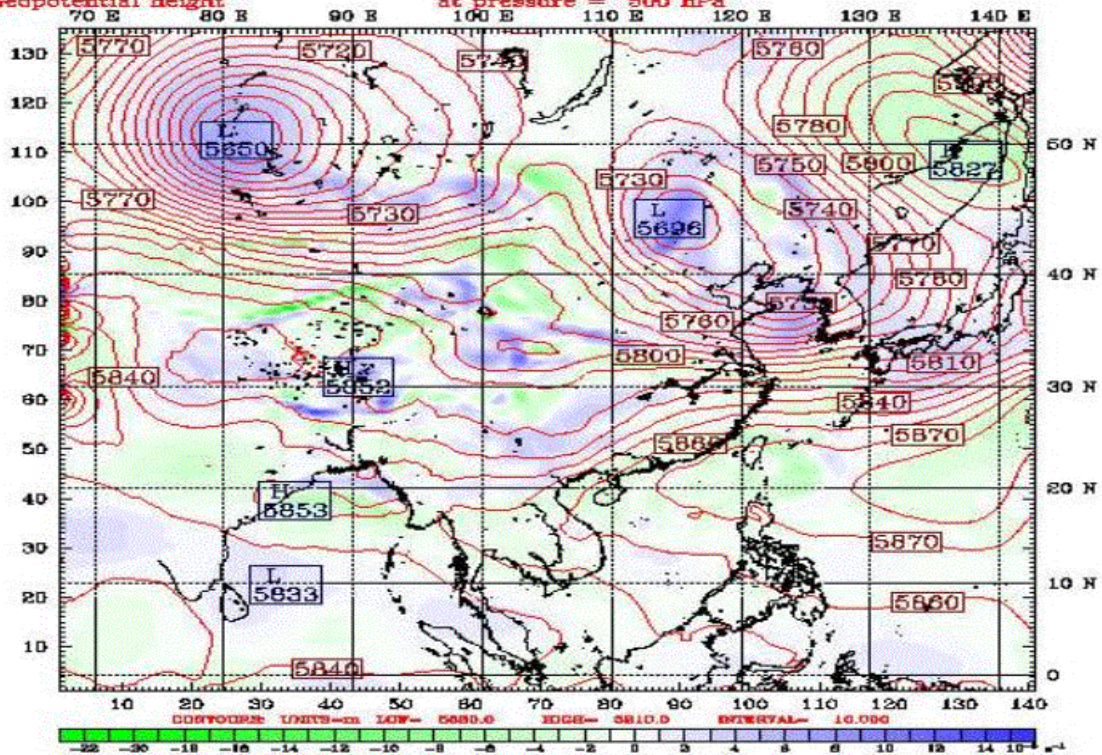
Valid: 0000 UTC Tue 21 Jul 98 (0900 LST Tue 21 Jul 98)
at pressure = 500 hPa
at pressure = 500 hPa



Fcst: *****

Relative vorticity
Geopotential height

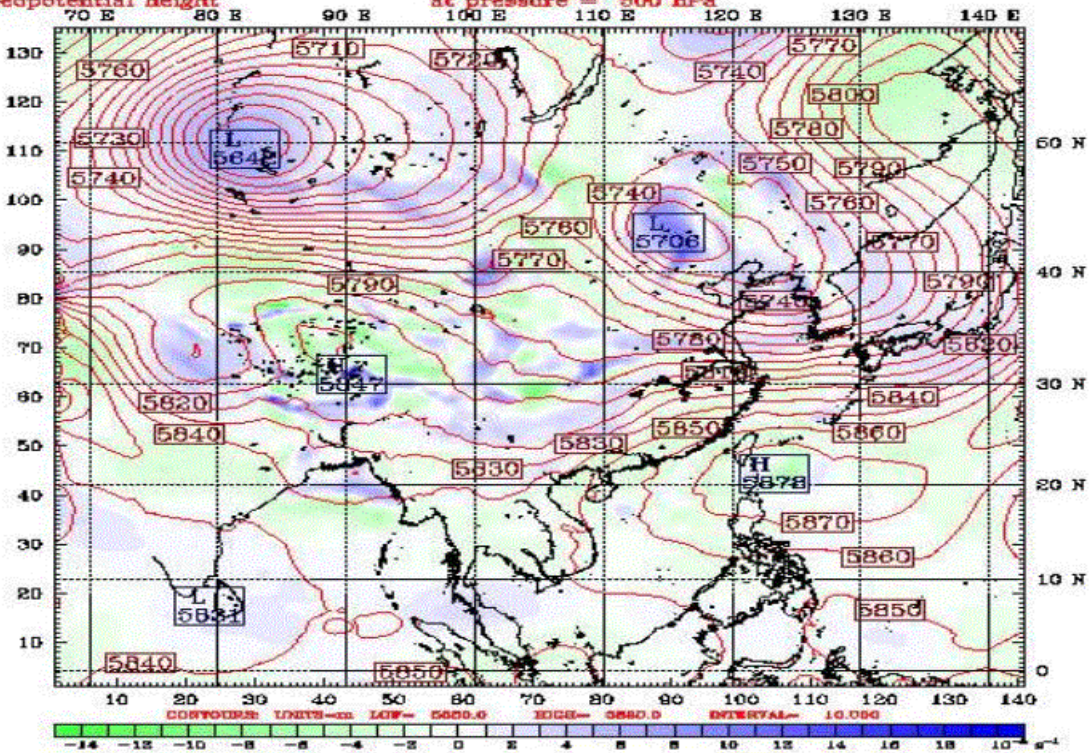
Valid: 1200 UTC Tue 21 Jul 98 (2100 LST Tue 21 Jul 98)
at pressure = 500 hPa
at pressure = 500 hPa

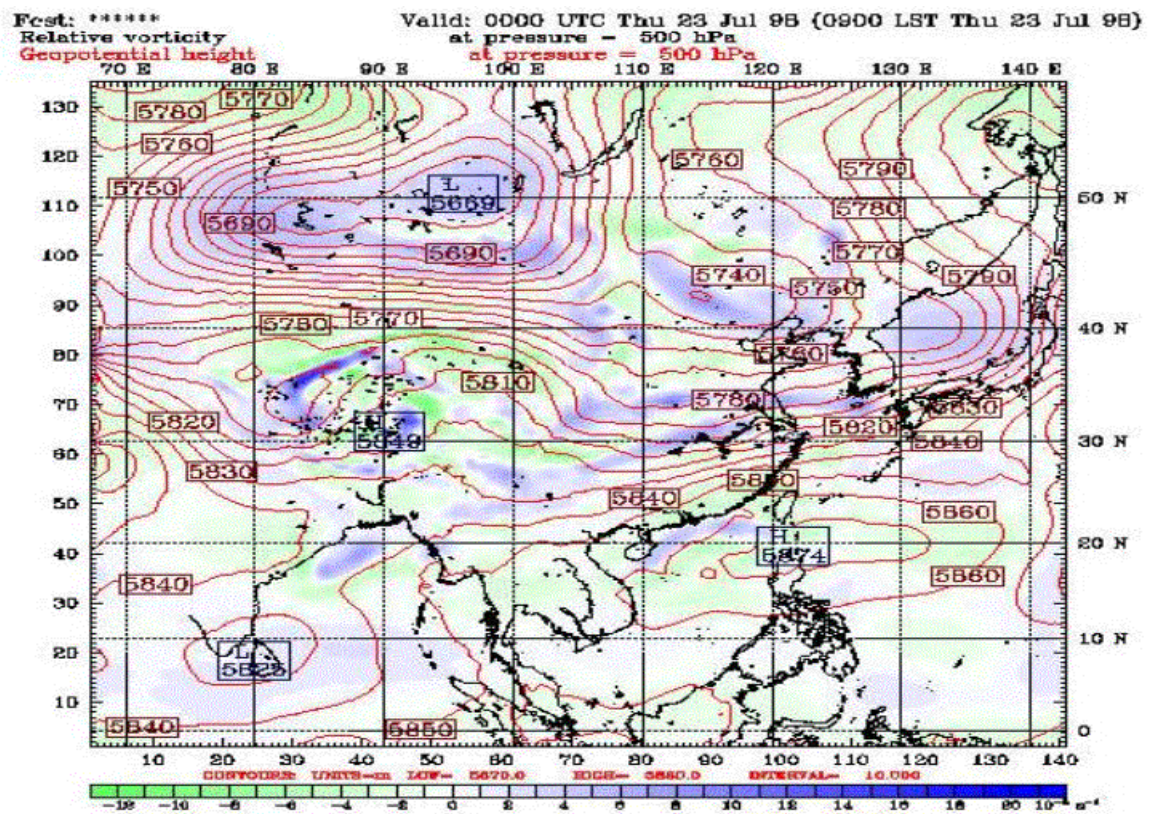
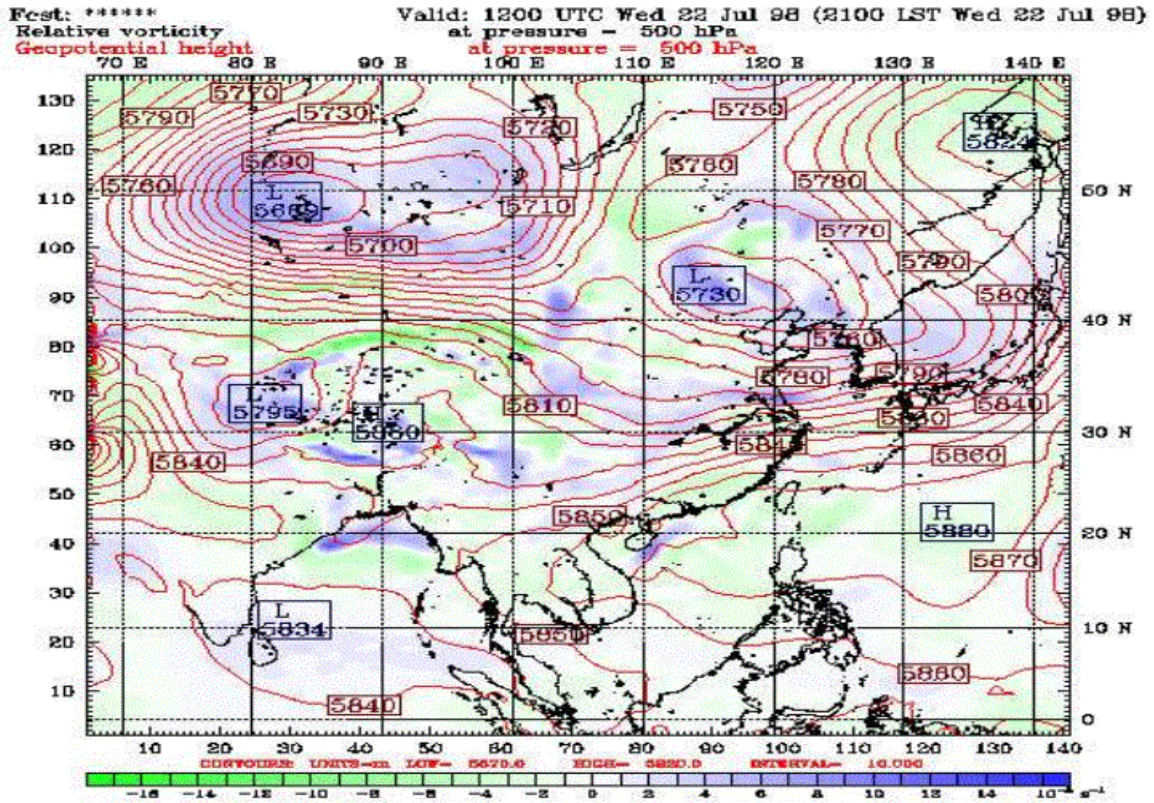


Fcst: *****

Relative vorticity
Geopotential height

Valid: 0000 UTC Wed 22 Jul 98 (0900 LST Wed 22 Jul 98)
at pressure = 500 hPa
at pressure = 500 hPa

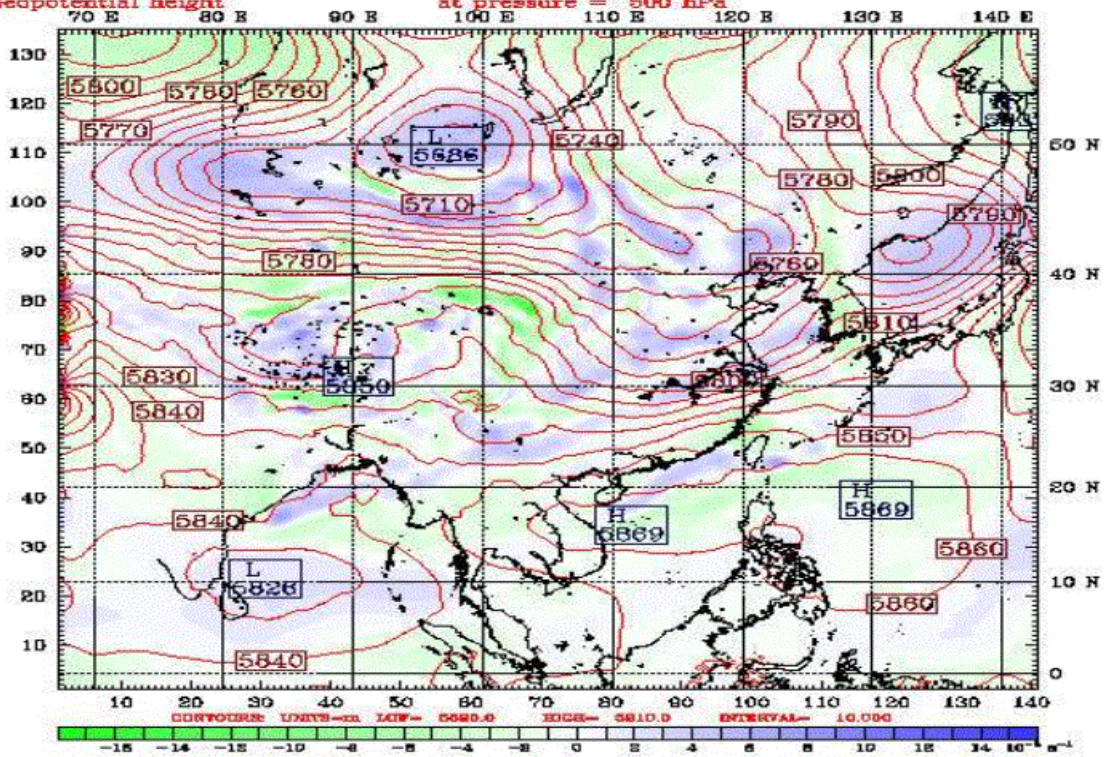




Fcst: *****

Relative vorticity
Geopotential height

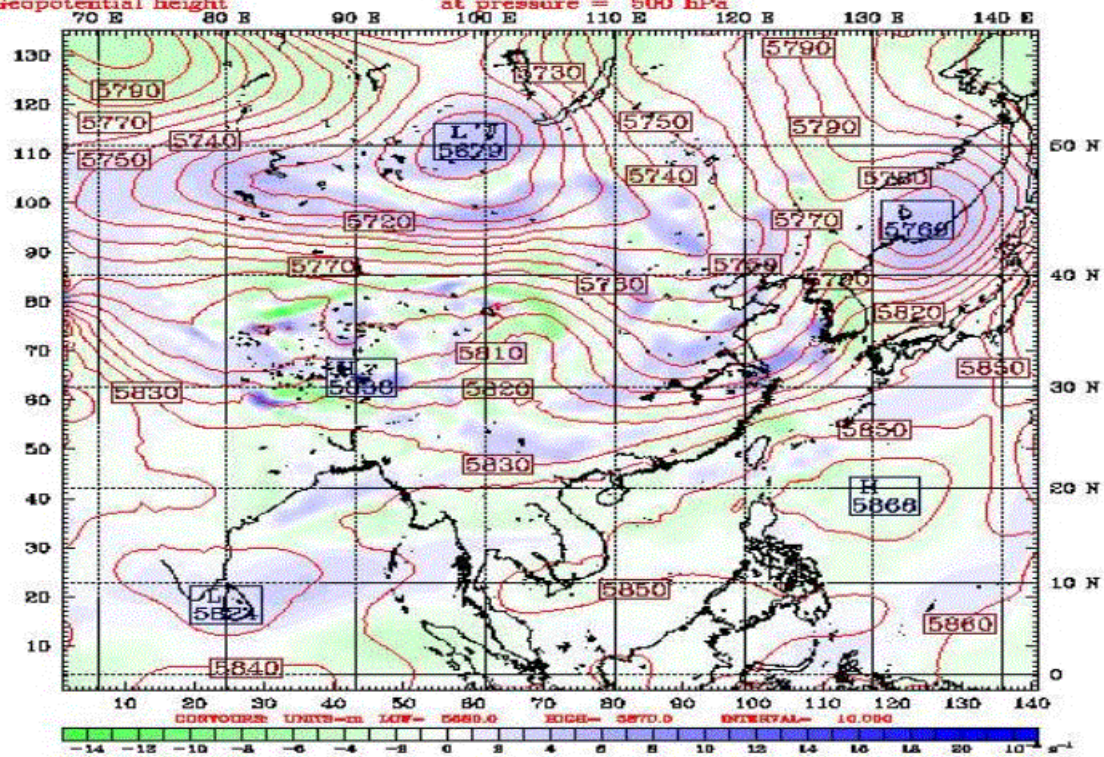
Valid: 1200 UTC Thu 23 Jul 98 (2100 LST Thu 23 Jul 98)
at pressure = 500 hPa
at pressure = 500 hPa



Fcst: *****

Relative vorticity
Geopotential height

Valid: 0000 UTC Fri 24 Jul 98 (0900 LST Fri 24 Jul 98)
at pressure = 500 hPa
at pressure = 500 hPa

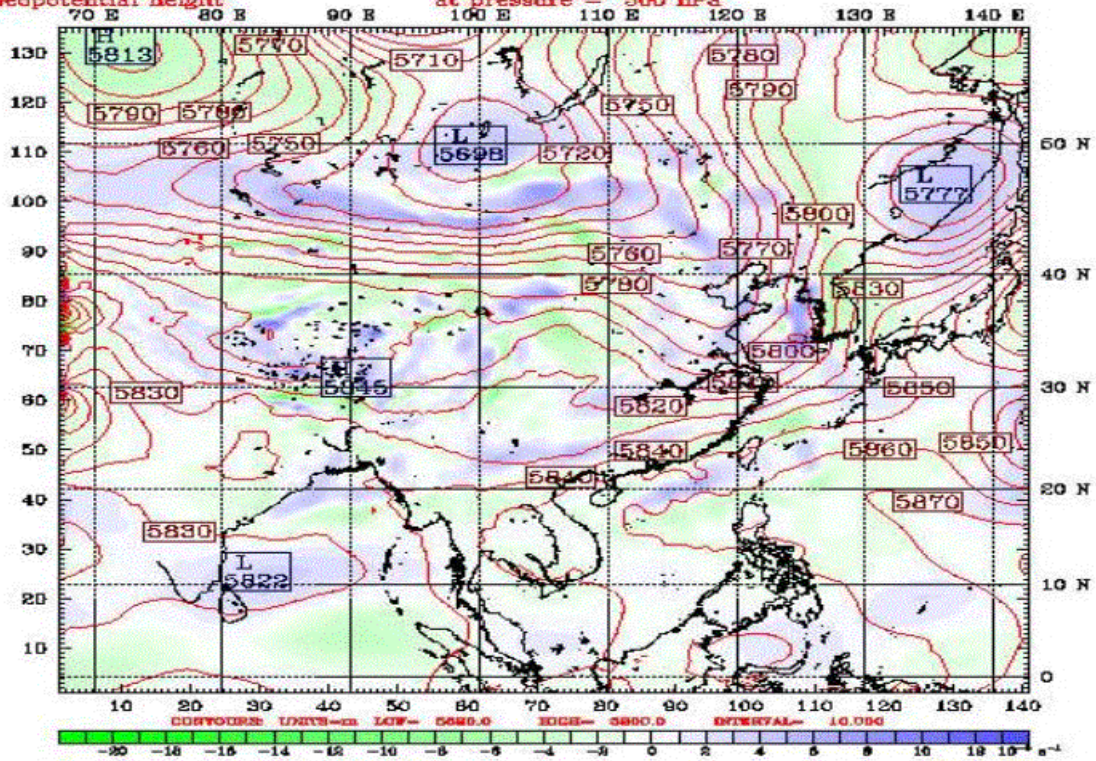


Fcst: *****

Relative vorticity
Geopotential height

Valid: 1200 UTC Fri 24 Jul 98 (2100 LST Fri 24 Jul 98)
at pressure = 500 hPa

at pressure = 500 hPa

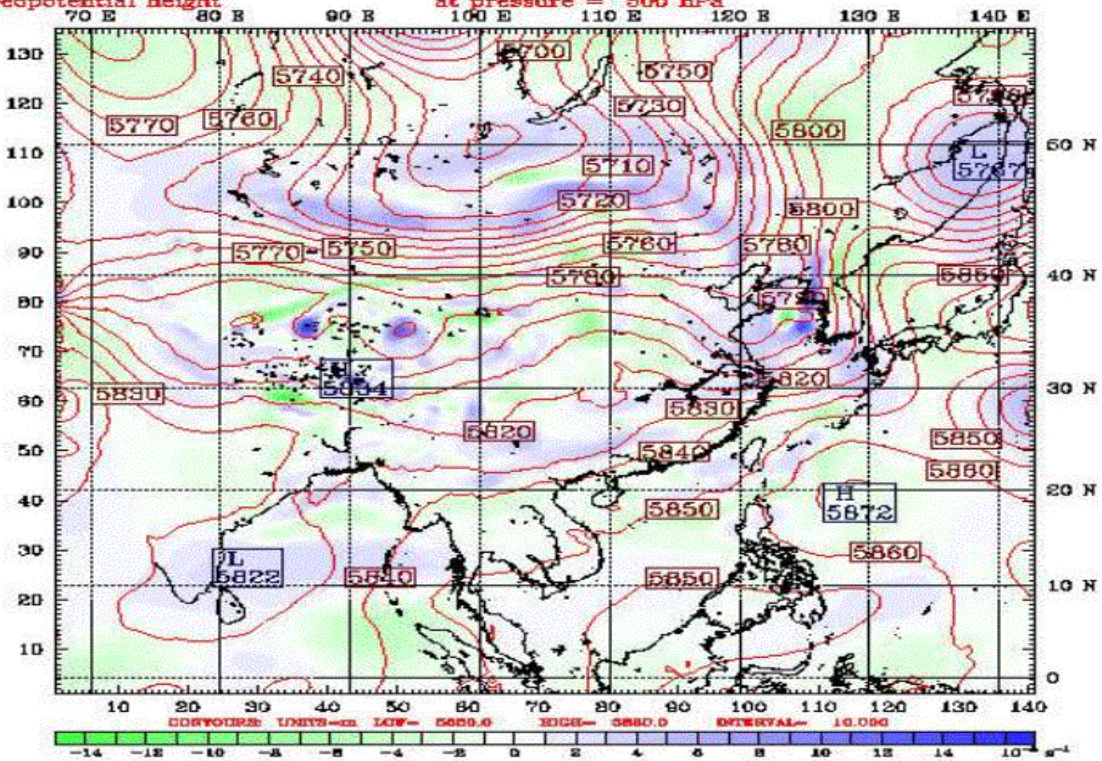


Fcst: *****

Relative vorticity
Geopotential height

Valid: 0000 UTC Sat 25 Jul 98 (0900 LST Sat 25 Jul 98)
at pressure = 500 hPa

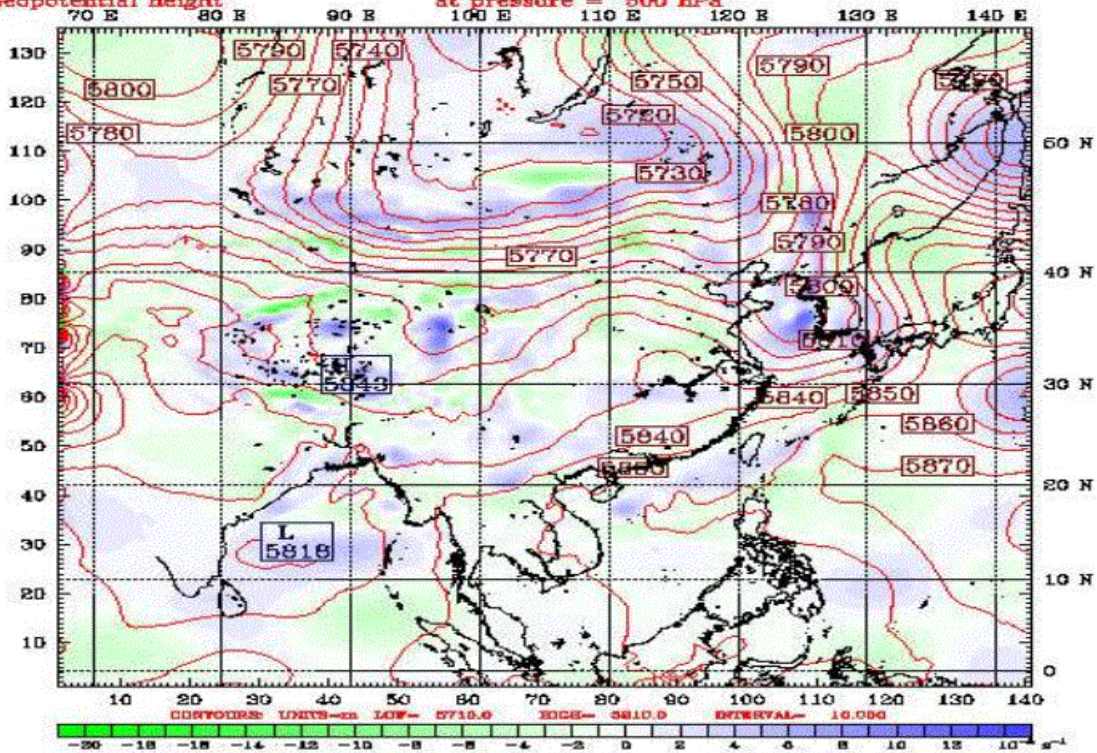
at pressure = 500 hPa



Fcst: *****

Relative vorticity
Geopotential height

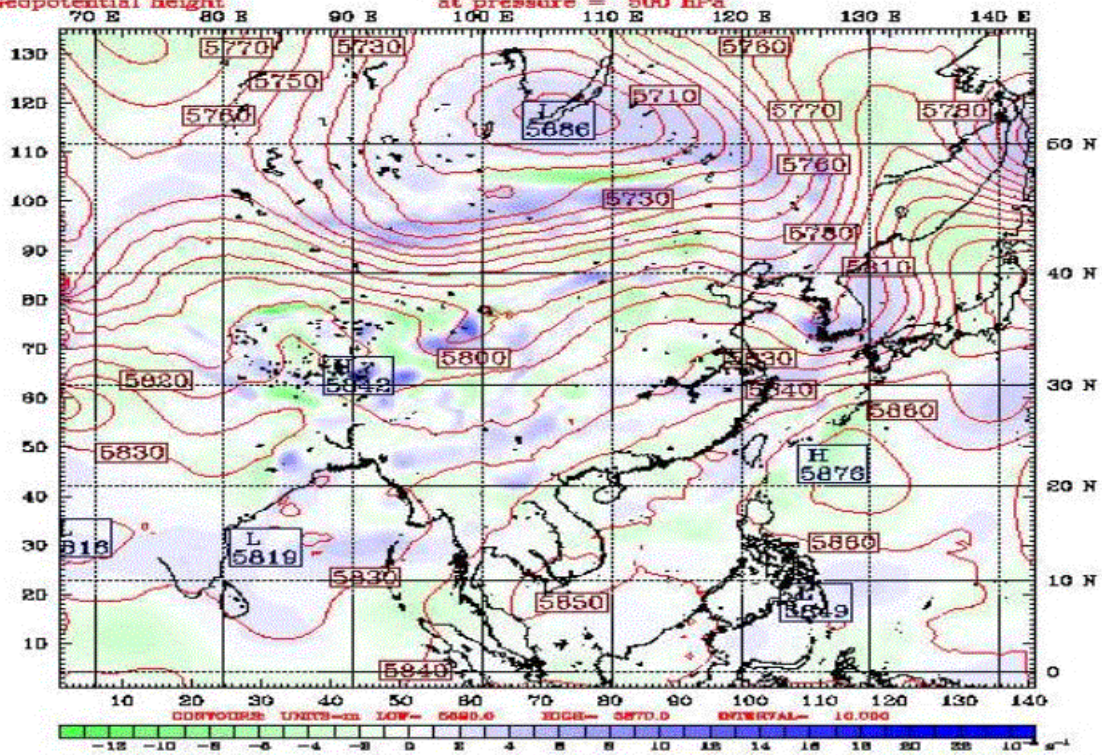
Valid: 1200 UTC Sat 25 Jul 98 (2100 LST Sat 25 Jul 98)
at pressure - 500 hPa
at pressure = 500 hPa



Fcst: *****

Relative vorticity
Geopotential height

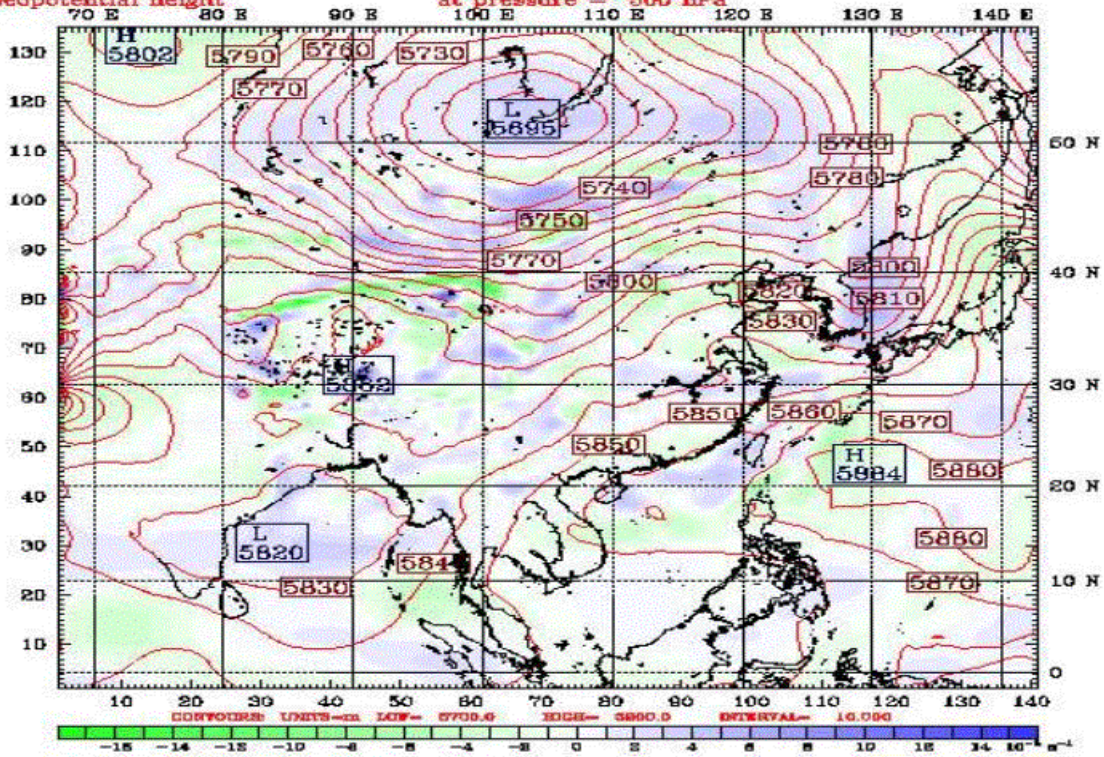
Valid: 0000 UTC Sun 26 Jul 98 (0900 LST Sun 26 Jul 98)
at pressure - 500 hPa
at pressure = 500 hPa



Fcst: *****

Relative vorticity
Geopotential height

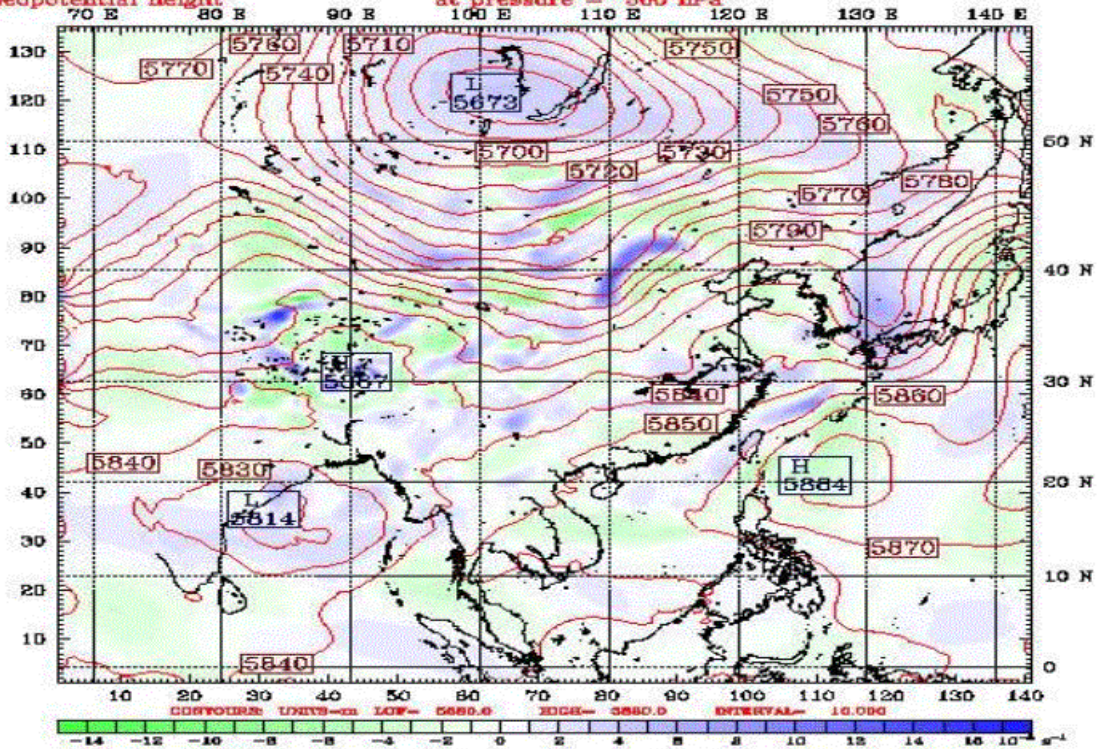
Valid: 1200 UTC Sun 26 Jul 98 (2100 LST Sun 26 Jul 98)
at pressure = 500 hPa
at pressure = 500 hPa



Fcst: *****

Relative vorticity
Geopotential height

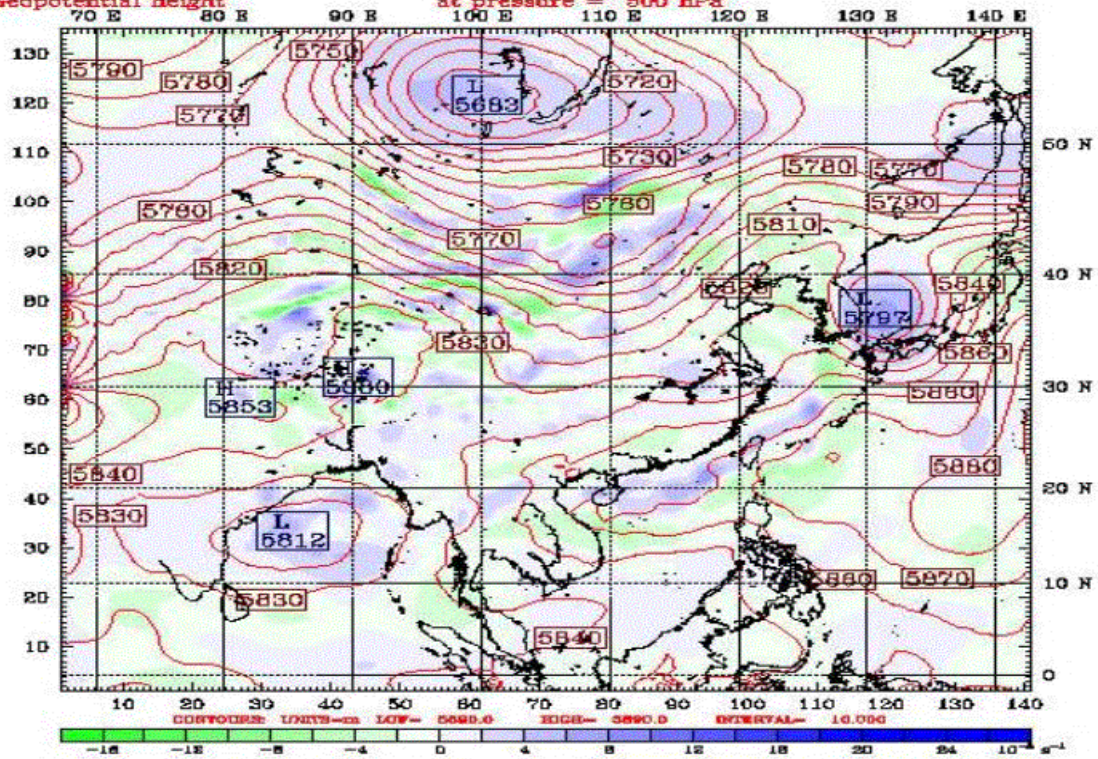
Valid: 0000 UTC Mon 27 Jul 98 (0900 LST Mon 27 Jul 98)
at pressure = 500 hPa
at pressure = 500 hPa



Fcst: *****

Relative vorticity
Geopotential height

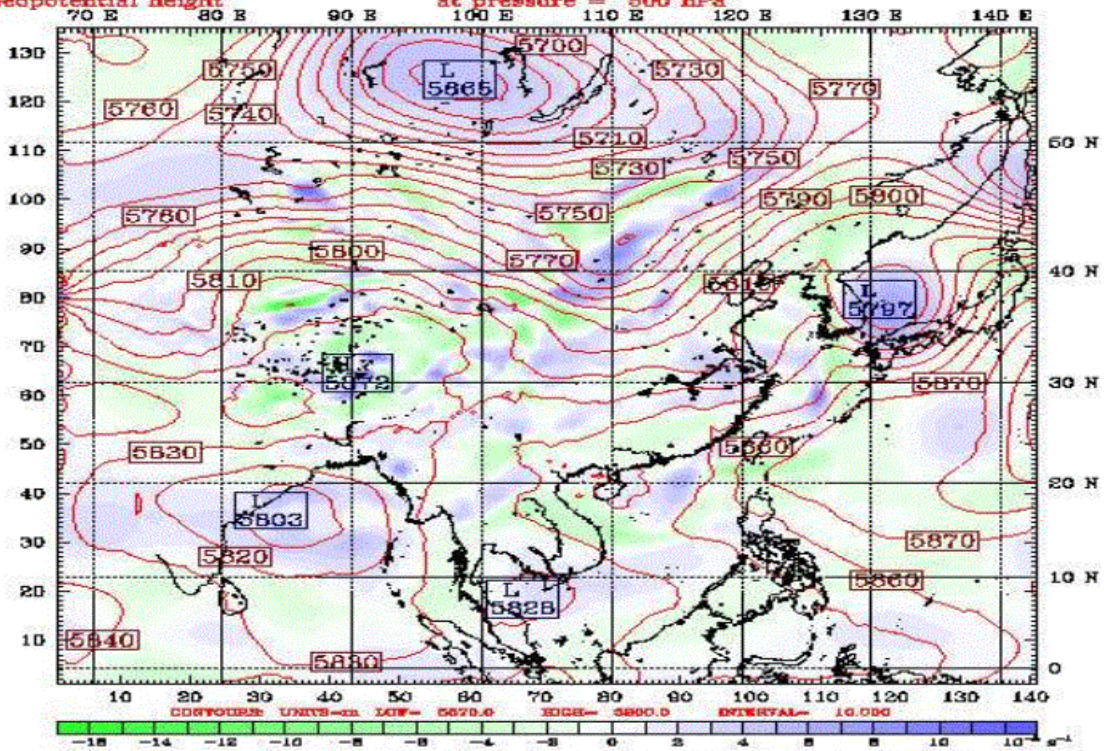
Valid: 1200 UTC Mon 27 Jul 98 (2100 LST Mon 27 Jul 98)
at pressure = 500 hPa
at pressure = 500 hPa



Fcst: *****

Relative vorticity
Geopotential height

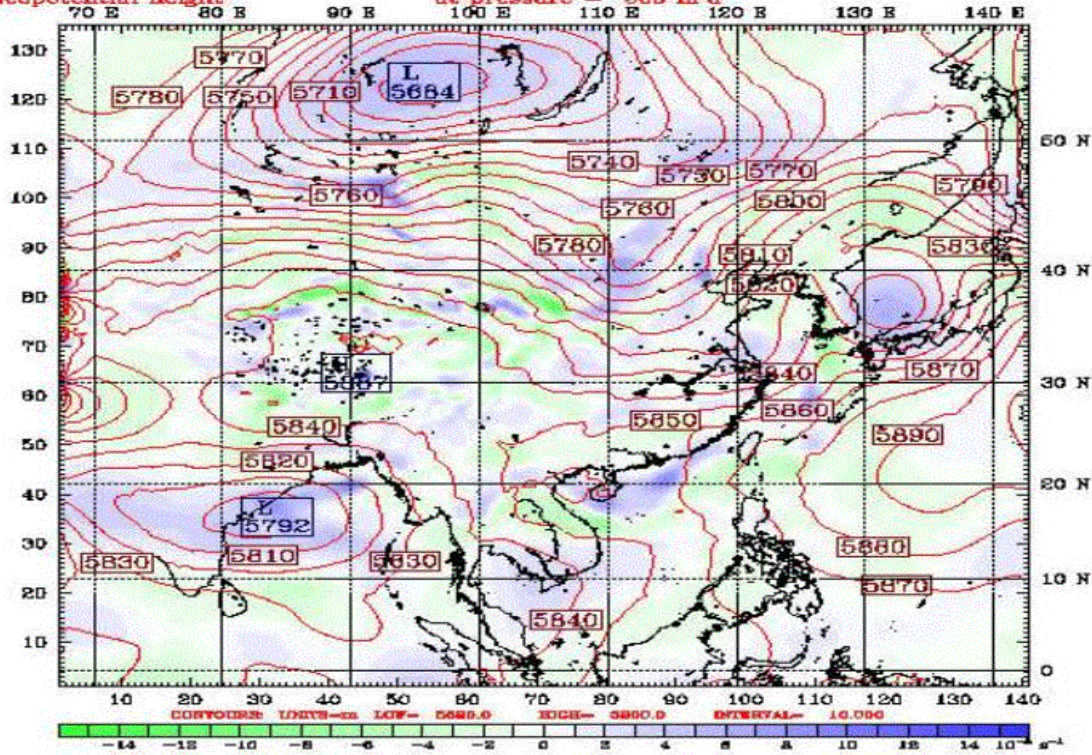
Valid: 0000 UTC Tue 28 Jul 98 (0900 LST Tue 28 Jul 98)
at pressure = 500 hPa
at pressure = 500 hPa



Fcst: *****

Relative vorticity
Geopotential height

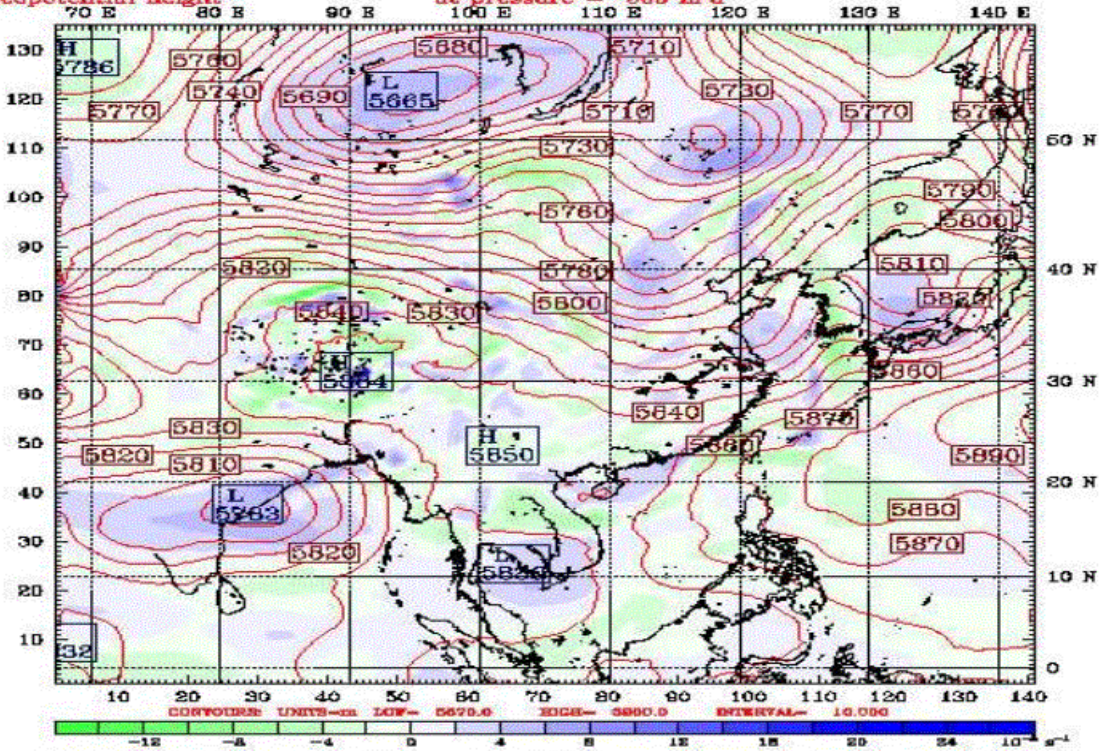
Valid: 1200 UTC Tue 28 Jul 98 (2100 LST Tue 28 Jul 98)
at pressure - 500 hPa
at pressure = 500 hPa



Fcst: *****

Relative vorticity
Geopotential height

Valid: 0000 UTC Wed 29 Jul 98 (0900 LST Wed 29 Jul 98)
at pressure - 500 hPa
at pressure = 500 hPa



Fcst: *****

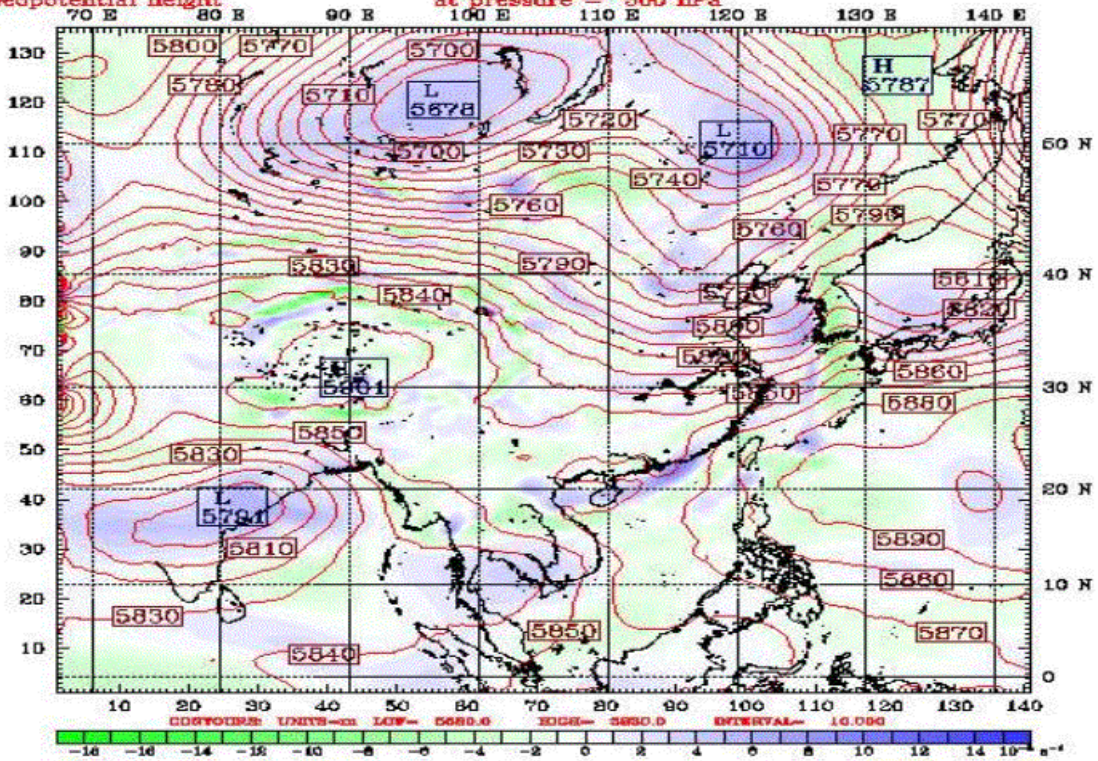
Valid: 1200 UTC Wed 29 Jul 98 (2100 LST Wed 29 Jul 98)

Relative vorticity

at pressure = 500 hPa

Geopotential height

at pressure = 500 hPa



Fcst: *****

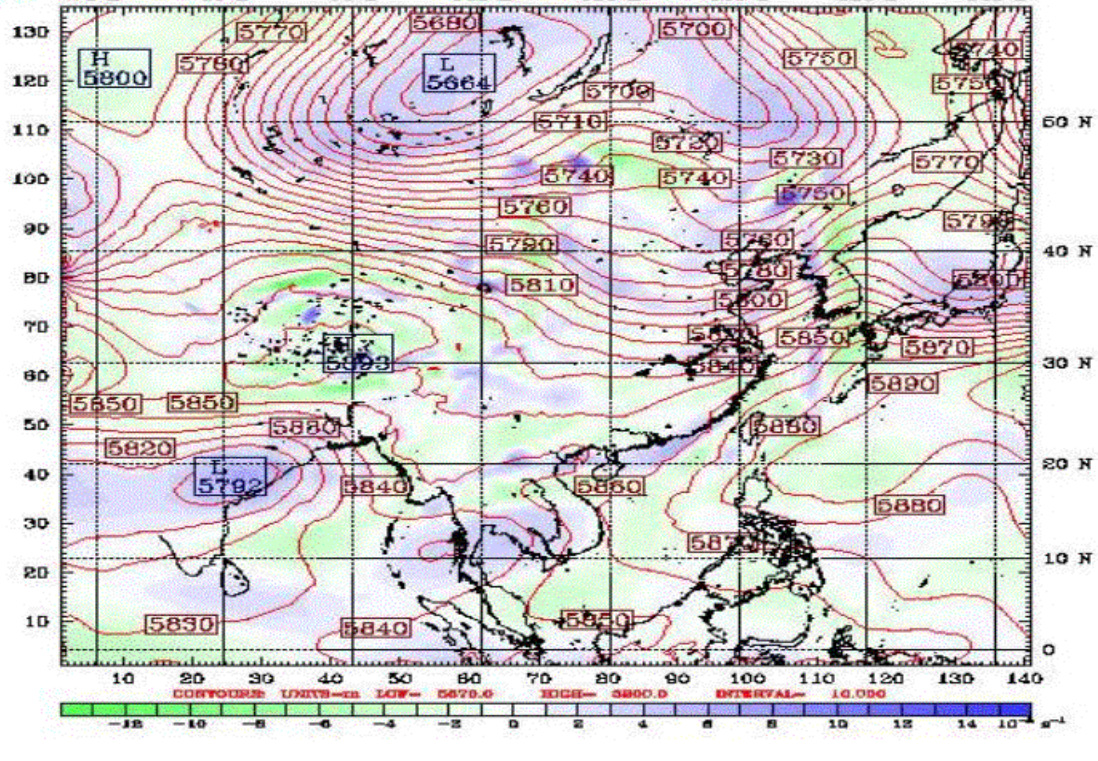
Valid: 0000 UTC Thu 30 Jul 98 (0900 LST Thu 30 Jul 98)

Relative vorticity

at pressure = 500 hPa

Geopotential height

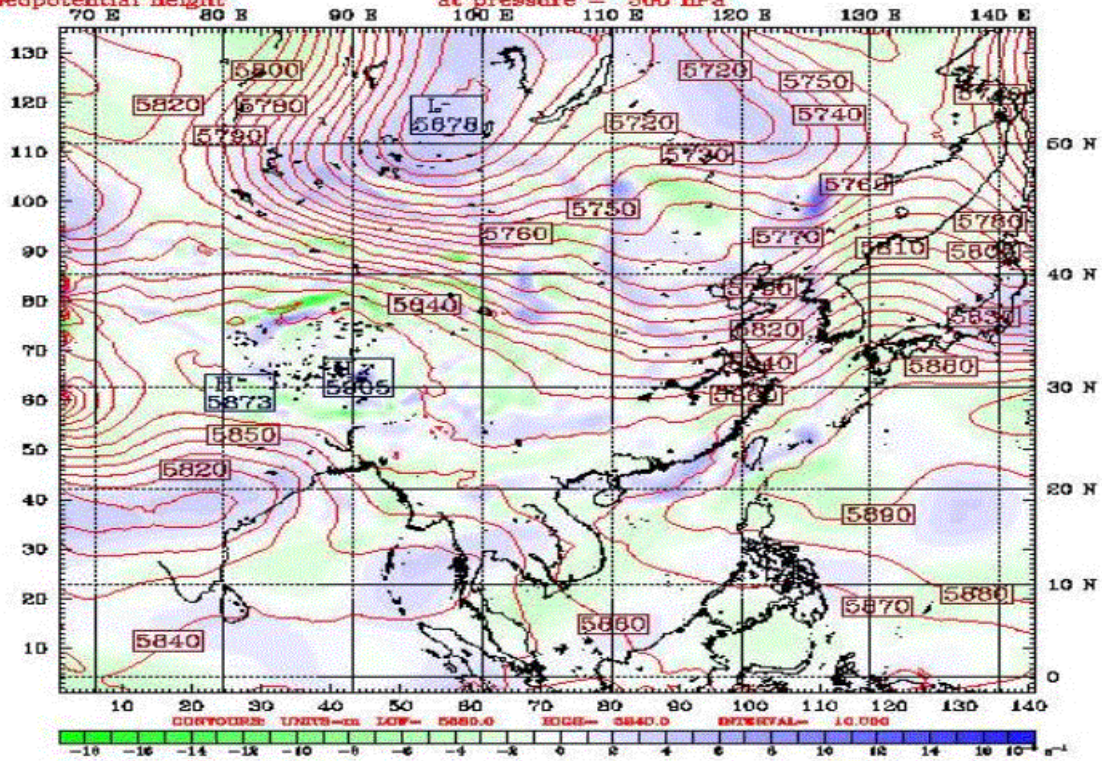
at pressure = 500 hPa



Fcst: *****

Relative vorticity
Geopotential height

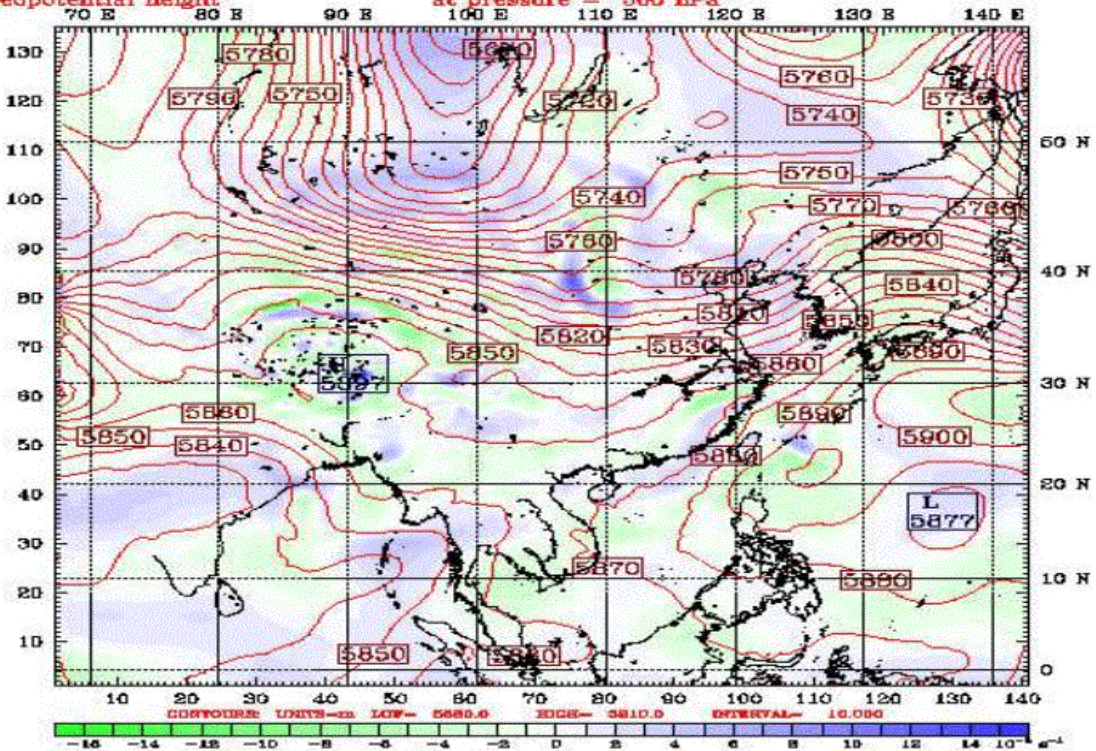
Valid: 1200 UTC Thu 30 Jul 98 (2100 LST Thu 30 Jul 98)
at pressure = 500 hPa
at pressure = 500 hPa



Fcst: *****

Relative vorticity
Geopotential height

Valid: 0000 UTC Fri 31 Jul 98 (0900 LST Fri 31 Jul 98)
at pressure = 500 hPa
at pressure = 500 hPa

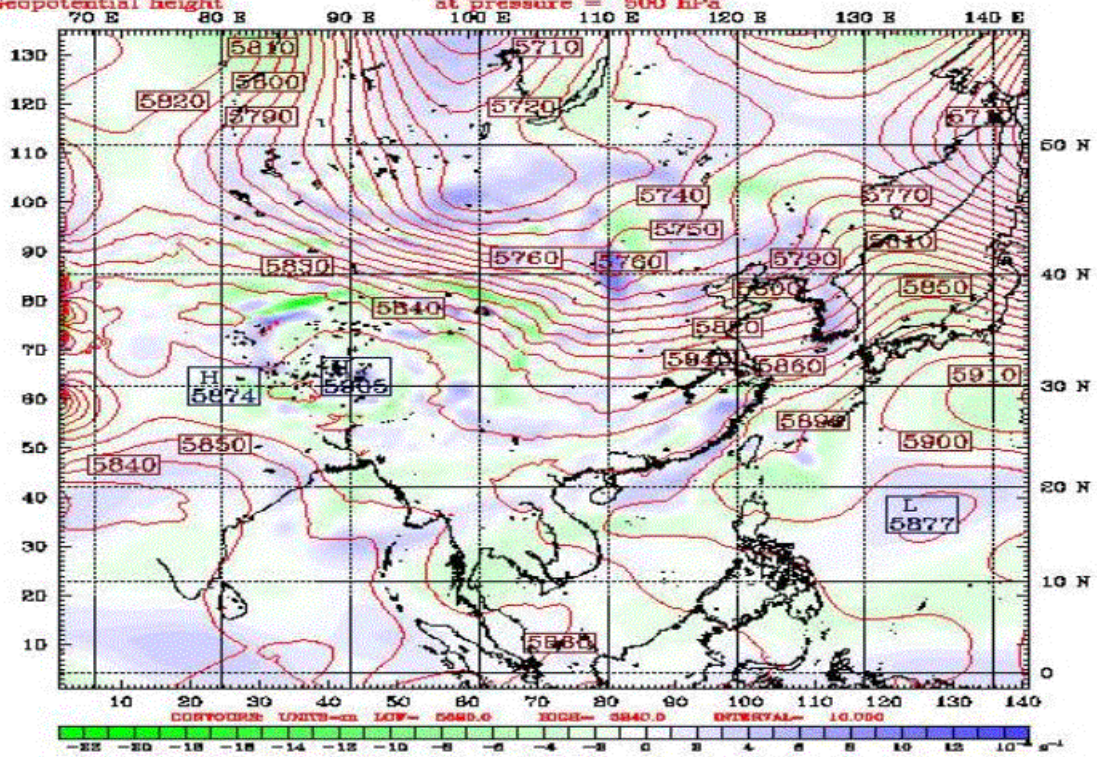


Fcst: *****

Relative vorticity
Geopotential height

Valid: 1200 UTC Fri 31 Jul 98 (2100 LST Fri 31 Jul 98)
at pressure = 500 hPa

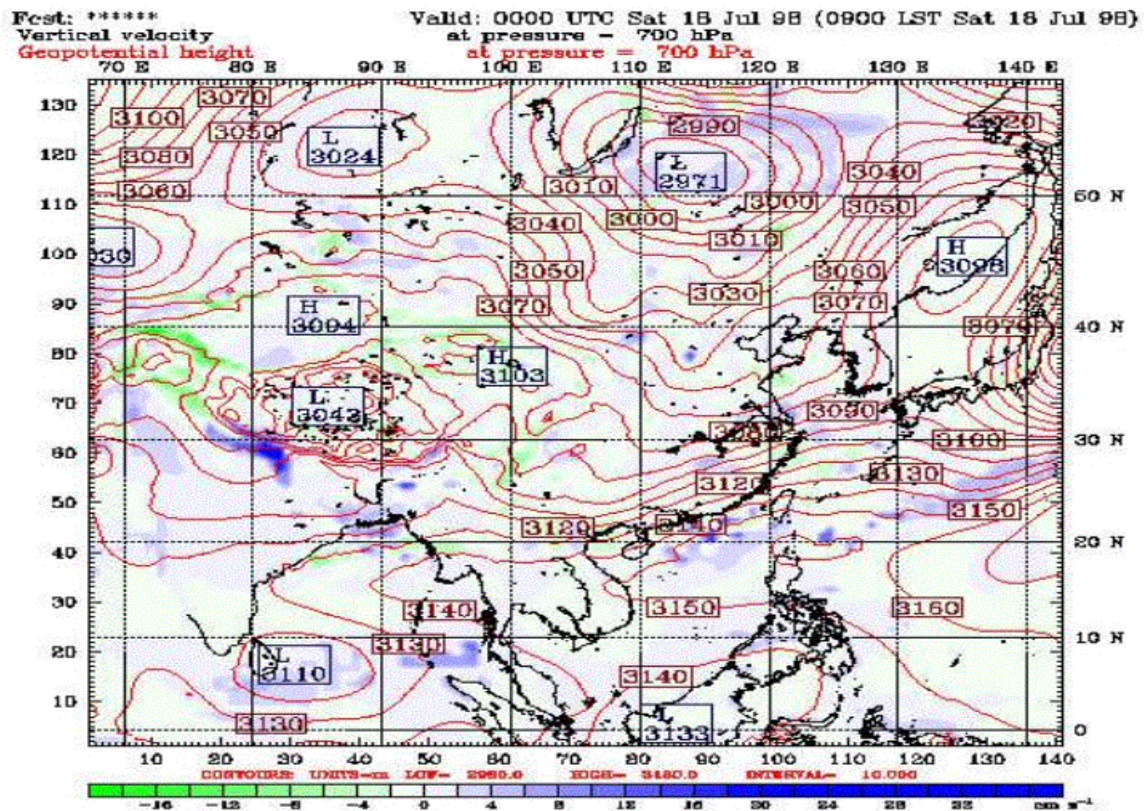
at pressure = 500 hPa



THIS PAGE INTENTIONALLY LEFT BLANK

APPENDIX W. 700-MB VERTICAL VELOCITY/GEOPOTENTIAL HEIGHT PLOTS OVER THE EAMS FOR THE JULY TIME PERIOD

Appendix W consists of 28 figures that show 700-mb vertical velocity and geopotential heights for the May time period over the EAMS. The figures are in time sequential order from July 18 through July 31.



Fcst: *****

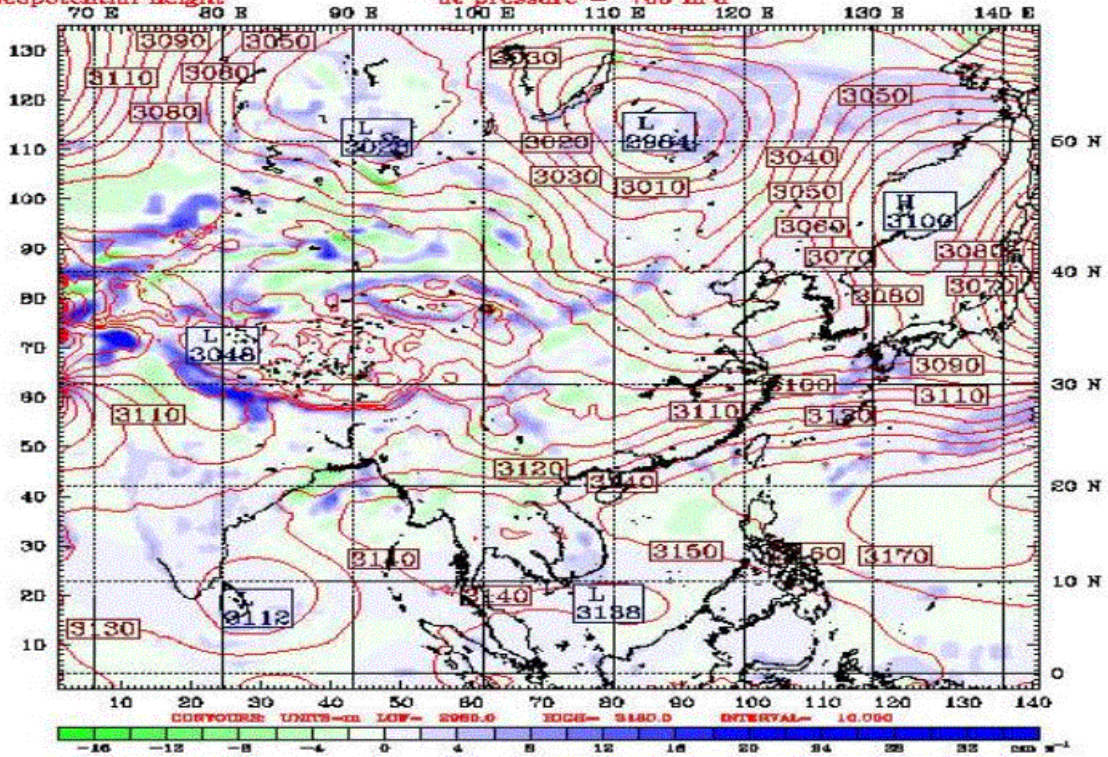
Valid: 1200 UTC Sat 18 Jul 98 (2100 LST Sat 18 Jul 98)

Vertical velocity

at pressure = 700 hPa

Geopotential height

at pressure = 700 hPa



Fcst: *****

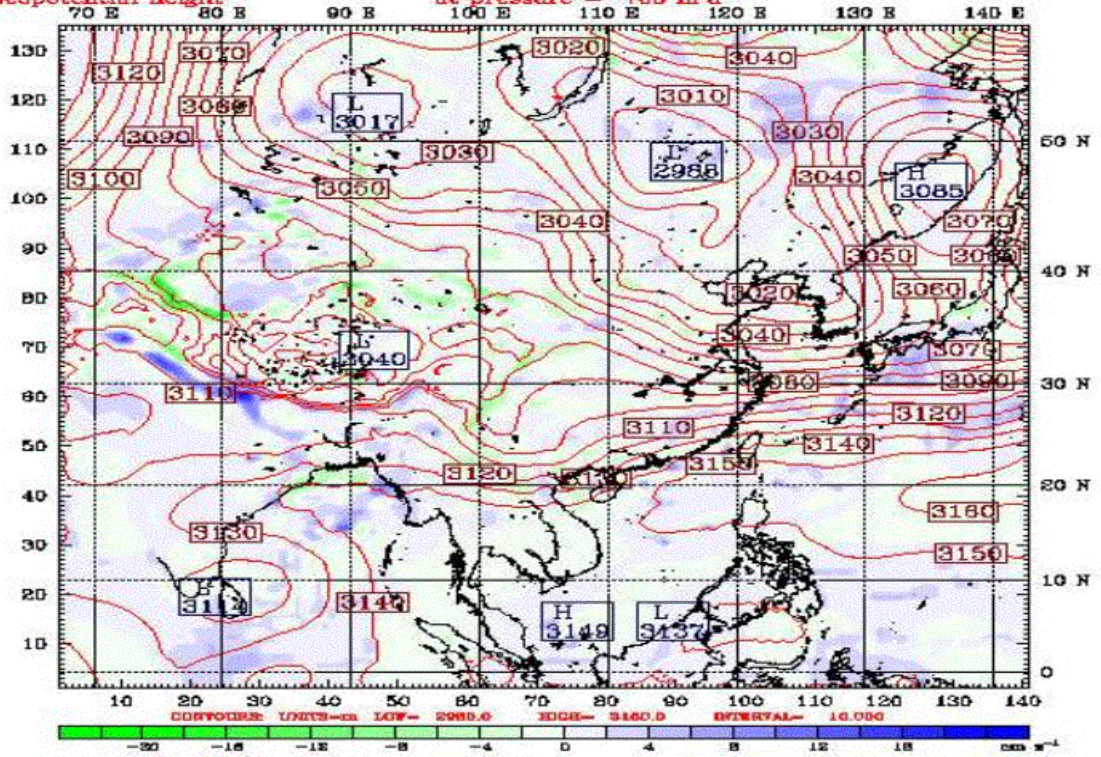
Valid: 0000 UTC Sun 19 Jul 98 (0900 LST Sun 19 Jul 98)

Vertical velocity

at pressure = 700 hPa

Geopotential height

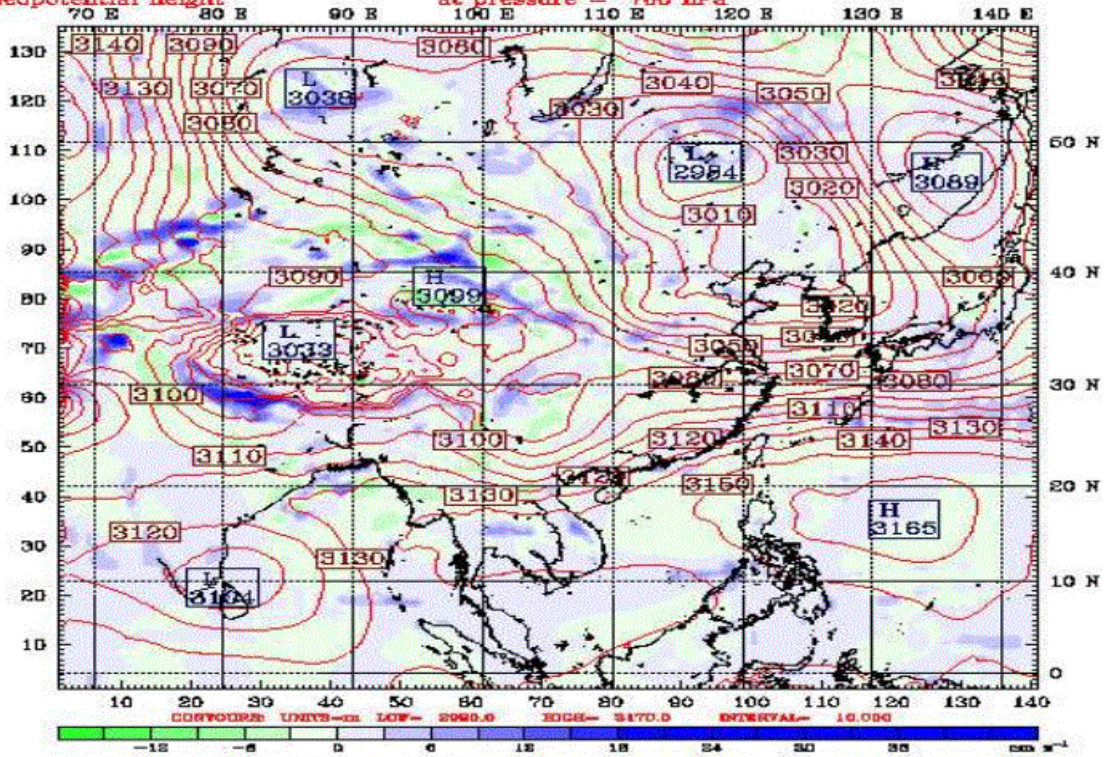
at pressure = 700 hPa



Fcst: *****

Vertical velocity
Geopotential height

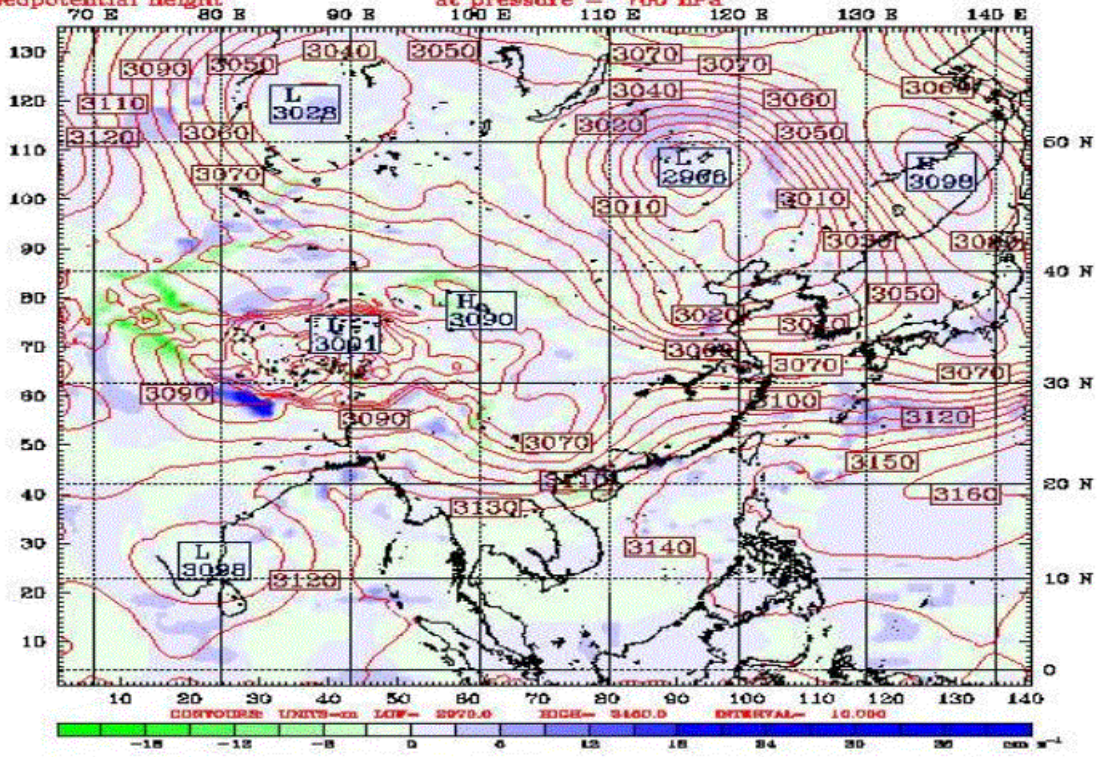
Valid: 1200 UTC Sun 19 Jul 98 (2100 LST Sun 19 Jul 98)
at pressure = 700 hPa
at pressure = 700 hPa



Fcst: *****

Vertical velocity
Geopotential height

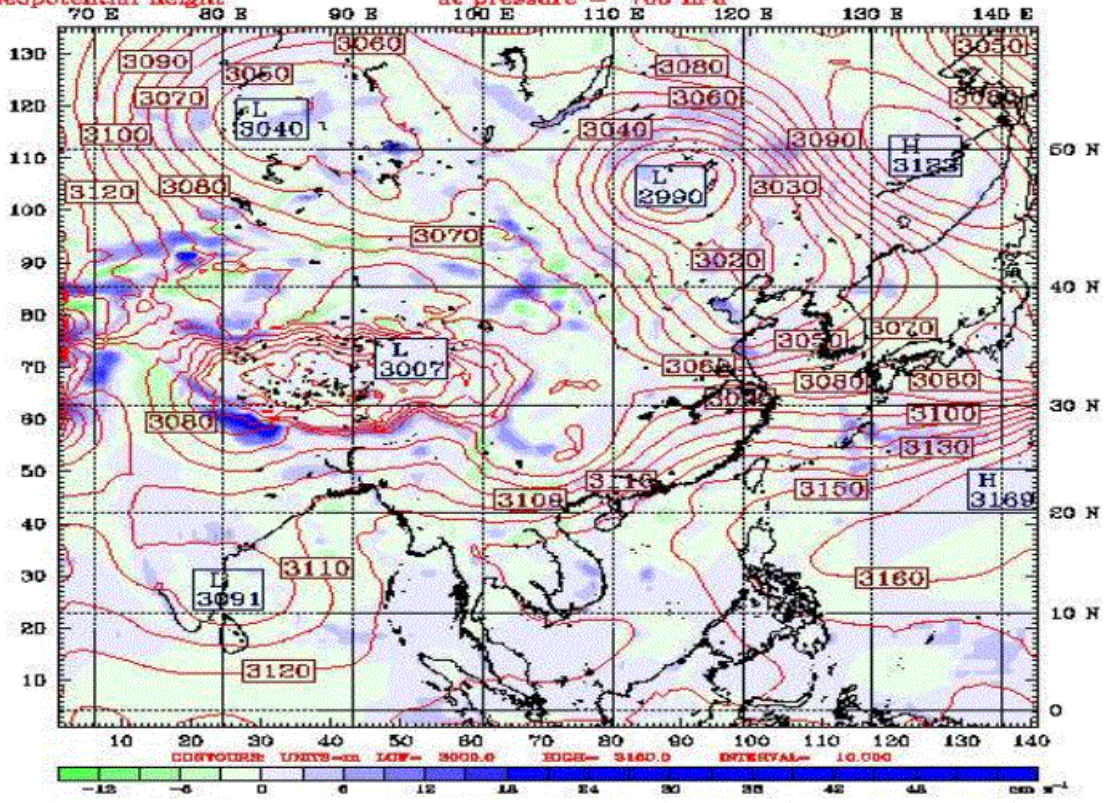
Valid: 0000 UTC Mon 20 Jul 98 (0900 LST Mon 20 Jul 98)
at pressure = 700 hPa
at pressure = 700 hPa



Fest: *****

Vertical velocity
Geopotential height

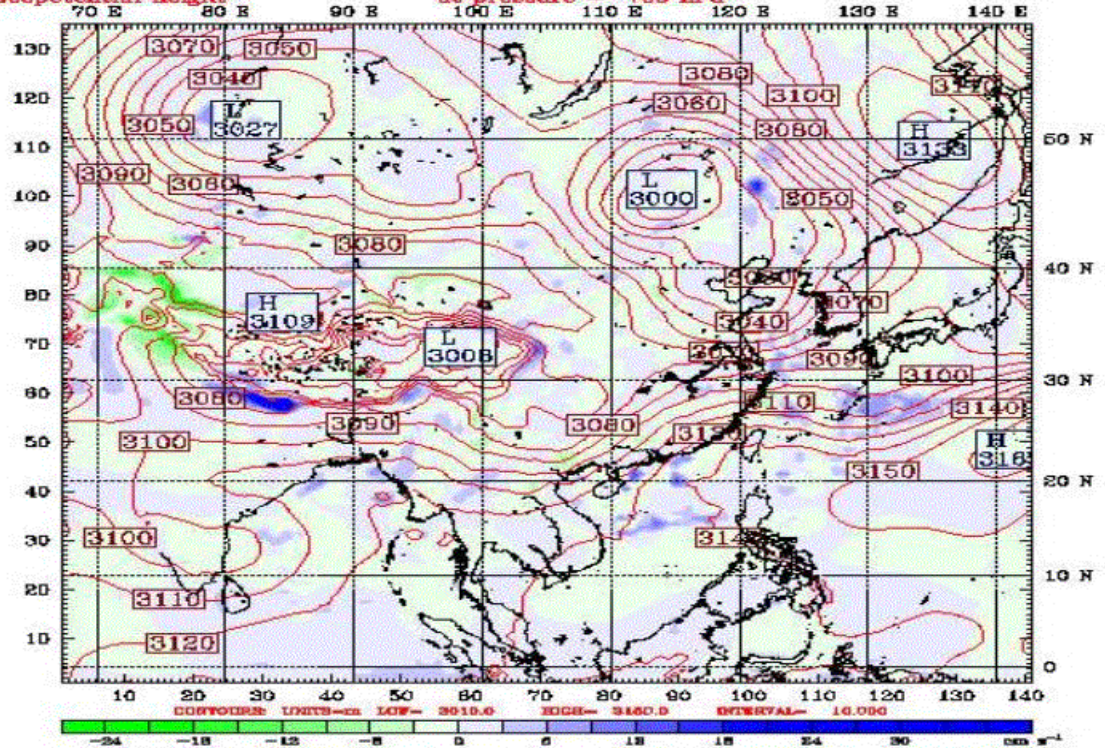
Valid: 1200 UTC Mon 20 Jul 98 (2100 LST Mon 20 Jul 98)
at pressure = 700 hPa
at pressure = 700 hPa



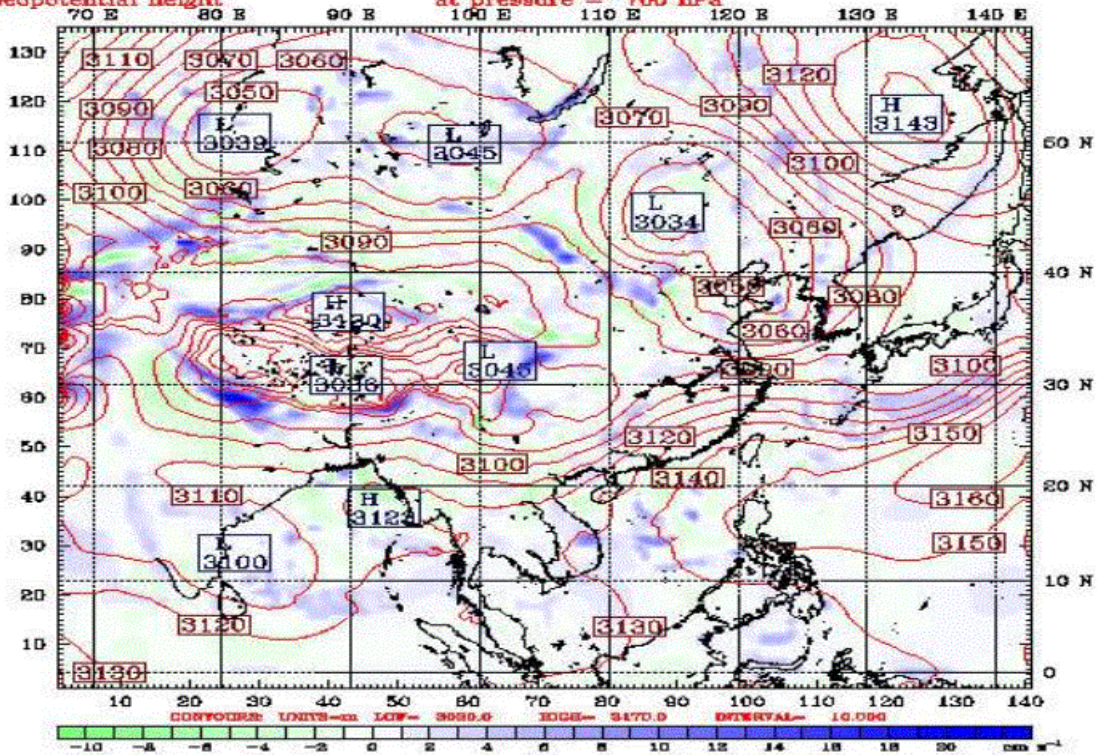
Fest: *****

Vertical velocity
Geopotential height

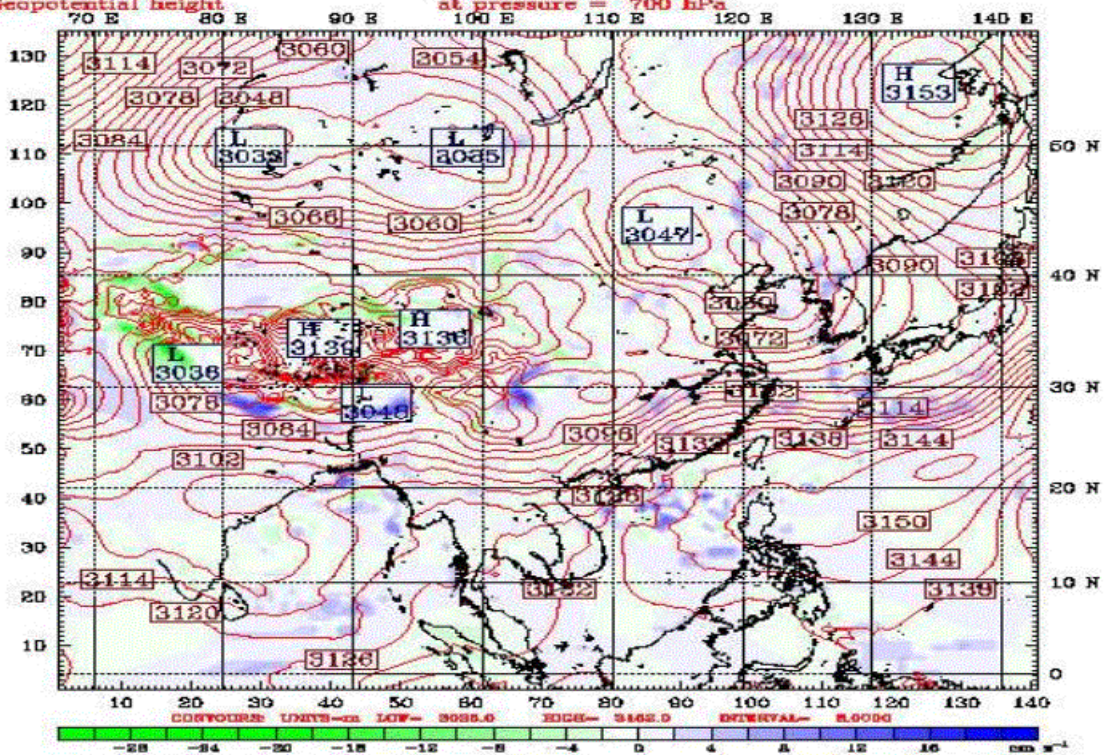
Valid: 0000 UTC Tue 21 Jul 98 (0900 LST Tue 21 Jul 98)
at pressure = 700 hPa
at pressure = 700 hPa

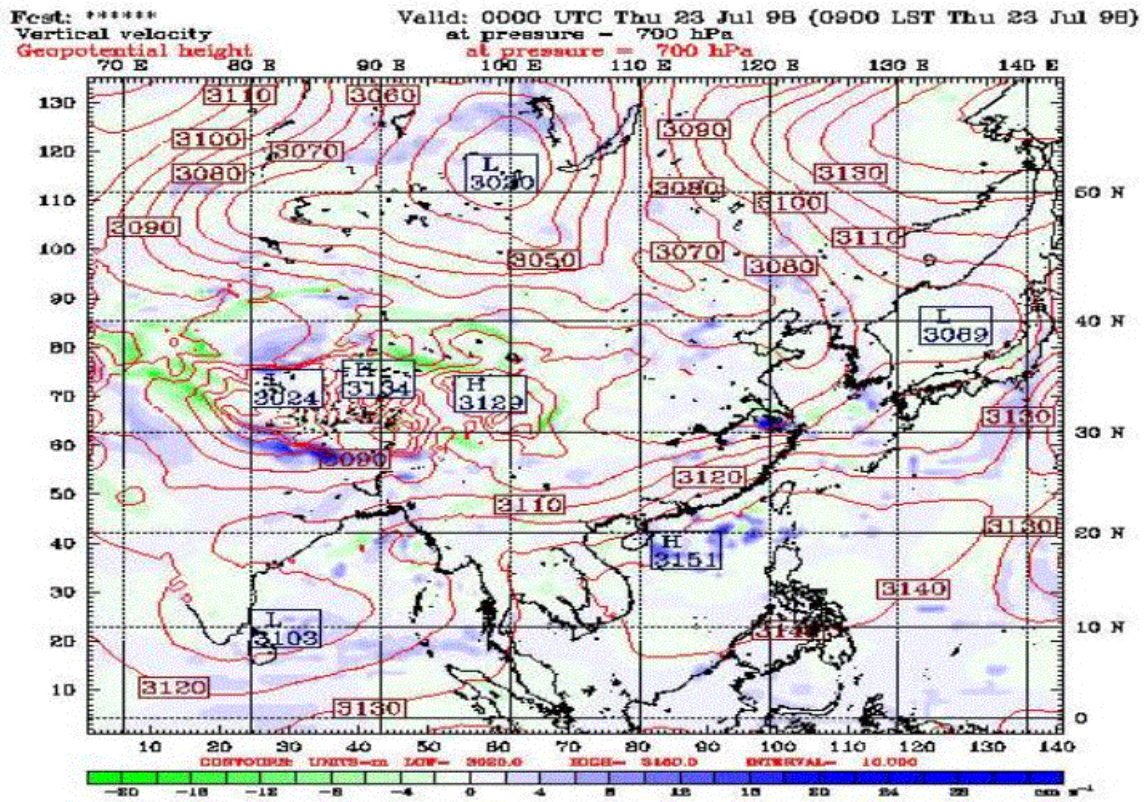
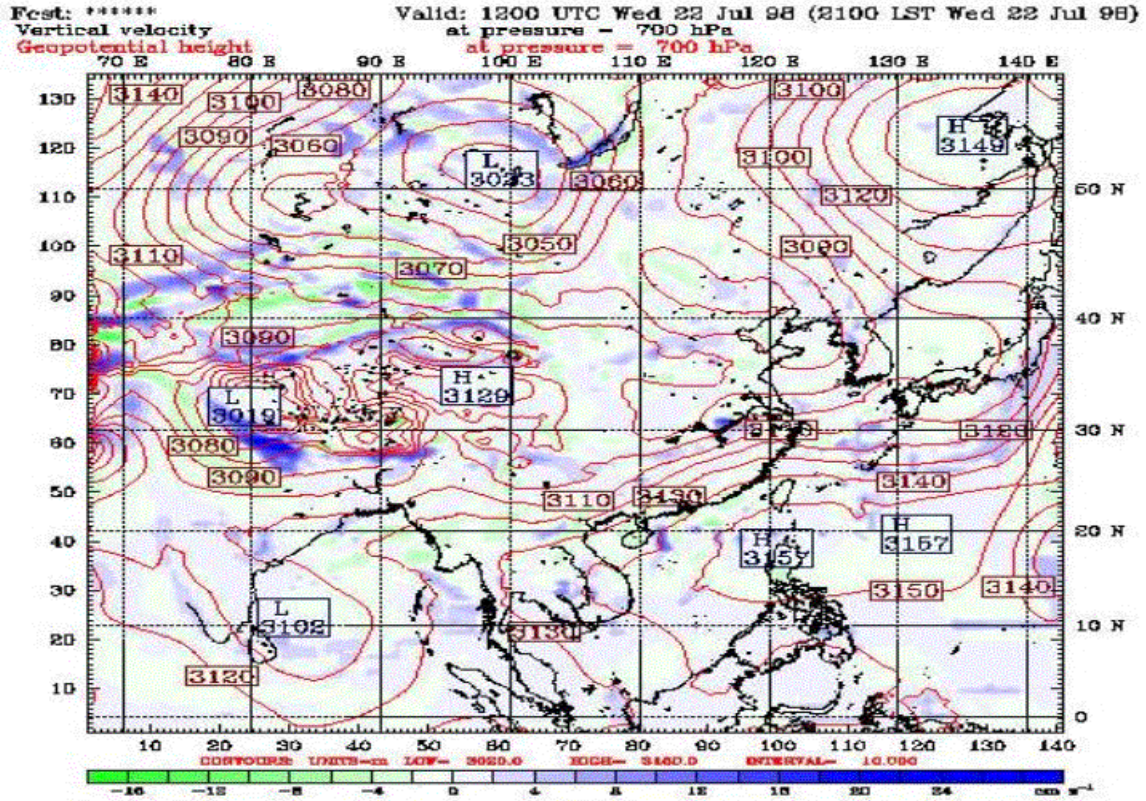


Fest: *****
 Vertical velocity
 Geopotential height
 Valid: 1200 UTC Tue 21 Jul 98 (2100 LST Tue 21 Jul 98)
 at pressure = 700 hPa
 at pressure = 700 hPa



Fest: *****
 Vertical velocity
 Geopotential height
 Valid: 0000 UTC Wed 22 Jul 98 (0900 LST Wed 22 Jul 98)
 at pressure = 700 hPa
 at pressure = 700 hPa

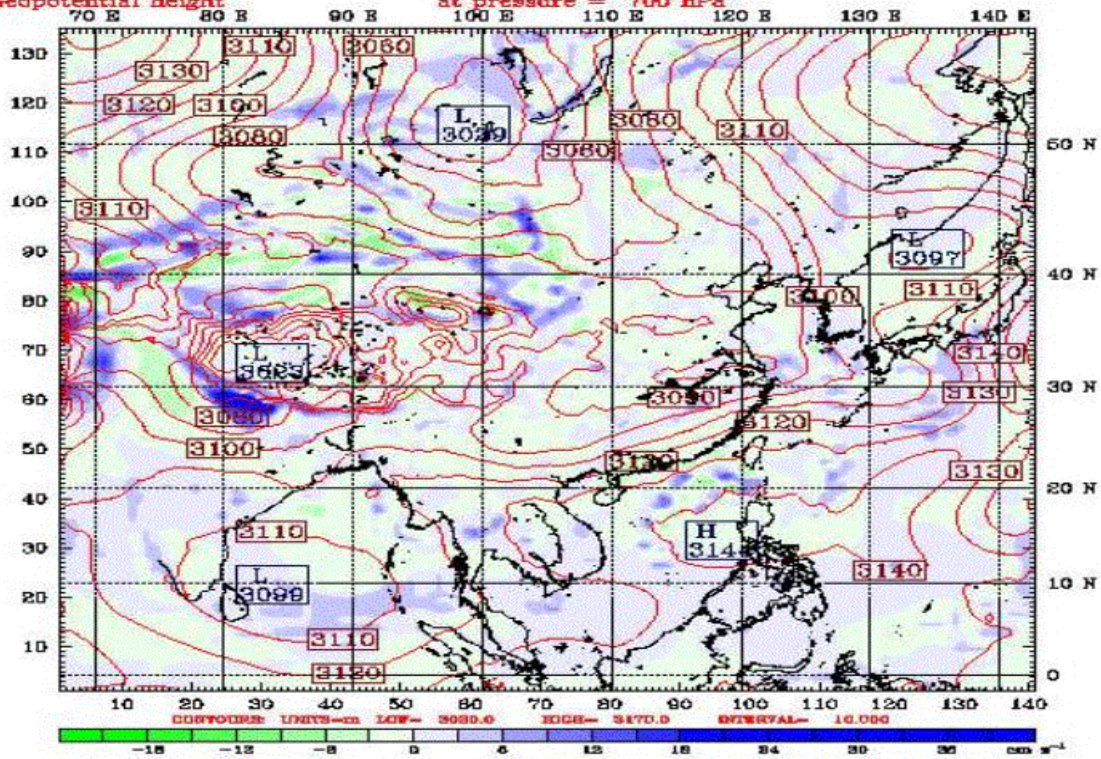




Fcst: *****

Vertical velocity
Geopotential height

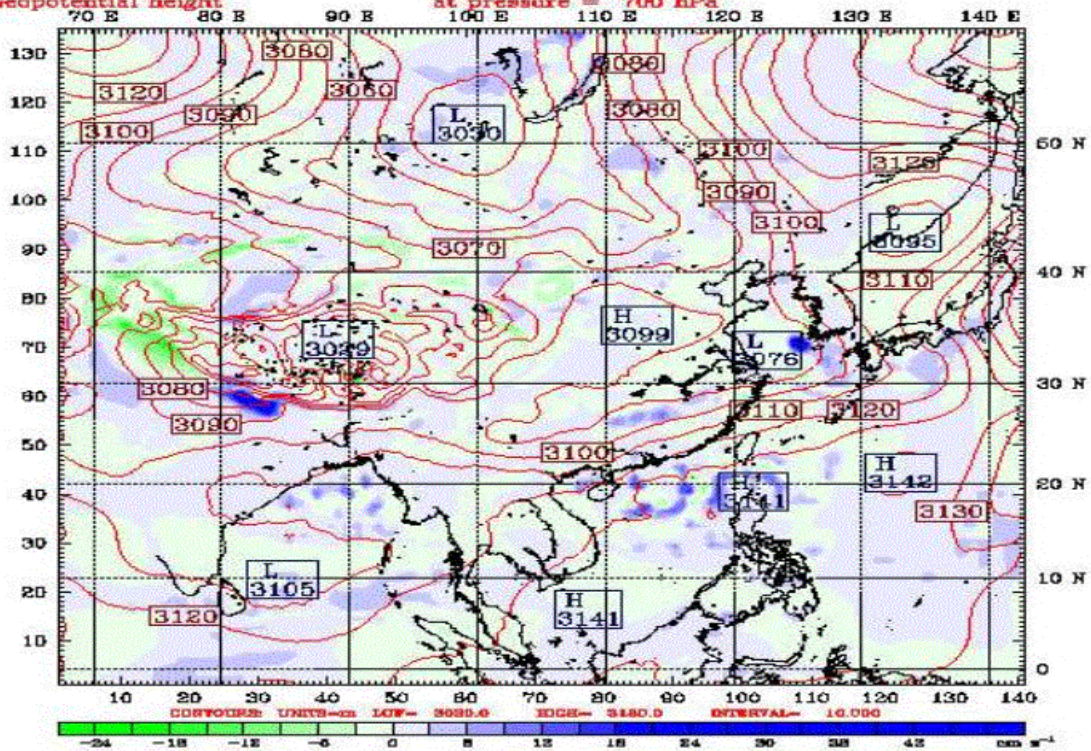
Valid: 1200 UTC Thu 23 Jul 98 (2100 LST Thu 23 Jul 98)
at pressure = 700 hPa
at pressure = 700 hPa

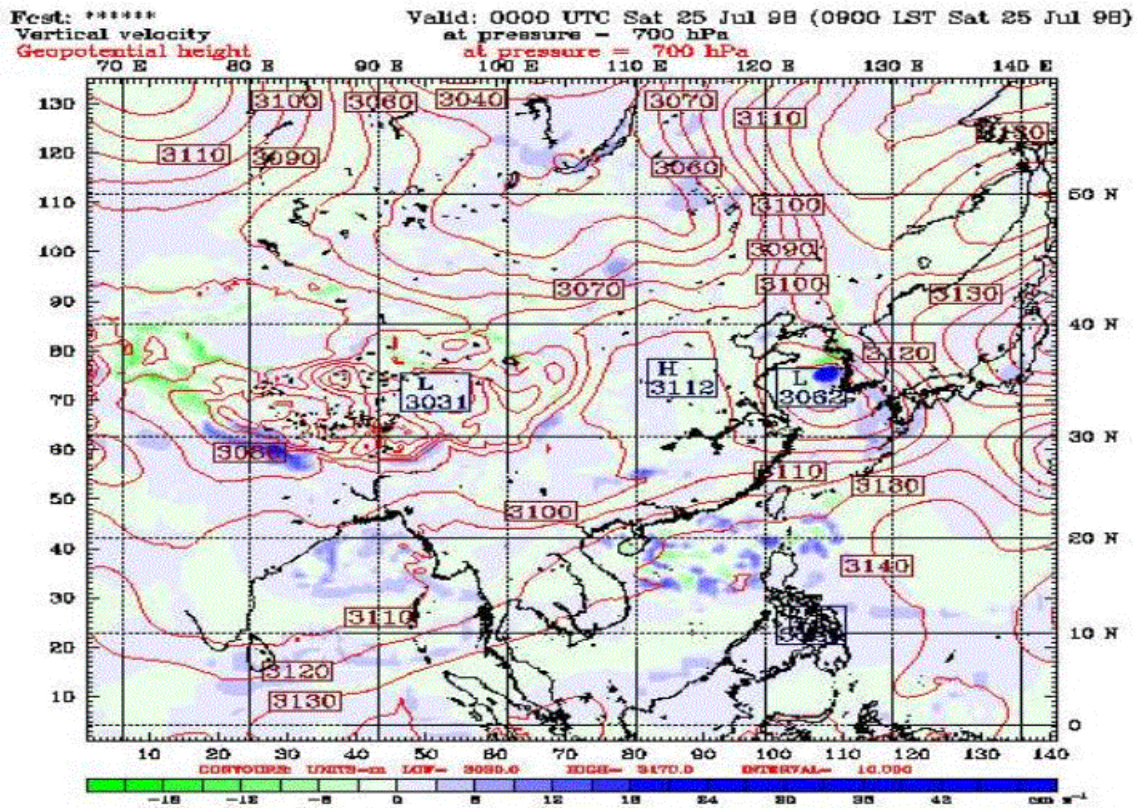
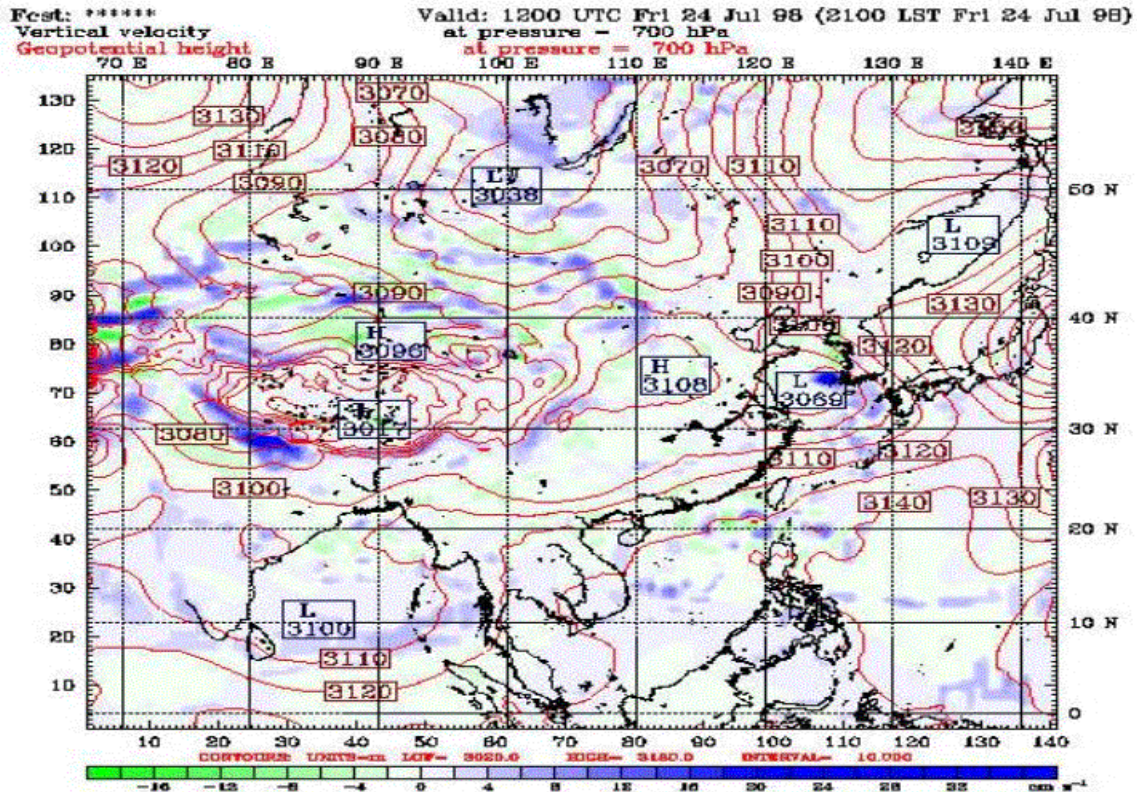


Fcst: *****

Vertical velocity
Geopotential height

Valid: 0000 UTC Fri 24 Jul 98 (0900 LST Fri 24 Jul 98)
at pressure = 700 hPa
at pressure = 700 hPa





Fest: *****

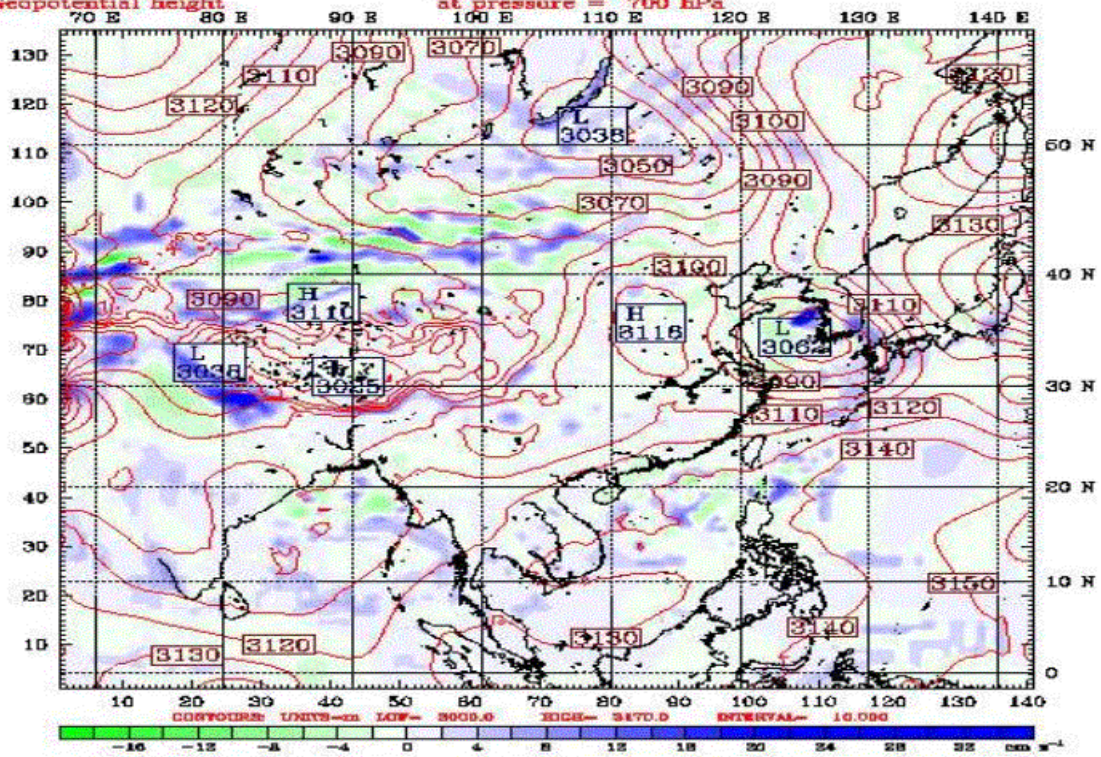
Vertical velocity

Geopotential height

Valid: 1200 UTC Sat 25 Jul 98 (2100 LST Sat 25 Jul 98)

at pressure = 700 hPa

at pressure = 700 hPa



Fest: *****

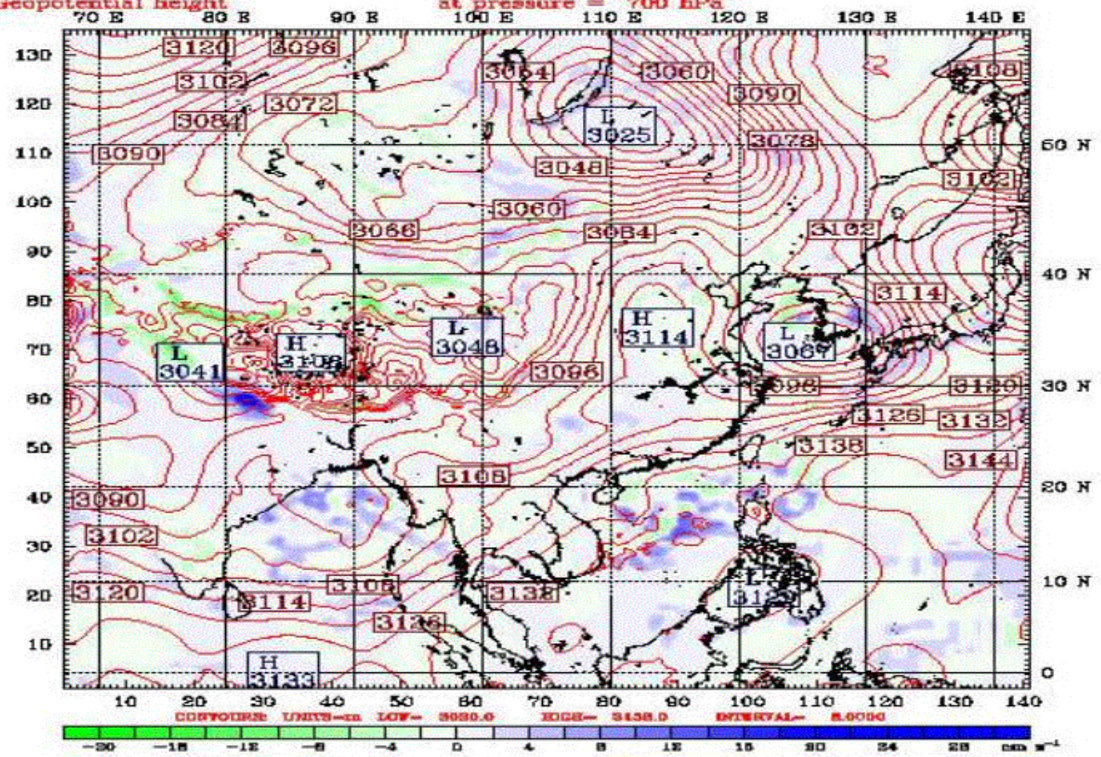
Vertical velocity

Geopotential height

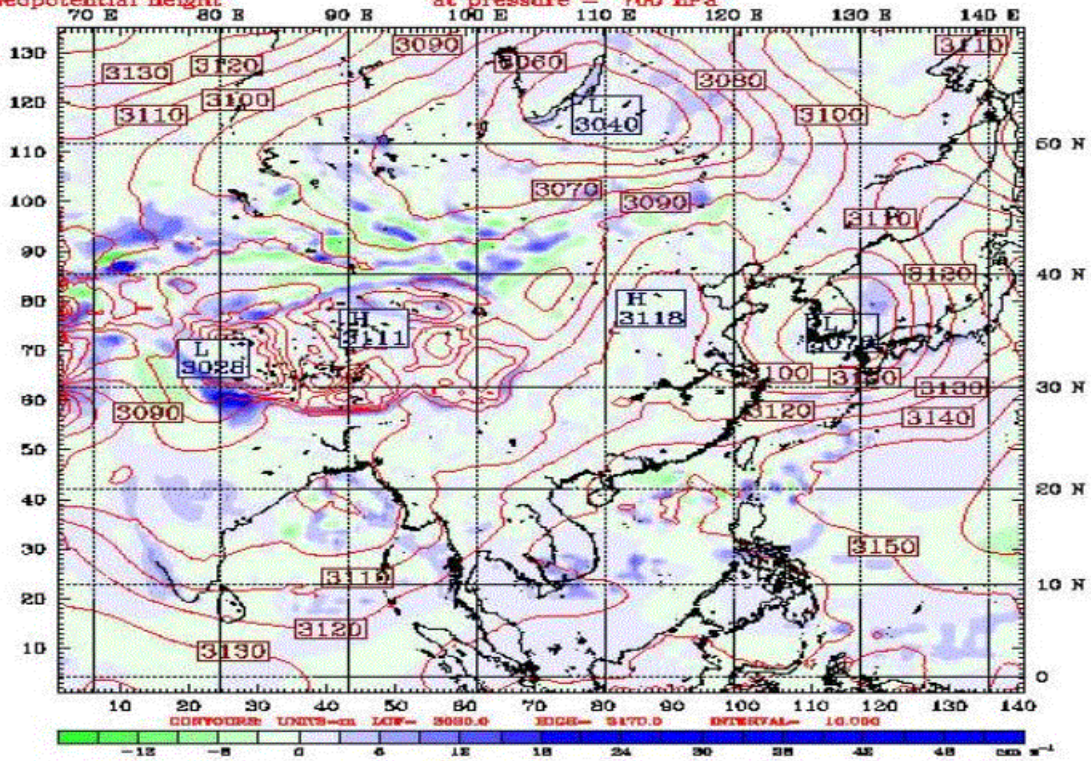
Valid: 0000 UTC Sun 26 Jul 98 (0900 LST Sun 26 Jul 98)

at pressure = 700 hPa

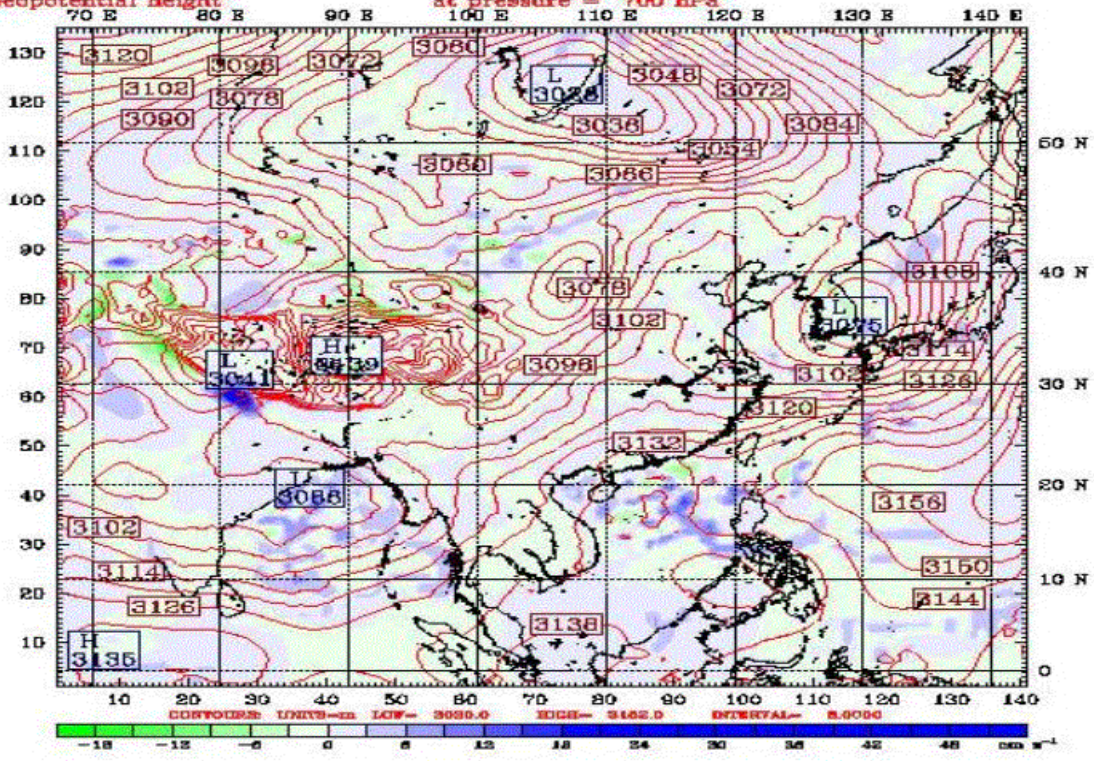
at pressure = 700 hPa

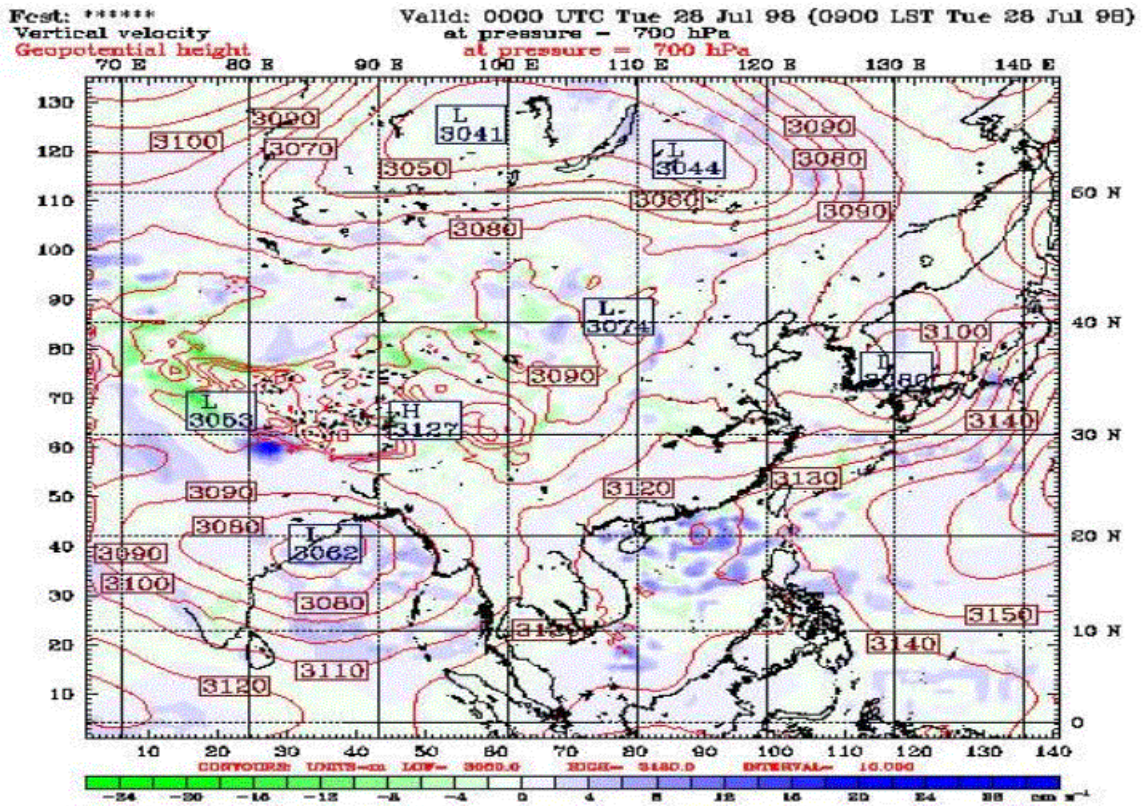
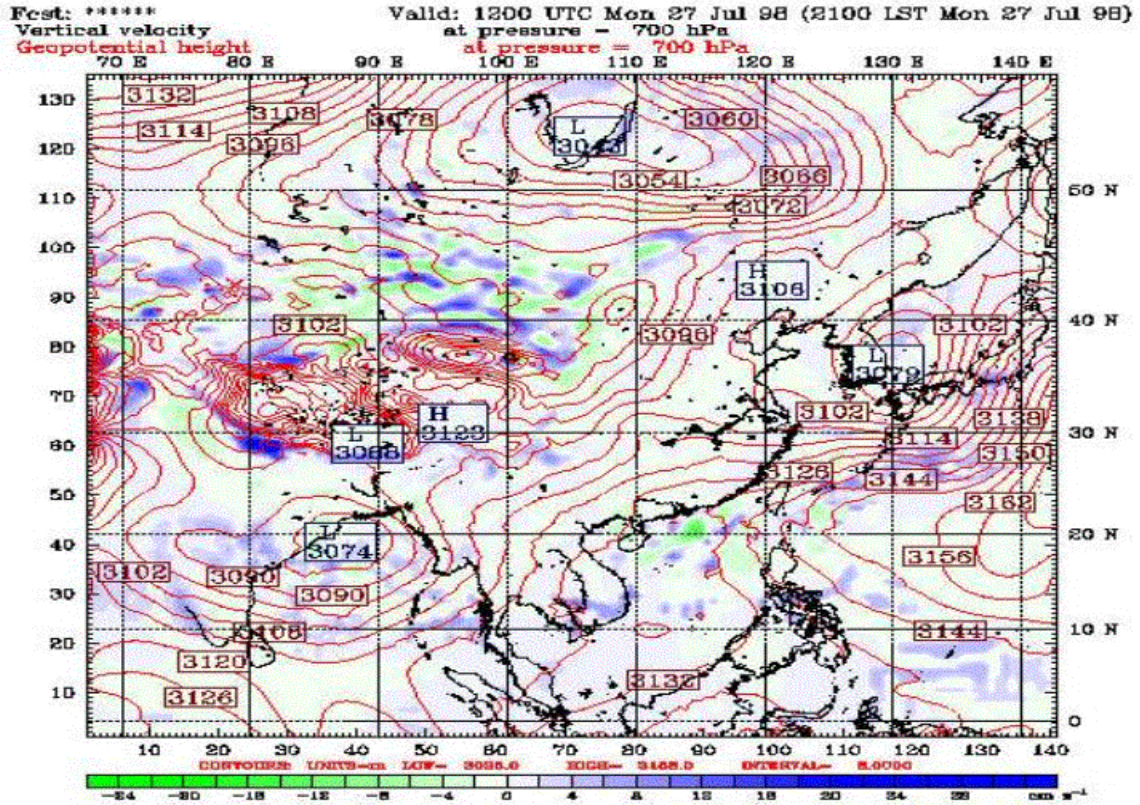


Fcst: *****
 Valid: 1200 UTC Sun 26 Jul 98 (2100 LST Sun 26 Jul 98)
 Vertical velocity
 at pressure = 700 hPa
 Geopotential height
 at pressure = 700 hPa



Fcst: *****
 Valid: 0000 UTC Mon 27 Jul 98 (0900 LST Mon 27 Jul 98)
 Vertical velocity
 at pressure = 700 hPa
 Geopotential height
 at pressure = 700 hPa





Fcst: *****

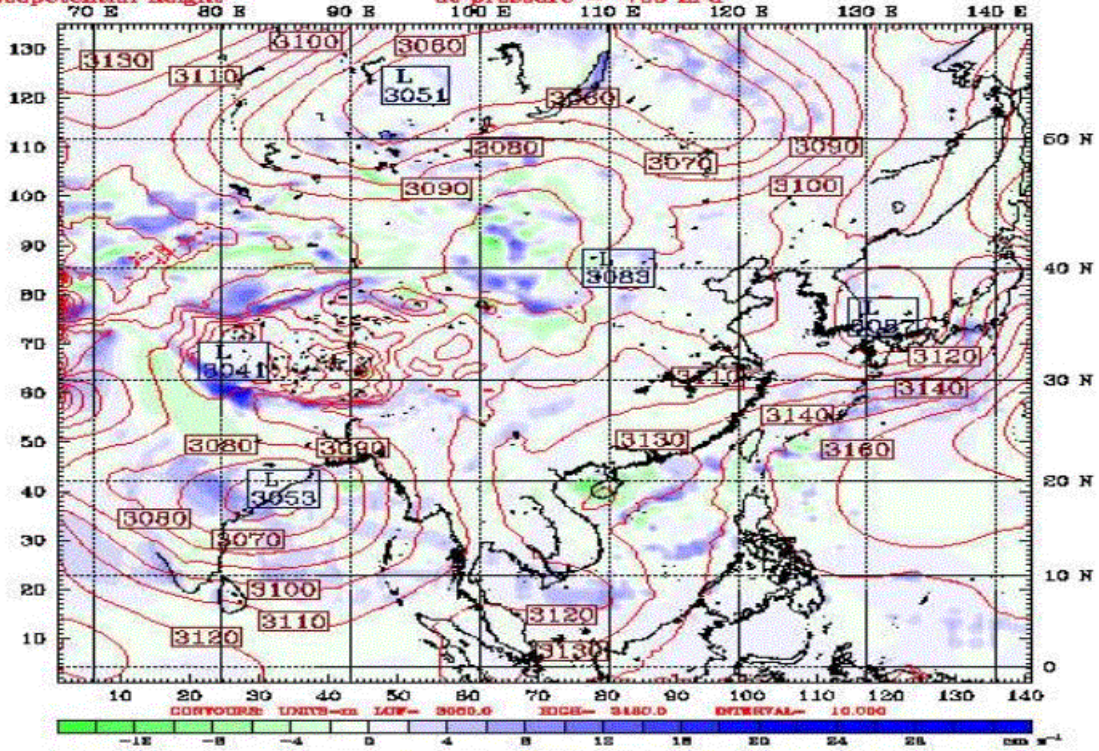
Valid: 1200 UTC Tue 28 Jul 98 (2100 LST Tue 28 Jul 98)

Vertical velocity

at pressure = 700 hPa

Geopotential height

at pressure = 700 hPa



Fcst: *****

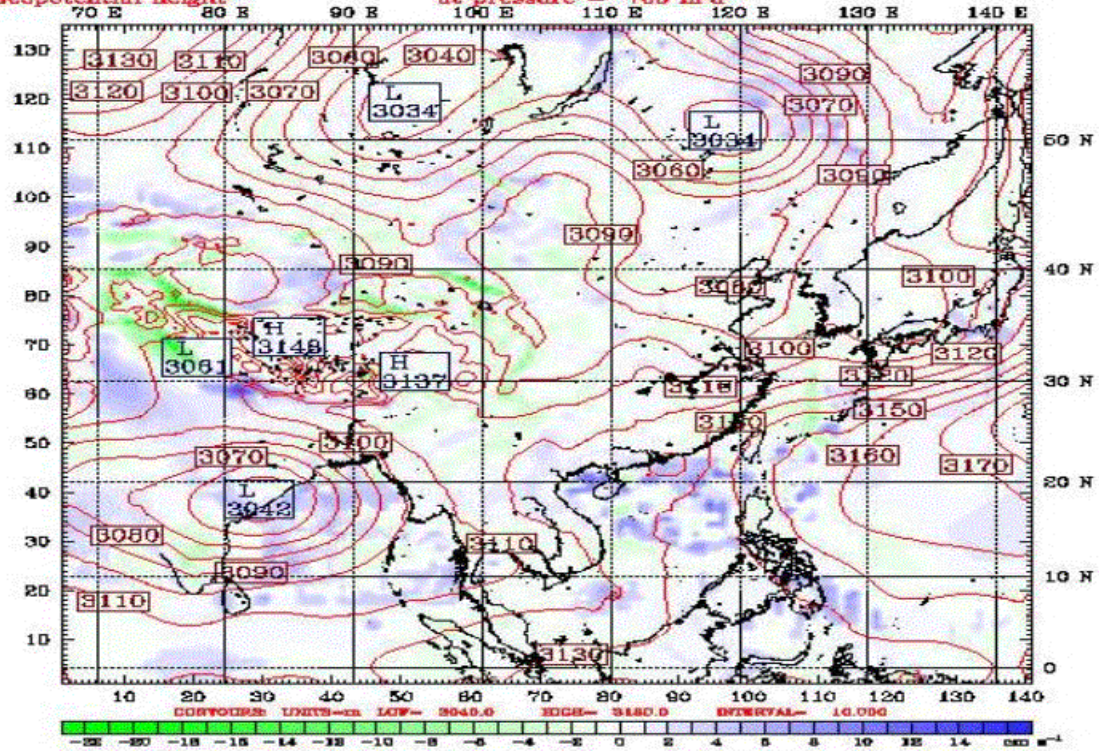
Valid: 0000 UTC Wed 29 Jul 98 (0900 LST Wed 29 Jul 98)

Vertical velocity

at pressure = 700 hPa

Geopotential height

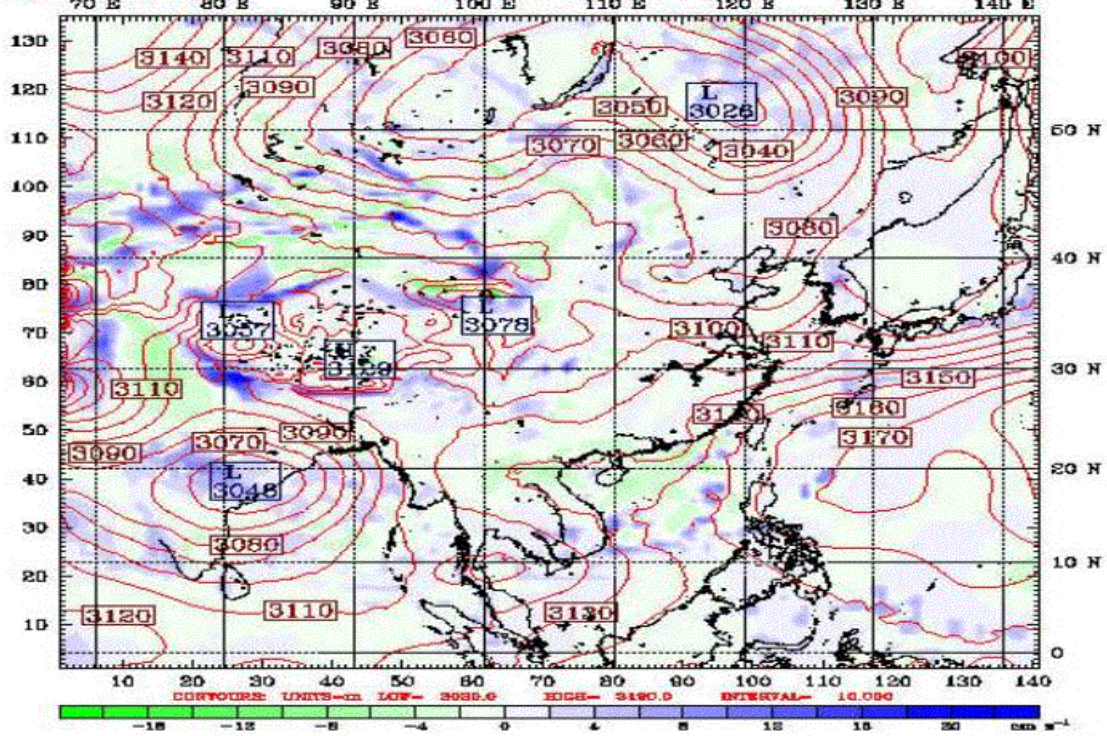
at pressure = 700 hPa



Fcst: *****

Vertical velocity
Geopotential height

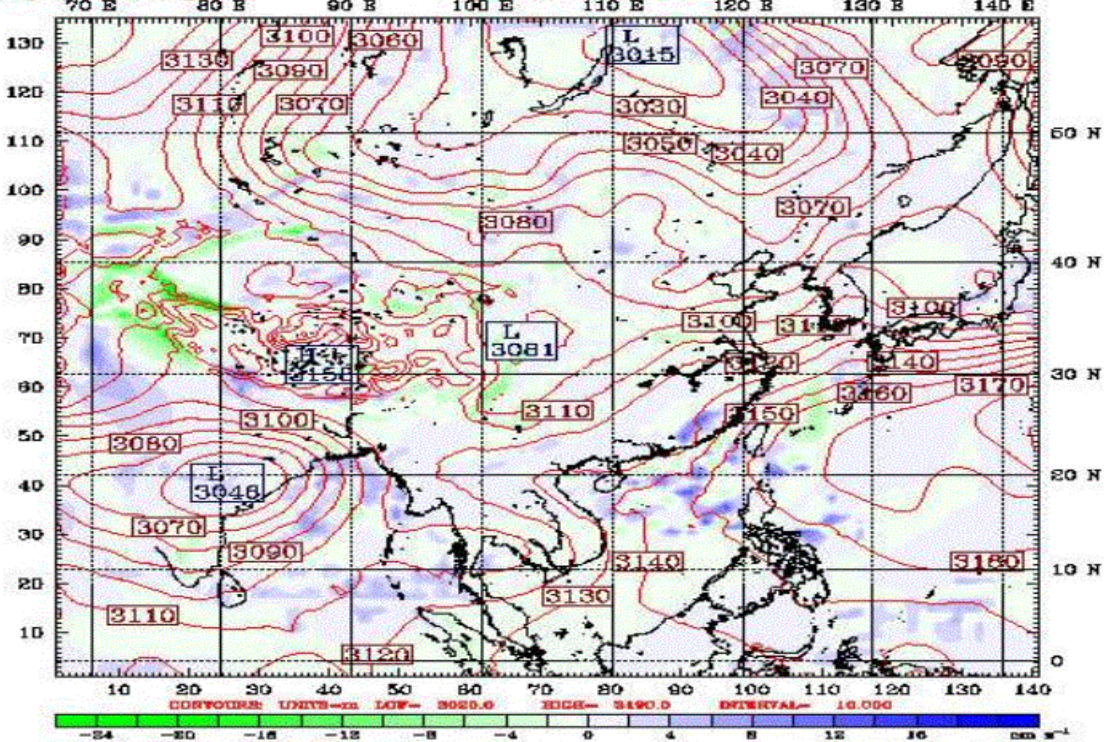
Valid: 1200 UTC Wed 29 Jul 98 (2100 LST Wed 29 Jul 98)
at pressure = 700 hPa
at pressure = 700 hPa

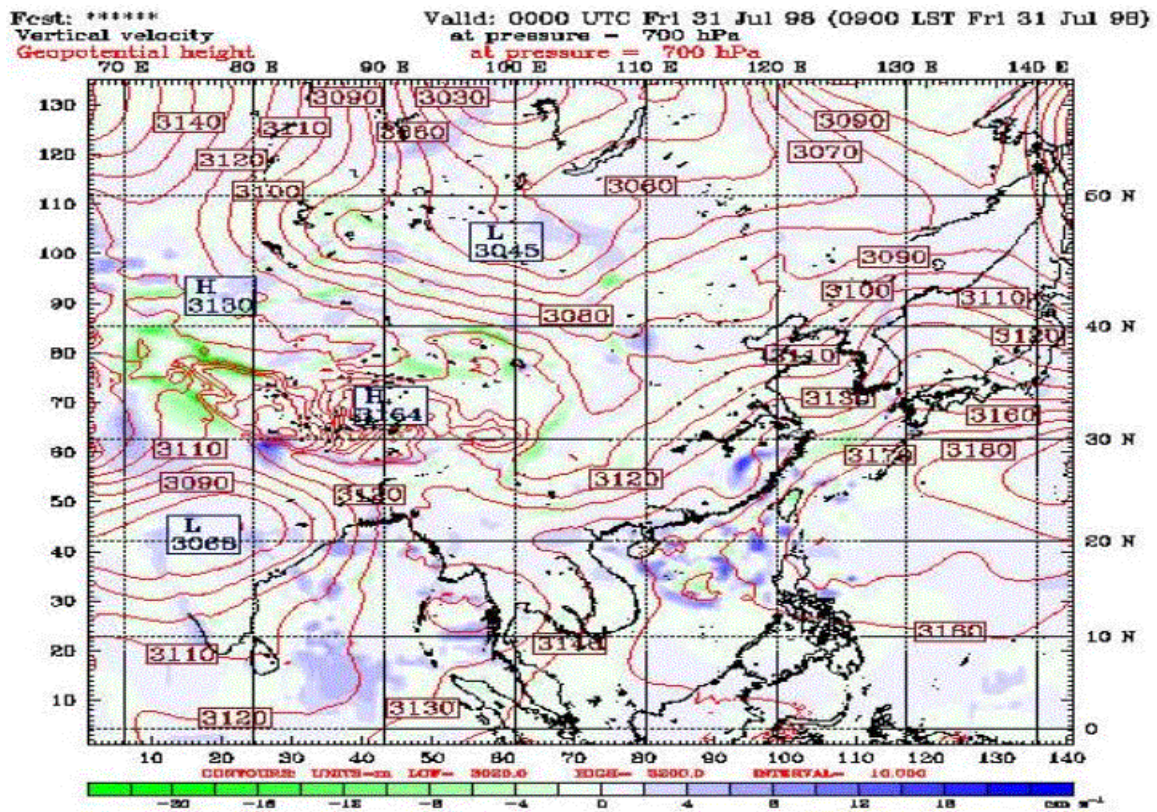
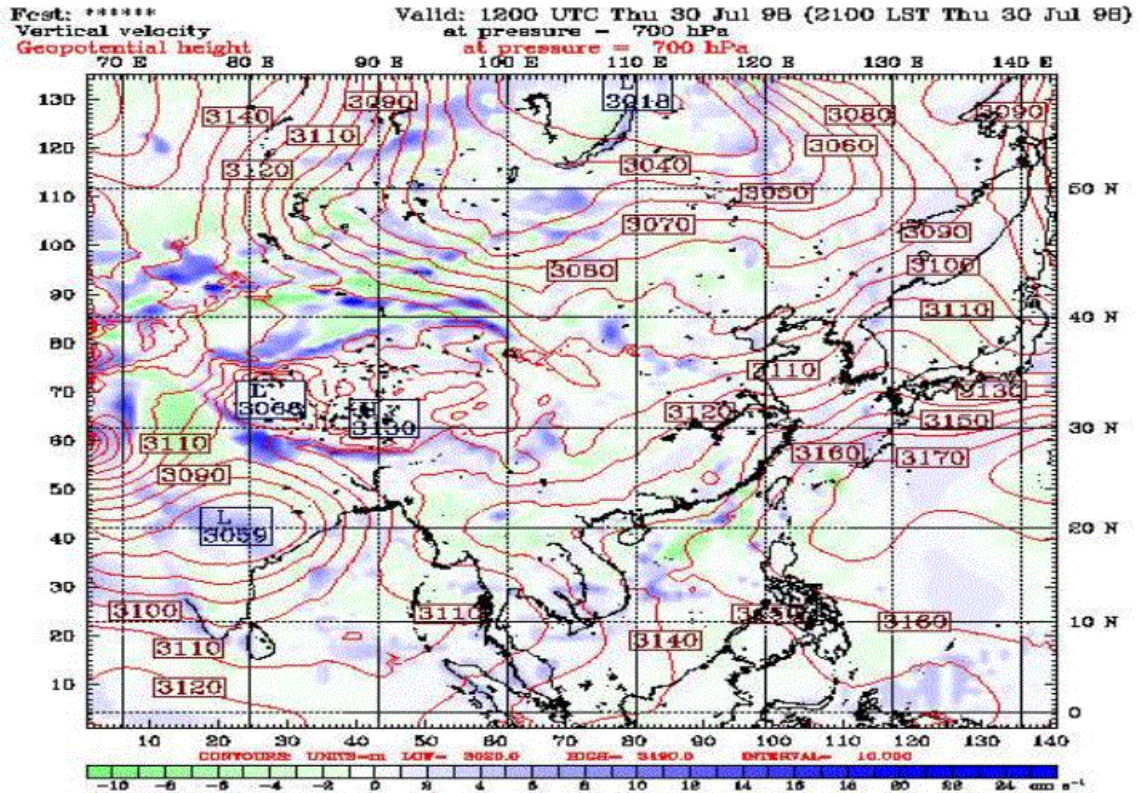


Fcst: *****

Vertical velocity
Geopotential height

Valid: 0000 UTC Thu 30 Jul 98 (0900 LST Thu 30 Jul 98)
at pressure = 700 hPa
at pressure = 700 hPa





Fest: *****

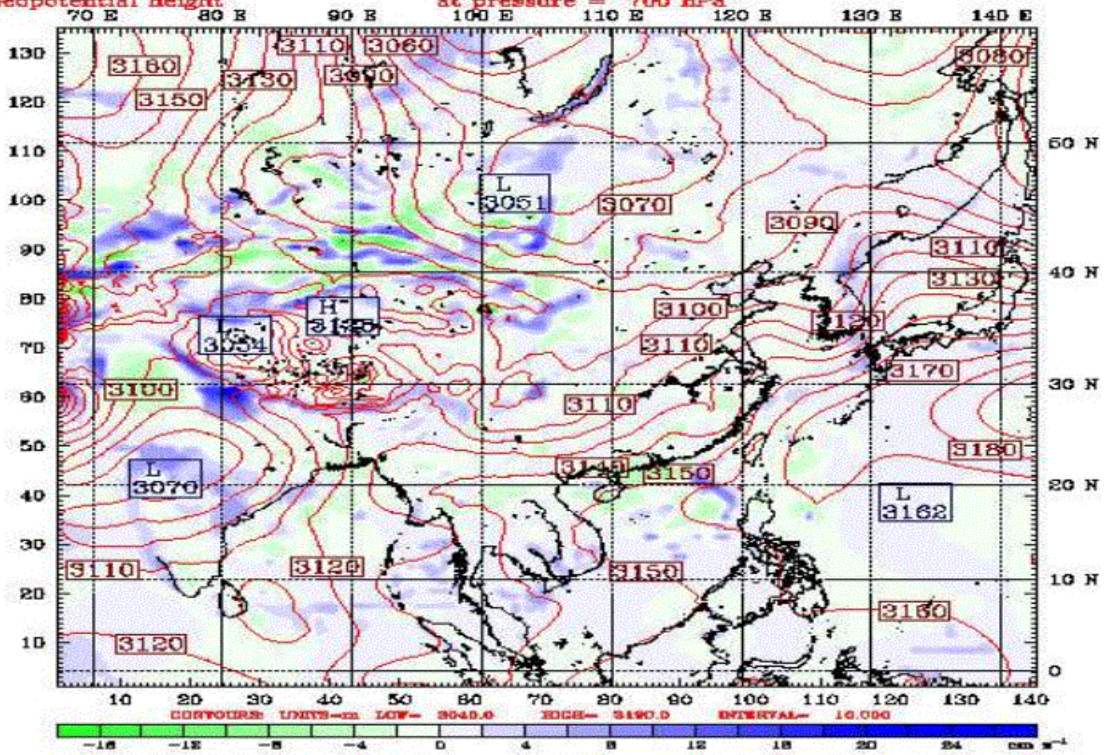
Valid: 1200 UTC Fri 31 Jul 98 (2100 LST Fri 31 Jul 98)

Vertical velocity

at pressure = 700 hPa

Geopotential height

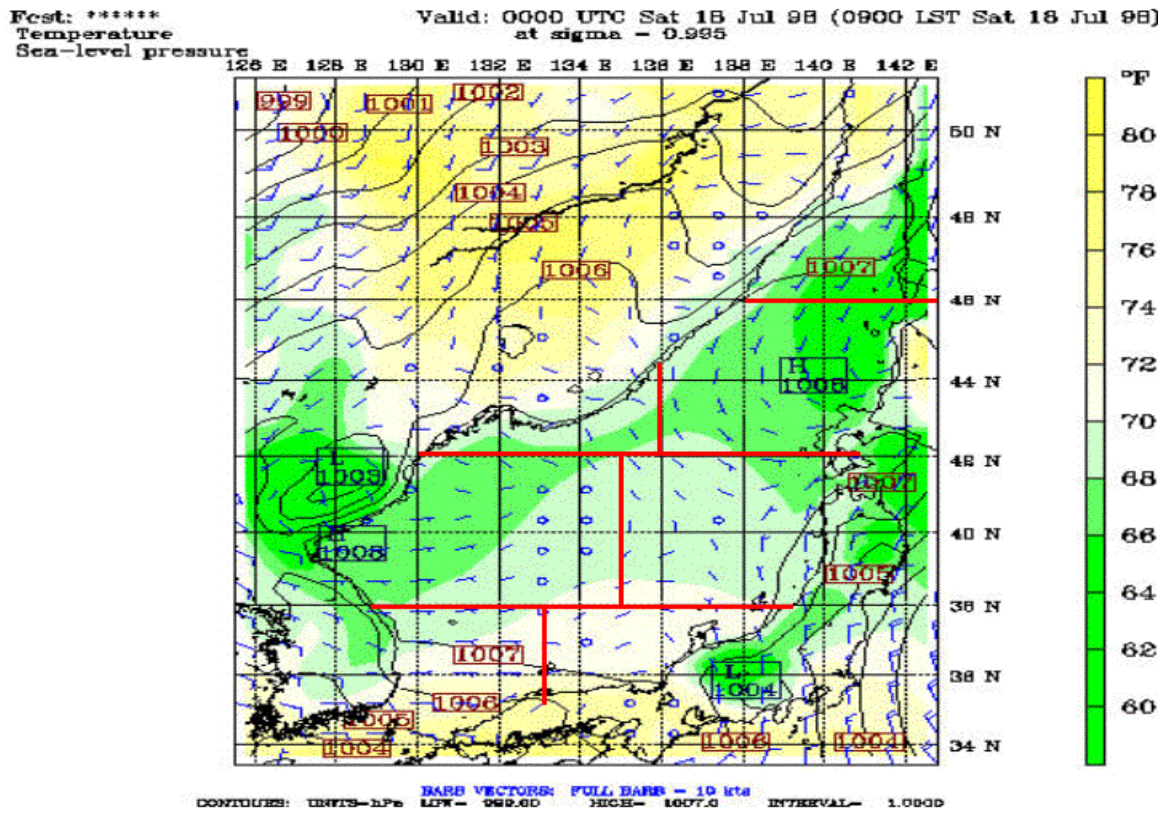
at pressure = 700 hPa



THIS PAGE INTENTIONALLY LEFT BLANK

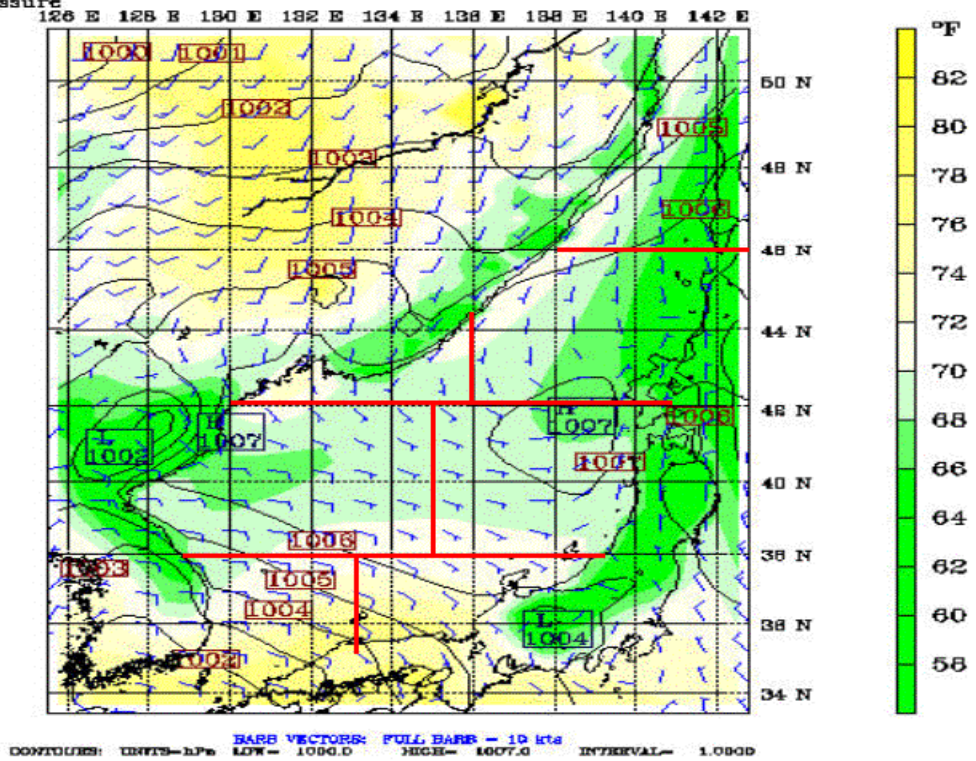
APPENDIX X. SEA LEVEL PRESSURE/SAT/SURFACE WIND PLOTS FOR THE JES FOR THE JULY TIME PERIOD

Appendix X consists of 28 figures that show sea level pressure, SAT, and surface winds for the July time period over the JES. The figures are in time sequential order from July 18 through July 31.



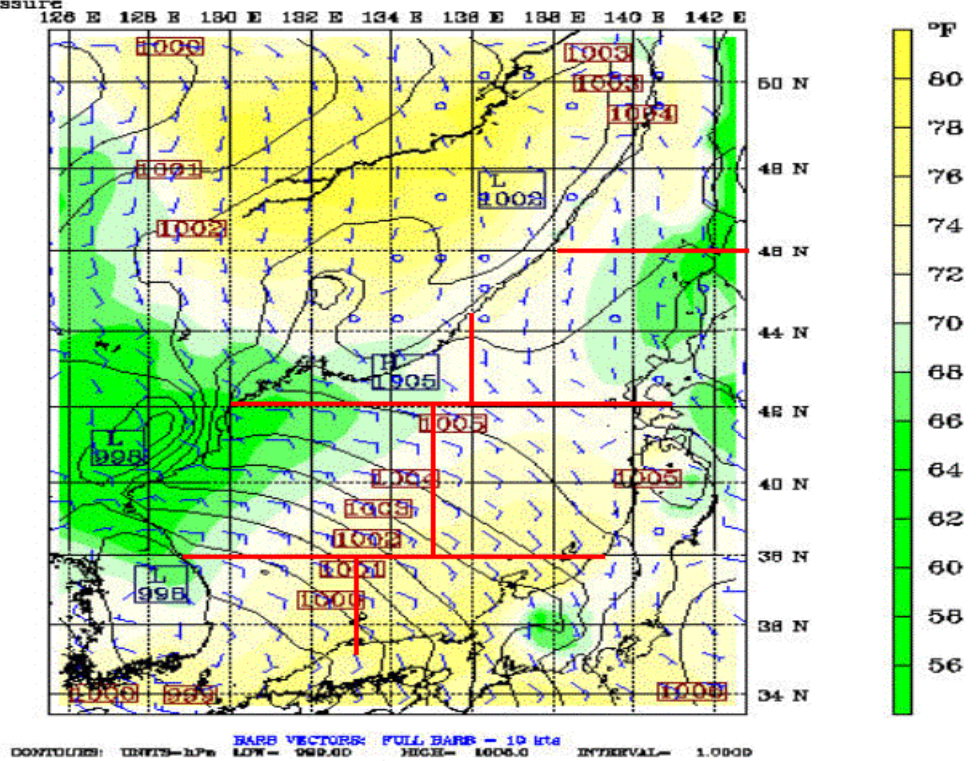
Fcst: *****
Temperature
Sea-level pressure

Valid: 1200 UTC Sat 18 Jul 98 (2100 LST Sat 18 Jul 98)
at sigma - 0.995



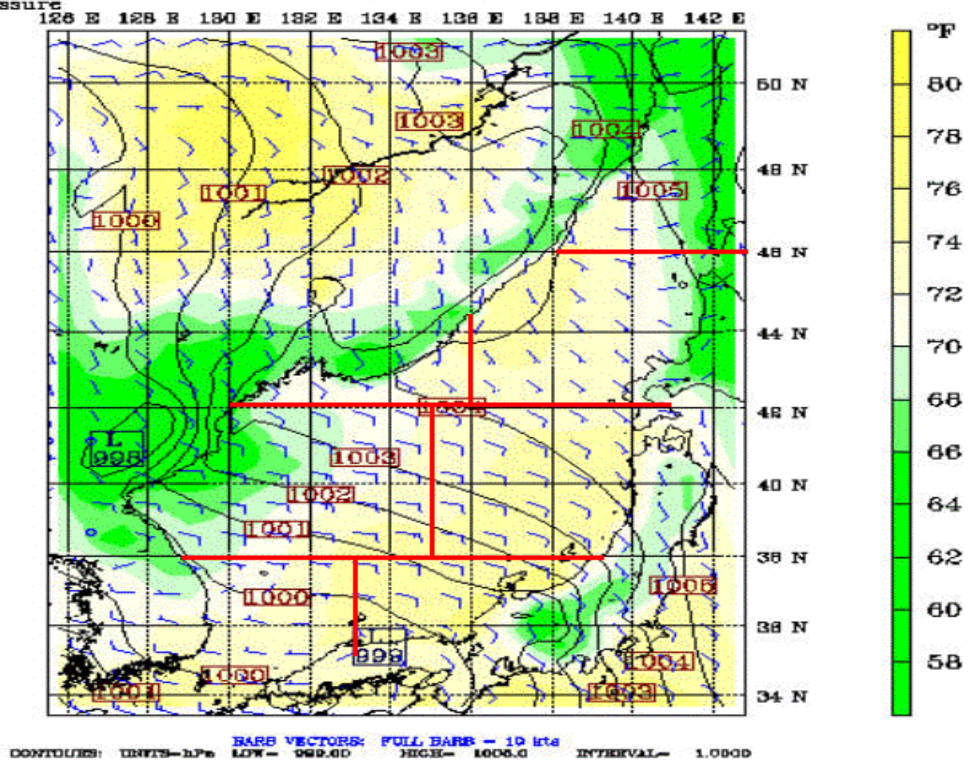
Fcst: *****
Temperature
Sea-level pressure

Valid: 0000 UTC Sun 19 Jul 98 (0900 LST Sun 19 Jul 98)
at sigma - 0.995



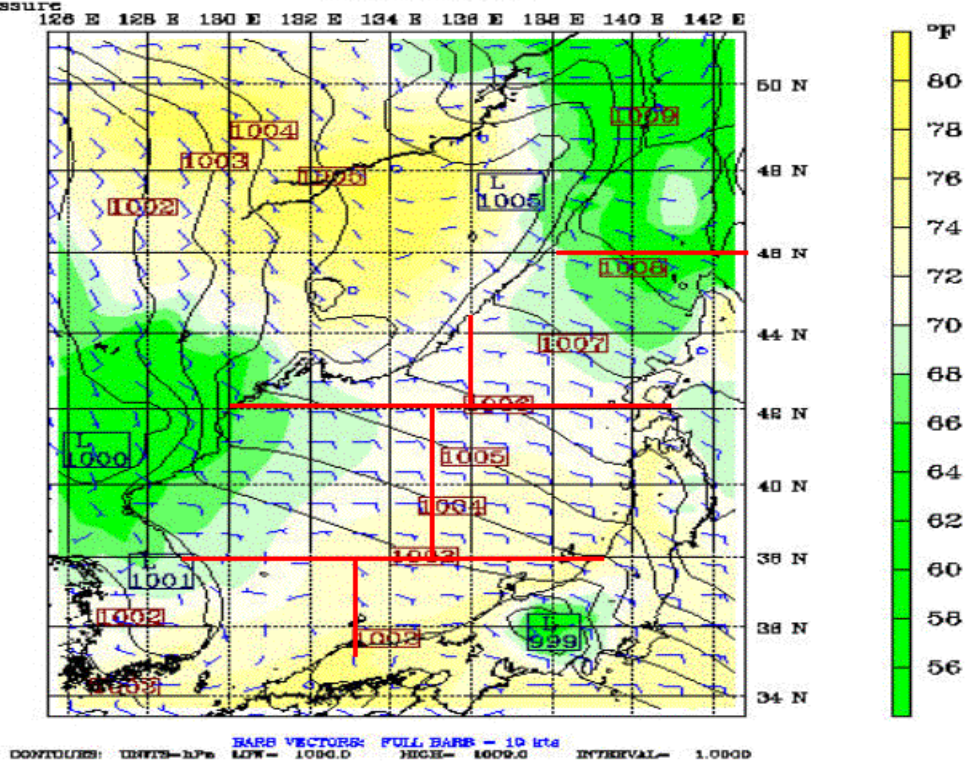
Fcst: *****
 Temperature
 Sea-level pressure

Valid: 1200 UTC Sun 19 Jul 98 (2100 LST Sun 19 Jul 98)
 at sigma - 0.995



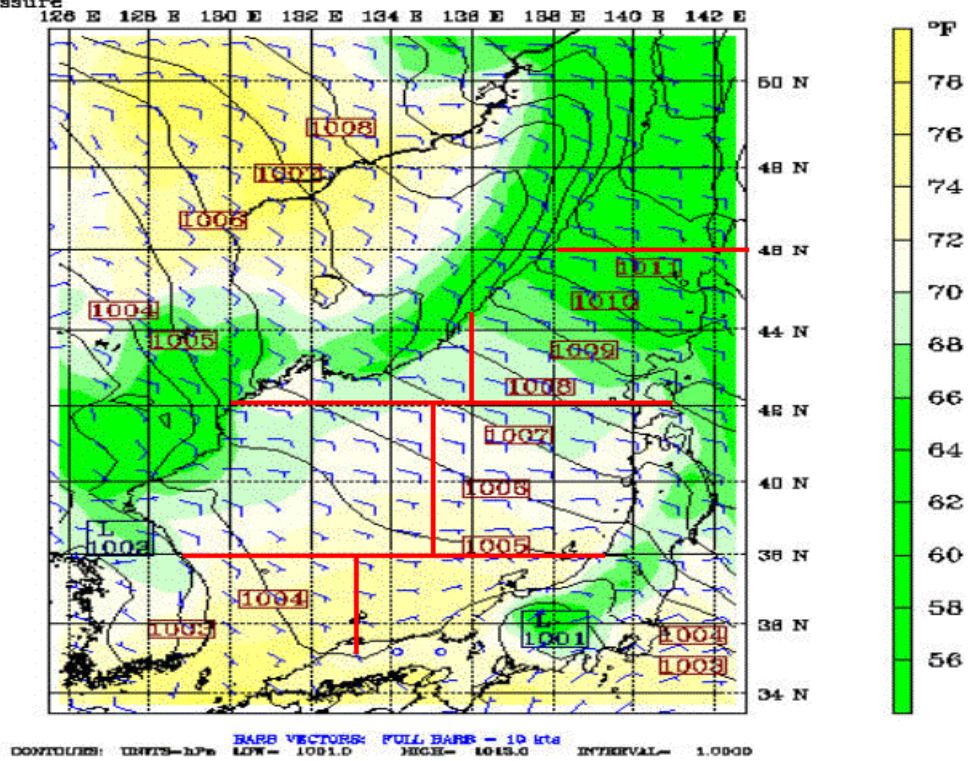
Fcst: *****
 Temperature
 Sea-level pressure

Valid: 0000 UTC Mon 20 Jul 98 (0900 LST Mon 20 Jul 98)



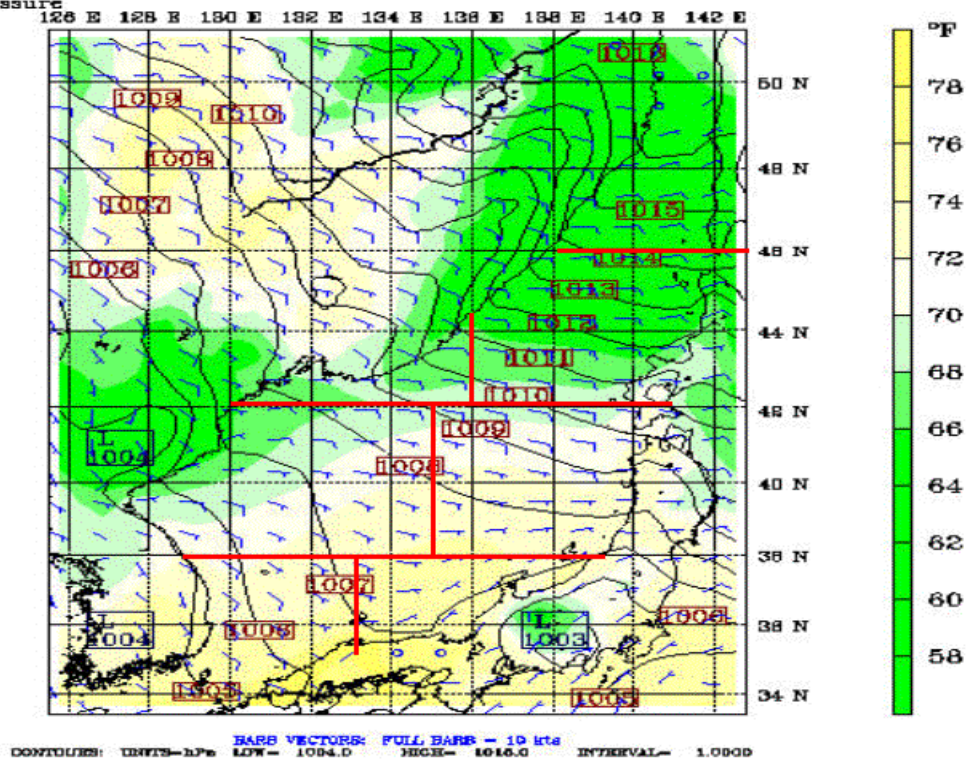
Fcst: *****
 Temperature
 Sea-level pressure

Valid: 1200 UTC Mon 20 Jul 98 (2100 LST Mon 20 Jul 98)
 at sigma - 0.995



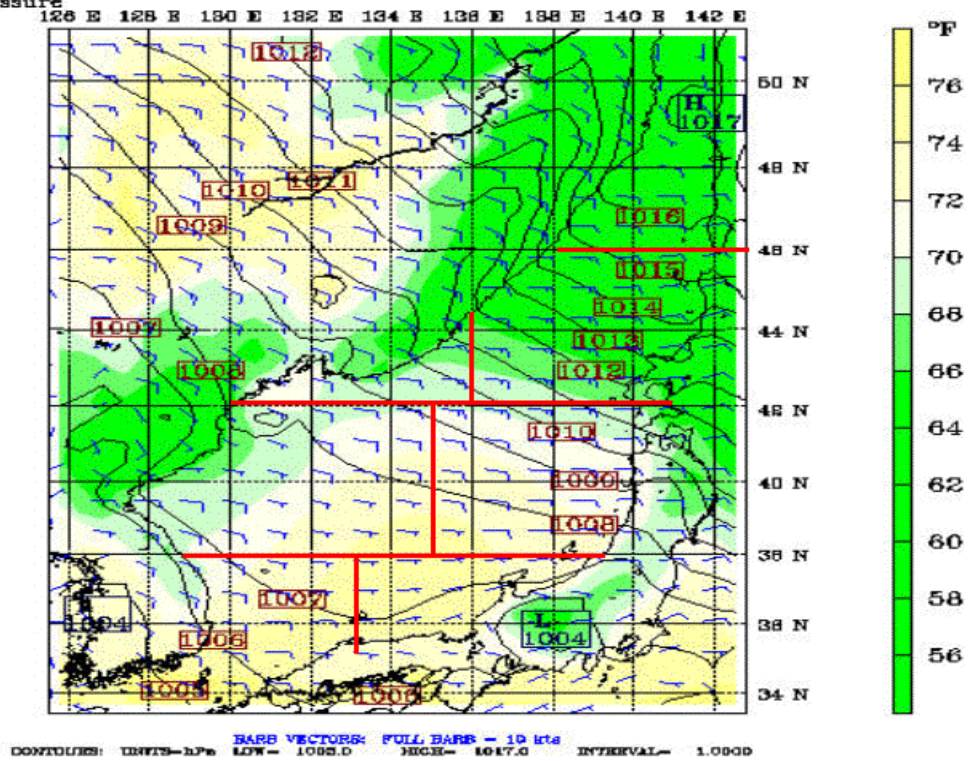
Fcst: *****
 Temperature
 Sea-level pressure

Valid: 0000 UTC Tue 21 Jul 98 (0900 LST Tue 21 Jul 98)



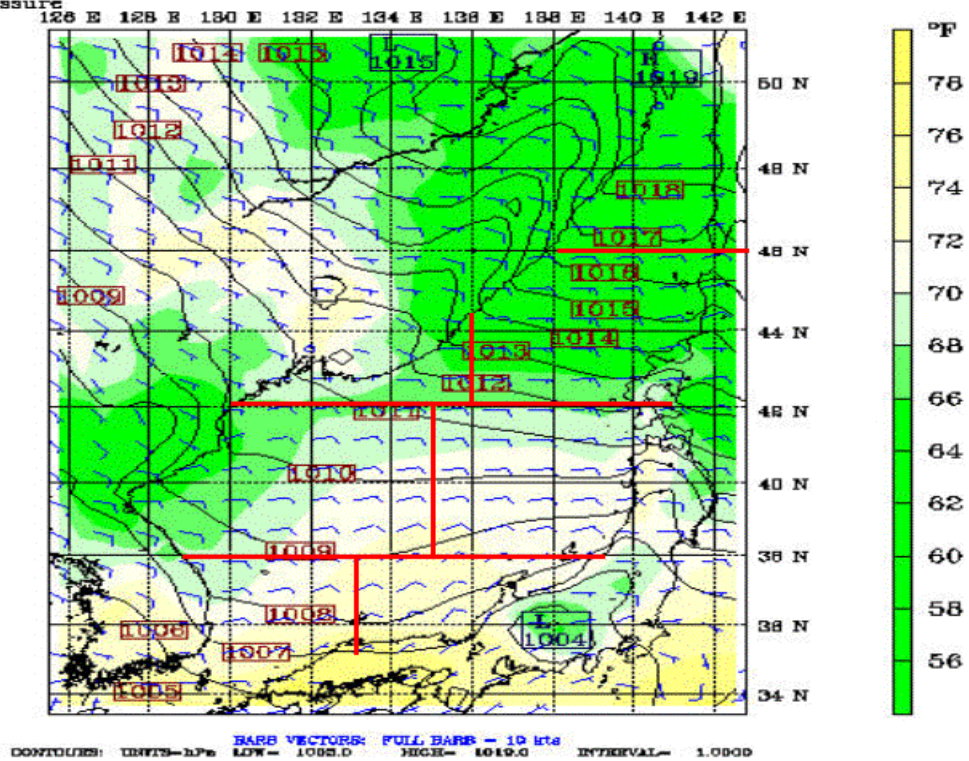
Fcst: *****
Temperature
Sea-level pressure

Valid: 1200 UTC Tue 21 Jul 98 (2100 LST Tue 21 Jul 98)
at sigma - 0.995



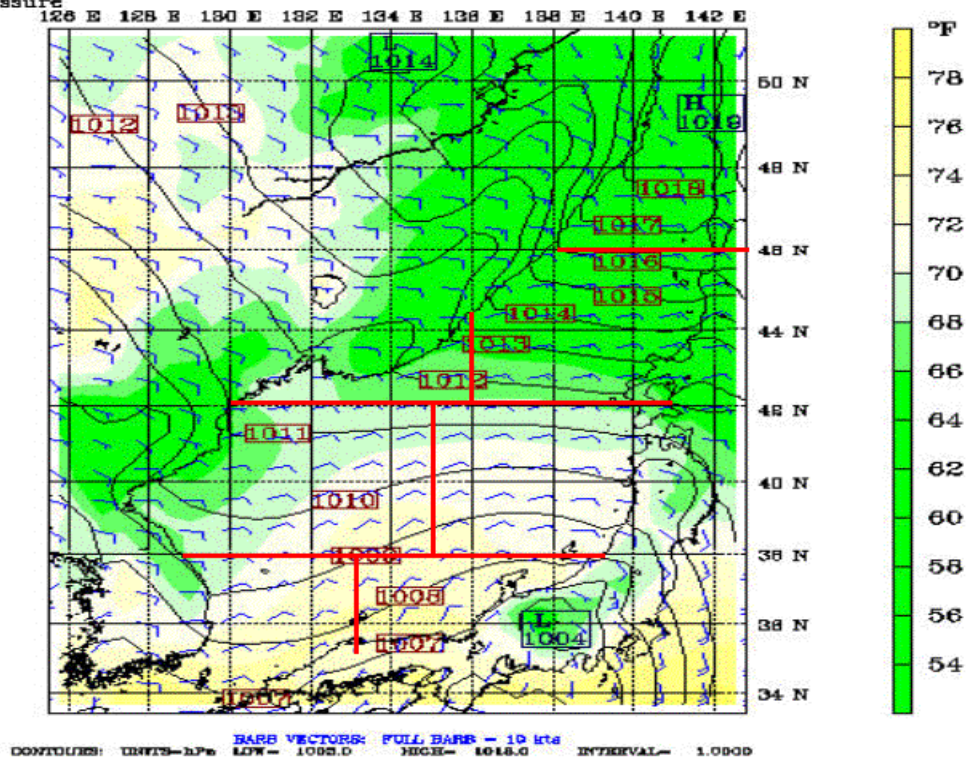
Fcst: *****
Temperature
Sea-level pressure

Valid: 0000 UTC Wed 22 Jul 98 (0900 LST Wed 22 Jul 98)
at sigma - 0.995



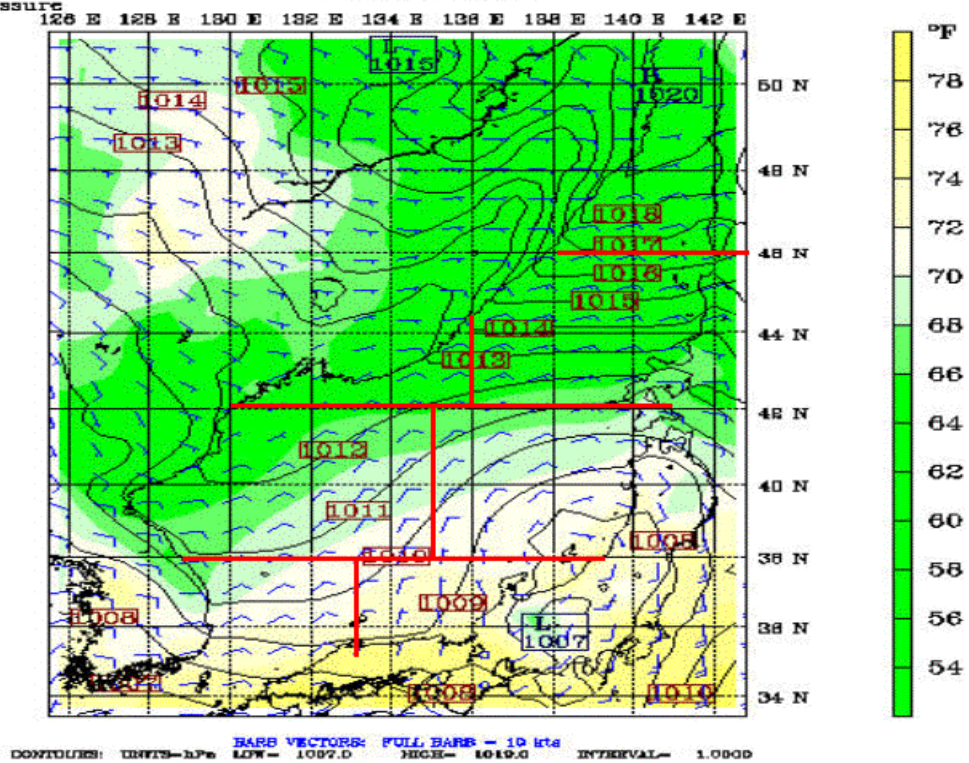
Feet: *****
Temperature
Sea-level pressure

Valid: 1200 UTC Wed 22 Jul 98 (2100 LST Wed 22 Jul 98)
at sigma - 0.995



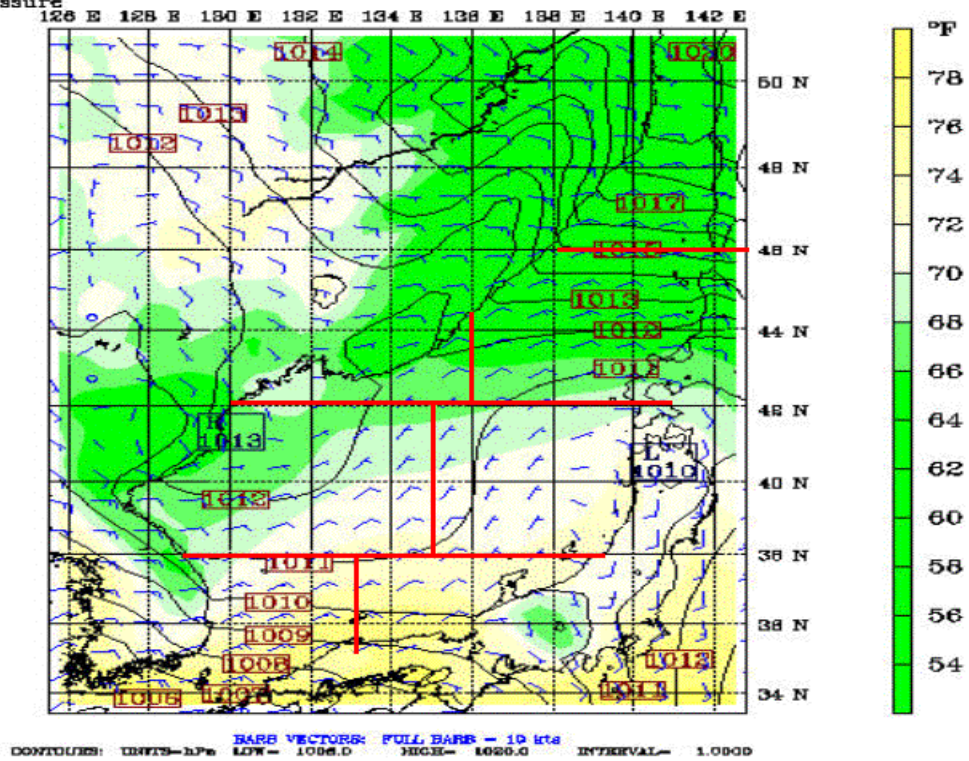
Feet: *****
Temperature
Sea-level pressure

Valid: 0000 UTC Thu 23 Jul 98 (0900 LST Thu 23 Jul 98)
at sigma - 0.995



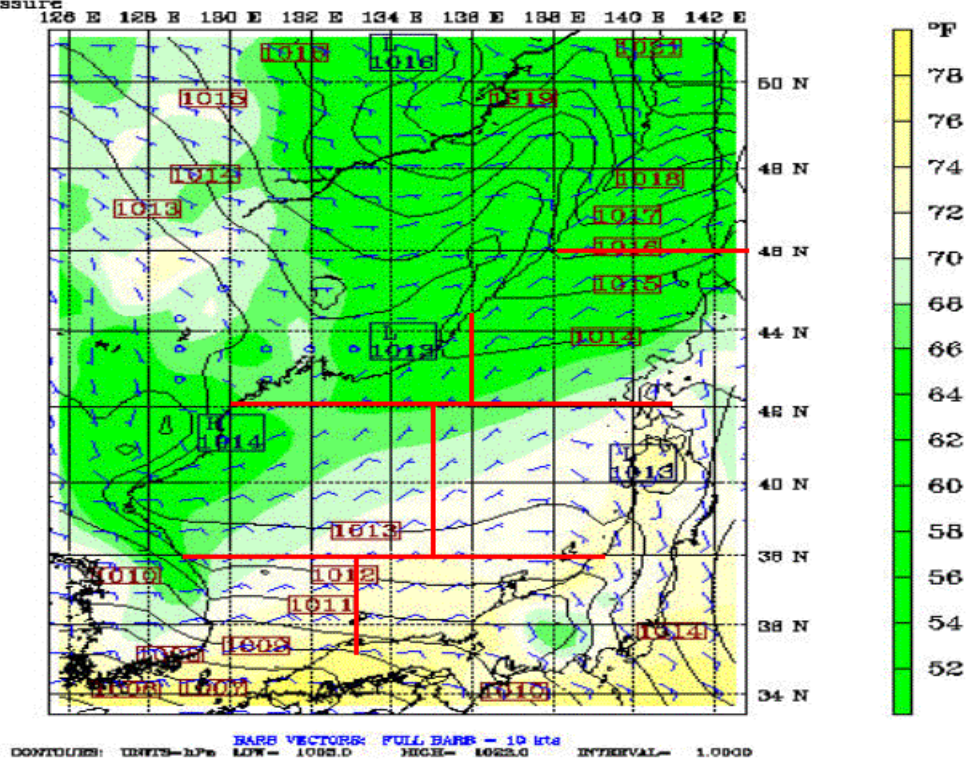
Fcst: *****
Temperature
Sea-level pressure

Valid: 1200 UTC Thu 23 Jul 98 (2100 LST Thu 23 Jul 98)
at sigma - 0.995



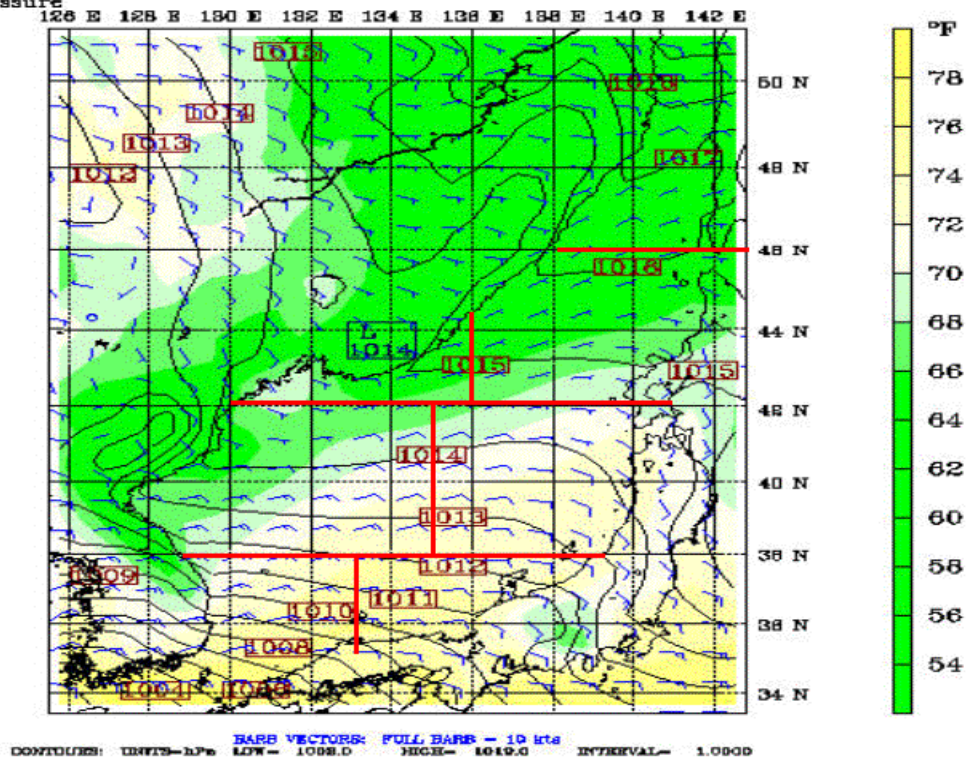
Fcst: *****
Temperature
Sea-level pressure

Valid: 0000 UTC Fri 24 Jul 98 (0900 LST Fri 24 Jul 98)
at sigma - 0.995



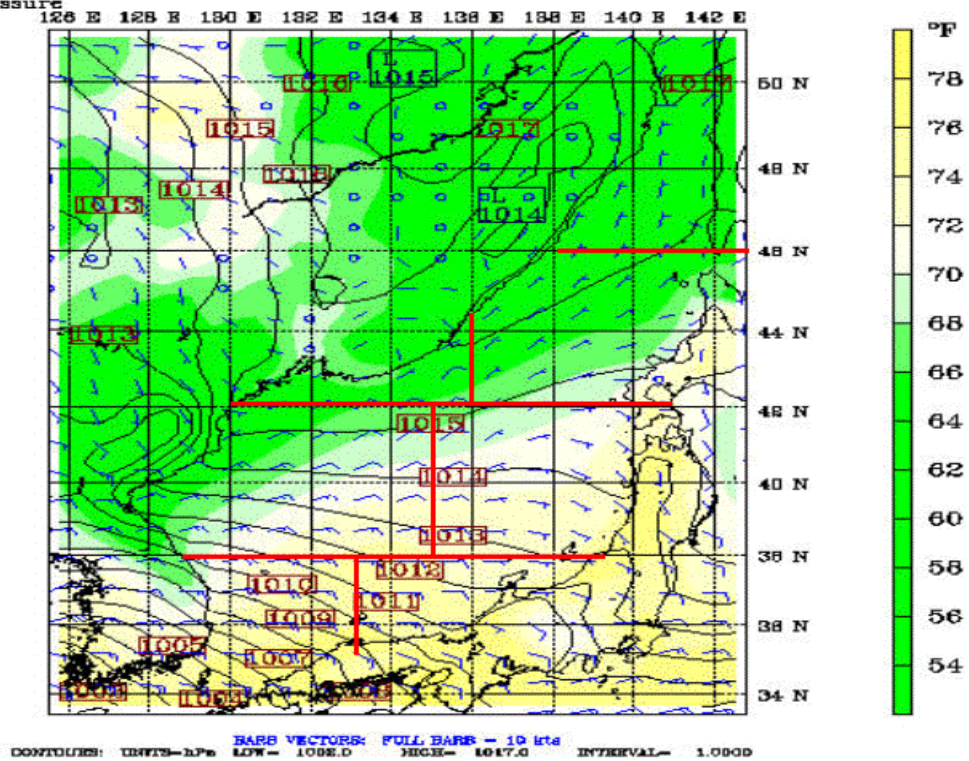
Fcst: *****
Temperature
Sea-level pressure

Valid: 1200 UTC Fri 24 Jul 98 (2100 LST Fri 24 Jul 98)
at sigma - 0.995



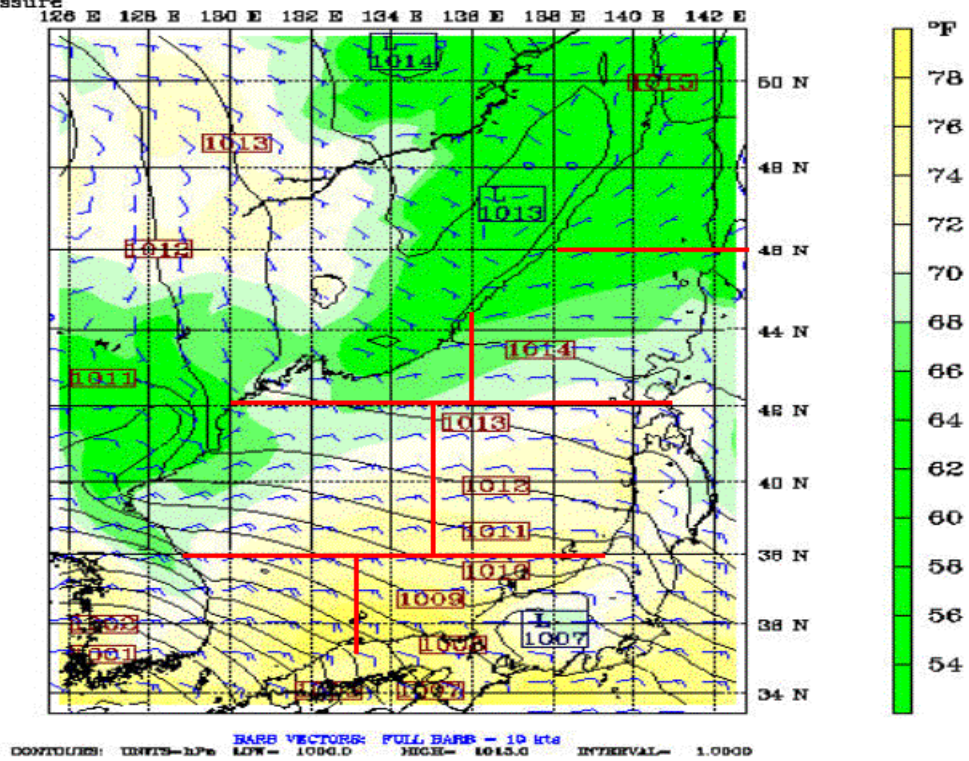
Fcst: *****
Temperature
Sea-level pressure

Valid: 0000 UTC Sat 25 Jul 98 (0900 LST Sat 25 Jul 98)
at sigma - 0.995



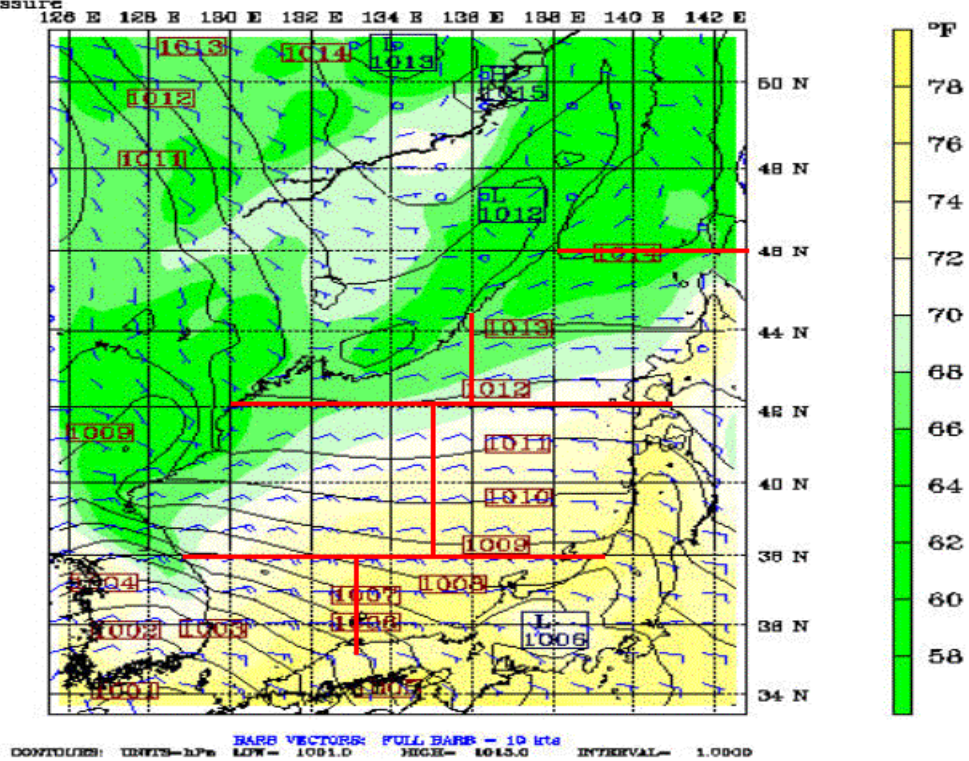
Fcst: *****
 Temperature
 Sea-level pressure

Valid: 1200 UTC Sat 25 Jul 98 (2100 LST Sat 25 Jul 98)
 at sigma - 0.995



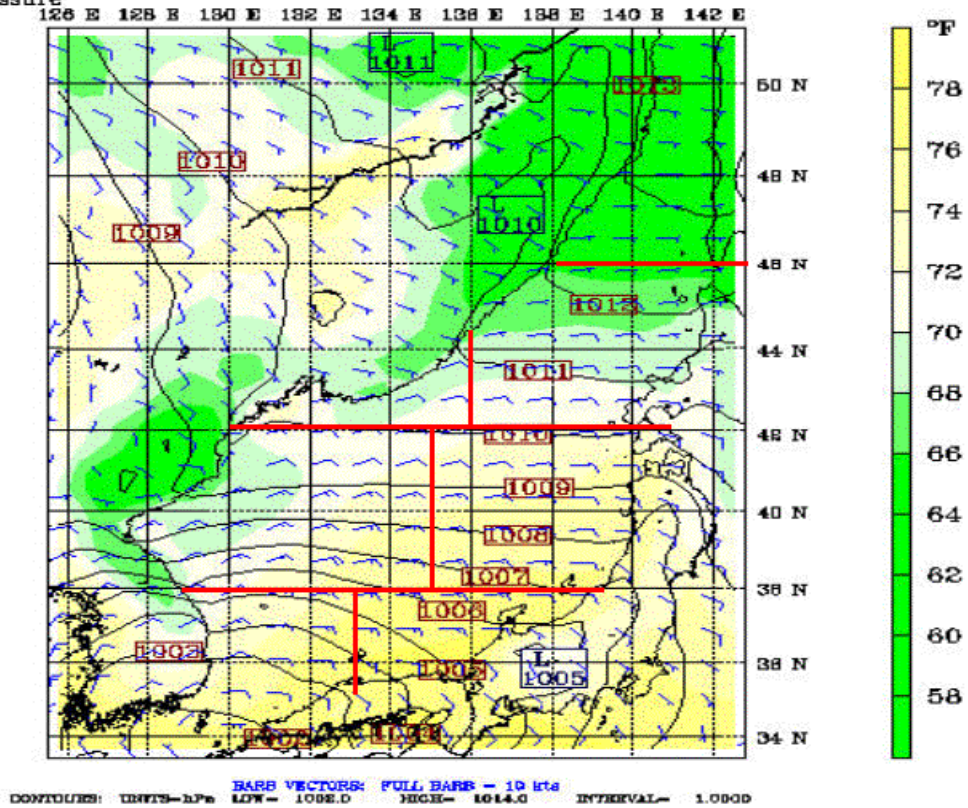
Fcst: *****
 Temperature
 Sea-level pressure

Valid: 0000 UTC Sun 26 Jul 98 (0900 LST Sun 26 Jul 98)
 at sigma - 0.995



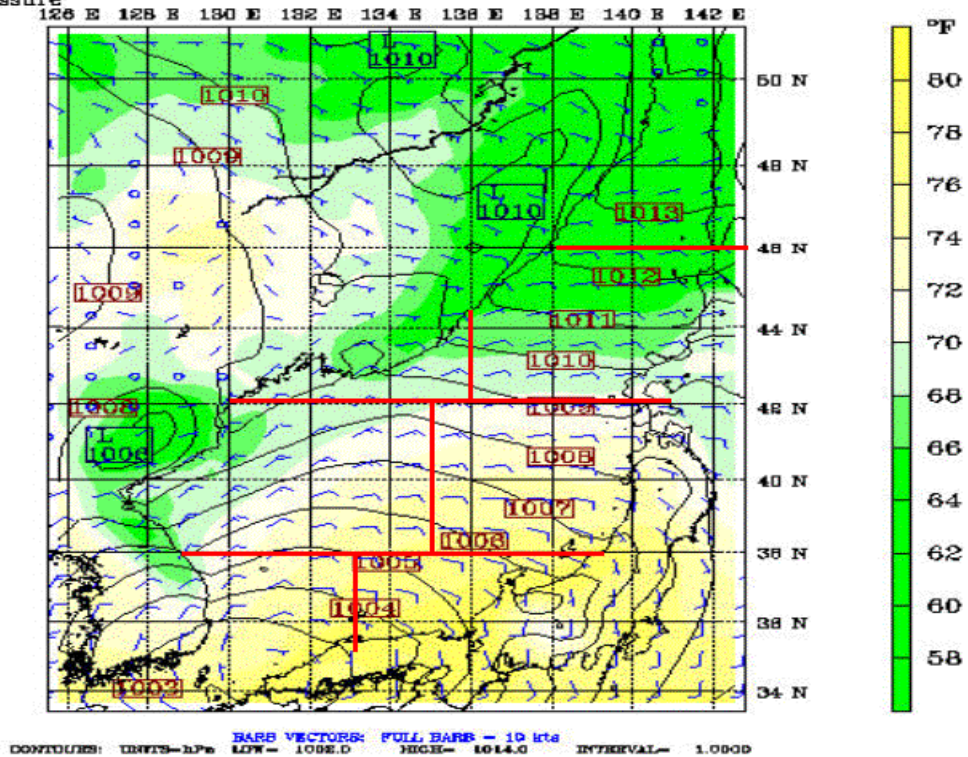
Fcst: *****
Temperature
Sea-level pressure

Valid: 1200 UTC Sun 26 Jul 98 (2100 LST Sun 26 Jul 98)
at sigma - 0.995



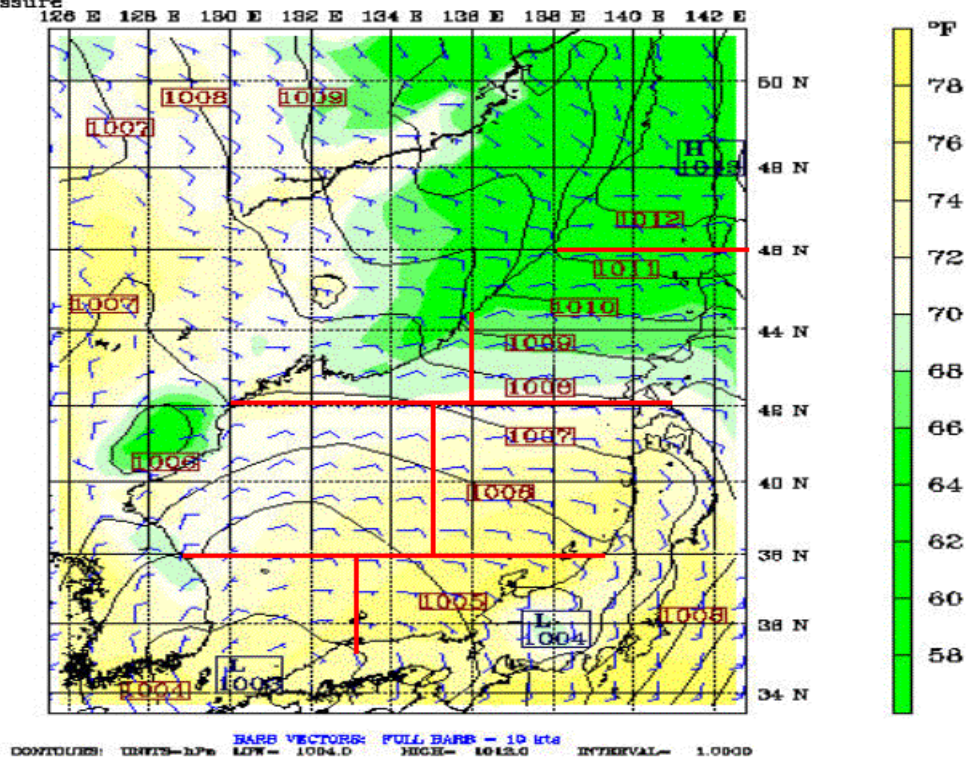
Fcst: *****
Temperature
Sea-level pressure

Valid: 0000 UTC Mon 27 Jul 98 (0900 LST Mon 27 Jul 98)
at sigma - 0.995



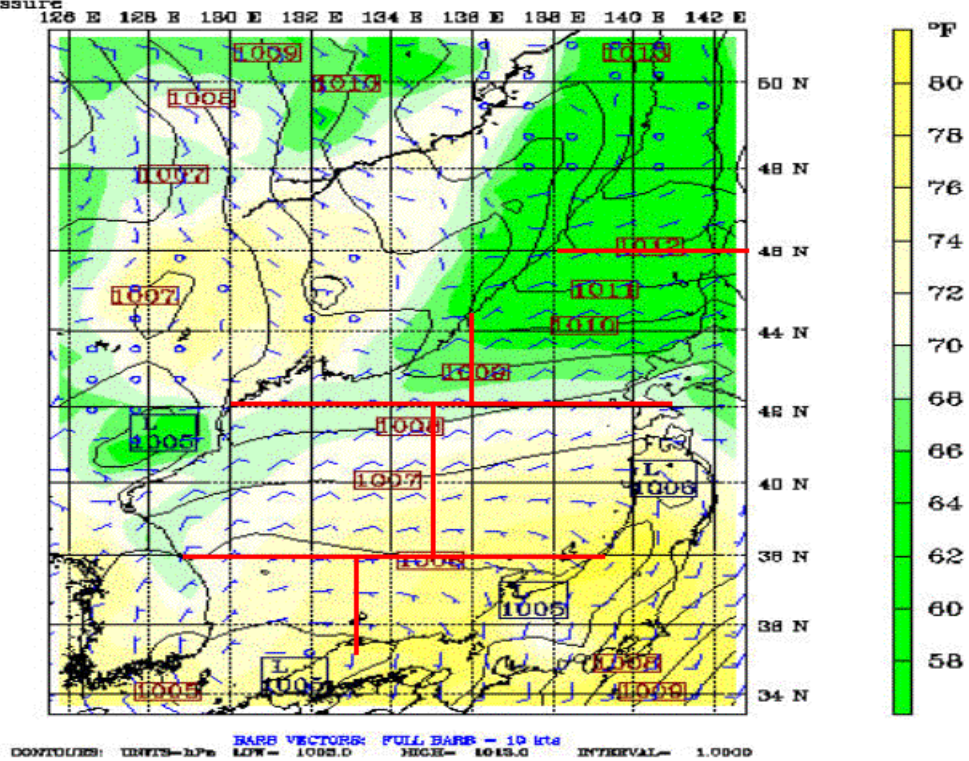
Feet: *****
Temperature
Sea-level pressure

Valid: 1200 UTC Mon 27 Jul 98 (2100 LST Mon 27 Jul 98)
at sigma - 0.995



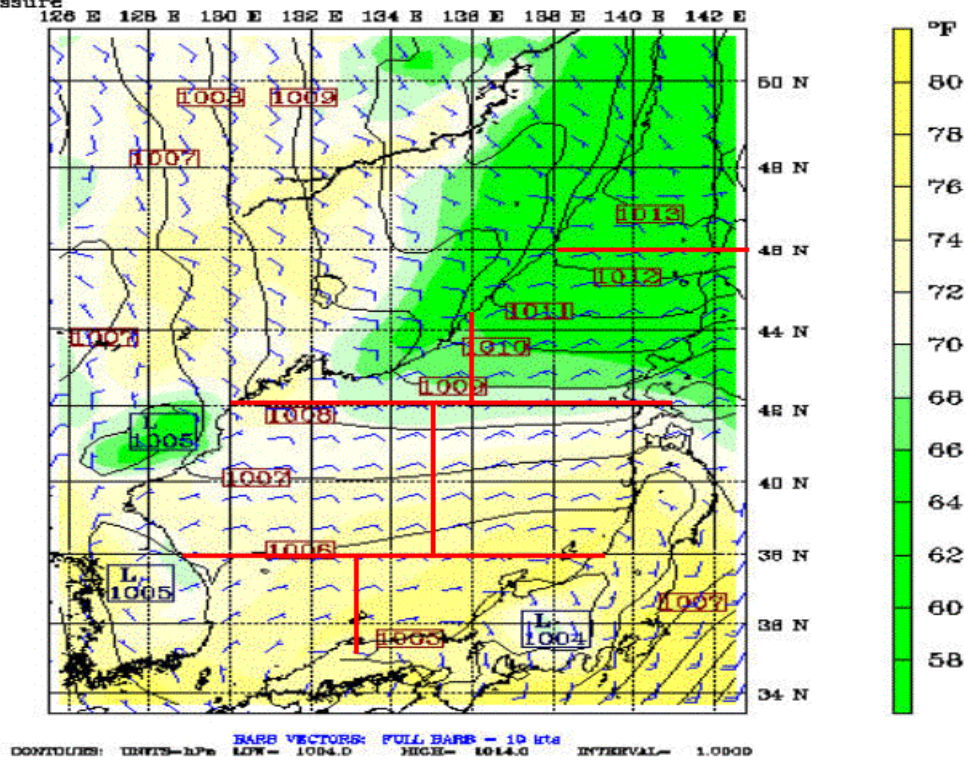
Feet: *****
Temperature
Sea-level pressure

Valid: 0000 UTC Tue 28 Jul 98 (0900 LST Tue 28 Jul 98)
at sigma - 0.995



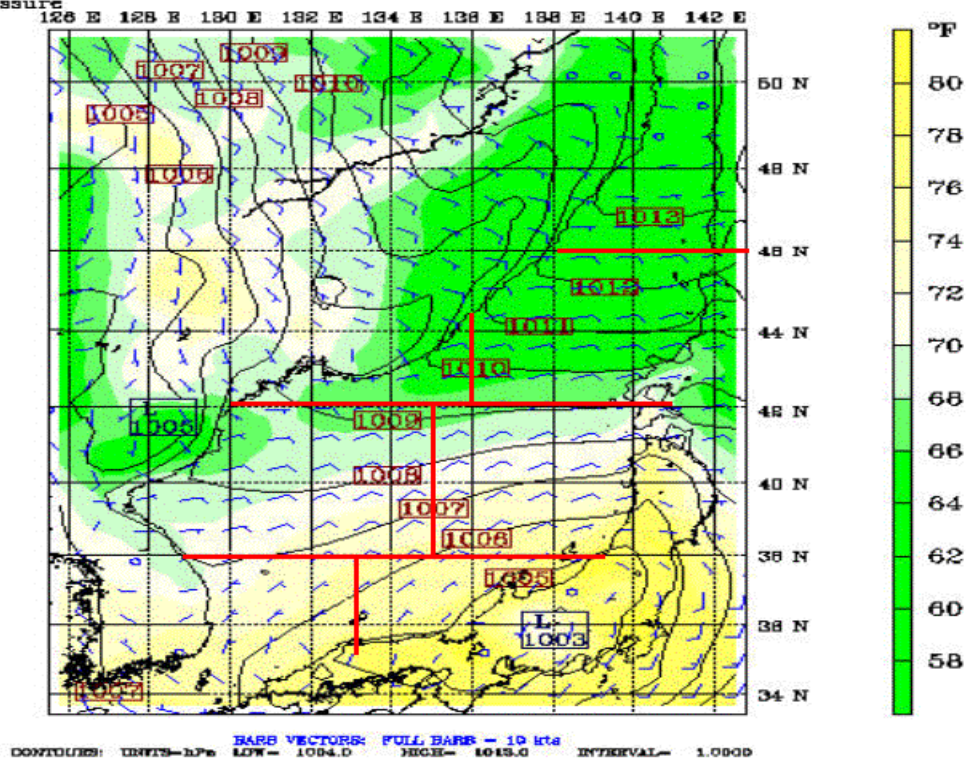
Fcst: *****
Temperature
Sea-level pressure

Valid: 1200 UTC Tue 28 Jul 98 (2100 LST Tue 28 Jul 98)
at sigma - 0.995



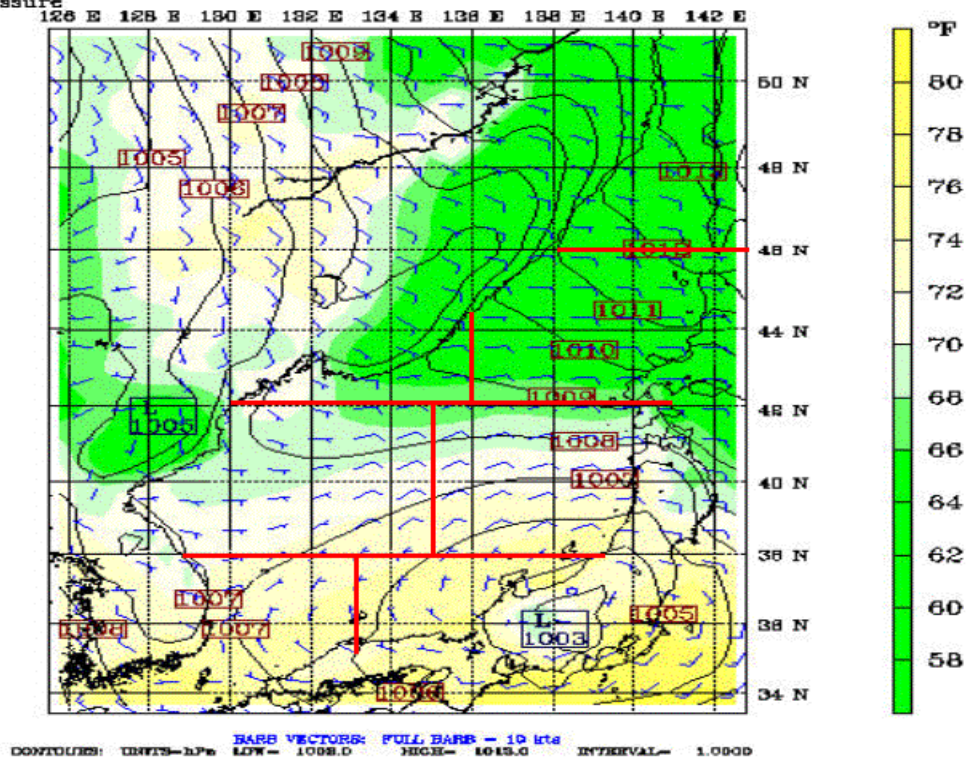
Fcst: *****
Temperature
Sea-level pressure

Valid: 0000 UTC Wed 29 Jul 98 (0900 LST Wed 29 Jul 98)
at sigma - 0.995



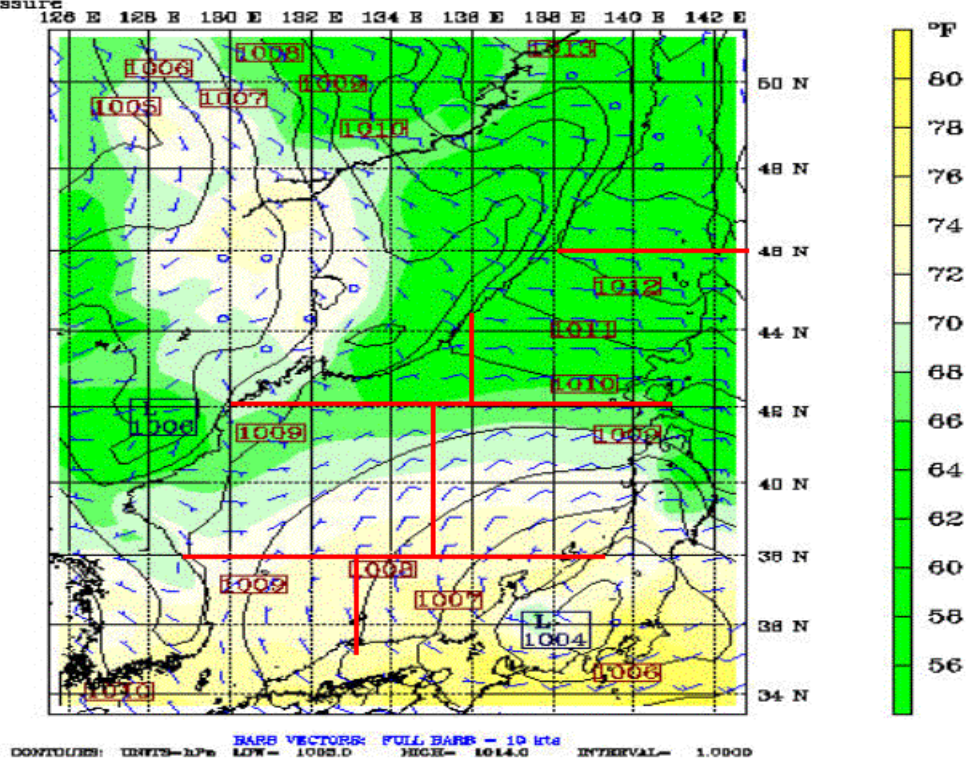
Fcst: *****
Temperature
Sea-level pressure

Valid: 1200 UTC Wed 29 Jul 98 (2100 LST Wed 29 Jul 98)
at sigma - 0.995



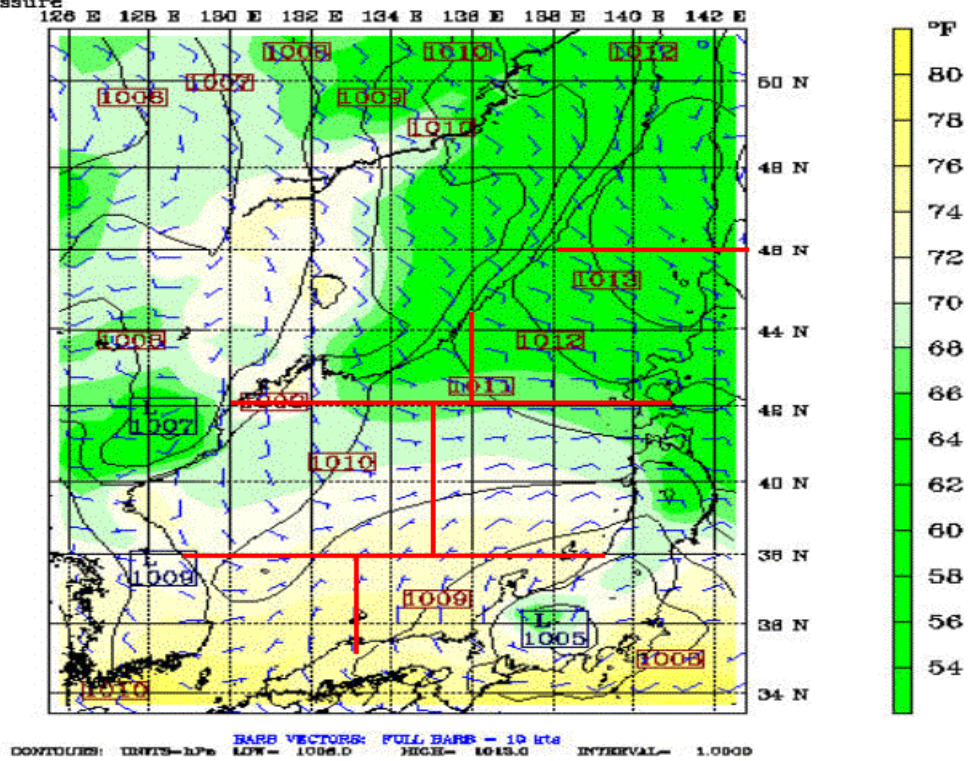
Fcst: *****
Temperature
Sea-level pressure

Valid: 0000 UTC Thu 30 Jul 98 (0900 LST Thu 30 Jul 98)
at sigma - 0.995



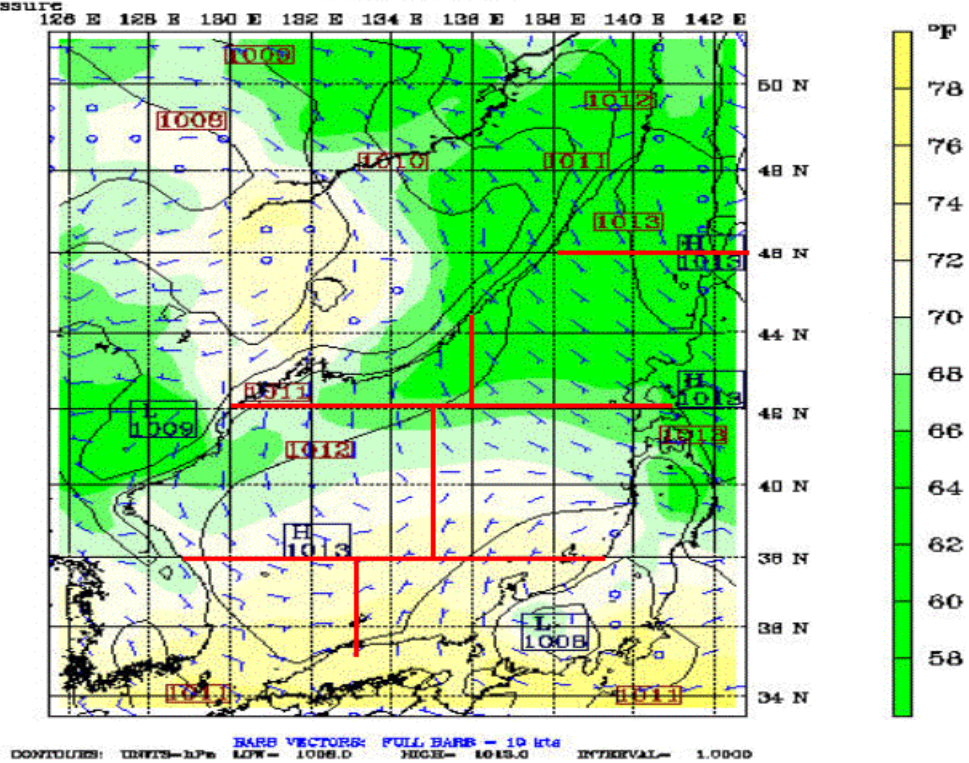
Fcst: *****
 Temperature
 Sea-level pressure

Valid: 1200 UTC Thu 30 Jul 98 (2100 LST Thu 30 Jul 98)
 at sigma - 0.995



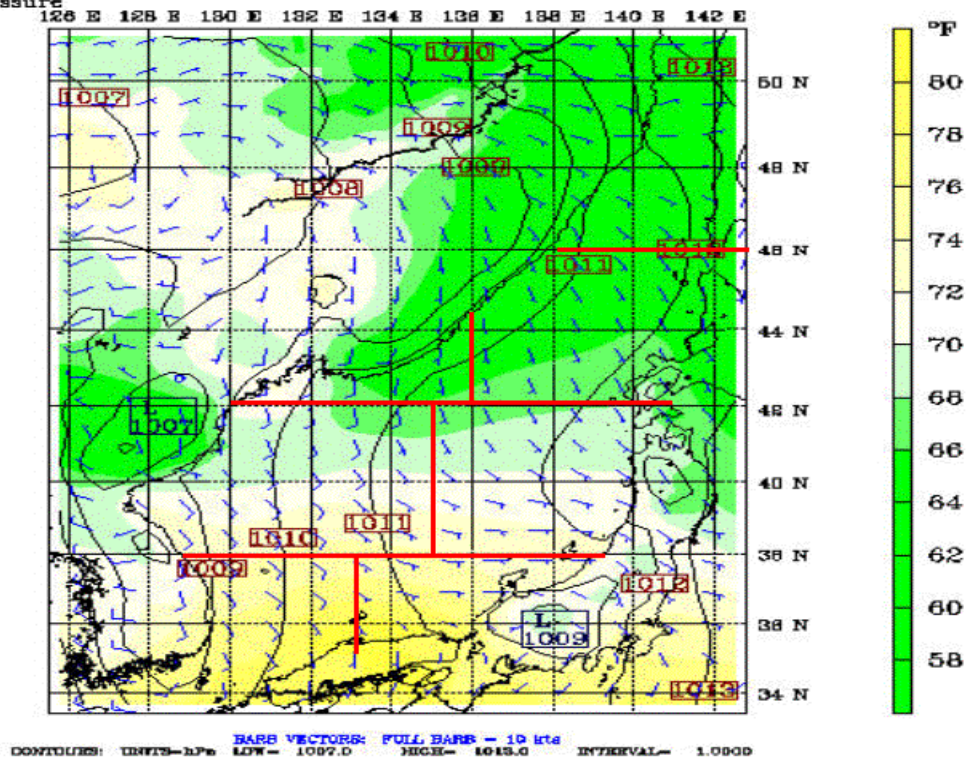
Fcst: *****
 Temperature
 Sea-level pressure

Valid: 0000 UTC Fri 31 Jul 98 (0900 LST Fri 31 Jul 98)
 at sigma - 0.995



Fest: *****
Temperature
Sea-level pressure

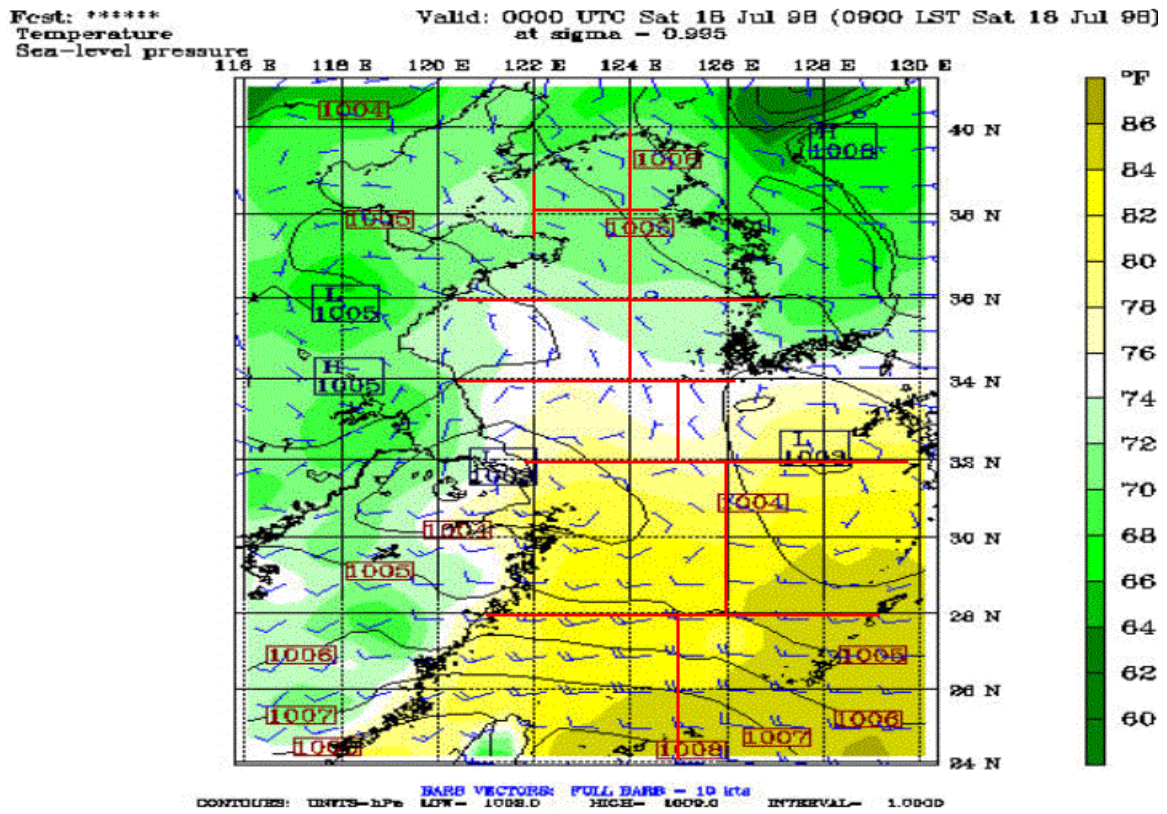
Valid: 1200 UTC Fri 31 Jul 98 (2100 LST Fri 31 Jul 98)
at sigma - 0.995



THIS PAGE INTENTIONALLY LEFT BLANK

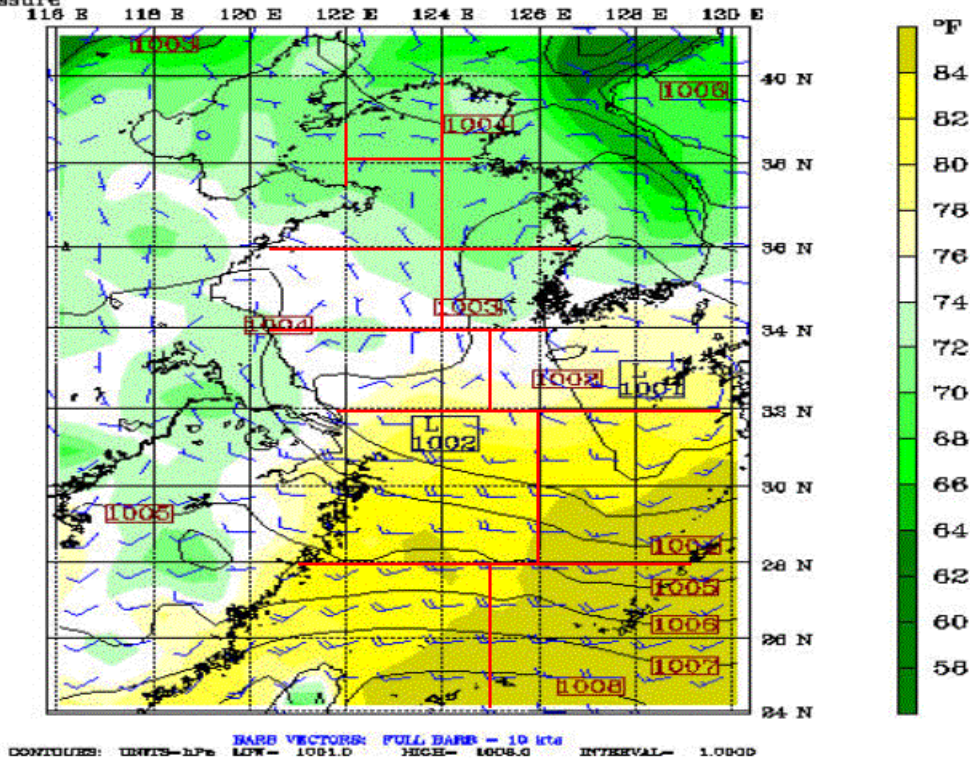
APPENDIX Y. SEA LEVEL PRESSURE/SAT/SURFACE WIND PLOTS FOR THE YES FOR THE JULY TIME PERIOD

Appendix Y consists of 28 figures that show sea level pressure, SAT, and surface winds for the July time period over the YES. The figures are in time sequential order from July 18 through July 31.



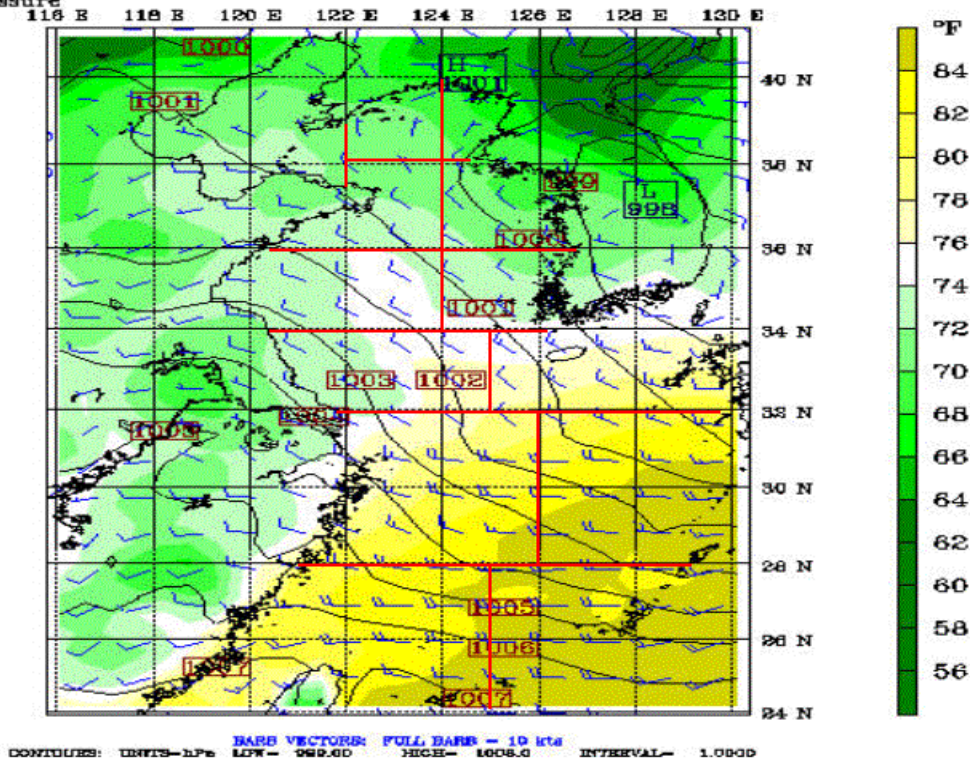
Post: *****
Temperature
Sea-level pressure

Valid: 1200 UTC Sat 15 Jul 98 (2100 LST Sat 15 Jul 98)
at sigma - 0.995



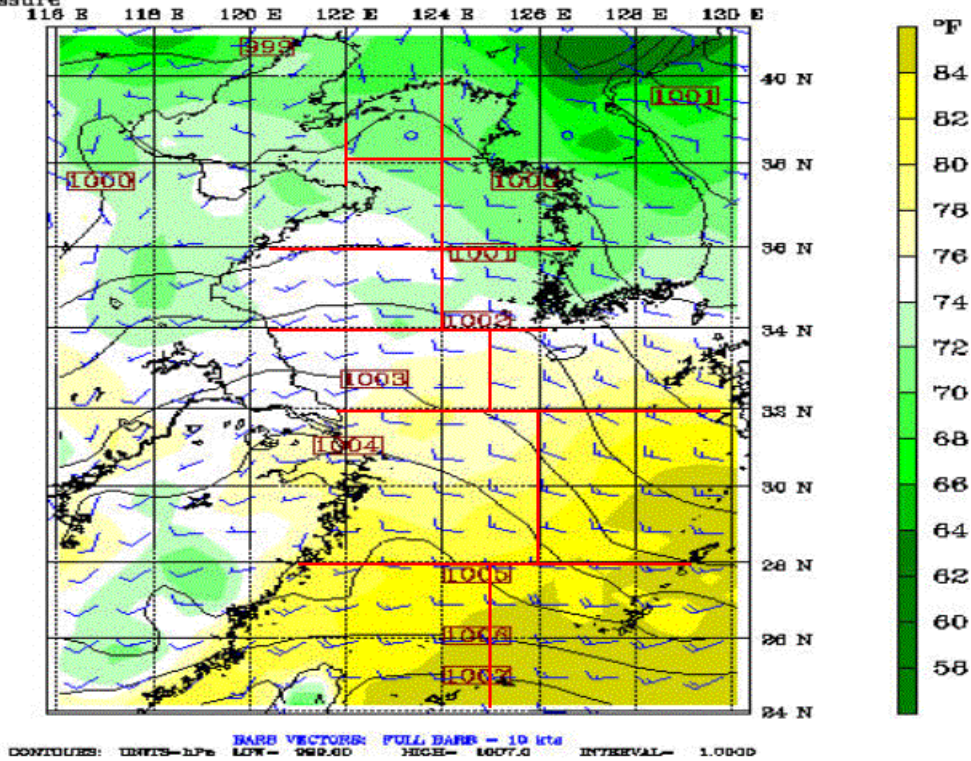
Post: *****
Temperature
Sea-level pressure

Valid: 0000 UTC Sun 19 Jul 98 (0900 LST Sun 19 Jul 98)
at sigma - 0.995



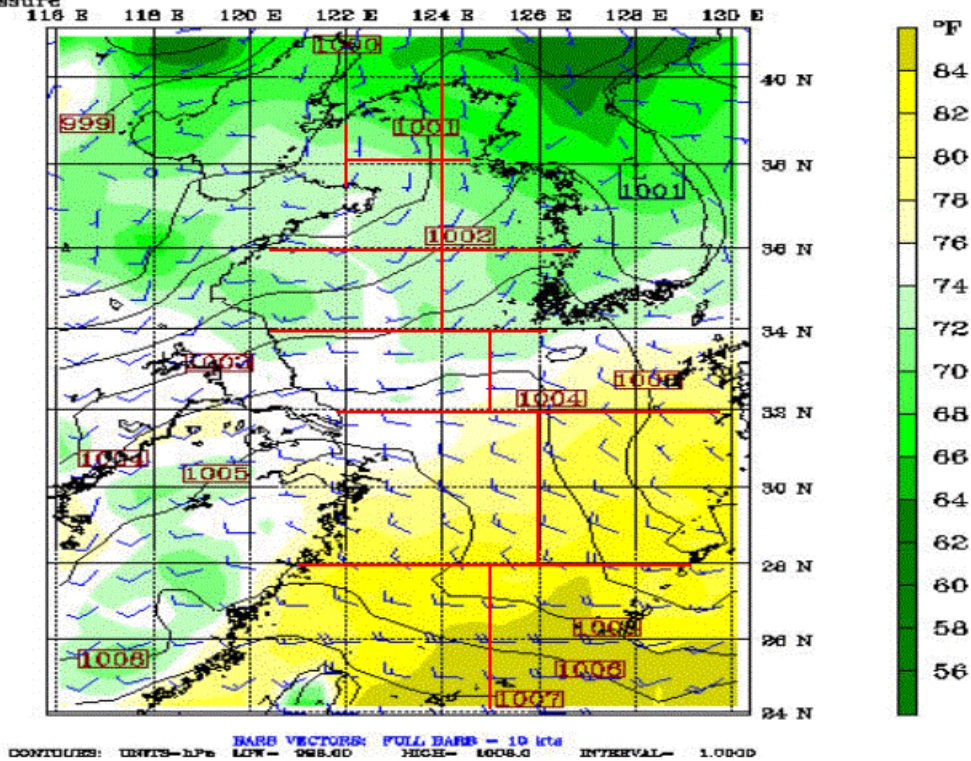
Post: *****
Temperature
Sea-level pressure

Valid: 1200 UTC Sun 19 Jul 98 (2100 LST Sun 19 Jul 98)
at sigma - 0.995



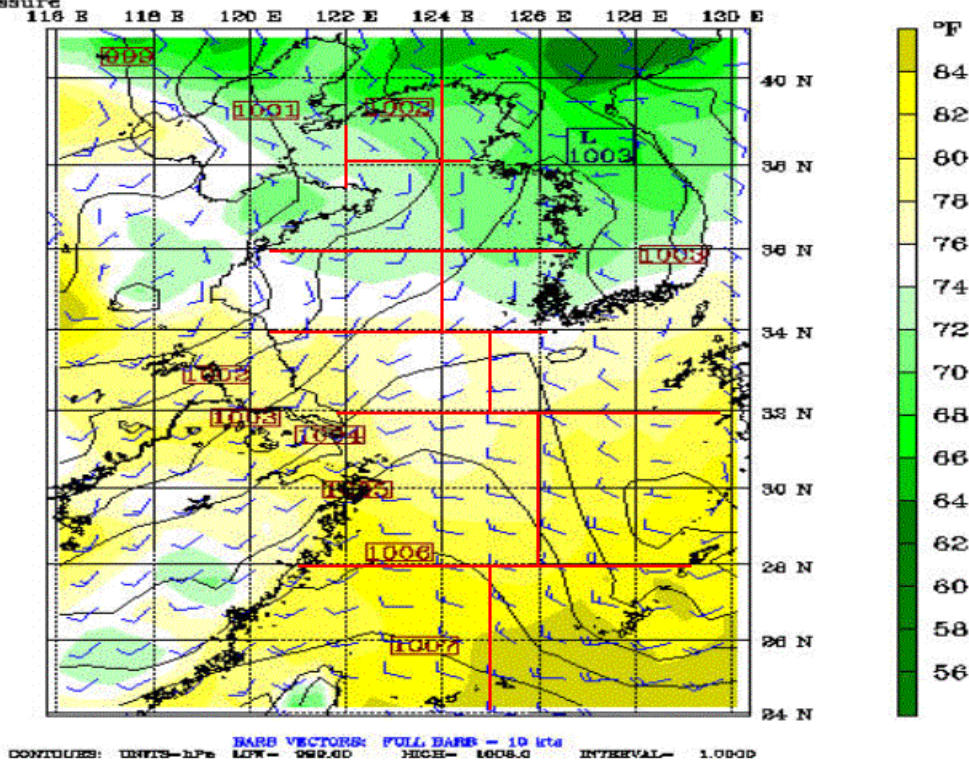
Post: *****
Temperature
Sea-level pressure

Valid: 0000 UTC Mon 20 Jul 98 (0900 LST Mon 20 Jul 98)
at sigma - 0.995



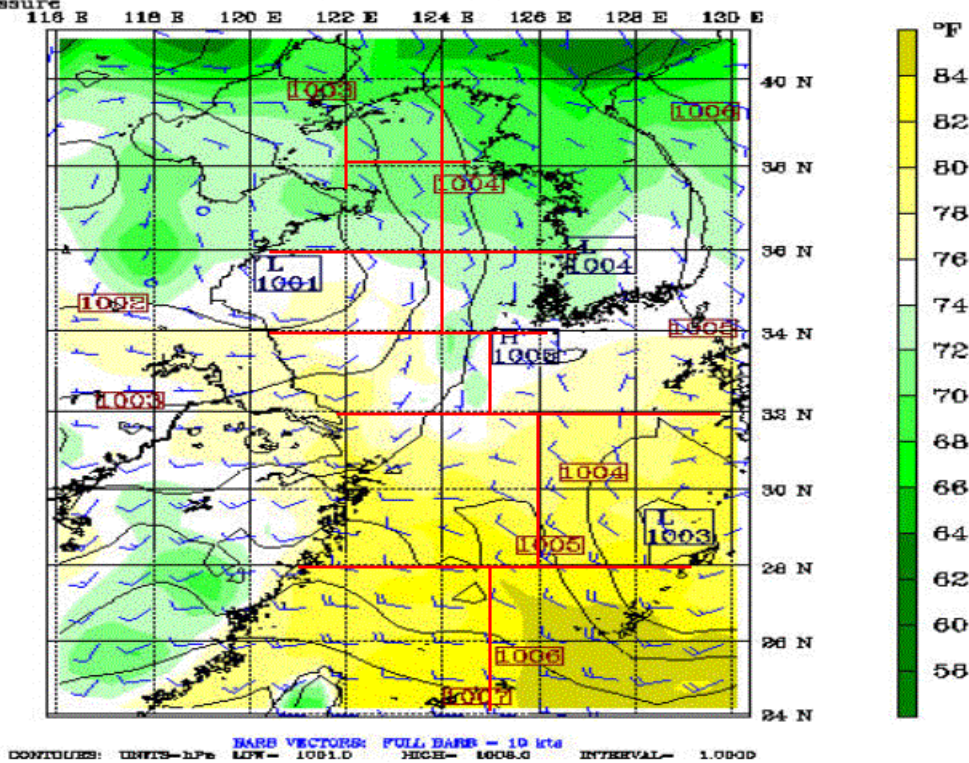
Post: *****
Temperature
Sea-level pressure

Valid: 1200 UTC Mon 20 Jul 98 (2100 LST Mon 20 Jul 98)
at sigma - 0.995



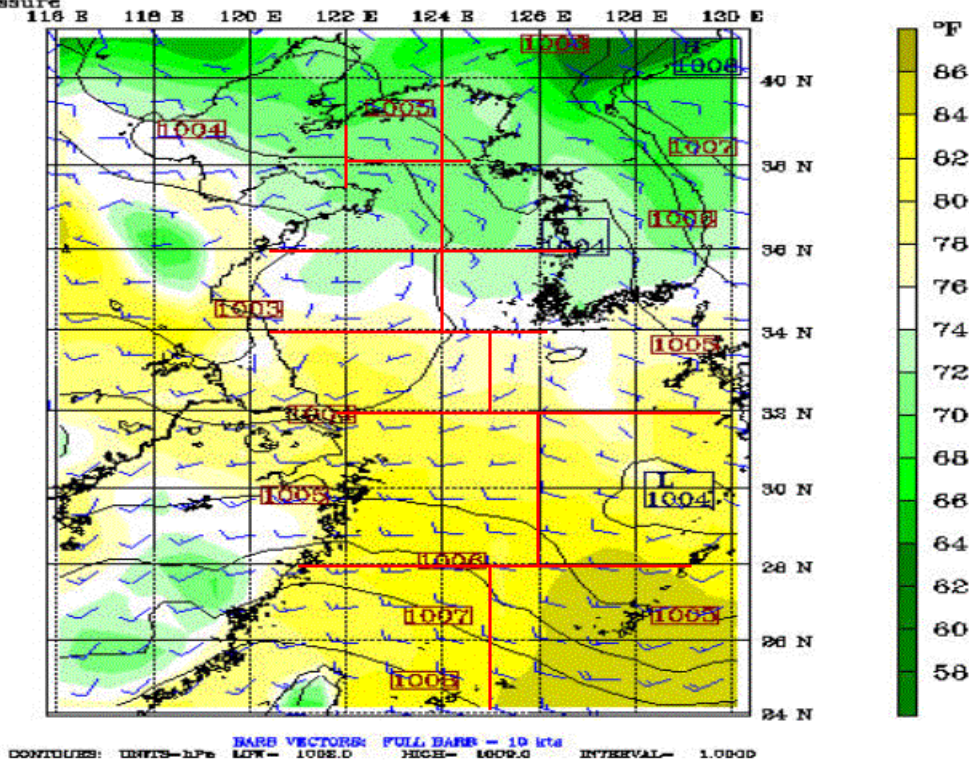
Post: *****
Temperature
Sea-level pressure

Valid: 0000 UTC Tue 21 Jul 98 (0900 LST Tue 21 Jul 98)
at sigma - 0.995



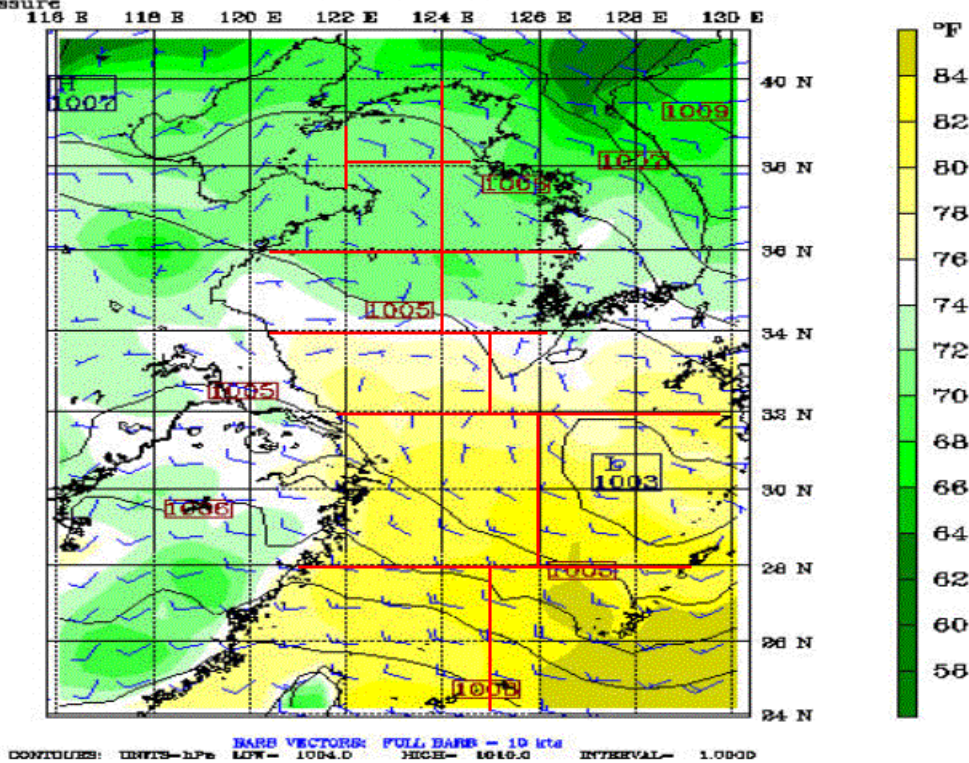
Post: *****
Temperature
Sea-level pressure

Valid: 1200 UTC Tue 21 Jul 98 (2100 LST Tue 21 Jul 98)
at sigma = 0.995



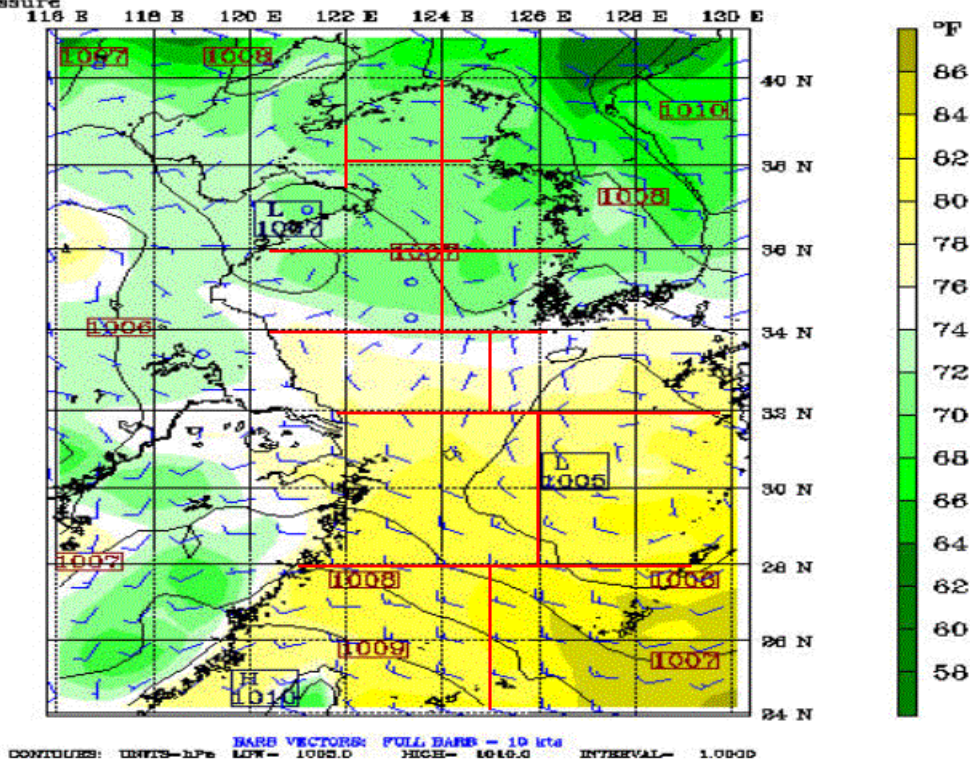
Post: *****
Temperature
Sea-level pressure

Valid: 0000 UTC Wed 22 Jul 98 (0900 LST Wed 22 Jul 98)
at sigma = 0.995



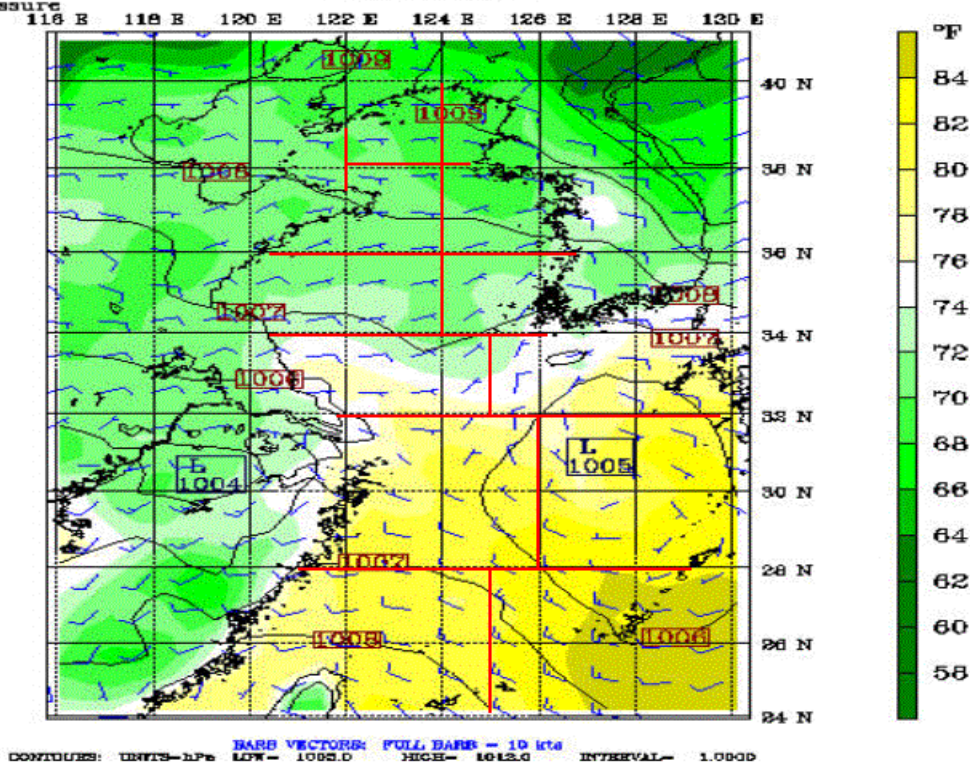
Post: *****
Temperature
Sea-level pressure

Valid: 1200 UTC Wed 22 Jul 98 (2100 LST Wed 22 Jul 98)
at sigma - 0.995



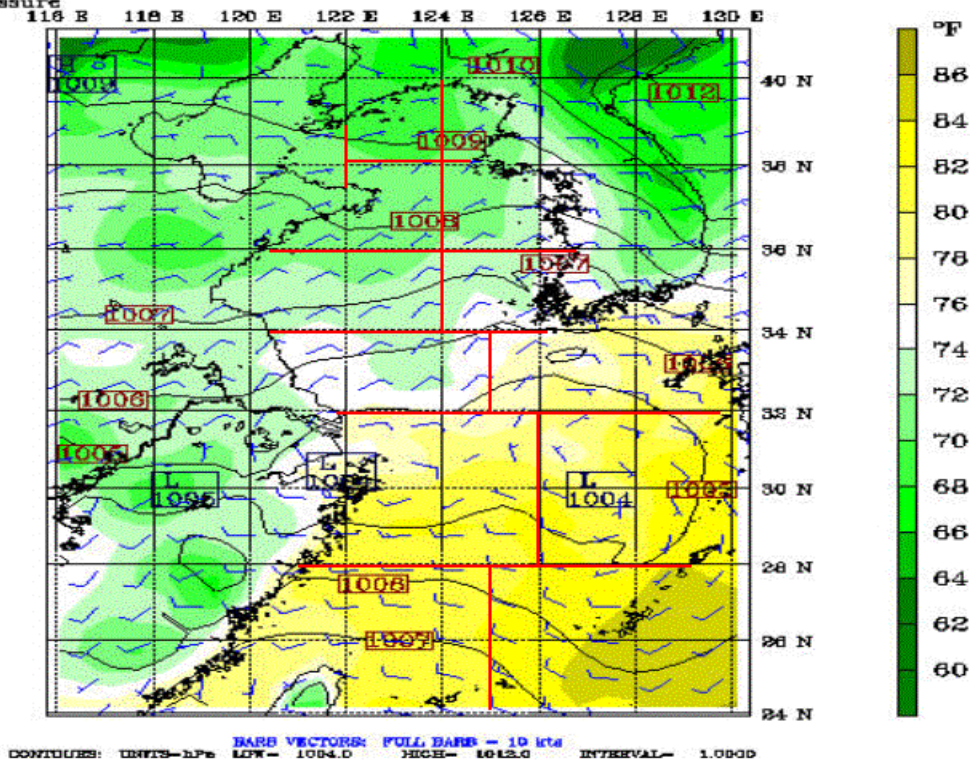
Post: *****
Temperature
Sea-level pressure

Valid: 0000 UTC Thu 23 Jul 98 (0900 LST Thu 23 Jul 98)
at sigma - 0.995



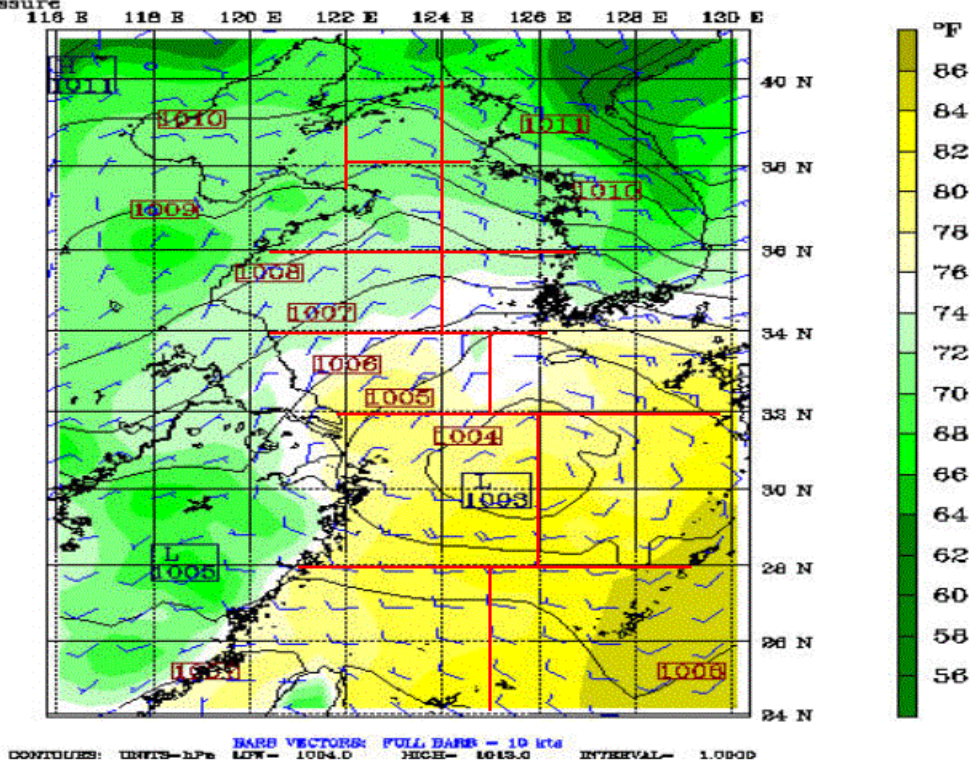
Post: *****
Temperature
Sea-level pressure

Valid: 1200 UTC Thu 23 Jul 98 (2100 LST Thu 23 Jul 98)
at sigma - 0.995



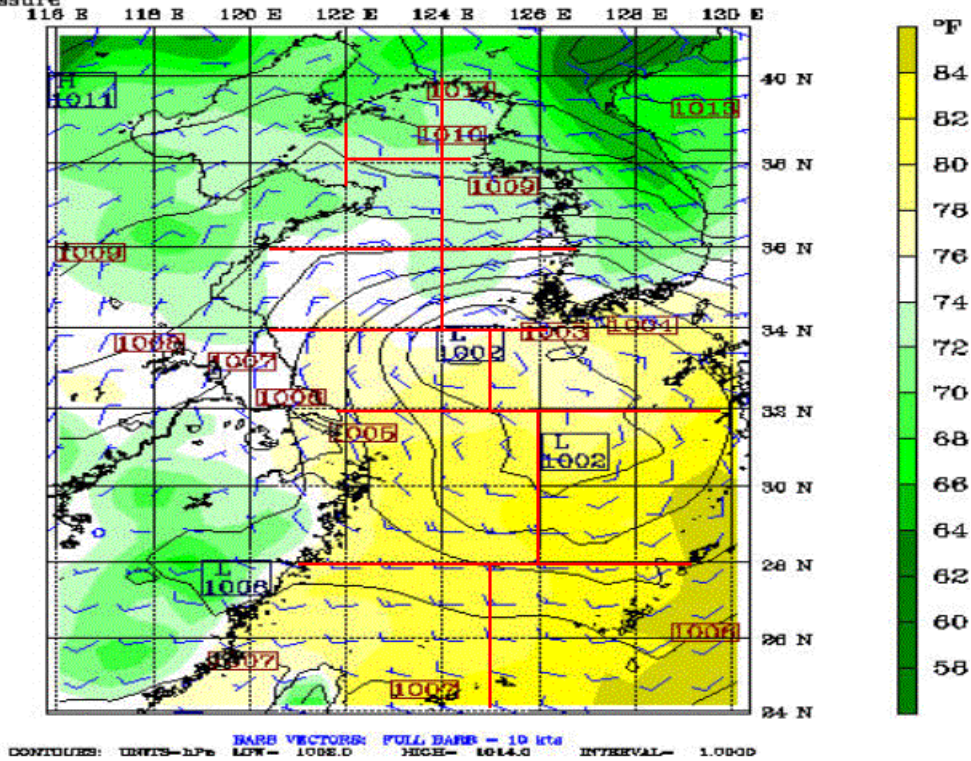
Post: *****
Temperature
Sea-level pressure

Valid: 0000 UTC Fri 24 Jul 98 (0900 LST Fri 24 Jul 98)
at sigma - 0.995



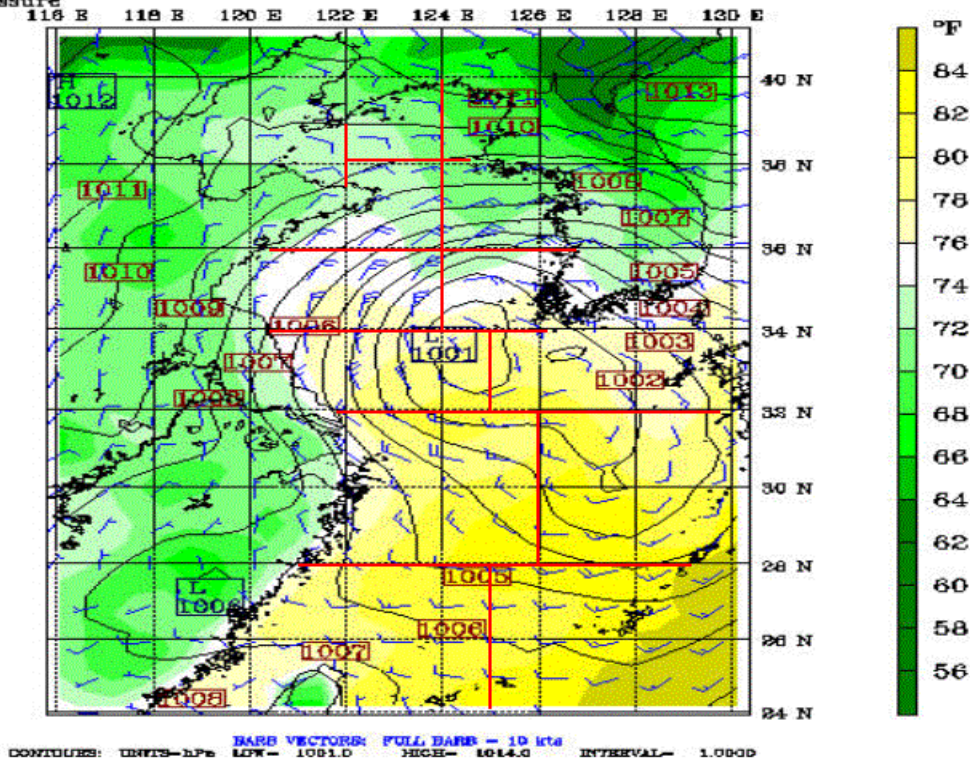
Post: *****
Temperature
Sea-level pressure

Valid: 1200 UTC Fri 24 Jul 98 (2100 LST Fri 24 Jul 98)
at sigma - 0.995



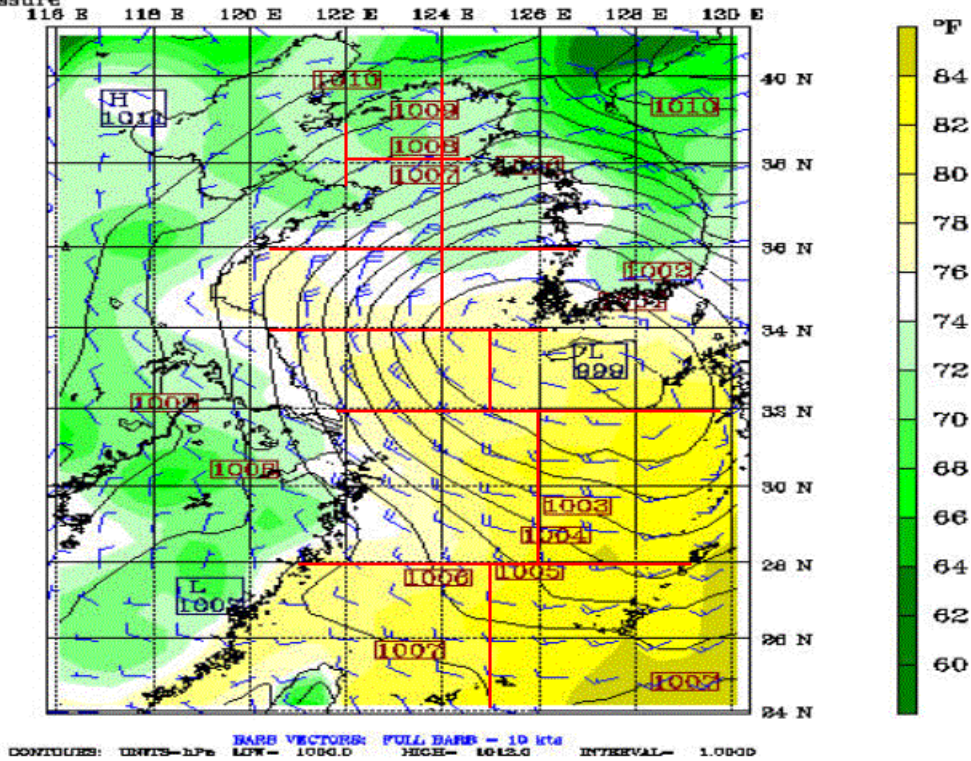
Post: *****
Temperature
Sea-level pressure

Valid: 0000 UTC Sat 25 Jul 98 (0900 LST Sat 25 Jul 98)
at sigma - 0.995



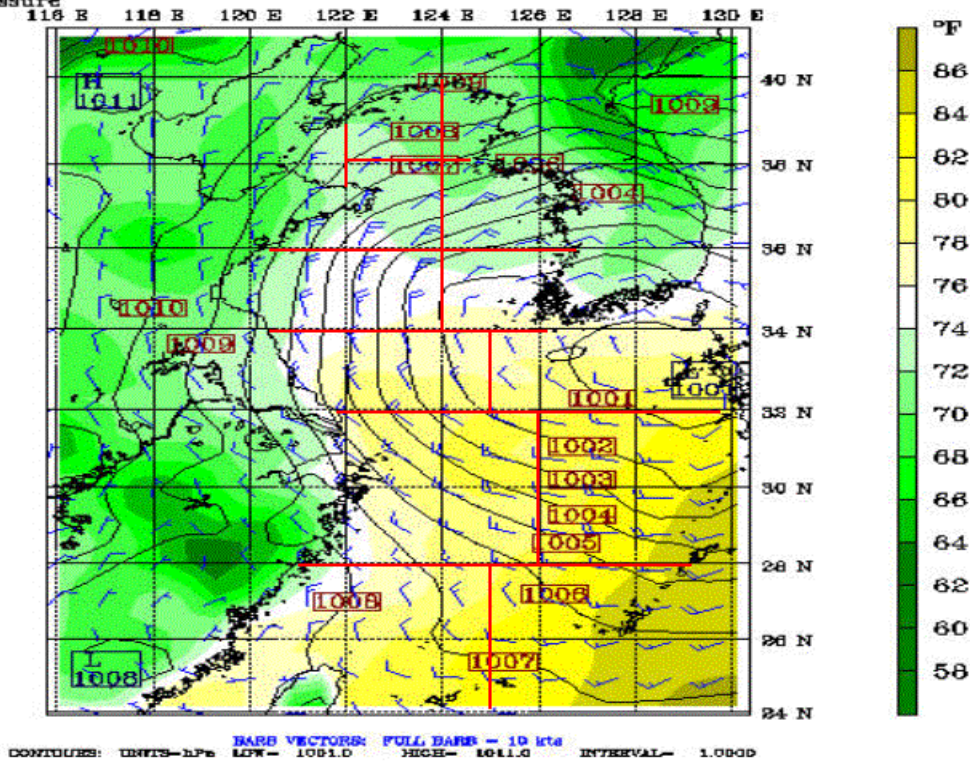
Post: *****
Temperature
Sea-level pressure

Valid: 1200 UTC Sat 25 Jul 98 (2100 LST Sat 25 Jul 98)
at sigma - 0.995



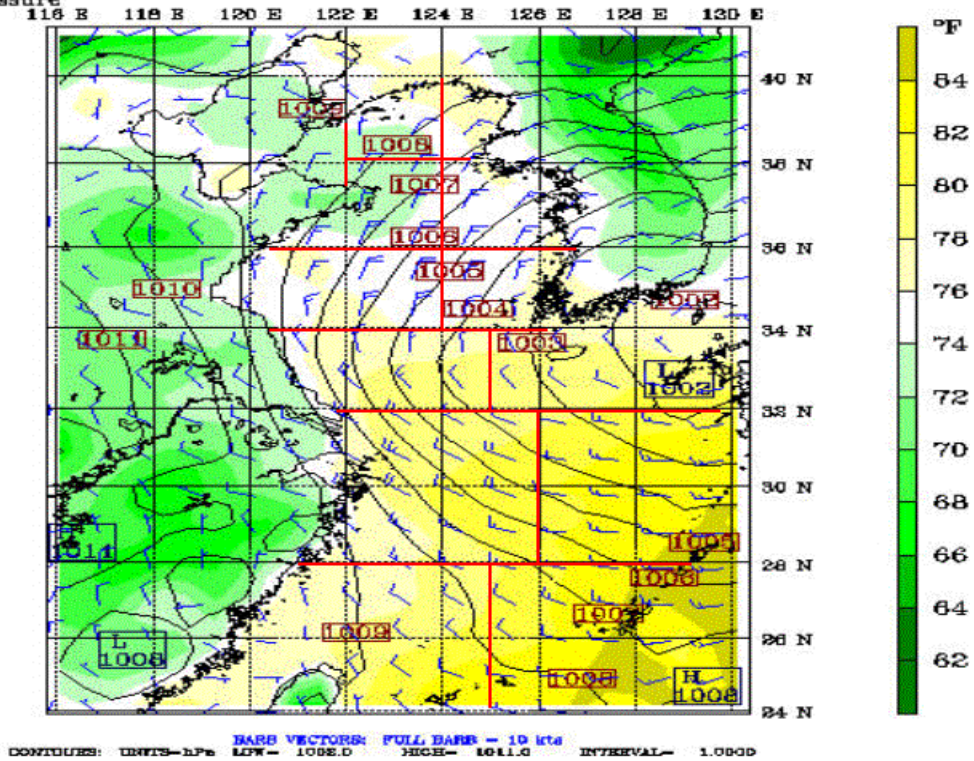
Post: *****
Temperature
Sea-level pressure

Valid: 0000 UTC Sun 26 Jul 98 (0900 LST Sun 26 Jul 98)
at sigma - 0.995



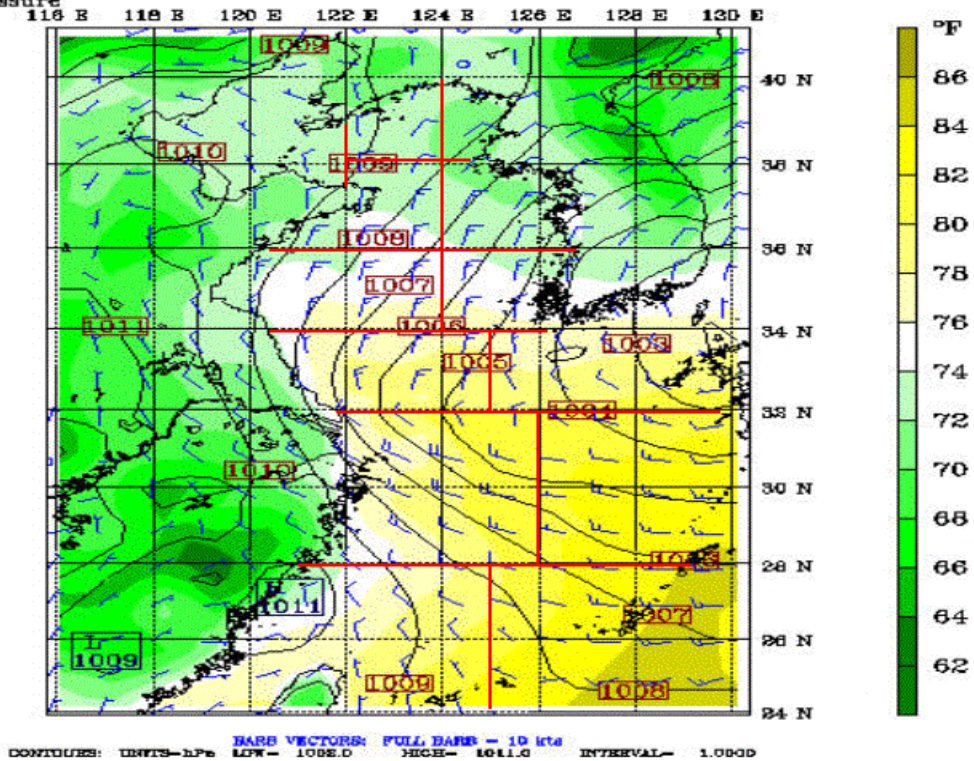
Post: *****
Temperature
Sea-level pressure

Valid: 1200 UTC Sun 26 Jul 98 (2100 LST Sun 26 Jul 98)
at sigma - 0.995



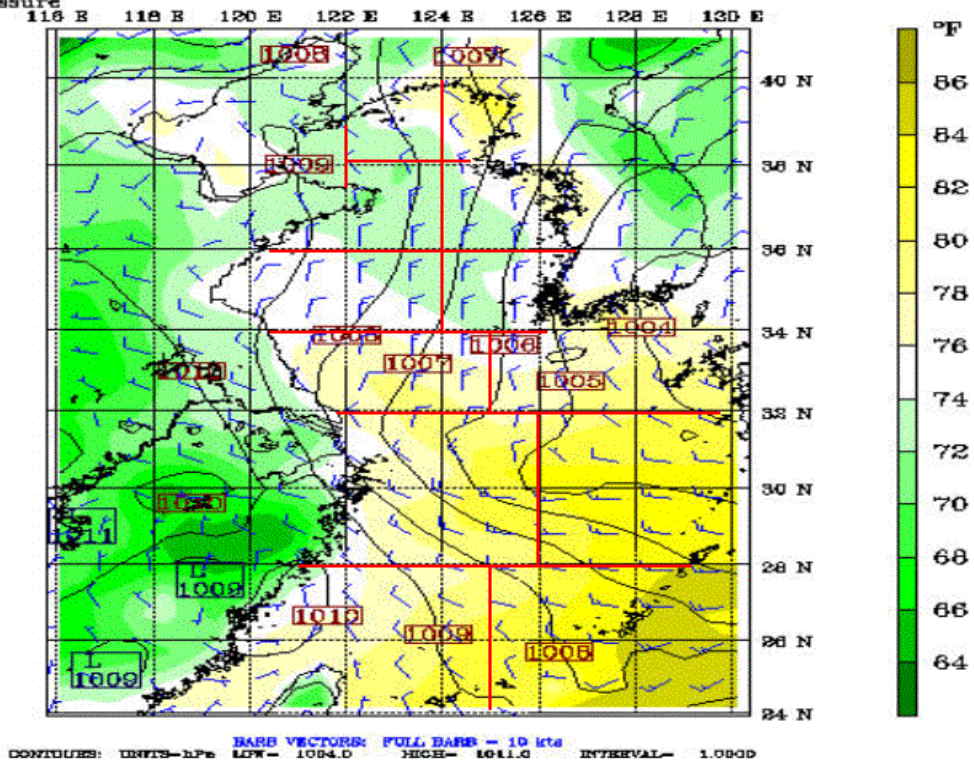
Post: *****
Temperature
Sea-level pressure

Valid: 0000 UTC Mon 27 Jul 98 (0900 LST Mon 27 Jul 98)
at sigma - 0.995



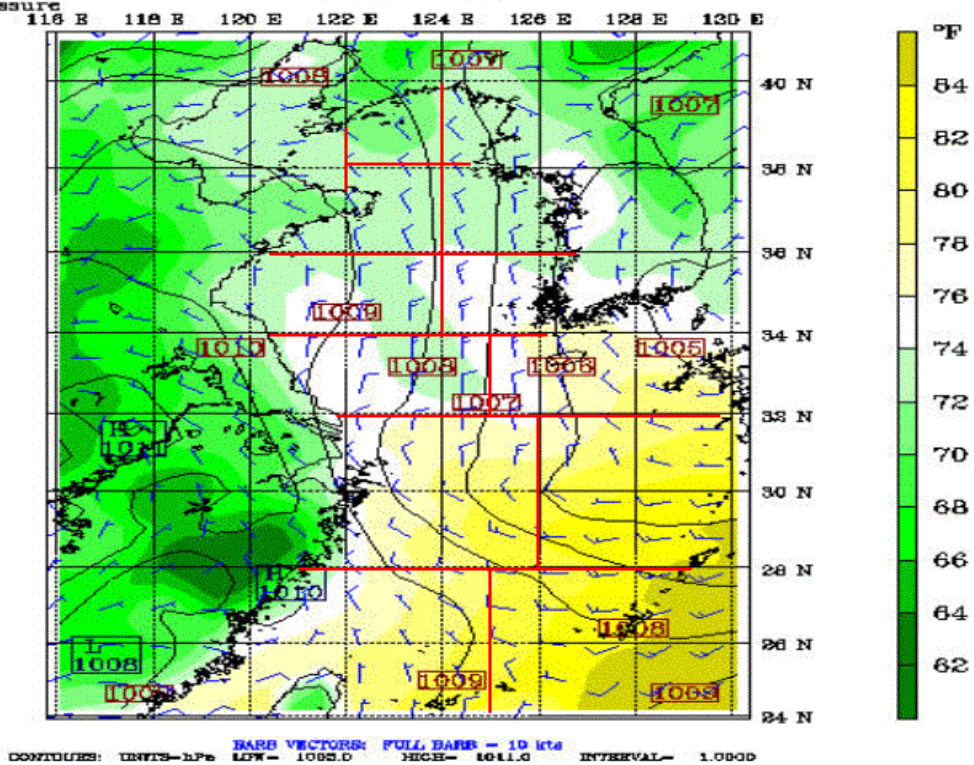
Post: *****
Temperature
Sea-level pressure

Valid: 1200 UTC Mon 27 Jul 98 (2100 LST Mon 27 Jul 98)
at sigma - 0.995



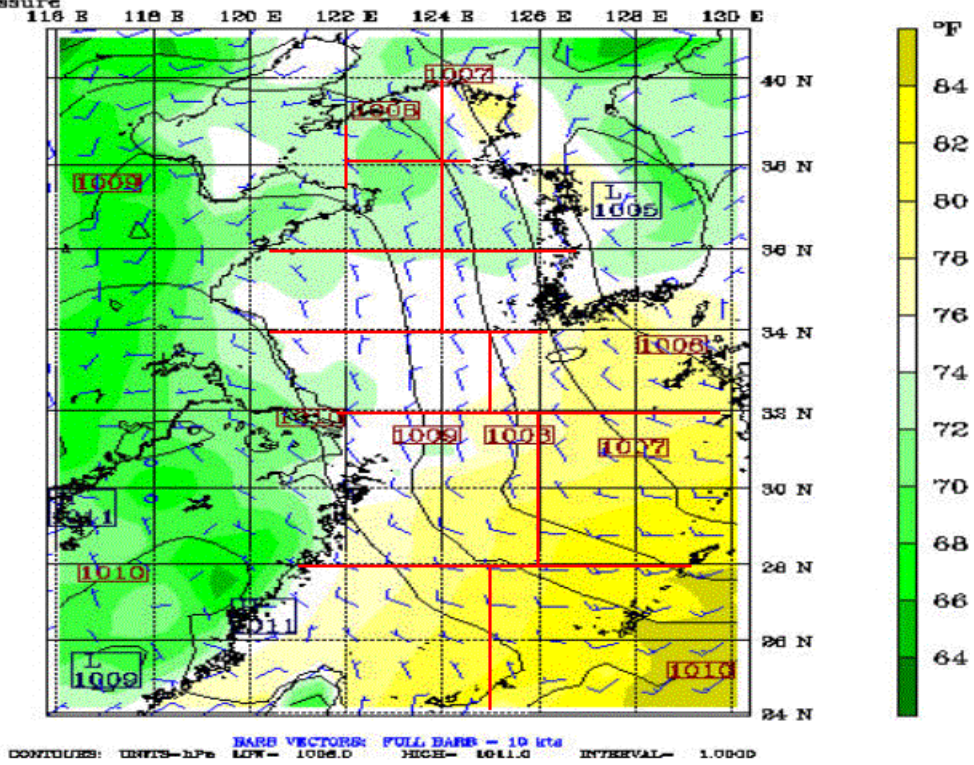
Post: *****
Temperature
Sea-level pressure

Valid: 0000 UTC Tue 28 Jul 98 (0900 LST Tue 28 Jul 98)
at sigma - 0.995



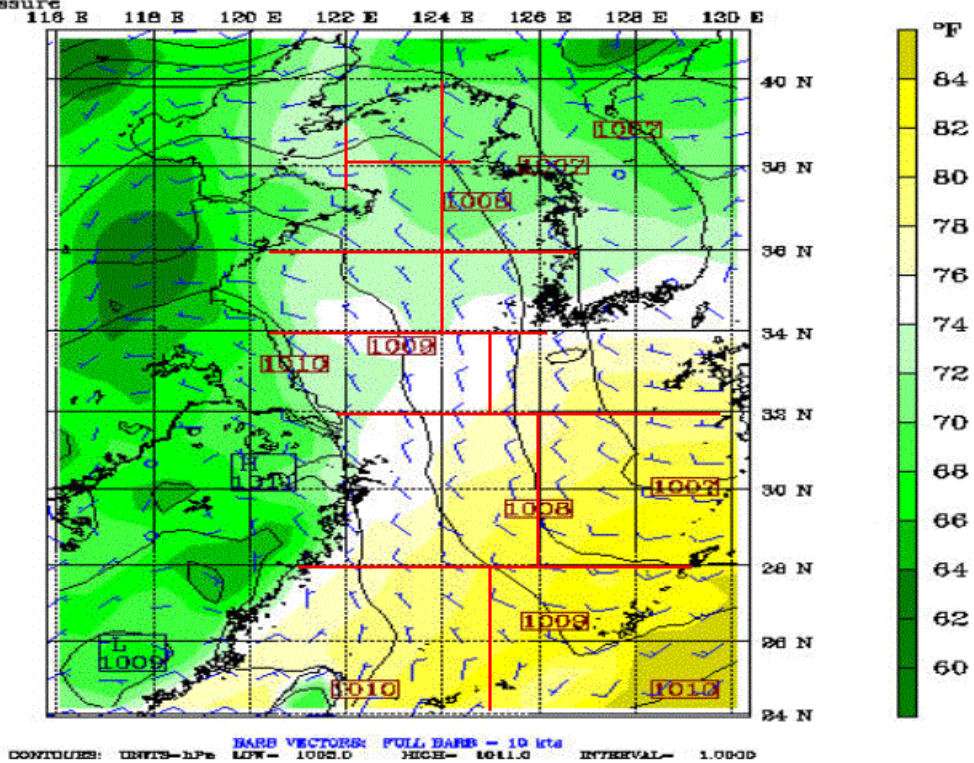
Post: *****
Temperature
Sea-level pressure

Valid: 1200 UTC Tue 28 Jul 98 (2100 LST Tue 28 Jul 98)
at sigma = 0.995



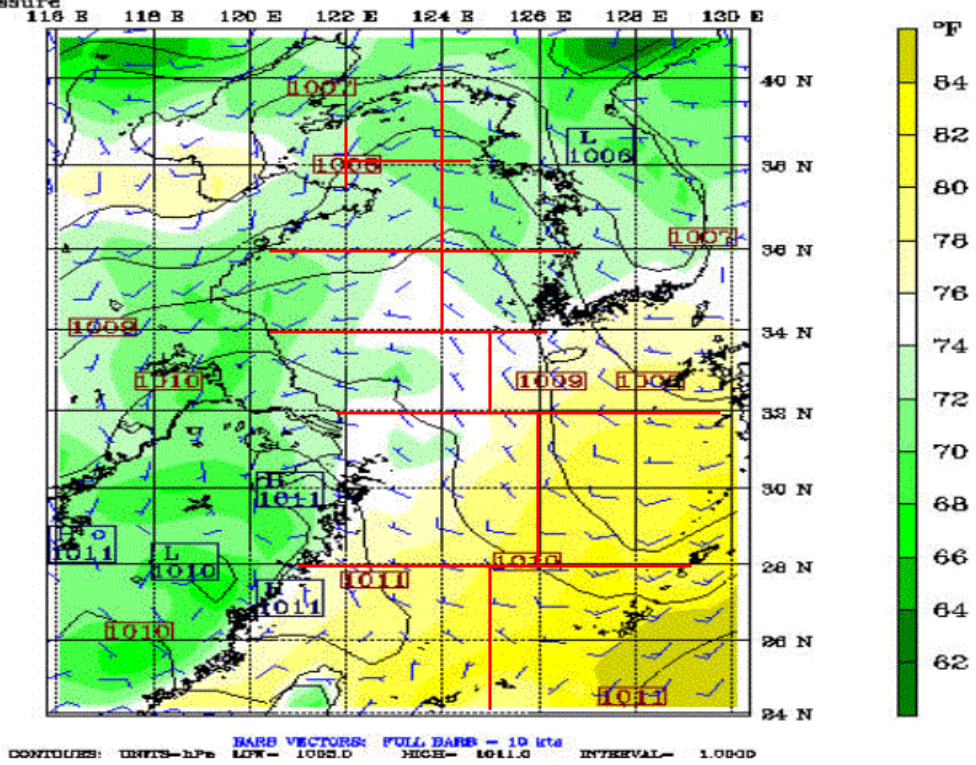
Post: *****
Temperature
Sea-level pressure

Valid: 0000 UTC Wed 29 Jul 98 (0900 LST Wed 29 Jul 98)
at sigma = 0.995



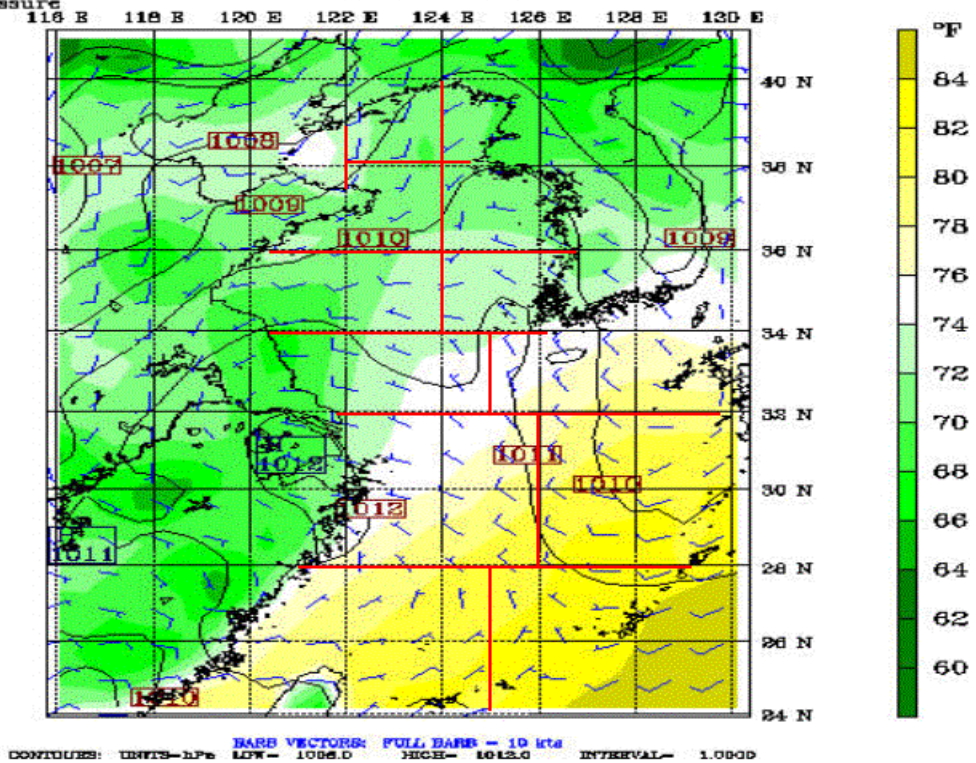
Post: *****
Temperature
Sea-level pressure

Valid: 1200 UTC Wed 29 Jul 98 (2100 LST Wed 29 Jul 98)
at sigma - 0.995



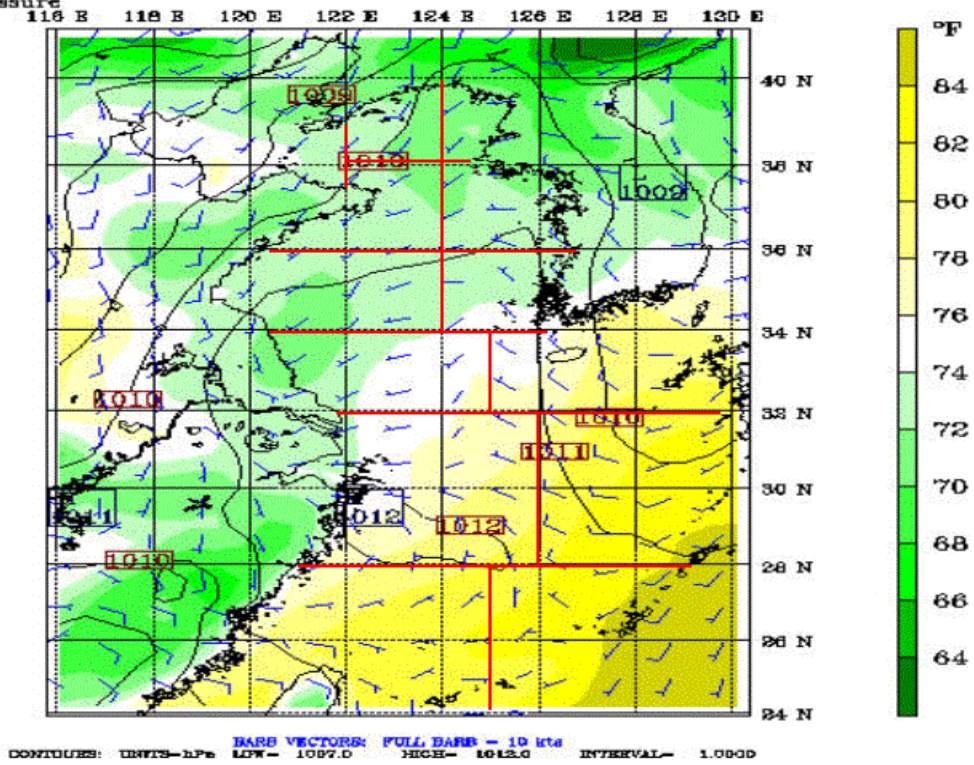
Post: *****
Temperature
Sea-level pressure

Valid: 0000 UTC Thu 30 Jul 98 (0900 LST Thu 30 Jul 98)
at sigma - 0.995



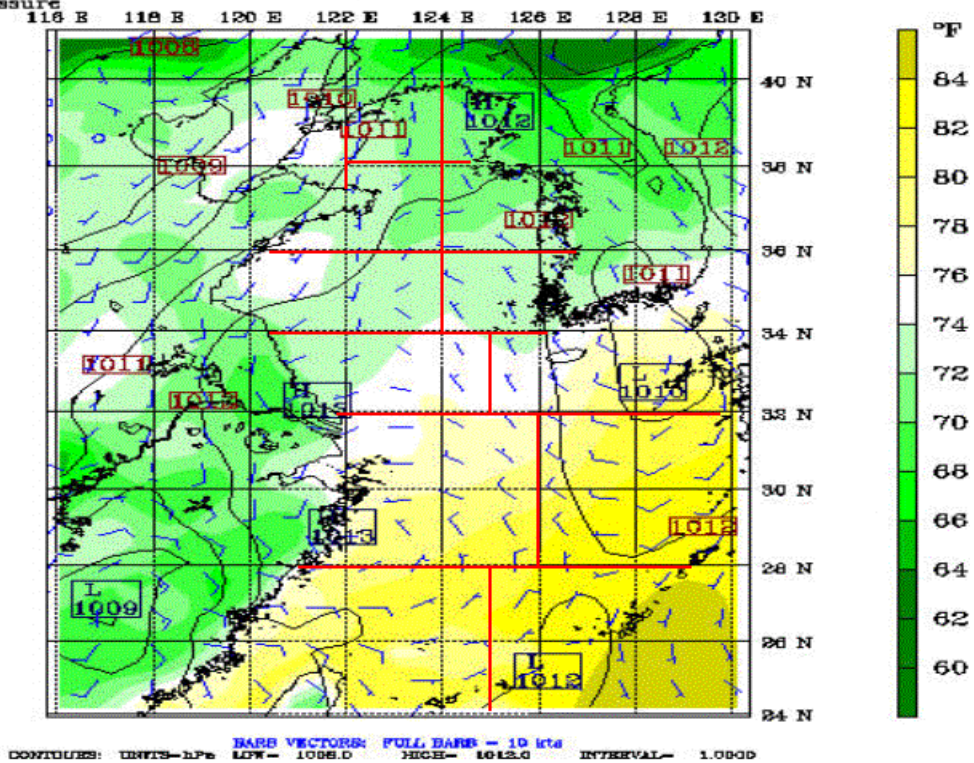
Post: *****
Temperature
Sea-level pressure

Valid: 1200 UTC Thu 30 Jul 98 (2100 LST Thu 30 Jul 98)
at sigma - 0.995



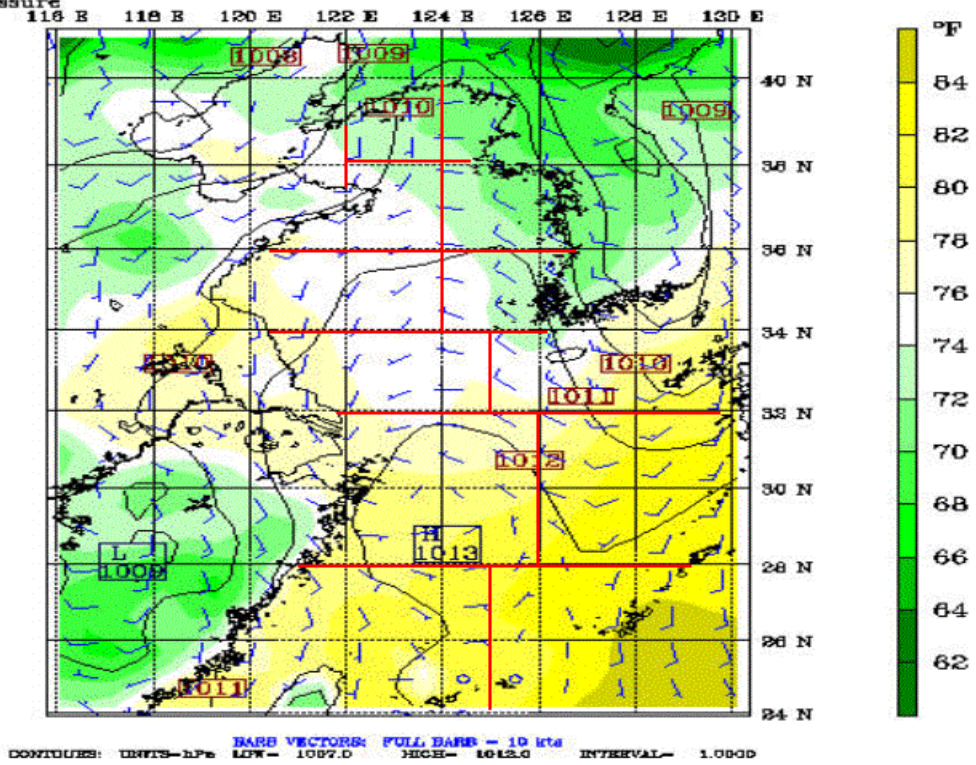
Post: *****
Temperature
Sea-level pressure

Valid: 0000 UTC Fri 31 Jul 98 (0900 LST Fri 31 Jul 98)
at sigma - 0.995



Post: *****
Temperature
Sea-level pressure

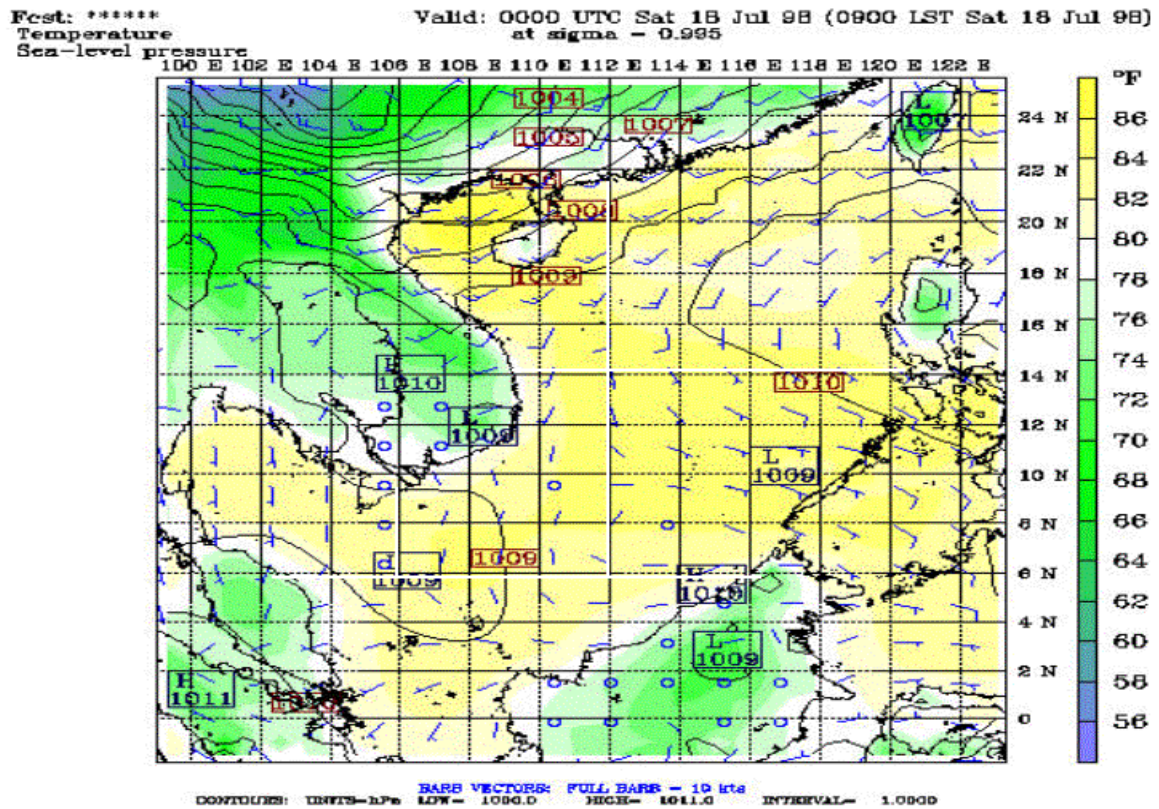
Valid: 1200 UTC Fri 31 Jul 98 (2100 LST Fri 31 Jul 98)
at sigma = 0.985



THIS PAGE INTENTIONALLY LEFT BLANK

APPENDIX Z. SEA LEVEL PRESSURE/SAT/SURFACE WIND PLOTS FOR THE SCS FOR THE JULY TIME PERIOD

Appendix Z consists of 28 figures that show sea level pressure, SAT, and surface winds for the July time period over the SCS. The figures are in time sequential order from July 18 through July 31.



Fcst: *****

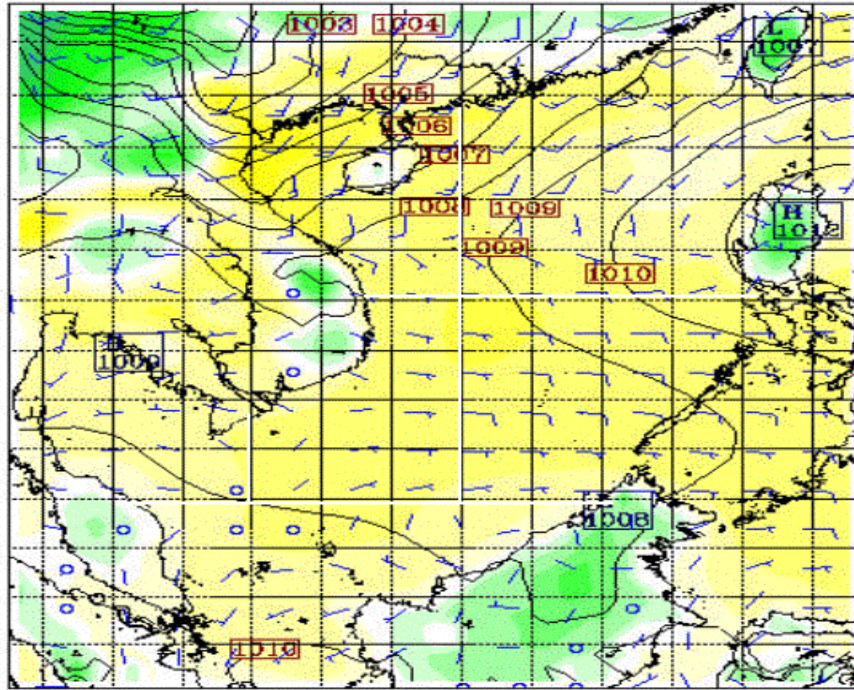
Valid: 1200 UTC Sat 18 Jul 98 (2100 LST Sat 18 Jul 98)

Temperature

at sigma - 0.995

Sea-level pressure

100 E 102 E 104 E 106 E 108 E 110 E 112 E 114 E 116 E 118 E 120 E 122 E



CONTOUTES: UNITS-hPa LOW- 1000.0 HIGH- 1011.0 INTERVAL- 1.0000
BARS VECTORS: FULL BARS - 10 kts

Fcst: *****

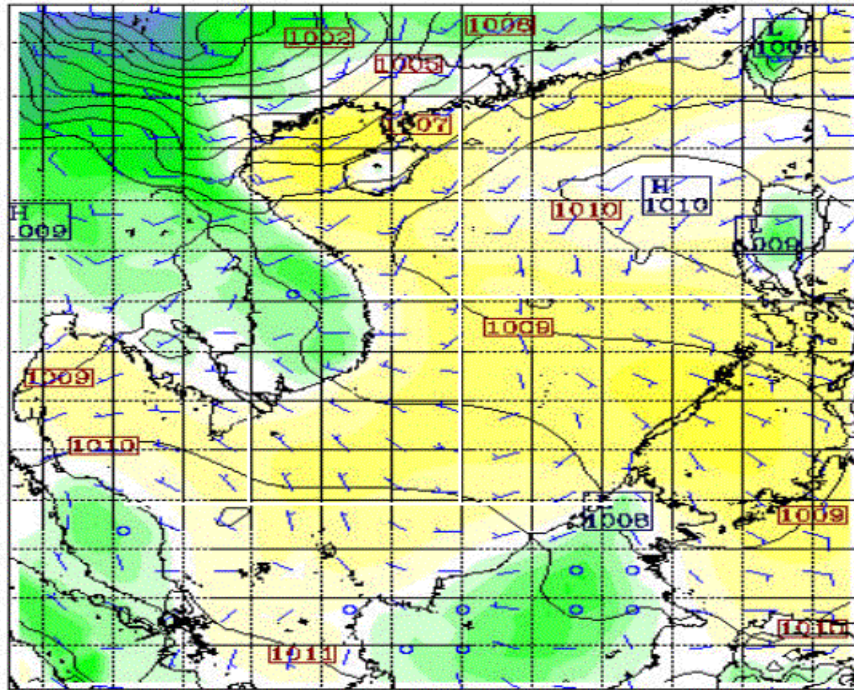
Valid: 0000 UTC Sun 19 Jul 98 (0900 LST Sun 19 Jul 98)

Temperature

at sigma - 0.995

Sea-level pressure

100 E 102 E 104 E 106 E 108 E 110 E 112 E 114 E 116 E 118 E 120 E 122 E



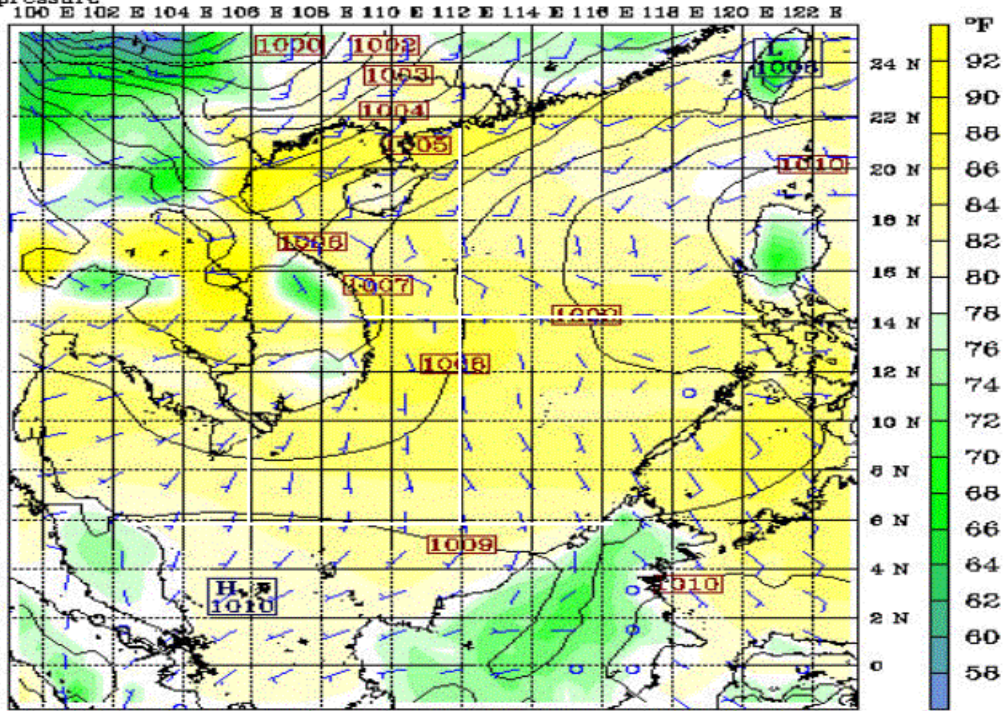
CONTOUTES: UNITS-hPa LOW- 999.00 HIGH- 1011.0 INTERVAL- 1.0000
BARS VECTORS: FULL BARS - 10 kts

Fcst: *****

Valid: 1200 UTC Sun 19 Jul 98 (2100 LST Sun 19 Jul 98)
at sigma - 0.995

Temperature

Sea-level pressure



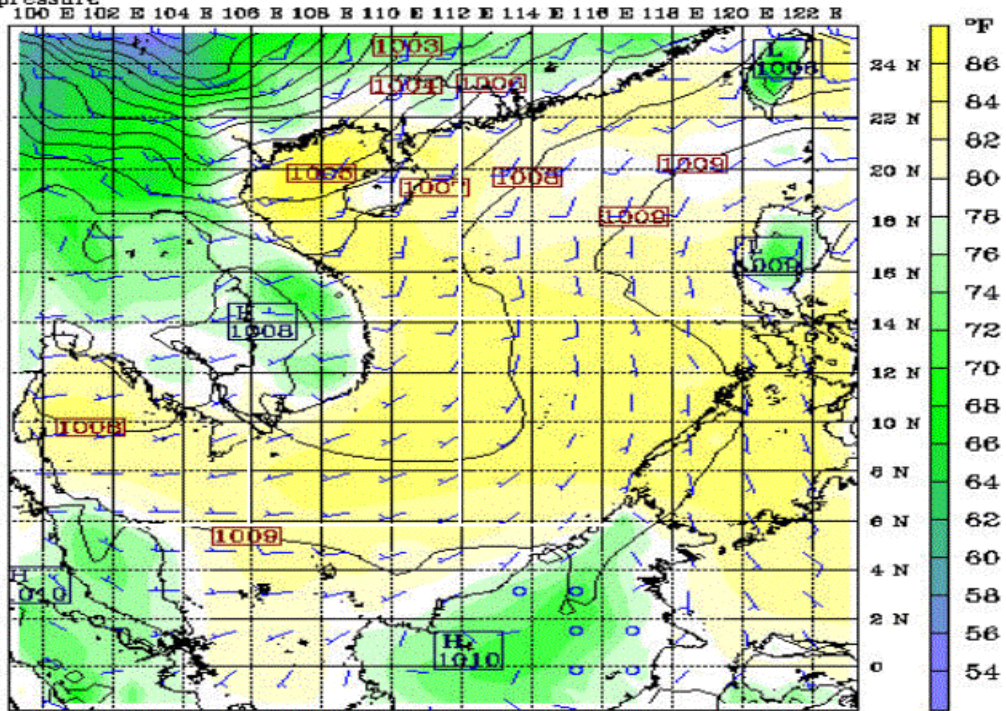
CONTOURS: UNITS-hPa LOW- 998.00 HIGH- 1011.0 INTERVAL- 1.0000
BARS VECTORS: FULL BARS - 10 kts

Fcst: *****

Valid: 0000 UTC Mon 20 Jul 98 (0900 LST Mon 20 Jul 98)
at sigma - 0.995

Temperature

Sea-level pressure



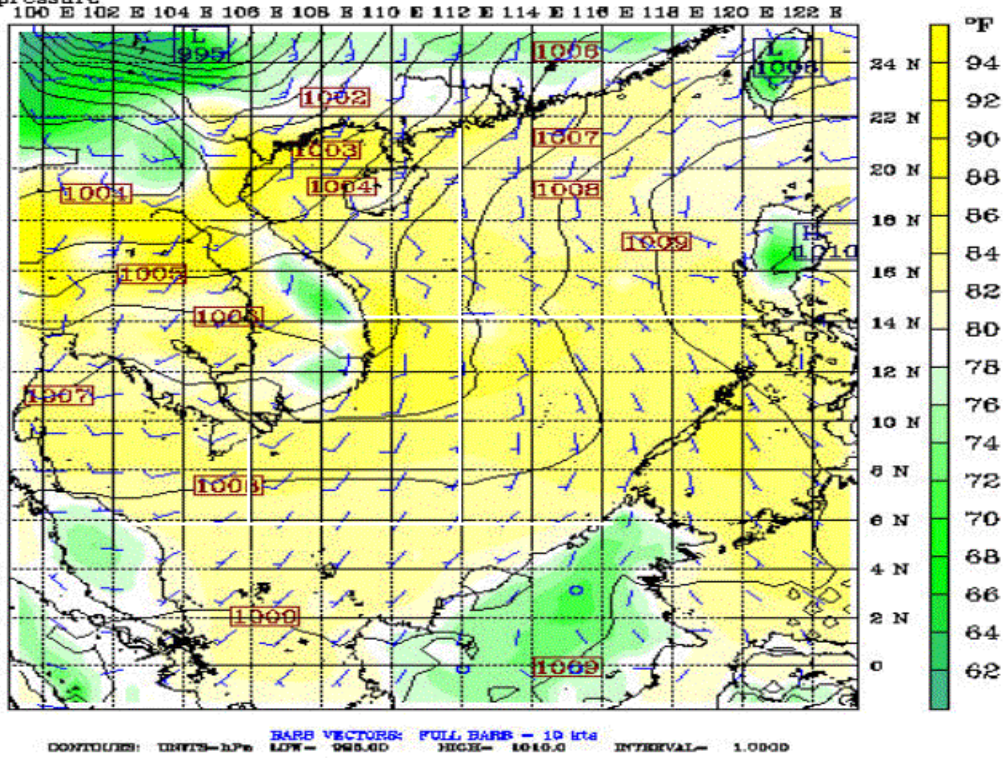
CONTOURS: UNITS-hPa LOW- 997.00 HIGH- 1010.0 INTERVAL- 1.0000
BARS VECTORS: FULL BARS - 10 kts

Fcst: *****

Temperature

Sea-level pressure

Valid: 1200 UTC Mon 20 Jul 98 (2100 LST Mon 20 Jul 98)
at sigma - 0.995

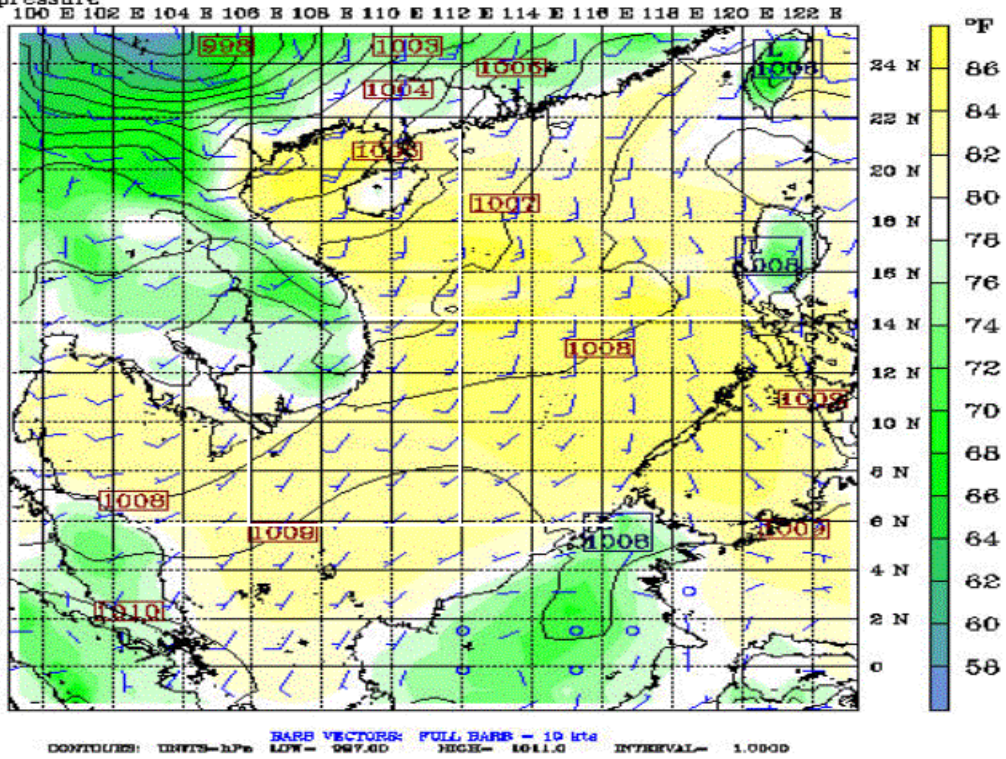


Fcst: *****

Temperature

Sea-level pressure

Valid: 0000 UTC Tue 21 Jul 98 (0900 LST Tue 21 Jul 98)
at sigma - 0.995

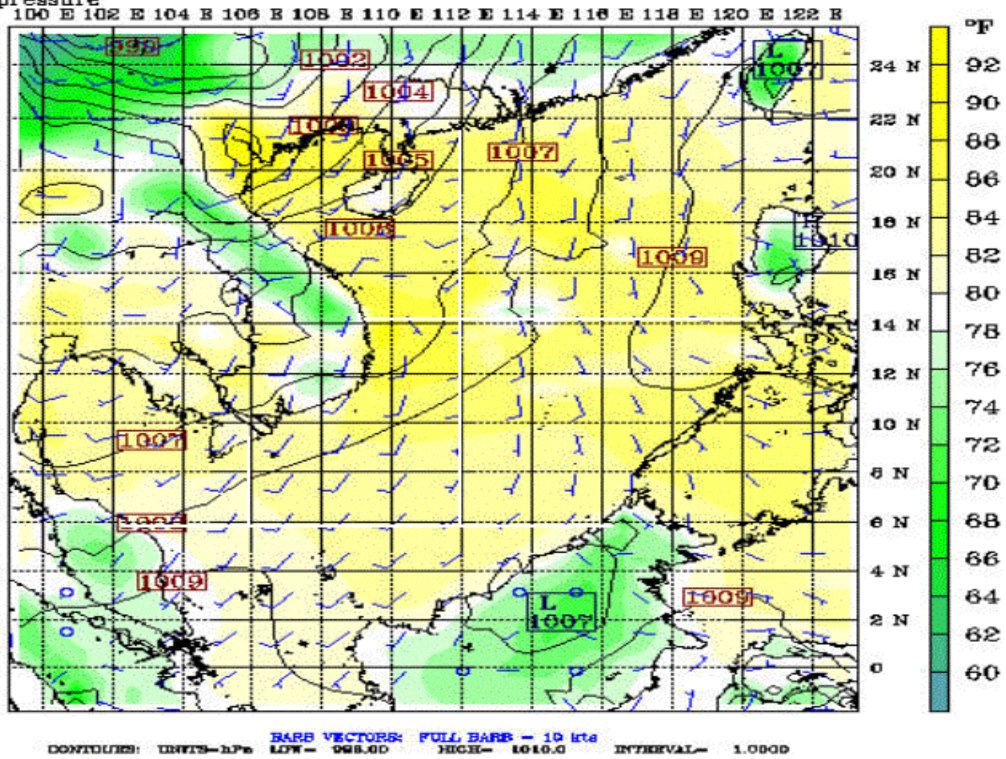


Fcst: *****

Temperature

Sea-level pressure

Valid: 1200 UTC Tue 21 Jul 98 (2100 LST Tue 21 Jul 98)
at sigma - 0.995

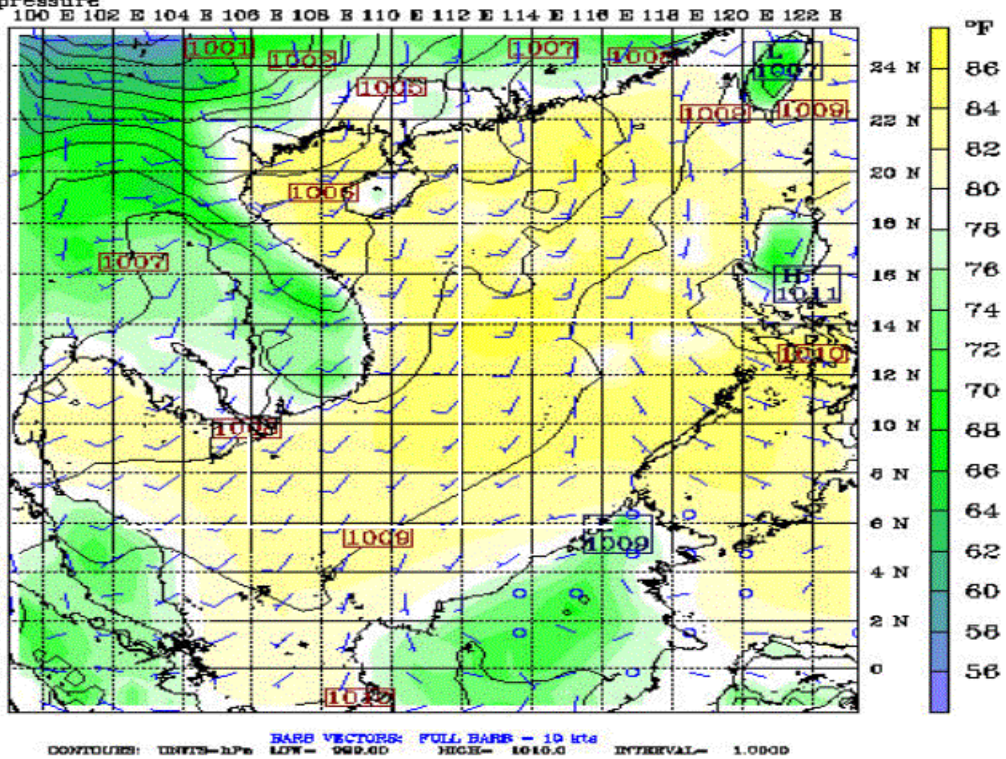


Fcst: *****

Temperature

Sea-level pressure

Valid: 0000 UTC Wed 22 Jul 98 (0900 LST Wed 22 Jul 98)
at sigma - 0.995

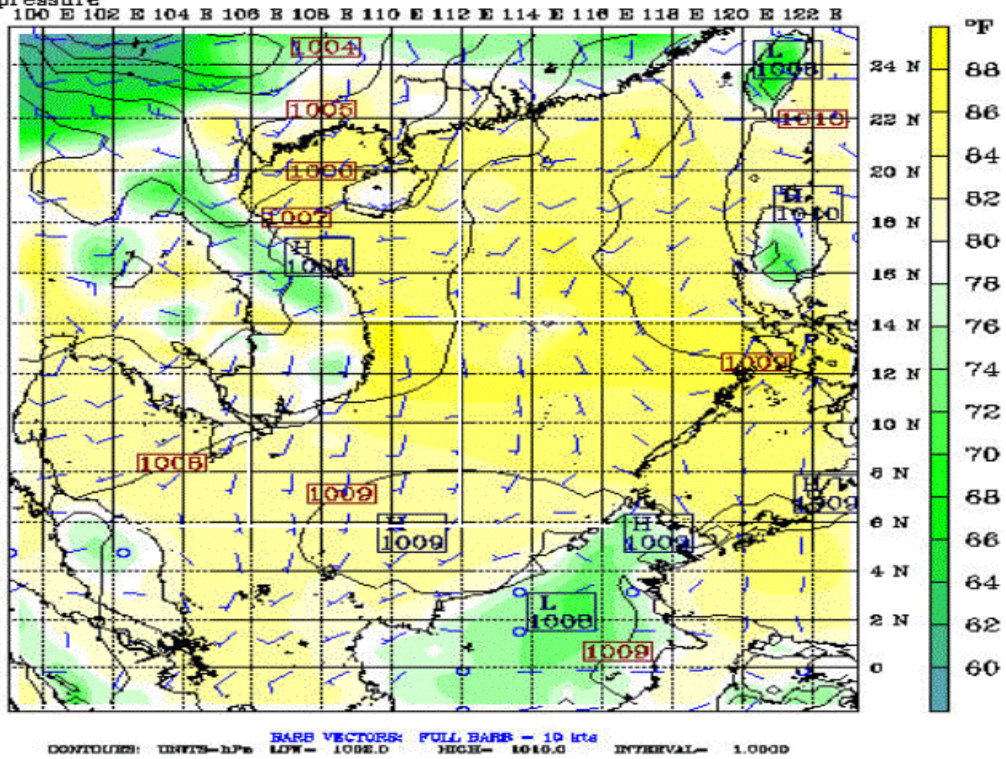


Fcst: *****

Temperature

Sea-level pressure

Valid: 1200 UTC Wed 22 Jul 98 (2100 LST Wed 22 Jul 98)
at sigma - 0.995

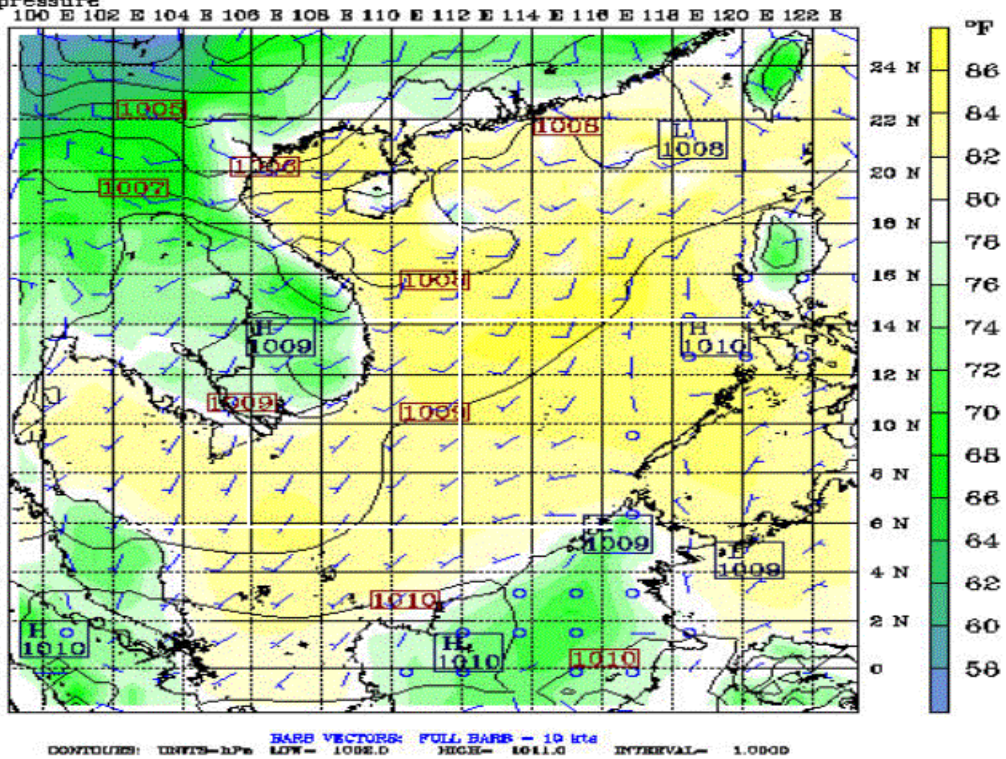


Fcst: *****

Temperature

Sea-level pressure

Valid: 0000 UTC Thu 23 Jul 98 (0900 LST Thu 23 Jul 98)
at sigma - 0.995



Fcst: *****

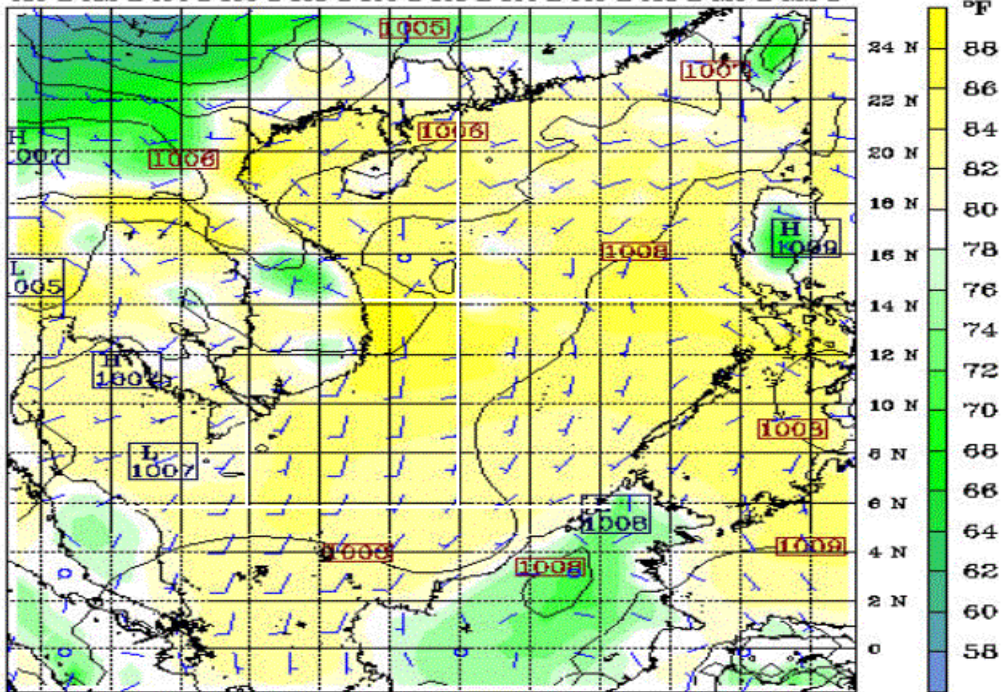
Valid: 1200 UTC Thu 23 Jul 98 (2100 LST Thu 23 Jul 98)

Temperature

at sigma - 0.995

Sea-level pressure

100 E 102 E 104 E 106 E 108 E 110 E 112 E 114 E 116 E 118 E 120 E 122 E



CONTOUTES: UNITS-hPa LOW- 1091.0 HIGH- 1010.0 INTERVAL- 1.0000
BARR VECTORS: FULL BARR - 10 kts INTERVAL- 1.0000

Fcst: *****

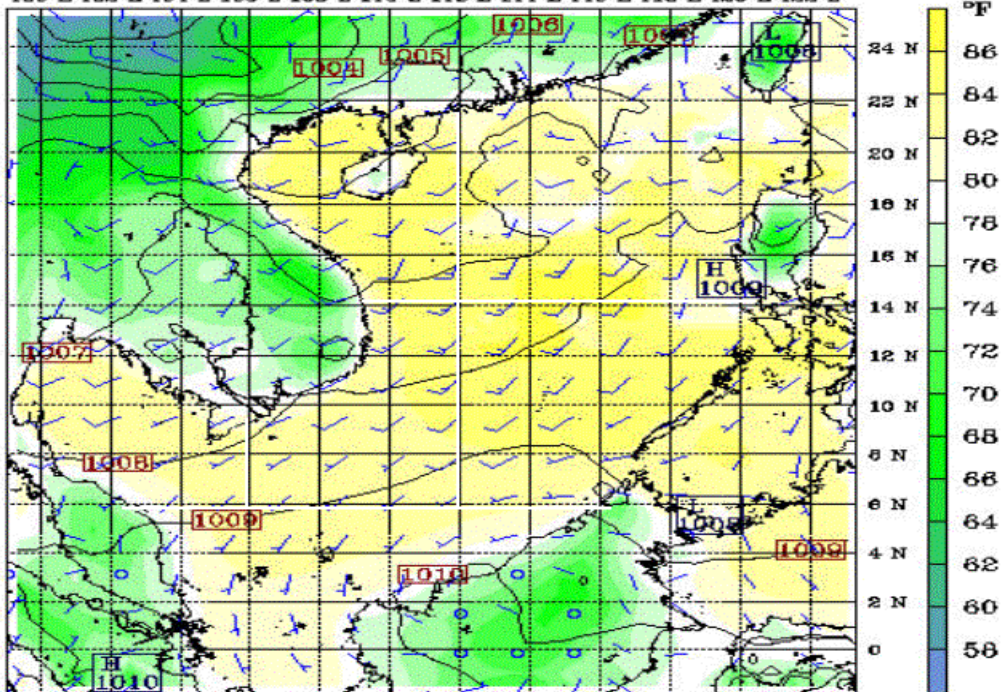
Valid: 0000 UTC Fri 24 Jul 98 (0900 LST Fri 24 Jul 98)

Temperature

at sigma - 0.995

Sea-level pressure

100 E 102 E 104 E 106 E 108 E 110 E 112 E 114 E 116 E 118 E 120 E 122 E



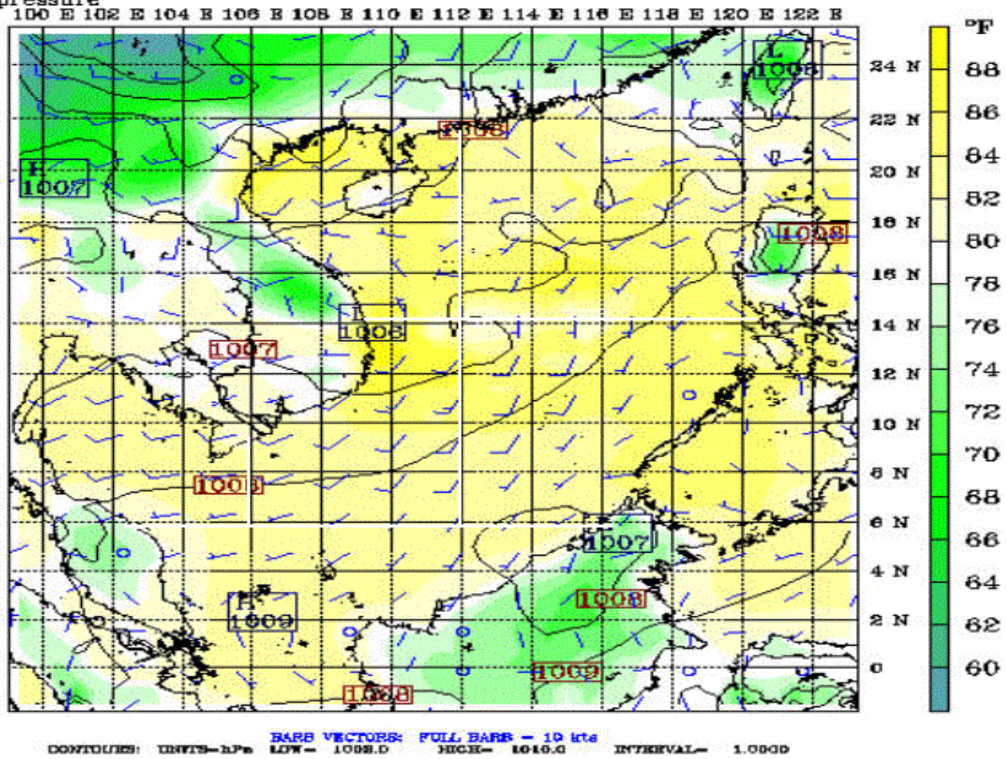
CONTOUTES: UNITS-hPa LOW- 1092.0 HIGH- 1011.0 INTERVAL- 1.0000
BARR VECTORS: FULL BARR - 10 kts INTERVAL- 1.0000

Fcst: *****

Temperature

Sea-level pressure

Valid: 1200 UTC Fri 24 Jul 98 (2100 LST Fri 24 Jul 98)
at sigma - 0.995

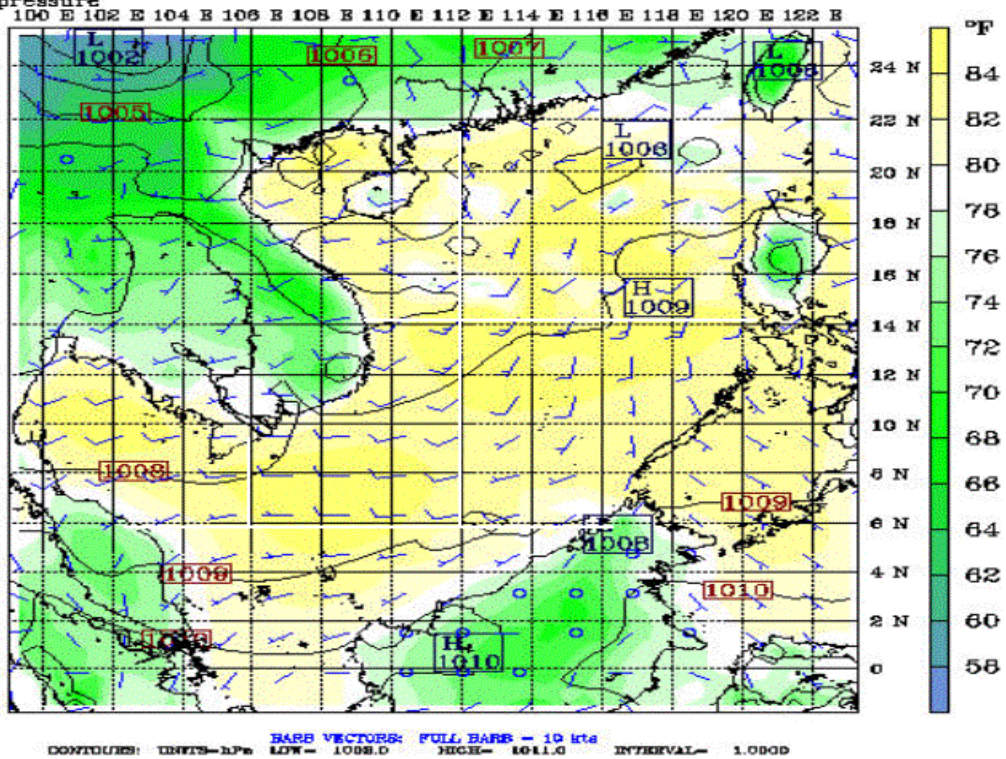


Fcst: *****

Temperature

Sea-level pressure

Valid: 0000 UTC Sat 25 Jul 98 (0900 LST Sat 25 Jul 98)
at sigma - 0.995



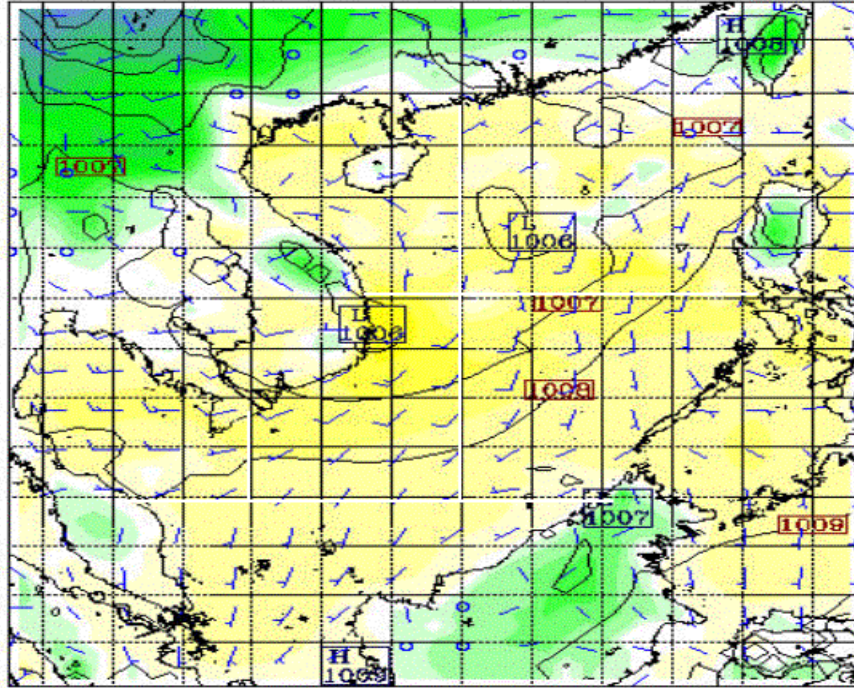
Fcst: *****

Valid: 1200 UTC Sat 25 Jul 98 (2100 LST Sat 25 Jul 98)
at sigma - 0.995

Temperature

Sea-level pressure

100 E 102 E 104 E 106 E 108 E 110 E 112 E 114 E 116 E 118 E 120 E 122 E



CONTOURS: UNITS-hPa LOW- 1098.0 HIGH- 1010.0 INTERVAL- 1.0000
BARB VECTORS: FULL BARB - 10 kts

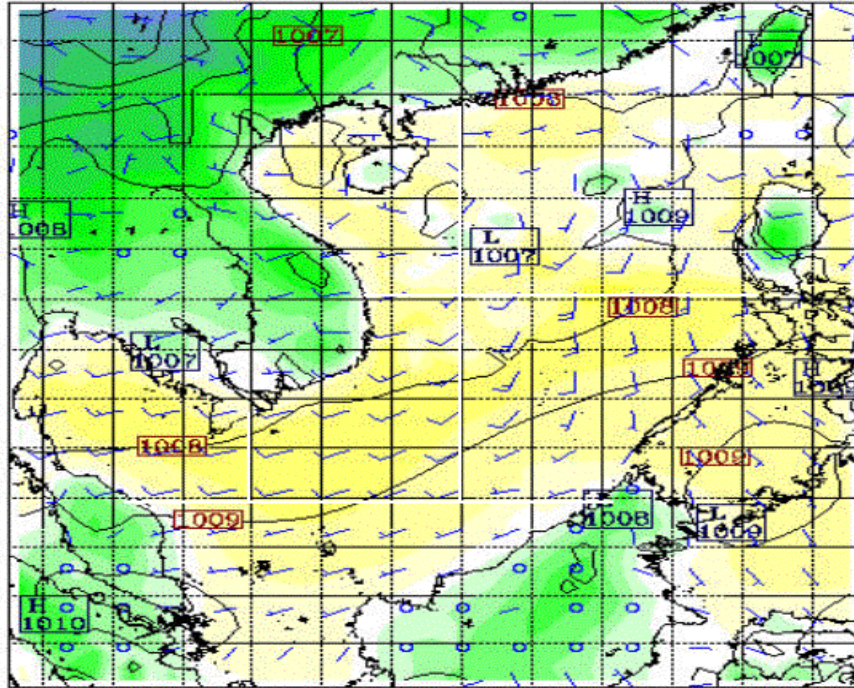
Fcst: *****

Valid: 0000 UTC Sun 26 Jul 98 (0900 LST Sun 26 Jul 98)
at sigma - 0.995

Temperature

Sea-level pressure

100 E 102 E 104 E 106 E 108 E 110 E 112 E 114 E 116 E 118 E 120 E 122 E



CONTOURS: UNITS-hPa LOW- 1098.0 HIGH- 1010.0 INTERVAL- 1.0000
BARB VECTORS: FULL BARB - 10 kts

Fcst: *****

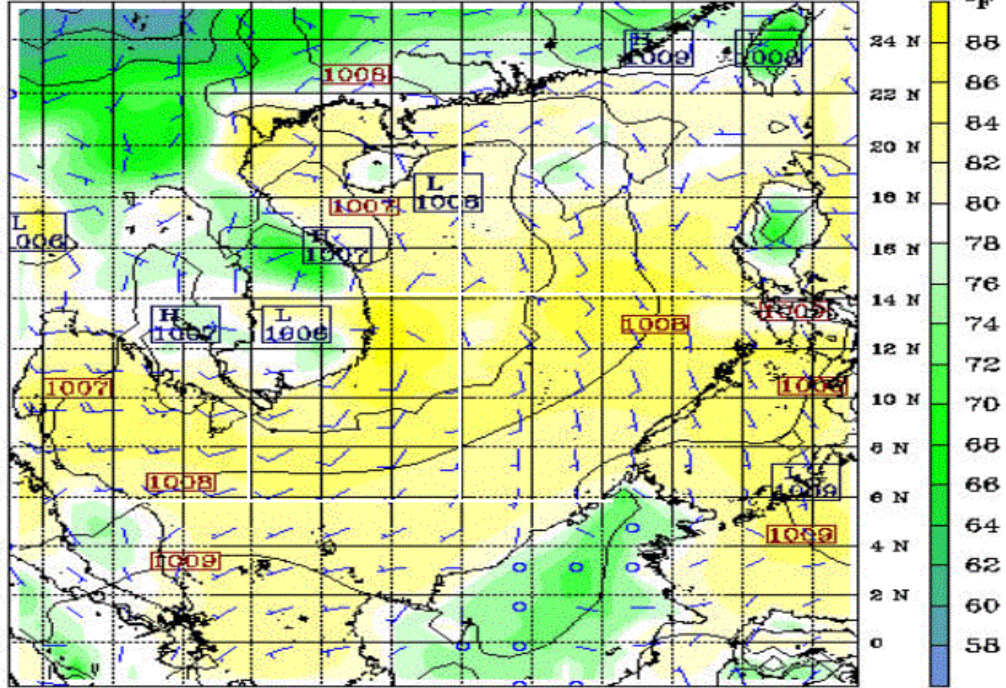
Valid: 1200 UTC Sun 26 Jul 98 (2100 LST Sun 26 Jul 98)

Temperature

at sigma - 0.995

Sea-level pressure

100 E 102 E 104 E 106 E 108 E 110 E 112 E 114 E 116 E 118 E 120 E 122 E



CONTOURS: UNITS-hPa LOW- 1004.0 HIGH- 1010.0 INTERVAL- 1.0000
BARB VECTORS: FULL BARB - 10 kts

Fcst: *****

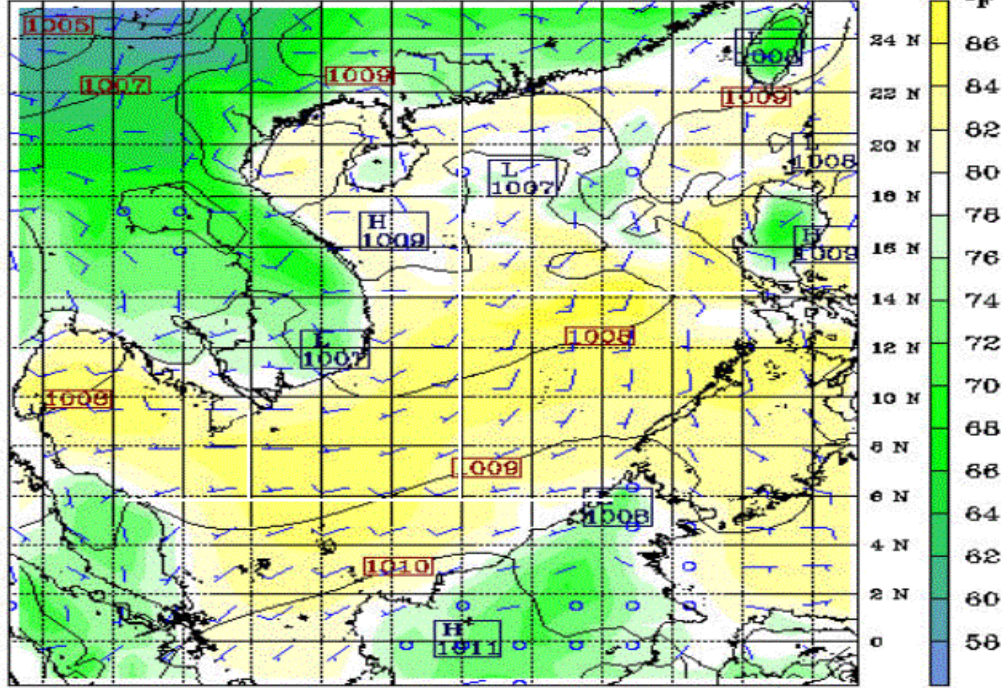
Valid: 0000 UTC Mon 27 Jul 98 (0900 LST Mon 27 Jul 98)

Temperature

at sigma - 0.995

Sea-level pressure

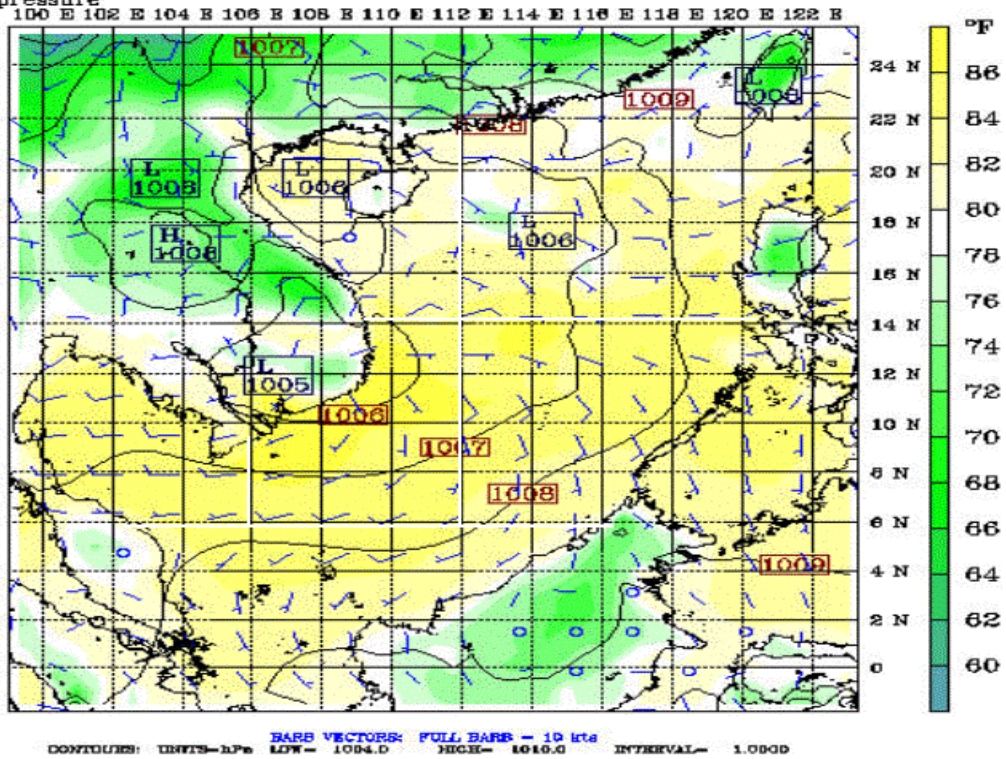
100 E 102 E 104 E 106 E 108 E 110 E 112 E 114 E 116 E 118 E 120 E 122 E



CONTOURS: UNITS-hPa LOW- 1004.0 HIGH- 1010.0 INTERVAL- 1.0000
BARB VECTORS: FULL BARB - 10 kts

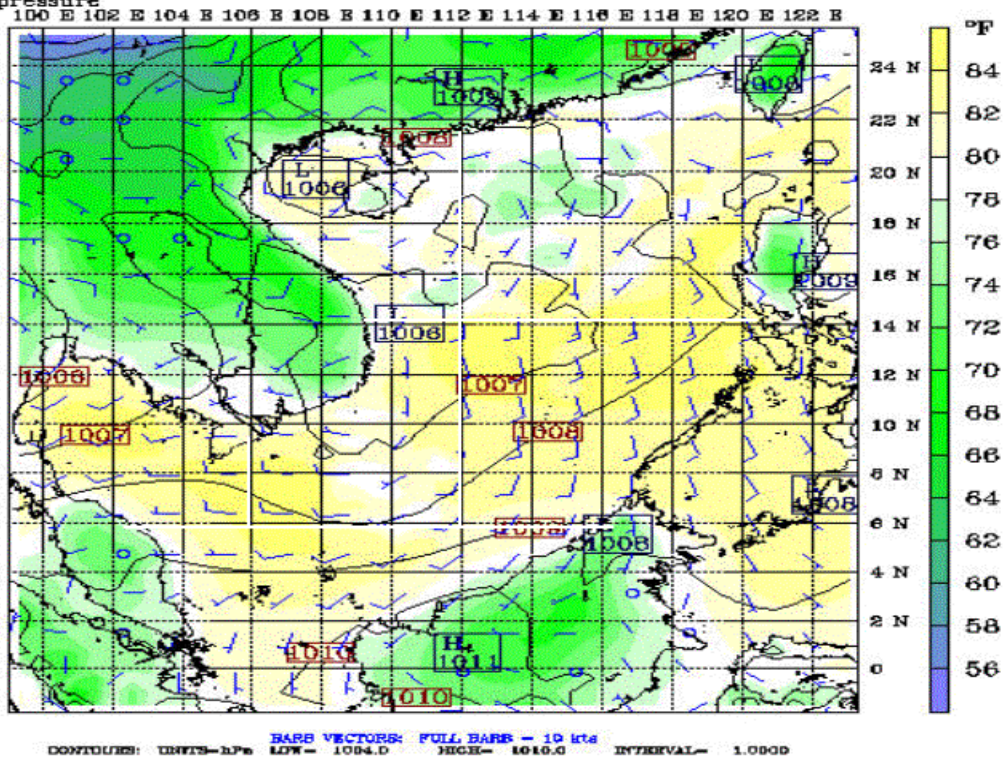
Fcst: *****
Temperature
Sea-level pressure

Valid: 1200 UTC Mon 27 Jul 98 (2100 LST Mon 27 Jul 98)
at sigma - 0.995



Fcst: *****
Temperature
Sea-level pressure

Valid: 0000 UTC Tue 28 Jul 98 (0900 LST Tue 28 Jul 98)
at sigma - 0.995

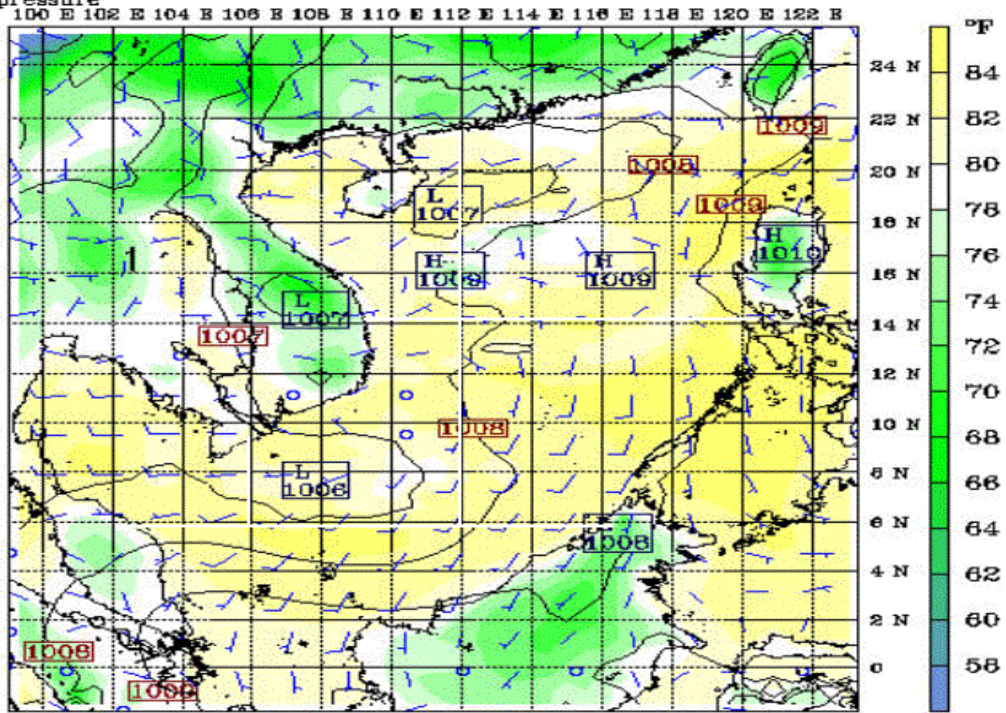


Fcst: *****

Temperature

Sea-level pressure

Valid: 1200 UTC Tue 28 Jul 98 (2100 LST Tue 28 Jul 98)
at sigma - 0.995



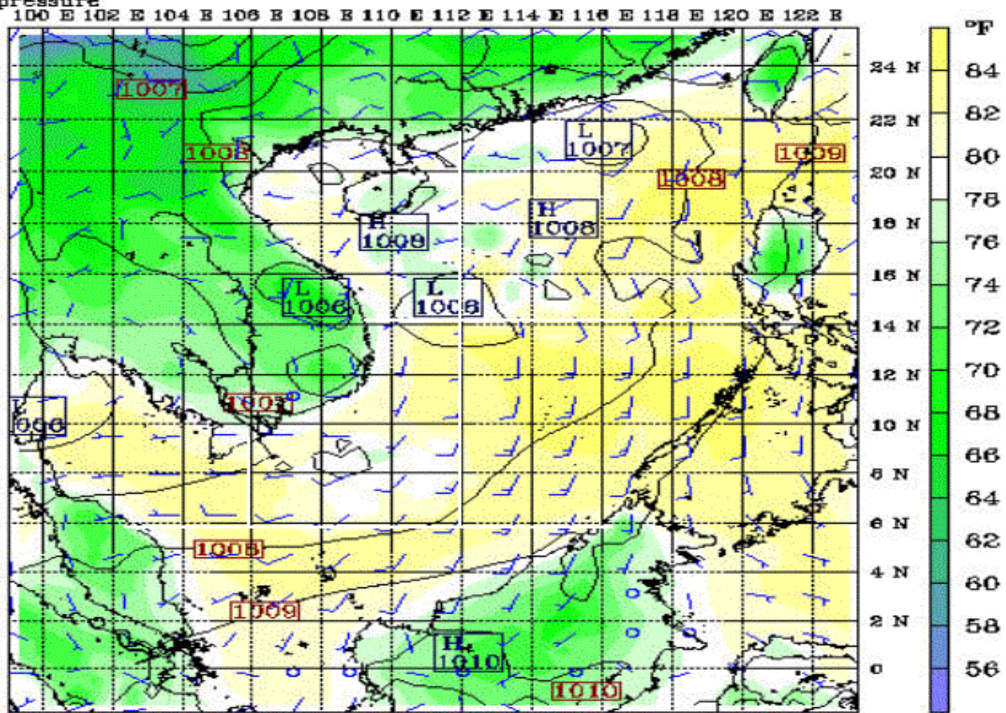
CONTIGUES: UNITS-hPa BARS VECTORS: FULL BARS - 10 kts
LOW- 1005.0 HIGH- 1010.0 INTERVAL- 1.0000

Fcst: *****

Temperature

Sea-level pressure

Valid: 0000 UTC Wed 29 Jul 98 (0900 LST Wed 29 Jul 98)
at sigma - 0.995



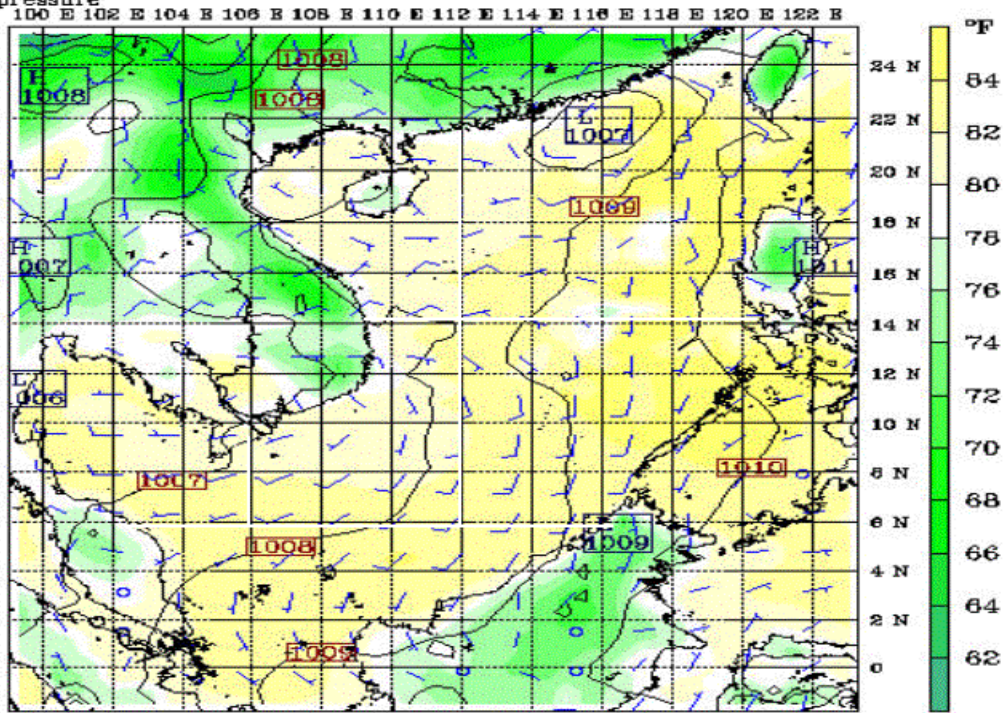
CONTIGUES: UNITS-hPa BARS VECTORS: FULL BARS - 10 kts
LOW- 1005.0 HIGH- 1010.0 INTERVAL- 1.0000

Fcst: *****

Valid: 1200 UTC Wed 29 Jul 98 (2100 LST Wed 29 Jul 98)
at sigma - 0.995

Temperature

Sea-level pressure



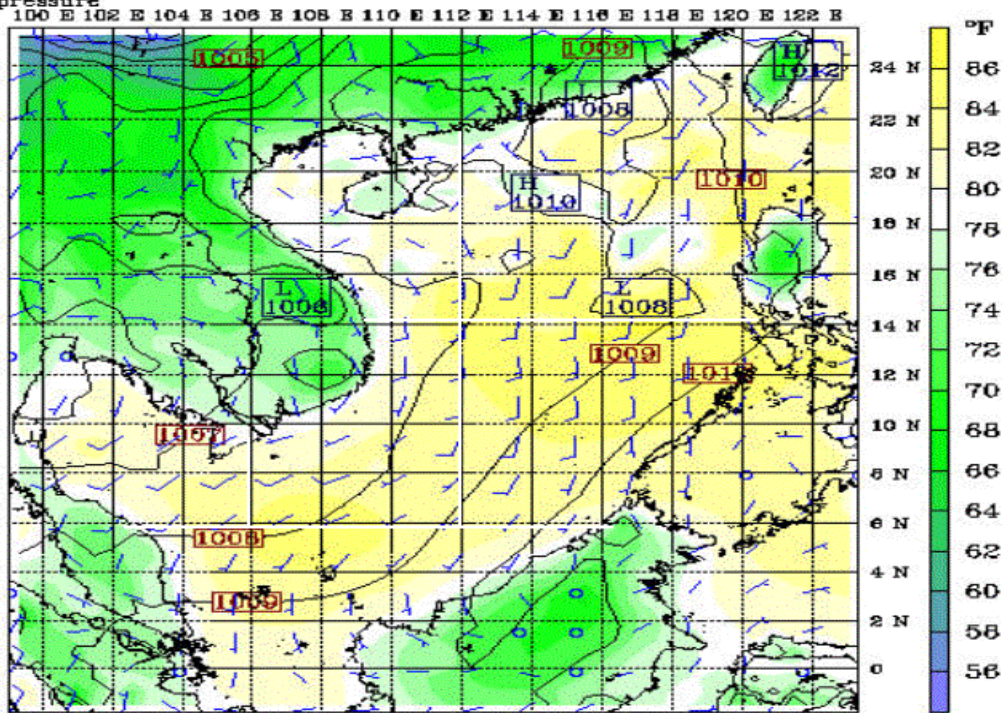
CONTOURS: UNITS-hPa LOW- 1005.0 HIGH- 1011.0 INTERVAL- 1.0000
BARB VECTORS: FULL BARB - 10 kts

Fcst: *****

Valid: 0000 UTC Thu 30 Jul 98 (0900 LST Thu 30 Jul 98)
at sigma - 0.995

Temperature

Sea-level pressure



CONTOURS: UNITS-hPa LOW- 1005.0 HIGH- 1011.0 INTERVAL- 1.0000
BARB VECTORS: FULL BARB - 10 kts

Fcst: *****

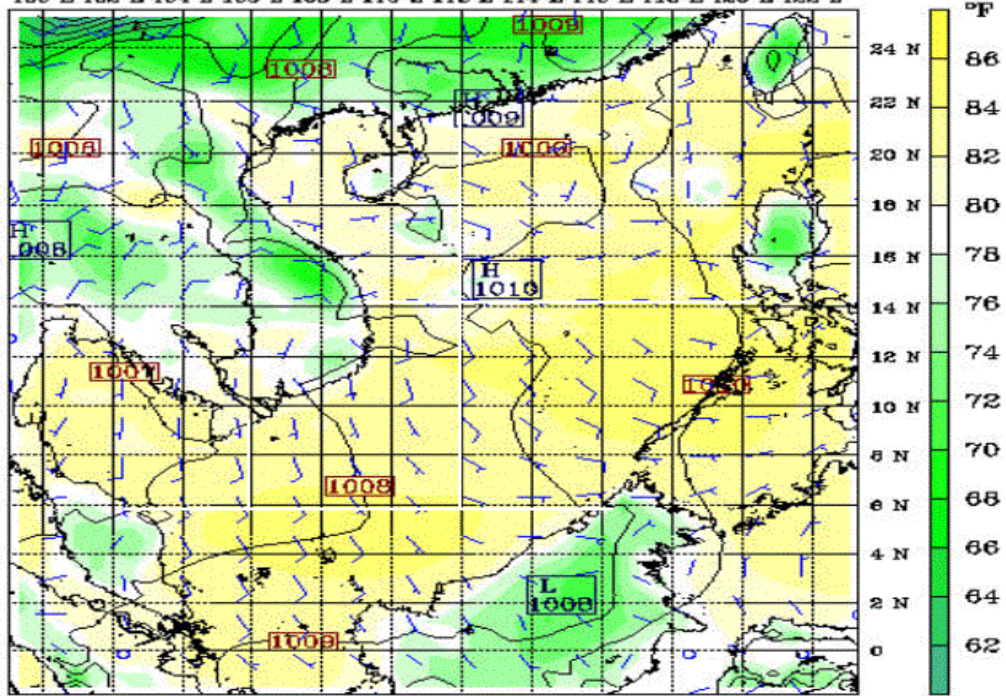
Valid: 1200 UTC Thu 30 Jul 98 (2100 LST Thu 30 Jul 98)

Temperature

at sigma - 0.995

Sea-level pressure

100 E 102 E 104 E 106 E 108 E 110 E 112 E 114 E 116 E 118 E 120 E 122 E



CONTOURS: UNITS-hPa LOW- 1002.0 HIGH- 1013.0 INTERVAL- 1.0000
BARS VECTORS: FULL BARS - 10 kts

Fcst: *****

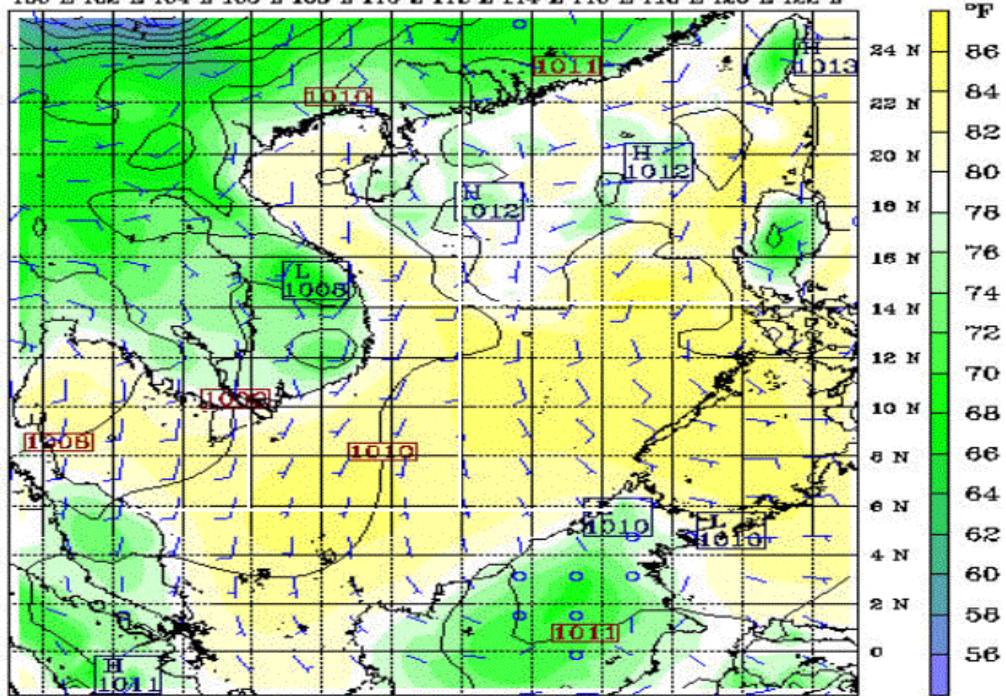
Valid: 0000 UTC Fri 31 Jul 98 (0900 LST Fri 31 Jul 98)

Temperature

at sigma - 0.995

Sea-level pressure

100 E 102 E 104 E 106 E 108 E 110 E 112 E 114 E 116 E 118 E 120 E 122 E



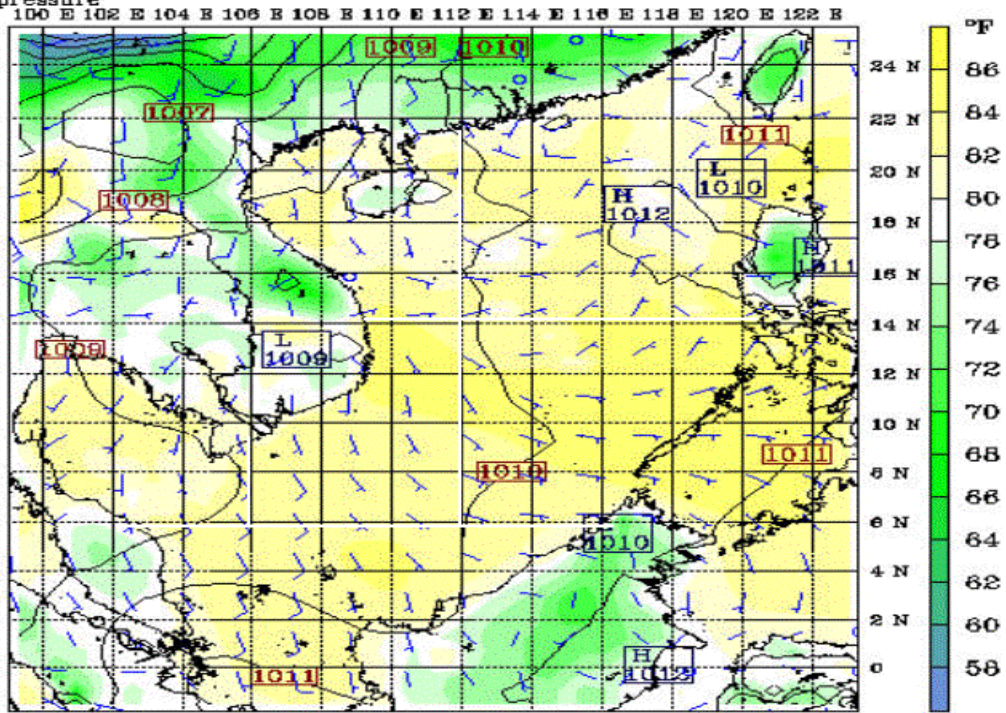
CONTOURS: UNITS-hPa LOW- 1002.0 HIGH- 1013.0 INTERVAL- 1.0000
BARS VECTORS: FULL BARS - 10 kts

Fcst: *****

Temperature

Sea-level pressure

Valid: 1200 UTC Fri 31 Jul 98 (2100 LST Fri 31 Jul 98)
at sigma - 0.995

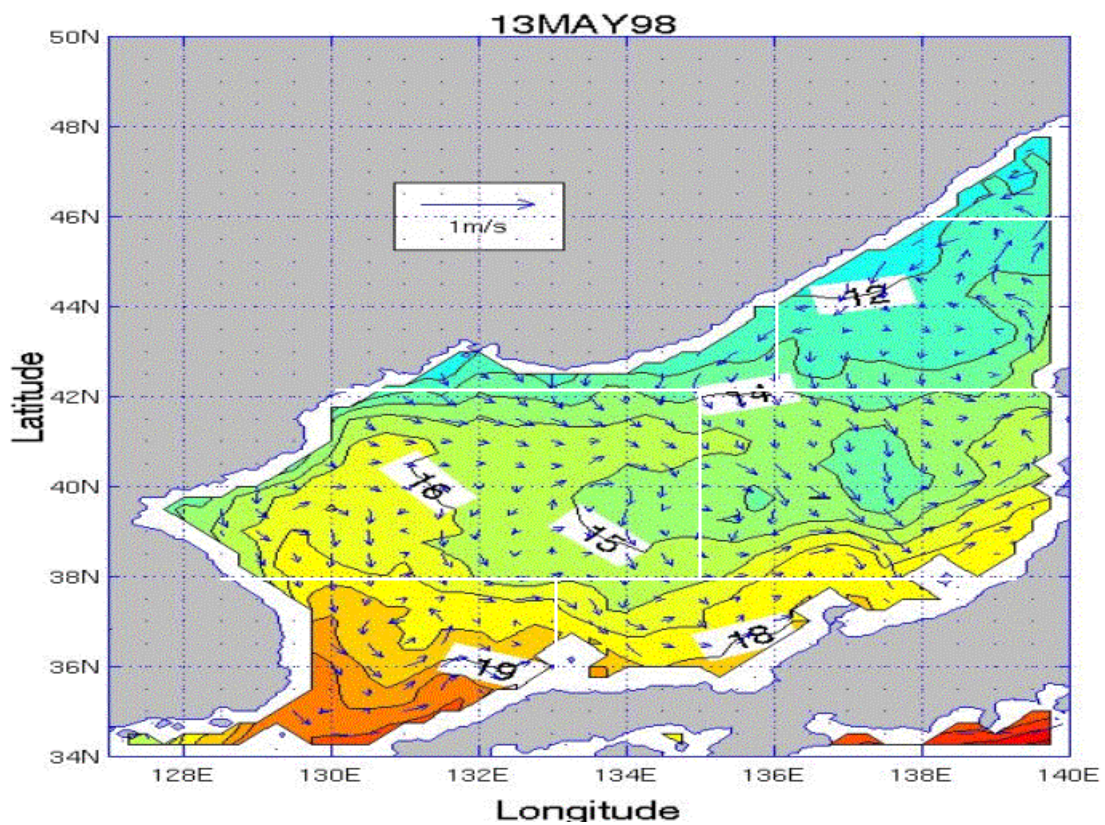


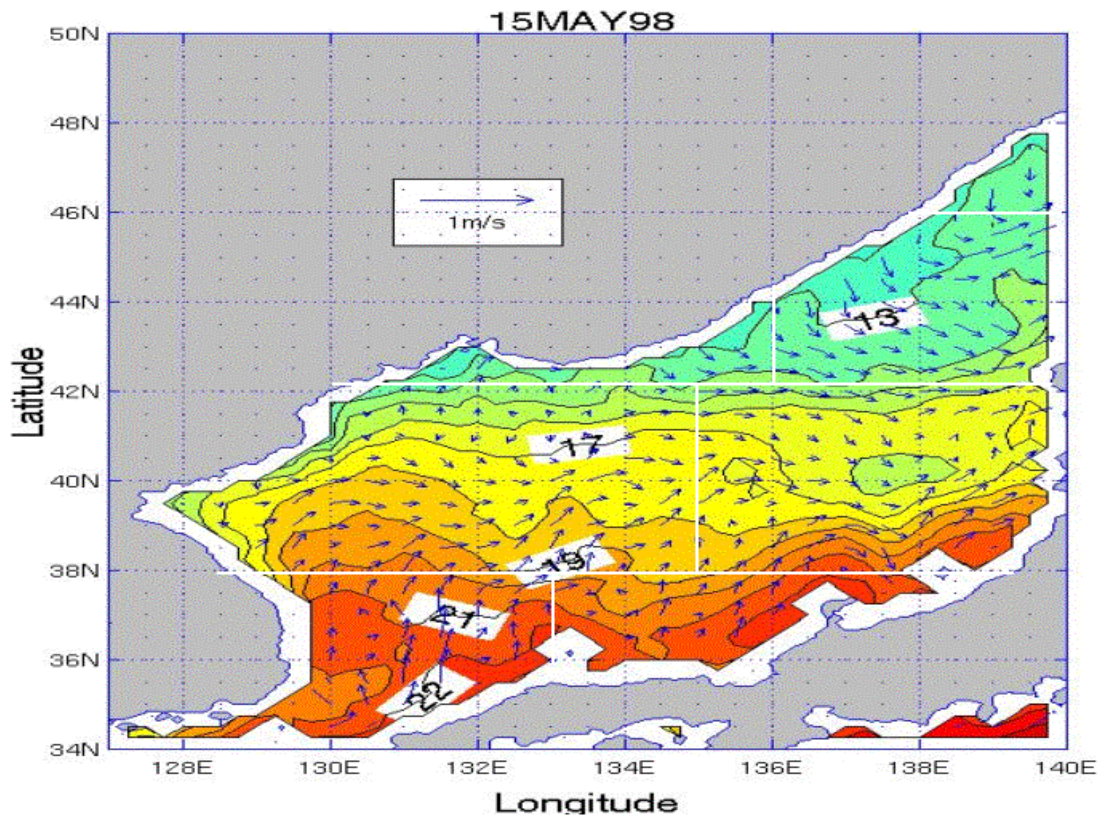
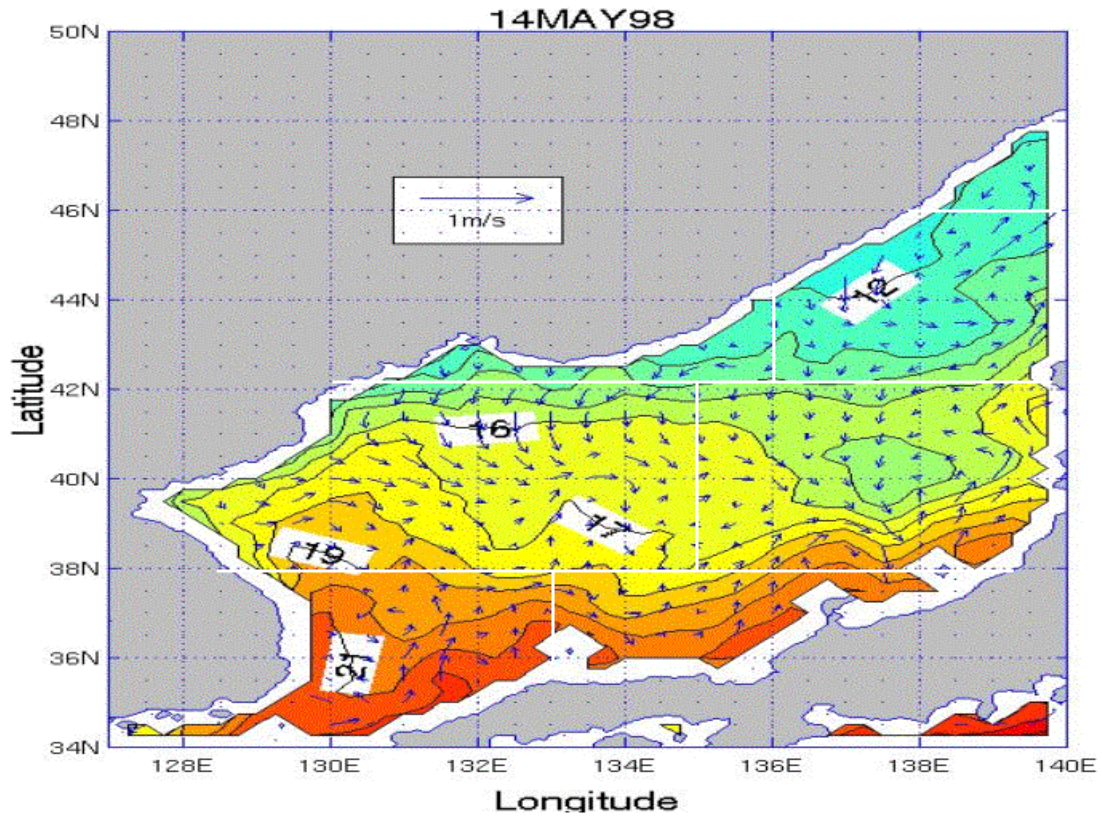
CONTIGUES: UNITS-hPa BARS VECTORS: FULL BARS - 10 kts
LOW- 1002.0 HIGH- 1012.0 INTERVAL- 1.0000

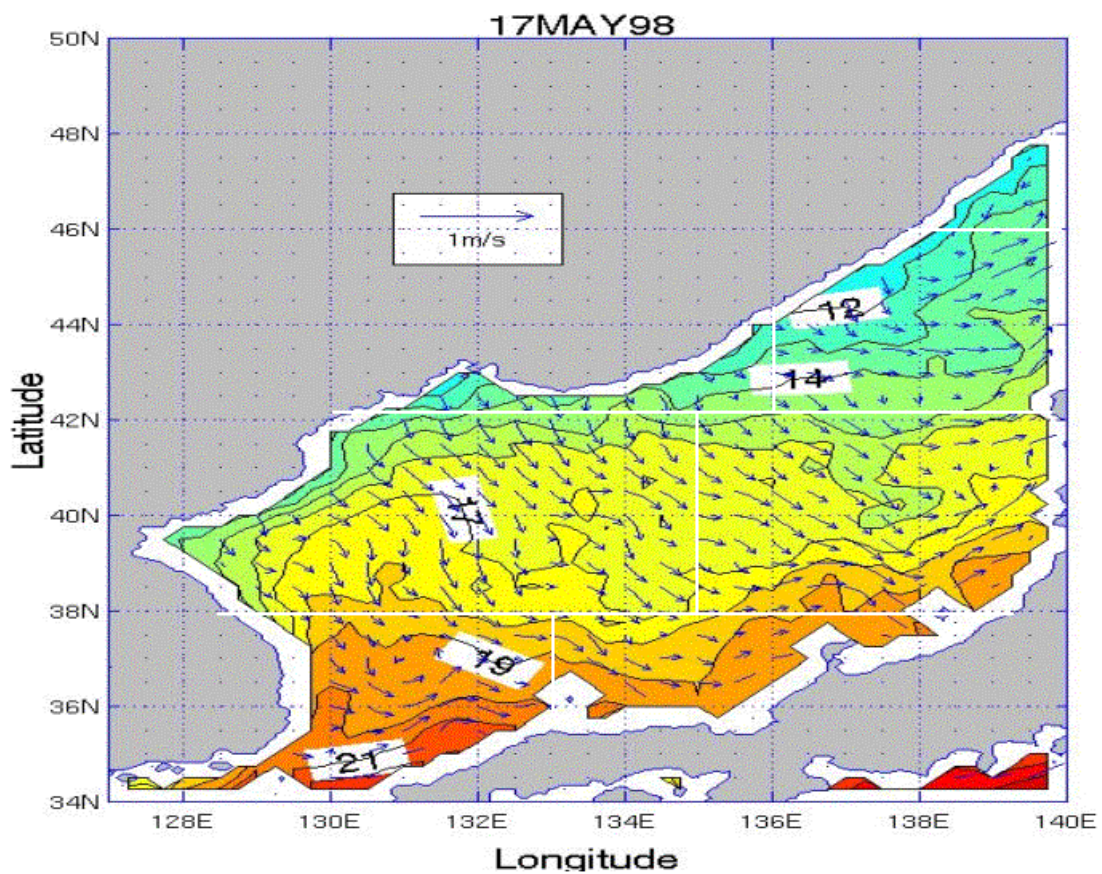
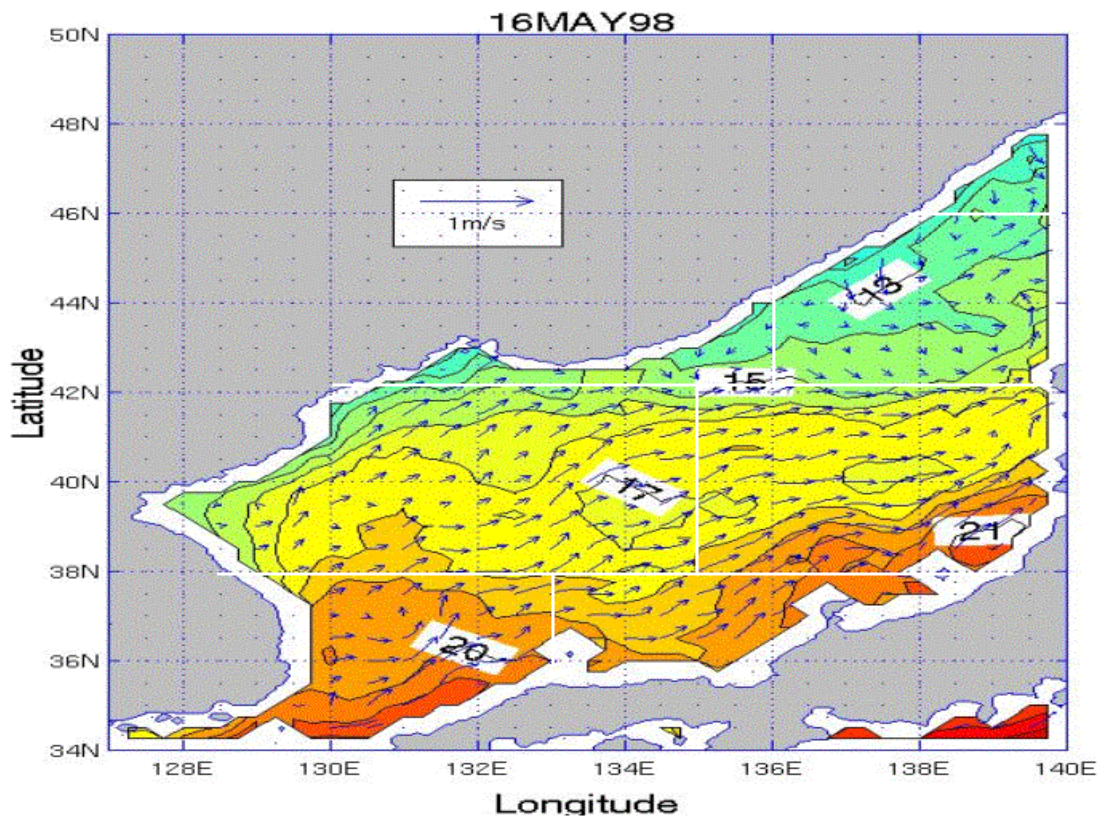
THIS PAGE INTENTIONALLY LEFT BLANK

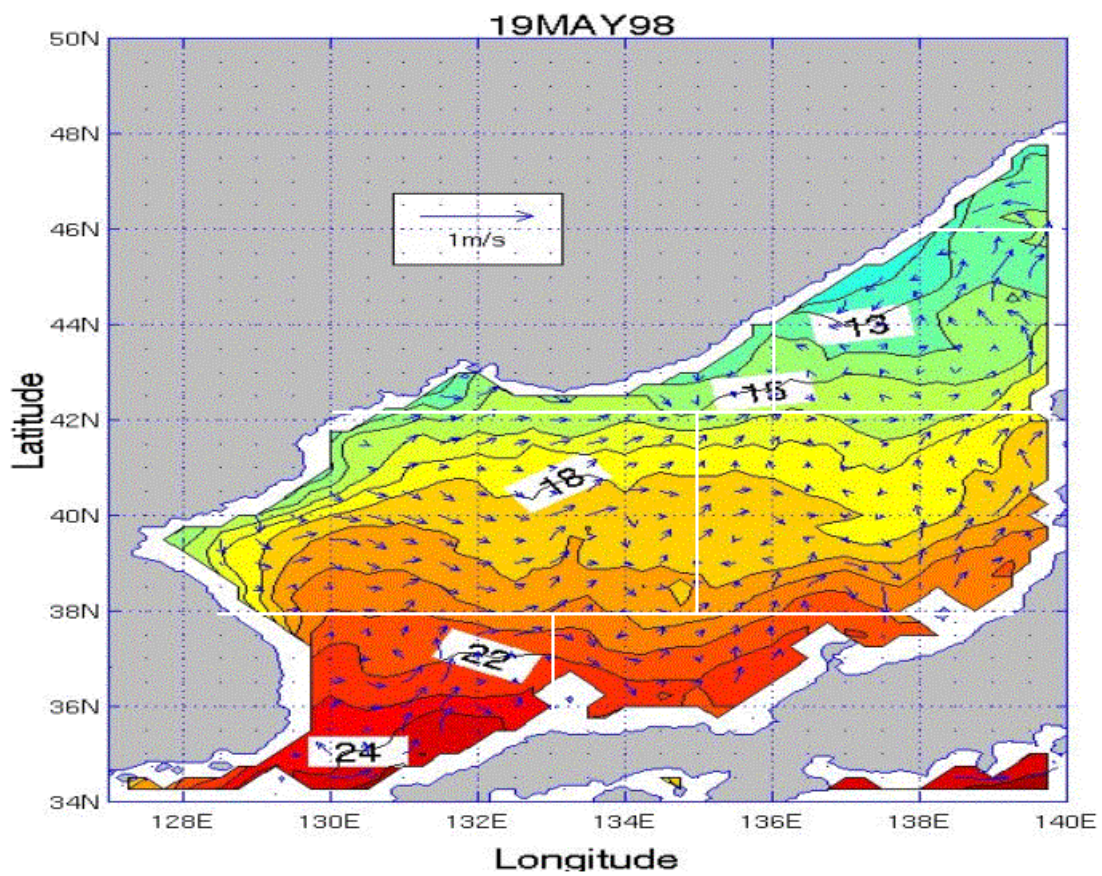
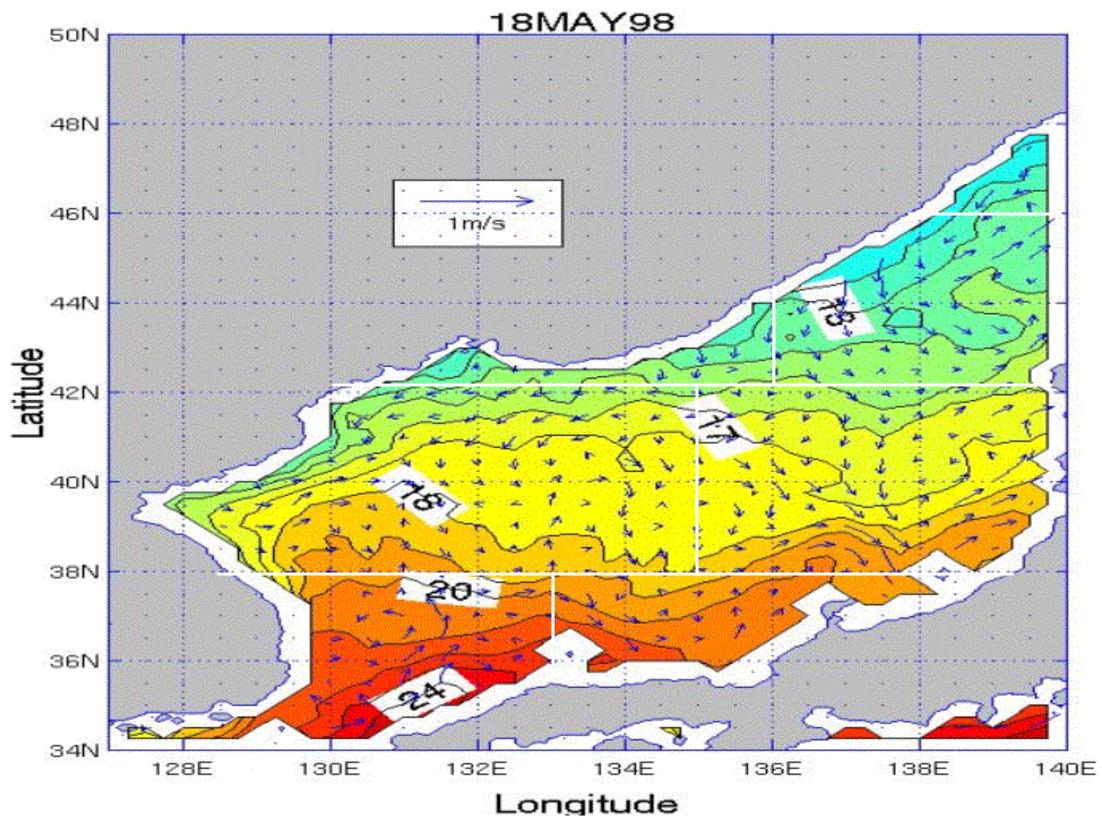
APPENDIX AA. SST AND SURFACE CURRENT VELOCITY PLOTS FOR THE JES FOR THE MAY TIME PERIOD

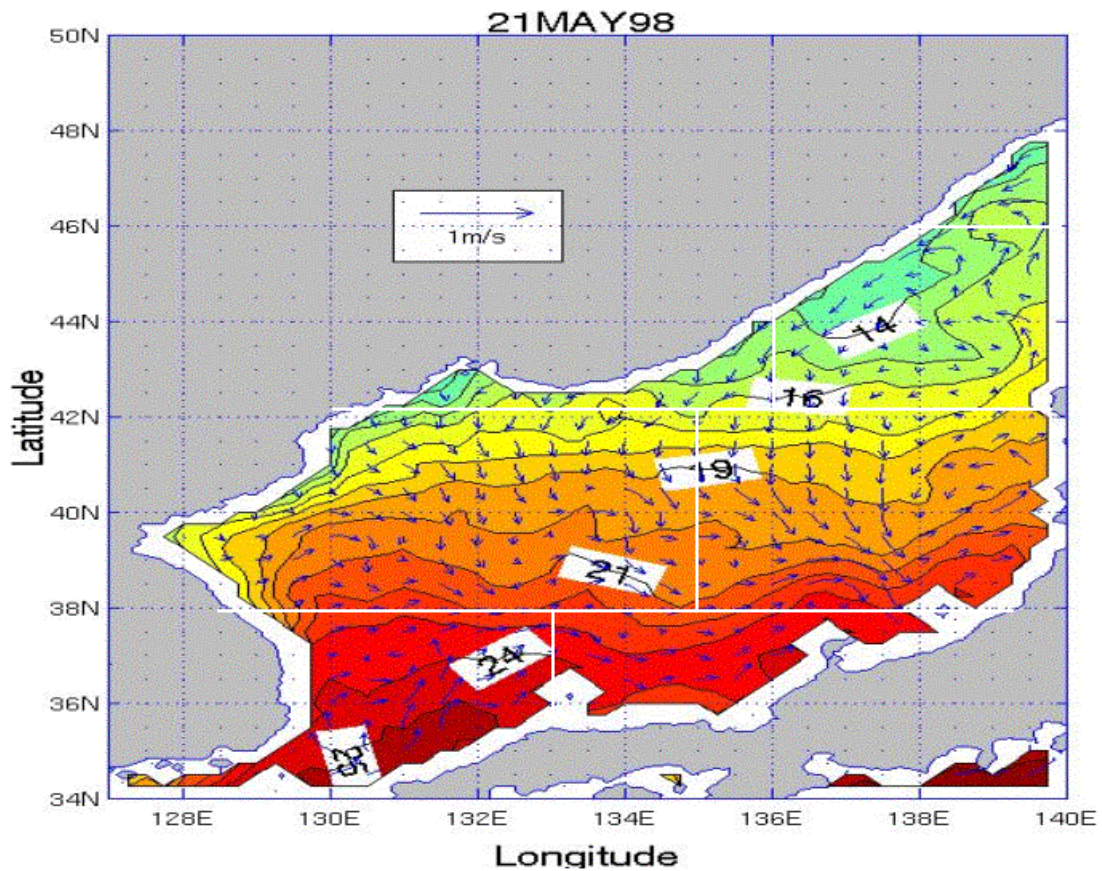
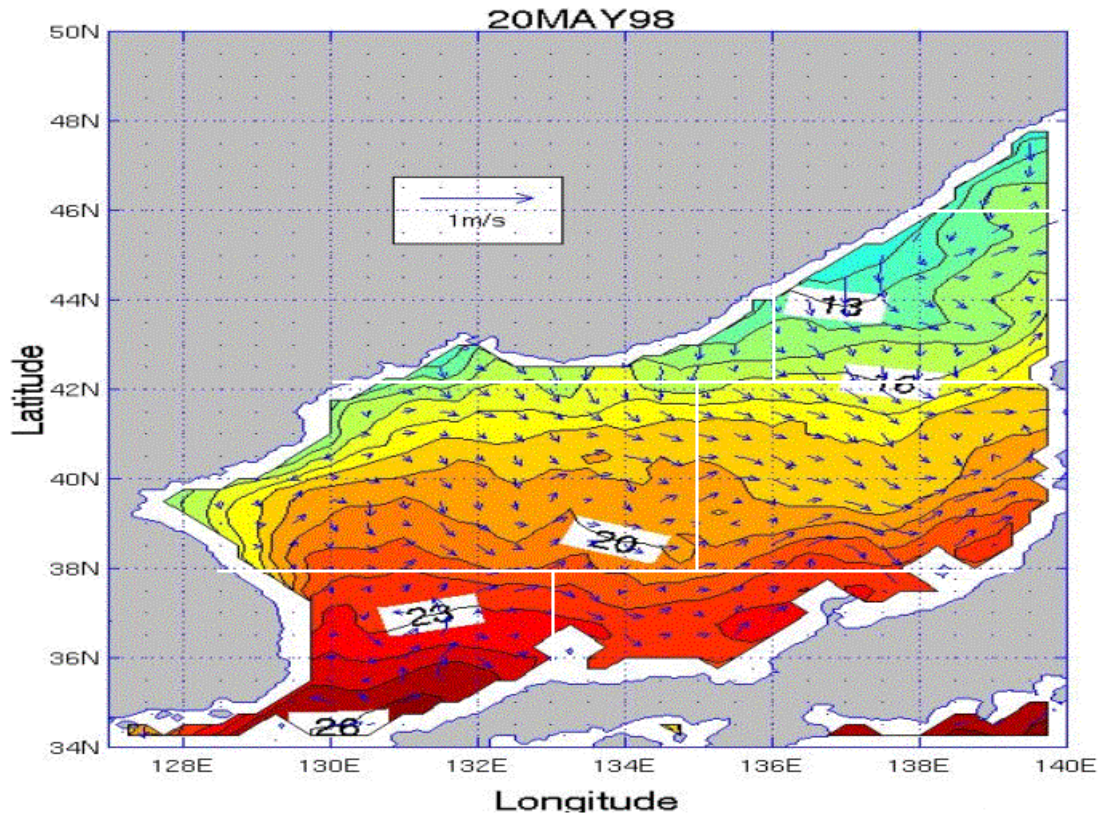
Appendix AA consists of 19 figures that show SST and surface current velocity for each day of the May time period for the JES. The figures are in time sequential order from May 13 through May 31.

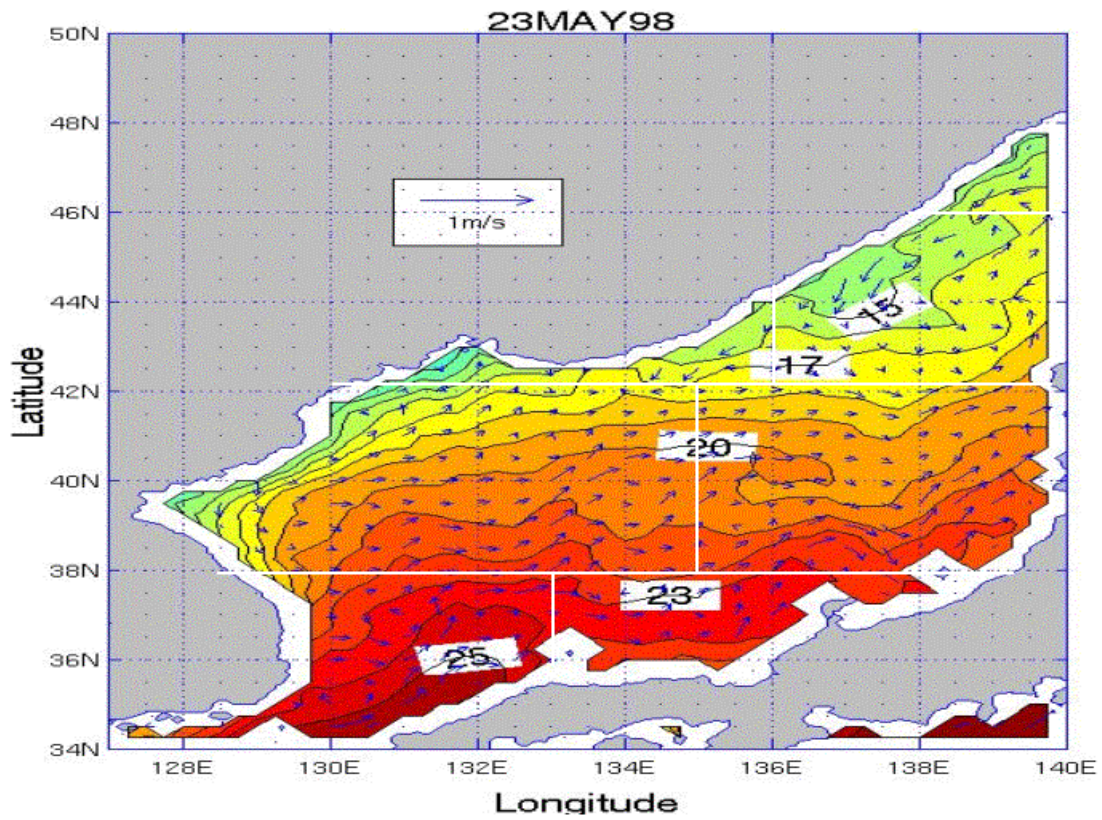
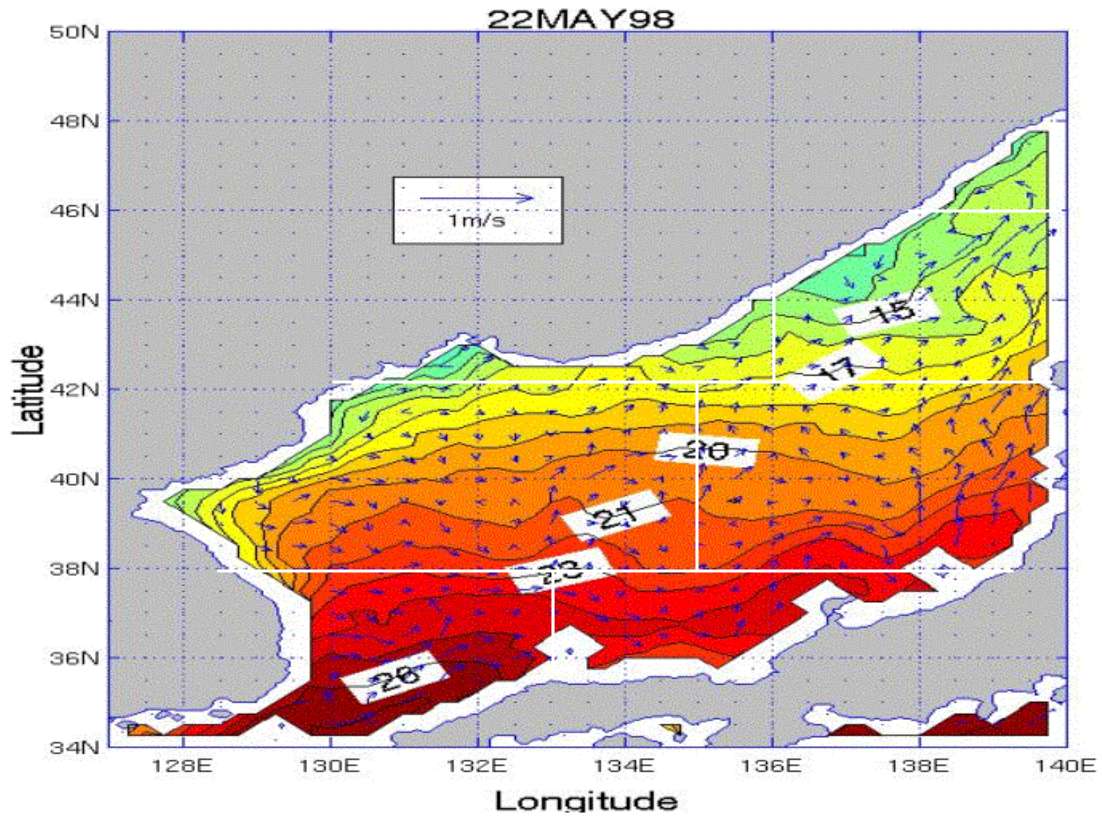


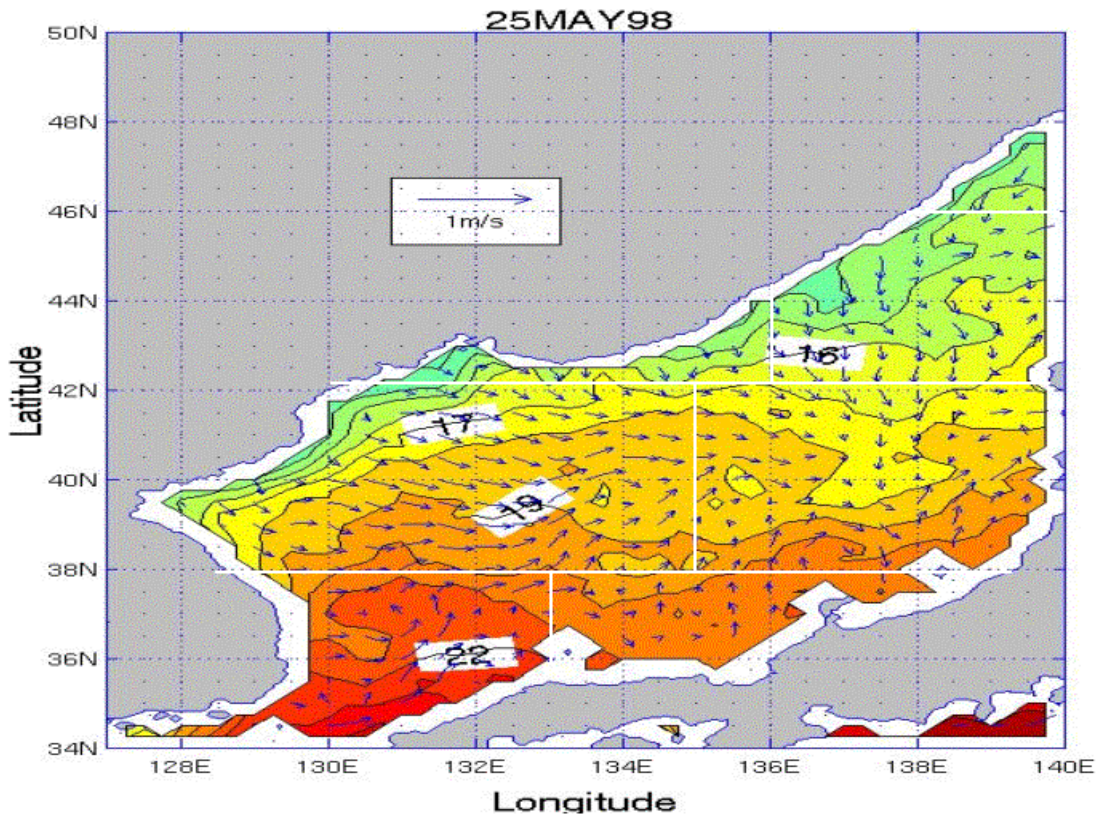
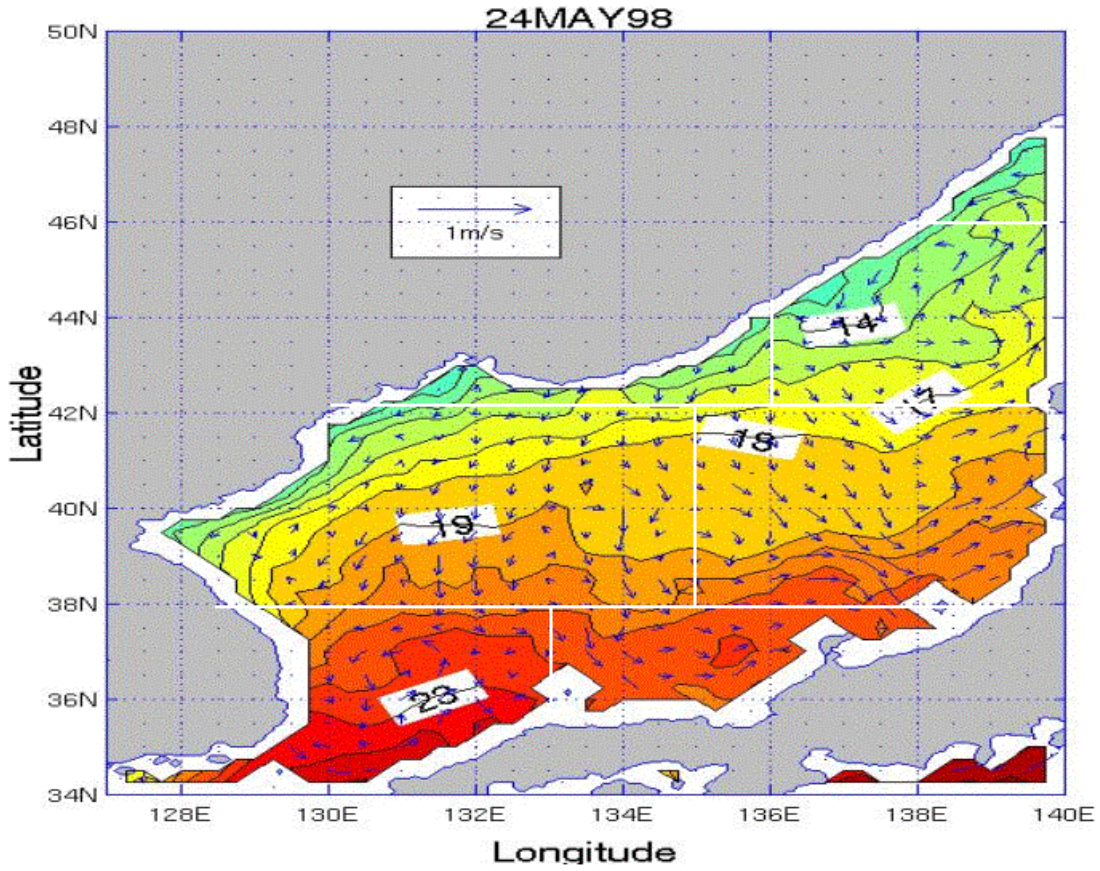


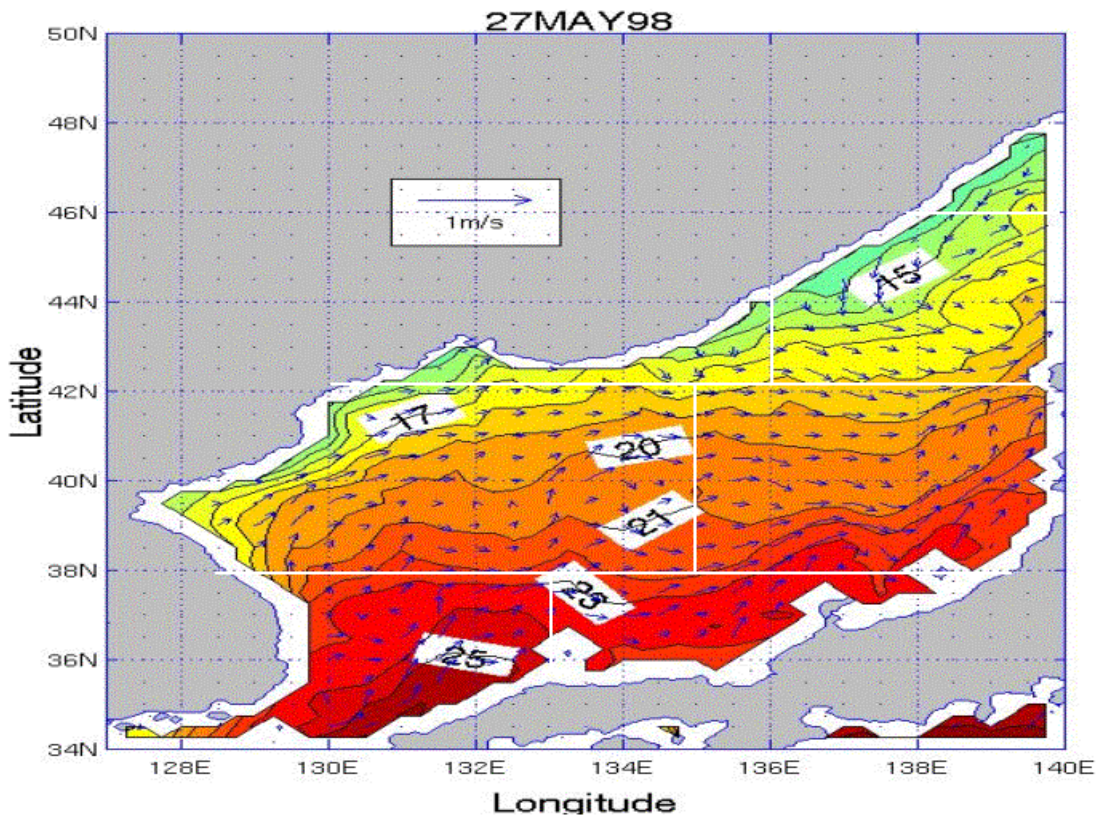
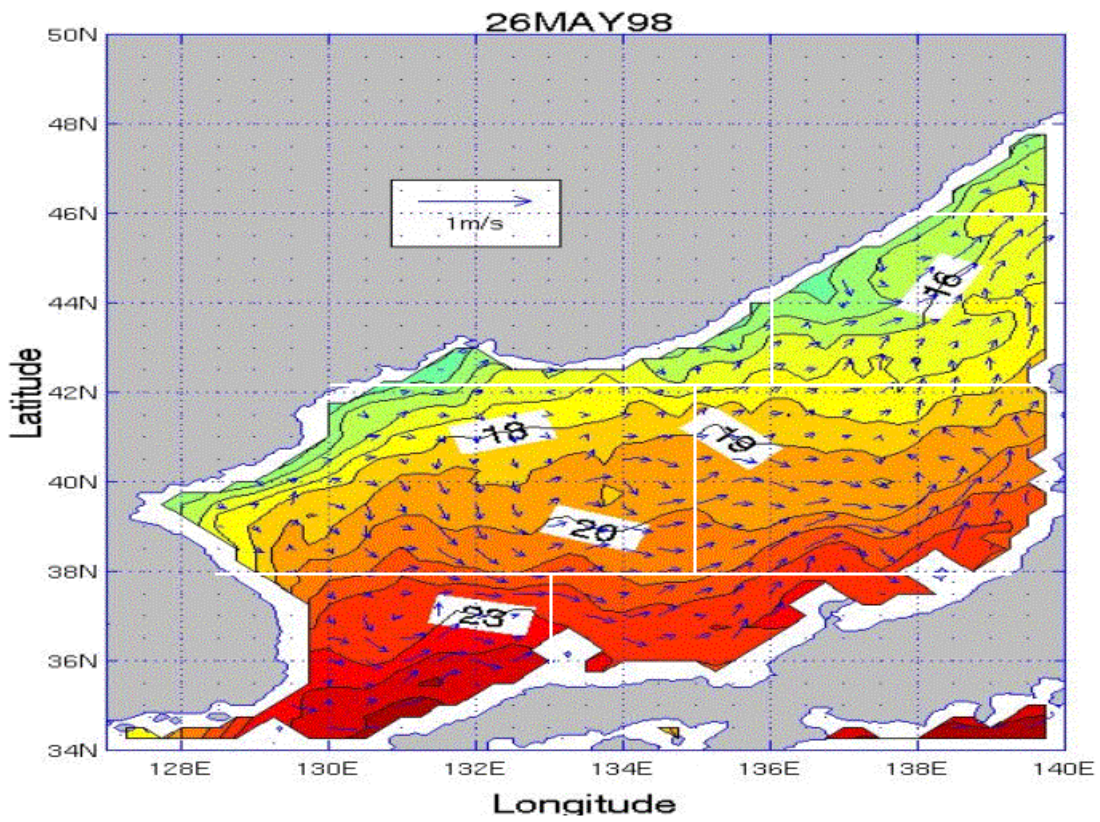


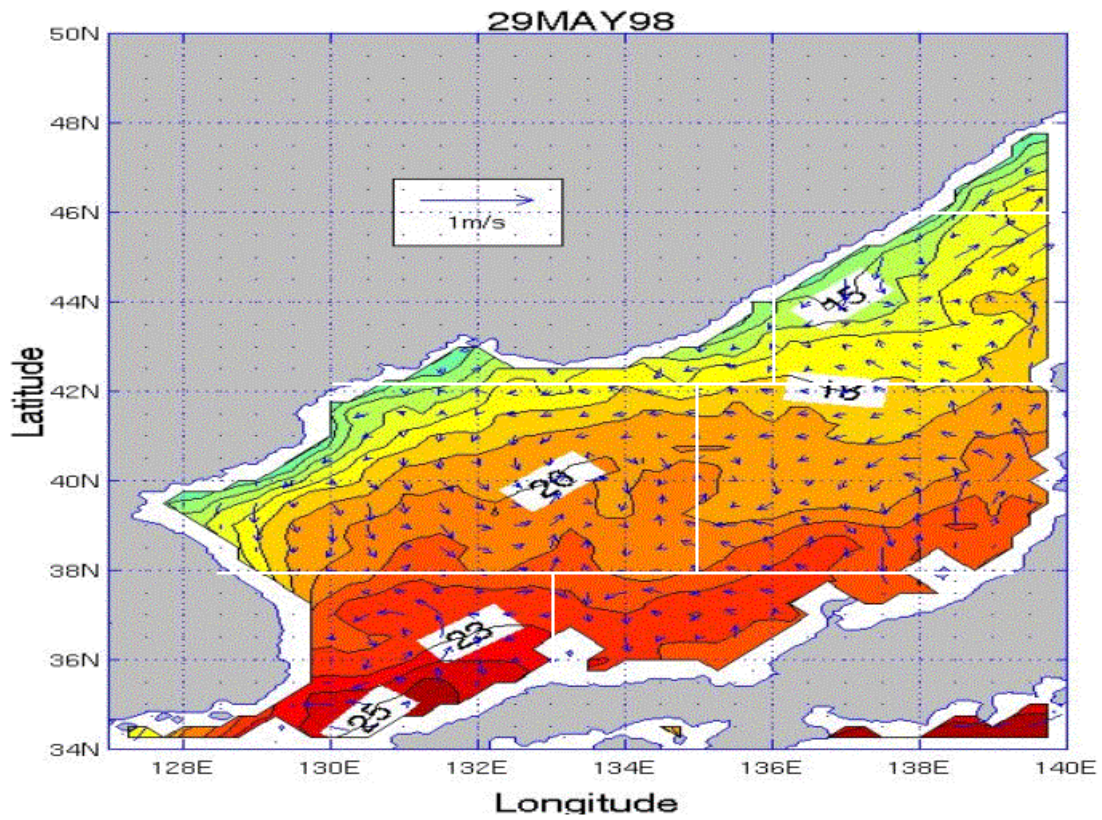
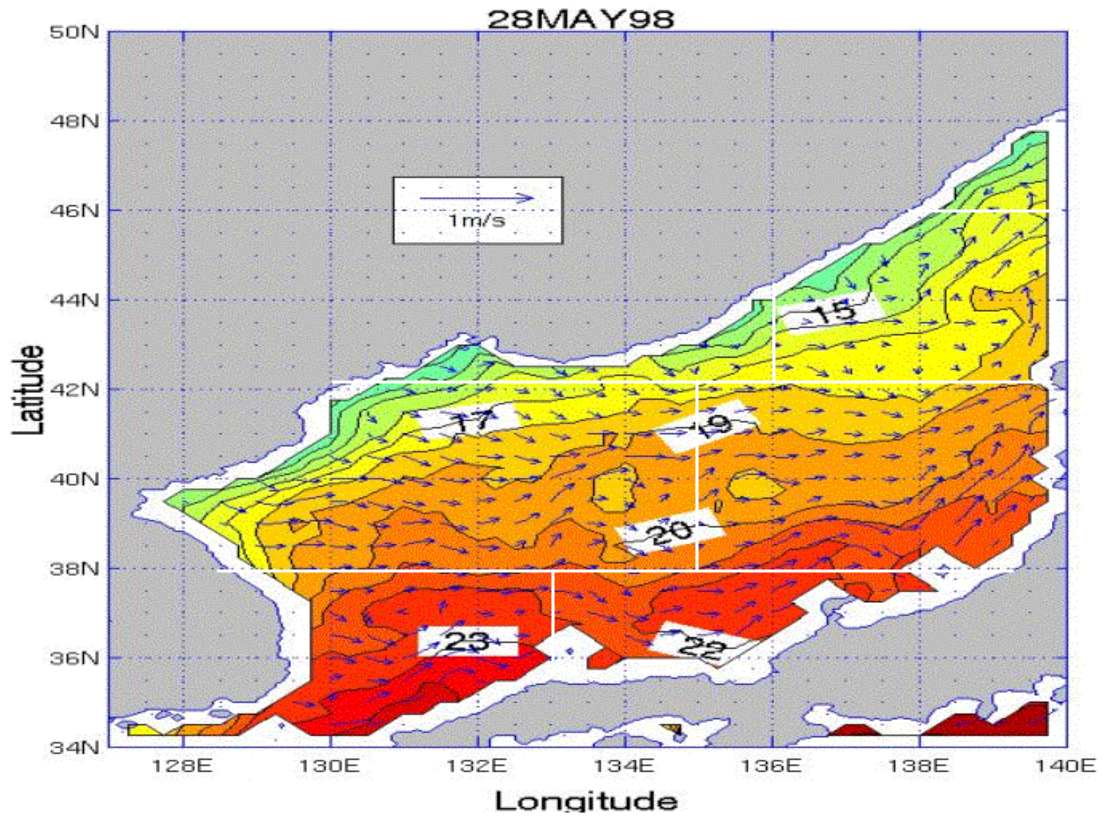


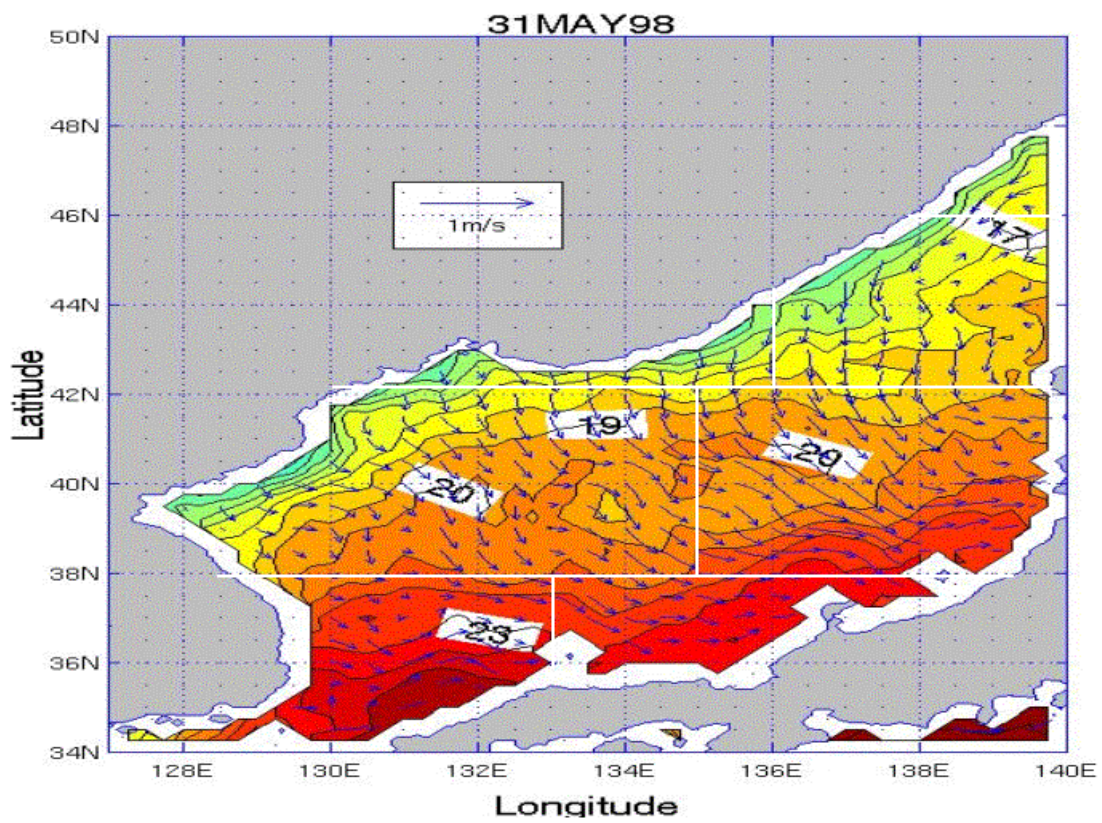
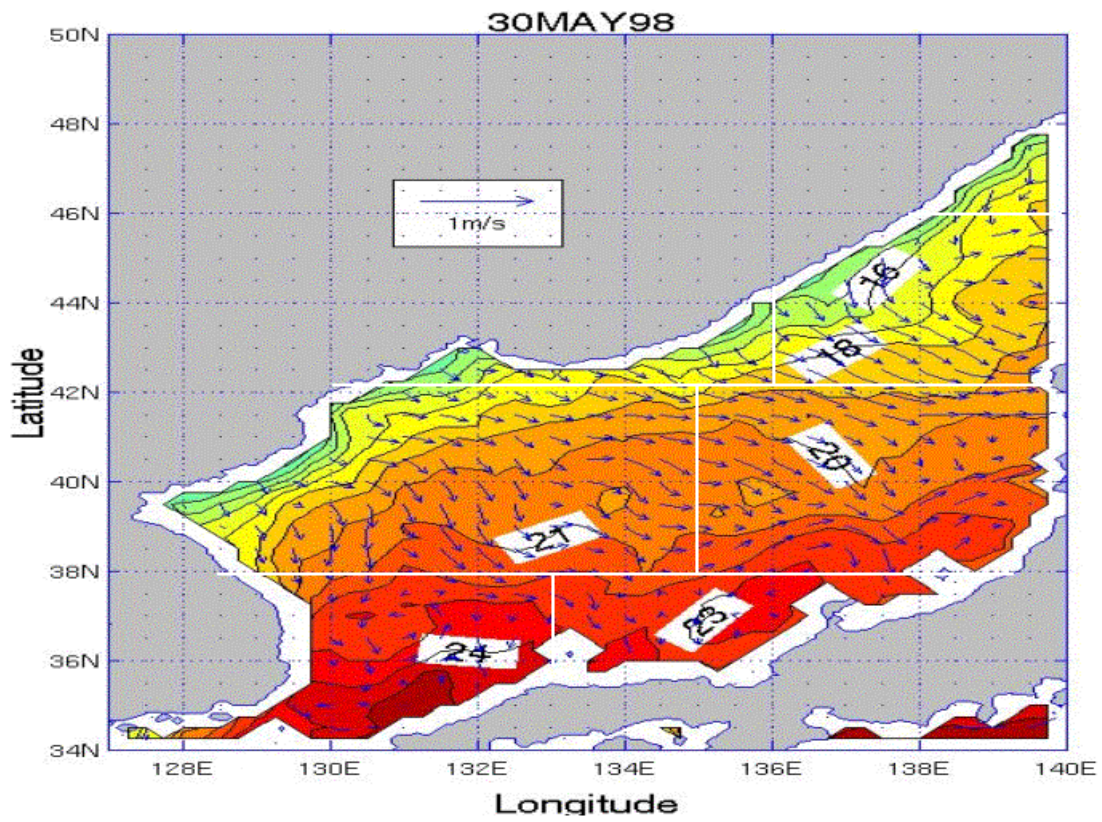






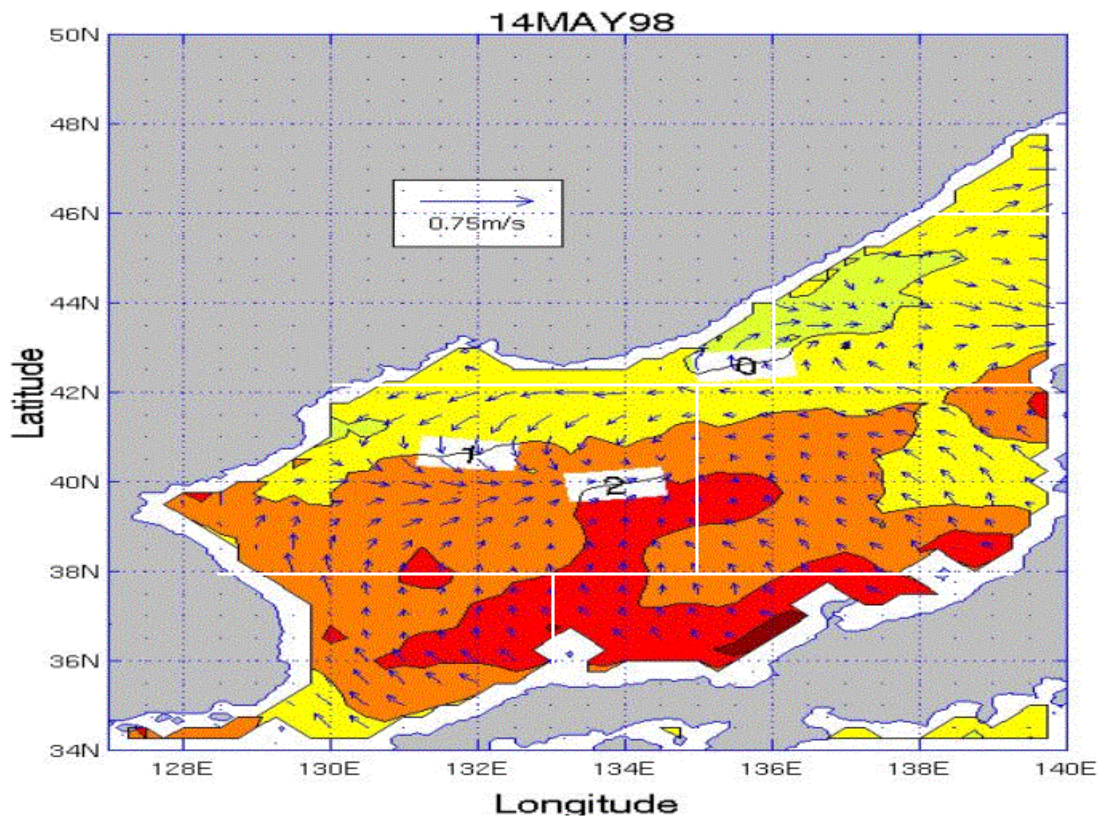


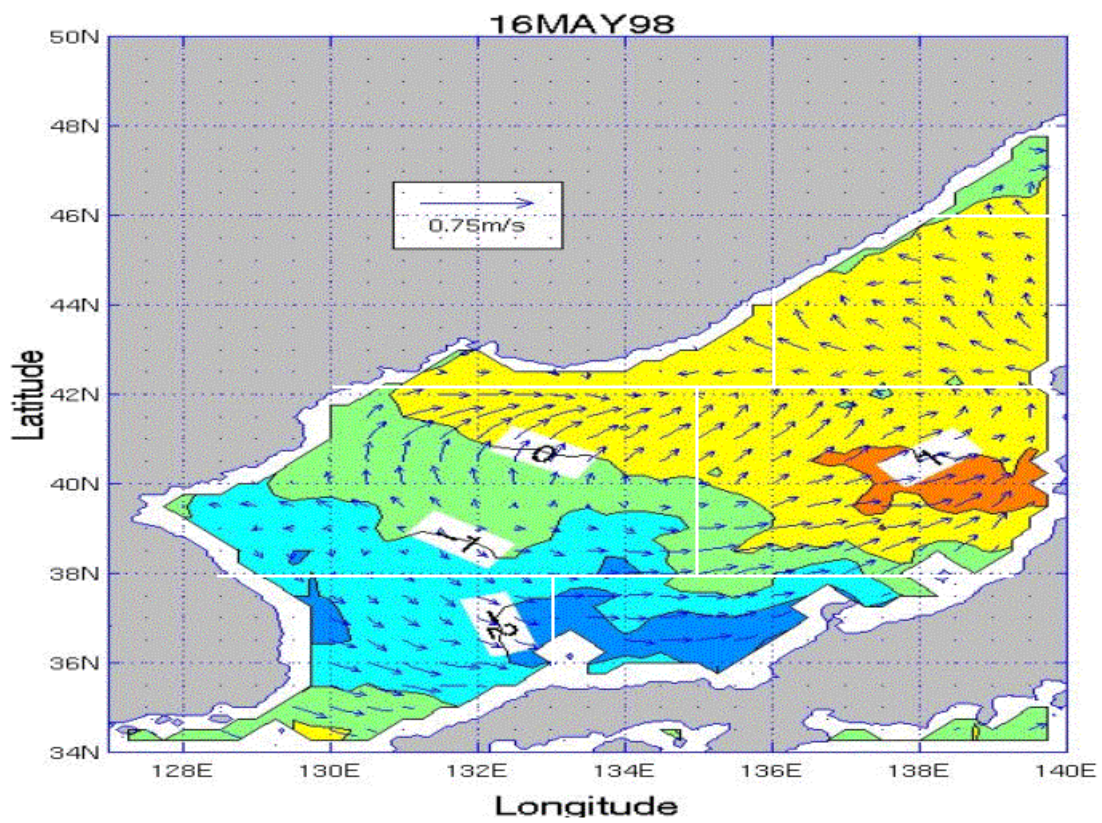
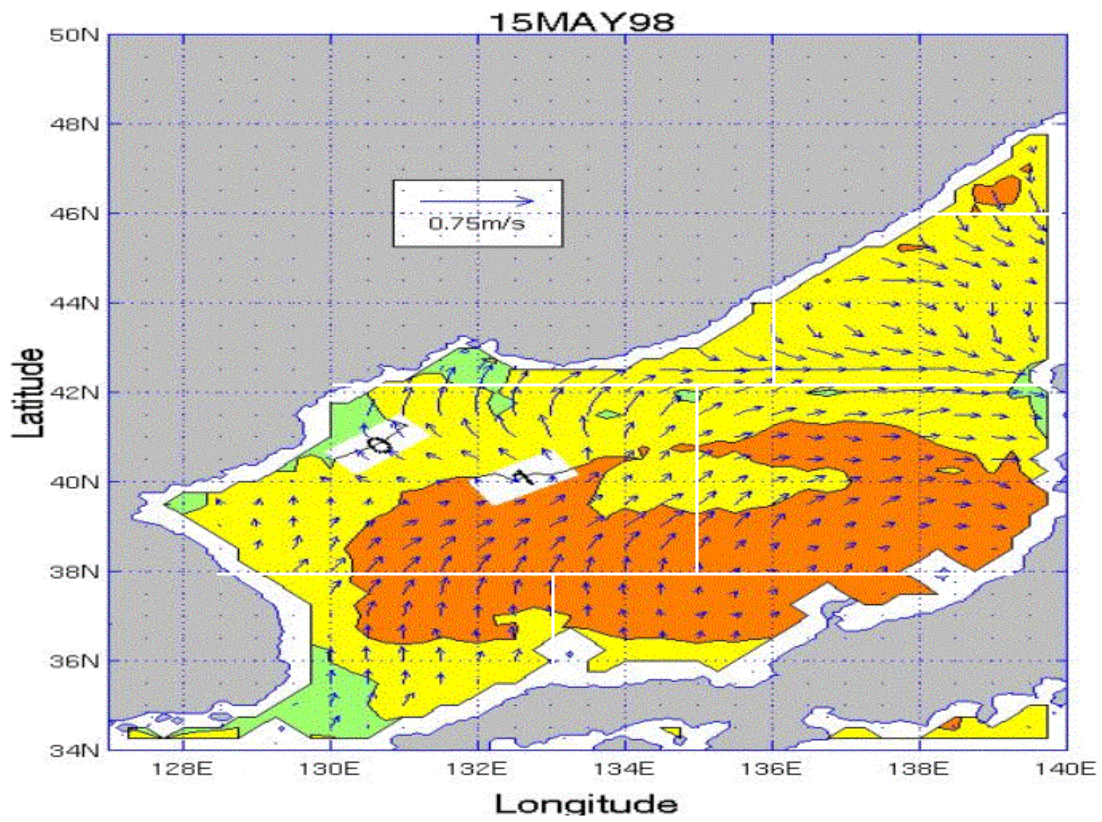


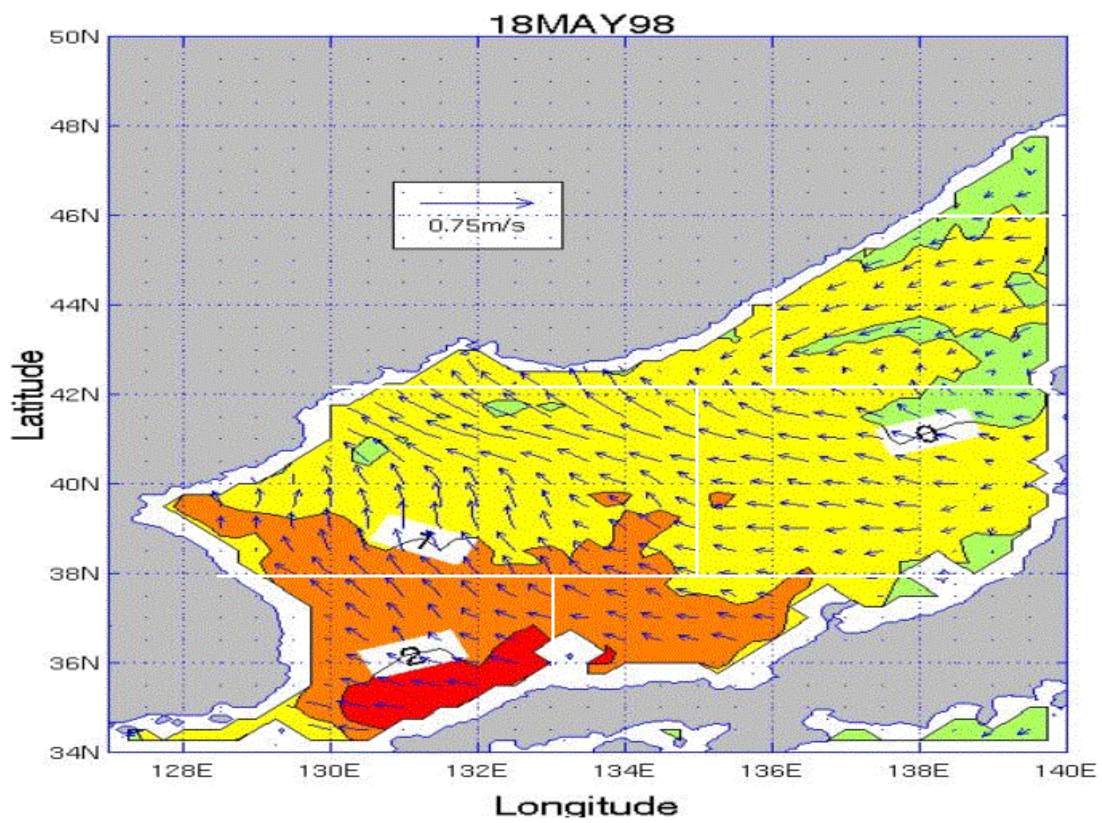
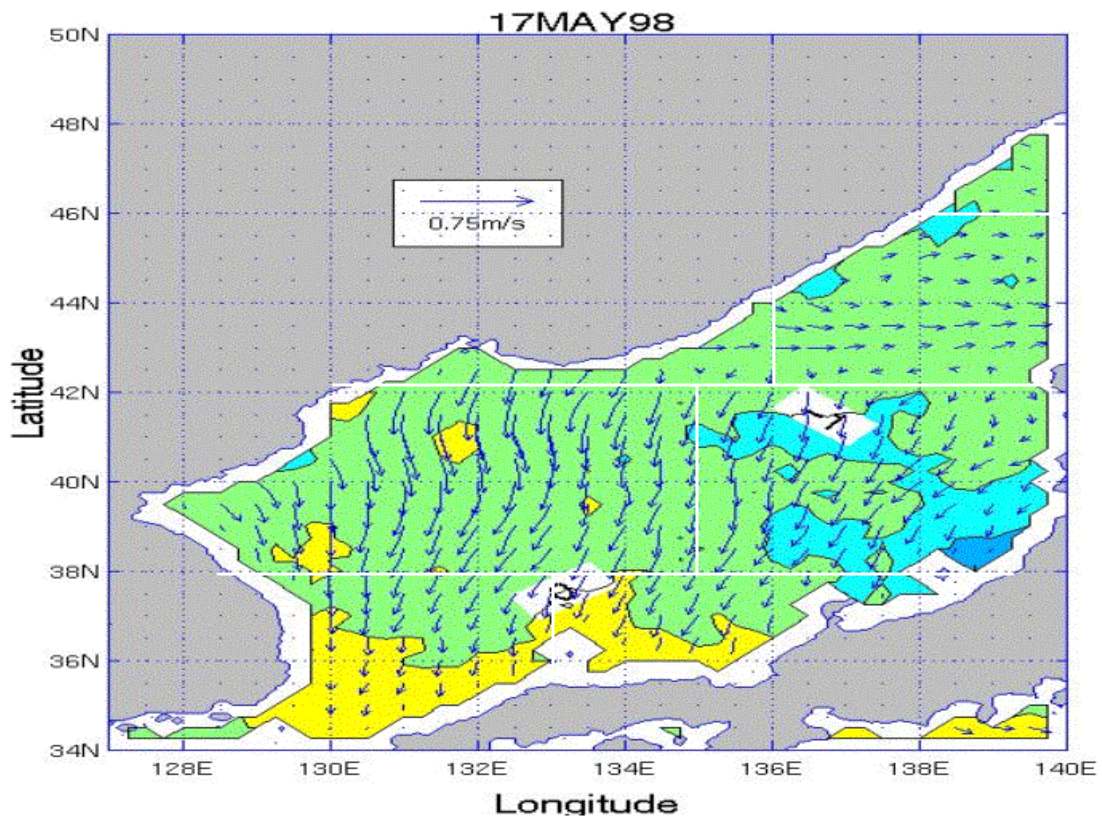


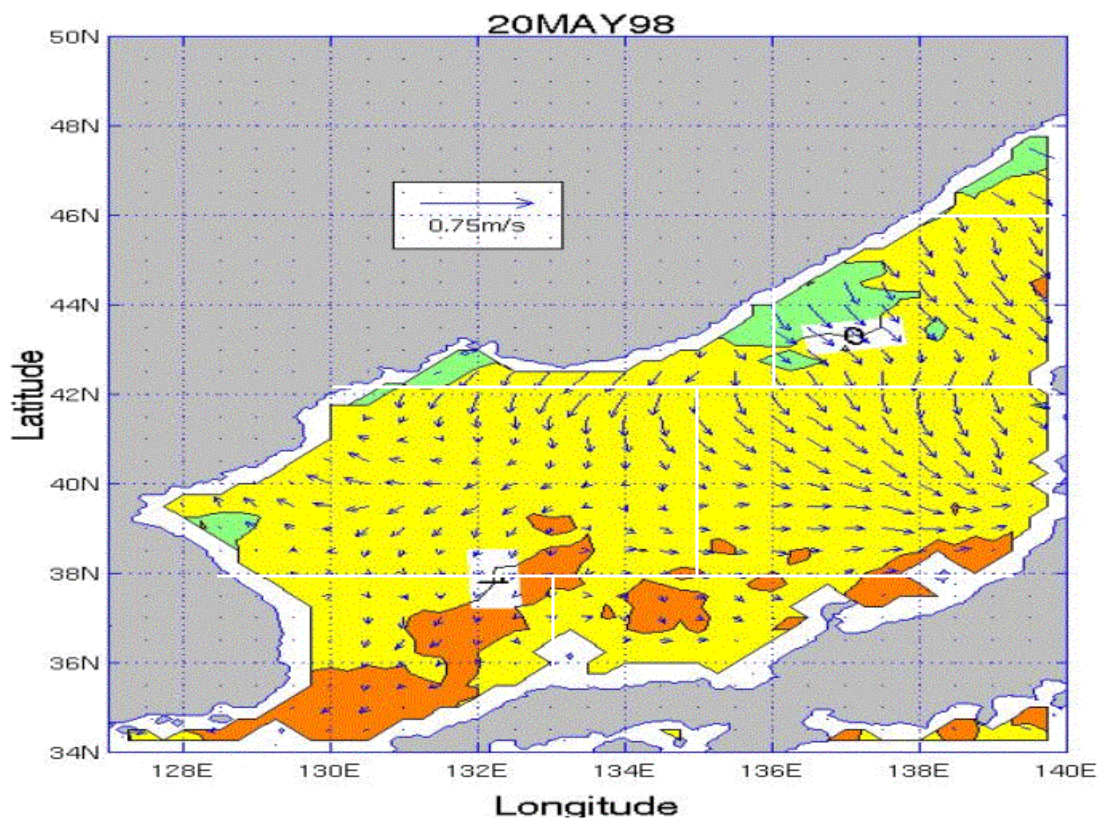
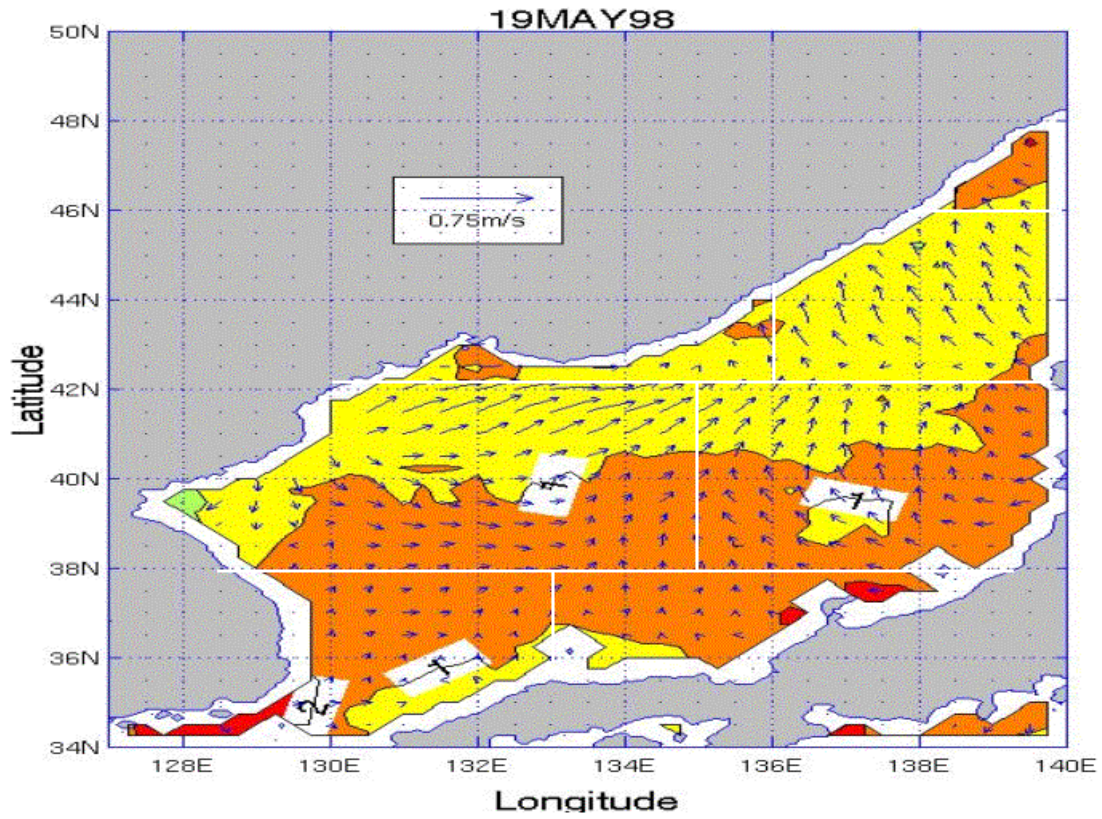
APPENDIX BB. SST AND SURFACE CURRENT VELOCITY TENDENCY PLOTS FOR THE JES FOR THE MAY TIME PERIOD

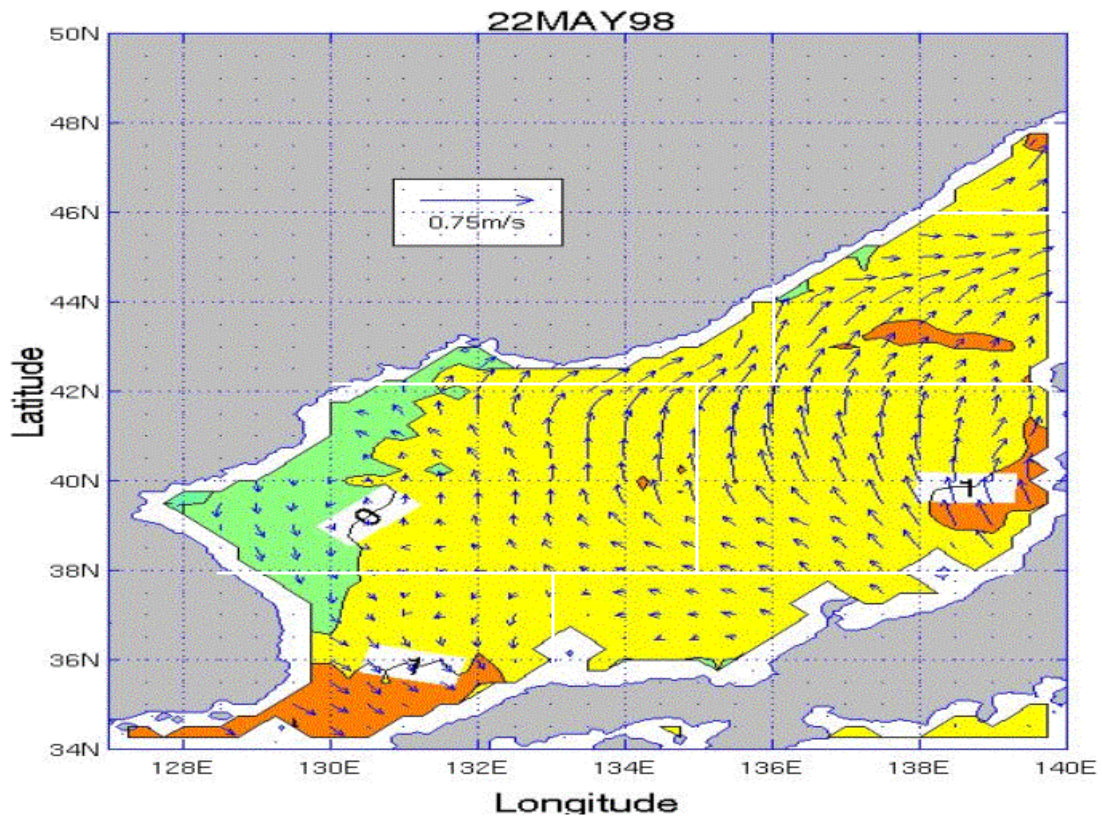
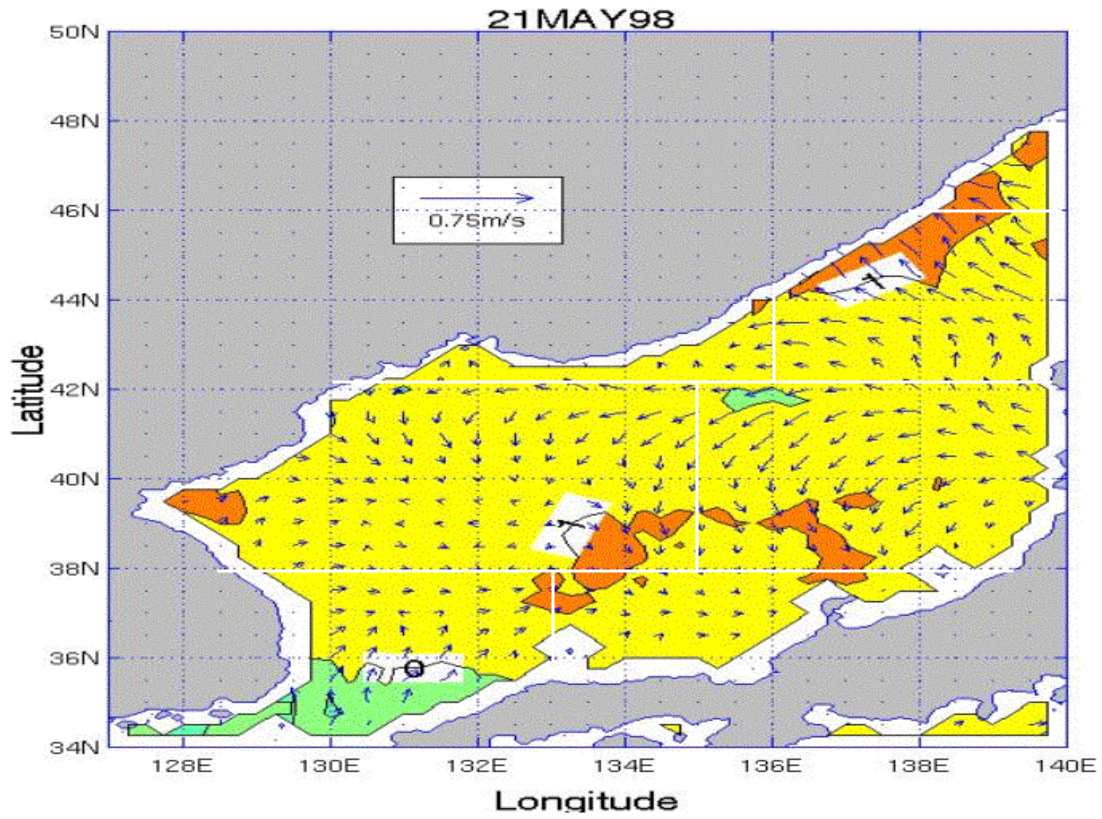
Appendix BB consists of 18 figures that show SST and surface current velocity day-to-day tendency for the May time period over the JES. The figures are in time sequential order from May 14 through May 31. Each plot represents the change between the previous day and the current day.

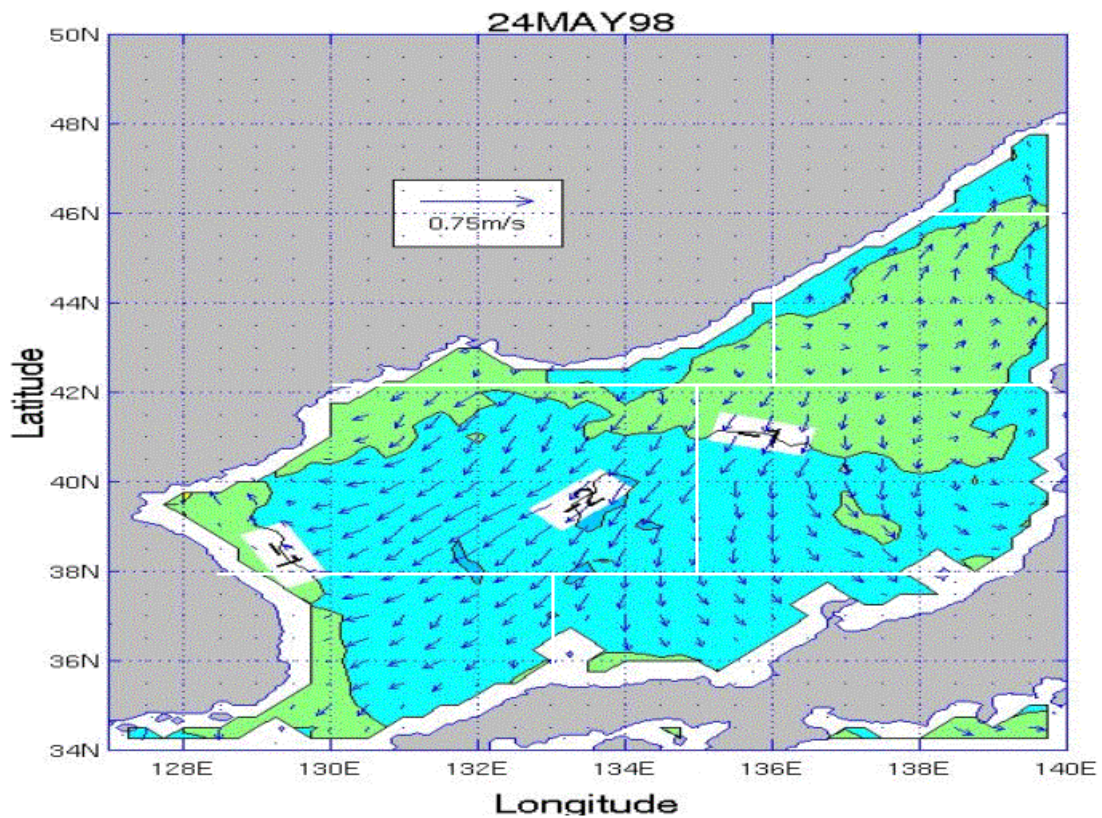
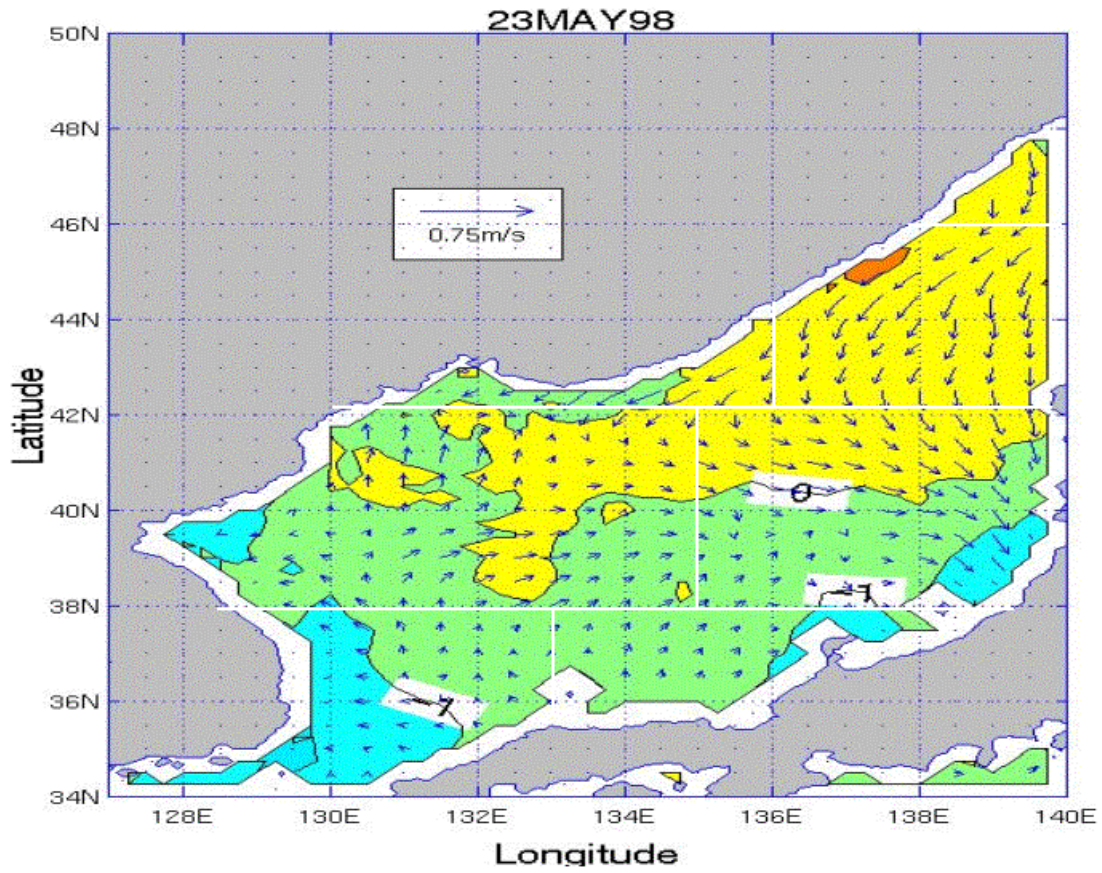


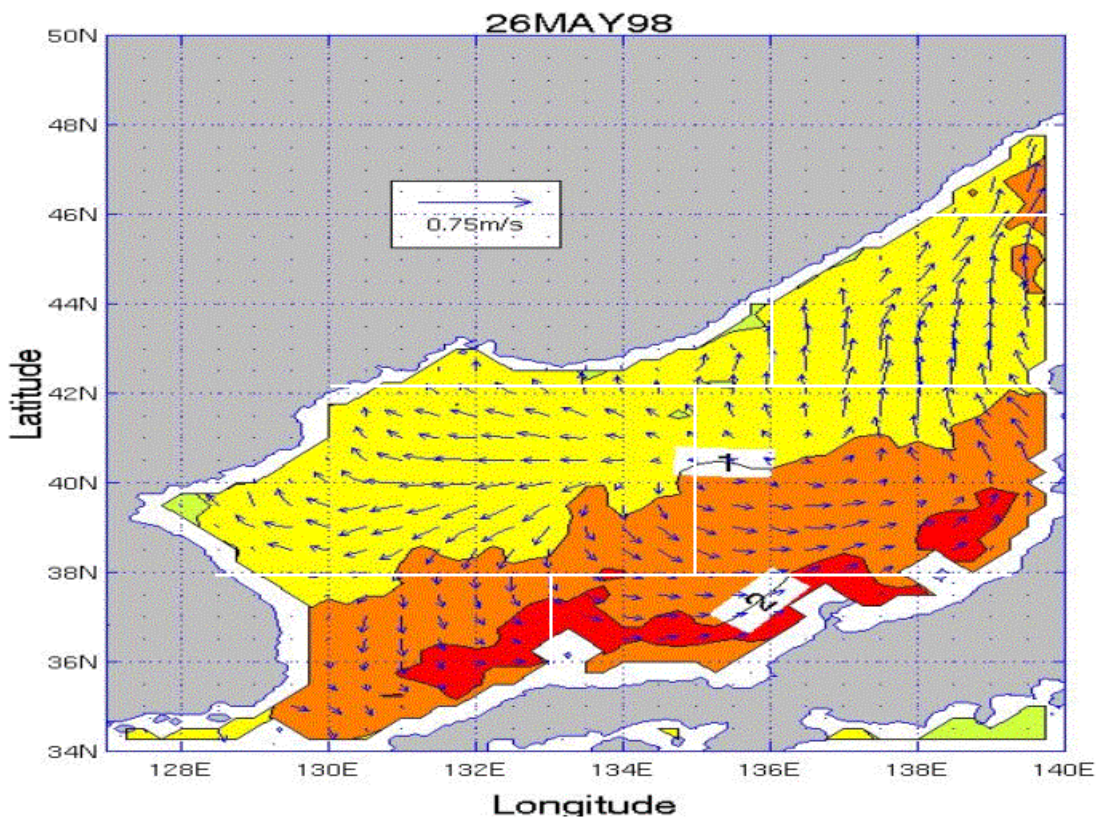
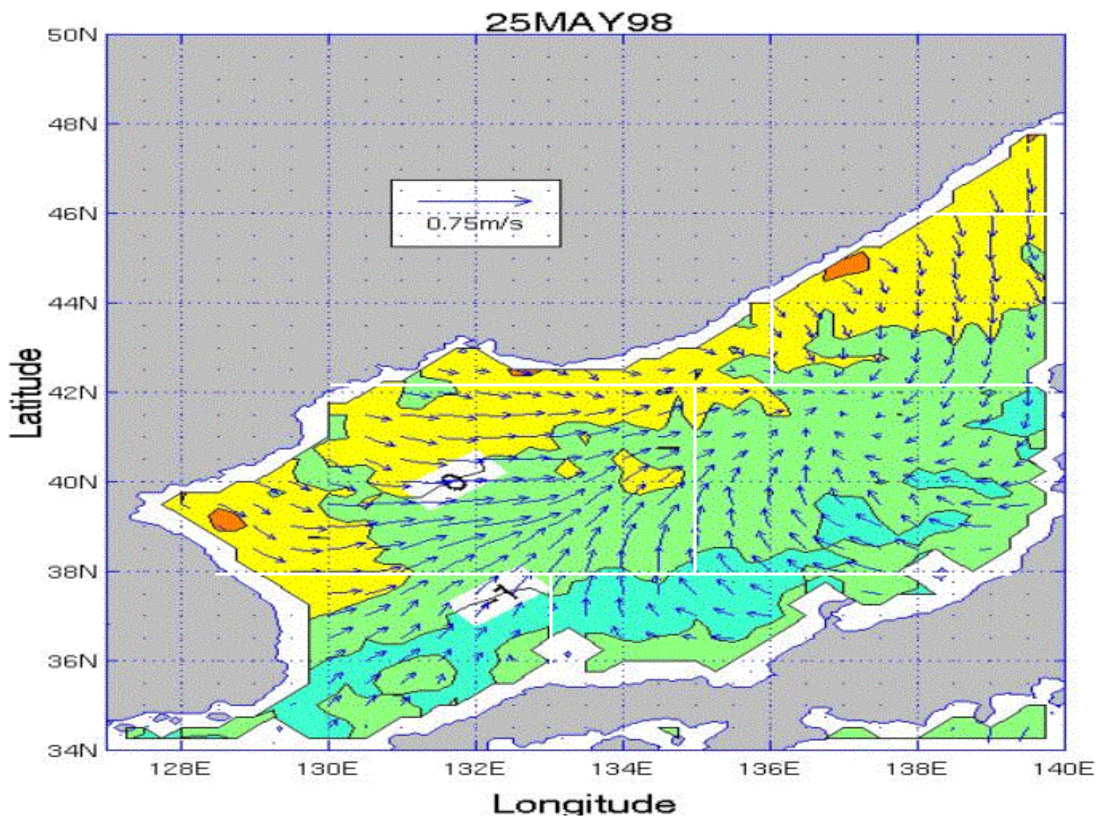


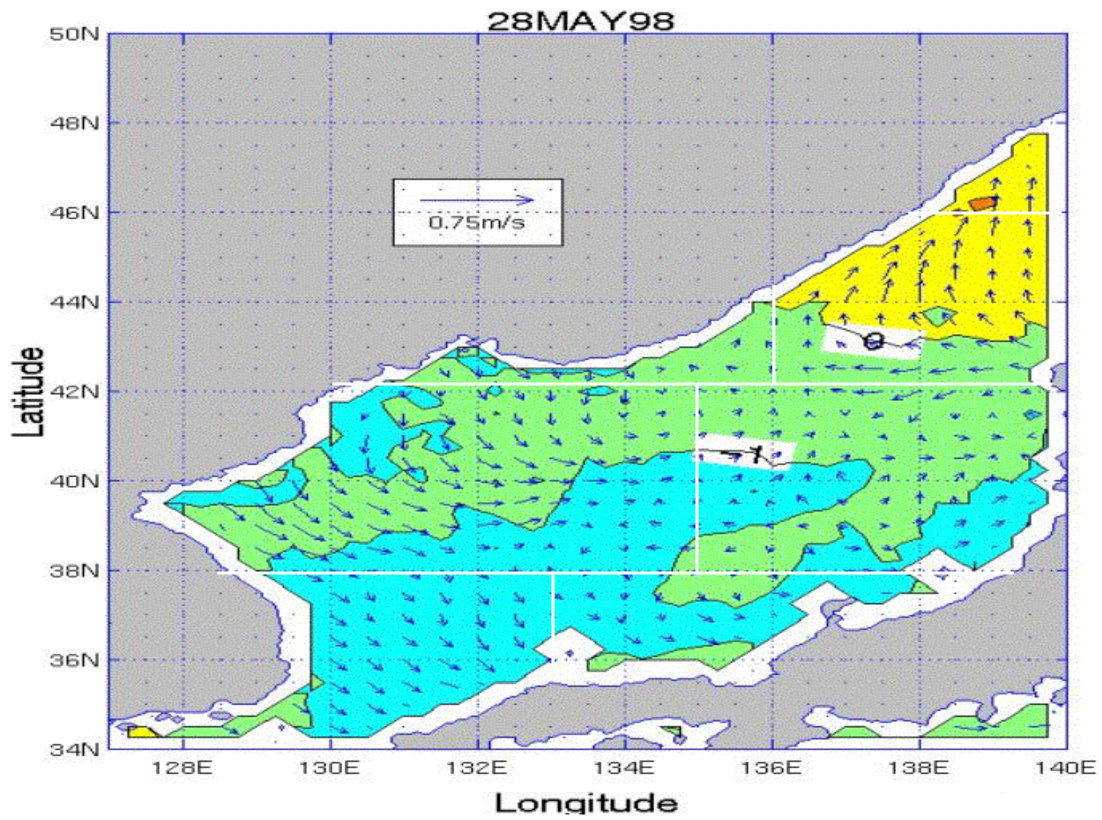
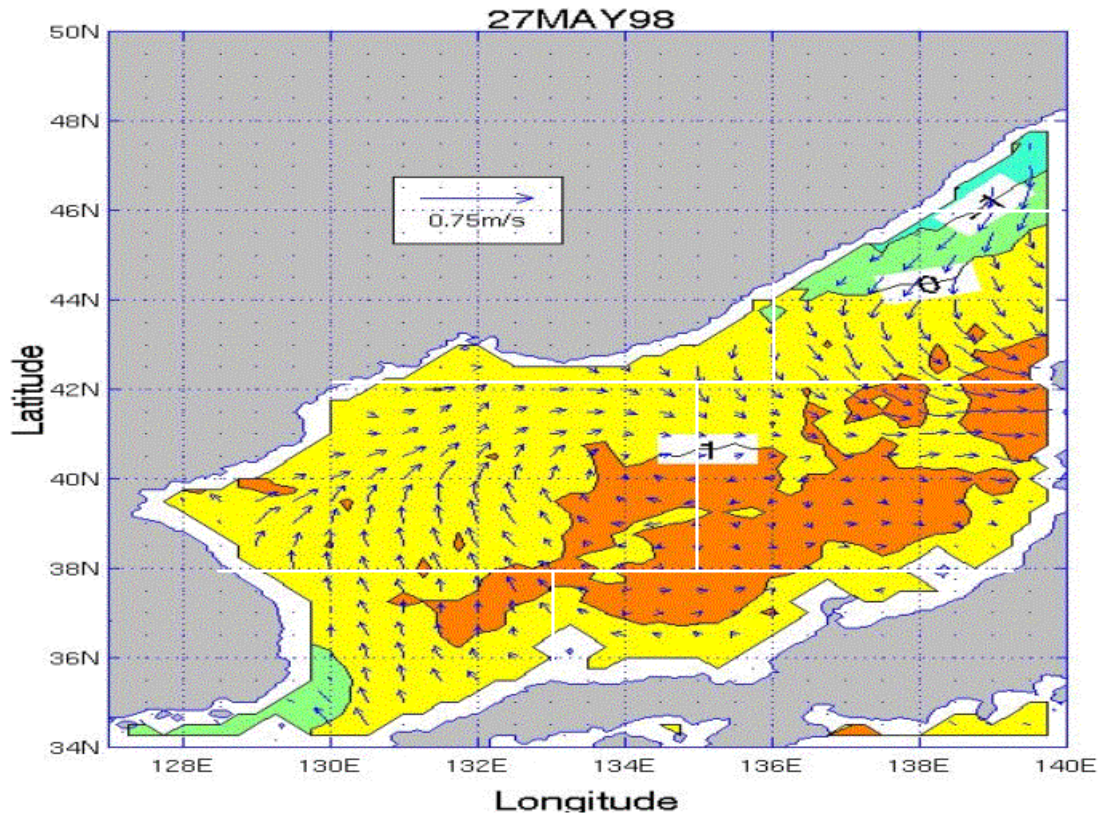


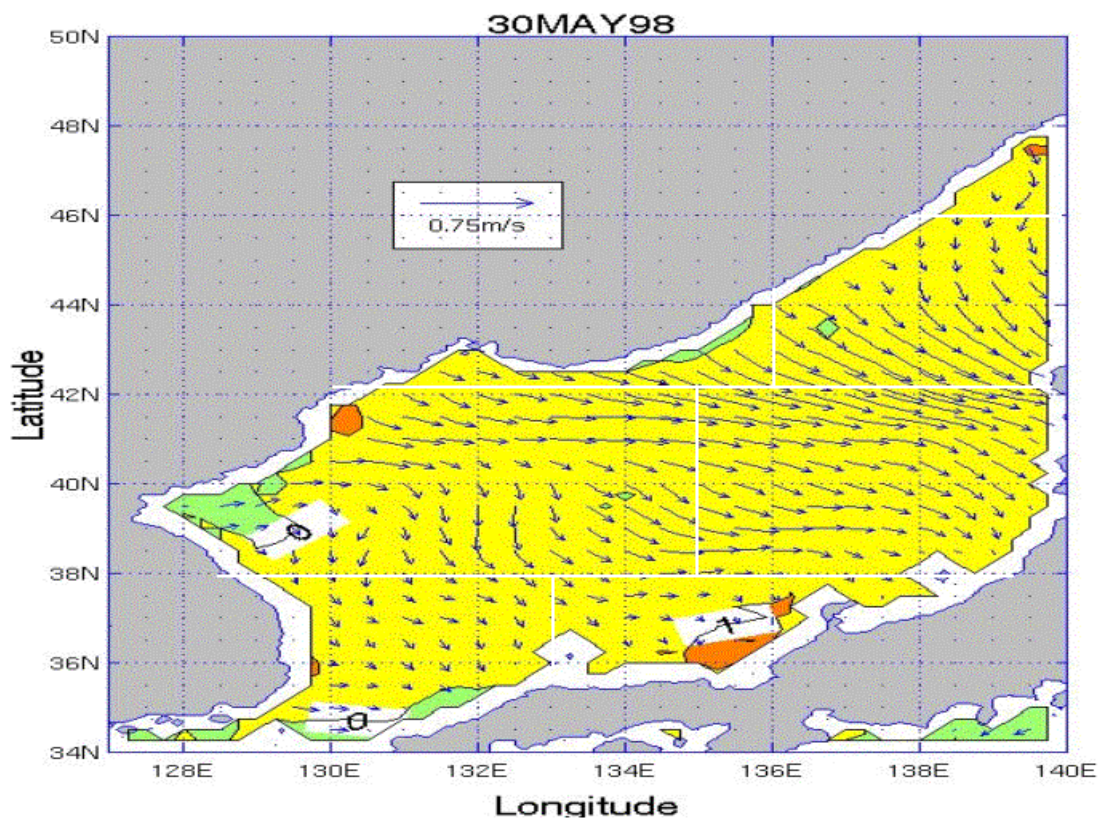
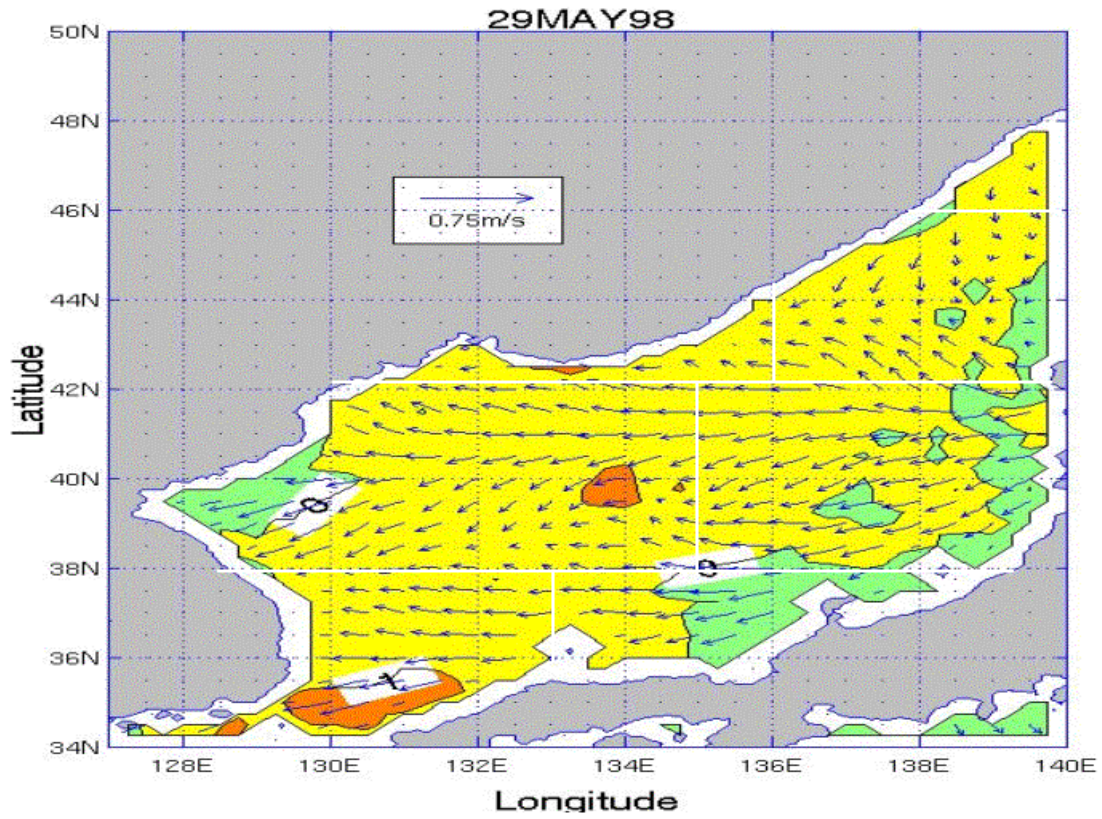


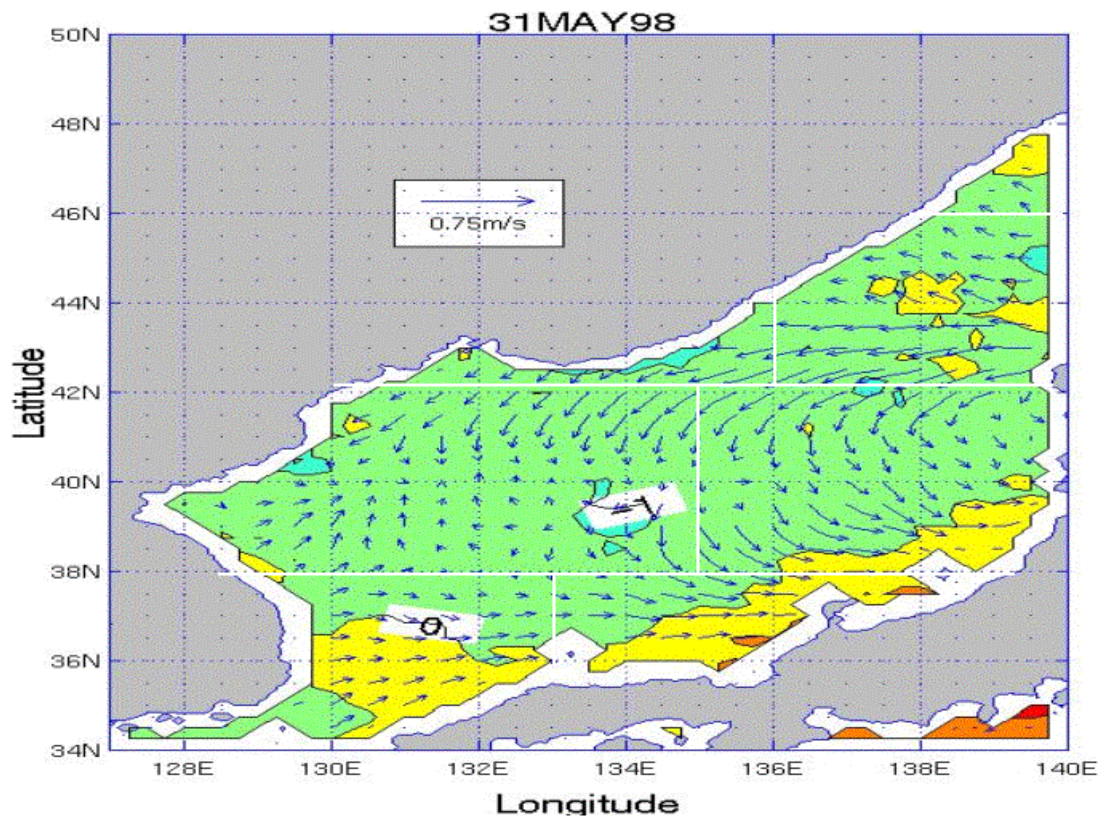






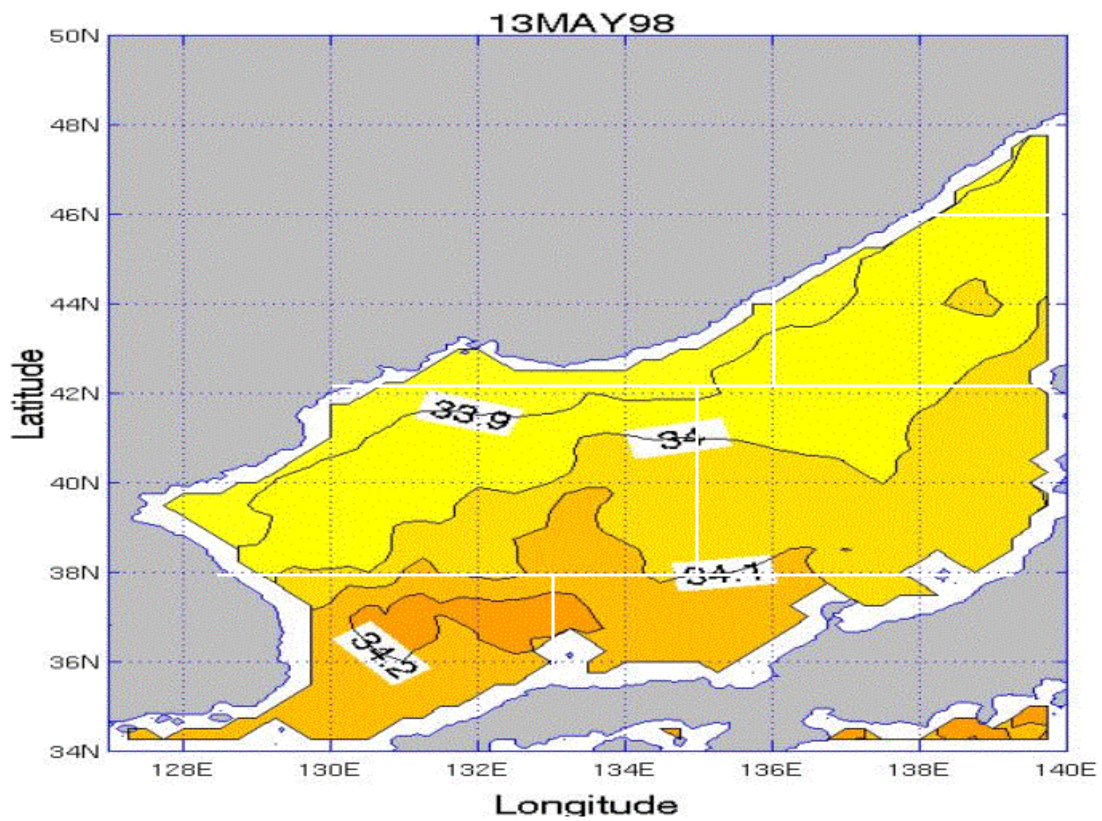


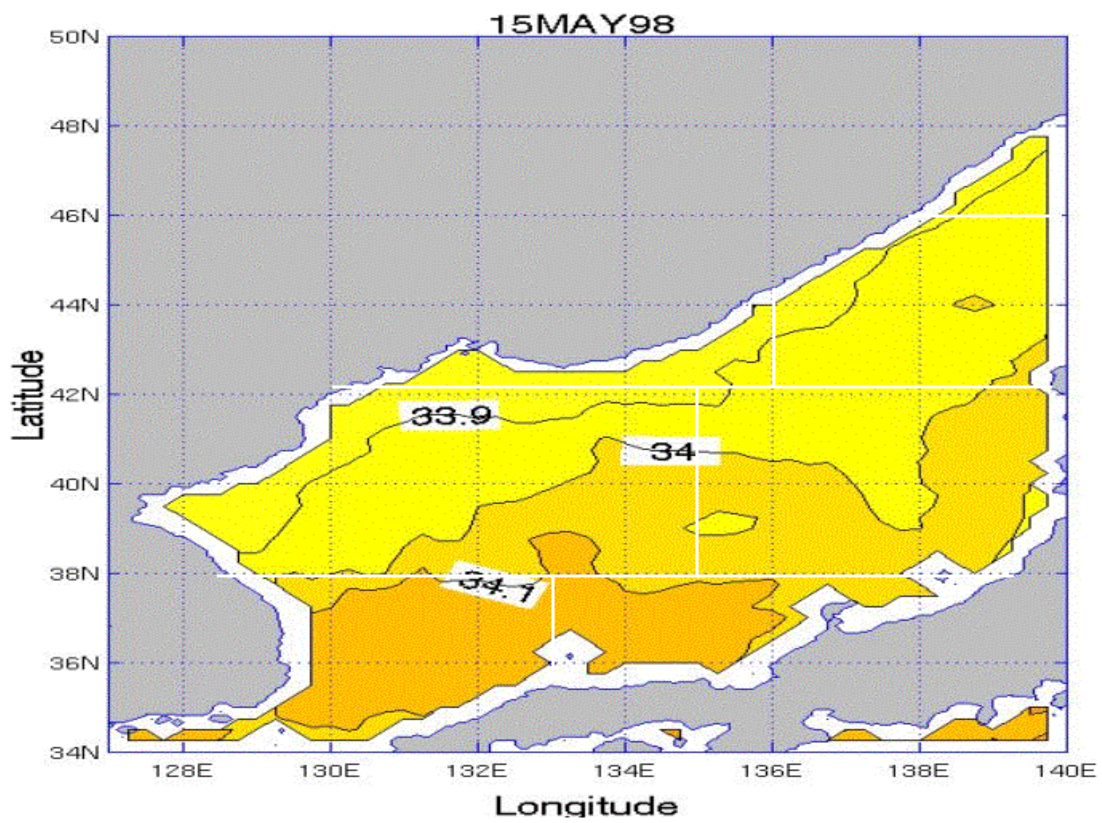
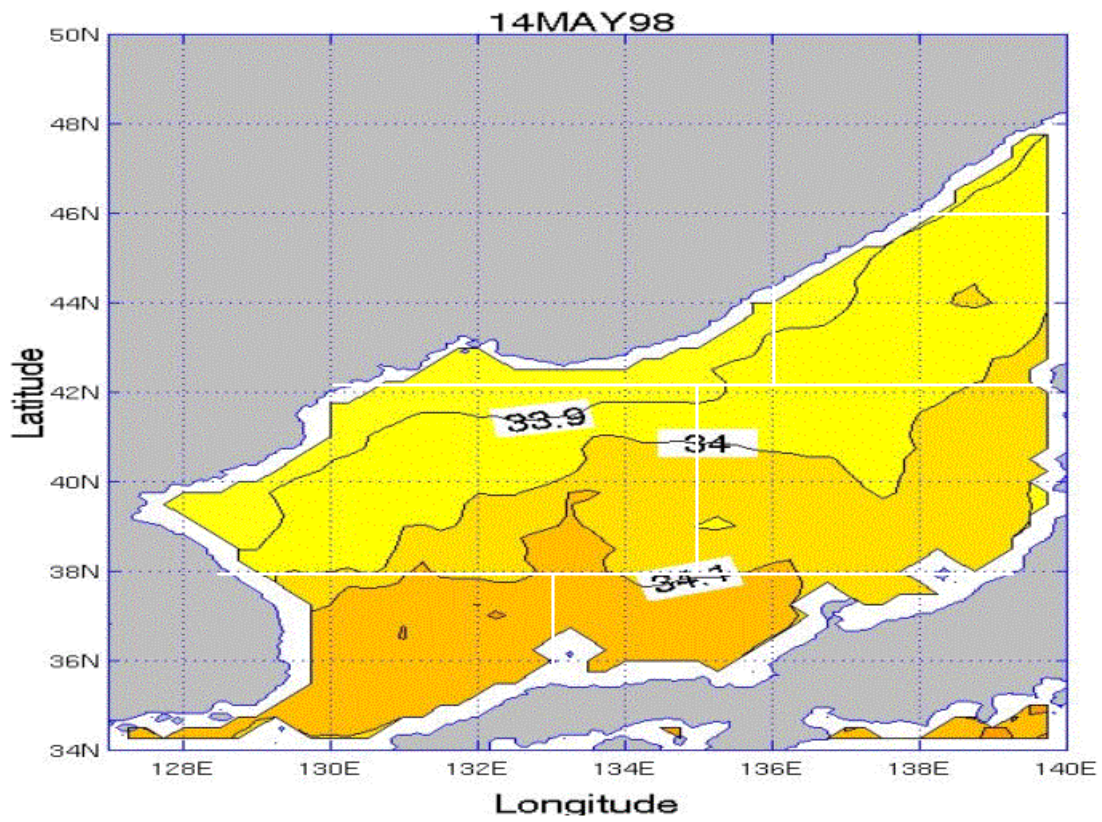


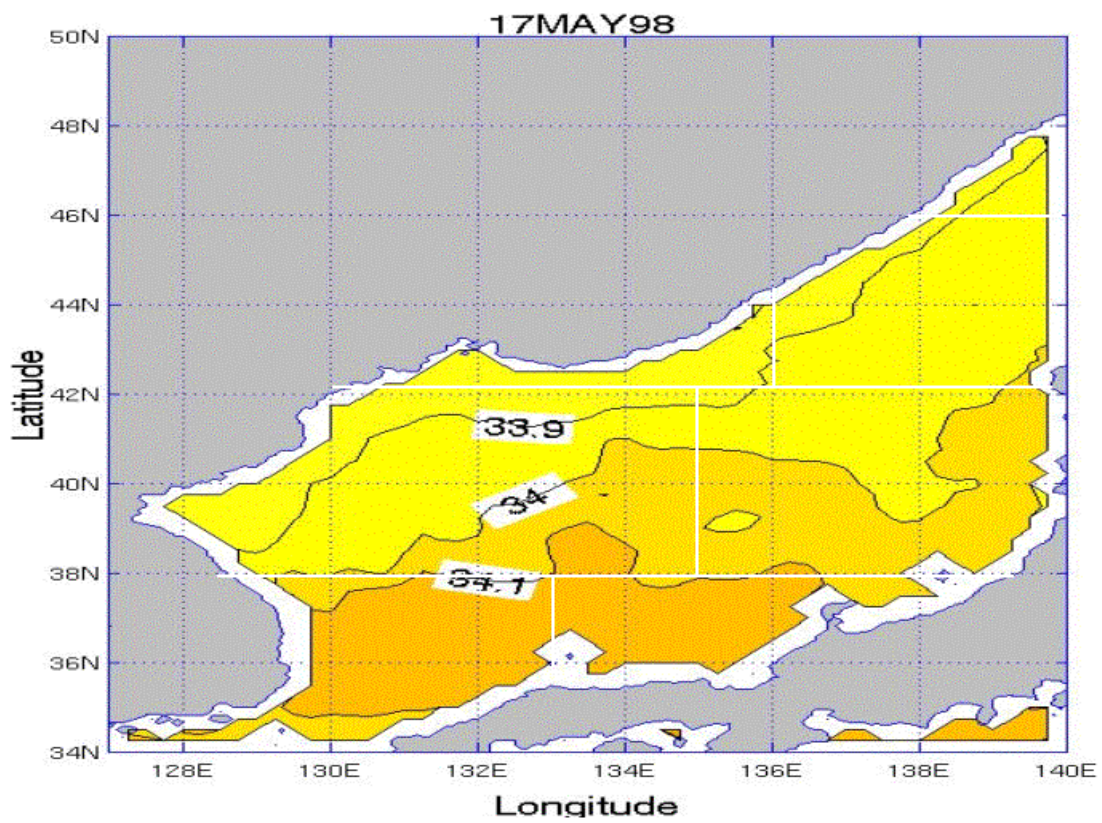
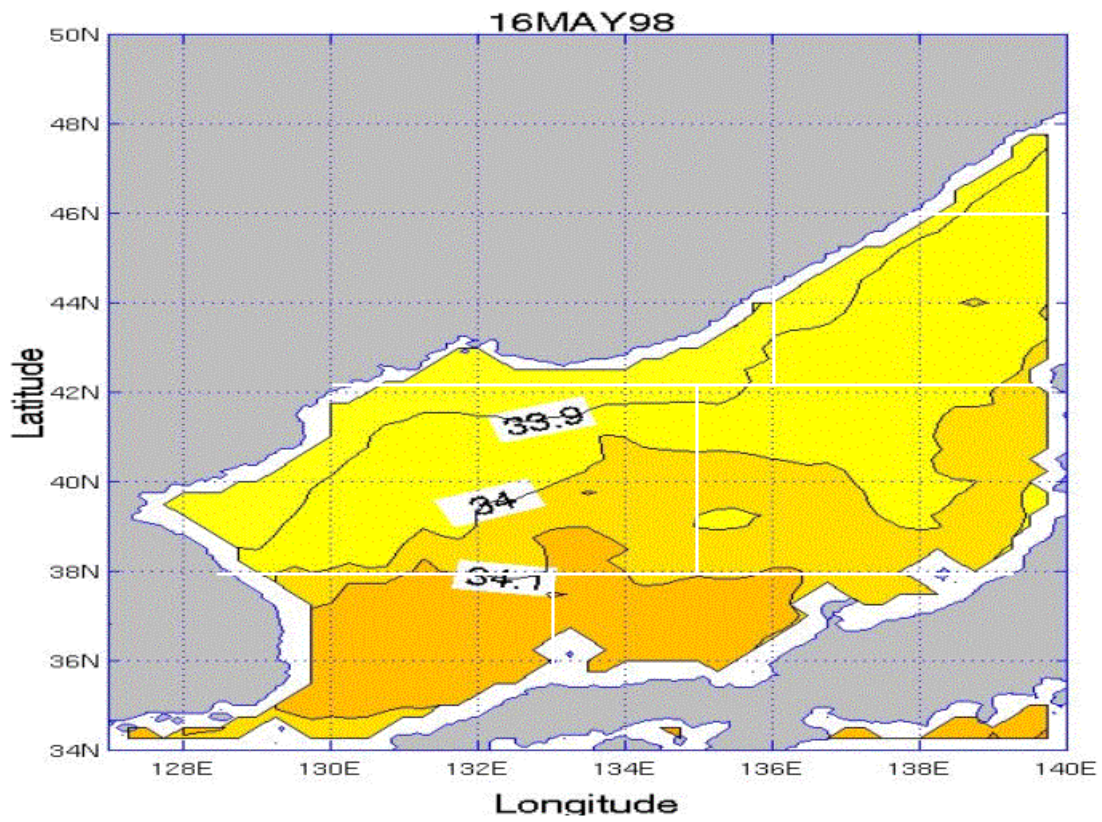


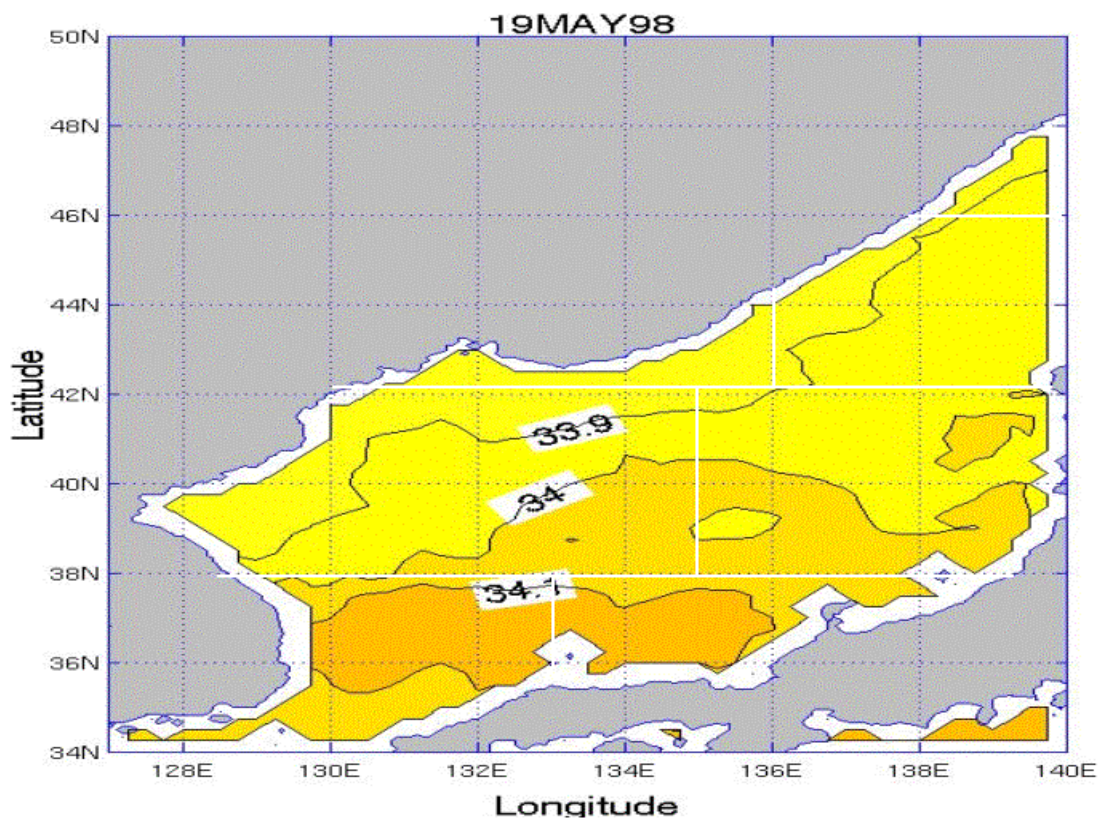
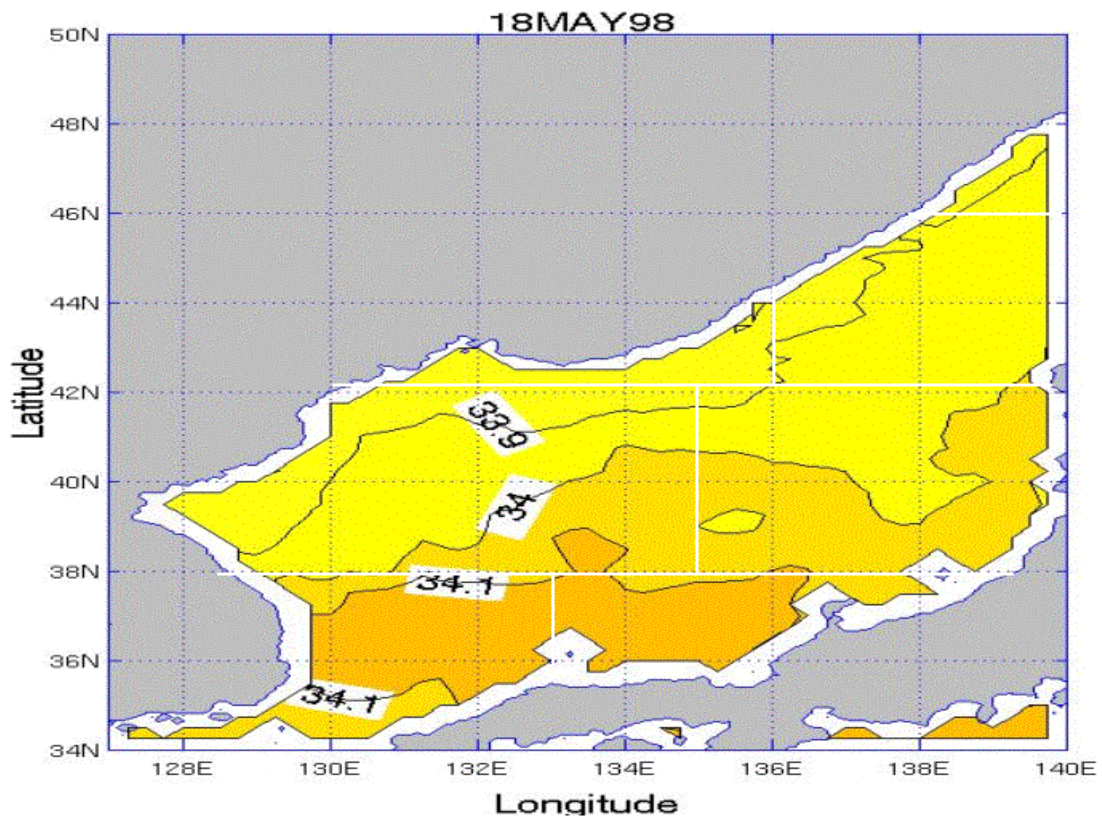
APPENDIX CC. SSS PLOTS FOR THE JES FOR THE MAY TIME PERIOD

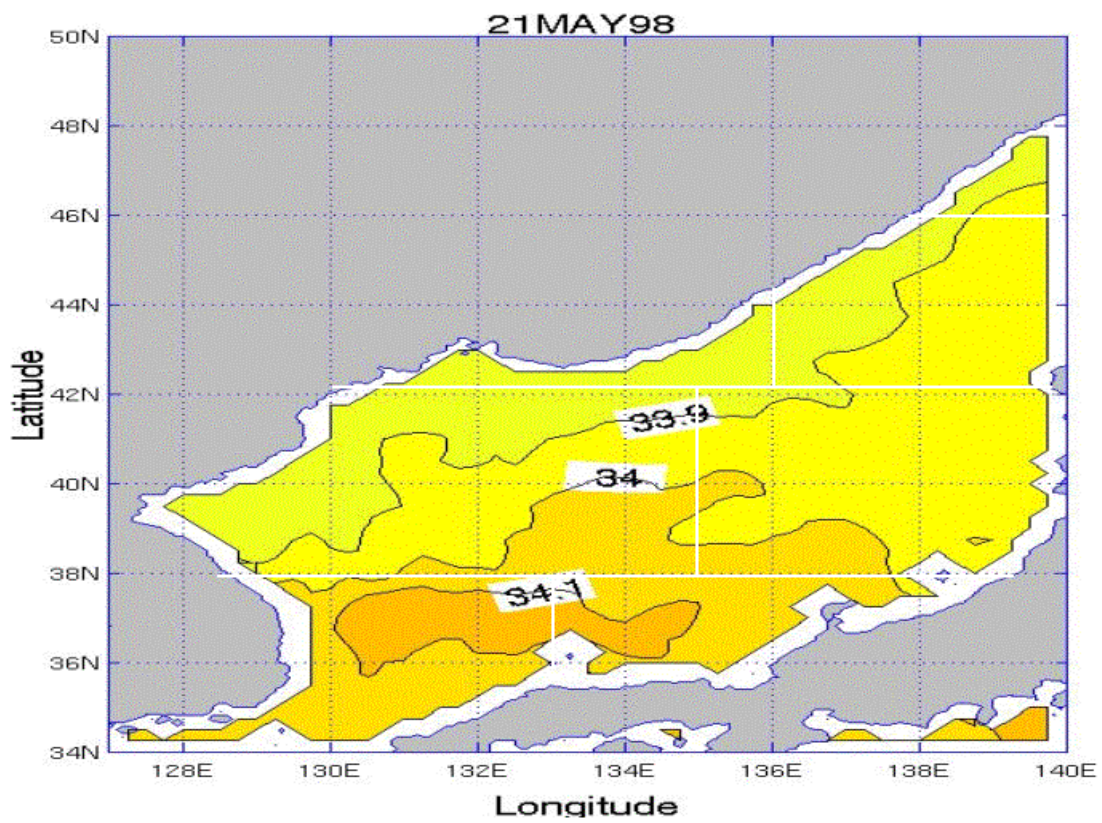
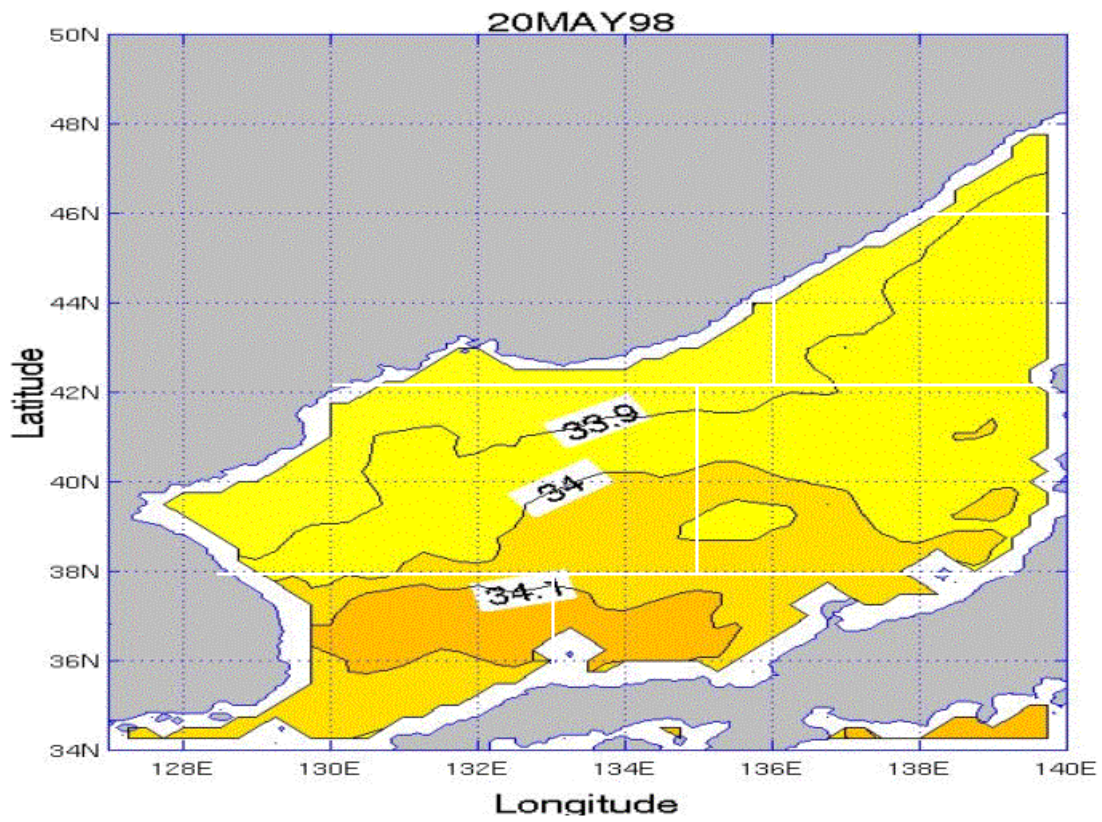
Appendix CC consists of 19 figures that show SSS for each day of the May time period for the JES. The figures are in time sequential order from May 13 through May 31.

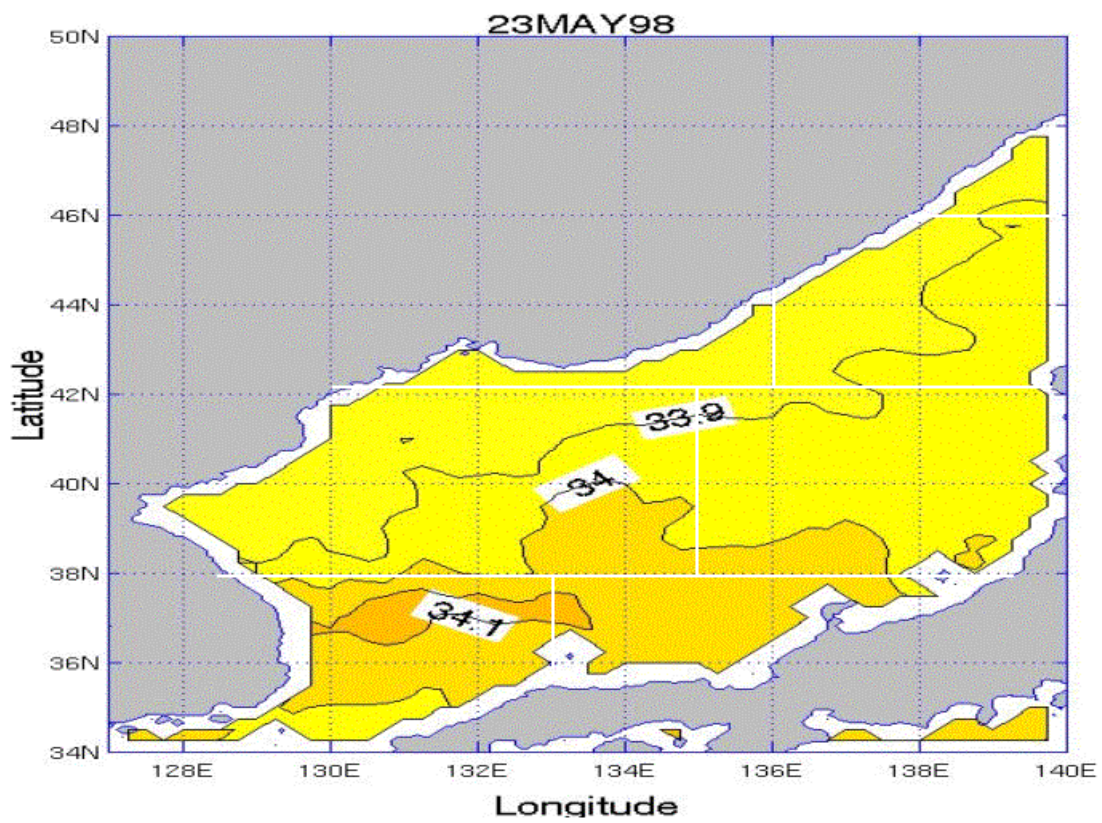
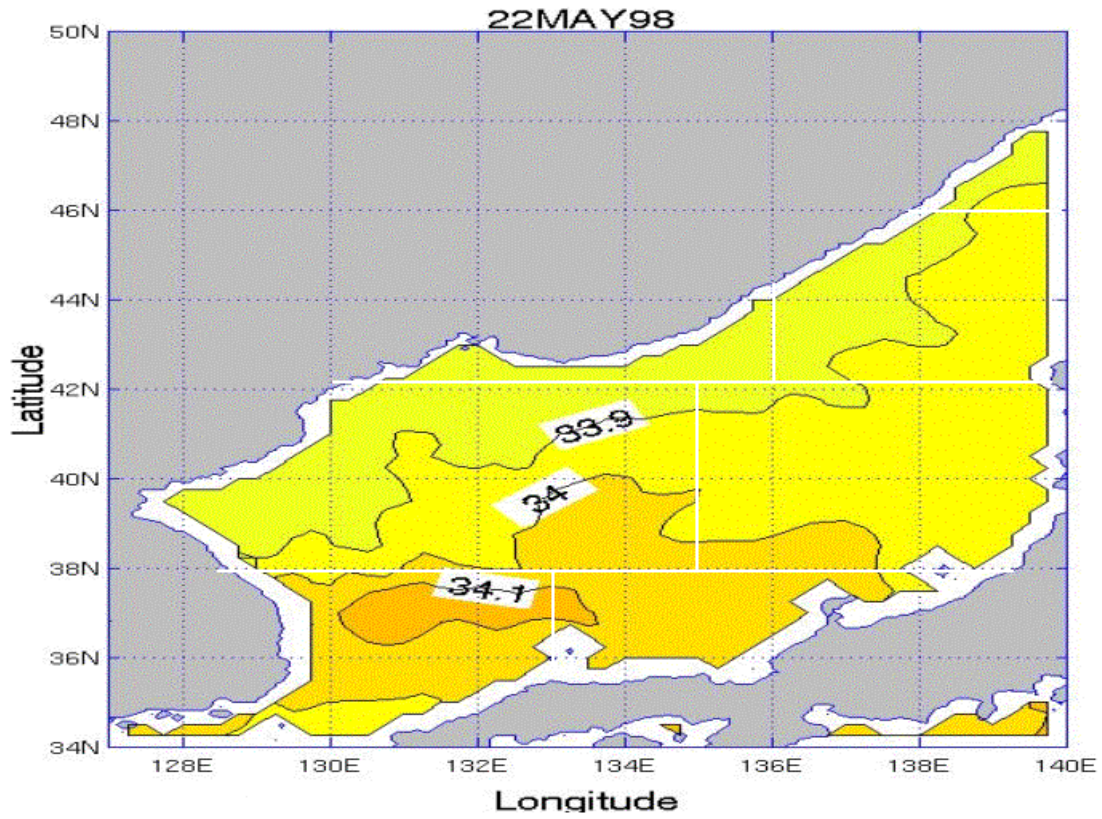


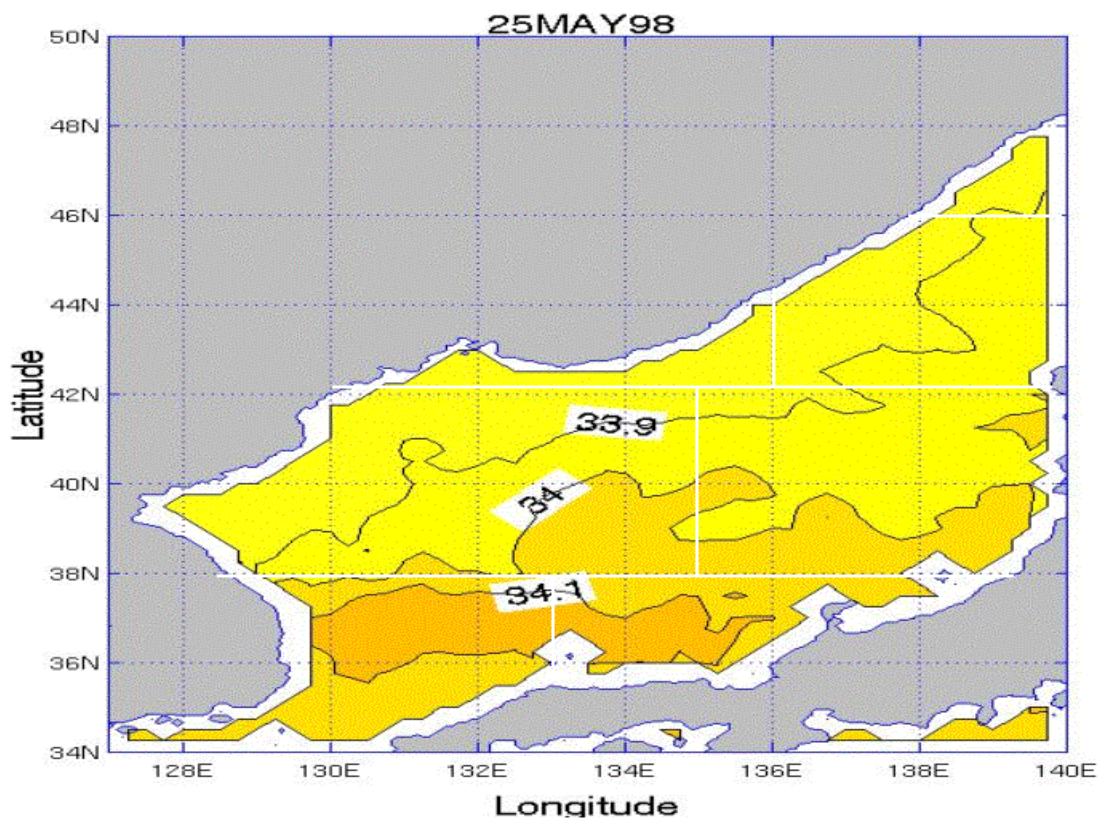
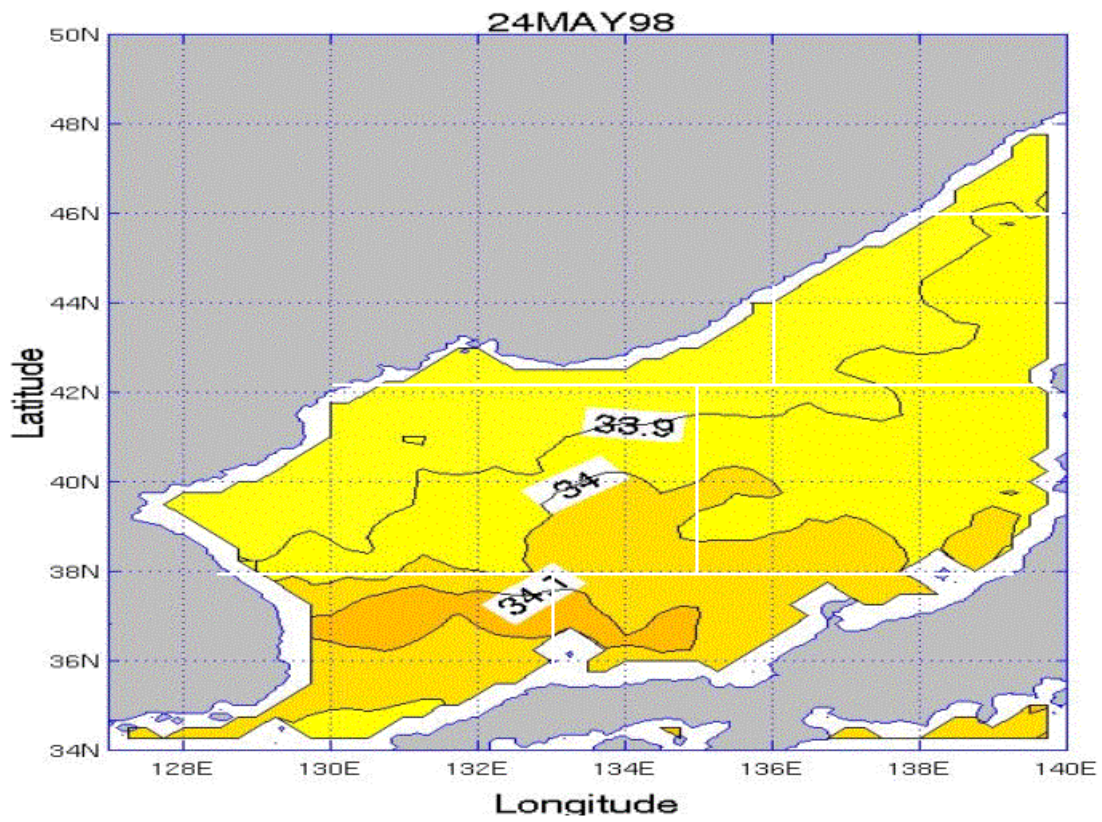


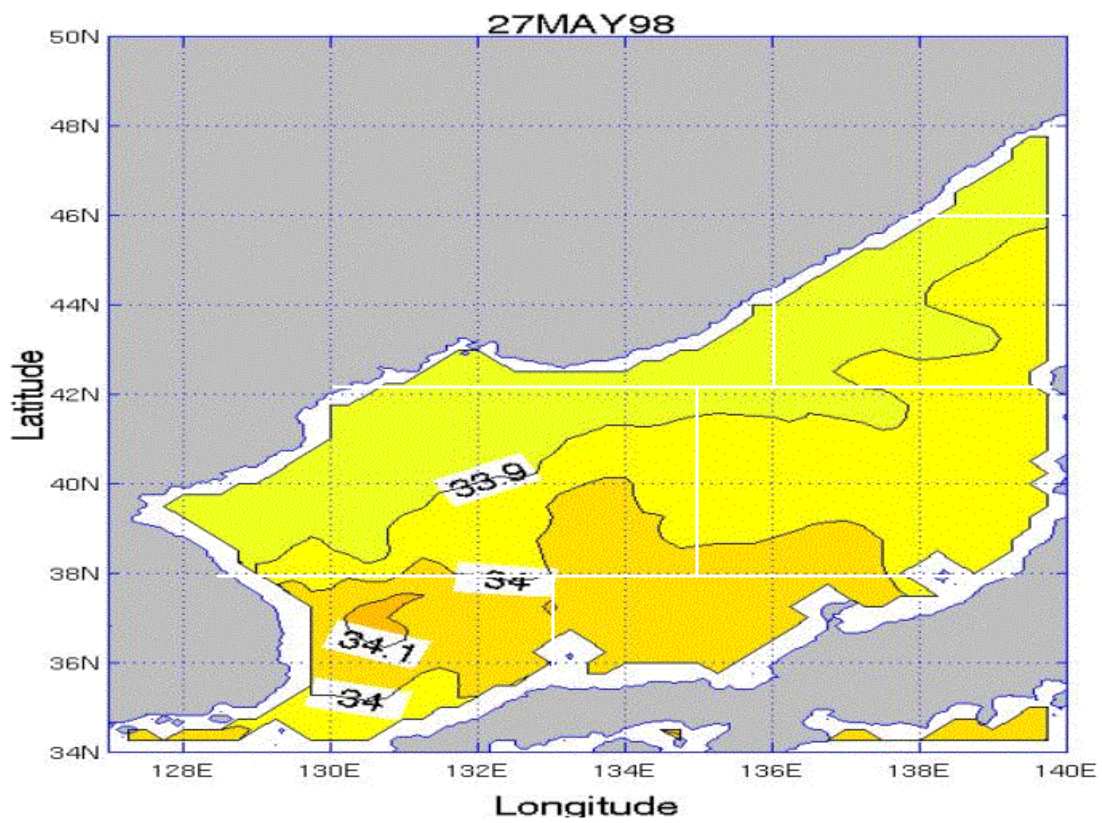
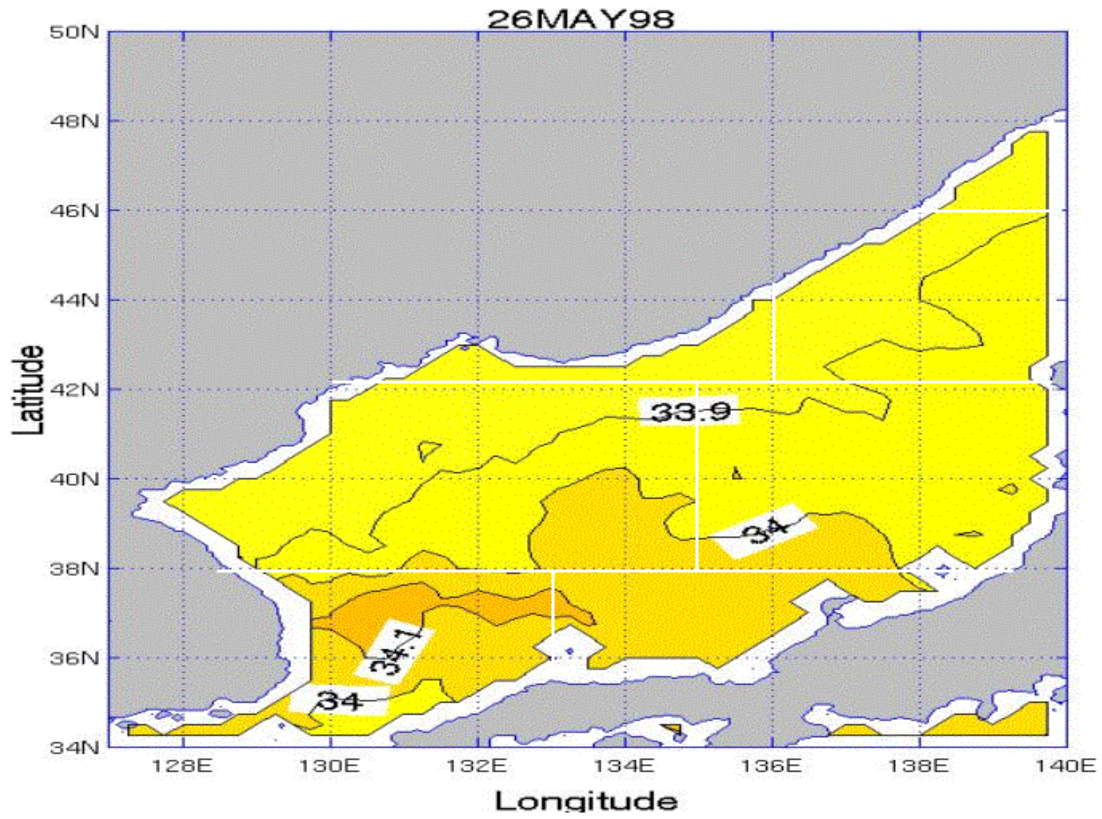


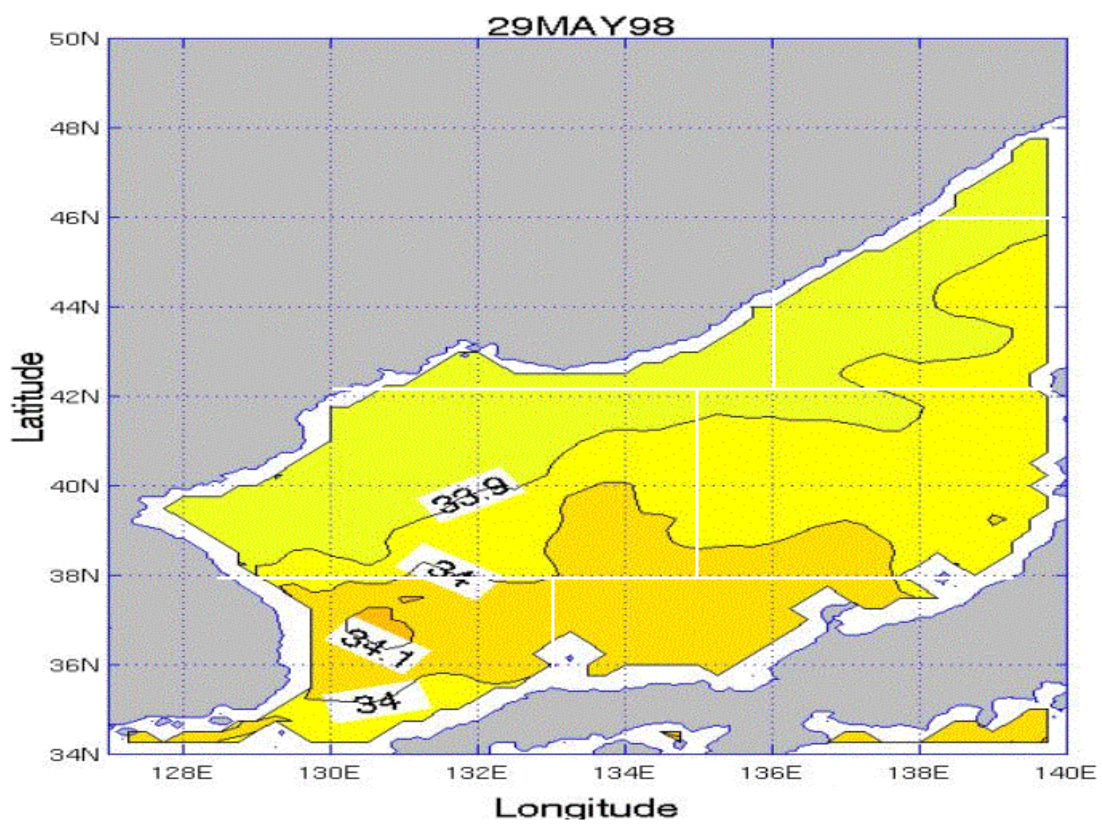
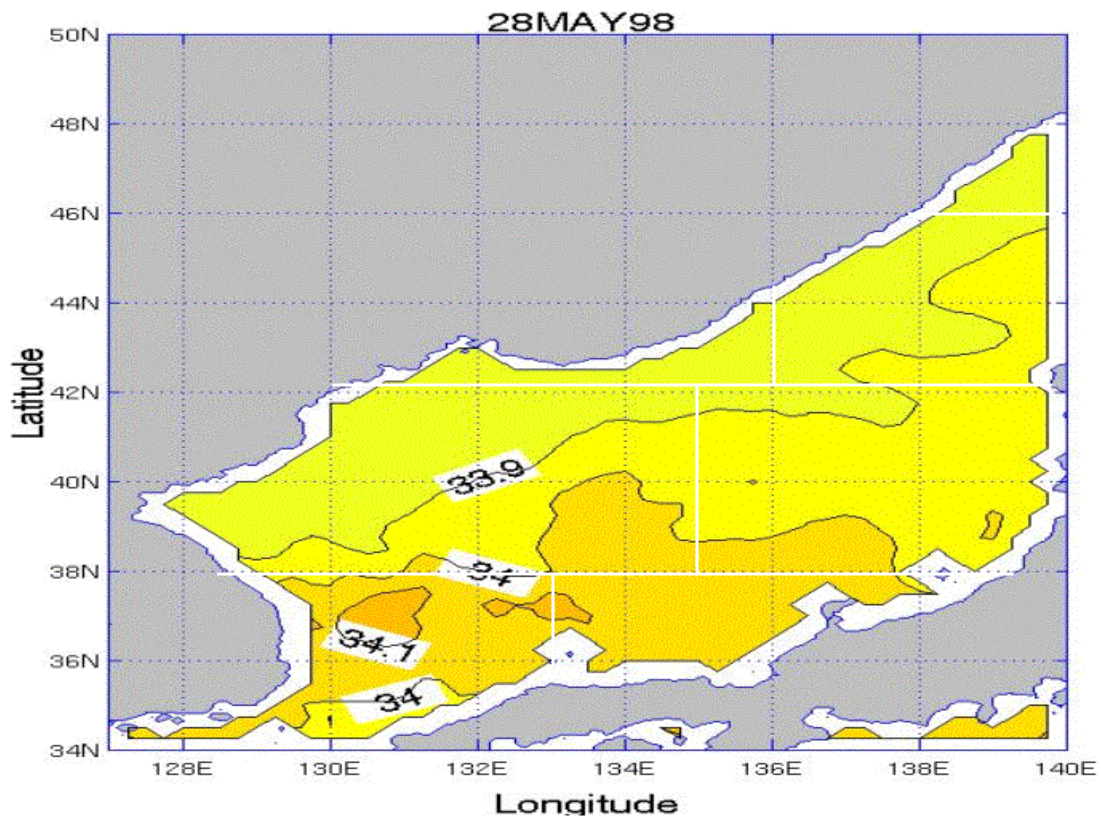


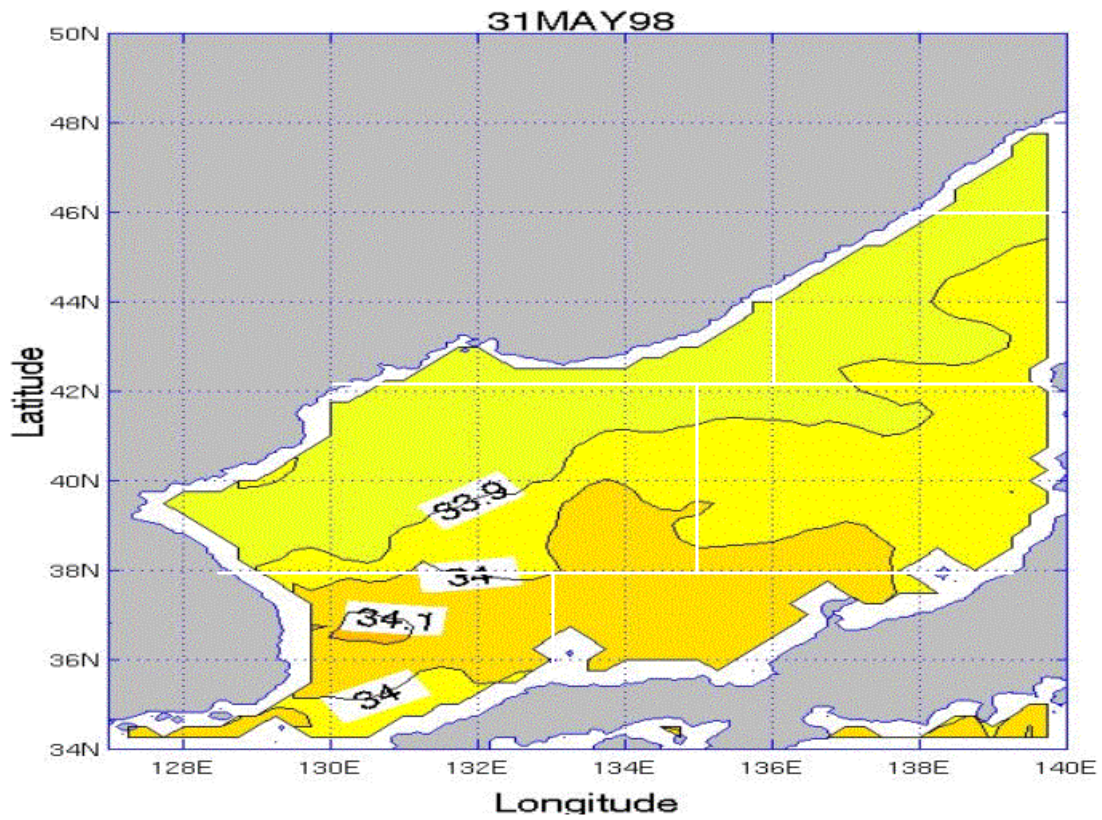
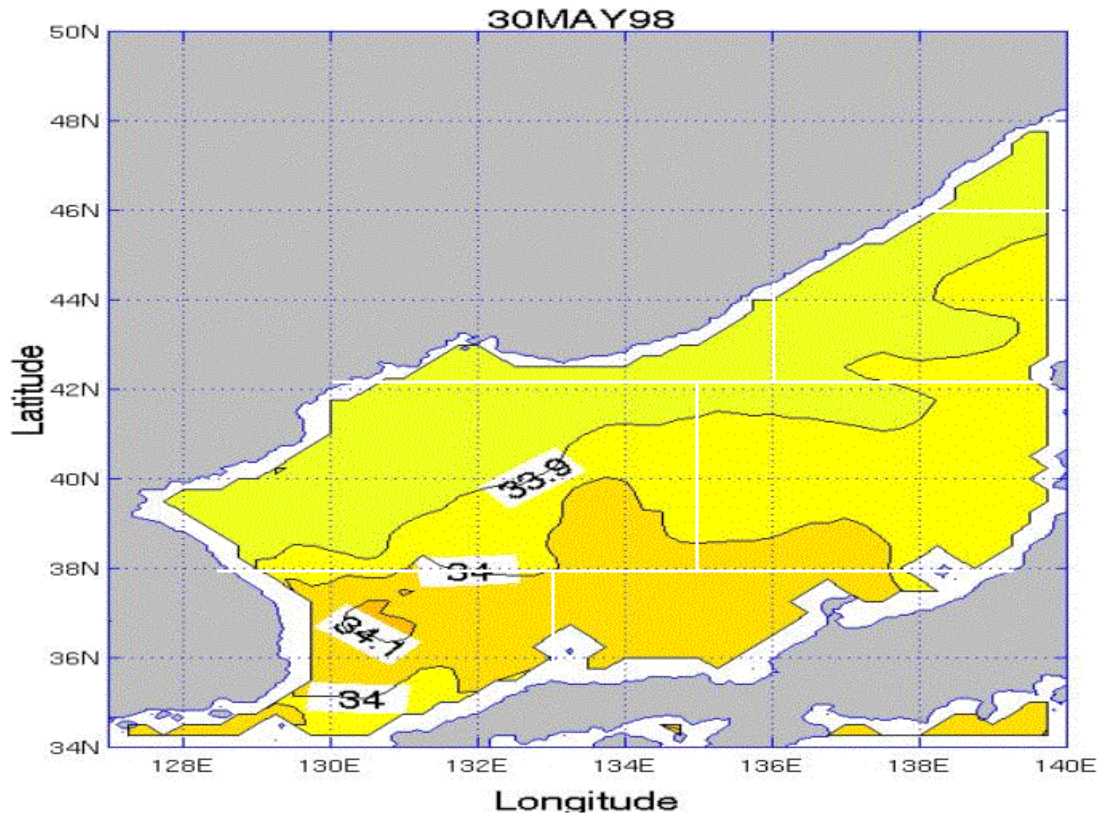






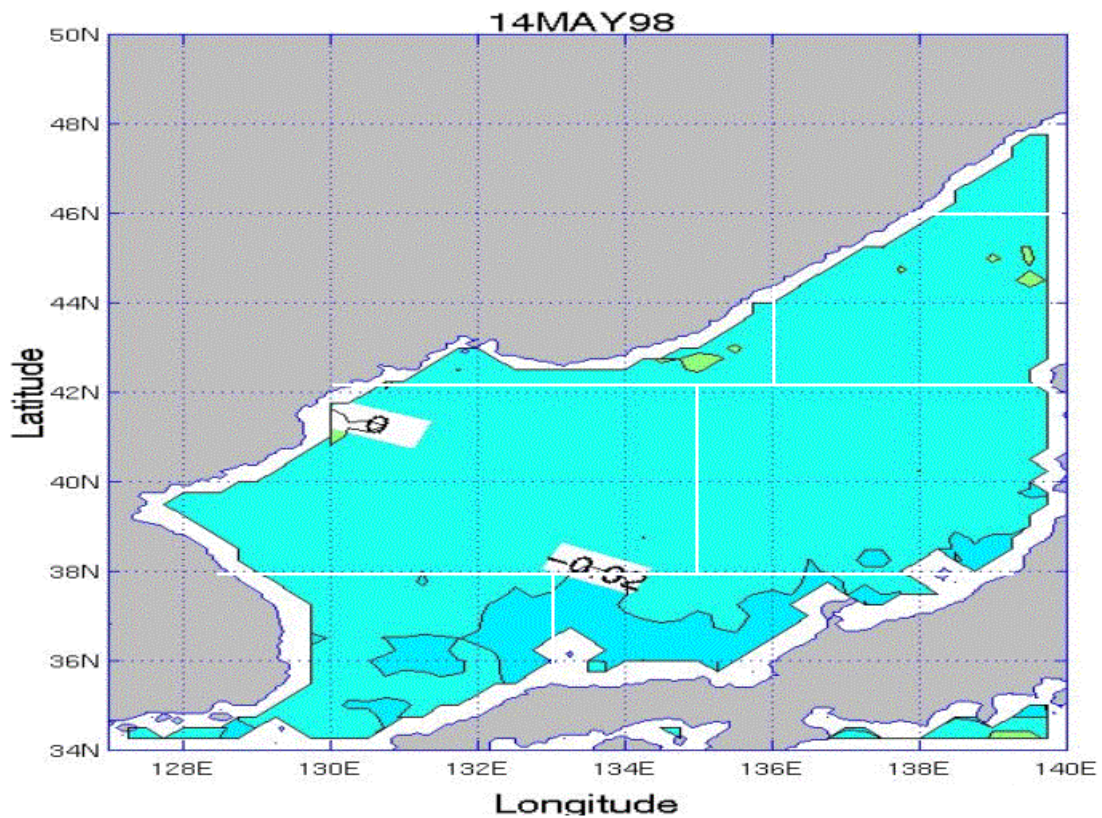


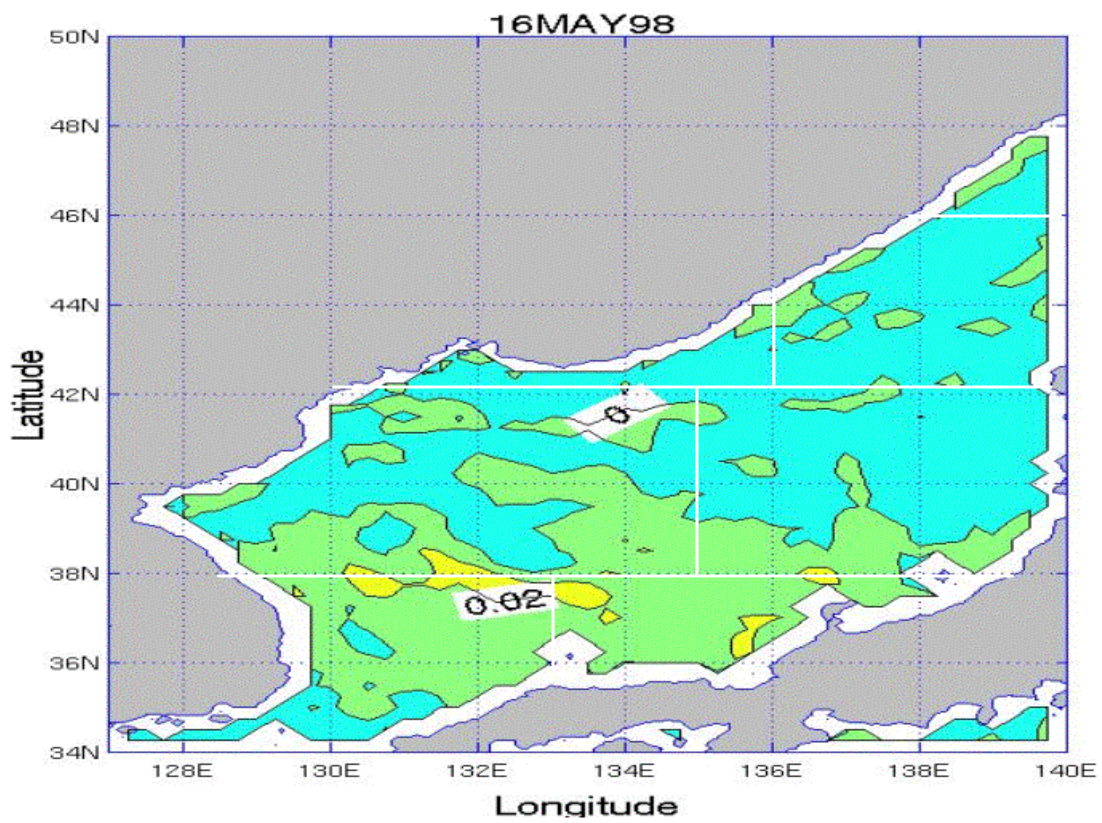
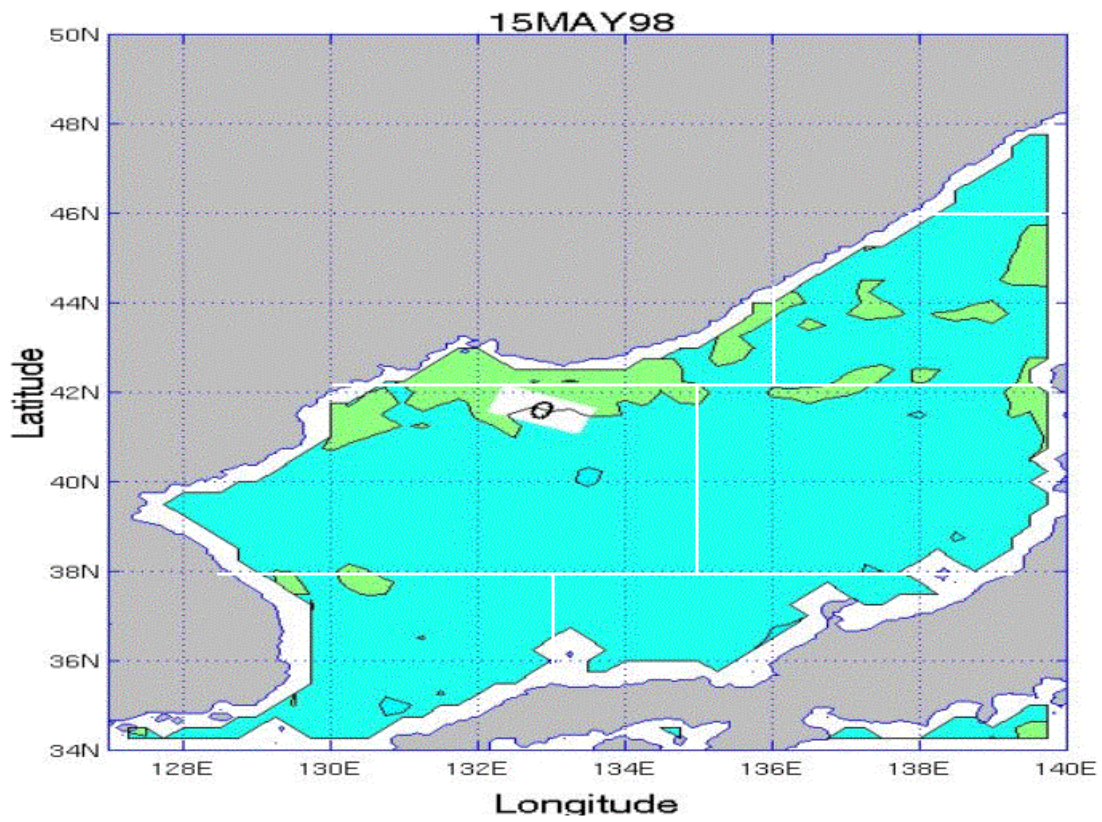


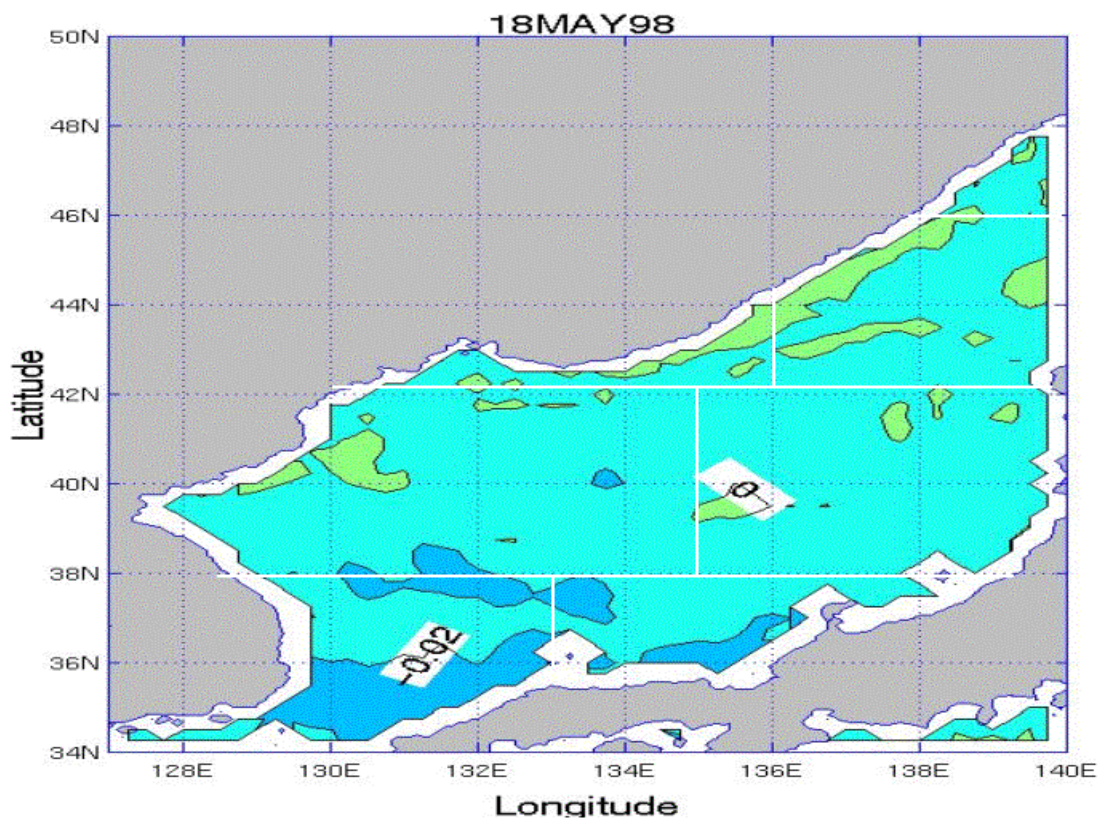
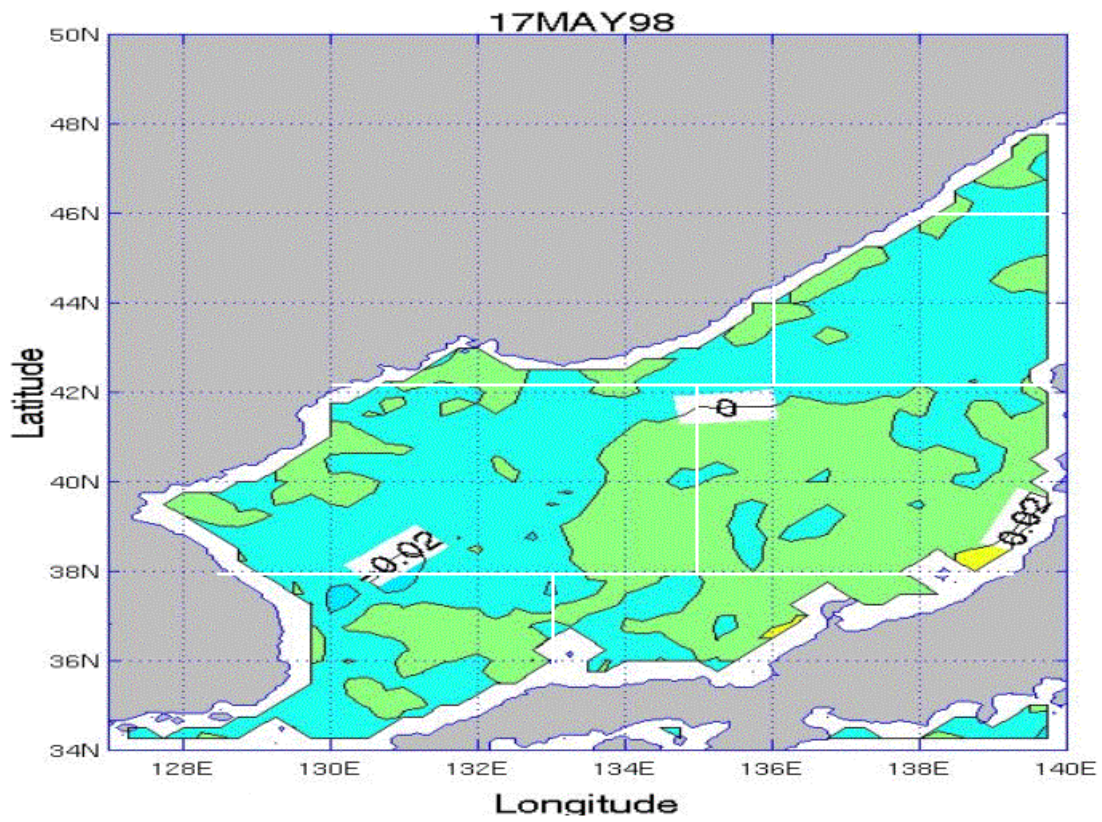


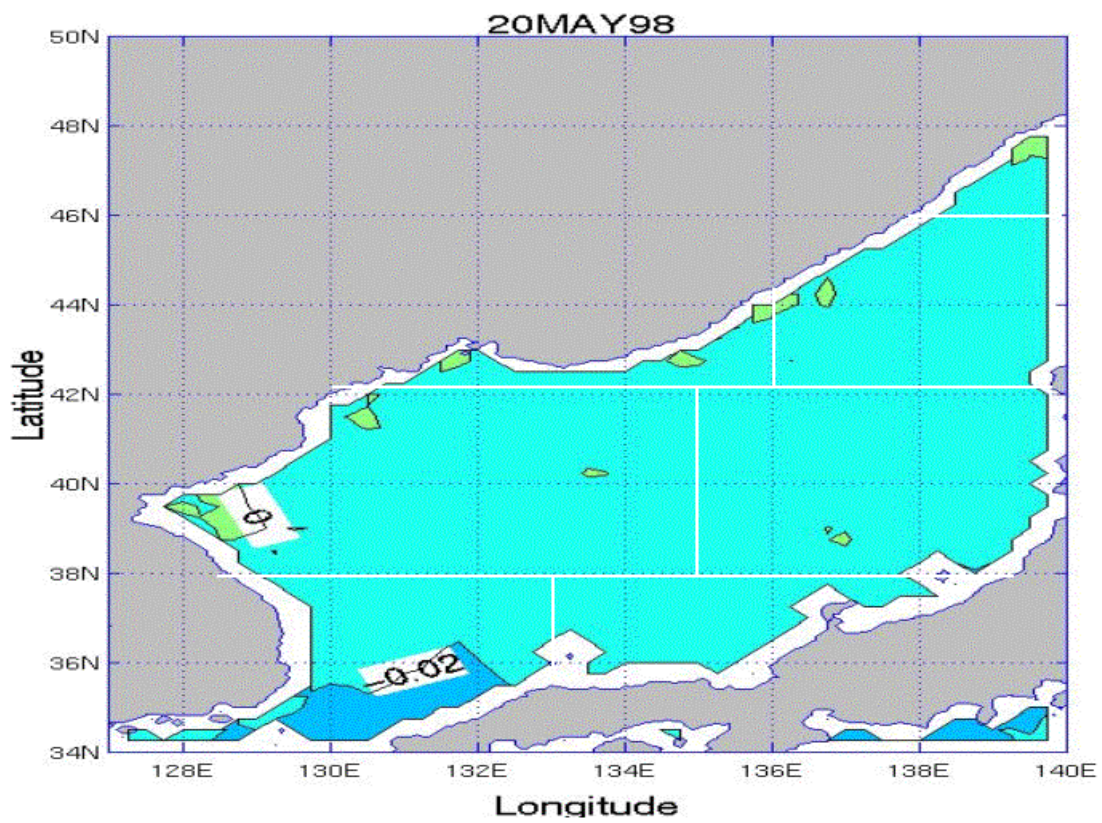
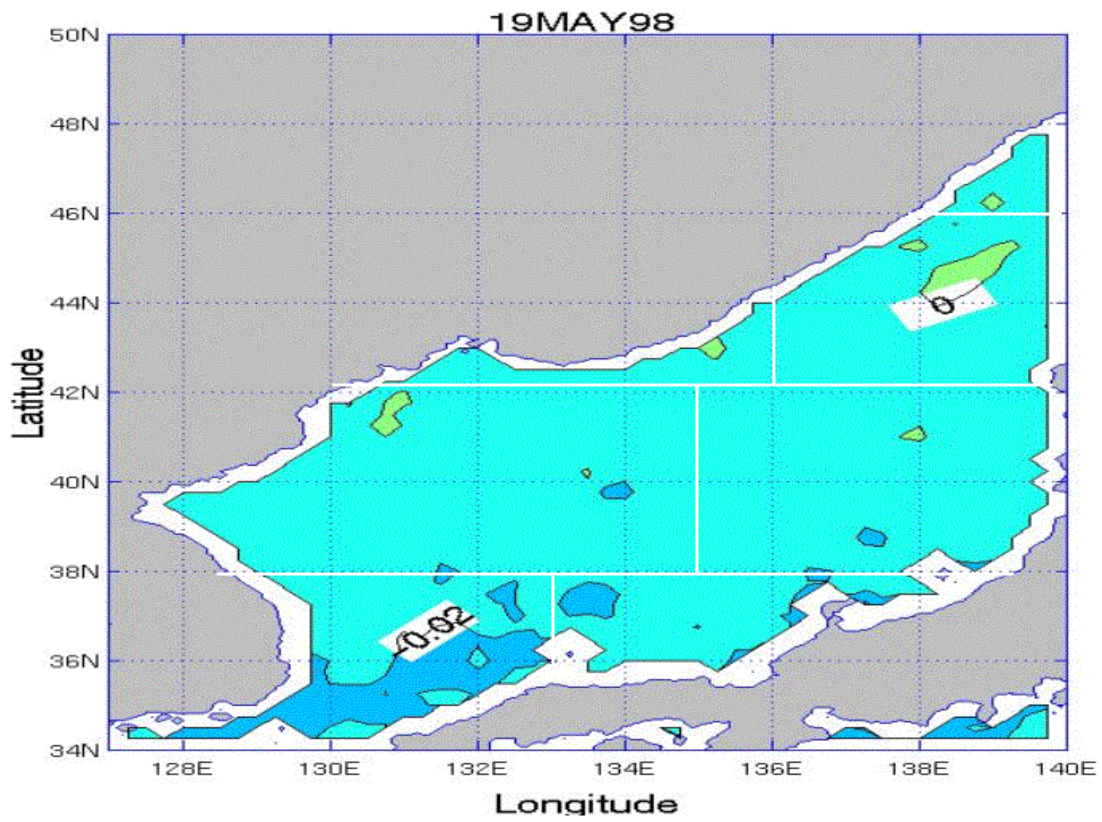
APPENDIX DD. SSS TENDENCY PLOTS FOR THE JES FOR THE MAY TIME PERIOD

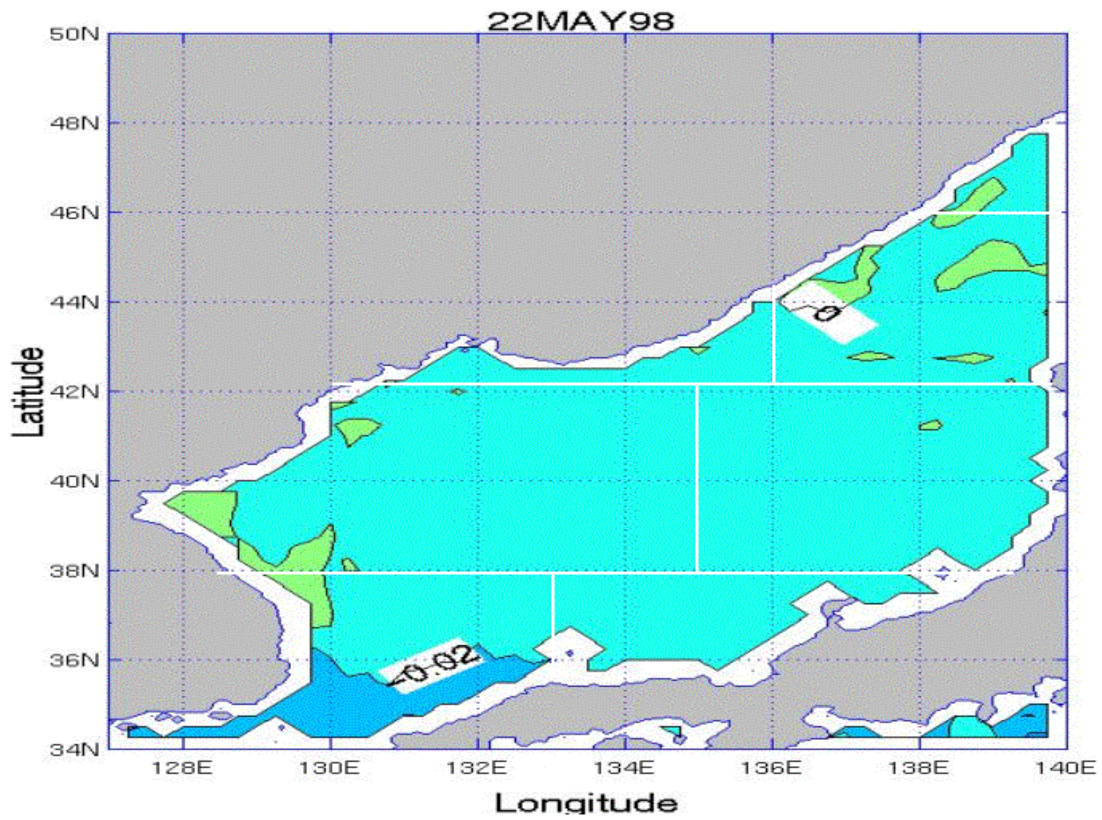
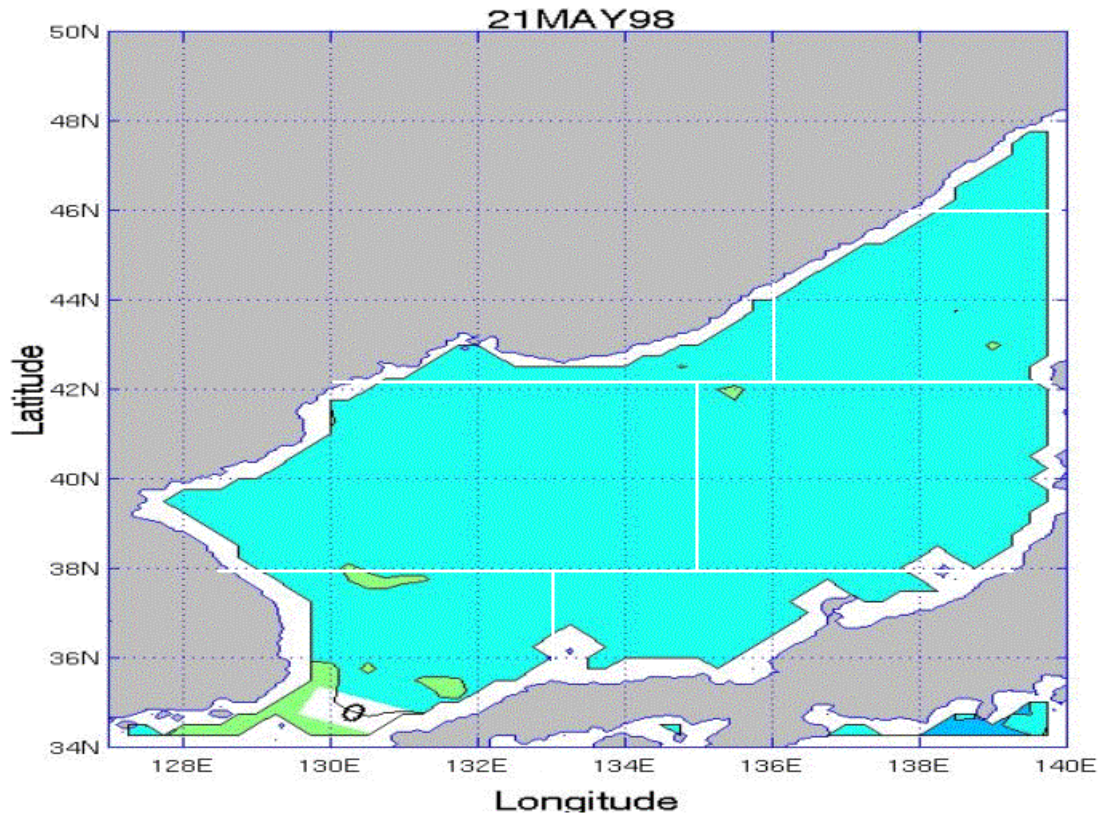
Appendix DD consists of 18 figures that show SSS day-to-day tendency for the May time period over the JES. The figures are in time sequential order from May 14 through May 31. Each plot represents the change between the previous day and the current day.

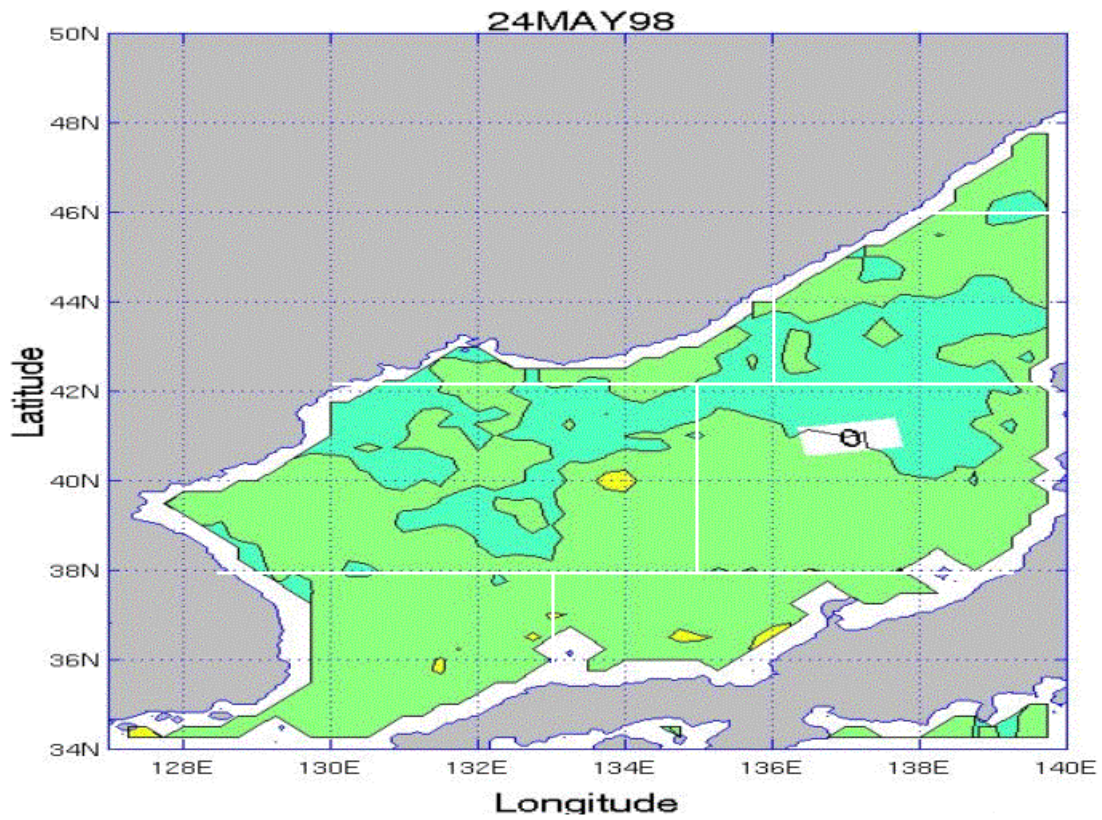
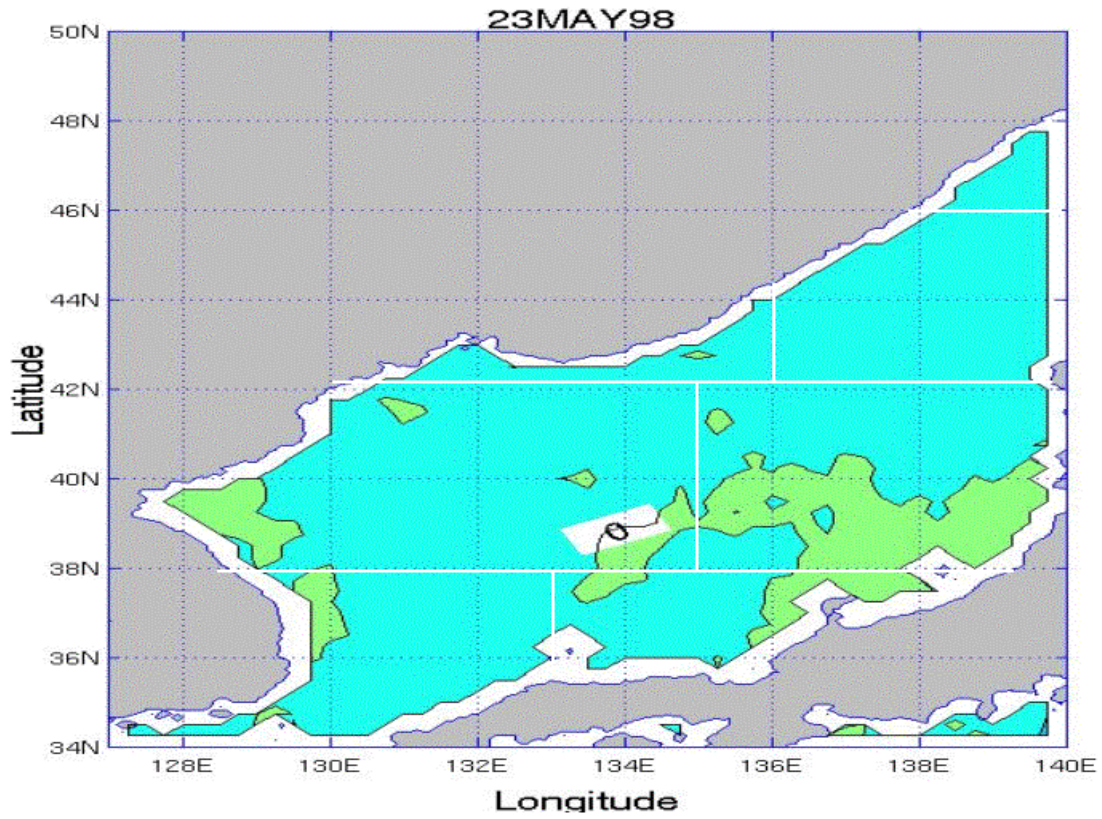


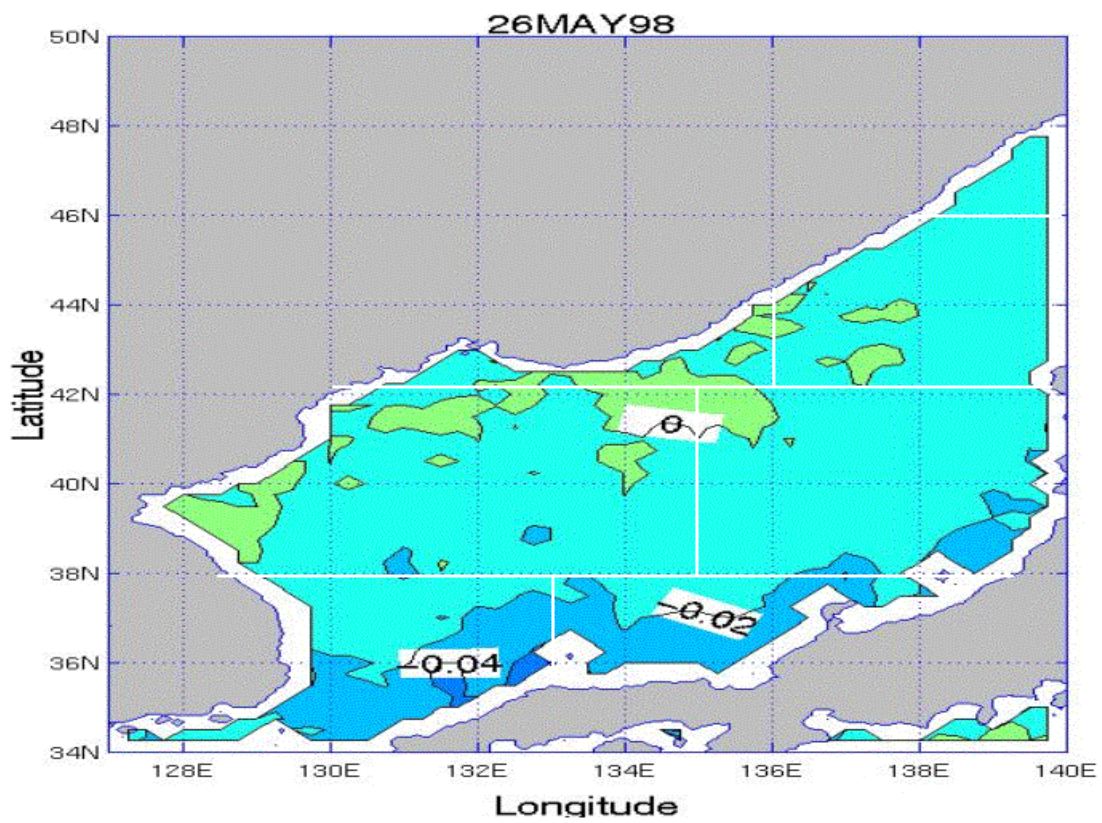
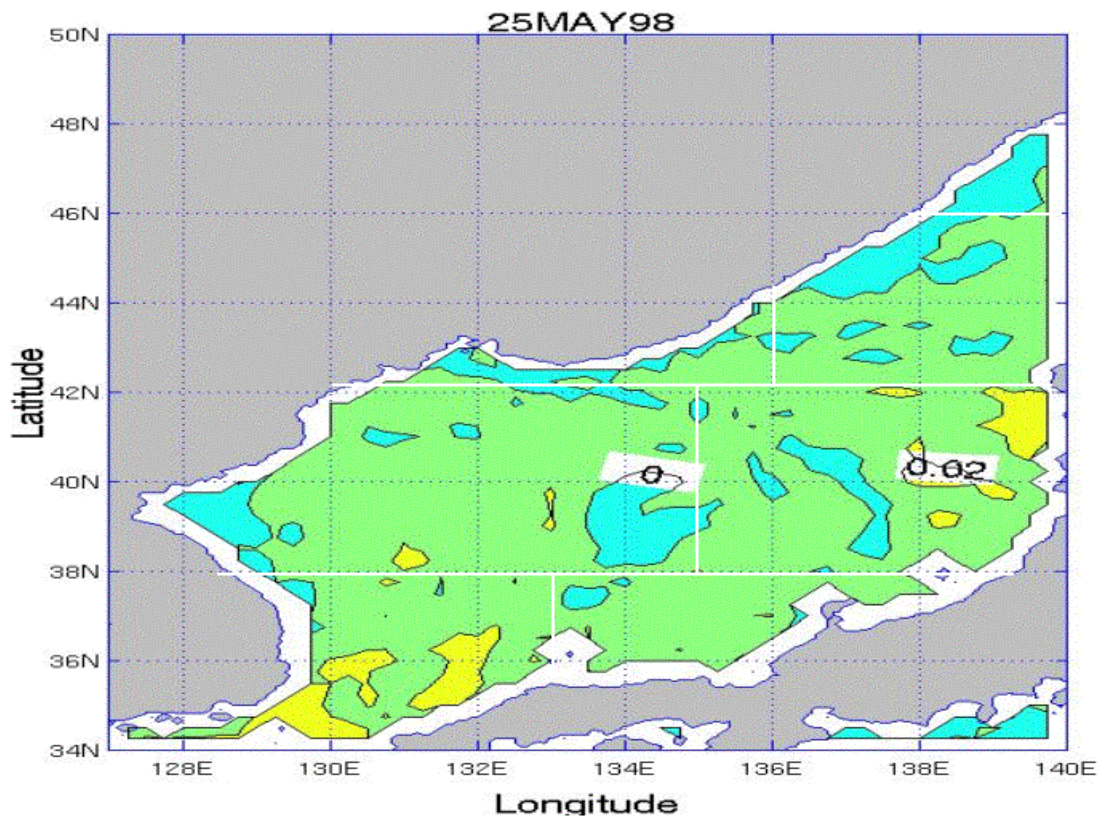


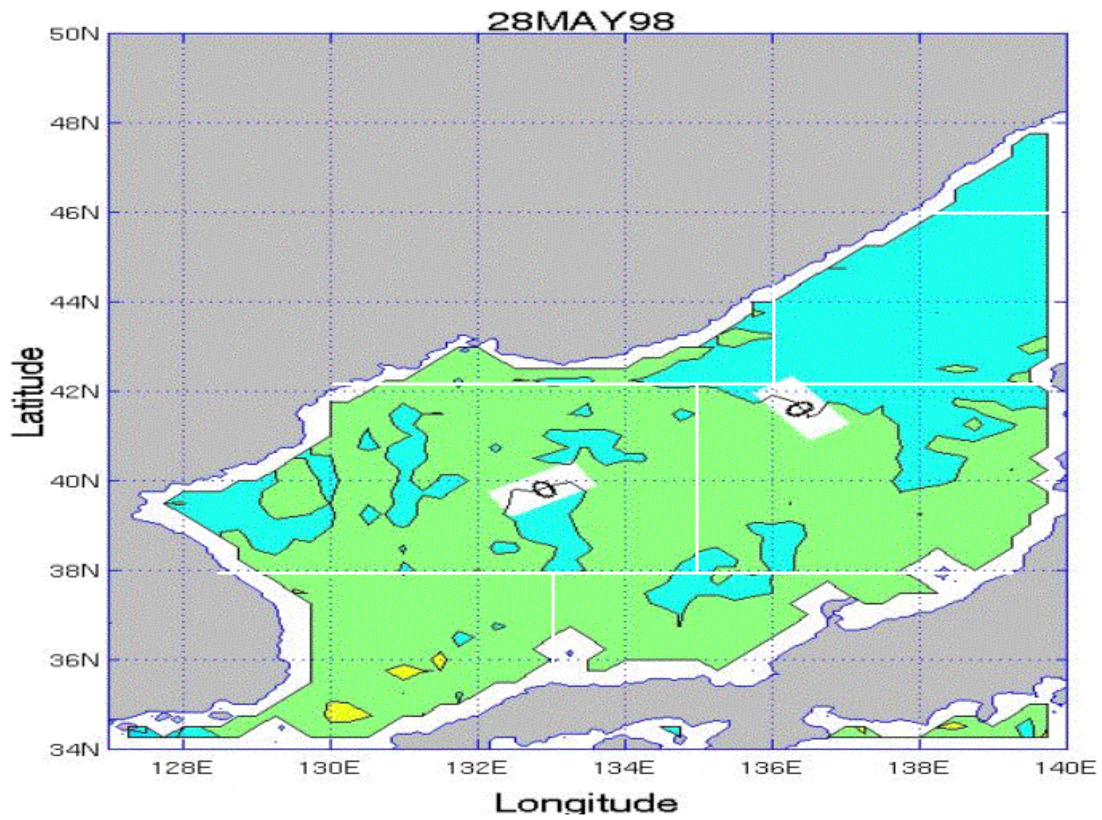
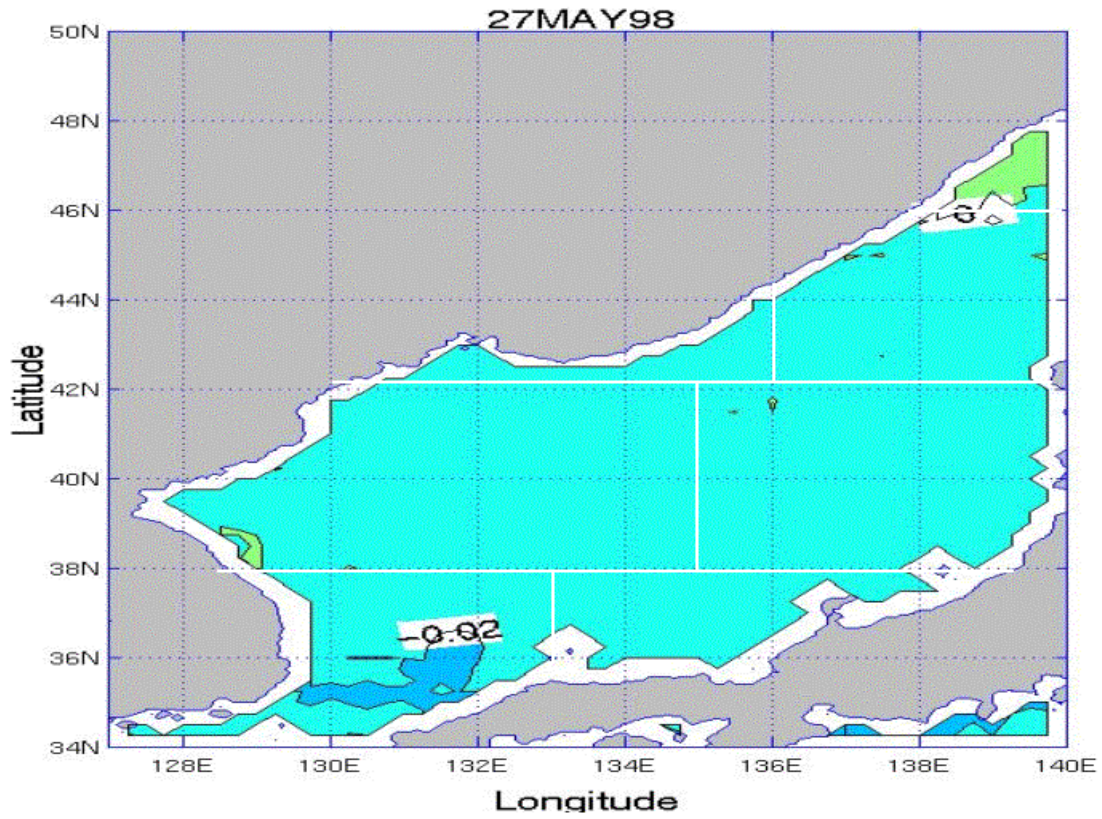


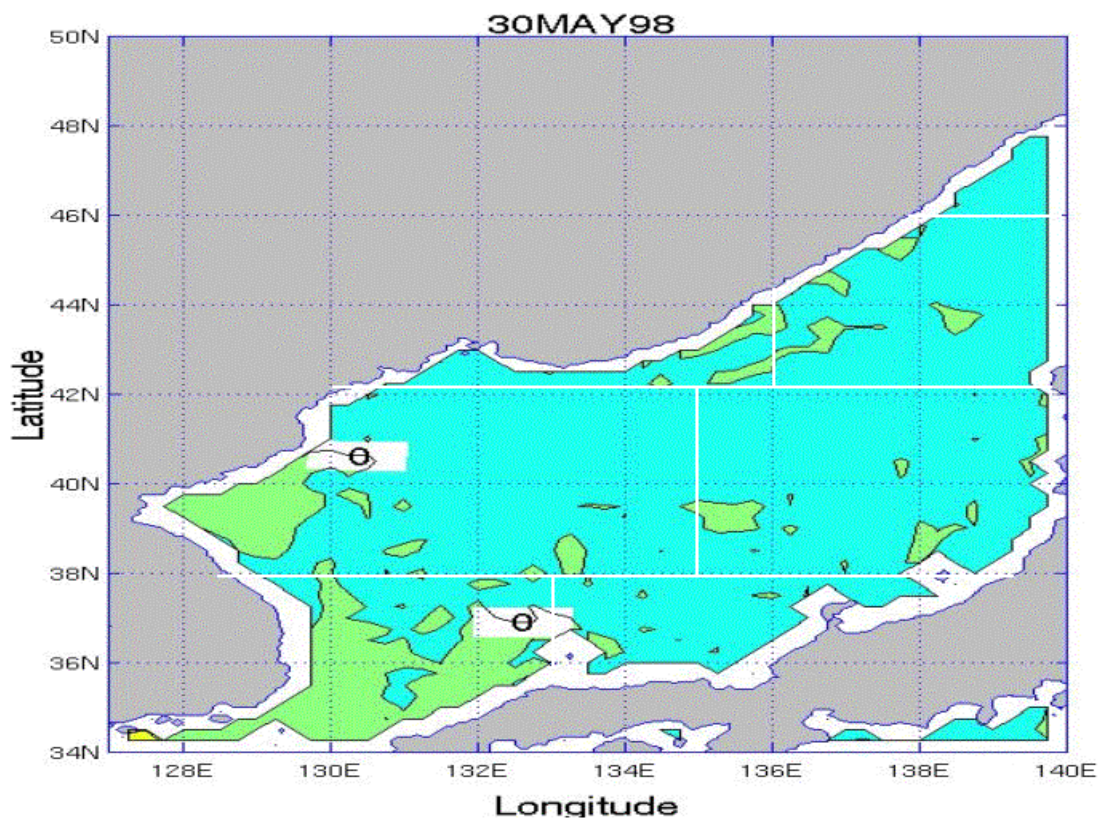
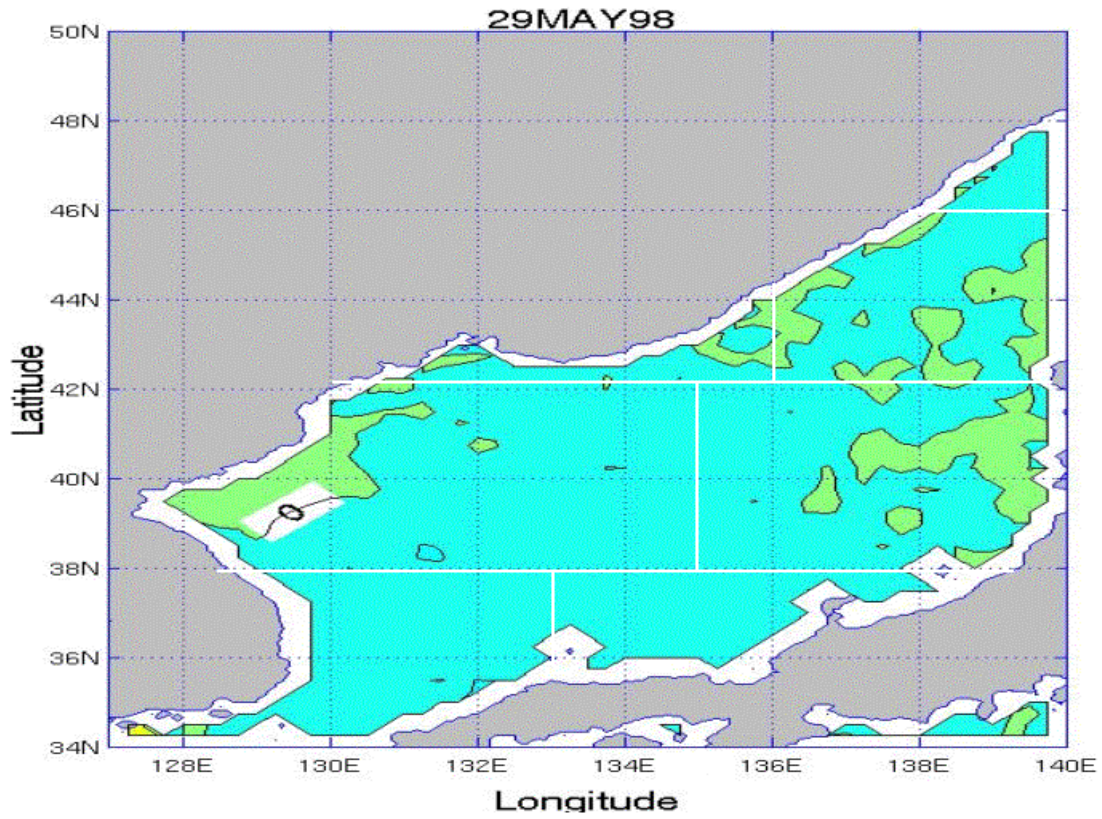


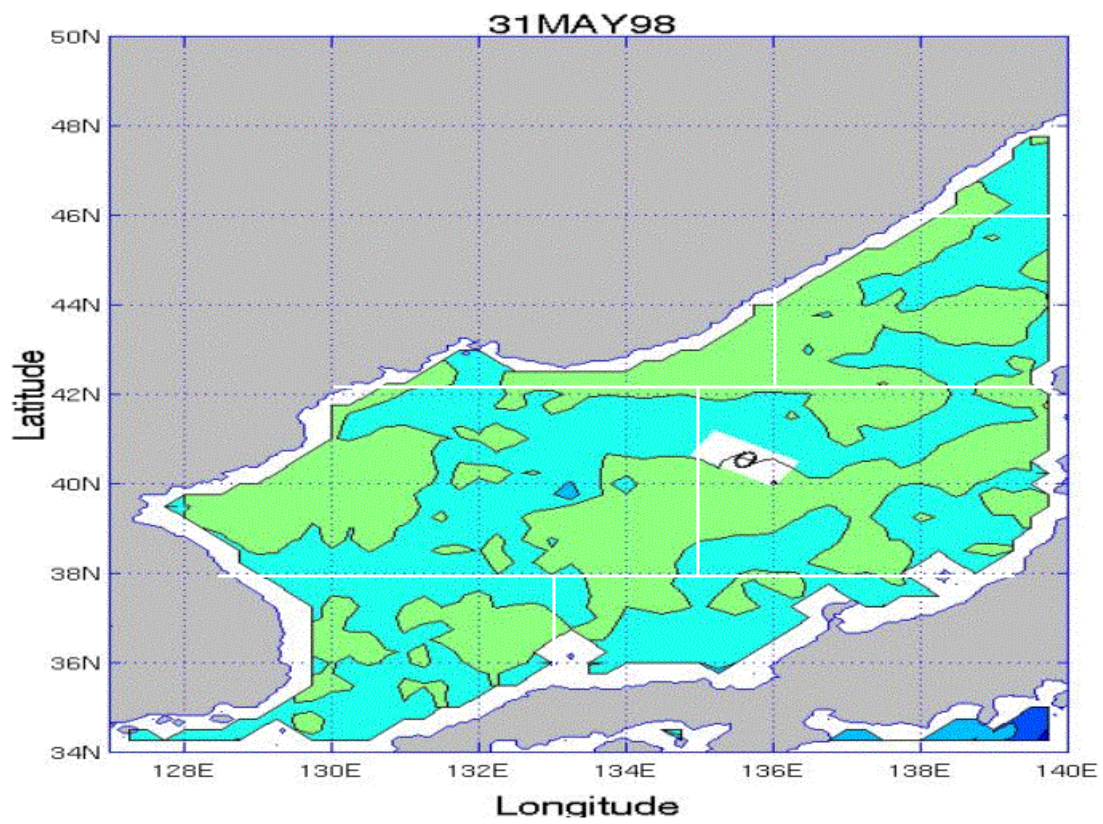






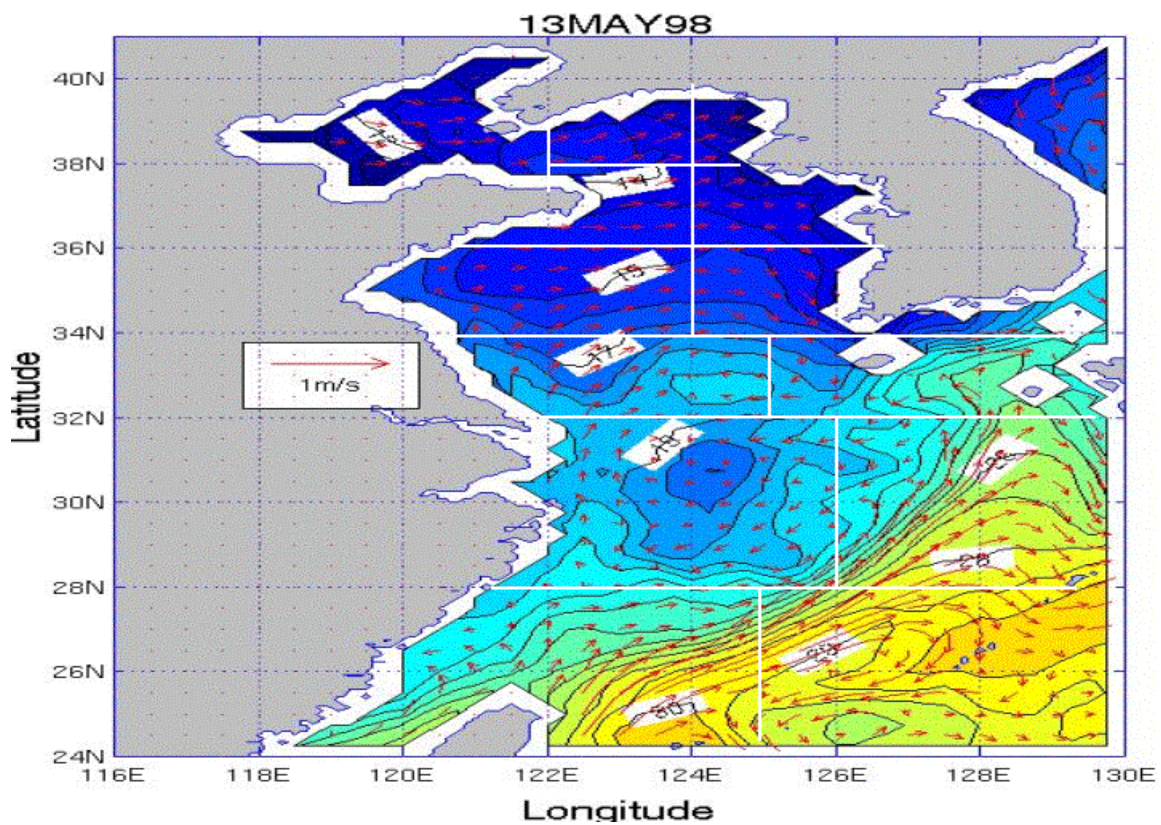


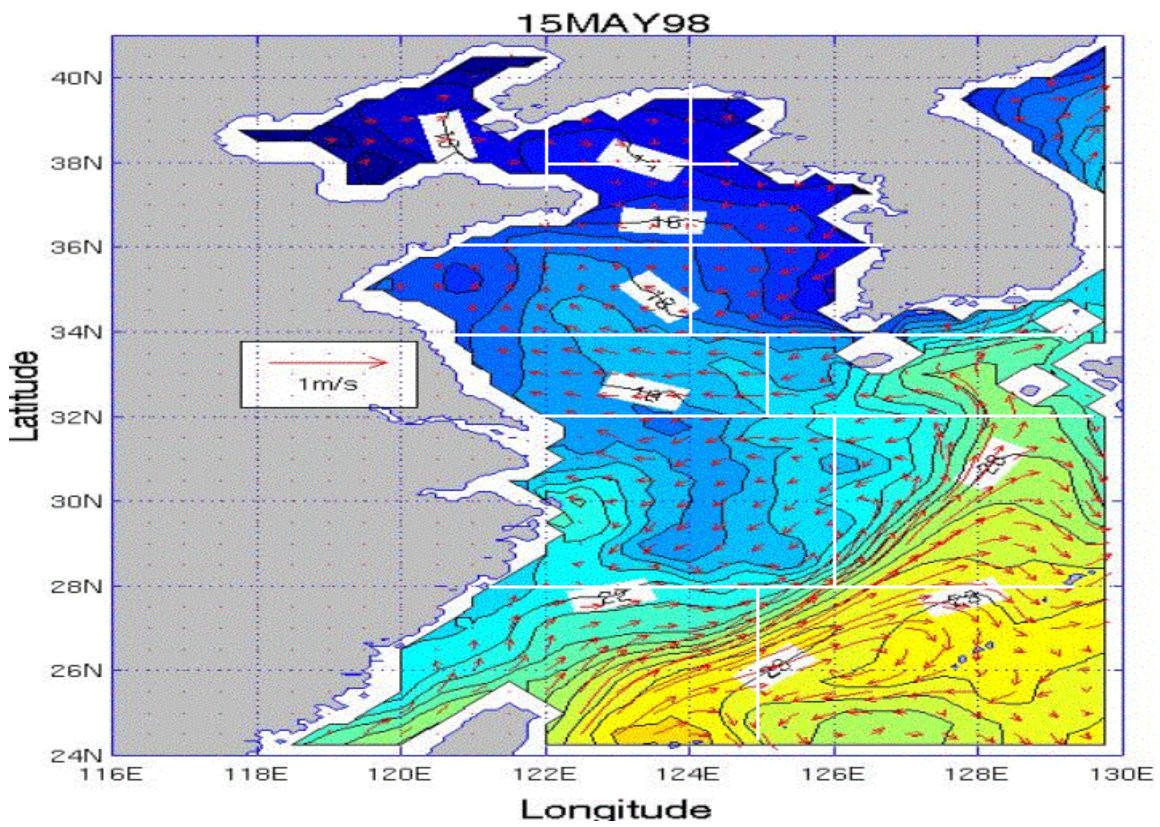
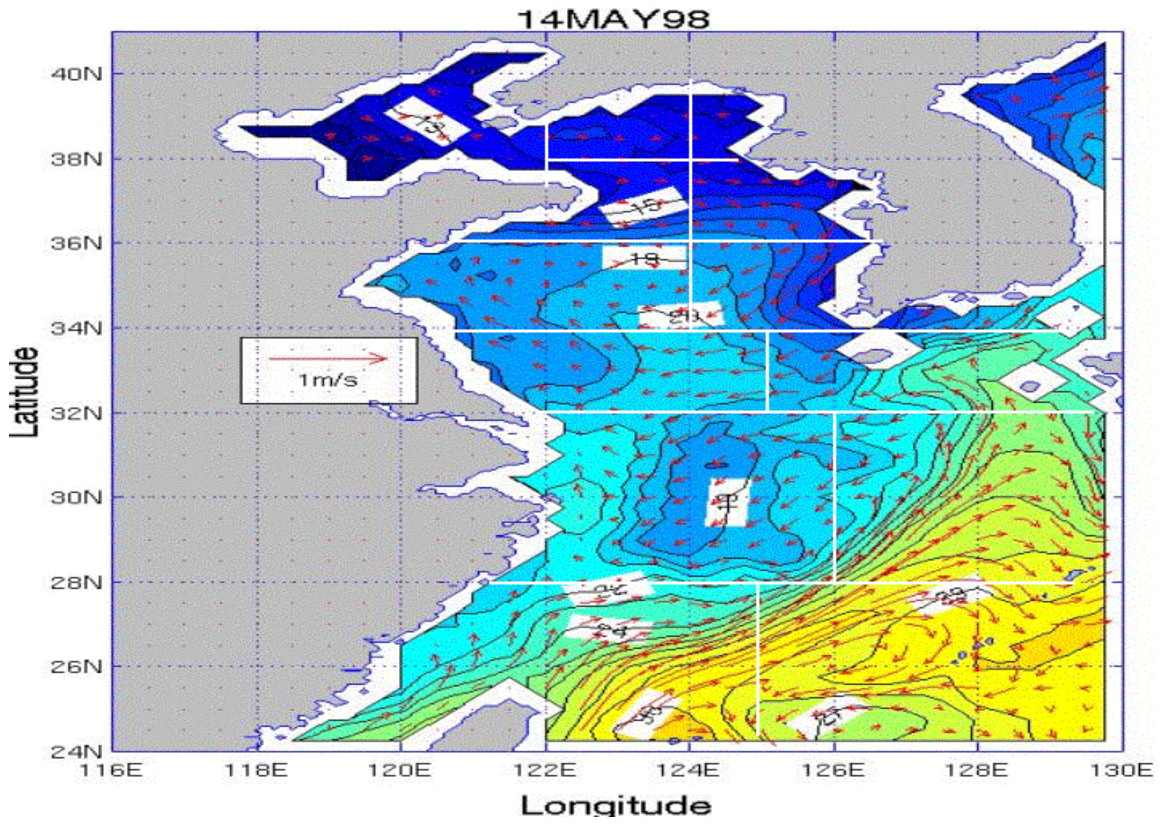


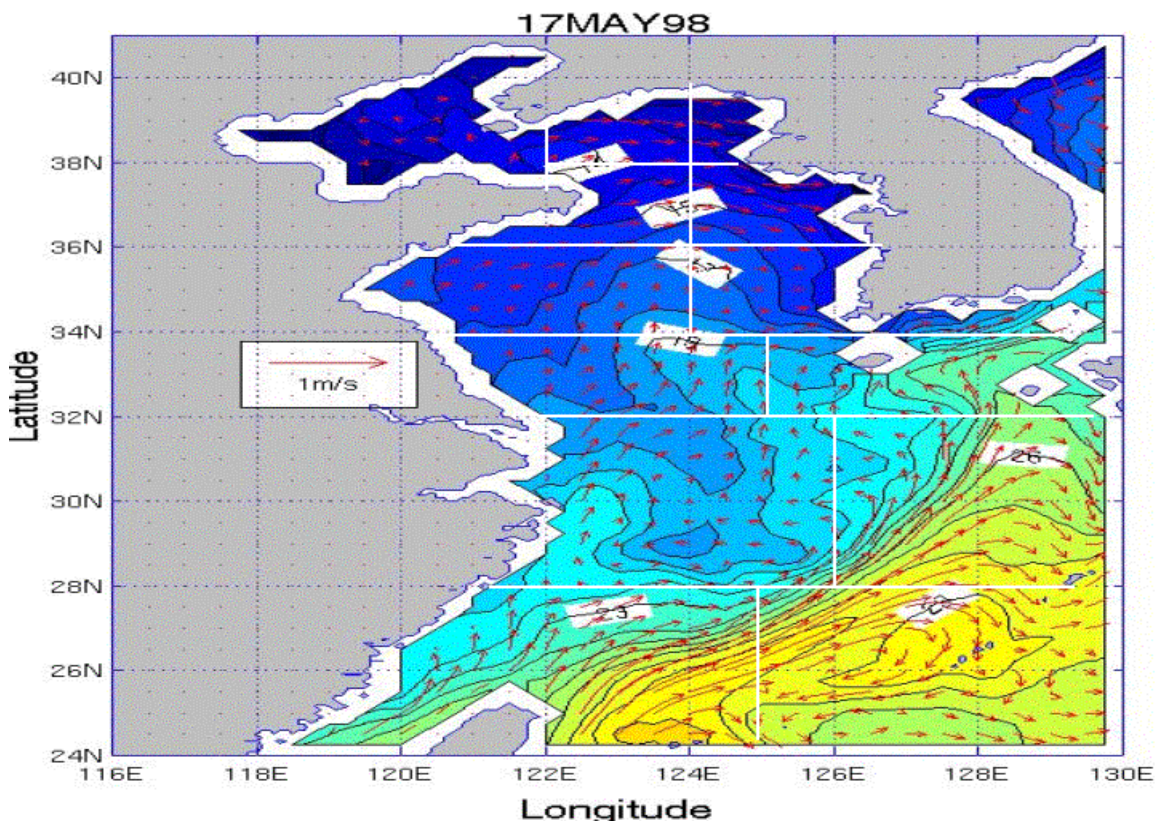
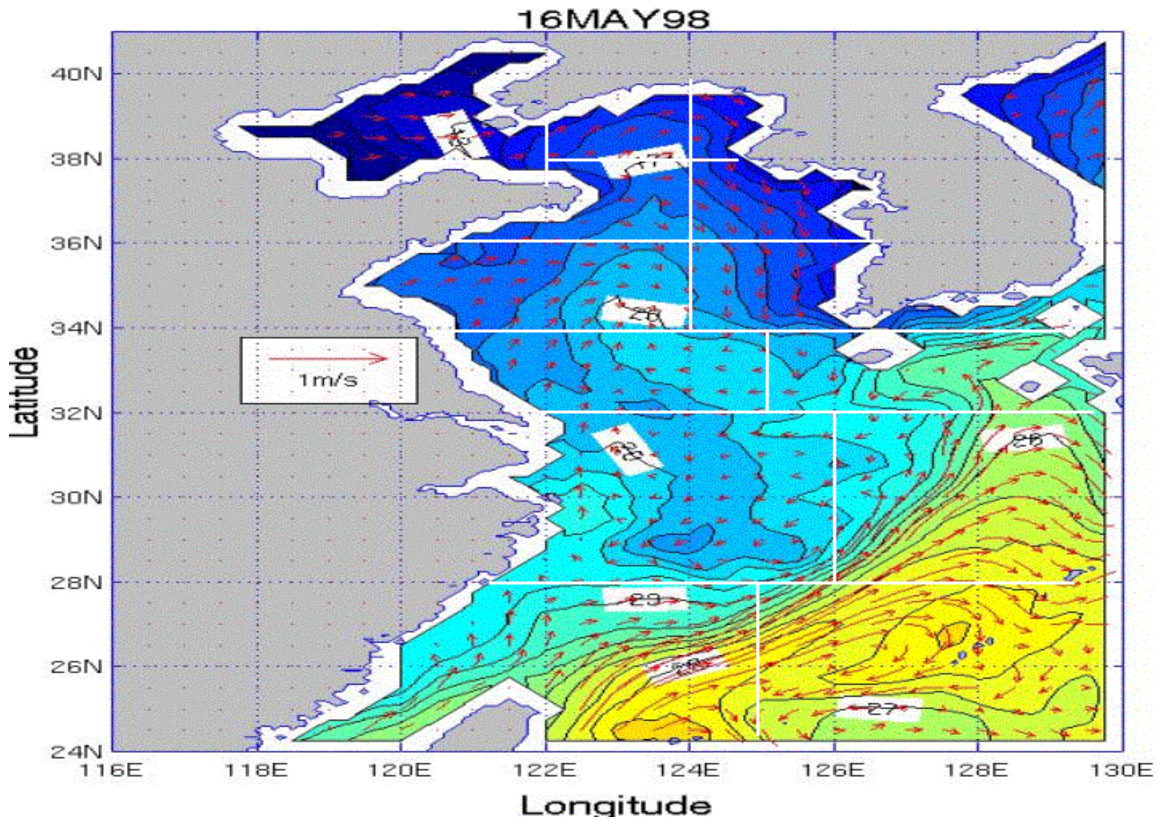


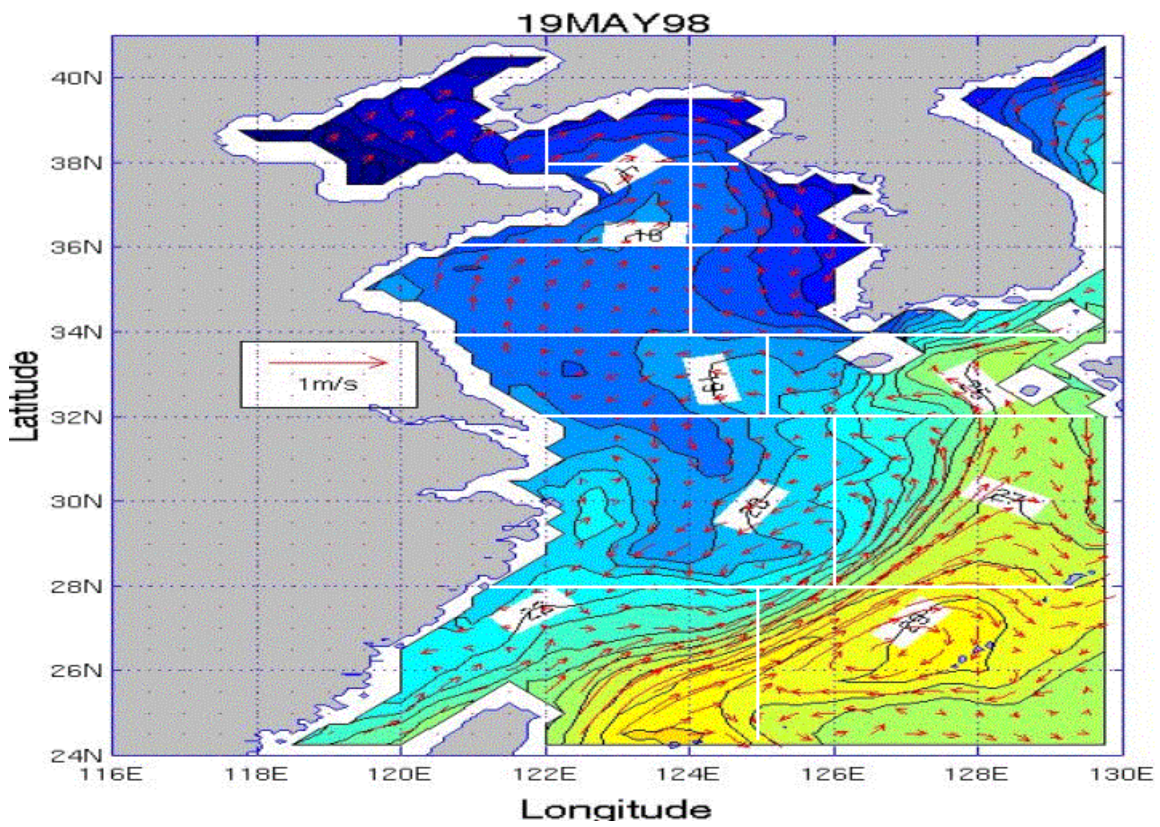
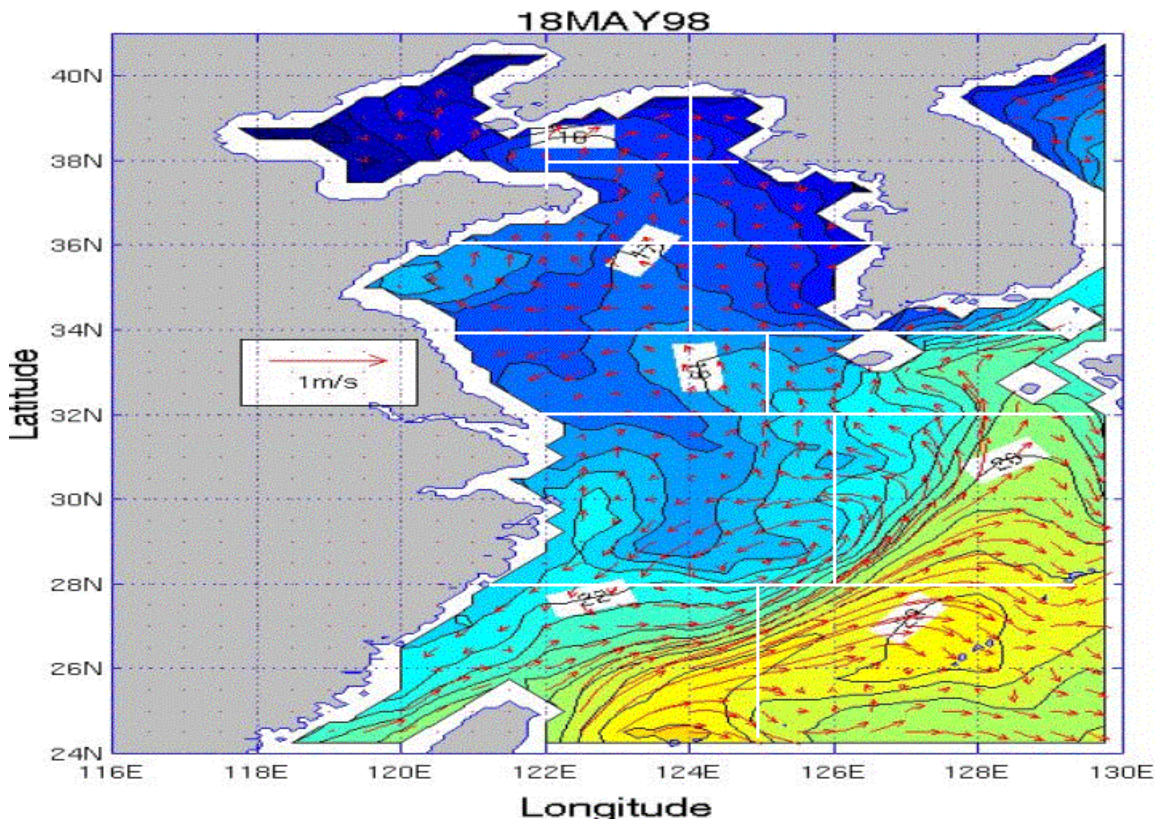
APPENDIX EE. SST AND SURFACE CURRENT VELOCITY PLOTS FOR THE YES FOR THE MAY TIME PERIOD

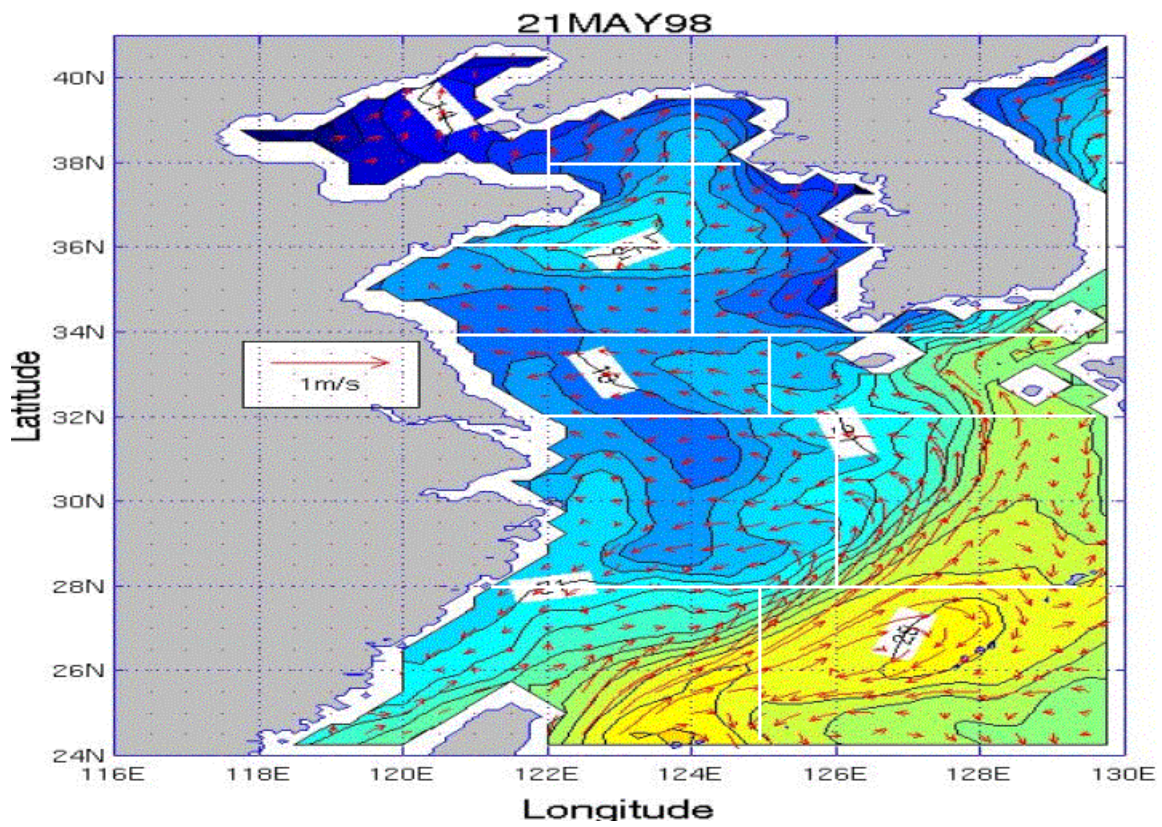
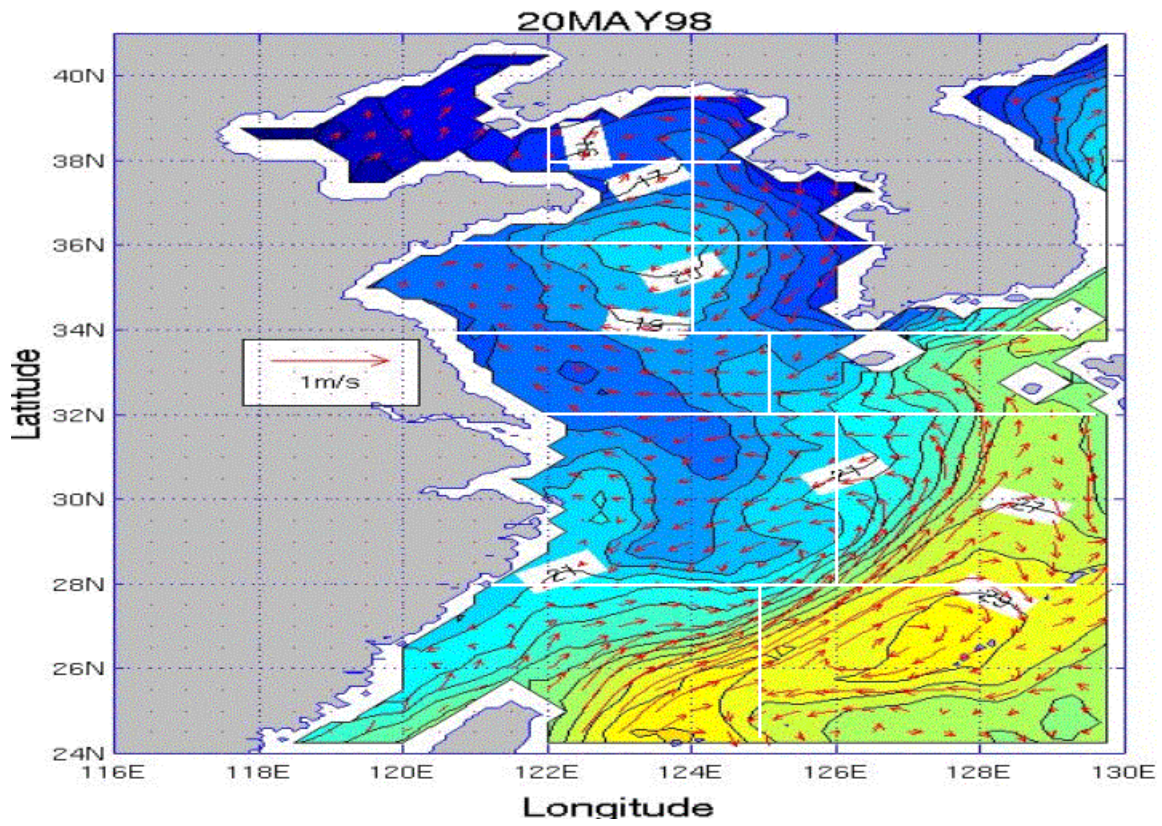
Appendix EE consists of 19 figures that show SST and surface current velocity for each day of the May time period for the YES. The figures are in time sequential order from May 13 through May 31.

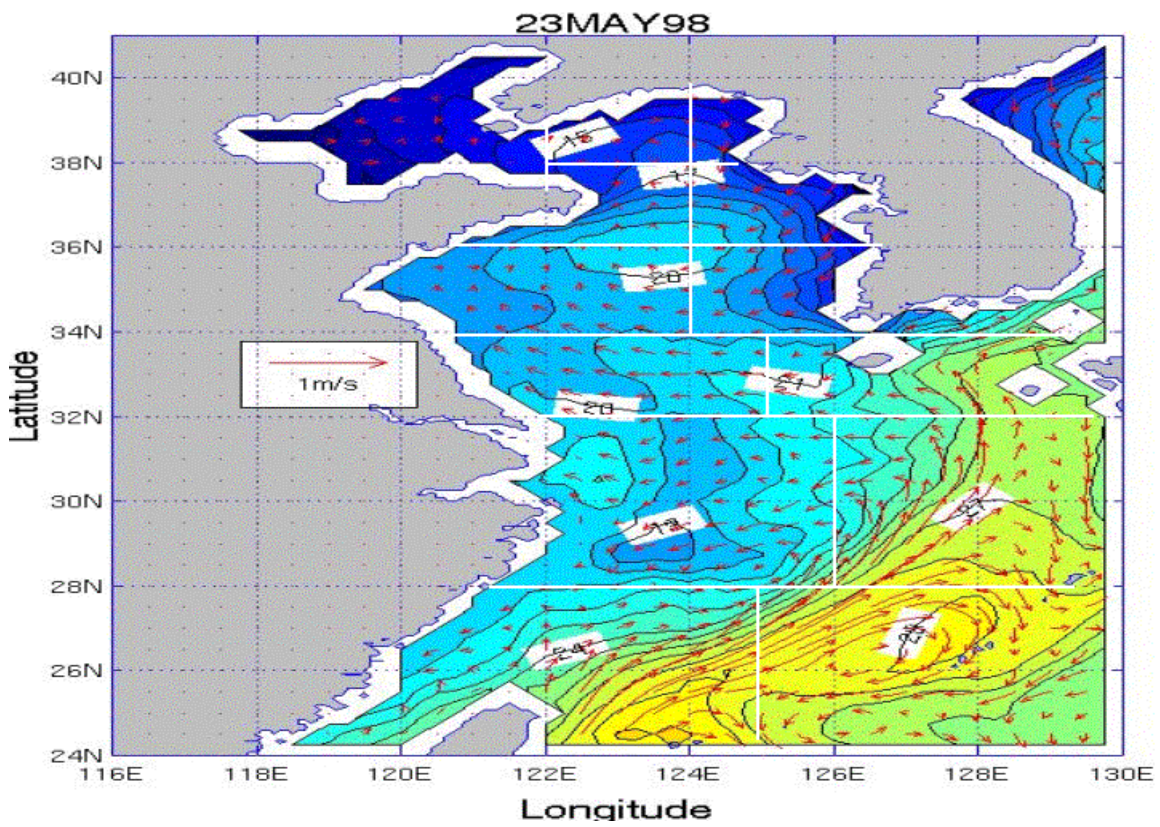
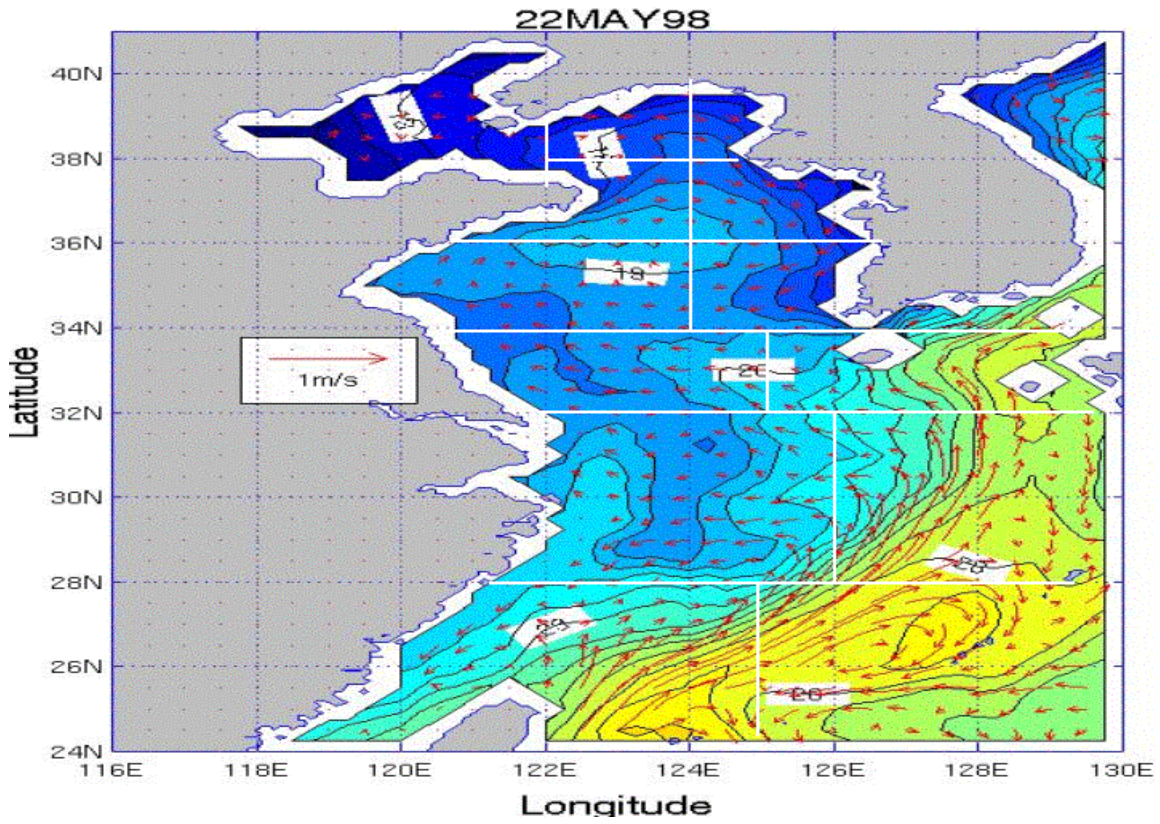


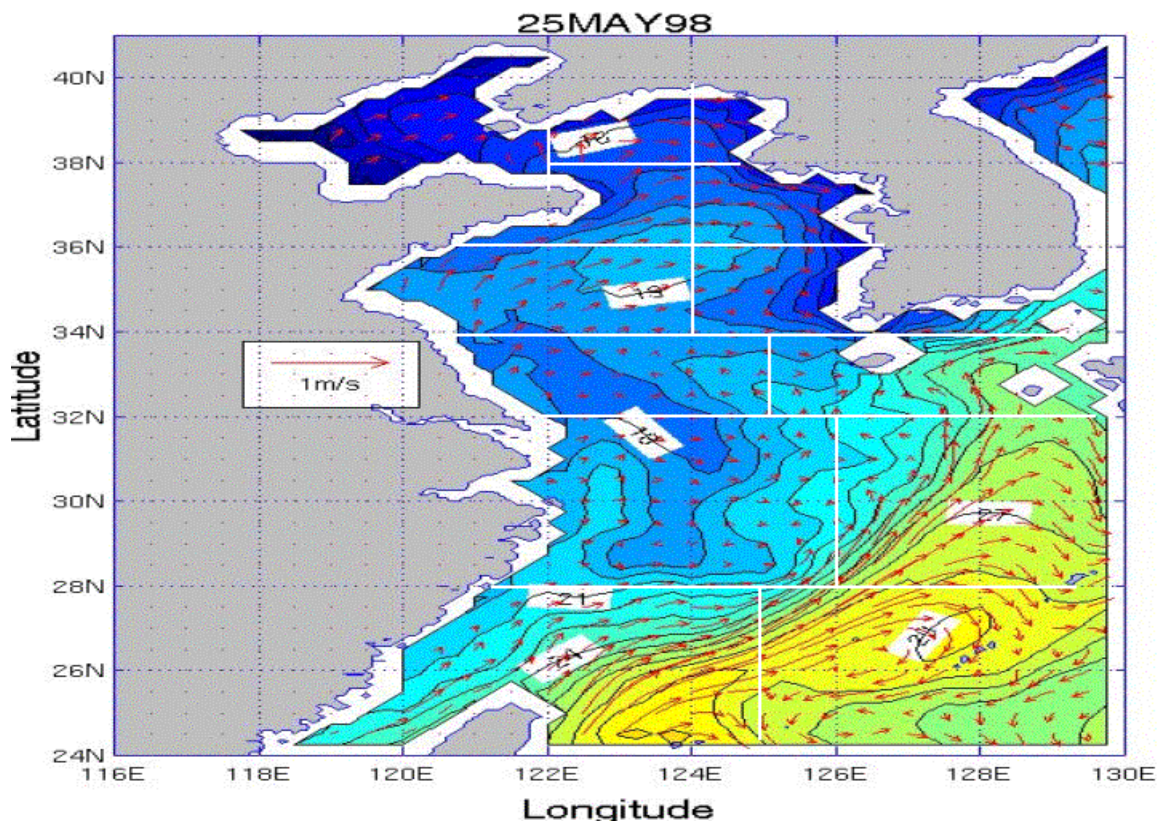
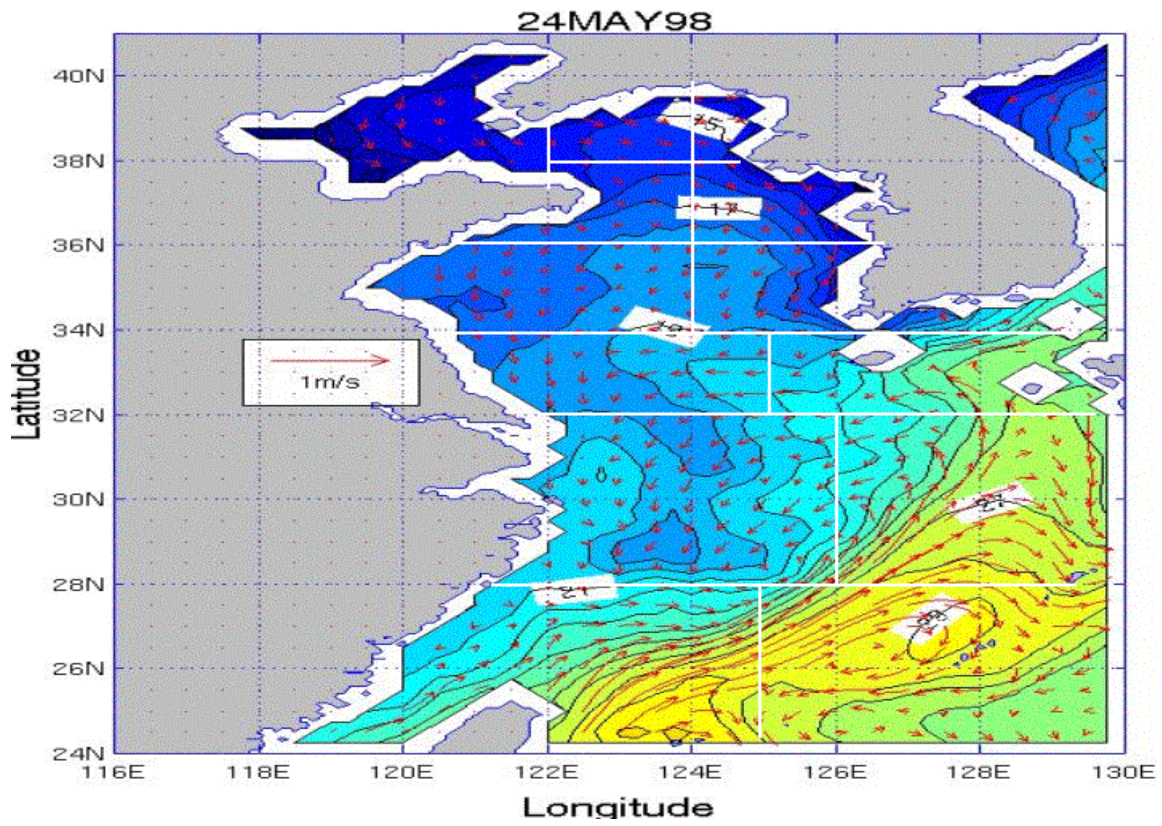


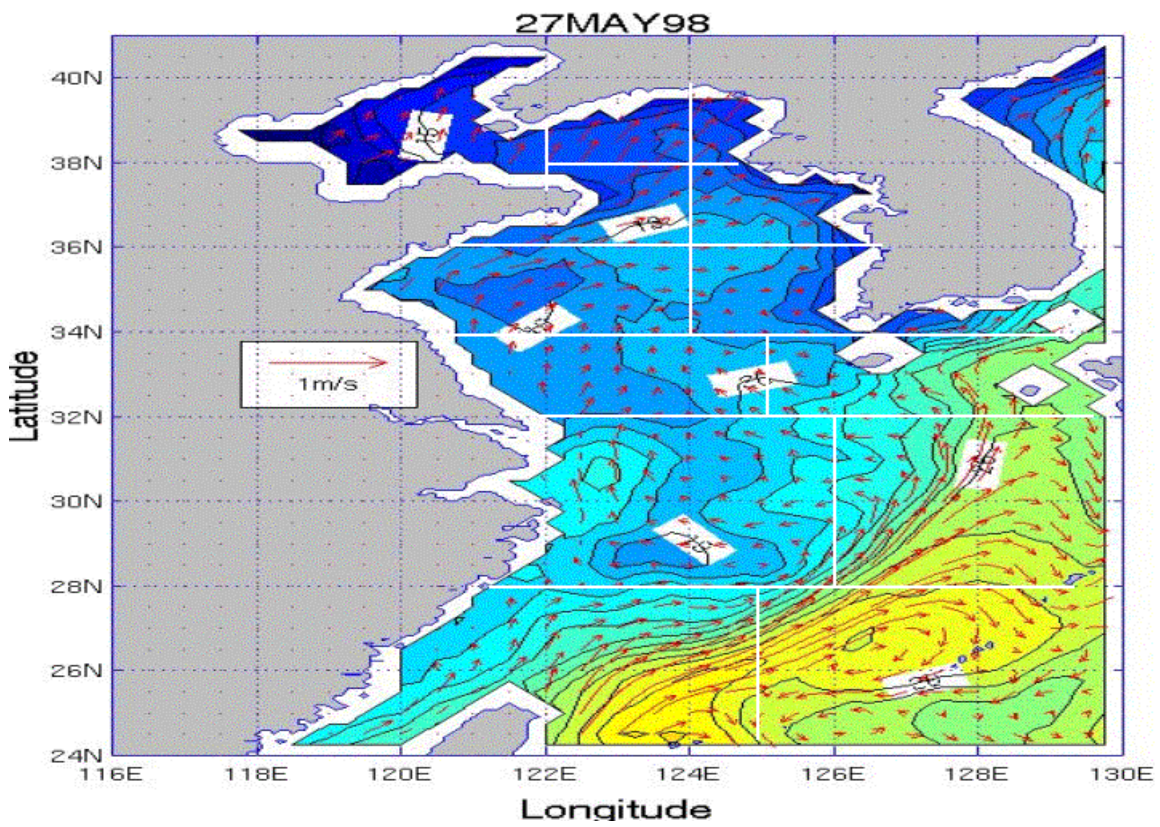
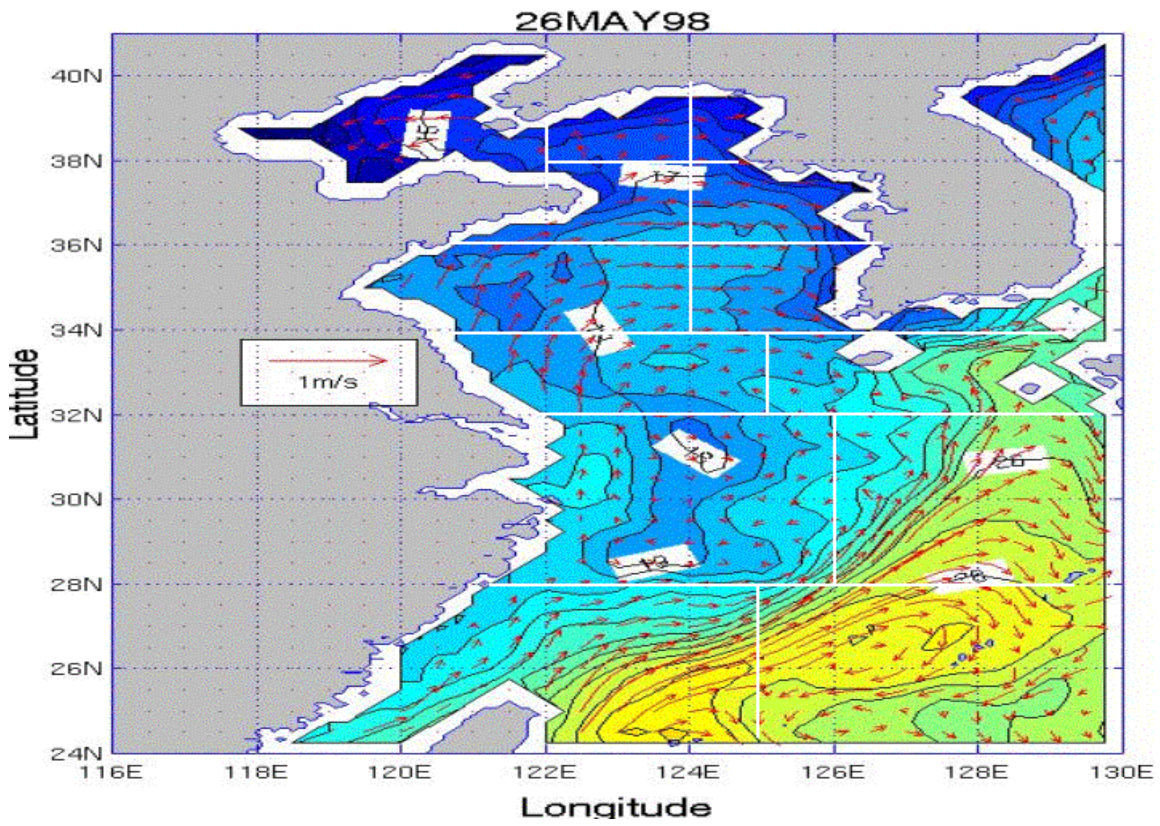


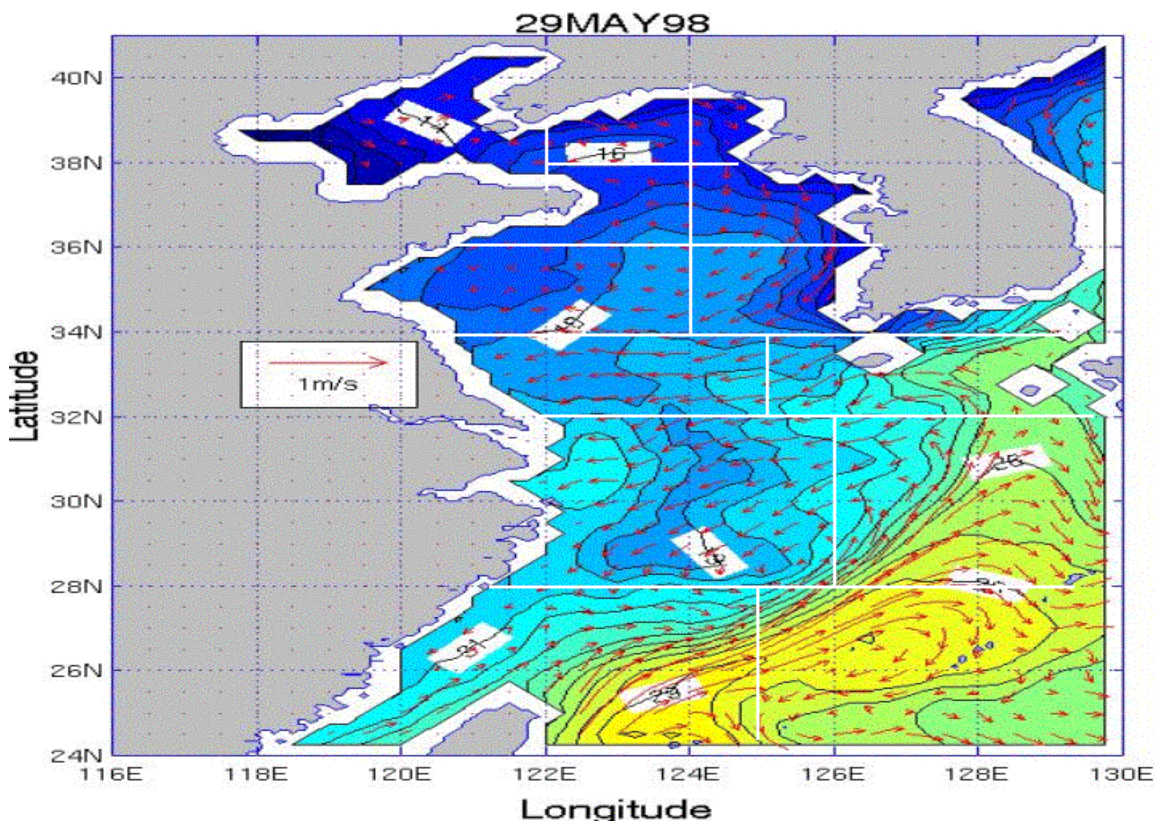
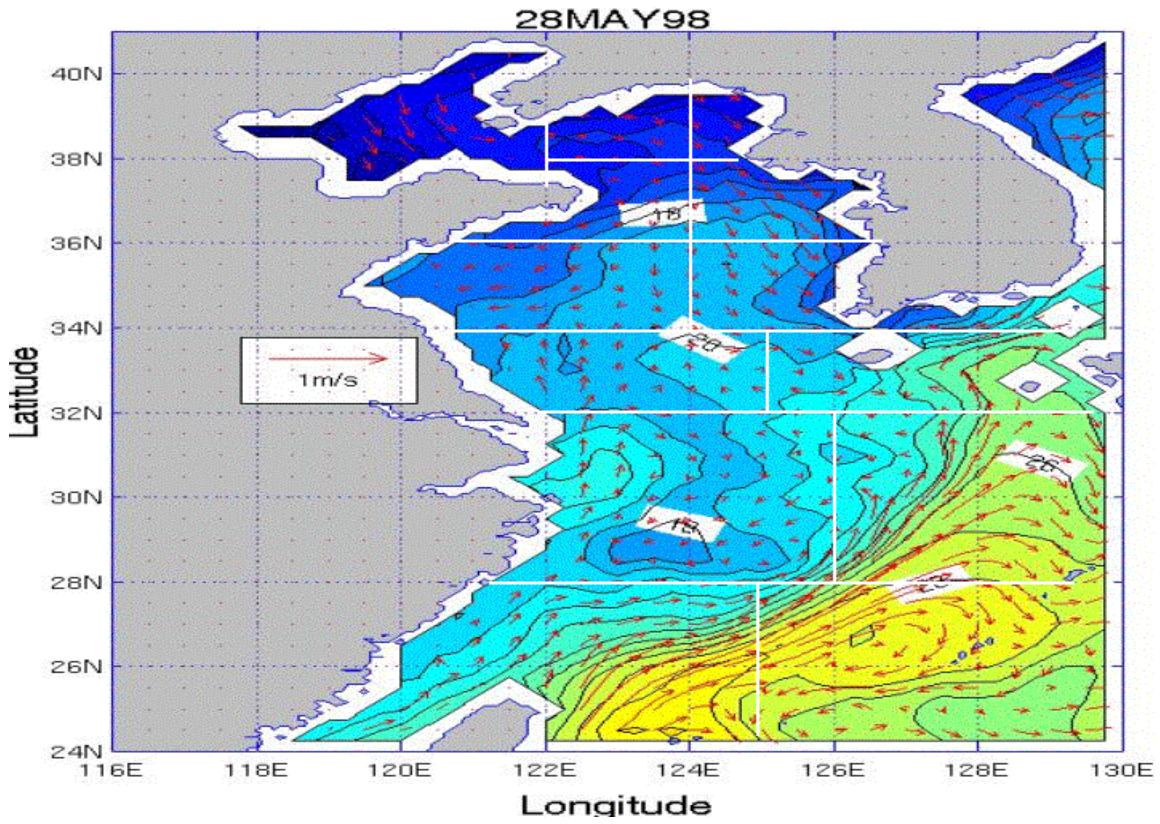


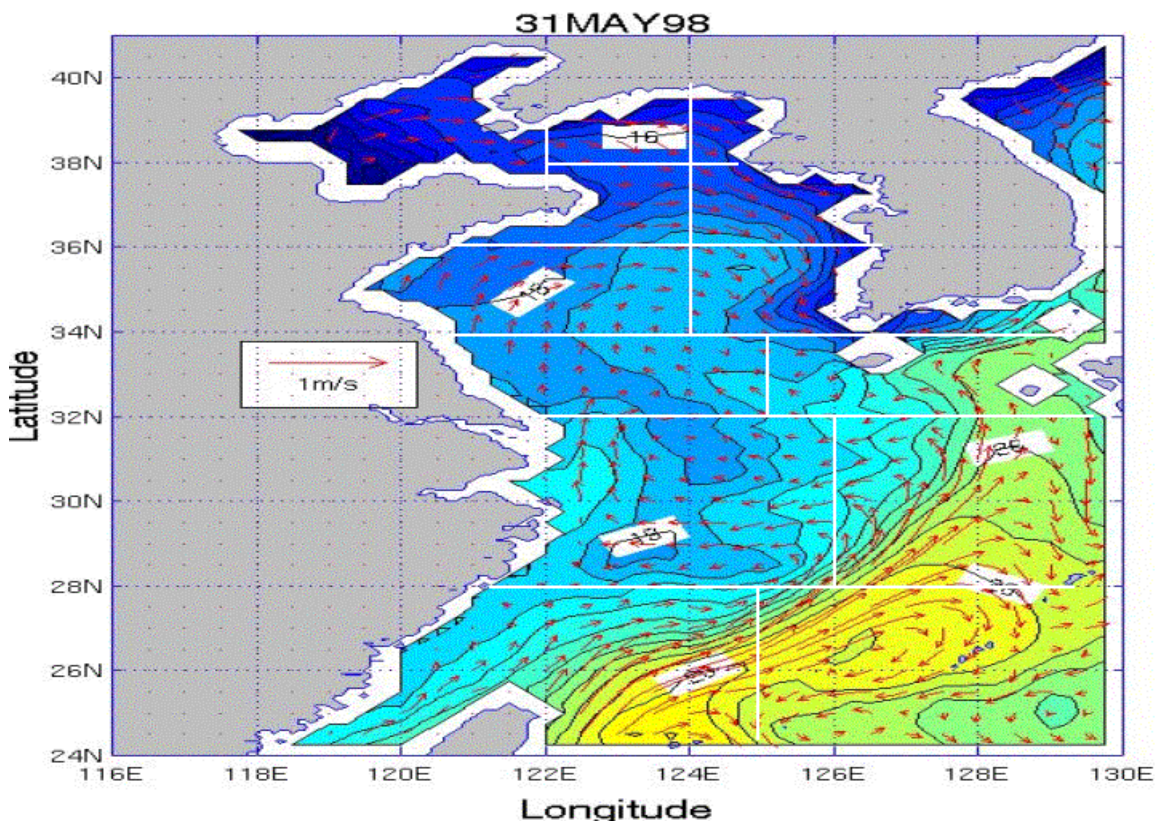
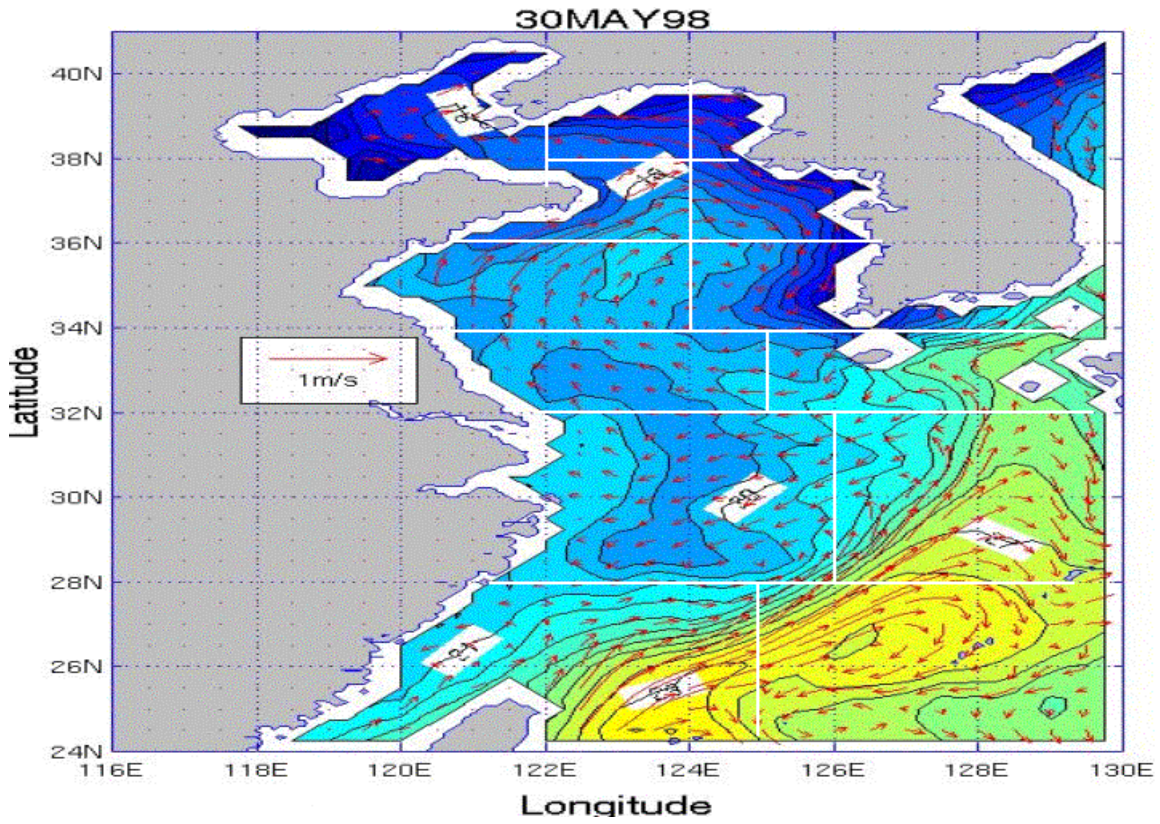






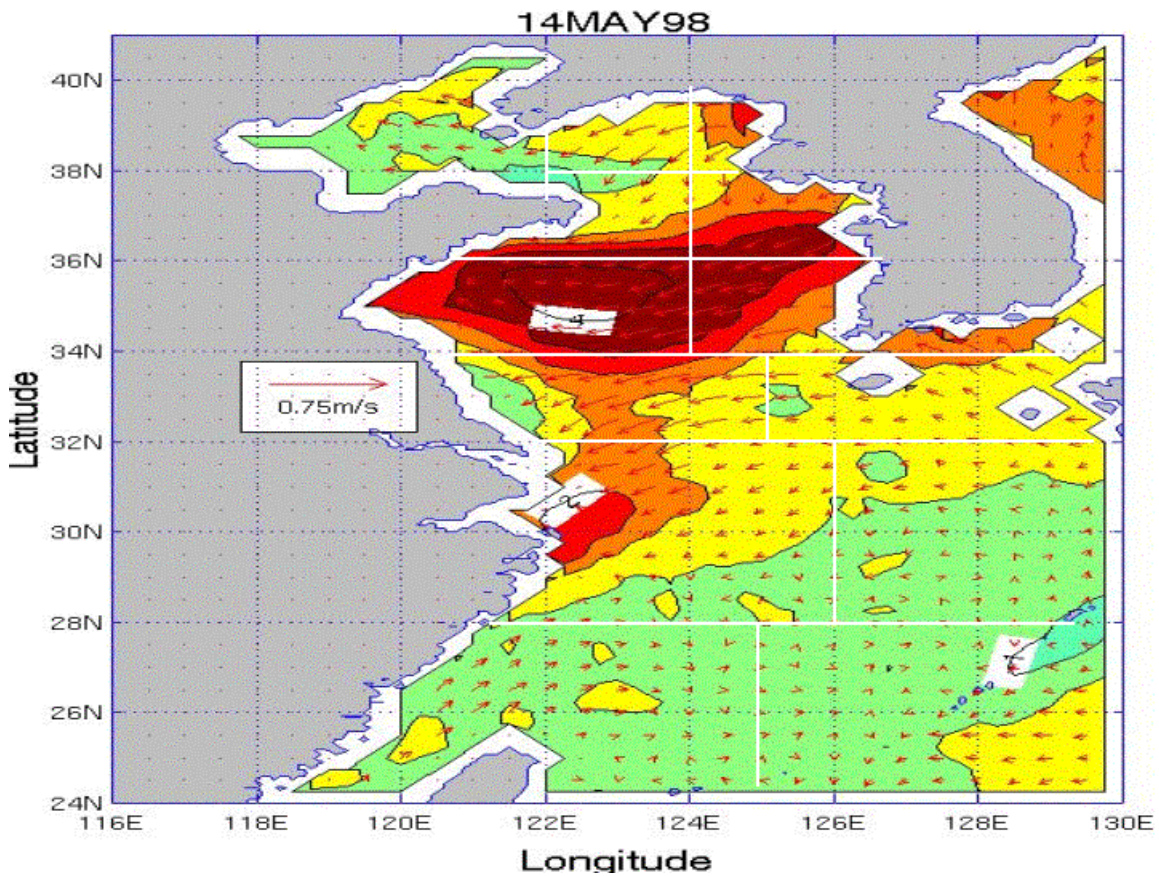


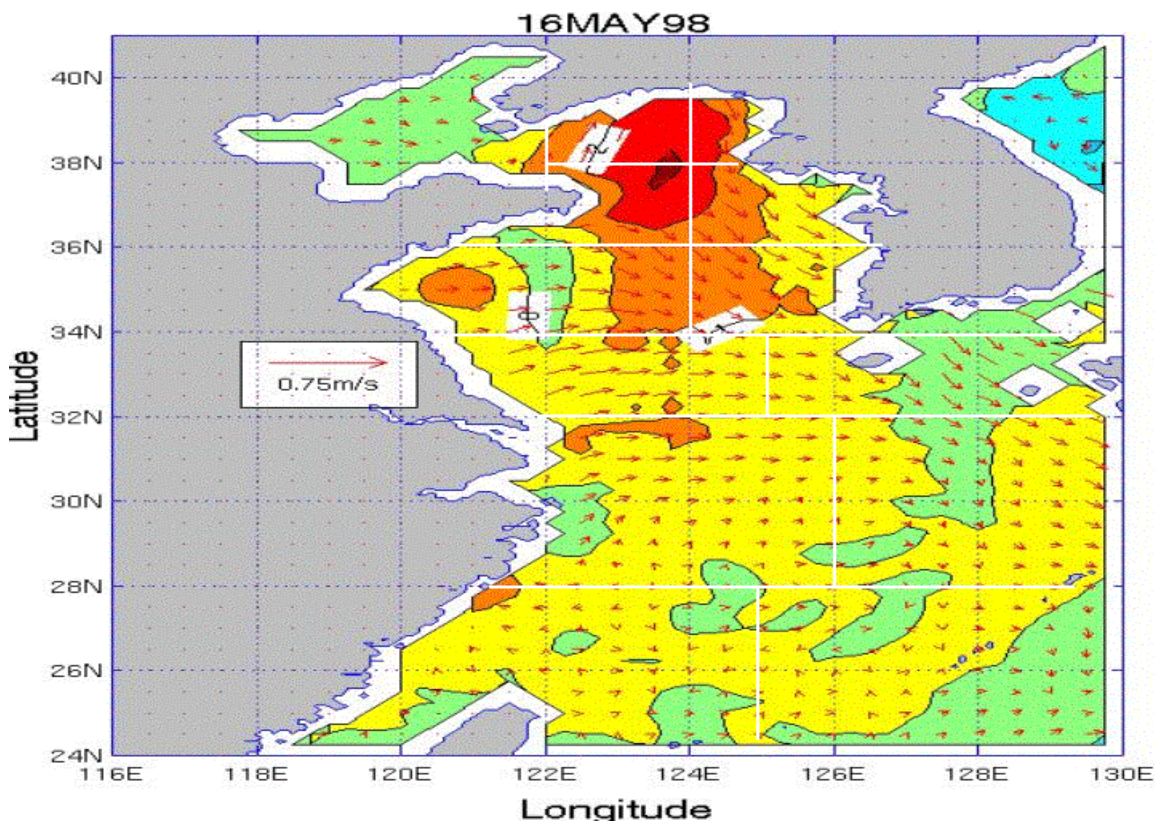
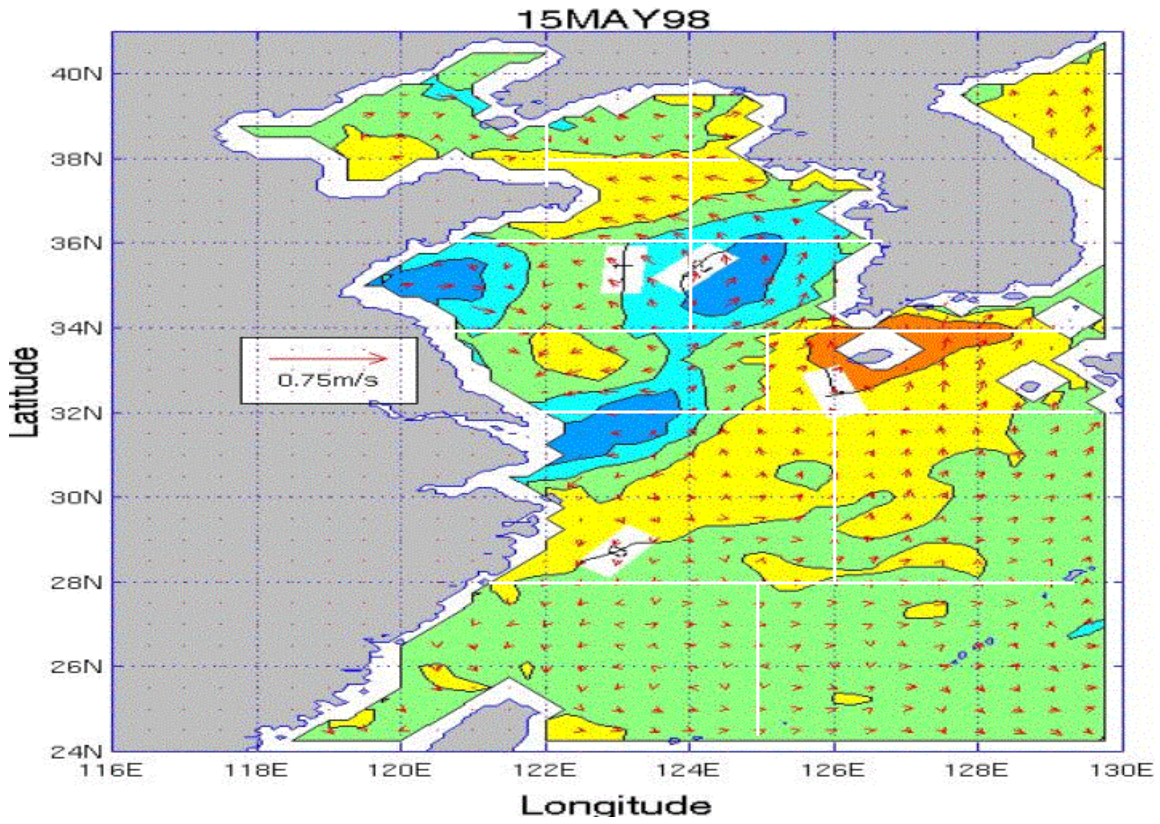


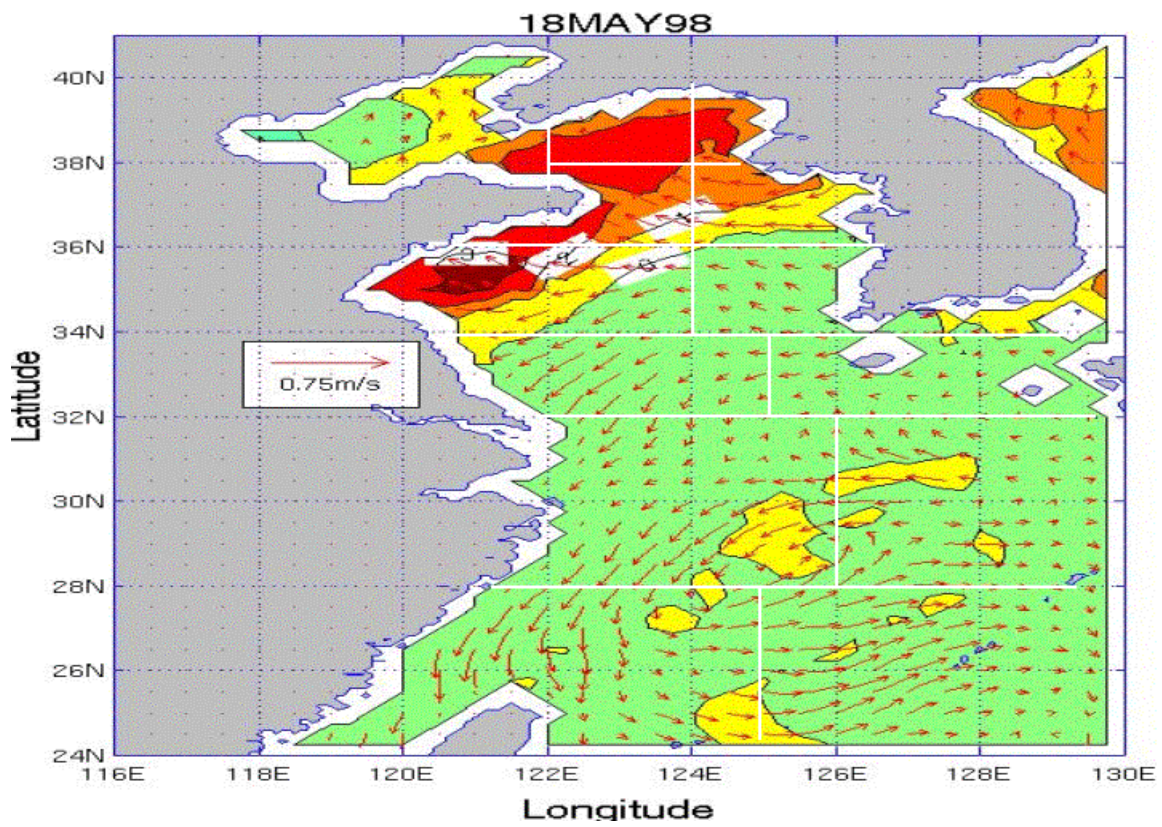
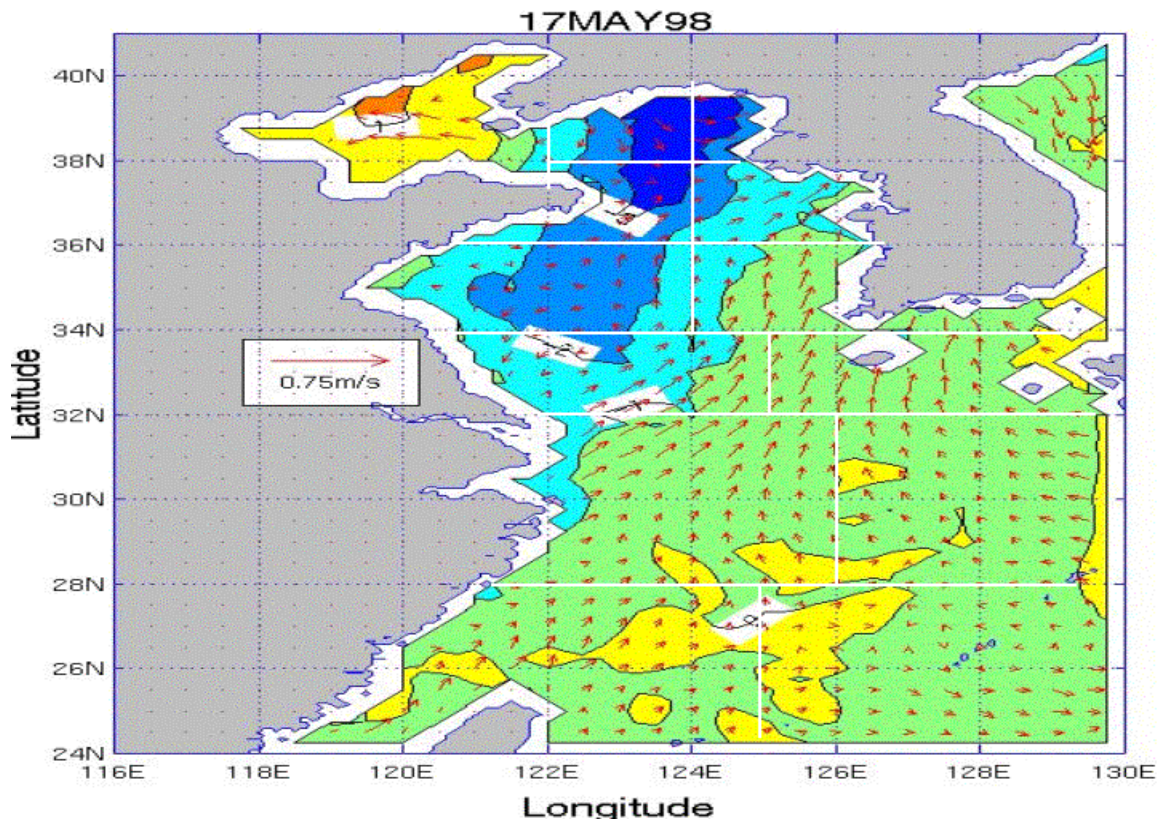


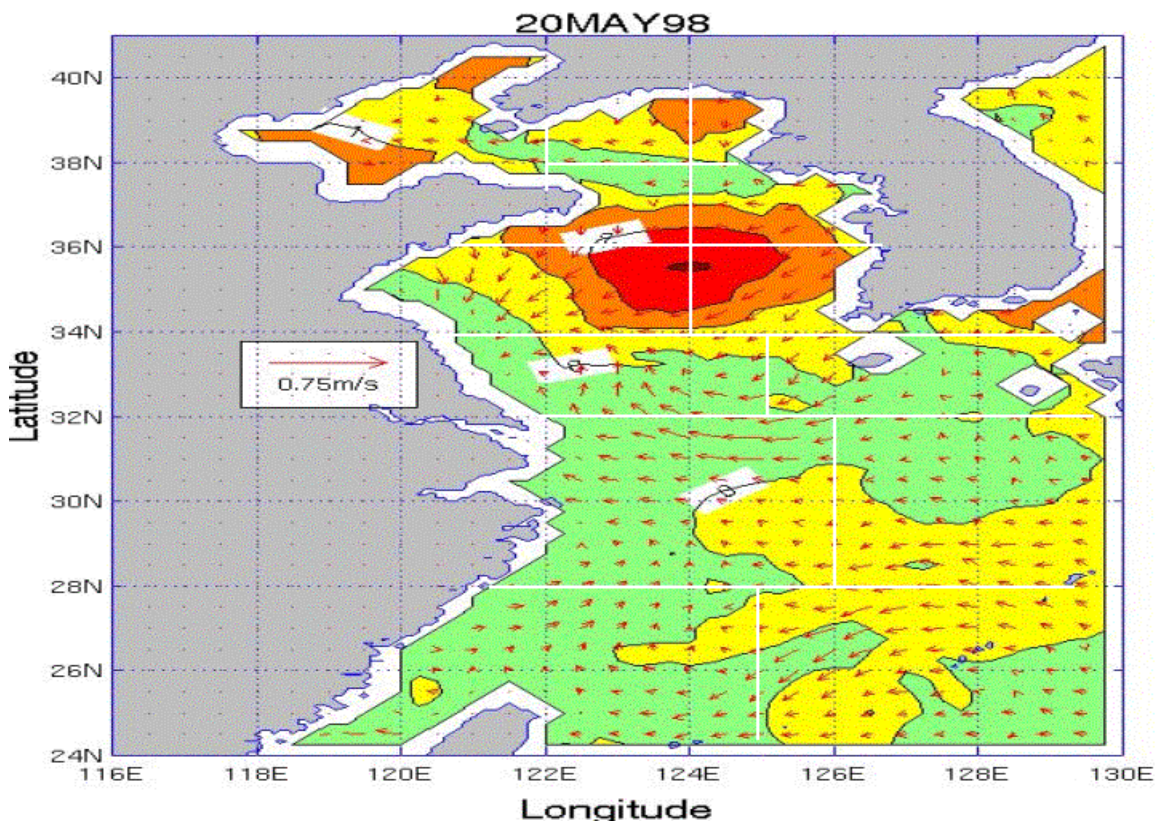
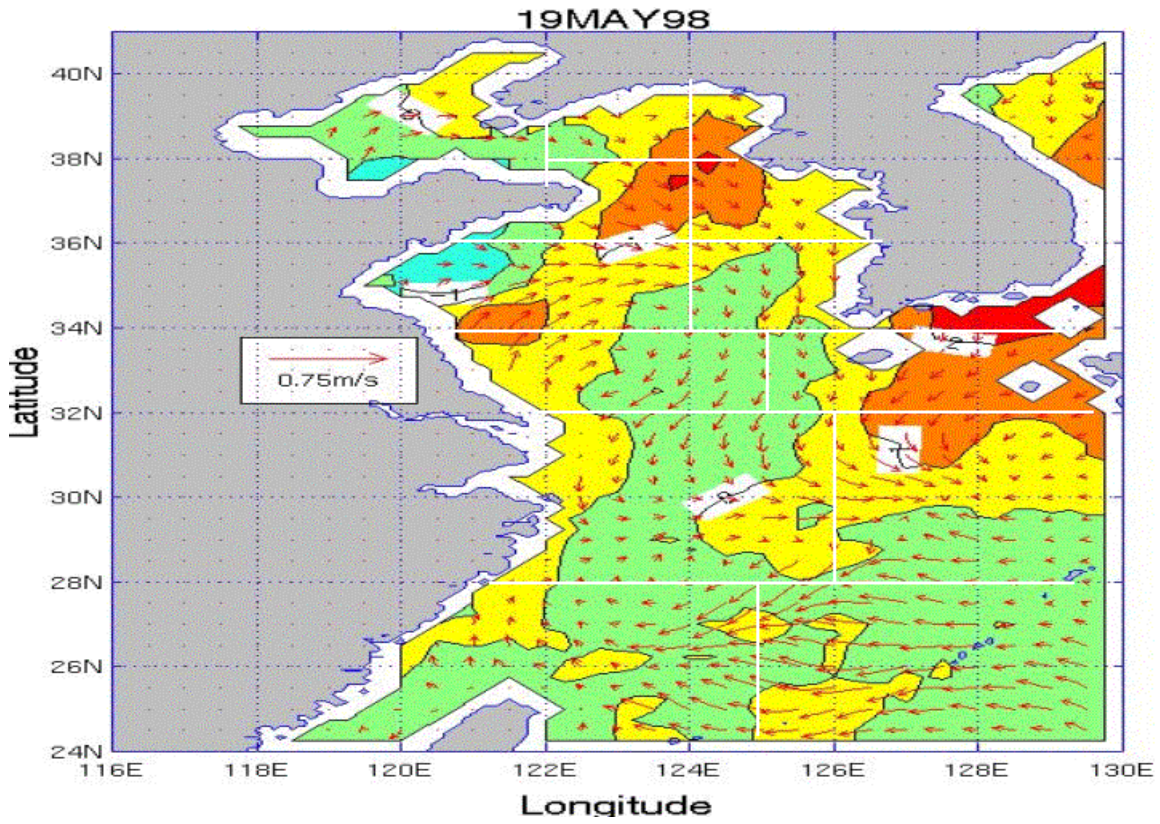
APPENDIX FF. SST AND SURFACE CURRENT VELOCITY TENDENCY PLOTS FOR THE YES FOR THE MAY TIME PERIOD

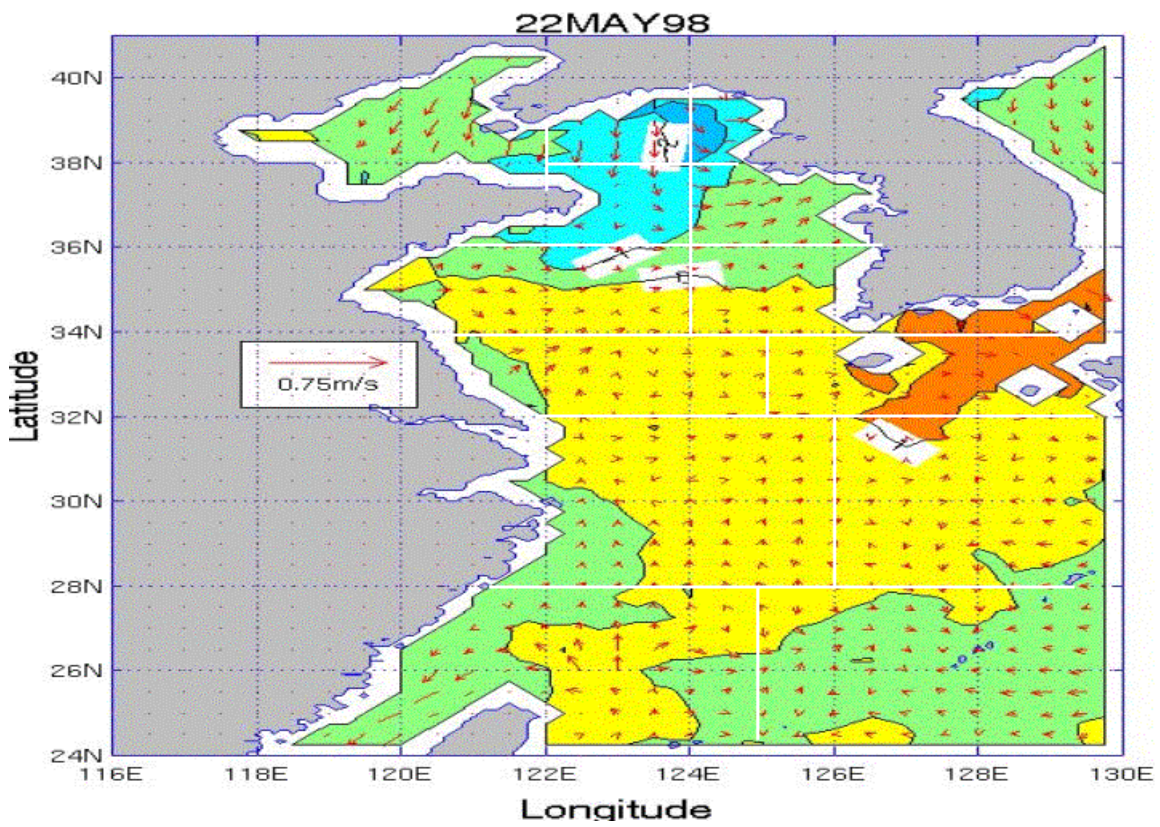
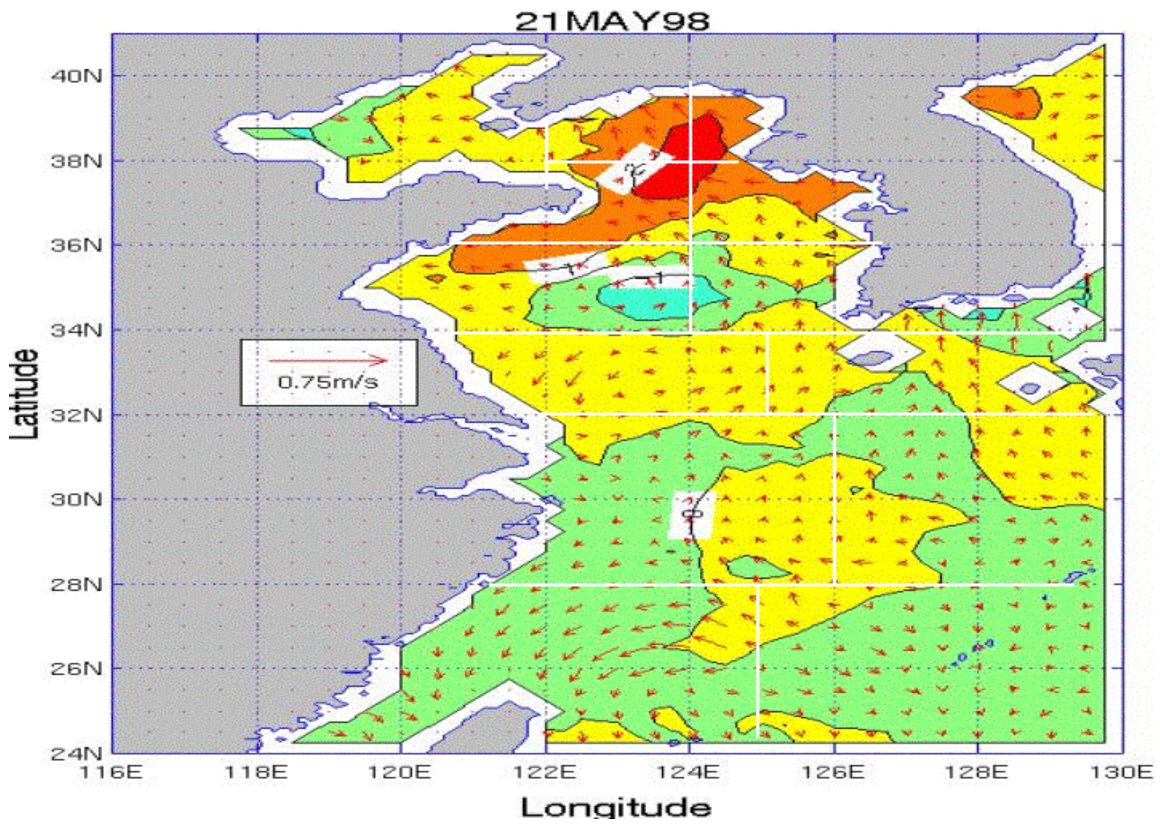
Appendix FF consists of 18 figures that show SST and surface current velocity day-to-day tendency for the May time period over the YES. The figures are in time sequential order from May 14 through May 31. Each plot represents the change between the previous day and the current day.

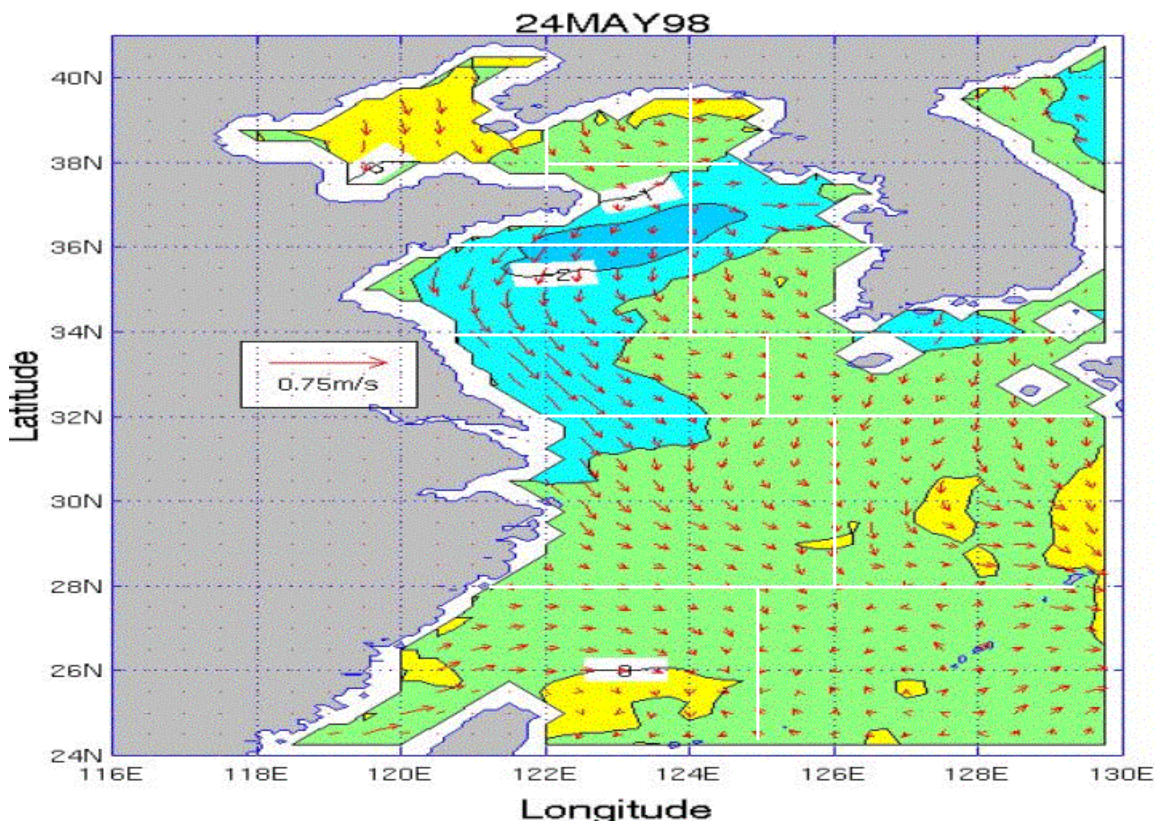
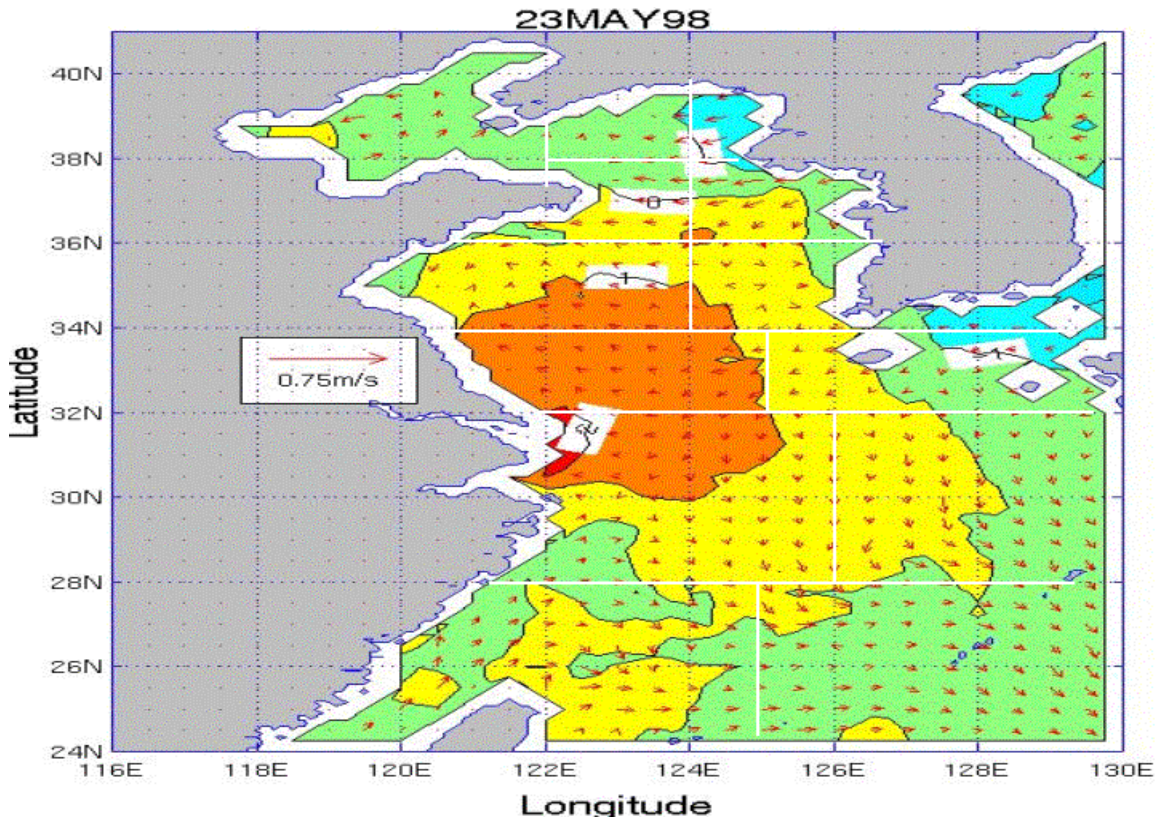


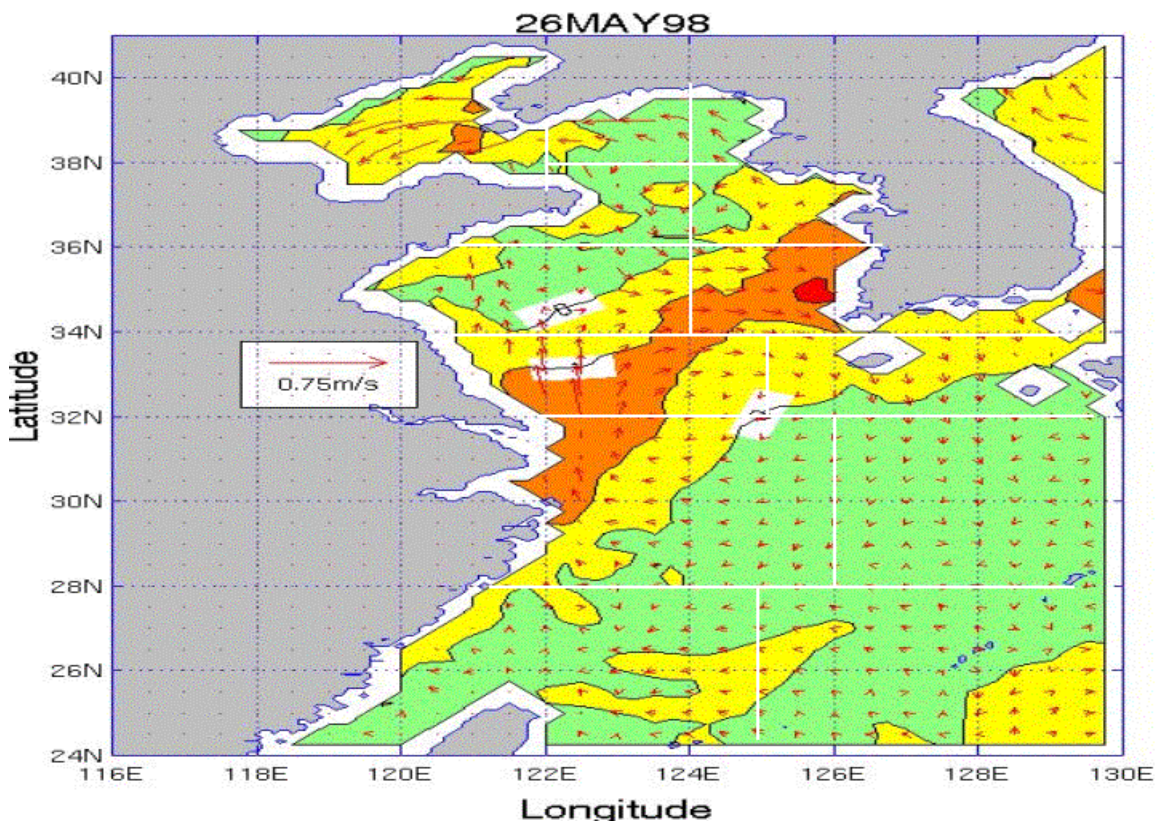
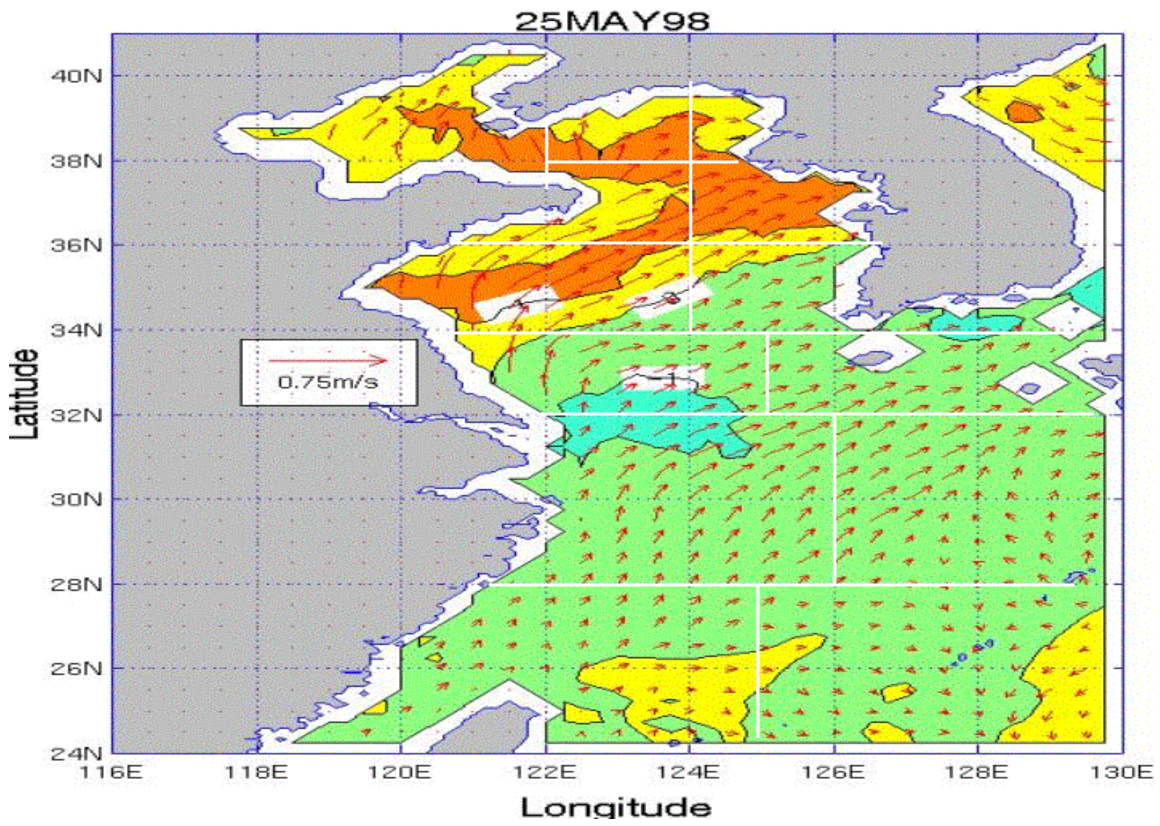


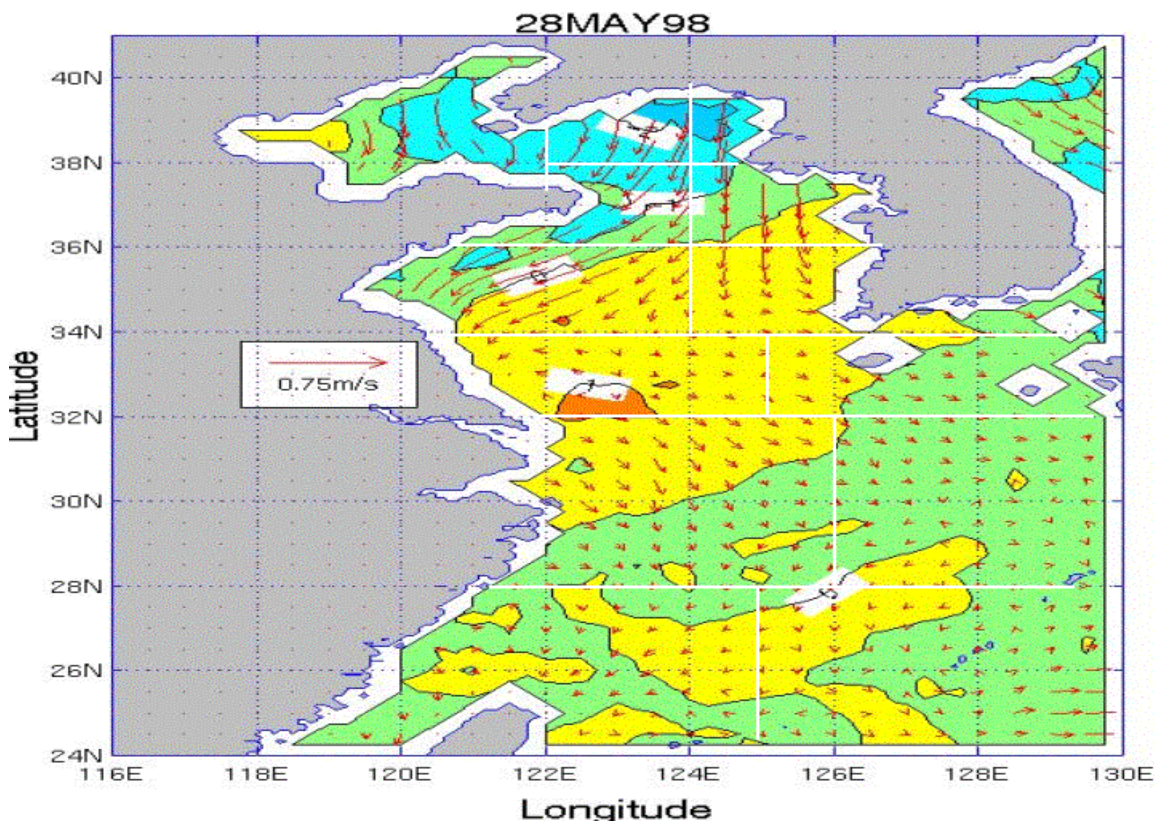
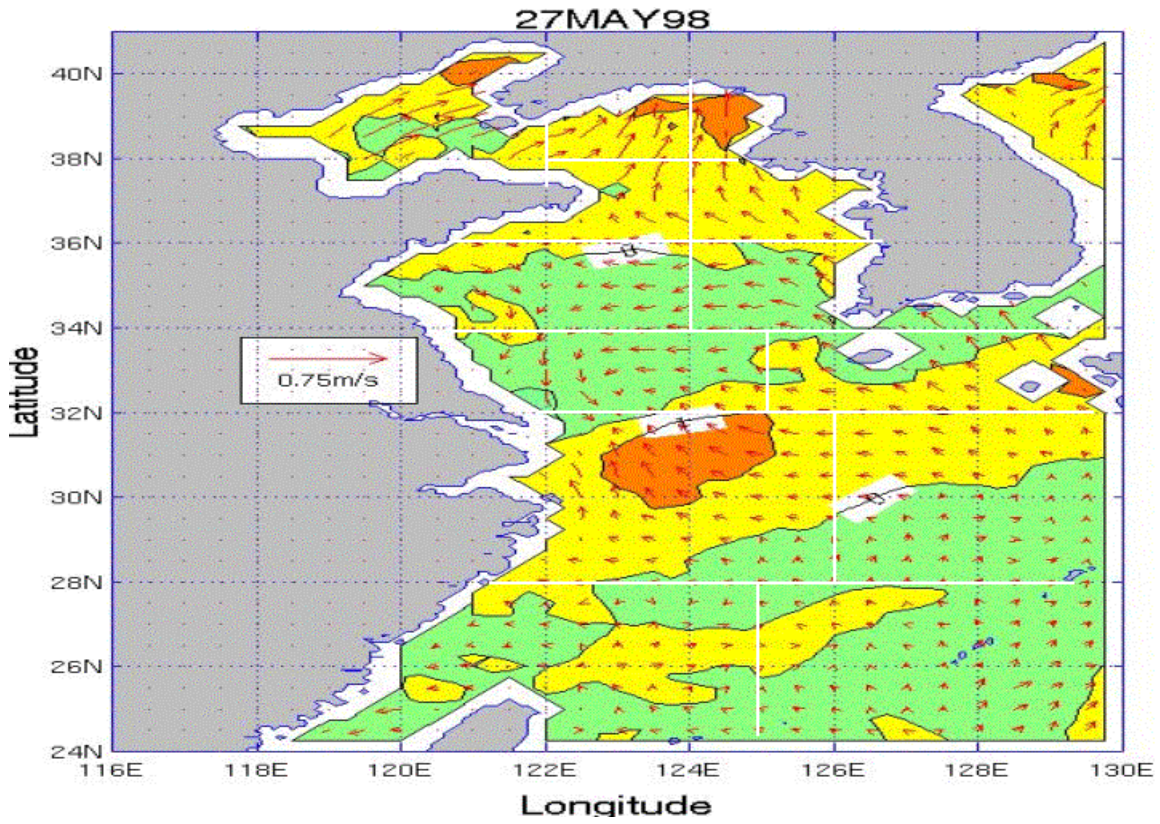


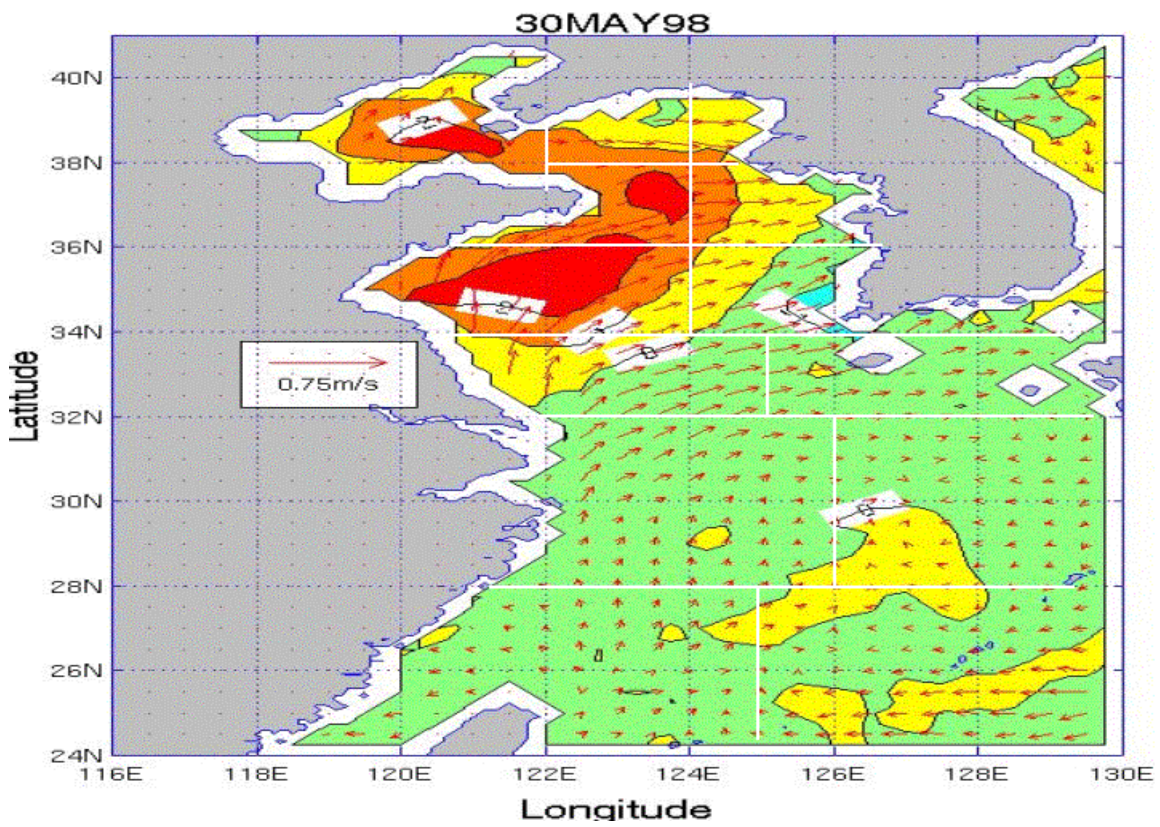
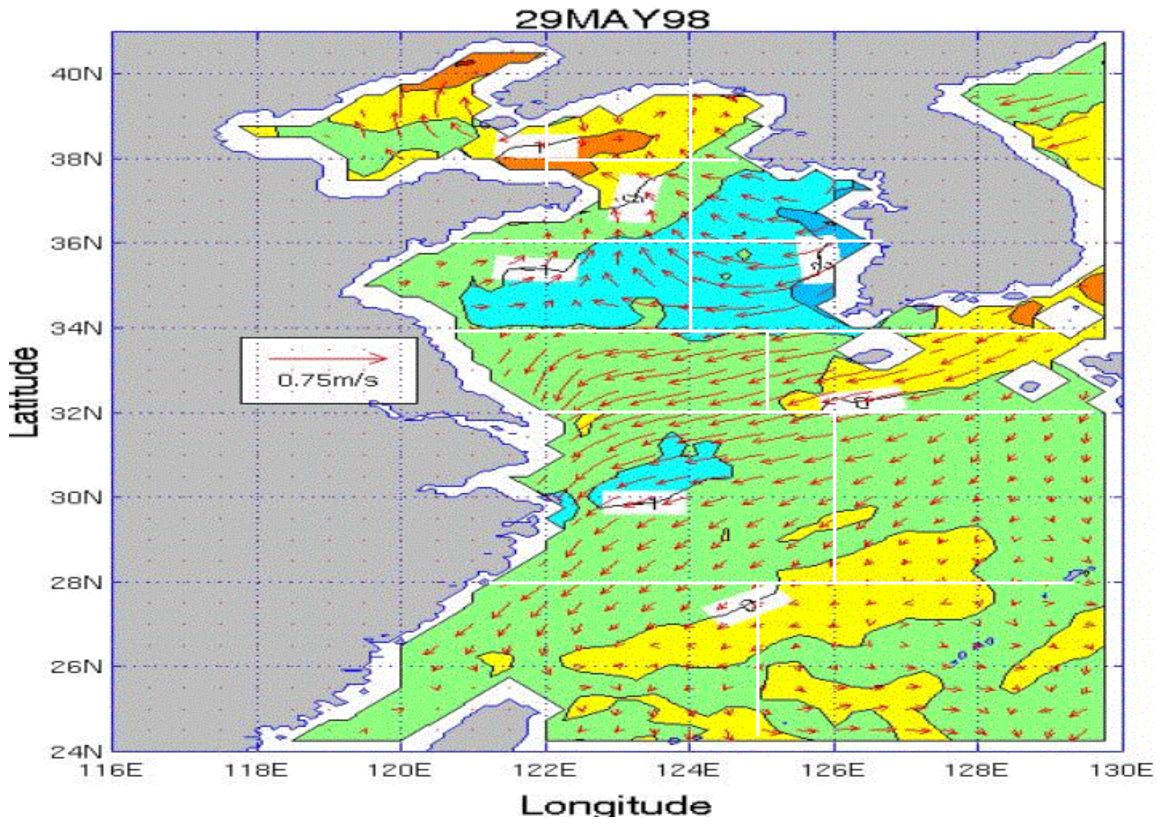


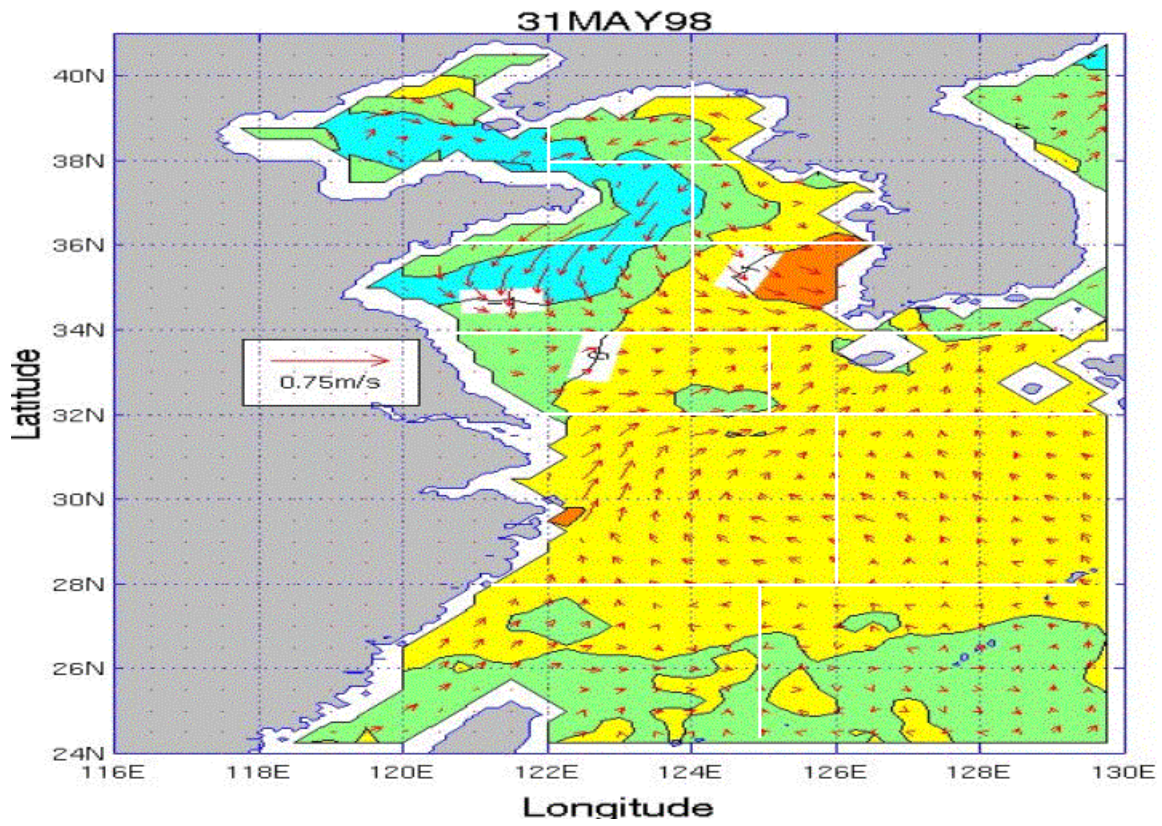






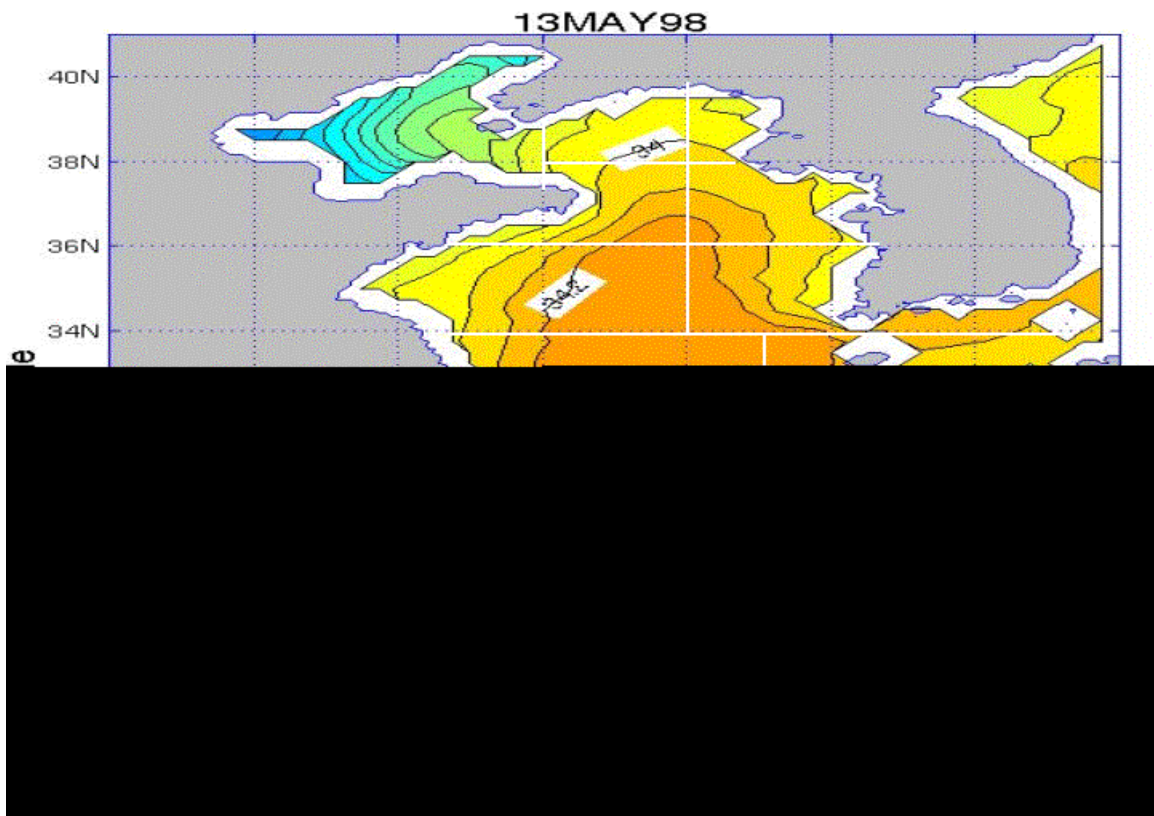


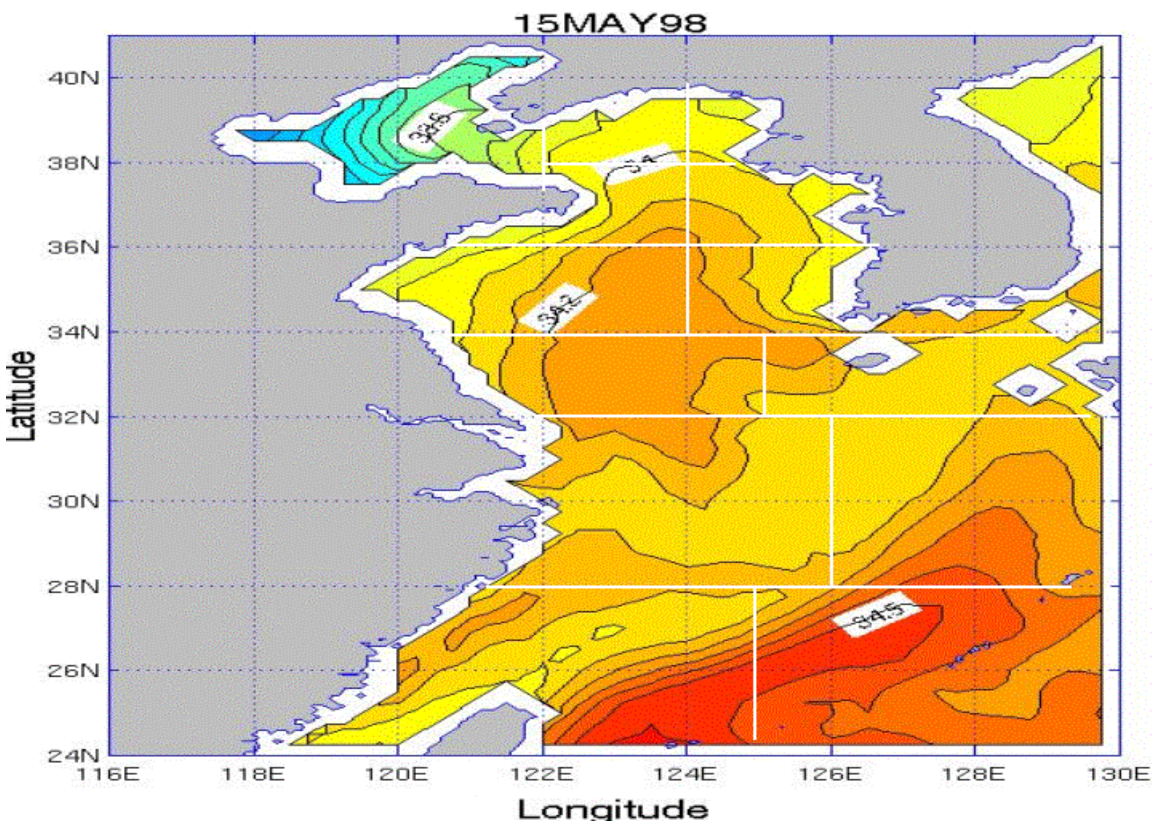
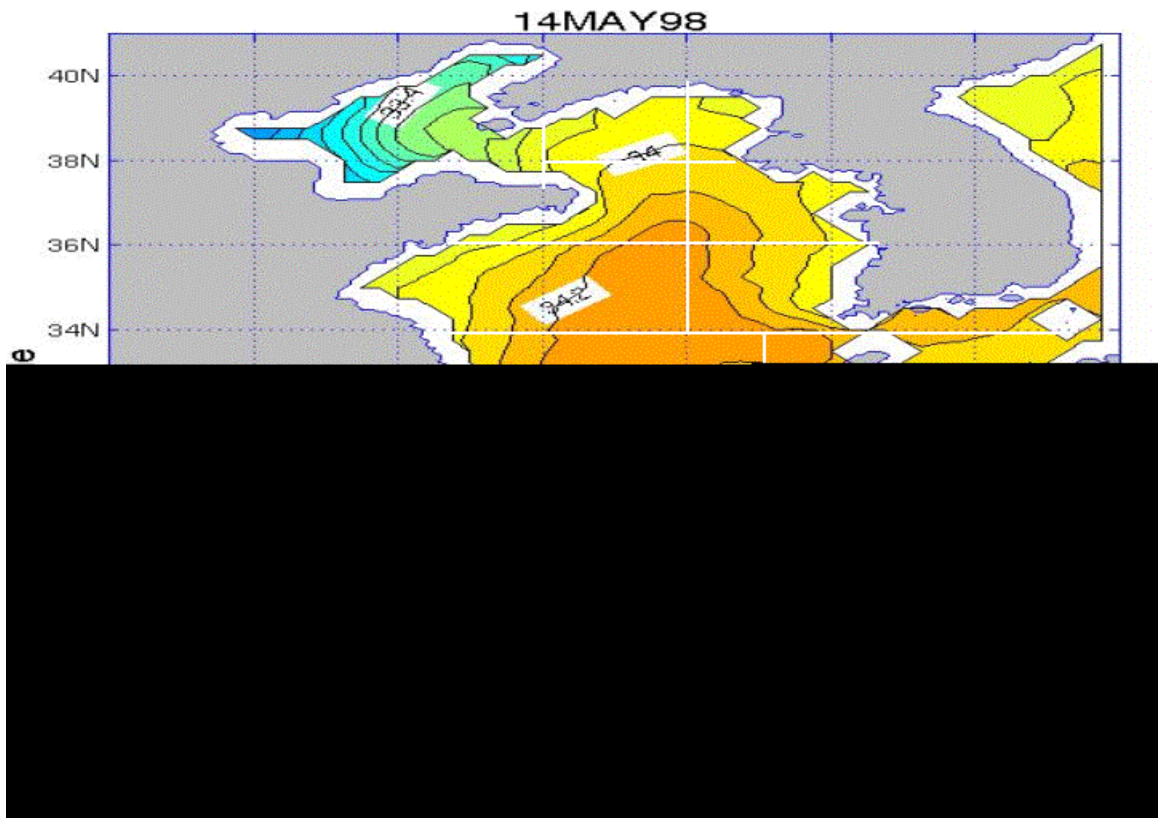


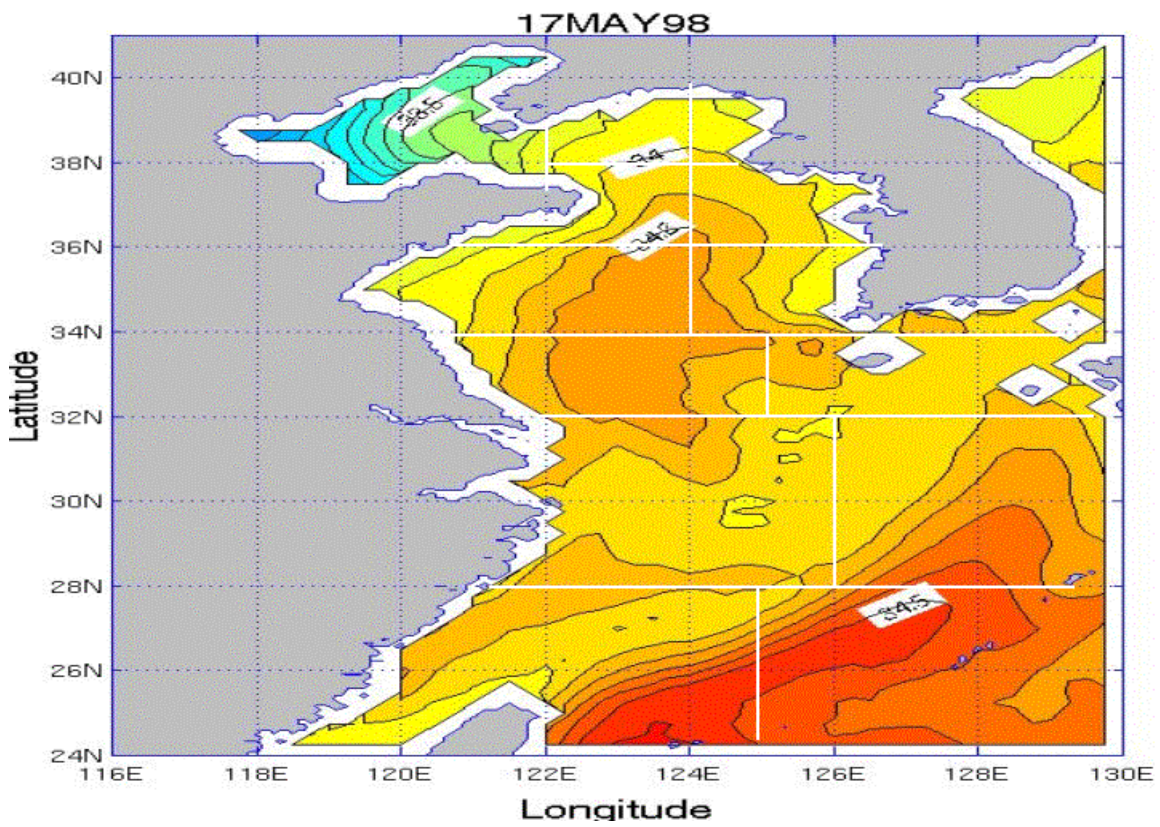
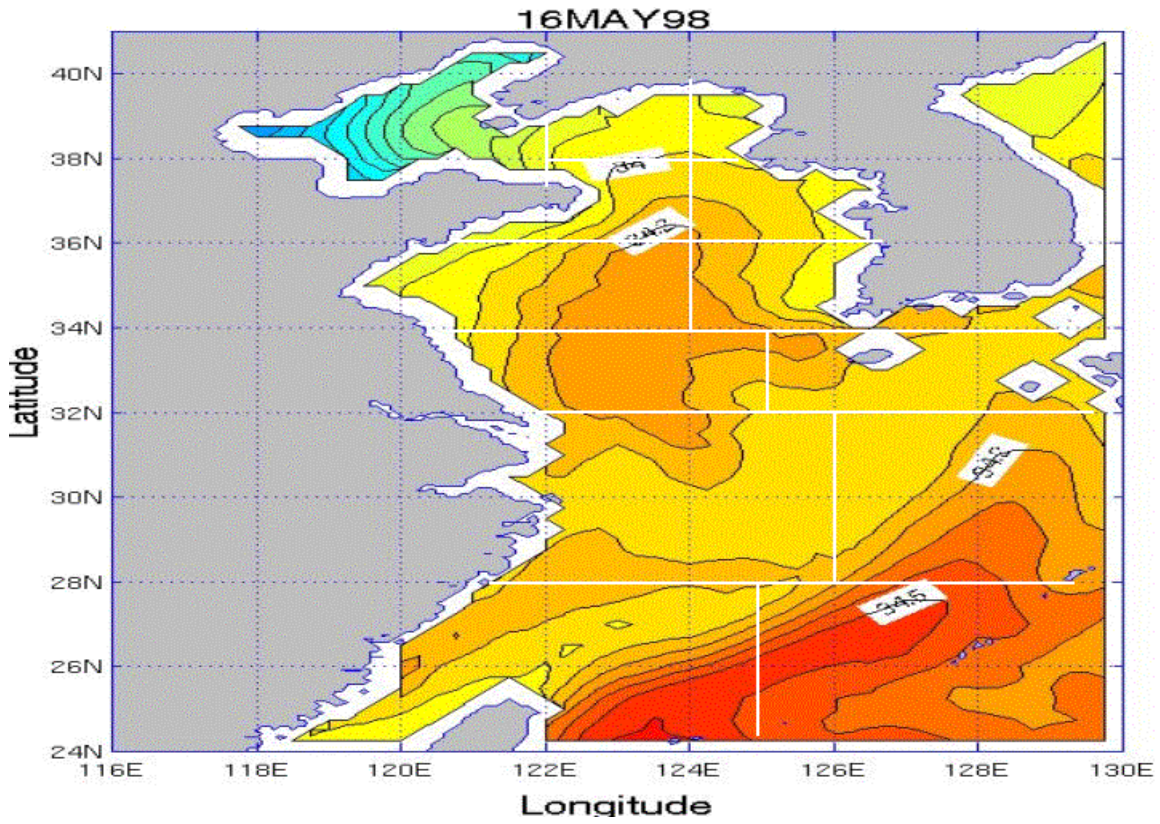


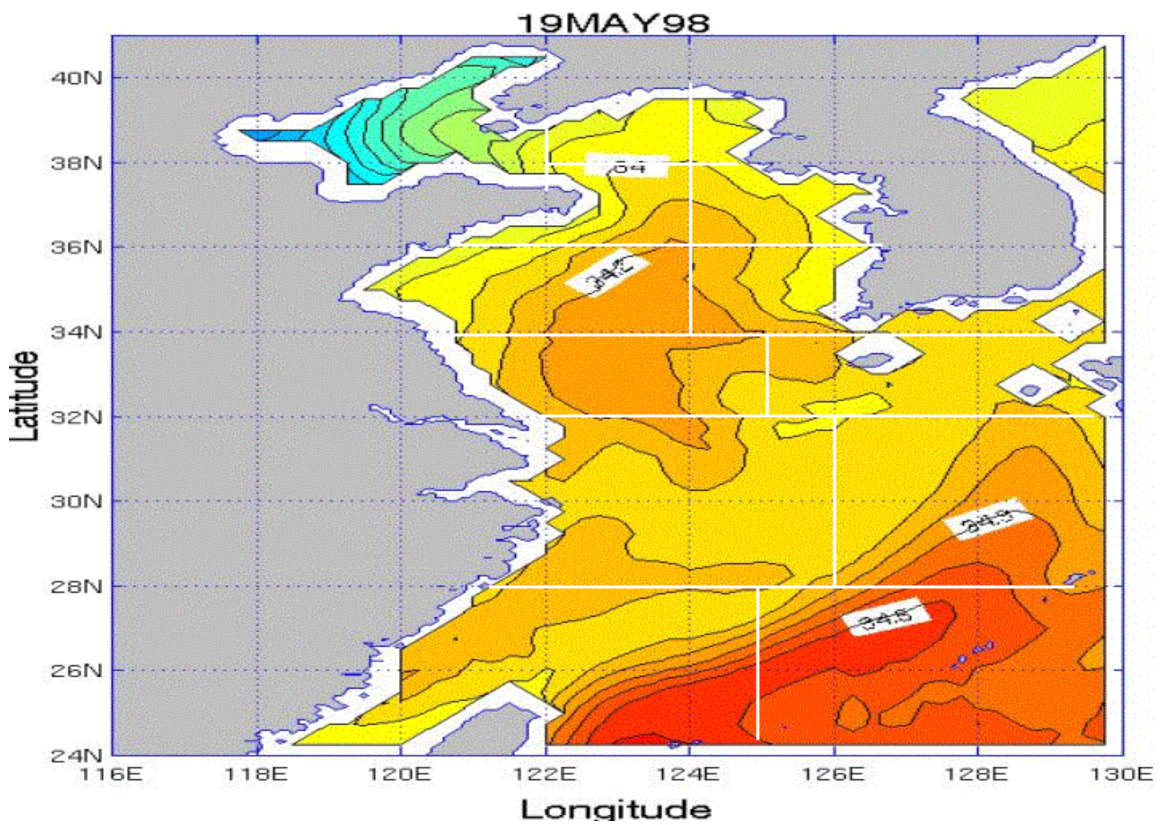
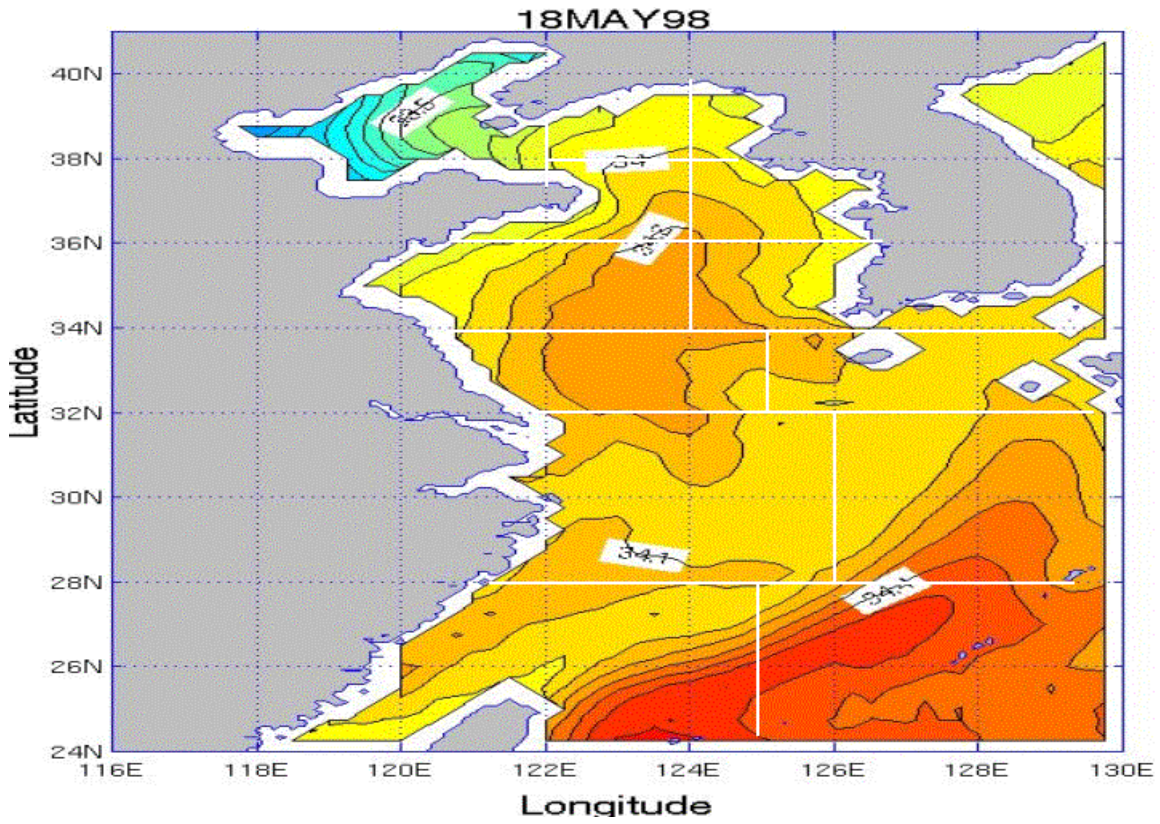
APPENDIX GG. SSS PLOTS FOR THE YES FOR THE MAY TIME PERIOD

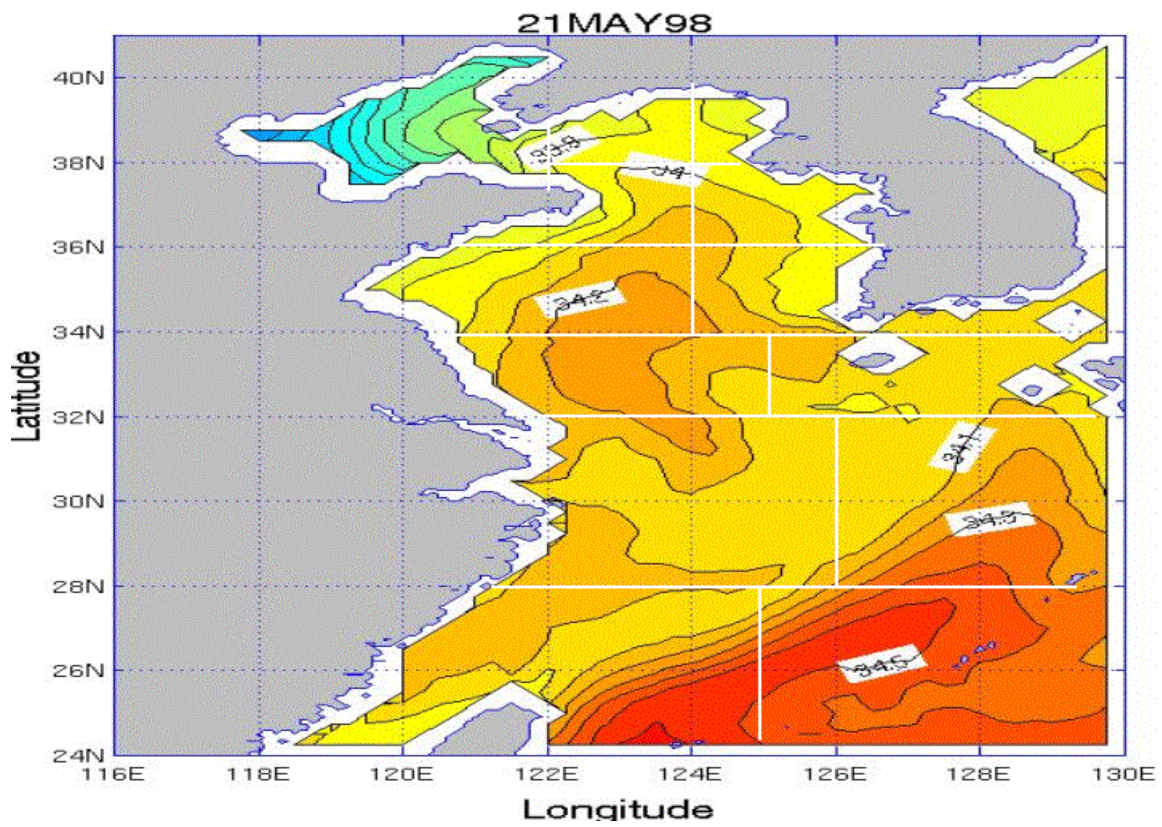
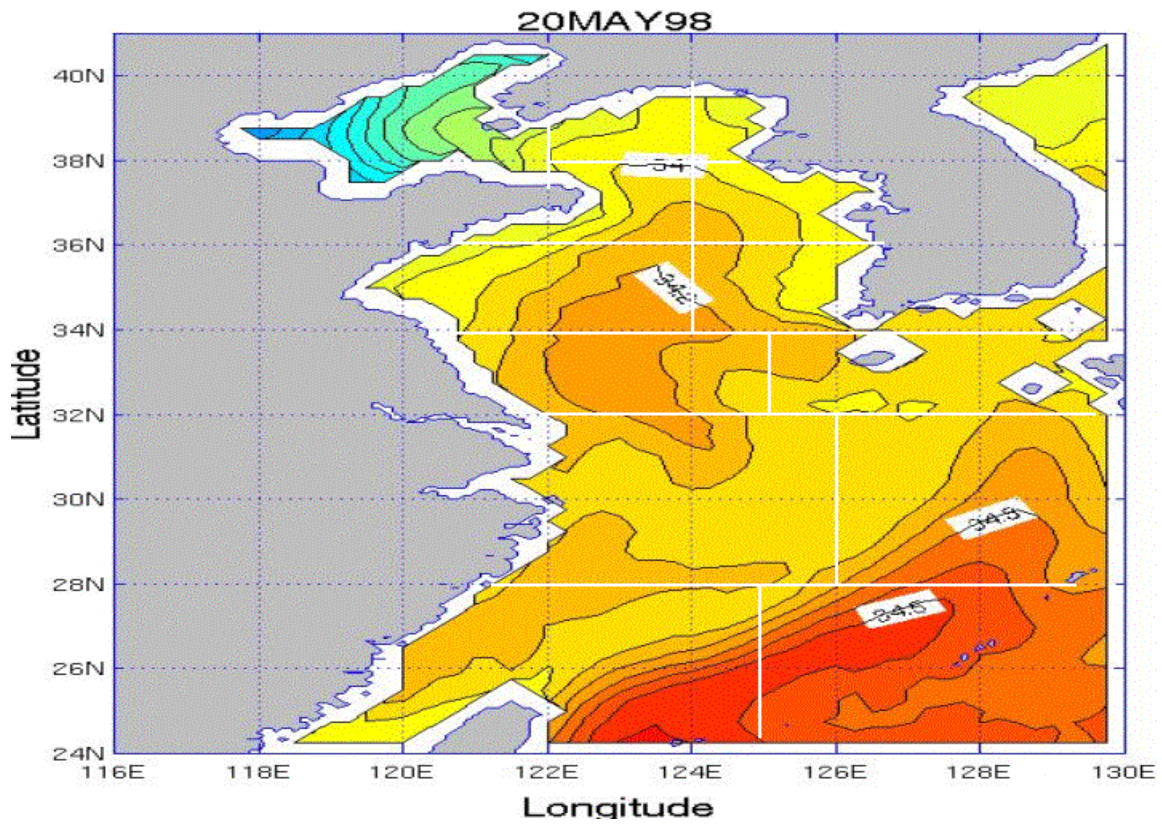
Appendix GG consists of 19 figures that show SSS for each day of the May time period for the YES. The figures are in time sequential order from May 13 through May 31.

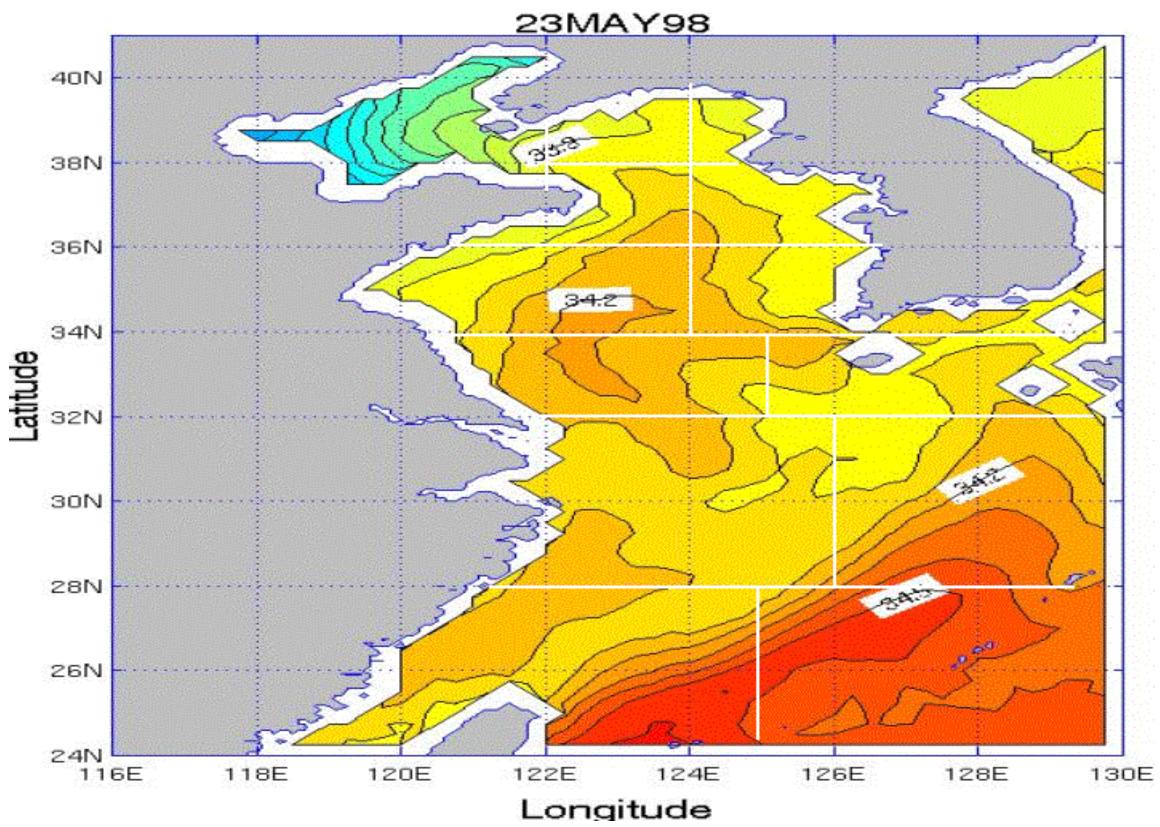
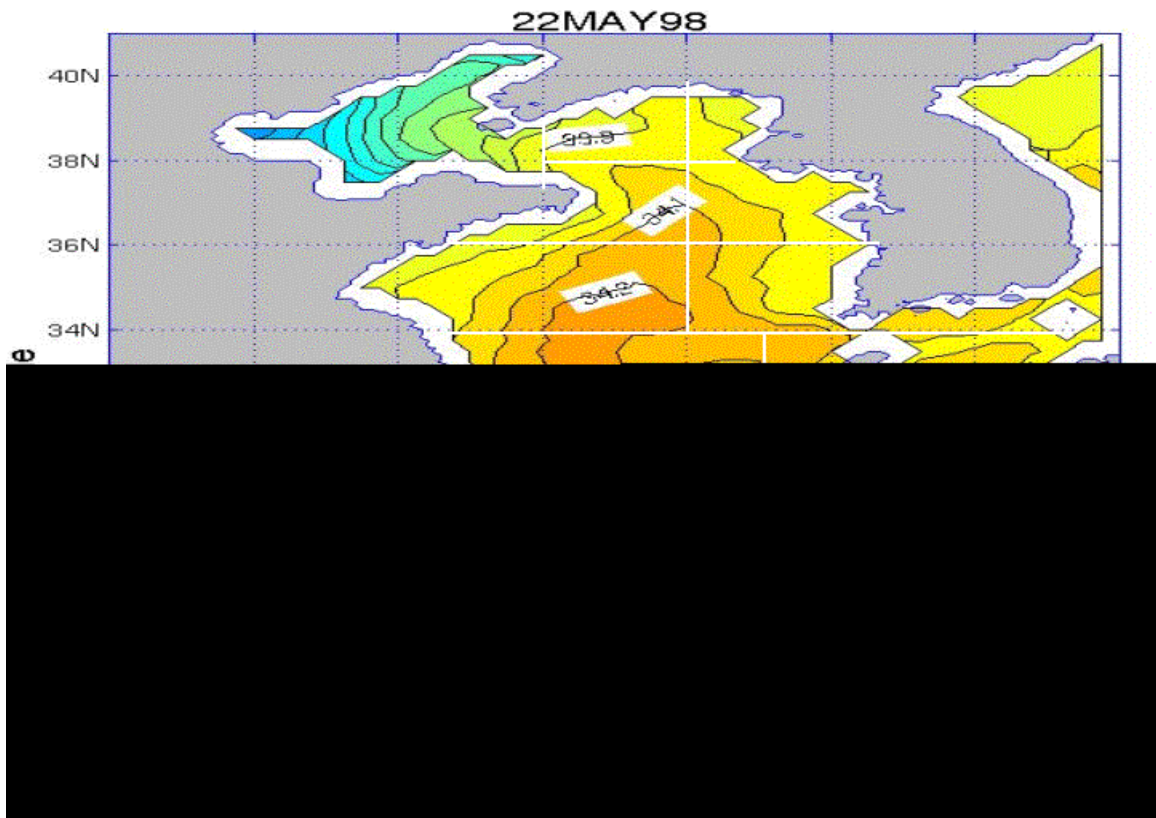


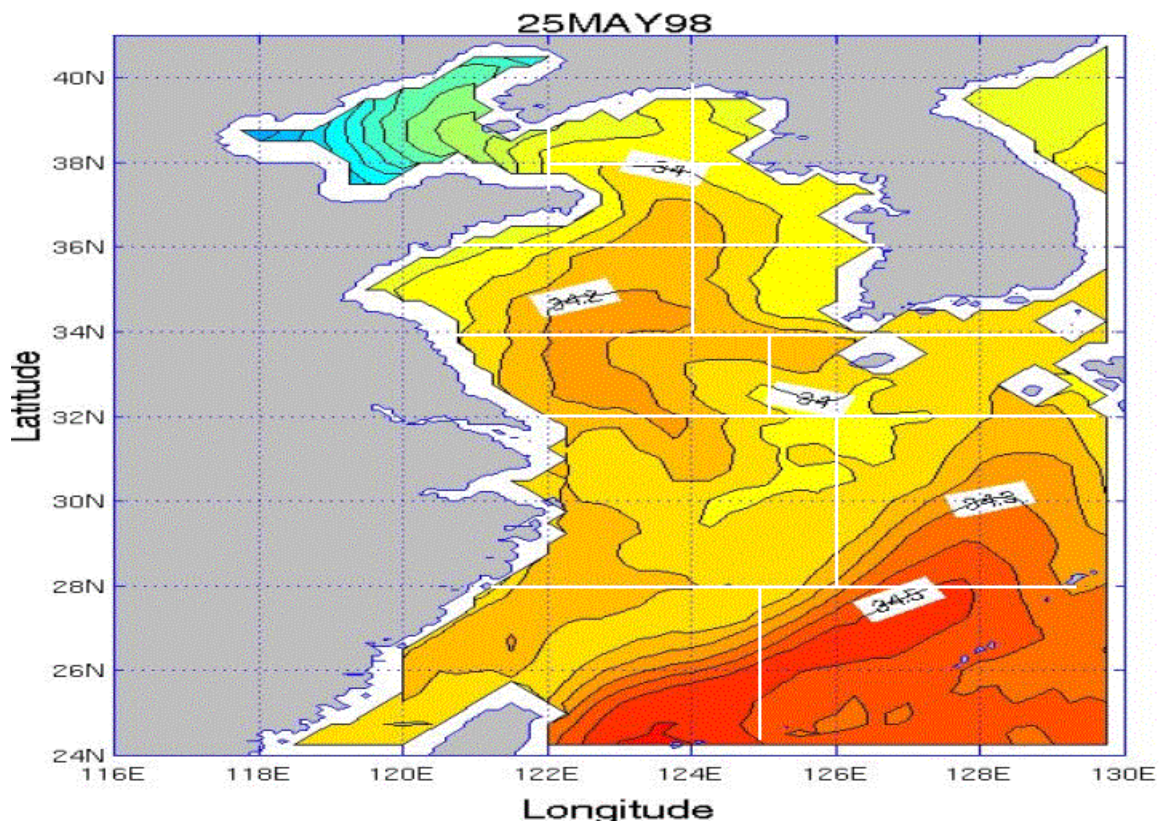
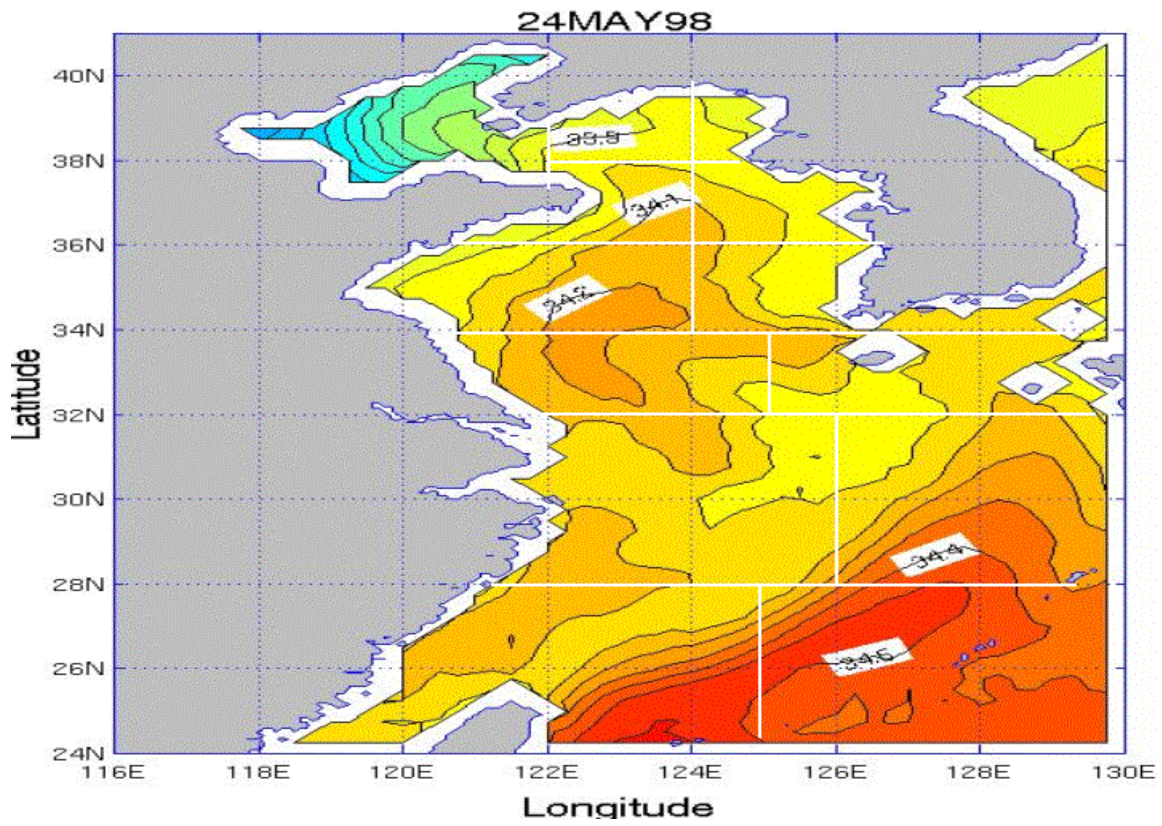


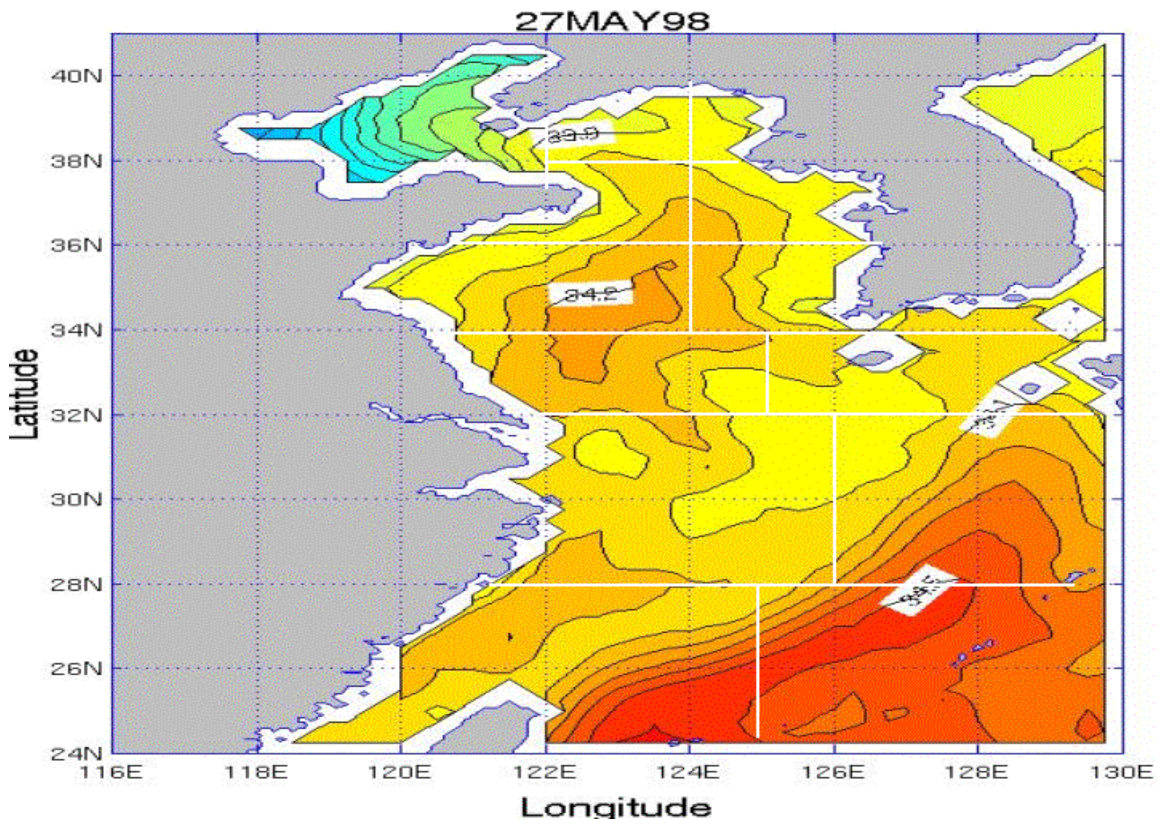
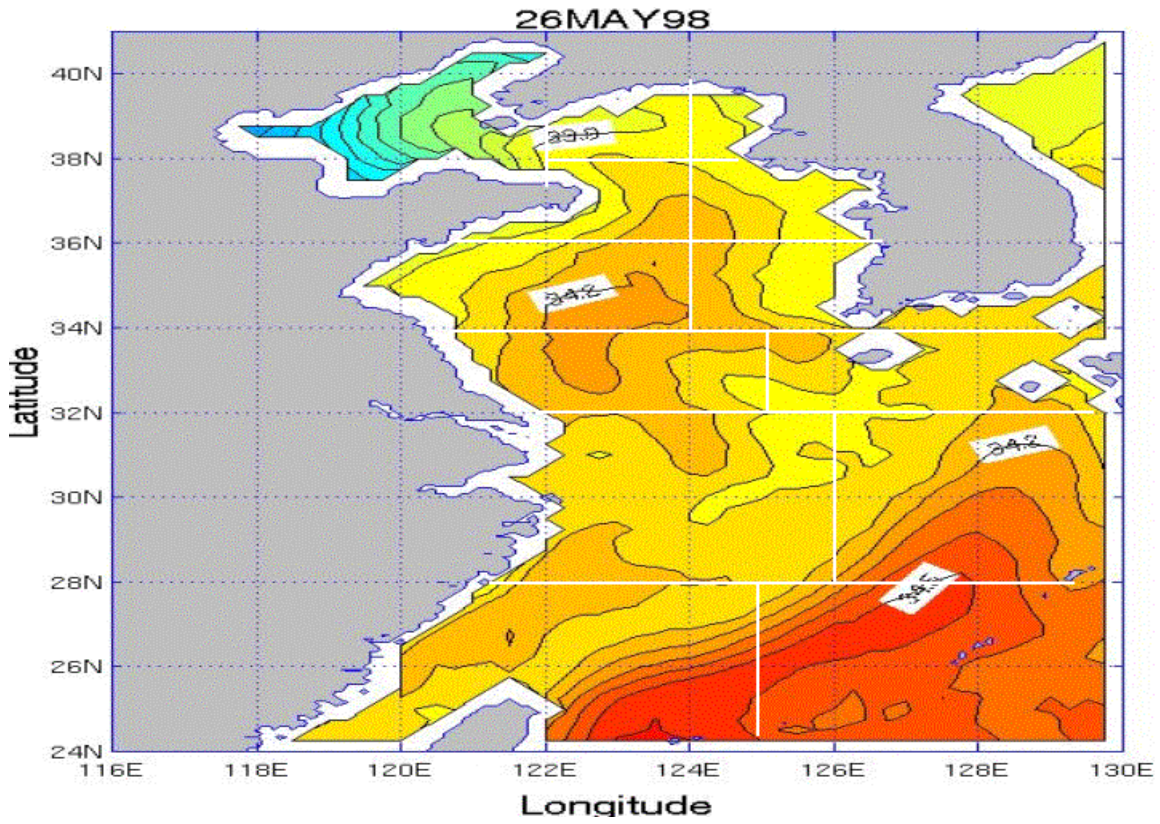


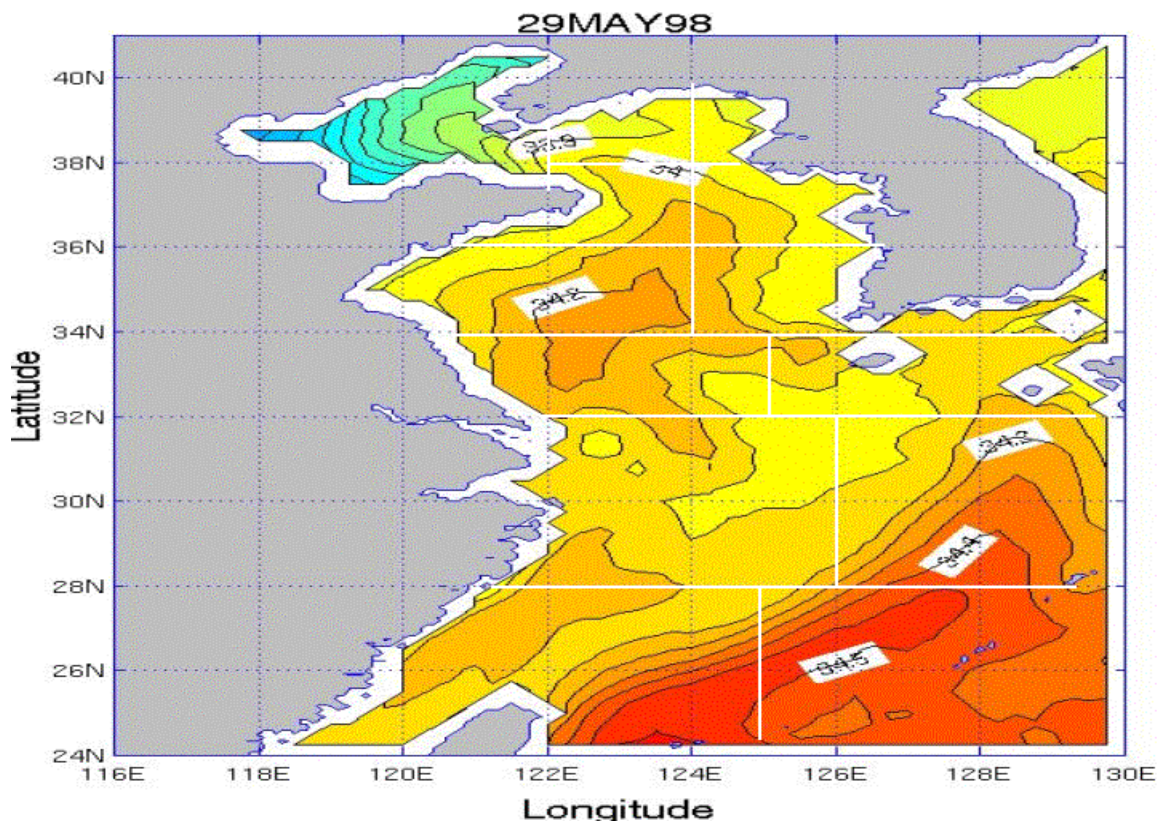
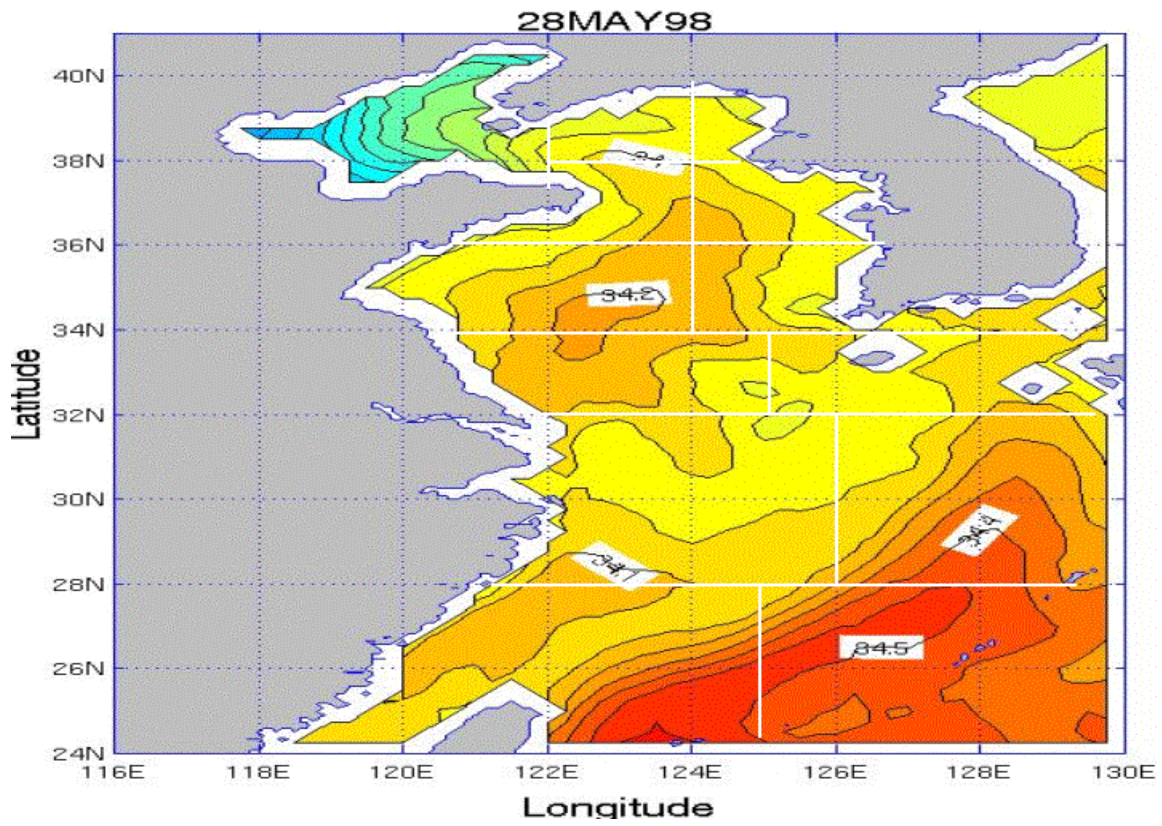


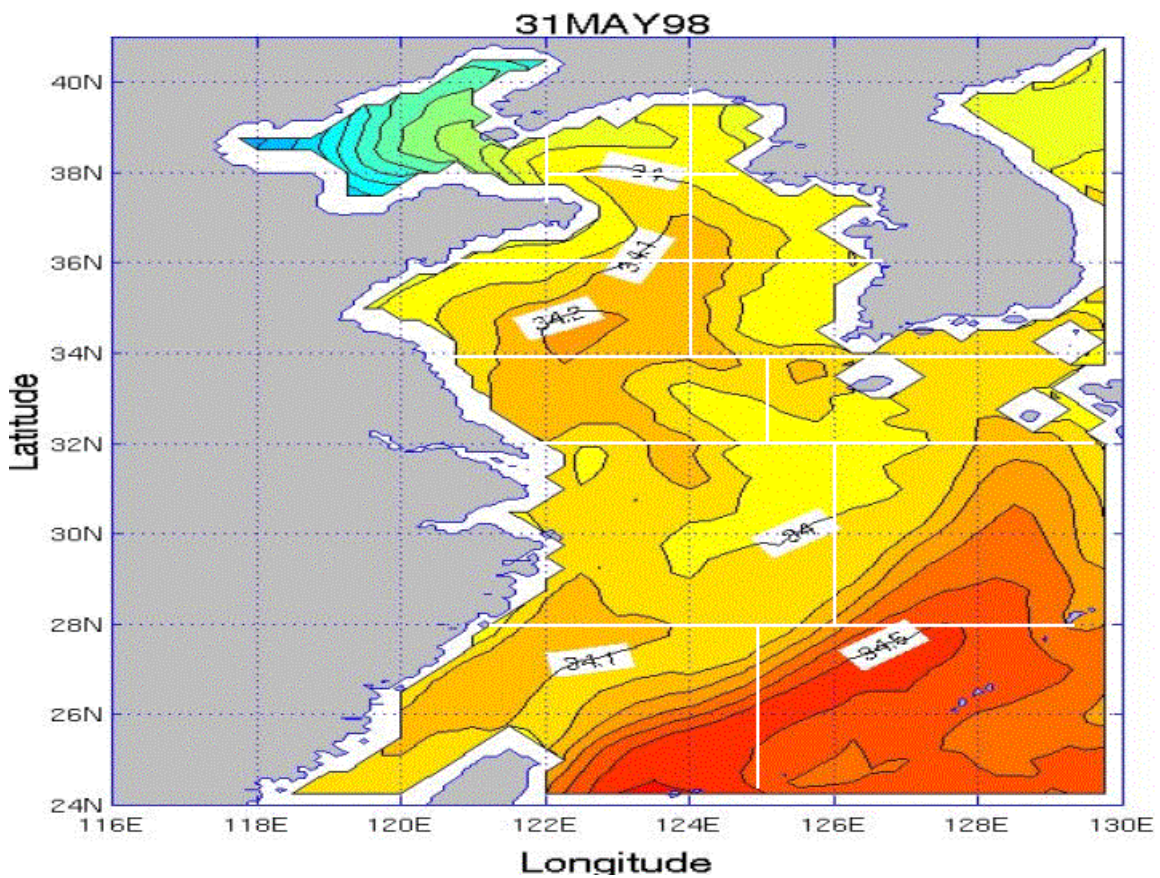
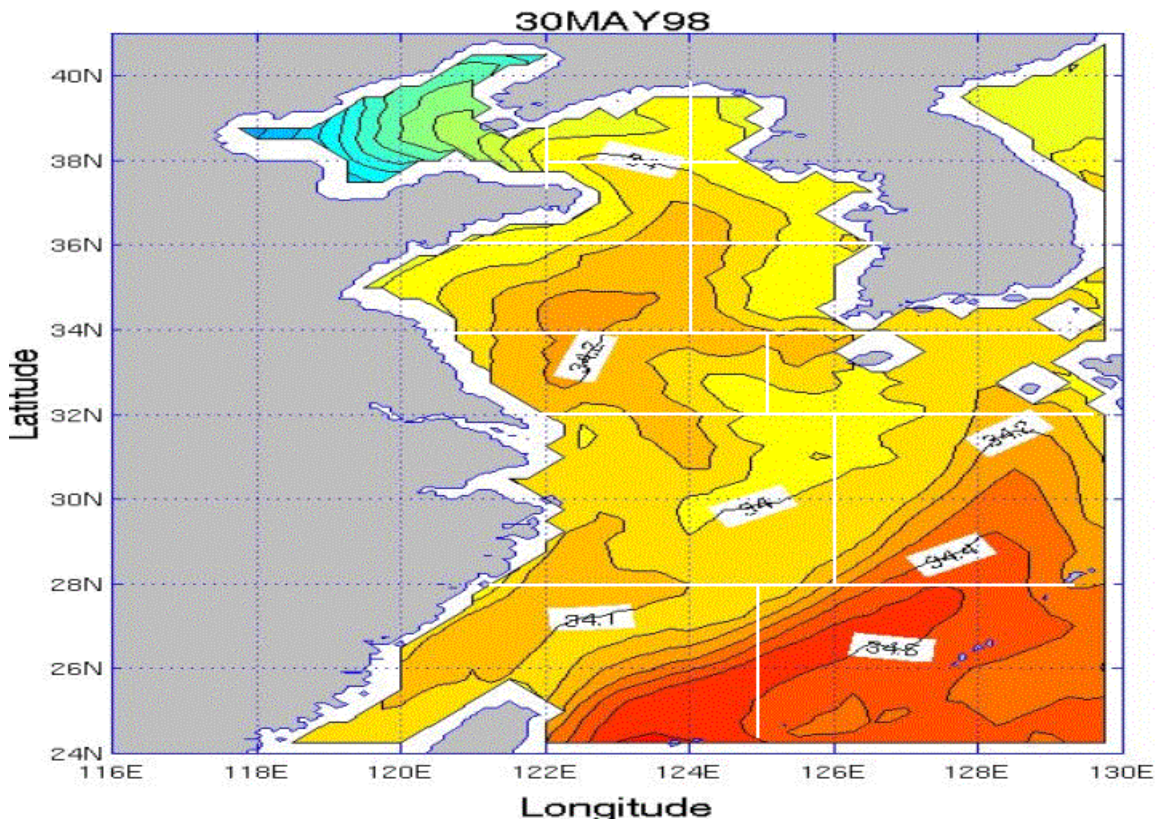






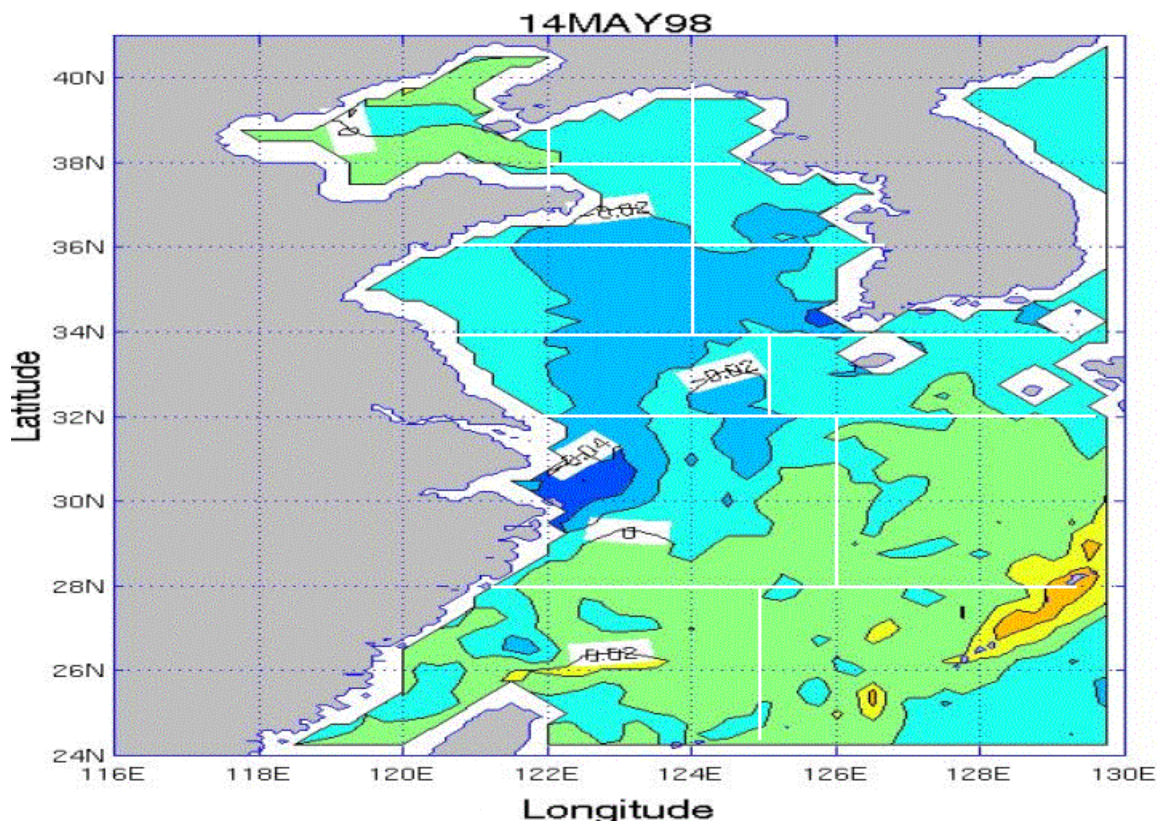


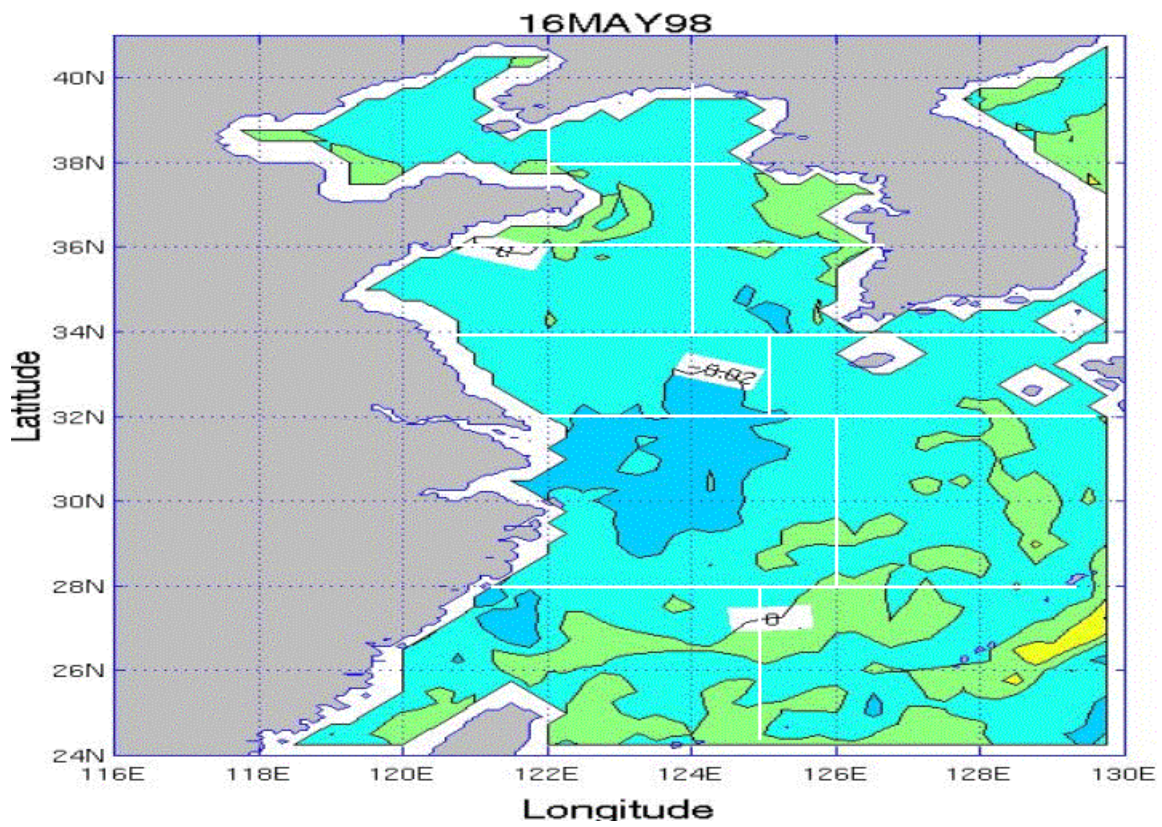
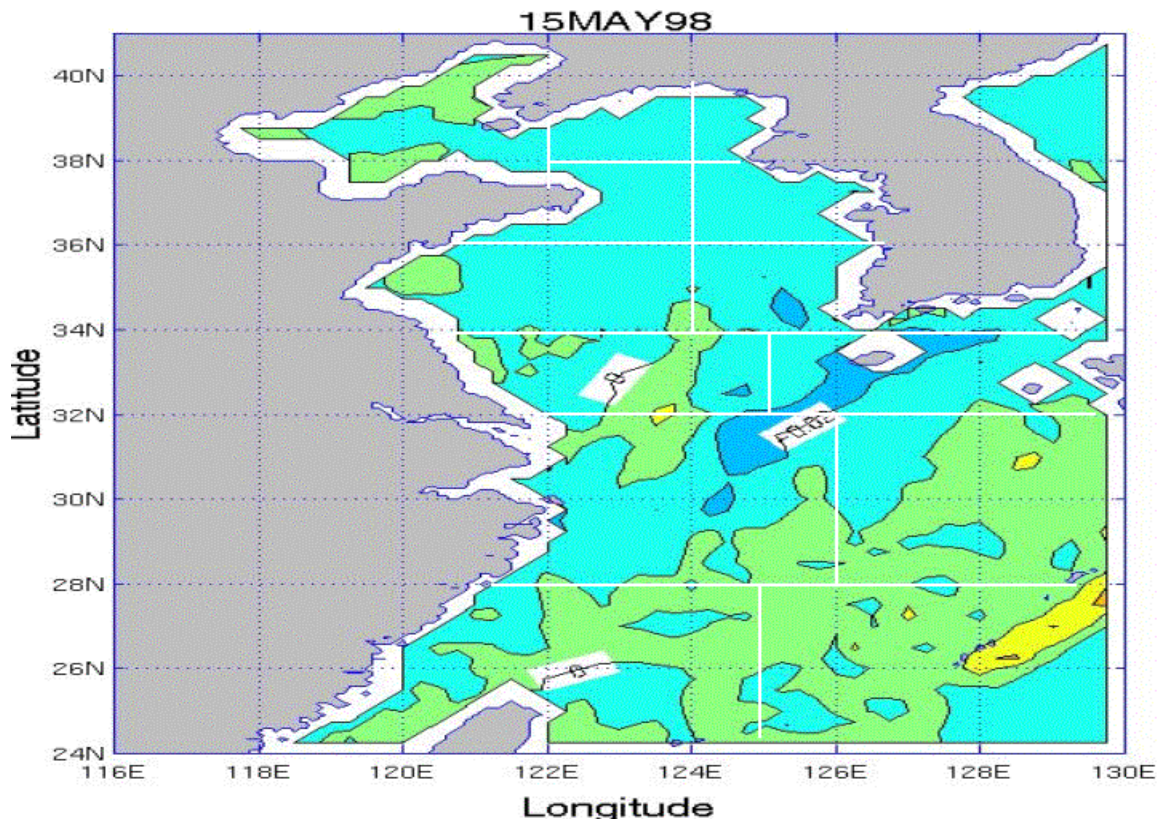


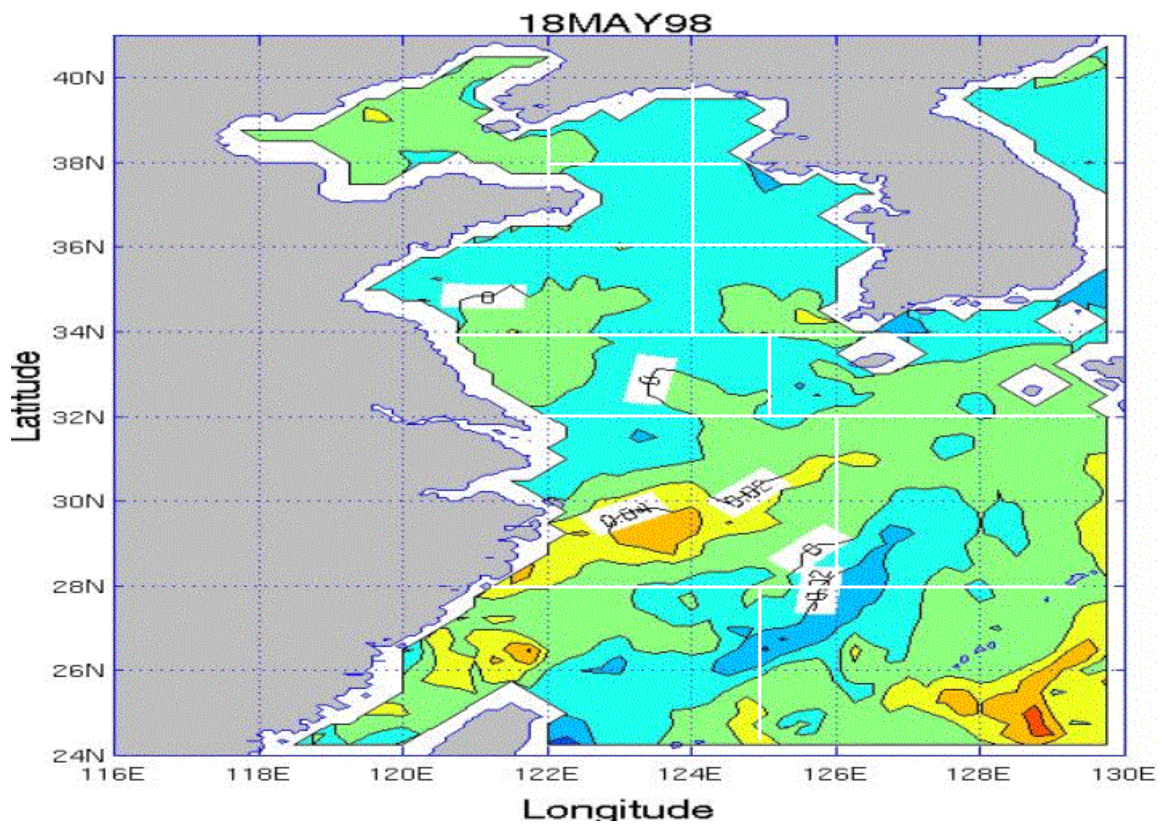
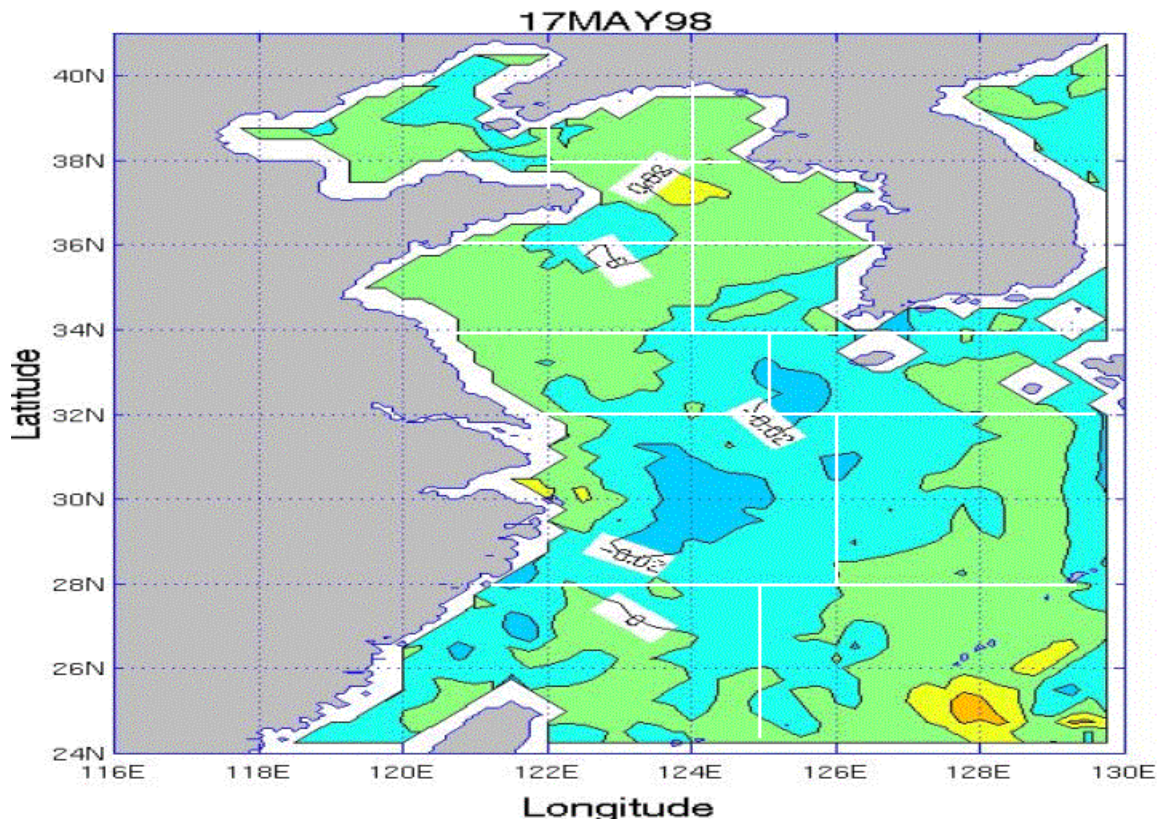


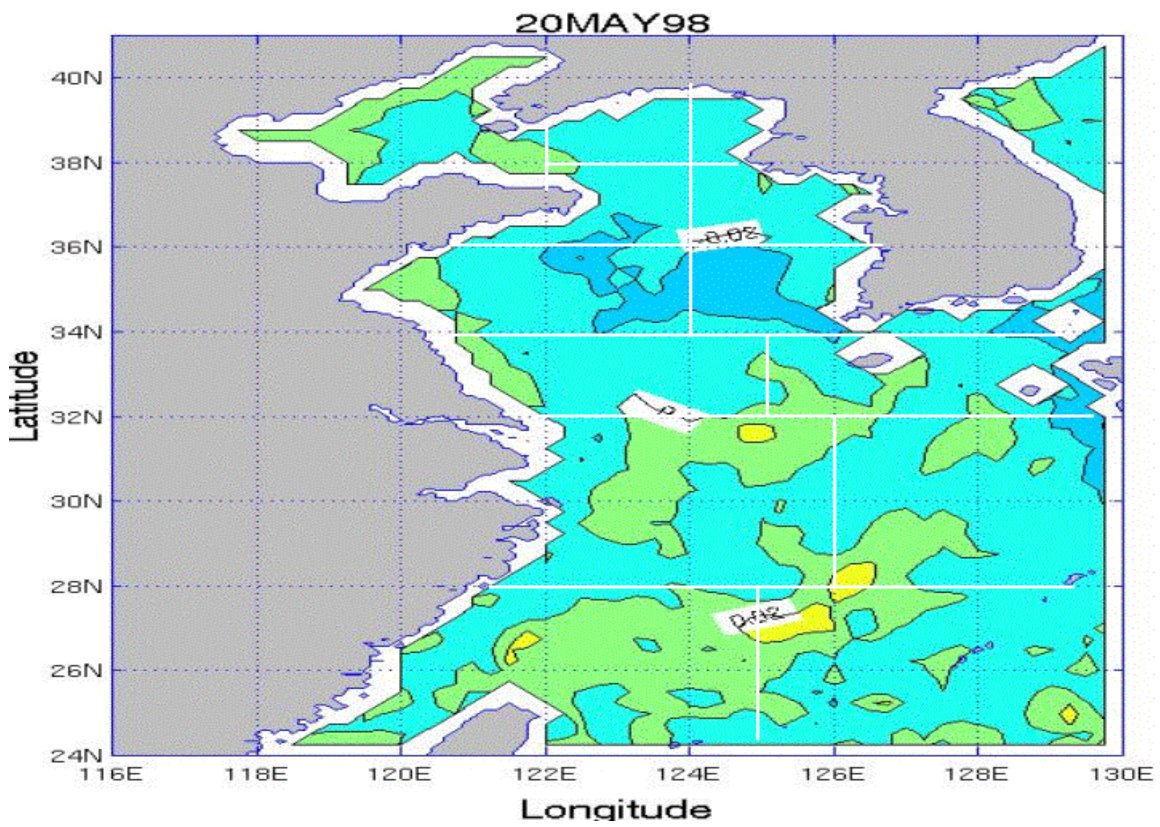
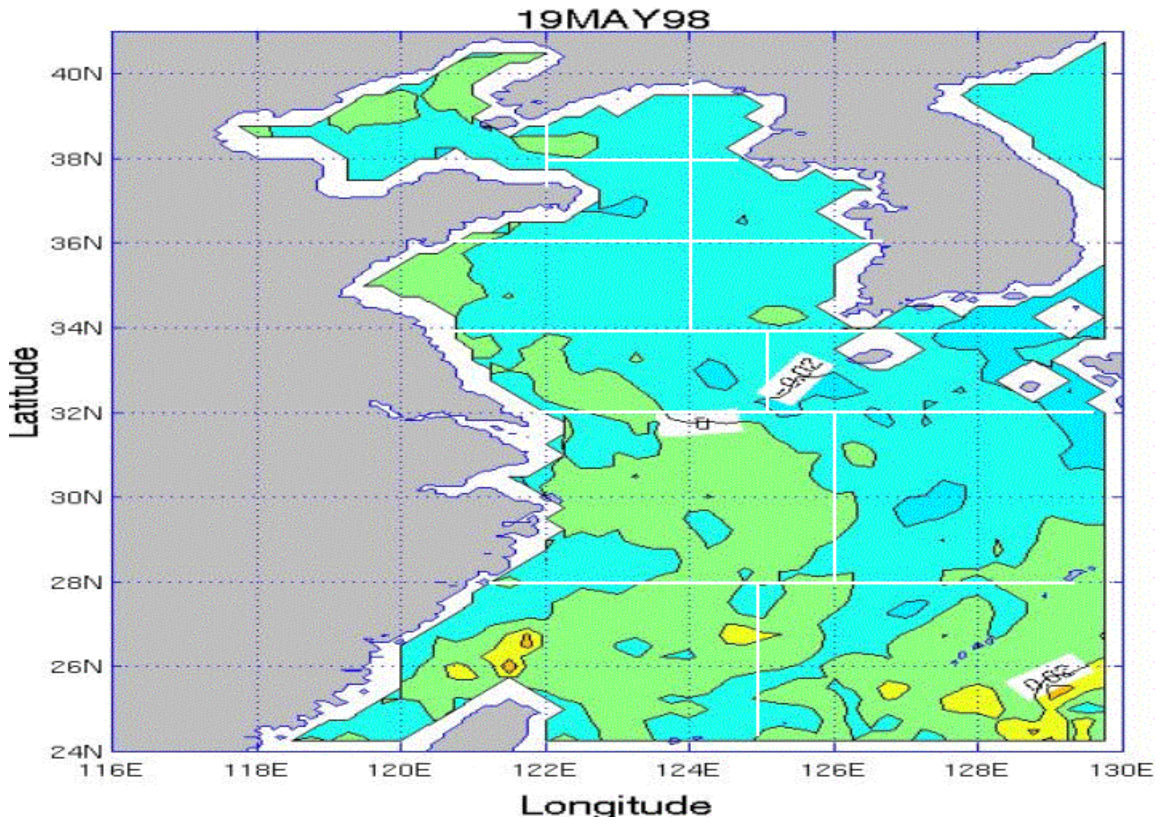
APPENDIX HH. SSS TENDENCY PLOTS FOR THE YES FOR THE MAY TIME PERIOD

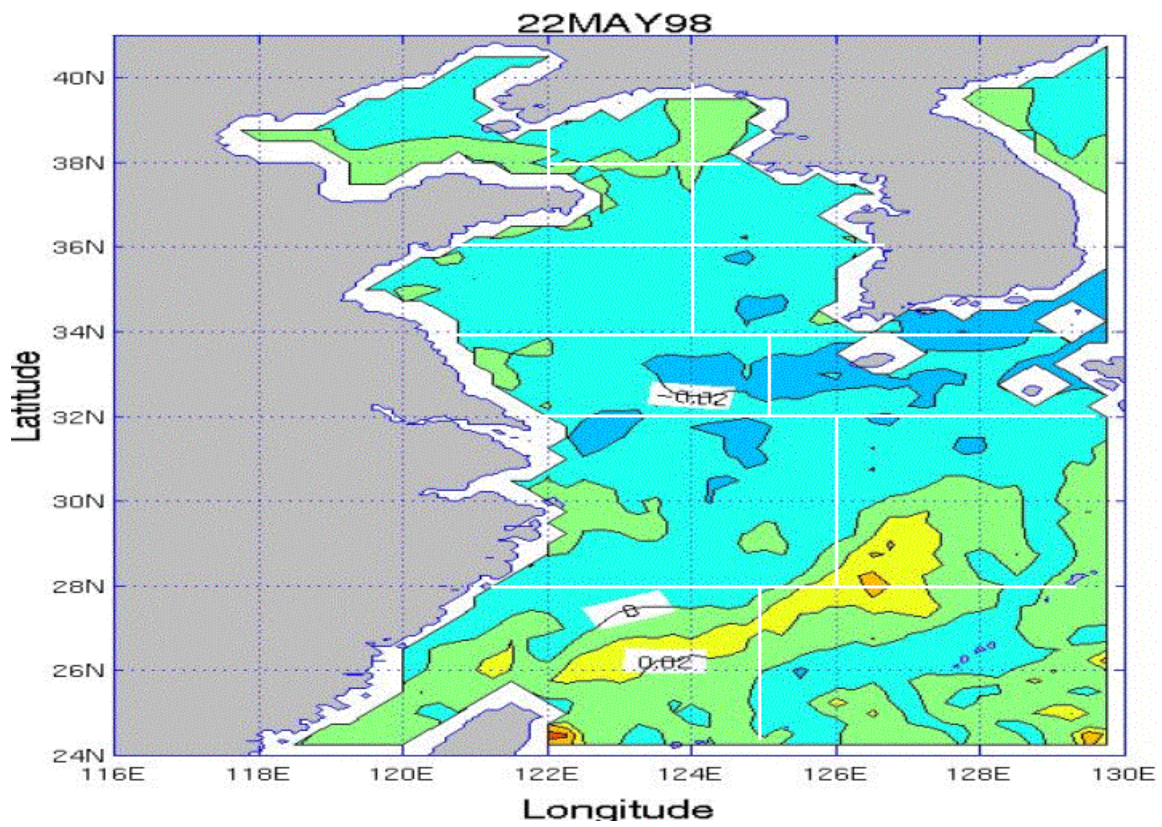
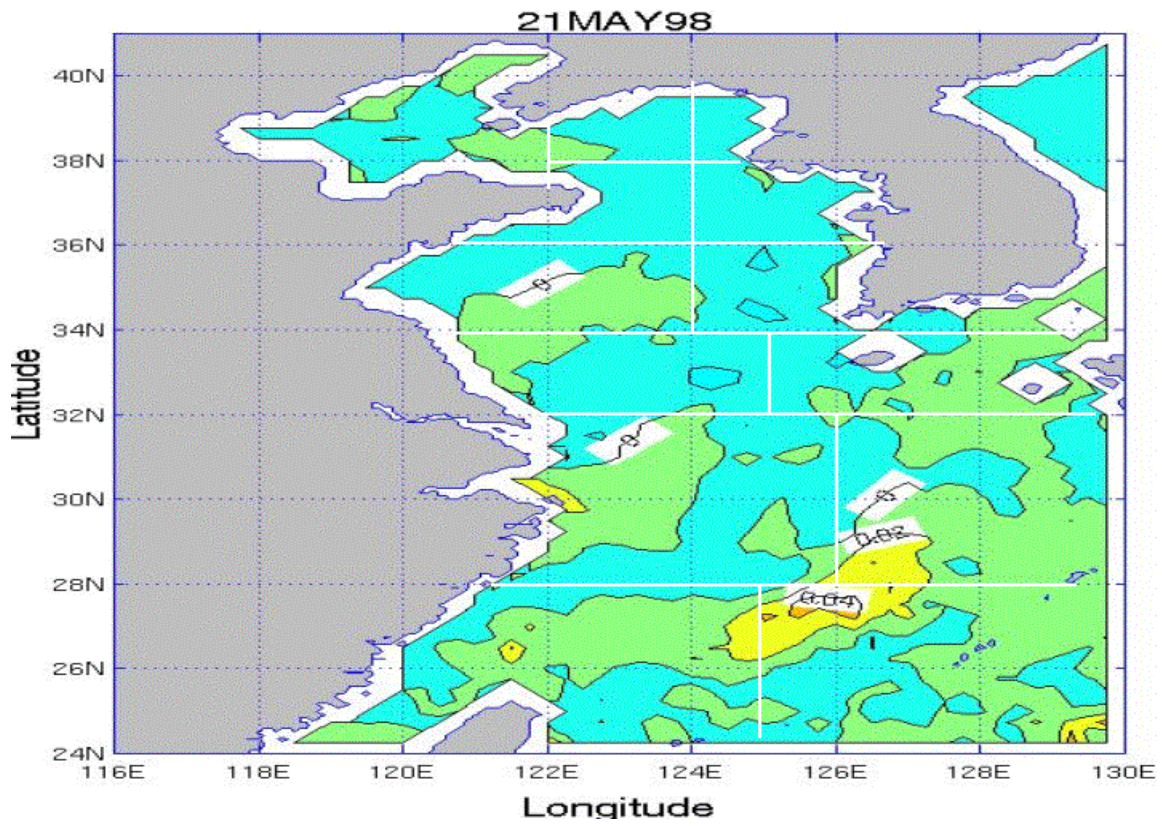
Appendix HH consists of 18 figures that show SSS day-to-day tendency for the May time period over the YES. The figures are in time sequential order from May 14 through May 31. Each plot represents the change between the previous day and the current day.

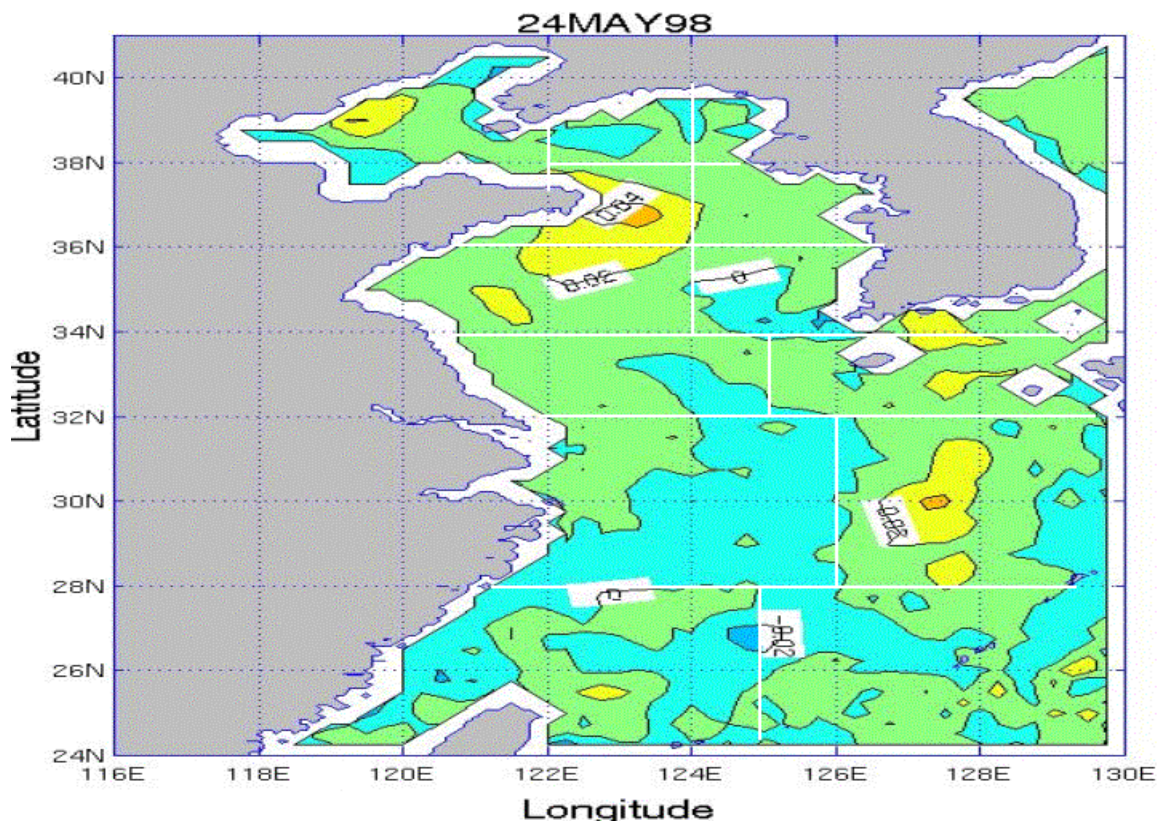
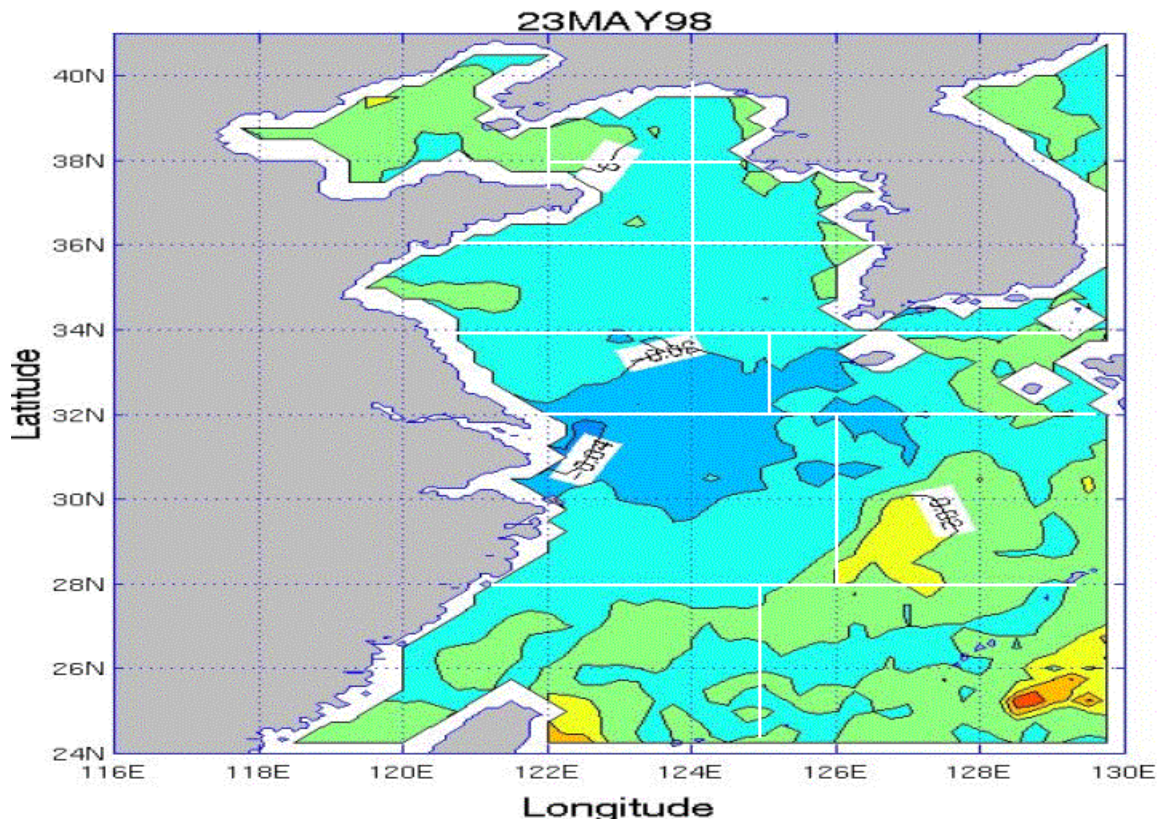


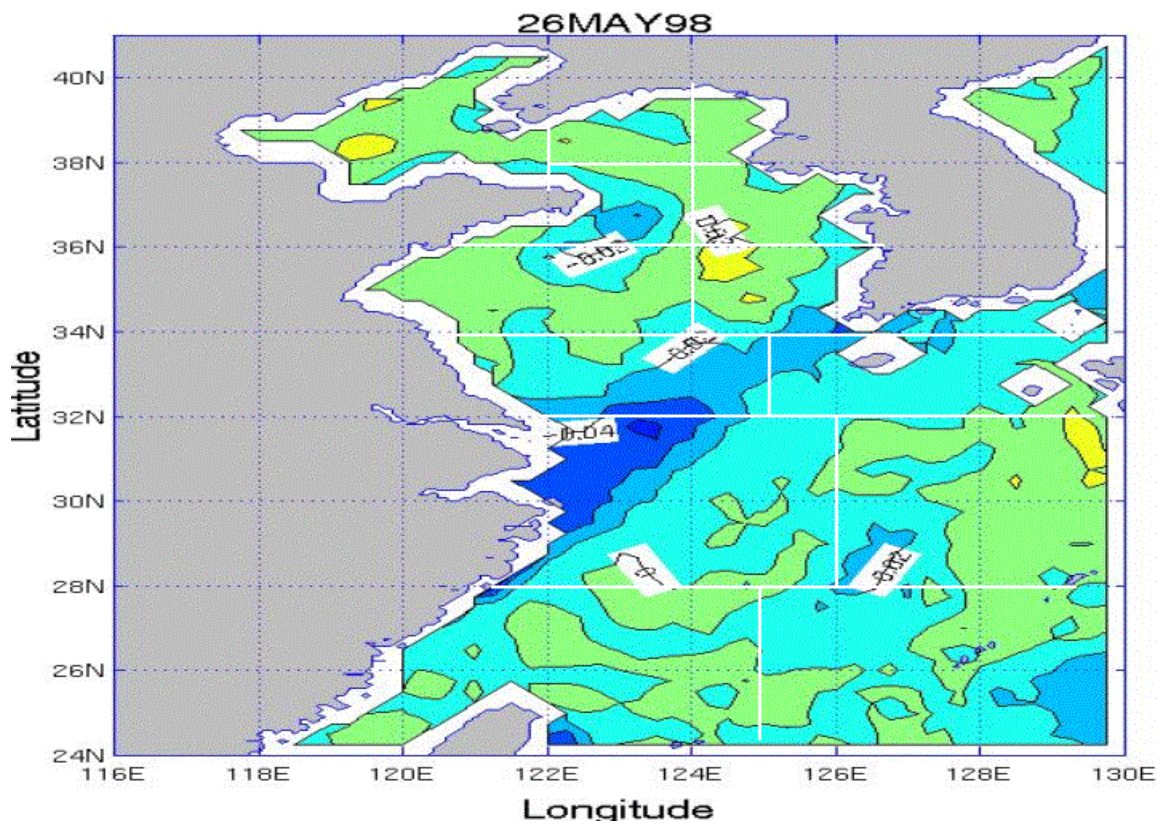
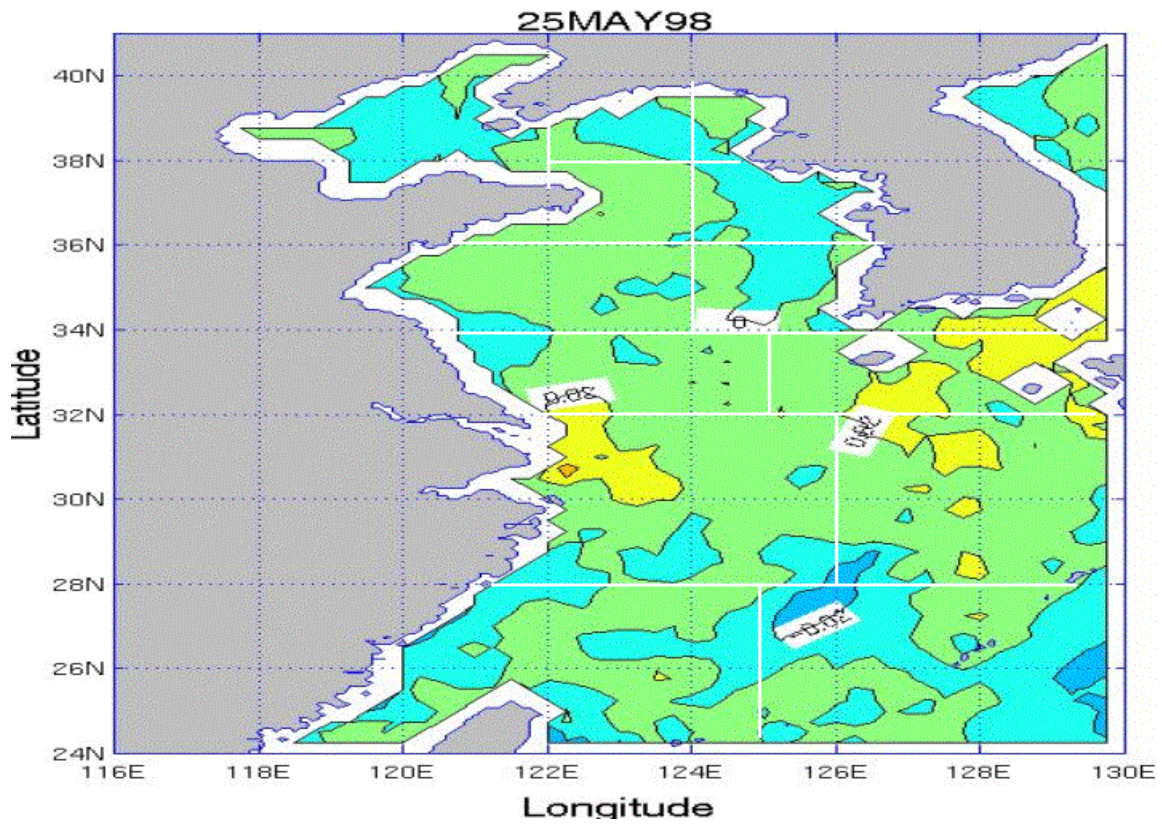


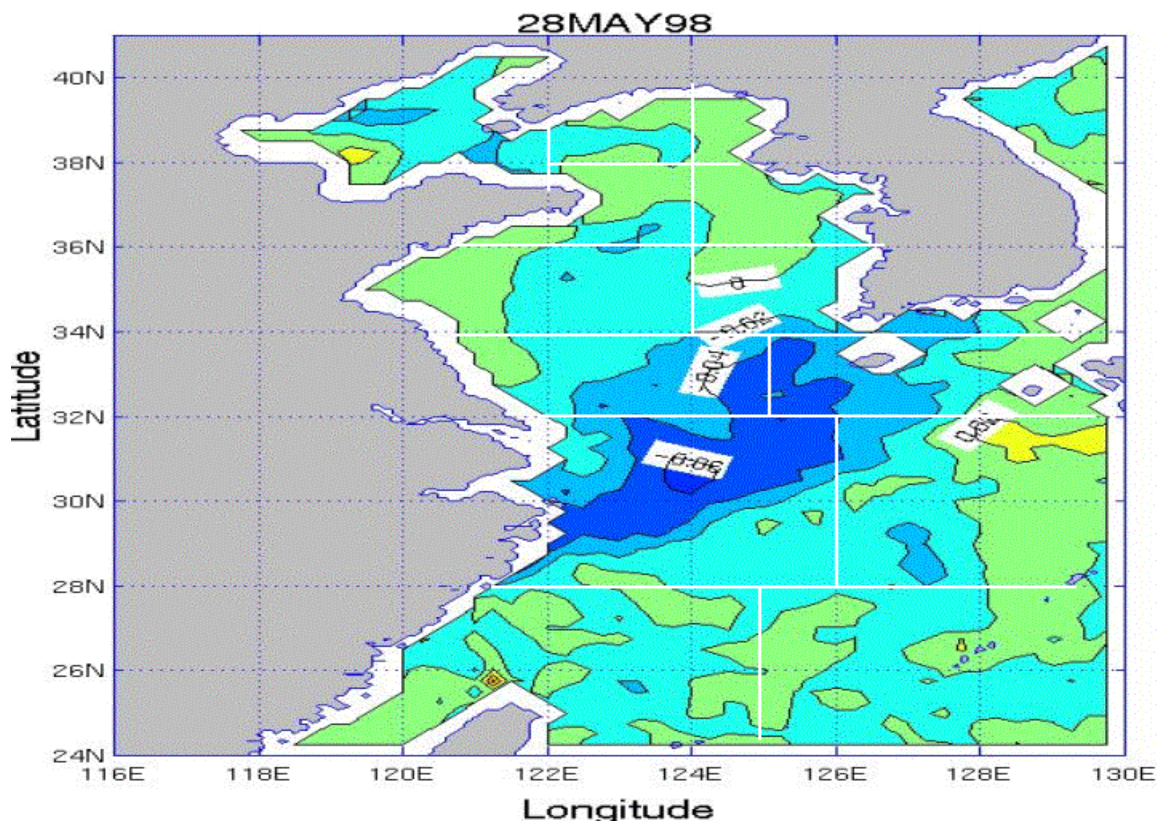
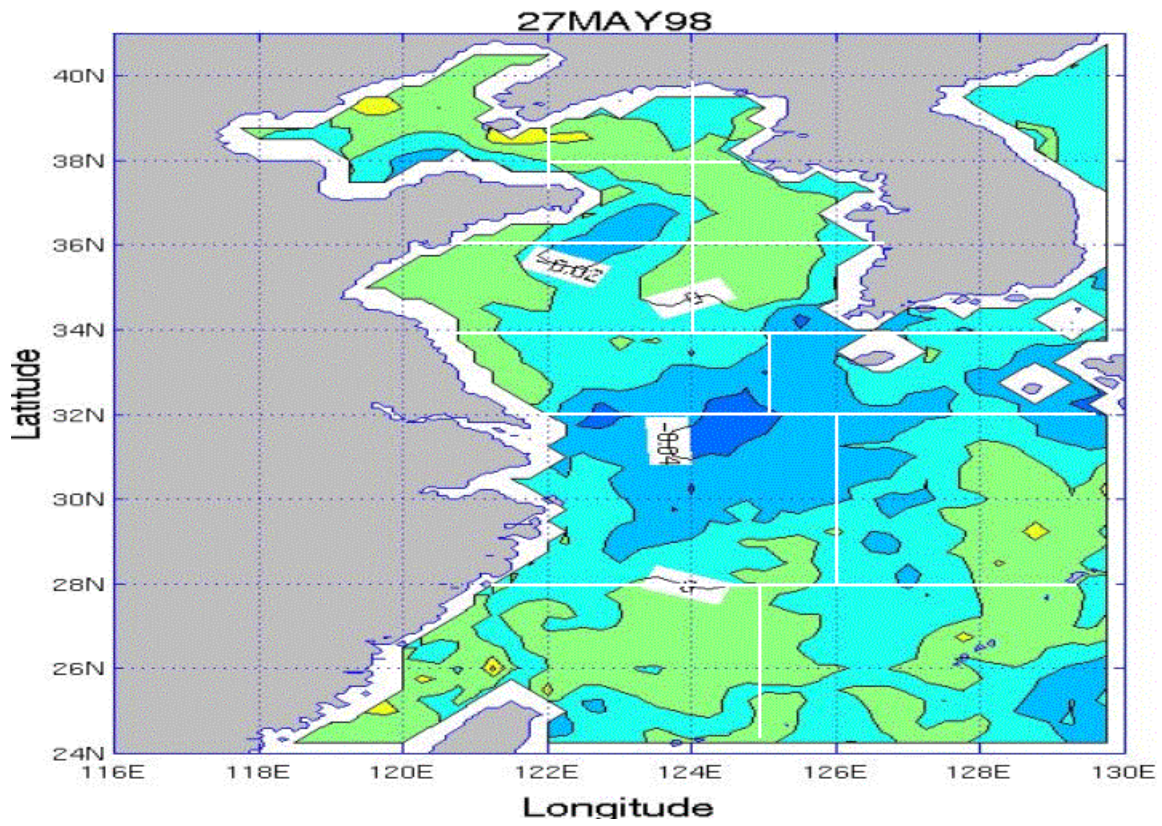


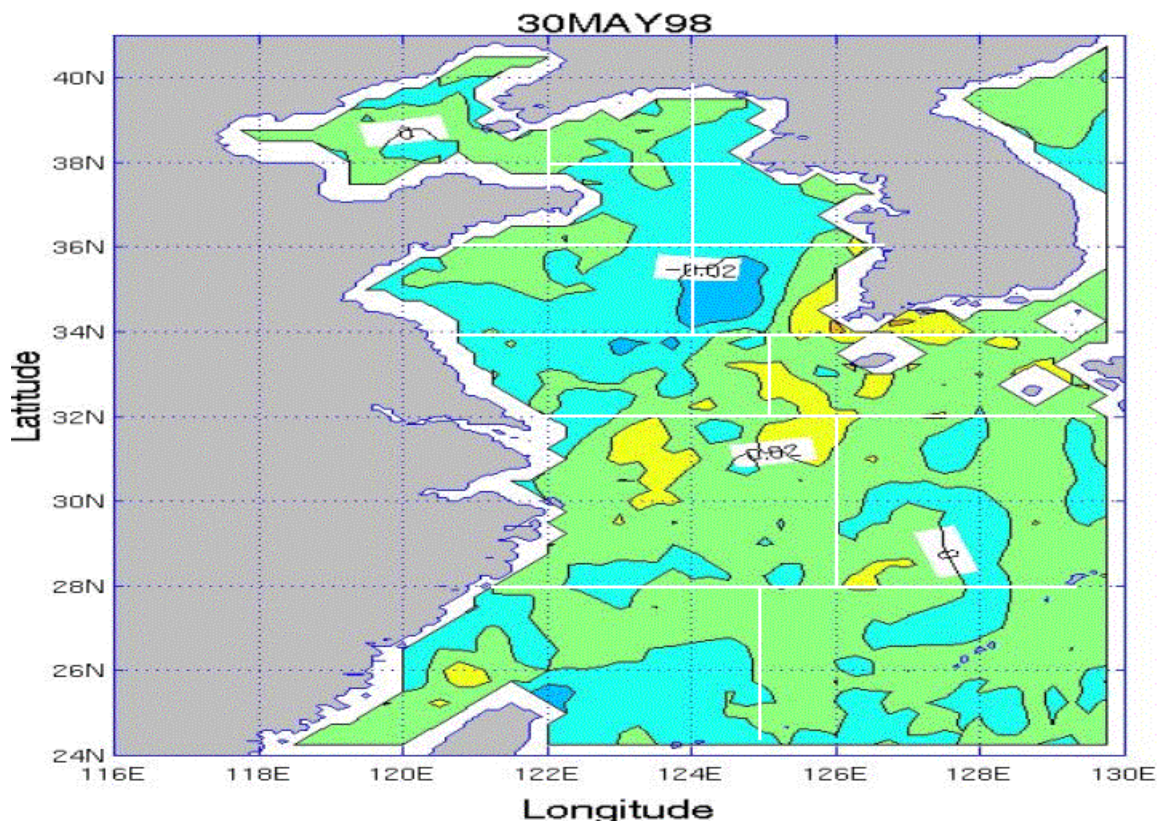
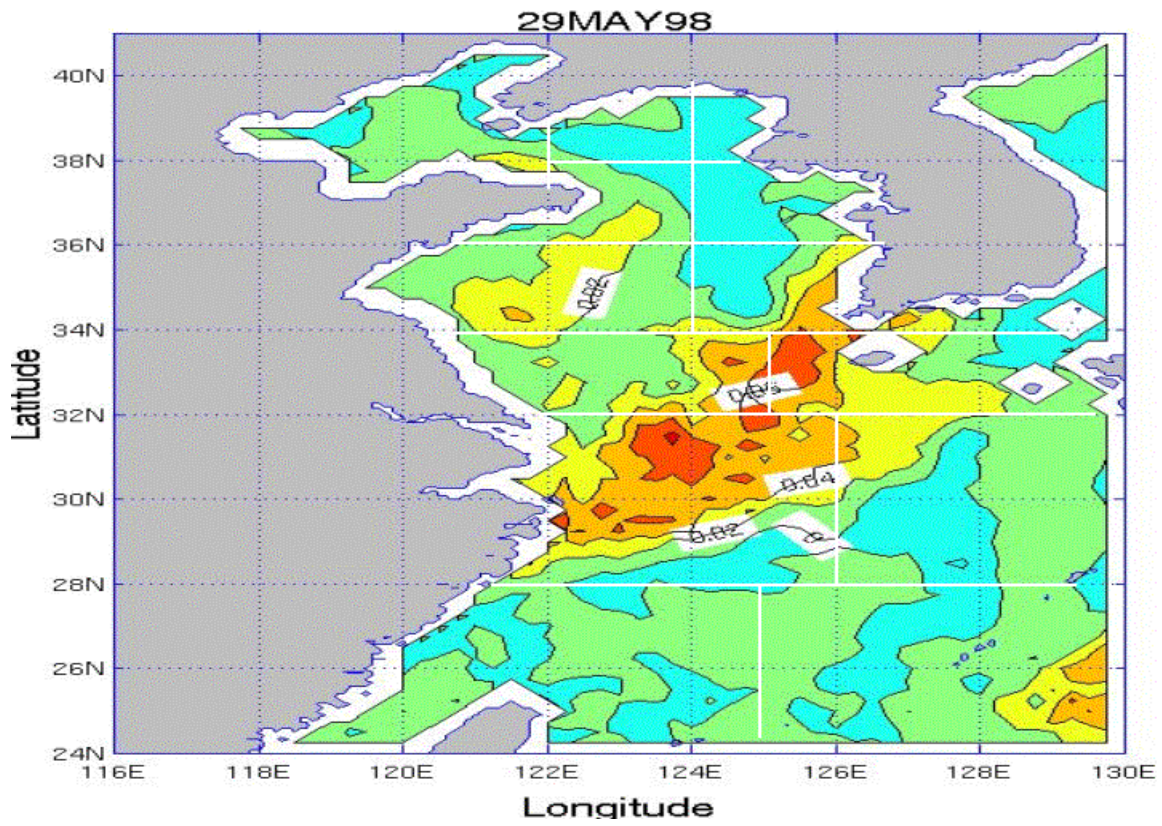


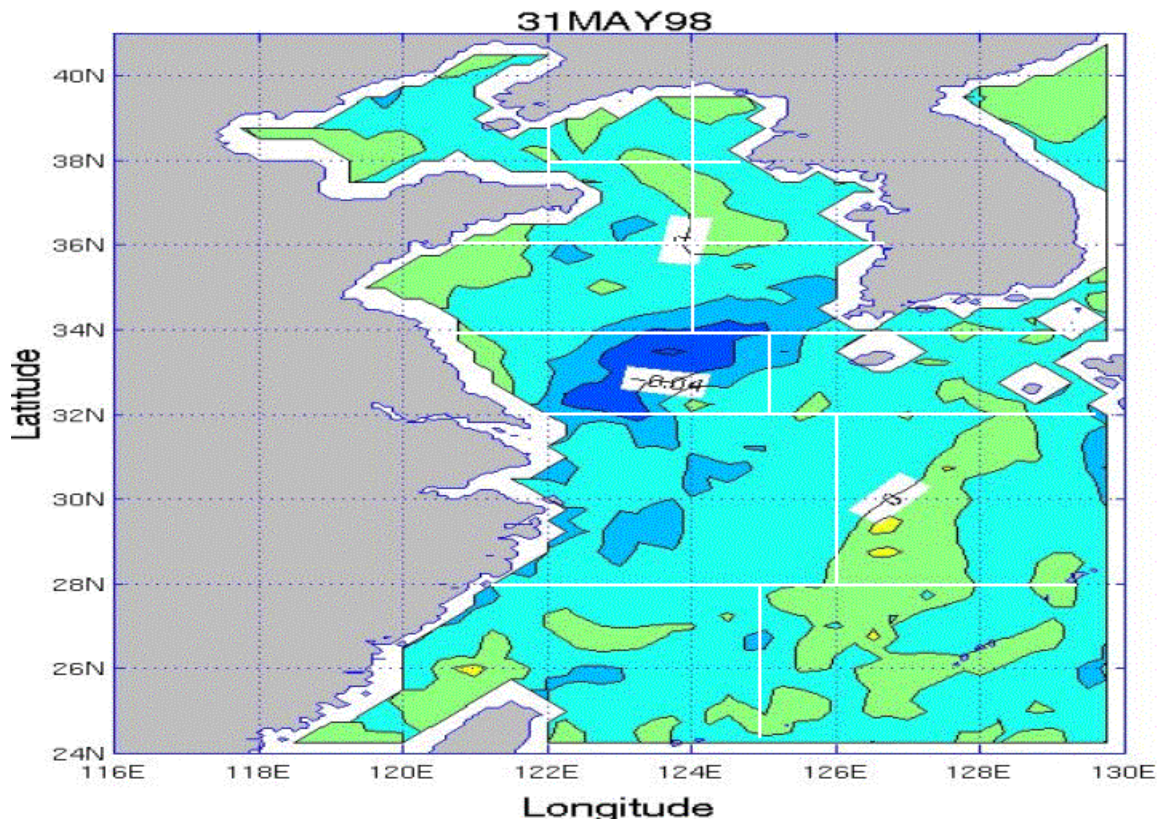






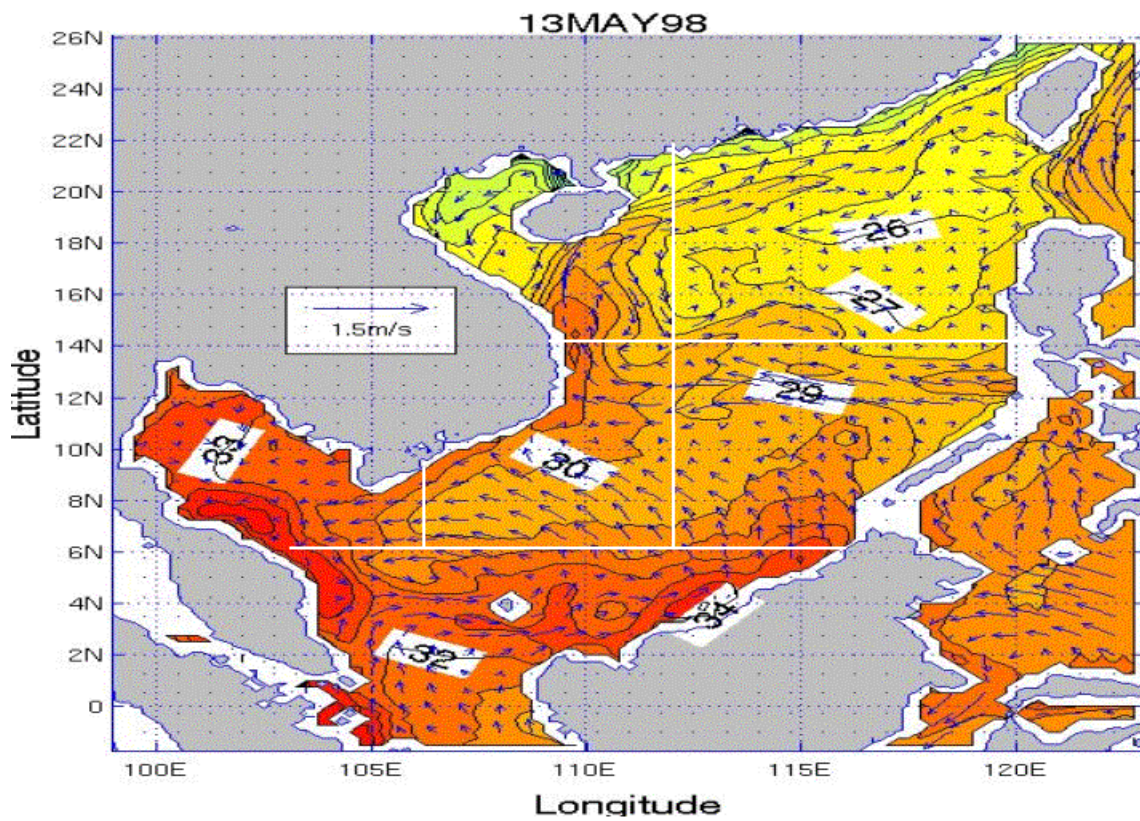


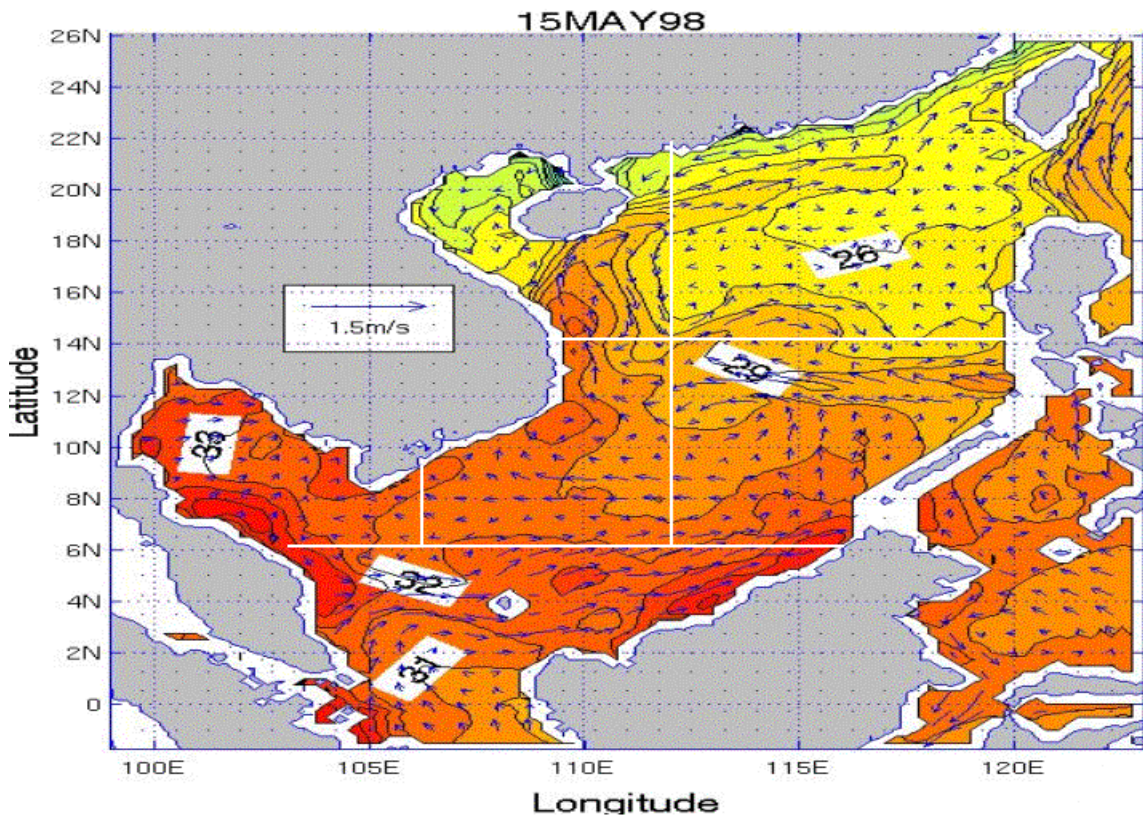
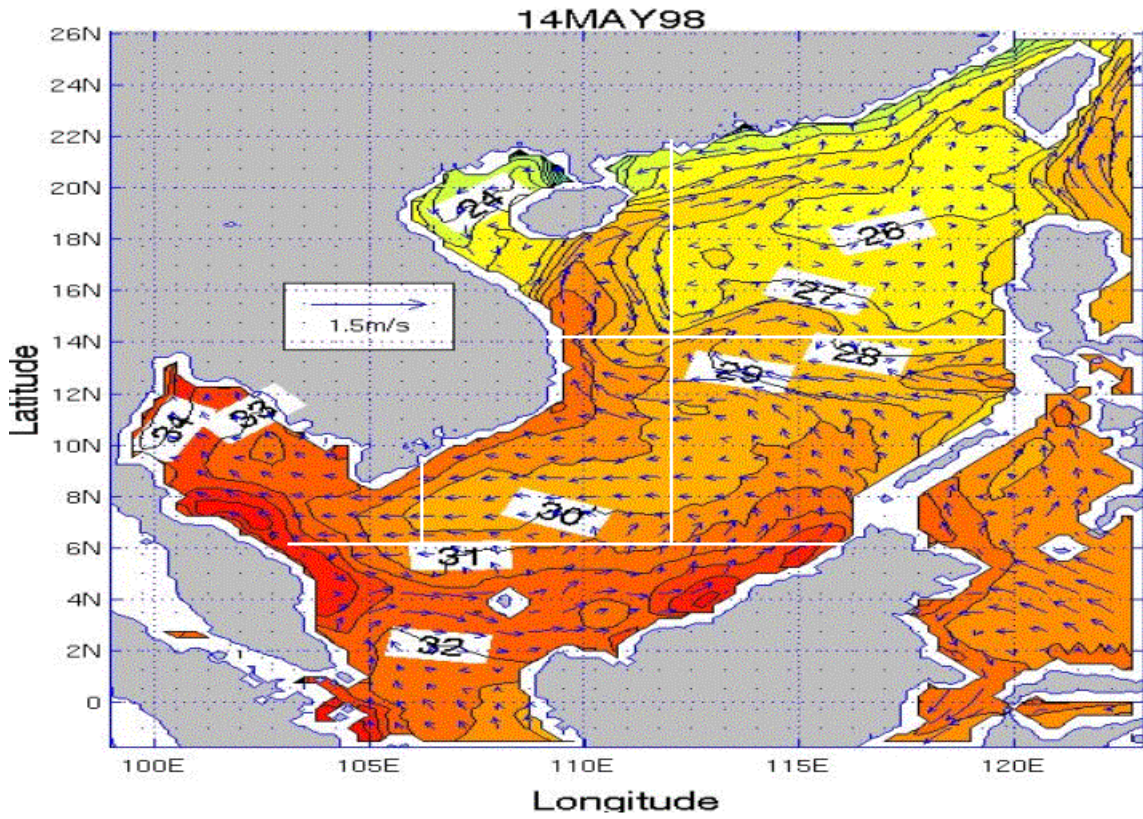


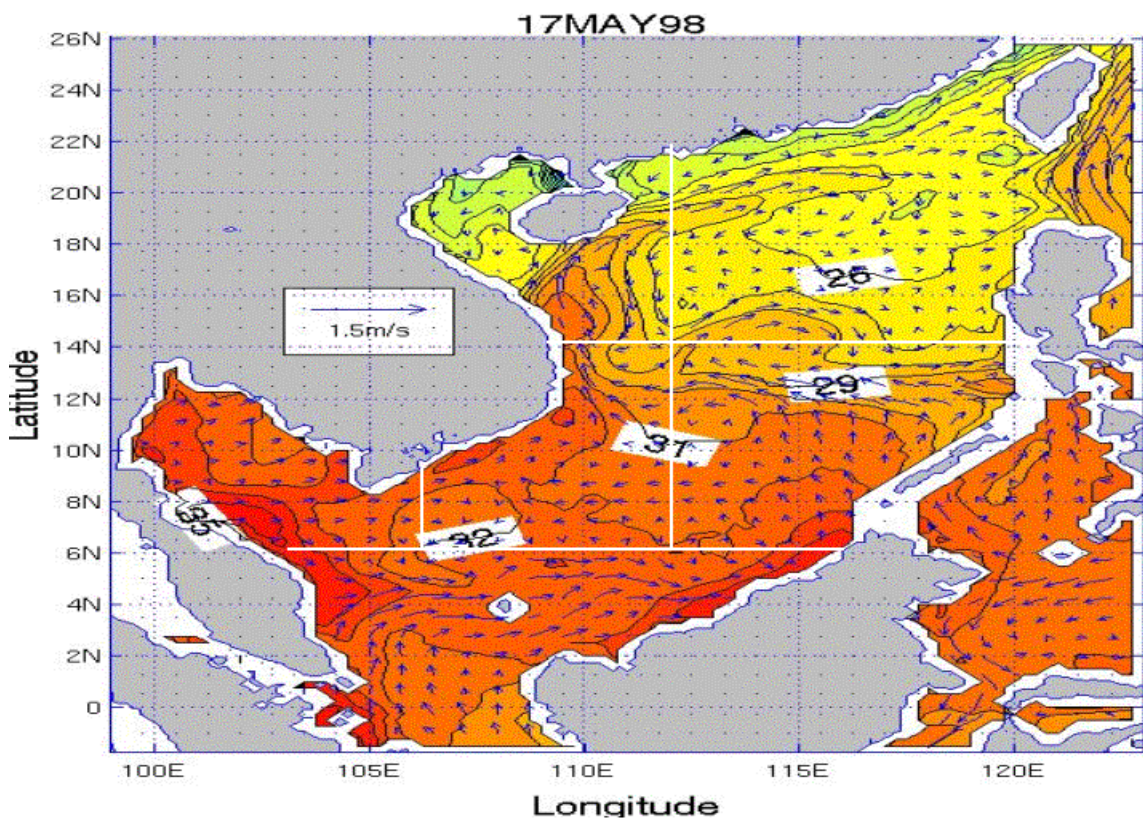
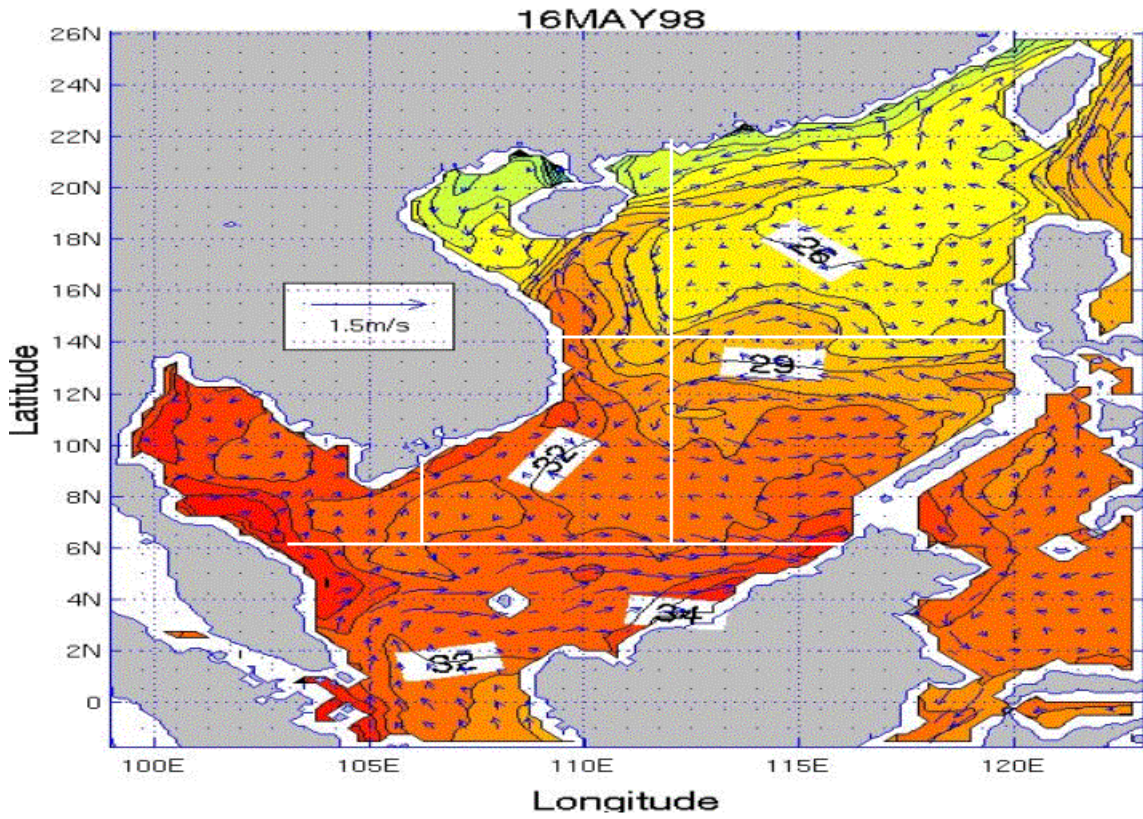


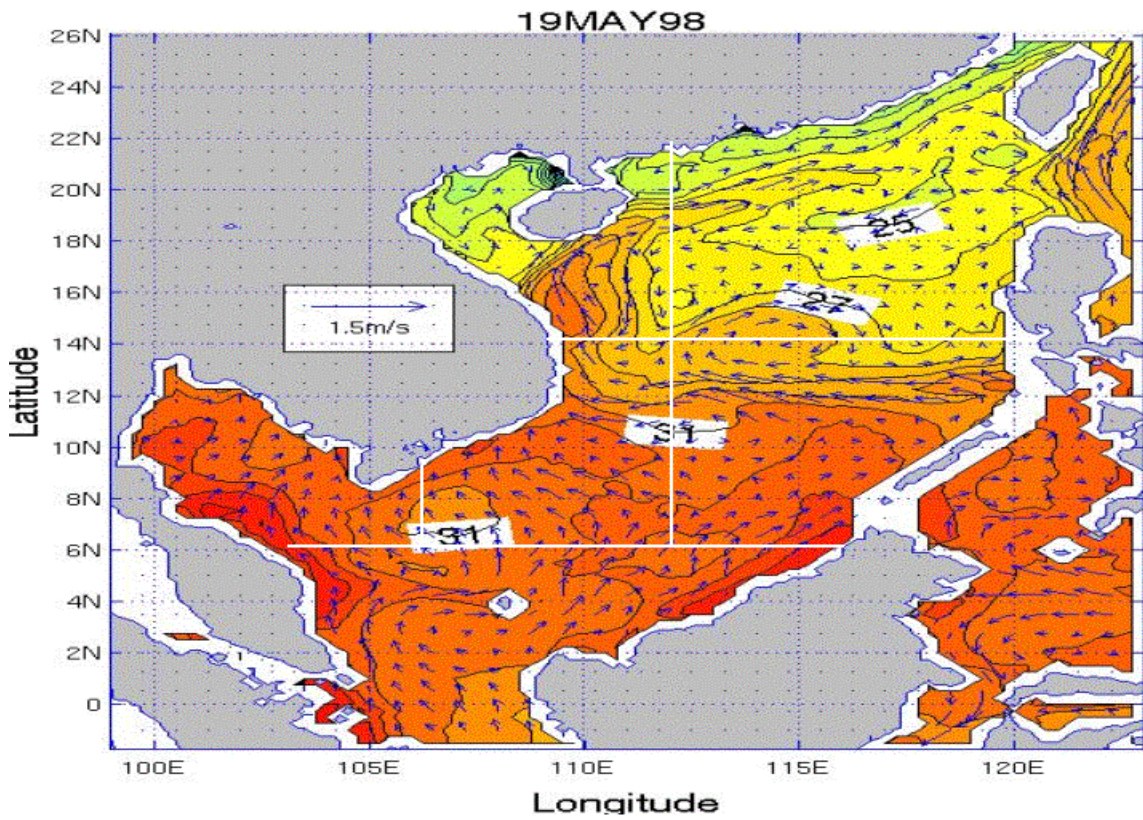
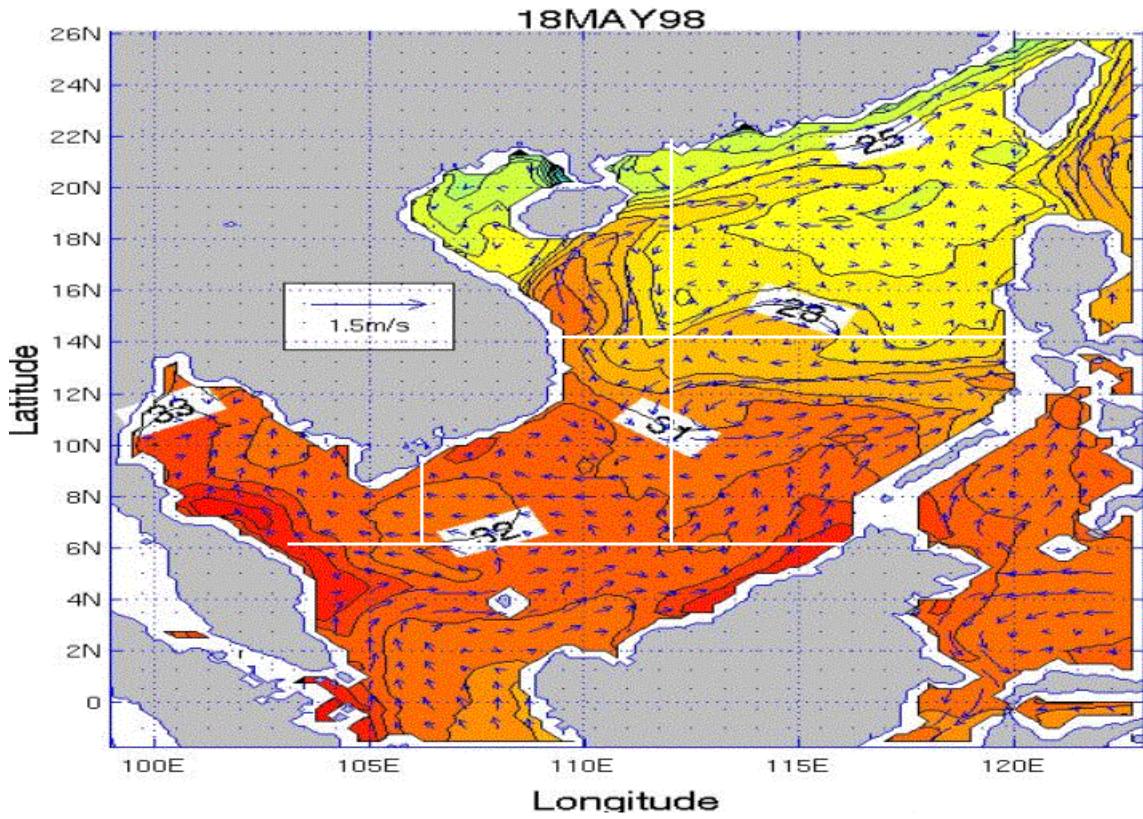
APPENDIX II. SST AND SURFACE CURRENT VELOCITY PLOTS FOR THE SCS FOR THE MAY TIME PERIOD

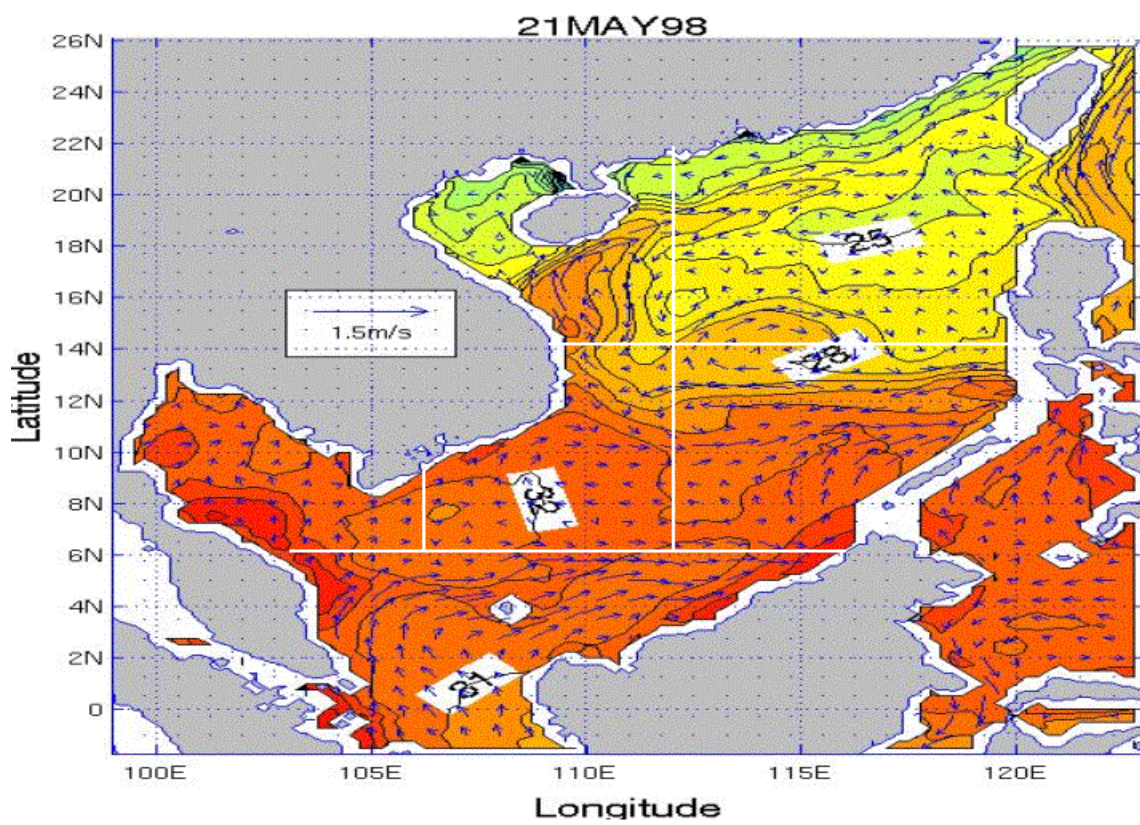
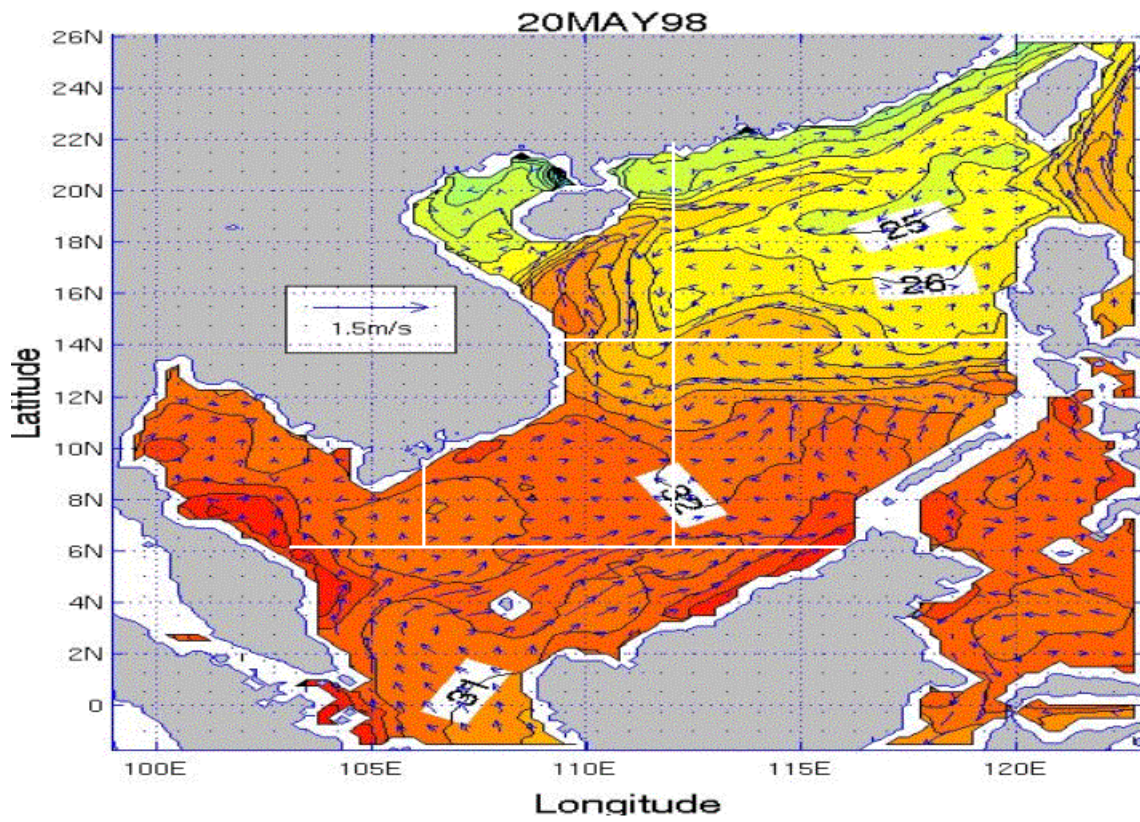
Appendix II consists of 19 figures that show SST and surface current velocity for each day of the May time period for the SCS. The figures are in time sequential order from May 13 through May 31.

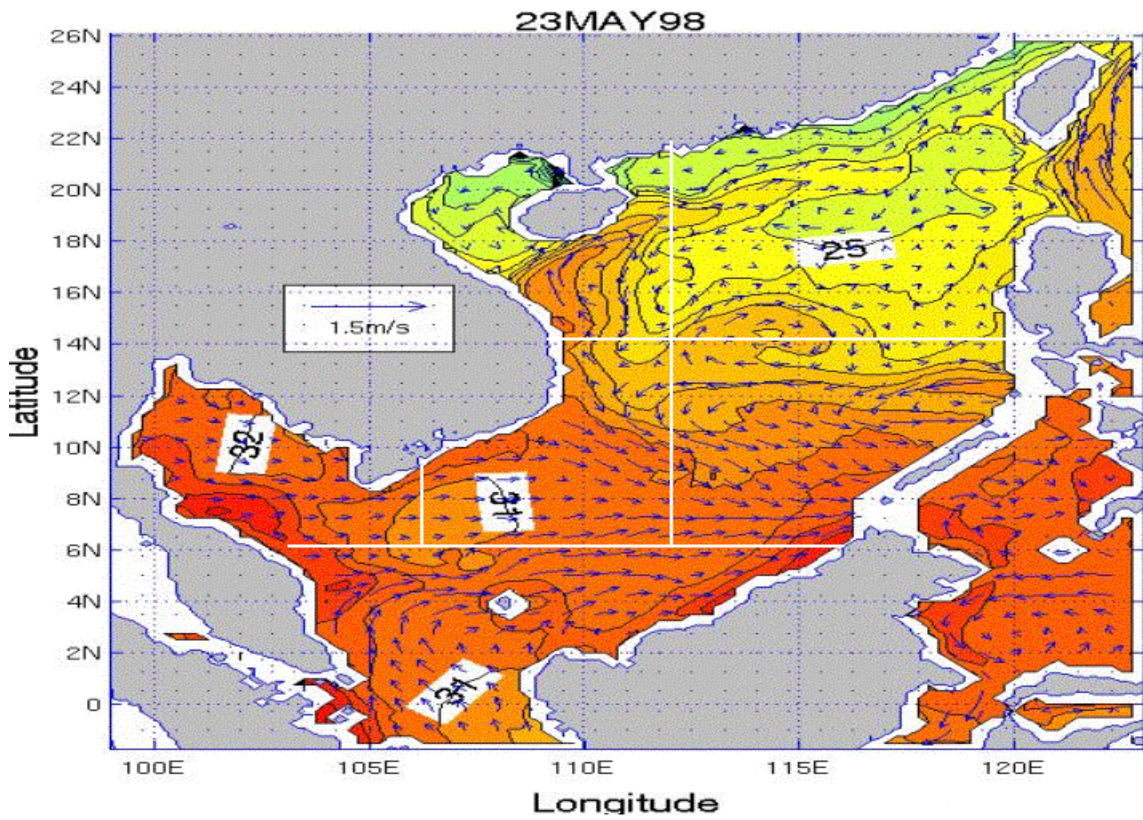
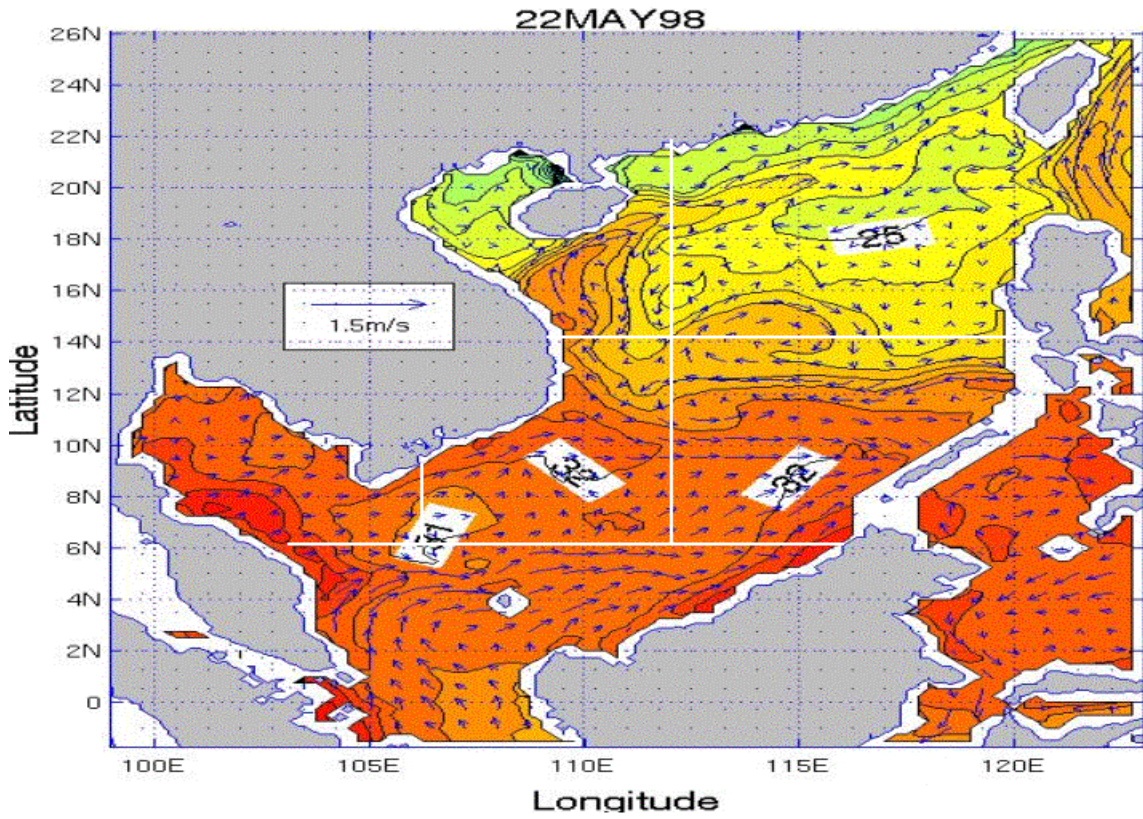


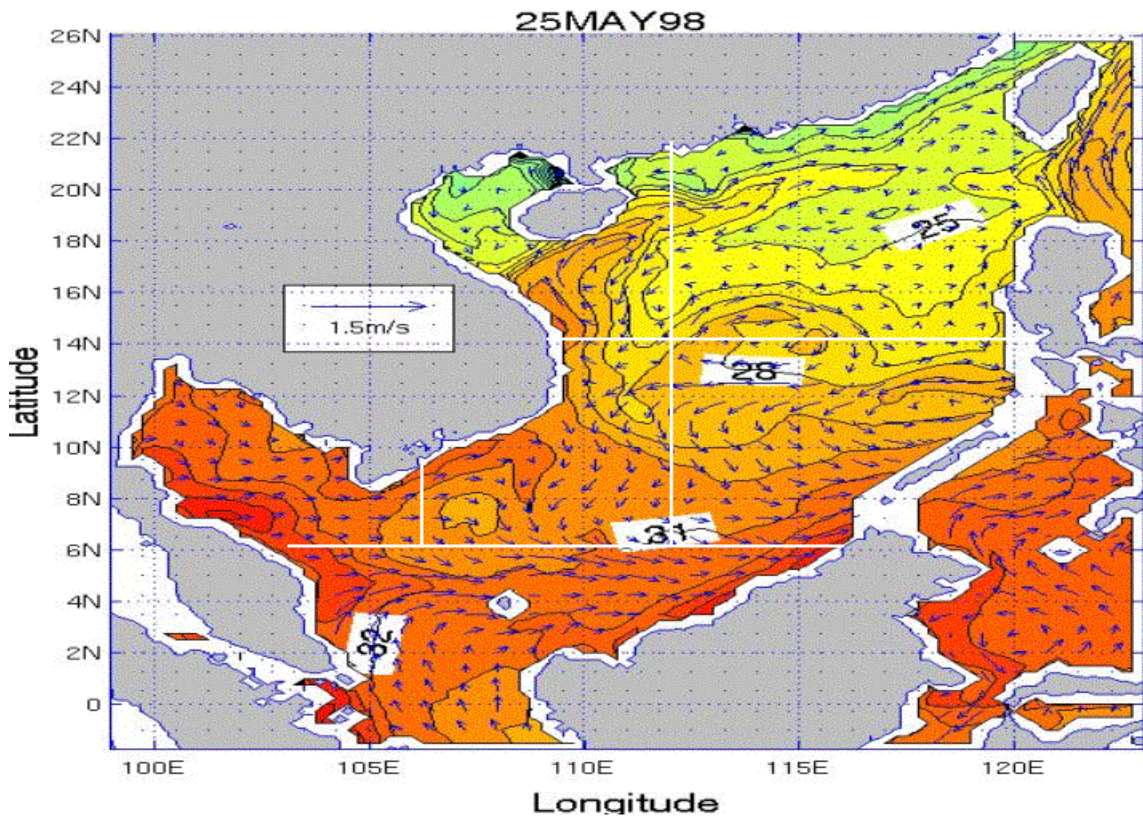
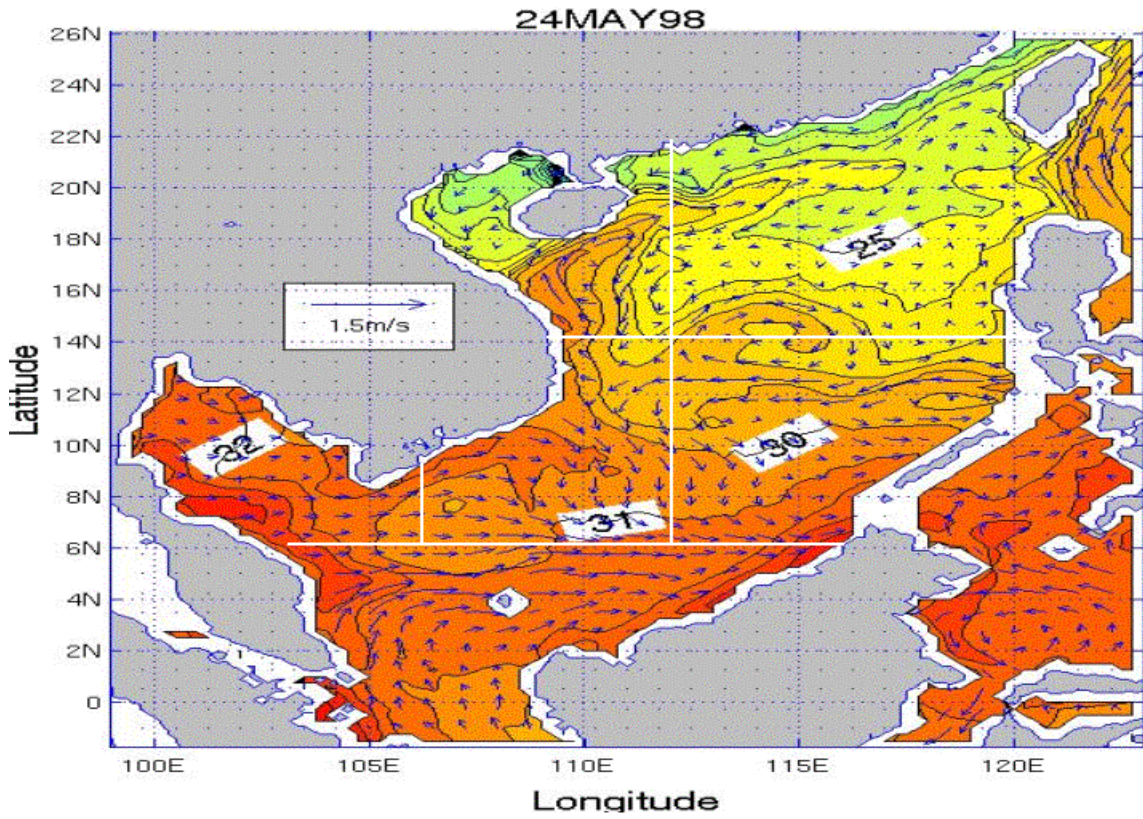


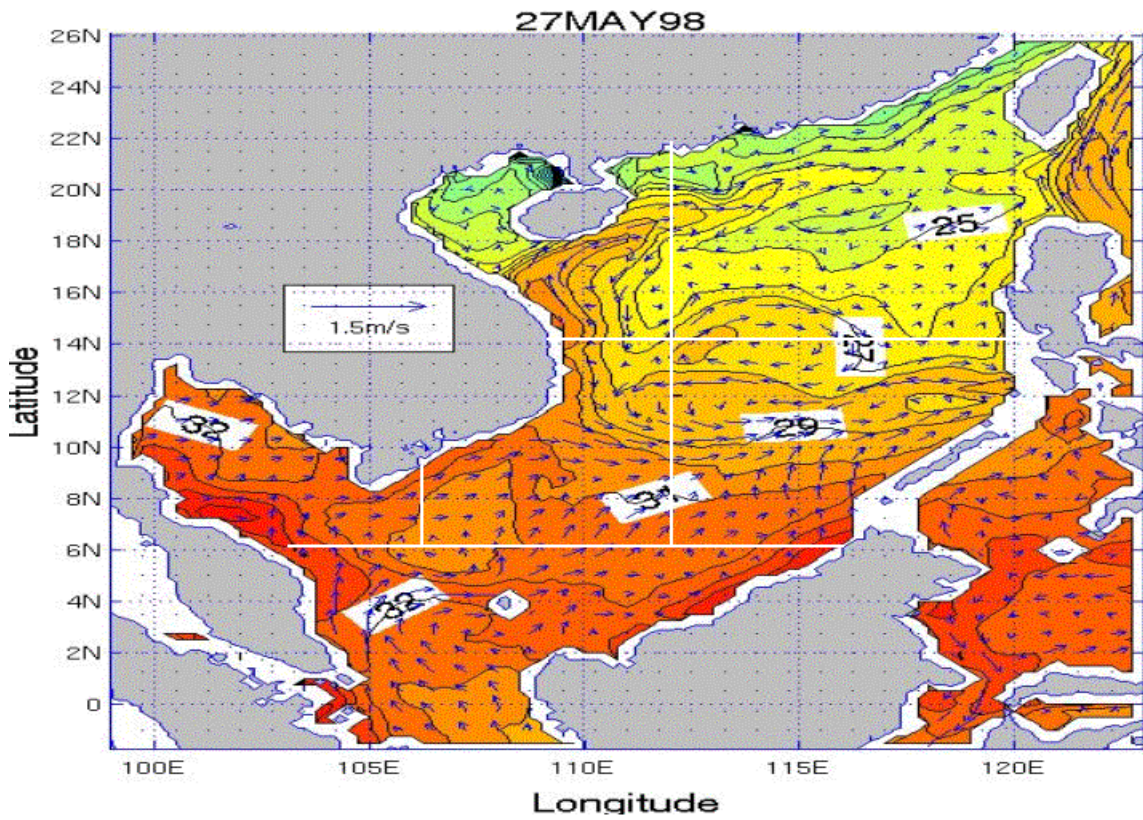
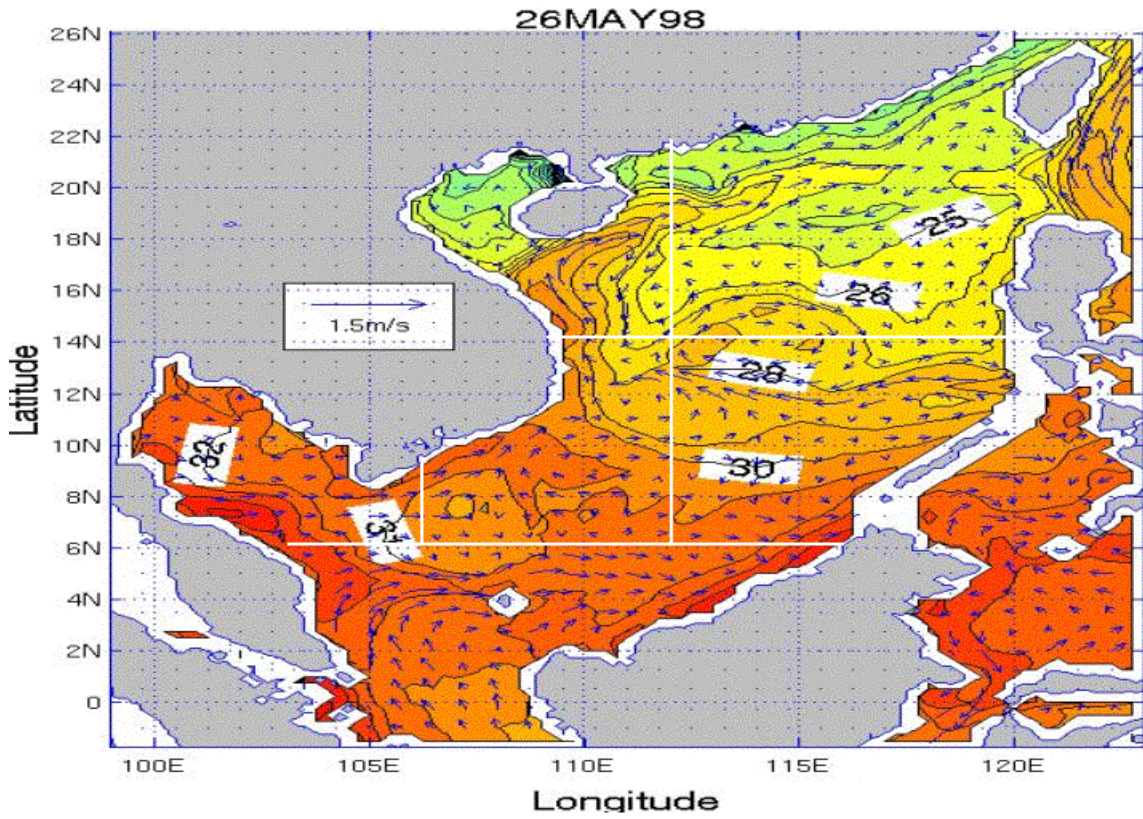


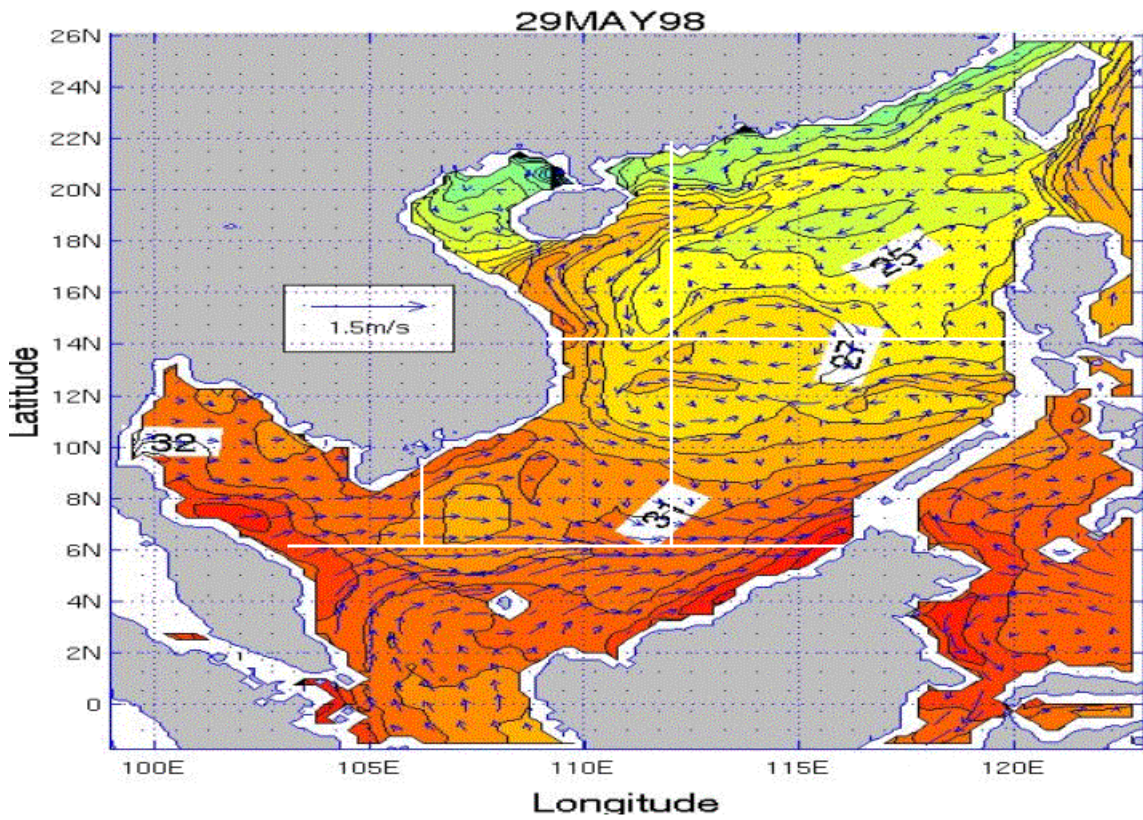
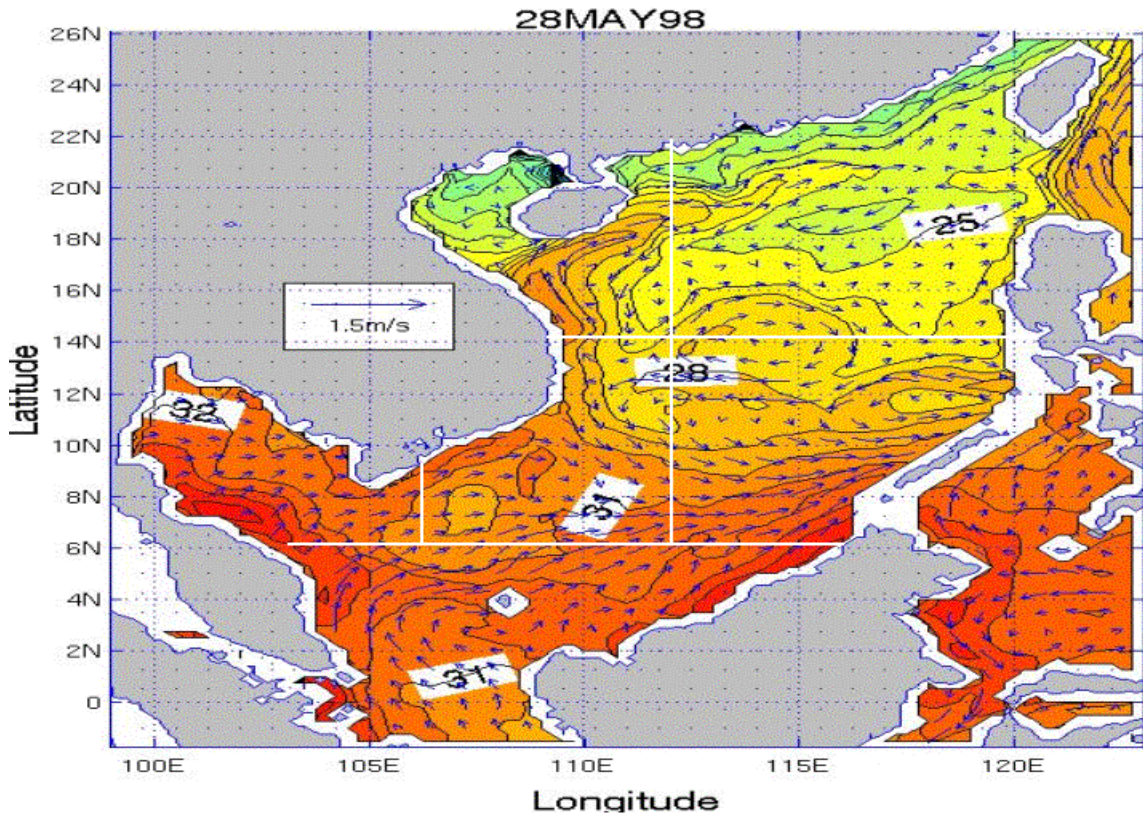


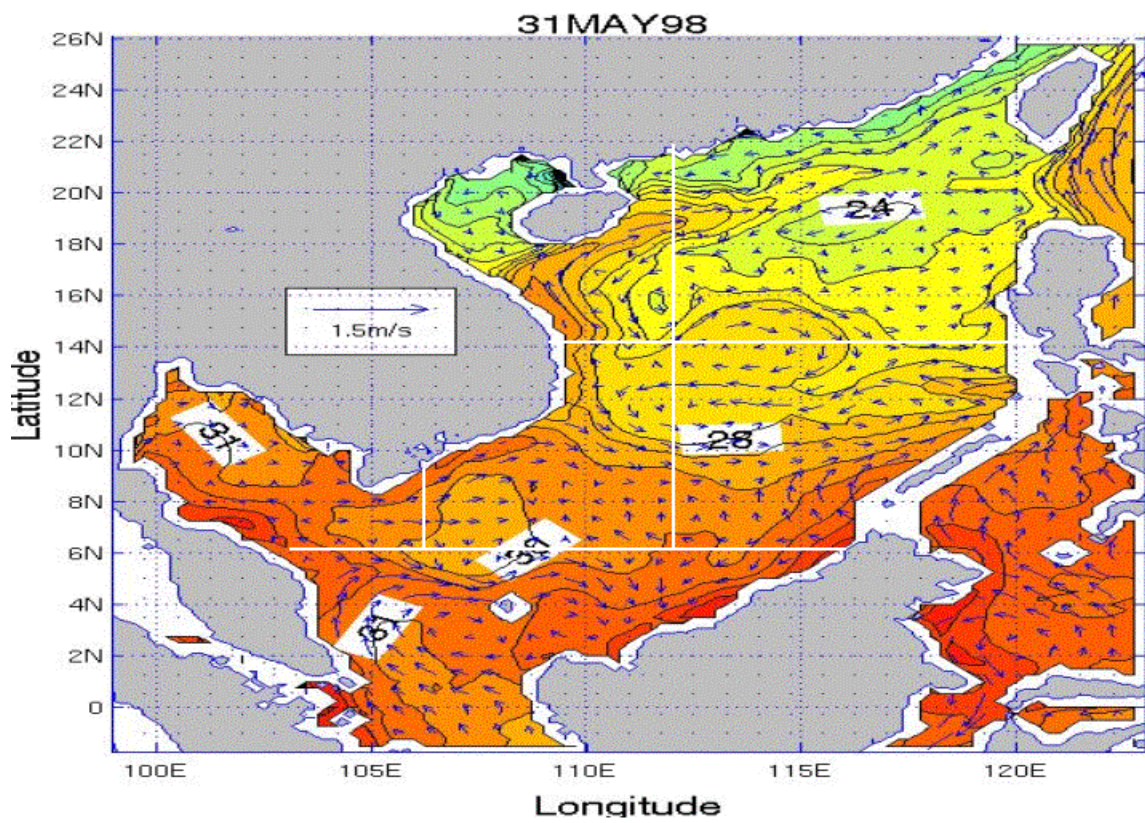
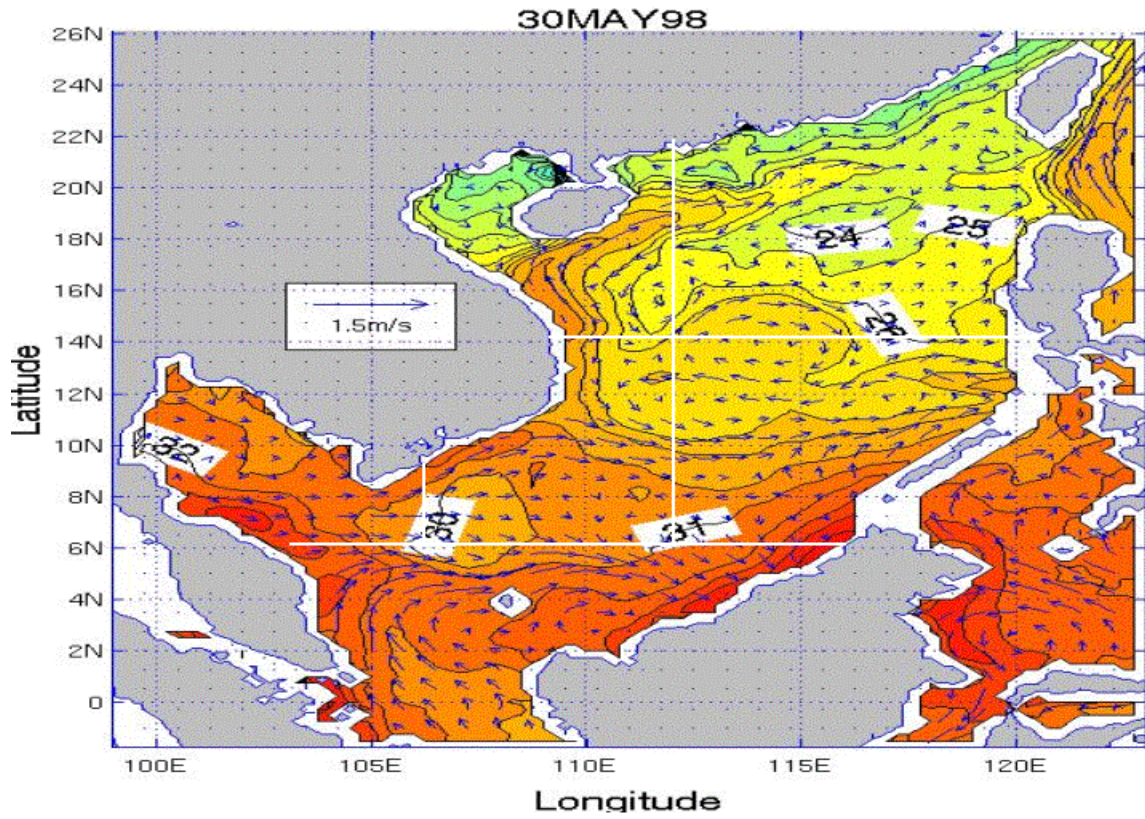






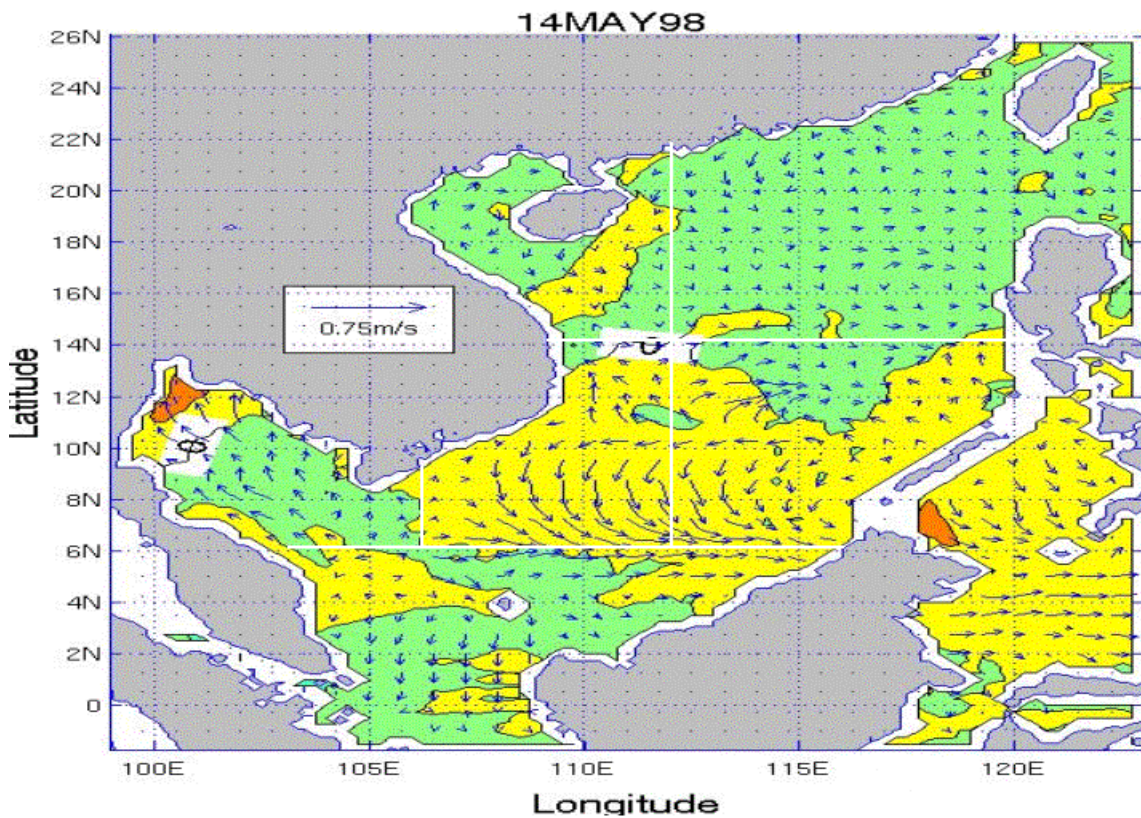


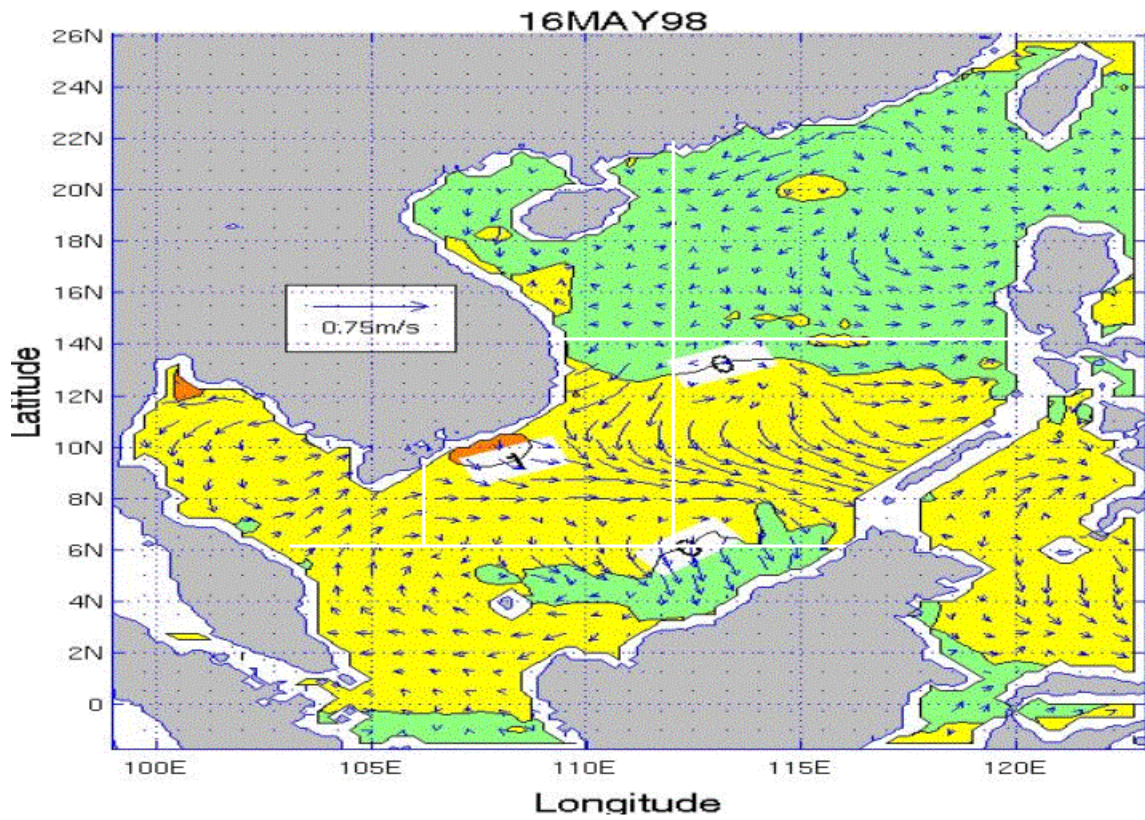
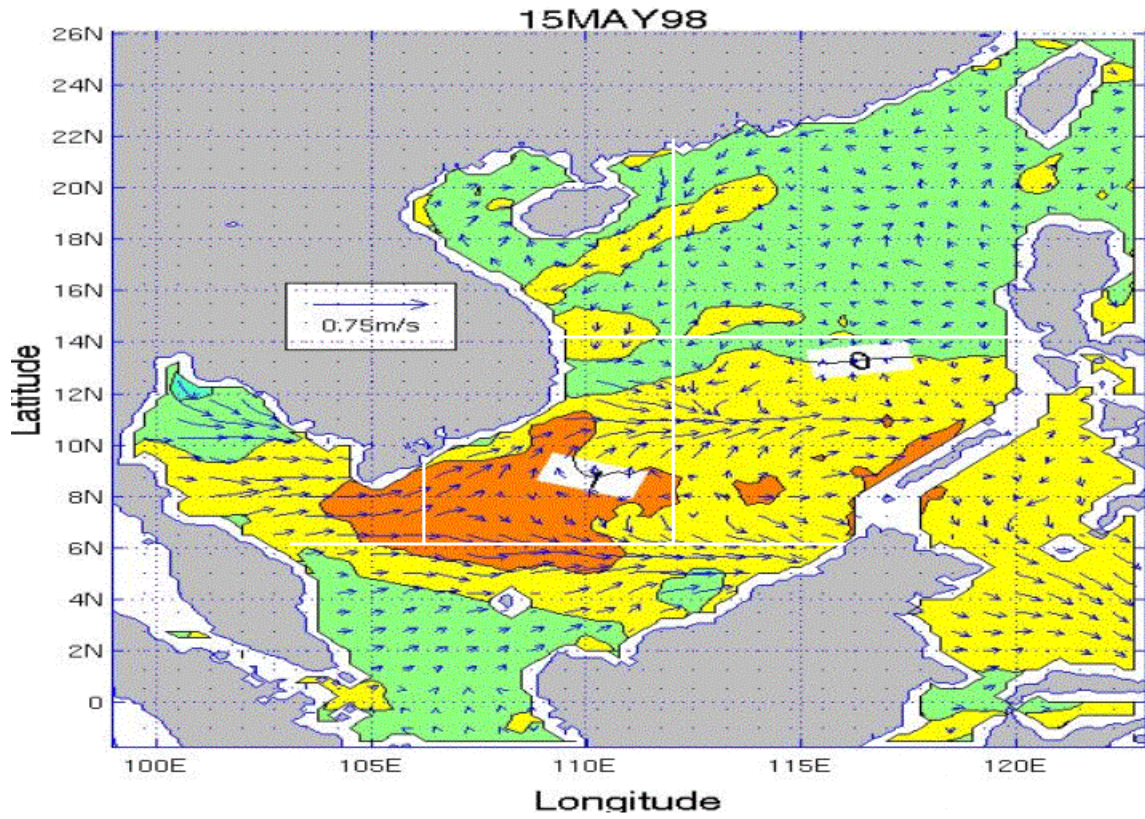


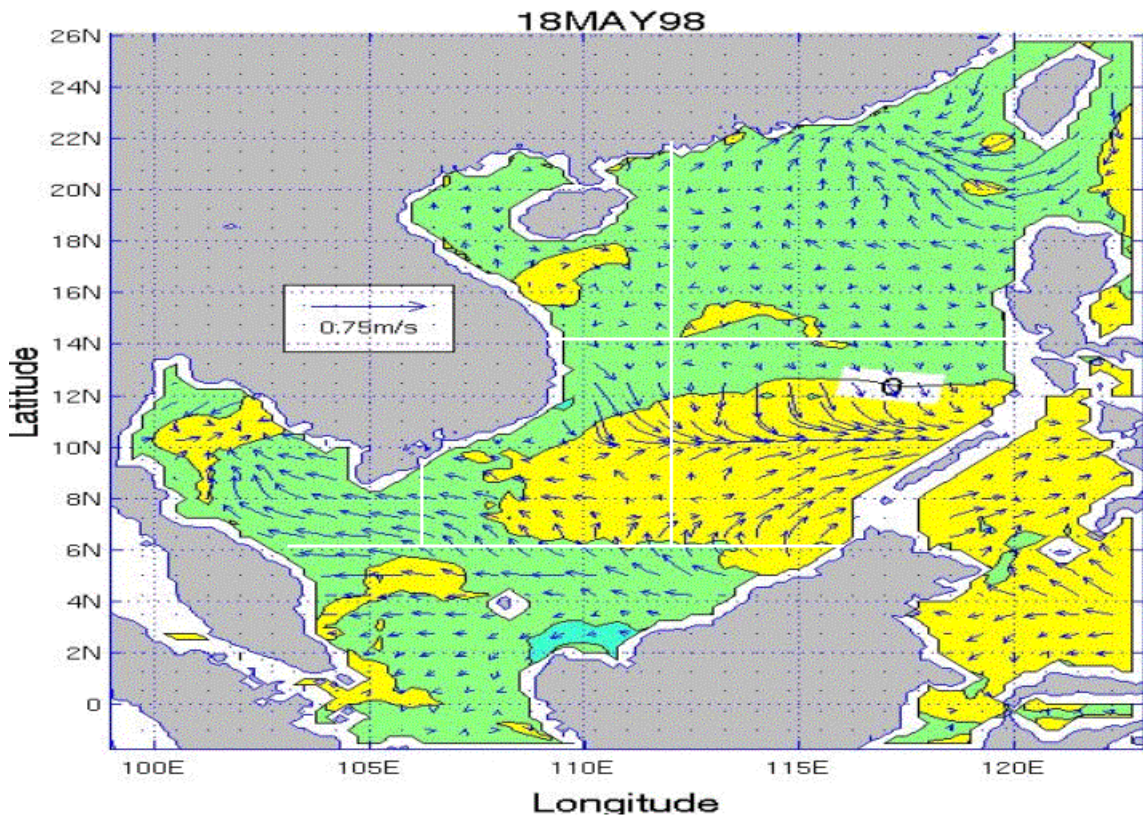
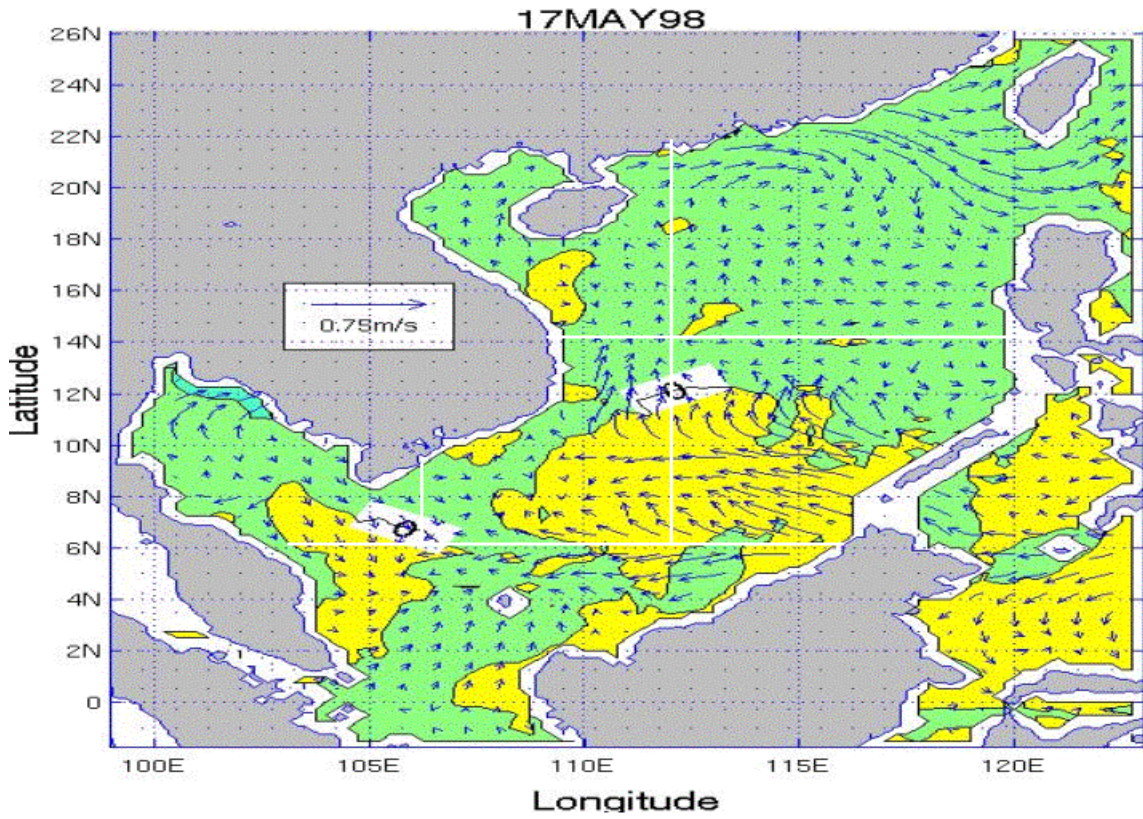


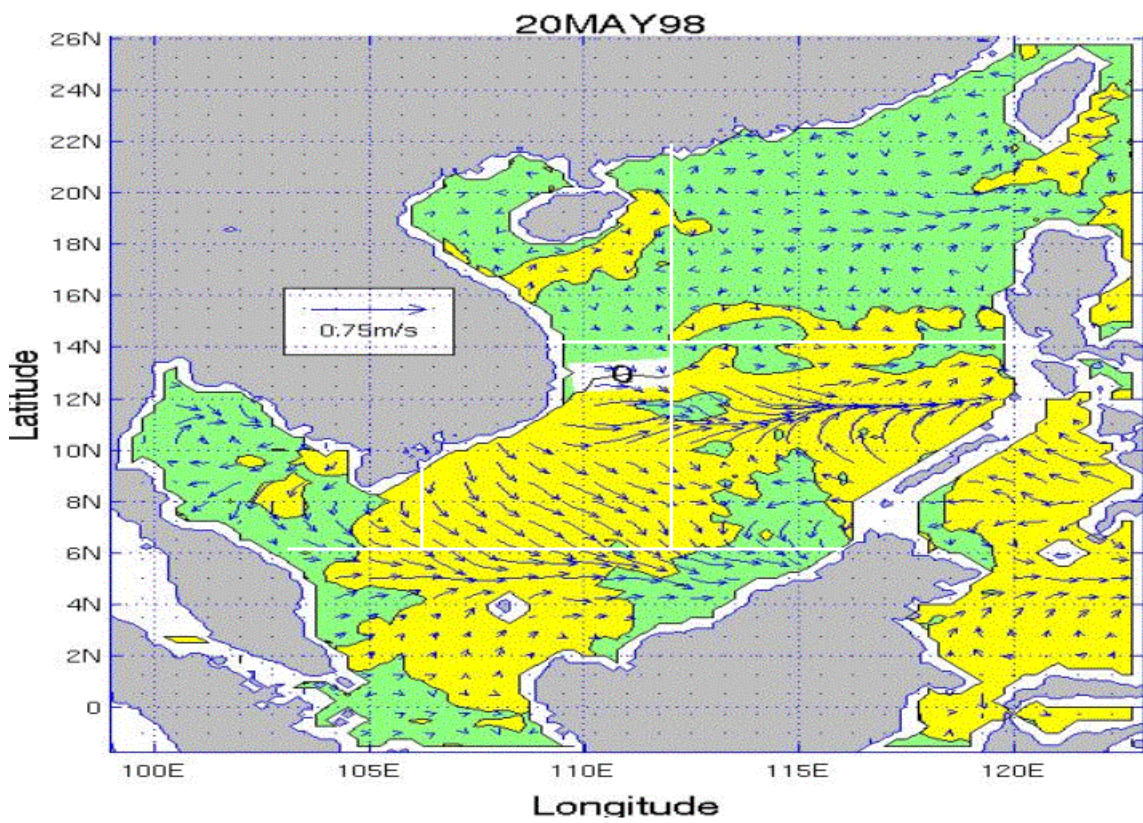
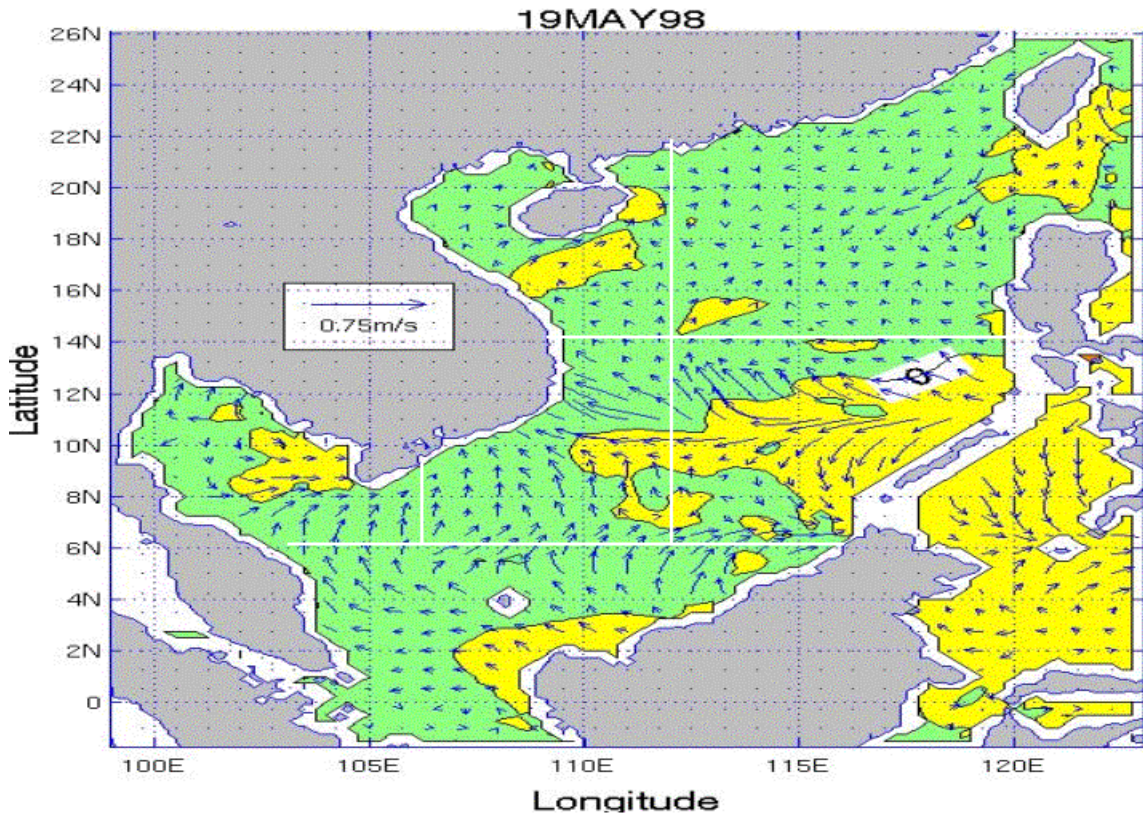
APPENDIX JJ. SST AND SURFACE CURRENT VELOCITY TENDENCY PLOTS FOR THE SCS FOR THE MAY TIME PERIOD

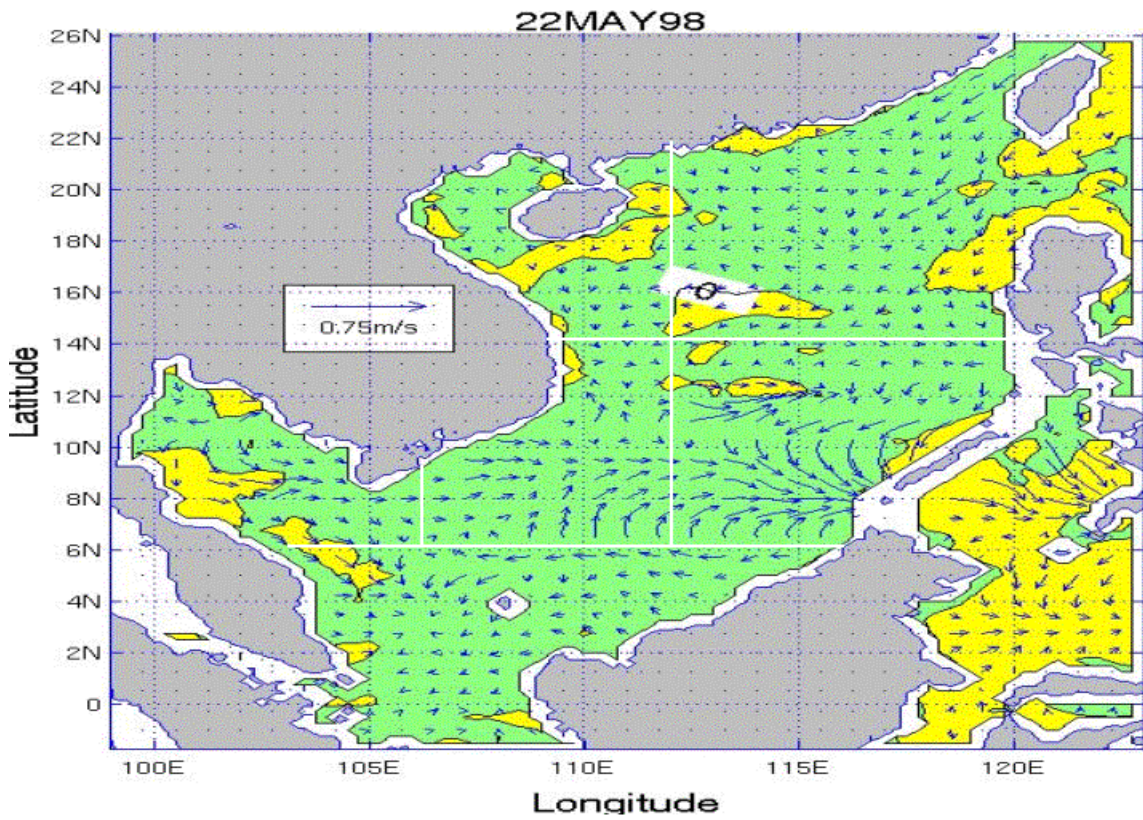
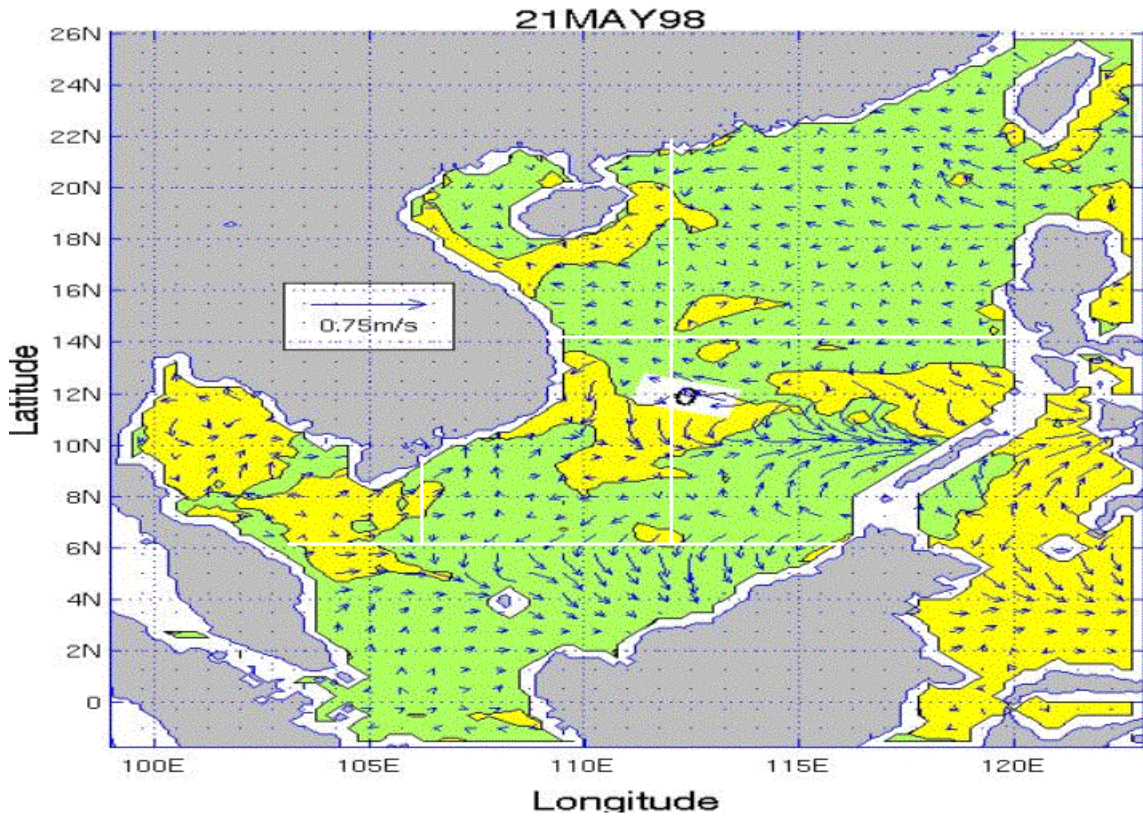
Appendix JJ consists of 18 figures that show SST and surface current velocity day-to-day tendency for the May time period over the SCS. The figures are in time sequential order from May 14 through May 31. Each plot represents the change between the previous day and the current day.

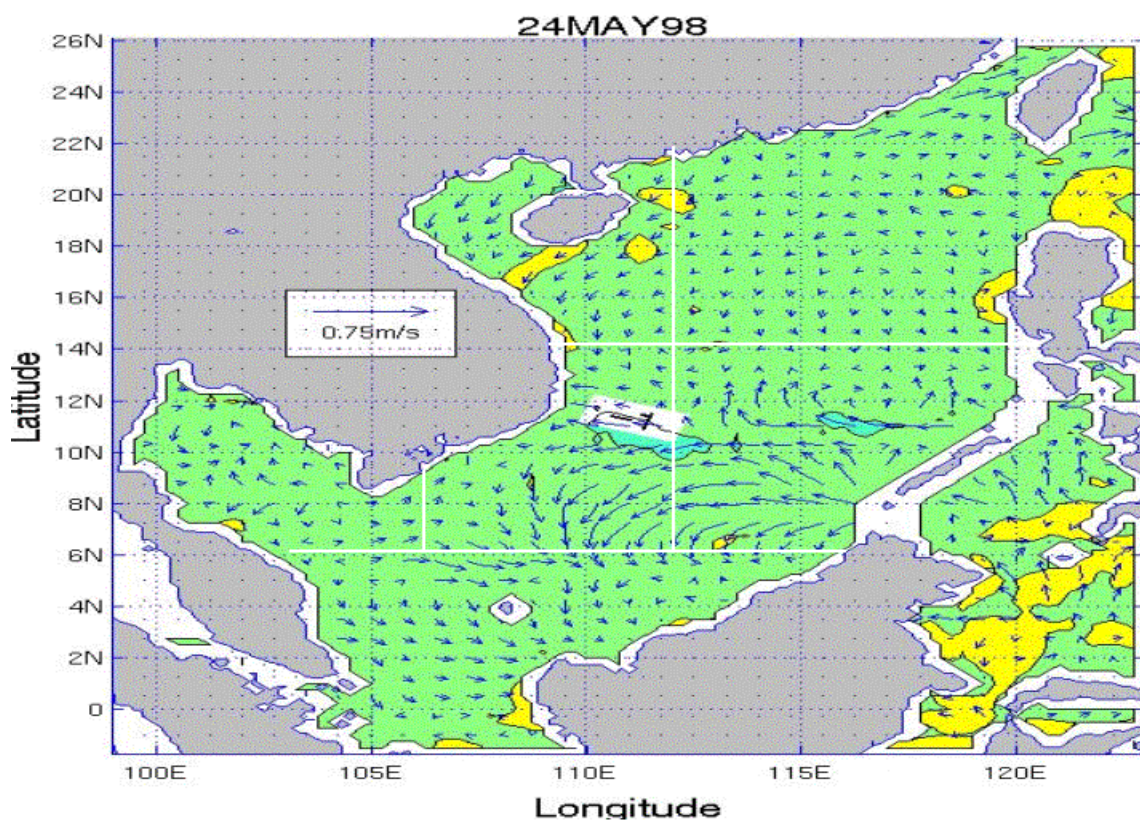
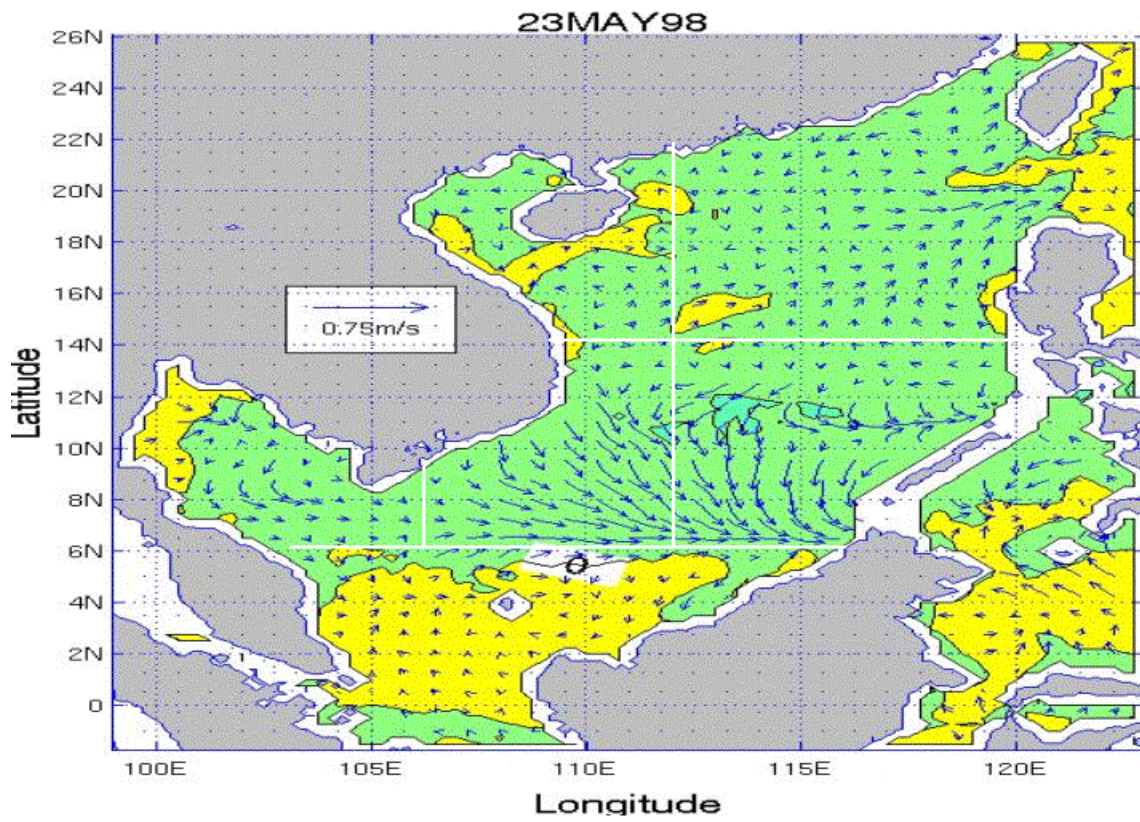


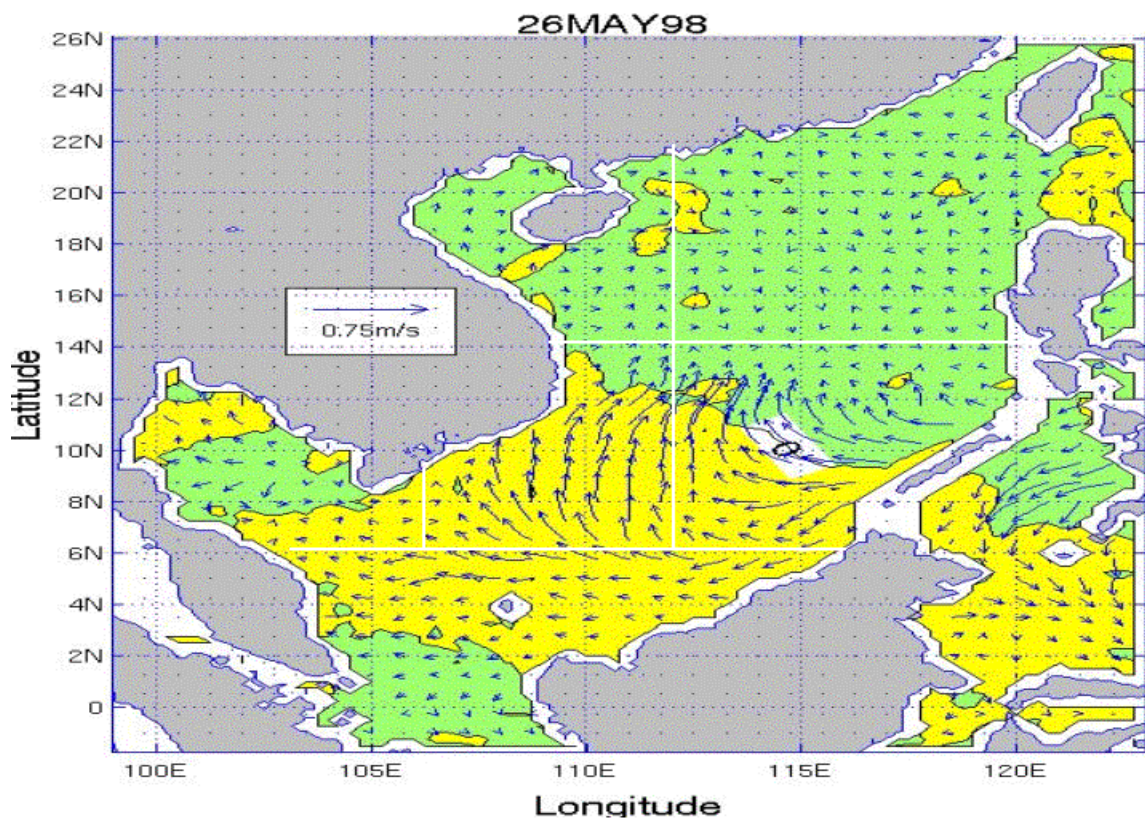
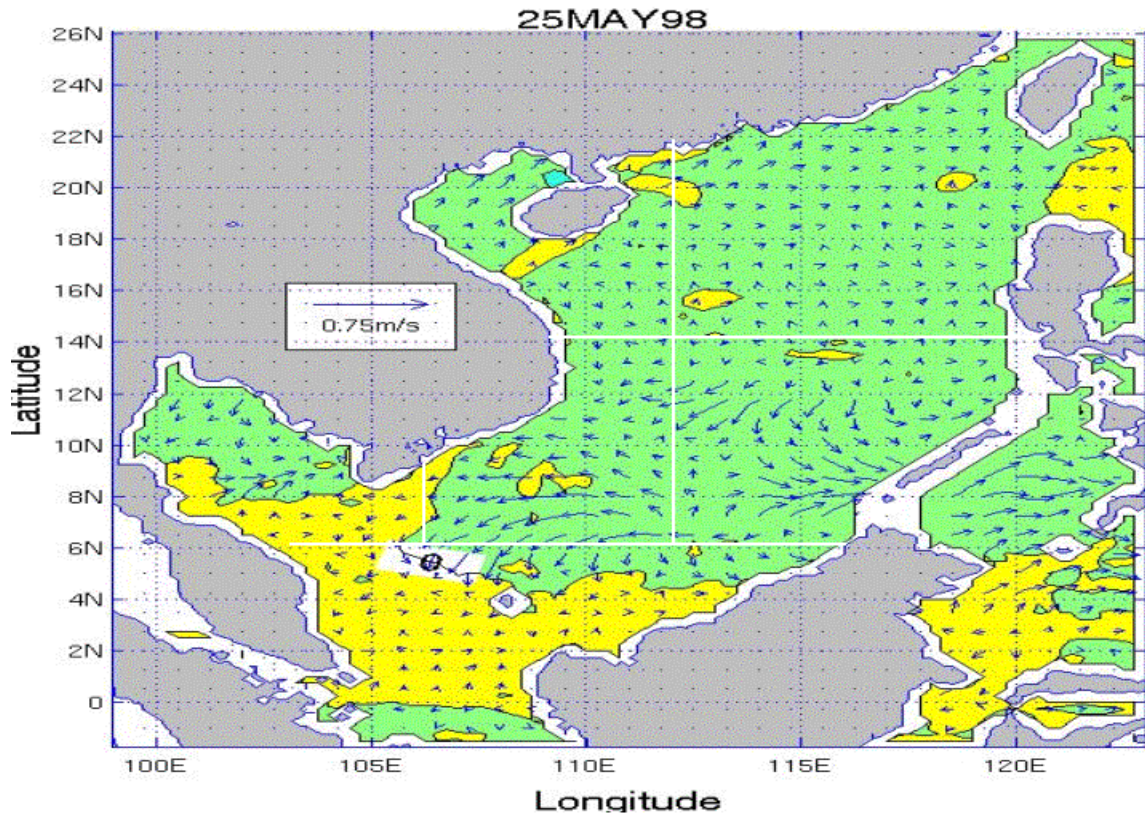


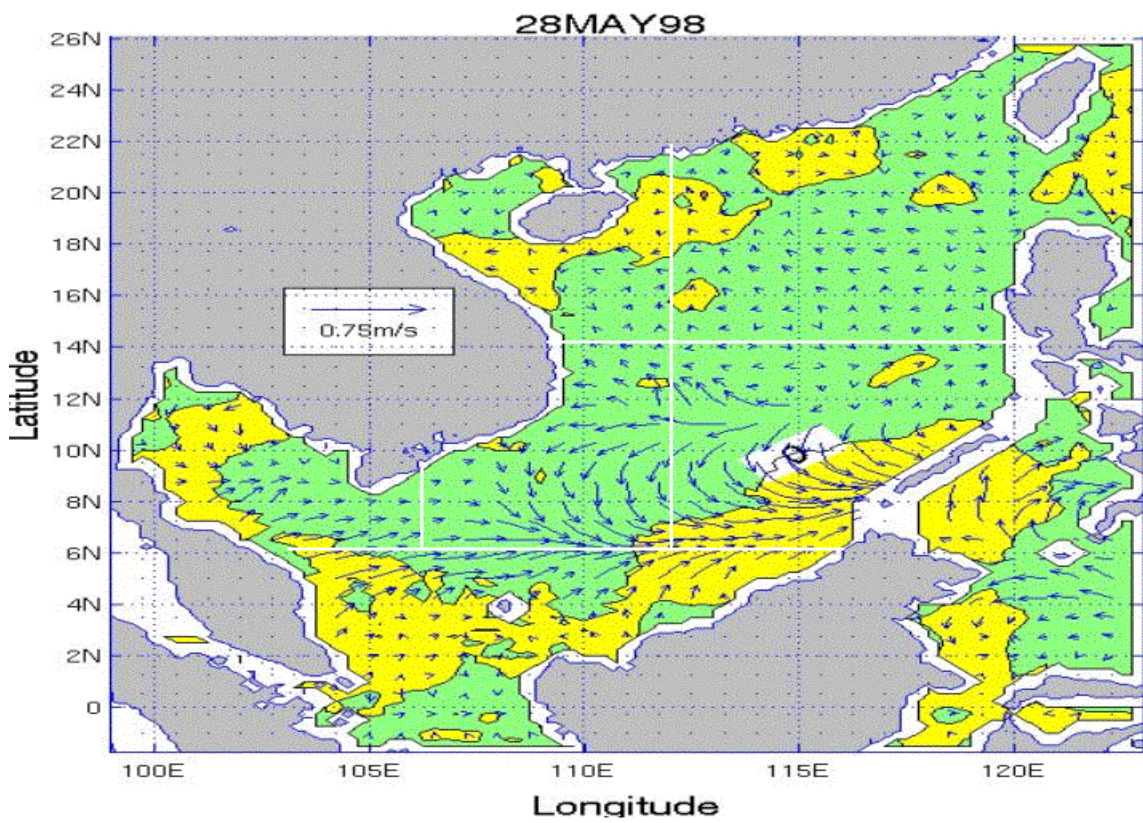
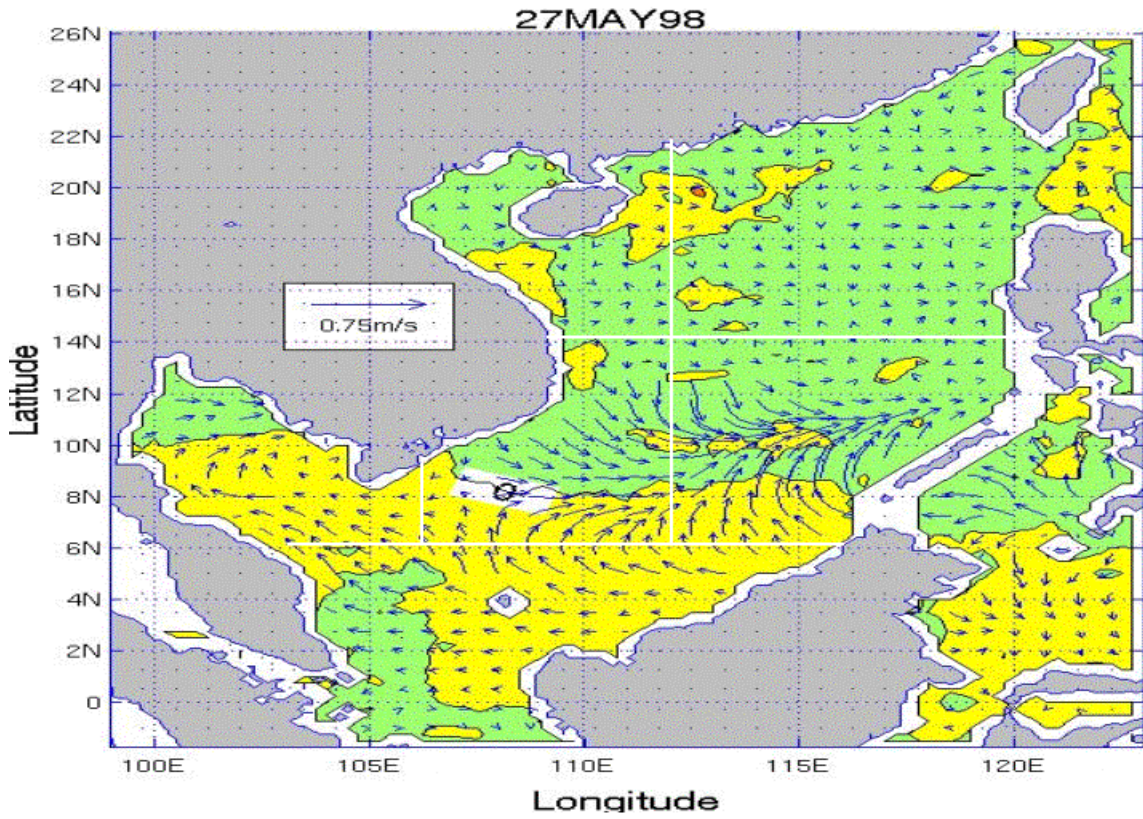


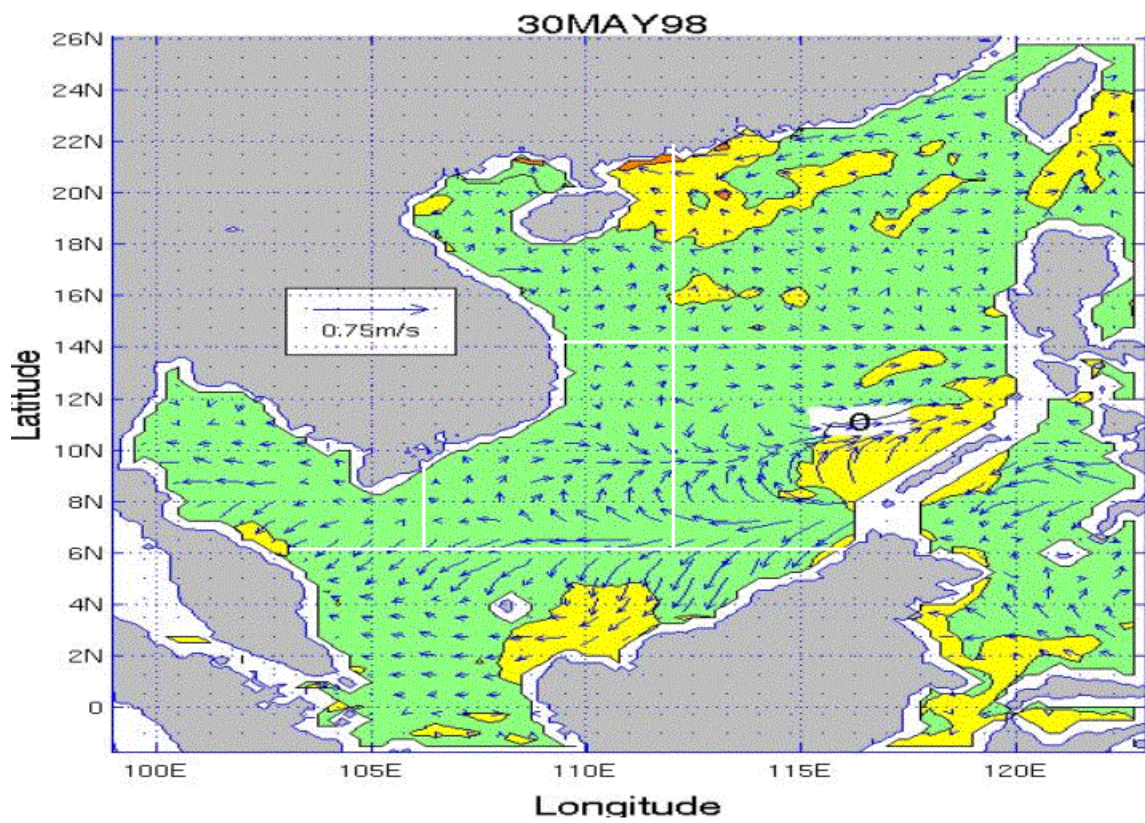
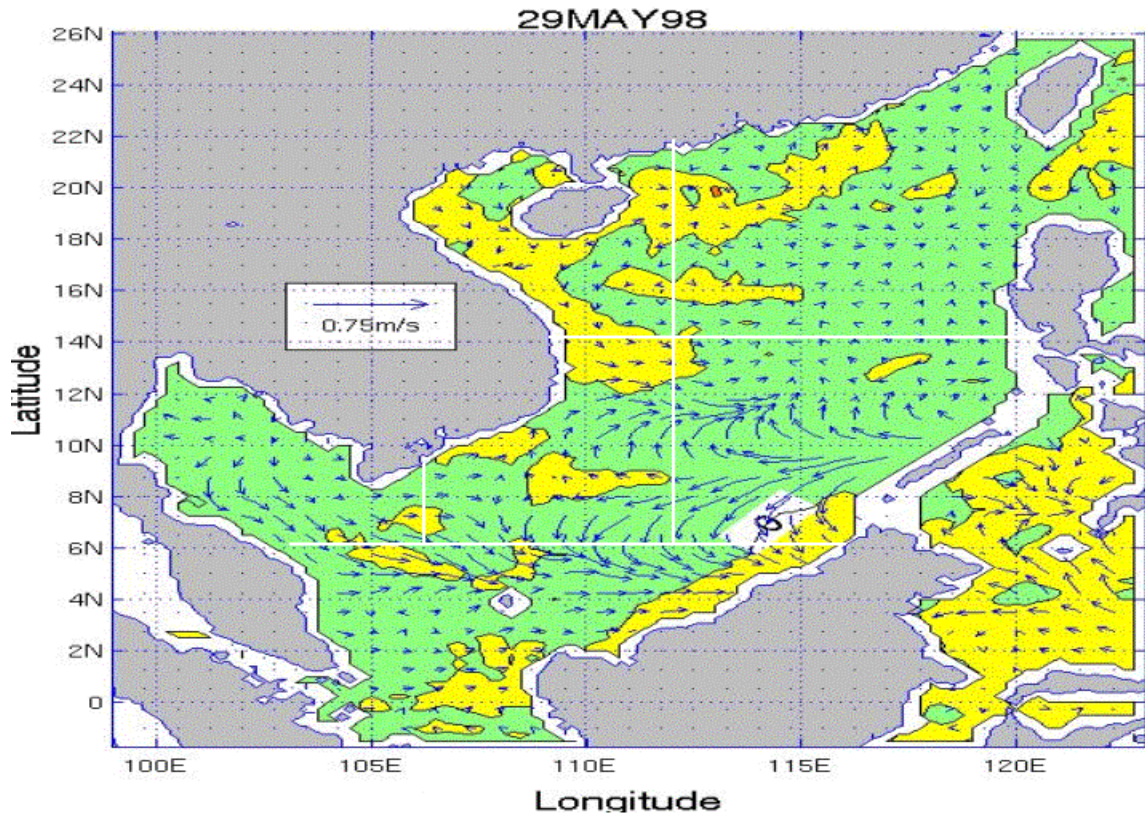


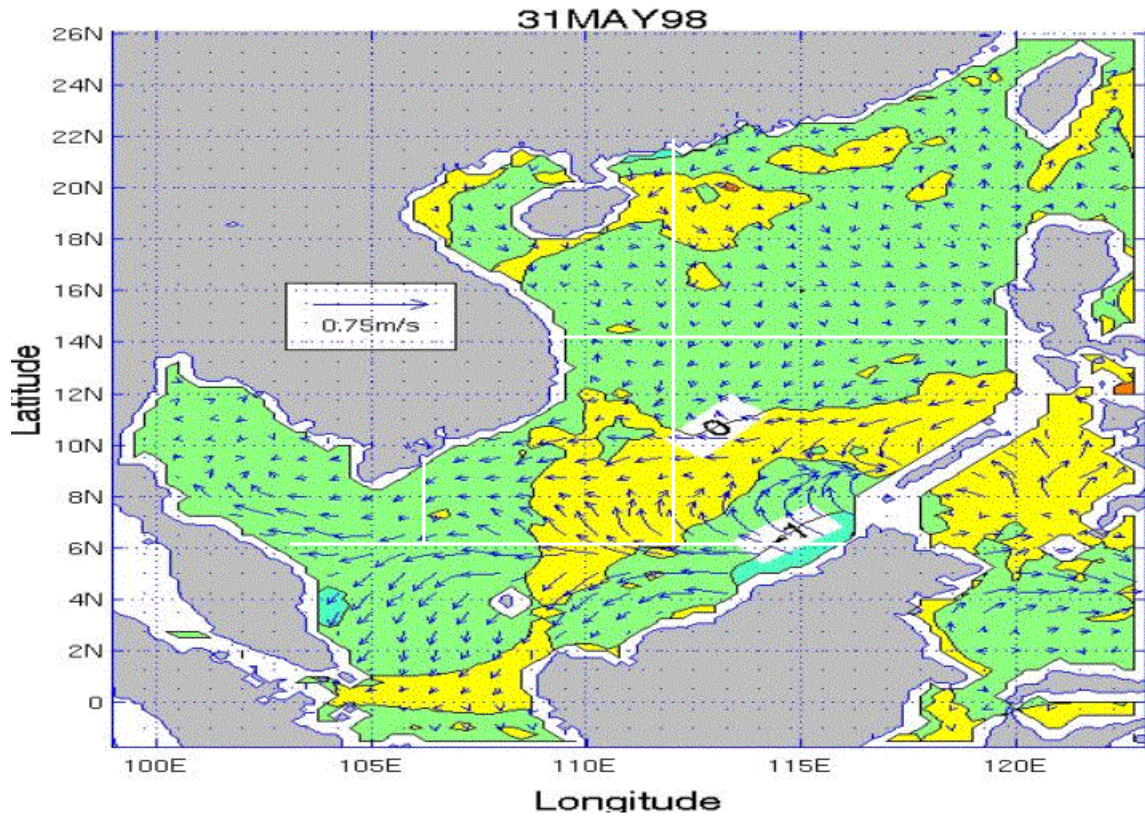






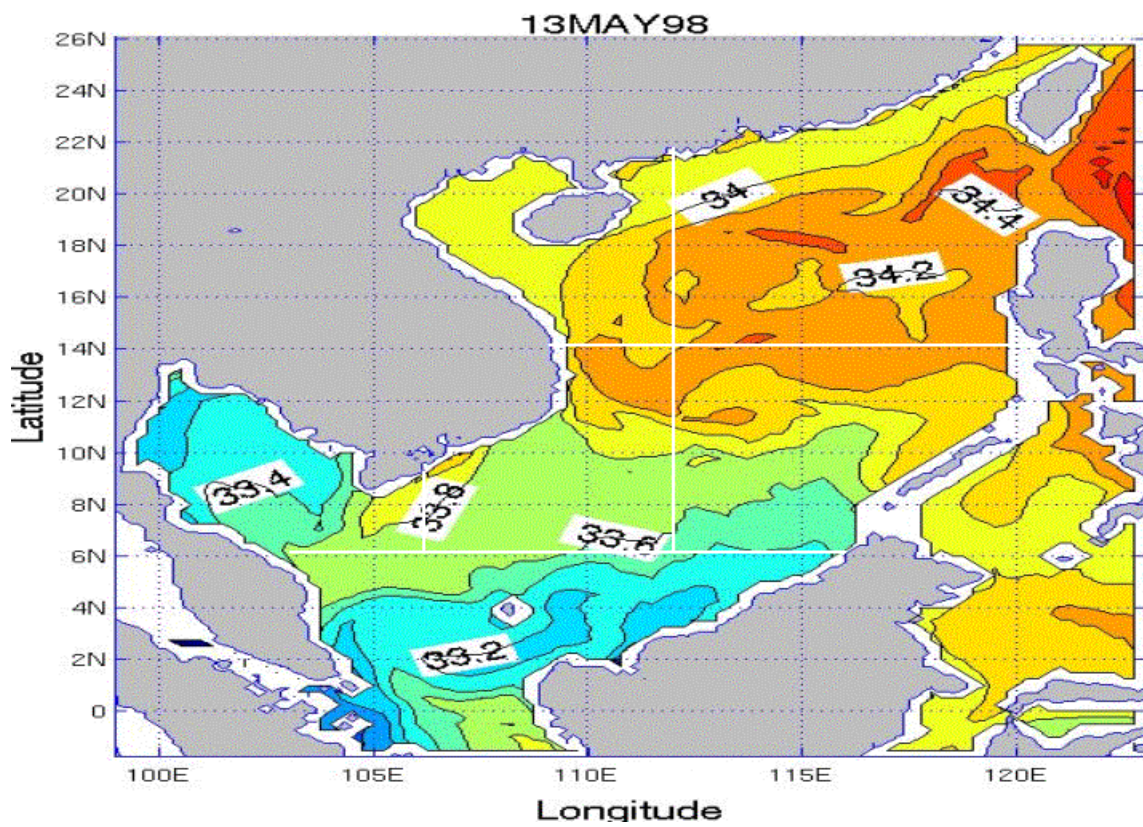


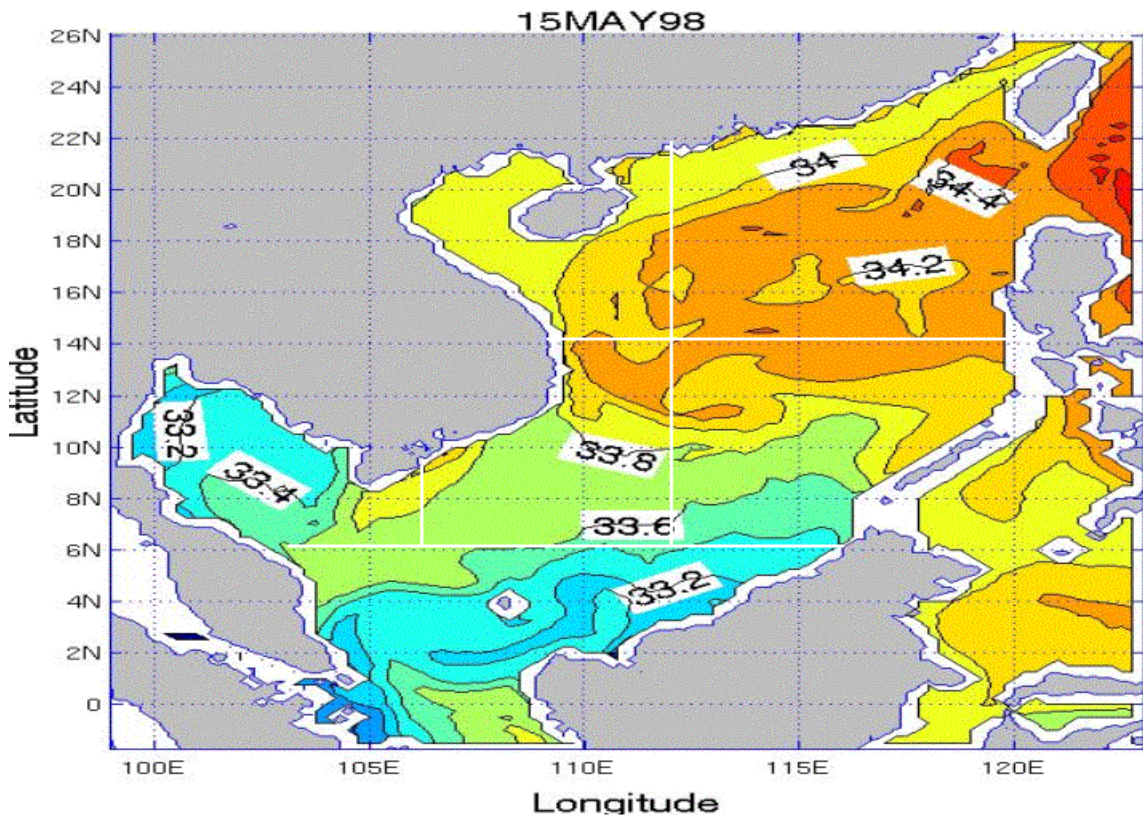
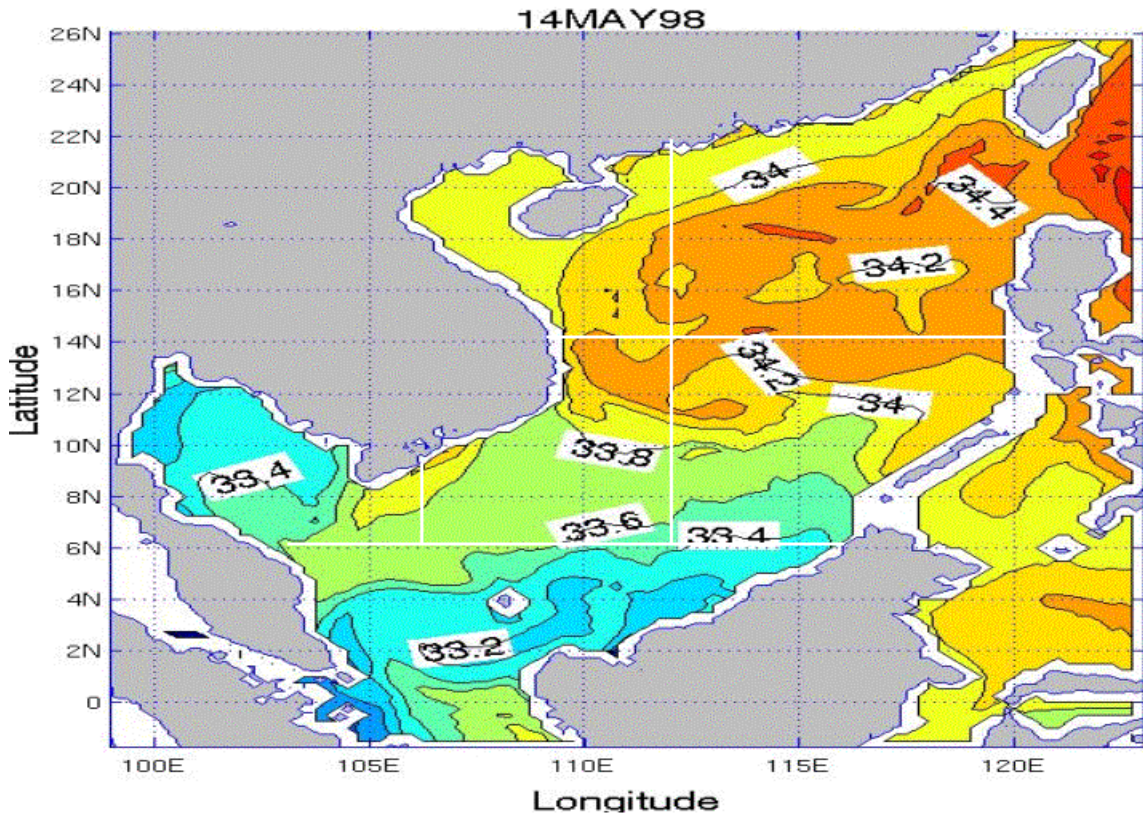


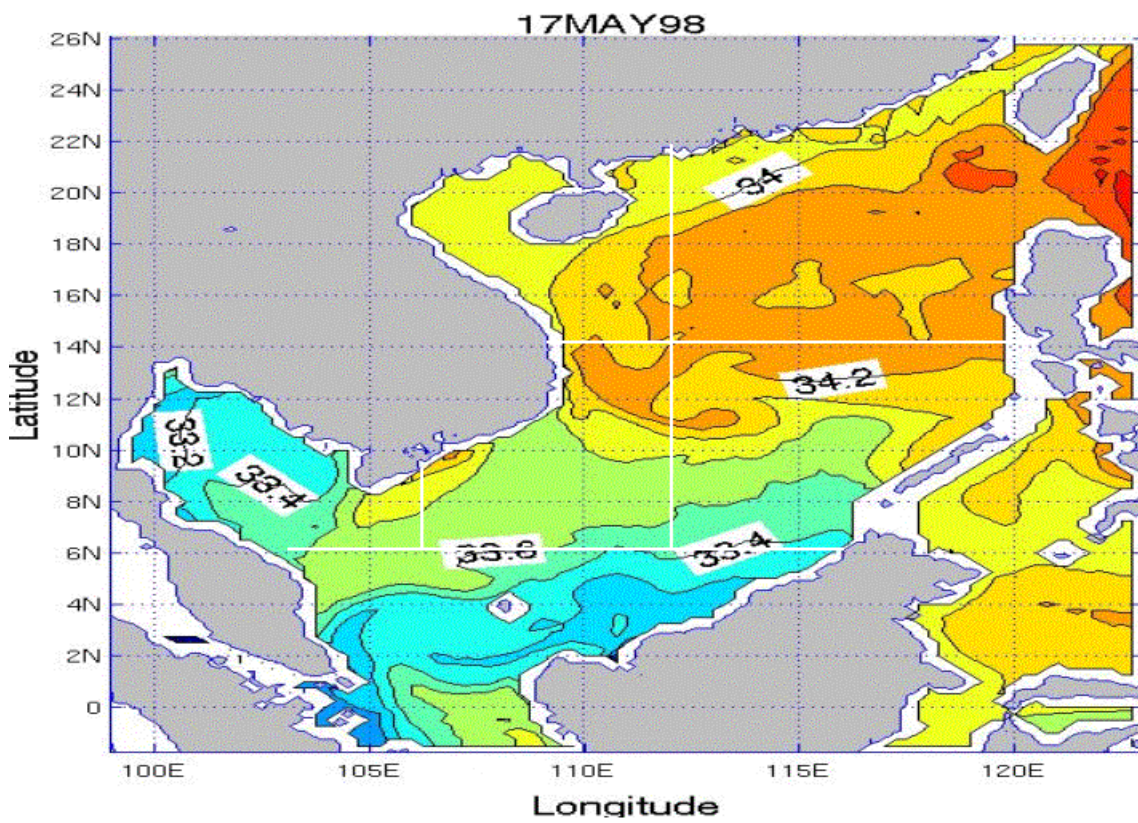
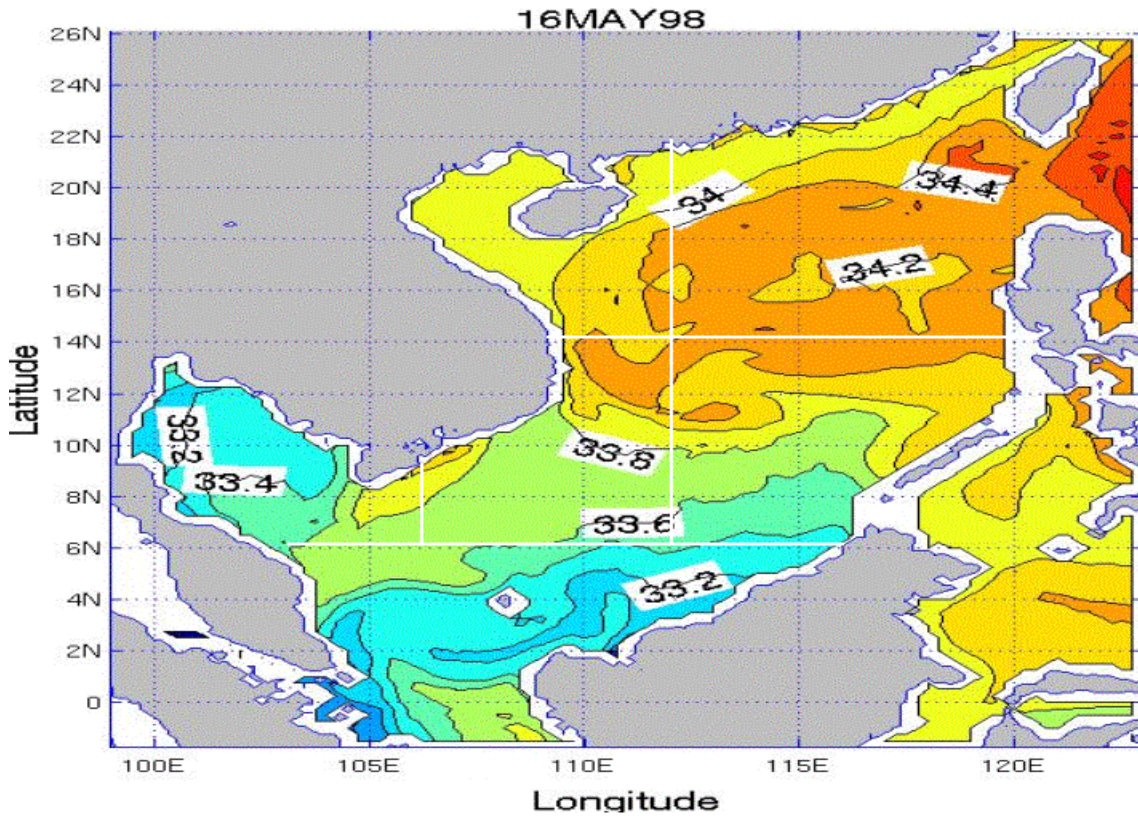


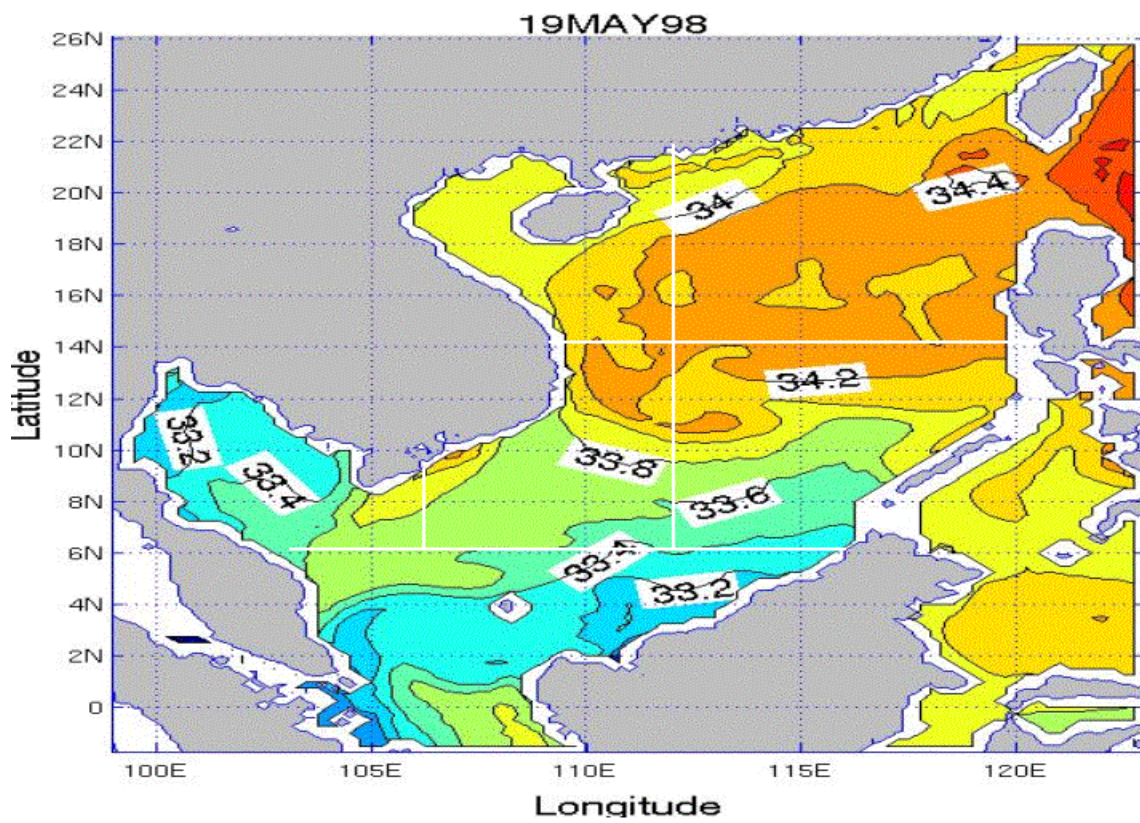
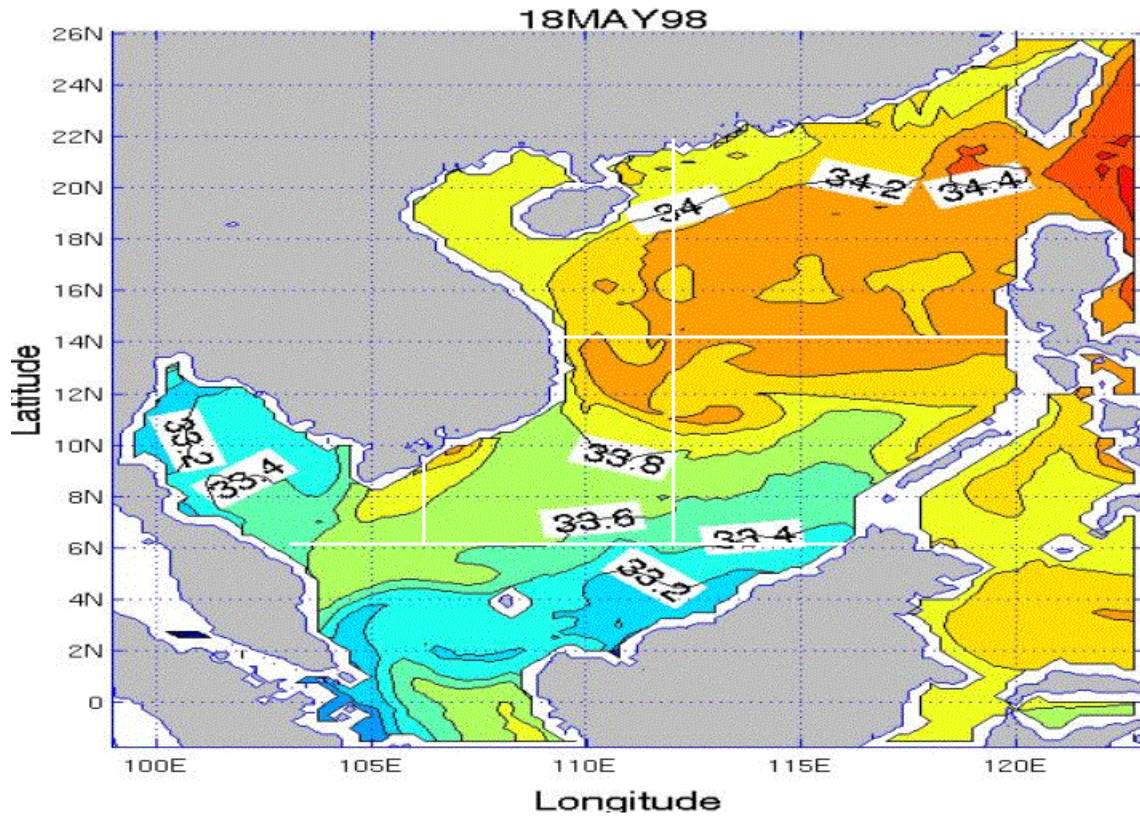
APPENDIX KK. SSS PLOTS FOR THE SCS FOR THE MAY TIME PERIOD

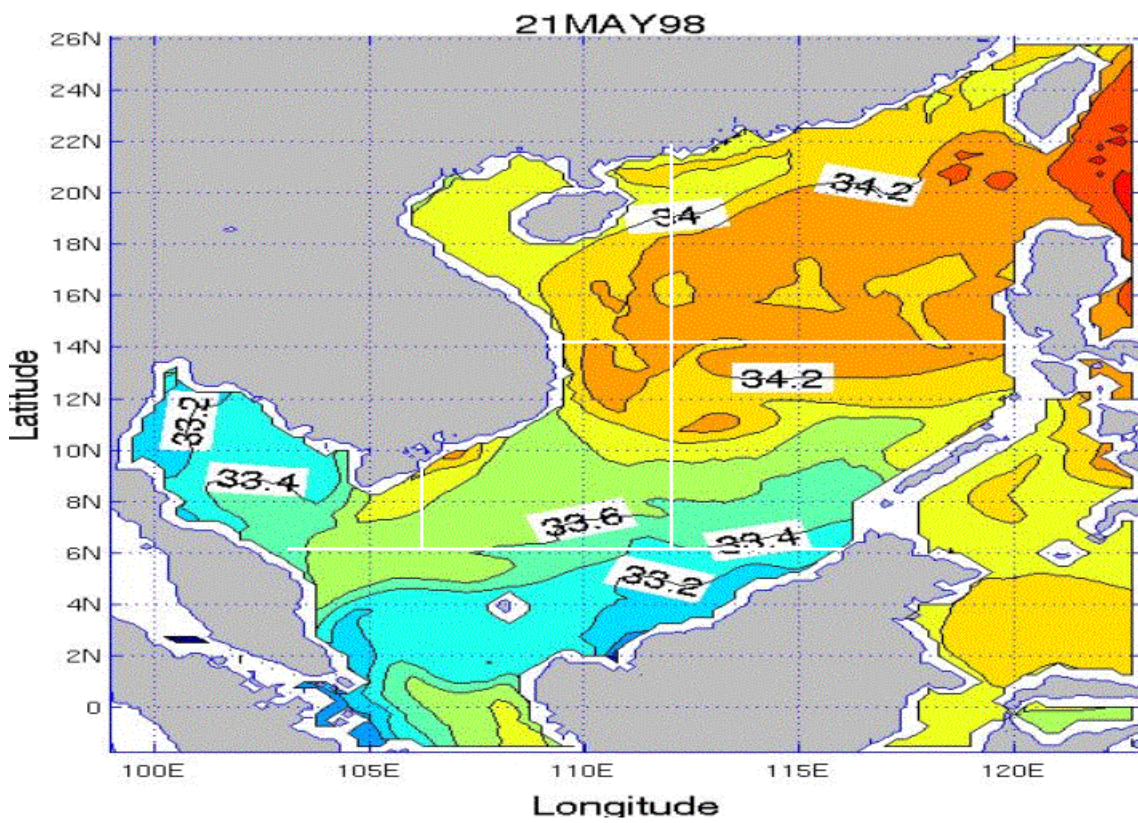
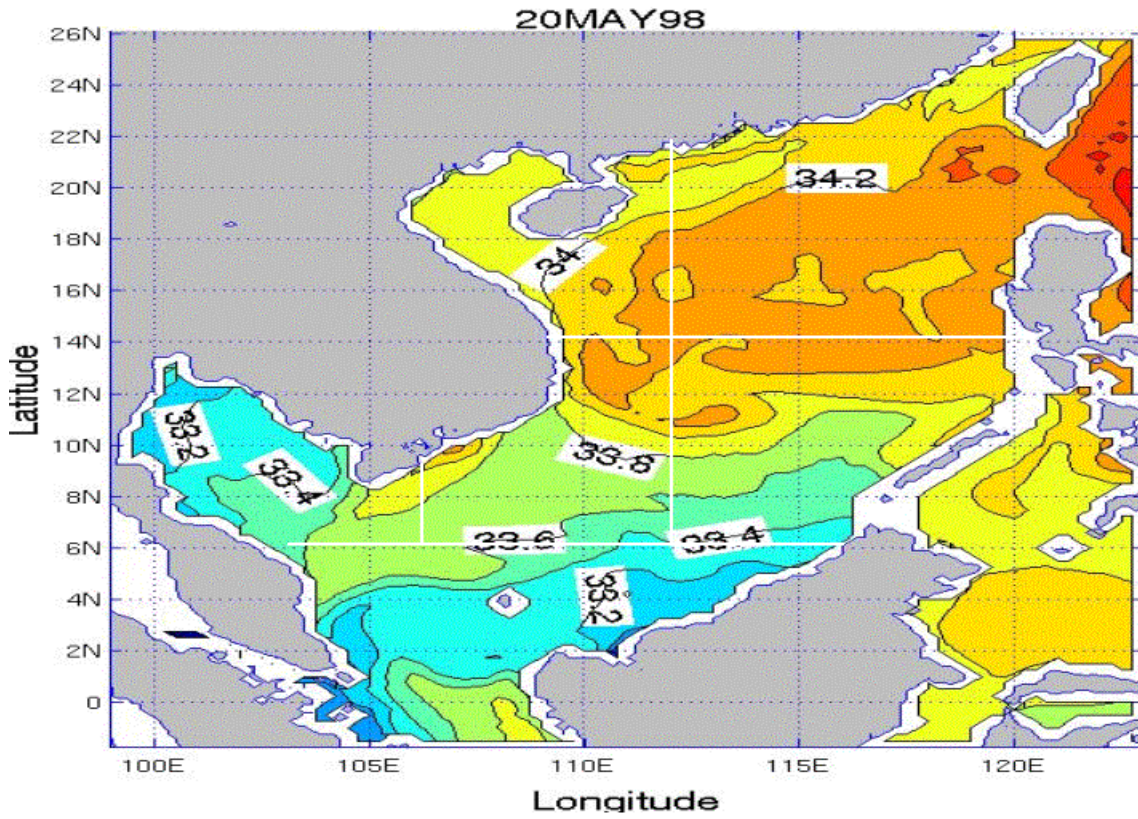
Appendix KK consists of 19 figures that show SSS for each day of the May time period for the SCS. The figures are in time sequential order from May 13 through May 31.

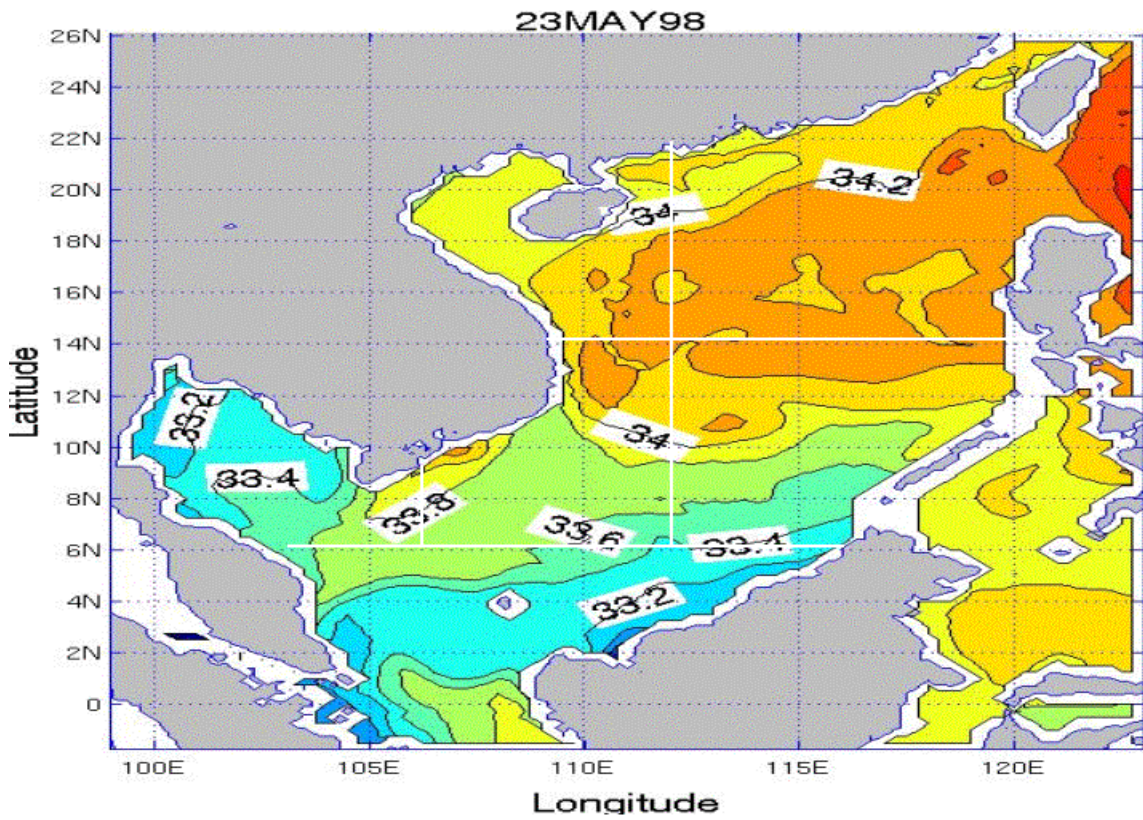
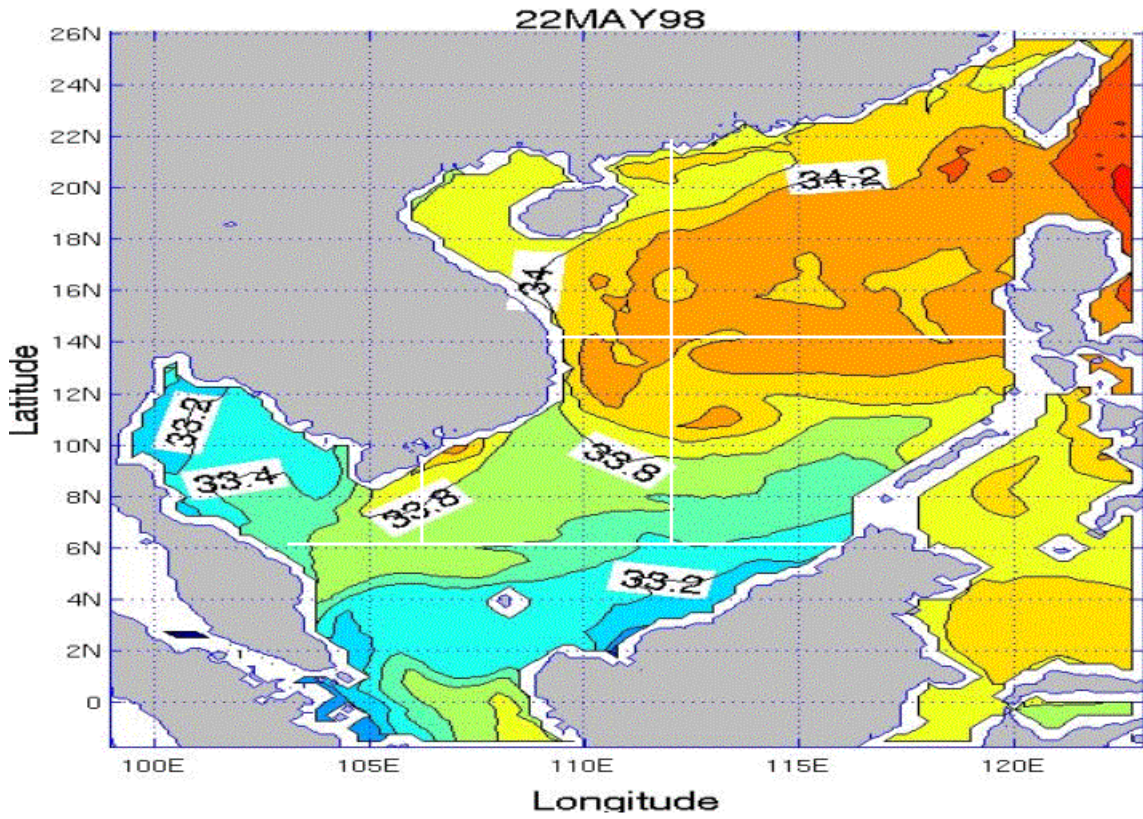


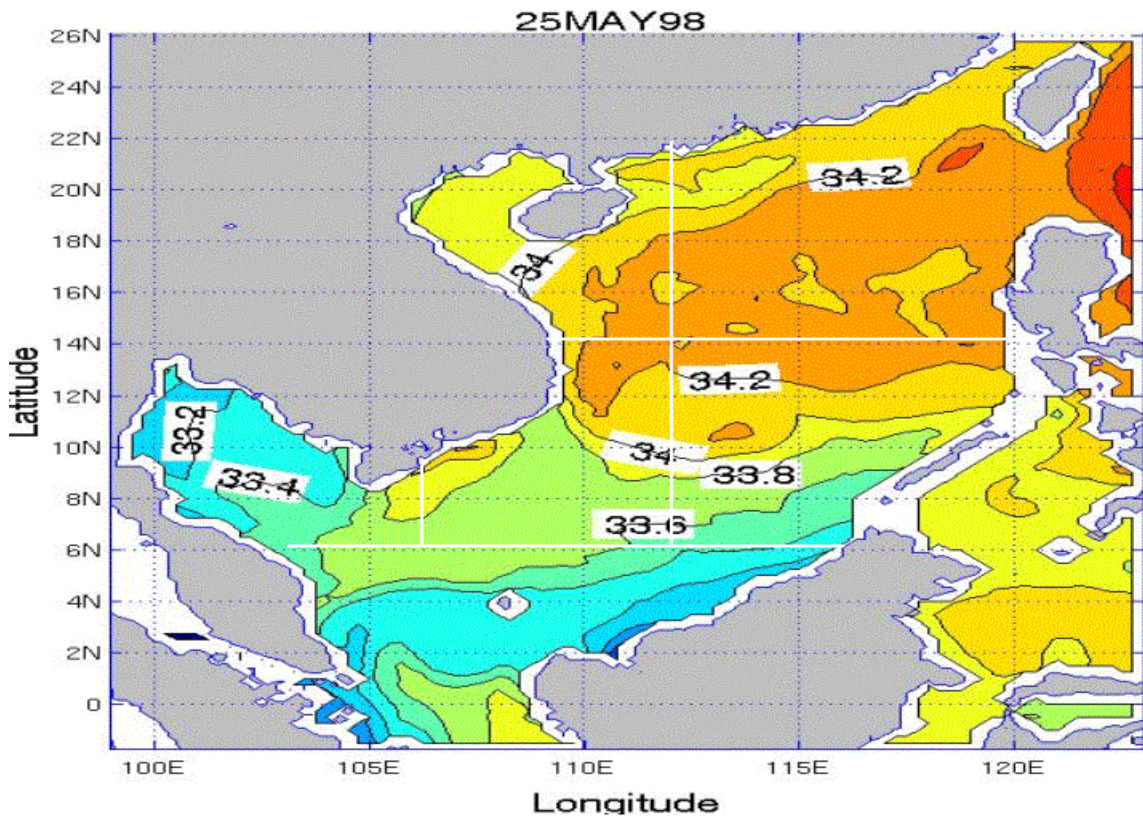
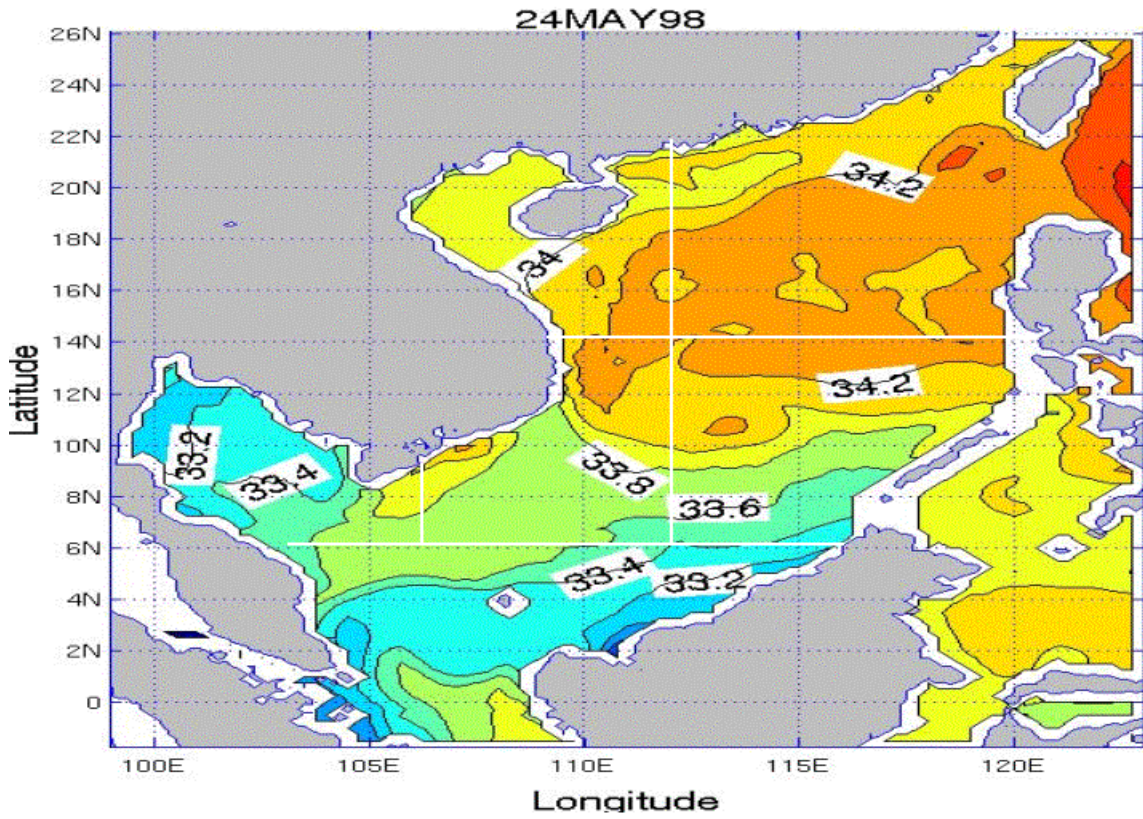


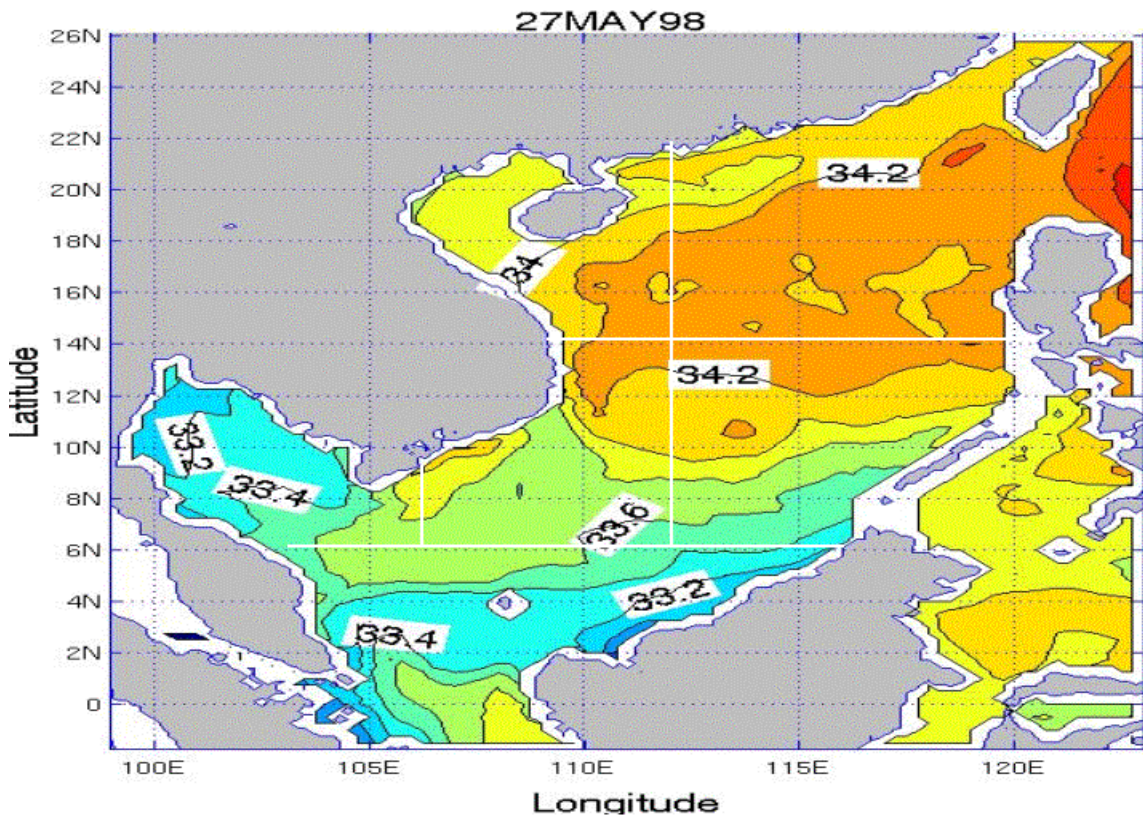
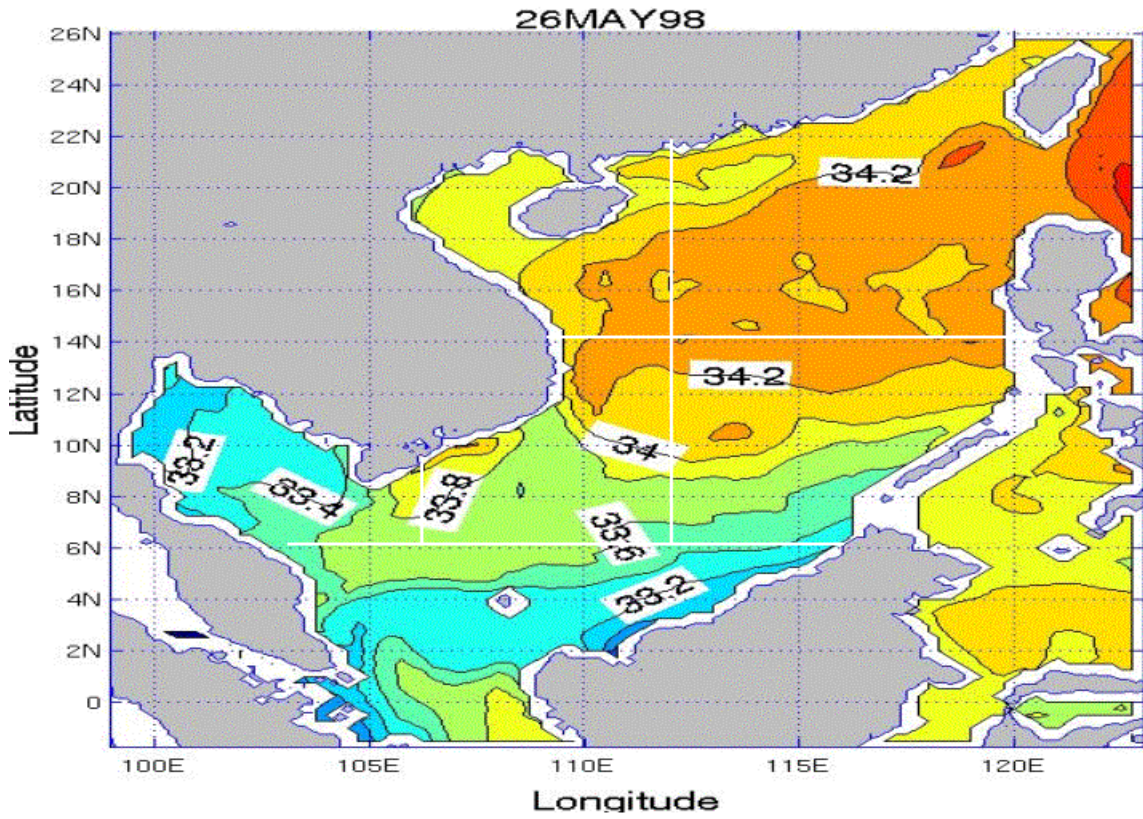


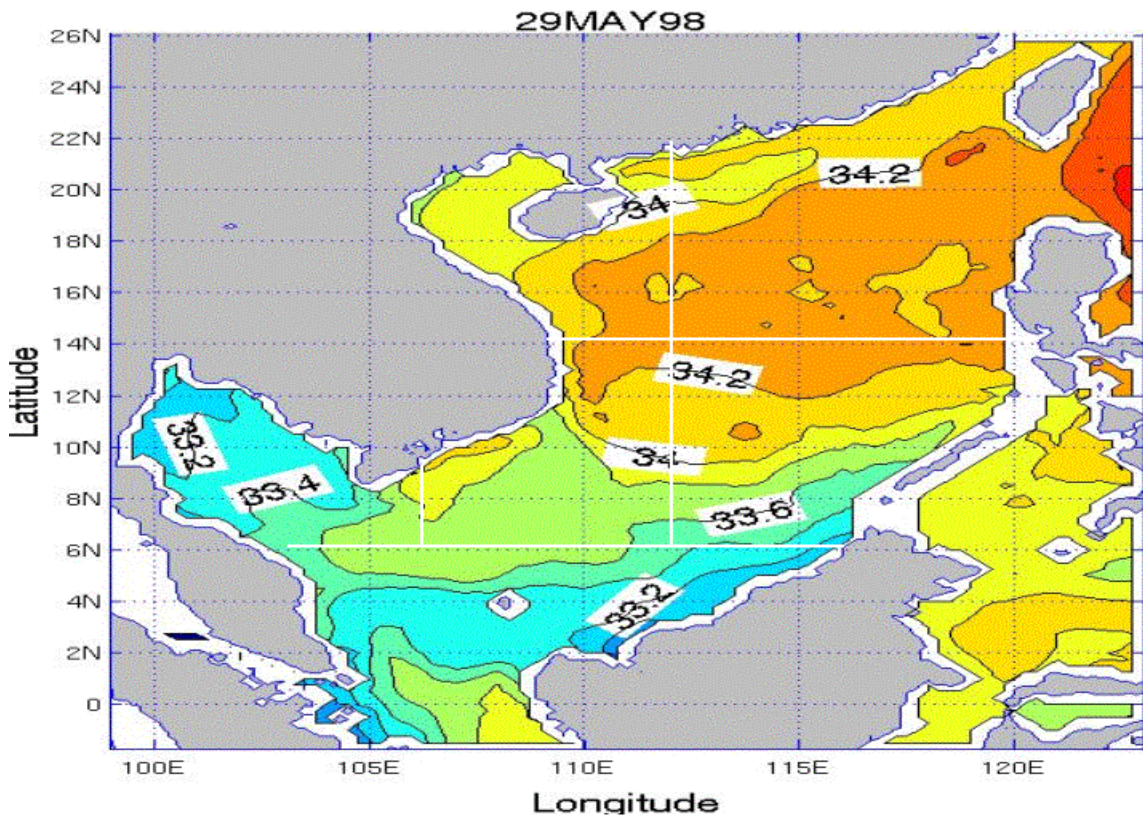
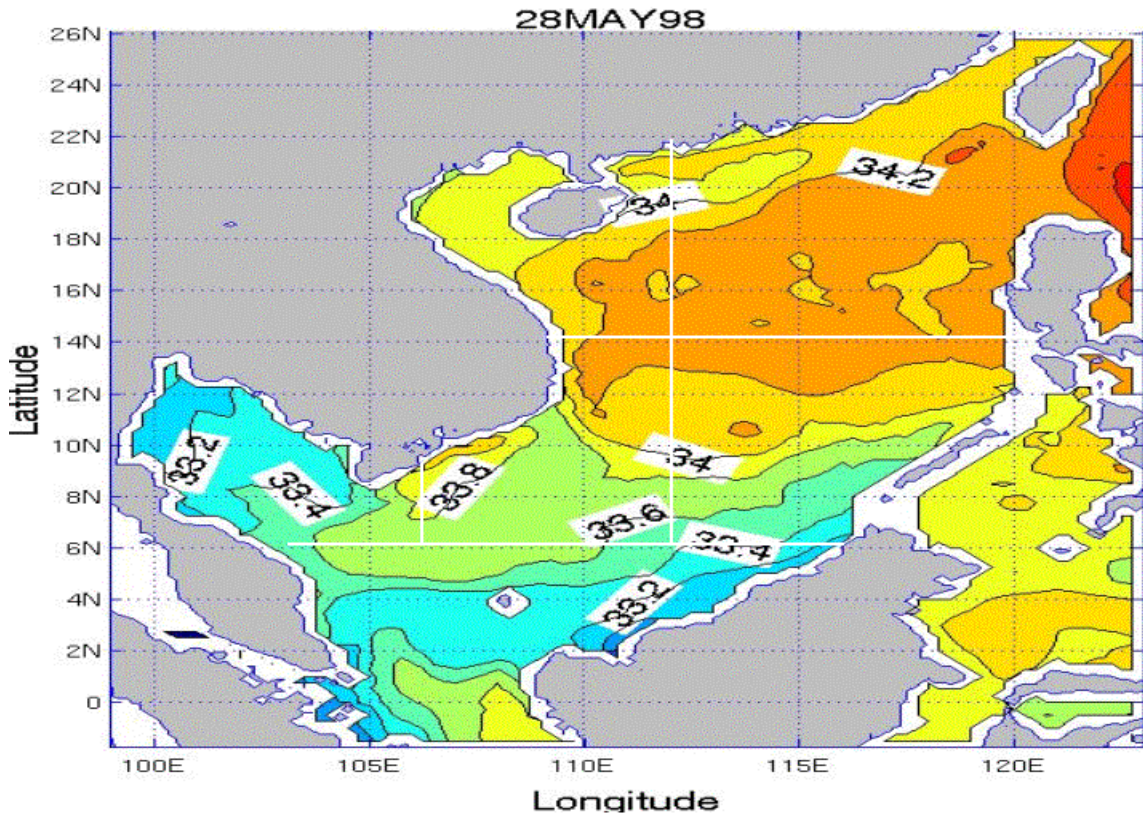


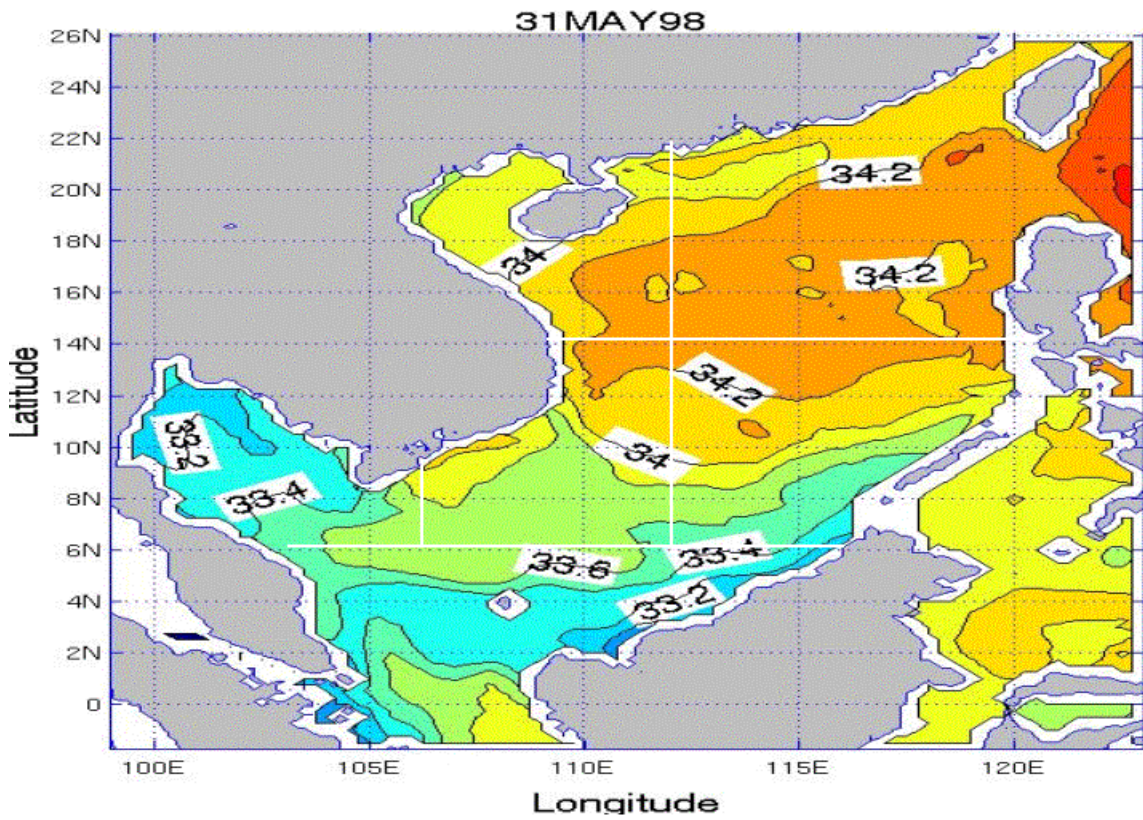
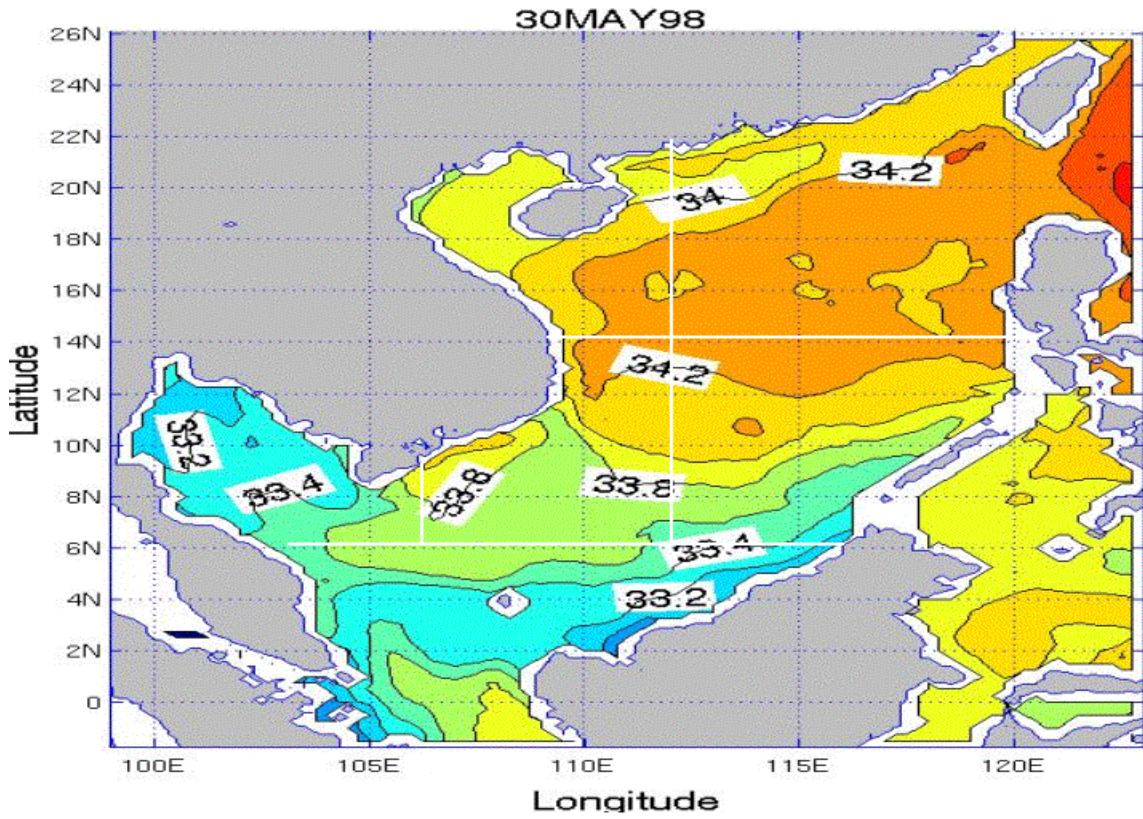






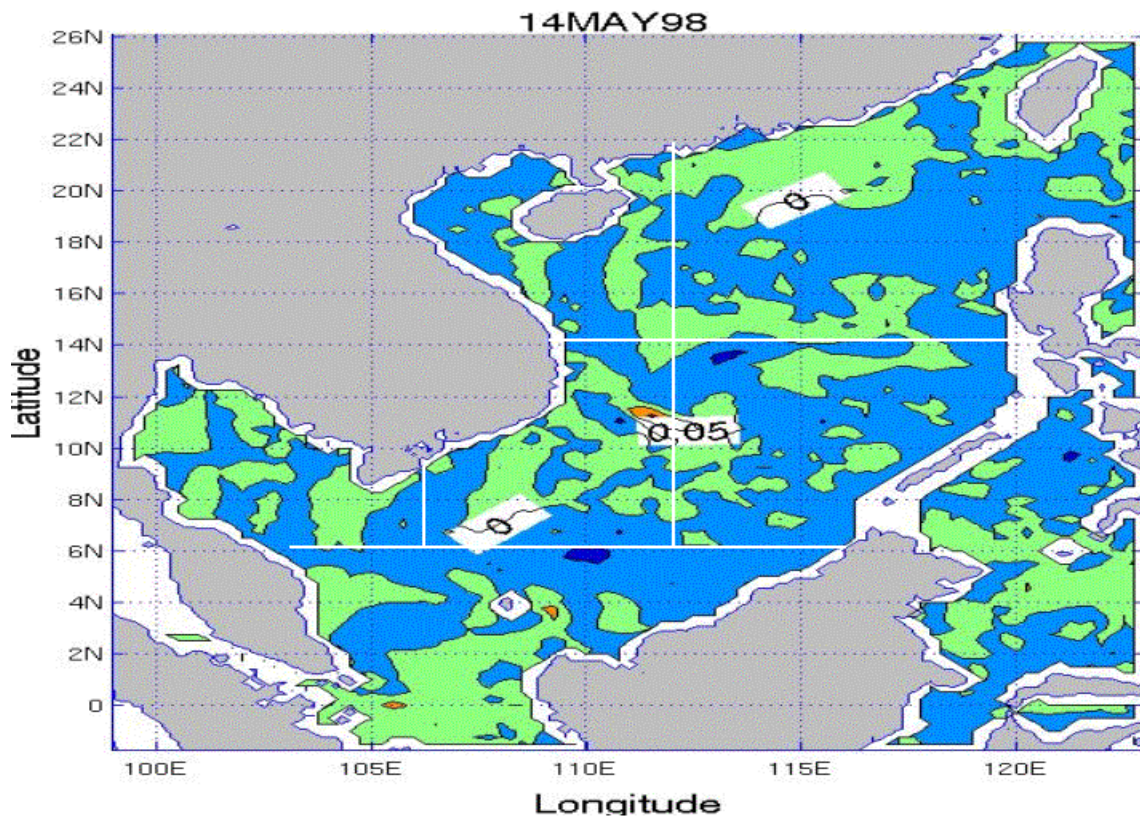


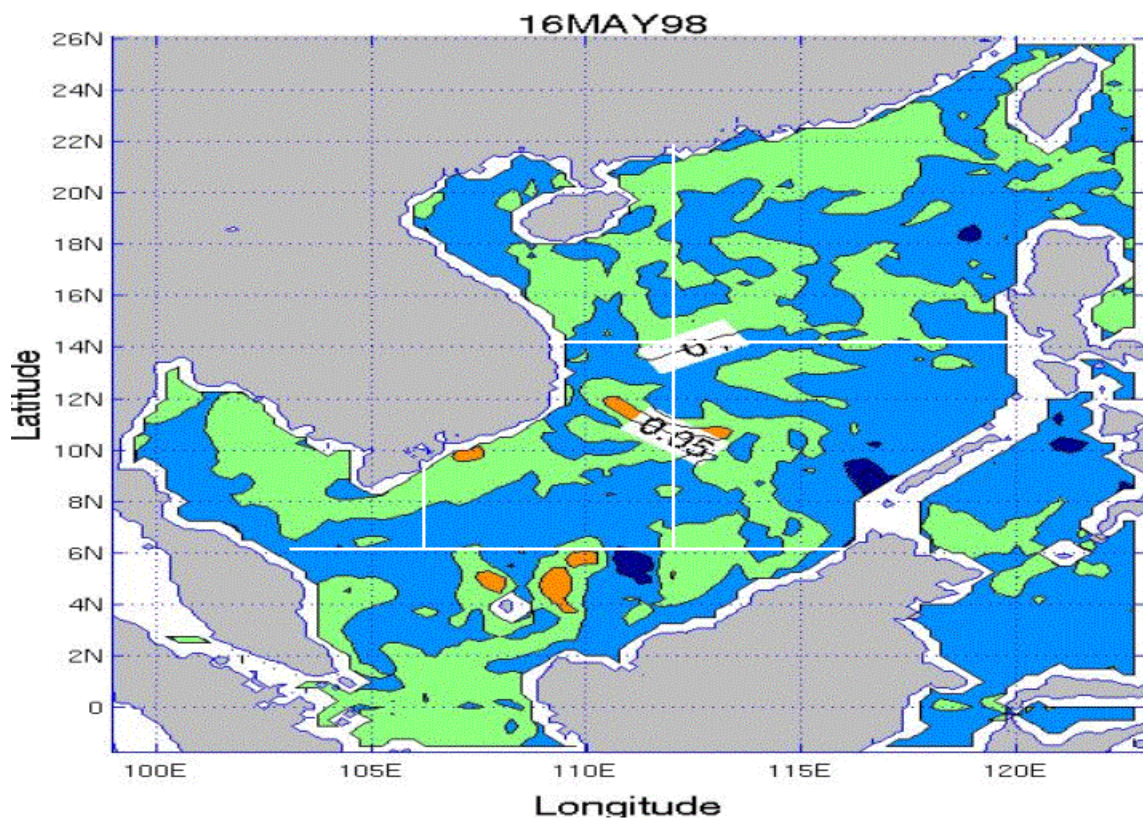
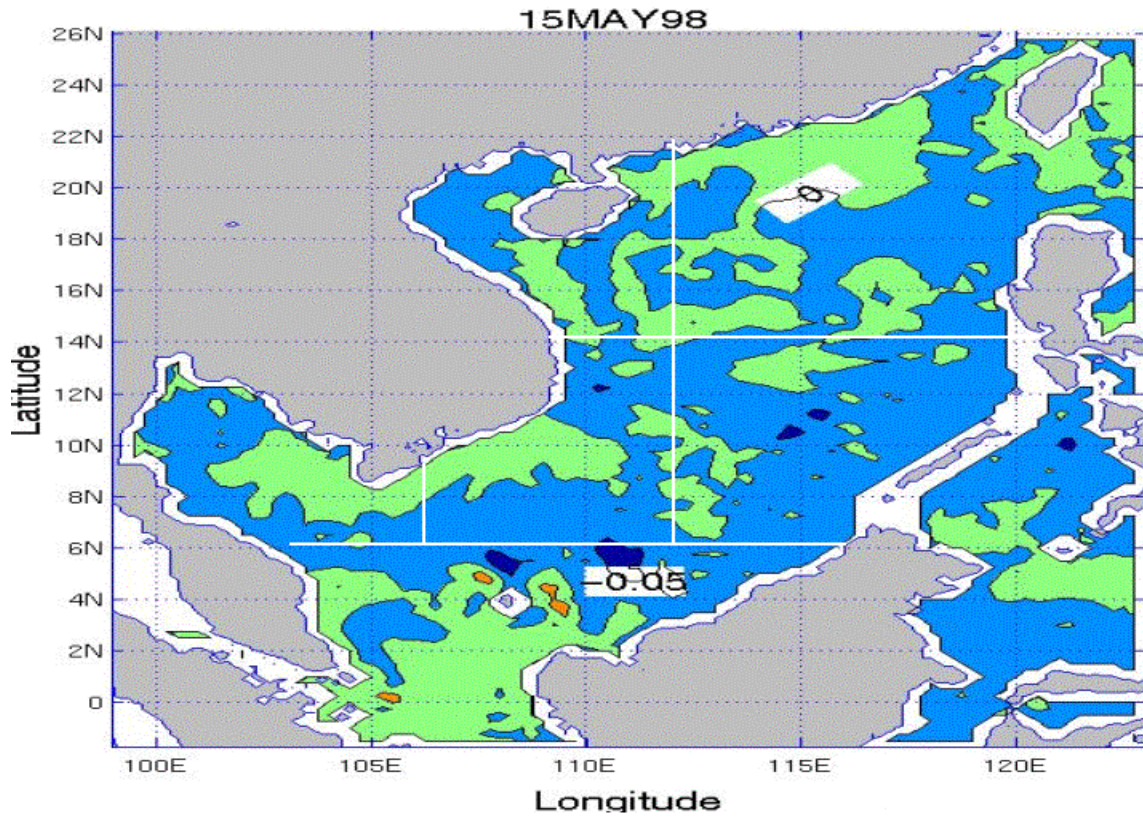


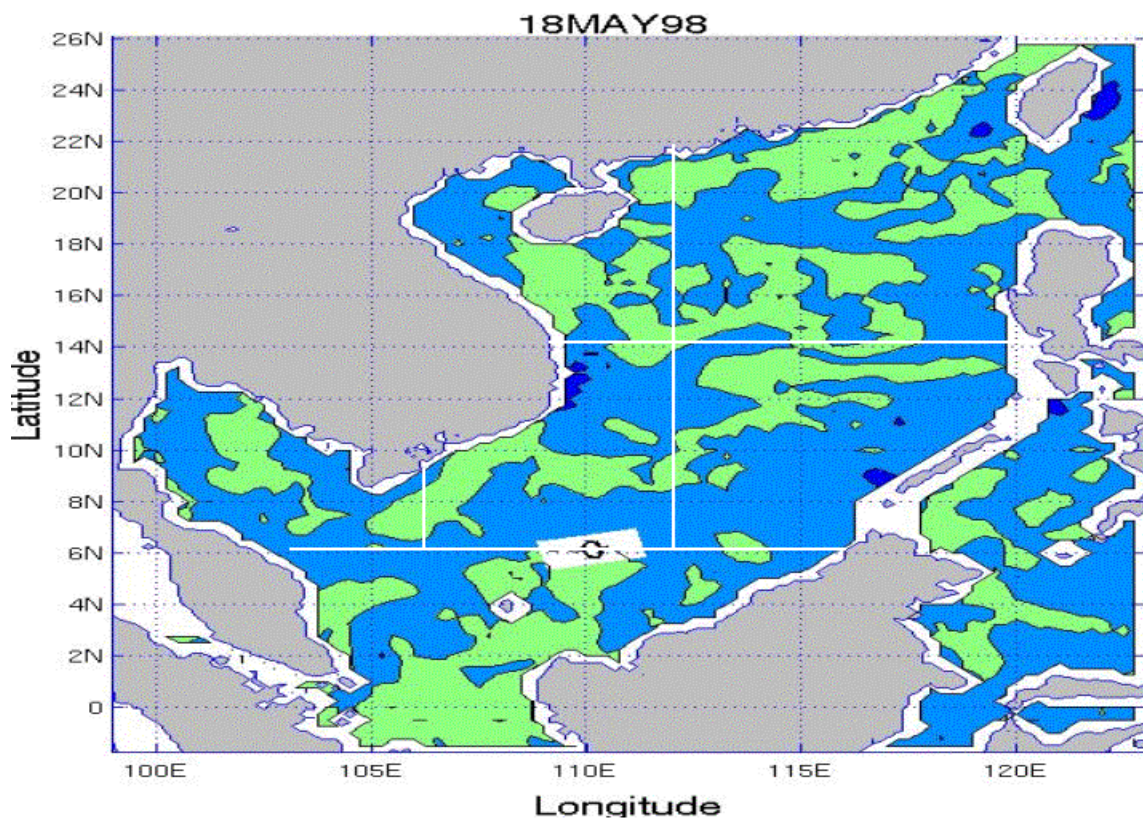
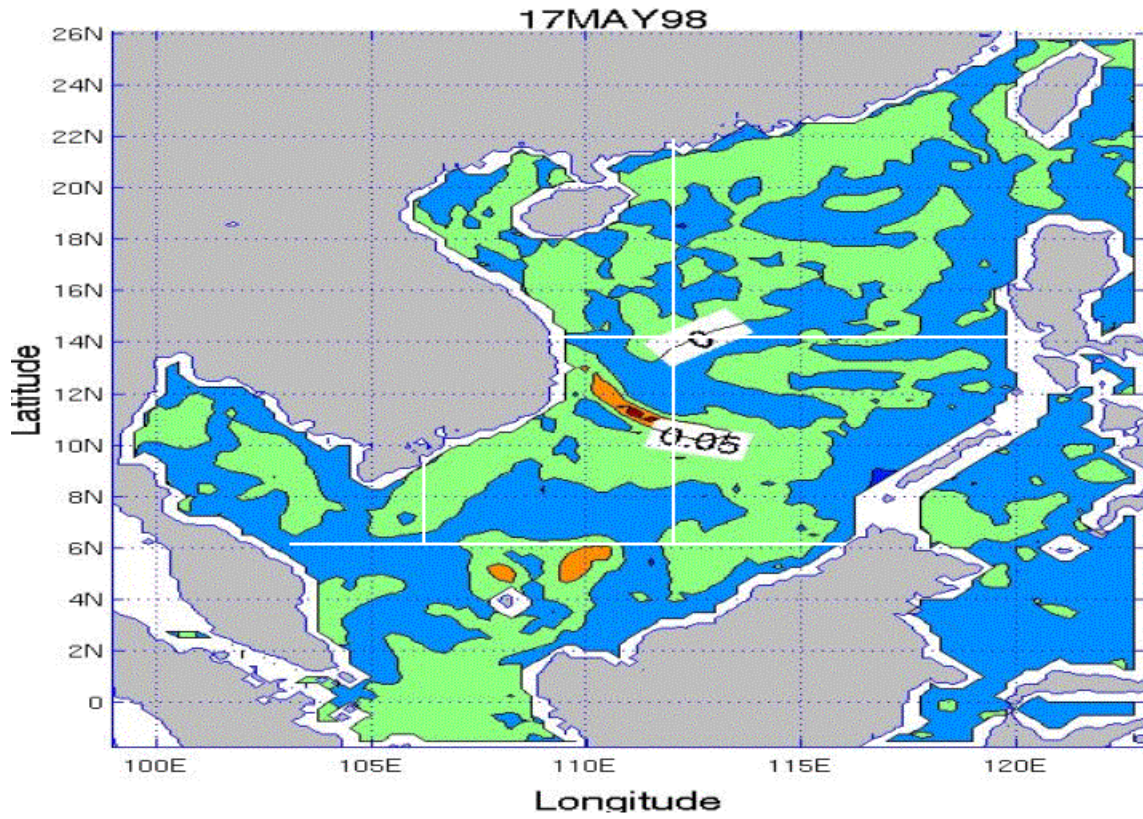


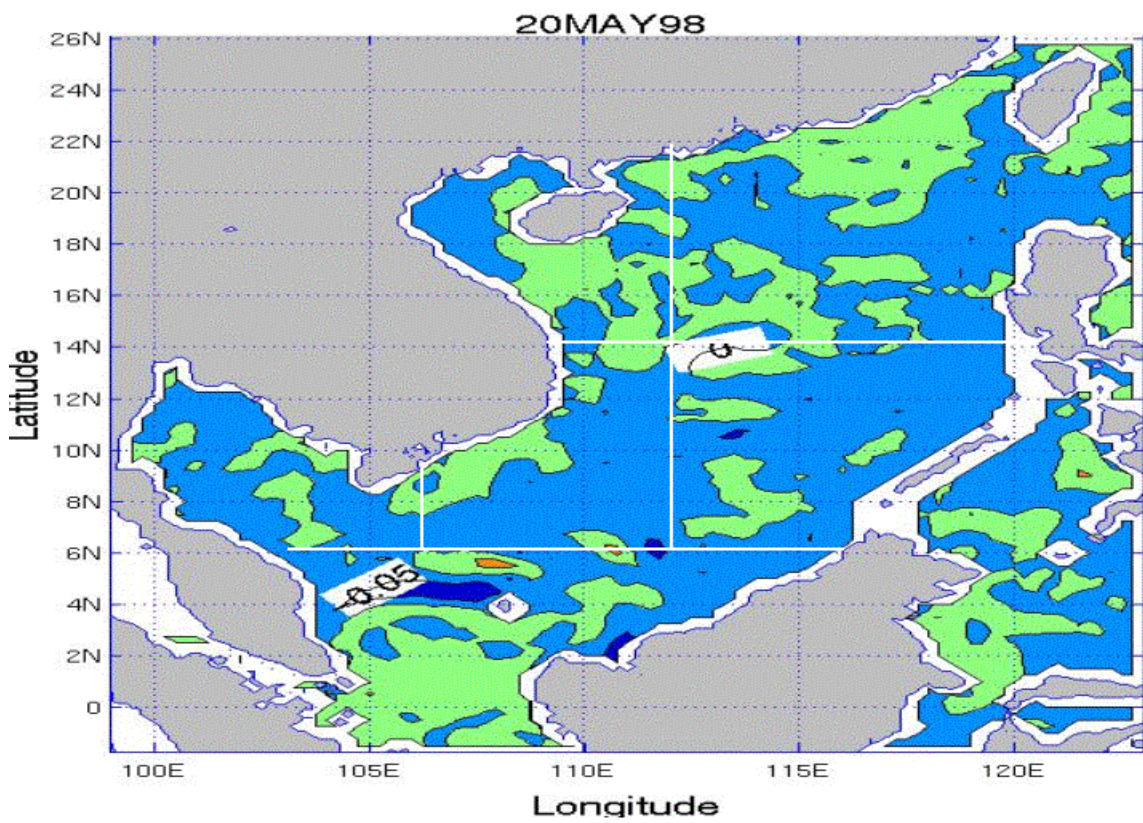
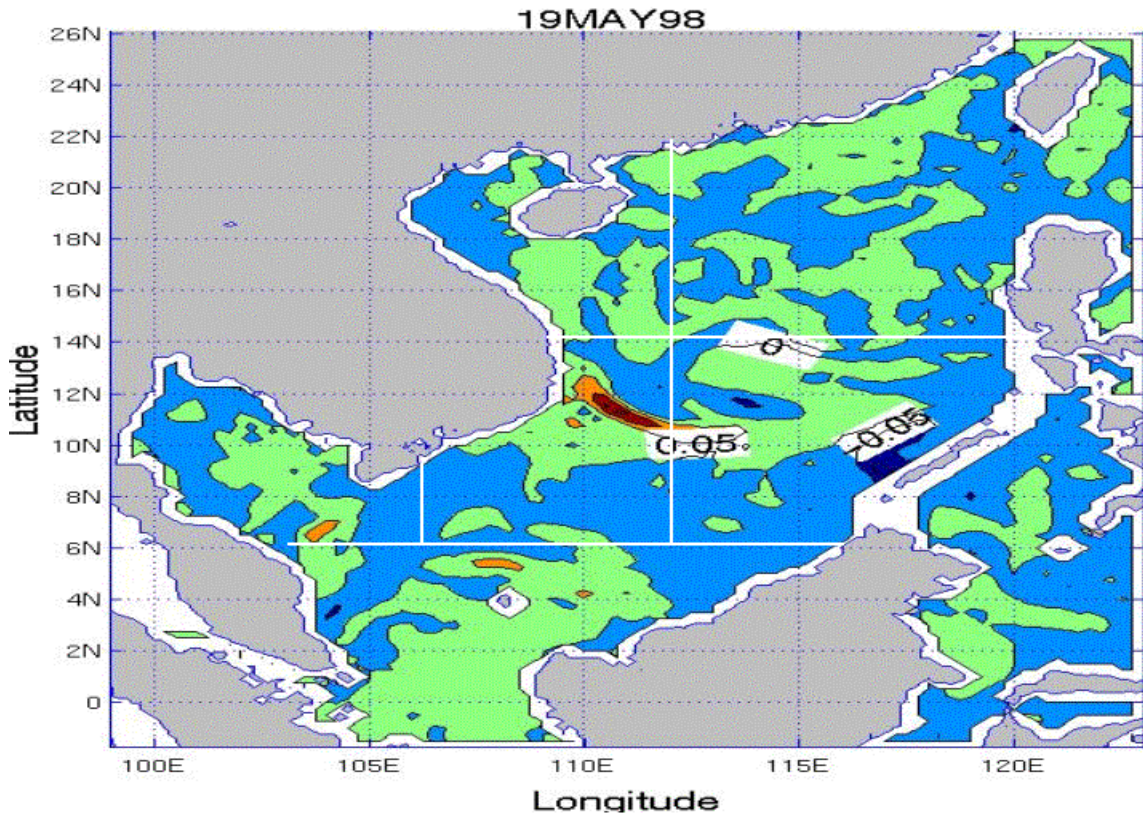
APPENDIX LL. SSS TENDENCY PLOTS FOR THE SCS FOR THE MAY TIME PERIOD

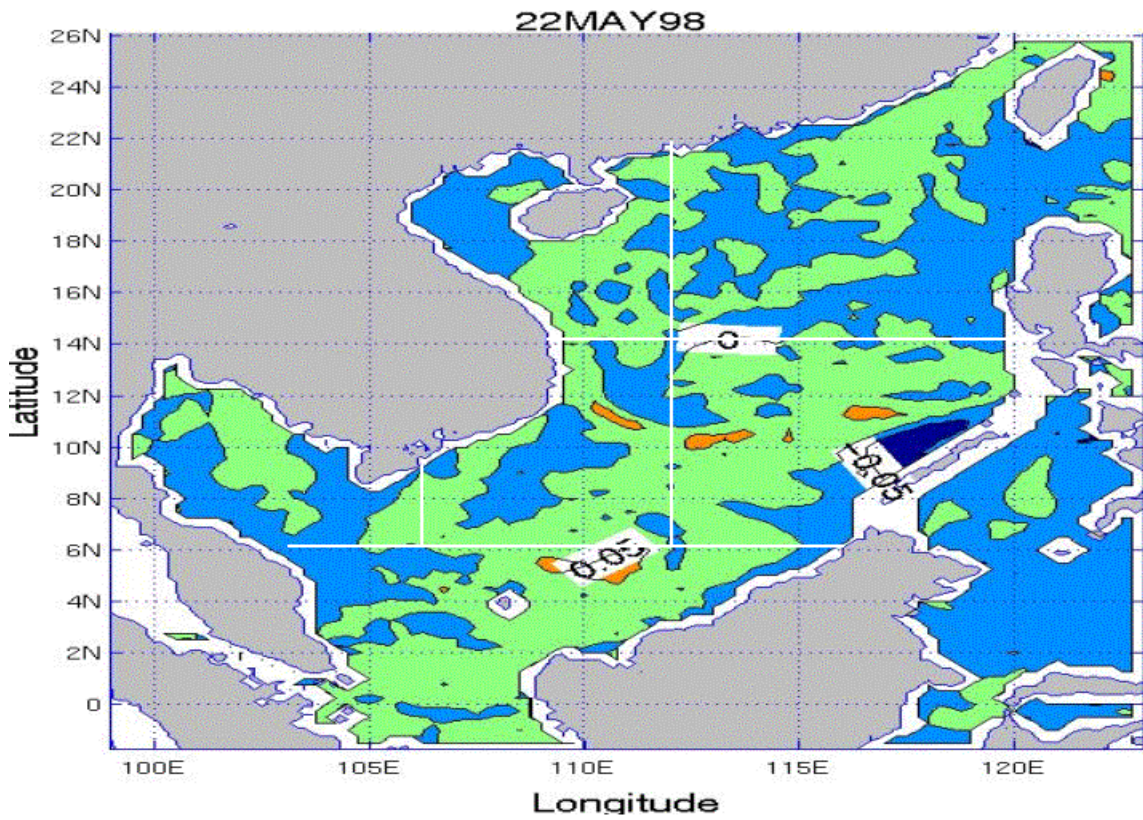
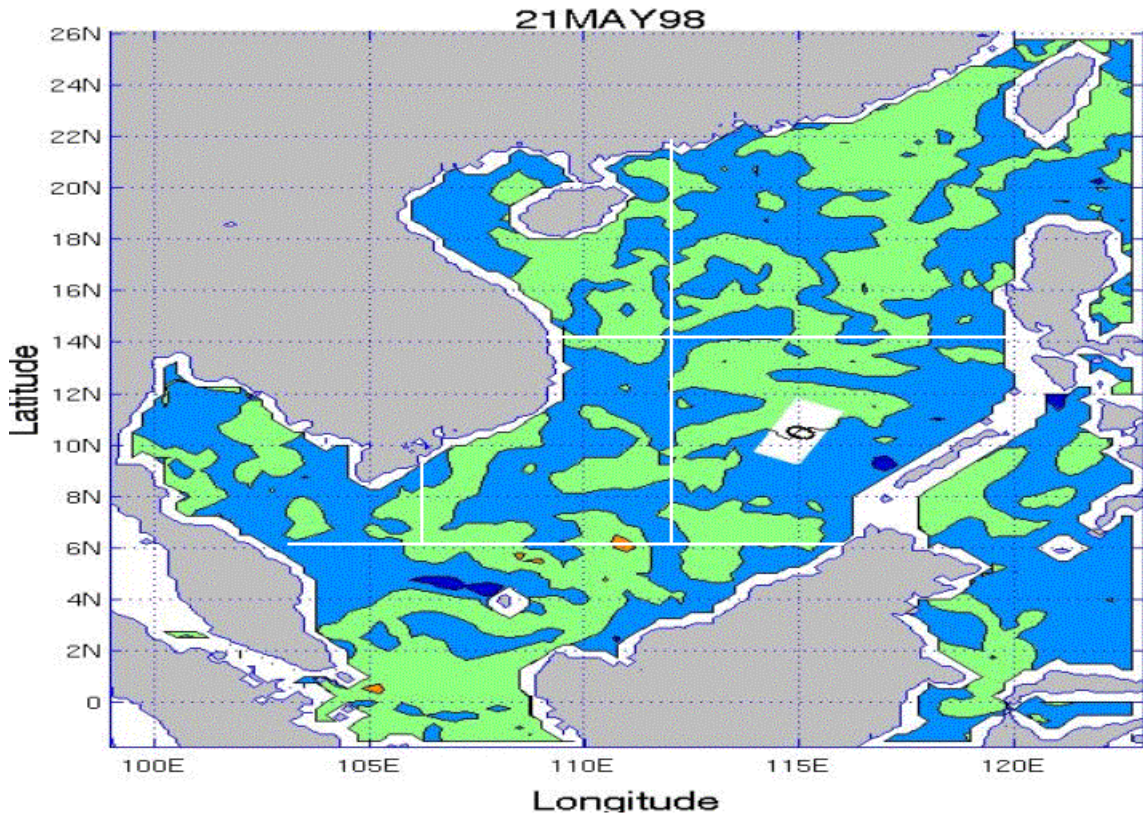
Appendix LL consists of 18 figures that show SSS day-to-day tendency for the May time period over the SCS. The figures are in time sequential order from May 14 through May 31. Each plot represents the change between the previous day and the current day.

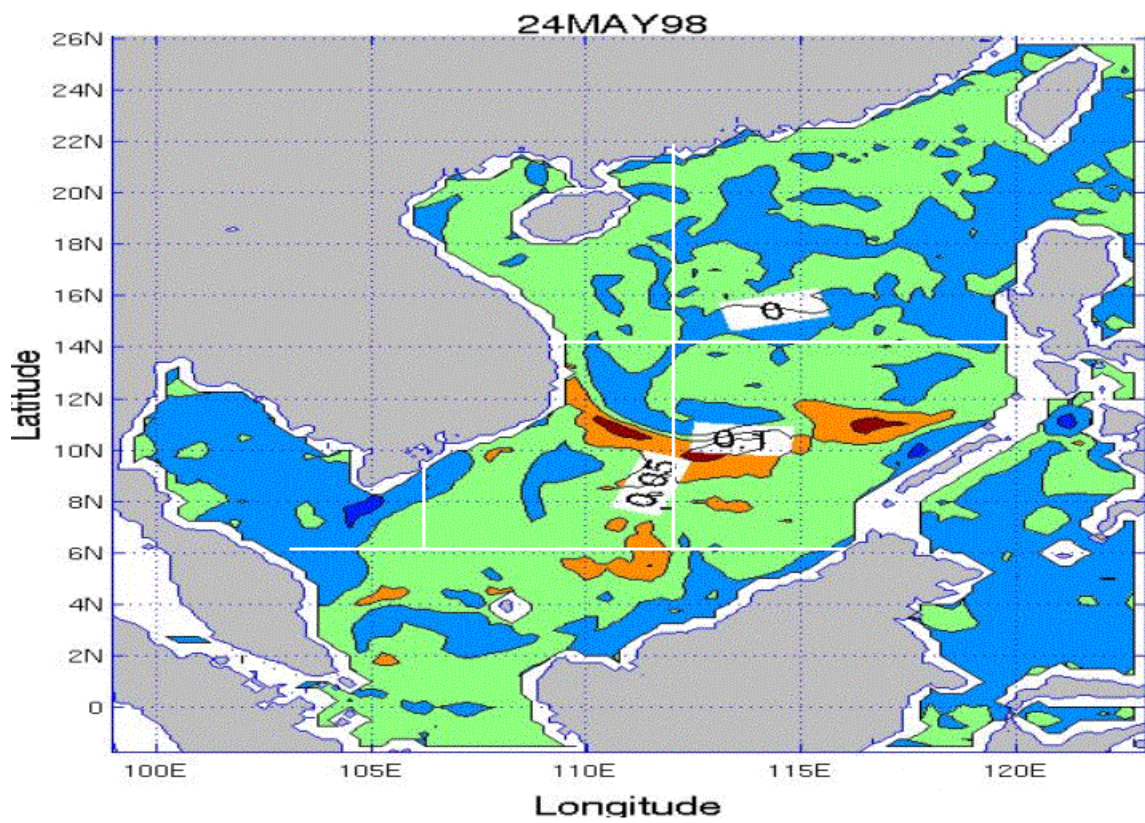
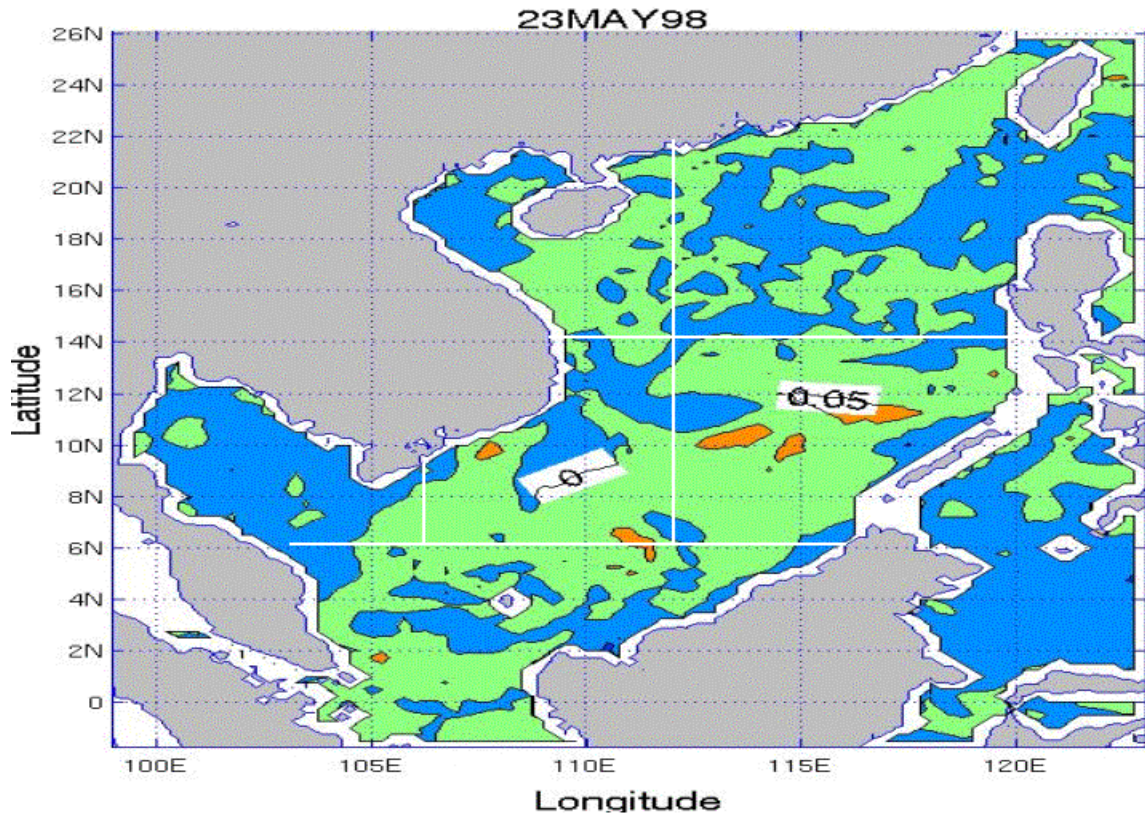


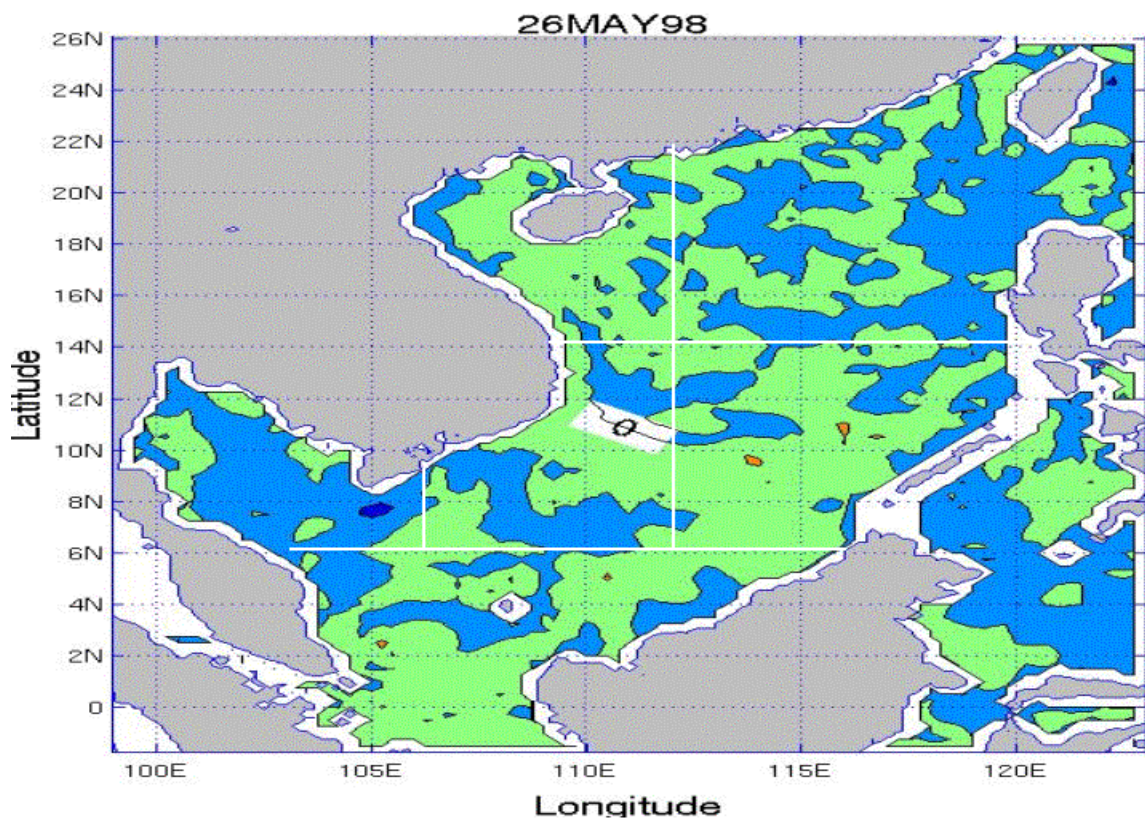
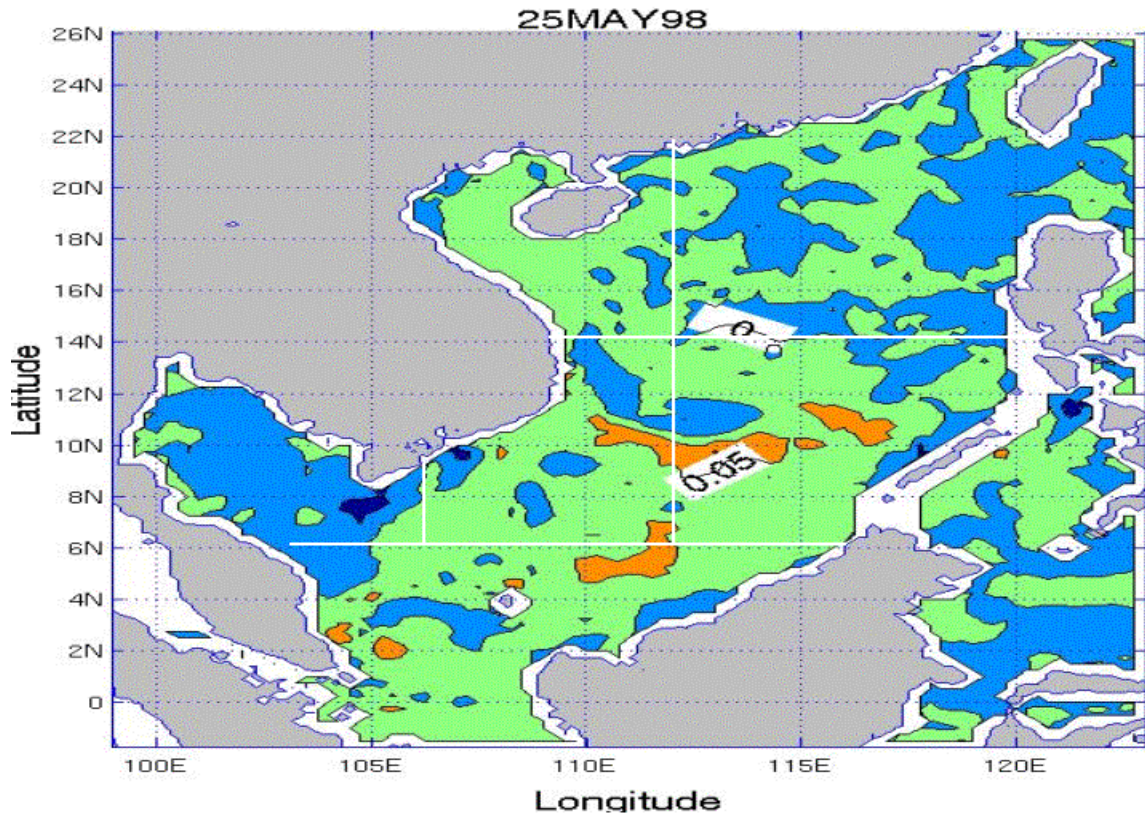


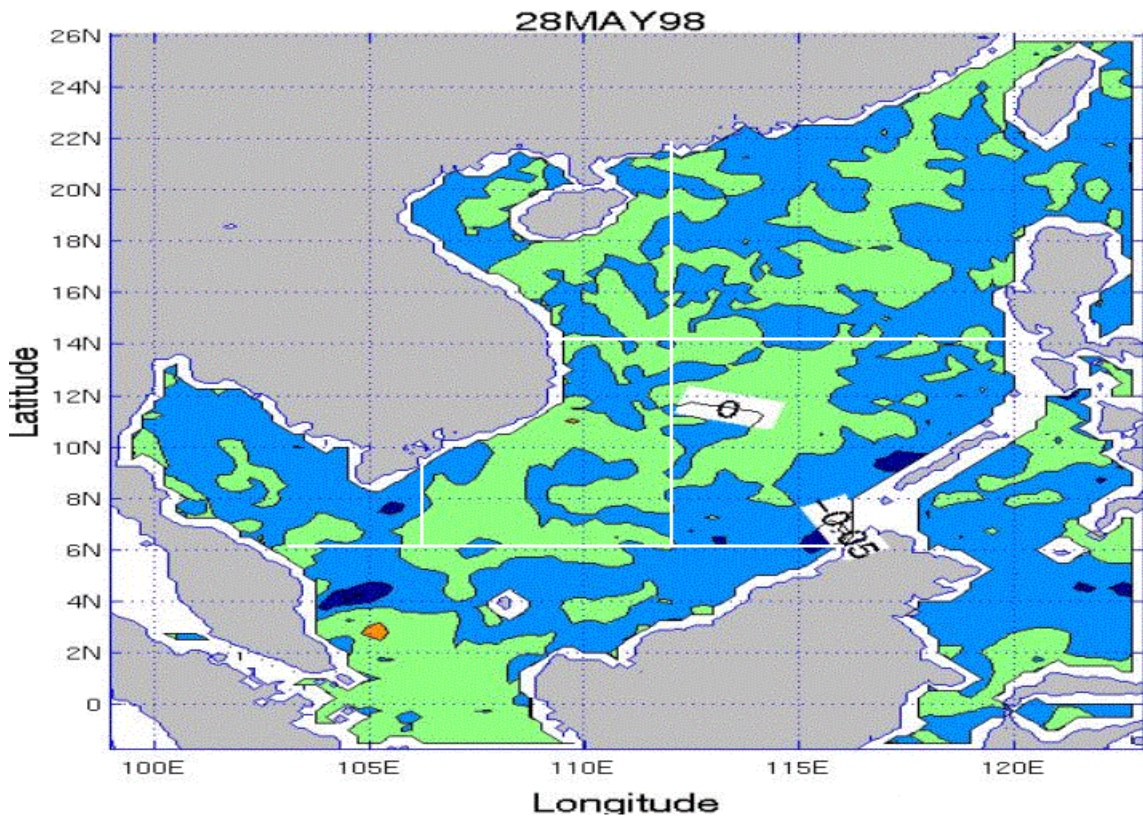
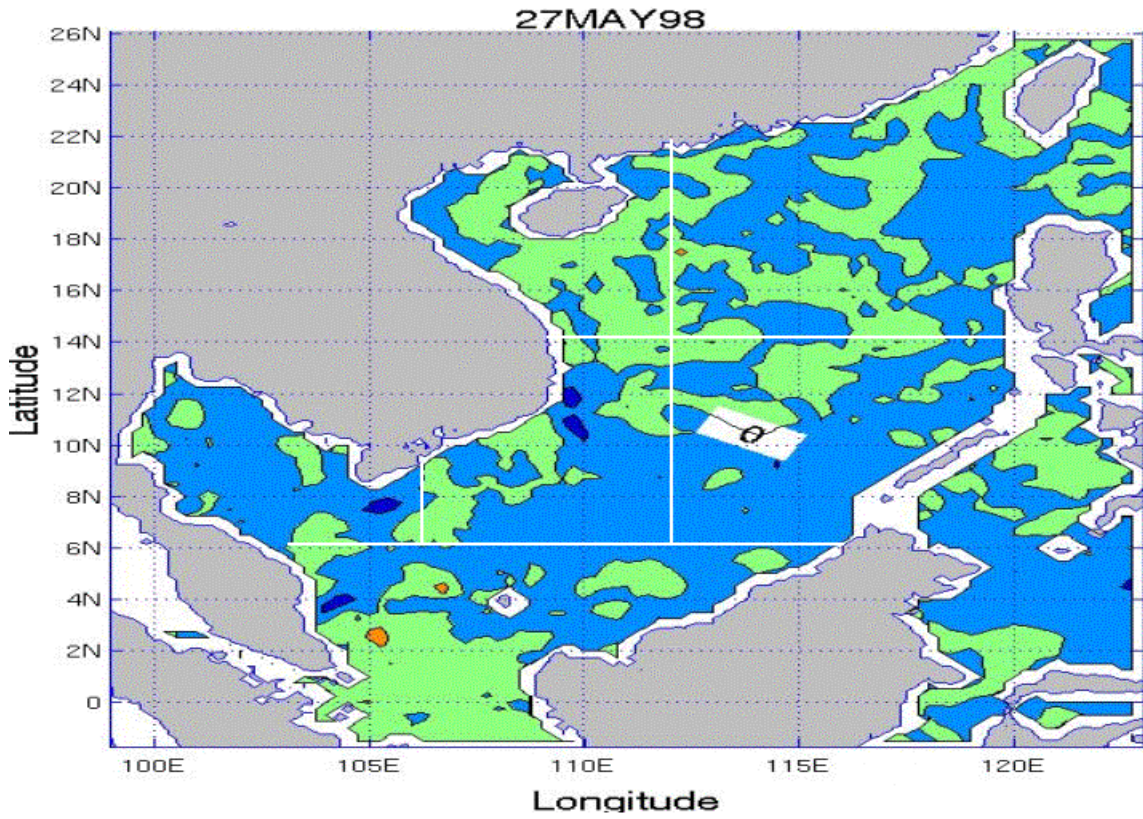


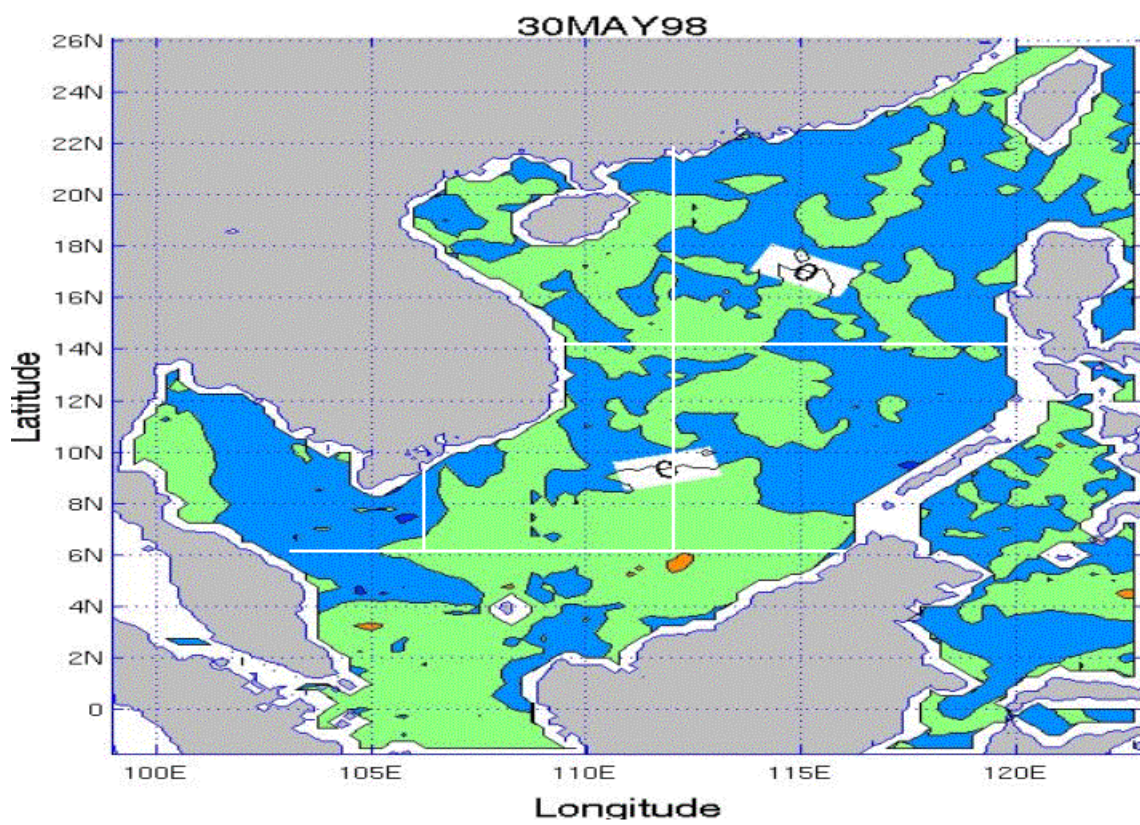
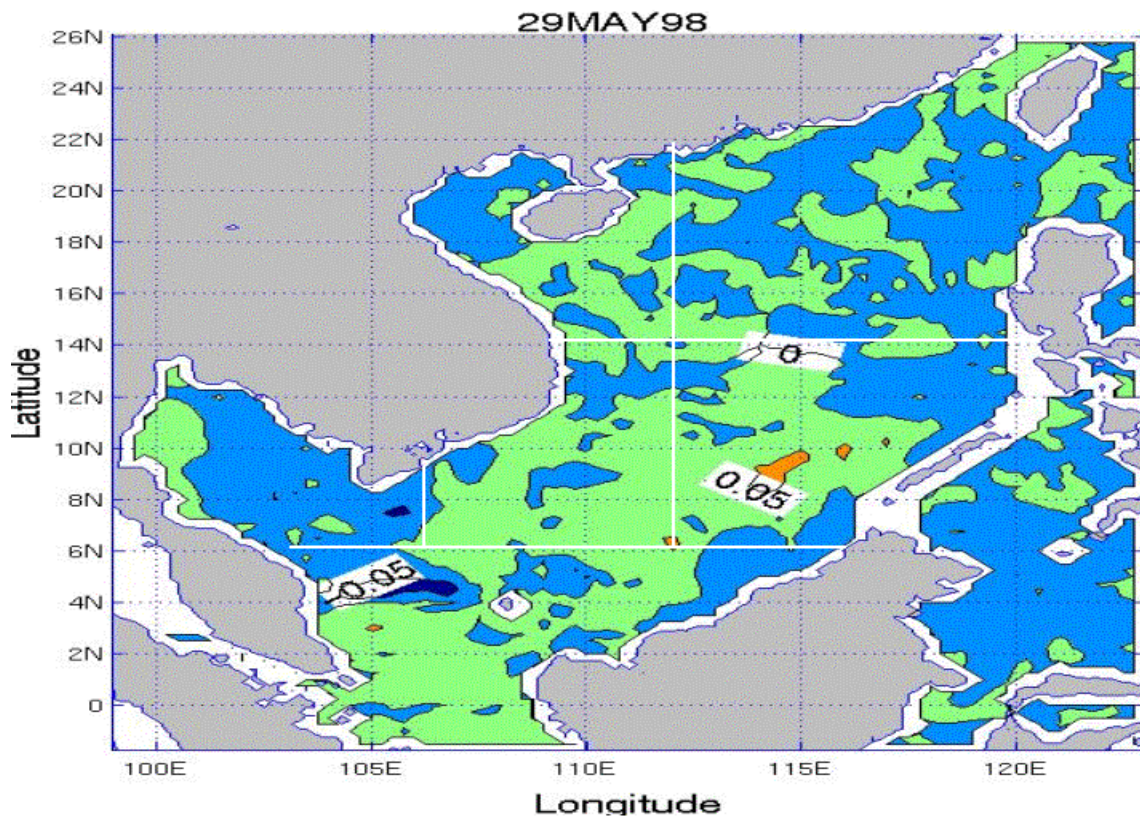


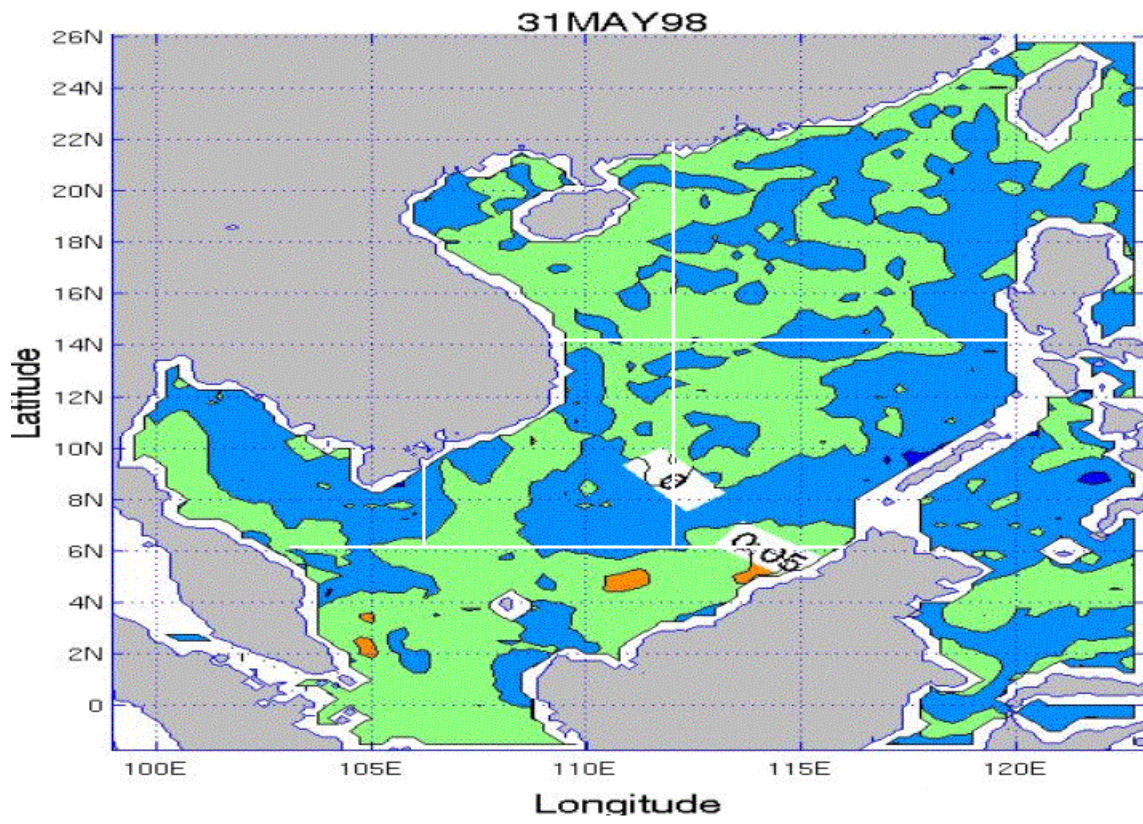






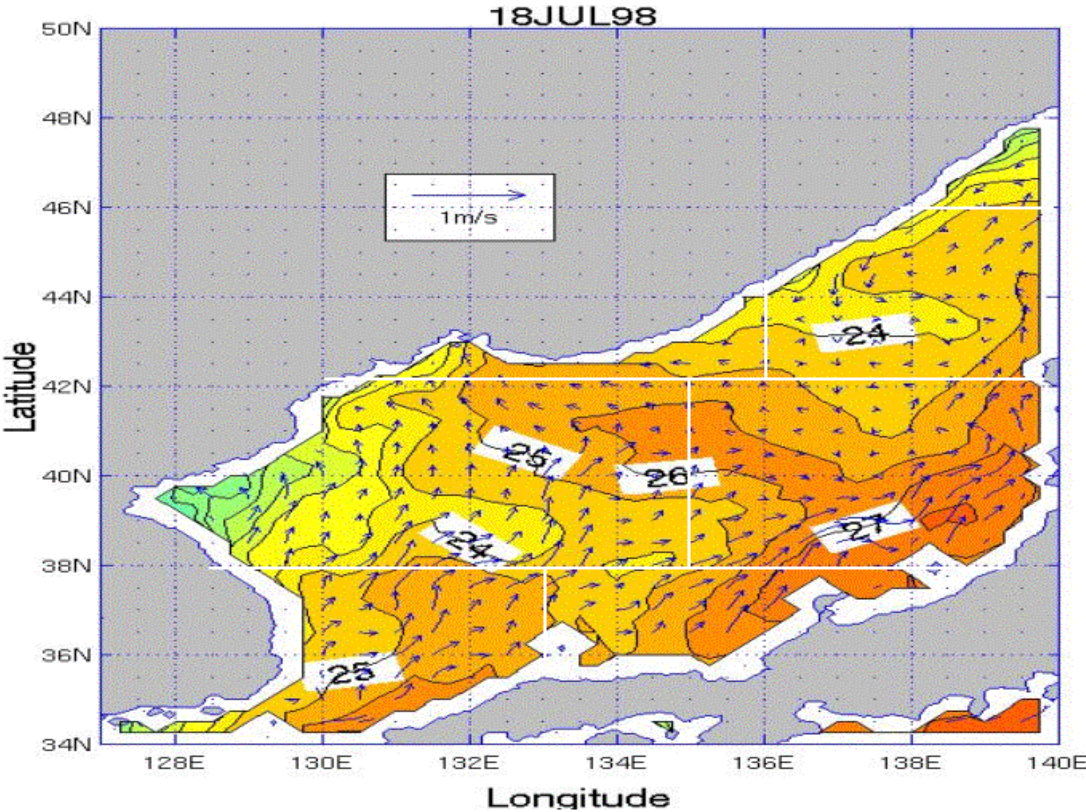


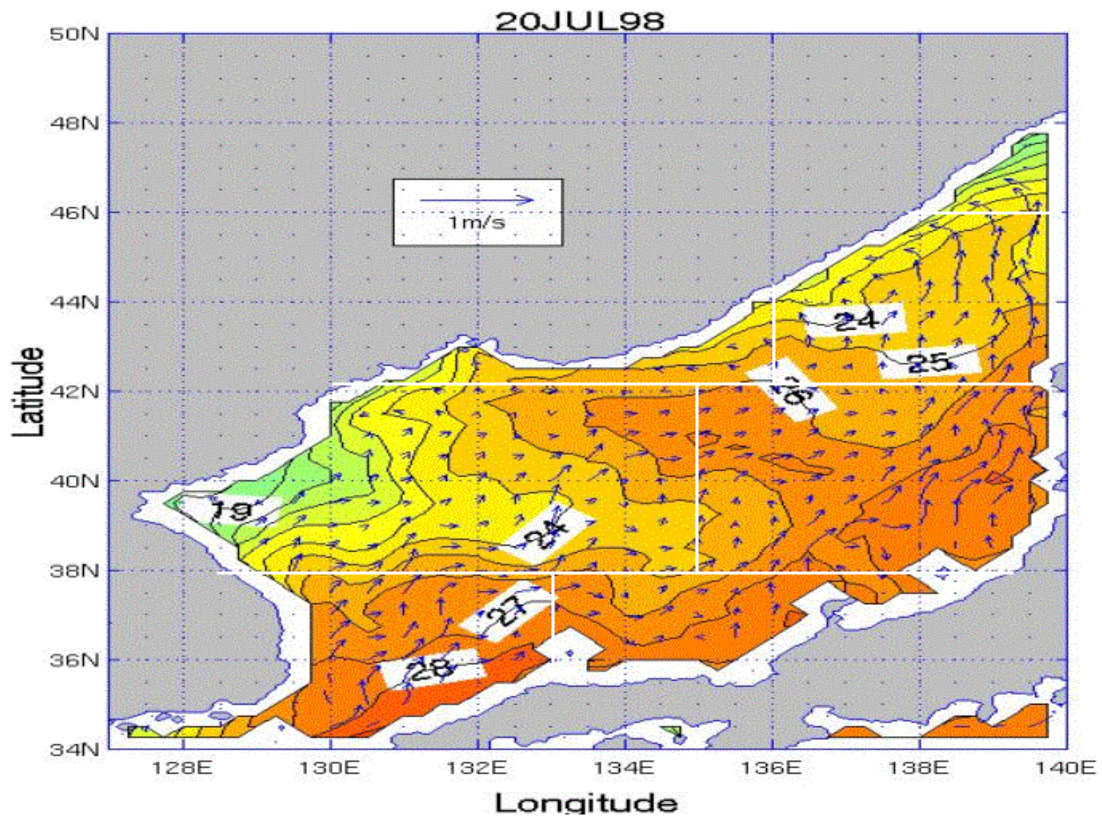
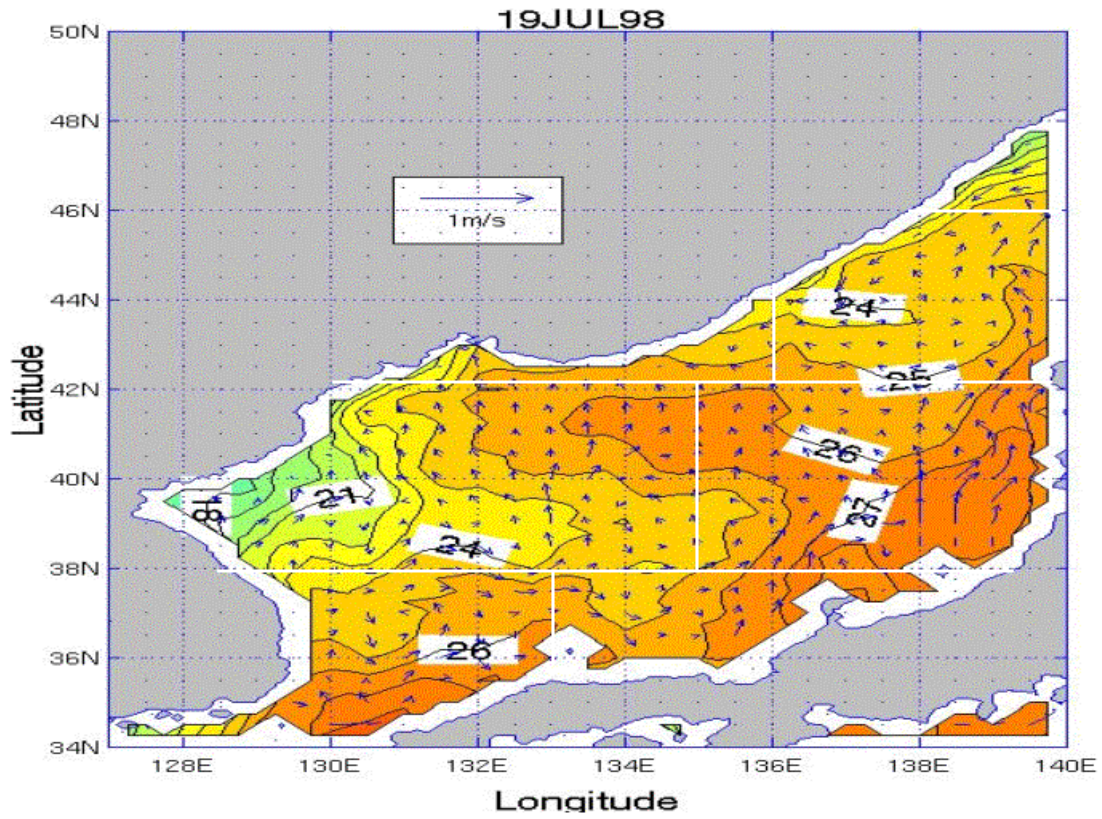


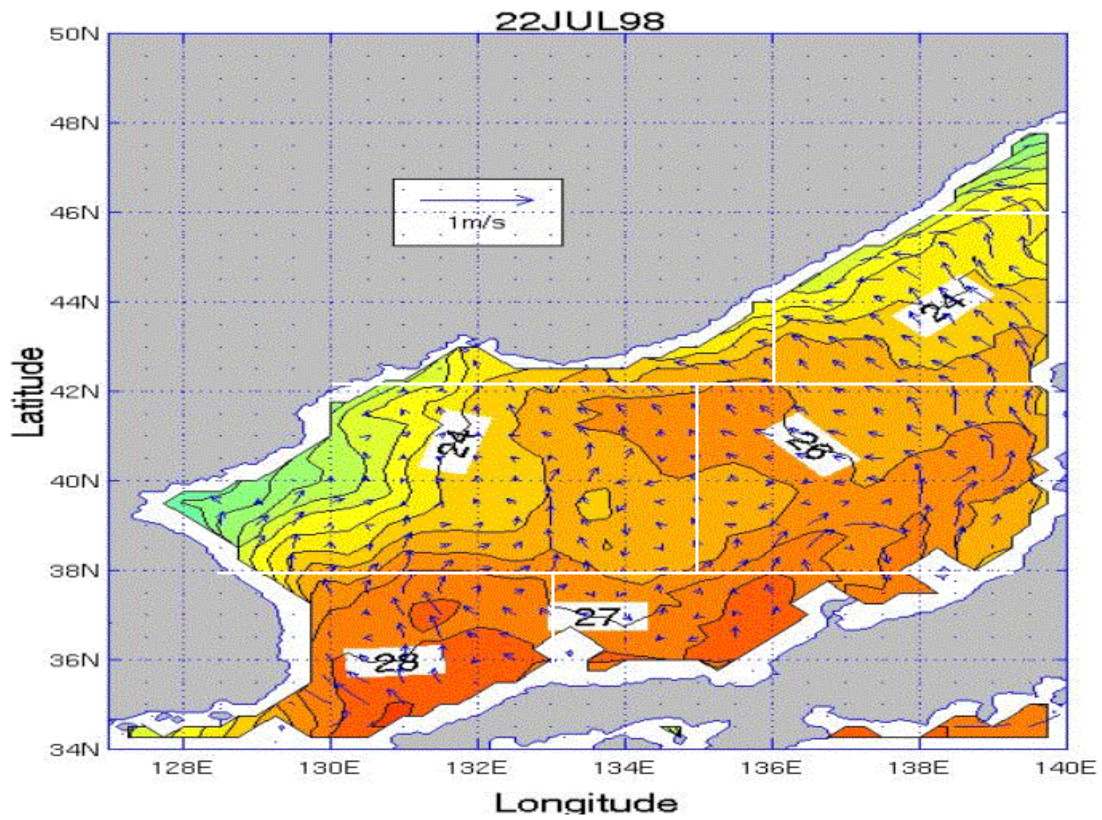
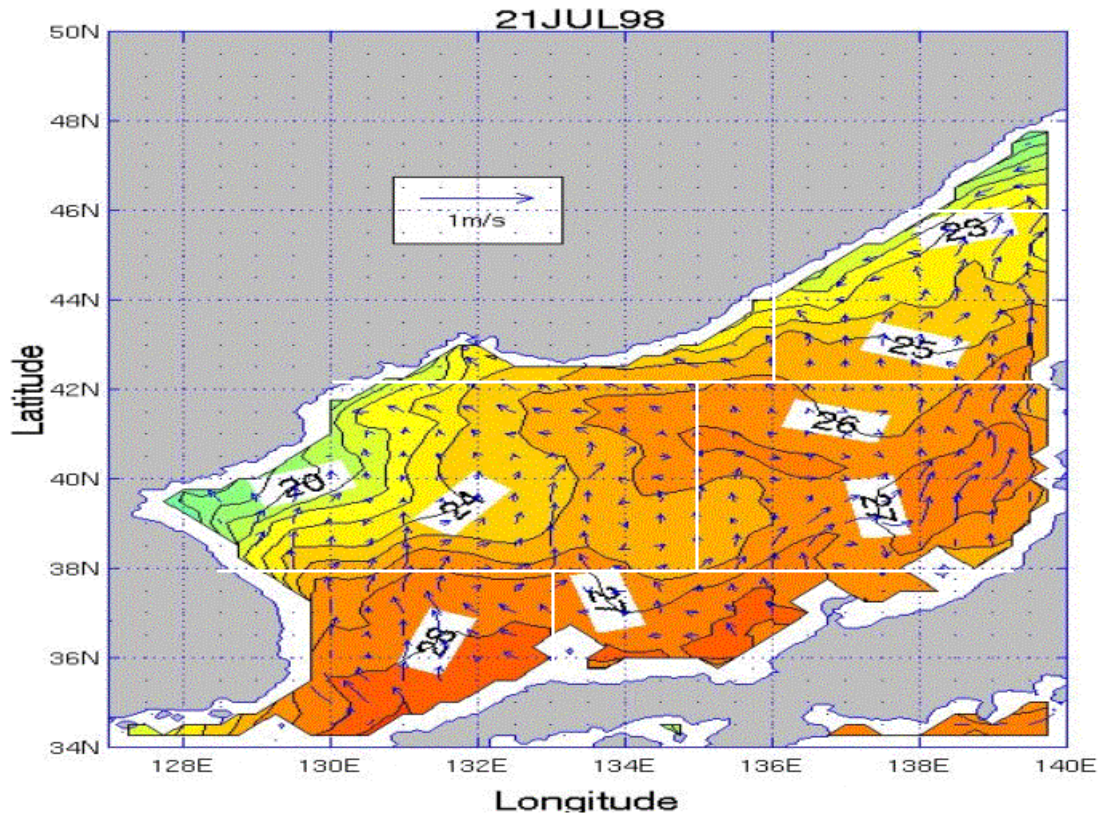


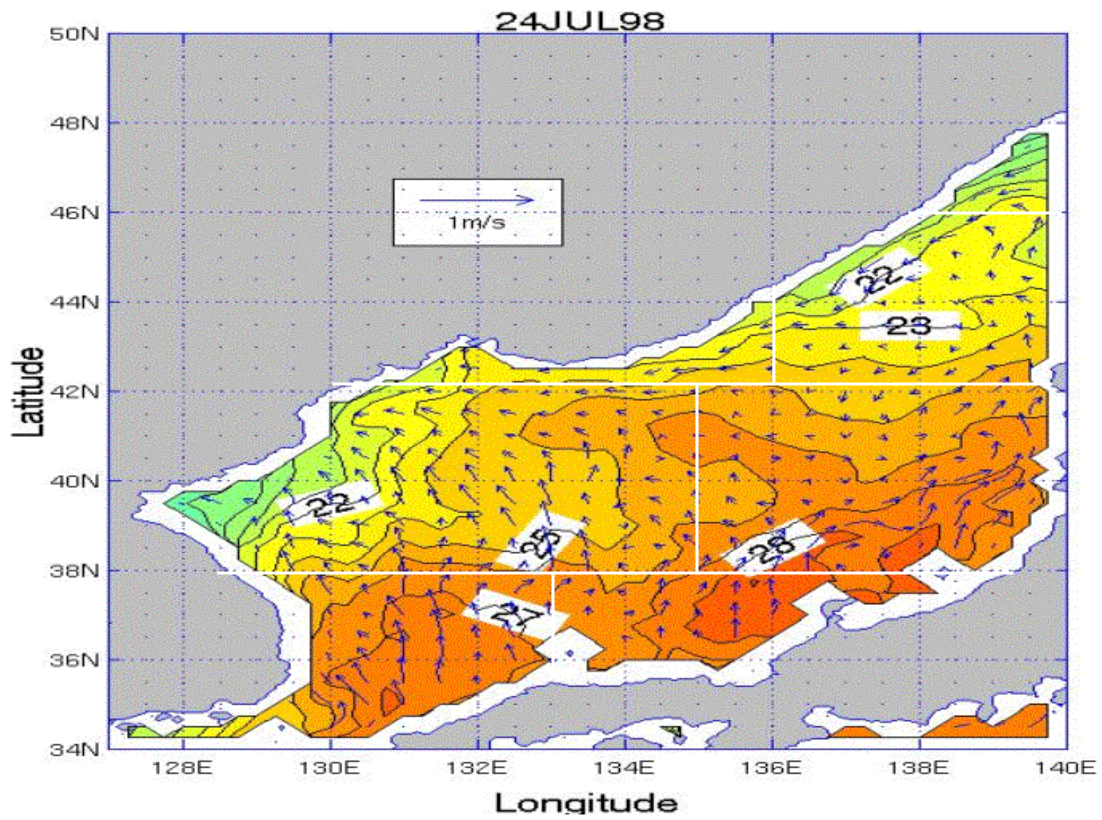
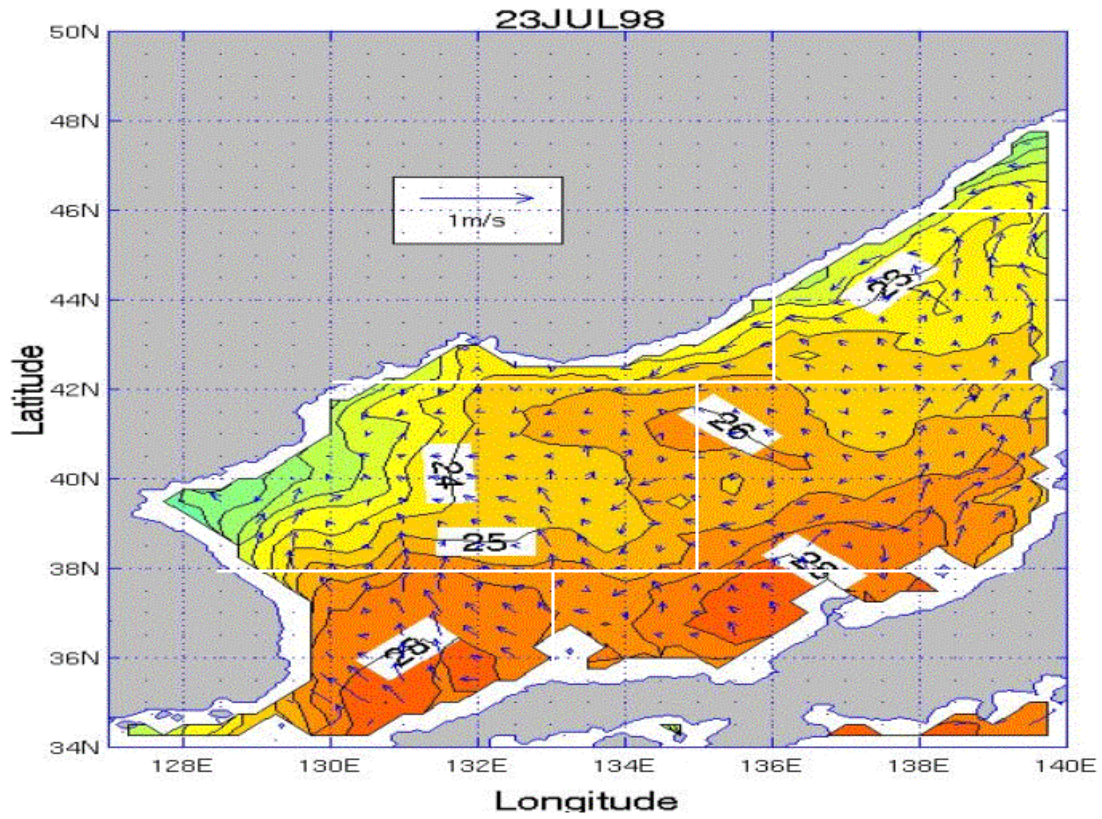
APPENDIX MM. SST AND SURFACE CURRENT VELOCITY PLOTS FOR THE JES FOR THE JULY TIME PERIOD

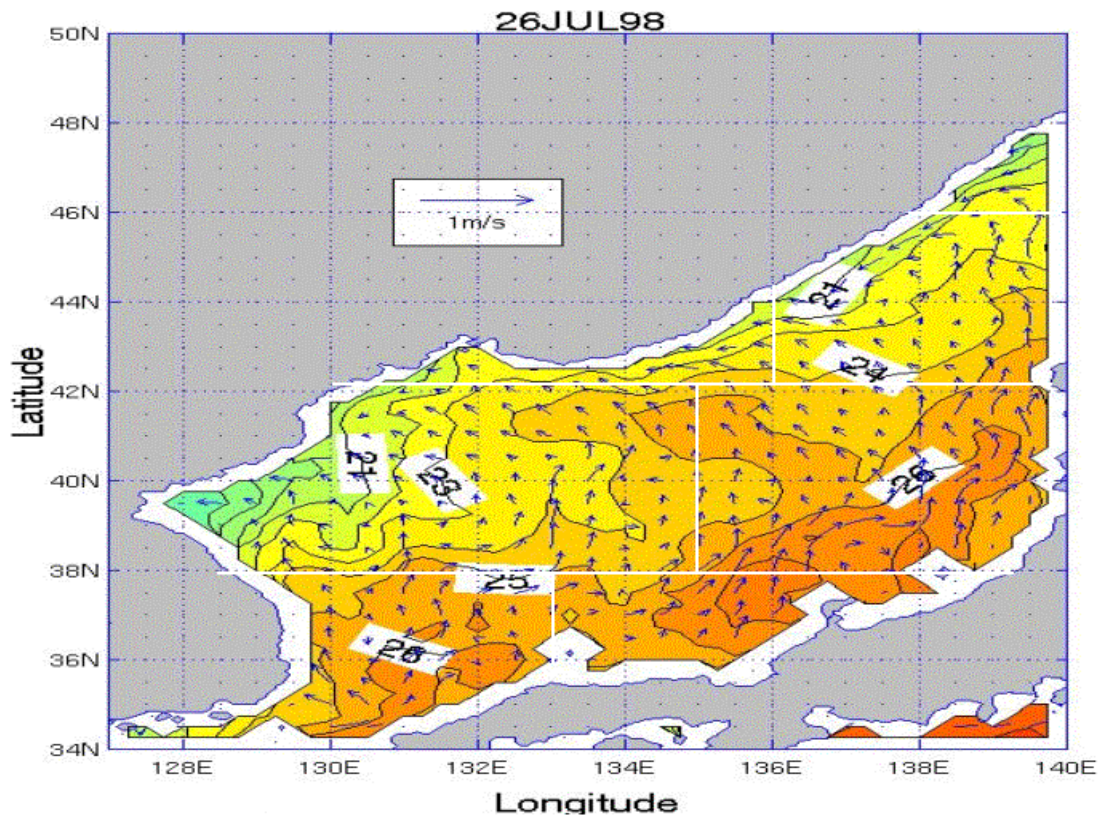
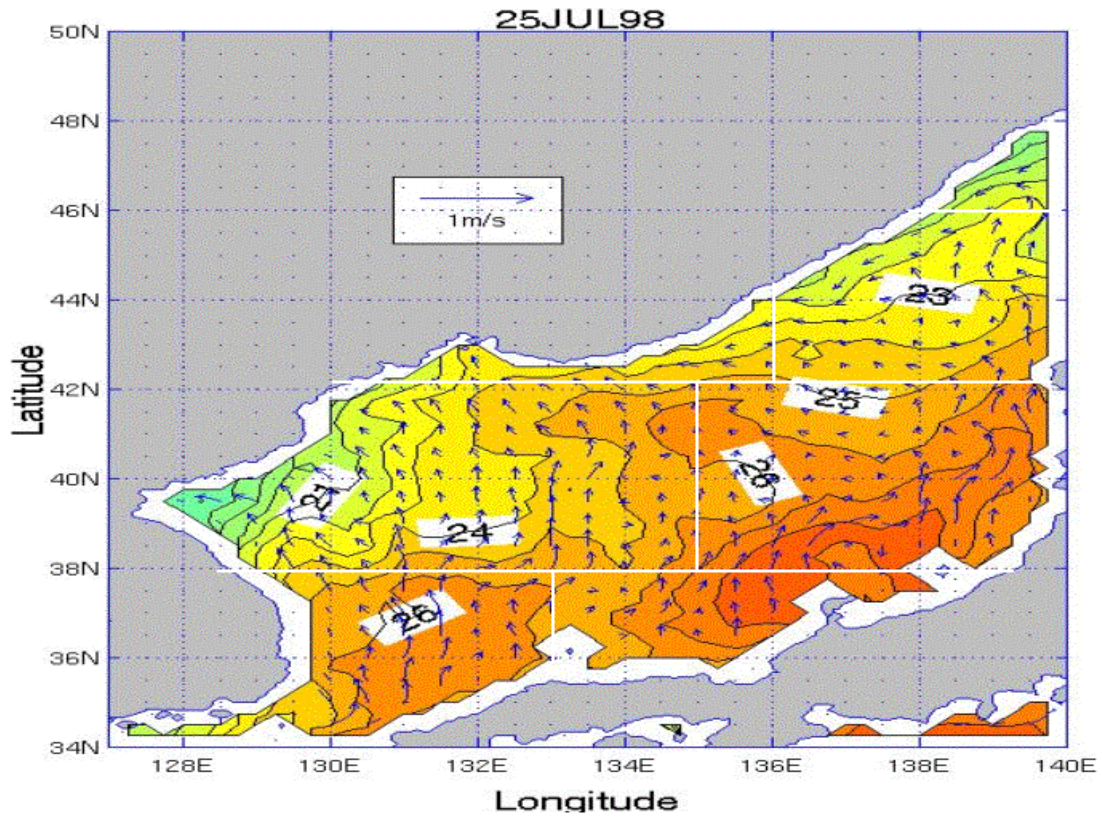
Appendix MM consists of 14 figures that show SST and surface current velocity for each day of the July time period for the JES. The figures are in time sequential order from July 18 through July 31.

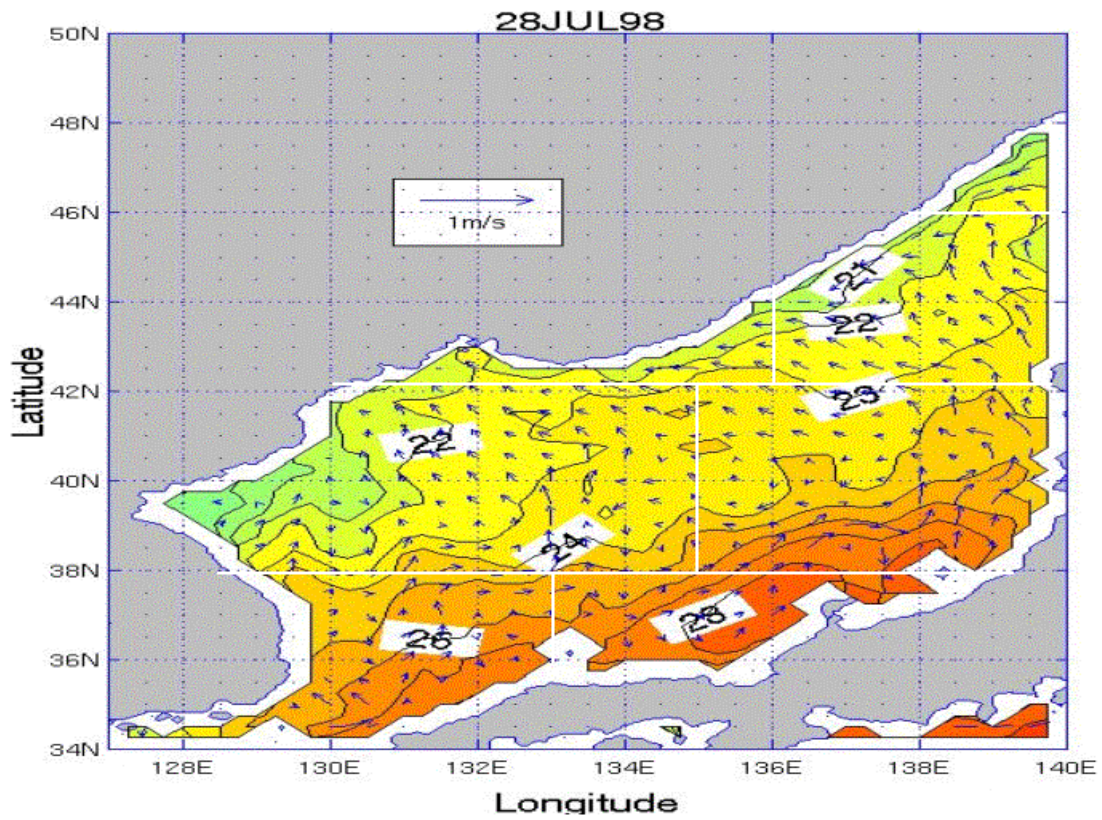
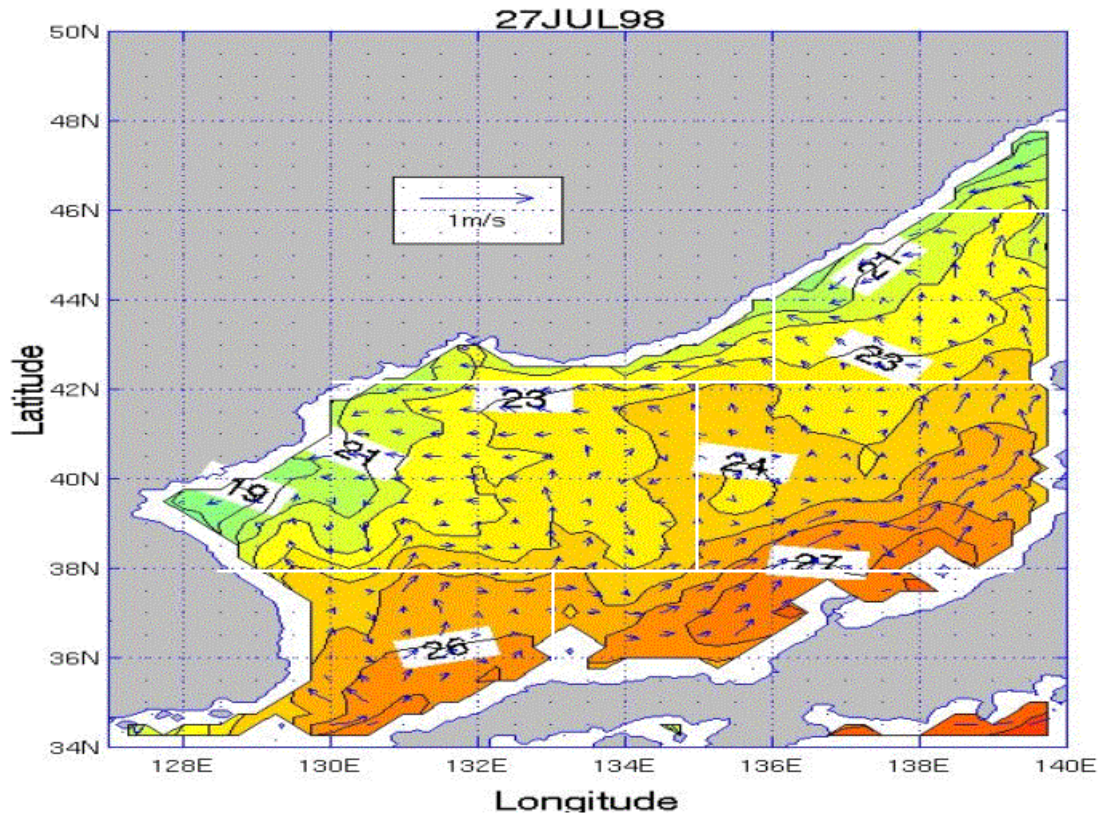


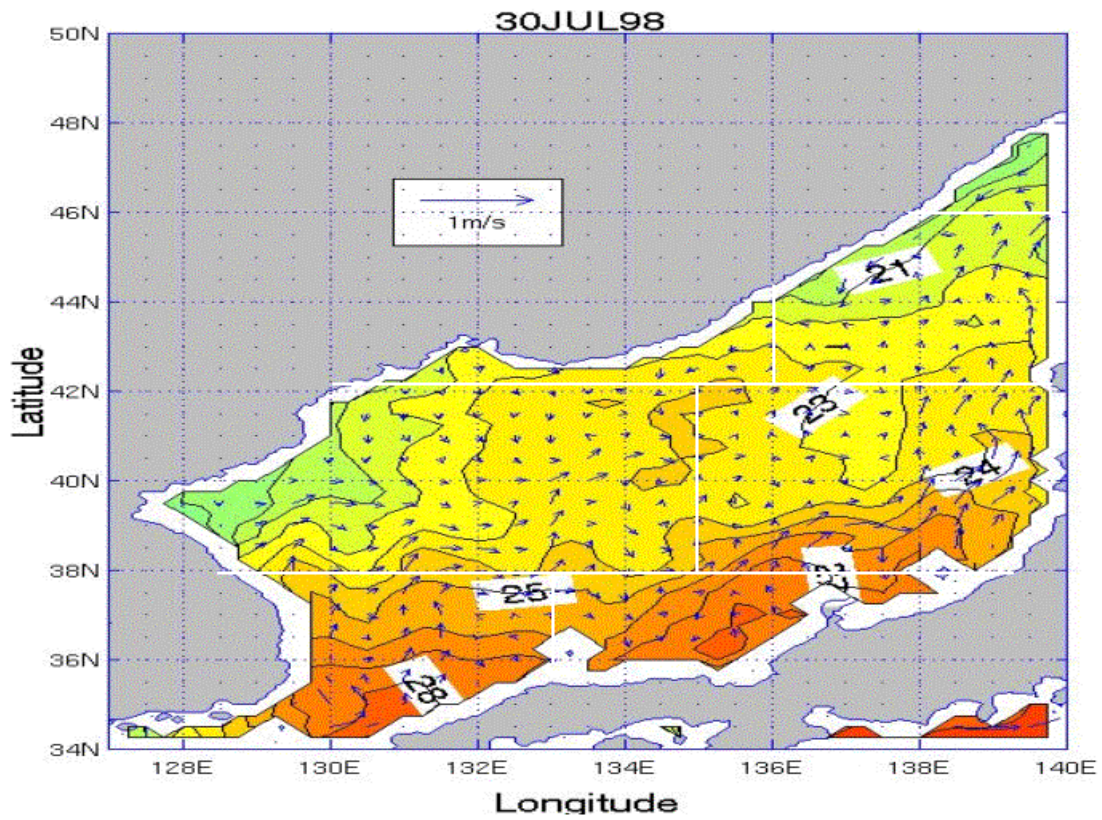
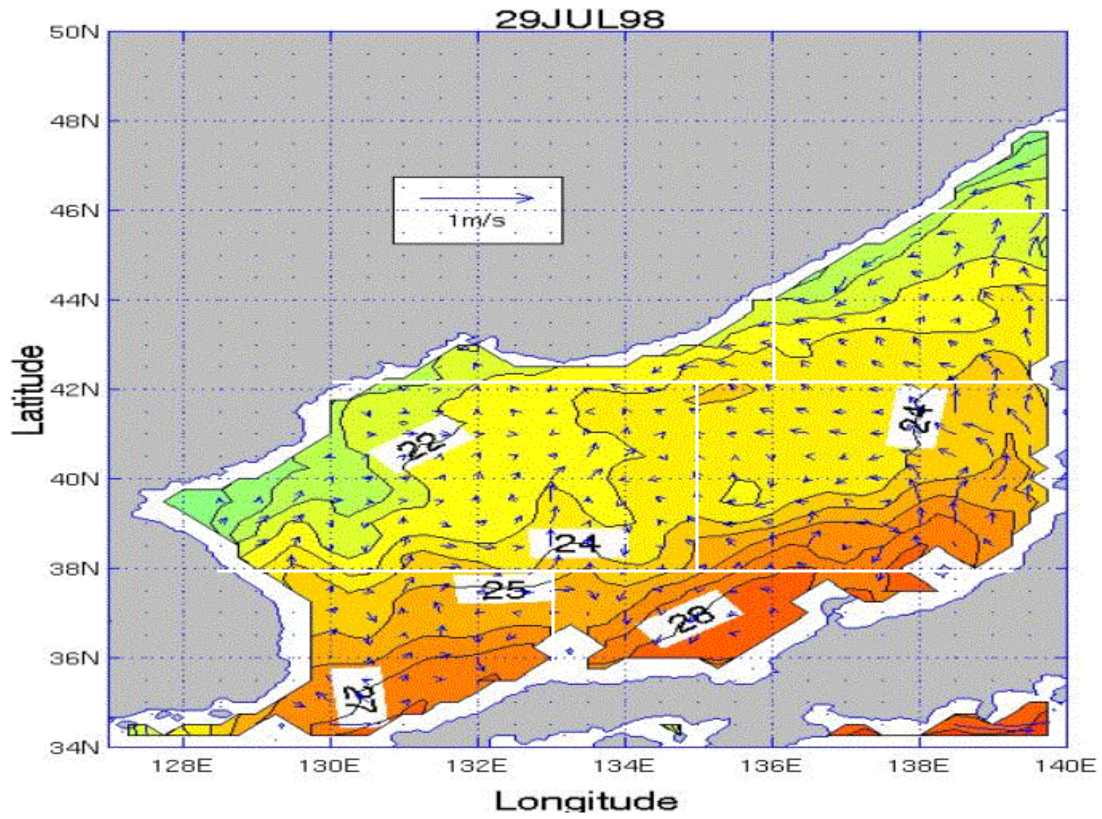


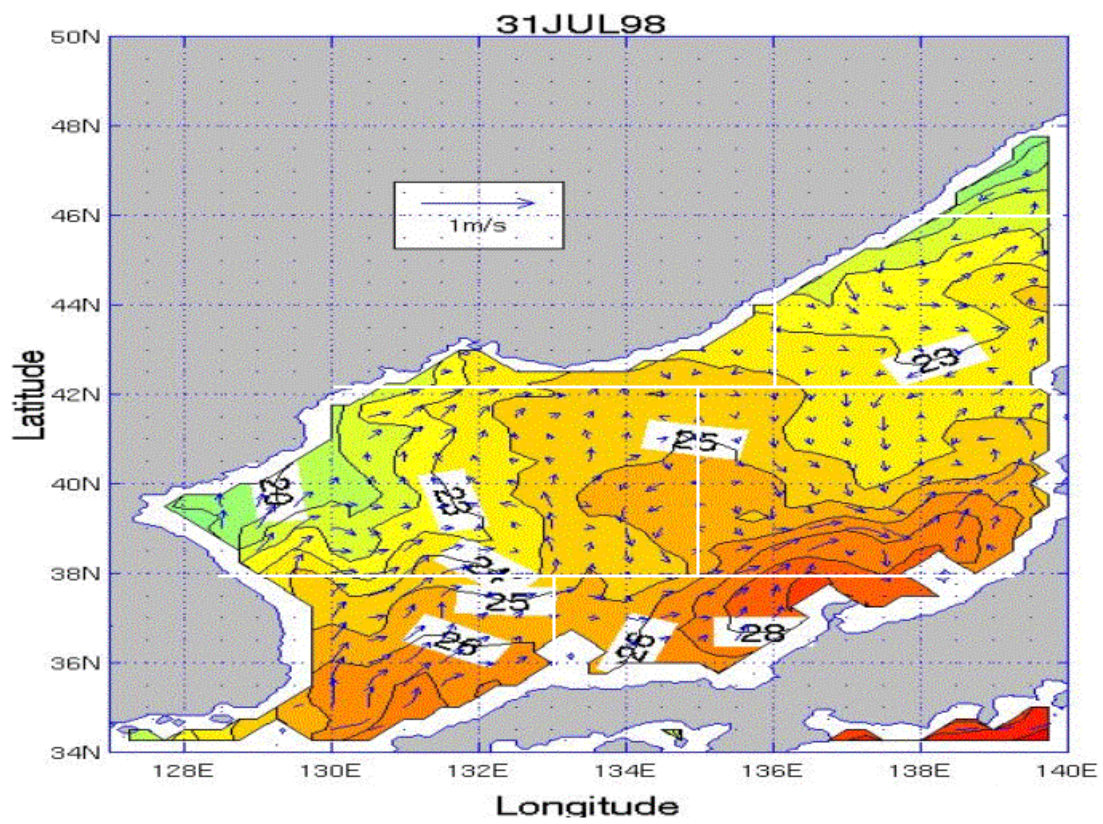






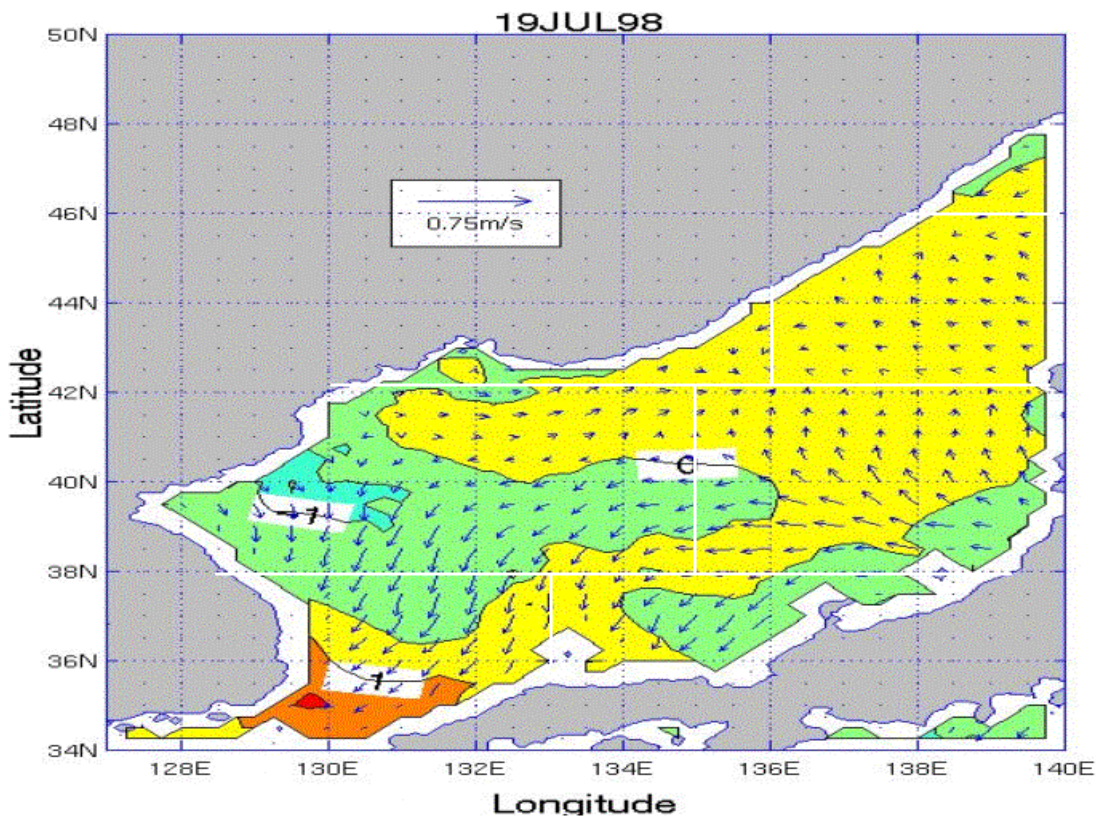


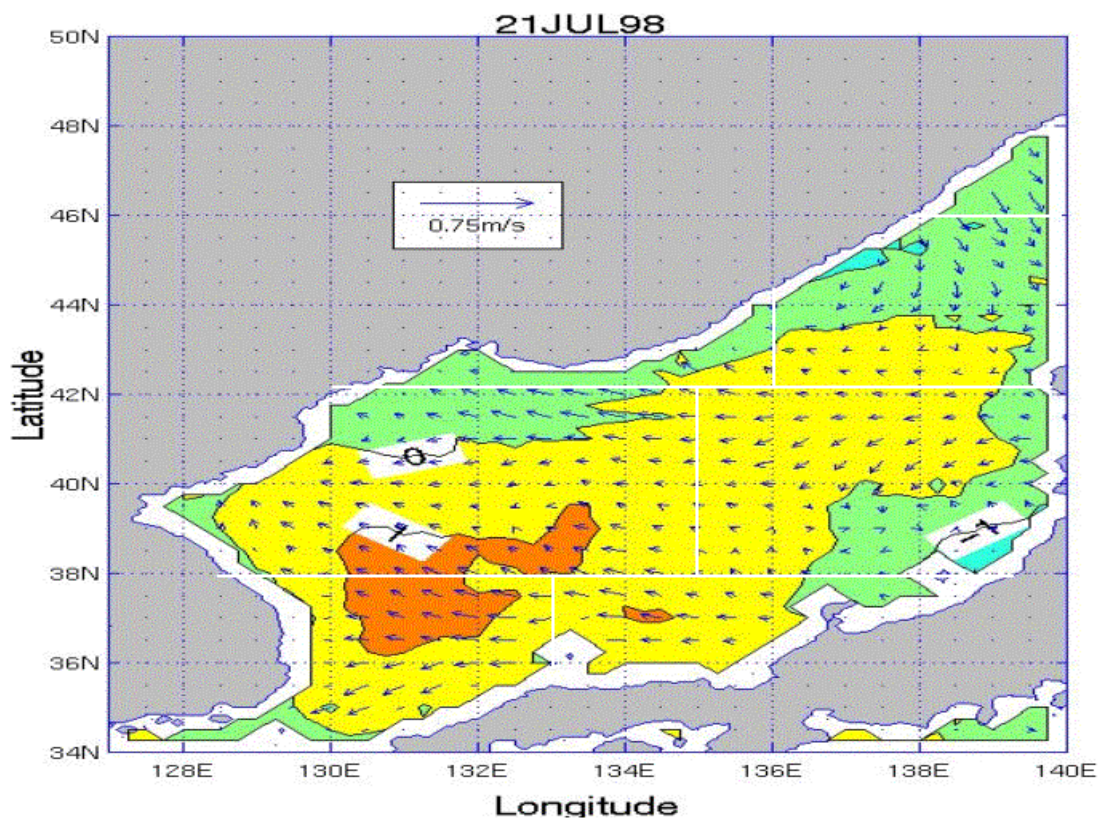
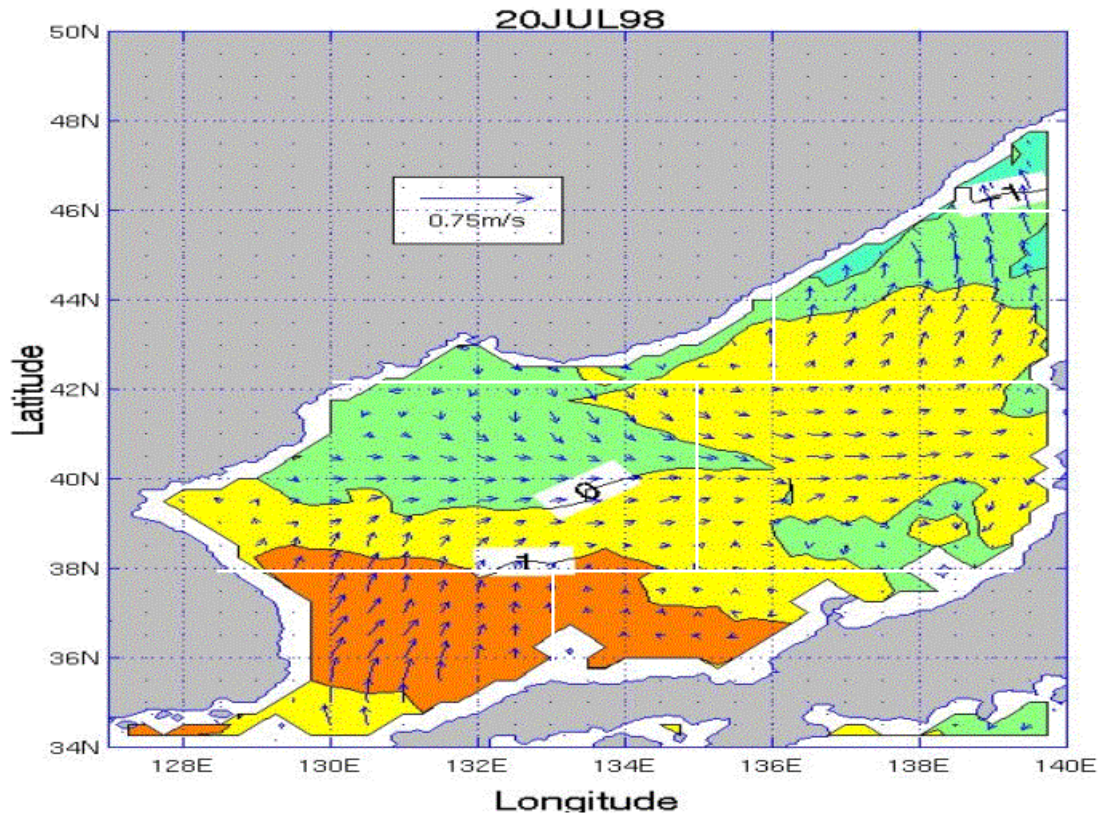


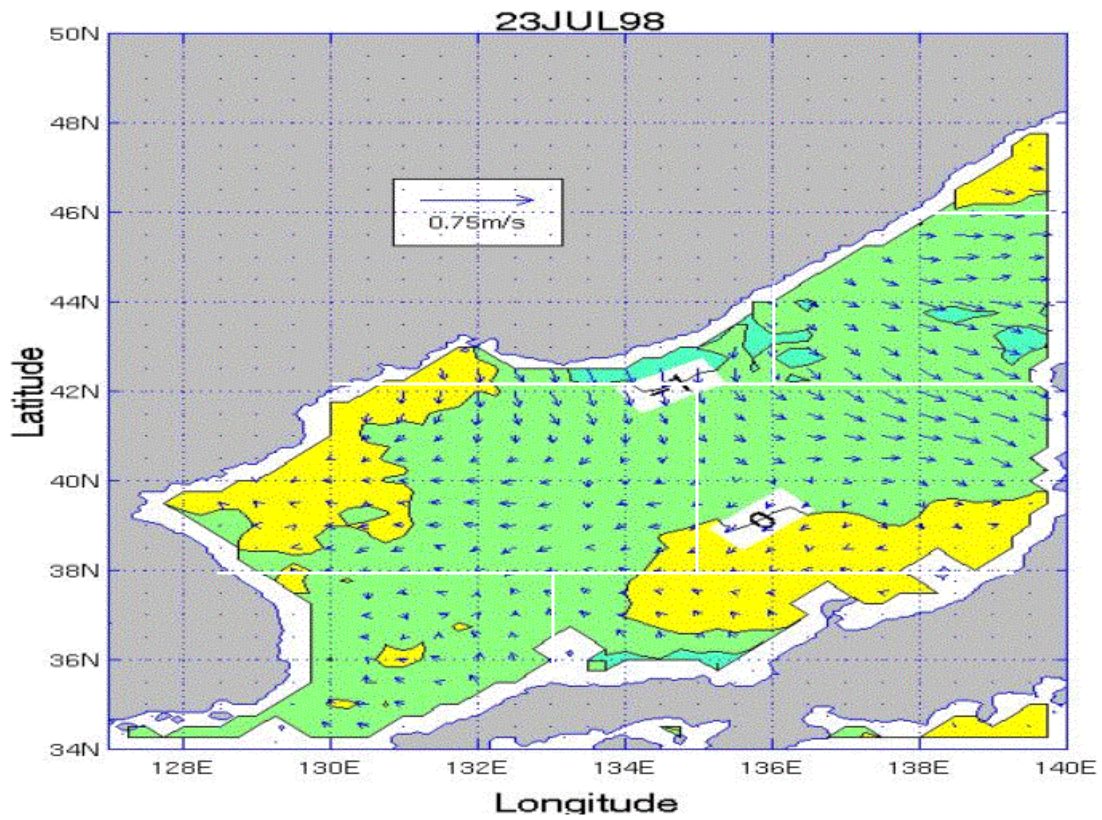
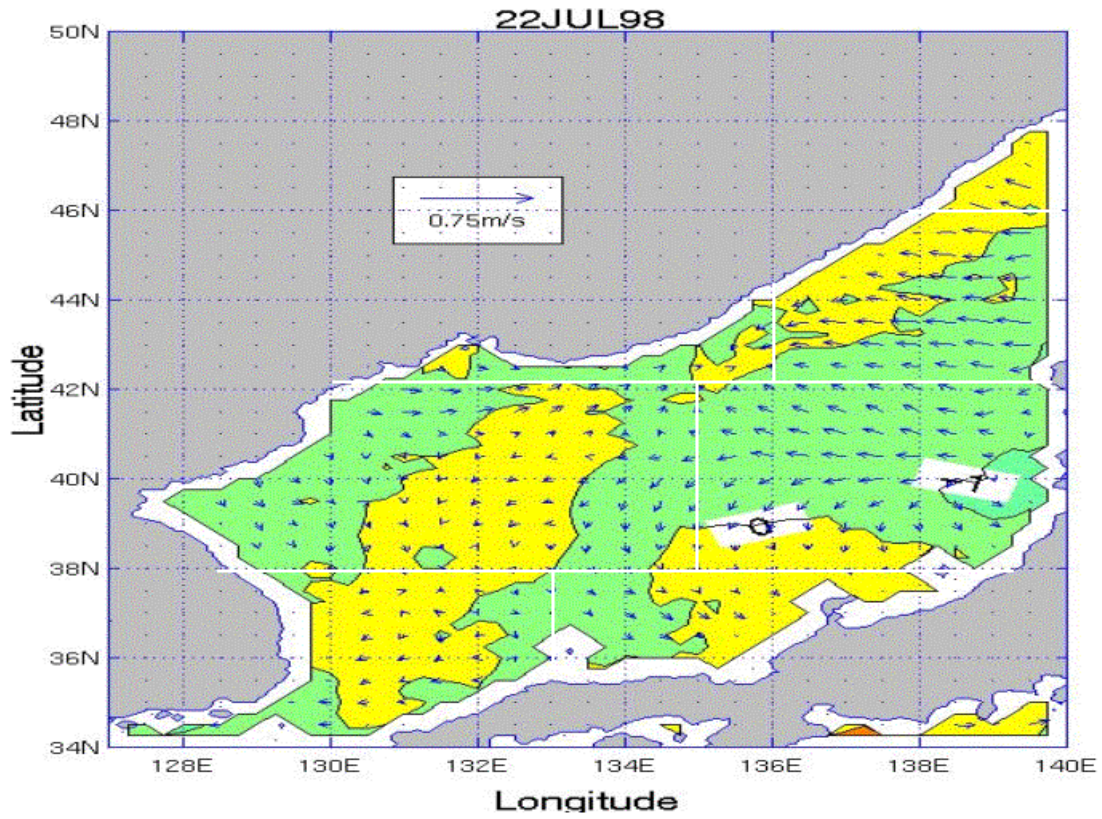


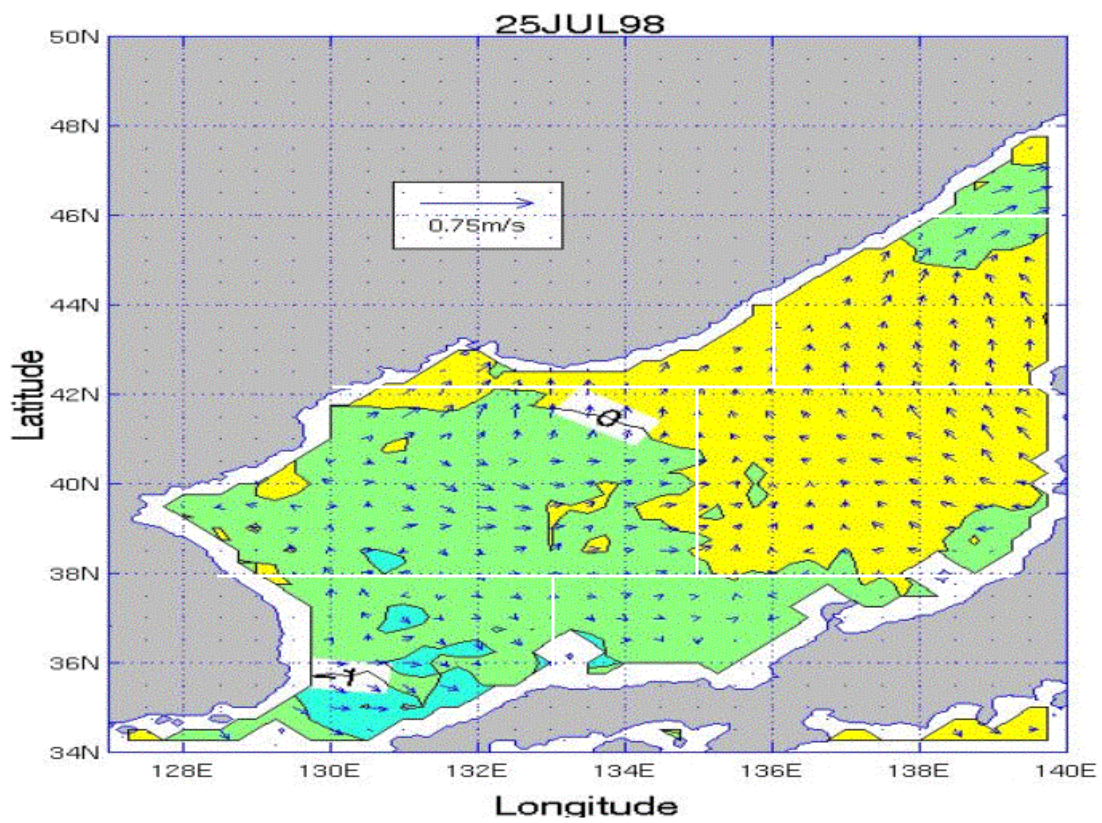
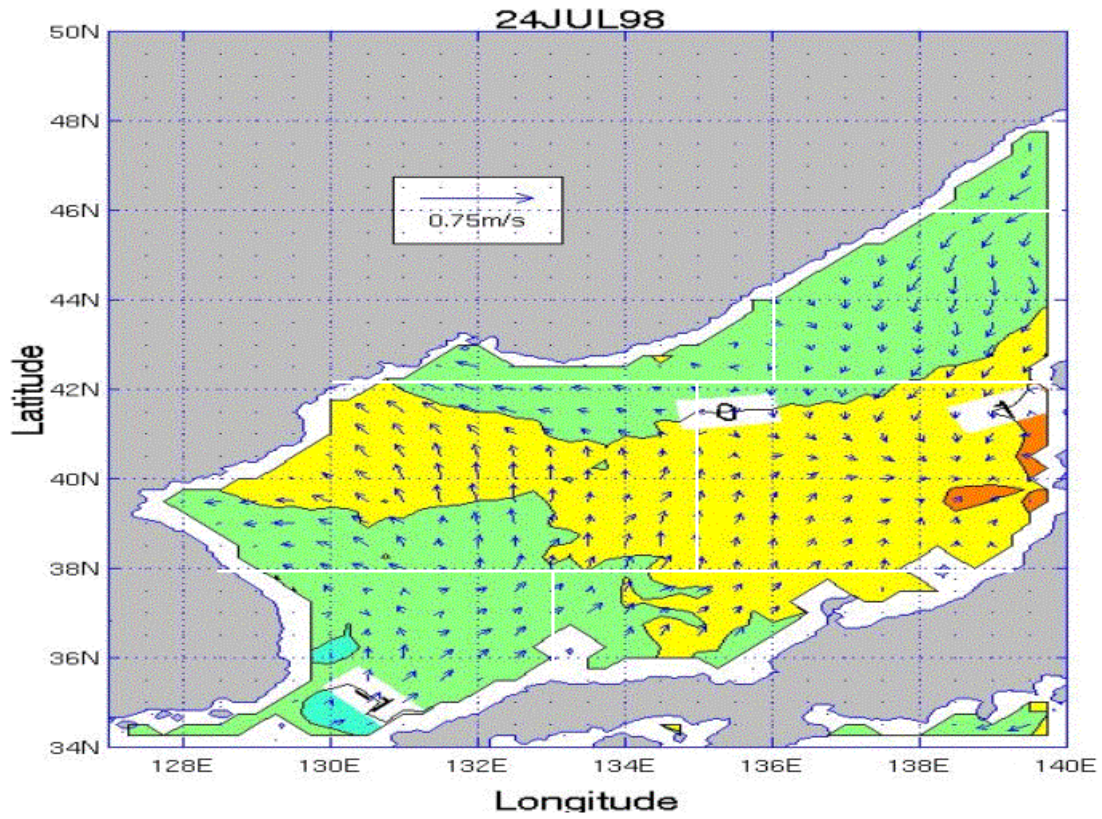
APPENDIX NN. SST AND SURFACE CURRENT VELOCITY TENDENCY PLOTS FOR THE JES FOR THE JULY TIME PERIOD

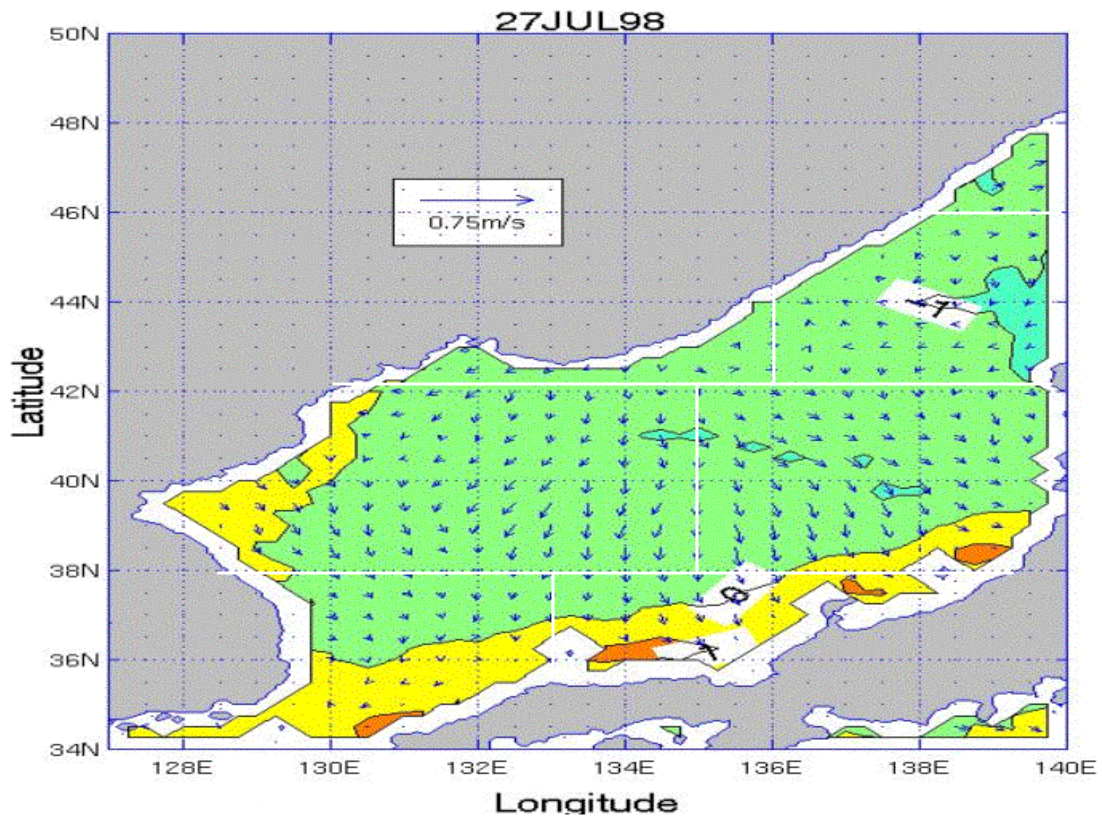
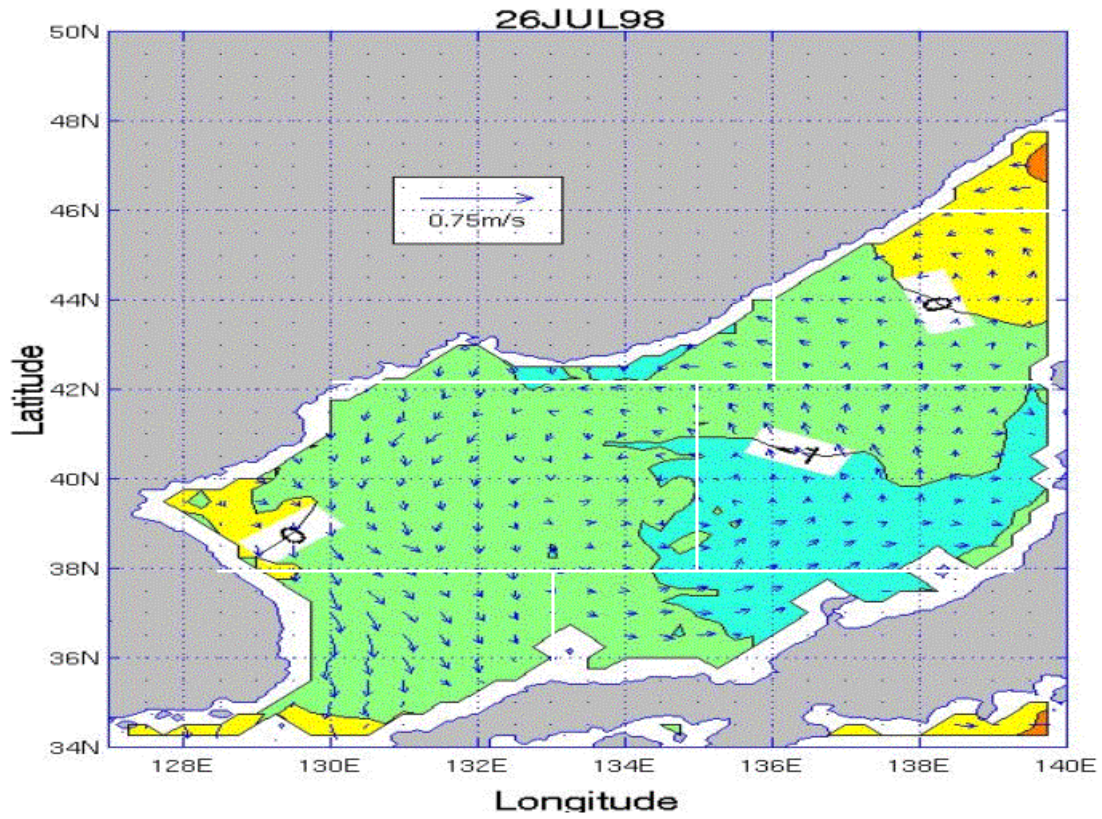
Appendix NN consists of 13 figures that show SST and surface current velocity day-to-day tendency for the July time period over the JES. The figures are in time sequential order from July 19 through July 31. Each plot represents the change between the previous day and the current day.

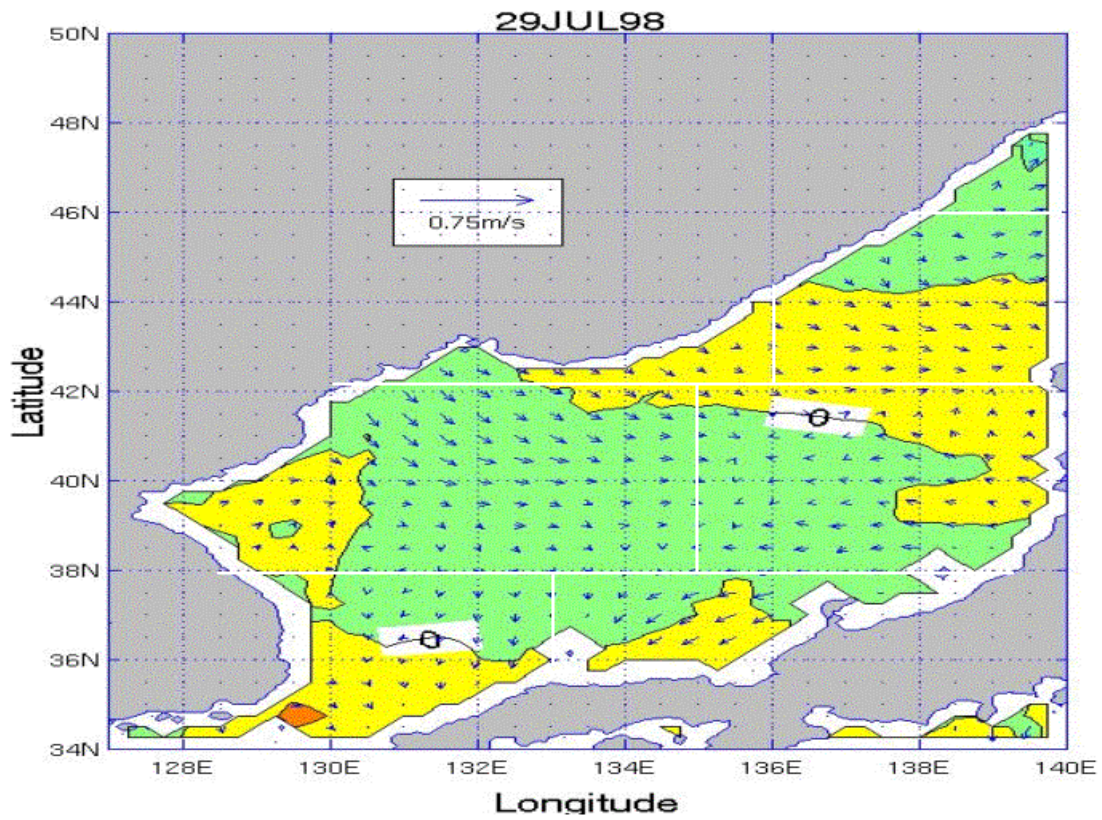
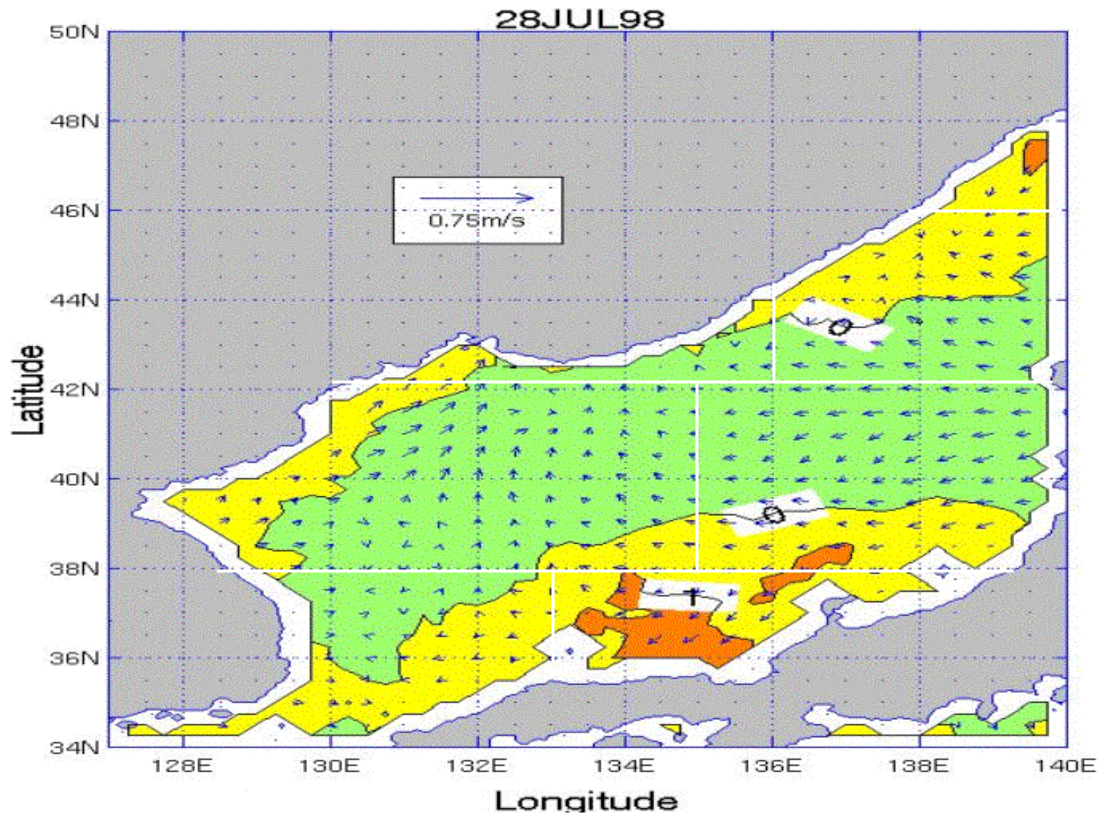


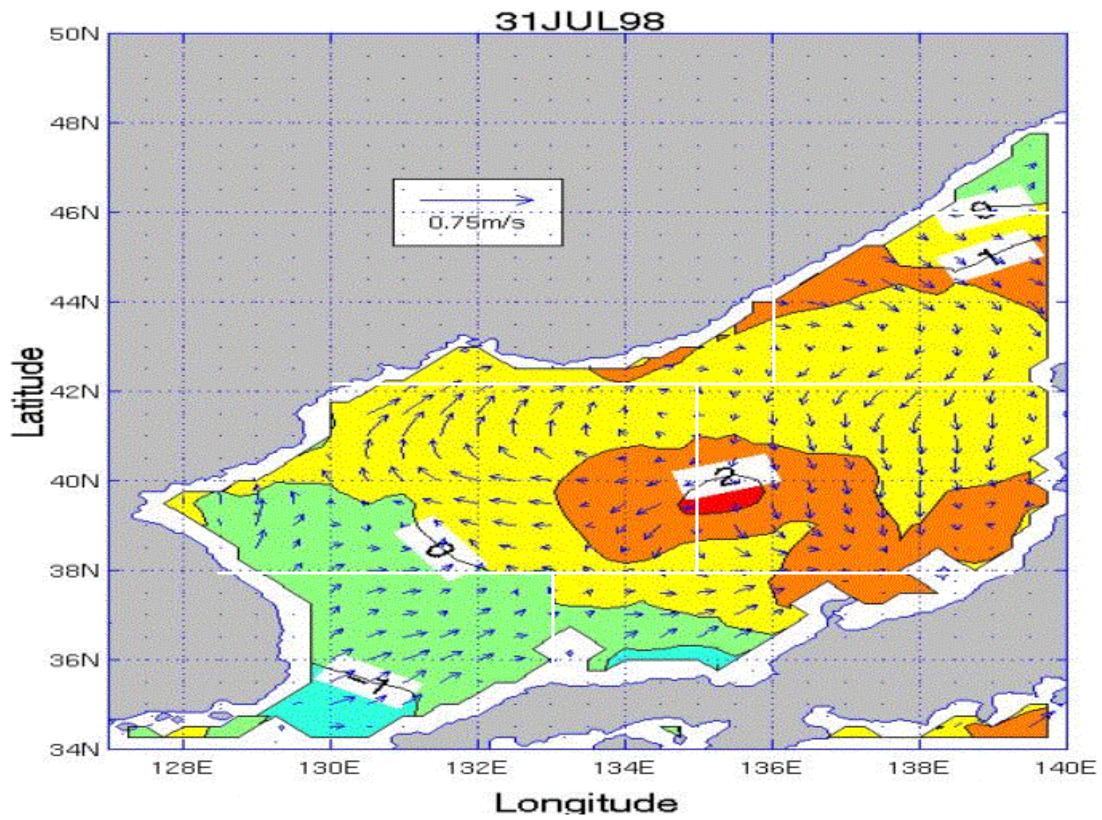
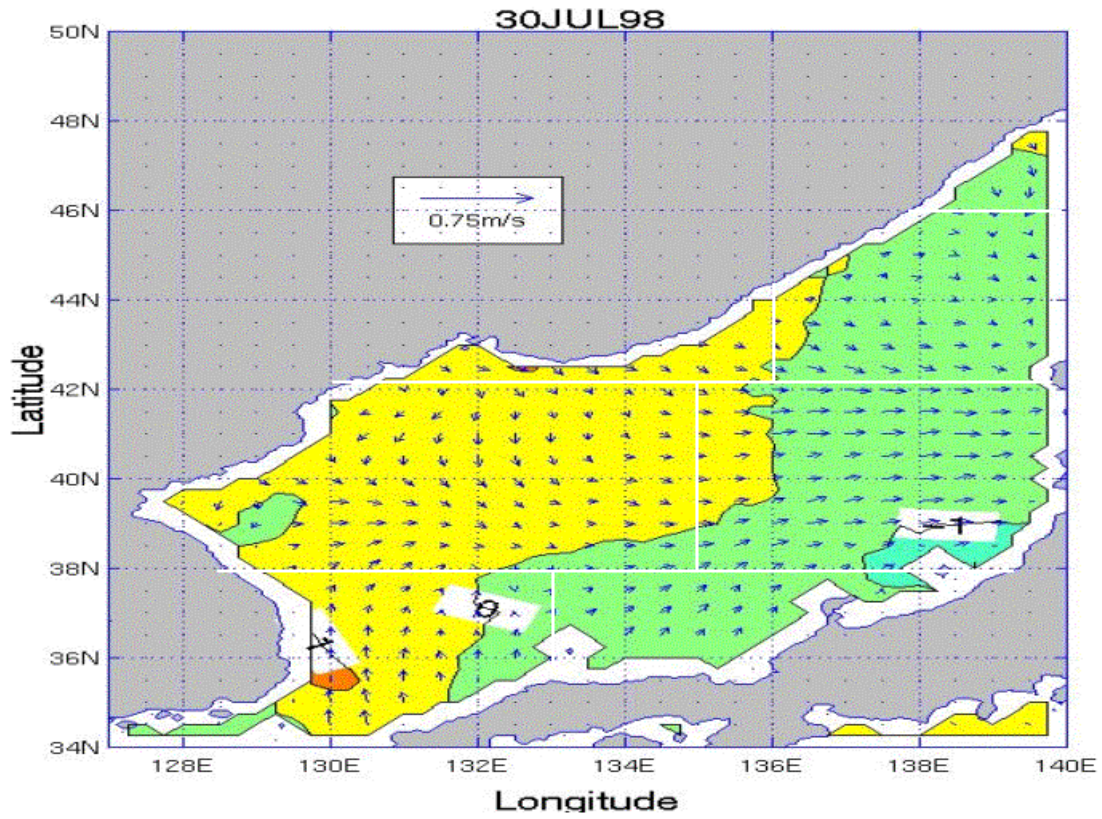








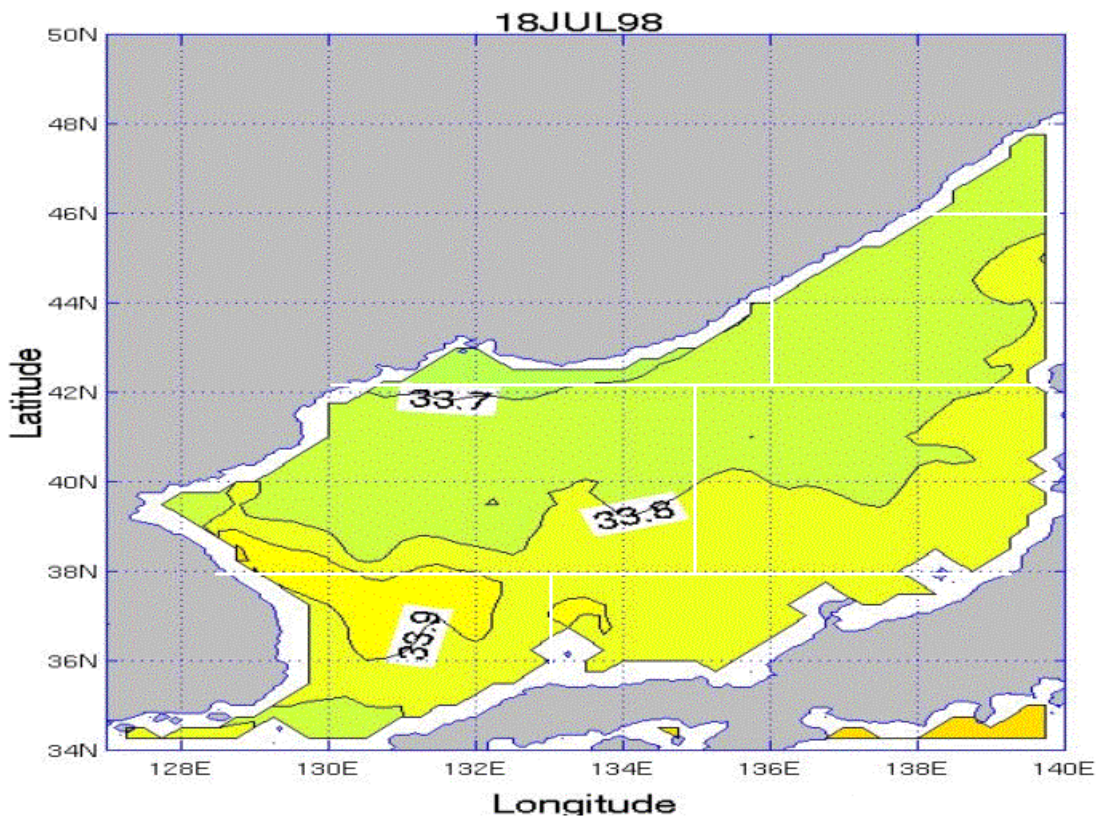


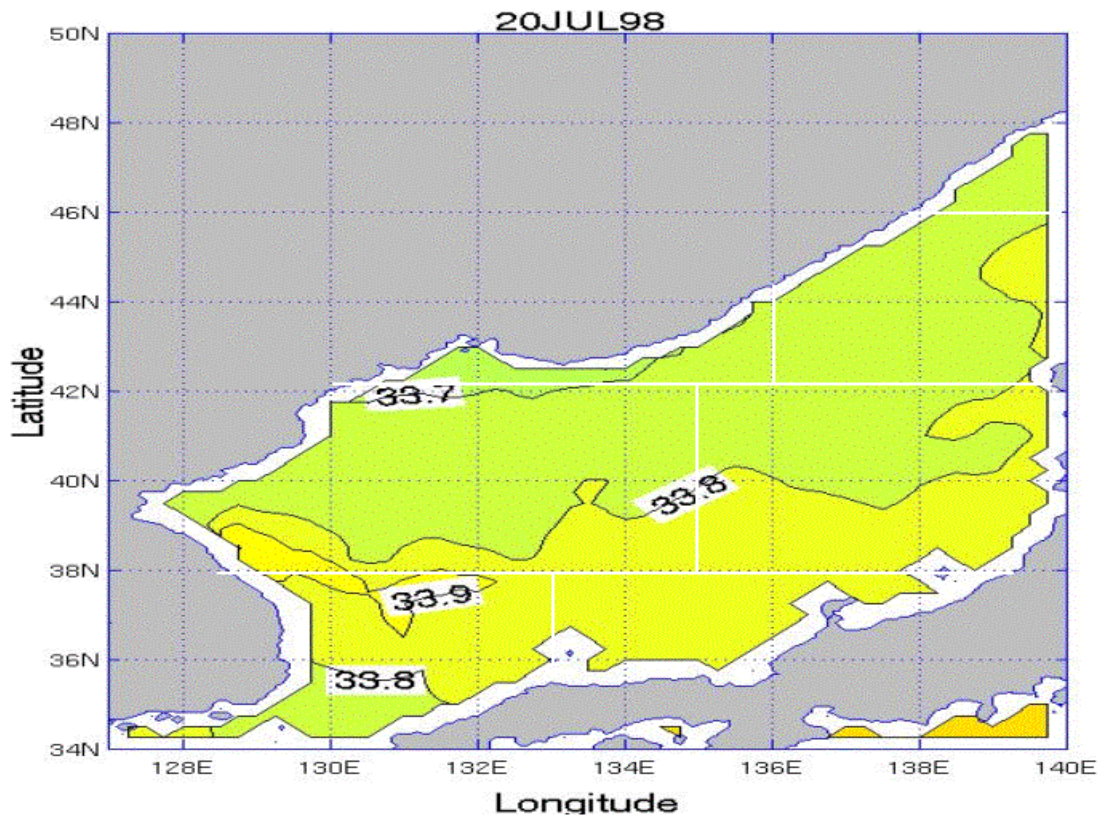
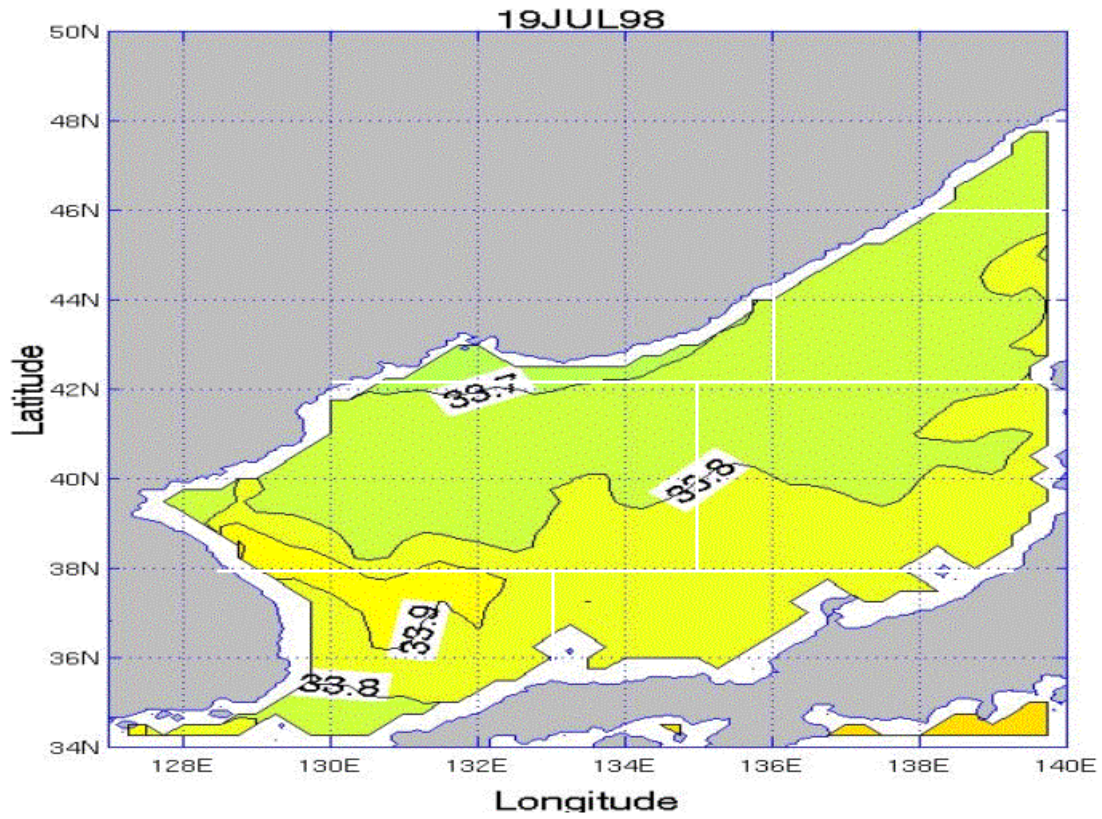


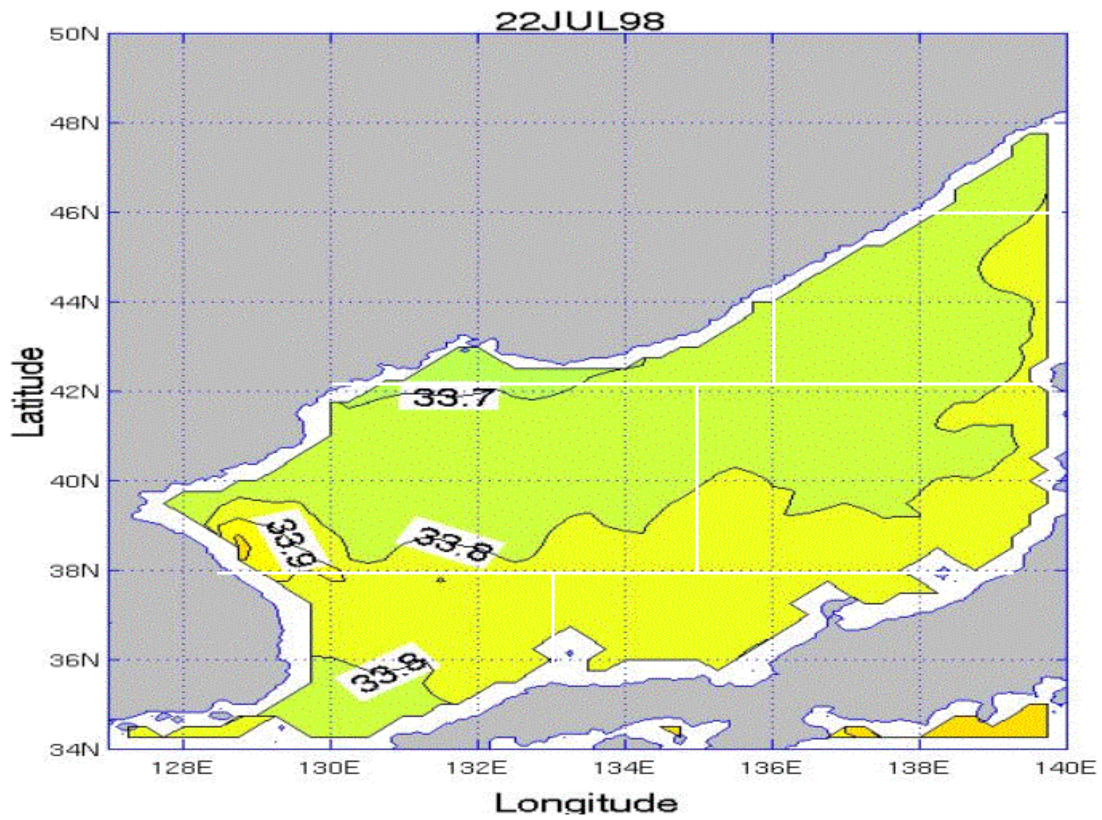
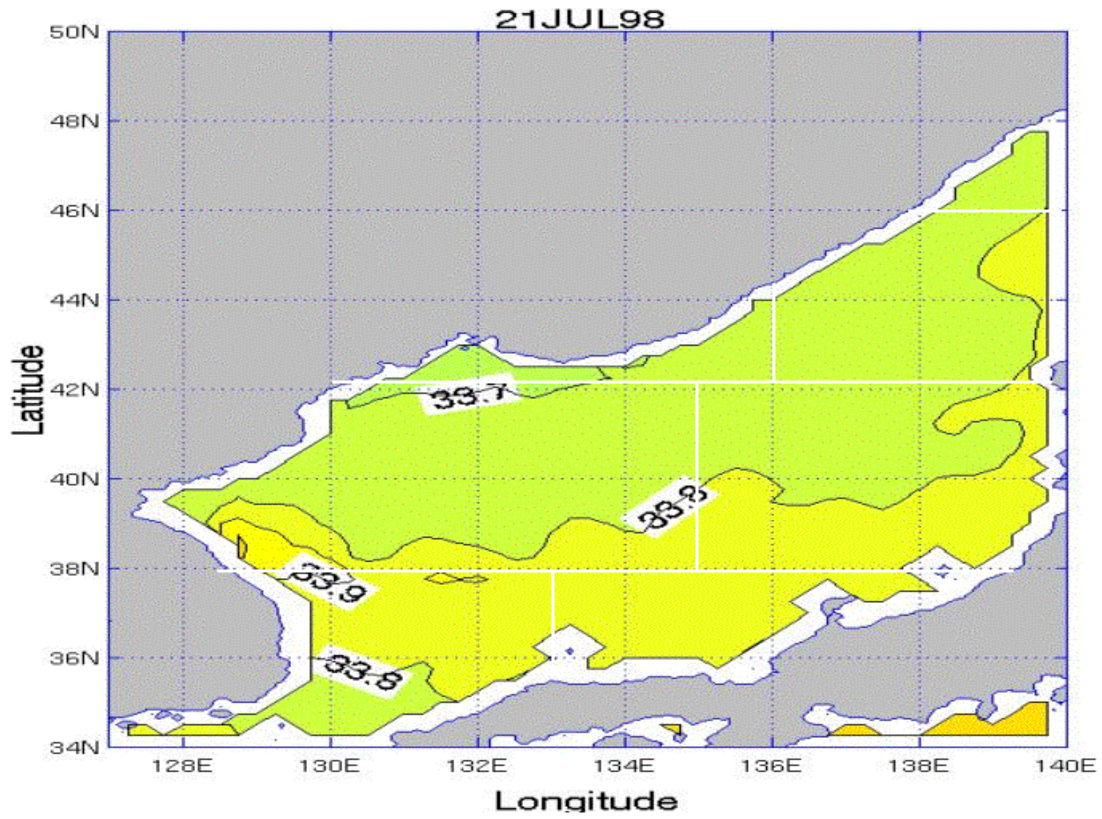
THIS PAGE INTENTIONALLY LEFT BLANK

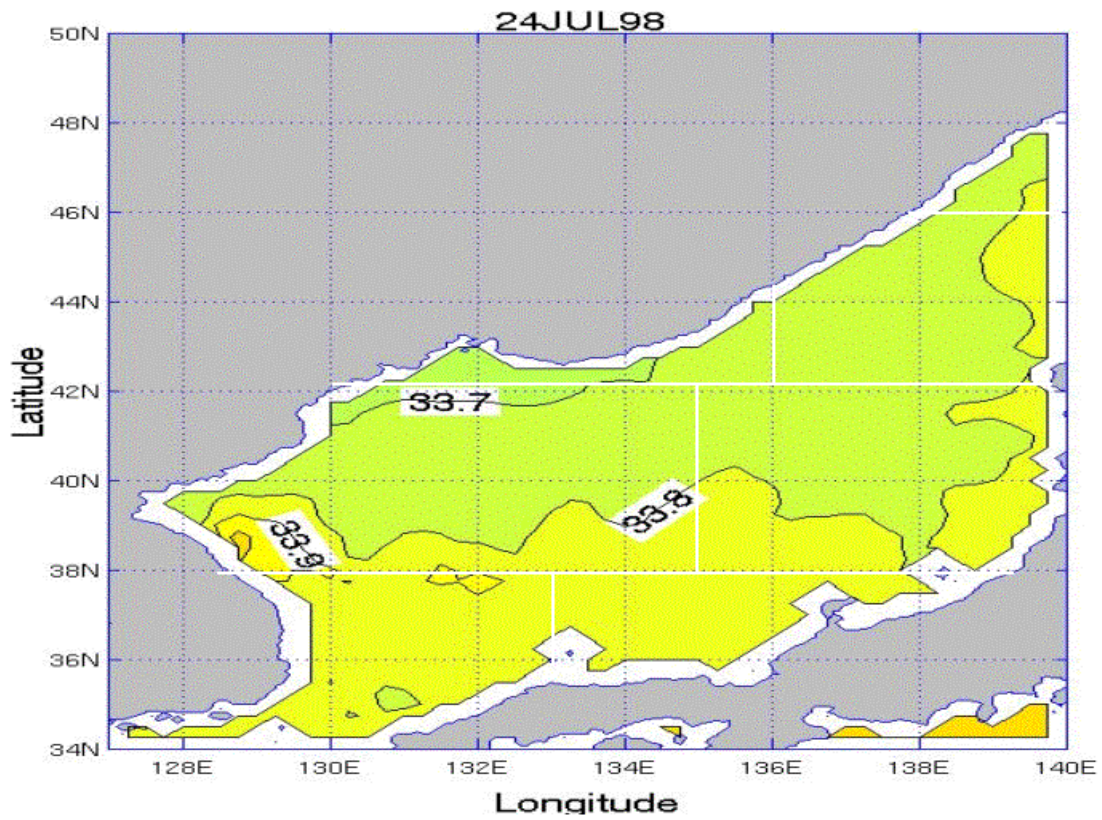
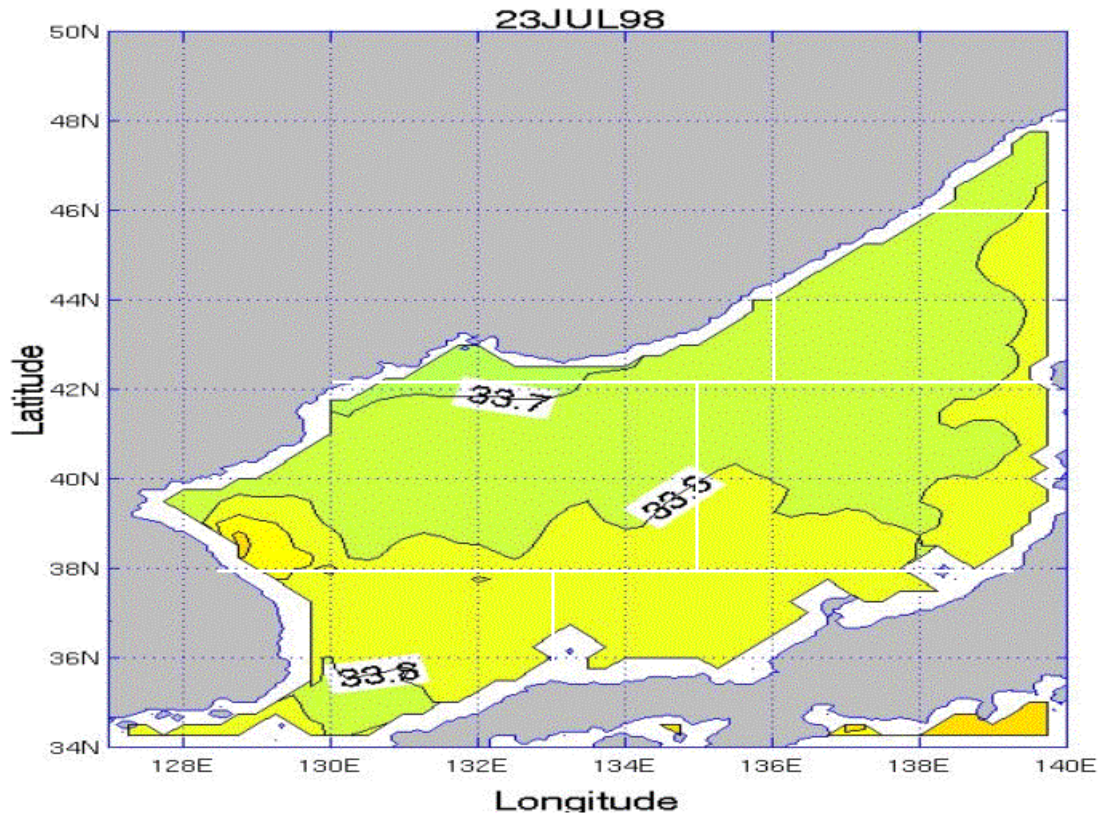
APPENDIX OO. SSS PLOTS FOR THE JES FOR THE JULY TIME PERIOD

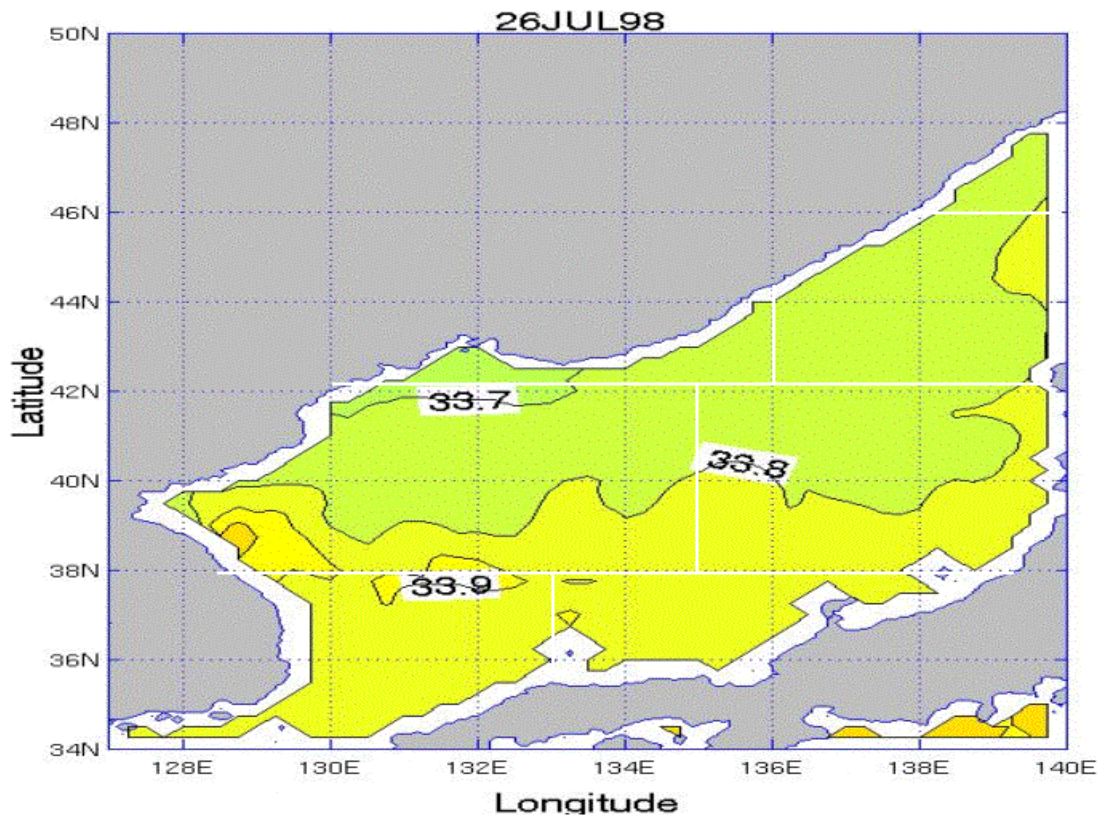
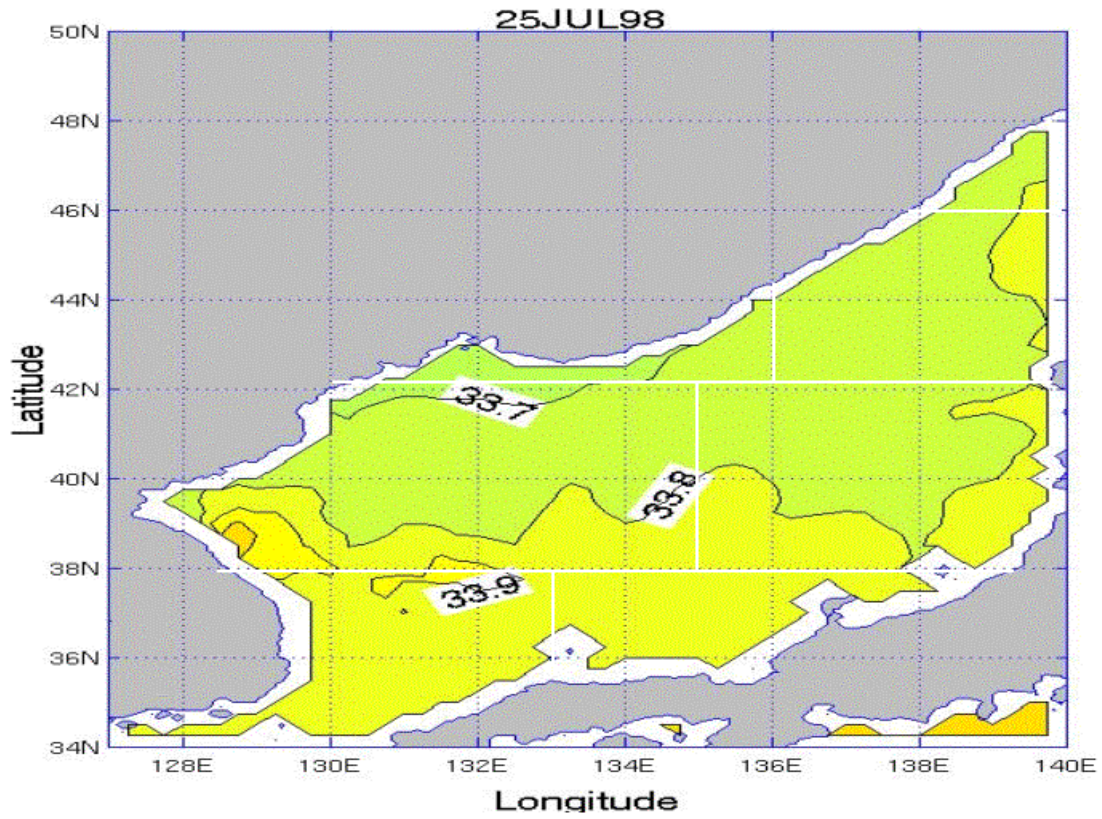
Appendix OO consists of 14 figures that show SSS for each day of the July time period for the JES. The figures are in time sequential order from July 18 through July 31.

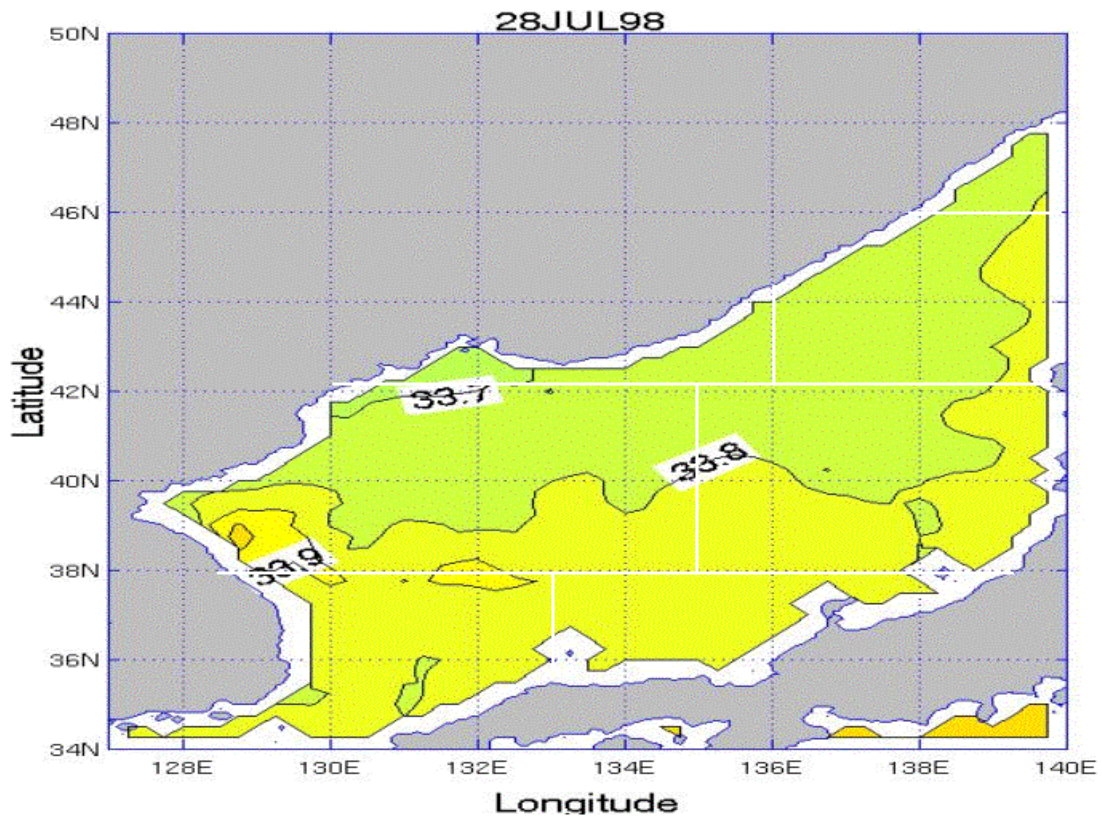
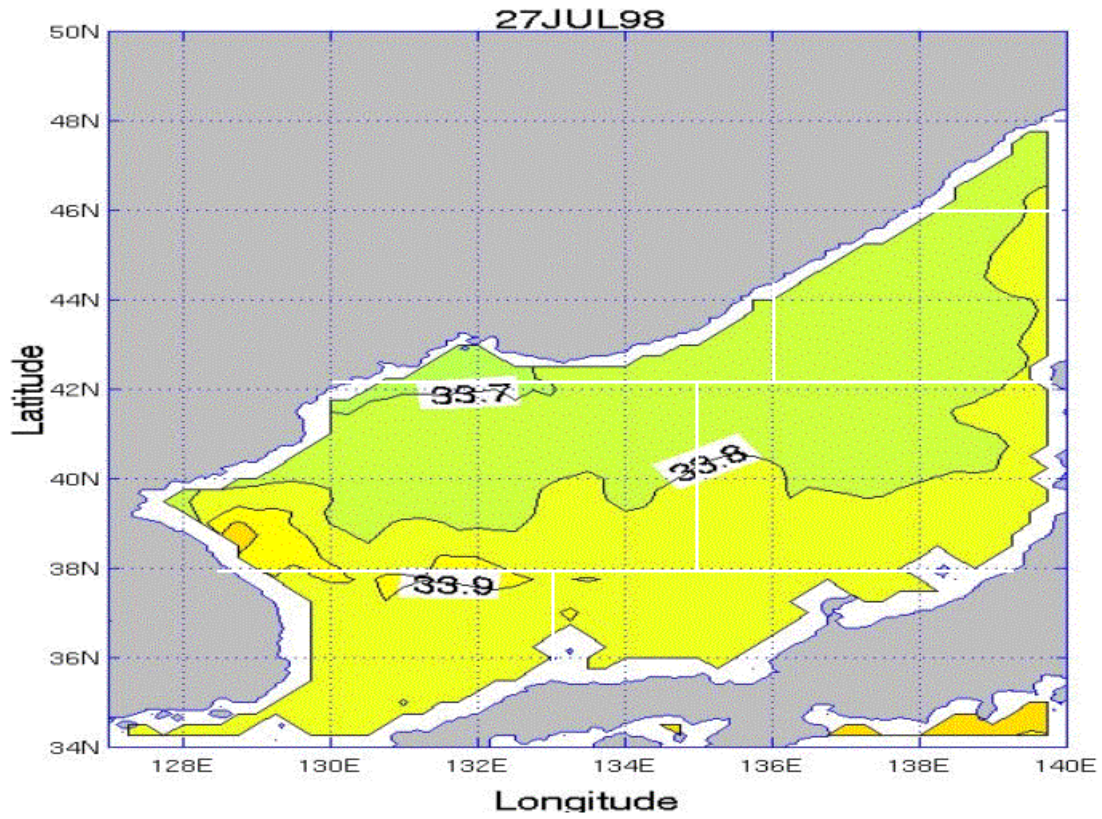


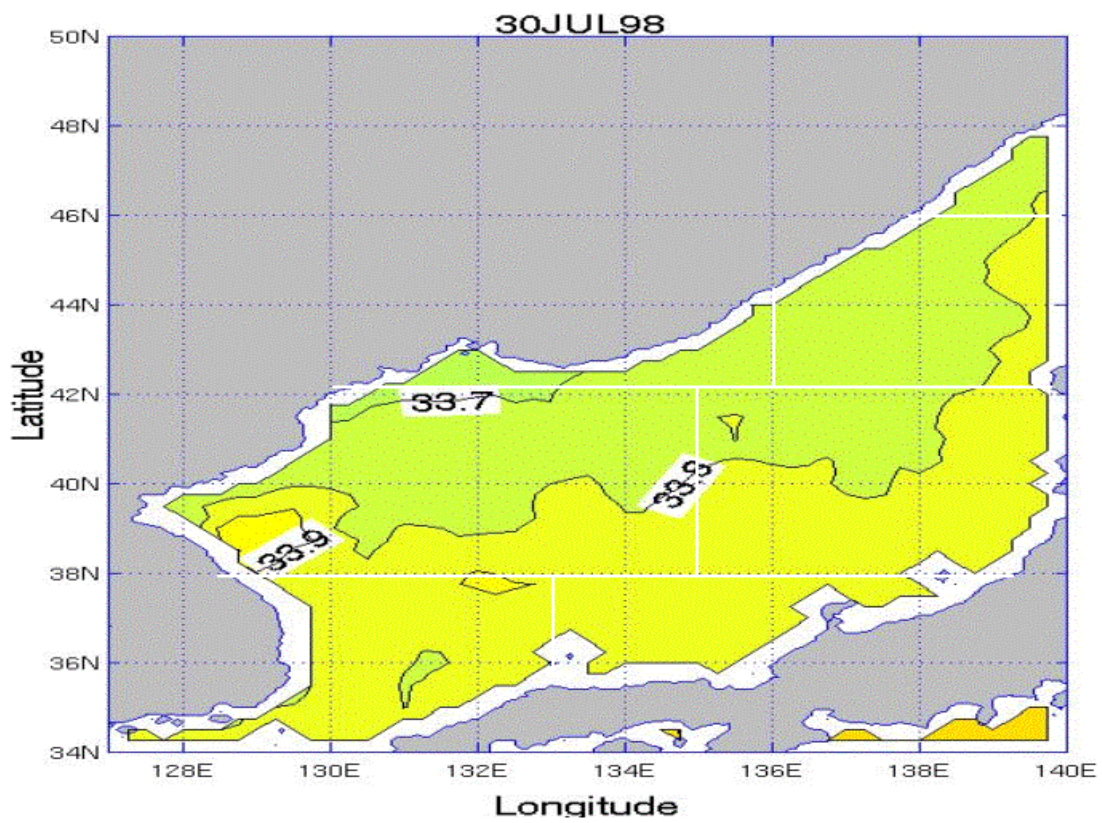
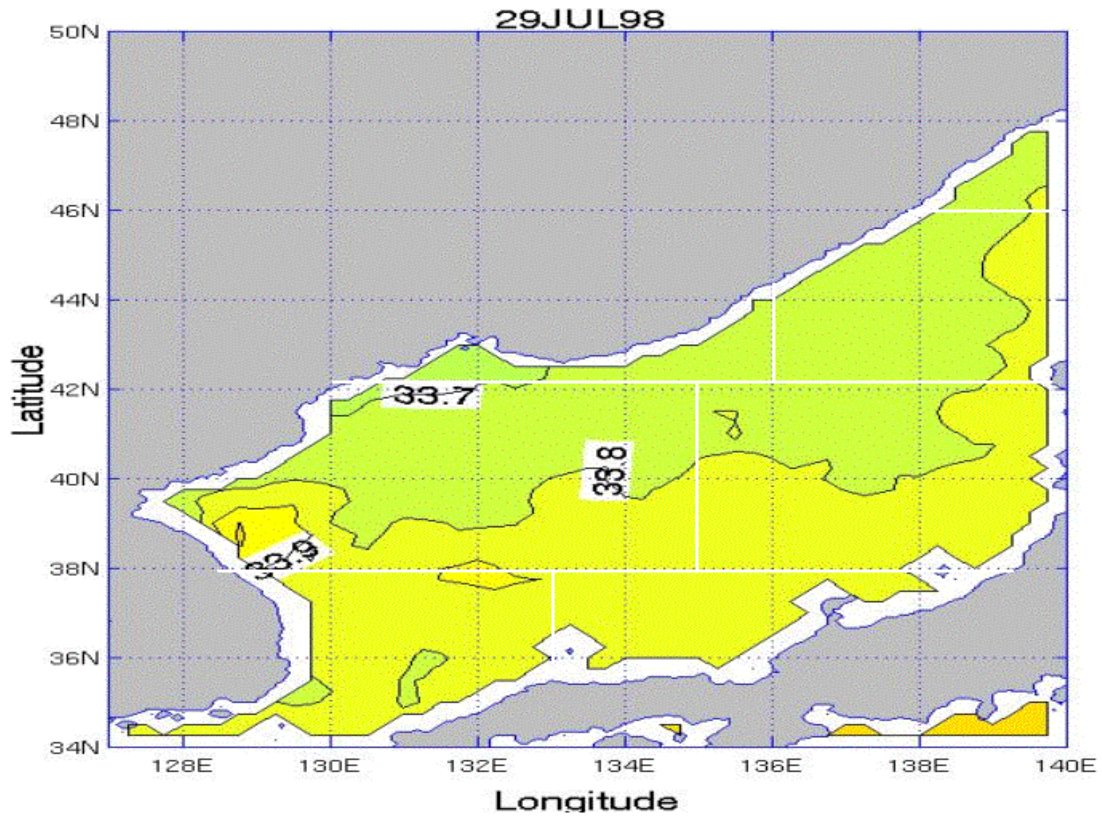


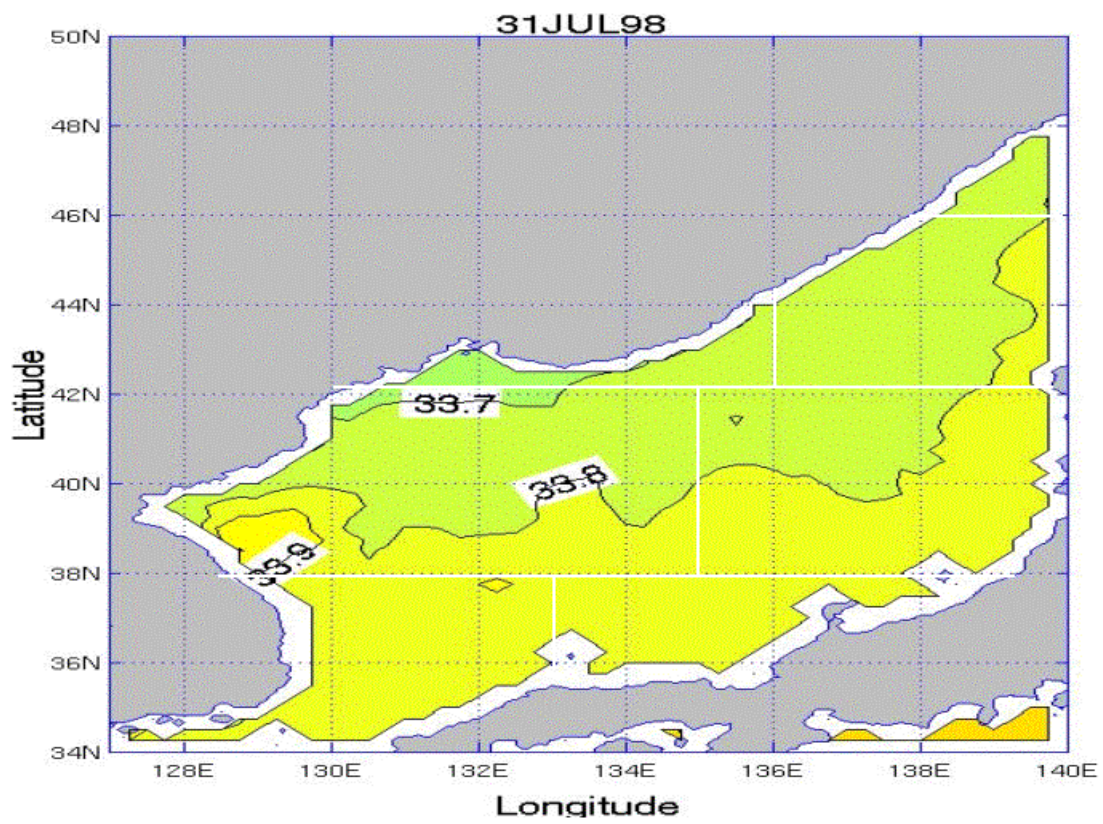






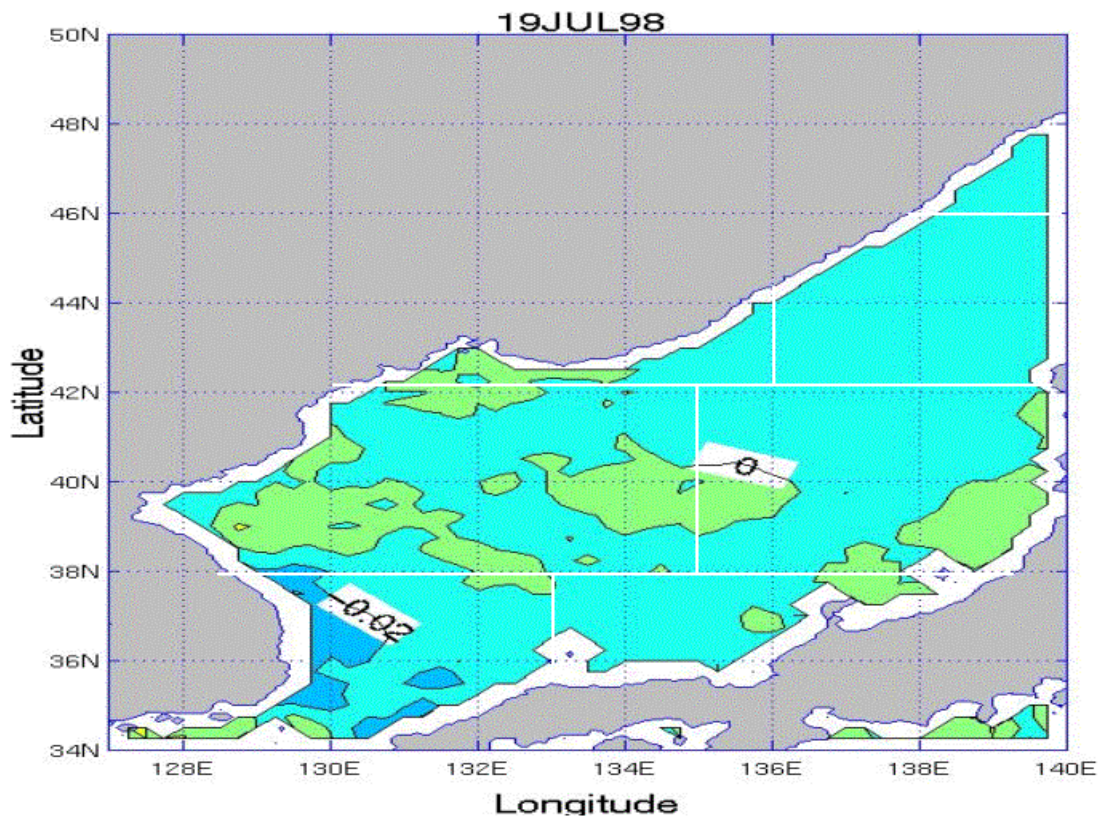


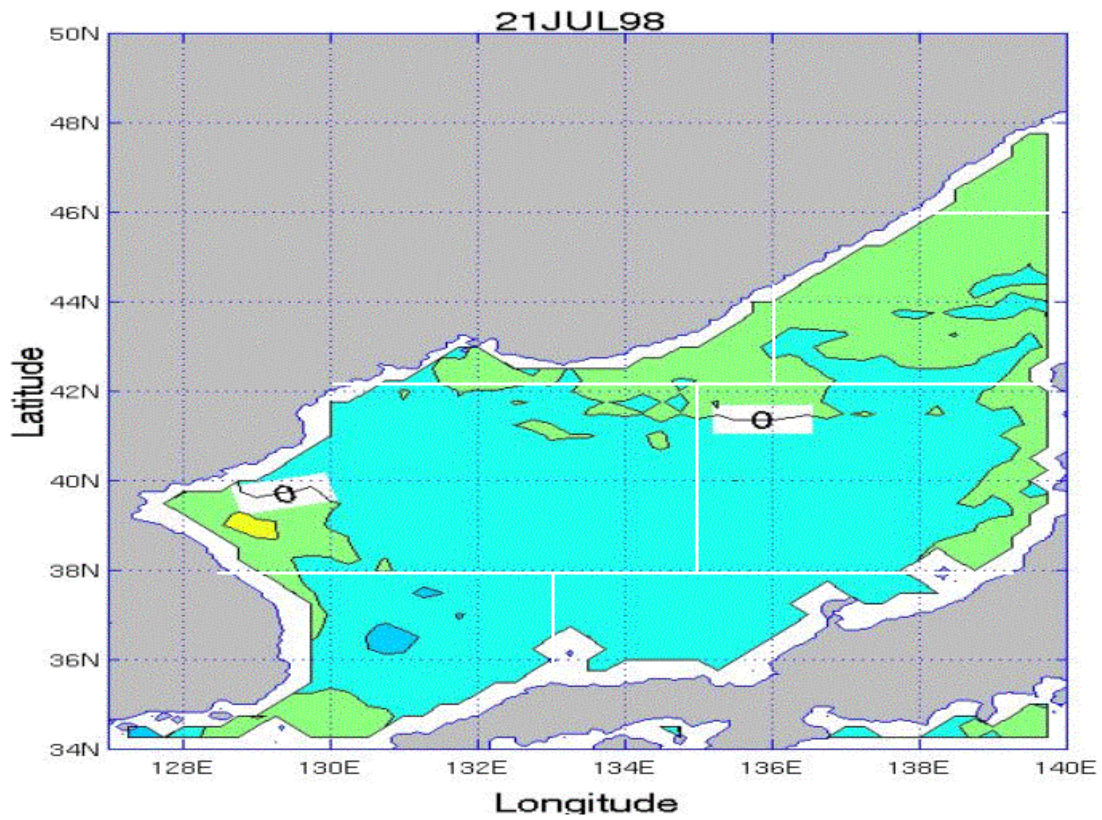
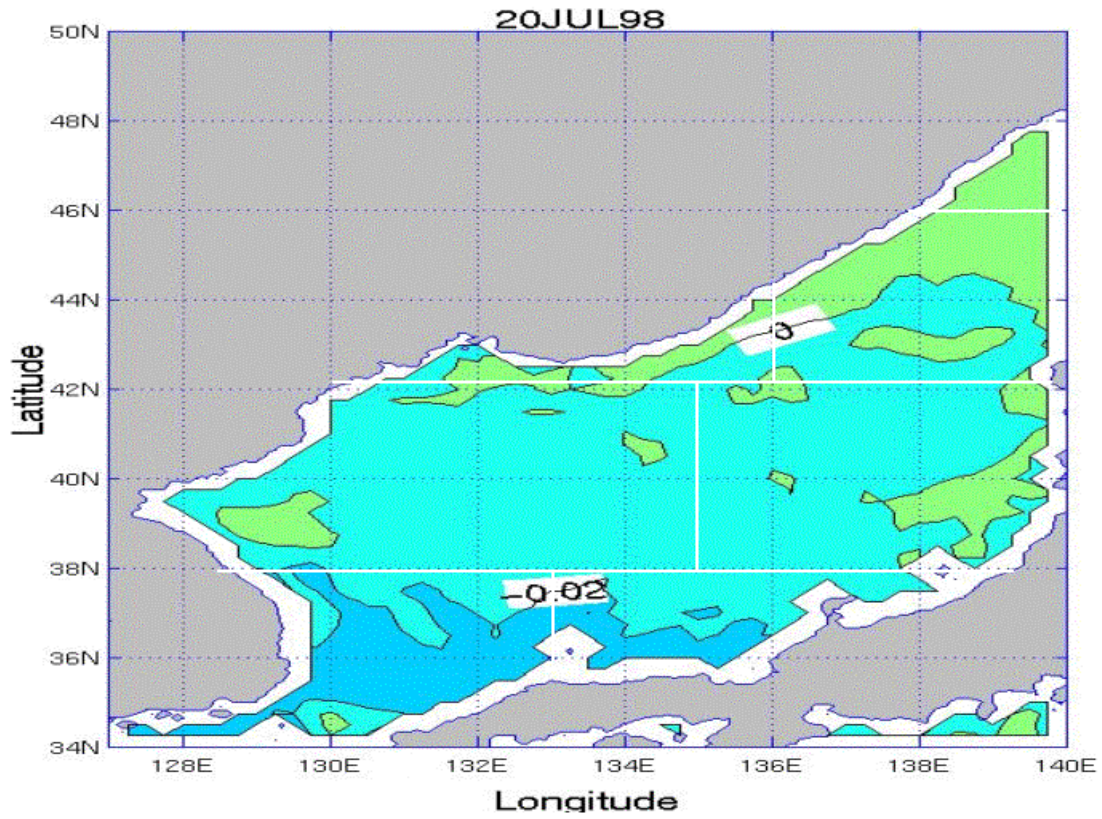


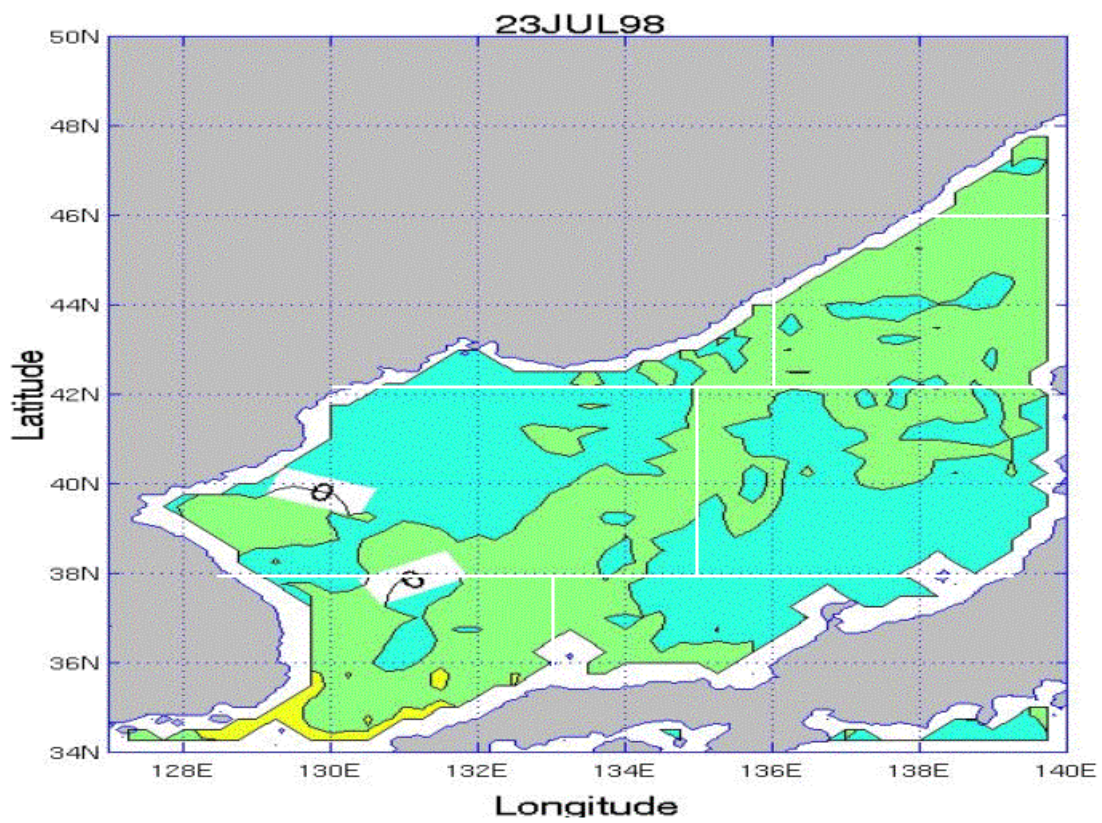
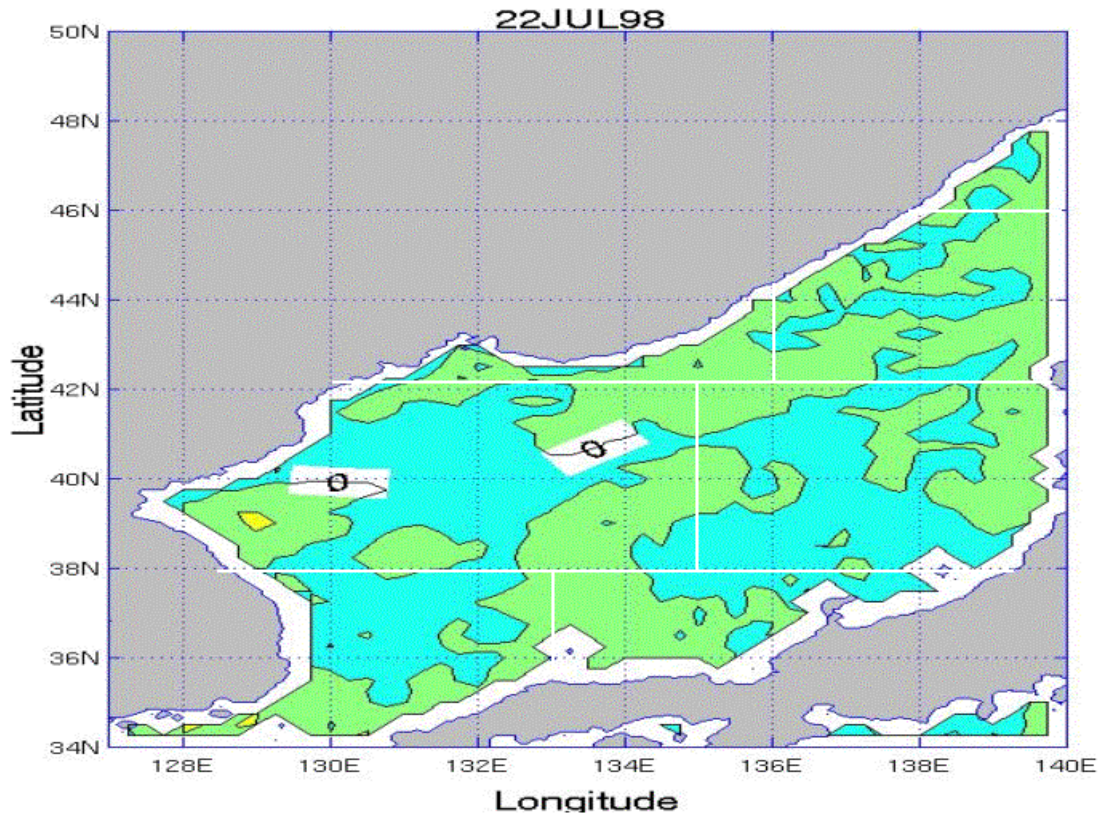


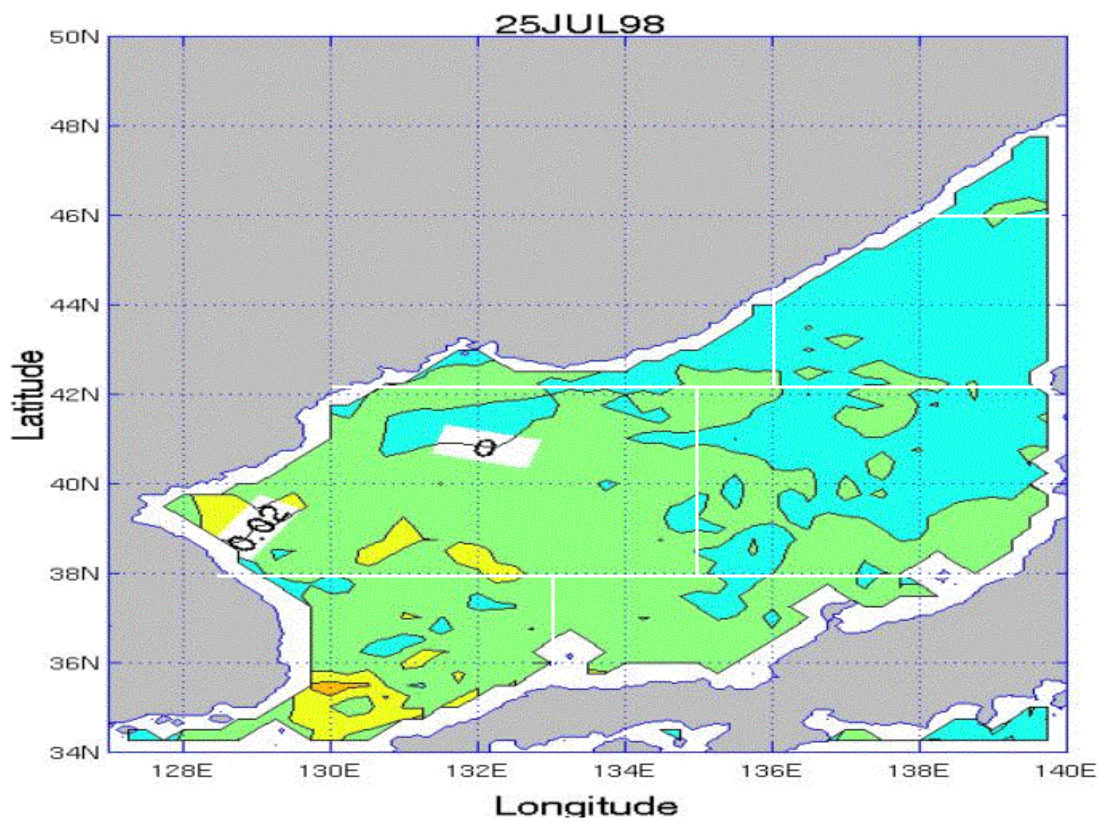
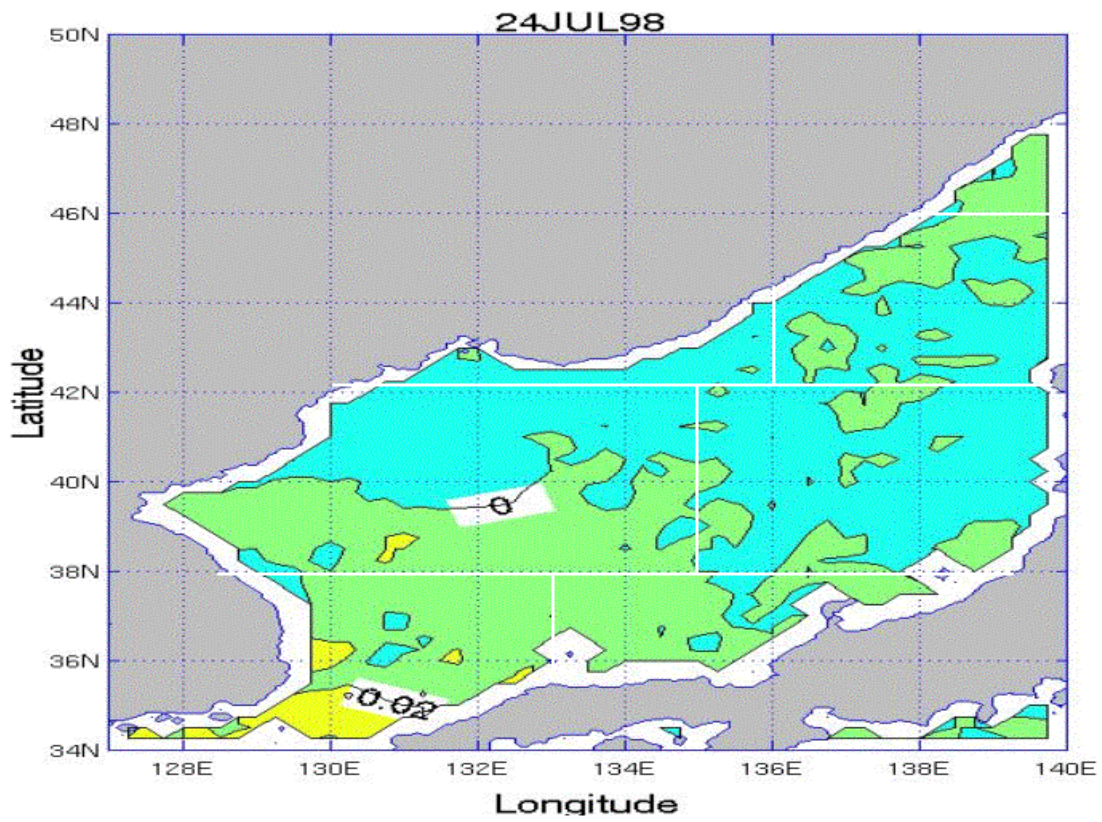
APPENDIX PP. SSS TENDENCY PLOTS FOR THE JES FOR THE JULY TIME PERIOD

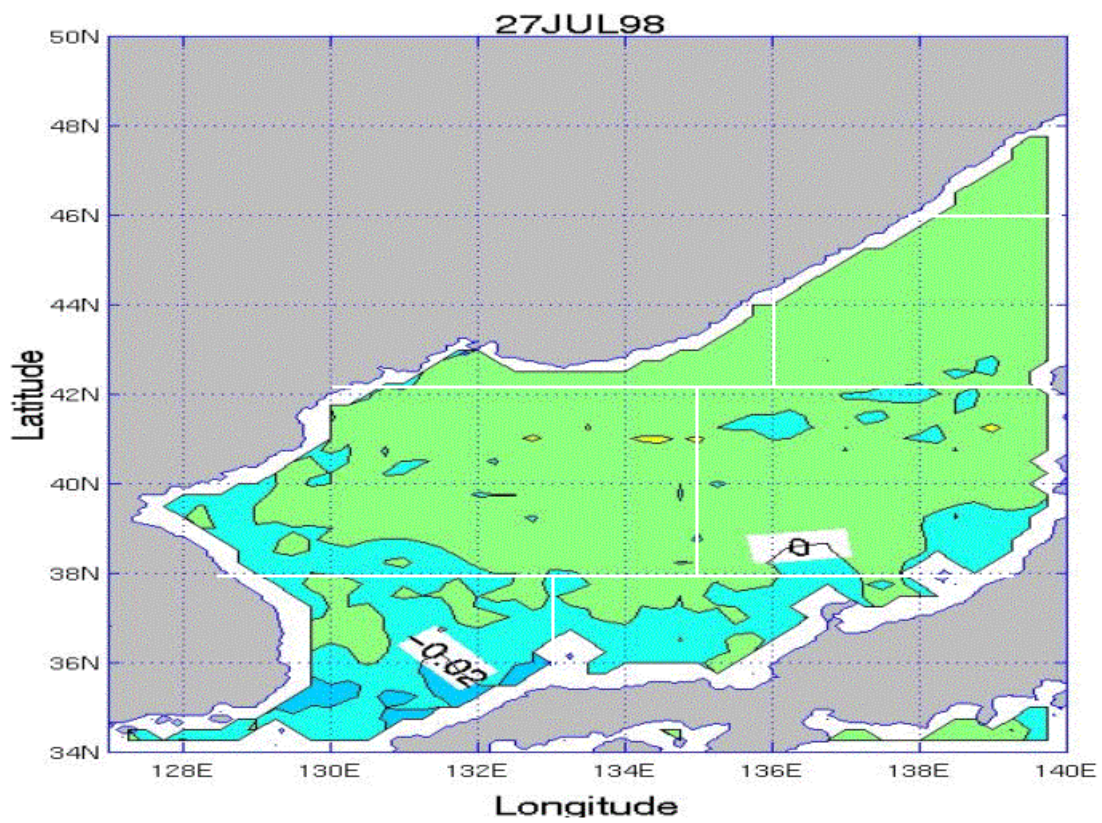
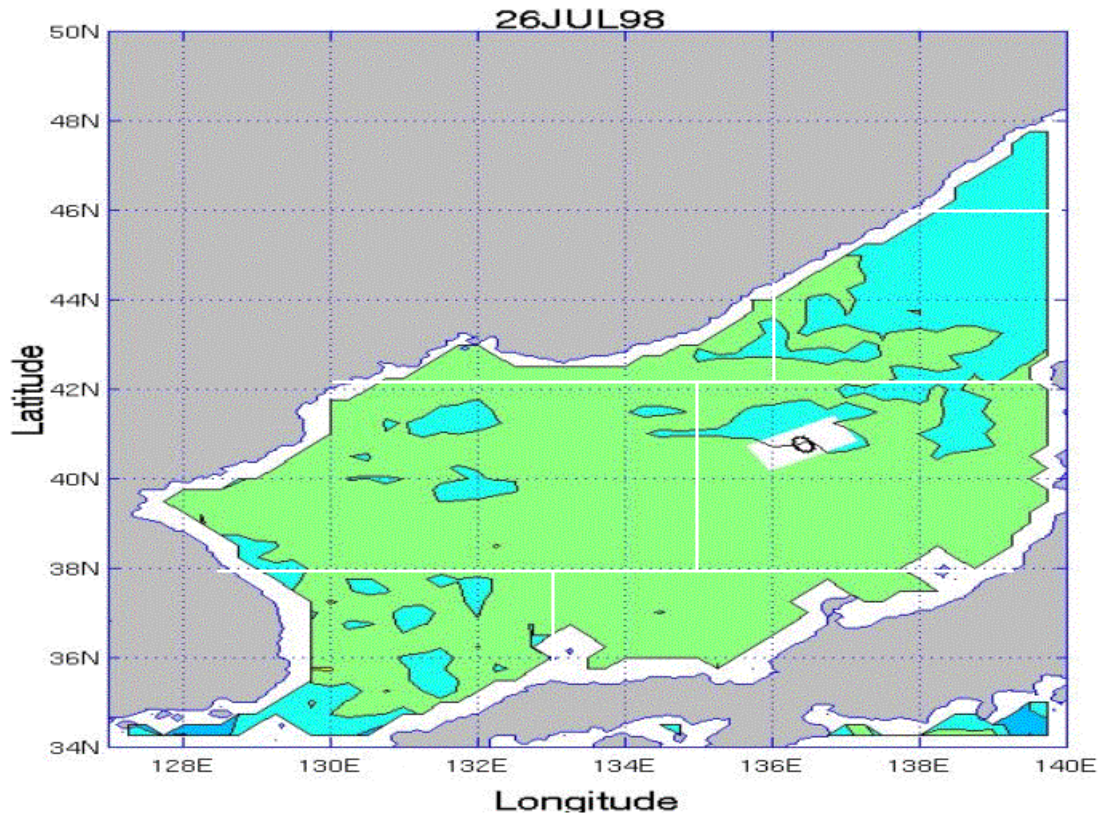
Appendix PP consists of 13 figures that show SSS day-to-day tendency for the July time period over the JES. The figures are in time sequential order from July 19 through July 31. Each plot represents the change between the previous day and the current day.

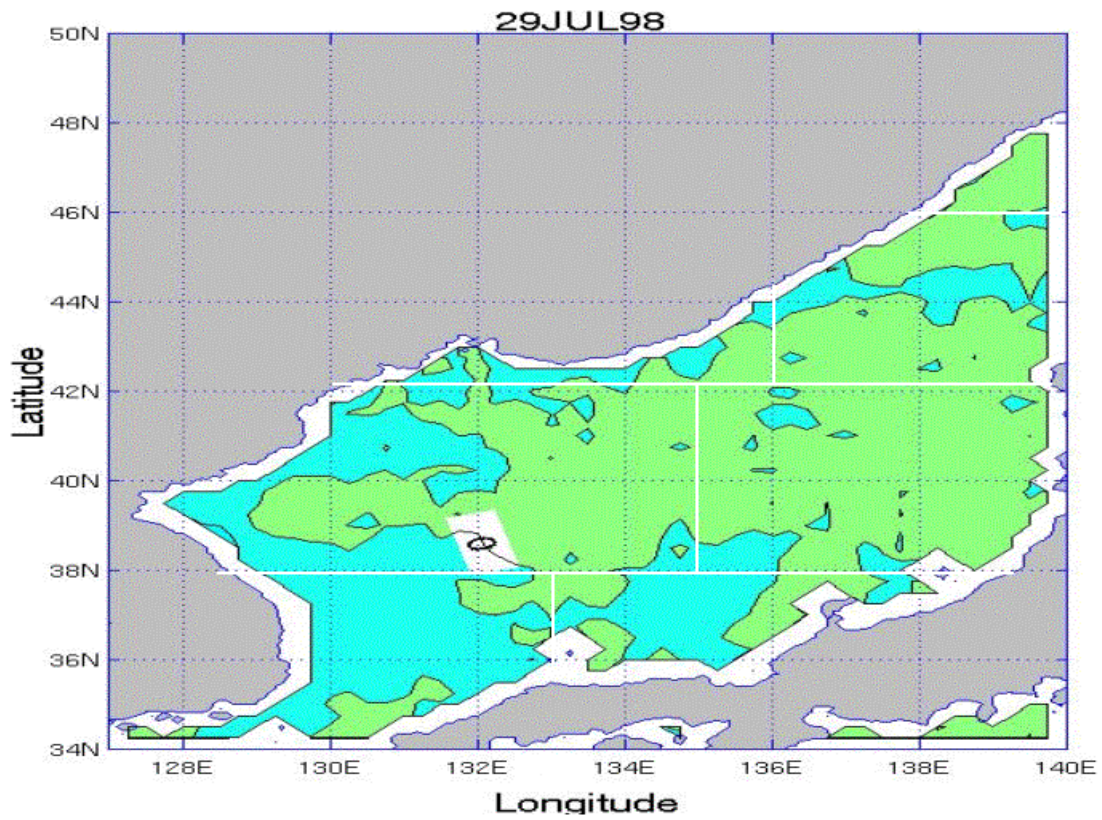
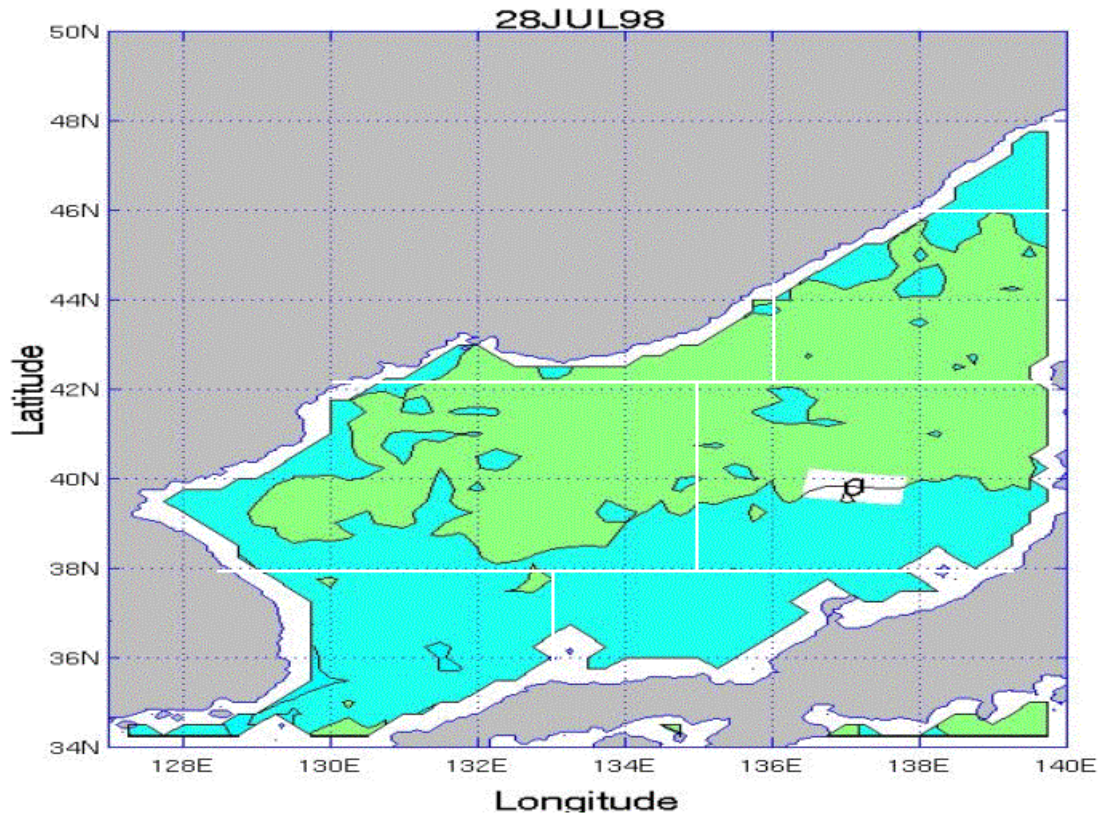


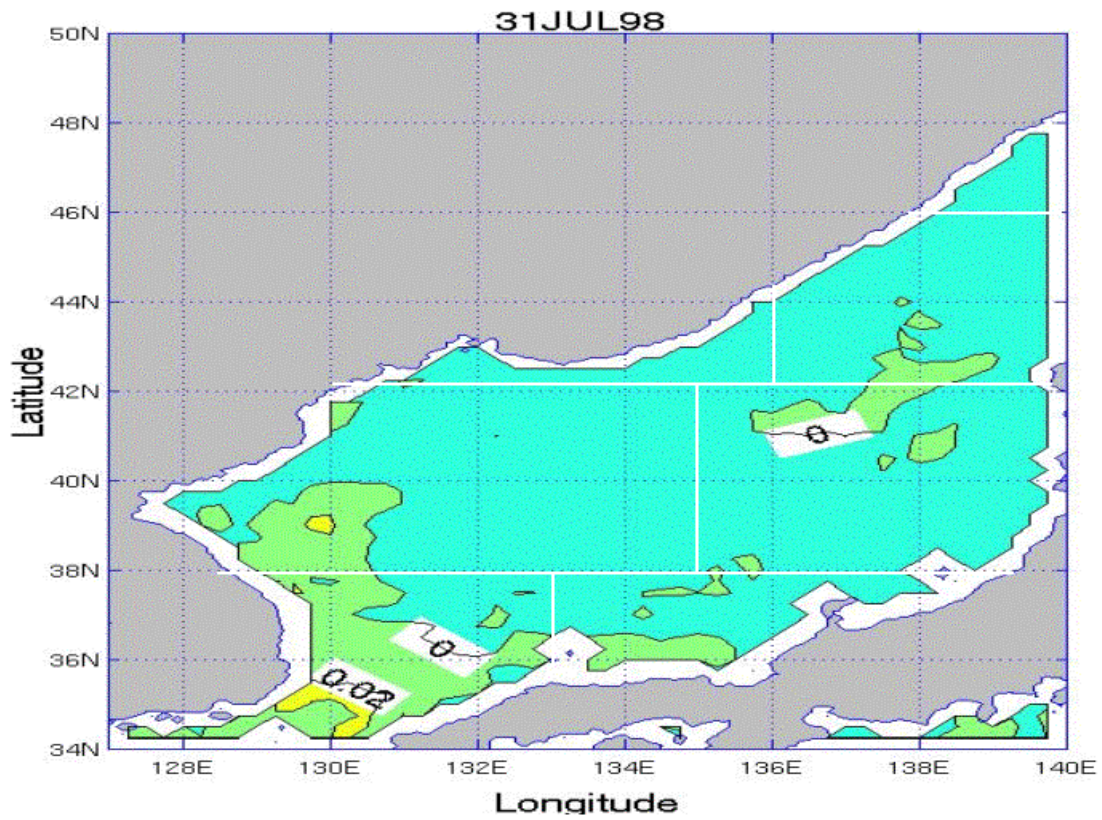
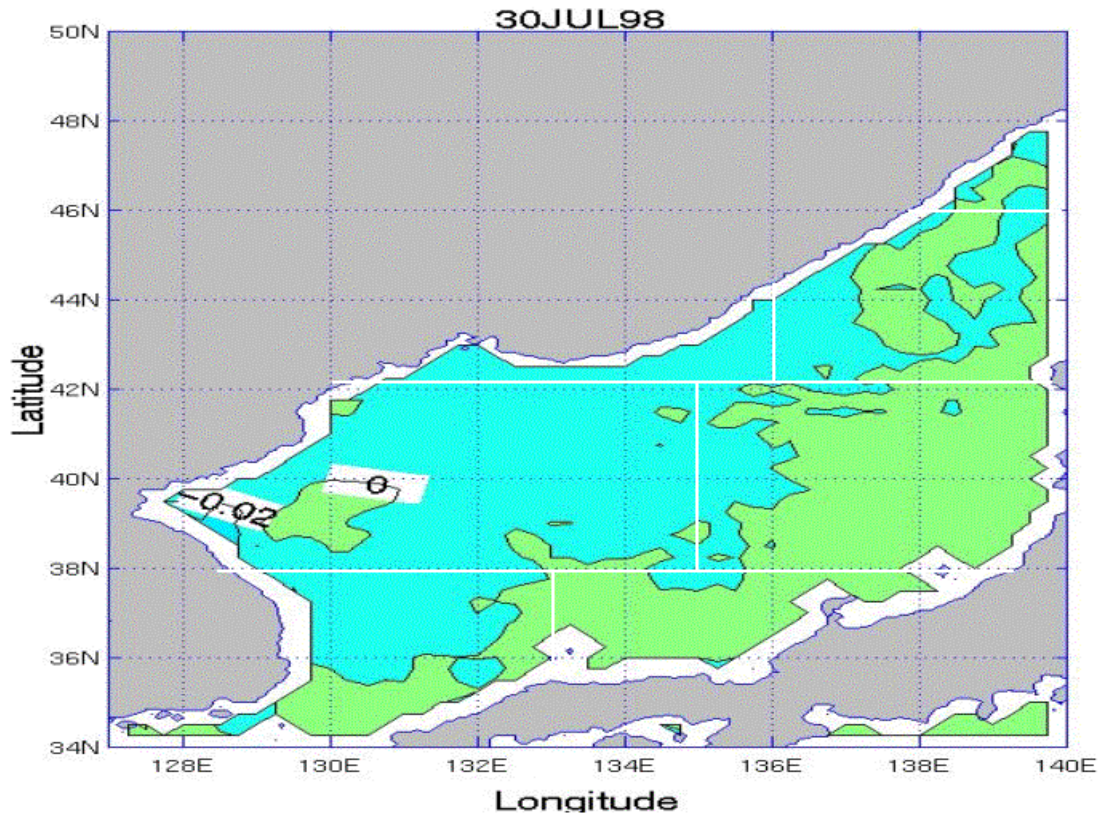








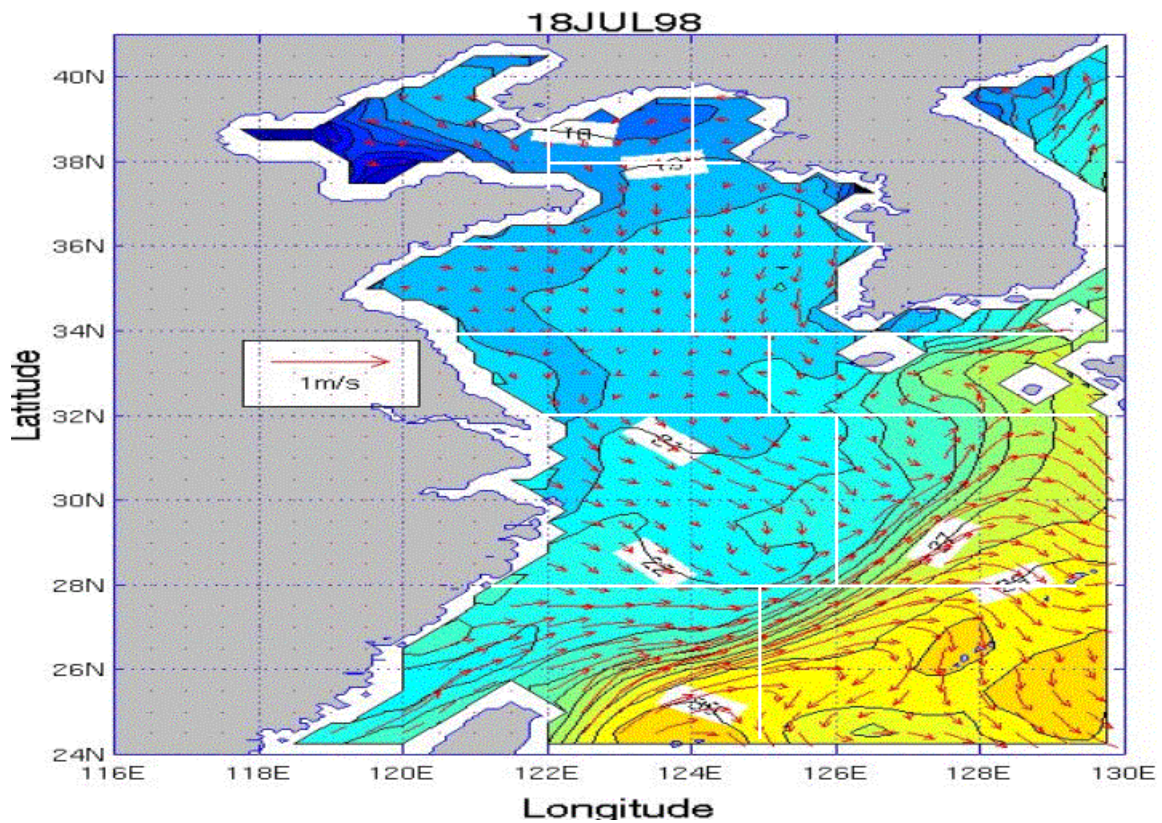


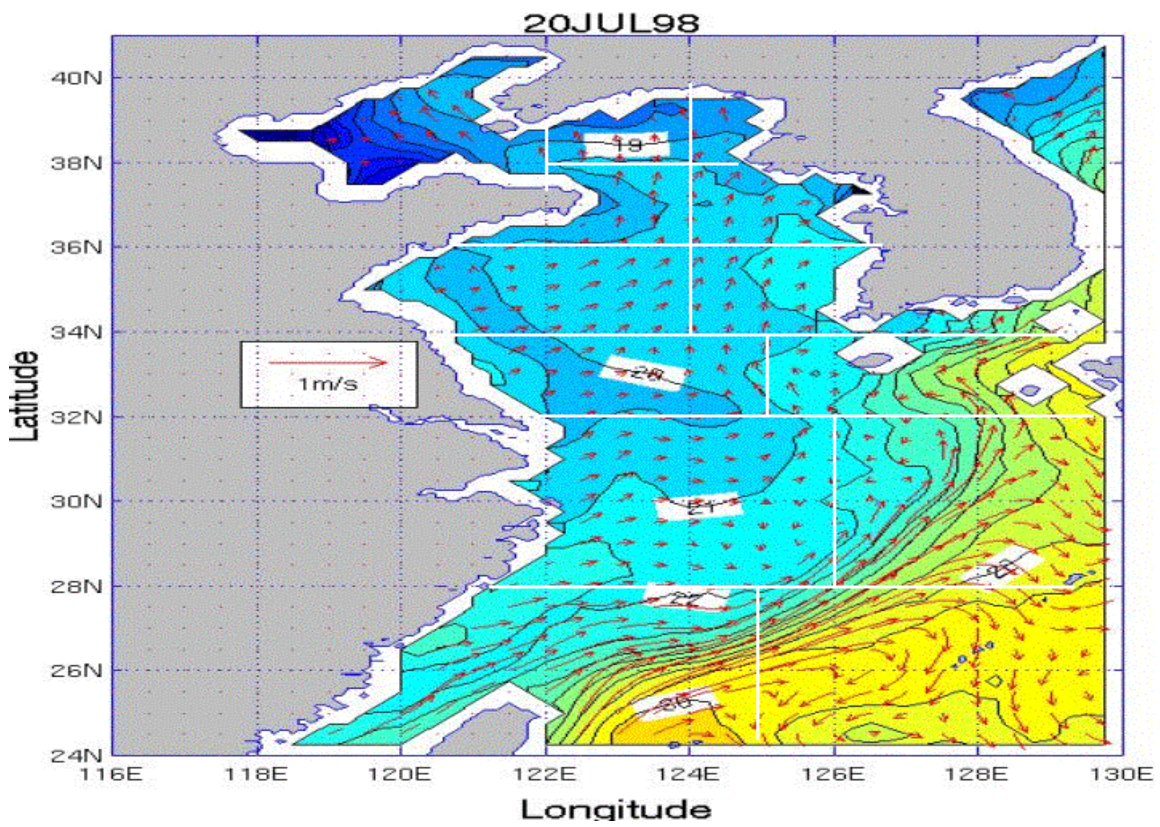
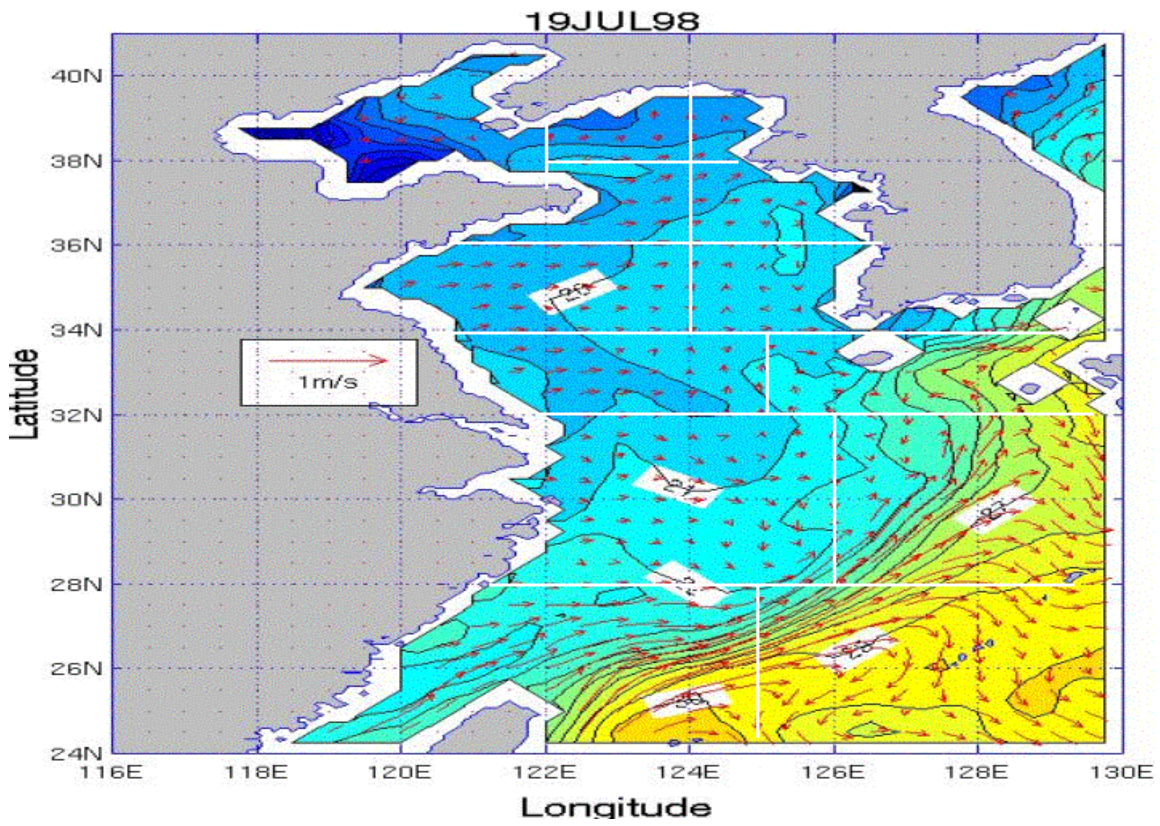


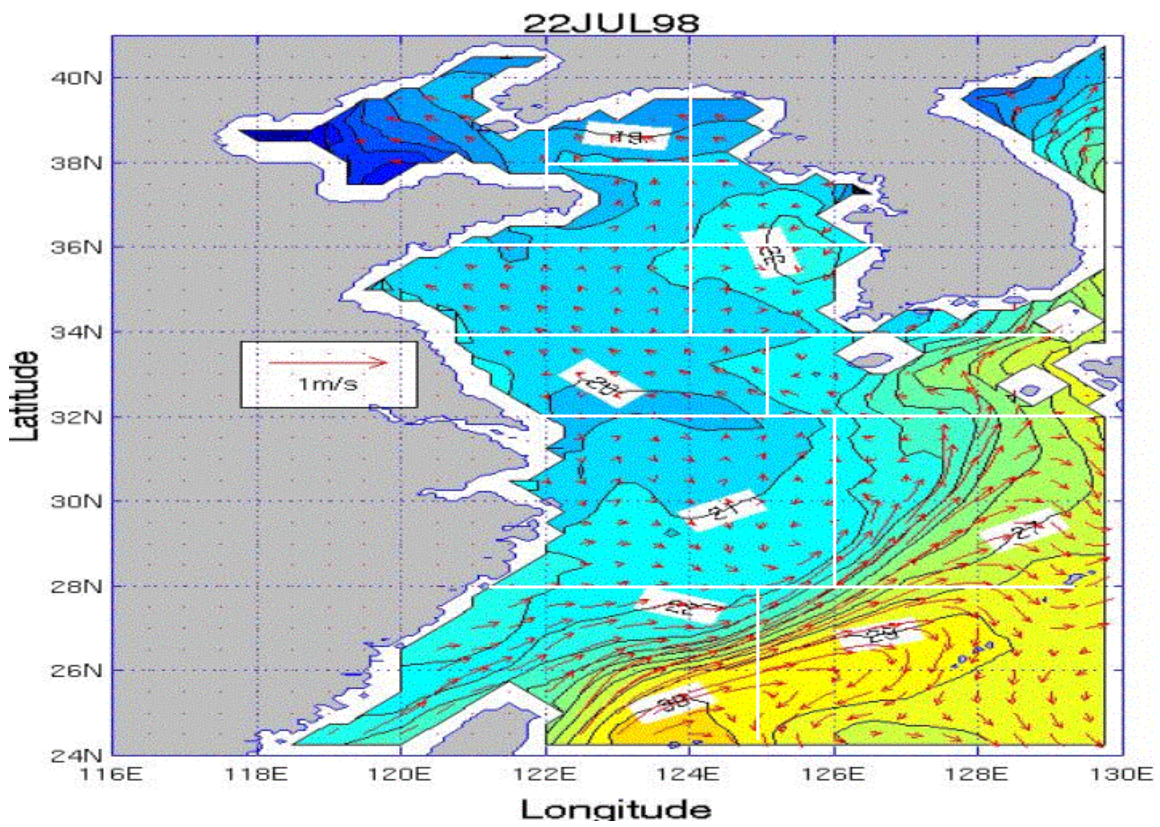
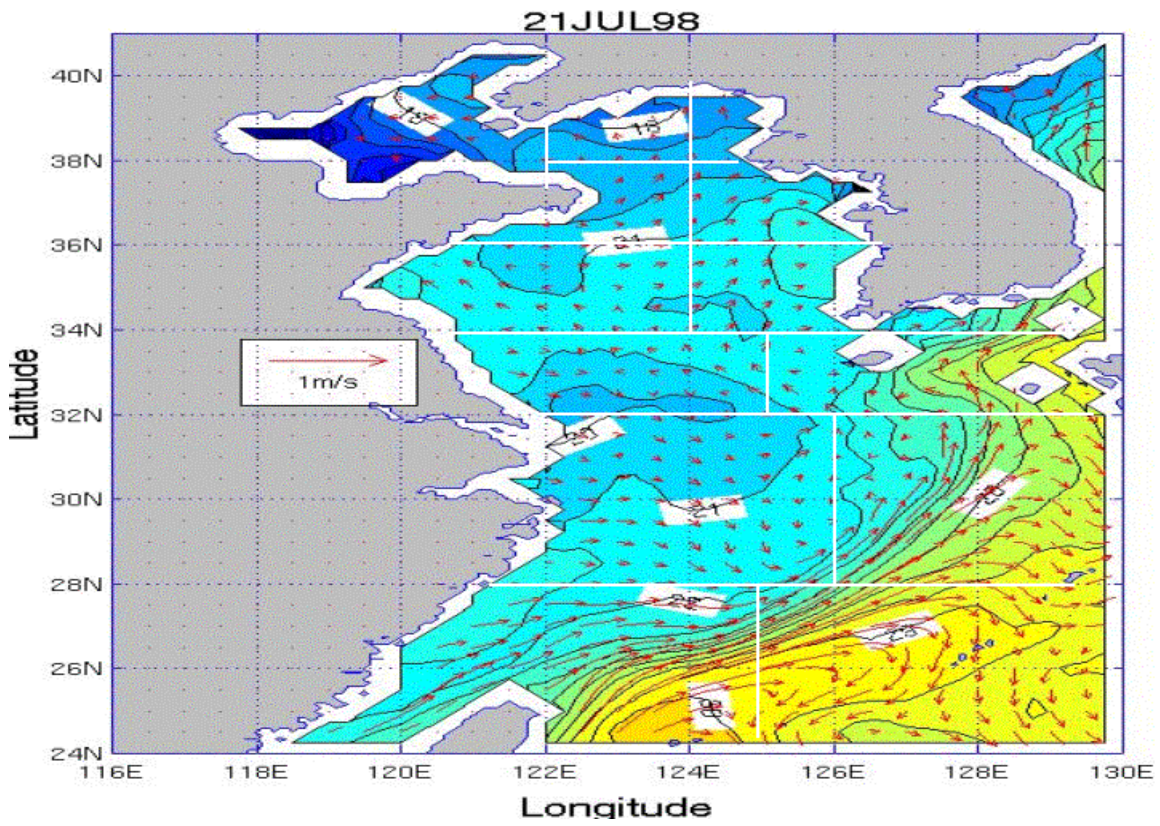
THIS PAGE INTENTIONALLY LEFT BLANK

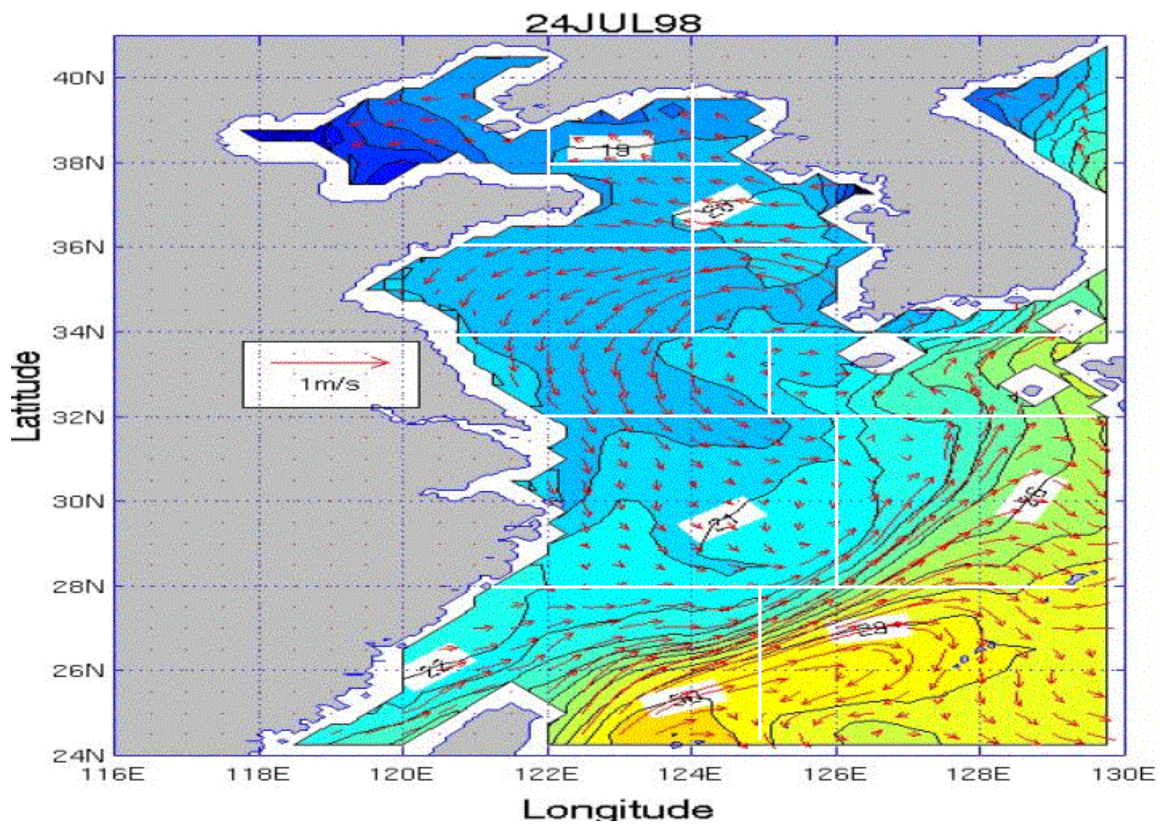
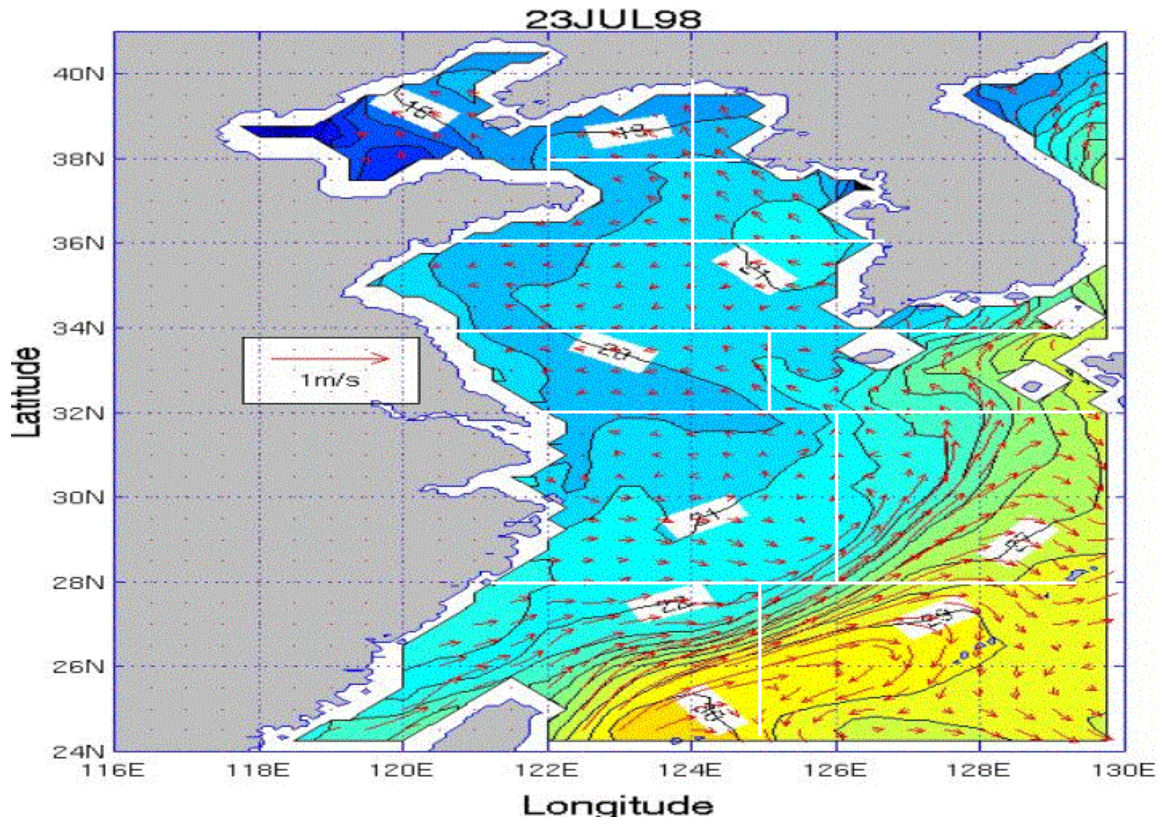
APPENDIX QQ. SST AND SURFACE CURRENT VELOCITY PLOTS FOR THE YES FOR THE JULY TIME PERIOD

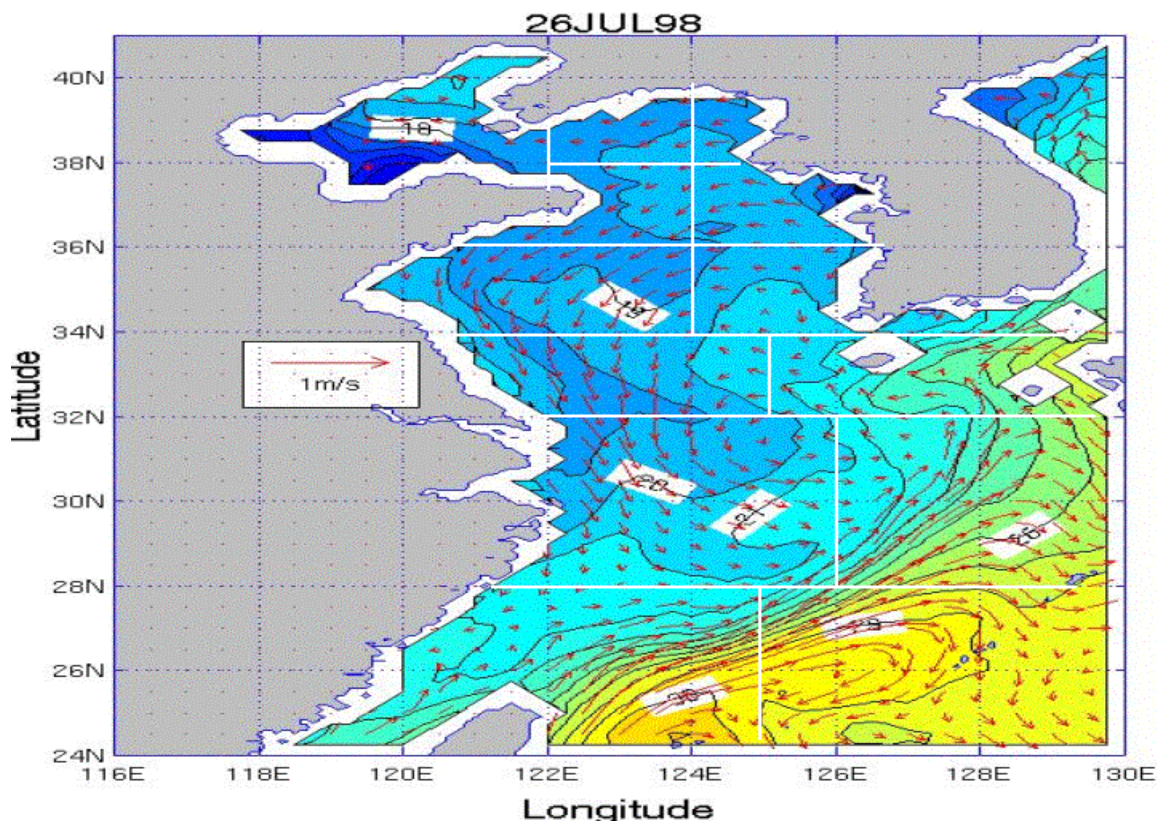
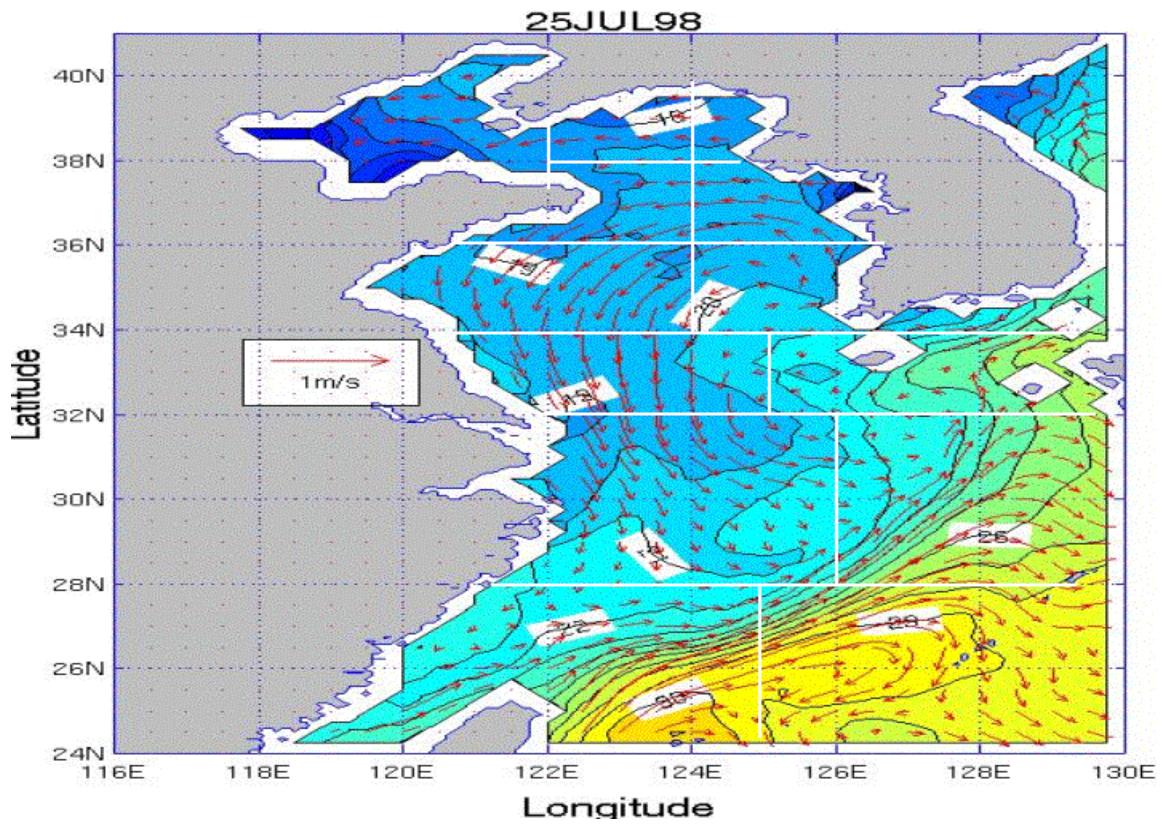
Appendix QQ consists of 14 figures that show SST and surface current velocity for each day of the July time period for the YES. The figures are in time sequential order from July 18 through July 31.

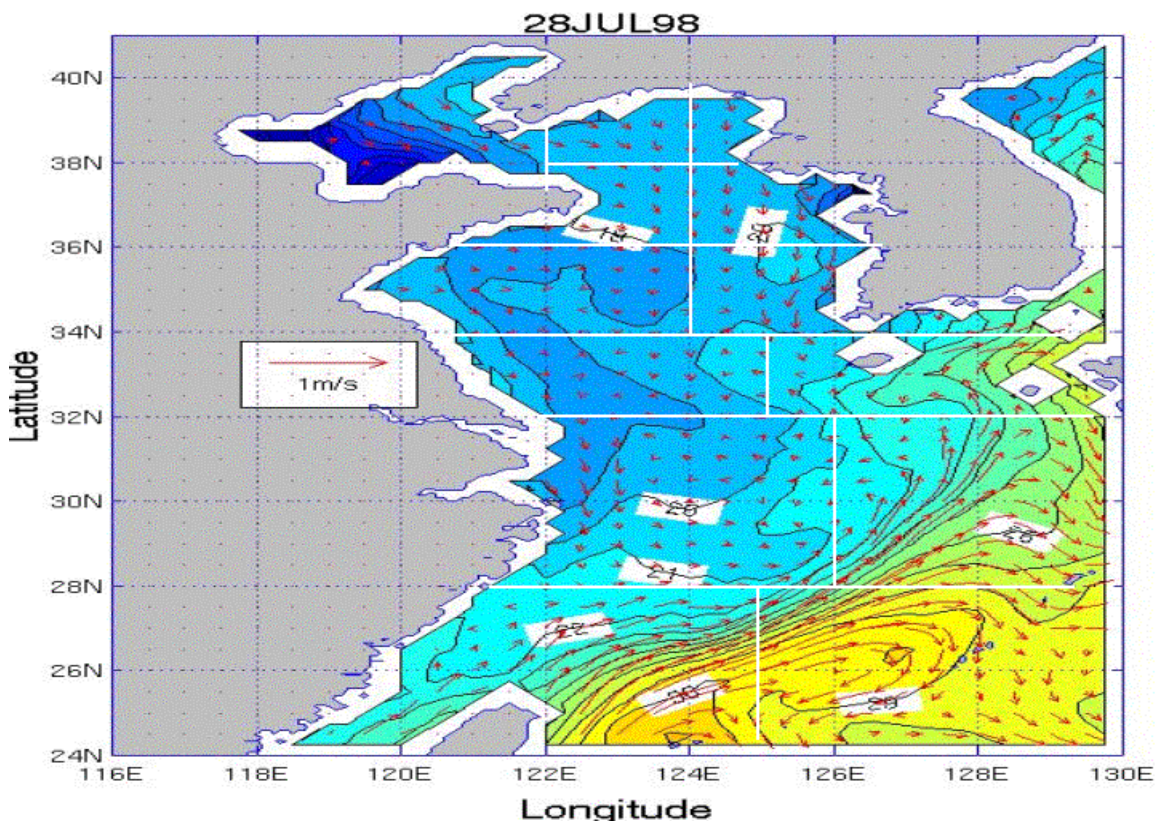
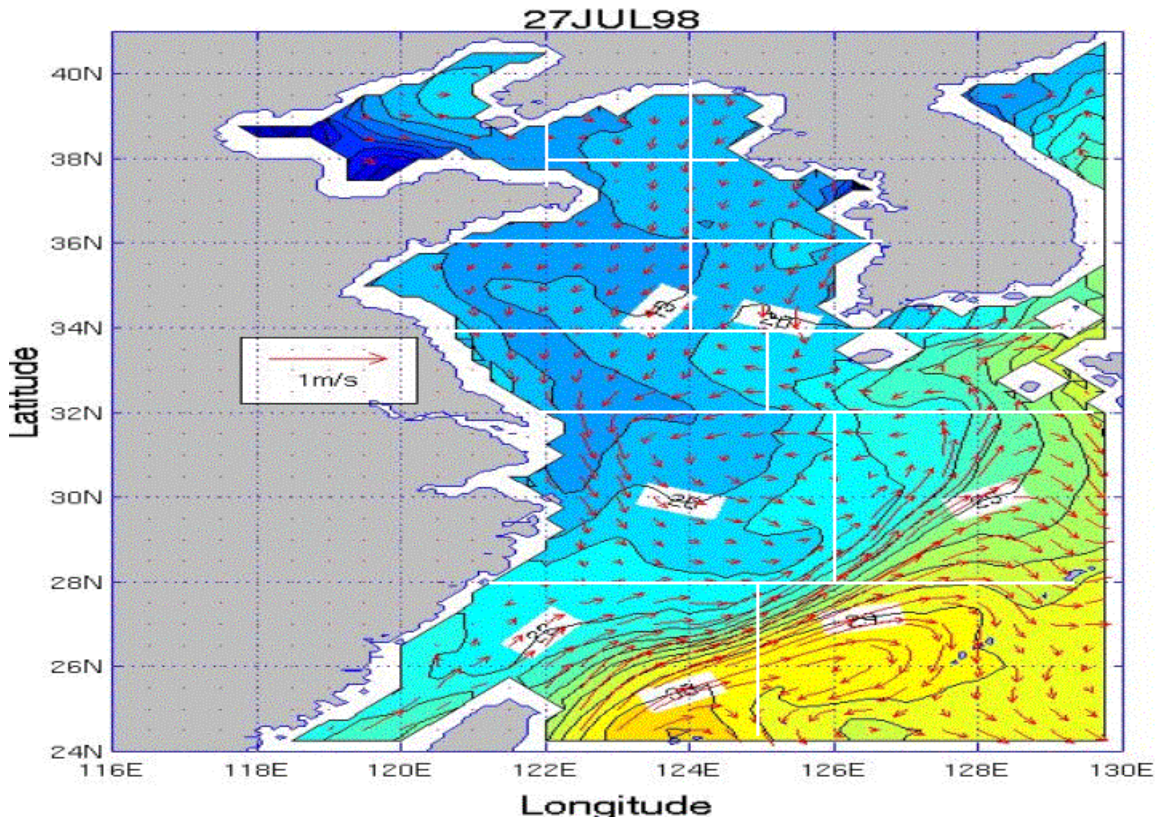


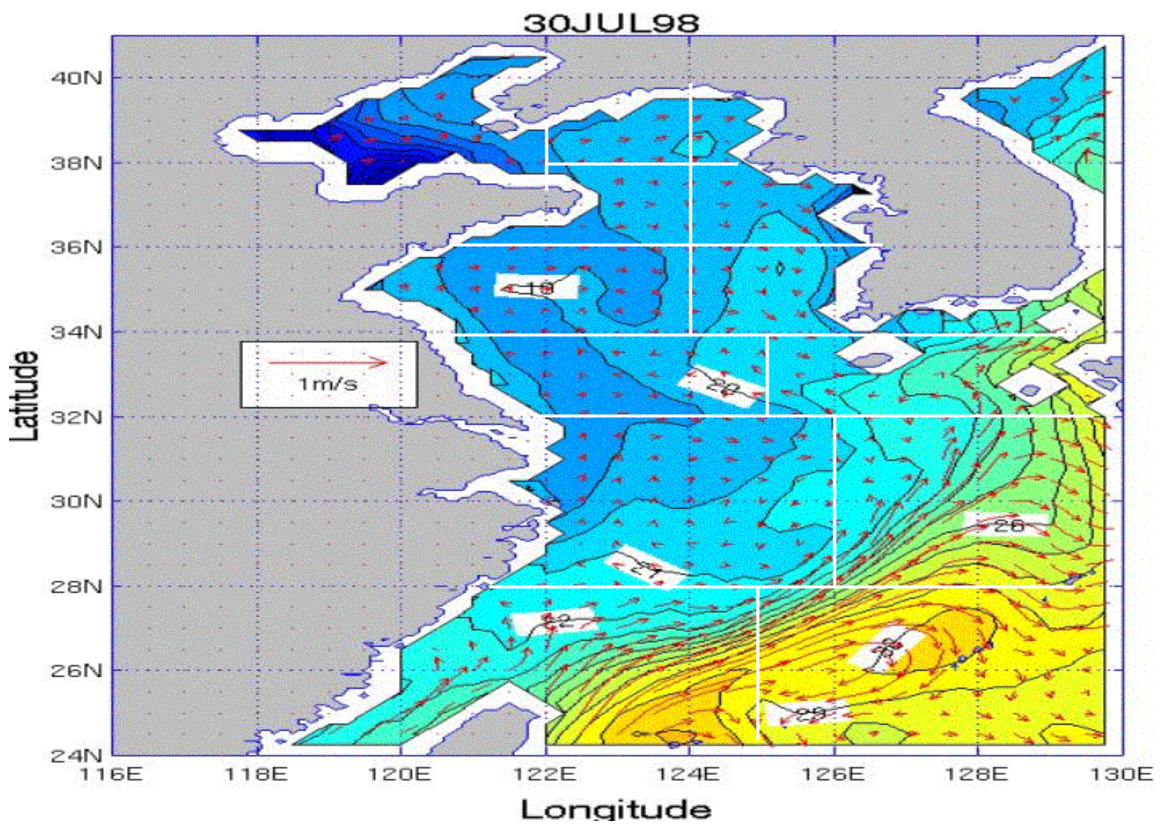
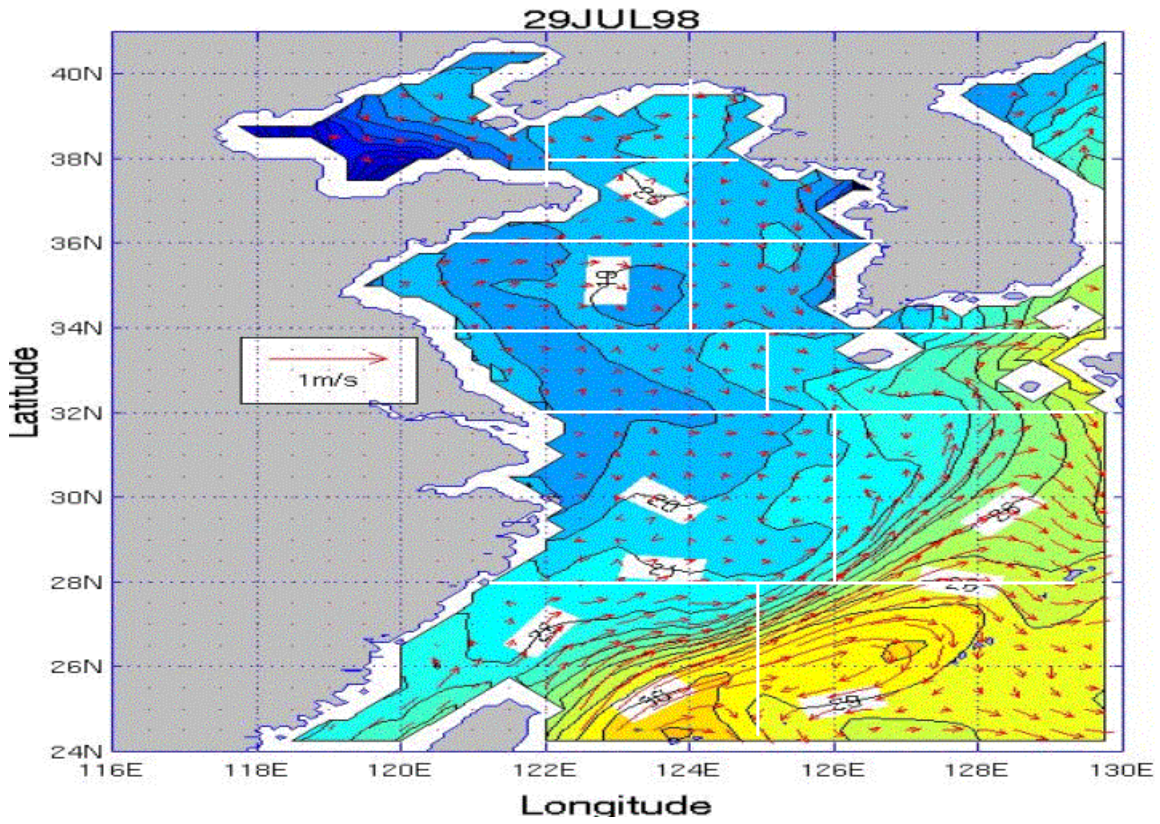


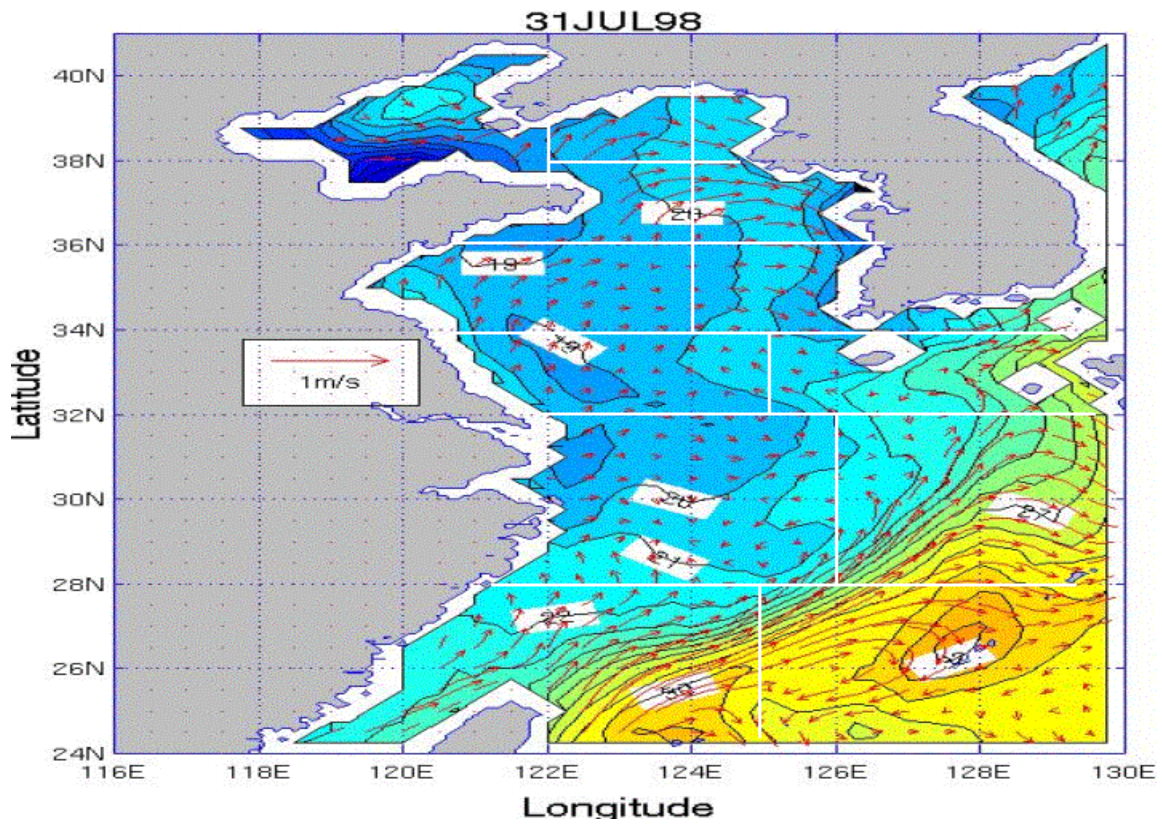






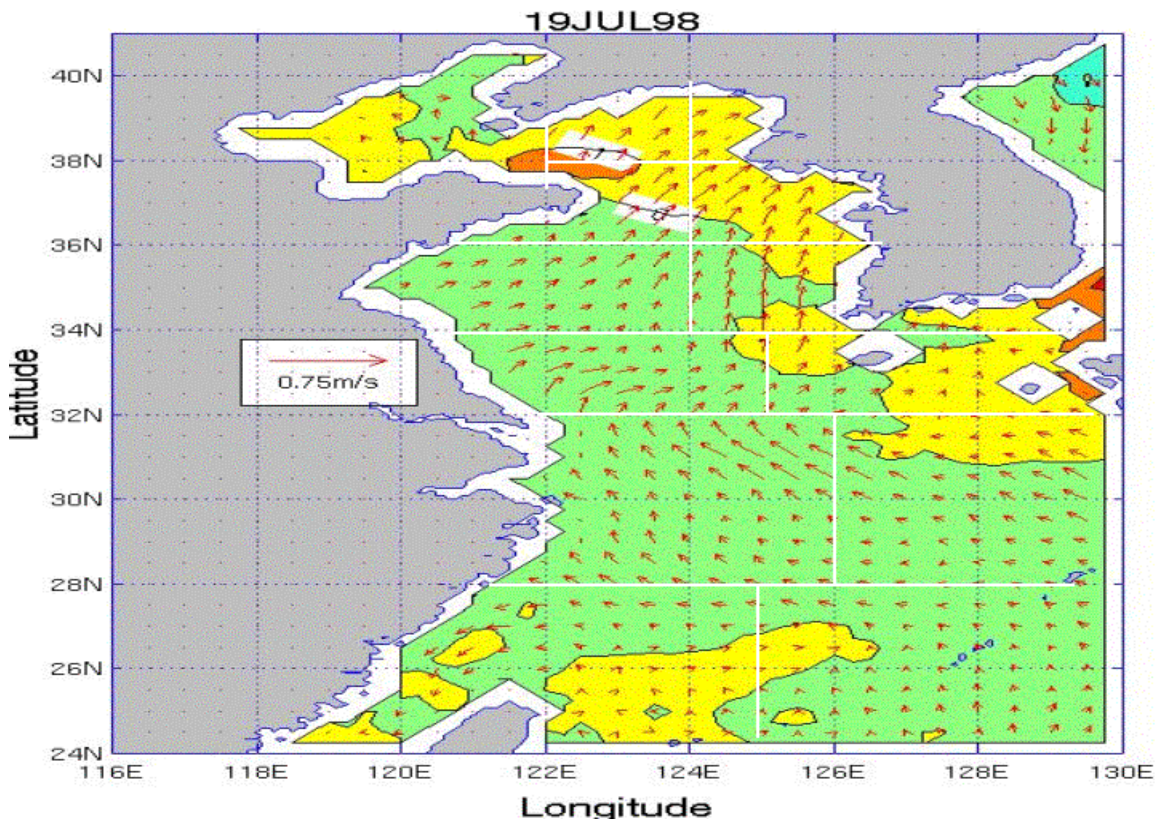


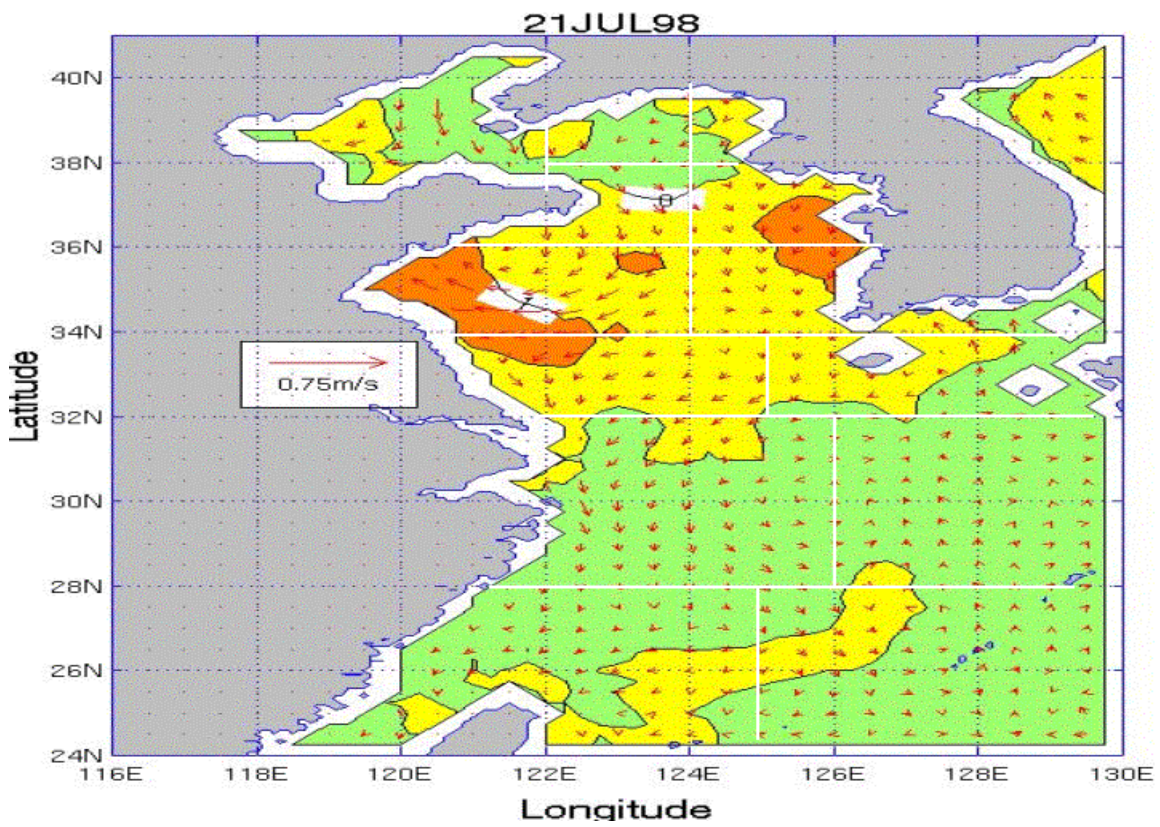
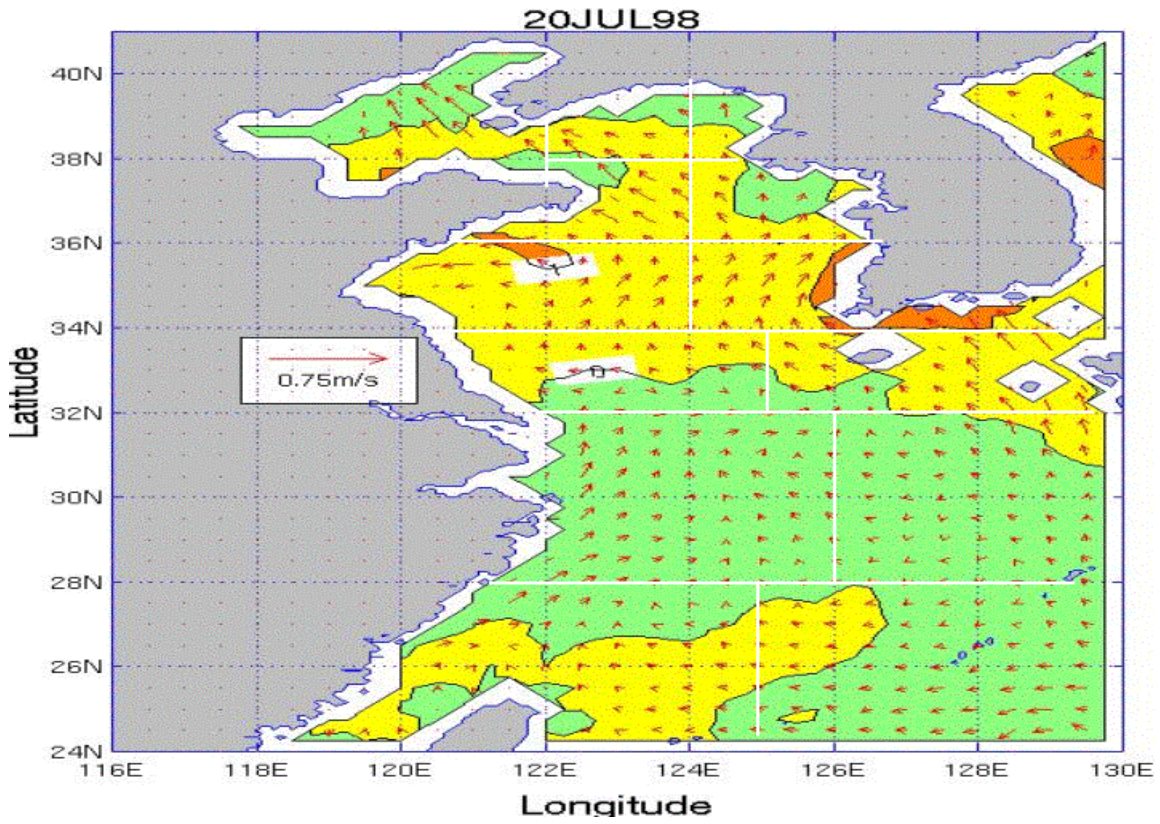


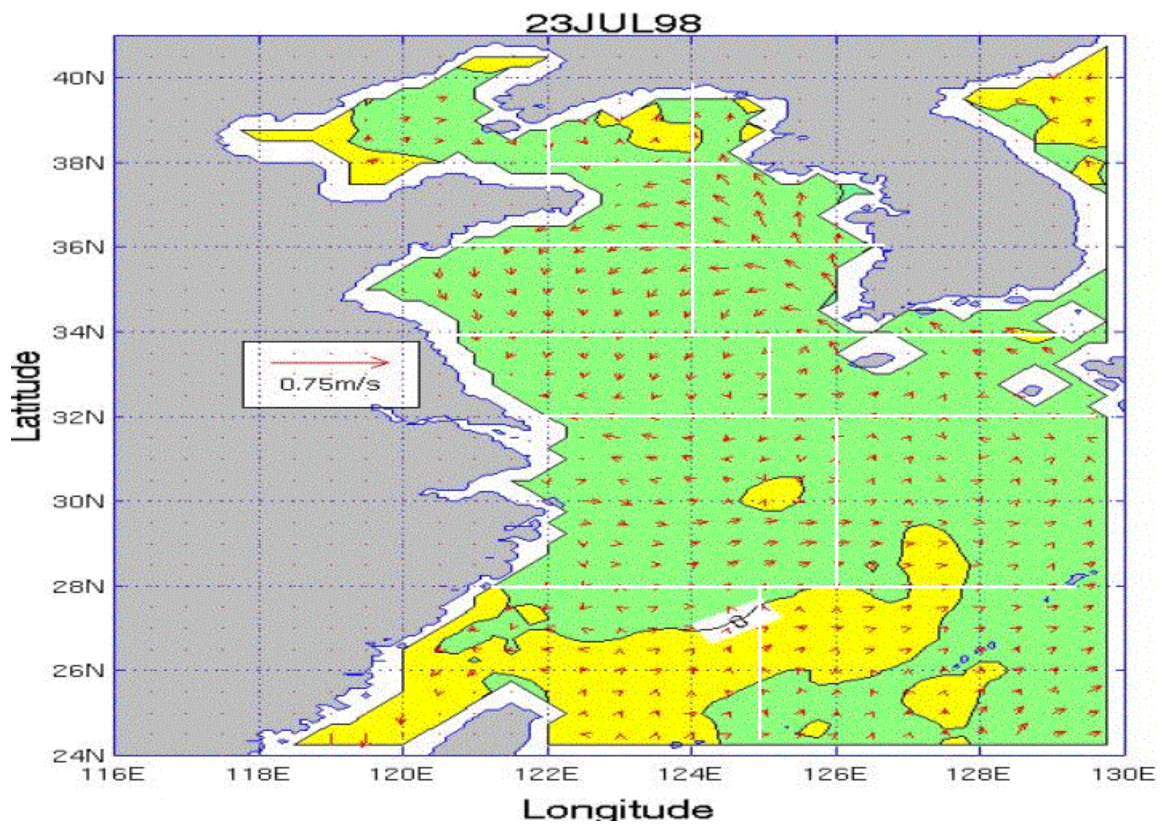
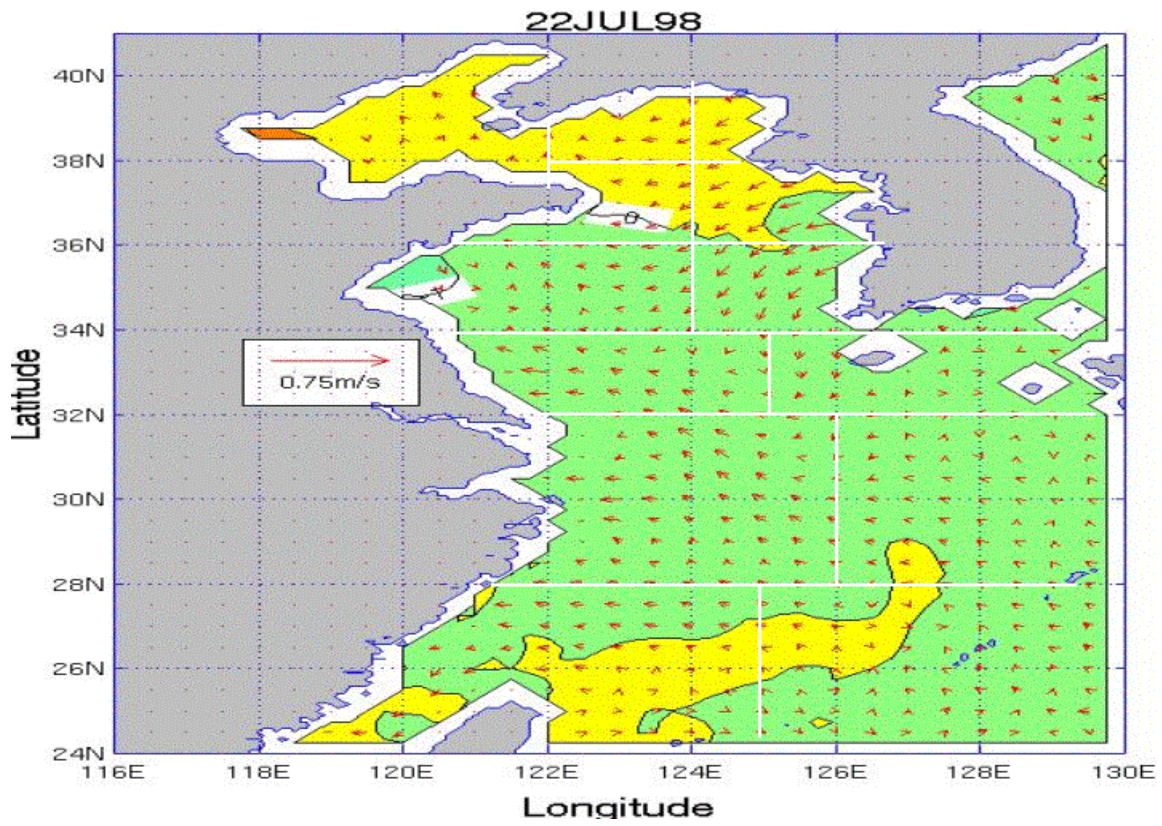


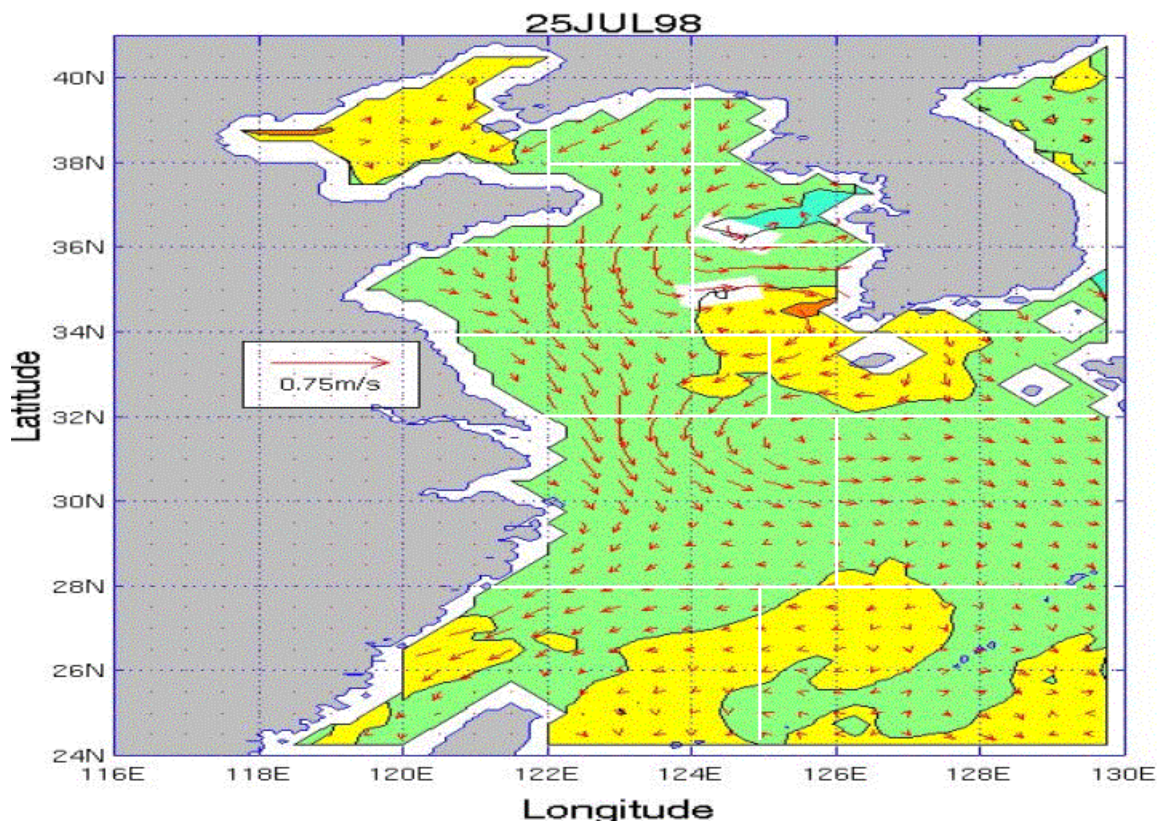
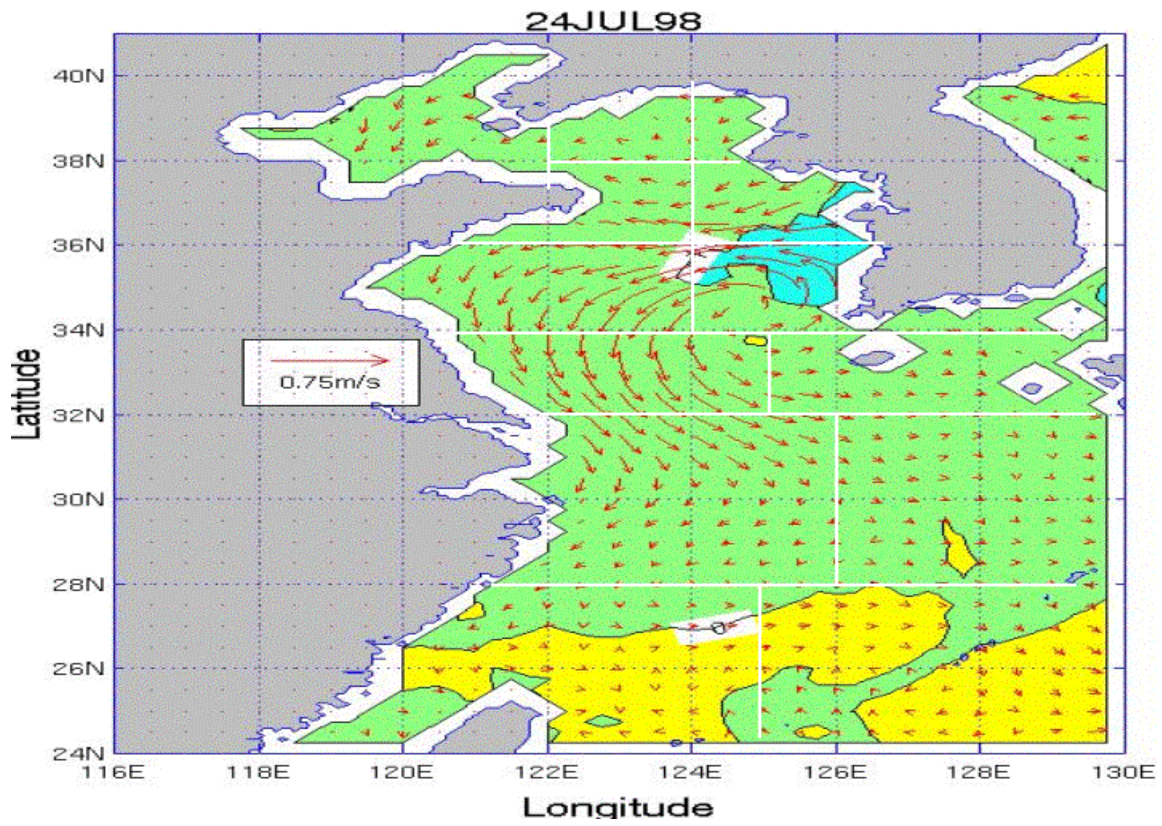
APPENDIX RR. SST AND SURFACE CURRENT VELOCITY TENDENCY PLOTS FOR THE YES FOR THE JULY TIME PERIOD

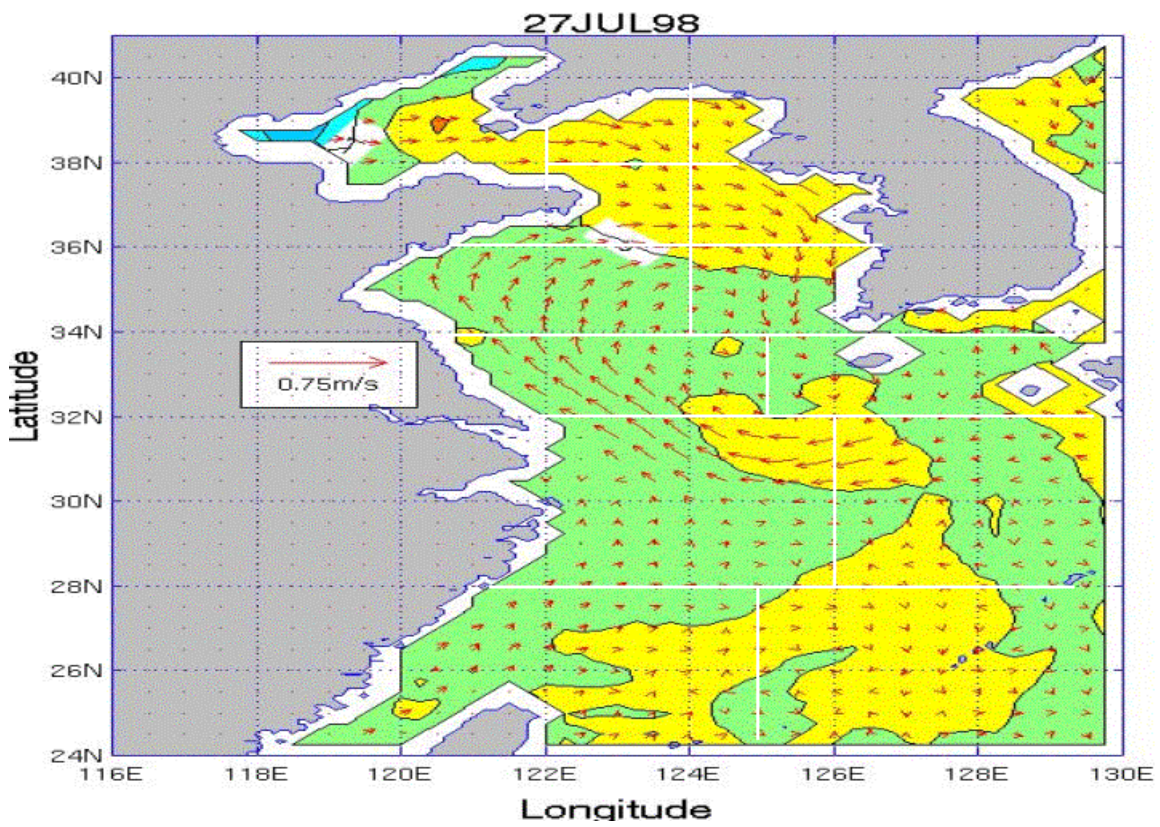
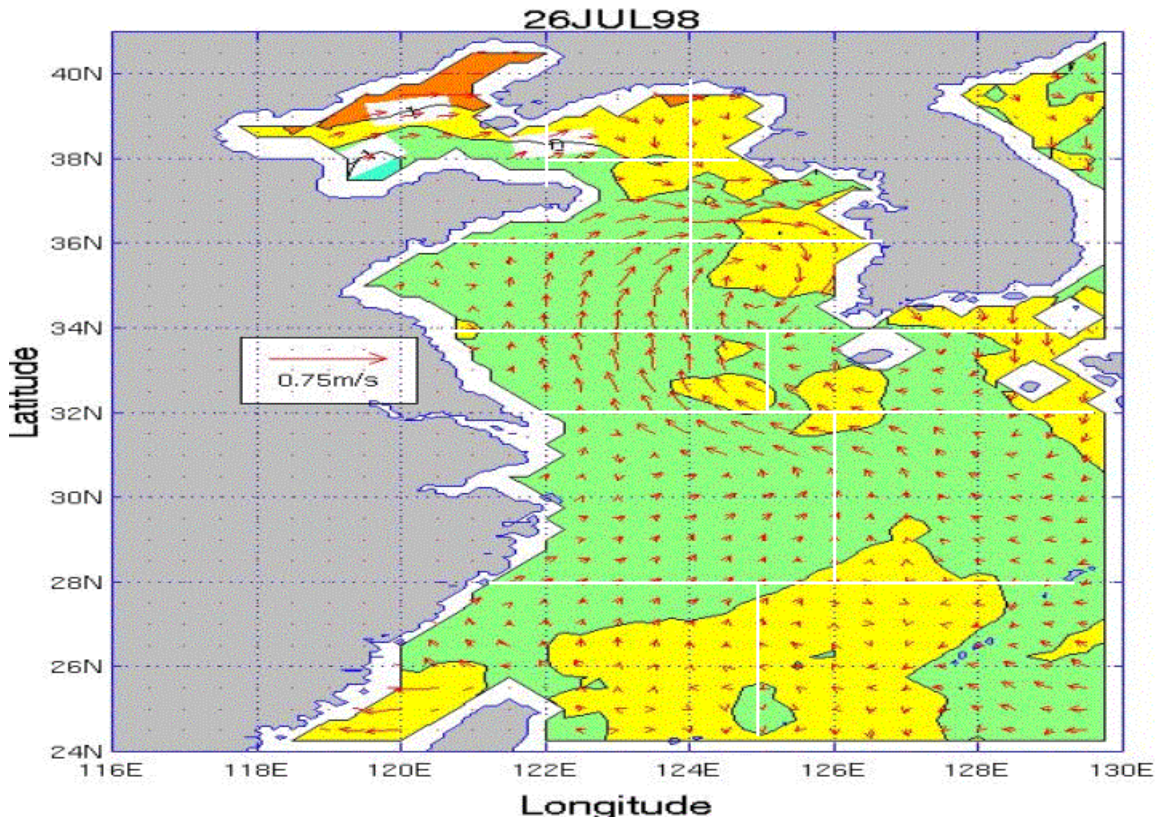
Appendix RR consists of 13 figures that show SST and surface current velocity day-to-day tendency for the July time period over the YES. The figures are in time sequential order from July 19 through July 31. Each plot represents the change between the previous day and the current day.

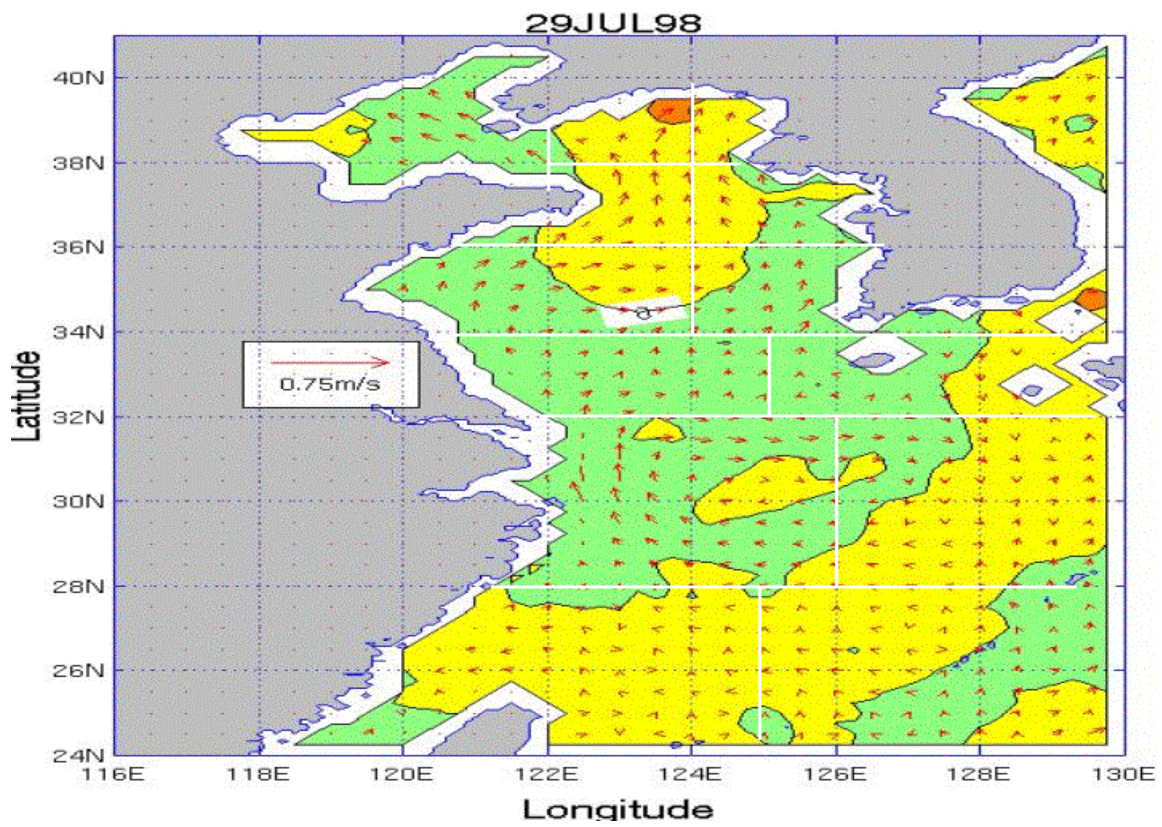
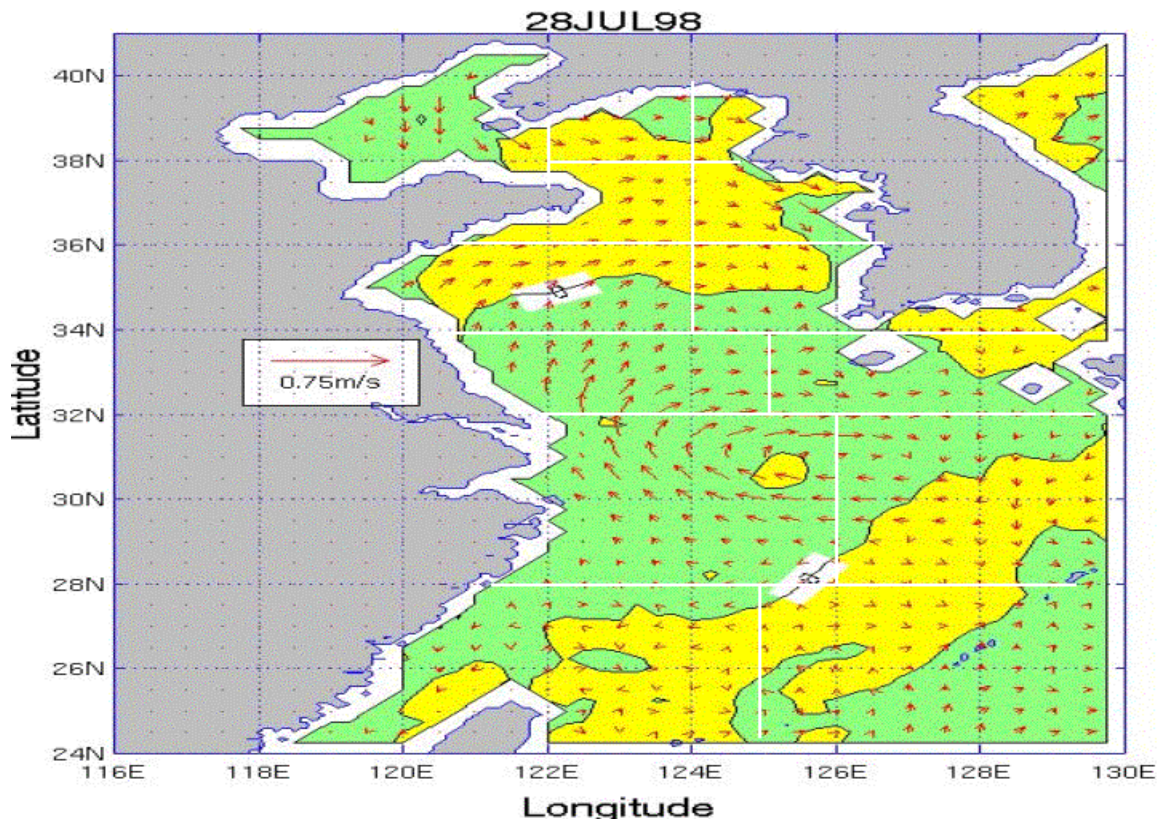


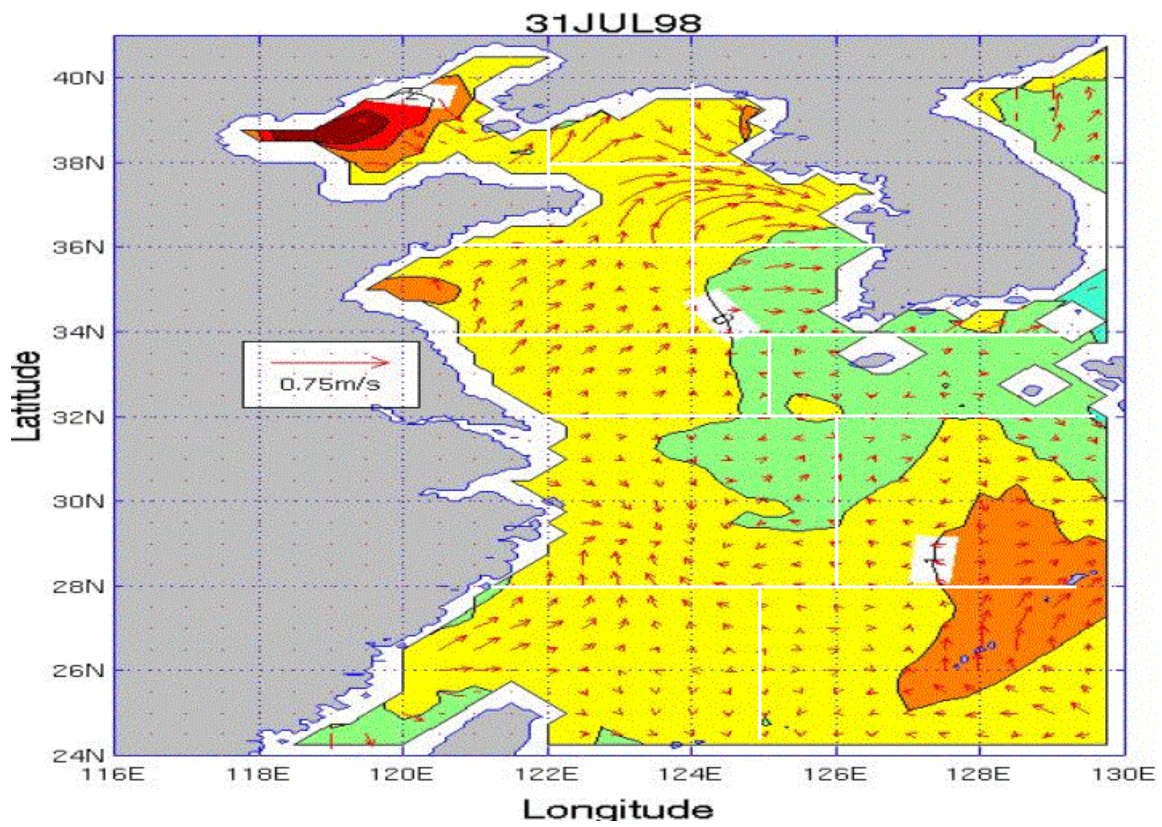
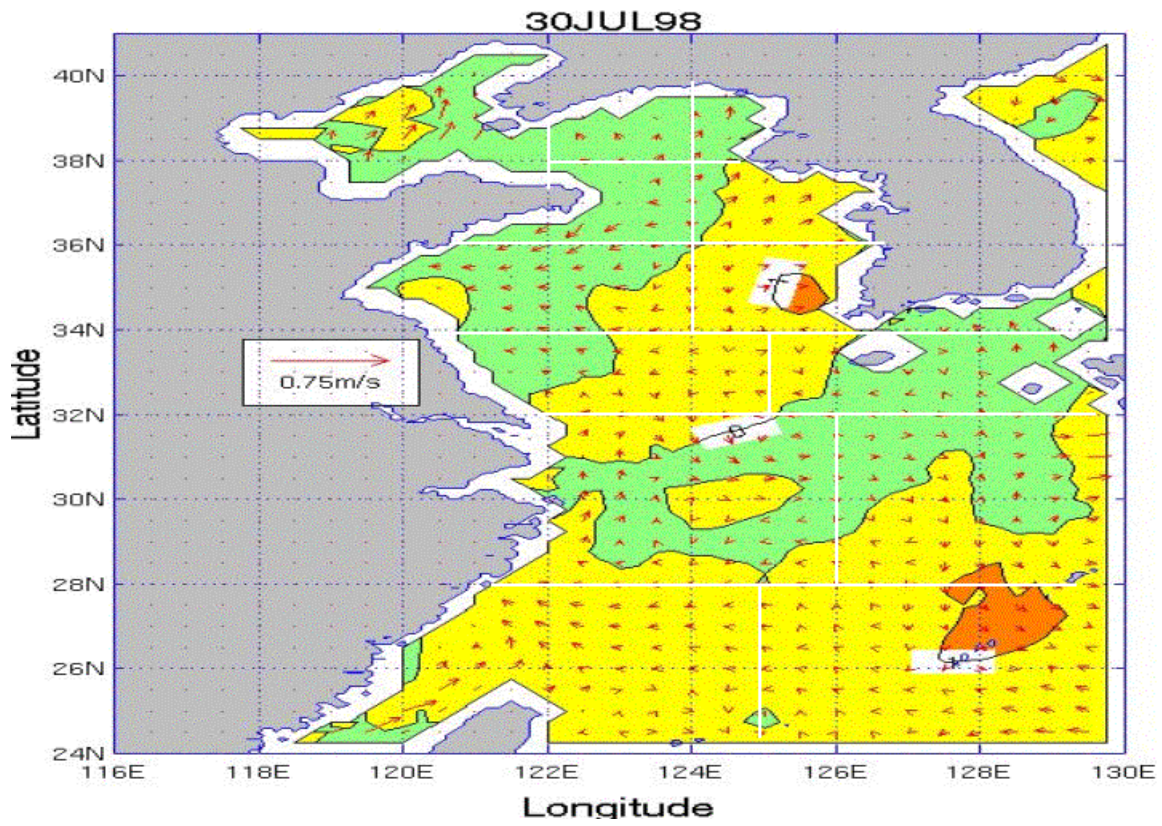








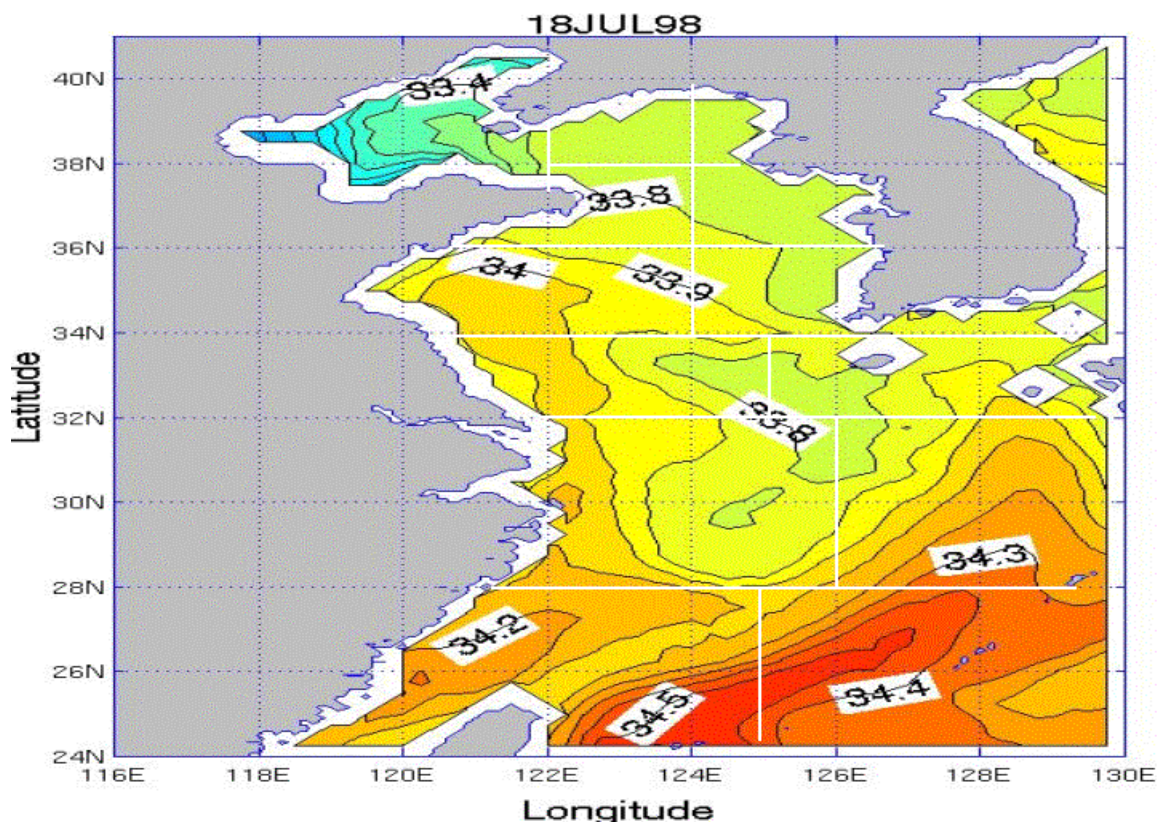


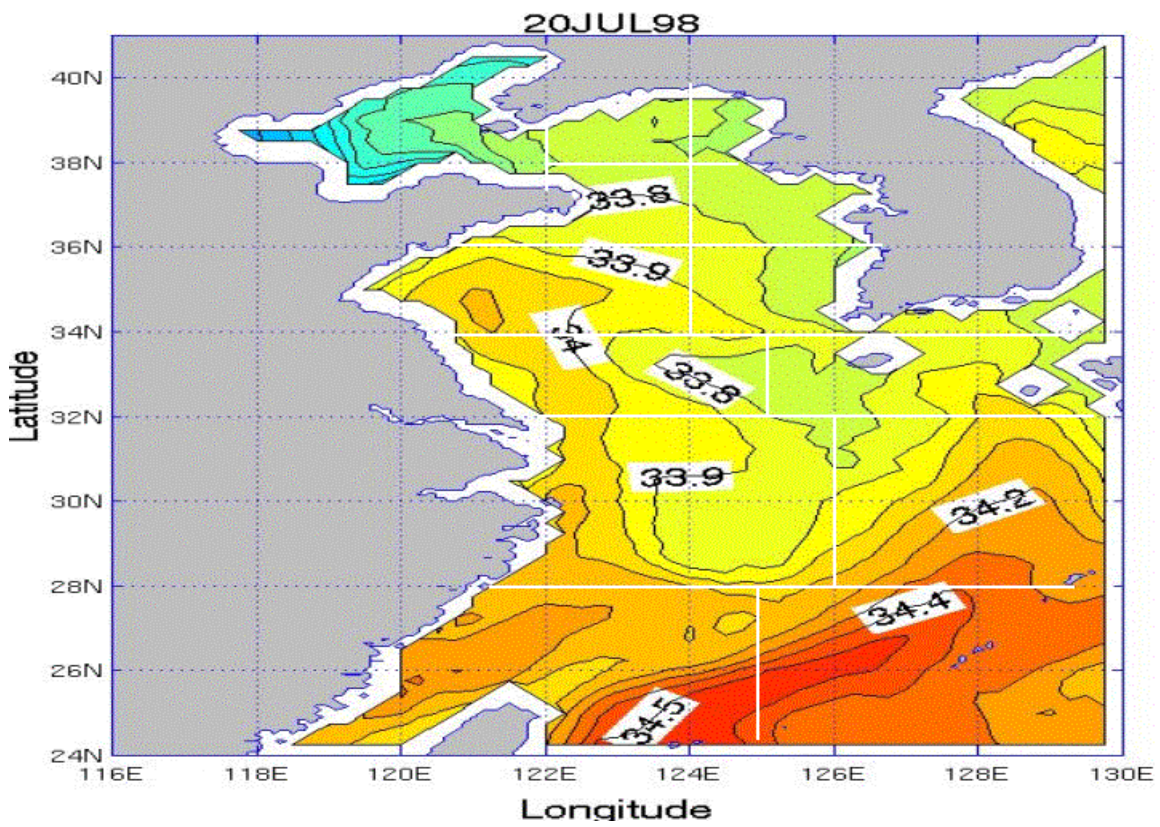
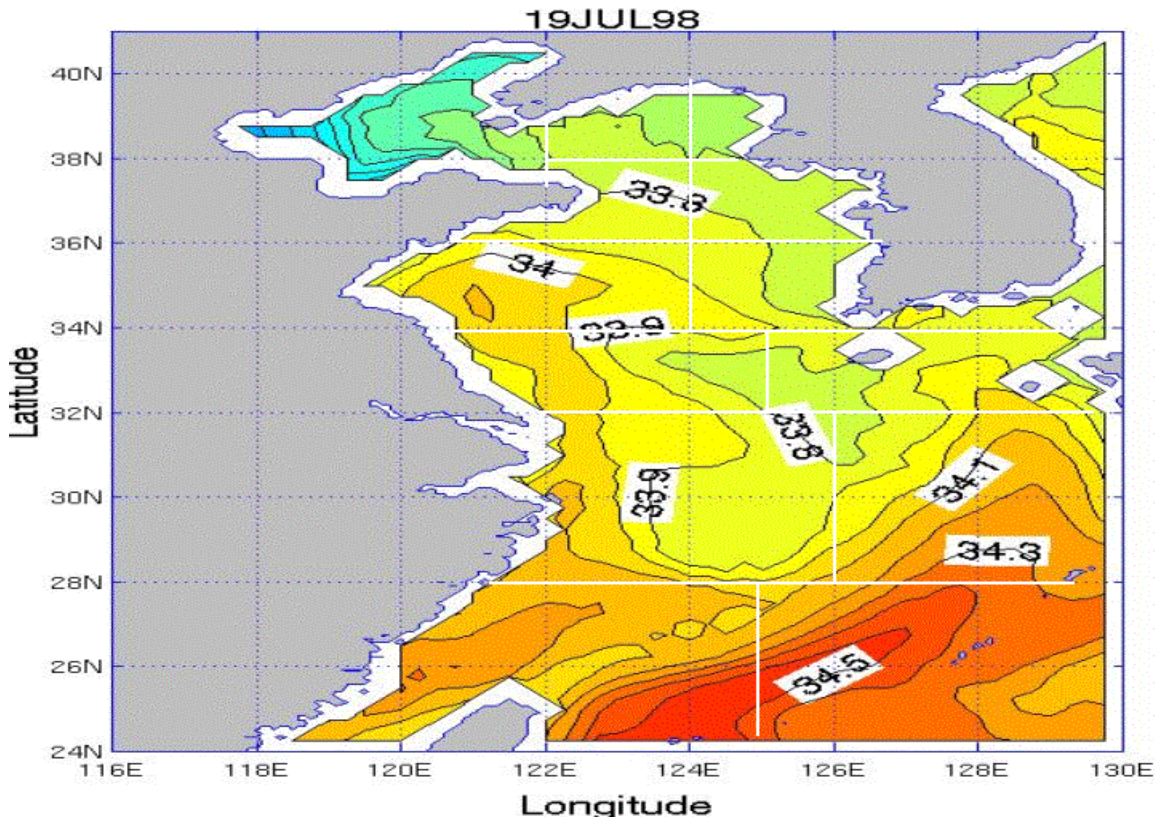


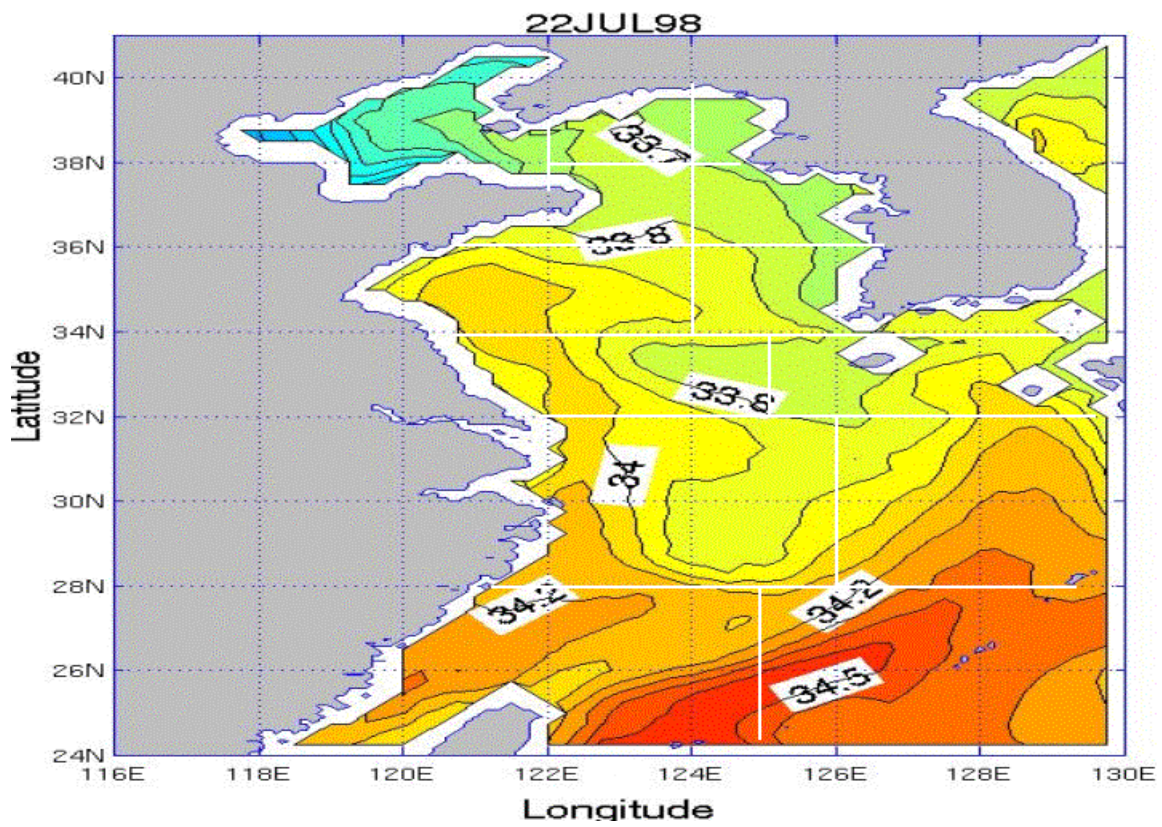
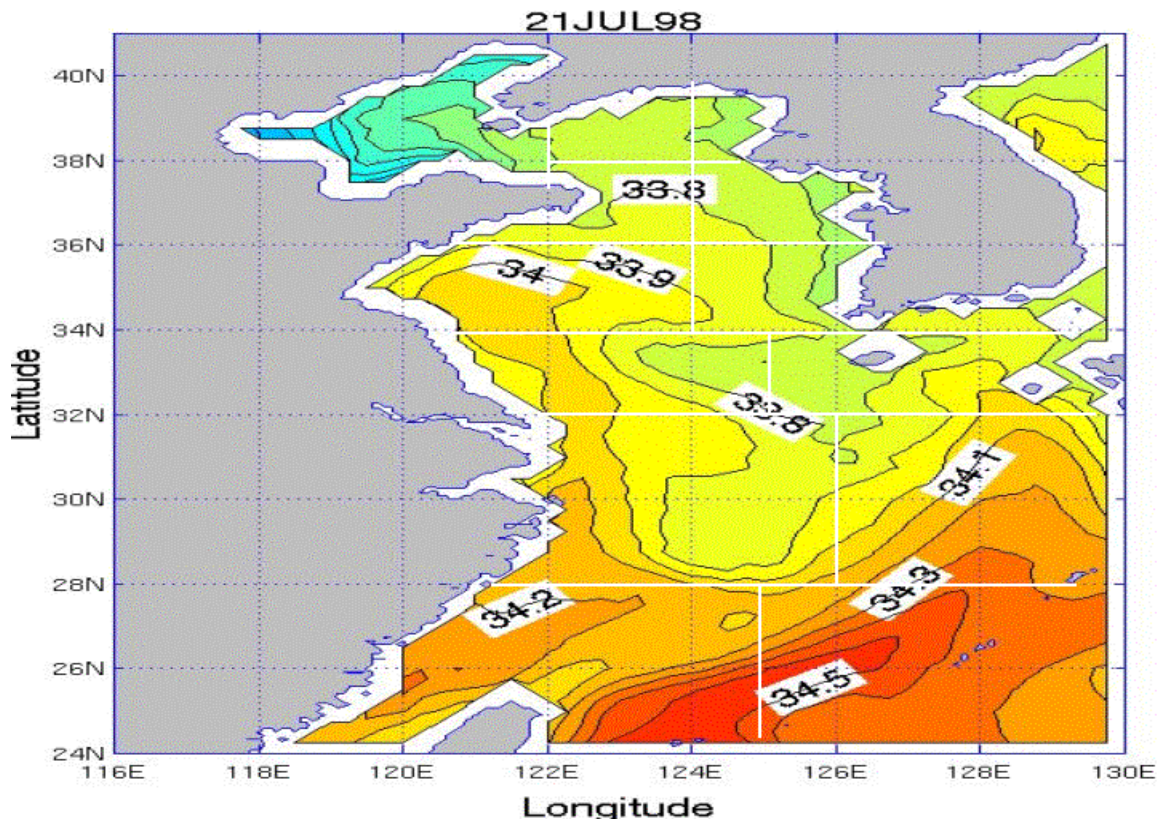
THIS PAGE INTENTIONALLY LEFT BLANK

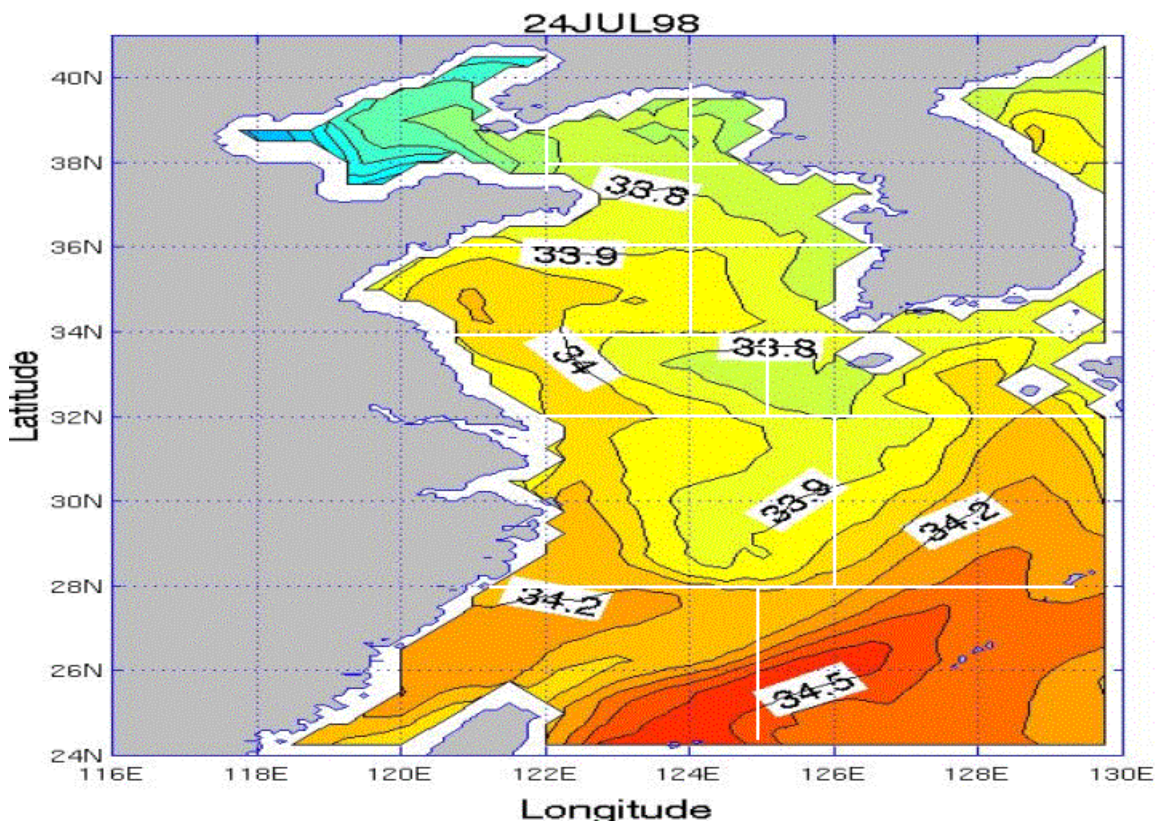
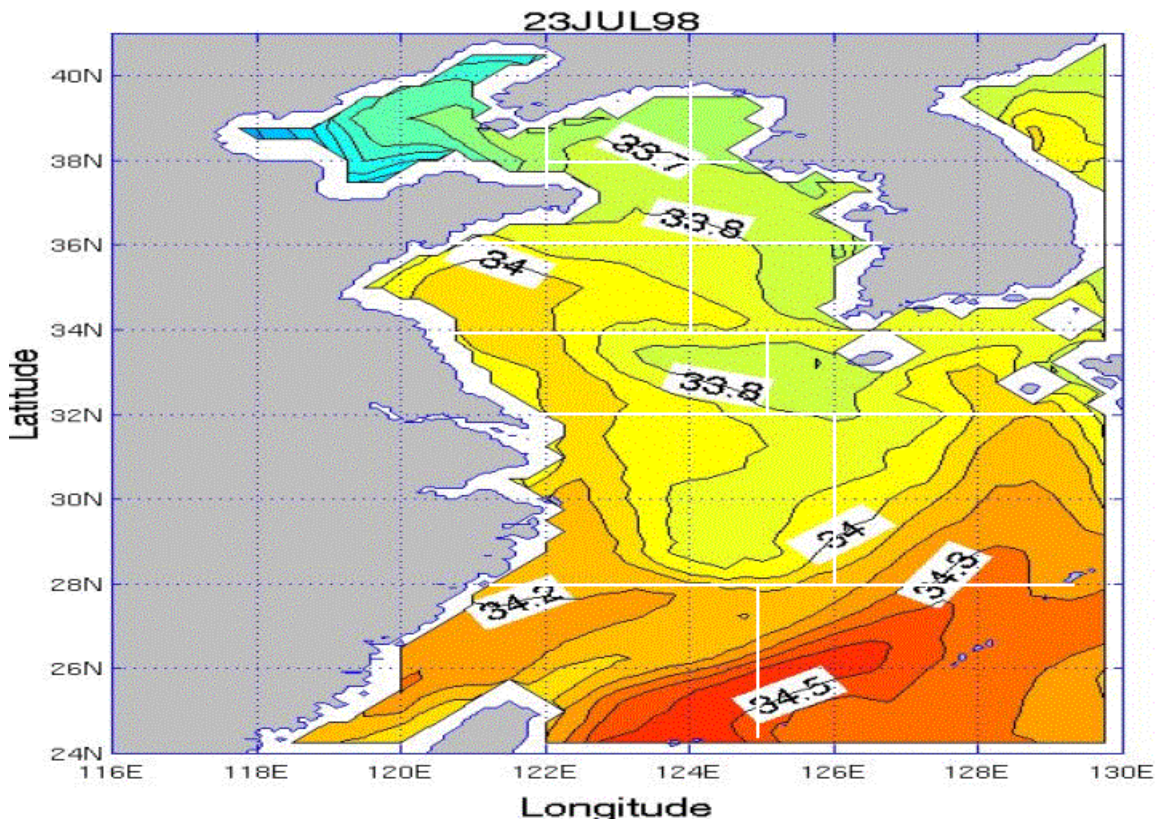
APPENDIX SS. SSS PLOTS FOR THE YES FOR THE JULY TIME PERIOD

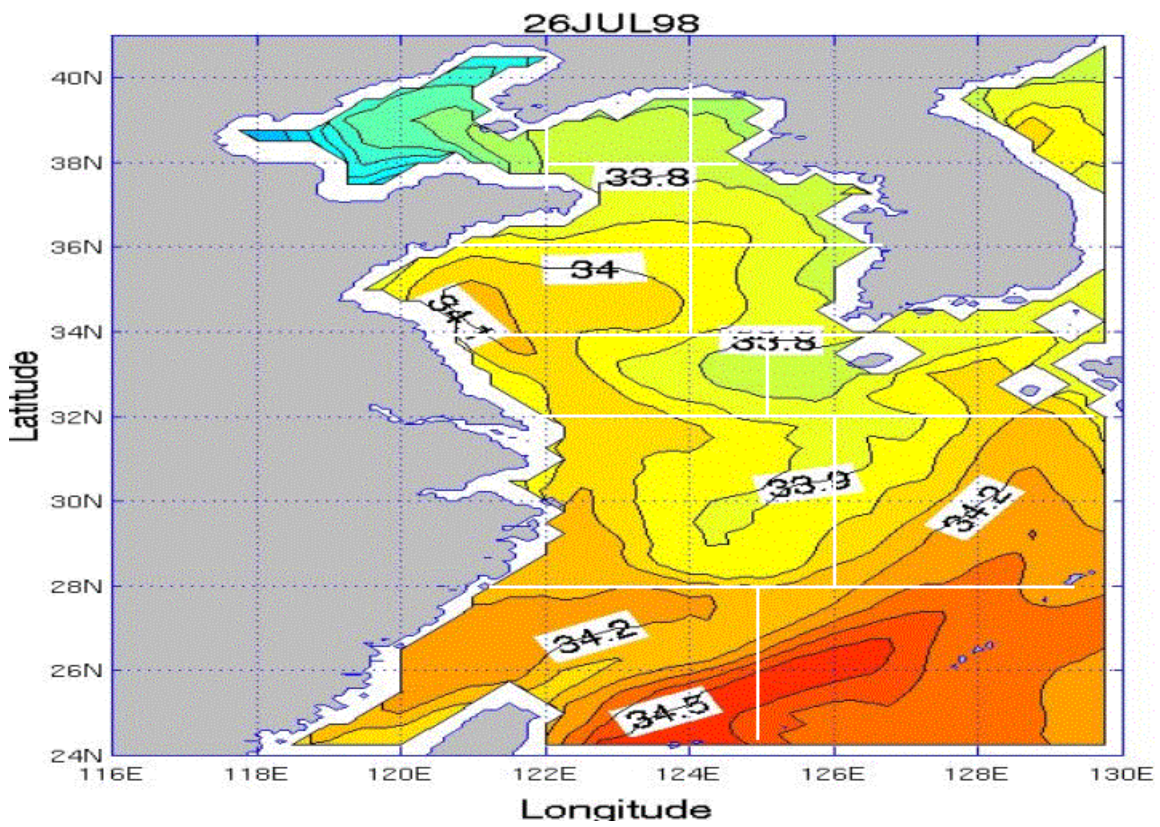
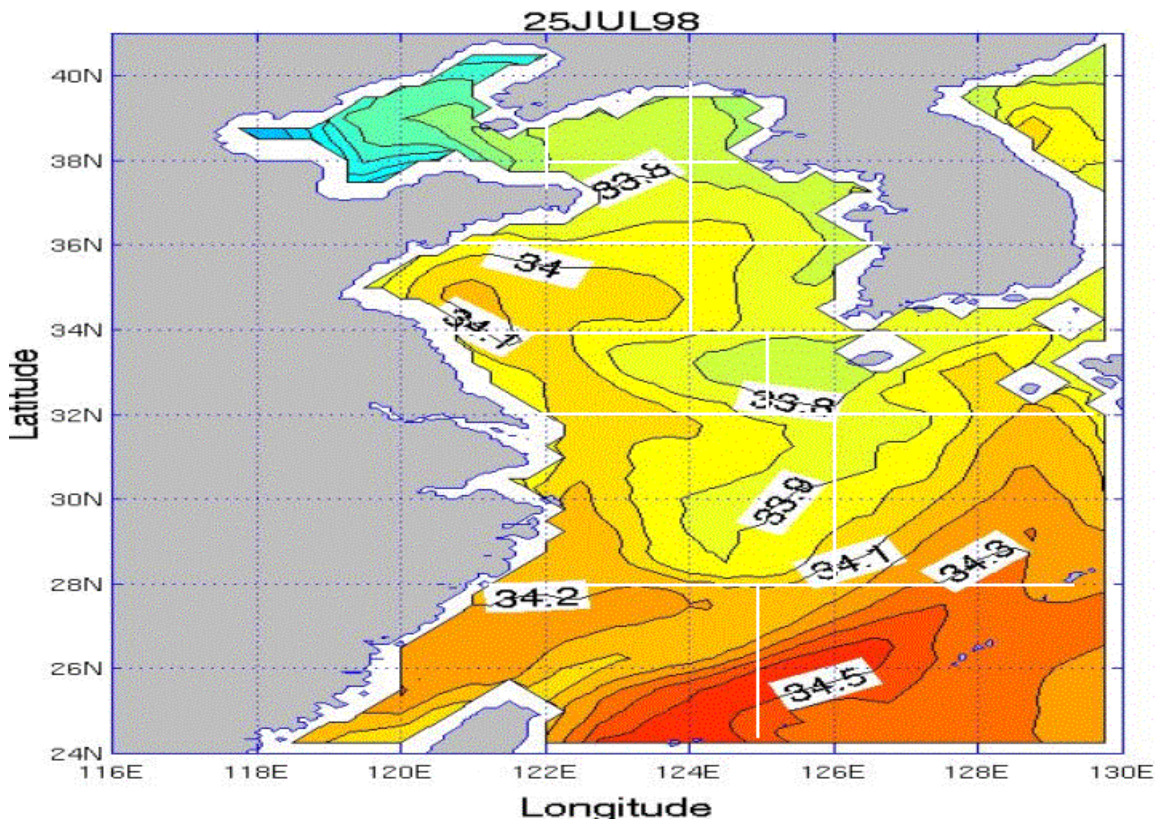
Appendix SS consists of 14 figures that show SSS for each day of the July time period for the YES. The figures are in time sequential order from July 18 through July 31.

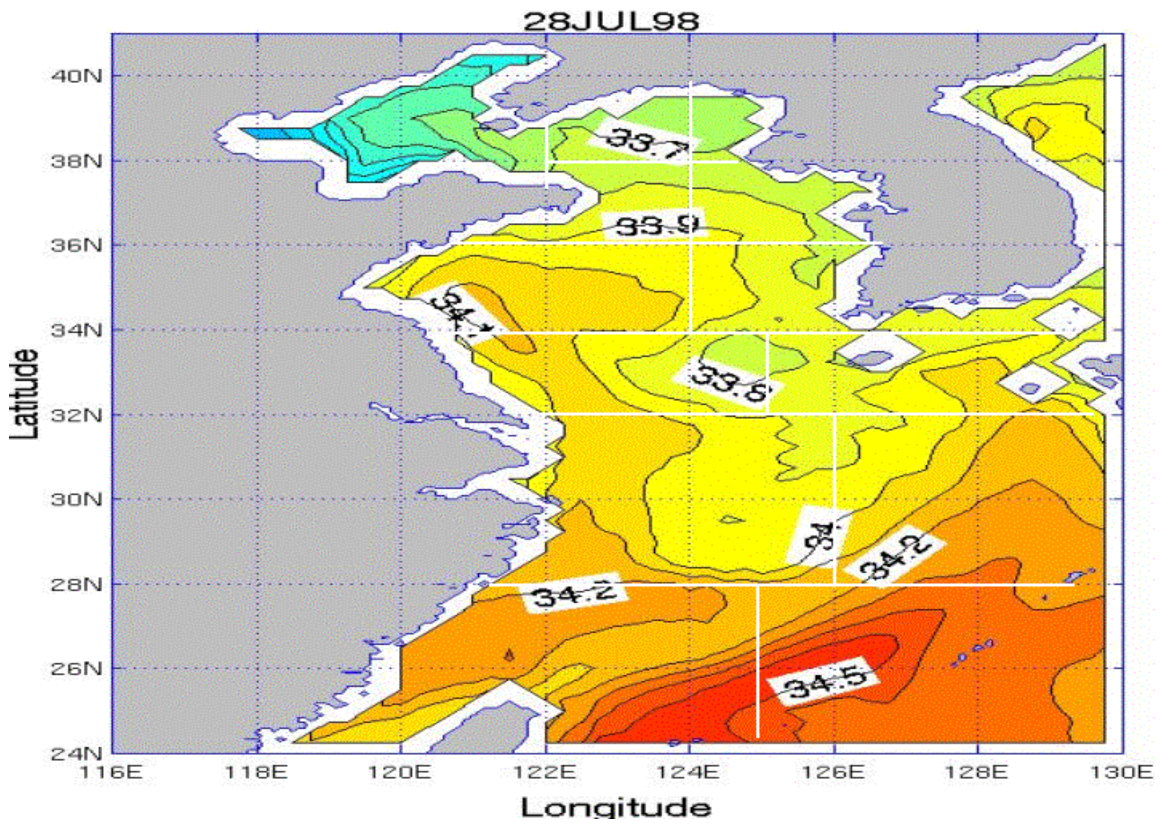
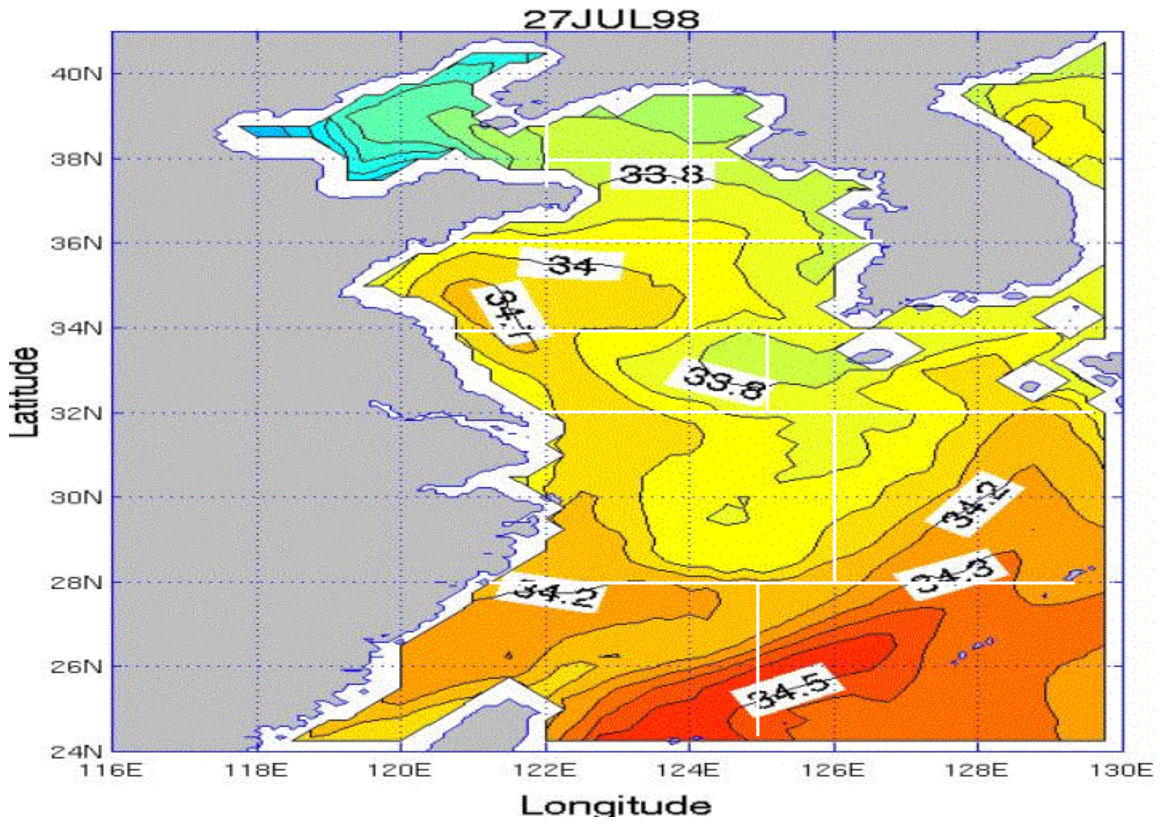


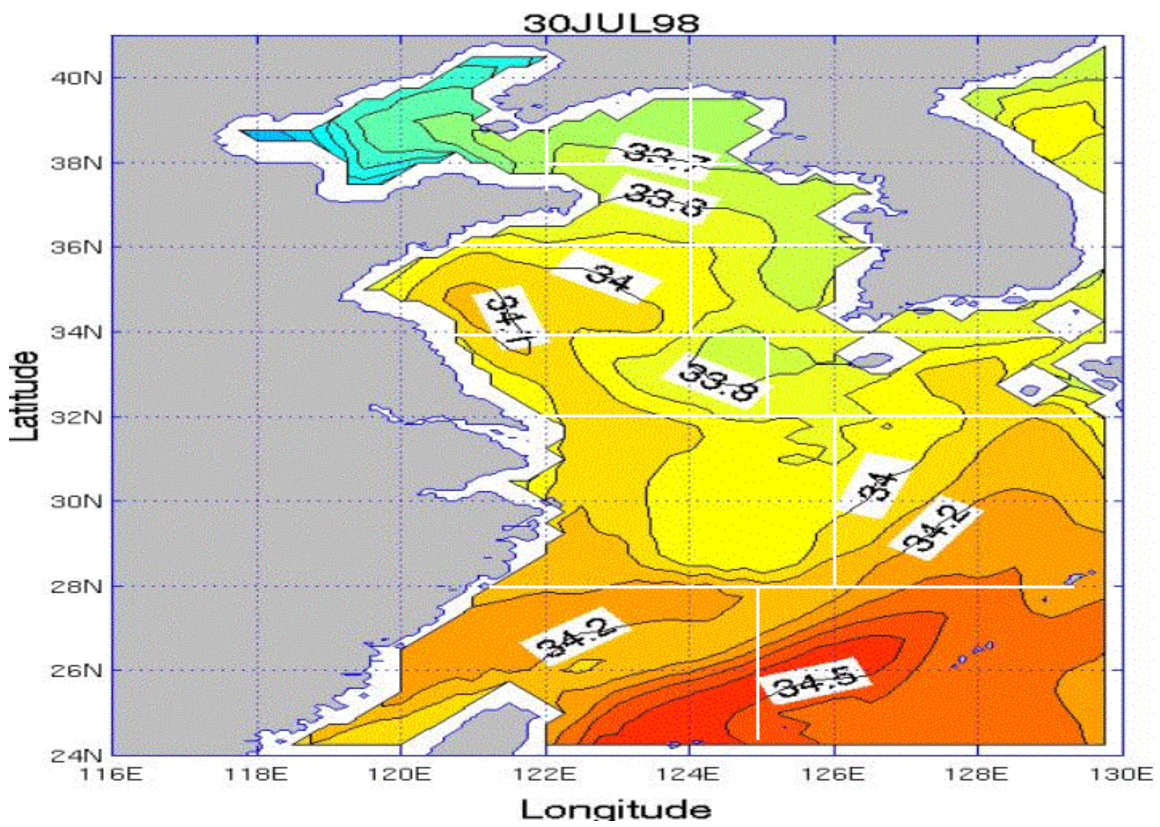
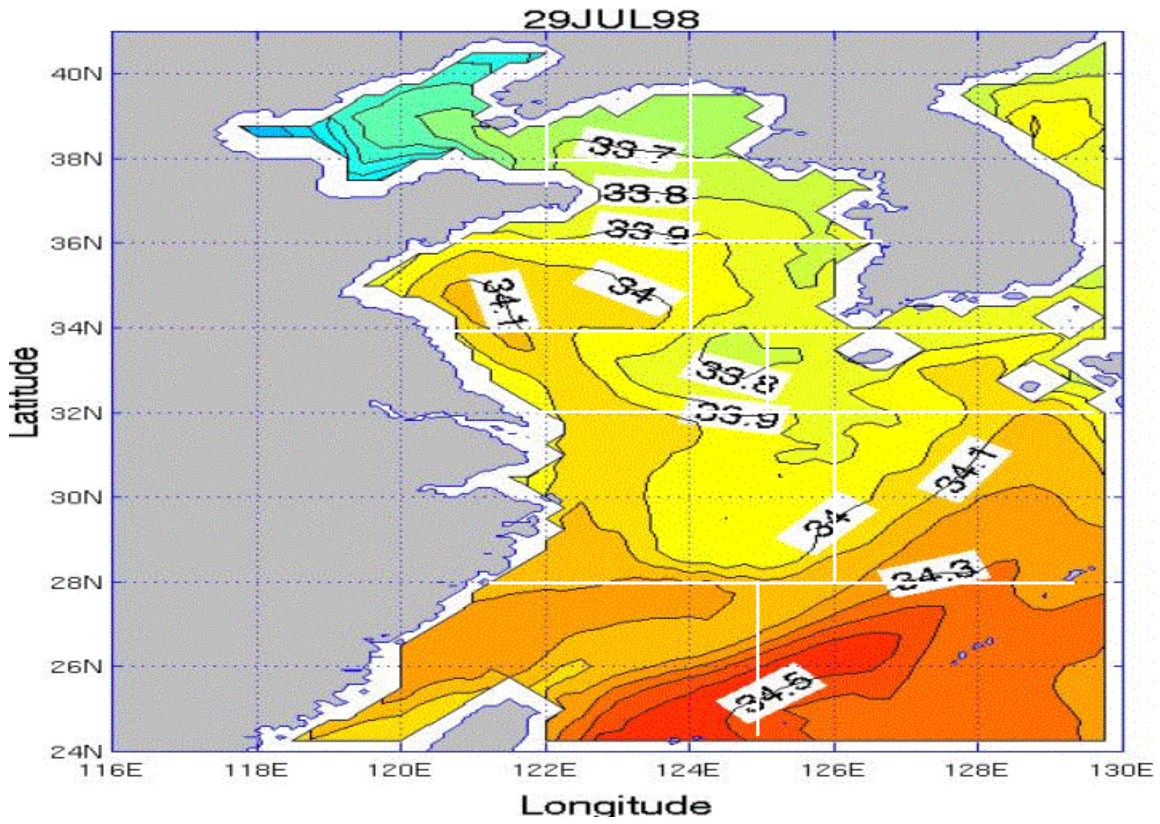


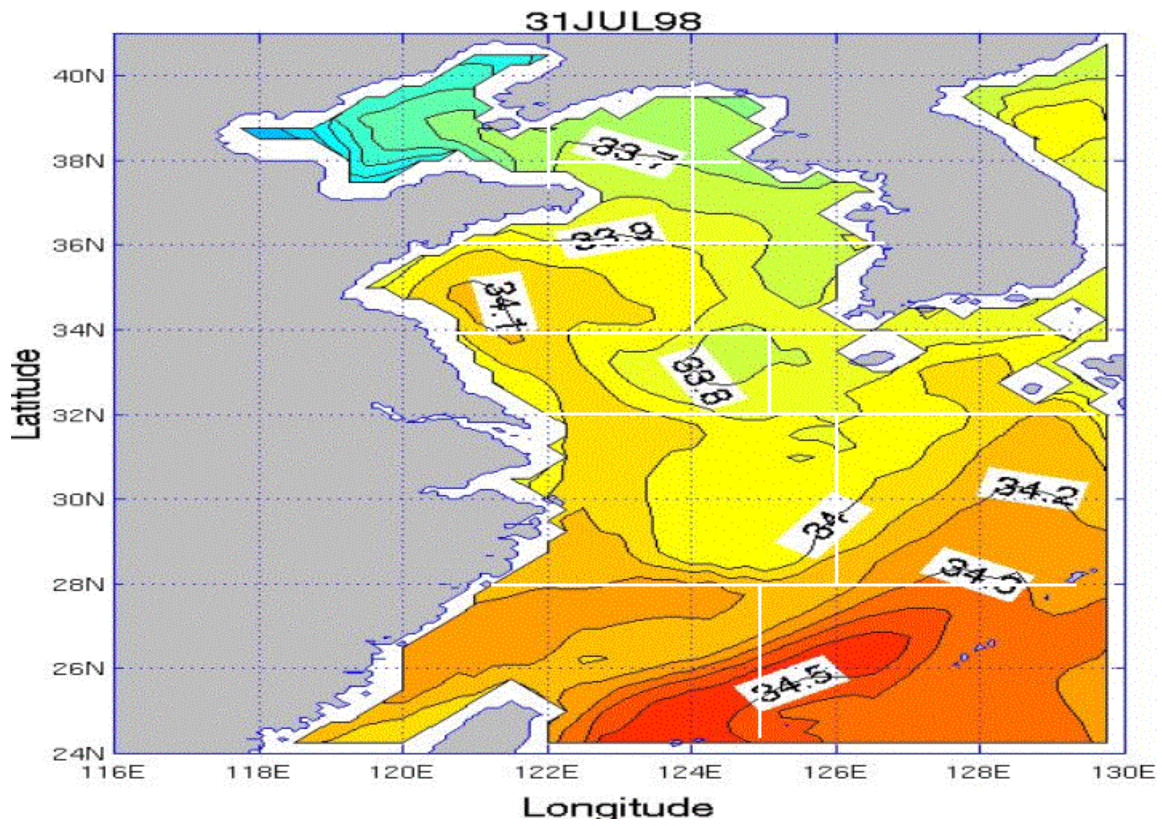






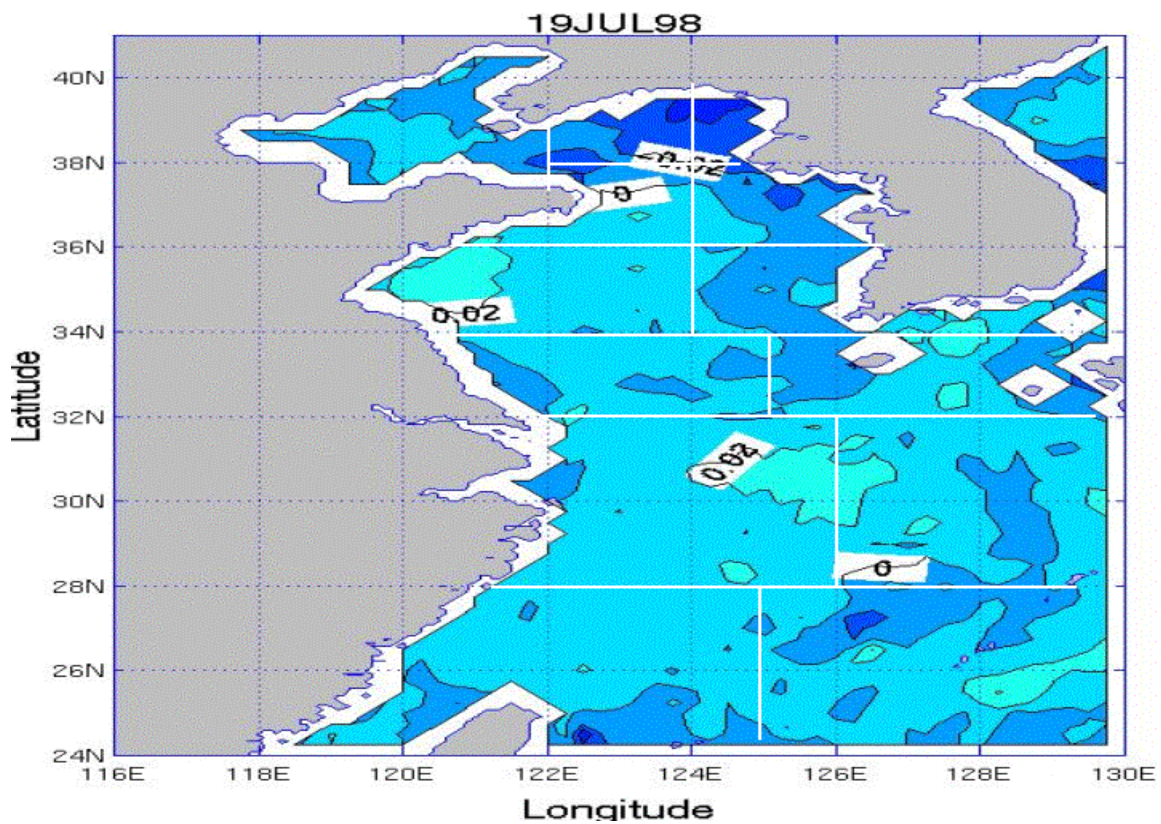


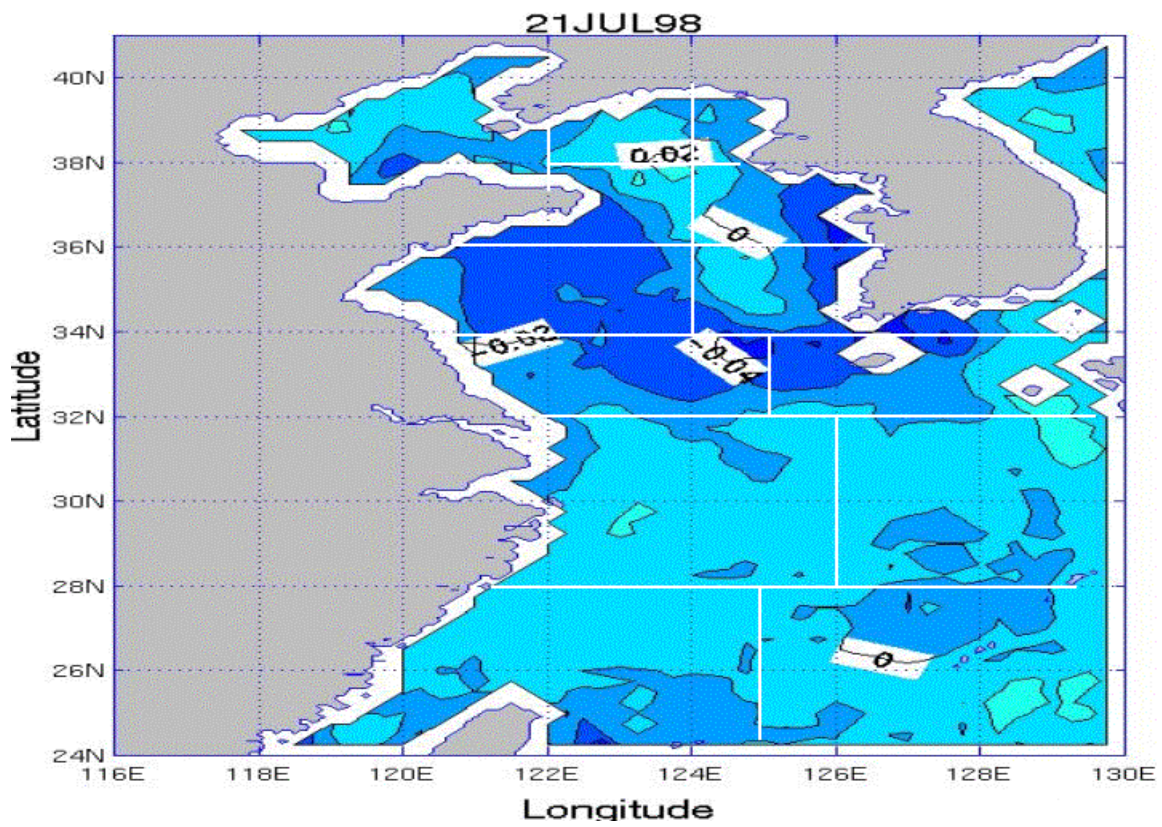
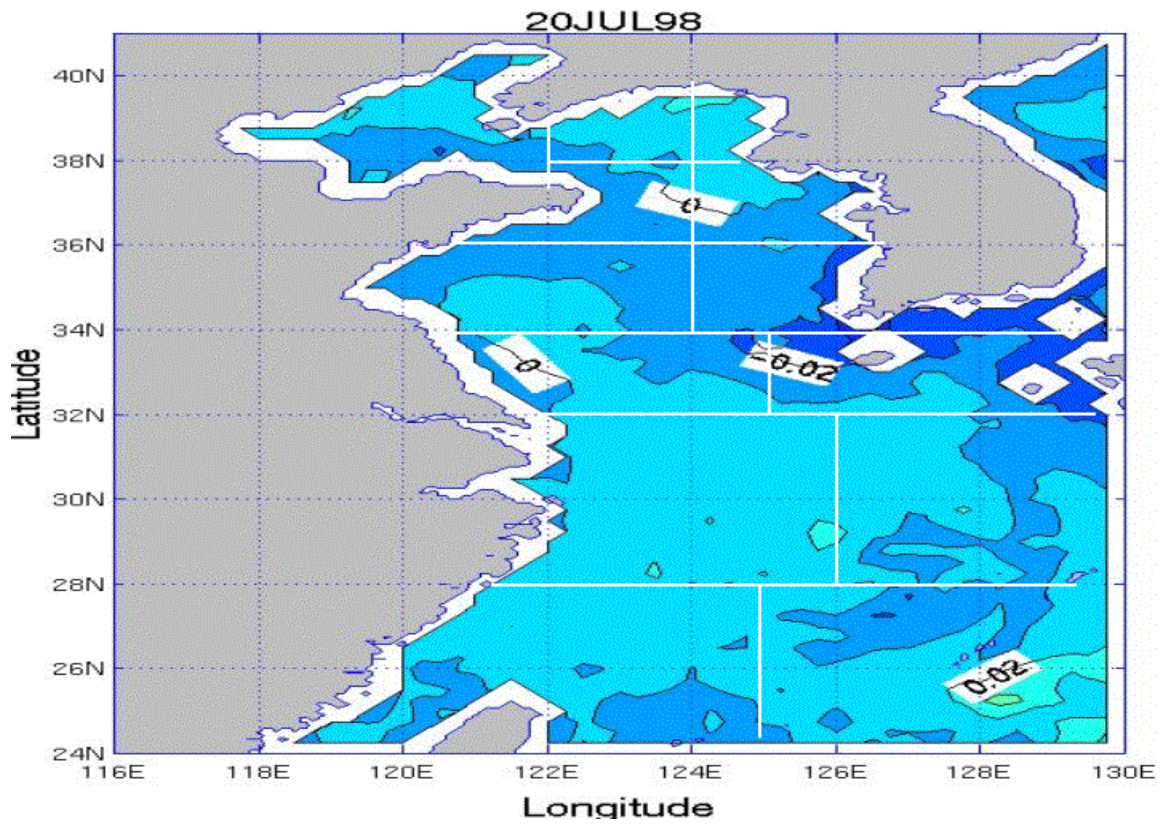


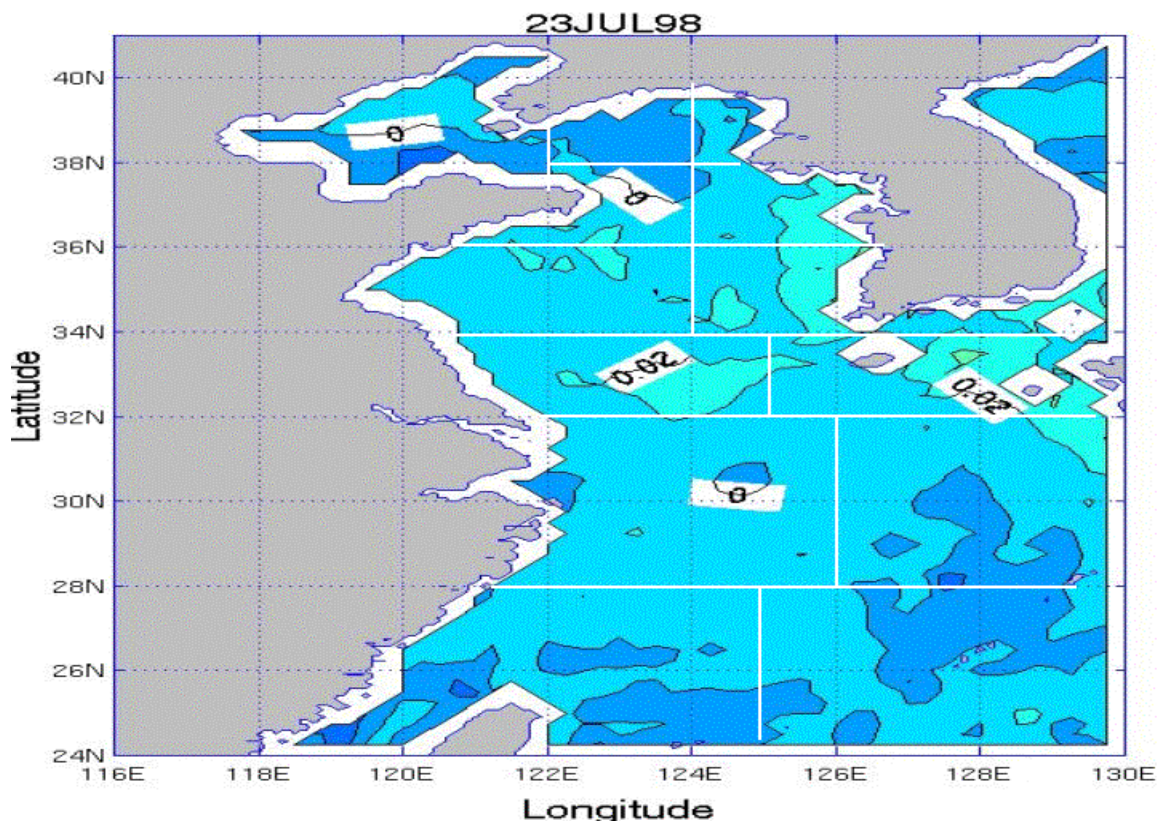
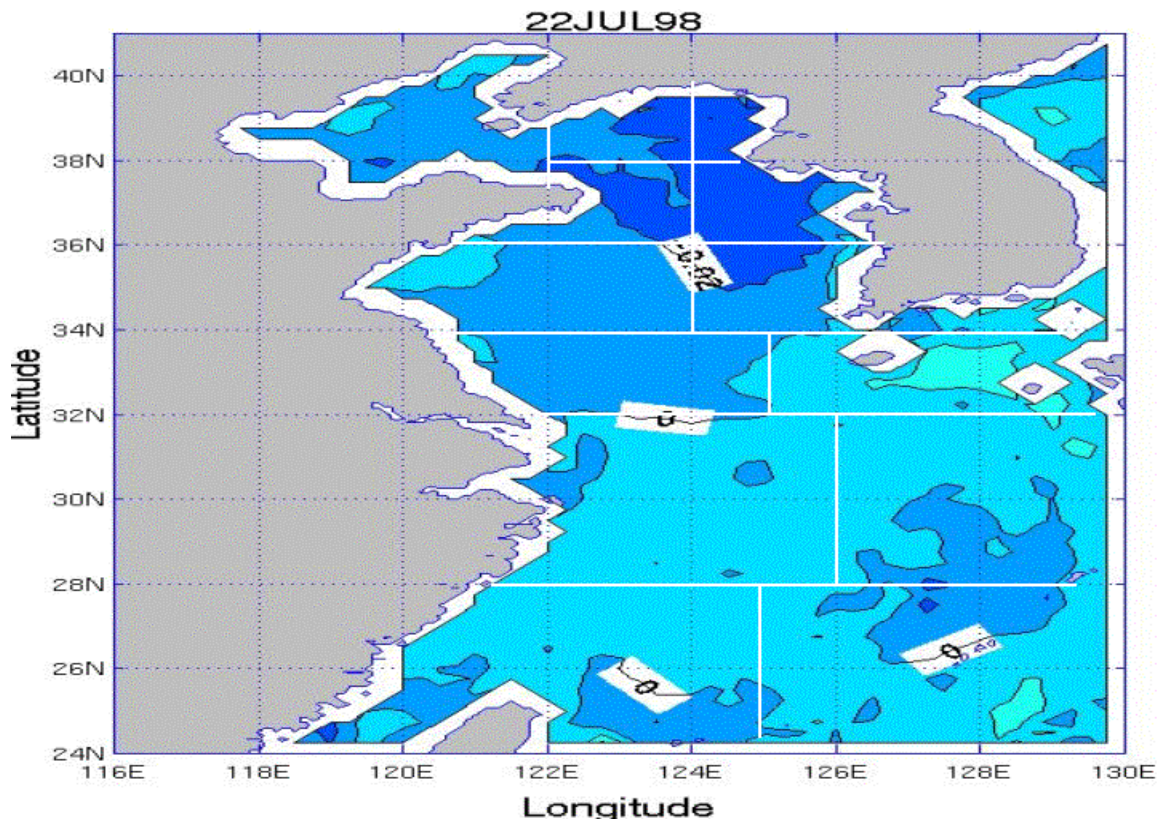


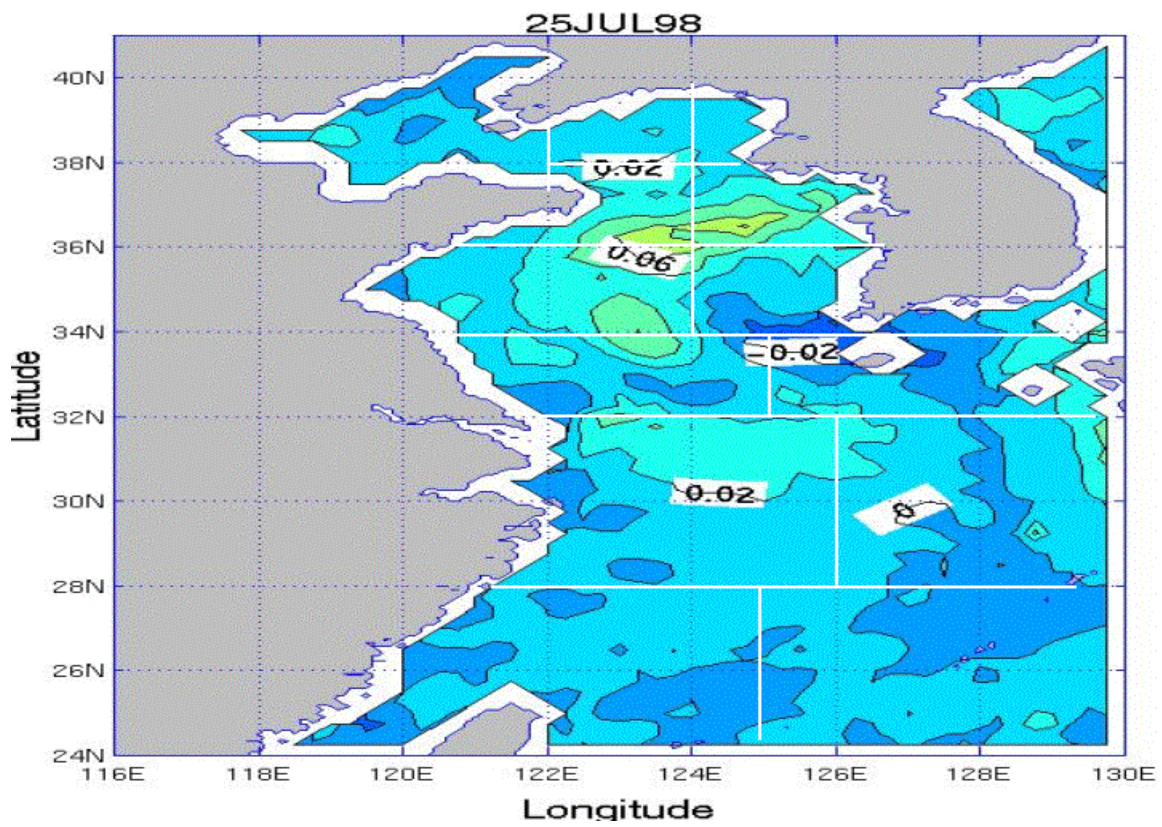
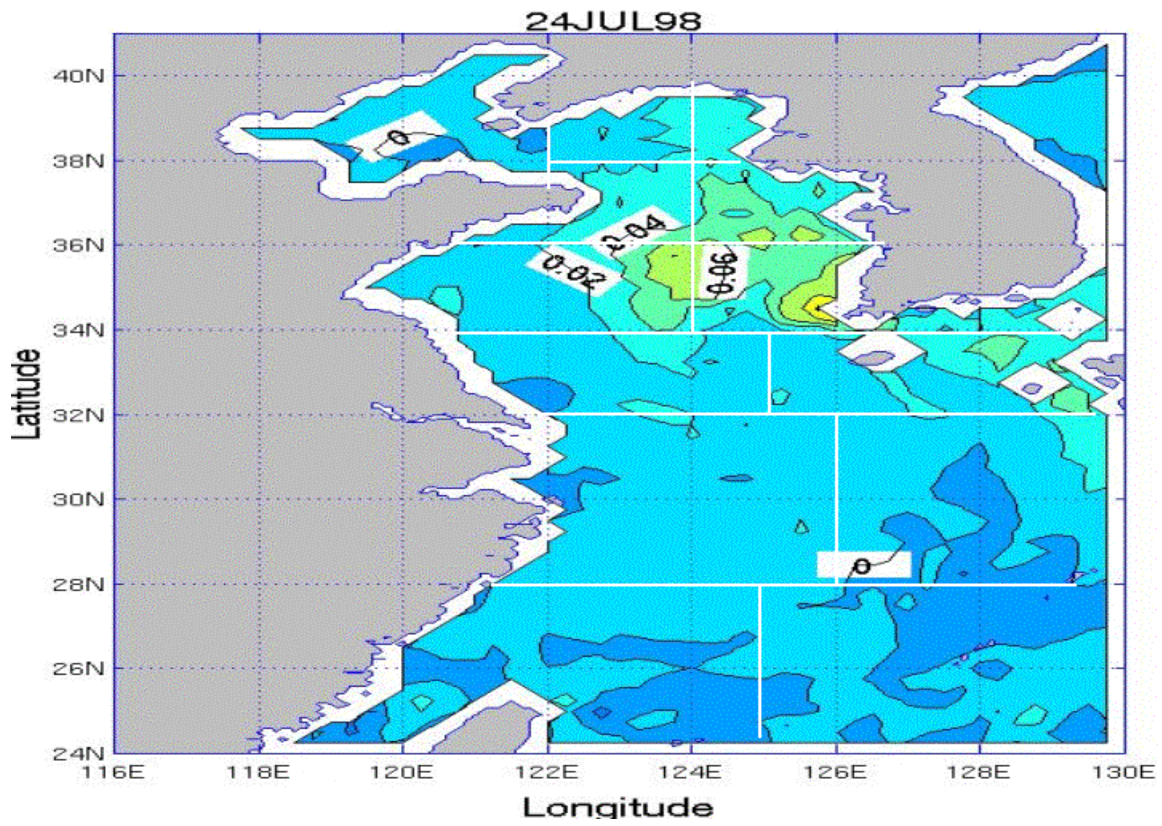
APPENDIX TT. SSS TENDENCY PLOTS FOR THE YES FOR THE JULY TIME PERIOD

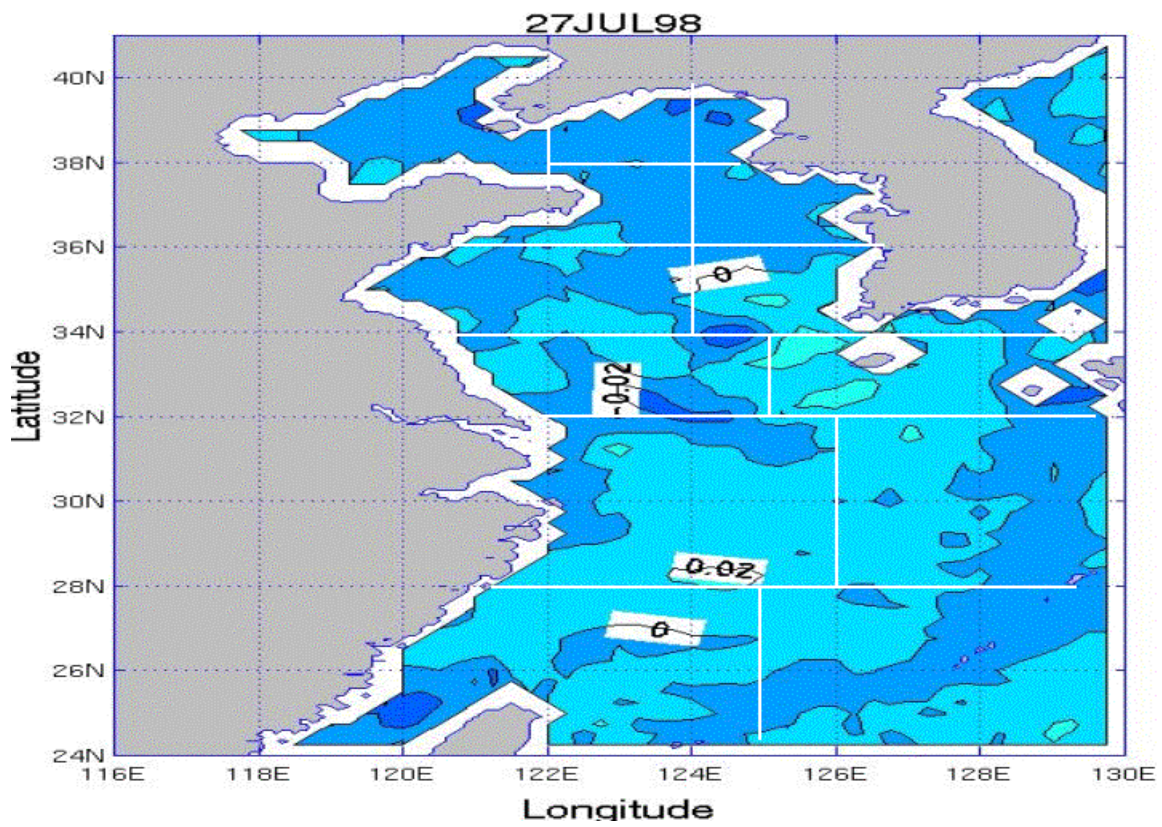
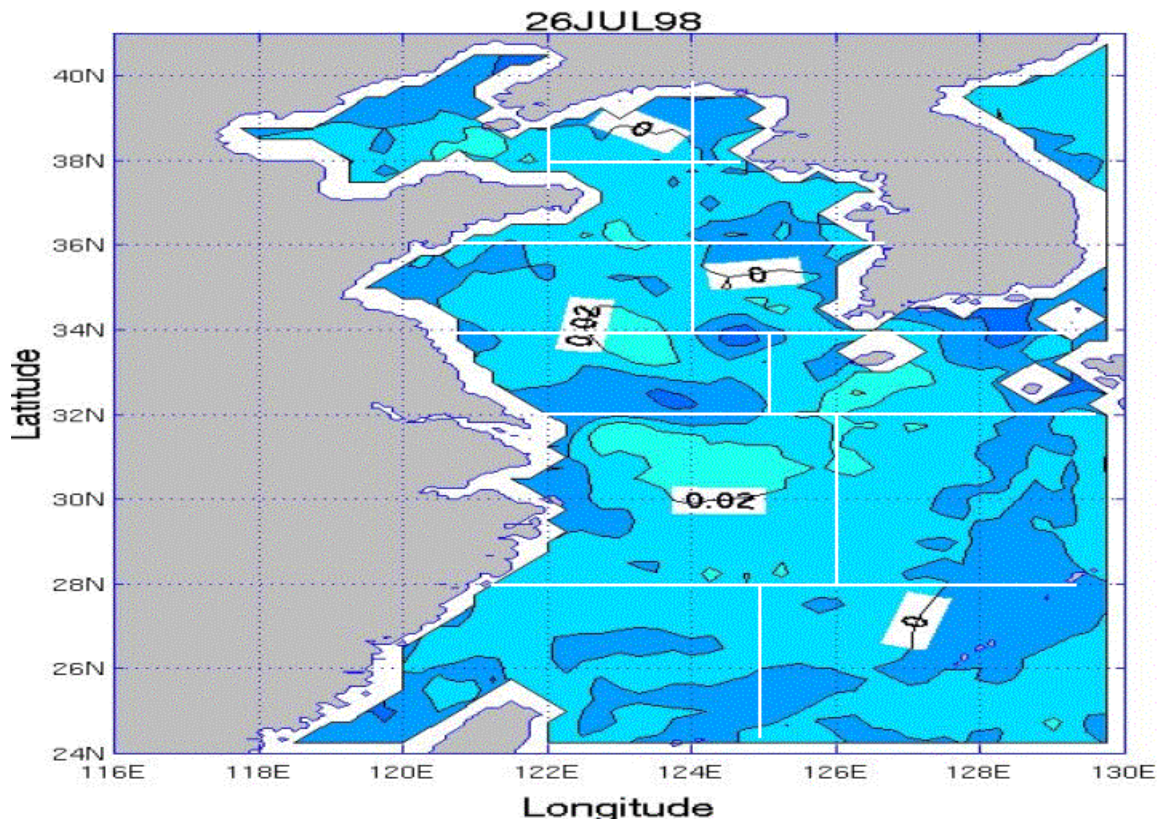
Appendix TT consists of 13 figures that show SSS day-to-day tendency for the July time period over the YES. The figures are in time sequential order from July 19 through July 31. Each plot represents the change between the previous day and the current day.

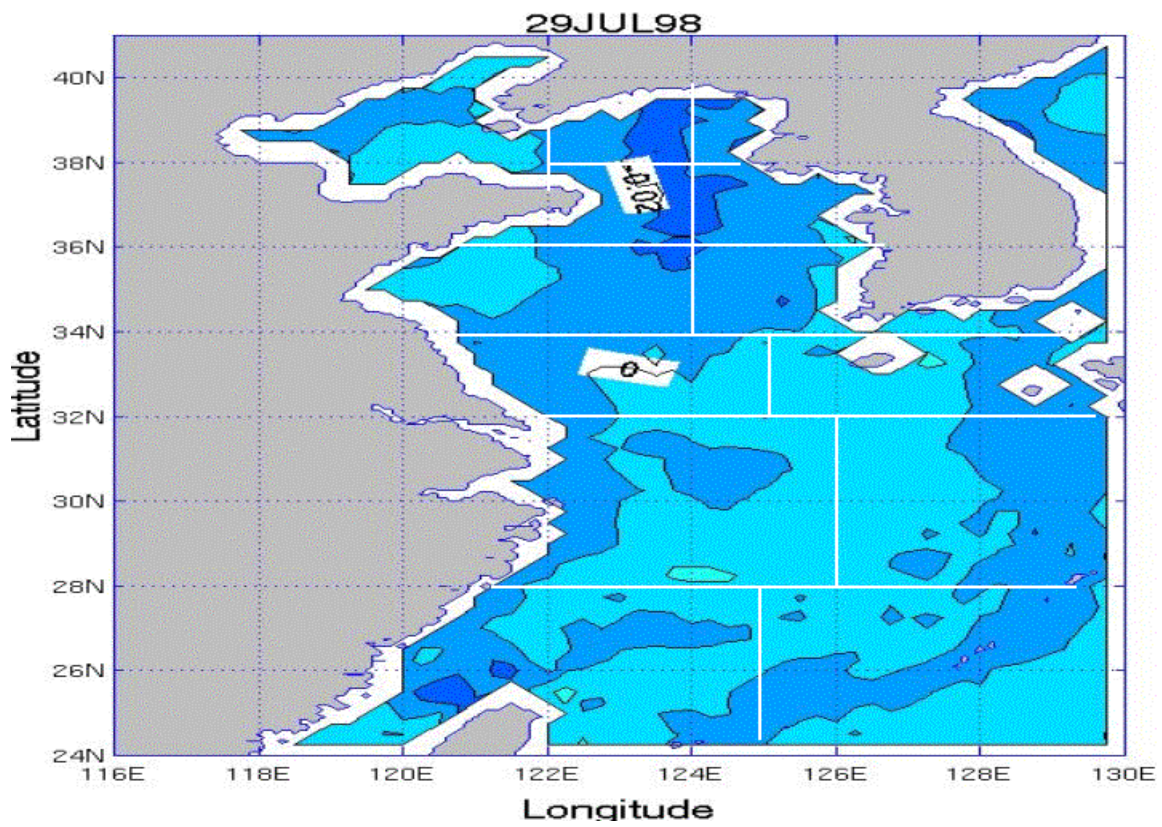
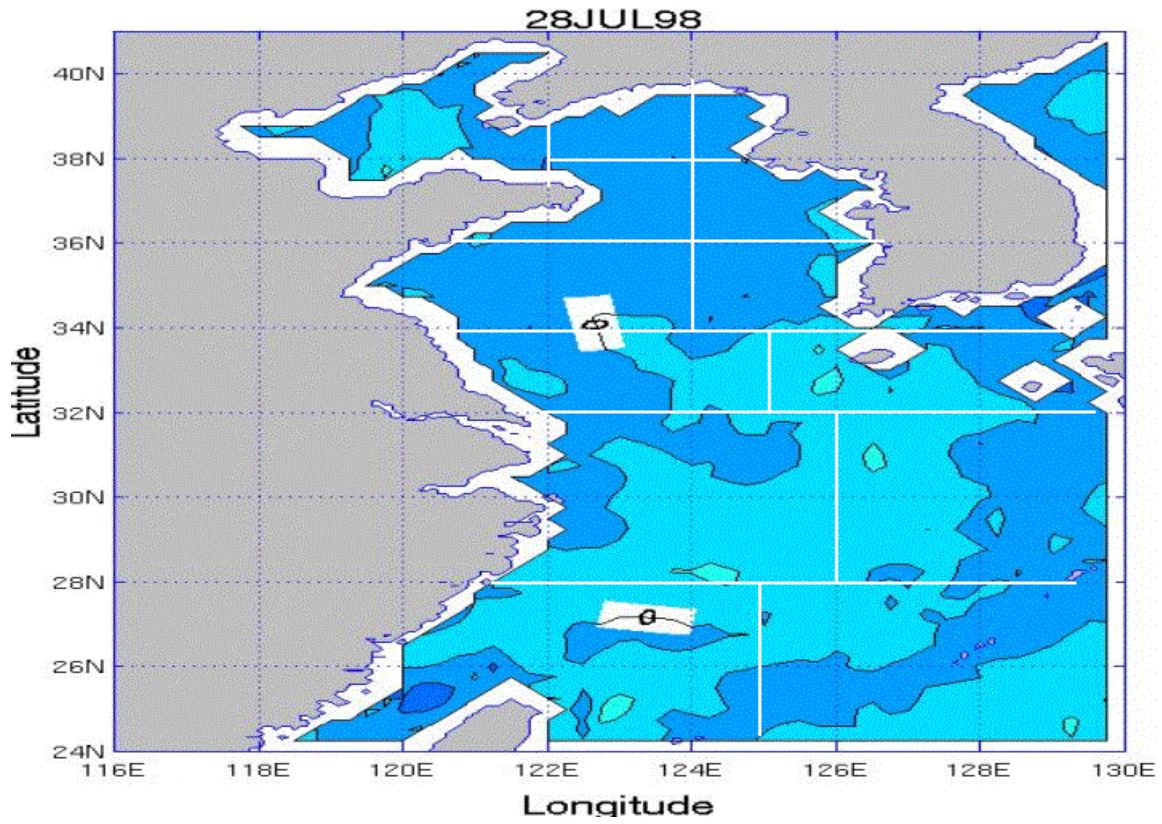


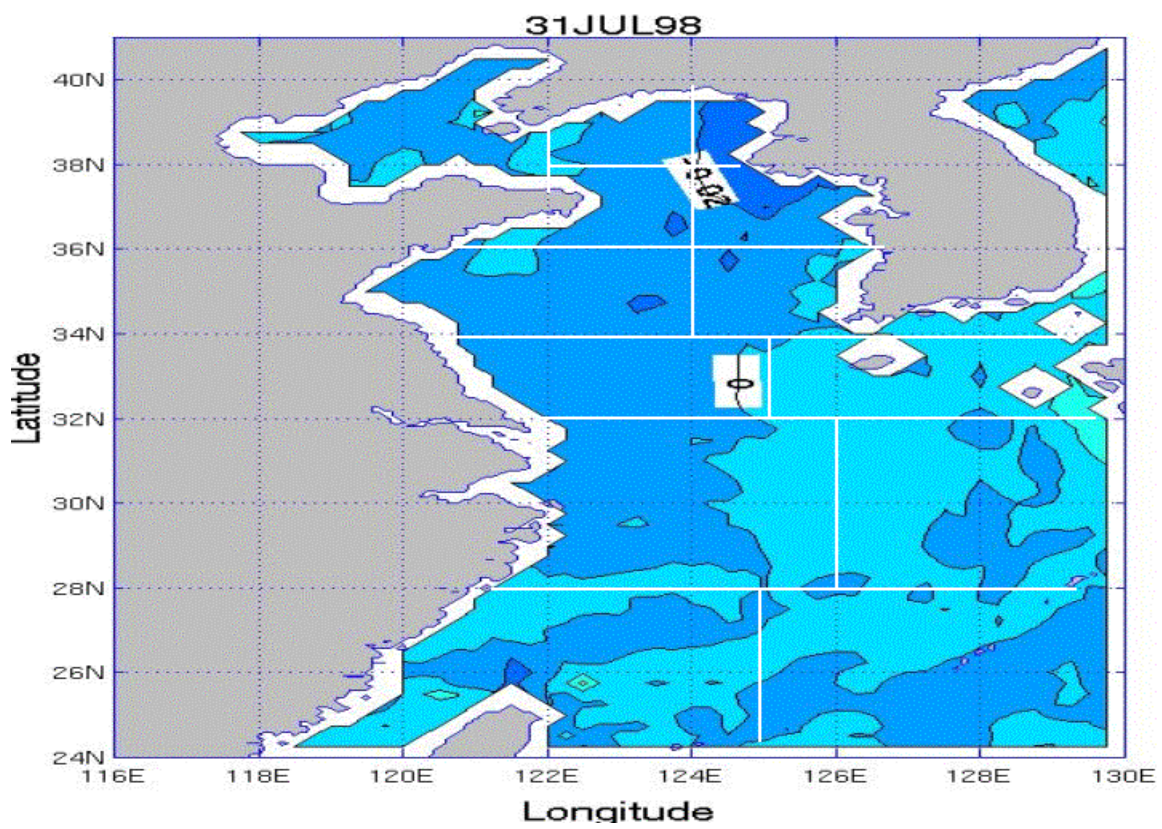
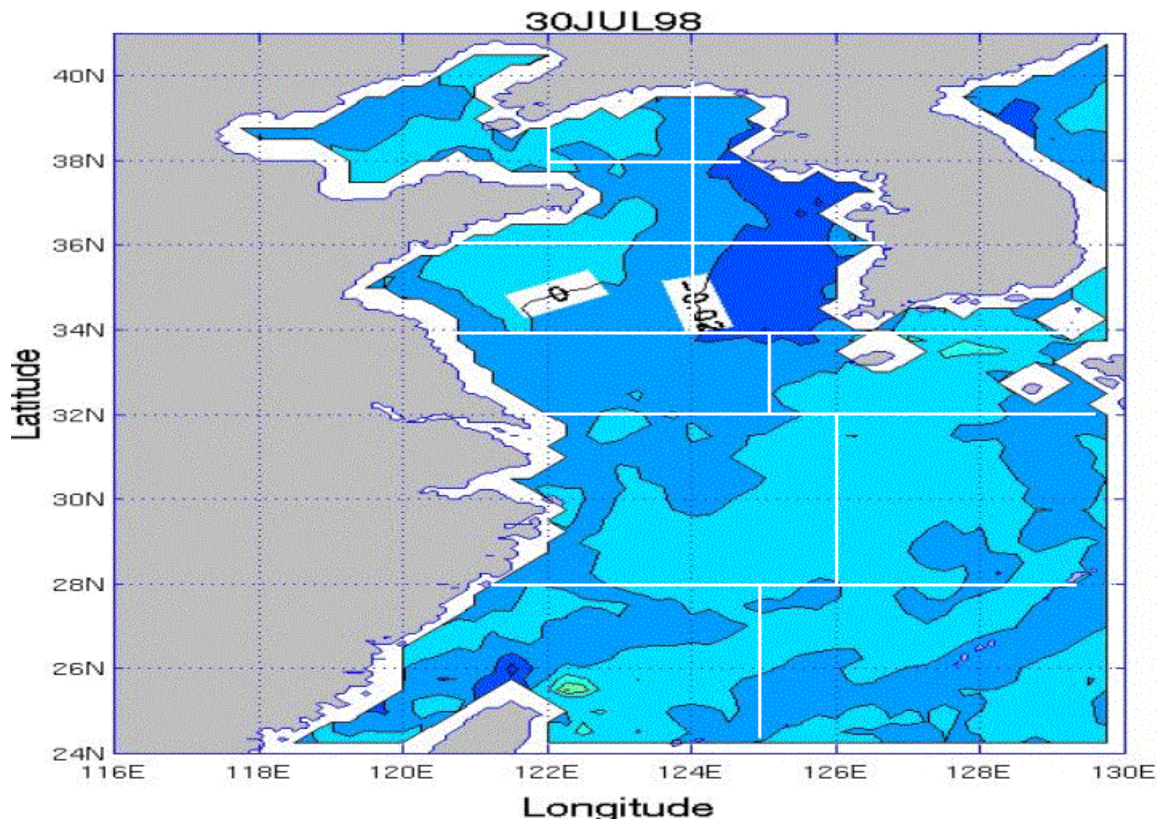








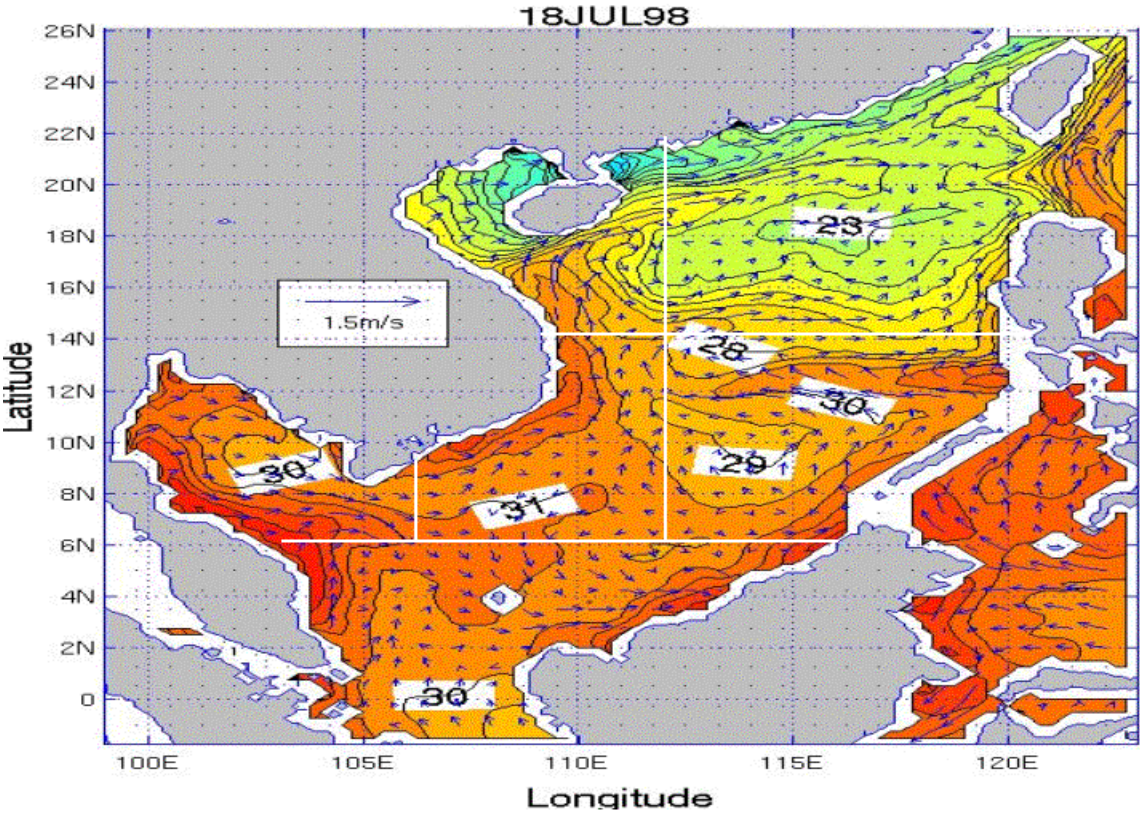


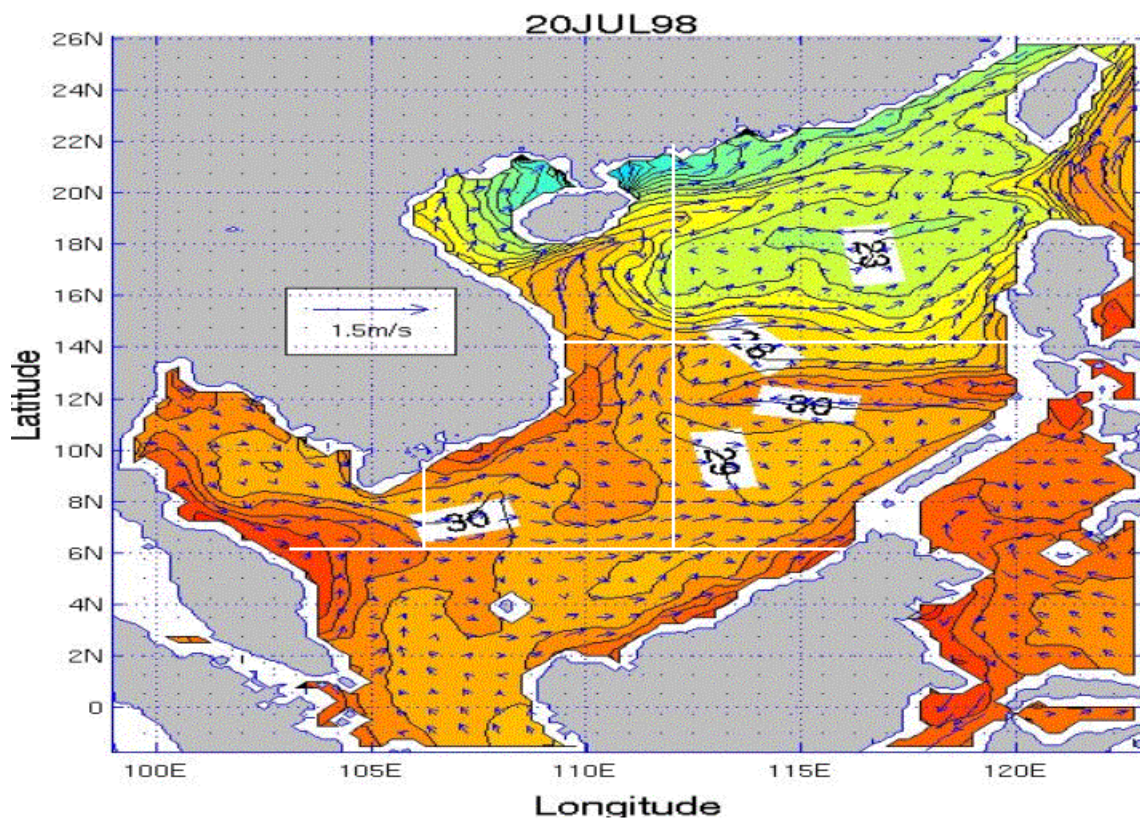
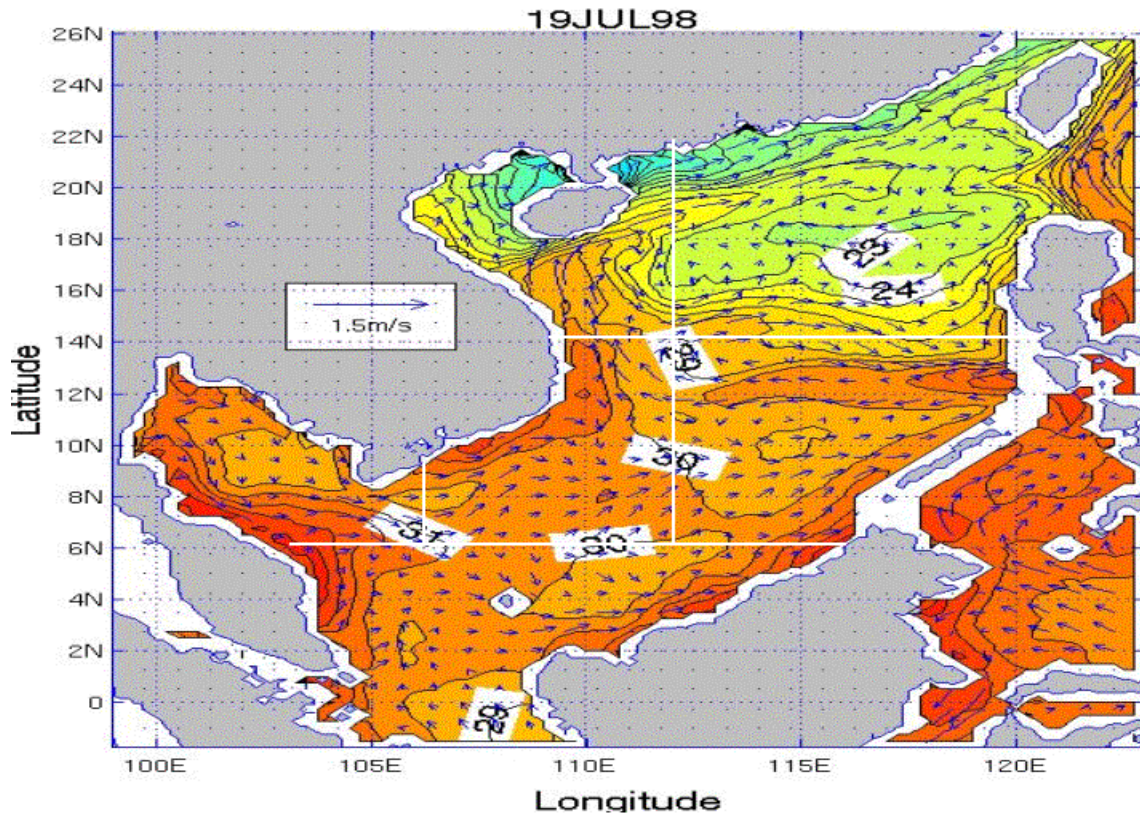


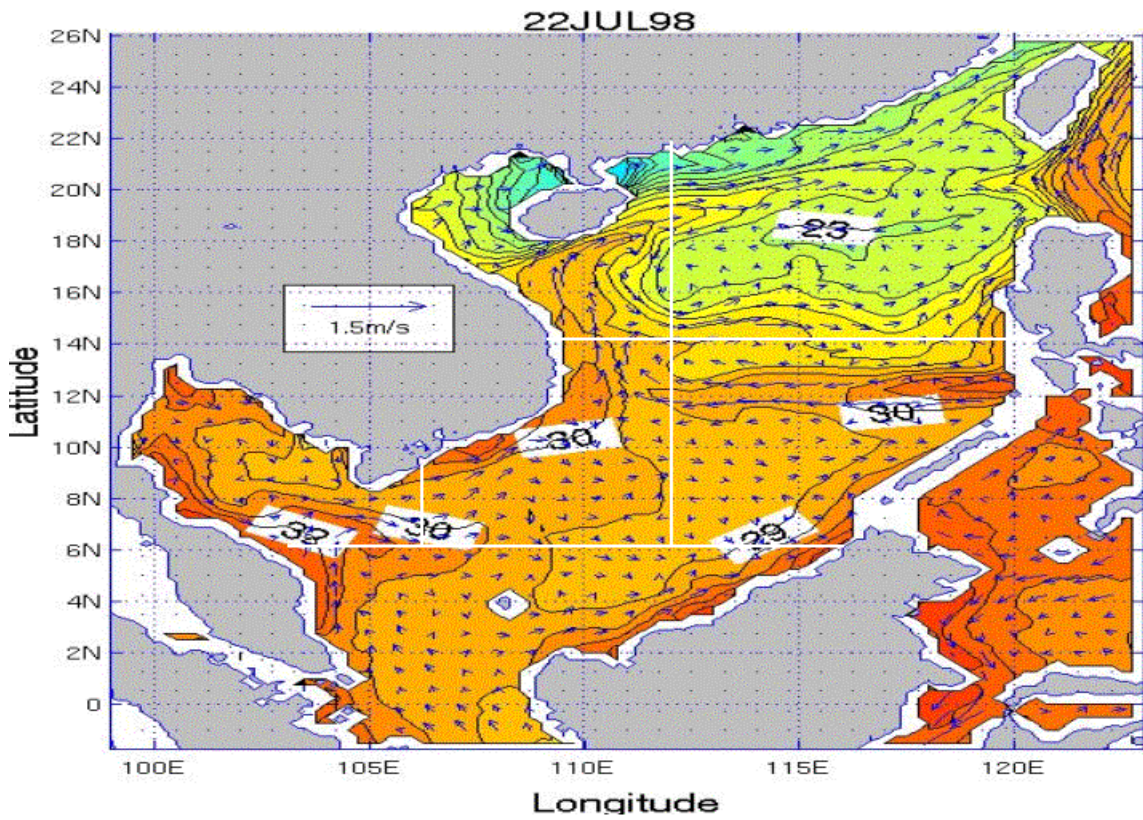
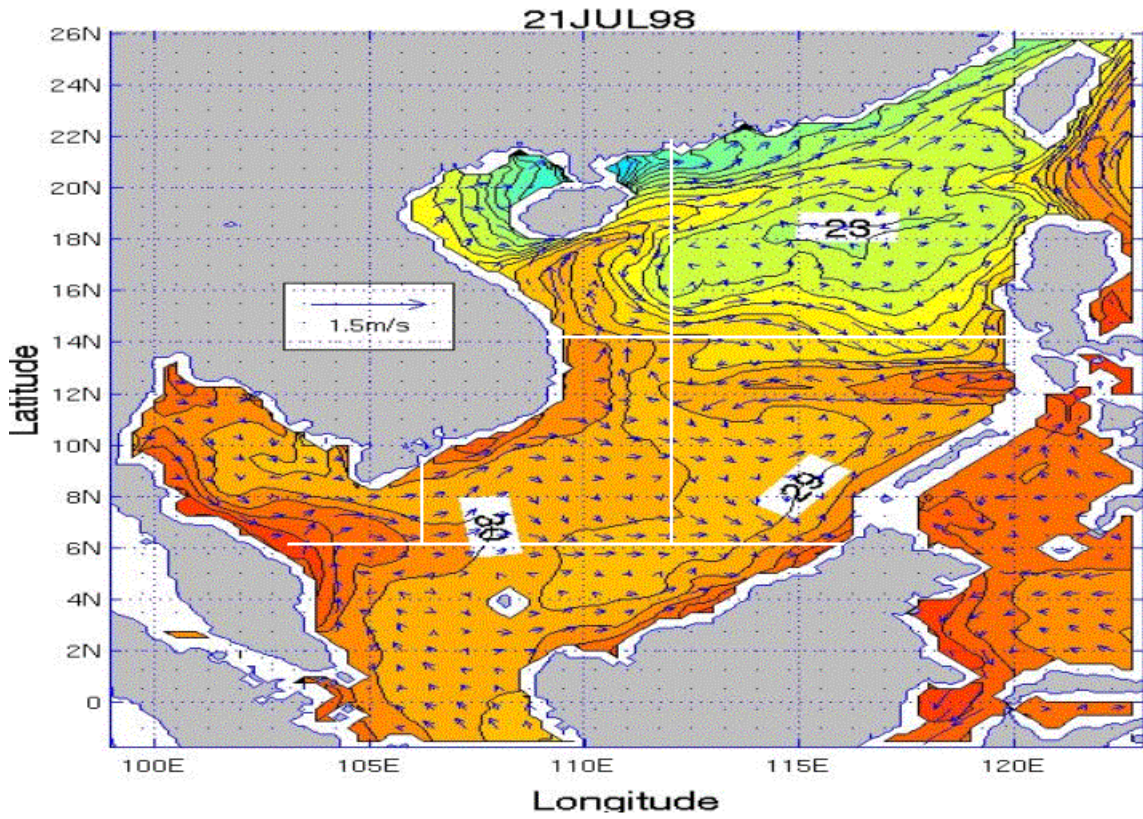
THIS PAGE INTENTIONALLY LEFT BLANK

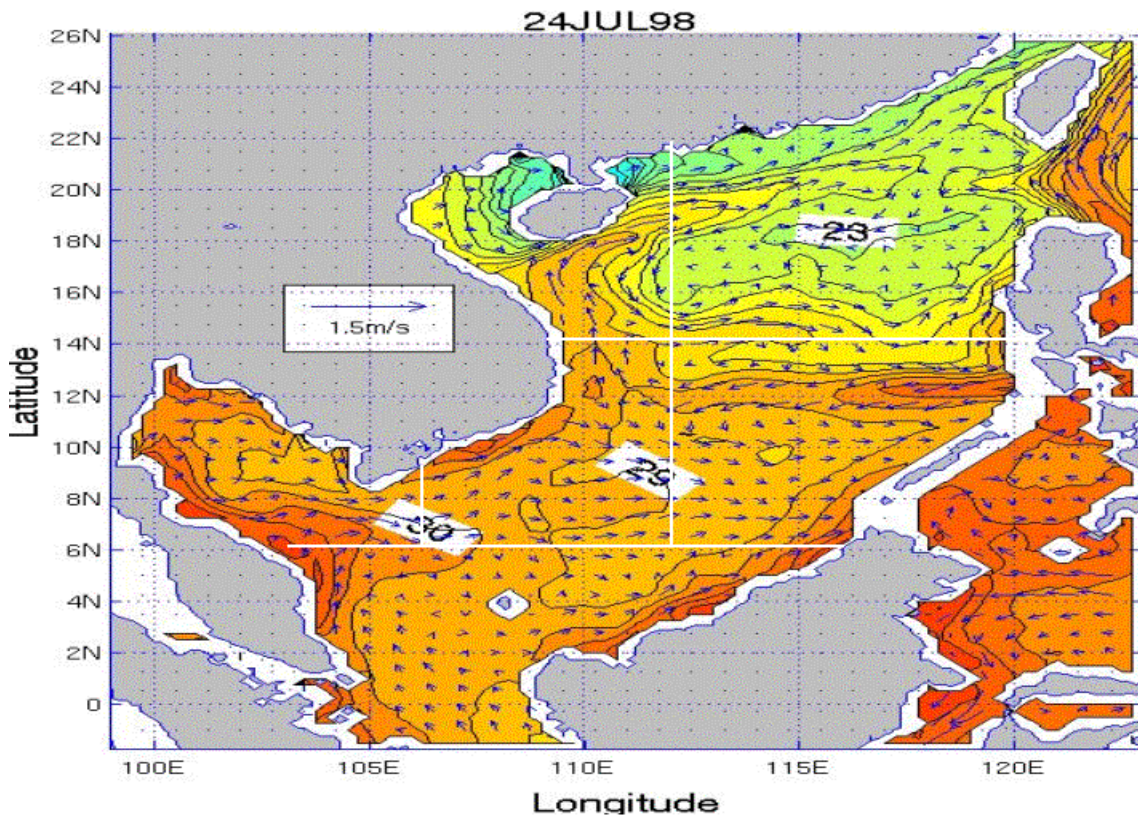
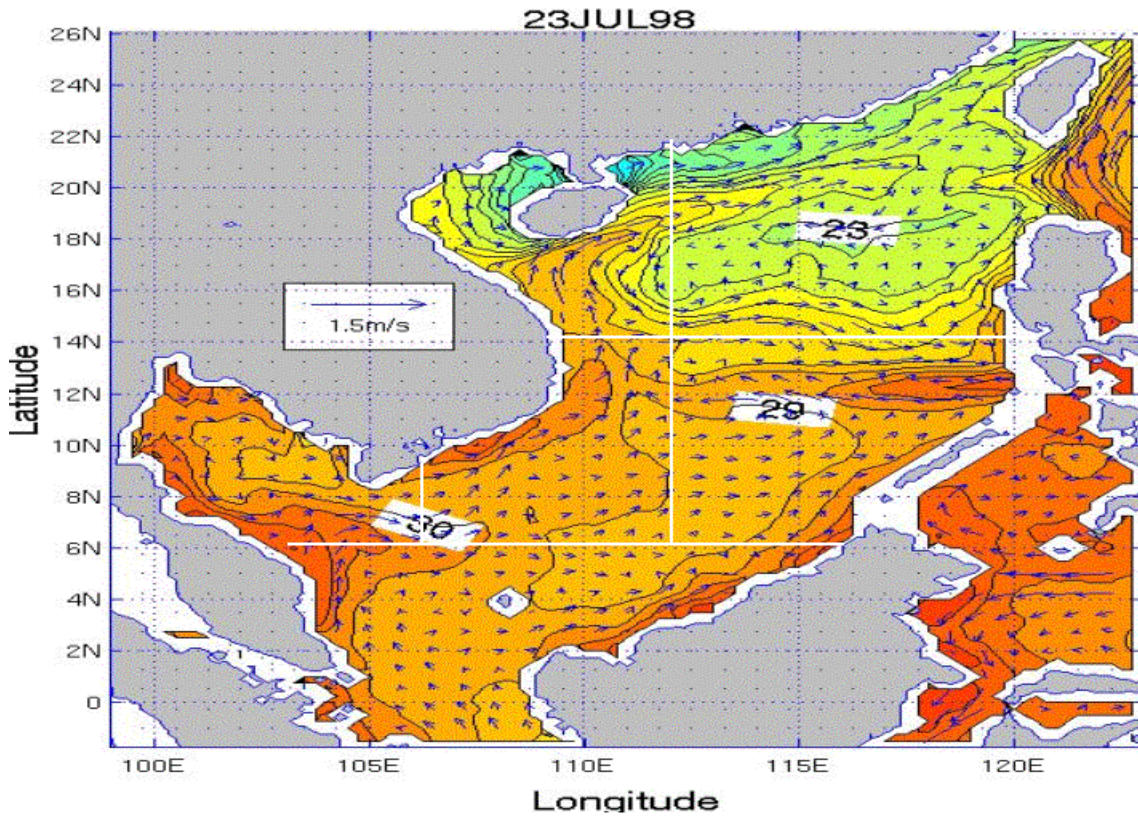
**APPENDIX UU. SST AND SURFACE CURRENT VELOCITY
PLOTS FOR THE SCS FOR THE JULY TIME PERIOD**

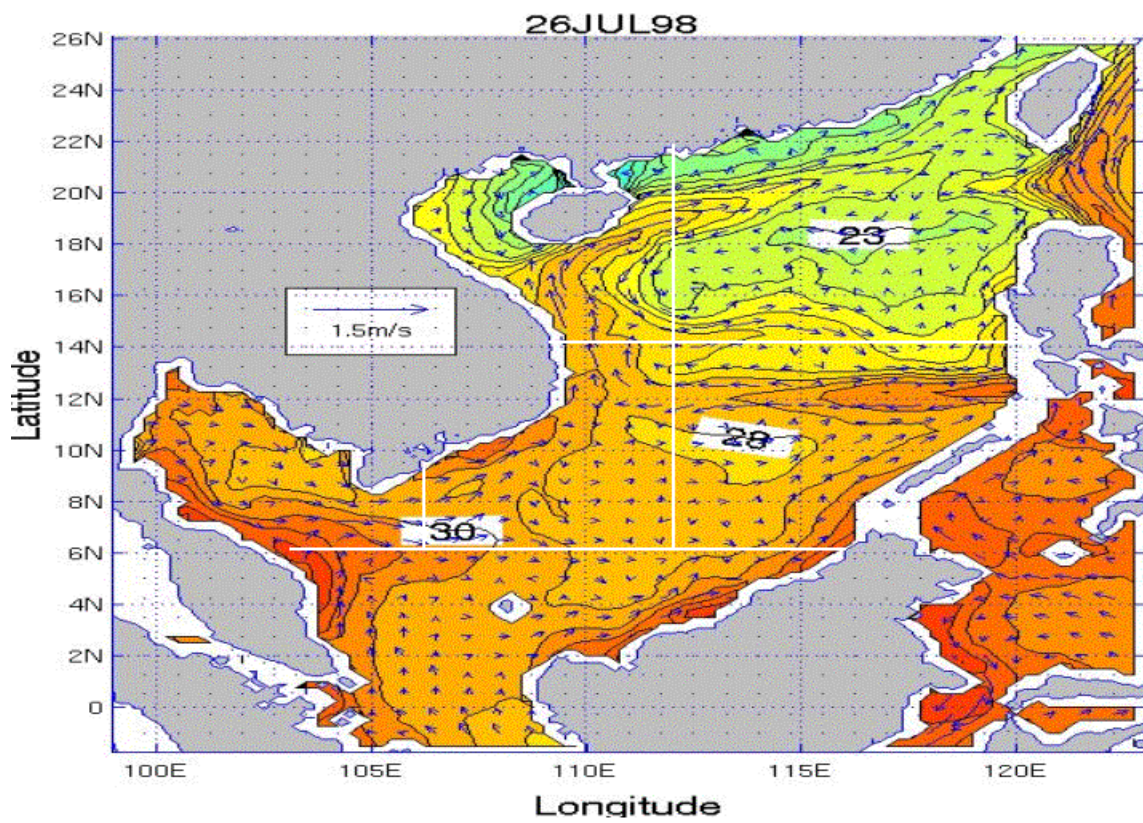
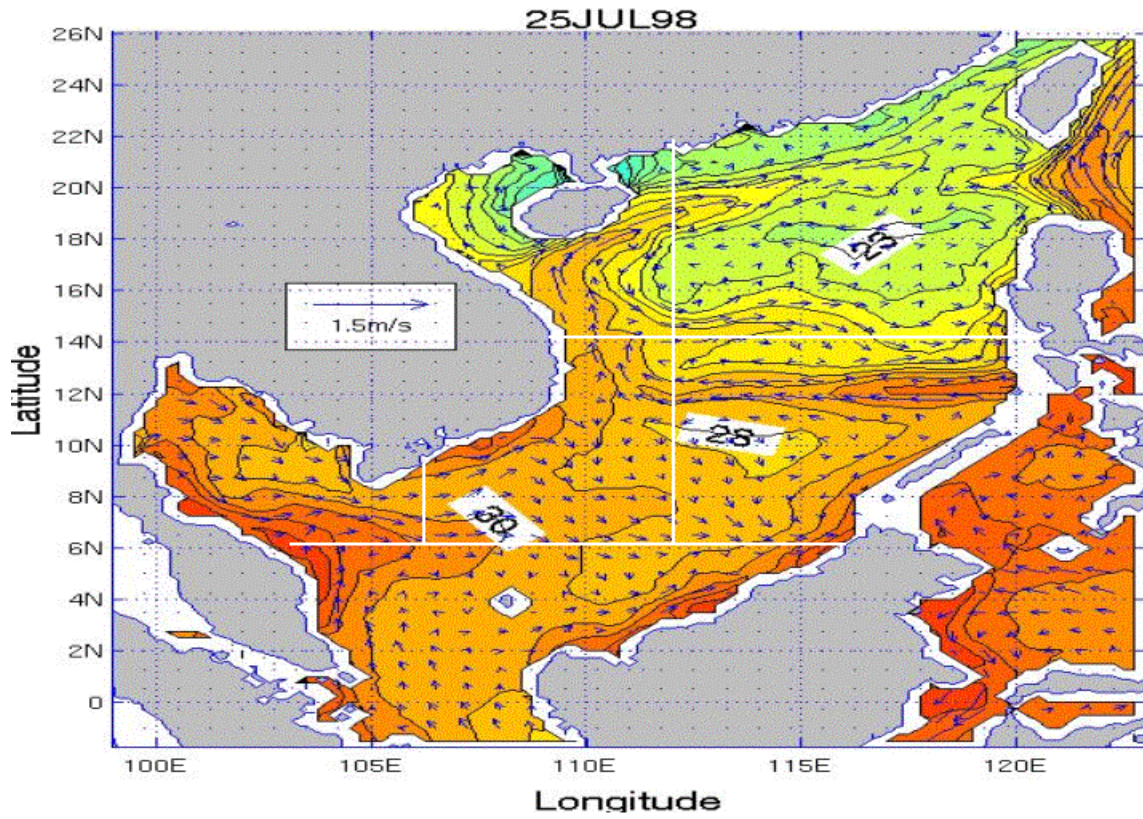
Appendix UU consists of 14 figures that show SST and surface current velocity for each day of the July time period for the SCS. The figures are in time sequential order from July 18 through July 31.

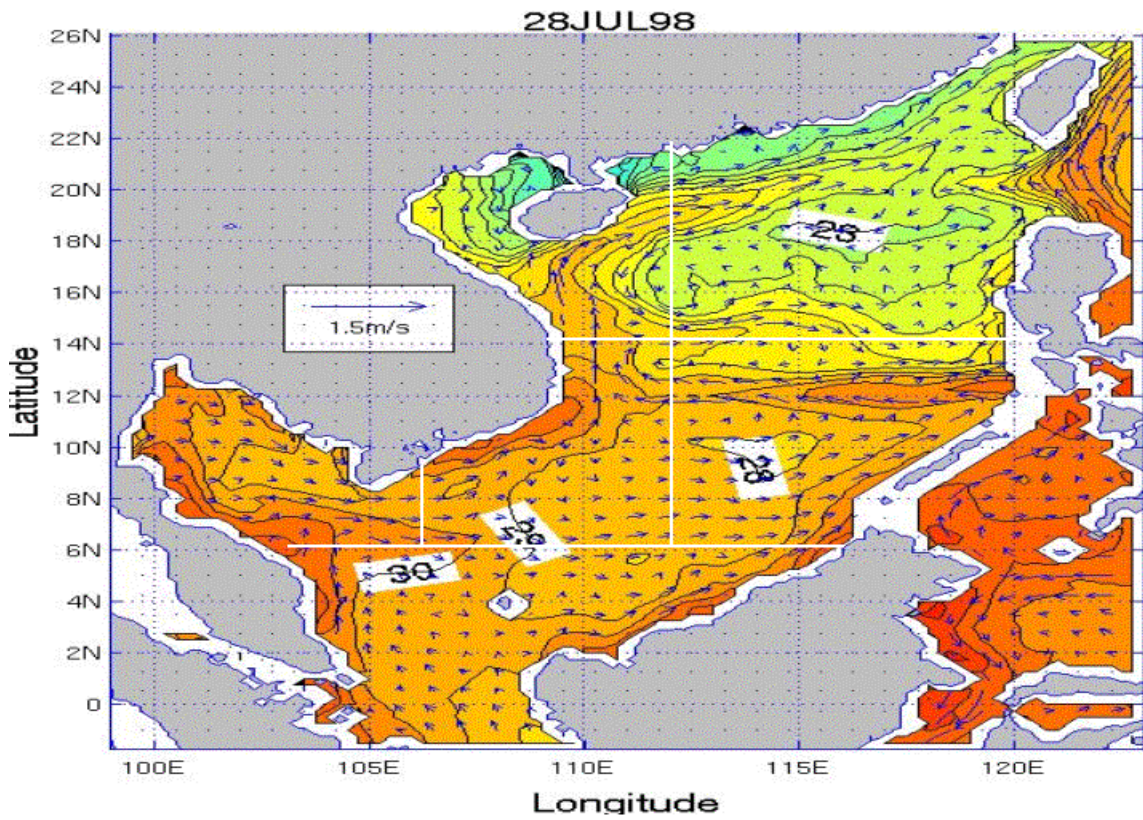
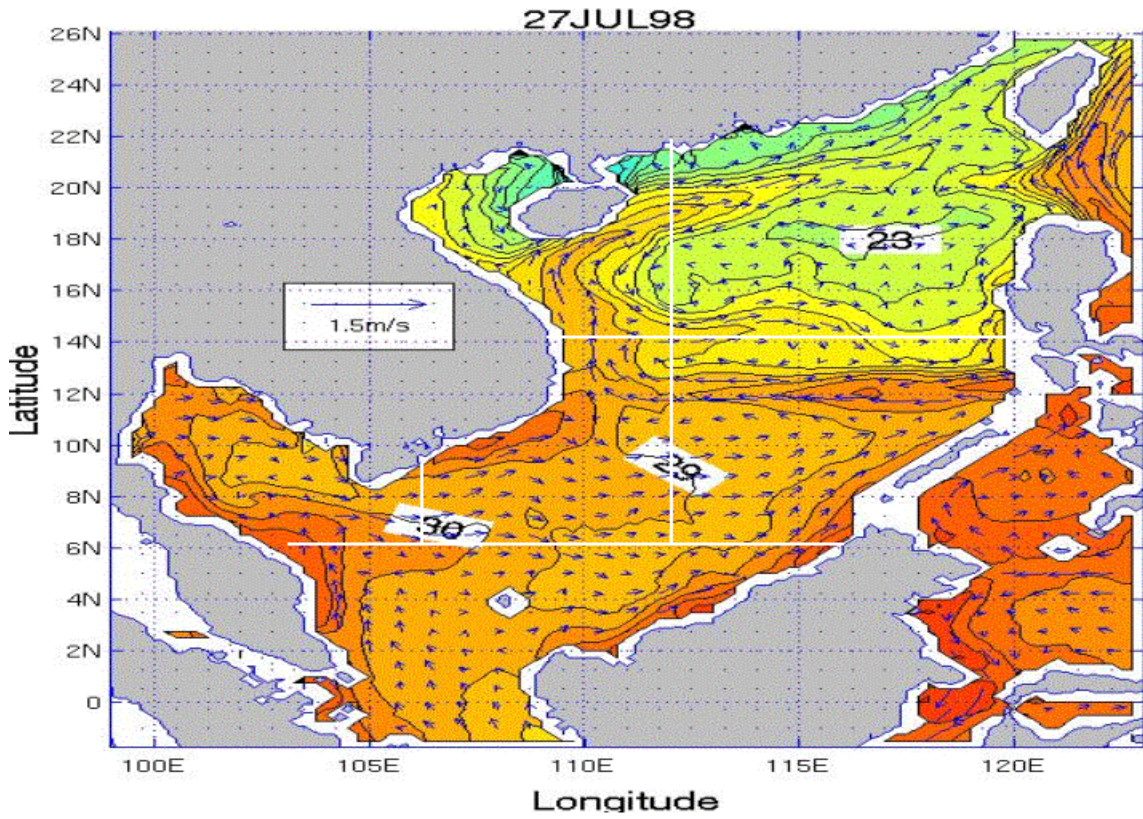


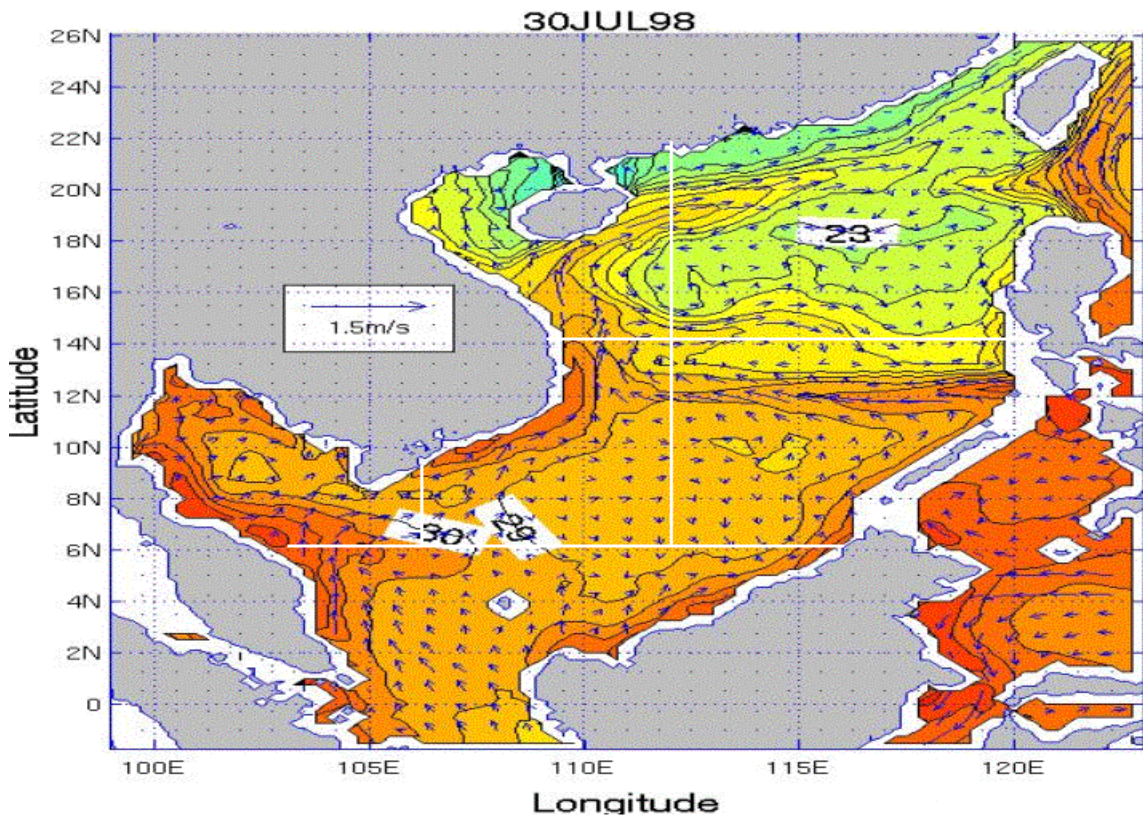
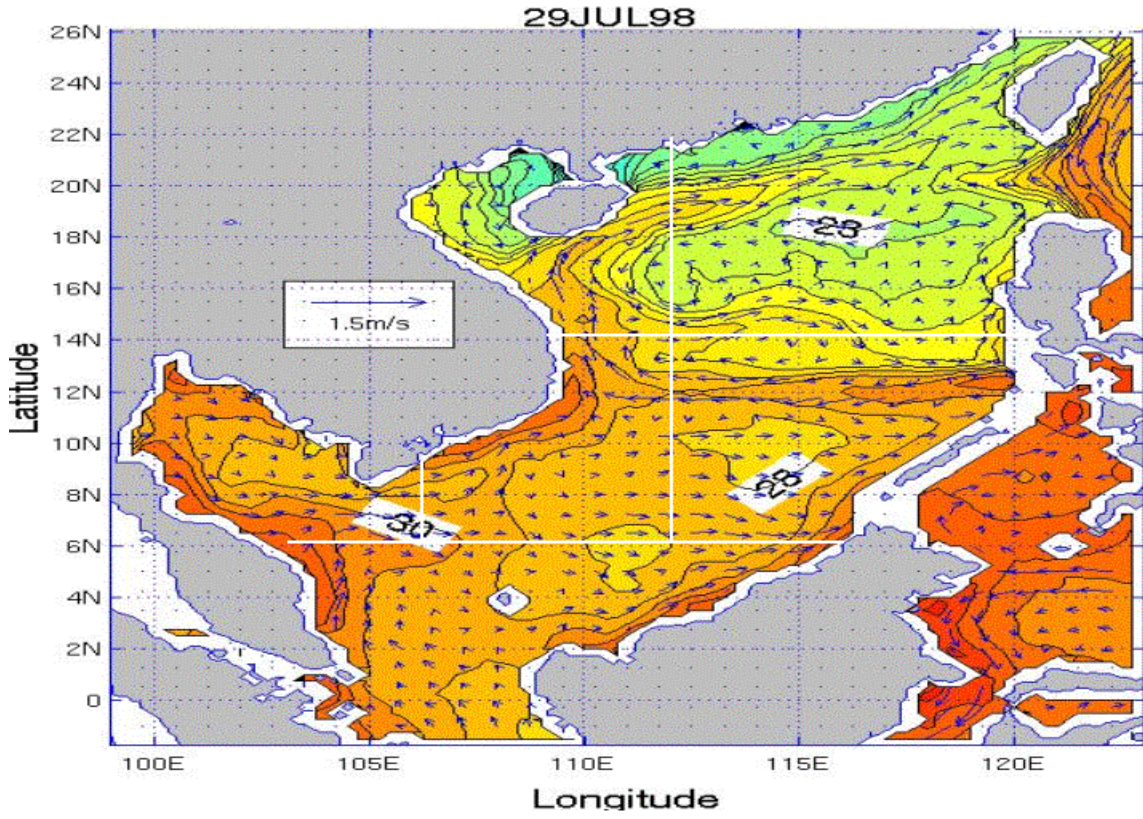


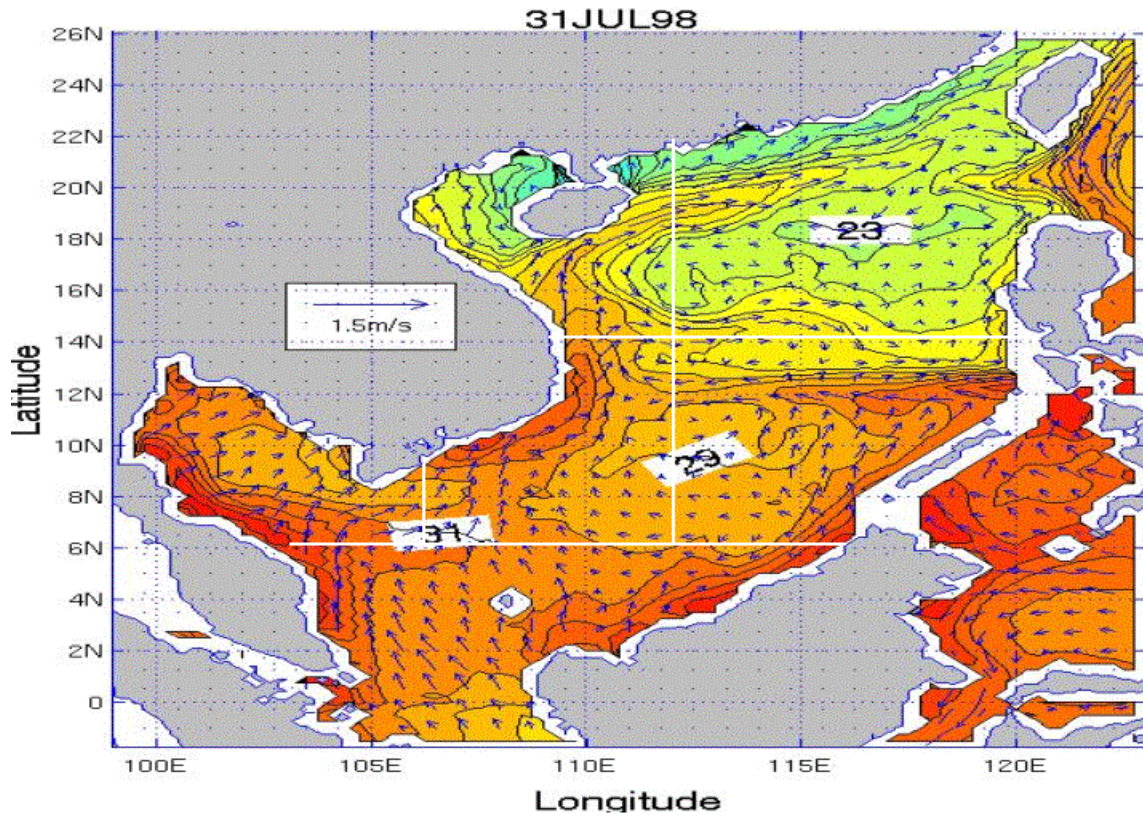






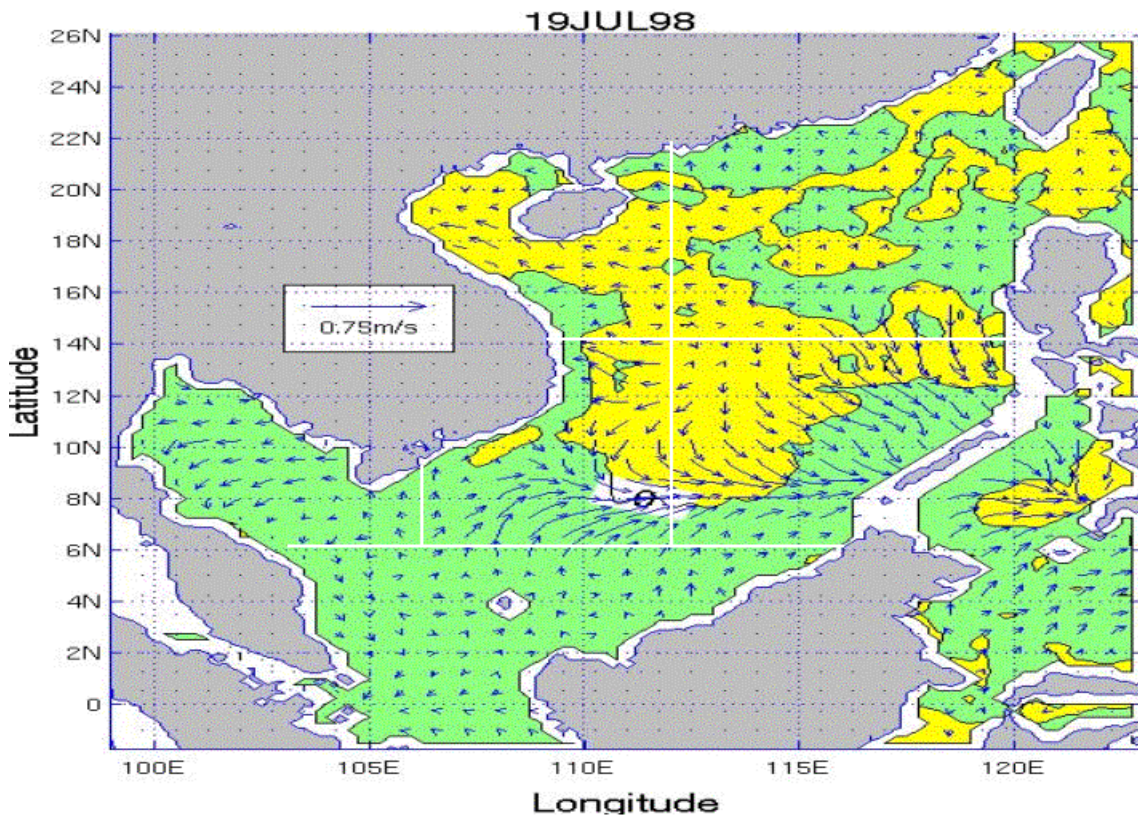


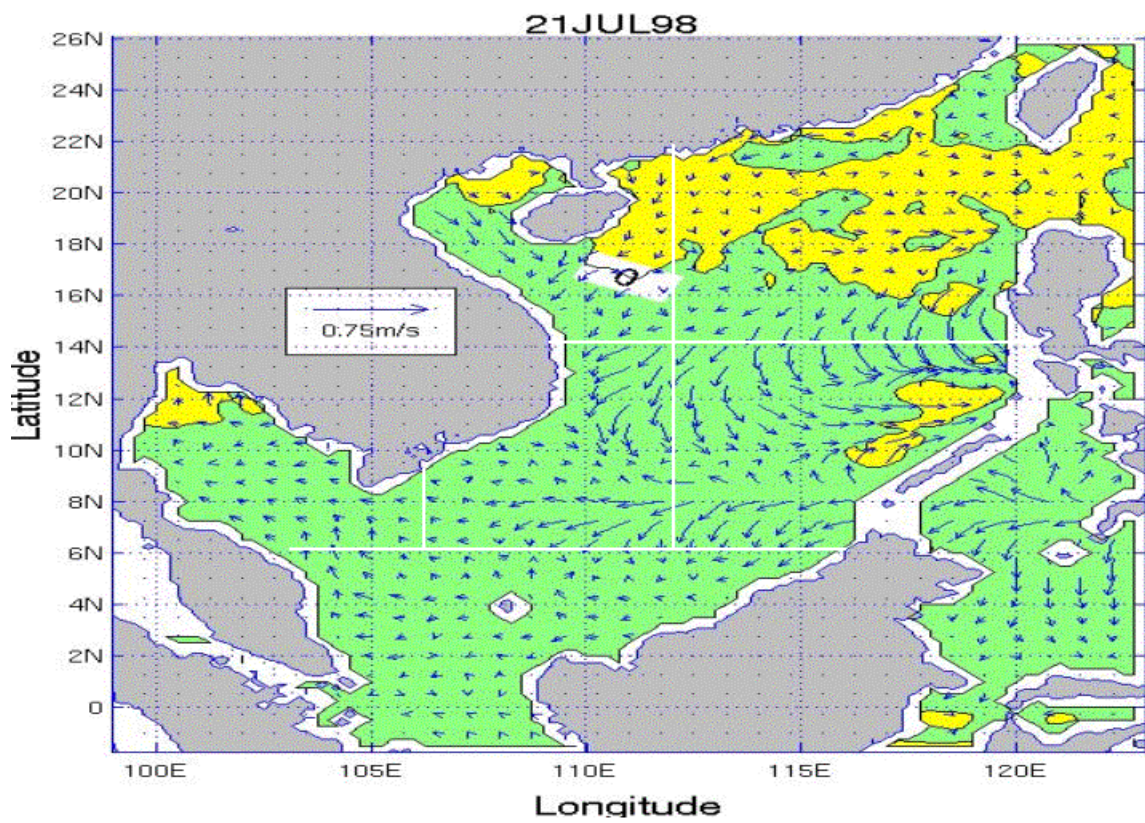
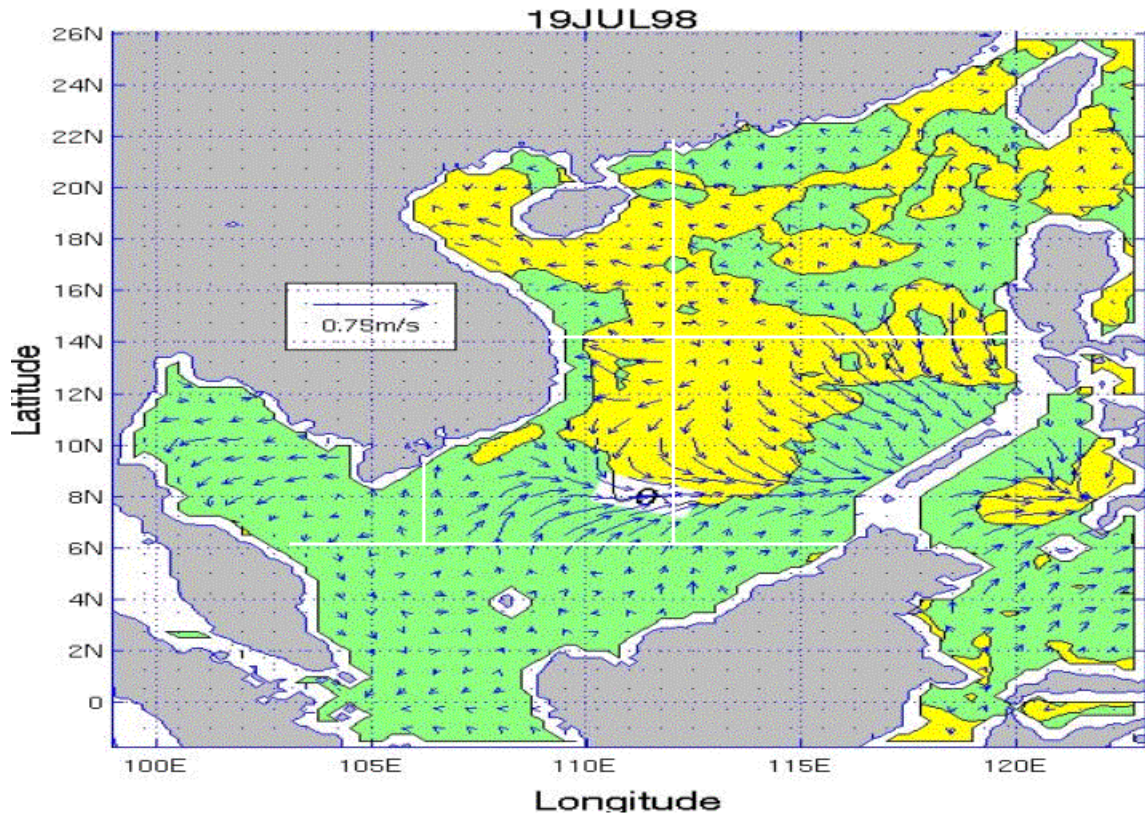


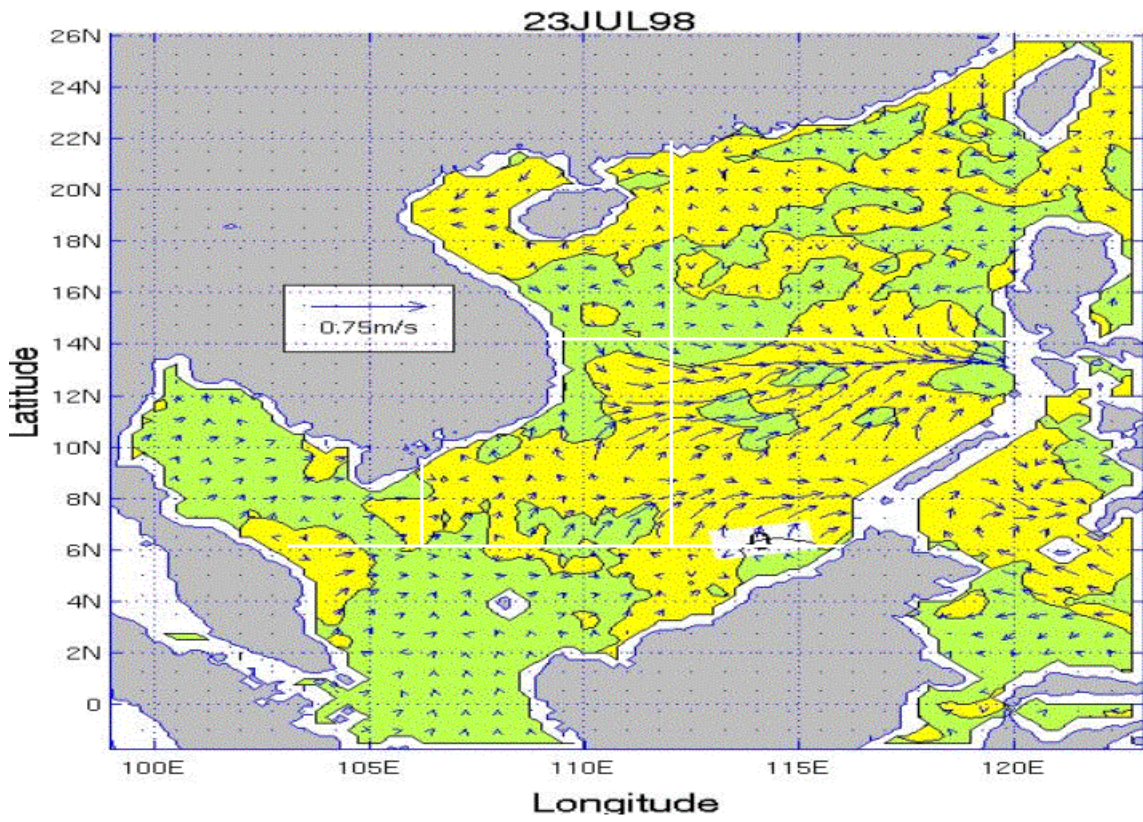
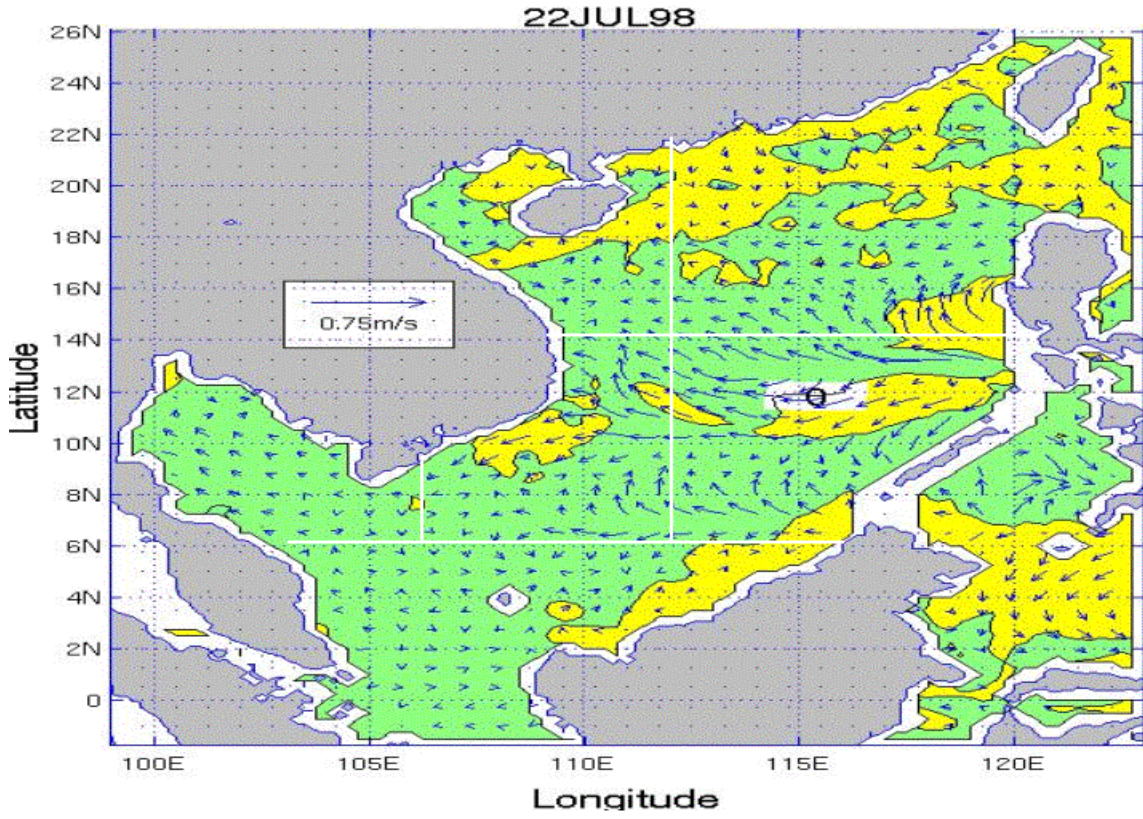


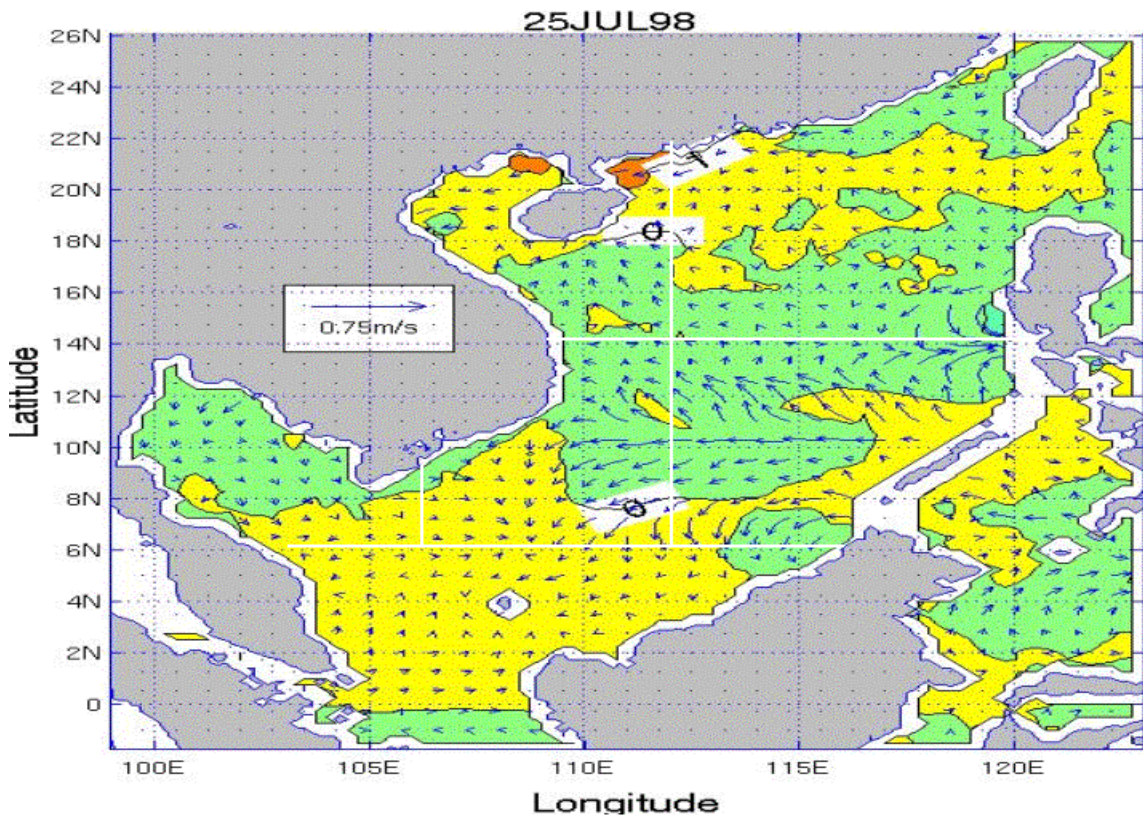
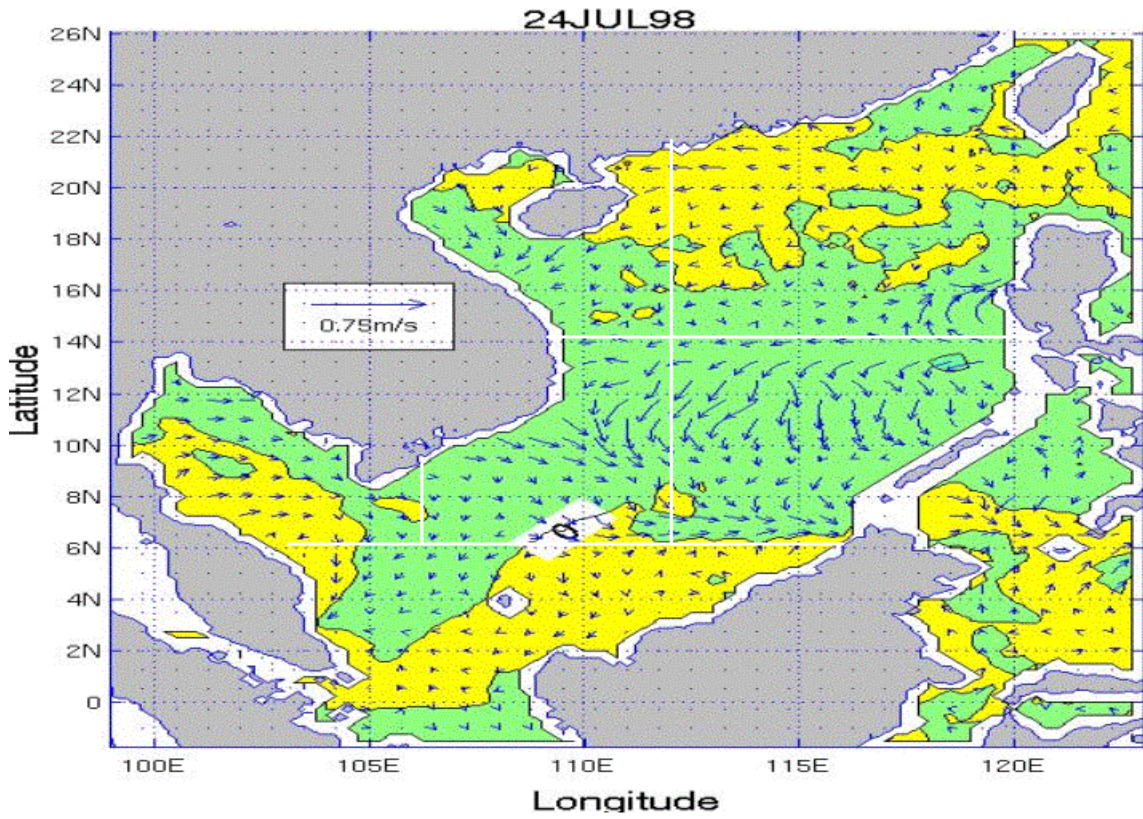
APPENDIX VV. SST AND SURFACE CURRENT VELOCITY TENDENCY PLOTS FOR THE SCS FOR THE JULY TIME PERIOD

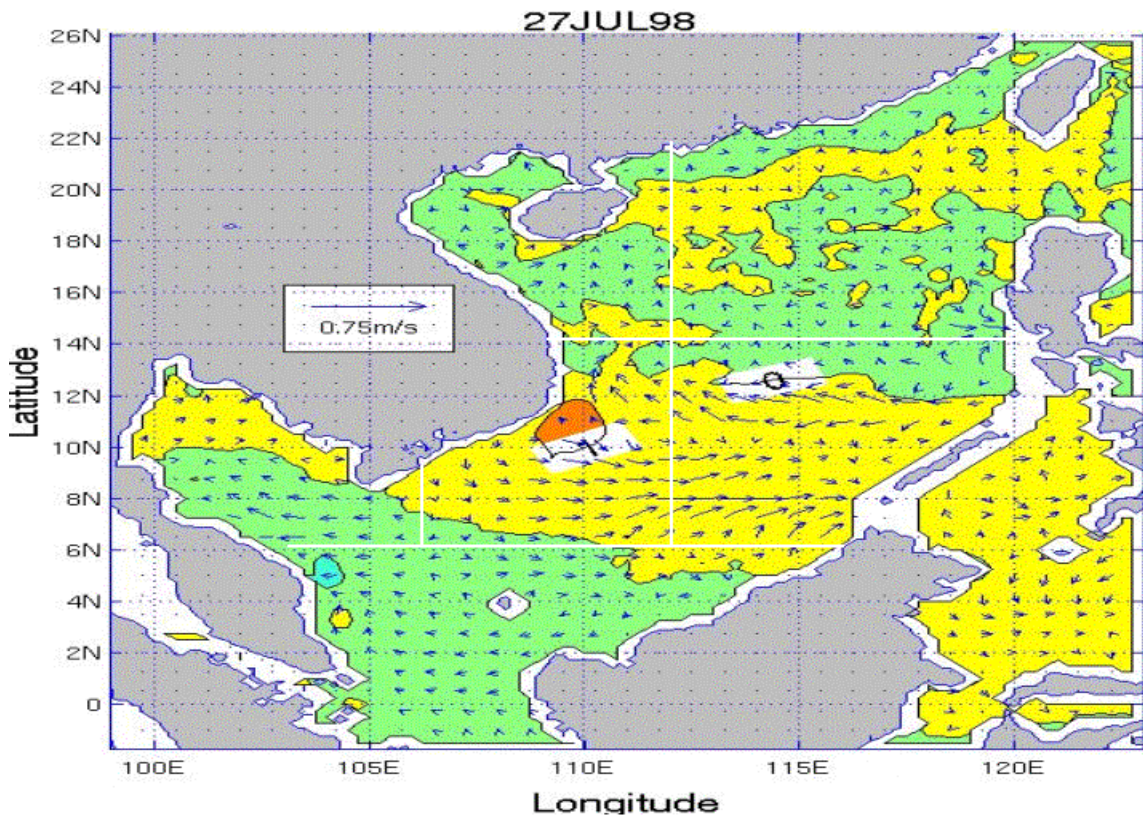
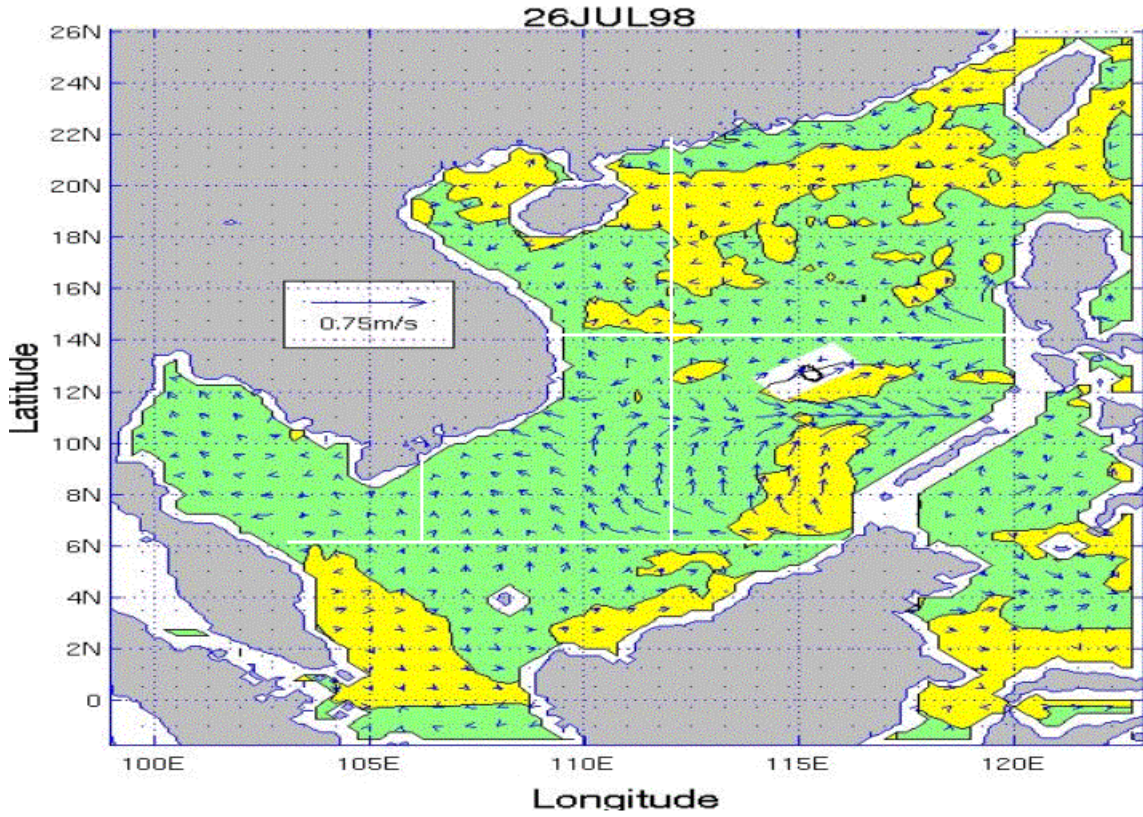
Appendix VV consists of 13 figures that show SST and surface current velocity day-to-day tendency for the July time period over the SCS. The figures are in time sequential order from July 19 through July 31. Each plot represents the change between the previous day and the current day.

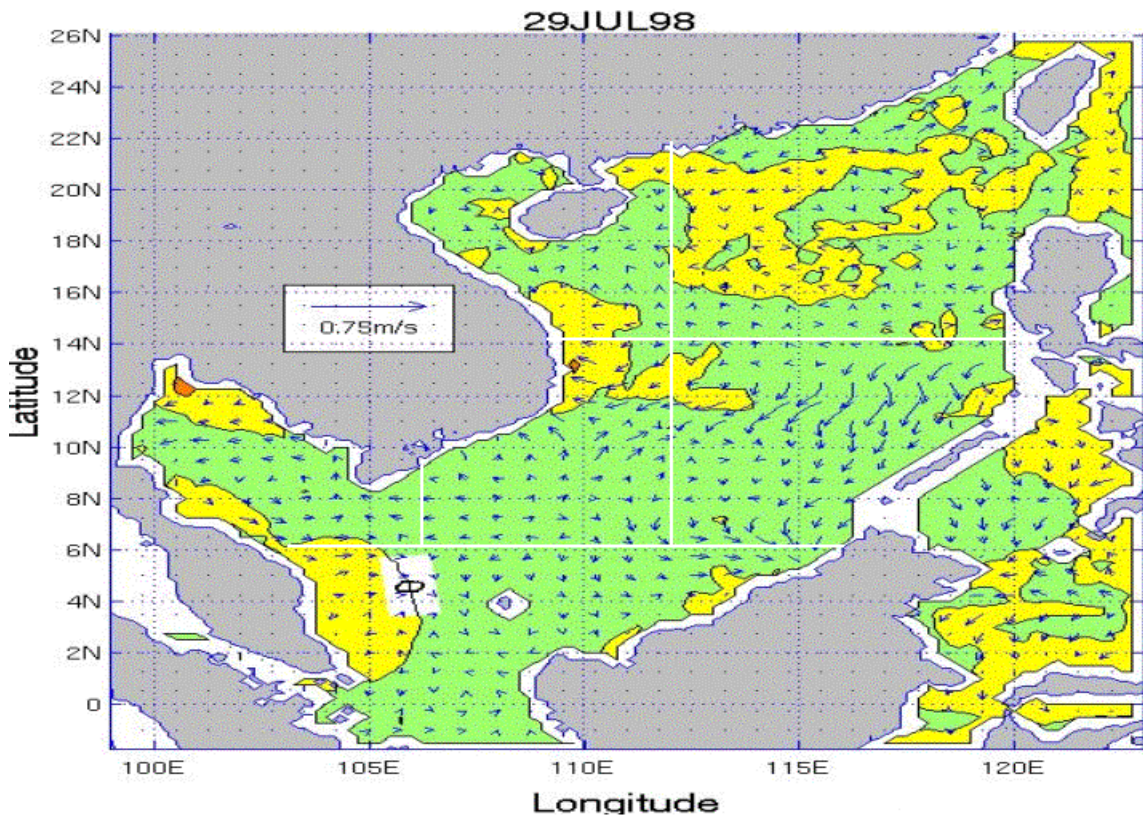
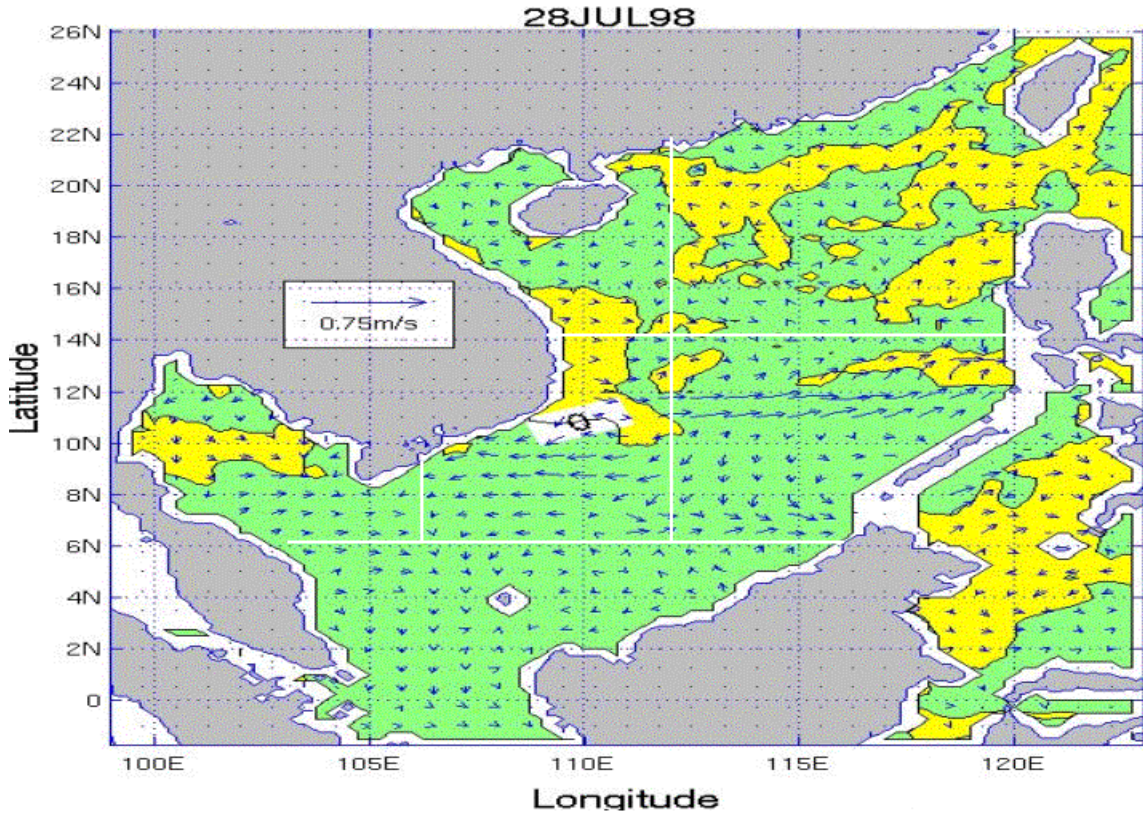


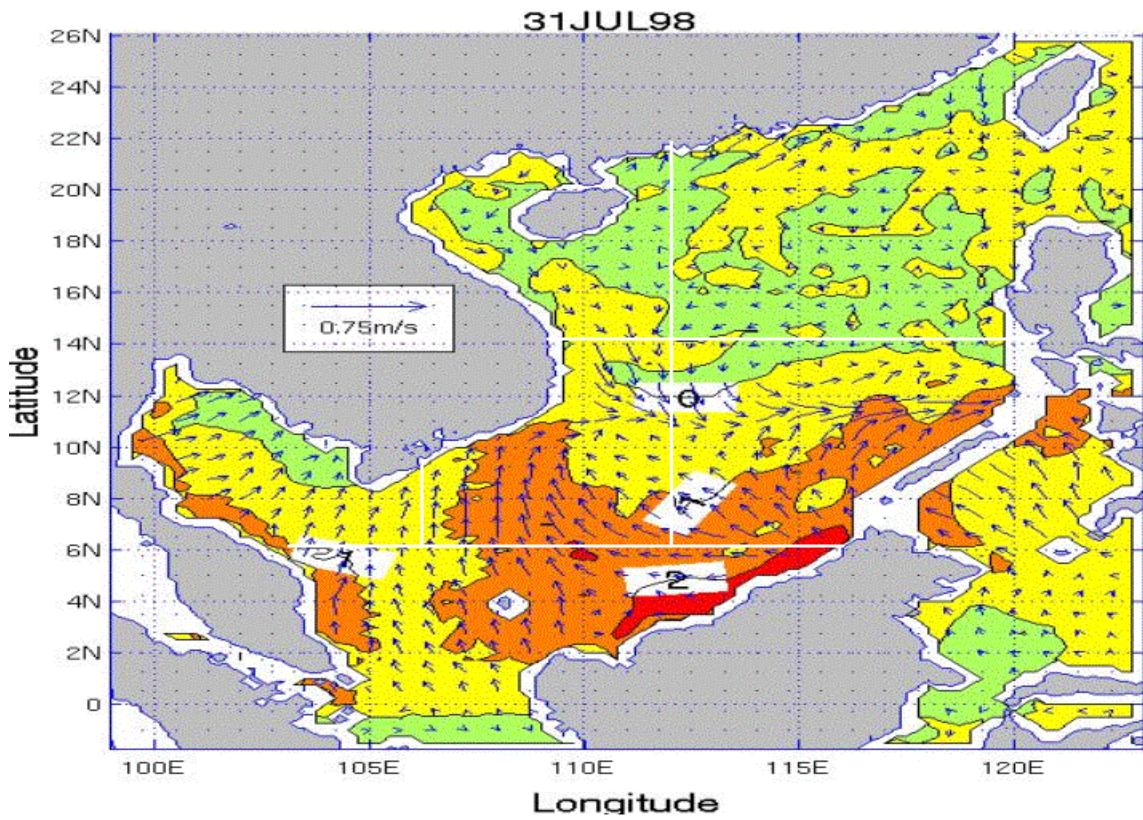
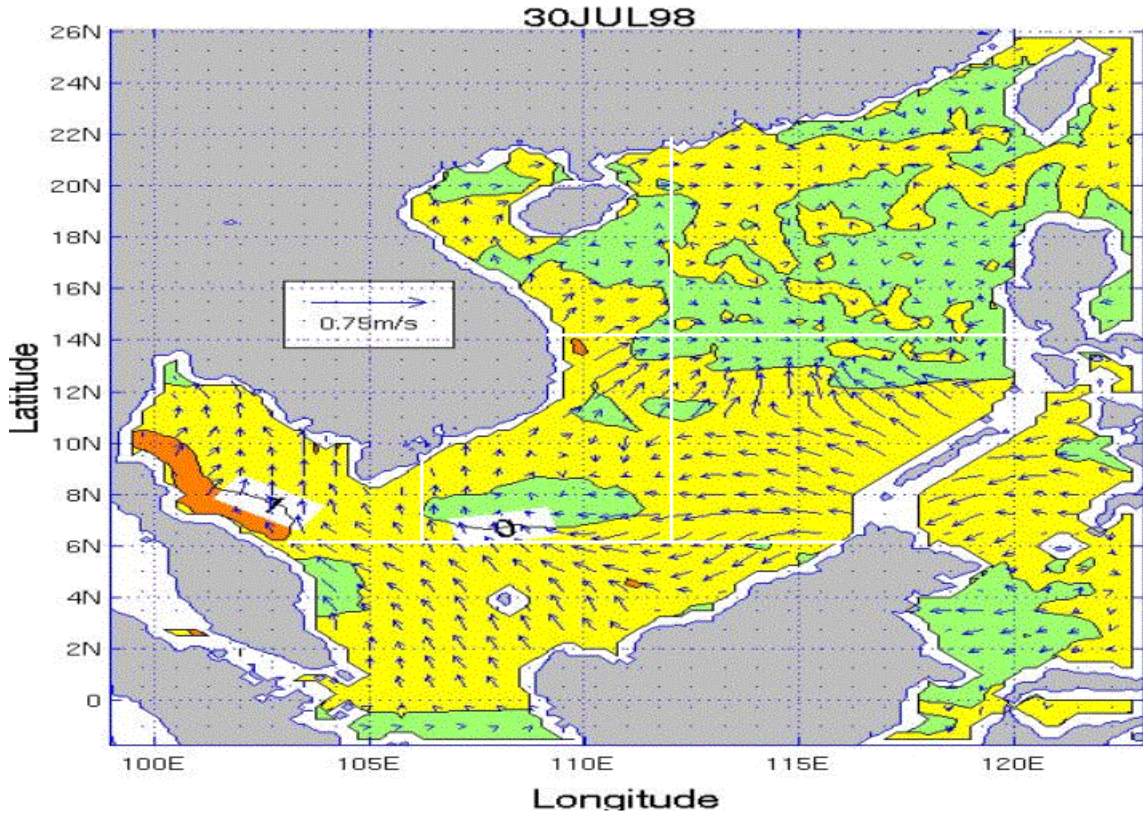








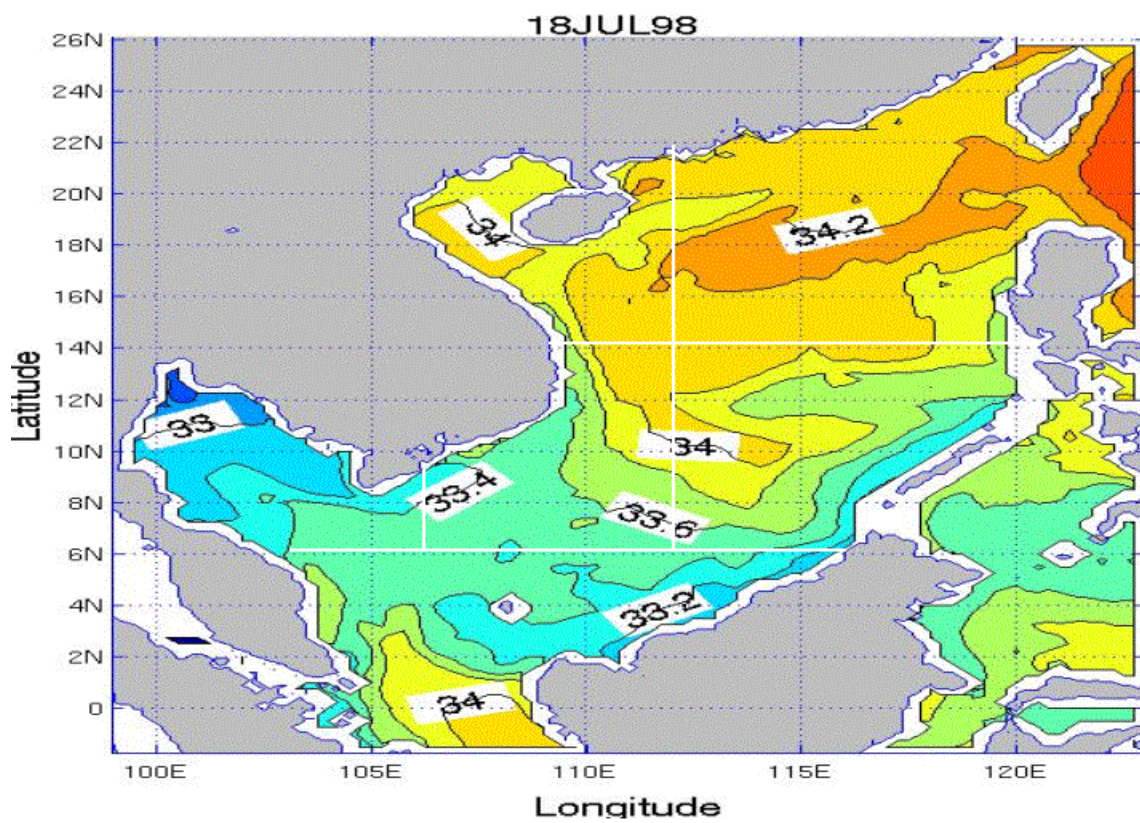


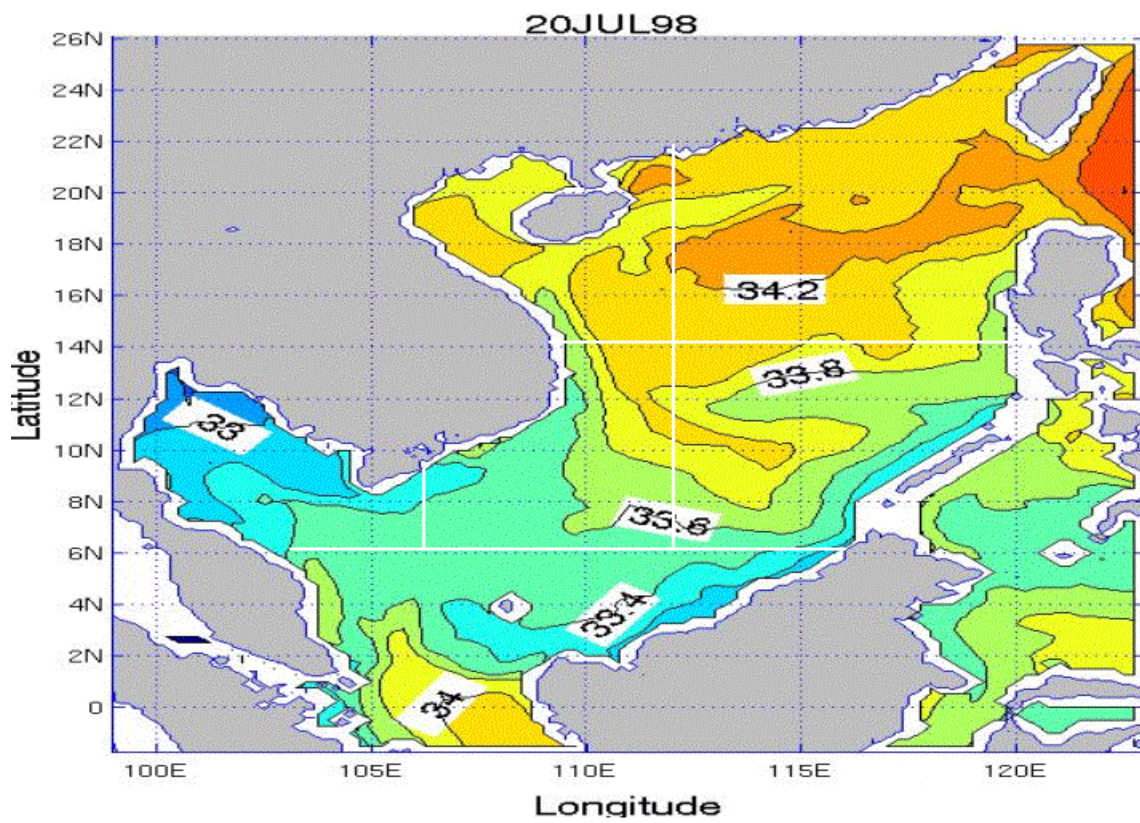
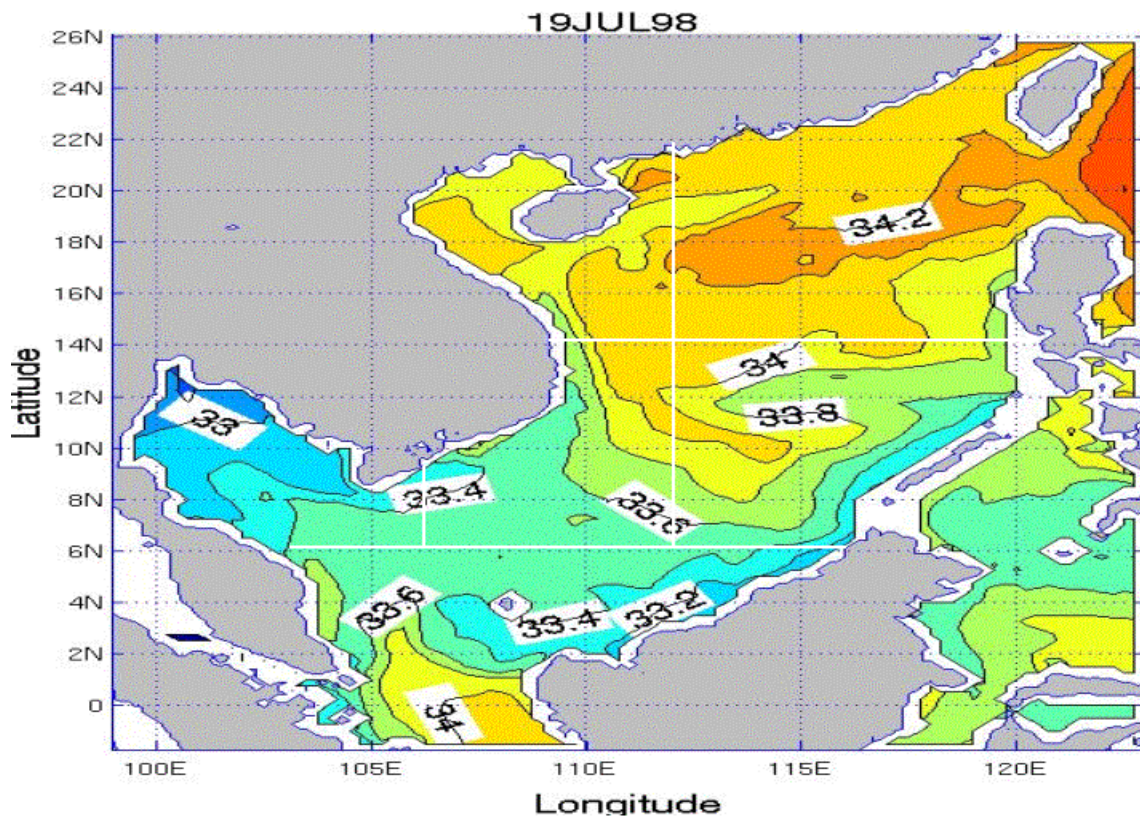


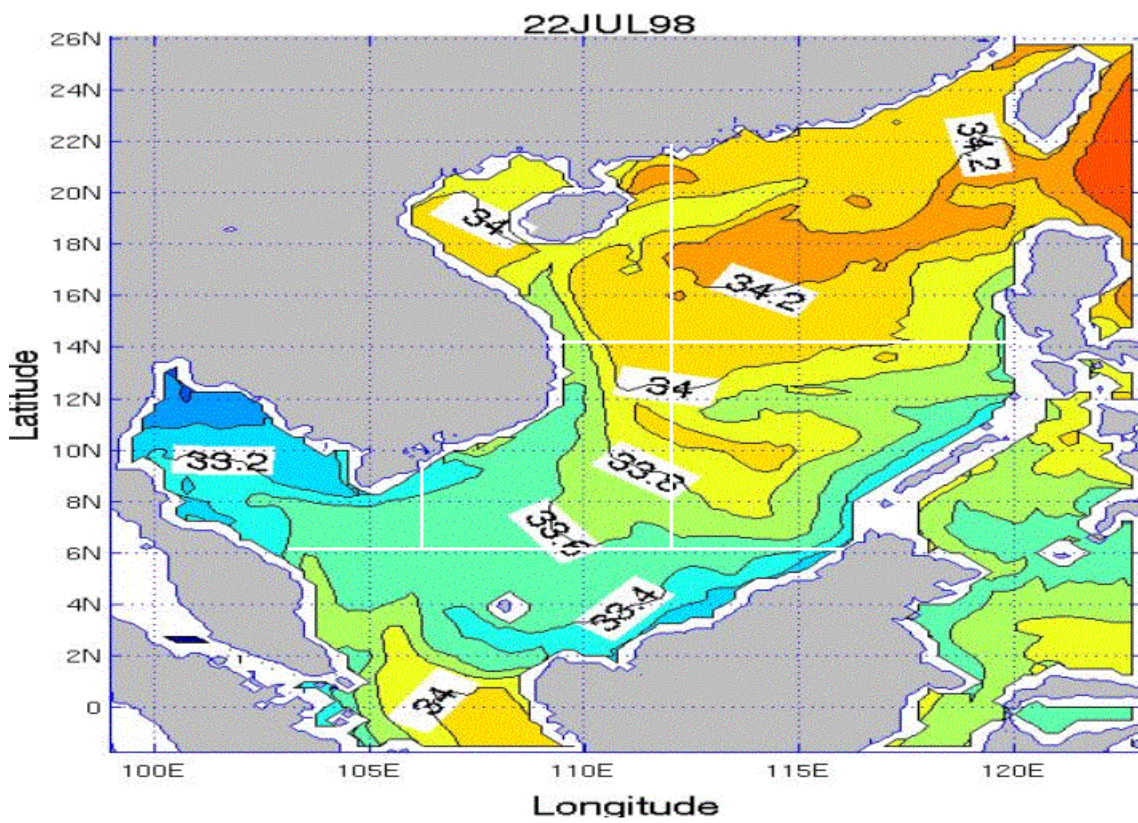
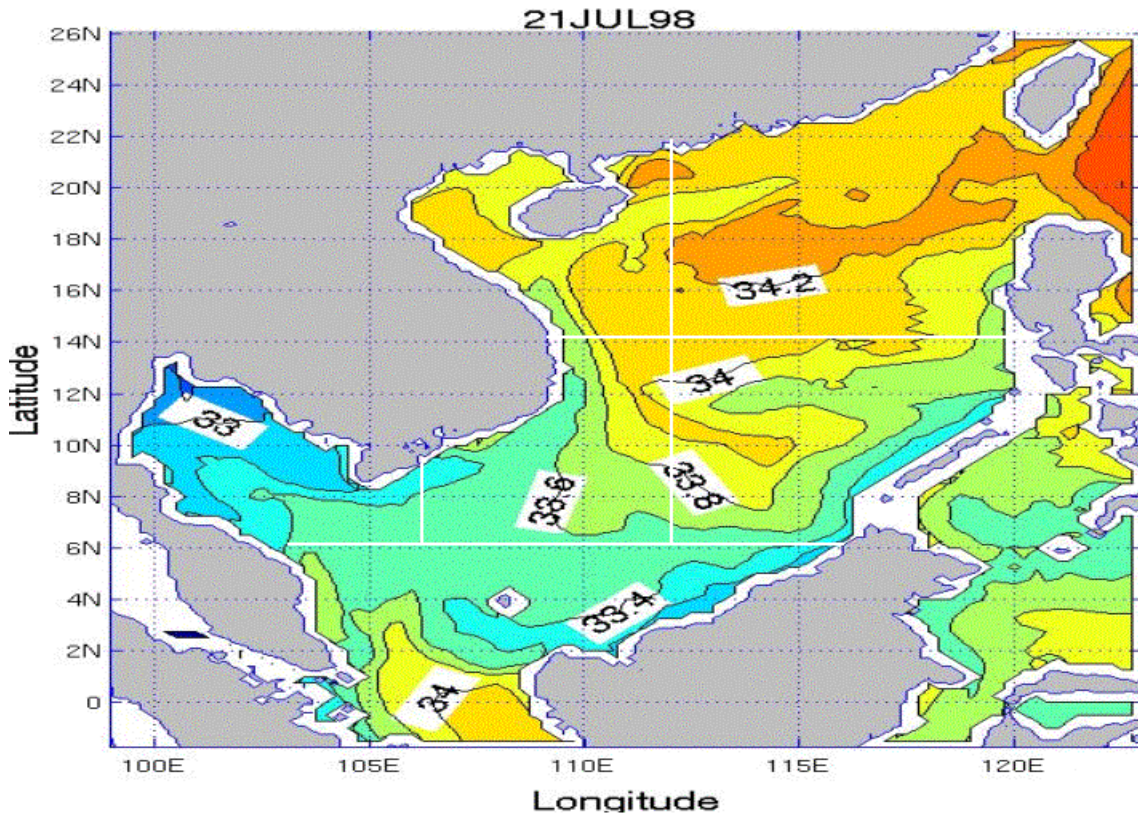
THIS PAGE INTENTIONALLY LEFT BLANK

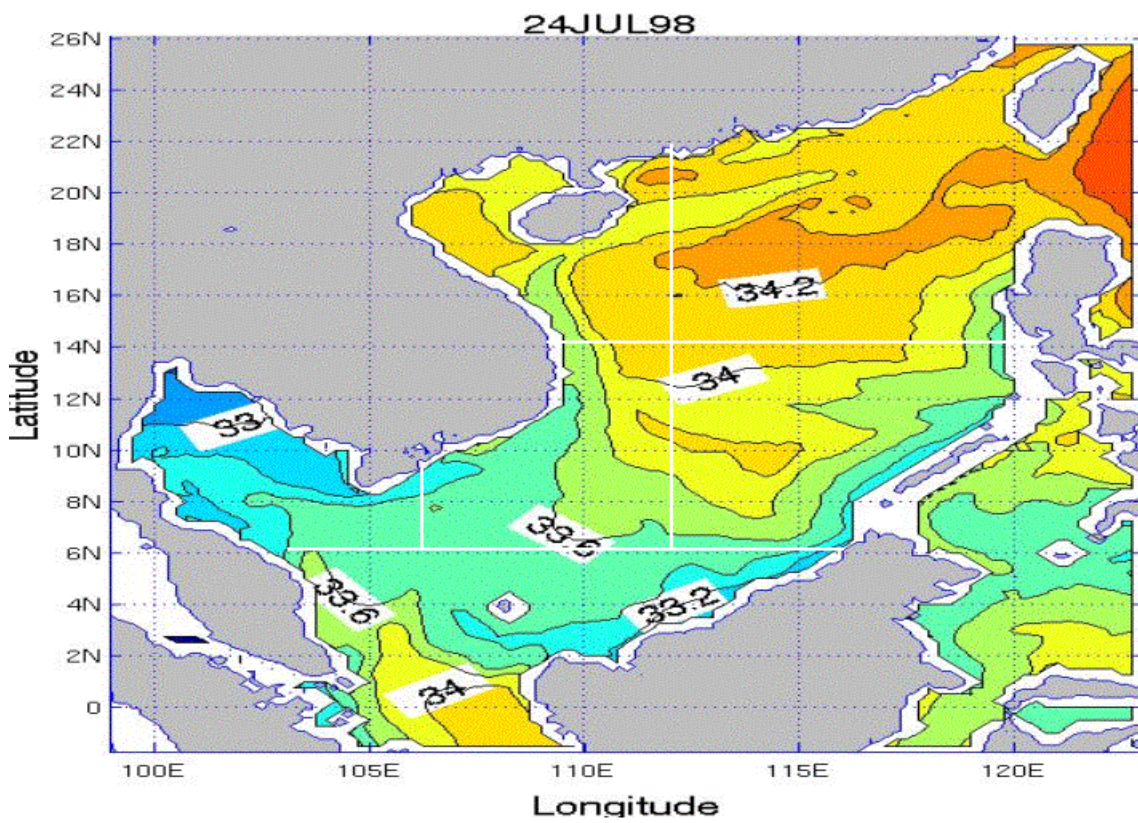
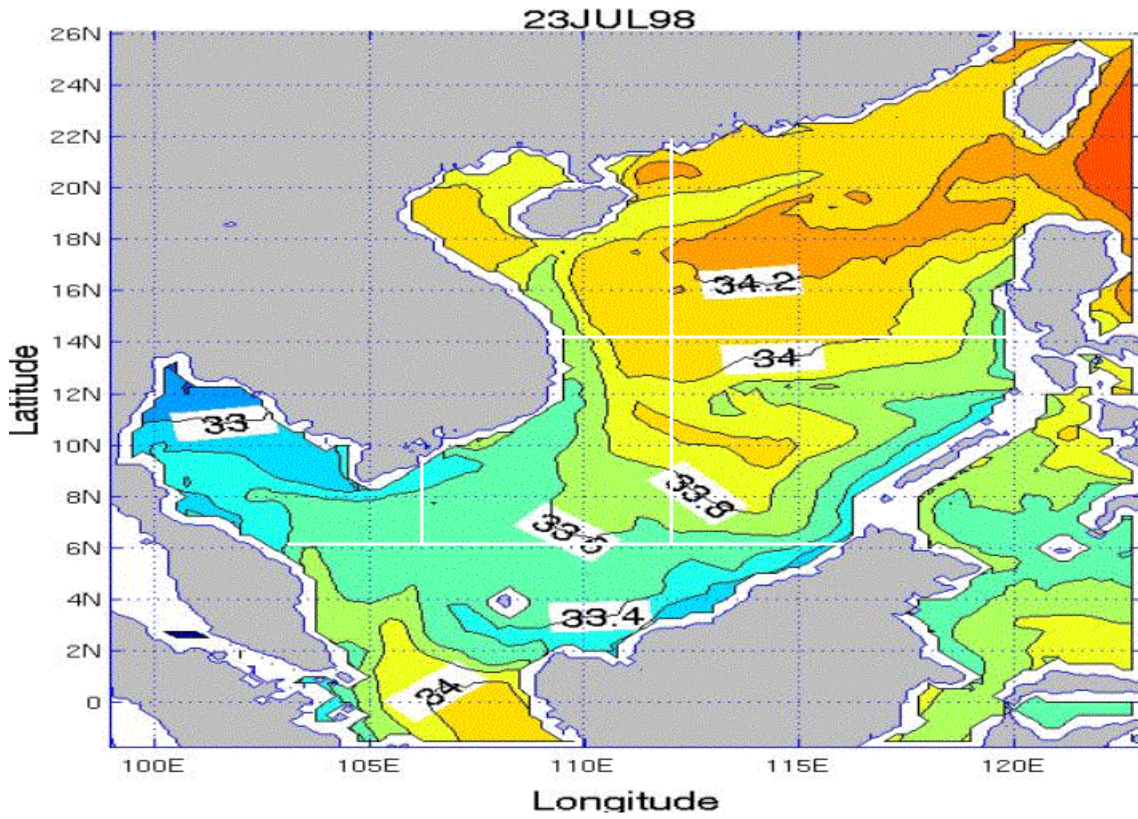
APPENDIX WW.SSS PLOTS FOR THE SCS FOR THE JULY TIME PERIOD

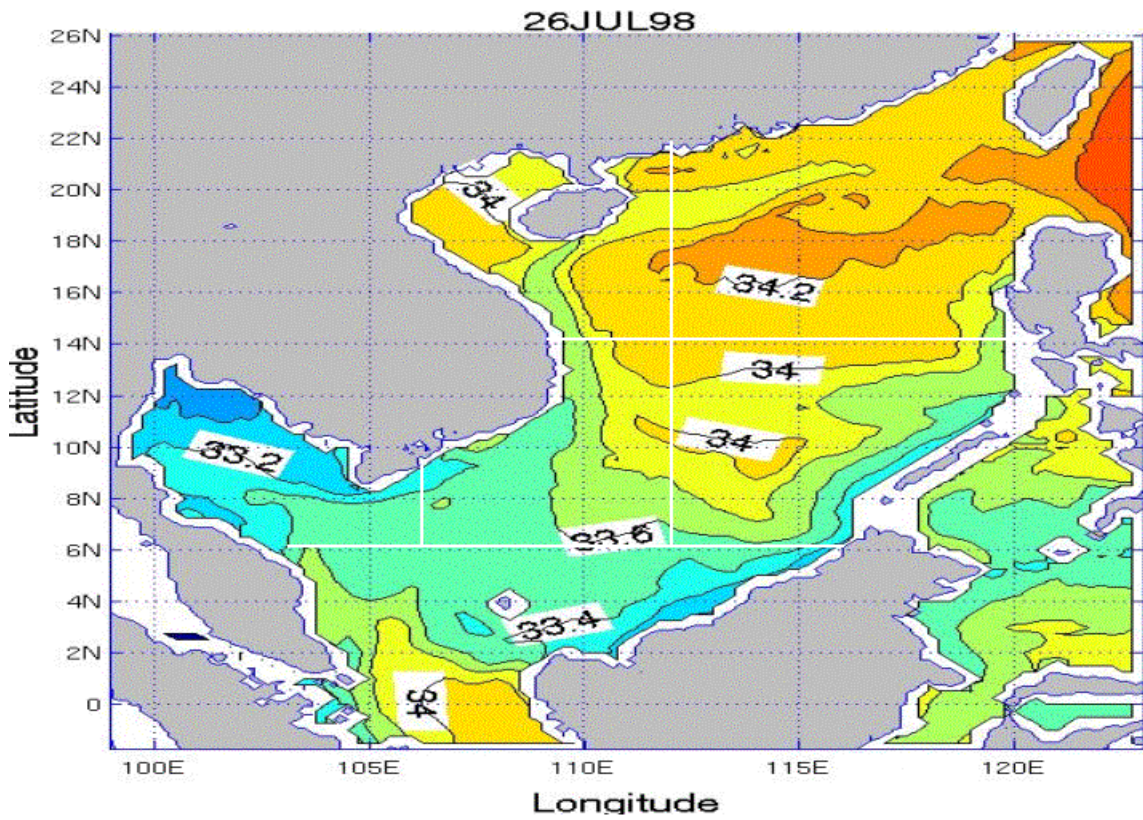
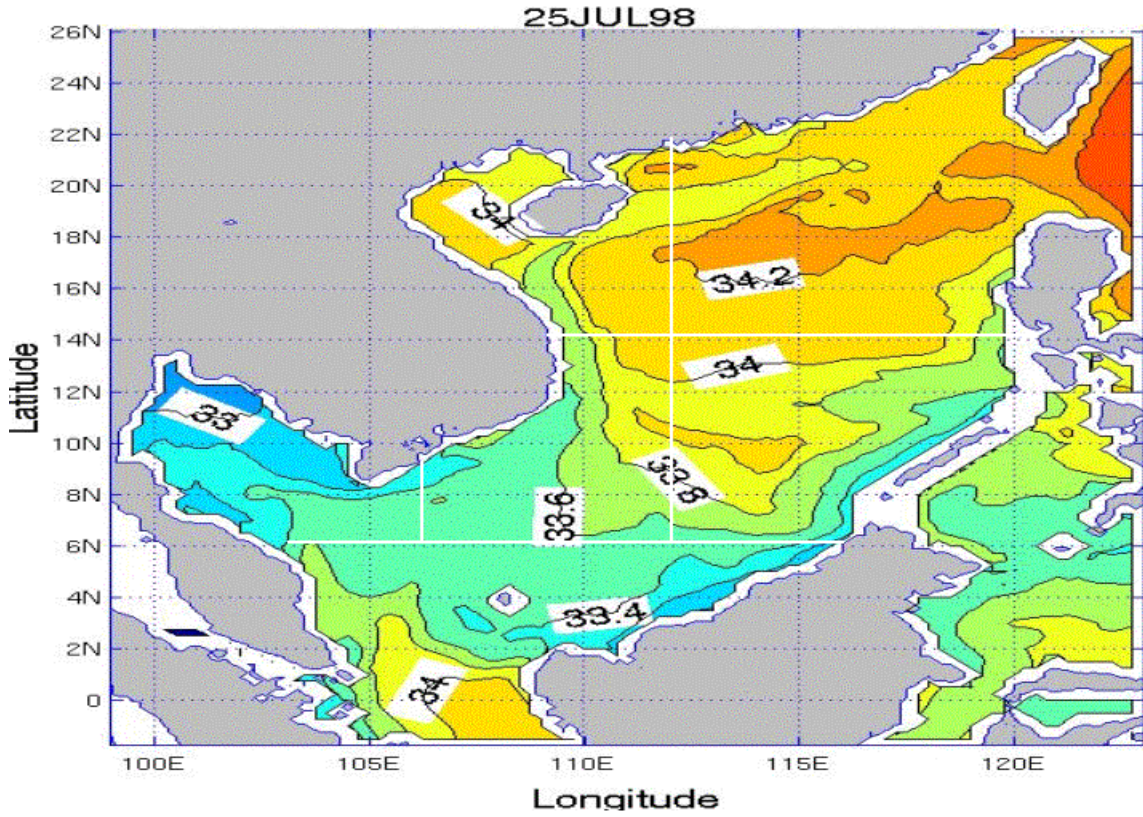
Appendix WW consists of 14 figures that show SSS for each day of the July time period for the SCS. The figures are in time sequential order from July 18 through July 31.

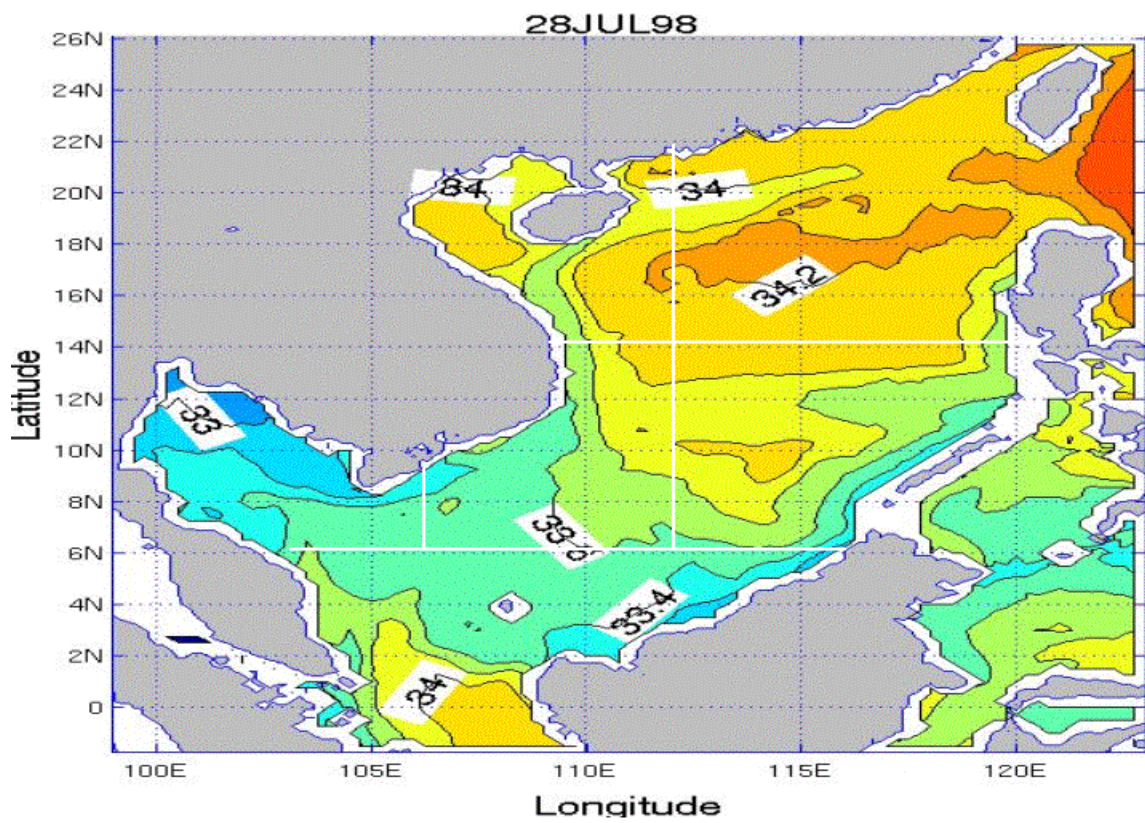
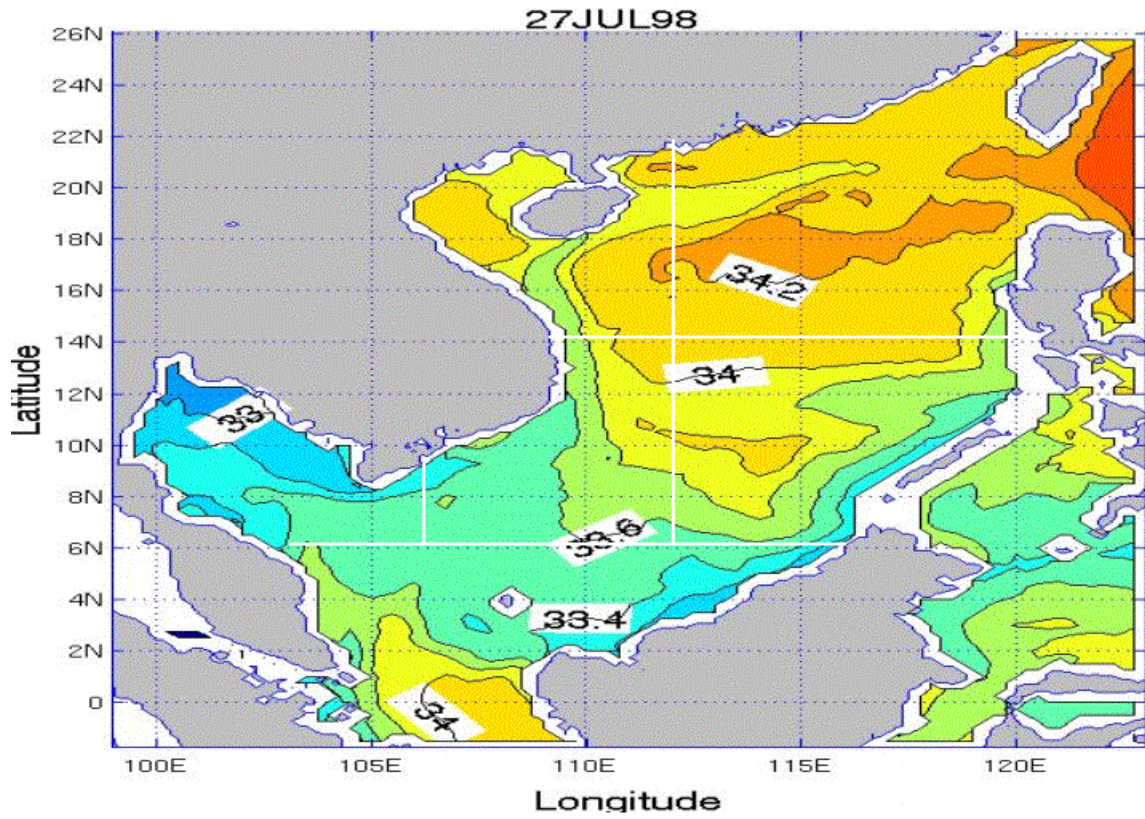


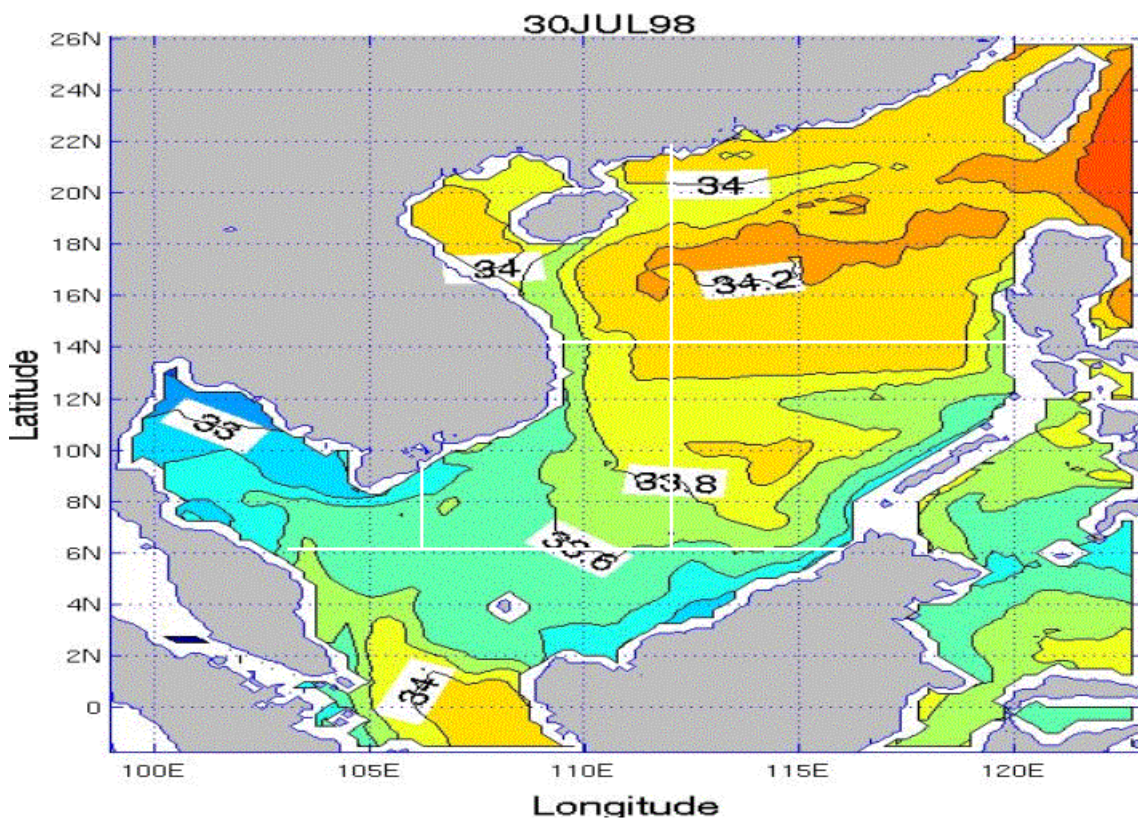
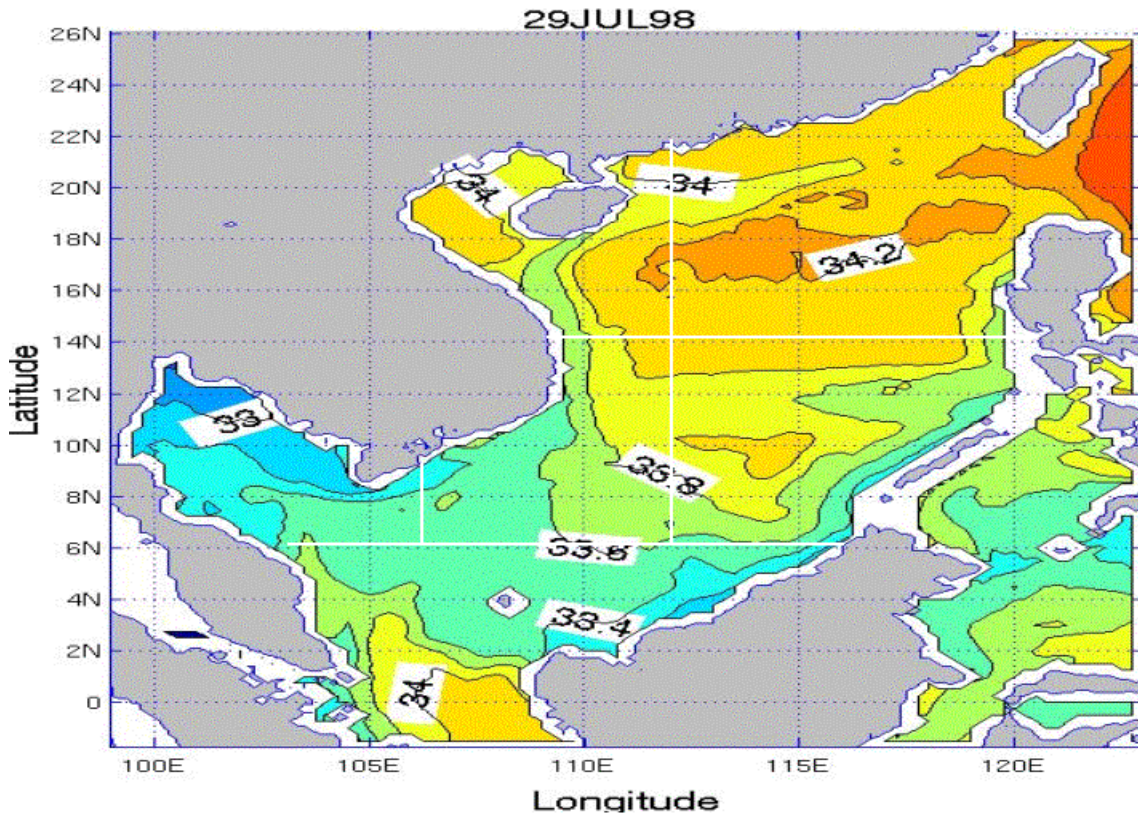


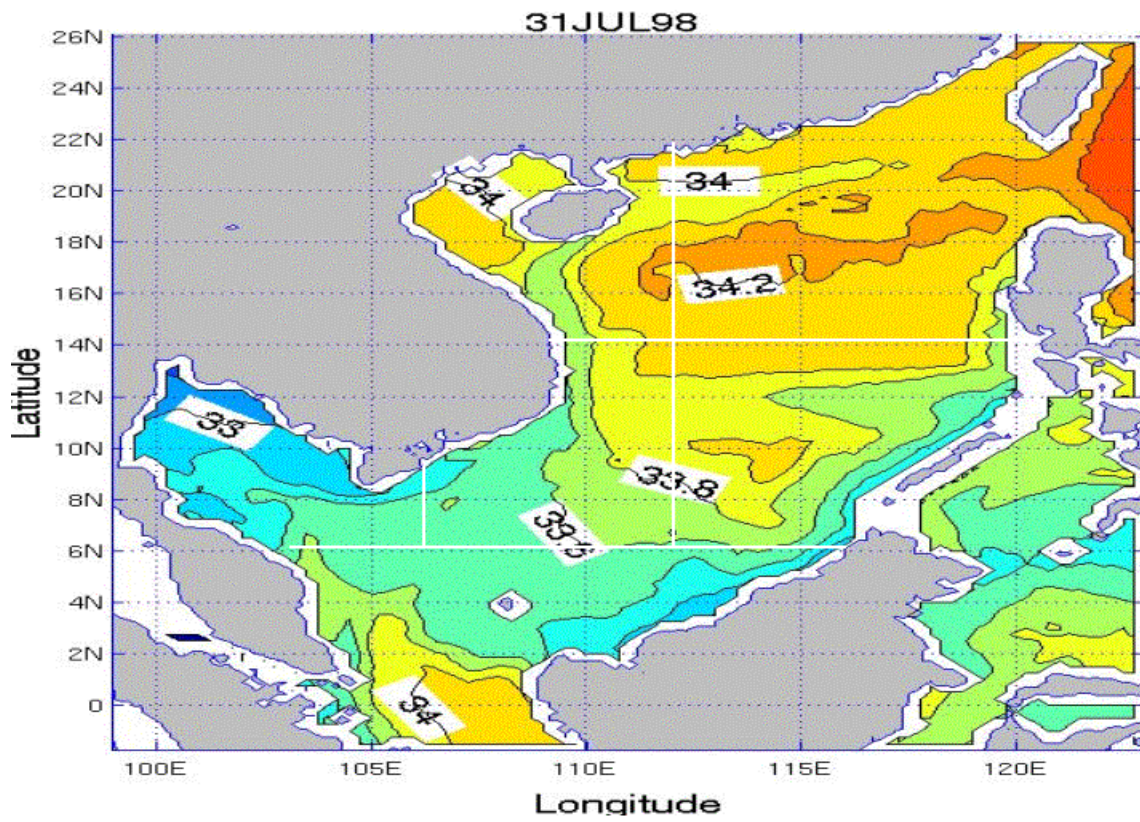






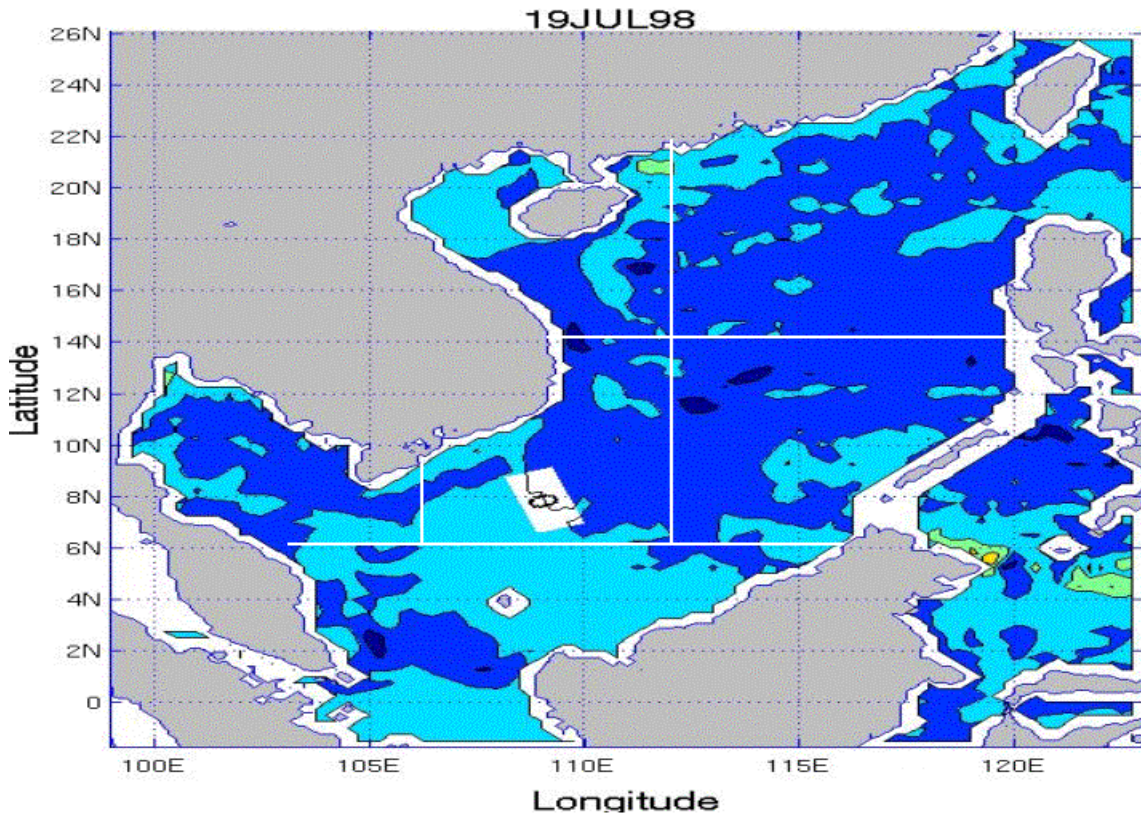


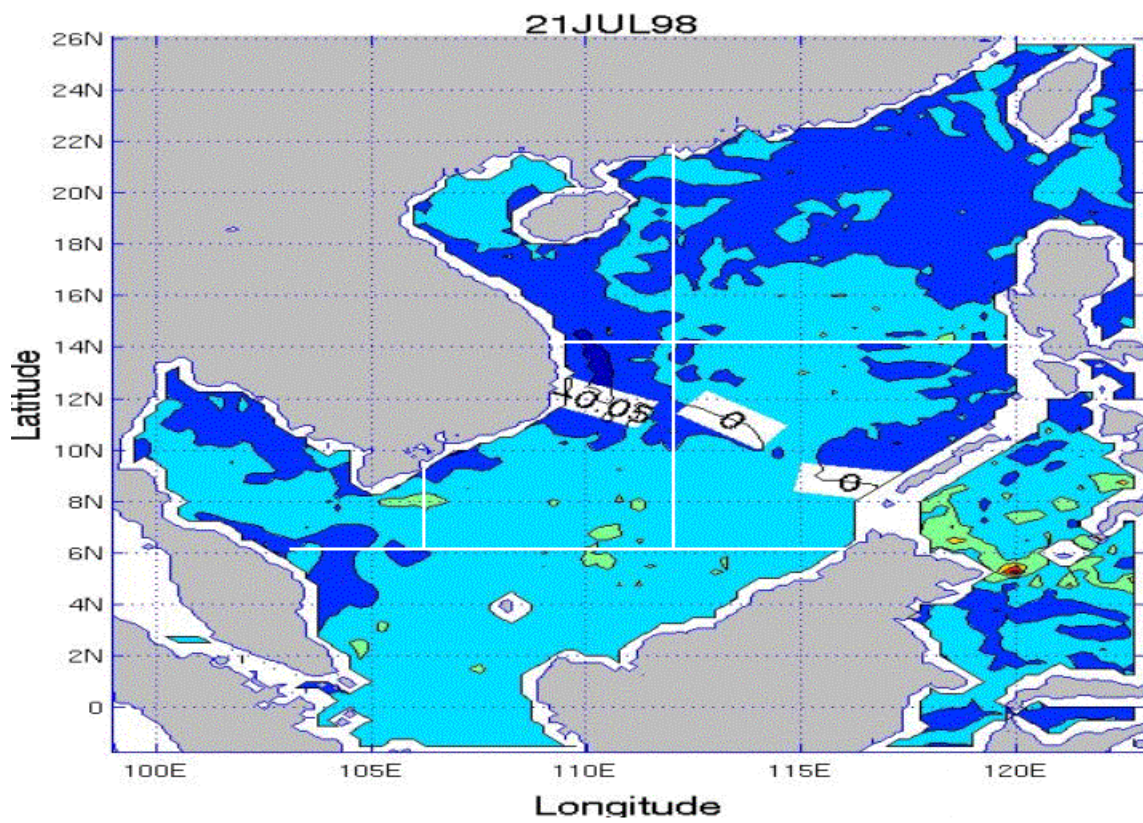
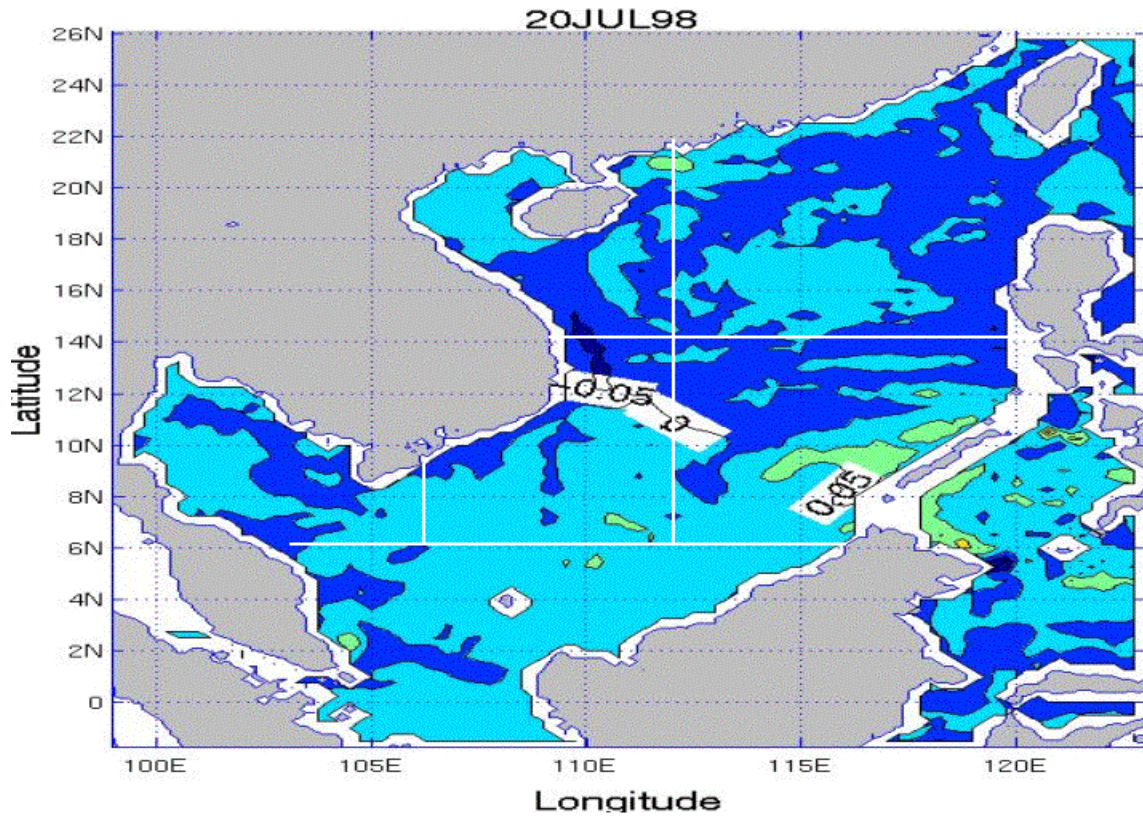


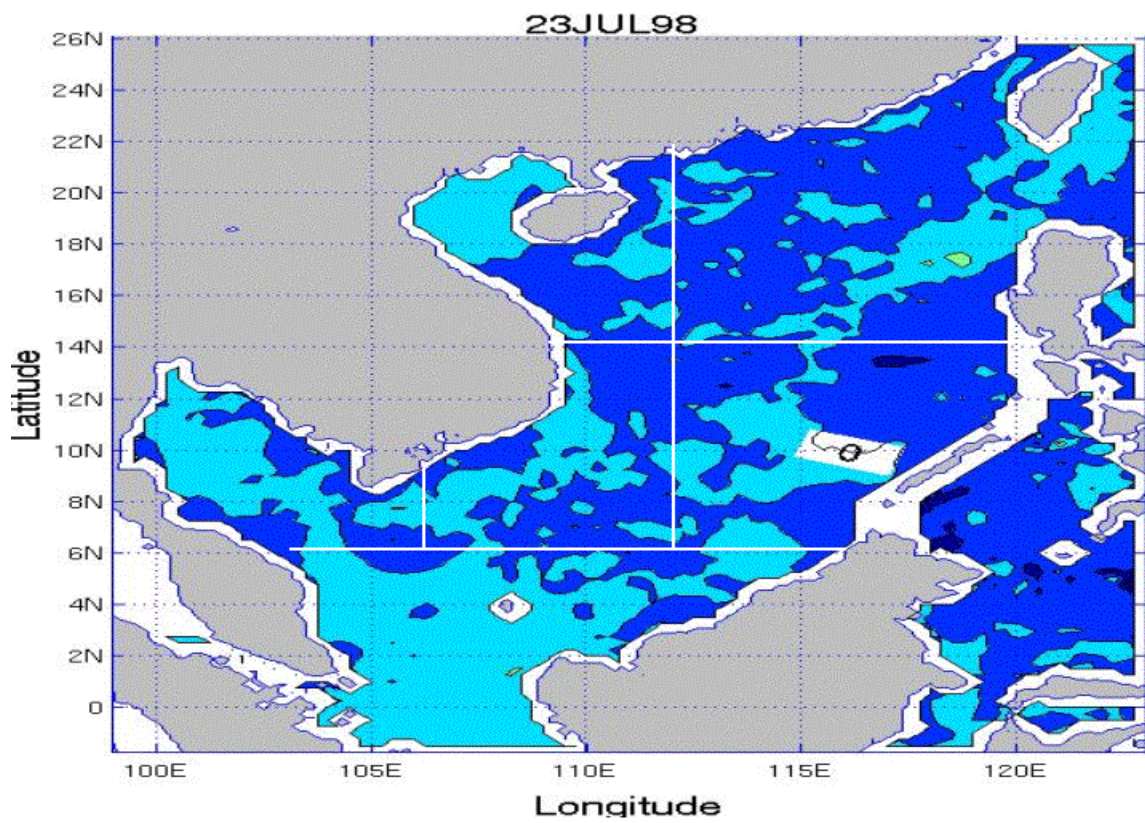
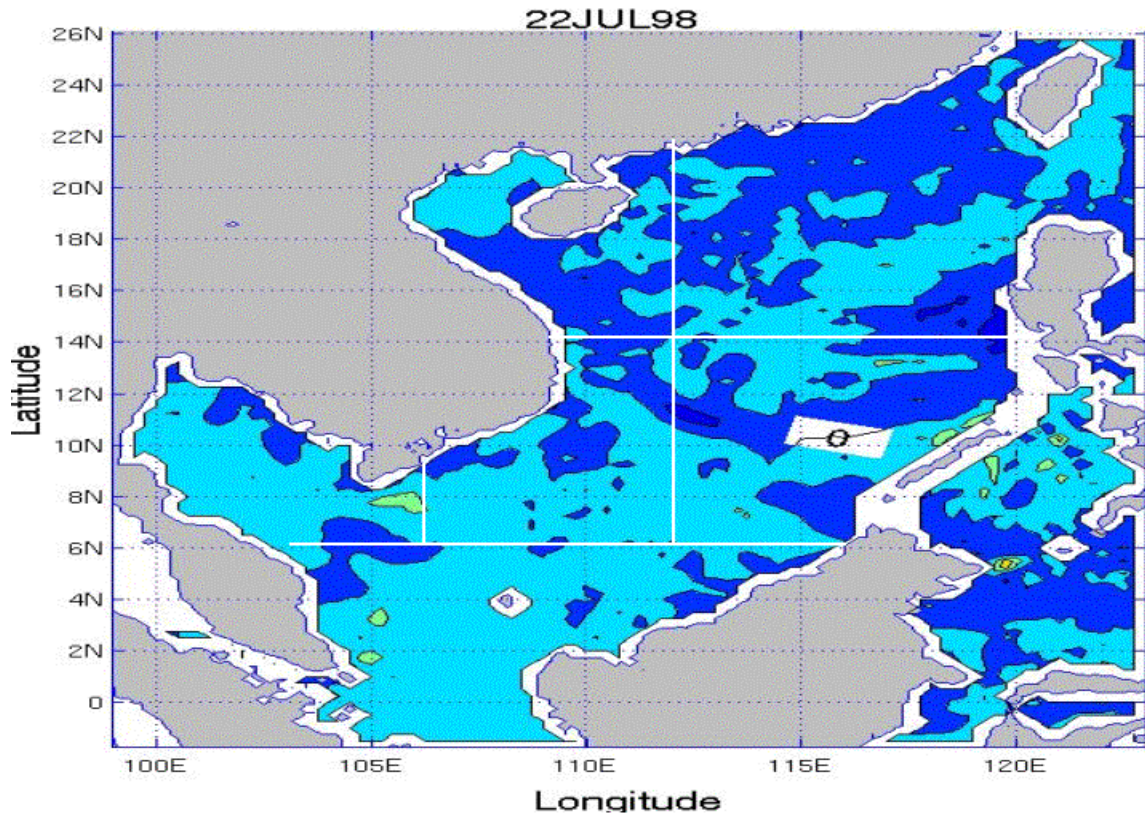


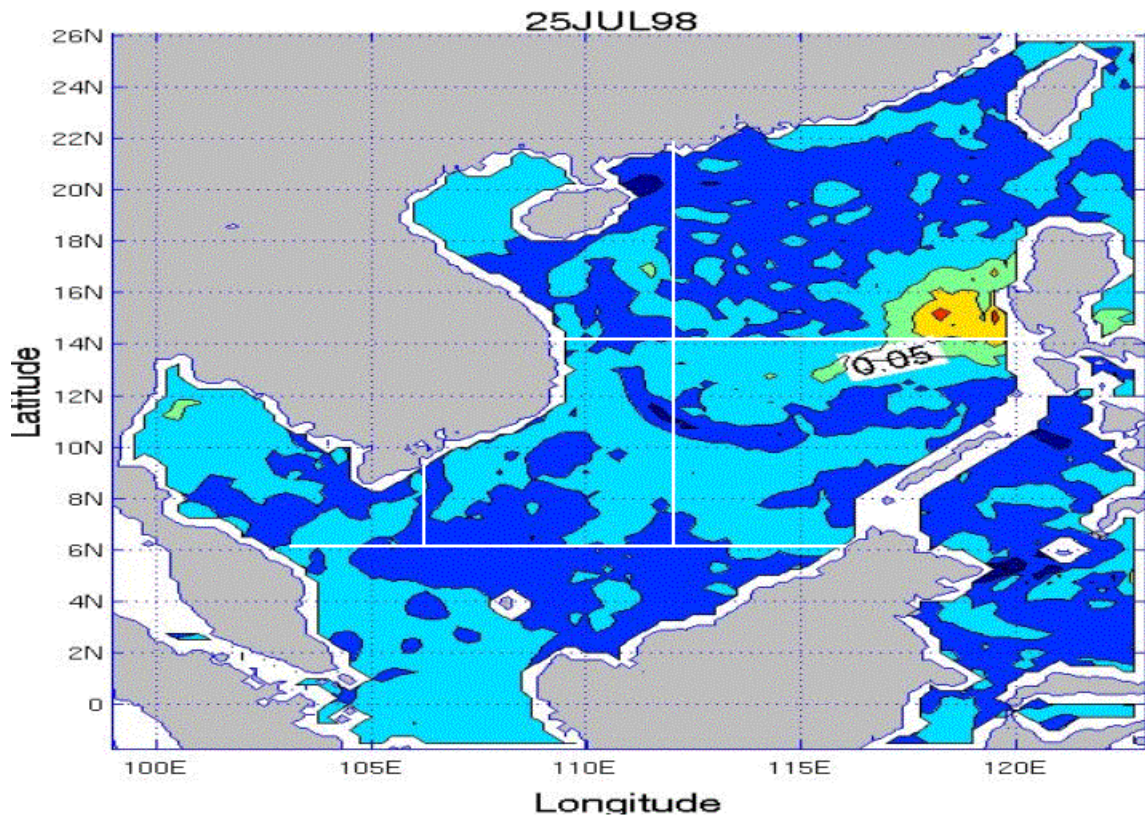
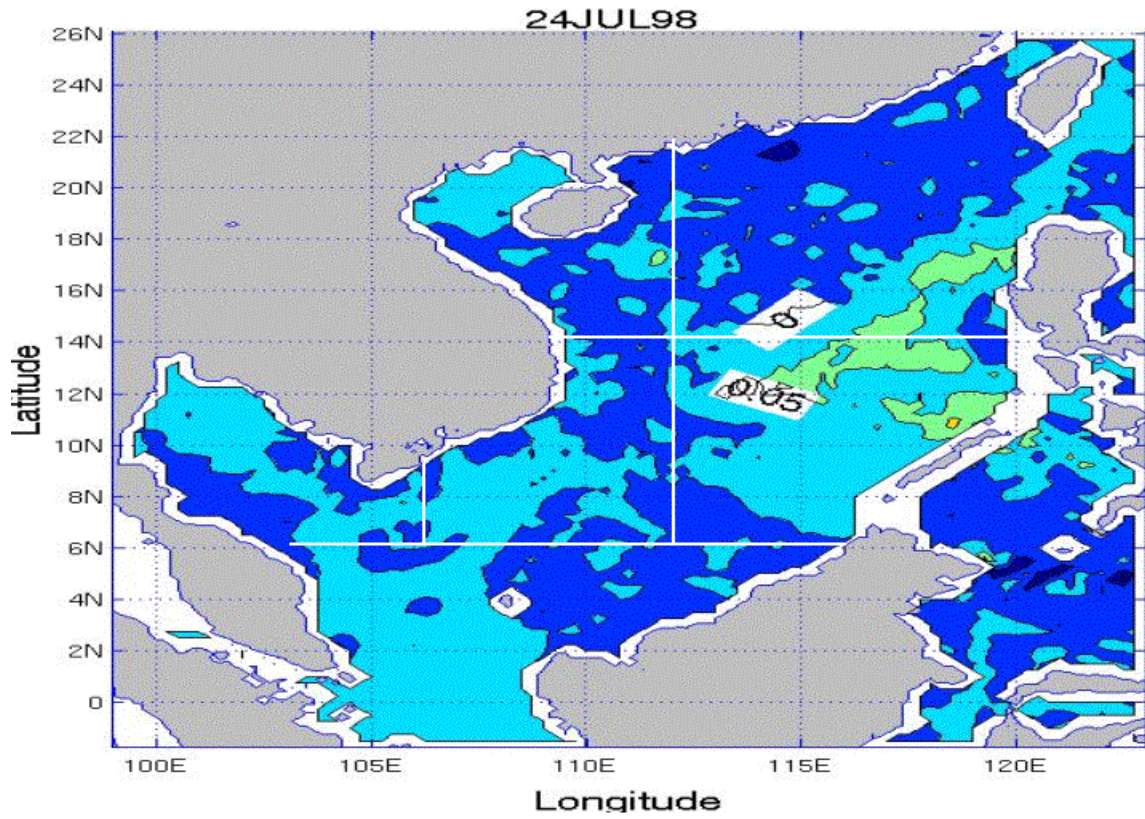
APPENDIX XX. SSS TENDENCY PLOTS FOR THE SCS FOR THE JULY TIME PERIOD

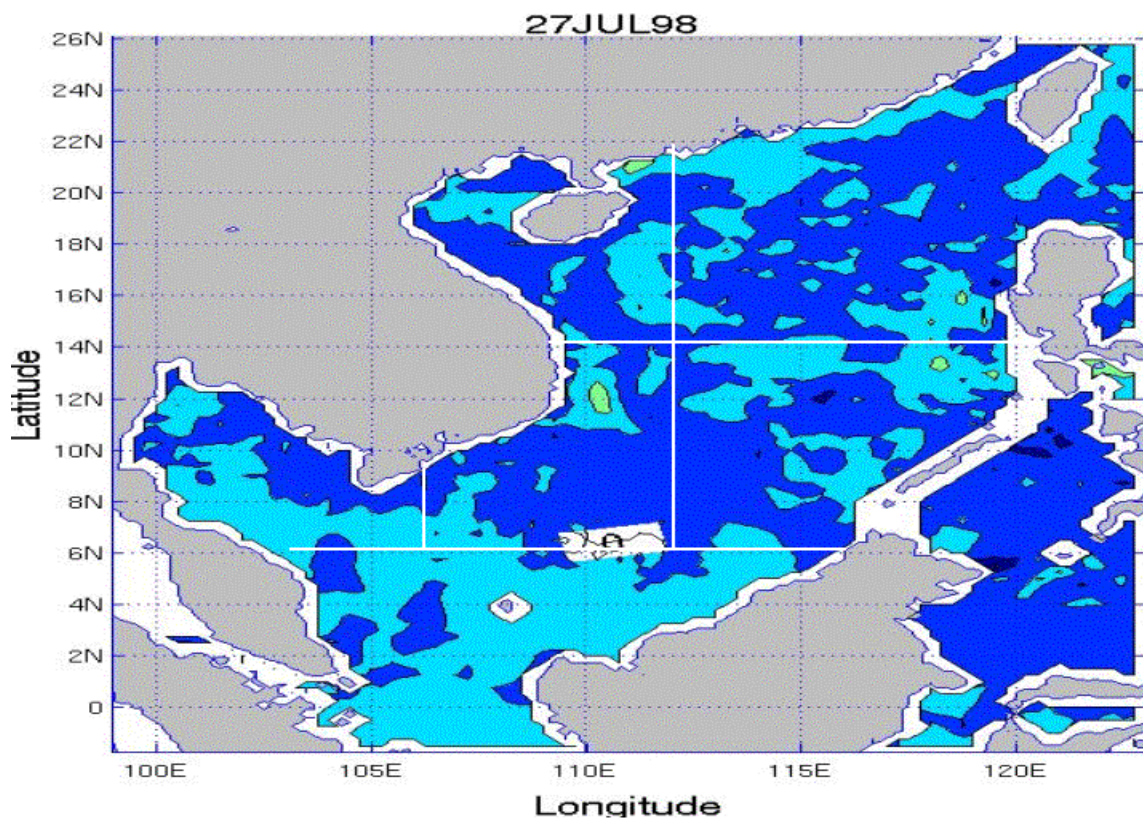
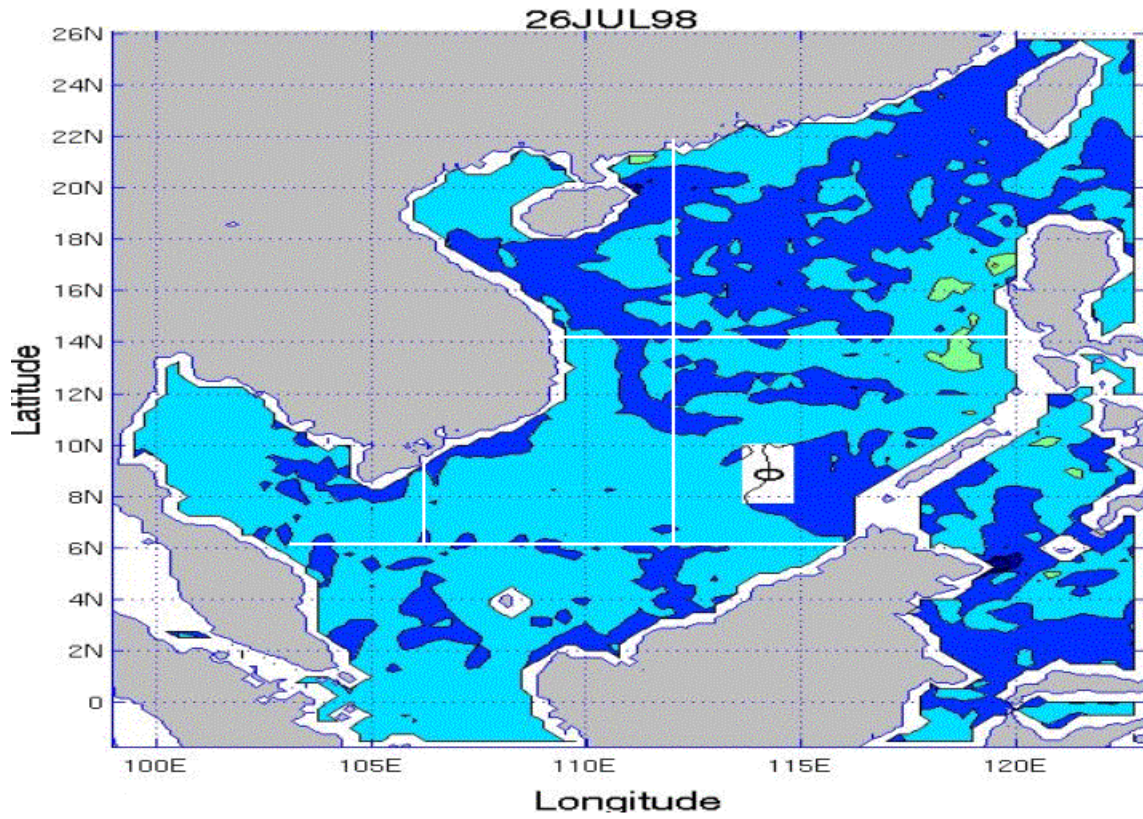
Appendix XX consists of 13 figures that show SSS day-to-day tendency for the July time period over the SCS. The figures are in time sequential order from July 19 through July 31. Each plot represents the change between the previous day and the current day.

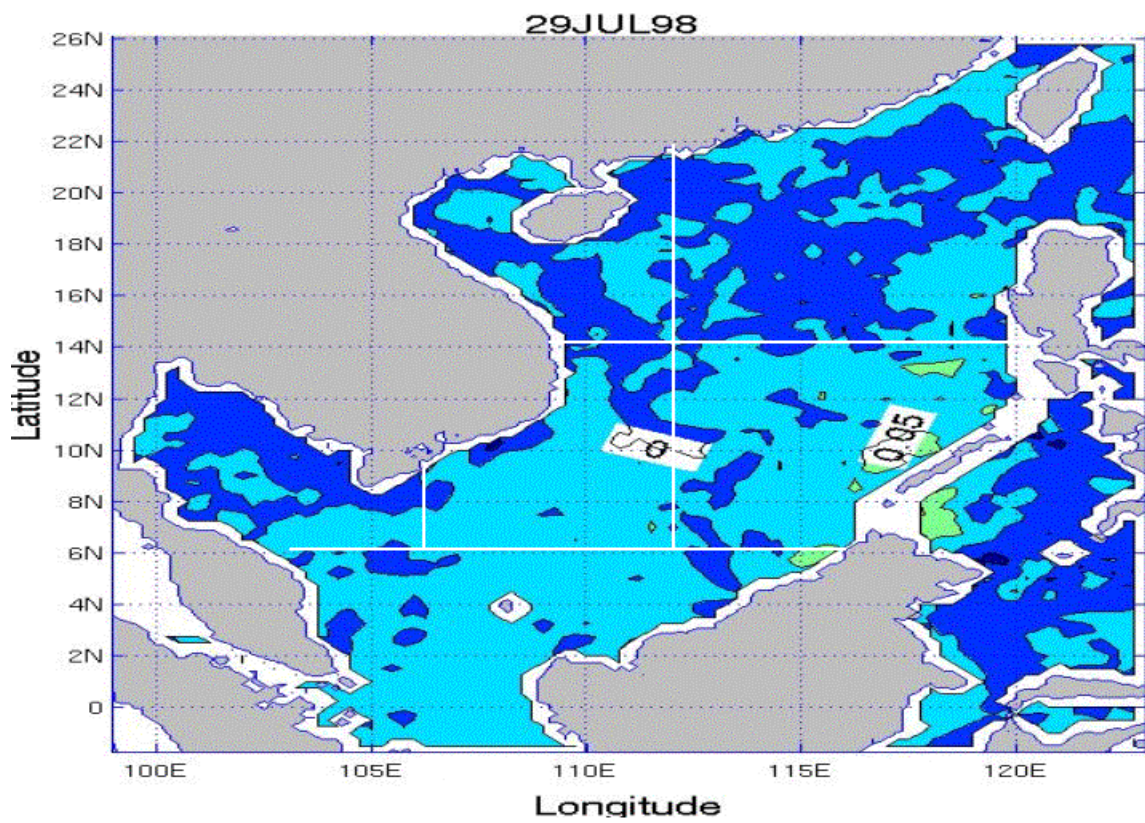
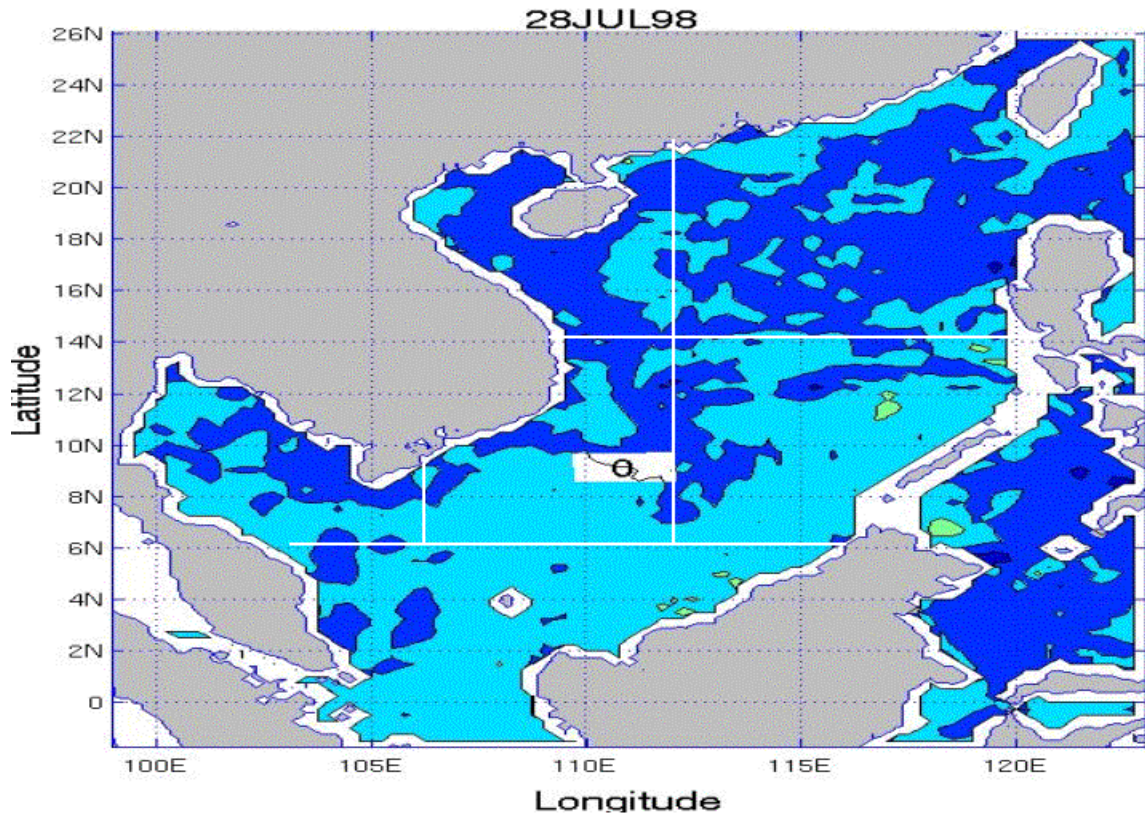


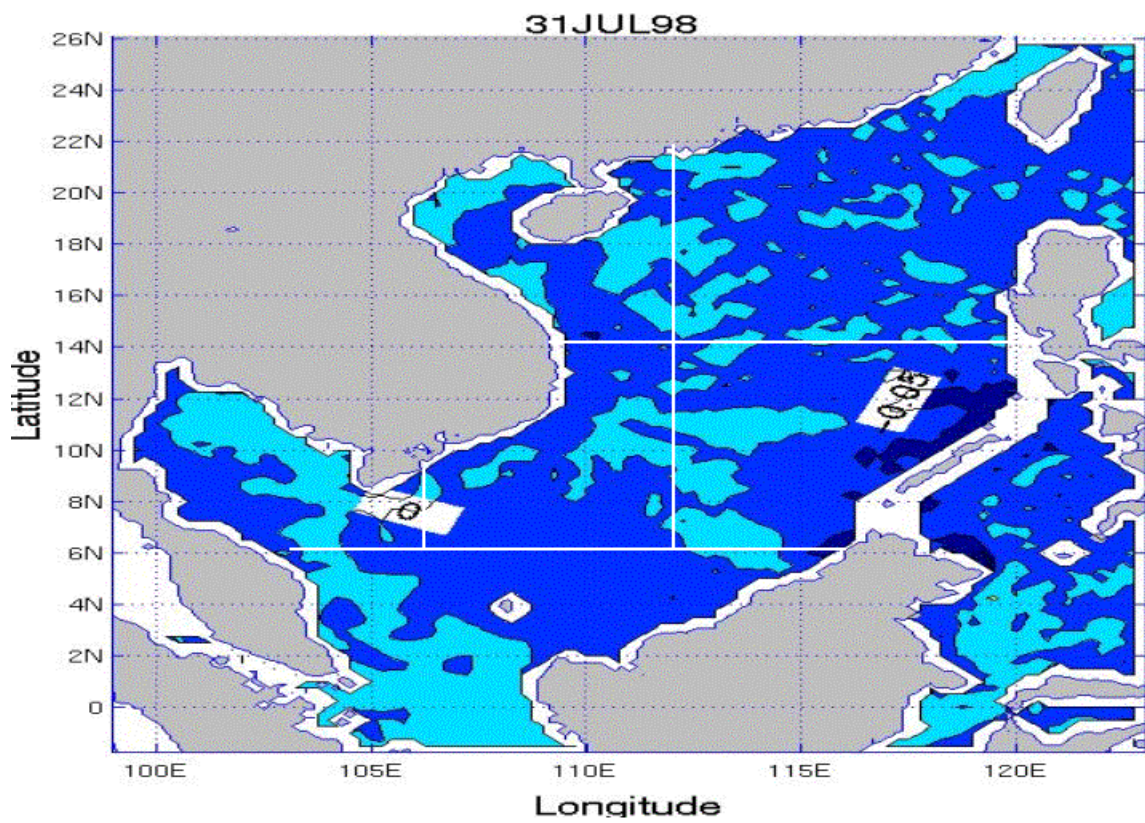
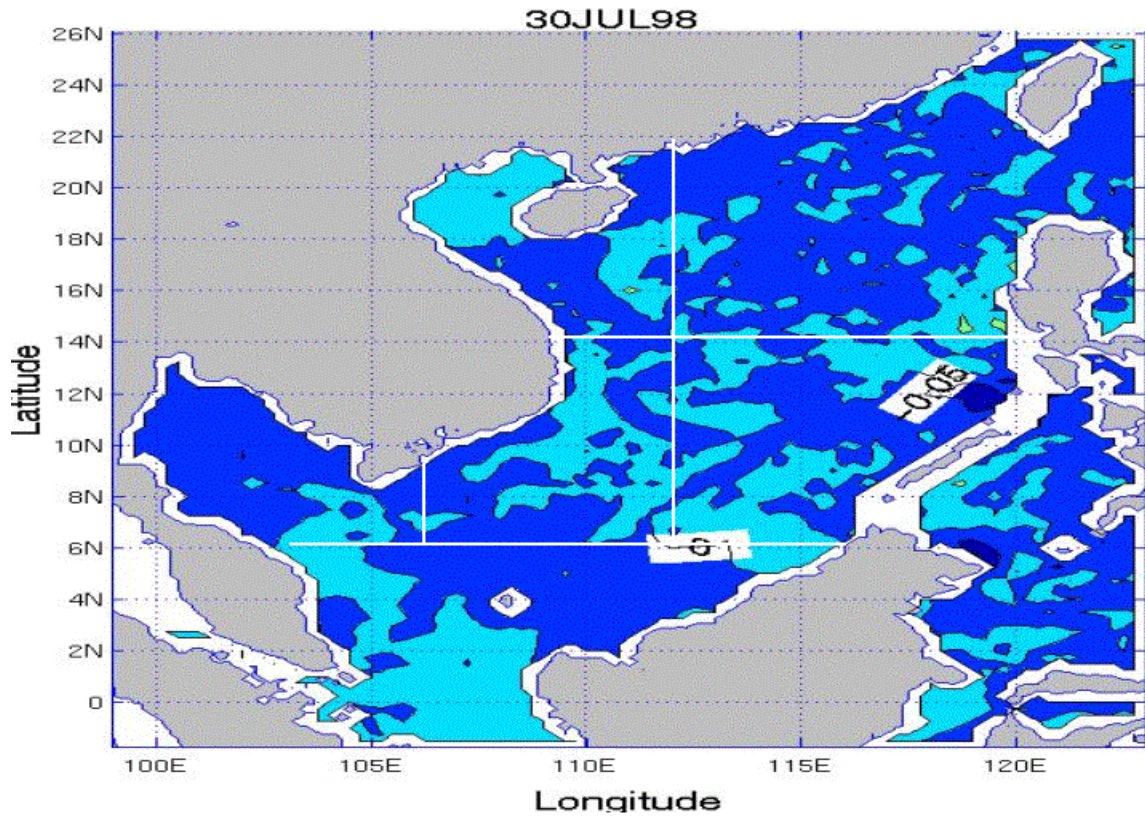












THIS PAGE INTENTIONALLY LEFT BLANK

LIST OF REFERENCES

- Bartz, P., 1972: South Korea. Oxford University Press, New York.
- Beardsley, R.C., R. Limeburner, H. Yu, and G.A. Cannon, 1985: Discharge of the Changjiang (Yangtze River) into the East China Sea. *Cont. Shelf Res.*, 4, 57-76.
- Blumberg, A. and G. Mellor, 1987: A description of a three dimensional coastal ocean circulation model. 1-16. In *Three-Dimensional Coastal Ocean Models*, ed. By N.S. Heaps, American Geophysics Union, Washington, D.C.
- Chu, P.C., J. Lan, and C. Fan, 2001: Japans Sea thermohaline structure and circulation. Part 1: Climatology. *J. Phys. Oceanogr.*, 31, 244-271.
- Chu, P.C. and C. Fan, 2001: Low salinity, cool core cyclonic eddy detected northwest of Luzon during the South China Sea Monsoon Experiment (SCSMEX) in July 1998. *J. Oceanogr.*, 57, 549-563.
- Chu, P.C. and R. Li, 2000: South China Sea isopycnal-surface circulation. *J. Phys. Oceanogr.*, 30, 2419-2438.
- Chu, P.C., S. Lu, and C. Fan, 2000: An air-ocean coupled nowcast/forecast system for the east Asian marginal seas. In *Symposium on advances in mathematical modeling of atmosphere and ocean dynamic*, ed. by P.F. Hodnett, Kluwer Academic Publishers, Dordrecht, Netherlans.
- Chu, P.C., S. Lu, and Y. Chen, 1999a: A coastal air ocean coupled system (CAOCS) evaluated using an airborne bathythermograph (AXBT) data set. *J. Oceanogr.*, 55, 543-558.
- Chu, P.C., N.L. Edmons, and C. Fan, 1999b: Dynamical mechanisms for the South China Sea seasonal circulation and thermohaline variabilities. *J. Phys. Oceanogr.*, 29, 2971-2989.
- Chu, P.C. and C.P. Chang, 1997: South China Sea warm pool in boreal spring. *Adv. Atmos. Sci.*, 14, 195-206.

Chu, P.C., S.K. Wells, S.D. Haeger, C. Szczechowski, and M. Carron, 1997a: Temporal and spatial scales of the Yellow Sea thermal variability. *J. Geophys. Res.*, 102, 5655-5667.

Chu, P.C., C.R. Fralick, S.D. Haeger, and M.J. Carron, 1997b: A parametric model for the Yellow Sea thermal variability. *J. Geophys. Res.*, 102, 10499-10507.

Chu, P.C., H.C. Tseng, C.P. Chang, and J.M. Chen, 1997c: South China Sea warm pool detected in spring from navy's Master Oceanographic Observational Data Set (MOODS). *J. Geophys. Res.*, 102, 15761-15771.

Commander Naval Meteorology and Oceanography Command, 2001: Available on-line at <https://www.cnmoc.navy.mil/>

Dale, W.L., 1956: Winds and drift currents in the South China Sea. *Malay J. Trop. Geogr.*, 8, 1-31.

Hu, J., H. Kawamura, H. Hong, and Y. Qi, 2000: A review on the currents in the South China Sea: Seasonal circulation, South China Sea Warm Current and Kuroshio intrusion. *J. Oceanogr.*, 56, 607-624.

Jacobs, G.A., H.B. Hur, and S.K. Riedlinger, 2000: Yellow and East China Seas response to winds and currents. *J. Geophys. Res.*, 105, 21947-21968.

Katoh, O., K. Teshima, O. Abe, H. Fujita, K. Miyaji, K. Morinaga, and N. Nakagawa, 1996: Process of the Tsushima Current formation revealed by ADCP measurements in summer. *J. Oceanogr.*, 52, 491-507.

Li, H. and Y. Yuan, 1992: On the formation and maintenance mechanisms of the cold water mass of the Yellow Sea. *Chin. J. Oceanol. Limnol.*, 10(2), 97-106.

Lie, H.J., C.H. Cho, J.H. Lee, P. Niiler, and J.H. Hu, 1998: Separation of the Kuroshio water and its penetration onto the continental shelf west of Kyushu. *J. Geophys. Res.*, 103, 2963-2976.

Lie, H.J. and C.H. Cho, 1994: On the origin of the Tsushima Warm Current. *J. Geophys. Res.*, 99, 25081-25091.

Metzger, E.J. and H.E. Hurlburt, 1996: Coupled dynamics of the South China Sea, the Sulu Sea, and the Pacific Ocean. *J. Geophys. Res.*, 101, 12331-12352.

Minami, H., Y. Kano, K. Ogawa, 1999: Long-term variations of potential temperature and dissolved oxygen of the Japan Sea Proper Water. *J. Oceanogr.*, 55, 197-205.

MM5 homepage, 2001: Available on-line at
<http://www.mmm.ucar.edu/mm5/mm5-home.html>

Naval Research Laboratory, 2001: Available on-line at
<http://www.nrlmry.navy.mil/projects/coamps/>

Park, K.-A. and J.Y. Chung, 1999: Spatial and temporal scale variations of sea surface temperature in the East Sea using NOAA/AVHRR data. *J. Oceanogr.*, 55, 271-288.

Park, Y.H., 1986: Water characteristics and movements of the Yellow Sea Warm Current in summer. *Prog. Oceanogr.*, 17, 243-254.

Ramage, C.S., 1971: Monsoon Meteorology. Academic Press, New York.

Riedlinger, S.K. and G.A. Jacobs, 2000: Study of the dynamics of wind driven transports into the Yellow Sea during winter. *J. Geophys. Res.*, 105, 28695-28708.

Seung, Y.-H., 1994: The separation of the East Korean Warm Current and the mechanism for the formation of the North Korean Cold Current (in Japanese). *Kaiyo Mon.*, 758-765.

Seung, Y.-H. and J.-H. Yoon, 1995: Some features of winter convection in the Japan Sea. *J. Oceanogr.*, 51, 61-73.

Shaw, P.-T., 1991: The seasonal variation of the intrusion of Phillipine Sea water into the South China Sea. *J. Geophys. Res.*, 96, 821-827.

Shaw, P.-T. and S.-Y. Chao, 1994: Surface circulation in the South China Sea. *Deep-Sea Res.*, 41, 1663-1683.

Stoelinga, M., 2000: A users' guide to RIP version 3.0: A guide to visualizing PSU/NCAR mesoscale modeling system output. Available on-line at <http://www.mmm.ucar.edu/mm5/documents/ripug.html>

Teague, W.J. and G.A. Jacobs, 2000: Current observations on the development of the Yellow Sea Warm Current. *J. Geophys. Res.*, 105, 3401-3411.

Uda, M. and T. Nakao, 1972: Water masses and currents in the South China Sea and their seasonal changes. *Third Cooperative Study of the Kuroshio and Adjacent Regions (CSK) Symp.*, Bangkok, Thailand, United Nations Educational, Scientific and Cultural Organization, 161-188.

Welch, 1999: The littoral challenge. *Surface Warfare Magazine*. Available on-line at http://surfacewarfare.nswc.navy.mil/magazine/so06_litchallenge.html#top

Wyrski, K. 1961: Scientific results of marine investigations of the South China Sea and Gulf of Thailand 1959-1961. *Naga Report*, Vol. 2.

Yanagi, T. and S. Takahashi, 1993: Seasonal variation of circulations in the East China Sea and the Yellow Sea. *J. Oceanogr.*, 49, 503-520.

Zheng, Q. and V. Klemas, 1982: Determination of winter temperature patterns, fronts, and surface currents in the Yellow Sea and East China Sea from satellite imagery. *Remote Sens. Environ.*, 12, 201-218.

INITIAL DISTRIBUTION LIST

1. Defense Technical Information Center
Ft. Belvoir, VA
2. Dudley Knox Library
Naval Postgraduate School
Monterey, CA
3. Dr. Mary Batteen
Naval Postgraduate School
Monterey, CA

4. Dr. Peter Chu
Naval Postgraduate School
Monterey, CA

5. Mr. Michael Clancy
Fleet Numerical Meteorology and Oceanographer Center
Monterey, CA

6. Mr. Steve Haeger
Naval Oceanographic Office
Stennis Space Center, MS

7. Atmospheric Dynamics and Prediction Branch
Naval Research Laboratory (Code 7530)
Monterey, CA

8. Ocean Dynamics and Prediction Division
Naval Research Laboratory (Code 7320)
Stennis Space Center, MS

9. Ocean, Atmosphere, and Space Science and Technology Division
Office of Naval Research
Arlington, VA

10. Dr. Richard Spinrad
Chief of Naval Operations (Code N96)
Washington, DC
-